VOLUME 26 / NUMBER 18
SEPTEMBER 23, 1988
ACC. NOS. N88-24573 TO N88-25430

STAR

AN ABSTRACT JOURNAL

Scientific and Technical Aerospace Reports

PRODUCED BY THE
SCIENTIFIC AND TECHNICAL
INFORMATION
DIVISION

NASA

NATIONAL AERONAUTICS AND SPACE ADMINISTRATION

WHAT YOU CAN DO FOR *STAR*

All users of this abstract service are urged to forward reports to be considered for announcement in *STAR*. This will aid NASA in its efforts to provide the fullest possible coverage of all scientific and technical publications that might support aeronautics and space research and development. If you have prepared relevant reports (other than those that you will transmit to NASA, DoD, or DOE through the usual contract- or grant-reporting channels), please send them for consideration to the NASA Scientific and Technical Information Facility, P.O. Box 8757, B.W.I. Airport, Maryland 21240.

Reprints of journal articles, book chapters, and conference papers are also welcome. These will be considered for announcement in *STAR's* companion journal, *International Aerospace Abstracts*.

You may specify a particular source to be included in a report announcement if you wish; otherwise the report will be placed on public sale at the National Technical Information Service. Copyrighted publications will be announced but not distributed or sold.

PURCHASE OF *STAR*

The semimonthly issues are available for sale by the Superintendent of Documents, U.S. Government Printing Office, Washington, D.C. 20402.

PUBLISHED BY:

UNITED STATES GOVERNMENT
NATIONAL AERONAUTICS AND SPACE ADMINISTRATION
SCIENTIFIC AND TECHNICAL INFORMATION DIVISION
Scientific and Technical Aerospace Reports, Volume 26, is prepared by the NASA Scientific and Technical Information Facility operated for the National Aeronautics and Space Administration by RMS Associates.

The Administrator of the National Aeronautics and Space Administration has determined that the publication of this periodical is necessary in the transaction of the public business required by law of this Agency. Use of funds for printing this periodical has been approved by the Director of the Office of Management and Budget through March 22, 1989.

US ISSN 0036-8741

INTRODUCTION

Scientific and Technical Aerospace Reports (STAR) is a major component of a comprehensive National Aeronautics and Space Administration information system covering aeronautics, space, and supporting disciplines. *STAR* is issued on the 8th and 23rd of each month and announces current publications of the following types:

- NASA, NASA contractor, and NASA grantee reports
- Reports issued by other U.S. Government Agencies, domestic and foreign institutions, universities, and private firms
- Translations in report form
- NASA-owned patents and patent applications
- Dissertations and theses

Journal, book, and conference literature, cover-to-cover journal translations, and certain foreign dissertations are announced in a companion journal, *International Aerospace Abstracts (IAA)*, available on subscription from the American Institute of Aeronautics and Astronautics, Technical Information Service, 555 West 57th Street, 12th Floor, New York, New York 10019.

SUBJECT SCOPE

Subject scope of *STAR*, and *IAA* includes all aspects of aeronautics and space research and development, supporting basic and applied research, and applications. Aerospace aspects of earth resources, energy development, conservation, oceanography, environmental protection, urban transportation, and other topics of high national priority are also covered.

OTHER NASA PUBLICATIONS

Other NASA publications and information services are described in the publication, *The NASA Scientific and Technical Information System ... and How to Use It*, available without charge from the NASA Scientific and Technical Information Facility, P.O. Box 8757, B.W.I. Airport, Maryland 21240.

HOW TO USE *STAR* SUBJECT CATEGORIES

STAR is categorized by 10 major subject divisions divided into 76 specific subject categories and one general category/division. The major subject divisions are listed in the Table of Contents, together with a note for each that defines its scope and provides any cross-references. For example:

AERONAUTICS

Includes aeronautics (general); aerodynamics; air transportation and safety; aircraft communications and navigation; aircraft design, testing and performance; aircraft instrumentation; aircraft propulsion and power; aircraft stability and control; and research and support facilities (air).

For related information see also *Astronautics*.

Each major division is further divided into as many as nine specific categories, which are identified by category numbers.

Abstracts in *STAR* are grouped by specific category, the categories appearing in sequential order. Category breaks in the abstract section are identified by the category number and title, and a scope note. Cross-references to other categories are provided as appropriate. For example:

02 AERODYNAMICS

Includes aerodynamics of bodies, combinations, wings, rotors, and control surfaces; and internal flow in ducts and turbomachinery.

For related information see also *34 Fluid Mechanics and Heat Transfer.*

CROSS-REFERENCES

Individual *STAR* abstracts are not ordinarily cross-referenced, except for certain conference reports or book translations that have had separate abstracts written for their component papers or chapters. Citations and abstracts of the components follow immediately after those of the parent document. When the subject content of a component differs sufficiently from the general content of the parent, a cross-reference citation also is printed at the end of the category to which it normally would have been assigned if it were independent.

DOCUMENTS ON MICROFICHE

Documents on microfiche(1) are designated by a pound sign (#) following the accession number. The pound sign is used without regard to the source or quality of the microfiche.

AVAILABILITIES

One or more sources from which a document announced in *STAR* is available to the public is given in each citation. The most commonly indicated sources and their acronyms or abbreviations are listed below. If the publication is available from a source other than those listed, the publisher and his address will be displayed on the availability line or in combination with the corporate source line.

Avail: NTIS. Sold by the National Technical Information Service. Prices for hard copy (HC) and microfiche (MF) are indicated by a price code following the letters HC or MF in the *STAR* citation. Current values for the price codes are given in the tables on page vii.

Initially distributed microfiche under the NTIS SRIM (Selected Research in Microfiche) is available at greatly reduced unit prices. For this service and for information concerning subscription to NASA printed reports, consult the NTIS Subscription Section, Springfield, Va. 22161.

NOTE ON ORDERING DOCUMENTS: When ordering NASA publications (those followed by the * symbol), use the N accession number. NASA patent applications (only the specifications are offered) should be ordered by the US-Patent-Appl-SN number. Non-NASA publications (no asterisk) should be ordered by the AD, PB, or other *report number* shown on the last line of the citation, not by the N accession number. It is also advisable to cite the title and other bibliographic identification.

Avail: SOD (or GPO). Sold by the Superintendent of Documents, U.S. Government Printing Office, in hard copy. The current price and order number are given following the availability line. (NTIS will fill microfiche requests, as indicated above, for those documents identified by a # symbol.)

(1) A microfiche is a transparent sheet of film, 105 by 148 mm in size, containing as many as 60 to 98 pages of information reduced to micro images (not to exceed 26:1 reduction).

Avail: BLL (formerly NLL): British Library Lending Division, Boston Spa, Wetherby, Yorkshire, England. Photocopies available from this organization at the price shown. (If none is given, inquiry should be addressed to the BLL.)

Avail: DOE Depository Libraries. Organizations in U.S. cities and abroad that maintain collections of Department of Energy reports, usually in microfiche form, are listed in *Energy Research Abstracts*. Services available from the DOE and its depositories are described in a booklet, *DOE Technical Information Center - Its Functions and Services* (TID-4660), which may be obtained without charge from the DOE Technical Information Center.

Avail: ESDU. Pricing information on specific data, computer programs, and details on ESDU topic categories can be obtained from ESDU International Ltd. Requesters in North America should use the Virginia address while all other requesters should use the London address, both of which are on page vi.

Avail: Fachinformationszentrum, Karlsruhe. Sold by the Fachinformationszentrum Energie, Physik, Mathematik GMBH, Eggenstein Leopoldshafen, Federal Republic of Germany, at the price shown in deutschmarks (DM).

Avail: HMSO. Publications of Her Majesty's Stationery Office are sold in the U.S. by Pendragon House, Inc. (PHI), Redwood City, California. The U.S. price (including a service and mailing charge) is given, or a conversion table may be obtained from PHI.

Avail: NASA Public Document Rooms. Documents so indicated may be examined at or purchased from the National Aeronautics and Space Administration, Public Documents Room (Room 126), 600 Independence Ave., S.W., Washington, D.C. 20546, or public document rooms located at each of the NASA research centers, the NASA Space Technology Laboratories, and the NASA Pasadena Office at the Jet Propulsion Laboratory.

Avail: Univ. Microfilms. Documents so indicated are dissertations selected from *Dissertation Abstracts* and are sold by University Microfilms as xerographic copy (HC) and microfilm. All requests should cite the author and the Order Number as they appear in the citation.

Avail: US Patent and Trademark Office. Sold by Commissioner of Patents and Trademarks, U.S. Patent and Trademark Office, at the standard price of $1.50 each, postage free. (See discussion of NASA patents and patent applications below.)

Avail: (US Sales Only). These foreign documents are available to users within the United States from the National Technical Information Service (NTIS). They are available to users outside the United States through the International Nuclear Information Service (INIS) representative in their country, or by applying directly to the issuing organization.

Avail: USGS. Originals of many reports from the U.S. Geological Survey, which may contain color illustrations, or otherwise may not have the quality of illustrations preserved in the microfiche or facsimile reproduction, may be examined by the public at the libraries of the USGS field offices whose addresses are listed in this Introduction. The libraries may be queried concerning the availability of specific documents and the possible utilization of local copying services, such as color reproduction.

Avail: Issuing Activity, or Corporate Author, or no indication of availability. Inquiries as to the availability of these documents should be addressed to the organization shown in the citation as the corporate author of the document.

NASA PATENTS AND PATENT APPLICATIONS

Patents and patent applications owned by NASA are announced in *STAR* under appropriate subject categories and are referenced in the *STAR* indexes. In the Report/Accession Number Index, patents are indexed by the NASA Case Number (which appears in lieu of the report number in other indexes), the U.S. Patent Number, the U.S. Patent Application Serial Number, and the U.S. Patent Class. Patent applications for which patents have not yet been issued are indexed by the NASA Case Number and the U.S. Patent Application Serial Number.

NASA *patent application specifications* are sold in paper copy by the National Technical Information Service at price code A02. Microfiche are sold at price code A01. The US-Patent-Appl-SN- number should be used in ordering either paper copy or microfiche from NTIS. Printed copies of *patents* (which are not microfiched) are available for purchase at $1.50 per copy from:

Commissioner of Patents and Trademarks
U.S. Patent and Trademark Office
Washington, D.C. 20231

When ordering patents, the U.S. Patent Number should be used, and payment must be remitted in advance, preferably by money order or check payable to the Commissioner of Patents and Trademarks. Prepaid purchase coupons for ordering are also available from the Patent and Trademark Office. The patents and patent applications announced in *STAR* are owned by NASA and are available for royalty-free licensing. Requests for licensing terms and further information should be addressed to:

Associate General Counsel for Intellectual Property/Code GP
National Aeronautics and Space Administration
Washington, D.C. 20546

ELIGIBILITY AND REGISTRATION FOR NASA INFORMATION PRODUCTS AND SERVICES

A variety of services is available to organizations of the following types that have registered with NASA to receive specific services or products:

1. NASA offices, research centers, contractors, subcontractors, grantees, and consultants;
2. Other U.S. Government agencies and their contractors;
3. Libraries in the United States that have arrangements with NASA to maintain collections of NASA documents for public reference;
4. Other organizations in the United States having a need for NASA documents in work related to aeronautics and space research;
5. Organizations abroad that have established reciprocal document exchange arrangements with NASA.

Only the central service points or central points of document acquisition and control within qualified organizations are eligible to register for NASA products and services. Domestic organizations that may be eligible to receive various classes of NASA publications and services should address their requests for registration or for further information to:

NASA Scientific and Technical Information Facility
ATTN: Registration Activity
P.O. Box 8757
B.W.I. Airport, Maryland 21240

Organizations abroad should direct requests to the same address, but to the attention of: International Exchange Program.

AVAILABILITY OF *STAR* ABSTRACTS ON MICROFICHE

Microfiche of the abstract sections of this issue and other issues of *STAR* are available on annual subscription from NTIS as PB88-911300, Attn: Subscriptions, 5285 Port Royal Road, Springfield, Virginia 22161. Annual subscription rates are $70.00 North America; $140.00 foreign. Abstract sections for previous years retroactive to 1964 are available at the current rates. Microfiche for individual *STAR* issue abstract sections are not available.

PUBLIC COLLECTIONS OF NASA DOCUMENTS

DOMESTIC: NASA and NASA-sponsored documents and a large number of aerospace publications are available to the public for reference purposes at the library maintained by the American Institute of Aeronautics and Astronautics, Technical Information Service, 555 West 57th Street, 12th Floor, New York, New York 10019

EUROPEAN: An extensive collection of NASA and NASA-sponsored publications is maintained by the British Library Lending Division, Boston Spa, Wetherby, Yorkshire, England for public access. The British Library Lending Division also has available many of the non-NASA publications cited in *STAR*. European requesters may purchase facsimile copy or microfiche of NASA and NASA-sponsored documents, those identified by both the symbols # and * from ESA - Information Retrieval Service European Space Agency, 8-10 rue Mario-Nikis, 75738 Paris CEDEX 15, France.

FEDERAL DEPOSITORY LIBRARY PROGRAM

In order to provide the general public with greater access to U.S. Government publications, Congress established the Federal Depository Library Program under the Government Printing Office (GPO), with 50 regional depositories responsible for permanent retention of material, inter-library loan, and reference services. At least one copy of nearly every NASA and NASA-sponsored publication, either in printed or microfiche format, is received and retained by the 50 regional depositories. A list of the regional GPO libraries, arranged alphabetically by state, appears on the inside back cover. These libraries are *not* sales outlets. A local library can contact a Regional Depository to help locate specific reports, or direct contact may be made by an individual.

ADDRESSES OF ORGANIZATIONS

American Institute of Aeronautics and Astronautics
Technical Information Service
555 West 57th Street, 12th Floor
New York, New York 10019

British Library Lending Division,
Boston Spa, Wetherby, Yorkshire,
England

Commissioner of Patents and Trademarks
U.S. Patent and Trademark Office
Washington, D.C. 20231

Department of Energy
Technical Information Center
P.O. Box 62
Oak Ridge, Tennessee 37830

ESA-Information Retrieval Service
ESRIN
Via Galileo Galilei
00044 Frascati (Rome) Italy

ESDU International, Ltd.
1495 Chain Bridge Road
McLean, Virginia 22101

ESDU International, Ltd.
251-259 Regent Street
London, W1R 7AD, England

Fachinformationszentrum Energie, Physik, Mathematik GMBH
7514 Eggenstein Leopoldshafen
Federal Republic of Germany

Her Majesty's Stationery Office
P.O. Box 569, S.E. 1
London, England

NASA Scientific and Technical Information Facility
P.O. Box 8757
B.W.I. Airport, Maryland 21240

National Aeronautics and Space Administration
Scientific and Technical Information Division (NTT-1)
Washington, D.C. 20546

National Technical Information Service
5285 Port Royal Road
Springfield, Virginia 22161

Pendragon House, Inc.
899 Broadway Avenue
Redwood City, California 94063

Superintendent of Documents
U.S. Government Printing Office
Washington, D.C. 20402

University Microfilms
A Xerox Company
300 North Zeeb Road
Ann Arbor, Michigan 48106

University Microfilms, Ltd.
Tylers Green
London, England

U.S. Geological Survey Library
National Center - MS 950
12201 Sunrise Valley Drive
Reston, Virginia 22092

U.S. Geological Survey Library
2255 North Gemini Drive
Flagstaff, Arizona 86001

U.S. Geological Survey
345 Middlefield Road
Menlo Park, California 94025

U.S. Geological Survey Library
Box 25046
Denver Federal Center, MS914
Denver, Colorado 80225

NTIS PRICE SCHEDULES

(Effective January 1, 1988)

Schedule A
STANDARD PRICE DOCUMENTS AND MICROFICHE

PRICE CODE	NORTH AMERICAN PRICE	FOREIGN PRICE
A01	$ 6.95	$13.90
A02	9.95	19.90
A03	12.95	25.90
A04-A05	14.95	29.90
A06-A09	19.95	39.90
A10-A13	25.95	51.90
A14-A17	32.95	65.90
A18-A21	38.95	77.90
A22-A25	44.95	89.90
A99	*	*
NO1	49.50	89.90
NO2	48.00	80.00

Schedule E
EXCEPTION PRICE DOCUMENTS AND MICROFICHE

PRICE CODE	NORTH AMERICAN PRICE	FOREIGN PRICE
E01	$ 8.50	17.00
E02	11.00	22.00
E03	12.00	24.00
E04	14.50	29.00
E05	16.50	33.00
E06	19.00	38.00
E07	21.50	43.00
E08	24.00	48.00
E09	26.50	53.00
E10	29.00	58.00
E11	31.50	63.00
E12	34.00	68.00
E13	36.50	73.00
E14	39.50	79.00
E15	43.00	86.00
E16	47.00	94.00
E17	51.00	102.00
E18	55.00	110.00
E19	61.00	122.00
E20	71.00	142.00
E99	*	*

* Contact NTIS for price quote.

IMPORTANT NOTICE

NTIS Shipping and Handling Charges
U.S., Canada, Mexico — ADD $3.00 per TOTAL ORDER
All Other Countries — ADD $4.00 per TOTAL ORDER

Exceptions — Does NOT apply to:
ORDERS REQUESTING NTIS RUSH HANDLING
ORDERS FOR SUBSCRIPTION OR STANDING ORDER PRODUCTS *ONLY*

NOTE: Each additional delivery address on an order requires a separate shipping and handling charge.

VOLUME 26 NUMBER 18 / SEPTEMBER 23, 1988

TABLE OF CONTENTS

AERONAUTICS

Includes aeronautics (general); aerodynamics; air transportation and safety; aircraft communications and navigation; aircraft design, testing and performance; aircraft instrumentation; aircraft propulsion and power; aircraft stability and control; and research and support facilities (air).

For related information see also *Astronautics.*

01 AERONAUTICS (GENERAL) 2455

02 AERODYNAMICS 2456

Includes aerodynamics of bodies, combinations, wings, rotors, and control surfaces; and internal flow in ducts and turbomachinery.

For related information see also *34 Fluid Mechanics and Heat Transfer*

03 AIR TRANSPORTATION AND SAFETY 2460

Includes passenger and cargo air transport operations; and aircraft accidents.

For related information see also *16 Space Transportation* and *85 Urban Technology and Transportation.*

04 AIRCRAFT COMMUNICATIONS AND NAVIGATION 2461

Includes digital and voice communication with aircraft; air navigation systems (satellite and ground based); and air traffic control.

For related information see also *17 Space Communications, Spacecraft Communications, Command and Tracking* and *32 Communications and Radar.*

05 AIRCRAFT DESIGN, TESTING AND PERFORMANCE 2463

Includes aircraft simulation technology.

For related information see also *18 Spacecraft Design, Testing and Performance* and *39 Structural Mechanics.* For land transportation vehicles see *85 Urban Technology and Transportation.*

06 AIRCRAFT INSTRUMENTATION 2465

Includes cockpit and cabin display devices; and flight instruments.

For related information see also *19 Spacecraft Instrumentation* and *35 Instrumentation and Photography.*

07 AIRCRAFT PROPULSION AND POWER 2466

Includes prime propulsion systems and systems components, e.g., gas turbine engines and compressors; and onboard auxiliary power plants for aircraft.

For related information see also *20 Spacecraft Propulsion and Power, 28 Propellants and Fuels,* and *44 Energy Production and Conversion.*

08 AIRCRAFT STABILITY AND CONTROL 2467

Includes aircraft handling qualities; piloting; flight controls; and autopilots.

For related information see also *05 Aircraft Design, Testing and Performance.*

09 RESEARCH AND SUPPORT FACILITIES (AIR) 2467

Includes airports, hangars and runways; aircraft repair and overhaul facilities; wind tunnels; shock tubes; and aircraft engine test stands.

For related information see also *14 Ground Support Systems and Facilities (Space).*

ASTRONAUTICS

Includes astronautics (general); astrodynamics; ground support systems and facilities (space); launch vehicles and space vehicles; space transportation; space communications, spacecraft communications, command and tracking; spacecraft design, testing and performance; spacecraft instrumentation; and spacecraft propulsion and power.

For related information see also *Aeronautics*

12 ASTRONAUTICS (GENERAL) 2469

For extraterrestrial exploration see *91 Lunar and Planetary Exploration.*

13 ASTRODYNAMICS N.A.

Includes powered and free-flight trajectories; and orbital and launching dynamics.

14 GROUND SUPPORT SYSTEMS AND FACILITIES (SPACE) 2469

Includes launch complexes, research and production facilities; ground support equipment, e.g., mobile transporters; and simulators.

For related information see also *09 Research and Support Facilities (Air).*

15 LAUNCH VEHICLES AND SPACE VEHICLES N.A.

Includes boosters; operating problems of launch/space vehicle systems; and reusable vehicles.

For related information see also *20 Spacecraft Propulsion and Power.*

16 SPACE TRANSPORTATION 2470

Includes passenger and cargo space transportation, e.g., shuttle operations; and space rescue techniques.

For related information see also *03 Air Transportation and Safety* and *18 Spacecraft Design, Testing and Performance.* For space suits see *54 Man/System Technology and Life Support.*

17 SPACE COMMUNICATIONS, SPACECRAFT COMMUNICATIONS, COMMAND AND TRACKING 2470

Includes telemetry; space communications networks; astronavigation and guidance; and radio blackout.

For related information see also *04 Aircraft Communications and Navigation* and *32 Communications and Radar.*

18 SPACECRAFT DESIGN, TESTING AND PERFORMANCE 2471

Includes satellites; space platforms; space stations; spacecraft systems and components such as thermal and environmental controls; and attitude controls.

For life support systems see *54 Man/System Technology and Life Support.* For related information see also *05 Aircraft Design, Testing and Performance, 39 Structural Mechanics,* and *16 Space Transportation.*

19 SPACECRAFT INSTRUMENTATION N.A.

For related information see also *06 Aircraft Instrumentation* and *35 Instrumentation and Photography.*

20 SPACECRAFT PROPULSION AND POWER 2474

Includes main propulsion systems and components, e.g. rocket engines; and spacecraft auxiliary power sources.

For related information see also *07 Aircraft Propulsion and Power, 28 Propellants and Fuels, 44 Energy Production and Conversion,* and *15 Launch Vehicles and Space Vehicles.*

CHEMISTRY AND MATERIALS

Includes chemistry and materials (general); composite materials; inorganic and physical chemistry; metallic materials; nonmetallic materials; propellants and fuels; and materials processing.

23 CHEMISTRY AND MATERIALS (GENERAL) 2477

24 COMPOSITE MATERIALS 2477

Includes physical, chemical, and mechanical properties of laminates and other composite materials.

For ceramic materials see *27 Nonmetallic Materials.*

25 INORGANIC AND PHYSICAL CHEMISTRY 2480

Includes chemical analysis, e.g., chromatography; combustion theory; electrochemistry; and photochemistry.

For related information see also *77 Thermodynamics and Statistical Physics.*

26 METALLIC MATERIALS 2484

Includes physical, chemical, and mechanical properties of metals, e.g., corrosion; and metallurgy.

27 NONMETALLIC MATERIALS 2489

Includes physical, chemical, and mechanical properties of plastics, elastomers, lubricants, polymers, textiles, adhesives, and ceramic materials.

For composite materials see *24 Composite Materials.*

28 PROPELLANTS AND FUELS 2494

Includes rocket propellants, igniters and oxidizers; their storage and handling procedures; and aircraft fuels.

For related information see also *07 Aircraft Propulsion and Power, 20 Spacecraft Propulsion and Power,* and *44 Energy Production and Conversion.*

29 MATERIALS PROCESSING 2496

Includes space-based development of products and processes for commercial application.

For biological materials see *55 Space Biology.*

ENGINEERING

Includes engineering (general); communications and radar; electronics and electrical engineering; fluid mechanics and heat transfer; instrumentation and photography; lasers and masers; mechanical engineering; quality assurance and reliability; and structural mechanics.

For related information see also *Physics.*

31 ENGINEERING (GENERAL) 2497

Includes vacuum technology; control engineering; display engineering; cryogenics; and fire prevention.

32 COMMUNICATIONS AND RADAR 2498

Includes radar; land and global communications; communications theory; and optical communications.

For related information see also *04 Aircraft Communications and Navigation* and *17 Space Communications, Spacecraft Communications, Command and Tracking.* For search and rescue see *03 Air Transportation and Safety,* and *16 Space Transportation.*

33 ELECTRONICS AND ELECTRICAL ENGINEERING 2503

Includes test equipment and maintainability; components, e.g., tunnel diodes and transistors; microminiaturization; and integrated circuitry.

For related information see also *60 Computer Operations and Hardware* and *76 Solid-State Physics.*

34 FLUID MECHANICS AND HEAT TRANSFER 2507

Includes boundary layers; hydrodynamics; fluidics; mass transfer and ablation cooling.

For related information see also *02 Aerodynamics* and *77 Thermodynamics and Statistical Physics.*

35 INSTRUMENTATION AND PHOTOGRAPHY 2515

Includes remote sensors; measuring instruments and gages; detectors; cameras and photographic supplies; and holography.

For aerial photography see *43 Earth Resources and Remote Sensing.* For related information see also *06 Aircraft Instrumentation* and *19 Spacecraft Instrumentation.*

36 LASERS AND MASERS 2520

Includes parametric amplifiers.

For related information see also *76 Solid-State Physics.*

37 MECHANICAL ENGINEERING 2522

Includes auxiliary systems (nonpower); machine elements and processes; and mechanical equipment.

38 QUALITY ASSURANCE AND RELIABILITY 2524

Includes product sampling procedures and techniques; and quality control.

39 STRUCTURAL MECHANICS 2526

Includes structural element design and weight analysis; fatigue; and thermal stress.

For applications see *05 Aircraft Design, Testing and Performance* and *18 Spacecraft Design, Testing and Performance.*

GEOSCIENCES

Includes geosciences (general); earth resources and remote sensing; energy production and conversion; environment pollution; geophysics; meteorology and climatology; and oceanography.

For related information see also *Space Sciences.*

42 GEOSCIENCES (GENERAL) **N.A.**

43 EARTH RESOURCES AND REMOTE SENSING **2531**

Includes remote sensing of earth resources by aircraft and spacecraft; photogrammetry; and aerial photography.

For instrumentation see *35 Instrumentation and Photography.*

44 ENERGY PRODUCTION AND CONVERSION **2535**

Includes specific energy conversion systems, e.g., fuel cells; global sources of energy; geophysical conversion; and windpower.

For related information see also *07 Aircraft Propulsion and Power, 20 Spacecraft Propulsion and Power,* and *28 Propellants and Fuels.*

45 ENVIRONMENT POLLUTION **2538**

Includes atmospheric, noise, thermal, and water pollution.

46 GEOPHYSICS **2540**

Includes aeronomy; upper and lower atmosphere studies; ionospheric and magnetospheric physics; and geomagnetism.

For space radiation see *93 Space Radiation.*

47 METEOROLOGY AND CLIMATOLOGY **2544**

Includes weather forecasting and modification.

48 OCEANOGRAPHY **2547**

Includes biological, dynamic, and physical oceanography; and marine resources.

For related information see also *43 Earth Resources and Remote Sensing.*

LIFE SCIENCES

Includes life sciences (general); aerospace medicine; behavioral sciences; man/system technology and life support; and space biology.

51 LIFE SCIENCES (GENERAL) **2548**

52 AEROSPACE MEDICINE **2550**

Includes physiological factors; biological effects of radiation; and effects of weightlessness on man and animals.

53 BEHAVIORAL SCIENCES **2551**

Includes psychological factors; individual and group behavior; crew training and evaluation; and psychiatric research.

54 MAN/SYSTEM TECHNOLOGY AND LIFE SUPPORT **2552**

Includes human engineering; biotechnology; and space suits and protective clothing.

For related information see also *16 Space Transportation.*

55 SPACE BIOLOGY **N.A.**

Includes exobiology; planetary biology; and extraterrestrial life.

MATHEMATICAL AND COMPUTER SCIENCES

Includes mathematical and computer sciences (general); computer operations and hardware; computer programming and software; computer systems; cybernetics; numerical analysis; statistics and probability; systems analysis; and theoretical mathematics.

59 MATHEMATICAL AND COMPUTER SCIENCES (GENERAL) **N.A.**

60 COMPUTER OPERATIONS AND HARDWARE **2554**

Includes hardware for computer graphics, firmware, and data processing.

For components see *33 Electronics and Electrical Engineering.*

61 COMPUTER PROGRAMMING AND SOFTWARE **2555**

Includes computer programs, routines, algorithms, and specific applications, e.g., CAD/CAM.

62 COMPUTER SYSTEMS **2559**

Includes computer networks and special application computer systems.

63 CYBERNETICS **2560**

Includes feedback and control theory, artificial intelligence, robotics and expert systems.

For related information see also *54 Man/System Technology and Life Support.*

64 NUMERICAL ANALYSIS **2562**

Includes iteration, difference equations, and numerical approximation.

65 STATISTICS AND PROBABILITY **2568**

Includes data sampling and smoothing; Monte Carlo method; and stochastic processes.

66 SYSTEMS ANALYSIS **N.A.**

Includes mathematical modeling; network analysis; and operations research.

67 THEORETICAL MATHEMATICS **2569**

Includes topology and number theory.

PHYSICS

Includes physics (general); acoustics; atomic and molecular physics; nuclear and high-energy physics; optics; plasma physics; solid-state physics; and thermodynamics and statistical physics.

For related information see also *Engineering.*

70 PHYSICS (GENERAL) **2569**

For precision time and time interval (PTTI) see *35 Instrumentation and Photography;* for geophysics, astrophysics or solar physics see *46 Geophysics, 90 Astrophysics,* or *92 Solar Physics.*

71 ACOUSTICS 2570
Includes sound generation, transmission, and attenuation.
For noise pollution see *45 Environment Pollution.*

72 ATOMIC AND MOLECULAR PHYSICS 2571
Includes atomic structure, electron properties, and molecular spectra.

73 NUCLEAR AND HIGH-ENERGY PHYSICS 2574
Includes elementary and nuclear particles; and reactor theory.
For space radiation see *93 Space Radiation.*

74 OPTICS 2574
Includes light phenomena and optical devices.
For lasers see *36 Lasers and Masers.*

75 PLASMA PHYSICS 2577
Includes magnetohydrodynamics and plasma fusion.
For ionospheric plasmas see *46 Geophysics.* For space plasmas see *90 Astrophysics.*

76 SOLID-STATE PHYSICS 2580
Includes superconductivity.
For related information see also *33 Electronics and Electrical Engineering* and *36 Lasers and Masers.*

77 THERMODYNAMICS AND STATISTICAL PHYSICS 2586
Includes quantum mechanics; theoretical physics; and Bose and Fermi statistics.
For related information see also *25 Inorganic and Physical Chemistry* and *34 Fluid Mechanics and Heat Transfer.*

SOCIAL SCIENCES

Includes social sciences (general); administration and management; documentation and information science; economics and cost analysis; law, political science, and space policy; and urban technology and transportation.

80 SOCIAL SCIENCES (GENERAL) 2587
Includes educational matters.

81 ADMINISTRATION AND MANAGEMENT 2587
Includes management planning and research.

82 DOCUMENTATION AND INFORMATION SCIENCE 2589
Includes information management; information storage and retrieval technology; technical writing; graphic arts; and micrography.
For computer documentation see *61 Computer Programming and Software.*

83 ECONOMICS AND COST ANALYSIS N.A.
Includes cost effectiveness studies.

84 LAW, POLITICAL SCIENCE AND SPACE POLICY 2590
Includes NASA appropriation hearings; aviation law; space law and policy; international law; international cooperation; and patent policy.

85 URBAN TECHNOLOGY AND TRANSPORTATION N.A.
Includes applications of space technology to urban problems; technology transfer; technology assessment; and surface and mass transportation.
For related information see *03 Air Transportation and Safety, 16 Space Transportation,* and *44 Energy Production and Conversion.*

SPACE SCIENCES

Includes space sciences (general); astronomy; astrophysics; lunar and planetary exploration; solar physics; and space radiation.
For related information see also *Geosciences.*

88 SPACE SCIENCES (GENERAL) 2590

89 ASTRONOMY 2592
Includes radio, gamma-ray, and infrared astronomy; and astrometry.

90 ASTROPHYSICS 2593
Includes cosmology; celestial mechanics; space plasmas; and interstellar and interplanetary gases and dust.
For related information see also *75 Plasma Physics.*

91 LUNAR AND PLANETARY EXPLORATION 2594
Includes planetology; and manned and unmanned flights.
For spacecraft design or space stations see *18 Spacecraft Design, Testing and Performance.*

92 SOLAR PHYSICS 2595
Includes solar activity, solar flares, solar radiation and sunspots.
For related information see *93 Space Radiation.*

93 SPACE RADIATION 2596
Includes cosmic radiation; and inner and outer earth's radiation belts.
For biological effects of radiation see *52 Aerospace Medicine.* For theory see *73 Nuclear and High-Energy Physics.*

GENERAL

Includes aeronautical, astronautical, and space science related histories, biographies, and pertinent reports too broad for categorization; histories or broad overviews of NASA programs.

99 GENERAL 2596

Note: N.A. means that no abstracts were assigned to this category for this issue.

SUBJECT INDEX I-1
PERSONAL AUTHOR INDEX I-51
CORPORATE SOURCE INDEX I-57
CONTRACT NUMBER INDEX I-69
REPORT/ACCESSION NUMBER INDEX I-73

TYPICAL CITATION AND ABSTRACT

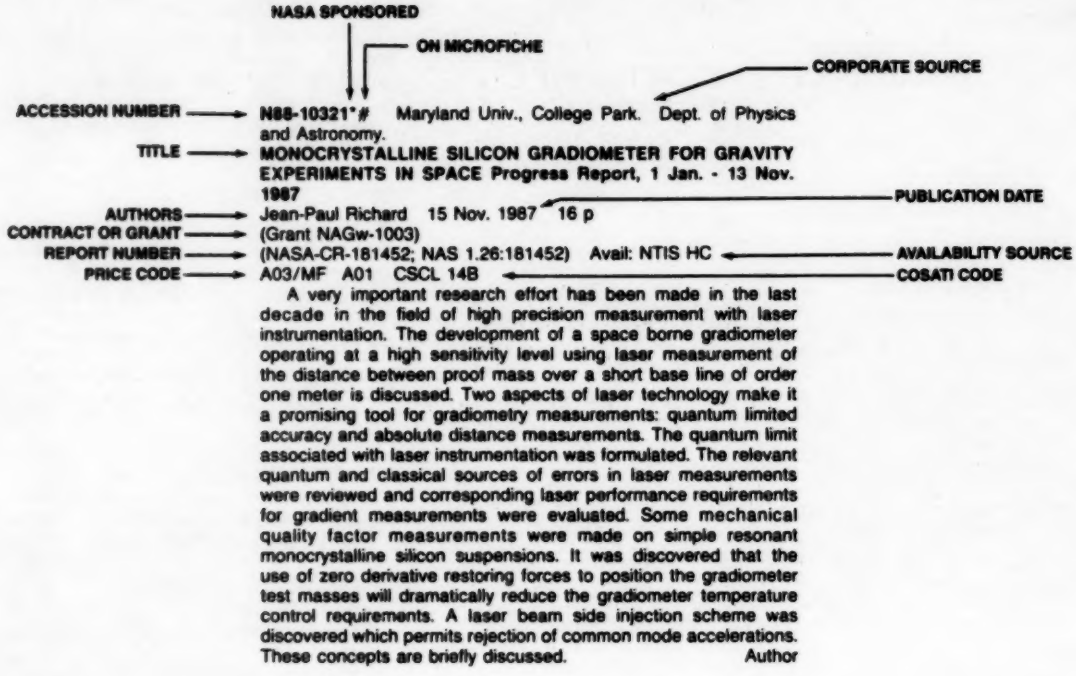
NASA SPONSORED
ON MICROFICHE
CORPORATE SOURCE
ACCESSION NUMBER
N88-10321*# Maryland Univ., College Park. Dept. of Physics and Astronomy.
TITLE
MONOCRYSTALLINE SILICON GRADIOMETER FOR GRAVITY EXPERIMENTS IN SPACE Progress Report, 1 Jan. - 13 Nov. 1987
PUBLICATION DATE
AUTHORS
Jean-Paul Richard 15 Nov. 1987 16 p
CONTRACT OR GRANT
(Grant NAGw-1003)
REPORT NUMBER
(NASA-CR-181452; NAS 1.26:181452) Avail: NTIS HC
AVAILABILITY SOURCE
PRICE CODE
A03/MF A01 CSCL 14B
COSATI CODE
A very important research effort has been made in the last decade in the field of high precision measurement with laser instrumentation. The development of a space borne gradiometer operating at a high sensitivity level using laser measurement of the distance between proof mass over a short base line of order one meter is discussed. Two aspects of laser technology make it a promising tool for gradiometry measurements: quantum limited accuracy and absolute distance measurements. The quantum limit associated with laser instrumentation was formulated. The relevant quantum and classical sources of errors in laser measurements were reviewed and corresponding laser performance requirements for gradient measurements were evaluated. Some mechanical quality factor measurements were made on simple resonant monocrystalline silicon suspensions. It was discovered that the use of zero derivative restoring forces to position the gradiometer test masses will dramatically reduce the gradiometer temperature control requirements. A laser beam side injection scheme was discovered which permits rejection of common mode accelerations. These concepts are briefly discussed. Author

VOLUME 26 NUMBER 18/ SEPTEMBER 23, 1988

Scientific and Technical Aerospace Reports

A Semimonthly Publication of the National Aeronautics and Space Administration

01 AERONAUTICS (GENERAL)

N88-24573# Air Force Wright Aeronautical Labs., Wright-Patterson AFB, Ohio.
COMPOSITE REPAIR OF CRACKED ALUMINUM ALLOY AIRCRAFT STRUCTURE Final Report, Oct. 1981 - Apr. 1984
Forrest A. Sandow and Raymond K. Cannon Sep. 1987 48 p
(AD-A190514; AFWAL-TR-87-3072) Avail: NTIS HC A03/MF A01 CSCL 01C

A bonded composite patch repair of fatigue-cracked aluminum on aircraft has advantages over a standard bolted metal patch repair, such as no severe stress concentrations (no bolt holes), fatigue-resistant patch, thinner patch, simple molding techniques, a sealed interface to help prevent corrosion, and usually no inspection (NDI) problems. The objective of this program was to determine the effect of composite patches on stress intensity and crack growth characteristics of aluminum. This was accomplished by studying metal thickness and patch parameters (area, thickness, and ply orientation) effects on crack growth rate of the composite patch/aluminum specimen. Both room temperature and elevated temperature (250 F) curing adhesives were studied. The testing procedure consists of edge cracking a 4-inch x 18-inch 2024-t3 aluminum specimen to a length of between 03 and 05 inch. The aluminum is then prepared for bonding, normally using the phosphoric acid non-tank anodize (PANTA) method, primed, and patched. The specimen then cycled to failure. Both constant amplitude and flight spectrum loading were used. Patch material for most specimens was 5521/4 boron/epoxy. Results have shown thickness of the metal being repaired to be the most significant factor in the repair process. There was also a significant difference in results between constant amplitude and spectrum tests. 1/8-inch thick aluminum constant amplitude tests showed lifetime extensions of about 15 times, while 1/16-inch and 1/8 inch thick spectrum waded specimens showed extensions of about 15 and 7 times respectively. GRA

N88-24574# International Trade Administration, Washington, D.C.
COMPETITIVE ASSESSMENT OF THE U.S. CIVIL HELICOPTER INDUSTRY
Apr. 1988 109 p
(PB88-186325) Avail: NTIS HC A06/MF A01 CSCL 01A

The competitive assessment of the U.S. civil helicopter industry is the 44th industry assessment published by the Trade Development unit of the U.S. Department of Commerce. Trade Development has major responsibility for developing U.S. government policy on competitiveness and export promotion. Contents by chapter are as follows: The U.S. Civil Helicopter Industry; Structure of the Industry; Economic Characteristics of the Industry; Factors Affecting Industry Growth; Foreign Competition; Industry Outlook; Implications of U.S. Government Policies on the Helicopter Industry. GRA

N88-24575# Air Force Systems Command, Wright-Patterson AFB, Ohio. Foreign Technology Div.
ACTA AERONAUTICA ET ASTRONAUTICA SINICA (SELECTED ARTICLES)
18 Feb. 1988 36 p Transl. into ENGLISH of Hangkong Xuebao (Peoples Republic of China), v. 8, no. 2, Feb. 1987 p 1-18
(AD-A191552; FTD-ID(RS)T-1193-87) Avail: NTIS HC A03/MF A01 CSCL 01C

This paper demonstrates the importance of stealth penetration ability for future military aircrafts via three areas such as the inspirations from war, the conclusions of a system engineering analysis and the threats from anti-stealth techniques, etc. The emphasis of this paper is placed on the analysis of the new content of tactical-technical requirements for military aircrafts in the early part of the 21st century—the three categories included in the stealth penetration ability are: (1) scattering and radiation characteristics of aircrafts; (2) electronic interference ability of aircrafts; (3) tactical stealth techniques used by aircrafts. GRA

N88-24576# Federal Aviation Administration, Atlantic City, N.J. Office of Aviation Policy and Plans.
FAA AVIATION FORECASTS FISCAL YEARS 1988-1999
Feb. 1988 195 p
(AD-A191711; FAA-APO-88-1) Avail: NTIS HC A09/MF A01 CSCL 01A

This report contains Fiscal Years 1988-1999 FAA forecasts of aviation activity at FAA facilities. These include airports with FAA control towers, air route traffic control centers, and flight service stations. Detailed forecasts were made for the four major users of the National Aviation System: air carriers, air taxi/commuters, general aviation and the military. The forecasts have been prepared to meet the budget and planning needs of the constituent units of the FAA and to provide information that can be used by state and local authorities, by the aviation industry, and by the general public. The overall outlook for the forecast period is for continued economic growth, rising real fuel prices, and moderate inflation. Based upon these assumptions, aviation activity by fiscal year 1999 is forecast to increase by 33.4 percent at towered airports, 33.5% at air route traffic control centers, and 11.7% in flight services performed. Hours flown by general aviation are forecast to increase 6.1% and helicopter hours flown, 33.3%. Scheduled domestic revenue passenger miles (RPMs) are forecast to increase by 81.3%, and regionals/commuters by 16.9%. percent. Scheduled domestic revenue passenger miles (RPM's) are forecast to increase 75.8 percent, with scheduled international RPM's forecast to increase by 81.3 percent, and regionals/commuters RPM's forecast to increase by 16.9 percent. GRA

N88-24577# Federal Aviation Administration, Washington, D.C. Office of Management Systems.
US CIVIL AIRMEN STATISTICS, 1987
Patricia W. Carter 31 Mar. 1988 39 p
(AD-A191714) Avail: NTIS HC A03/MF A01 CSCL 05I

The U.S. Civil Airmen Statistics is an annual study published to meet the demands of FAA, other government agencies, and industry for more detailed airmen statistics than those published in other FAA reports. Statistics pertaining to airmen, both pilot and nonpilot, were obtained from the official airman certification records maintained at the FAA Aeronautical Center, Oklahoma City, Oklahoma. An active Airmen is one holding both an airmen certificate and a valid medical certificate. Airmen who must have a valid medical exam to exercise the privileges of their certificate are all airplane pilots, control tower operators, and flight navigators. Lighter-than-air pilots are not required to have a medical examination but the numbers represent only those who had a

valid medical certificate. Mechanics, parachute riggers, ground instructors, and dispatchers certificates represent all certificates on record at the Aeronautical Center. GRA

N88-24578* National Aeronautics and Space Administration, Washington, D.C.
AERONAUTICAL ENGINEERING: A CONTINUING BIBLIOGRAPHY WITH INDEXES (SUPPLEMENT 227)
Jun. 1988 122 p
(NASA-SP-7037(227); NAS 1.21:7037(227)) Avail: NTIS HC A06 CSCL 01B

This bibliography lists 418 reports, articles, and other documents introduced into the NASA scientific and technical information system in May, 1988. Author

N88-24579*# National Aeronautics and Space Administration. Ames Research Center, Moffett Field, Calif.
PROGRESS AND FUTURE DIRECTIONS IN COMPUTATIONAL FLUID DYNAMICS
Paul Kutler and Anthony R. Gross Jun. 1988 17 p
(NASA-TM-100091; A-88128; NAS 1.15:100091) Avail: NTIS HC A03/MF A01 CSCL 01B

Computational fluid dynamics (CFD) has made great strides in the detailed simulation of complex fluid flows, including the fluid physics of flows heretofore not understood. It is now being routinely applied to some rather complicated problems, and starting to impact the design cycle of aerospace vehicles and their components. In addition, it is being used to complement and is being complemented by experimental studies. In this paper some major elements of contemporary CFD research, such as code validation, turbulence physics, and hypersonic flows are discussed, along with a review of the principal pacing items that currently govern CFD. Several examples are presented to illustrate the current state of the art. Finally, prospects for the future of the development and application of CFD are suggested. Author

02 AERODYNAMICS

Includes aerodynamics of bodies, combinations, wings, rotors, and control surfaces; and internal flow in ducts and turbomachinery.

For related information see also *34 Fluid Mechanics and Heat Transfer.*

N88-24580*# National Aeronautics and Space Administration. Langley Research Center, Hampton, Va.
AERODYNAMIC PERFORMANCE AND PRESSURE DISTRIBUTIONS FOR A NASA SC(2)-0714 AIRFOIL TESTED IN THE LANGLEY 0.3-METER TRANSONIC CRYOGENIC TUNNEL
Renaldo V. Jenkins, Acquilla S. Hill, and Edward J. Ray Jul. 1988 300 p Sponsored by NASA, Washington
(NASA-TM-4044; L-16384; NAS 1.15:4044) Avail: NTIS HC A13/MF A01 CSCL 01A

This report presents in graphic and tabular forms the aerodynamic coefficient and surface pressure distribution data for a NASA SC(2)-0714 airfoil tested in the Langley 0.3-Meter Transonic Cryogenic Tunnel. The test was another in a series of tests involved in the joint NASA/U.S. Industry Advanced Technology Airfoil Tests program. This 14% thick supercritical airfoil was tested at Mach numbers from 0.6 to 0.76 and angles of attack from -2.0 to 6.0 degrees. The test Reynolds numbers were 4 million, 6 million, 10 million, 15 million, 30 million, 40 million, and 45 million. Author

N88-24581# Princeton Univ., N. J. Dept. of Mechanical and Aerospace Engineering.
FUNDAMENTAL ASPECTS OF THE STRUCTURE OF SUPERSONIC TURBULENT BOUNDARY LAYERS Final Report, Jan. 1985 - Jan. 1988
A. J. Smits 21 Jan. 1988 38 p
(Grant AF-AFOSR-0126-85)
(AD-A191494; AFOSR-88-0028TR) Avail: NTIS HC A03/MF A01 CSCL 20D

This three-year contract originally had two tasks: to investigate the structure of flat plate supersonic turbulent boundary layers (Task A), and to investigate longitudinal curvature effects in turbulent boundary layers (Task B). As a result of the work performed under these task headings, we identified a need to study the structure of simple, wall-bounded vortex loops. This investigation (Task C) commenced in the third year, and we feel that it has made a major contribution to our understanding of the ensemble-averaged structure of low and high speed turbulent boundary layers. The progress reported here is that achieved in completing these three tasks. GRA

N88-24582# Air Force Systems Command, Wright-Patterson AFB, Ohio. Foreign Technology Div.
EXPERIMENT INVESTIGATION ON LONGITUDINAL CHARACTERISTICS OF THE FORWARD SWEPT WING
Yaobin Guo, Xuejian Wang, and Binjiang Zhang 10 Mar. 1988 29 p Transl. into ENGLISH from Hangkong Xuebao (Peoples Republic of China), v. 8, no. 6, Jun. 1987 p 227-238 Original language document was announced in IAA as A88-16336
(AD-A191553; FTD-ID(RS)T-1364-87) Avail: NTIS HC A03/MF A01 CSCL 01C

Based on testing results of aerodynamic forces and pressures from a wind tunnel, the longitudinal aerodynamics characteristics of a forward swept wing are discussed in this paper. The results are also compared with the data of an associated aft swept wing. Measures of improving the inboard flowfield of a forward swept wing are also investigated, and the results are discussed. Under a low speed situation, an appropriate sweptback of the root section can improve the flow consequently obtaining higher aerodynamic performances. GRA

N88-24583# Harry Diamond Labs., Adelphi, Md.
AN ANALYTIC MODEL FOR AERODYNAMIC SHAPES Final Report, Oct. 1986 - Oct. 1987
Michael J. Vrabel Mar. 1988 66 p Sponsored by Army Lab. Command, Adelphi, Md.
(AD-A191573; HDL-TR-140) Avail: NTIS HC A04/MF A01 CSCL 01A

Exact analytical models represent a viable alternative for applications requiring geometric constructs with a level of surface perfection unachievable with traditional polynomial techniques. To avoid the limitations in shape complexity normally associated with traditional analytic models, a model based upon a topological transformation of a lofted surface was developed. The consequence is, if not an equation of all shapes, then, at least, an equation describing a great many arbitrarily complicated shapes. A full theoretical development of the model is presented along with a model-implementing FORTRAN source module and some example geometries. GRA

N88-24584# Purdue Univ., West Lafayette, Ind. Sciences and Propulsion Center.
RESEARCH ON AERO-THERMODYNAMIC DISTORTION INDUCED STRUCTURAL DYNAMIC RESPONSE OF MULTI-STAGE COMPRESSOR BLADING Final Technical Report, Apr. 1983 - Nov. 1987
Sanford Fleeter 15 Jan. 1988 237 p
(Contract F49620-83-K-0029)
(AD-A192169; ME-TSPC-TR-88-10; AFOSR-88-0045TR) Avail: NTIS HC A11/MF A01 CSCL 01A

The overall objective of this research program was to quantitatively investigate the fundamental phenomena relevant to aero-thermodynamic distortion induced structural dynamic blade responses in multi-stage gas turbine engine components. The technical approach involved both experiment and analysis. The flow physics of multi-stage blade row interactions has been experimentally investigated, with unique high reduced frequency unsteady aerodynamic data obtained to understand, quantify, and discriminate the fundamental flow phenomena as well as to direct

the modeling of advanced analyses. The development of an unsteady viscous flow analysis appropriate for aerodynamic forced response predictions was initiated. A structural dynamics model based on an energy balance techniques coupled with the unsteady aerodynamic analyses under development is being utilized to investigate aerodynamically forced response of turbomachine blade rows. GRA

N88-24585# Aeronautical Research Inst. of Sweden, Stockholm. Aerodynamics Dept.
WIND TUNNEL INVESTIGATION OF WING AND CONTROL PANEL LOADS AT TRANSONIC AND SUPERSONIC SPEEDS ON SOME SCHEMATIC CRUCIFORM MISSILE CONFIGURATIONS
Sven Erik Gudmundson and Lars Torngren Sep. 1987 207 p
(Contracts FMV-FlygFL-82223-74-001-07-001; FMV-FlygFL-82223-75-007-07-001)
(FFA-TN-1986-43; ETN-88-92491) Avail: NTIS HC A10/MF A01

Transonic and supersonic wind tunnel tests investigated the loads on one wing panel and one control panel at different positions on schematic body-wing, body-tail, and body-wing-tail cruciform missile configurations for 0 and 45 deg roll position. The Mach number range was 0.7 to 3.0 and the angle of attack varied between minus 3 degrees and plus 24 degrees. The tail controls were tested at different angles from 0 deg to -20 deg with 5 deg steps. The result is given in diagram and tables. Interference coefficients and downwash figures were evaluated. ESA

N88-24586# Aeronautical Research Inst. of Sweden, Stockholm. Aerodynamics Dept.
INCOMPRESSIBLE EULER SOLUTION ON A MULTIBLOCK GRID AROUND A CAR CONFIGURATION
Torsten Berglind 16 Nov. 1987 28 p
(Contract STU-87-0472)
(FFA-TN-1987-65; ETN-88-92493) Avail: NTIS HC A03/MF A01

A patched multiblock grid around a car-like configuration above a flat ground plane was constructed by transfinite interpolation. The flow region is divided into eight computational blocks, so that each coordinate side of a block contains exactly one type of boundary condition. The grid is of O-O type with four 3/4 type mapping singularities. A finite-volume Euler solver using explicit Runge-Kutta time stepping was coded to handle general multiblock structures. The symmetrical flow around a bluff body with fundamental vehicle shape, Davis A1 model, serves as a test case. The computed example does not converge completely due to nonphysical vortices generated at interface boundaries. Interface boundaries with slope discontinuities intersect regions with high flow gradients implying large truncation errors and large artificial viscosity. The solution to this is either to change the mapping concept so that grid defects are located in regions with low flow gradients, or interpolate values at block interfaces so that all interface boundaries have metric continuity. ESA

N88-24587# Aeronautical Research Inst. of Sweden, Stockholm. Aerodynamics Dept.
WAVE GROWTH ASSOCIATED WITH TURBULENT SPOTS IN PLANE POISEUILLE FLOW
Dan S. Henningson 22 Jan. 1988 32 p Sponsored by the Swedish Board for Technical Development
(FFA-TN-1988-08; ETN-88-92496) Avail: NTIS HC A03/MF A01

Numerical simulations show that the waves at the wingtips of plane Poiseuille spots grow rapidly as they propagate into the turbulent region. Kinematic wave theory is used to investigate the growth mechanism by calculating the amplitude of waves along rays defined by the group velocity. A dispersion relation is found by solving an extended form of the Orr-Sommerfeld equation using spatially averaged mean velocity profiles. The results indicate that the waves grow due to a combination of wave energy focusing and cross flow type instability. The exponential growth resulting from the cross flow inflexional profiles is the dominating factor. Good agreement between the wave characteristics calculated by the theory and those found in the simulations is found. ESA

N88-24588 Rensselaer Polytechnic Inst., Troy, N.Y.
PASSIVE SHOCK WAVE-BOUNDARY LAYER CONTROL FOR THE BELL FX69-H-098 AIRFOIL Ph.D. Thesis
Timothy John Bidlack 1987 269 p
Avail: Univ. Microfilms Order No. DA8729296

Passive shock wave-boundary layer control involves using a porous surface for the portion of an airfoil in the region of a sufficiently strong shock wave and positioning a cavity beneath it. Such a combination allows for some of the flow compressed by the shock waves to recirculate upstream. The suction created downstream of the shock wave by the difference in pressure accross it and the removal of flow in this region helps thin the boundary layer and reduces the possiblity of flow separation. In addition, the injection of flow upstream of the normal shock wave results in the formation of a lambda shock wave. This reduces the strength of the normal shock wave and its corresponding effects. As cruise speeds of helicopters increase, the transonic flow effects experienced by rotor blades becomes more pronounced. To determine the feasibility of applying passive shock wave-boundary layer control to a typical rotor blade, this research was conducted. The effects of varying the depth of the cavity was also investigated. The Bell FX69-H-098 airfoil was selected as a representative helicopter rotor blade. Its profile is typical of airfoils designed for high lift-to-drag ratios in hover, high maximum lift coefficients at retreating blade Mach numbers, and has favorable drag divergence characteristics. Dissert. Abstr.

N88-24589 Iowa Univ., Iowa City.
PREDICTION OF LAMINAR AND TURBULENT FLOWS PAST SINGLE AND TWIN AIRFOILS Ph.D. Thesis
Kemakolam M. Obasih [1987] 366 p
Avail: Univ. Microfilms Order No. DA8729497

A numerical solution of the incompressible, two dimensional, constant property, ensemble averaged Navier Stokes equations, including a transition to turbulence model, is obtained for a single and twin airfoil in a nearly orthogonal boundary-fitted coordinate system. The Navier Stokes equations are solved by the finite analytic method. The turbulent transport properties are determined by a k-epsilon-E turbulence model and the Reynolds stresses are modelled by the algebraic eddy viscosity model. The transition from laminar to turbulent flow is determined from an empirical correlation based on the growth of the momentum thickness Reynolds number of the flow as it develops. A numerical computer program called FANS-2DEF is developed. For verification, finite analytic solutions are first obtained for laminar and turbulent flows over a finite flat plate at Reynolds numbers of 10,000 and 1,700,000 respectively. Results are verified by experimental data. Then results were obtained for laminar flow over a NACA 0012 airfoil at various angles of attack and Reynolds numbers. Good agreement with experimental results was obtained. Laminar and turbulent flow past a twin airfoil were also obtained. Predicted results agree well with the expected physical flow situation. Dissert. Abstr.

N88-24590# George Washington Univ., Washington, D.C. School of Engineering and Applied Science.
A TRANSONIC SMALL DISTURBANCE WING DESIGN METHODOLOGY M.S. Thesis
Pamela Susan Phillips May 1987 70 p
Avail: NTIS HC A04/MF A01

A predictor-corrector wing/airfoil design code was developed that predicts surface contour modifications to achieve a specified pressure distribution. The design code is comprised of an existing small distrubance wing-body-pod-pylon-winglet code and a version of existing design algorithm. Several two-and three-dimensional design test cases were successfully run demonstrating the subject code. Included in these cases are two design tasks previously completed by using a cut and try approach. These results and a description of the formulation of the design code are presented.

Also included is background information on optimization, fictitious gas, predictor-correlator, and inverse methods. Author

N88-24591*# Eloret Corp., Sunnyvale, Calif.
EXPERIMENTAL INVESTIGATION OF HYPERSONIC AERODYNAMICS Final Report, 1 Apr. 1987 - 30 Jun. 1988
Peter F. Intrieri 5 Jul. 1988 37 p
(Contract NCC2-475)
(NASA-CR-182973; NAS 1.26:182973) Avail: NTIS HC A03/MF A01 CSCL 01A

An extensive series of ballistic range tests were conducted at the Ames Research Center to determine precisely the aerodynamic characteristics of the Galileo entry probe vehicle. Figures and tables are presented which summarize the results of these ballistic range tests. Drag data were obtained for both a nonablated and a hypothesized ablated Galileo configuration at Mach numbers from about 0.7 to 14 and at Reynolds numbers from 1000 to 4 million. The tests were conducted in air and the experimental results were compared with available Pioneer Venus data since these two configurations are similar in geometry. The nonablated Galileo configuration was also tested with two different center-of-gravity positions to obtain values of pitching-moment-curve slope which could be used in determining values of lift and center-of-pressure location for this configuration. The results indicate that the drag characteristics of the Galileo probe are qualitatively similar to that of Pioneer Venus, however, the drag of the nonablated Galileo is about 3 percent lower at the higher Mach numbers and as much as 5 percent greater at transonic Mach numbers of about 1.0 to 1.5. Also, the drag of the hypothesized ablated configuration is about 3 percent lower than that of the nonablated configuration at the higher Mach numbers but about the same at the lower Mach numbers. Additional tests are required at Reynolds numbers of 1000, 500, and 250 to determine if the dramatic rise in drag coefficient measured for Pioneer Venus at these low Reynolds numbers also occurs for Galileo, as might be expected. Author

N88-24592*# National Aeronautics and Space Administration. Lewis Research Center, Cleveland, Ohio.
EFFECT OF INITIAL TANGENTIAL VELOCITY DISTRIBUTION ON THE MEAN EVOLUTION OF A SWIRLING TURBULENT FREE JET
S. Farokhi, R. Taghavi (Kansas Univ., Lawrence.), and E. J. Rice [1988] 10 p Prepared for presentation at the 1st National Fluid Dynamics Congress, Cincinnati, Ohio, 24-28 Jul. 1988; sponsored in part by AIAA, ASME, ASCE, SIAM, and ASP
(Grant NCC3-56)
(NASA-TM-100934; E-4211; NAS 1.15:100934) Avail: NTIS HC A02/MF A01 CSCL 01A

An existing cold jet facility at NASA-Lewis was modified to produce swirling flows with controllable initial tangential velocity distribution. Distinctly different swirl velocity profiles were produced, and their effects on jet mixing characteristics were measured downstream of an 11.43 cm diameter convergent nozzle. It was experimentally shown that in the near field of a swirling turbulent jet, the mean velocity field strongly depends on the initial swirl profile. Two extreme tangential velocity distributions were produced. The two jets shared approximately the same initial mass flow rate of 5.9 kg/s, mass averaged axial Mach number and swirl number. Mean centerline velocity decay characteristics of the solid body rotation jet flow exhibited classical decay features of a swirling jet with $S = 0.48$ reported in the literature. It is concluded that the integrated swirl effect, reflected in the swirl number, is inadequate in describing the mean swirling jet behavior in the near field. Author

N88-24593# Direction des Armements Terrestres, Toulouse (France).
PARACHUTE FOR IN-FLIGHT TRAINING ON PARACHUTE EJECTION [PARACHUTE POUR L'INSTRUCTION EN VOL A LA LIBERATION DE VOILURE]
M. Carol Sep. 1987 239 p In FRENCH
(Rept-87-11; ETN-88-91996) Avail: NTIS HC A11/MF A01

A parachute was designed for ejection training in conditions close to reality in a military environment. The design is implemented with known components from operating parachutes and selected control components. The in-flight tests show that the functional specifications are respected both for the training qualities and for the safety aspects. ESA

N88-24594# Poitiers Univ. (France). Lab. de Mecanique des Fluides.
UNSTEADY FLOW AROUND A PROFILE SUBJECTED TO PULSED MOTIONS Final Report [ECOULEMENT INSTATIONNAIRE AUTOUR D'UN PROFIL SOUMIS IMPULSIVEMENT A DIFFERENTS MOUVEMENTS]
Madeleine Coutanceau, Kazuo Ohmi, Alain Texier, Ta Phuoc Loc (Paris-Sud Univ., Orsay, France), Olivier Daube, and Annie Dulieu Jul. 1987 110 p In FRENCH
(Contract DRET-84-020)
(ETN-88-92151) Avail: NTIS HC A06/MF A01

The wake produced by a thin profile subjected to combined translation and rotation pulsed motions is studied. Wind tunnel experimental data and numerical simulation data were obtained. Flow visualization methods are described. Motion frequency is identified as the main parameter. When the frequency increases the relative importance of rotation increases and becomes predominant. The mutual interference of translation and rotation vortices is discussed. ESA

N88-24595# Centre d'Etudes et de Recherches, Toulouse (France). Dept. d'Etudes et de Recherches en Aerothermodynamique.
BOUNDARY LAYER TRANSITION [TRANSITION DE LA COUCHE LIMITE]
D. Arnal Jan. 1987 56 p In FRENCH
(Contract DRET-86-002)
(CERT-OA-37/5018-AYD; DERAT-37/5018-DY; ETN-88-92163)
Avail: NTIS HC A04/MF A01

Transition mechanisms in three-dimensional and compressible flow were studied using infinite swept wings and calculations of stability on a thermal wall up to Mach 10 respectively. The possibilities of using spanwise blowing to control and maintain a laminar regime, downstream of a backward facing step or on a swept wing, were examined. High velocity transition is reviewed and the extension to compressible flow of a method developed for low velocity is outlined. Experimental results on the effects of isolated rough spots are given. ESA

N88-24596# Centre d'Etudes et de Recherches, Toulouse (France). Dept. d'Etudes et de Recherches en Aerothermodynamique.
SUPPLEMENTS TO THE STUDY OF THE WAKE OF A MIRAGE G8 MODEL AT F2 [COMPLEMENTS A L'ETUDE DU SILLAGE DE LA MAQUETTE DU MIRAGE G8 A F2]
C. Gleyzes and G. Pailhas Nov. 1987 52 p In FRENCH
(Contract STPA-85-95-004)
(CERT-RT-OA-20/5025-AYD; ETN-88-92547) Avail: NTIS HC A04/MF A01

Two dimensional laser velocimeter and hot-wire probe measurements were made on a wind tunnel model of a Mirage G8 aircraft. Wake and drag results are obtained in spite of the wide spacing of measuring points. The results show that the relative contributions to drag are: fuselage 58 percent; wings 24 percent; tailplane 12 percent; and 6 percent drift. For turbulent drag (11 percent of the total) the figures are 6, 74, 15, and 5 percent respectively. ESA

N88-24597*# National Aeronautics and Space Administration. Lewis Research Center, Cleveland, Ohio.
SUMMARY OF LOW-SPEED WIND TUNNEL RESULTS OF SEVERAL HIGH-SPEED COUNTERROTATION PROPELLER CONFIGURATIONS
Christopher E. Hughes and John A. Gazzaniga (Sverdrup Technology, Inc., Cleveland, Ohio.) 1988 35 p Presented at the 24th Joint Propulsion Conferences, Boston, Mass., 11-13 Jul.

1988; sponsored by AIAA, ASME, SAE and ASEE
(NASA-TM-100945; E-4234; NAS 1.15:100945; AIAA-88-3149)
Avail: NTIS HC A03/MF A01 CSCL 01A

The low speed aerodynamic performance characteristics of several advanced counterrotation pusher propeller configurations with cruise design Mach numbers of 0.72 and 0.80 were investigated in the NASA Low Speed Wind Tunnel. The tests were conducted at Mach numbers representative of the takeoff and landing flight regime. The investigation included: (1) the propeller performance characteristics over a range of blade angle settings and rotational speeds at a Mach number of 0.20; (2) the effect on the propeller performance of varying the axial rotor spacing and mismatching the power and rotational speeds on the propeller rotors; (3) determining the reverse thrust performance characteristics at Mach numbers of 0.0, 0.10, 0.15 and 0.20. The results of the investigation indicated that the overall low speed performance of the counterrotation propeller configurations was reasonable. Author

N88-24598*# National Aeronautics and Space Administration. Langley Research Center, Hampton, Va.
AIRCRAFT AEROELASTICITY AND STRUCTURAL DYNAMICS RESEARCH AT THE NASA LANGLEY RESEARCH CENTER: SOME ILLUSTRATIVE RESULTS
Robert V. Doggett, Jr. and F. W. Cazier, Jr. May 1988 13 p Proposed for presentation at the 16th Congress of the International Council of the Aeronautical Sciences (ICAS), Jerusalem, Israel, 28 Aug. - 2 Sep. 1988
(NASA-TM-100627; NAS 1.15:100627) Avail: NTIS HC A03/MF A01 CSCL 01A

Highlights of nine different research studies are described. Five of these topics relate directly to fixed-wing aircraft and range from flutter studies using relatively simple and inexpensive wind-tunnel models to buffet studies of the vertical tails of an advanced high performance configuration. The other four topics relate directly to rotary-wing aircraft and range from studies of the performance and vibration characteristics of an advanced rotor design to optimization of airframe structures for vibration attenuation. Author

N88-24599# Tokyo Univ. (Japan). Inst. of Space and Astronautical Science.
HIGH SPEED AND HIGH ANGLE OF ATTACK AERODYNAMIC CHARACTERISTICS OF WINGED SPACE VEHICLE
Yoshifumi Inatani Dec. 1987 46 p
(ISSN-0285-6808; ISAS-RN-624) Avail: NTIS HC A03/MF A01

Static aerodynamic characteristics of winged space vehicles are investigated through a series of wind tunnel tests. A summary of the test results and associated considerations are included. The tests were conducted and supported by the Working Group for Winged Space Vehicles of the Institute of Space and Astronautical Science (ISAS). Attention was concentrated on both longitudinal and lateral/directional, high angle of attack flight capability at the high speed flight conditions of the vehicle for the accomplishment of the reentry flight, so that three types of tail configurations are investigated (single, double, and tip-fin configurations). Test results are summarized in terms of aerodynamic coefficients and their derivatives. Discussions based on the test results are made to find out the relations between vehicle configuration and various aerodynamic and flight dynamics characteristics, which compare the high angle of attack flight criteria of current high-performance aircrafts. Author

N88-24600*# National Aeronautics and Space Administration. Ames Research Center, Moffett Field, Calif.
A FORMULATION FOR THE BOUNDARY-LAYER EQUATIONS IN GENERAL COORDINATES
Joseph L. Steger, William R. VanDalsem, Argyris G. Panaras, and K. V. Rao Jun. 1988 27 p
(NASA-TM-100079; A-88114; NAS 1.15:100079) Avail: NTIS HC A03/MF A01 CSCL 01A

This is a working paper in which a formulation is given for solving the boundary-layer equations in general body-fitted curvilinear coordinates while retaining the original Cartesian dependent variables. The solution procedure does not require that any of the coordinates be orthogonal, and much of the software developed for many Navier-Stokes schemes can be readily used. A limited number of calculations has been undertaken to validate the approach. Author

N88-24601*# National Aeronautics and Space Administration. Ames Research Center, Moffett Field, Calif.
SOME ROTORCRAFT APPLICATIONS OF COMPUTATIONAL FLUID DYNAMICS
W. J. McCroskey Mar. 1988 25 p Presented at the 2nd International Conference on Basic Rotorcraft Research, College Park, Md., Feb. 1988 Prepared in cooperation with Army Aviation Research and Development Command, Moffett Field, Calif.
(NASA-TM-100066; A-88094; NAS 1.15:100066; USAAVSCOM-TR-88-A-001) Avail: NTIS HC A03/MF A01 CSCL 01A

The growing application of computational aerodynamics to nonlinear rotorcraft problems is outlined, with particular emphasis on the development of new methods based on the Euler and thin-layer Navier-Stokes equations. Rotor airfoil characteristics can now be calculated accurately over a wide range of transonic flow conditions. However, unsteady 3-D viscous codes remain in the research stage, and a numerical simulation of the complete flow field about a helicopter in forward flight is not now feasible. Nevertheless, impressive progress is being made in preparation for future supercomputers that will enable meaningful calculations to be made for arbitrary rotorcraft configurations. Author

N88-24602*# National Aeronautics and Space Administration. Ames Research Center, Moffett Field, Calif.
APPLICATIONS OF THE NAVIER-STOKES EQUATIONS TO WINGS AND COMPLEX CONFIGURATIONS USING A ZONAL APPROACH
Jolen Flores Jun. 1988 12 p
(NASA-TM-100080; A-88115; NAS 1.15:100080) Avail: NTIS HC A03/MF A01 CSCL 01A

The simulation of a transonic viscous flow over a series of 3-D configurations, ranging from isolated wings to relatively complete aircraft, is presented. A fast, diagonalized Beam-Warming algorithm is used in conjunction with a zonal approach to solve the Euler/Navier-Stokes equations for these applications. The computer code, called Transonic Navier-Stokes, uses four zones for wing configurations and up to 19 zones for more complete aircraft configurations. For the inner zones adjacent to no-slip surfaces, the thin-layer Navier-Stokes equations are solved, while in the outer zones the Euler equations are solved. Numerical results are presented and compared with experiment (when available) for wing calculations and a more complete configuration based on the F-16A aircraft. Author

N88-24603*# National Aeronautics and Space Administration. Ames Research Center, Moffett Field, Calif.
A DECADE OF COMPUTER SIMULATIONS FOR SPACE SHUTTLE AERODYNAMICS
Mamoru Inouye May 1988 11 p
(NASA-TM-100990; A-88150; NAS 1.15:100990) Avail: NTIS HC A03/MF A01 CSCL 01A

Ten years ago computer simulations of the flow field around the Space Shuttle Orbiter were limited to inviscid calculations for the windward side of the forebody and viscous calculations for selected 2-D problems. Advances in computer hardware and numerical methods during the past ten years made it possible to calculate viscous flow over the complete orbiter configuration at angle of attack. The equations solved are the Reynolds-averaged, Navier-Stokes equation, simplified by either the thin-layer or parabolized approximation. An algebraic eddy viscosity model is used for turbulent flow. The free stream is assumed to be a perfect gas for wind tunnel conditions and a real gas in thermodynamic equilibrium for flight conditions. Four examples of recent computer simulations are presented. Flow field results include oil flow patterns

on the surface and Mach number contours, isobars, and cross-flow velocity vectors in the shock layer. Author

N88-24604 Virginia Univ., Charlottesville.
COMPRESSIBLE FLOW IN A PIE-SHAPED CYLINDER ROTATING ABOUT THE VERTEX Ph.D. Thesis
Richard Joseph Babarsky 1986 145 p
Avail: Univ. Microfilms Order No. DA8801110

A solution technique was developed for predicting the axial mass flux for a gas contained in a pie shaped cylinder rotating rapidly about the vertex. This problem has application to a conventional cylindrical gas centrifuge with radial walls. The mathematical model is obtained by using the theory of matched asymptotic expansions which exploits the boundary layer character of the flow. Three different types of boundary layers exist in the flow; Ekman layers on the top and bottom, buoyancy layers on the radial walls, and cylindrical pancake layer on the outer wall of the container. A single sixth order partial differential equation is obtained for the axial velocity in the cylindrical layer and the other layers provide matching conditions. The problem is formulated for no slip and prescribed temperature conditions on the solid surfaces, and for zero shear stress, zero pressure, and zero heat conduction at the inner free surface. Approximate solutions are obtained for the case of nonhomogeneous end conditions corresponding to mass throughput and heat flux and or shear. Dissert. Abstr.

N88-24605 Michigan Univ., Ann Arbor.
UNSTEADY FLOW IN A SUPERCRITICAL SUPERSONIC INLET Ph.D. Thesis
Robert Thomas Biedron 1987 160 p
Avail: Univ. Microfilms Order no. DA8801282 CSCL 01A

Unsteady flow through a two dimensional supersonic inlet diffuser, with a normal shock wave in the diffuser is analyzed using asymptotic methods. Two time regimes are considered, the first corresponding to fundamentally unsteady flow, the second to quasisteady flow; a unified solution containing both time regimes is also presented. An ordinary differential equation describing the shock wave motion is found. Examples show the motion of a shock wave resulting from impressed back pressure oscillations and from changes in flow area due to a separated flow region. For cases involving separated flow, additional numerical solutions are employed to give typical wall shapes as functions of time. Unstarts and self sustained oscillations are considered.
Dissert. Abstr.

N88-24606 California Univ., Santa Barbara.
THE CALCULATION OF TRANSONIC FLOW OVER THE SHUTTLE ORBITER USING SLENDER BODY THEORY Ph.D. Thesis
Karunamurthy Rajagopal 1987 98 p
Avail: Univ. Microfilms Order No. DA8729687

Transonic flow over the Shuttle Orbiter was modeled with the use of slender body theory. In the theory, the original three-dimensional problem is divided into two simpler component problems, the near field and the far field. The near field problem represents a cross flow which is almost incompressible and is defined by Laplace's equation with a flow tangency boundary condition on the body. A nonlinear transonic small disturbance approximation is the basis for the far field problem and described the flow over a body of revolution having the same longitudinal area distribution as the asymmetric vehicle. Both the near and far field problems are two-dimensional boundary value problems. A boundary element method is used to solve the near field problem. The solution for the axisymmetric far field problem is obtained by a successive line overrelaxation (SLOR) method. The two component solutions are combined to obtain the complete solution. To take into account viscous effects near the body in a qualitative sense, an effective wing surface which includes the displacement effect of the viscous layer was used in the calculations. The computed fuselage and wing pressure results are compared with experiments for Mach numbers (1.25 and 0.9). Dissert. Abstr.

N88-24607*# Army Aviation Systems Command, Hampton, Va.
INFLOW MEASUREMENTS MADE WITH A LASER VELOCIMETER ON A HELICOPTER MODEL IN FORWARD FLIGHT. VOLUME 1: RECTANGULAR PLANFORM BLADES AT AN ADVANCE RATION OF 0.15
Joe W. Elliott, Susan L. Althoff, and Richard H. Sailey (PRC Kentron, Inc., Hampton, Va.) Apr. 1988 323 p
(NASA-TM-100541; AVSCOM-TM-88-B-004; NAS 1.15:100541)
Avail: NTIS HC A14/MF A01 CSCL 01A

An experimental investigation was conducted in the 14- by 22-Foot Subsonic Tunnel at NASA Langley to measure the inflow into a scale model helicopter rotor in forward flight (microinf = 0.15). The measurements were made with a two component Laser Velocimeter (LV) one chord above the plane formed by the path of the rotor tips (tip path plane). A conditional sampling technique was employed to determine the azimuthal position of the rotor at the time each velocity measurement was made so that the azimuthal fluctuations in velocity could be determined. Measurements were made at a total of 147 separate locations in order to clearly define the inflow character. This data is presented without analysis. In order to increase the availability of the resulting data, both the mean and azimuthally dependent values are included as part of this report on two 5.25 inch floppy disks in Microsoft Corporation MS-DOS format. Author

N88-24608*# National Aeronautics and Space Administration. Langley Research Center, Hampton, Va.
ACCURATE MULTIGRID SOLUTION OF THE EULER EQUATIONS ON UNSTRUCTURED AND ADAPTIVE MESHES Final Report
Dimitri J. Mavriplis Jun. 1988 33 p Submitted for publication
(Contract NAS1-18107)
(NASA-CR-181679; ICASE-88-40; NAS 1.26:181679) Avail: NTIS HC A03/MF A01 CSCL 01A

A method for accurately solving inviscid compressible flow in the subcritical and supercritical regimes about complex configurations is presented. The method is based on the use of unstructured triangular meshes in two dimensions, and special emphasis is placed on the accuracy and efficiency of the solutions. High accuracy is achieved by careful scaling of the artificial dissipation terms, and by reformulating the inner and outer boundary conditions for both the convective and dissipative operators. An adaptive grid refinement strategy is presented which enhances the solution accuracy for complex flows. When coupled with an unstructured multigrid algorithm, this method is shown to produce an efficient solver for flows about arbitrary configurations. Author

03 AIR TRANSPORTATION AND SAFETY

Includes passenger and cargo air transport operations; and aircraft accidents.

For related information see also *16 Space Transportation* and *85 Urban Technology and Transportation.*

N88-24609# General Accounting Office, Washington, D. C. Information Management and Technology Div.
FAA (FEDERAL AVIATION ADMINISTRATION) TECHNICAL CENTER: MISSION AND ROLE IN NATINAL AIRSPACE SYSTEM PLAN IMPLEMENTATION
Jan. 1988 45 p
(PB88-169818; GAO/IMTEC-88-6BR) Avail: NTIS HC A03/MF A01 CSCL 01C

A survey was conducted of the mission and operations of the Federal Aviation Administration's (FAA) Technical Center located in Pomona, New Jersey. The review notes that the FAA has proceeded to production with several high cost systems in its $15 billion National Airspace System plan without adequately testing and validating their operational capability. It also investigates the overall mission of the Center, its role in modernizing the air traffic control system (implementing the National Airspace System plan),

and the way in which the Center allocates and uses resources.
Author

N88-24610# Federal Aviation Agency, Atlantic City, N.J.
STUDY OF BENEFITS OF PASSENGER PROTECTIVE BREATHING EQUIPMENT FROM ANALYSIS OF PAST ACCIDENTS Final Report
Louise Speitel and Richard G. Hill Mar. 1988 246 p
(DOT/FAA/CT-88/03) Avail: NTIS HC A11/MF A01

A computer model was developed and utilized for calculating the benefits of passenger protective breathing devices and other fire safety improvements based on an analysis of accidents involving fire occurring from 1966 to 1986. The results of exercising this model on 20 past accidents indicate that the lives saved is very sensitive to assumptions. It was determined that seat cushion fire blocking (FB) would have saved almost half the lives. Floor proximity lighting (FPL) is much less effective than FB, saving 3 to 4 percent of fire deaths. Protective breathing equipment (PBE), assuming no donning delay and 100 percent usage by passengers is more effective than FPL. However, a 15 second donning delay of PBE may have resulted in a net disbenefit. Author

N88-24611# Anco Engineers, Inc., Culver City, Calif.
PEAK ACCELERATION DEVICE (PAD) Final Report, 1 Apr. 1985 - 19 Dec. 1986
Paul Ibanez and John F. Gray Oct. 1987 146 p
(Contract DAAK51-85-C-0009; DA Proj. 1L6-65502-MM-40)
(AD-A191639; AD-F800025; ANCO-1663.11;
USAAVSCOM-TM-87-D-3) Avail: NTIS HC A07/MF A01
CSCL 01D

Each year a number of aircraft are involved in incidents/accidents of varying ground impact severity. The object of this project was to develop a small, passive, low-cost triaxial indicator that in the event of an incident/accident would record the magnitude of the acceleration experienced at their location in the aircraft. Analysis of this data would provide an insight into the performance of crashworthy structures and vehicles, thereby contributing to efforts to reduce loss of life, injury and equipment damage. Three basic concepts for the design of the Peak Acceleration Device (PAD) were examined. Initially, the use of foam that would crush predictably under the action of a metal rod was explored. Unfortunately, this arrangement was found to be impracticable as was a variation of the same concept where metal foils were to be pierced by pointed rods. The drawback in each case being primarily related to material characteristics. The third approach utilized a filament under tensile stress as a g-force indicator. Testing showed that this mechanism provided predictable and repeatable measure of impact levels and therefore it was this concept that was developed into the PAD. The final configuration of the Peak g indicator conforms to the target criteria established for the device. It has the capability to measure impacts of 15-100 g in each of three axes, will fit within a 2-1/4-in. cube, has a mechanical filter system that isolates the indicators from energy at frequencies above 100 Hz, and is housed in a rugged aluminum casing that provides high resistance to mechanical damage.
GRA

N88-24612# National Transportation Safety Board, Washington, D. C.
AIRCRAFT ACCIDENT/INCIDENT, COPPERHILL, TENNESSEE, FEBRUARY 22, 1986 Summary Report, 1986
30 Mar. 1988 9 p
(PB88-910407; NTSB/AAR-88/02/SUM) Avail: NTIS HC
A02/MF A01 CSCL 01C

This is the report of an aircraft accident investigated by the National Transportation Safety Board. The accident occurred at Copperhill, Tennessee, 22 February, 1986. Author

04 AIRCRAFT COMMUNICATIONS AND NAVIGATION

Includes digital and voice communication with aircraft; air navigation systems (satellite and ground based); and air traffic control.

For related information see also *17 Space Communications, Spacecraft Communications, Command and Tracking* and *Communications and Radar.*

N88-24613# Federal Aviation Administration, Washington, D.C.
CESSNA 172 MLS (MICROWAVE LANDING SYSTEM) TERMINAL INSTRUMENT PROCEDURES (TERPS) APPROACH DATA COLLECTION AND PROCESSING DATA REPORT Technical Note, Jun. 1986 - Jun. 1987
Edward J. Pugacz Oct. 1987 207 p
(AD-A191241; DOT/FAA/CT-TN87/36) Avail: NTIS HC
A10/MF A01 CSCL 17G

This report documents the approaches portion of the Fixed Wing Microwave Landing System (MLS) Terminal Instrument Procedures (TERPS) data collection and processing project using a Cessna 172 (C-172) aircraft. This is one part of the Fixed Wing MLS TERPS data collection and processing program being performed at the Federal Aviation Administration (FAA) Technical Center. The program was undertaken to collect flight test data in various aircraft to establish a data base for development of MLS TERPS criteria. Data were collected during both missed approaches and landings using glideslopes of 3 deg, 4 deg, and 5 deg with all flights being tracked by ground based tracking systems. Statistical processing was performed on both the airborne and tracker data, and various graphical plots were produced. The processed data were delivered to AVN-120 for inclusion in the MLS TERPS criteria development data base. GRA

N88-24614# Federal Aviation Administration, Atlantic City, N.J.
ROTORCRAFT TCAS (TRAFFIC ALERT AND COLLISION AVOIDANCE SYSTEM) EVALUATION: GROUP 3 RESULTS Technical Note, Sep. - Dec. 1985
Albert J. Rehmann Oct. 1987 67 p
(AD-A191719; DOT/FAA/CT-TN87/21) Avail: NTIS HC
A04/MF A01 CSCL 01D

This report documents the operational flight test of a prototype Traffic Alert and Collision Avoidance System (TCAS) installed in a Sikorsky S-76 helicopter. The prototype TCAS, programmed to encompass the functions of a TCAS 1, was flown to five east coast terminal cities, and operated along defined helicopter routes therein. The test results validated the minimum proposed TCAS 1 configuration. Further results recommend enhancements, to be included as options to improve the usefulness of TCAS 1. GRA

N88-24615# Federal Aviation Administration, Atlantic City, N.J.
OPTIMIZATION OF THE DILATION CHARACTERISTIC ON THE CONTROL JURISDICTION OF AN AREA CONTROL FACILITY
Robert G. Mulholland Jan. 1988 65 p
(AD-A191720; DOT/FAA/CT-TN87/39) Avail: NTIS HC
A04/MF A01 CSCL 17G

In an air traffic control environment such as the National Airspace System the control function is based on stereographic representations of aircraft positions in a plane tangent to a sphere with a center collocated with the center of an ellipsoidal model of the geoid. The variation of the dilation (i.e., the discrepancy between the length of an infinitesimal arc on the model surface and the image of the arc in the plane) over the control jurisdiction of an air traffic control facility is one of many factors that adversely affect the ability of the facility to maintain separation standards. Techniques are disclosed for selecting a tangency point and a radius for the spherical support of the stereographic plane that minimize the variation of the dilation over the control jurisdiction about a predetermined constant. The constant can be viewed as a specification of the scale of the map that is the stereographic image in the plane of the portion of the surface of the earth model underlying controlled airspace. GRA

N88-24616# Federal Aviation Administration, Atlantic City, N.J.
MICROWAVE LANDING SYSTEM MATHEMATICAL MODELING STUDY FOR MIDWAY AIRPORT RUNWAY 22L, CHICAGO, ILLINOIS Technical Note, Aug. - Oct. 1987
Jesse D. Jones and Linda Epstein Jan. 1988 65 p
(AD-A191721; DOT/FAA/CT-TN87/49) Avail: NTIS HC A04/MF A01 CSCL 17G

This technical note describes Microwave Landing System (MLS) mathematical modeling performed for runway 22L, Midway Airport, Chicago, Illinois. This study considered multipath and shadowing effects of buildings and aircraft. Results are provided as plots showing the multipath levels and separation angles and error plots showing the resultant errors. GRA

N88-24617# Naval Ocean Systems Center, San Diego, Calif.
WESTERN PACIFIC OMEGA VALIDATION: PROJECT DESCRIPTION Professional Paper, period ending Aug. 1986
Carl P. Kugel Nov. 1987 5 p
(AD-A191753) Avail: NTIS HC A02/MF A01 CSCL 17G

The Naval Ocean Systems Center (NOSC) in San Diego, California, has been tasked by the Omega Navigation System Center (ONSC) to perform the validation of the Omega System in the Western Pacific Ocean Area. In early April 1986, a Coast Guard C-130H aircraft based at Clearwater, Florida was outfitted with specially-designed receiving equipment as used in previous validations for the Indian and the South Pacific Oceans and proceeded to gather approximately 120 fight hours of Omega signal information throughout the Western Pacific. These flights were performed in conjunctions with simultaneous ground and shipboard measurements from several of ONSC's on-going monitor sites and ships operating in the region. Because no meaningful data analysis has been accomplished by this writing, this paper will be confined to describing the aircraft flight itinerary, ground monitor operations and qualitative observations from the overall mission. GRA

N88-24618# Coast Guard Research and Development Center, Groton, Conn.
DESCRIPTIONS OF HF AND VHF LORAN-C BUOYS AND EVALUATIONS AS POTENTIAL DATUM MARKER BUOYS Interim Report
Arthur A. Allen, Sandra L. Eynon, and R. Q. Robe Sep. 1987 45 p
(AD-A192069; CGR/DC-09/87; USGC-D-02-88) Avail: NTIS HC A03/MF A01 CSCL 17G

The U.S. Coast Guard R and D Center tested two types of Loran-C drifting buoys as prototype replacements for the presently used Radio Direction Finder (RDF) type Datum Marker Buoys (DMB). The buoys used HF or VHF transmission of the buoy's Loran-C Time Differences to a shore/ship based receiver at 10 to 100 minute intervals. Field testing of the buoys at sea occurred off Cape Cod, MA; Cape May, NJ; and Georges Bank, MA. Of the two types of buoys the one using VHF technology proved to be more suitable for future development than that using HF technology. The main reasons for the better results with the VHF versus HF buoys was simplicity and reliability. Results indicated that the VHF buoys can survive severe weather, transmit data reliably, and have sufficient range for useful tracking and data collection. Tests indicated reliable data reception at 20 nautical miles (nm) from a vessel and 50-60 nm from an airborne receiver. The advantage of the Loran-C buoys over the RDF DMB is the increased data collection rate and that the data collection does not interrupt the ongoing search. The Loran-C buoys are being incorporated into a system to be used to establish a working search datum and for defining the sea surface currents of the search area in real time. GRA

N88-24619*# Charles River Analytics, Inc., Cambridge, Mass.
USER'S GUIDE TO THE FAULT INFERRING NONLINEAR DETECTION SYSTEM (FINDS) COMPUTER PROGRAM
A. K. Caglayan, P. M. Godiwala, and H. S. Satz Jun. 1988 89 p
(Contract NAS1-17719)
(NASA-CR-178410; R8801; NAS 1.26:178410) Avail: NTIS HC A05/MF A01 CSCL 14B

Described are the operation and internal structure of the computer program FINDS (Fault Inferring Nonlinear Detection System). The FINDS algorithm is designed to provide reliable estimates for aircraft position, velocity, attitude, and horizontal winds to be used for guidance and control laws in the presence of possible failures in the avionics sensors. The FINDS algorithm was developed with the use of a digital simulation of a commercial transport aircraft and tested with flight recorded data. The algorithm was then modified to meet the size constraints and real-time execution requirements on a flight computer. For the real-time operation, a multi-rate implementation of the FINDS algorithm has been partitioned to execute on a dual parallel processor configuration: one based on the translational dynamics and the other on the rotational kinematics. The report presents an overview of the FINDS algorithm, the implemented equations, the flow charts for the key subprograms, the input and output files, program variable indexing convention, subprogram descriptions, and the common block descriptions used in the program. Author

N88-24620*# National Aeronautics and Space Administration. Langley Research Center, Hampton, Va.
NAVIGATION SYSTEM FOR LAND VEHICLES Patent Application
H. Douglas Garner, inventor (to NASA) 18 May 1988 10 p
(NASA-Case-LAR-13322-1; NAS 1.71:LAR-13322-1; US-Patent-Appl-SN-195221) Avail: NTIS HC A02/MF A01 CSCL 17G

The invention is a navigation system for land vehicles. Prior methods of determining vehicle heading have been either too expensive or too inaccurate for widespread use in automotive vehicles. The novel aspect of this invention is that it determines vehicle heading by utilizing an inexpensive angle-of-deflection transducer connected to the vehicle steering wheel, and a microcomputer with a look-up table to compensate for the nonlinear relationship between the angle of deflection of the steering wheel or linkage and that of the road wheel. The system comprises a distance transducer, a steering wheel look-up table, and a positioning display. The signal processor operates on distance information and heading information from the transducers, the look-up table compensates for the nonlinear relationship between the steering wheel angle and the angle of the road wheel, and the resulting position information is displayed. NASA

N88-24621*# National Aeronautics and Space Administration. Langley Research Center, Hampton, Va.
AIRPLANE RUNWAY PERFORMANCE MONITORING SYSTEM Patent Application
David B. Middleton, inventor (to NASA), Raghavachari Srivatsan, inventor (to NASA) (Kansas Univ., Lawrence.), and Lee H. Person, Jr., inventor (to NASA) 11 May 1988 43 p
(NASA-Case-LAR-13854-1-CU; NAS 1.71:LAR-13854-1-CU; US-Patent-Appl-SN-192562) Avail: NTIS HC A03/MF A01 CSCL 17G

The invention is a real-time takeoff and landing performance monitoring system for an aircraft which provides a pilot with graphic and metric information to assist in decisions related to achieving rotation speed within the safe zone of a runway, or stopping the aircraft on the runway after landing or takeoff abort. By comparing the present performance of the aircraft with a predicted nominal performance based upon given conditions, performance deficiencies are detected by the system. The system provides a head-down display and a head-up display. The head-up display is projected onto a partially reflective transparent surface through which the pilot views the runway. Hence, the system supplies the pilot with critical status information while allowing the pilot to continue to view the runway. NASA

N88-24622# Data Transformation Corp., Silver Spring, Md.
NEW YORK TRACON DEMONSTRATION OF PROGRAM RECODING REQUIREMENTS ANALYSIS DOCUMENT Final Report

Aug. 1987 267 p
(Contract DTFA03-85-C-0058)
(DOT/FAA/CT-87/34) Avail: NTIS HC A12/MF A01

This document is an intermediate deliverable in a project whose objective was to convert portions of the current New York (N.Y.) TRACON software written in ULTRA to a higher order transportable language. A combination of ADA/PDL leading to PASCAL as the higher order language was chosen. The document consists of four main parts: (1) a detailed analysis of the N.Y. TRACON demonstration project software requirements for software version A5.04; (2) a description of the demonstration system architecture, in contrast with the current N.Y. TRACON hardware; (3) a description and rationale for the demonstration system operational software architecture; and (4) a data dictionary of the current system. The output of this document led to the next step which was the actual writing of the new software. Author

N88-24936# Deutsche Forschungs- und Versuchsanstalt fuer Luft- und Raumfahrt, Brunswick (West Germany).
INERTIAL REFERENCE SYSTEM WITH GLOBAL POSITIONING SYSTEM (GPS) SUPPORT [INERTIALES REFERENZSYSTEM MIT GPS-STUETZUNG]
Eberhard Schlemper *In its* Optics: Perspectives for Measurement Techniques and Signal Processing for Flight Guidance Aug. 1987 p 193-220 In GERMAN (For primary document see N88-24928 18-35)
Avail: NTIS HC A13/MF A01; DFVLR, VB-PL-DO, 90 60 58, 5000 Cologne, Fed. Republic of Germany 88 Deutsche marks

05 AIRCRAFT DESIGN, TESTING AND PERFORMANCE

Includes aircraft simulation technology.

For related information see also *18 Spacecraft Design, Testing and Performance* and *39 Structural Mechanics*.For land transportation vehicles see *85 Urban Technology and Transportation.*

N88-24623*# National Aeronautics and Space Administration. Langley Research Center, Hampton, Va.
NONLINEAR PROGRAMMING EXTENSIONS TO RATIONAL FUNCTION APPROXIMATION METHODS FOR UNSTEADY AERODYNAMIC FORCES
Sherwood H. Tiffany and William M. Adams, Jr. Jul. 1988 55 p Previously announced in IAA as A87-33694 Sponsored by NASA, Washington
(NASA-TP-2776; L-16205; NAS 1.60:2776) Avail: NTIS HC A04/MF A01 CSCL 01C

The approximation of unsteady generalized aerodynamic forces in the equations of motion of a flexible aircraft are discussed. Two methods of formulating these approximations are extended to include the same flexibility in constraining the approximations and the same methodology in optimizing nonlinear parameters as another currently used extended least-squares method. Optimal selection of nonlinear parameters is made in each of the three methods by use of the same nonlinear, nongradient optimizer. The objective of the nonlinear optimization is to obtain rational approximations to the unsteady aerodynamics whose state-space realization is lower order than that required when no optimization of the nonlinear terms is performed. The free linear parameters are determined using the least-squares matrix techniques of a Lagrange multiplier formulation of an objective function which incorporates selected linear equality constraints. State-space mathematical models resulting from different approaches are described and results are presented that show comparative evaluations from application of each of the extended methods to a numerical example. Author

N88-24624# Air Force Inst. of Tech., Wright-Patterson AFB, Ohio. School of Engineering.
A SYSTEM STATUS MONITOR FOR THE NATIONAL AEROSPACE PLANE M.S. Thesis
James M. Baumann Dec. 1987 129 p
(AD-A190681; AFIT/GCE/ENG/87D-1) Avail: NTIS HC A07/MF A01 CSCL 01C

The purposes of this study were to develop a model for an in-flight diagnostic system that could be applied to the National Aerospace Plane, and to implement a computer program to demonstrate the feasibility of that model as a basis for a system status monitor. The diagnostic system model which was developed features a double hierarchy structure, one for the aircraft functions to be diagnosed, and another for the diagnostic functions to be performed. The hierarchical nature of both the system knowledge and the functions that use the knowledge allow decomposition of the diagnostic task into relatively independent and manageable parts. The demonstration program which was developed includes a subset of the diagnostic system model. This program was implemented in Zetalisp on a Symbolics 3600 computer. It will simulate monitoring the dynamic performance parameters of an aircraft's subsystems, report any readings that fall outside of predetermined limits, reason about components responsible for the fault, display to the aircrew the other aircraft functions which may be affected by the component failure, and recommend actions that may remedy the fault situation. GRA

N88-24625# Fluid Dynamics International, Inc., Evanston, Ill.
SIMULATIONS OF A MISSILE WITH LIQUID PAYLOAD UNDER LAUNCH CONDITIONS Contractor Report, Sep. 1986 - Sep. 1987
Simon Rosenblat Jan. 1988 31 p
(Contract DAAD05-86-M-0985)
(AD-A191479; CRDEC-CR-88020) Avail: NTIS HC A03/MF A01 CSCL 16B

A numerical simulation of the flow of a liquid in the annular region between two coaxial circular cylinders was performed. This simulation corresponds to the actual behavior of a missile with a liquid payload during its launch phase. The simulation was performed in two parts. The first part was to determine if the payload liquid, which comprised both Newtonian and non-Newtonian fluids, would achieve full spin up relative to the missile during launch. During the second part, the despin moments acting on the spinning and nutating missile with a fully spun up liquid payload were determined from the steady-state Navier-Stokes equations relative to an aeroballistic reference frame. The simulations were performed with a finite element software package FIDAP. The majority of the computations were done on an HP9000 minicomputer; some were done on a Microvax workstation. GRA

N88-24626# Naval Air Test Center, Patuxent River, Md.
METHOD FOR PREDICTION AND DETERMINATION OF TAKEOFF PERFORMANCE FOR VECTORED THRUST VEHICLES
J. F. Calvert 5 Jan. 1988 18 p
(AD-A191809; NATC-TM-87-171-SA) Avail: NTIS HC A03/MF A01 CSCL 01B

YAV-8B and AV-8B Short Takeoff(STO) test results had indicated that STO techniques for the Harrier 2 could be further optimized, particularly for operations at higher hover weight ratios (1.3 and above). This paper documents a method to predicte and determine optimum land-based STO performance with minimum flight testing required. The method was applied during the determination of the optimum STO performance of the AV-8B, and is tailored generally toward thrust vectored vehicles with rapid thrust vectoring capability. With certain assumptions accounted for this approach can also be used in less restricted cases. Emphasis was placed on developing a repeatable task terminating with sufficient flight path acceleration at 50 ft AGL. STO tests conducted using the revised STO procedures validated the improvement in STO performance. Changes to the AV-8B flight operations manual were recommended in order to implement the revised STO task. GRA

N88-24627# Honeywell Systems and Research Center, Minneapolis, Minn.
NONLINEAR FLYING QUALITY PARAMETERS BASED ON DYNAMIC INVERSION Final Report, Jun. 1986 - Jun. 1987
B. G. Morton, M. R. Elgersma, C. A. Harvey, and G. Hines 30 Oct. 1987 169 p
(Contract F33615-86-C-3612)
(AD-A192146; F0231-FR; AFWAL-TR-87-3079) Avail: NTIS HC A08/MF A01 CSCL 01A

This report documents the results of efforts to develop that can be used for the computation of nonlinear flying quality parameters. A variety of candidate nonlinear flying quality parameters and candidate specifications for them were developed. These parameters are genuinely different from expressions derived from linearized models. They depend on the nonlinear aerodynamic functions themselves and not their derivatives, and these parameters can be computed directly from preliminary nonlinear aircraft models. GRA

N88-24628*# National Aeronautics and Space Administration. Langley Research Center, Hampton, Va.
ACTUATED FOREBODY STRAKES Patent Application
Daniel G. Murri, inventor (to NASA) 11 May 1988 22 p
(NASA-Case-LAR-13983-1; NAS 1.71:LAR-13983-1; US-Patent-Appl-SN-192563) Avail: NTIS HC A03/MF A01 CSCL 01C

Actuated forebody strakes provide yaw control at high angles of attack. In one embodiment, the strakes are axially slidable in the forebody to be deployed out of slots provided for the strakes in the forebody. In another embodiment, the strakes are pivotally connected at the tip of the strakes to pivot radially outwardly out of the slots provided in the forebody. In another embodiment, the forebody is provided with either a single strake or two strakes and the forebody is rotatable to vary the radial location of the strake or strakes. All embodiments achieve significant yaw control capability over a wide angle of attack and sideslip ranges. NASA

N88-24629*# Kansas Univ., Lawrence. Design Team.
CLASS 2 DESIGN UPDATE FOR THE FAMILY OF COMMUTER AIRPLANES
Thomas R. Creighton and Louis J. Hendrich May 1987 284 p
(Grant NGT-8001)
(NASA-CR-182681; NAS 1.26:182681) Avail: NTIS HC A13/MF A01 CSCL 01C

This is the final report of seven on the design of a family of commuter airplanes. This design effort was performed in fulfillment of NASA/USRA grant NGT-8001. Its contents are as follows: (1) the class 1 baseline designs for the commuter airplane family; (2) a study of takeoff weight penalties imposed on the commuter family due to implementing commonality objectives; (3) component structural designs common to the commuter family; (4) details of the acquisition and operating economics of the commuter family, i.e., savings due to production commonality and handling qualities commonality are determined; (5) discussion of the selection of an advanced turboprop propulsion system for the family of commuter airplanes, and (6) a proposed design for an SSSA controller design to achieve similar handling for all airplanes. Final class 2 commuter airplane designs are also presented. Author

N88-24630*# West Virginia Univ., Morgantown. Dept. of Mechanical and Aerospace Engineering.
COMPUTATIONAL DESIGN OF LOW ASPECT RATIO WING-WINGLET CONFIGURATIONS FOR TRANSONIC WIND-TUNNEL TESTS Progress Report, 1 Jan. - 30 Jun. 1988
John M. Kuhlman and Christopher K. Brown 6 Jul. 1988 64 p
(Grant NAG1-625)
(NASA-CR-183021; NAS 1.26:183021) Avail: NTIS HC A04/MF A01 CSCL 01C

A computational design has been performed for three different low aspect ratio wing planforms fitted with nonplanar winglets; one of the three planforms has been selected to be constructed as a wind tunnel model for testing in the NASA LaRC 7 x 10 High Speed Wind Tunnel. A design point of M = 0.8, CL approx = 0.3 was selected, for wings of aspect ratio equal to 2.2, and leading edge sweep angles of 45 and 50 deg. Winglet length is 15 percent of the wing semispan, with a cant angle of 15 deg, and a leading edge sweep of 50 deg. Winglet total area equals 2.25 percent of the wing reference area. This report summarizes the design process and the predicted transonic performance for each configuration. Author

N88-24631 Virginia Polytechnic Inst. and State Univ., Blacksburg.
PERIODIC SOLUTIONS IN AIRCRAFT CRUISE-DASH OPTIMIZATION Ph.D. Thesis
Uday J. Shankar 1987 171 p
Avail: Univ. Microfilms Order No. DA8802734

The problem of obtaining optimal cruise-dash trajectories for atmospheric aircraft flight is investigated. Periodic solutions are sought. The problem amounts to finding the trajectories that give the best range performance while achieving a specified average velocity. The cost functional is the weighted sum of the fuel spent and the time taken averaged over the range traversed. The aircraft model is quite complex and all solutions are obtained numerically. It is known that the nonconvexity of the energy hodograph results in a relaxed steady state solution for the energy model, chattering cruise dash. This solution has limited practical application. More realistic solutions in terms of an averaging model are sought. The fast dynamics are modeled as oscillatory solutions with ripples that do not die out, but move along with the progression of the slow motions. These are unsuccessful for the particular aircraft example worked out. A better approximation, relaxation oscillations, which encompasses slow energy changes alternating with fast altitude transitions is proposed. Numerical solutions is obtained. Finally optimal periodic solutions for the point-mass-model are obtained for some values of the cost weighting parameter. Dissert. Abstr.

N88-24632*# Taylor and Associates, Inc., Wrightwood, Calif.
SPACE STATION ARCHITECTURAL ELEMENTS MODEL STUDY
T. C. Taylor, J. S. Spencer, C. J. Rocha, E. Kahn, E. Cliffton, and C. Carr Washington NASA Jan. 1987 155 p
(NASA-CR-4027; NAS 1.26:4027) Avail: NTIS HC A08/MF A01 CSCL 01C

The worksphere, a user controlled computer workstation enclosure, was expanded in scope to an engineering workstation suitable for use on the Space Station as a crewmember desk in orbit. The concept was also explored as a module control station capable of enclosing enough equipment to control the station from each module. The concept has commercial potential for the Space Station and surface workstation applications. The central triangular beam interior configuration was expanded and refined to seven different beam configurations. These included triangular on center, triangular off center, square, hexagonal small, hexagonal medium, hexagonal large and the H beam. Each was explored with some considerations as to the utilities and a suggested evaluation factor methodology was presented. Scale models of each concept were made. The models were helpful in researching the seven beam configurations and determining the negative residual (unused) volume of each configuration. A flexible hardware evaluation factor concept is proposed which could be helpful in evaluating interior space volumes from a human factors point of view. A magnetic version with all the graphics is available from the author or the technical monitor. Author

N88-24633*# National Aeronautics and Space Administration. Hugh L. Dryden Flight Research Center, Edwards, Calif.
CURRENT FLIGHT TEST EXPERIENCE RELATED TO STRUCTURAL DIVERGENCE OF FORWARD-SWEPT WINGS
Lawrence S. Schuster and William A. Lokos Aug. 1988 15 p Presented at the 1988 International Symposium of Flight Test Engineers, Arlington, Tex., 14-18 Aug. 1988
(NASA-TM-100445; H-1500; NAS 1.15:100445) Avail: NTIS HC A03/MF A01 CSCL 01C

Flight testing the X-29A forward-swept wing aircraft has required development of new flight test techniques to accomplish subcritical extrapolations to the actual structural divergence dynamic pressure of the aircraft. This paper provides current experience related to applying these techniques to analysis of flight data from the forward-swept wing in order to assess the applicability of these techniques to flight test data. The measurements required, maneuvers flown, and flight test conditions are described. Supporting analytical predictions for the techniques are described and the results using flight data are compared to these predictions. Use of the results during envelope expansion and the resulting modifications to the techniques are discussed. Some of the analysis challenges that occurred are addressed and some preliminary conclusions and recommendations are made relative to the usefulness of these techniques in the flight test environment. Author

N88-24634*# National Aeronautics and Space Administration. Ames Research Center, Moffett Field, Calif.

ANALYSIS PROCEDURES AND SUBJECTIVE FLIGHT RESULTS OF A SIMULATOR VALIDATION AND CUE FIDELITY EXPERIMENT

Peter C. Carr and Burnell T. McKissick (National Aeronautics and Space Administration. Langley Research Center, Hampton, Va.) Jul. 1988 31 p

(NASA-TM-88270; H-1371; NAS 1.15:88270) Avail: NTIS HC A03/MF A01 CSCL 01C

A joint experiment to investigate simulator validation and cue fidelity was conducted by the Dryden Flight Research Facility of NASA Ames Research Center (Ames-Dryden) and NASA Langley Research Center. The primary objective was to validate the use of a closed-loop pilot-vehicle mathematical model as an analytical tool for optimizing the tradeoff between simulator fidelity requirements and simulator cost. The validation process includes comparing model predictions with simulation and flight test results to evaluate various hypotheses for differences in motion and visual cues and information transfer. A group of five pilots flew air-to-air tracking maneuvers in the Langley differential maneuvering simulator and visual motion simulator and in an F-14 aircraft at Ames-Dryden. The simulators used motion and visual cueing devices including a g-seat, a helmet loader, wide field-of-view horizon, and a motion base platform. Author

06 AIRCRAFT INSTRUMENTATION

Includes cockpit and cabin display devices; and flight instruments.

For related information see also *19 Spacecraft Instrumentation* and *35 Instrumentation and Photography.*

N88-24635# Army Aeromedical Research Lab., Fort Rucker, Ala.

EVALUATION OF THE US ARMY FITTING PROGRAM FOR THE INTEGRATED HELMET UNIT OF THE INTEGRATED HELMET AND DISPLAY SIGHTING SYSTEM

Clarence E. Rash, John S. Martin, Daniel W. Gower, Jr., Joseph R. Licina, and John V. Barson Jul. 1987 80 p

(AD-A191616; USAARL-87-8) Avail: NTIS HC A05/MF A01 CSCL 25C

In June 1985, the US Army began fielding a new aircraft known as the Advanced Attack Helicopter, the AH-64. Integral to this new aircraft is a monocular helmet-mounted display system, the Integrated Helmet and Display Sighting System (IHADSS). Along with various electronic components, the IHADSS includes a helmet referred to as the Integrated Helmet Unit (IHU). The purpose of the IHU is to provide the aviator with basic impact and noise protection. In addition, it serves as a platform for the display system, composed of a miniature, 1-inch diameter, Cathode Ray Tube (CRT) and an optical relay device, the Helmet Display Unit (HDU). The basic fitting process involves numerous steps including, but not limited to, adjustments to the suspension system, proper location and alignment to the HDU, and final trimming of the helmet visor to accommodate the HDU when in the operating position. The objectives of the fitting procedure are to: a) obtain a comfortable, stable fit of the IHU, which will enable the aviator to achieve the maximum field-of-view provided by the HDU when it is mounted on the helmet and b) achieve boresight, which permits accurate engagement of weapons systems. This report documents the fitting program established at USAARL, its successes and deficiencies, and presents recommendations for designing a fitting program which, will ensure that the man-machine interface, as provided by the helmet, is optimized. GRA

N88-24636# Aeronautical Systems Div., Wright-Patterson AFB, Ohio.

AN EVALUATION OF THREE LINEAR SCALE RADAR ALTIMETER DISPLAYS Final Report

Larry A. Carr Jan. 1988 102 p

(AD-A192173; ASD-TR-87-5005) Avail: NTIS HC A06/MF A01 CSCL 17G

Twelve fighter pilots were used as subjects to fly six low altitude missions in a full mission F-16 simulator with a visual system projected on a head-up display. The subjects were required to accomplish three descents to one of two altitudes (300' or 1000') on each of the missions and to maintain that altitude before then climbing back to cruising altitude were used as measures of performance. A Modified Cooper Harper scale was used to assess workload and a questionnaire was also used to ascertain subjective opinion concerning each scale. The original scale was compared with two alternative scales that both had an expanded lower portion and one of the two had an expanded upper altitude range. The results indicated that none of the performance measures were significant with respect to the scales being used. Accuracy for reading and plotting altitudes was better using the original scale apparently due to its larger number of scale markings. Workload ratings showed lower workload associated with the expanded upper scale in transitioning into and out of low altitude. Questionnaire data was not significant, but did result in key comments that showed distinct preference for the two alternatives scales with the expanded low altitude regions. A separate alternative scale was recommended for further testing. GRA

N88-24637*# Research Triangle Inst., Research Triangle Park, N.C.

DEVELOPMENT OF A MULTIPURPOSE SMART RECORDER FOR GENERAL AVIATION AIRCRAFT

J. H. White and J. F. Finger Mar. 1988 93 p

(Contract NAS1-16098)

(NASA-CR-168353; NAS 1.26:168353) Avail: NTIS HC A05/MF A01 CSCL 01D

An intelligent flight recorder, called the Smart Recorder, was fabricated and installed on a King Air aircraft used in standard commercial charter service. This recorder was used for collection of data toward two objectives: (1) the characterization of the typical environment encountered by the aircraft; and (2) research in the area of trend monitoring. Data processing routines and data presentation formats were defined that are applicable to commuter size aircraft. The feasibility of a cost-effective, multipurpose recorder for general aviation aircraft was successfully demonstrated. Implementation of on-board environmental data processing increased the number of flight hours that could be stored on a single data cartridge and simplified the data management problem by reducing the volume of data to be processed in the laboratory. Trend monitoring algorithms showed less variability in the trend plots when compared against plots of manual data. J.P.B.

07 AIRCRAFT PROPULSION AND POWER

Includes prime propulsion systems and systems components, e.g., gas turbine engines and compressors; and onboard auxiliary power plants for aircraft.

For related information see also *20 Spacecraft Propulsion and Power, 28 Propellants and Fuels,* and *44 Energy Production and Conversion.*

N88-24638# Battelle Columbus Labs., Ohio.
AIRCRAFT EMISSIONS CHARACTERIZATION: TF41-A2, TF30-P103 AND TF30-P109 ENGINES Final Report, Dec. 1985 - Mar. 1987
C. W. Spicer, M. W. Holdren, S. E. Miller, D. L. Smith, and R. N. Smith Dec. 1987 76 p
(Contract F08635-85-C-0122)
(AD-A192053; AFESC/ESL-TR-87-27) Avail: NTIS HC A05/MF A01 CSCL 24A

Assessment of the environmental impact of aircraft operations is required by Air Force regulations. This program was undertaken with the aim of quantifying the gaseous and articulate emissions associated with three Air Force turbine engines. These engines were 41-A2, TF30-P103, and TF30-P109. The emissions tests were carried out, using a test cell Tinker AFP, Oklahoma City, OK. All tests employed JP-4 as the fuel, and fuel samples were characterized by standard tests and analyzed for composition. Emissions were measured at power settings of idle, 30 percent, 75 percent, 100 percent, and afterburner (where appropriate). Measurements were made of detailed organic composition, CO, CO2, NO, NOx, smoke number, particle concentration, and particle size distribution. A multiport sampling rake was used to sample the exhaust, and heated Teflon tubing was used to transfer exhaust to the monitoring instrumentation. Measured and calculated fuel/air ratios were compared to assure representative sampling of the exhaust. GRA

N88-24639*# National Aeronautics and Space Administration. Lewis Research Center, Cleveland, Ohio.
PARTICLE-LADEN WEAKLY SWIRLING FREE JETS: MEASUREMENTS AND PREDICTIONS
Daniel L. Bulzan, Jian-Shun Shuen, and Gerard M. Faeth (Michigan Univ., Ann Arbor.) 1988 22 p Presented at the 24th Joint Propulsion Conference, Boston, Mass., 11-13 Jul. 1988; sponsored by AIAA, ASEE, ASME and SAE
(NASA-TM-100920; E-4176; NAS 1.15:100920; AIAA-88-3138)
Avail: NTIS HC A03/MF A01 CSCL 21E

A theoretical and experimental investigation of particle-laden, weakly swirling, turbulent free jets was conducted. Glass particles, having a Sauter mean diameter of 39 microns with a standard deviation of 15 microns, were used. A single loading ratio of 0.2 was used in the experiments. Measurements are reported for three swirl numbers, ranging from 0.0 to 0.3. The measurements included mean and fluctuating velocities of both phases, and particle mass flux distributions. Measurements were compared with predictions from three types of multiphase flow analysis: locally homogeneous flow (LHF); deterministic separated flow (DSF); and stochastic separated flow (SSF). For the particle-laden jets, the LHF and DSF models did not provide very satisfactory predictions. The LHF model generally overestimated the rate of decay of particle mean axial and angular velocities with streamwise distance, due to the neglect of particle inertia. The LHF model predictions of particle mass flux also showed poor agreement with measurements due to the assumption of no-slip between phases. The DSF model also performed quite poorly for predictions of particle mass flux, because turbulent dispersion of the particles was neglected. The SSF model, which accounts for both particle inertia and turbulent dispersion of the particles, yielded reasonably good predictions throughout the flow field for the particle-laden jets. Author

N88-24640*# National Aeronautics and Space Administration. Lewis Research Center, Cleveland, Ohio.
AN EMPIRICAL MODEL OF THE EFFECTS OF CURVATURE AND CONVERGENCE ON DILUTION JET MIXING
James D. Holdeman, Ram Srinivasan, and Craig D. White (Garrett Engine Co., Phoenix, Ariz.) [1988] 20 p Presented at the 24th Joint Propulsion Conference, Boston, Mass., 11-13 Jul. 1988; sponsored in part by AIAA, ASME, SAE and ASEE Original document contains color illustrations
(NASA-TM-100896; E-4143; NAS 1.15:100896; AIAA-88-3180)
Avail: NTIS HC A03/MF A01 CSCL 21E

An existing empirical model of the temperature field downstream of single and multiple rows of jets injected into a confined crossflow has been extended to model the effects of curvature and convergence on the mixing. This extension is based on the results of a numerical study of these effects using a 3-D turbulent flow computer code. Temperature distributions calculated with the empirical model are presented to show the effects of flow area convergence, radius of curvature, and inner and outer wall injection for single and opposed rows of jets. Author

N88-24641*# National Aeronautics and Space Administration. Lewis Research Center, Cleveland, Ohio.
NASA/INDUSTRY ADVANCED TURBOPROP TECHNOLOGY PROGRAM
Joseph A. Ziemianski and John B. Whitlow, Jr. [1988] 26 p Prepared for presentation at the 16th Congress of the International Council of Aeronautical Sciences, Jerusalem, Israel, 28 Aug. - 2 Sep. 1988
(NASA-TM-100929; E-4198; NAS 1.15:100929) Avail: NTIS HC A03/MF A01 CSCL 21E

Experimental and analytical effort shows that use of advanced turboprop (propfan) propulsion instead of conventional turbofans in the older narrow-body airline fleet could reduce fuel consumption for this type of aircraft by up to 50 percent. The NASA Advanced Turboprop (ATP) program was formulated to address the key technologies required for these thin, swept-blade propeller concepts. A NASA, industry, and university team was assembled to develop and validate applicable design codes and prove by ground and flight test the viability of these propeller concepts. Some of the history of the ATP project, an overview of some of the issues, and a summary of the technology developed to make advanced propellers viable in the high-subsonic cruise speed application are presented. The ATP program was awarded the prestigious Robert J. Collier Trophy for the greatest achievement in aeronautics and astronautics in America in 1987. Author

N88-24642*# National Aeronautics and Space Administration. Lewis Research Center, Cleveland, Ohio.
EXPERIMENTAL VIBRATION DAMPING CHARACTERISTICS OF THE THIRD-STAGE ROTOR OF A THREE-STAGE TRANSONIC AXIAL-FLOW COMPRESSOR
Frederick A. Newman [1988] 24 p Presented at the 24th Joint Propulsion Conference, Boston, Mass., 11-13 Jul. 1988; sponsored in part by AIAA, ASME, SAE and ASEE
(NASA-TM-100948; E-4240; NAS 1.15:100948; AIAA-88-3229)
Avail: NTIS HC A03/MF A01 CSCL 21E

Rotor blade aerodynamic damping is experimentally determined in a three-stage transonic axial flow compressor having design aerodynamic performance goals of 4.5:1 pressure ratio and 65.5 lbm/sec weight flow. The combined damping associated with each mode is determined by a least squares fit of a single degree of freedom system transfer function to the nonsynchronous portion of the rotor blade strain gage output power spectra. The combined damping consists of the aerodynamic damping and the structural and mechanical damping. The aerodynamic damping varies linearly with the inlet total pressure for a given corrected speed, weight flow, and pressure ratio while the structural and mechanical damping is assumed to remain constant. The combined damping is determined at three inlet total pressure levels to obtain the aerodynamic damping. The third-stage rotor blade aerodynamic damping is presented and discussed for the design equivalent speed with the stator blades reset for maximum efficiency. The

compressor overall preformance and experimental Campbell diagrams for the third-stage rotor blade row are also presented.
Author

08 AIRCRAFT STABILITY AND CONTROL

Includes aircraft handling qualities; piloting; flight controls; and autopilots.

For related information see also *05 Aircraft Design, Testing and Performance.*

N88-24643 Texas Univ., Austin.
ATTITUDE CONTROL LAWS FOR GAS-JET SPACECRAFT Ph.D. Thesis
Edward Raymond Avila 1987 263 p
Avail: Univ. Microfilms Order No. DA8728512

A digital control algorithm is presented for attitude stabilization during maneuvering (thrust vector control) of reaction-jet spacecraft, whose rotational dynamics may be closely approximated by two kinematic integrators about each control axis (negligible dynamic inter-axis coupling). The algorithm is called the Control Law for Orientation Using Thrusters (CLOUT). CLOUT is a good candidate for control of spacecraft continuously maneuvering under low thrust, although it is also appropriate for maneuvering units with shorter acceleration times. CLOUTS uses noisy angle measurements and a third-order observer (in each axis) to estimate angle, angular rate, and the two components of center-of-gravity offset from the geometric center of the four translational jets. The control law uses these estimates to implement parabolic phase plane switching boundaries which adapt the center-of-gravity offset estimates, and achieve very tight thrust vector control. The CLOUT scheme evolved from the study of the implementation of ideal-limit-cycle control in the presence of a known environmental distrubing torque. During coasting flight, or for control about the unaffected axis during a translational acceleration, CLOUT is designed to revert to a single-axis ideal-limit-cycle control law. Thus, CLOUT provides both coasting flight attitude hold, and thrust vector control, and is fuel conservative. Six degrees-of-freedom simulation results verify the performance of the CLOUT system. Dissert. Abstr.

N88-24644*# Old Dominion Univ., Norfolk, Va. Dept. of Electrical and Computer Engineering.
GUIDANCE AND CONTROL STRATEGIES FOR AEROSPACE VEHICLES Progress Report, 1 Jan. - 30 Jun. 1988
Desineni S. Naidu and Joseph L. Hibey Jul. 1988 61 p
(Grant NAG1-736)
(NASA-CR-183032; NAS 1.26:183032) Avail: NTIS HC A04/MF A01 CSCL 01C

The optimal control problem arising in coplanar, orbital transfer employing aeroassist technology is addressed. The maneuver involves the transfer from high Earth orbit to low Earth orbit. A performance index is chosen the minimize the fuel consumption for the transfer. Simulations are carried out for establishing a corridor of entry conditions which are suitable for flying the spacecraft through the atmosphere. A highlight of the paper is the application of an efficient multiple shooting method for taming the notorious nonlinear, two-point, boundary value problem resulting from optimization procedure. Author

09 RESEARCH AND SUPPORT FACILITIES (AIR)

Includes airports, hangars and runways; aircraft repair and overhaul facilities; wind tunnels; shock tubes; and aircraft engine test stands.

For related information see also *14 Ground Support Systems and Facilities (Space).*

N88-24645# Air Force Inst. of Tech., Wright-Patterson AFB, Ohio. School of Engineering.
PARAMETER-ADAPTIVE MODEL-FOLLOWING FOR IN-FLIGHT SIMULATION M.S. Thesis
Luis A. Pineiro Dec. 1987 320 p
(AD-A190567; AFIT/GE/ENG/87D-74) Avail: NTIS HC A14/MF A01 CSCL 01C

This thesis implements an adaptive, fast-sampling control law to compensate for changing aircraft parameters. The step-response matrix which is required for this implementation is identified recursively using a recently developed technique which does not require special test signals and which automatically discounts old data depending on the input excitation detected. Tracking fidelity is maintained despite parameter changes which occur either abruptly or slowly. Simulations are conducted, using a model of the AFTI/F-16 aircraft and the control design package MATRIX, to test the resulting adaptive system. Actuator position and rate limits are discussed. The performance of the resulting system is excellent and demonstrates the relative advantages of adaptive controllers for in-flight simulation. Recommendations are made for future analysis including the use of moving-bank estimators.
GRA

N88-24646# Oak Ridge National Lab., Tenn. Metals and Ceramics Div.
SHaRE: COLLABORATIVE MATERIALS SCIENCE RESEARCH
Edward A Kenik and Karren L. More (Oak Ridge Associated Universities, Inc., Tenn.) 1988 3 p Presented at the MAS/EMSA Microbeam Analysis Conference, Milwaukee, Wisc., 7 Aug. 1988
(Contracts DE-AC05-84OR-21400; DE-AC05-76OR-00033)
(DE88-007175; CONF-880841-2) Avail: NTIS HC A02/MF A01

The Shared Research Equipment (SHaRE) Program provides access to the wide range of advanced equipment and techniques available in the Metals and Ceramics Division of ORNL to researchers from universities, industry, and other national laboratories. All SHaRE projects are collaborative in nature and address materials science problems in areas of mutual interest to the internal and external collaborators. While all facilities in the Metals and Ceramics Division are available under SHaRE, there is a strong emphasis on analytical electron microscopy (AEM), based on state-of-the-art facilities, techniques, and recognized expertise in the Division. The microscopy facilities include four analytical electron microscopes (one 300 kV, one 200 kV, and two 120 kV instruments), a conventional transmission electron microscope with a low field polepiece for examination of ferromagnetic materials, a high voltage (1 MV) electron microscope with a number of in situ capabilities, and a variety of EM support facilities. An atom probe field ion microscope provides microstructural and elemental characterization at atomic resolution. Other facilities utilized under SHaRE include several Auger electron spectroscopy/surface analytical instruments, a triple beam Van de Graaff accelerator facility for nuclear microanalysis techniques, various x-ray diffraction instruments, a Nanoindenter for high spatial resolution mechanical property measurements, and a host of other advanced and unique facilities. DOE

N88-24647# Carnegie-Mellon Univ., Pittsburgh, Pa. Software Engineering Inst.
AN OOD (OBJECT-ORIENTED DESIGN) PARADIGM FOR FLIGHT SIMULATORS Final Report
Kenneth J. Lee, Michael S. Rissman, Richard DIppolito, Charles Plinta, and Roger VanScoy Dec. 1987 104 p
(Contract F19628-85-C-0003)

(AD-A191097; CMU/SEI-87-TR-43; ESD-TR-87-206) Avail: NTIS HC A06/MF A01 CSCL 01B

This report presents a paradigm for object-oriented implementations of flight simulators. It is a result of work on the Ada Simulator Validation Program (ASVP) carried out by members of the technical staff at the Software Engineering Institute (SEI). Object-oriented design predominates discussions about Ada-based software engineering. The identification of objects and implementation of objects are two separate issues. This paradigm is a model for implementing systems of objects. The objects are described in a form of specification called an object dependency diagram. The paradigm is not about how to create the specification. Although much has been written on object-oriented design, SEI project members could find no examples of object-oriented implementations relevant to flight simulators. Examples were required for two reasons. First, object-orientation was new to both of the contractors on the ASVP. A methodology which leads to a specification of objects is useful only if developers know how to implement what is specified. Second, managers were skeptical about the benefits of object-oriented design. Examples were needed to determine whether benefits outweight costs. GRA

N88-24648# Essex Corp., Orlando, Fla.
SIMULATOR EVALUATION OF LINEUP VISUAL LANDING AIDS FOR NIGHT CARRIER LANDING Final Report, Aug. 1986 - Mar. 1987
Daniel J. Sheppard, Lawrence J. Hettinger, Daniel P. Westra, and Sherrie A. Jones 10 Mar. 1987 63 p
(Contract N613339-85-D-0026)
(AD-A191212; EOTR-88-1) Avail: NTIS HC A04/MF A01 CSCL 05I

A simulator performance experiment was conducted to evaluate three lineup visual landing aids for night carrier landing at the Visual Technology Research Simulator (VTRS), Naval Training Systems Center (NAVTRASYSCEN), Orlando, Florida. They were a strobe light (string of sequentially flashed lights) extending down the centerline of the landing deck, a searchlight mounted forward of the landing deck on the centerline, and a crossbar lineup system (a linear array of nine lights mounted on the fantail of the ship perpendicular to the drop lights). The searchlight and crossbar were also combined to form an additional VLA condition. A bare deck condition that represented the standard carrier deck lighting configuration was used as the control comparison. Night carrier landing experience (zero night traps versus approximately 50 night traps), and a difficulty factor (axial winds versus angle wind), were also manipulated in the experiment. Ten naval aviators each performed 60 simulated night carrier landings under all experimental conditions. Lineup performance was significantly more accurate with the crossbar and crossbar/searchlight combination system than with the bare deck for the far and middle segments of the approach. There appeared to be no advantage in performance near the ramp and at touchdown. There was no difference in performance between the crossbar and crossbar/searchlight combination. GRA

N88-24649# Anacapa Sciences, Inc., Fort Rucker, Ala.
AN ENUMERATION OF RESEARCH TO DETERMINE THE OPTIMAL DESIGN AND USE OF ARMY FLIGHT TRAINING SIMULATORS Final Report, Feb. 1984 - Feb. 1985
Kenneth D. Cross and Charles A. Gainer Oct. 1987 22 p
(Contract MDA903-81-C-0504; DA Proj. 2Q2-63744-A-795)
(AD-A191242; ASI479-066-85; ARI-TR-763) Avail: NTIS HC A03/MF A01 CSCL 05I

This document lists and describes research the authors judged necessary to determine the optimal design and use of Army flight training simulators. Two major lines of research are described; the first addresses the design fidelity issue. Specifically, research is described that is judged necessary to determine the most cost- and training-effective level of fidelity for four simulator components: the visual system, the motion systems, the math models that determine the handling qualities of the flight simulator, and the cockpit displays and controls. The purpose of the second line of research is to determine how best to use production simulators that have been or are soon to be acquired by the Army. This line of research focuses primarily on the use of production simulators for field unit aviators who have completed institutional training and have been assigned to an operational field unit. However, the second line of research addresses some issues associated with the use of flight simulators for institutional training at the U.S. Army Aviation Center received before the aviator's first assignment to an operational unit. GRA

N88-24650# Von Karman Inst. for Fluid Dynamics, Rhode-Saint-Genese (Belgium).
THE PERFORMANCE OF THE VKI LONGSHOT HYPERSONIC WIND TUNNEL
G. Simeonides Jun. 1987 59 p
(VKI-TN-161; ETN-88-92481) Avail: NTIS HC A04/MF A01

A method to predict the piston cycle of a hypersonic facility is described. Predictions of reservoir temperature are satisfactory; discrepancies between predicted and measured reservoir pressures are attributed to an empirical chambrage correction factor. Predictions of the total compressed volume of the nitrogen test gas are considered valid, as this is rather insensitive to reservoir pressure. They were used to confirm the possibility to nearly double the present reservoir volume and consequently the running time of the facility. The predictions of the method are presented in the form of charts which may be used as guidelines in the definition of operating conditions. Improvement of the method with respect to the chambrage correction is recommended and a possible procedure is proposed. Determination of the test section conditions and their variation during a test are discussed. ESA

N88-24651# Blocher-Motor G.m.b.H. and Co. K.G., Metzingen (West Germany).
DESIGN STUDY. MANIPULATOR SYSTEMS FOR MODEL HANDLING IN EUROPEAN TRANSONIC WIND TUNNELS [KONZEPTSTUDIE. MANIPULATORSYSTEM FUER MODELHANDHABUNG IM EUROPAEISCHEN TRANSSCHALL-WINDKANAL]
Reiner Blocher and Eberhard Weiss 25 May 1987 199 p In GERMAN
(ETN-88-91944) Avail: NTIS HC A09/MF A01

Electrical master slave manipulators in cryogenic temperatures and under pressure are proposed for remote model handling. Economy of time and energy can be achieved without thermal stresses in model and wind tunnel. Manipulator design consists of two arms and seven degrees of freedom. Control is achieved by frequency regulated asynchronous motors. Digital electronics procures total automation for the study of collision protection and special handling cycles. Viewing and associated audio-systems are provided by stereo and monosystems giving optimal global view of the operating field. Mechanical properties of construction parts in cryogenic environment are studied. ESA

N88-24652# Army Engineer Waterways Experiment Station, Vicksburg, Miss. Geotechnical Lab.
DESIGN OF OVERLAYS FOR RIGID AIRPORT PAVEMENTS Final Report, Jan. 1982 - Jun. 1987
Raymond S. Rollings Apr. 1988 277 p
(Contract DTFA01-81-Y-10523)
(DOT/FAA/PM-87/19) Avail: NTIS HC A13/MF A01

Existing rigid and flexible overlay pavement design methods are empirical, and they use specific levels of cracking or visual deflection as the defined failure condition. The existing empirical designs are based on tests run 30 years ago, and current analytical models provide greatly improved abilities to examine the overlay pavement structure. Emphasis by many agencies on life-cycle cost analysis and more sophisticated maintenance and rehabilitation strategies require methods of predicting pavement performance rather than simply developing safe designs. A layered-elastic analytical model was selected to evaluate stresses from applied loads in the pavement structure. Pavement performance was measured in terms of a structural condition index (SCI) which related to the type, degree, and severity of pavement cracking and spalling on a scale of 0 to 100. Models were developed to

represent the effect of cracking in base slabs under the overlay, to account for fatigue damage of previous traffic on the base pavement, and to account for the effects of substandard load transfer at slab joints. The predicted performance of rigid overlays and pavements using this technique was checked against the results of full-scale accelerated traffic tests conducted by the Corps of Engineers and against current overlay design methods and was found to provide reasonab le agreement. Author

12 ASTRONAUTICS (GENERAL)

For extraterrestrial exploration see *91 Lunar and Planetary Exploration.*

N88-24653# British Aerospace Public Ltd. Co., Bristol (England). Configuration Control Dept.
P-PLUS: POLAR PLATFORM UTILIZATION STUDY, EXECUTIVE SUMMARY
C. P. Lee Paris, France ESA Jul. 1987 49 p Prepared in cooperation with Dornier Werke GmbH, Friedrichshafen, Fed. Republic of Germany; Matra Espace, Toulouse, France; Telespazio S.p.A., Rome, Italy; Logica Ltd., London, England; and Laben Space Instrumentation and Systems, Milan, Italy
(Contract ESA-6608/85)
(BAe-TP-8391; ESA-CR(P)-2507; ETN-88-92552) Copyright Avail: NTIS HC A03/MF A01

Space Station Polar Platform users and their requirements were identified. Earth observations and solar terrestrial physics are the main users. The STS system provides a more flexible servicing capability than Hermes. The ground segment, particularly data systems, is the main cost and utilization aspect for users. Data management must be studied closely. ESA

N88-24654*# Draper (Charles Stark) Lab., Inc., Cambridge, Mass.
A DESIGN STUDY OF ONBOARD NAVIGATION AND GUIDANCE DURING AEROCAPTURE AT MARS M.S. Thesis
Douglas Paul Fuhry May 1988 200 p
(Contract NAS9-17560)
(NASA-CR-172053; NAS 1.26:172053; CSDL-T-986) Avail: NTIS HC A09/MF A01 CSCL 22A

The navigation and guidance of a high lift-to-drag ratio sample return vehicle during aerocapture at Mars are investigated. Emphasis is placed on integrated systems design, with guidance algorithm synthesis and analysis based on vehicle state and atmospheric density uncertainty estimates provided by the navigation system. The latter utilizes a Kalman filter for state vector estimation, with useful update information obtained through radar altimeter measurements and density altitude measurements based on IMU-measured drag acceleration. A three-phase guidance algorithm, featuring constant bank numeric predictor/corrector atmospheric capture and exit phases and an extended constant altitude cruise phase, is developed to provide controlled capture and depletion of orbital energy, orbital plane control, and exit apoapsis control. Integrated navigation and guidance systems performance are analyzed using a four degree-of-freedom computer simulation. The simulation environment includes an atmospheric density model with spatially correlated perturbations to provide realistic variations over the vehicle trajectory. Navigation filter initial conditions for the analysis are based on planetary approach optical navigation results. Results from a selection of test cases are presented to give insight into systems performance. Author

13 ASTRODYNAMICS

Includes powered and free-flight trajectories; and orbital and launching dynamics.

No abstracts in this category.

14 GROUND SUPPORT SYSTEMS AND FACILITIES (SPACE)

Includes launch complexes, research and production facilities; ground support equipment, e.g., mobile transporters; and simulators.

For related information see also *09 Research and Support Facilities (Air).*

N88-24655# GT-Devices, Alexandria, Va.
ANALYTIC AND NUMERICAL MODELING OF HEAT AND MATERIAL TRANSPORT IN ELECTRICAL HYPERVELOCITY GUNS Final Report, 5-6 Sep. 1986
Niels K. Winsor 4 Dec. 1987 85 p
(Contract F49620-85-C-0134)
(AD-A192178; AFOSR-88-0257TR) Avail: NTIS HC A05/MF A01 CSCL 20C

A computer simulation code has been developed. The physical transport processes of radiation transport, viscosity, electrical and thermal conductivity and turbulence were included in the study. The code benchmarked against material erosion experiments with metals and insulators. The processes occurring near the bore wall of an electrothermal gun have been evaluated. The studies have demonstrated the utility of a gun system redesign which lowers the propelling gas temperature near the wall. This has resulted in the experimental reduction of gun bore erosion to levels at or below the erosion in conventional powder guns. The code results have also been interpreted for the electromagnetic (rail) gun case. Here the unavoidable high propelling gas temperatures cause a more severe erosion problem. GRA

N88-24656 Texas Univ., Austin.
FUNDAMENTAL LIMITS TO THE VELOCITY OF SOLID ARMATURES IN RAILGUNS Ph.D. Thesis
Glen Carl Long, Jr. 1987 314 p
Avail: Univ. Microfilms Order No. DA8728605

The fundamental limits to the velocity of solid armatures in railguns are dependent upon the increase in temperature which melts the conducting medium or lower the yield strength of the material. A two dimensional transient finite element electrothermal model is developed to determine the magnetic and temperature fields in the rails and armature of a railgun. The solution for the magnetic and temperature fields is based upon the fundamentals of Maxwell's equations and Fourier's law of heat conduction with no apriori assumptions about the current density distribution in the rails or the armature. The magnetic field and temperature field spatial variations are calculated using finite differencing methods. A thermal diffusion iteration is performed between each magnetic diffusion iteration. Joule heating information is provided by solving the magnetic diffusion problem and temperature data for calculating material properties such as the electrical resistivity, thermal conductivity, and specific heat is provided by solving the thermal diffusion problem. Various types of rail and armature designs are simulated to include solid armatures consisting of different homogeneous materials, resistive rails, and a graded resistance armature. The analysis also includes different solid armature shapes such as the square, curved, and chevron designs. The results of the transient finite element electrothermal model are compared with the laboratory test results. Dissert. Abstr.

N88-24657# New Mexico Univ., Albuquerque. Dept. of Mechanical Engineering.
USE OF A TWO-STAGE LIGHT-GAS GUN AS AN INJECTOR FOR ELECTROMAGNETIC RAILGUNS
M. Shahinpoor, J. R. Asay, C. H. Konrad, and C. A. Hall Apr. 1988 6 p Presented at the 4th Symposium on Electromagnetic Launch Technology, Austin, Tex., 12 Apr. 1988 Prepared in cooperation with Sandia National Labs., Albuquerque, N. Mex.
(Contract DE-AC04-76DP-00789)
(DE88-007200; SAND-87-2314C; CONF-880478-5) Avail: NTIS HC A02/MF A01

Ablation of wall materials is known to be a major factor limiting the performance of railguns. To minimize this effect, it is desirable

to inject projectiles into railgun at velocities greater than the ablation threshold velocity (6 to 8 km/s for copper rails). Because two-stage light-gas guns are capable of achieving such velocities, a program was initiated to design, build and evaluate the performance of a two-stage light gas gun, utilizing hydrogen gas, for use as an injector to an electromagnetic railgun. This effort is part of a project to develop a hypervelocity electromagnetic launcher (HELEOS) for use in equation-of-state studies. In this paper, the specific design features that enhance compatibility of the injector with the railgun, including a slip-joint between the injector launch tube and the coupling section to the railgun are described. The operational capabilities for using all major projectile velocity measuring techniques, such as in-bore pressure gauges, laser and CW X-ray interrupt techniques, flash x-ray and continuous in-bore velocity measurements using VISAR interferometry are also discussed. Finally an internal ballistics code for optimizing gun performance has been utilized to interpret performance data of the gun. DOE

N88-24658# Lawrence Livermore National Lab., Calif.
FABRICATION ISSUES AND TECHNOLOGY DEVELOPMENT FOR HELEOS (HYPERVELOCITY ELECTROMAGNETIC LAUNCHER FOR EQUATION OF STATE)
A. R. Susoeff, R. S. Hawke, J. K. Balk, C. A. Hall, and M. J. McDonald (Sandia National Labs., Albuquerque, N. Mex.) Feb. 1988 6 p Presented at the 4th Symposium on Electromagnetic Launch Technology, Austin, Tex., 12 Apr. 1988
(Contracts W-7405-eng-48; DE-AC04-76DP-00789)
(DE88-007419; UCRL-98228; CONF-880478-6; SAND-88-0843C)
Avail: NTIS HC A02/MF A01

Starfire is a joint railgun project of Lawrence Livermore National Laboratory and Sandia National Laboratory and Sandia National Laboratory (Albuquerque). Its goal is to develop a Hypervelocity Electromagnetic Launcher for Equation of State (HELEOS) experiments. A two-stage light-gas gun is used as pre-injector. Each round-bore HELEOS railgun module is 12.7 mm in diameter and 2.4 m long. The muzzle end of the railgun is connected to a vacuum tank. Common materials and fabrication technology are used in the manufacture of all components, and modular design allows for extending the length of the railgun as progress dictates. The launcher uses a vee block geometry, which is designed to: provide compressive preload; operate with a 300-MPa (3-kbar) internal bore pressure; and easily accommodate interchangeable materials in the bore support structure and rail. We have performed full-scale material testing of the railgun and have developed a precision round-bore fabrication process. Air-gage inspection is used to determine bore diameter and straightness. We have also developed a surface mapping system to document the surface topography of the bore before and after an experiment. This paper presents fabrication details, results of tests conducted, and areas for potential improvement. DOE

N88-24659*# National Aeronautics and Space Administration. Lewis Research Center, Cleveland, Ohio.
EXPERIMENTAL RADIO FREQUENCY LINK FOR Ka-BAND COMMUNICATIONS APPLICATIONS
Gene Fujikawa, Martin J. Conray, Alan L. Saunders, and Dale E. Pope Jun. 1988 16 p
(NASA-TM-100824; E-4012; NAS 1.15:100824) Avail: NTIS HC A03/MF A01 CSCL 17B

An experimental radio frequency link has been demonstrated to provide two-way communication between a remote user ground terminal and a ground-based Ka-band transponder. Bit-error-rate performance and radio frequency characteristics of the communication link were investigated. Author

15 LAUNCH VEHICLES AND SPACE VEHICLES

Includes boosters; operating problems of launch/space vehicle systems; and reusable vehicles.

For related information see also *20 Spacecraft Propulsion and Power.*

No abstracts in this category.

16 SPACE TRANSPORTATION

Includes passenger and cargo space transportation, e.g., shuttle operations; and space rescue techniques.

For related information see also *03 Air Transportation and Safety* and *18 Spacecraft Design, Testing and Performance.* For space suits see *54 Man/System Technology and Life Support.*

N88-24660*# National Aeronautics and Space Administration. Lyndon B. Johnson Space Center, Houston, Tex.
PAYLOAD DEPLOYMENT METHOD AND SYSTEM Patent Application
Clifford J. Barnett, inventor (to NASA), John E. Greenwood, inventor (to NASA), and Earl V. Holman, inventor (to NASA) (Rockwell International Corp., Houston, Tex.) 15 Apr. 1988 14 p
(NASA-Case-MSC-21330-1; NAS 1.71:MSC-21330-1; US-Patent-Appl-SN-182000) Avail: NTIS HC A03/MF A01 CSCL 22B

A method and apparatus for deploying the payload of space shuttle or the like is described. It is referred to as the Stabilized Payload Deployment System (SPDS). The payload is rotated about an axis outside of the payload but approximately longitudinally with the cargo bay of the shuttle craft. The payload may thus be rotated through ninety degrees. In this case, that is, in its rotated position, the payload may or may not have a small portion located within the cargo bay. Alternatively, the payload may be located completely outside of the bay. According to the apparatus two separable hinge-like devices connect at one longitudinal side or edge of the payload to respective ones of the payload trunnions at different longitudinally spaced locations along the length of the payload. Separation of the payload from the cargo bay is made by unlatching a latch and by the use of a repulsion spring at the position of each hinge-like device. Two four-link mechanisms allow movement between payload and bay. Such accommodative movement is required especially during launch when considerable vibration is encountered. NASA

17 SPACE COMM., SPACECRAFT COMM., COMMAND & TRACKING

Includes telemetry; space communications networks; astronavigation and guidance; and radio blackout.

For related information see also *04 Aircraft Communications and Navigation* and *32 Communications and Radar.*

N88-24661# Woods Hole Oceanographic Institution, Mass.
AN FSK (FREQUENCY SHIFT KEYING) TELEMETRY MODULE FOR VECTOR MEASURING CURRENT METERS Technical Report
Paul D. Fucile and James R. Valdes Dec. 1987 48 p
(Contract N00014-84-C-0134)
(AD-A192142; WHOI-87-55) Avail: NTIS HC A03/MF A01 CSCL 20N

The EG&G Vector Measuring Current Meter (VMCM) used in mooring work provides a 20 ma Serial ASCII Instrumentation Loop (SAIL) communication system. A projected application of the VMCM is to have a surface mooring communicate with a series of VMCMs

via a Frequency Shift Keying (FSK) link. While an FSK modem can communicate with the VMCM, a problem exists with the general operation of the VMCM. If the VMCM is addressed to dump data, it remains on until the unit is re-addressed. If a failure in the link occurs, then the VMCM stays on in a higher power mode and the batteries will be depleted early. The insertion of a processing block between the modem and the VMCM provides a way to look at incoming data, qualify it and re-transmit it to the VMCM. The VMCM will reply and the preprocessor can channel the data to the modem. In the event of a VMCM malfunction, the preprocessor has a timeout function and will turn off the carrier keeping the line quiet. GRA

N88-24662*# National Aeronautics and Space Administration. Lyndon B. Johnson Space Center, Houston, Tex.
ADAPTIVE DATA ACQUISITION MULTIPLEXING SYSTEM AND METHOD Patent Application
R. L. Sinderson, inventor (to NASA), G. A. Salazar, inventor (to NASA), C. M. Haddick, Jr., inventor (to NASA), C. J. Spahn, inventor (to NASA), and C. N. Venkatesh, inventor (to NASA) (Lockheed Engineering and Management Services Co., Inc., Houston, Tex.) 15 Apr. 1988 27 p
(NASA-Case-MSC-21170-1; NAS 1.71:MSC-21170-1; US-Patent-Appl-SN-182266) Avail: NTIS HC 03/MF A01 CSCL 09F

A reconfigurable telemetry multiplexer is discribed which includes a monitor-terminal and a plurality of remote terminals. The remote terminals each include signal conditioning for a plurality of sensors for measuring parameters which are converted by an analog to digital converter. CPU's in the remote terminals store instructions for prompting system configuration and reconfiguration commands. The measurements, instructions and the terminal's present configuration and status data are transmitted to the monitor-terminal and displayed. In response to menu-driven prompts generated and displayed at the monitor-terminal, data generation request commands, status and health commands, and the like are input at the monitor-terminal and transmitted to the remote terminals. The CPU in each remote terminal receives the various commands, stores them in electrically alterable memory and reacts in accordance with the commands to reconfigure a plurality of aspects of the system, generate parameter measurements, status and health signals, and the like; and transmits these signals of the respective terminals to the monitor-terminal for low data rate operator viewing and to higher rate external transmission/monitor equipment. Reconfiguration may be in real time during the general period of parameter measurement acquisition, and may include alteration of the gain, automatic gain rescaling, bias, and or sampling rates associated with one or more of the parameter measurements made by the remote terminals. NASA

N88-24663*# National Aeronautics and Space Administration. Lewis Research Center, Cleveland, Ohio.
SERVICE OFFERINGS AND INTERFACES FOR THE ACTS NETWORK OF EARTH STATIONS
Thom A. Coney 1988 22 p Presented at the 12th International Communication Satellite Systems Conference, Arlington, Va., 13-17 Mar. 1988; sponsored by AIAA
(NASA-TM-100809; E-3989; NAS 1.15:100809) Avail: NTIS HC A03/MF A01 CSCL 09F

The Advanced Communications Satellite (ACTS) is capable of two modes of communication. Mode 1 is a mesh network of Earth stations using baseband-switched, time-division multiple-access (BBS-TDMA) and hopping beams. Mode 2 is a mesh network using satellite-switched, time-division multiple-access (SS-TDMA) and fixed (or hopping) beams. The purpose of this paper is to present the functional requirements and the design of the ACTS Mode 1 Earth station terrestrial interface. Included among the requirements are that: (1) the interface support standard telecommunications service offerings (i.e., voice, video and data at rates ranging from 9.6 kbps to 44 Mbps); (2) the interface support the unique design characteristics of the ACTS communications systems (e.g., the real time demand assignment of satellite capacity); and (3) the interface support test hardware capable of validating ACTS communications processes. The resulting interface design makes use of an appropriate combination of T1 or T3 multiplexers and a small central office (maximum capacity 56 subscriber lines per unit). Author

18 SPACECRAFT DESIGN, TESTING AND PERFORMANCE

Includes satellites; space platforms; space stations; spacecraft systems and components such as thermal and environmental controls; and attitude controls.

For life support systems see *54 Man/System Technology and Life Support.* For related information see also *05 Aircraft Design, Testing and Performance, 39 Structural Mechanics,* and *16 Space Transportation.*

N88-24664# Los Alamos National Lab., N. Mex.
ARCING AND RF SIGNAL GENERATION DURING TARGET IRRADIATION BY A HIGH-ENERGY, PULSED NEUTRAL PARTICLE BEAM
R. T. Robiscoe Feb. 1988 81 p
(Contract W-7405-eng-36)
(DE88-007169; LA-10958-MS) Avail: NTIS HC A05/MF A01

We present a theory describing the dynamics of arc discharges in bulk dielectric materials on board space-based vehicles. Such punch-through arcs can occur in target satellites irradiated by high-energy (250 MeV), pulsed (100 mA x 10 ms) neutral particle beams. We treat the arc as a capacitively limited avalanche current in the target dielectric material, and we find expressions for the arc duration, charge transport, currents, and discharge energy. These quantities are adjusted to be consistent with known scaling laws for the area of charge depleted by the arc. After a brief account of the statistical distribution of voltages at which the arc starts and stops, we calculate the signal strength and frequency spectrum of the electromagnetic radiation broadcast by the arc. We find that arcs from thick (approx. 1 cm) targets can generate rf signals detectable up to 1000 km from the target, by a radio receiver operating at frequency 80 MHz, bandwidth 100 kHz, and detection threshold -105 dBm. These thick-target arc signals are 10 to 20 dB above ambient noise at the receiver, and they provide target hit assessment if the signal spectrum can be sampled at several frequencies in the nominal range 30-200 MHz. Thin-target (approx. 1 mm) arc signals are much weaker, but when they are detectable in conjunction with thick-target signals, target discrimination is possible by comparing the signal frequency spectra. DOE

N88-24665# Innovative Sciences, Inc., San Leandro, Calif.
ELECTROMAGNETIC DAMPING AND VIBRATION ISOLATION OF SPACE STRUCTURES Final Report, 1 Feb. - 30 Sep. 1987
J. K. Hulbert and Bruce W. Maxfield 5 Aug. 1987 66 p
(Contract F49620-87-C-0029)
(AD-A191492; AF080722A.DOC; AFOSR-88-0063TR) Avail: NTIS HC A04/MF A01 CSCL 10A

Structures used in the vacuum, zero gravity environment of space are quite different from earth-bound system. Vibrations induced in a space structure by the operation of equipment internal to the structure should, to the greatest extent possible, be dissipated through heat generation so that this vibrational energy is not simply redistributed throughout the structure. The usual restricted fluid flow dashpot damping system has several serious drawbacks when operating within a space environment. Phase 1 proposed the quantitative assessment of electromagnetic damping that results when conducting but non-magnetic body moves through a region of localized magnetic field. It was shown theoretically in the Phase 1 proposal that this damping should depend quadratically upon both the velocity and the magnetic field seen by the moving conducting body. From this, it follows that electromagnetic damping (ED) has the potential for both large energy and power dissipation. Although our initial approximate theoretical estimate predicted strong damping under ideal circumstances, the appropriate partial

differential equations (PDE) had not been solved at the onset of Phase 1. Consequently, one could not calculate the damping magnitude that might be realized under practical conditions.
GRA

N88-24666# Oklahoma Univ., Norman. Dept. of Mathematics.
ESTIMATION AND CONTROL OF DISTRIBUTED MODELS FOR CERTAIN ELASTIC SYSTEMS ARISING IN LARGE SPACE STRUCTURES Final Report, 1 Jul. 1984 - 30 Sep. 1987
Luther W. White 30 Sep. 1987 62 p
(Grant AF AFOSR-0271-84)
(AD-A192120; AFOSR-88-0245TR) Avail: NTIS HC A04/MF A01 CSCL 22B

The goal of this research was to study estimation and control of elastic systems composed of beams and plates. Specifically, the research considered the problem of locating the optimal placement of controllers on a beam or plate and the problem of controlling general three-dimensional elastic models that incorporate nonlinear friction and contact laws on the boundary conditions. This final report summarizes those results. GRA

N88-24667 State Univ. of New York, Buffalo.
LOW AUTHORITY CONTROL OF LARGE SPACE STRUCTURES USING A CONSTRAINED THRESHOLD CONTROL FORMULATION Ph.D. Thesis
David C. Zimmerman [1987] 208 p
Avail: Univ. Microfilms Order No. DA8727761

A new active control strategy for the vibration control of large space structures is presented. In this Low Authority-Threshold Control (LATC) method, the total energy requirement of the active controller is minimized by use of a threshold control formulation and by determining the control which minimizes an appropriate cost functional. The minimization results in a piecewise constant feedback control law and is suited for a distributed processing architecture because the designer is free to choose the allowable feedback structure. LATC is developed for single- and multi-degree of freedom structural models. The necessary conditions which define the optimal control law are determined using variational methods. Closed form and quasi-closed form solutions are developed to aid in the determination of the optimal control. The effect of observer-induced errors on LATC are investigated. The robustness of the control method in light of modelling errors is addressed. Finally, LATC has been compared with and contrasted to other similar control methods. Dissert. Abstr.

N88-24668*# Draper (Charles Stark) Lab., Inc., Cambridge, Mass.
A FEEDBACK LINEARIZATION APPROACH TO SPACECRAFT CONTROL USING MOMENTUM EXCHANGE DEVICES Ph.D. Thesis
John Edward Dzielski Apr. 1988 219 p
(Contract NAS9-17560)
(NASA-CR-172057; NAS 1.26:172057; CSDL-T-977) Avail: NTIS HC A10/MF A01 CSCL 22B

Recent developments in the area of nonlinear control theory have shown how coordiante changes in the state and input spaces can be used with nonlinear feedback to transform certain nonlinear ordinary differential equations into equivalent linear equations. These feedback linearization techniques are applied to resolve two problems arising in the control of spacecraft equipped with control moment gyroscopes (CMGs). The first application involves the computation of rate commands for the gimbals that rotate the individual gyroscopes to produce commanded torques on the spacecraft. The second application is to the long-term management of stored momentum in the system of control moment gyroscopes using environmental torques acting on the vehicle. An approach to distributing control effort among a group of redundant actuators is described that uses feedback linearization techniques to parameterize sets of controls which influence a specified subsystem in a desired way. The approach is adapted for use in spacecraft control with double-gimballed gyroscopes to produce an algorithm that avoids problematic gimbal configurations by approximating sets of gimbal rates that drive CMG rotors into desirable configurations. The momentum management problem is stated as a trajectory optimization problem with a nonlinear dynamical constraint. Feedback linearization and collocation are used to transform this problem into an unconstrainted nonlinear program. The approach to trajectory optimization is fast and robust. A number of examples are presented showing applications to the proposed NASA space station. Author

N88-24669# Erno Raumfahrttechnik G.m.b.H., Bremen (West Germany).
SEARCH AND RESCUE SATELLITE SYSTEM (SERES), PHASE A0 Final Report
1988 116 p In GERMAN Prepared in cooperation with ANT Nachrichtentechnik, Backnang, Fed. Republic of Germany and Dornier-Werke GmbH, Friedrichshafen, Fed. Republic of Germany
(Contract BMFT-01-YY-043-3)
(ETN-88-92335) Avail: NTIS HC A06/MF A01

Phase A0 of the feasability study of the Search and Rescue satellite program is presented, with the objectives to be attained, the alternative design satellite concepts, and a comparison with the SERES-COSPAS/SARSAT System. Navigation aids for the SERES satellite in association with alternative localization systems using the Dornier system are described. ESA

N88-24670# European Space Agency. European Space Research and Technology Center, ESTEC, Noordwijk (Netherlands).
SIMULATIONS OF THE ELECTROSTATIC CHARGING OF ESA COMMUNICATIONS SATELLITES
E. J. Daly and W. R. Burke Dec. 1987 45 p
(ESA-STM-239; ISSN-0379-4067; ETN-88-92555) Avail: NTIS HC A03/MF A01

The NASA Charging Analyzer Program (NASCAP) was used to investigate the electrostatic charging of three-axis stabilized satellites in geostationary plasma environments. Capabilities and limitations are discussed and the use of NASCAP in anomaly investigations is described. Three-dimensional charging simulations were performed for eclipse and sunlight conditions, with various plasma environments. The importance of three-dimensional effects is demonstrated. Differential charging on the solar arrays during eclipse and immediately following eclipse are predicted to be significant. Charging is strongly dependent on exposed material parameter values, since these determine the magnitudes of the seven basic components of the current to a surface. The effects of changes in the properties of exposed materials on the charging of the satellite were investigated to identify ways of reducing the differential charging. The associated program MATCHG was also used to investigate material response to charging environments (including laboratory electron beams) at a more basic level, without consideration of the geometrical or photoemission effects. It proves a useful tool in aiding the interpretation and reconciliation of material testing results before a full NASCAP run is undertaken. ESA

N88-24671*# National Aeronautics and Space Administration. Lyndon B. Johnson Space Center, Houston, Tex.
HATCH COVER Patent Application
Charles Allton, inventor (to NASA) and James H. OKane, inventor (to NASA) 9 Mar. 1988 14 p
(NASA-Case-MSC-21356-1; NAS 1.71:MSC-21356-1; US-Patent-Appl-SN-165956) Avail: NTIS HC A03/MF A01 CSCL 22B

This invention relates to a hatch and more particularly to a hatch for a space vehicle where the hatch has a low volume sweep and can be easily manipulated from either side of the hatch. The hatch system includes an elliptical opening in a bulkhead and an elliptical hatch member. The hatch cover system includes an elliptical port opening in a housing and an elliptical cover member supported centrally by a rotational bearing for rotation about a rotational axis normal to the cover member and by pivot pins in a gimbal member for pivotal movement about axes perpendicular to the rotational axis. Arm members support the gimbal member pivotally by pivot members so that upon rotation and manipulation the cover member can be articulatedly moved

from a closed position to the port opening to an out of the way position with a minimum of volume sweep by the cover member.
NASA

N88-24672*# National Aeronautics and Space Administration. Marshall Space Flight Center, Huntsville, Ala.
STRUCTURAL MARGINS ASSESSMENT APPROACH
Robert S. Ryan Jun. 1988 56 p
(NASA-TM-100332; NAS 1.15:100332) Avail: NTIS HC A04/MF A01 CSCL 22B

A general approach to the structural design and verification used to determine the structural margins of the space vehicle elements under Marshall Space Flight Center (MSFC) management is described. The Space Shuttle results and organization will be used as illustrations for techniques discussed. Given also are: (1) the system analyses performed or to be performed by, and (2) element analyses performed by MSFC and its contractors. Analysis approaches and their verification will be addressed. The Shuttle procedures are general in nature and apply to other than Shuttle space vehicles. Author

N88-24673# Tokyo Univ. (Japan). Inst. of Space and Astronautical Science.
DYNAMICS OF A FLEXIBLE ORBITING PLATFORM WITH MRMS
Yasuhiro Morita and Vinod J. Modi (British Columbia Univ., Vancouver.) Feb. 1988 79 p
(ISSN-0285-6808; ISAS-RN-625) Avail: NTIS HC A05/MF A01

A relatively general formulation for studying dynamics of a flexible Mobile Remote Manipulator System (MRMS), supported by an orbiting flexible platform, is developed using the Lagrangian approach with generalized forces accounting for the environmental effects, damping, and control. The flexible members are treated as continuum and their flexural deformations represented by a series of admissible functions. The highly nonlinear, nonautonomous and coupled equations of motion, being not amenable to any known closed-form solution, are solved numerically. The computational algorithm is so structured as to isolate the effects of various system parameters thus helping in assessment of their relative importance. Effectiveness of the general formulation is illustrated by studying complex interactions between vibrational and librational degrees of freedom in the presence of MRMS maneuver over a range of system parameters and initial conditions. Results suggest that the MRMS maneuver can affect librational and vibrational response substantially and under critical combinations of parameters the system can become unstable. The information is fundamental to the design of a control strategy which, for a flexible system in the presence of generalized forces, has received virtually no attention. Author

N88-24674 North Carolina State Univ., Raleigh.
AUTOMATIC FEEDBACK CONTROL OF A RIGID BODY FOR FINITE DISPLACEMENTS Ph.D. Thesis
Sunil Shrikrishna Kulkarni 1987 93 p
Avail: Univ. Microfilms Order No. DA8800119

A control law for a suspended rigid body with a fixed support is described for large angular displacements. This control law is a function of angular velocities and quaternions, also known as Euler's parameters. Several missions forseen for the next generation of spacecraft require rapid large angle maneuvers followed by extremely accurate attitude acquisition upon completion of each maneuver. The control law is also useful for attitude control for space stations. This control law is also useful for suppressing swinging of translating rapid body with two degrees of freedom. The examples of objects which swing during transport range from a crane unloading cargo from a ship to manipulators handling artillery shells to a robot performing pick and place operations. In general, it is required to attenuate or suppress this swinging during all phases of the transport. Numerical simulations of this automatic feedback control system are made for a rigid body on Earth's surface and in orbit. It is shown that control algorithm is simple to implement and system stability is extremely robust with respect to external disturbances and inertial variations. Mass and inertial variation is eight to one. Dissert. Abstr.

N88-25391*# Science and Engineering Associates, Inc., Englewood, Colo.
NEUTRAL ENVIRONMENT FOR SPACE STATION
R. O. Rantanen *In* NASA, Langley Research Center, A Study of Space Space Station Contamination Effects May 1988 p 1-9 (For primary document see N88-25390 18-88)
Avail: NTIS HC A07/MF A01 CSCL 22B

N88-25392*# National Aeronautics and Space Administration. Lyndon B. Johnson Space Center, Houston, Tex.
SPACE STATION NEUTRAL EXTERNAL ENVIRONMENT
H. Ehlers and L. Leger *In* NASA, Langley Research Center, A Study of Space Station Contamination Effects May 1988 p 11-17 (For primary document see N88-25390 18-88)
Avail: NTIS HC A07/MF A01 CSCL 22B

N88-25393*# Iowa Univ., Iowa City. Dept. of Physics and Astronomy.
CONTAMINANT IONS AND WAVES IN THE SPACE STATION ENVIRONMENT
G. B. Murphy *In* NASA, Langley Research Center, A Study of Space Space Station Contamination Effects May 1988 p 19-29 (For primary document see N88-25390 18-88)
Avail: NTIS HC A07/MF A01 CSCL 22B

N88-25395*# Alabama Univ., Huntsville. Center for Space Plasma and Aeronomic Research.
SPACE STATION CONTAMINATION STUDY: ASSESSMENT OF CONTAMINANT SPECTRAL BRIGHTNESS
D. G. Torr *In* NASA, Langley Research Center, A Study of Space Station Contamination Effects May 1988 p 43-59 (For primary document see N88-25390 18-88)
Avail: NTIS HC A07/MF A01 CSCL 22B

N88-25396*# Physical Sciences, Inc., Andover, Mass.
CALCULATION OF SPACE STATION INFRARED IRRADIANCE FROM ATMOSPHERE-INDUCED EMISSIONS
M. E. Fraser, A. Gelb, B. D. Green, and D. G. Torr (Alabama Univ., Huntsville.) *In* NASA, Langley Research Center, A Study of Space Station Contamination Effects May 1988 p 61-69 (For primary document see N88-25390 18-88)
(Grant NAGw-922)
Avail: NTIS HC A07/MF A01 CSCL 22B

N88-25397*# National Aeronautics and Space Administration. Marshall Space Flight Center, Huntsville, Ala.
SPACE STATION PARTICULATE CONTAMINATION ENVIRONMENT
E. R. Miller and K. S. Clifton *In* NASA, Langley Research Center, A Study of Space Station Contamination Effects May 1988 p 71-77 (For primary document see N88-25390 18-88)
Avail: NTIS HC A07/MF A01 CSCL 22B

N88-25398*# Physical Sciences, Inc., Andover, Mass.
THE PARTICULATE ENVIRONMENT SURROUNDING THE SPACE STATION: ESTIMATES FROM THE PACS DATA
Byron David Green *In* NASA, Langley Research Center, A Study of Space Station Contamination Effects May 1988 p 79-90 (For primary document see N88-25390 18-88)
Avail: NTIS HC A07/MF A01 CSCL 22B

N88-25399*# Science and Engineering Associates, Inc., Englewood, Colo.
EFFECTS OF METEOROIDS AND SPACE DEBRIS ON THE PARTICULATE ENVIRONMENT FOR SPACE STATION
W. R. Seebaugh *In* NASA, Langley Research Center, A Study of Space Station Contamination Effects May 1988 p 91-99 (For primary document see N88-25390 18-88)
Avail: NTIS HC A07/MF A01 CSCL 22B

N88-25400*# Aerospace Corp., Los Angeles, Calif. Chemistry and Physics Lab.
CONTAMINATION OF OPTICAL SURFACES
Graham S. Arnold and David F. Hall *In* NASA, Langley Research Center, A Study of Space Station Contamination Effects May 1988 p 101-108 (For primary document see N88-25390 18-88)
Avail: NTIS HC A07/MF A01 CSCL 22B

N88-25401*# Washington State Univ., Pullman. Dept. of Physics.
SURFACE INTERACTIONS RELEVANT TO SPACE STATION CONTAMINATION PROBLEMS
J. T. Dickinson *In* NASA, Langley Research Center, A Study of Space Station Contamination Effects May 1988 p 109-121 (For primary document see N88-25390 18-88)
(Grant NSF DMR-86-01281)
Avail: NTIS HC A07/MF A01 CSCL 22B

N88-25402*# Physical Sciences, Inc., Andover, Mass.
LABORATORY EXPERIMENTS OF RELEVANCE TO THE SPACE STATION ENVIRONMENT
G. E. Caledonia *In* NASA, Langley Research Center, A Study of Space Station Contamination Effects May 1988 p 123-130 (For primary document see N88-25390 18-88)
Avail: NTIS HC A07/MF A01 CSCL 22B

N88-25403*# Naval Research Lab., Washington, D.C. Geophysical and Plasma Dynamics Branch.
CONTAMINATION OF THE SPACE STATION ENVIRONMENT BY VENTED CHEMICALS
Paul A. Bernhardt *In* NASA, Langley Research Center, A Study of Space Station Contamination Effects May 1988 p 131-140 (For primary document see N88-25390 18-88)
Avail: NTIS HC A07/MF A01 CSCL 22B

19 SPACECRAFT INSTRUMENTATION

For related information see also *06 Aircraft Instrumentation* and *35 Instrumentation and Photography.*

No abstracts in this category.

20 SPACECRAFT PROPULSION AND POWER

Includes main propulsion systems and components, e.g., rocket engines; and spacecraft auxiliary power sources.

For related information see also *07 Aircraft Propulsion and Power, 28 Propellants and Fuels, 44 Energy Production and Conversion,* and *15 Launch Vehicles and Space Vehicles.*

N88-24675*# Scientific Research Associates, Inc., Glastonbury, Conn.
SOLID ROCKET MOTOR AFT FIELD JOINT FLOW FIELD ANALYSIS Final Technical Report
Jayant S. Sabnis, Edward J. Gibeling, and Henry McDonald Sep. 1987 37 p
(Contract NAS8-36185)
(NASA-CR-179288; NAS 1.26:179288; R87-900063-F) Avail: NTIS HC A03/MF A01 CSCL 21H

An efficient Navier-Stokes analysis was successfully applied to simulate the complex flow field in the vicinity of a slot in a solid rocket motor with segment joints. The capability of the computer code to resolve the flow near solid surfaces without using a wall function assumption was demonstrated. In view of the complex nature of the flow field in the vicinity of the slot, this approach is considered essential. The results obtained from these calculations provide valuable design information, which would otherwise be extremely difficult to obtain. The results of the axisymmetric calculations indicate the presence of a region of reversed axial flow at the aft-edge of the slot and show the over-pressure in the slot to be only about 10 psi. The results of the asymmetric calculations indicate that a pressure asymmetry more than two diameters downstream of the slot has no noticeable effect on the flow field in the slot. They also indicate that the circumferential pressure differential caused in the slot due to failure of a 15 deg section of the castable inhibitor will be approximately 1 psi.
Author

N88-24676*# Remtech, Inc., Huntsville, Ala.
RESEARCH STUDY: SPACE SHUTTLE MAIN ENGINE PLUME FLOWFIELD MODEL Final Report, 20 Nov. 1981 - 1 Apr. 1988
Robert L. Bender 1 Apr. 1988 23 p
(Contract NAS8-34135)
(NASA-CR-179336; NAS 1.26:179336; RTR-056-07) Avail: NTIS HC A03/MF A01 CSCL 21H

The initial research effort was an in-depth analysis of the shuttle main engine plumes in an effort to improve the flowfield model and to enhance shuttle base heating equipment predictions during ascent. A prediction methodology code was developed incorporating the improved plume model into a predictive tool which could consider different trajectoreis and engine perfromance variables. Various plume flow model improvement studies were ongoing at the time of the 51-L accident. Since that time, base heating and plume methodology improvements have continued as part of the overall emphasis on Shuttle design assurance before resuming flight schedule.
Author

N88-24677# Jet Propulsion Lab., California Inst. of Tech., Pasadena.
PERFORMANCE AND LONG DURATION TEST OF A 30 KW THERMAL ARCJET ENGINE Final Report, 28 Dec. 1984 - 30 Nov. 1986
T. J. Pivirotto, D. Q. King, J. R. Brophy, and W. D. Deininger Nov. 1987 99 p
(AF Proj. 3058)
(AD-A190962; JPL-D-4643; AFAL-TR-87-010) Avail: NTIS HC A05/MF A01 CSCL 21C

The objective of this effort was to evaluate the lifetime and performance of a 30-kWe constricted arc ammonia arcjet. This engine was based on a design developed by Avco Corporation in 1963 that delivered 978 seconds of specific impulse with ammonia during a 50-hour test. After 573 hours of operation, a short circuit between the cathode and anode of JPL's thruster forced the life test to end. Throughout the 573-hour test, the thruster operated at 24.9 kWe, delivering 2.29 N (0.15 lbs) of thrust, 865 seconds of specific impulse, and 37% efficiency. Although the lifetime of JPL's thruster fell short of AFAL's original 1500-hour goal for the effort, the arcjet demonstrated a duration of over eleven times the lifetime of the 1963 Avco arcjet. Further, the demonstrated lifetime of 576 hours is adequate for many orbit raising missions.
GRA

N88-24678# Naval Postgraduate School, Monterey, Calif.
TVC (THRUST VECTOR CONTROL) JET VANE THERMAL MODELING USING PARAMETRIC SYSTEM IDENTIFICATION
Robert H. Nunn 18 Mar. 1988 63 p
(AD-A191518; AD-E500953; NPS69-88-001) Avail: NTIS HC A04/MF A01 CSCL 21H

Parametric system identification procedures, using the software package MATRIXx, are applied to the problem of simulating the thermal response of a TVC jet vane. The jet vane is discretized into thermal lumps and energy balances are written to develop the governing mathematical relationships. Boundary layer convection and stagnation point heating are considered as thermal inputs, and the associated resistances are estimated. System identification is used to determine the appropriate values for the convective resistances and the vane mount thermal sink. The identified model, which is linear time-variant, closely predicts the thermal response of the jet vane shaft, surface and tip.
GRA

N88-24679# GT-Devices, Alexandria, Va.
PERFORMANCE OF A HYDROGEN PULSED ELECTROTHERMAL THRUSTER. STRATEGIC DEFENSE INITIATIVE ORGANIZATION INNOVATIVE SCIENCE AND TECHNOLOGY. SBIR, PHASE 1 Final Report, 12 Jan. - 12 Jul. 1987
Rodney L. Burton, Shyke A. Goldstein, and Shih-Ying Wang 28 Sep. 1987 47 p
(Contract F49620-87-C-0028)
(AD-A191999; AFOSR-88-0196TR) Avail: NTIS HC A03/MF A01 CSCL 21C

This report describes effort to determine the technical feasibility of measuring the performance of a pulsed electrothermal thruster on liquid hydrogen propellant. The design of a 5 kW thruster is presented, including the capacitive pulse forming network, arc discharge characteristics, nozzle performance and predicted specific impulse and thrust. A thermal model is discussed which treats and solves the problem of liquid hydrogen. It is concluded that a Phase 2 test should concentrate on water and/or hydrazine, and liquid hydrogen testing should be postponed to Phase 3. GRA

N88-24680# Aerospace Corp., El Segundo, Calif. Materials Sciences Lab.
THERMOGRAPHIC DETECTION OF BURIED DEBONDS
Mary T. Quinn, John R. Hribar, Raymond L. Ruiz, and Gary F. Hawkins 1 Mar. 1988 21 p
(Contract F04701-85-C-0086)
(AD-A192115; TR-0086A(2935-08)-1; SD-TR-88-35) Avail: NTIS HC A03/MF A01 CSCL 17E

This study was done to improve the reliability of solid rocket motors by testing infrared video imaging for detecting adhesive bonding flaws. The flaws, buried beneath 0.3 in. of steel and 0.2 in. of rubber in these motors, have been difficult to detect by conventional pulse-echo ultrasonic techniques. Ultrasonic inspection has been ineffective because of the large acoustical impedance mismatched at the steel-rubber interface. To detect buried flaws in spite of the impedance mismatch, infrared video imaging was investigated. GRA

N88-24681# Edgerton, Germeshausen and Grier, Inc., Idaho Falls, Idaho.
ADVANCED NUCLEAR ROCKET ENGINE MISSION ANALYSIS
J. Ramsthaler, G. Farbman, T. Sulmeisters, D. Buden, and P. Harris (Rockwell International Corp., Canoga Park, Calif.) Dec. 1987 11 p Presented at the JANNAF Propulsion Conference, San Diego, Calif., 15 Dec. 1987
(Contract DE-AC07-76ID-01570)
(DE88-006797; EGG-M-41087; CONF-871274-1) Avail: NTIS HC A03

The use of a derivative of the NERVA engine developed from 1955 to 1973 was evluated for potential application to Air Force orbital transfer and maneuvering missions in the time period 1995 to 2020. The NERVA stge was found to have lower Life Cycle Costs (LCC) than an advanced chemical stage for performing Low Earth Orbit (LEO) to geosynchronous orbit (GEO) missions at any level of activity greater than three missions per year. It had lower life cycle costs than a high performance nuclear electric engine at any level of LEO to GEO mission activity. An examination of all unmanned orbital transfer and maneuvering missions from the Space Transportation Architecture Study (STAS 111-3) indicated a LCC advantage for the NERVA stage over the advanced chemical stage of fifteen million dollars. The cost advance accured from both the orbital transfer and maneuvering missions. Parametric analyses showed that the specific impulse of the NERVA stage and the cost of delivering material to low earth orbit were the most significant factors in the LCC advantage over the chemical stage. Lower development costs and a higher thrust gave the NERVA engine an LCC advantage over the nuclear electric stage. DOE

N88-24682*# National Aeronautics and Space Administration. Lewis Research Center, Cleveland, Ohio.
EVALUATION OF THE COMMUNICATIONS IMPACT OF A LOW POWER ARCJET THRUSTER
Lynnette M. Carney 1988 26 p Presented at the 24th Joint Propulsion Conference, Boston, Mass., 11-13 Jul. 1988; sponsored by AIAA, ASME, SAE and ASEE
(NASA-TM-100926; E-4179; NAS 1.15:100926; AIAA-88-3105)
Avail: NTIS HC A03/MF A01 CSCL 21H

The interaction of a 1 kW arcjet thruster plume with a communications signal is evaluated. A two-parameter, source flow equation has been used to represent the far flow field distribution of the arcjet plume in a realistic spacecraft configuration. Modelling the plume as a plasma slab, the interaction of the plume with a 4 GHz communications signal is then evaluated in terms of signal attenuation and phase shift between transmitting and receiving antennas. Except for propagation paths which pass very near the arcjet source, the impacts to transmission appear to be negligible. The dominant signal loss mechanism is refraction of the beam rather than absorption losses due to collisions. However, significant reflection of the signal at the sharp vacuum-plasma boundary may also occur for propagation paths which pass near the source. Author

N88-24683# Technische Univ., Berlin (West Germany). Inst. fuer Luft- und Raumfahrt.
POSSIBILITIES AND LIMITS FOR USE OF LASER PROPULSION SYSTEMS IN INTERORBITAL SPACE FLIGHT [MOEGLICHKEITEN UND GRENZEN DES EINSATZES VON LASER-ANTRIEBEN BEI INTERORBITALEN RAUMFAEHREN]
Andreas Lindenthal 20 Aug. 1987 109 p In GERMAN
(ILR-Mitt-185; ETN-88-91933) Avail: NTIS HC A06/MF A01

State of the art of laser propulsion and developments for the year 2000 are presented. Market simulation gives a guideline for identification and quantification of geostationary space power systems. System analysis concerning space flights and laser space stations in association with operating and economic factors is used for the evaluation of propulsion alternatives. Sensitivity analysis performed for the whole system shows the effects of construction modifications on the state of development of the laser. ESA

N88-24684*# National Aeronautics and Space Administration. Lyndon B. Johnson Space Center, Houston, Tex.
NOZZLE FABRICATION TECHNIQUE Patent Application
Dennis L. Wells, inventor (to NASA) 1 Apr. 1988 18 p
(NASA-Case-MSC-21299-1; NAS 1.71:MSC-21299-1; US-Patent-Appl-SN-176587) Avail: NTIS HC A03/MF A01 CSCL 21H

This invention relates to techniques for fabricating hour glass throat or convergent divergent nozzle shapes, and more particularly to new and improved techniques for forming rocket nozzles from electrically conductive material and forming cooling channels in the wall thereof. The concept of positioning a block of electrically conductive material so that its axis is set at a predetermined skew angle with relation to a travelling electron discharge machine electrode and thereafter revolving the body about its own axis to generate a hyperbolic surface of revolution, either internal or external is novel. The method will generate a rocket nozzle which may be provided with cooling channels using the same control and positioning system. The configuration of the cooling channels so produced are unique and novel. Also the method is adaptable to nonmetallic material using analogous cutting tools, such as, water jet, laser, abrasive wire and hot wire. NASA

N88-24685*# National Aeronautics and Space Administration. Langley Research Center, Hampton, Va.
DUAL-FUEL, DUAL-MODE ROCKET ENGINE Patent Application
James A. Martin, inventor (to NASA) 9 Mar. 1988 14 p
(NASA-Case-LAR-13773-1; NAS 1.71:LAR-13773-1; US-Patent-Appl-SN-165946) Avail: NTIS HC A03/MF A01 CSCL 21H

The invention relates to a dual fuel, dual mode rocket engine

designed to improve the performance of earth-to-orbit vehicles. For any vehicle that operates from the earth's surface to earth orbit, it is advantageous to use two different fuels during its ascent. A high density impulse fuel, such as kerosene, is most efficient during the first half of the trajectory. A high specific impulse fuel, such as hydrogen, is most efficient during the second half of the trajectory. The invention allows both fuels to be used with a single rocket engine. It does so by adding a minimum number of state-of-the-art components to baseline single made rocket engines, and is therefore relatively easy to develop for near term applications. The novelty of this invention resides in the mixing of fuels before exhaust nozzle cooling. This allows all of the engine fuel to cool the exhaust nozzle, and allows the ratio of fuels used throughout the flight depend solely on performance requirements, not cooling requirements. NASA

N88-24686*# National Aeronautics and Space Administration. Lewis Research Center, Cleveland, Ohio.

THERMODYNAMIC MODELING OF THE NO-VENT FILL METHODOLOGY FOR TRANSFERRING CRYOGENS IN LOW GRAVITY

David J. Chato [1988] 10 p Prepared for presentation at the 24th Joint Propulsion Conference, Boston, Mass., 11-13 Jul. 1988; sponsored in part by AIAA, ASME, SAE, and ASEE
(NASA-TM-100932; E-4206; NAS 1.15:100932; AIAA-88-3403)
Avail: NTIS HC A02/MF A01 CSCL 21H

The filling of tanks with cryogens in the low-gravity environment of space poses many technical challenges. Chief among these is the inability to vent only vapor from the tank as the filling proceeds. As a potential solution to this problem, the NASA Lewis Research Center is researching a technique known as No-Vent Fill. This technology potentially has broad application. The focus is the fueling of space based Orbital Transfer Vehicles. The fundamental thermodynamics of the No-Vent Fill process to develop an analytical model of No-Vent Fill is described. The model is then used to conduct a parametric investigation of the key parameters: initial tank wall temperature, liquid-vapor interface heat transfer rate, liquid inflow rate, and inflowing liquid temperatures. Liquid inflowing temperature and the liquid-vapor interface heat transfer rate seem to be the most significant since they influence the entire fill process. The initial tank wall temperature must be sufficiently low to prevent a rapid pressure rise during the initial liquid flashing stage, but then becomes less significant. Author

N88-24687*# National Aeronautics and Space Administration. Lewis Research Center, Cleveland, Ohio.

AN EXTENDED LIFE AND PERFORMANCE TEST OF A LOW-POWER ARCJET

Francis M. Curran and Thomas W. Haag [1988] 23 p Presented at the 24th Joint Propulsion Conference, Boston, Mass., 11-13 Jul. 1988; sponsored by AIAA, ASME, SAE and ASEE
(NASA-TM-100942; E-4230; NAS 1.15:100942; AIAA-88-3106)
Avail: NTIS HC A03/MF A01 CSCL 21C

An automated, cyclic life test was performed to demonstrate the reliability and endurance of a low power dc cycle arcjet thruster. Over 1000 hr and 500 on-off cycles were accumulated which would represent the requirements for about 15 years of on-orbit lifetime. A hydrogen/nitrogen propellant mixture was used to simulate decomposed hydrazine propellant and the power level was nominally 1.2 kW after the burn-in period. The arcjet operated in a very repeatable fashion from cycle to cycle. The steady state voltage increased by approximately 6 V over the first 300 hr, and then by only 3 V through the remainder of the test. Thrust measurements taken before, during, and after the test verified that the thruster performed in a consistent fashion throughout the tests at a specific impulse of 450 to 460 sec. Post-test component evaluation revealed limited erosion on both the anode and cathode. Other thruster components, including graphite seals, appeared undamaged. Author

N88-24688*# National Aeronautics and Space Administration. Lewis Research Center, Cleveland, Ohio.

INTERNAL EROSION RATES OF A 10-kW XENON ION THRUSTER

Vincent K. Rawlin [1988] 30 p Presented at the 24th Joint Propulsion Conference, Boston, Mass., 11-23 Jul. 1988; sponsored in part by AIAA, ASME, SAE, and ASEE
(NASA-TM-100954; E-4228; NAS 1.15:100954; AIAA-88-2912)
Avail: NTIS HC A03/MF A01 CSCL 21C

A 30 cm diameter divergent magnetic field ion thruster, developed for mercury operation at 2.7 kW, was modified and operated with xenon propellant at a power level of 10 kW for 567 h to evaluate thruster performance and lifetime. The major differences between this thruster and its baseline configuration were elimination of the three mercury vaporizers, use of a main discharge cathode with a larger orifice, reduction in discharge baffle diameter, and use of an ion accelerating system with larger acceleration grid holes. Grid thickness measurement uncertainties, combined with estimates of the effects of reactive residual facility background gases gave a minimum screen grid lifetime of 7000 h. Discharge cathode orifice erosion rates were measured with three different cathodes with different initial orifice diameters. Three potential problems were identified during the wear test: the upstream side of the discharge baffle eroded at an unacceptable rate; two of the main cathode tubes experienced oxidation, deformation, and failure; and the accelerator grid impingement current was more than an order of magnitude higher than that of the baseline mercury thruster. The charge exchange ion erosion was not quantified in this test. There were no measurable changes in the accelerator grid thickness or the accelerator grid hole diameters. Author

N88-24689*# National Aeronautics and Space Administration. Lewis Research Center, Cleveland, Ohio.

CATALYTIC IGNITION OF HYDROGEN AND OXYGEN PROPELLANTS

Robert L. Zurawski and James M. Green (Sverdrup Technology, Inc., Arnold Air Force Station, Tenn.) [1988] 20 p Presented at the 24th Joint Propulsion Conference, Boston, Mass., 11-13 Jul. 1988; sponsored in part by AIAA, ASME, SAE, and ASEE
(NASA-TM-100957; E-4104; NAS 1.15:100957; AIAA-88-3300)
Avail: NTIS HC A03/MF A01 CSCL 21B

An experimental program was conducted to evaluate the catalytic ignition of gaseous hydrogen and oxygen propellants. Shell 405 granular catalyst and a monolithic sponge catalyst were tested. Mixture ratio, mass flow rate, propellant temperature, and back pressure were varied parametrically in testing to determine the operational limits of the catalytic igniter. The test results show that the gaseous hydrogen and oxygen propellant combination can be ignited catalytically using Shell 405 catalyst over a wide range of mixture ratios, mass flow rates, and propellant injection temperatures. These operating conditions must be optimized to ensure reliable ignition for an extended period of time. A cyclic life of nearly 2000, 2 sec pulses at nominal operating conditions was demonstrated with the catalytic igniter. The results of the experimental program and the established operational limits for a catalytic igniter using the Shell 405 catalyst are presented.
Author

N88-24690*# National Aeronautics and Space Administration. Lewis Research Center, Cleveland, Ohio.

THRUST CHAMBER THERMAL BARRIER COATING TECHNIQUES

Richard J. Quentmeyer [1988] 19 p Prepared for presentation at the 72nd Specialists' Meeting of the Propulsion and Energetics Panel, Bath, England, 3-5 Oct. 1988; sponsored by AGARD
(NASA-TM-100933; E-4204; NAS 1.15:100933) Avail: NTIS HC A03/MF A01 CSCL 21H

Methods for applying thermal barrier coatings to the hot-gas side wall of rocket thrust chambers in order to significantly reduce the heat transfer in high heat flux regions was the focus of technology efforts for many years. This paper describes a successful technique developed by the Lewis Research Center

that starts with the coating of a mandrel and then builds the thrust chamber around it by electroforming appropriate materials. This results in a smooth coating with exceptional adherence, demonstrated in hot fire rig tests. The low cycle fatigue life of chambers with coatings applied in this manner was increased dramatically compared to uncoated chambers. Author

23 CHEMISTRY AND MATERIALS (GENERAL)

N88-24691# Colorado Univ., Boulder. Dept. of Chemistry and Biochemistry.
TOPOLOGICAL STEREOCHEMISTRY Final Report, 1 Feb. 1985 - 31 Jan. 1988
David M. Walba 29 Jan. 1988 8 p
(Contract N00014-85-K-0228)
(AD-A191867) Avail: NTIS HC A02/MF A01 CSCL 11F

Results of research on two novel problems in organic stereochemistry are described: (1) topological stereochemistry; and (2) design and synthesis of novel organic optoelectronic materials. In the topological stereochemistry project, new methods for understanding the symmetries of topologically complex molecular structures were developed, and the total synthesis of several such structures was achieved. New strategies for the synthesis of the first molecular knotted ring, a long sought but still illusive target, have been tested and are under development. In the optoelectronic materials project, work has focussed on design and synthesis of new ferroelectric liquid crystals (FLCs), a novel class of fluid materials possessing polar symmetry. Such materials have important potential utility in flat panel video and devices for optical computing. A predictive model for the molecular origins of the ferroelectric polarization in FLCs has been developed and demonstrated, and several new FLC classes have been invented. Also, the model is being applied to design of the first liquid phases with high second order hyperpolarizability for ultra fast electro-optic applications. GRA

N88-24692* National Aeronautics and Space Administration. Ames Research Center, Moffett Field, Calif.
AROMATIC CYCLOTRIPHOSPHAZENES Patent
Devendra Kamar, inventor (to NASA) (National Academy of Sciences - National Research Council, Washington, D. C.), George M. Fohlen, inventor (to NASA), and John A. Parker, inventor (to NASA) 31 May 1988 20 p Filed 29 Oct. 1986 Division of US-Patent-Appl-SN-760374, Jul. 30, 1985, US-Patent-4,634,759, which is a division of US-Patent-Appl-SN-599126, Apr. 11, 1984, US-Patent-4,550,177
(NASA-Case-ARC-11428-3; US-Patent-4,748,263; US-Patent-Appl-SN-924467; US-Patent-Class-558-80; US-Patent-Class-564-13; US-Patent-Appl-SN-760374; US-Patent-4,634,759; US-Patent-Appl-SN-599126; US-Patent-4,550,177) Avail: US Patent and Trademark Office CSCL 07A

Four-Aminophenoxy cyclotriphosphazenes are reacted with maleic anhydride to produce maleamic acids which are converted to the maleimides. The maleimides are polymerized. By selection of starting materials (e.g., hexakis amino or trisaminophenoxy trisphenoxy cyclotrisphosphazenes), selection of molar porportions of reactants, use of mixtures of anhydrides and use of dianhydrides as bridging groups a variety of maleimides and polymers are produced. The polymers have high limiting oxygen indices, high char yields and other useful heat and fire resistant properties making them useful as, for example, impregnants of fabrics.
Official Gazette of the U.S. Patent and Trademark Office

24 COMPOSITE MATERIALS

Includes physical, chemical, and mechanical properties of laminates and other composite materials.
For ceramic materials see *27 Nonmetallic Materials*.

N88-24693# American Society for Composites, Dayton, Ohio.
PROCEEDINGS OF THE AMERICAN SOCIETY FOR COMPOSITES Final Report
1987 111 p Proceedings of the Biotechnology Aided Synthesis of Aerospace Composite Resins Symposium Workshop, Dayton, Ohio, 25-26 Aug. 1987
(Grant AF-AFOSR-0245-87)
(AD-A189861; AFOSR-87-1884TR) Avail: NTIS HC A06/MF A01 CSCL 11D

Topics addressed include: biotechnology; carbon matrix composites; aerospace organic matrix resin; current and future needs; synthetic chemistry; hydrocarbon bioconversion technology; and combination of biochemical and chemical concepts to produce polyphenylene. For individual titles, see N88-24694 through N88-24699.

N88-24694# Air Force Wright Aeronautical Labs., Wright-Patterson AFB, Ohio.
CARBON MATRIX COMPOSITES PROSPECTIVE ROLES FOR BIOTECHNOLOGY
L. Scott Theibert and Don L. Schmidt (Schmidt, Don L., Beavercreek, Ohio) *In* American Society for Composites, Proceedings of the American Society for Composites 1987 p 3-26 (For primary document see N88-24693 18-24)
Avail: NTIS HC A06/MF A01 CSCL 11D

Carbon matrix composites (CMC) are composed of a carbonaceous binder, a reinforcing fiber, and sometimes a filler. The CMCs are manufactured by the controlled pyrolysis of organic constituents to yield composites with extraordinary properties. The role of carbon matrices in CMC is discussed, including their functions, methods of formation, and properties. Matrix precursors based on thermosetting resins and thermoplastic pitches, and their influence on the generated carbon structures is also described. Some highly speculative roles for biotechnology are also discussed to stimulate original thinking in the interdisciplinary materials field. Author

N88-24695# Air Force Wright Aeronautical Labs., Wright-Patterson AFB, Ohio.
CURRENT AND FUTURE MOLECULAR STRUCTURES OF AEROSPACE ORGANIC MATRIX RESINS Abstract Only
Fred E. Arnold *In* American Society for Composites, Proceedings of the American Society for Composites 1987 p 27 (For primary document see N88-24693 18-24)
Avail: NTIS HC A06/MF A01 CSCL 11D

Research in both industrial and governmental laboratories has provided a variety of thermally stable polymers. During the last decade the primary effort was in the development of cure chemistry to provide matrix resins with improved moisture resistance, thermal and thermooxidative stability, and toughness. Material concepts also played an important role instructurally tailoring macromolecules for advanced future aerospace system. Both thermoset and high molecular weight polymer systems which are of considerable interest to the Air Force are examined. Synthetic aspects to thermoset endcapping agents will be discussed as well as monomers required in the ordered polymer technologies. Paramount to the success of a polymer technology is low cost organic intermediates which are required for a successful transition to the commercial market place. It is anticipated that biotechnology could play an important role in the low cost manufacturing of these materials. Author

N88-24696# Shell Development Co., Houston, Tex.
INDUSTRIAL PERSPECTIVE ON CURRENT AND FUTURE NEEDS IN AEROSPACE MATRIX RESIN CHEMISTRY
Ronald S. Bauer *In* American Society for Composites, Proceedings of the American Society for Composites 1987

p 28-42 (For primary document see N88-24693 18-24)
Avail: NTIS HC A06/MF A01 CSCL 11D

The chemistry of the state-of-the-art and emerging aircraft/aerospace matrix resin systems are reviewed. Areas will be identified where biotechnology assisted chemical synthesis can be applied to commercial high performance composite matrix resins. Author

N88-24697# SRI International Corp., Menlo Park, Calif. Bio-Organic Chemistry Lab.
APPLICATIONS OF BIOTECHNOLOGY TO SYNTHETIC CHEMISTRY FOR AEROSPACE MATRIX RESINS DEVELOPMENT
Masato Tanabe *In* American Society for Composites, Proceedings of the American Society for Composites 1987 p 43-47 (For primary document see N88-24693 18-24)
Avail: NTIS HC A06/MF A01 CSCL 11D

The focus of this presentation is on the potential use of the enzymes from primary or secondary metabolism that are either constitutive or induced enzyme systems available from mammalian, microbial, or plant sources. Several areas are examined including: material cost reduction through biosynthesis; materials not otherwise obtainable; learning the mechanism of a biophenomenon (biosynthesis) and mimicing the process in the non-biological system; and what is feasible today and tomorrow. B.G.

N88-24698# Bio-Technical Resources, Inc., Manitowoc, Wisc.
THE APPLICATION OF HYDROCARBON BIOCONVERSION TECHNOLOGY TO AEROSPACE MATERIALS PRODUCTION
Ronald J. Huss and Paul E. Swanson *In* American Society for Composites, Proceedings of the American Society for Composites 1987 p 48-52 (For primary document see N88-24693 18-24)
Avail: NTIS HC A06/MF A01 CSCL 11D

Bio-Technical Resources, Inc. (BTR) is a 25 year old, privately held biotechnology company with its origin in the malting and brewing industries. The primary business has evolved into product and process development for the fermentation, pharmaceutical, chemical, and food industries. Past experience, current research programs, and future expectations in the area of hydrocarbon bioconversions are highlighted. B.G.

N88-24699# Imperial Chemical Industries Ltd., Runcorn (England).
THE SYNTHESIS OF POLYPHENYLENE FROM A CIS-DIHYDROCATECHOL BIOLOGICALLY PRODUCED MONOMER **c27**
D. G. H. Ballard, A. Courtis, I. M. Shirley, and S. C. Taylor (ICI Biological Products Business, Billingham, England) *In* American Society for Composites, Proceedings of the American Society for Composites 1987 p 53-94 (For primary document see N88-24693 18-24)
Avail: NTIS HC A06/MF A01 CSCL 11B

Benzene is oxidized by oxygen utilizing the dioxygenase enzyme contained in the microorganism Pseudomonas Putida. Genetic manipulation produced a variant which gave exclusively the initial oxidation product of cis-dihydrocatechol in practical quantities. Derivatives of the latter, in particular the methyl carbonate can be obtained pure and are very stable. The derivatives polymerize in the absence of solvent with radical initiators to give a polymer. The latter is soluable and readily forms coherent coatings and films. On heating methanol and CO2 are expelled and polyphenylene chloride is formed as a coating or film. The aromatization process is catalyzed by bases and can occur well below the glass transition temperature of the precursor polymer of 192 C. The aromatization can occur under homogeneous conditions in the basic solvent N-methyl pyrrolidone. Surprisingly, these partially aromatized moles are soluble even at conversion to 30 percent phenyl groups. The latter studies can be used to measure the glass transition of polyphenylene which was found to be 283 C. Neutron scattering studies have shown that the precursor polymer is a random coil. Viscosity measurements show that there is a coil-rod transition on aromatization in N-methyl pyrrolidone. Crystallographic data on polyphenylene crystallized above its glass transistion and the thermal and electrical properties are described. Author

N88-24700# Drexel Univ., Philadelphia, Pa. Dept. of Mechanical Engineering and Mechanics.
MIXED-MODE FRACTURE OF UNIAXIAL FIBER REINFORCED COMPOSITES Final Report, 1 Jul. 1985 - 31 Dec. 1986
A. S. Wang, B. Binienda, E. S. Reddy, and Y. Zhong Apr. 1987 147 p
(Contract N62269-85-C-0246)
(AD-A191629; NADC-87133-60) Avail: NTIS HC A07/MF A01 CSCL 11D

Mixed-mode matrix fracture in notched off-axis undirectional composite is investigated. First the problem is treated by an exact formulation based on elastic fracture mechanics. It is then simulated by a finite element model. Correlation with experiment suggests a fracture criterion based on total strain energy release rate as the fracture parameter. GRA

N88-24701# Pennsylvania State Univ., University Park. Dept. of Materials Science and Engineering.
SOL/GEL PROCESSING TECHNIQUES FOR GLASS MATRIX COMPOSITES Final Report, Jun. 1986 - Jun. 1987
C. G. Pantano, G. L. Messing, D. Qi, and W. Minehan Nov. 1987 34 p
(Contract F29601-85-C-0056)
(AD-A191748; AFWL-TN-86-59) Avail: NTIS HC A03/MF A01 CSCL 11D

This report summarizes the first year of a two-year effort on sol/gel processing techniques for glass matrix composites. The emphasis in this program is on sol/gel fabrication techniques and their influence upon the composite properties. The program did not try to develop new matrices or reinforcements. Special emphasis was placed on the reduction in processing temperature and more uniform distribution of the glass matrix between the fibers. GRA

N88-24702# Cincinnati Univ., Ohio. Dept. of Aerospace Engineering and Engineering Mechanics.
INTERACTION OF ULTRASONIC WAVES WITH COMPOSITE PLATES Annual Technical Report, 15 Dec. 1986 - 15 Dec. 1987
Adnan H. Nayfeh 15 Dec. 1987 41 p
(Grant AF AFOSR-0052-86)
(AD-A191879; AFOSR-88-0259TR) Avail: NTIS HC A03/MF A01 CSCL 11D

During the second year of our reporting period we continued our close cooperation with the NDE Branch on the Material's Lab at Wright-Patterson Air Force Base. For our part, we continued developing analytical and computational methods on the modeling of the mechanical behavior of fibrous composites for applications in the NDE field. Specifically, we extended our theoretical models which were developed to describe the behavior of single unidirectional fiber-reinforced plates, to more general plates. These included single and multilayered plates. For the single laminated plate the solutions are extended for arbitrary azimuthal angles and hence resulted in three dimensional analysis. GRA

N88-24703# Centre d'Essais Aeronautique Toulouse (France). Lab. des Materiaux Composites et Organiques.
ELEMENTARY CHARACTERIZATION OF PREIMPREGNATED CARBON EPOXY T400H/DA0506 FROM STRUCTIL. TEST REPORT M6-577100 Final Report [CARACTERISATION ELEMENTAIRE DU PREIMPREGNE CARBONE/EPOXY T400H/DA0506 DE STRUCTIL. PROCES-VERBAL M6-577100]
M. Loriot 11 Sep. 1987 46 p In FRENCH
(CEAT-047426; M6-577100; ETN-88-92538) Avail: NTIS HC A03/MF A01

Compression, tensile, and shear properties of T400H-DA0506 preimpregnated carbon epoxy resin composite were tested, including laminates. Results show that fiber T400H improves tensile strength by 40 percent compared to T300 fiber with the same

resin. The hole coefficient for standard 28 fold ply is low (0.54). With T400H, the DA0506 resin confirms its low sensitivity to warm, moist aging. ESA

N88-24704# Aeronautical Research Inst. of Sweden, Stockholm. Structures Dept.
DETECTING DELAMINATIONS IN CFRP SPECIMENS USING X-RAY TECHNIQUES
Leif Carlsson Jan. 1988 16 p
(Contract FMV-FFL-82223-80-183-21-001)
(FFA-TN-1988-04; ETN-88-92495) Avail: NTIS HC A03/MF A01

Constant amplitude fatigue testing of carbon fiber/epoxy-laminates was carried out. Compression fatigue tests were carried out on laminates, with the stacking sequence (+ or - 45/02/ + or - 45/90/03/+ or - 45/02)S (28 plies) notched with a 6 mm circular hole, at R = - infinity and with an amplitude of 78 percent of the compressive strength. After a certain number of load cycles the laminates were removed from the testing machine and X-rayed. Tetrabromoethane was used as contrast fluid. The results show that it is possible to get a very detailed picture of the damage. After relatively few load cycles matrix-cracks are noted in the 0 deg plies at the hole boundary. After a larger number of loading cycles delamination is initiated at the hole boundary and propagates transverse to the loading direction. The X-ray radiography thus gives a good description of the damage growth in the composite laminate at compression fatigue. ESA

N88-24705 Societe Nationale Industrielle Aerospatiale, Suresnes (France). Lab. Central.
HARMFULNESS OF DEFECTS: BEHAVIOUR IN SERVICE OF A DELAMINATION IN A COMPOSITE CONTAINING MANY DIFFERENTLY ORIENTED LAYERS Final Report
J. Odorico and D. Lang 2 Jul. 1987 65 p In FRENCH
Sponsored by Direction des Recherches, Etudes et Techniques, Paris, France
(PB88-124714; PROCES-VERBAL-47/363/F) Avail: NTIS HC E04/MF E04 CSCL 11D

Experimental results are presented of the progression of defects and the rupture of samples with delaminating defects in stratified composites of carbon-epoxy of two different compositions and with 16 layers either almost isotropic or markedly oriented (50 percent at 0 deg). The presence of a defect had no effect on tensile strength. In compression, 5 to 40 percent of resistance to rupture was lost. The least effect was produced by a defect in the plane symmetry. In this case, as in tension, no progression or blistering of the defect was seen. Dissert. Abstr.

N88-24706 Rensselaer Polytechnic Inst., Troy, N.Y.
SHAPE STABILITY IN COMPOSITES Ph.D. Thesis
Donald W. Radford 1987 275 p
Avail: Univ. Microfilms Order No. DA8729319

Work was undertaken to investigate shape instabilities in anisotropic laminated composites. Both theoretical and experimental studies were carried out. The experimental segments made use of carbon fiber/epoxy composites, and investigated the effects of both temperature and moisture. Long term cyclic environmental conditioning was performed to check the reproducibility of the shape instabilities and to monitor laminate degradation. Curvatures of classical asymmetric laminates were used to aid in evaluating the internal stress of the laminates throughout the test. Safe operating conditions were determined within the time/temperature/moisture domain. This information was subsequently used to predict the long term reproducibility of the shape instabilities. A model was derived, based on a closed form analytical technique, which allows the prediction of the degree of shape instability and warpage in a composite semi-cylindrical shell of unsymmetric geometry. Further extension of this model allowed the prediction of optimized laminate stacking sequences which resulted in shape stable composite components. This shape stability was gained by balancing the unsymmetric geometry with an asymmetric laminate. Both experimental and computer numerical techniques were used to verify the results of these models. This analytical technique is not limited to epoxy based laminated composites. The equations presented are applicable to composites utilizing any material systems, and, in general, to any anisotropic material. Dissert. Abstr.

N88-24707# Societe Nationale des Poudres et Explosifs, Vert-Le-Petit (France). Centre de Recherches du Bouchet.
AGING OF CARBON FIBERS [VIEILLISSEMENT DES FIBRES DE CARBONE]
Christiane Gourdin and Jean Marcel Dartyge 10 Mar. 1986 82 p In FRENCH
(Contract DRET-84-34-302)
(SNPE-NT-10/86/CRB/NP; CPR-93-13-203.00; ETN-88-92152)
Avail: NTIS HC A05/MF A01

The physical, chemical, and mechanical properties of different types of carbon fibers aged at 250 C in an air environment are reported. High performance fibers such as IM6, X636 and T700 were also studied. A correlation is found between the increase in specific surface and the weight loss. High performance fibers have more carbon and less sodium than normal ones. In all cases the carbon atoms show low crystallinity with a high molecular orientation. ESA

N88-24708# Lockheed Missiles and Space Co., Palo Alto, Calif. Research and Development Div.
CHEMICAL COMPATIBILITY BETWEEN SILICON CARBIDE AND A NICKEL ALUMINIDE
T. G. Nieh, J. J. Stephens, J. Wadsworth, and C. T. Liu 1988 10 p Presented at the International Conference on Composite Interfaces, Cleveland, Ohio, 13 Jun. 1988 Prepared in cooperation with ORNL, Tenn.
(Contract DE-AC05-84OR-21400)
(DE88-006188; CONF-880671-1) Avail: NTIS HC A02/MF A01

The chemical compatability between a nickel aluminide (IC-50) and silicon carbide, in both fiber and bulk forms, has been studied over the temperature range from 700 to 1100 C. In general, there are four reaction layers formed at the interface. The elemental distribution in each layer was analyzed using electron microprobe techniques. Nickel is apparently the dominant diffusing species controlling the overall reaction. The chemical reaction between SiC and nickel aluminide is similar to that between SiC and Ni-base superalloys. Aluminum oxide is an effective diffusion barrier in inhibiting SiC-nickel aluminide reaction. DOE

N88-24709# Edgerton, Germeshausen and Grier, Inc., Idaho Falls, Idaho.
INTERFACIAL SHEAR PHENOMENA IN GRAPHITE EPOXY COMPOSITES UNDER IMPACT LOADING USING DYNAMIC MOIRE INTERFEROMETRY
V. A. Deason, J. S. Epstein, and M. Abdallah 1987 7 p Presented at the SPIE International Conference on Photomechanics and Speckle Metrology, San Diego, Calif., 17 Aug. 1987 Prepared in cooperation with Hercules Aerospace Corp., Magna, Utah
(Contract DE-AC07-76ID-01570)
(DE88-006773; EGG-M-02187; CONF-8708213-4) Avail: NTIS HC A02/MF A01

As advanced structural materials (e.g., graphite epoxy, metal matrix and ceramic matrix composites) or optical mirror substrate materials (e.g., beryllium and silicon carbide) are increasingly used in high performance systems, their ability to withstand environments that will cause loss of system survivability must be taken into account. The concept of survivability includes cases where the system is not destroyed, but is inoperable because of subtle effects on it. These effects can be delamination from weak shock events, critical platform misalignment from large slew motions, or even mirror coating and substrate deformations of as little as a fraction of a micron from their specifications. All the effects listed above, in the system survivability realm, are very subtle and are due to transient deformations at a local or micromechanical level. This paper describes recent work to understand the transient mechanisms in composite interfaces that lead to impact delamination. The principal tool of investigation was dynamic moire interferometry coupled with continuum analysis. Results for two

configurations under impact loading are presented. Results for two configurations under impact loading are presented. The first result shows dynamic interfacial shears in an AS43501-6 [090]/sub s/ composite. The second result shows similar effects in a [090]/sub s/ configuration of the same material. Similarities and dissimilarities will be discussed. DOE

N88-24710*# National Aeronautics and Space Administration, Washington, D.C.
FUNCTIONAL AND MECHANICAL ANALYSIS OF CONTINUOUS MEDIA-APPLICATION TO THE STUDY OF ELASTIC COMPOSITES WITH PERIODIC STRUCTURE: HOMOGENIZATION
G. Duvaut Jun. 1988 31 p Transl. into ENGLISH of Analyse Fonctionnelle et Mechanique des Millieuz Continue - Application a l'etude des Materiaux Composites Elastiques a Structure Periodique: Homogeneisation presented at the 14th International Congress, 1987 p 119-132 Congress held in Delft, Netherlands, 30 Aug. - 4 Sep. 1987 Original language document was announced in IAA as A78-13997 Transl. by Scientific Translation Service, Santa Barbara, Calif.
(Contract NASw-4307)
(NASA-TT-20188; NAS 1.77:20188) Avail: NTIS HC A03/MF A01 CSCL 11D

After a review of the functional analysis of problems of continuum mechanics, the paper examines applications of the analysis to elastic composites with fine periodic structure. The limit homogeneous behavior of the composites as the period tends to zero is studied using either an asymptotic expansion combined with functional analysis or an energy method. Homogenization coefficients are calculated explicitly for the case of linear 3-D elasticity and for the case of plates in flexure. Author

N88-24711 California Univ., Los Angeles.
LOCAL DELAMINATION BUCKLING IN LAYERED STRUCTURES Ph.D. Thesis
Erdogan Madenci 1987 95 p
Avail: Univ. Microfilms Order No. DA8800611

An analytical model was developed within the scope of elasticity theory in order to address the local buckling and growth of delamination in layered structures. Delamination buckling and growth is a frequently observed failure mode in laminated composites subjected to compressive load. The three-dimensional theory of elasticity permits the equilibrium equations of the buckled state to be posed in terms of a linear eigenvalue problem. This new problem statement then leads to the desired solution upon using solution methods appropriate to mixed boundary value problems in the theory of elasticity. The buckling stress of a perfect and the stress intensity factor of an initially imperfect delamination between the homogeneous and isotropic layers under axisymmetric and uniaxial loading conditions are studied. Solution of these problems permit the study of the effect of delamination damage upon compressive strength of composites, assessment of structural approximations to this problem, and establishes benchmark solutions for evaluation of future numerical solutions of related problems. Dissert. Abstr.

N88-24712*# National Aeronautics and Space Administration. Lewis Research Center, Cleveland, Ohio.
THE 700 F PROPERTIES OF AUTOCLAVE CURED PMR-2 COMPOSITES
Raymond D. Vannucci and Diane Cifani 1988 17 p Proposed for presentation at the 20th International SAMPE Technical Conference, Minneapolis, Minn., 27-29 Sep. 1988; sponsored by the Society for Advancement of Material and Processing Engineering
(NASA-TM-100923; E-4186; NAS 1.15:100923) Avail: NTIS HC A03/MF A01 CSCL 11D

Studies were conducted to develop autoclave processing parameters for graphite reinforced PMR-2 resin composite materials intended for use in applications at temperatures up to 371 degrees (700 F). The effect of resin composition on autoclaveability was investigated. The effect of various graphite fibers and resin composition on 343 C (650 F) and 371 C (700 F) thermo-oxidative stability and mechanical properties was also investigated. The results of the processing studies show that PMR-2 resin composites can be easily fabricated under autoclave conditions. Autoclaved laminates exposed to 1 atm of air at 343 C (650 F) and 371 C (700 F) exhibited less than 5 percent weight loss after 750 hr exposure to 650 F air and 8 percent weight loss during exposure to 700 F air for 500 hr. After 500 hr exposure, autoclaved laminates exhibited greater than 90 percent retention of initial 650 and 700 F flexural and interlaminar shear strengths. The effect of resin formulated molecular weight and postcure conditions on laminate glass transition temperature is also discussed. Author

N88-24713*# National Aeronautics and Space Administration. Langley Research Center, Hampton, Va.
ANALYSIS OF NOTCHED METAL MATRIX COMPOSITES UNDER TENSION LOADING
C. A. Bigelow Jun. 1988 44 p Submitted for publication
(NASA-TM-100629; NAS 1.15:100629) Avail: NTIS HC A03/MF A01 CSCL 11D

Presented are techniques based on 3-D finite-element analysis for the examination of continuous fiber reinforced metal matrix composites. Examples are shown for specific metal matrix composites such as boron/aluminum and silicon-carbide/aluminum. Specimen stress-strain behavior and stress at first fiber failure were predicted for boron/aluminum laminates containing circular holes and crack-like slits. The predictions compared very well for (+ or - 45) sub 2s laminates. Mesh configuration was shown to have an effect on the calculation of stresses local to the notch. The presence of thin interface layers of matrix material had a significant influence on the slit-tip stress state, causing sharper stress gradients near the notch. Interface layers reduced the slit-tip fibers stresses in a (+ or - 45) sub s silicon-carbide/aluminum laminate but increased them in a (0/90) sub s laminate. Author

25 INORGANIC AND PHYSICAL CHEMISTRY

Includes chemical analysis, e.g., chromatography; combustion theory; electrochemistry; and photochemistry.

For related information see also *77 Thermodynamics and Statistical Physics.*.

N88-24714# Wayne State Univ., Detroit, Mich. Dept. of Chemistry.
SURFACE COMPOSITION-REACTIVITY RELATIONSHIPS IN HETEROGENEOUS CATALYSIS Final Report
A. Brenner 25 Nov. 1987 27 p
(Contract DE-AC02-79ER-10381)
(DE88-006679; DOE/ER-10381/9) Avail: NTIS HC A03/MF A01

There were three objectives to this research program, listed below in order of priority. (1) Prepare and determine the activity of well dispersed and low valent catalysts of supported base metals. (2) Determine the activity for H/sub 2/-D/sub 2/ exchange of some transition metals and oxides. (3) Develop the concept of reactive characterization to see if it can be used to assess the morphology of catalysts containing very small metal ensembles. This report contains a brief summary of results for the period March 1985 through September 1987. Limited background information is also provided to indicate the rationale for the experiments. DOE

N88-24715# Brookhaven National Lab., Upton, N. Y.
UPDATE OF LOW TEMPERATURE CATALYST DEVELOPMENT
D. Mahajan, R. S. Sapienza, T. E. OHare, and G. T. Skaperdas May 1987 15 p Presented at the 12th Annual EPRI Contractors; Conference on Fuel Science and Conversion, Palo Alto, Calif., 13 May 1987
(Contract DE-AC02-76CH-00016)
(DE88-007032; BNL-40685; CONF-8705261-1) Avail: NTIS HC A03/MF A01

A highly active catalyst system for the synthesis of methanol from synthesis gas has been under development. A combination of low temperature (greater than or equal to 70 C), low pressure (greater than or equal to 100 psi), and liquid phase performance makes it possible to achieve high conversion per pass, typically >90% with feed gas composed of hydrogen to carbon monoxide ratio of 2 with this new catalyst. High selectivity to methanol (greater than 95%) has been routinely achieved with methyl formate, a value added product, being the by-product. In addition to temperature and pressure, activity of the new catalyst is sensitive to catalyst formulation, solvent medium, and concentration of product methanol. The catalyst is inert to most impurities normally present in coal-derived syngas, although the carbon dioxide to carbon monoxide ratio is a critical factor. DOE

N88-24716# Delaware Univ., Newark. Dept. of Chemistry.
STRUCTURE/PROPERTY/REACTIVITY RELATIONS AMONG NITRAMINE AND OTHER ENERGETIC MATERIALS Annual Report, 1 Oct. 1986 - 30 Sep. 1987
Thomas B. Brill 1 Oct. 1987 12 p
(Grant AF AFOSR-0033-87)
(AD-A190878; AFOSR-88-0169TR) Avail: NTIS HC A03/MF A01 CSCL 07C

High heating rate thermoylsis studies of energetic materials using rapid-scan Fourier transform infrared spectroscopy as the diagnostic technique have yielded considerable information on the origins of the pressure dependence of the process and structure/property/reactivity relationships. The pressure dependence of the observed gas products up to 1000 psi was shown for the first time to originate from heterogeneous gas/condensed phase reactions. The formation of NH3 from alkylammonium nitrate salts occurs only if the O/H ratio is less than one. The thermochemistry of cyclic and acyclic nitramines is shown to be different in the condensed phase as a result of the different global molecular shapes. Hydrogen bonding as a stabilizing feature in the impact sensitivity of an energetic material was shown to be overridden by the presence of energetic functional groups. GRA

N88-24717# Rome Air Development Center, Griffiss AFB, N.Y.
A SCIENTIFIC BASIS FOR AN ALTERNATE CATHODE ARCHITECTURE Report, for Sep. 1984 - Dec. 1987
E. J. Daniszewski Feb. 1988 153 p
(AD-A191498; RADC-TR-88-33) Avail: NTIS HC A08/MF A01 CSCL 07D

The main effort of this research has been to try to bring together in a simplified manner both theoretical and experimental studies basic to the analysis of thermionic emission from Impregnated Dispenser Cathodes (IDC) as it is understood at this time. This study revealed two major areas of uncertainty: (1) the electronic and steric nature of the cathode emissive surface, and (2) the lack of a reproducible impregnation procedure. Mossbauer Spectroscopy was used to probe cathode surfaces and revealed that enhanced thermionic emission was concomitant with the presence of a low-spin state transition metal ion. The existence of the low-spin Mossbauer probe led to a formulation of a hypothetical surface considerations. This model had a striking parallelism with similar systems in the field of heterogeneous supported catalysis (HSC), viz., the hexagonal barium titanates (HBT). GRA

N88-24718# Air Force Wright Aeronautical Labs., Wright-Patterson AFB, Ohio.
SELECTIVE DETECTION IN GAS CHROMATOGRAPHY Final Report, Jan. - Mar. 1985
Edward W. Pitzer Dec. 1987 25 p
(AD-A191499; AFWAL-TR-86-2039) Avail: NTIS HC A03/MF A01 CSCL 07D

High-resolution gas chromatography (HRGC) is capable of separating a very complex hydrocarbon liquid such as jet propulsion fuel into nearly all of its individual components. However, there is no guarantee that what appears to be a single chromatographic peak is in fact a single fuel component. The method of detecting these HRGC eluents is very often the flame ionization detector (FID), a very sensitive and universally responding hydrocarbon detector. Neither the separating power of HRGC, or the sensitivity of the FID, however, lend information as to the identity of the eluting component. The need to specifically identify HRGC eluents, especially those containing heteroatoms such as nitrogen, sulfur, phosphorus, oxygen, halogens and some materials has been well-documented. The purpose of this report is to review the progress in the area of selective gas chromatographic detectors and to recommend selective detectors for use in the HRGC analysis of jet propulsion fuels. This report will present 24 different selective gas chromatographic detectors. These detectors, while not all directly applicable to the HRGC analysis of jet propulsion fuel, all show the concept of selective detection in gas chromatography. The applicability of these detectors to jet propulsion fuel analyses is determined from a comparison of their complexity and cost versus their effectiveness as high-resolution gas chromatographic detectors. GRA

N88-24719# Cornell Univ., Ithaca, N.Y. Dept. of Chemistry.
ELECTROCHEMISTRY IN LIQUID CRYSTALS Final Report, 15 Aug. 1986 - 15 Feb. 1988
Hector D. Abruna 15 Feb. 1988 4 p
(Contract N00014-84-K-0656)
(AD-A191554) Avail: NTIS HC A02/MF A01 CSCL 07D

Over the last two years our studies have focused on further studies of electrochemical reactions in liquid crystals as well as the use of x rays as insitu probes of electrochemical interfaces. In the area of liquid crystals, we have studied the electrochemical response of electrodes modified with cholesteryl oleyl carbonate (COC; a cholestric phase with optical activity) and on the differences in the electrochemical responses of the optically resolved forms of Ru(bpy)3+2 at such electrode surfaces. We have investigated a wide range of preparations including the modification of electrode surfaces with polymer films containing COC as a dopant and have found these to exhibit a high degree of enantioselective discrimination (ca.20%) in the oxidation of (+) and (-) (Ru(bpy)3)+2. We have also investigated the effect of adding chiral supporting electrolytes such as 2,3 dimethoxy bis 1,4 dimethlamino butane and again, significant chiral discrimination was observed. GRA

N88-24720# California Univ., Berkeley. Dept. of Engineering.
APPLICATION OF RAYLEIGH SCATTERING TO TURBULENT FLOW WITH HEAT TRANSFER AND COMBUSTION Final Report, 1 Apr. 1984 - 30 Sep. 1987
L. Talbot 11 Dec. 1987 10 p
(Grant AF AFOSR-0124-84)
(AD-A191565; AFOSR-88-0270TR) Avail: NTIS HC A02/MF A01 CSCL 21B

A comprehensive investigation has been carried out of the structure and statistical properties of unconfined turbulent flames, both V-shaped and conical. Measurement techniques included conditioned velocity measurements using two component LDV, flow visualization techniques, and Rayleigh scattering. Additionally, a new time resolved technique, LARS(Linear Array for Rayleigh Scattering) was developed which makes possible the determination of the instantaneous location of the flame sheet within the turbulent flame brush. A major objective of these flame studies was to access the appropriateness of models such as the Bray-Moss-Libby (BLM) model for describing the structure of planar turbulent combustion zones. The results of these investigation have revealed that many of the predictions of the BML model accord reasonably well with experimental observations, although some of the constants chosen in the theory are not verified experimentally. Agreement is better for the V-shaped planar flame than for the conical flame, particularly in the vicinity of the flame tip. Studies of the flame stabilization region in the wake of flameholders showed evidence of vortex shedding in the wake and of diminished fluctuation intensity with increased heat release. It was also observed that reaction in the shear layer bounding the recirculating products does not occur until a finite distance downstream of the

flameholder. This observation is confirmed by CH fluorescence imaging of the flame region. GRA

N88-24721# California Univ., Irvine. Dept. of Mechanical Engineering.
ANALYSIS OF MOLECULAR MIXING AND CHEMICAL REACTION IN MIXING LAYER
B. M. Cetegen and W. A. Sirignano 14 Jan. 1988 9 p
(Grant AF AFOSR-0016-86)
(AD-A191600; AFOSR-88-0242TR) Avail: NTIS HC A02/MF A01 CSCL 07D

This paper concerns an analytical study of molecular mixing and finite rate chemical reactions in an infinite row of vortices representing a mixing layer. Diffusion equations for reacting and non-reacting species are solved locally in the Lagrangian frame of reference following material elements. The flowfield is a given for the problem. The concentration distributions in the vortex structure are composed from these analytical solutions and presented for several cases. The probability density functions constructed from these distributions are compared with the mixing layer experiments. For the cases studied, the comparisons indicate encouraging agreement for the reacting flow case. However, some differences are present for the non-reacting flows. GRA

N88-24722# Georgia Univ., Athens. Dept. of Chemistry.
PHOTOIONIZATION DYNAMICS AND ABUNDANCE PATTERNS IN LASER VAPORIZED TIN AND LEAD CLUSTERS
K. LaiHing, R. G. Wheeler, W. L. Wilson, and M. A. Ducan 15 Sep. 1987 10 p
(Contract DAAG29-85-K-0040)
(AD-A191604; ARO-21783.8-CH) Avail: NTIS HC A02/MF A01 CSCL 07B

Tin and lead clusters are produced by laser vaporization in a pulsed nozzle source and studied with laser photoionization mass spectroscopy. Magic numbers are observed in both cluster size distributions under a variety of laser wavelength and power conditions which can be understood in terms of ionization thresholds, relative ionization cross sections, and multiphoton-induced fragmentation . After investigation of the photoionization dynamics, relative abundances of different sized clusters are estimated. Abundance patterns of tin and lead clusters are compared to those reported previously for other group 4 elements (C, Si, Ge) to investigate the role of periodicity in cluster growth and bonding properties. Especially abundant 10-atom cluster species are observed for both tin and lead, as has been observed previously for both silicon and germanium. Other features not observed for silicon and germanium, such as abundance patterns characteristic of atom close packing geometries, are observed to a limited degree for tin clusters and are more prominent in lead clusters. GRA

N88-24723# Texas Univ., Austin. Dept. of Chemistry.
ELECTROCHEMISTRY IN NEAR-CRITICAL AND SUPERCRITICAL FLUIDS. 6: THE ELECTROCHEMISTRY OF FERROCENE AND PHENAZINE IN ACETONITRILE BETWEEN 25C AND 300C
Richard M. Crooks and Allen J. Bard Jul. 1987 26 p
(Contract N00014-84-K-0428)
(AD-A192171; TR-8) Avail: NTIS HC A03/MF A01 CSCL 07C

Cyclic voltammetry in MeCN at various temperatures and pressure, including supercritical conditions, are described. The reduction wave of phenazine in MeCN/CF3SO3Na was reversible or nearly reversible up to 200 C. Above 200 C the second reduction wave coalesced with the first. The oxidation of ferrocene in CH3CN was quasi-reversible between 25 and 285 C. Above the critical temperature (Tc) the standard heterogeneous electron transfer (k) decreased. The diffusion coefficients (D) of phenazine and ferrocene up to Tc are reported, and the determination of viscosity of high temperature/high pressure liquids and fluids based on the measurements of D via and Stokes-Einstein equation is suggested. GRA

N88-24724# Chemical Research and Development Center, Aberdeen Proving Ground, Md.
OPTICAL CONSTANTS OF MINERALS AND OTHER MATERIALS FROM THE MILLIMETER TO THE ULTRAVIOLET Contractor Report, Jun. 1985 - May 1987
Marvin Querry Nov. 1987 330 p
(Contract DAAA15-85-K-0004)
(AD-A192210; CRDEC-CR-88009) Avail: NTIS HC A15/MF A01 CSCL 20F

Reflectance spectra of near normal incidence and/or transmittance spectra of 29 materials were acquired in the ultraviolet, visible, and infrared spectra regions. Optical constants of the materials were determined primarily by use of Kramers-Kronig analysis of reflectance or extinction coefficient spectra. The materials were: Sodium chloride, Potassium chloride, Cesium iodide, Cesium bromide, Zinc sulfide, Zinc selenide, Barium fluoride, Zinc, Manganese, Molybdenum, Zirconium, Anhydrite, Dolomite, Montomorillonite, Kaolin, Illite, Composite of clays, Lanthanum hexaboride, Diesel soot, Polydimethylsiloxane, Dimethyl methylphosphonate, Diethyl sulfite, Diisopropyl methyl phosphonate, and Diethylphthalate. GRA

N88-24725# Imperial Coll. of Science and Technology, London (England). Computational Fluid Dynamics Unit.
COMPUTER SIMULATION OF TURBULENT COMBUSTION IN RECIPROCATING ENGINES
D. Brian Spalding Aug. 1987 26 p Presented at the PHOENICS User Conference, London, England, 23-25 Nov. 1987
(Contracts MOD-NSN/13A/1A-90762; RDMFE-7/87; Grants SERC-GR/D/68139; SERC-GR/D/24371)
(CFDU/87/11; ETN-88-92506) Avail: NTIS HC A03/MF A01

The PHOENICS computer code was applied to simulate premixed combustion in idealized reciprocating engines. A one-dimensional idealization shows that the two-fluid model alone can predict the turbulence which can arise in the absence of mean-flow velocity gradients. A two-dimensional idealization of the same phenomenon, with the addition of swirl, squish and other initiators of Rayleigh-Taylor instability, is also described. The studies show how turbulence, combustion, density fluctuations, and pressure gradients may interact in reciprocating-engines. Implications are discussed, together with suggestions on how the two-fluid model may be developed. ESA

N88-24726# Institut d'Aeronomie Spatiale de Belgique, Brussels.
TEMPERATURE DEPENDENCE OF ULTRAVIOLET ABSORPTION CROSS SECTIONS OF CHLOROFLUOROETHANES
P. C. Simon, D. Gillotay, N. Vanlaethem-Meuree, and J. Wisemberg 1988 35 p Submitted for publication
(Contract EEC-303-78-1)
(Aeronomica-Acta-A-325-1987; ISSN-0065-3713; ETN-88-92485)
Avail: NTIS HC A03/MF A01

Absorption cross sections of 3 haloethanes (C2F5Cl, C2F4Cl2 (CF2Cl-CF2Cl), and C2F3Cl3 (CF2Cl-CFCl2)) measured between 172 and 250 nm for temperatures from 225 to 295 K, are presented with uncertainties between 2 and 4 percent. They are compared with measurements at room temperature and at only one low temperature (208 K). The largest temperature effects which take place near the absorption threshold can be up to 50 percent for C2F3Cl3, and 70 percent for C2F4Cl2; temperature effect, if any, is too small to be detected in the case of C2F5Cl. Extrapolated values for temperatures of aeronomical interest are presented as well as parametrical formulas which give absorption cross section values for given wavelength and temperature useful in stratospheric modeling calculations. Photodissociation coefficients are presented and their temperature dependence is discussed. ESA

N88-24727 Office National d'Etudes et de Recherches Aerospatiales, Paris (France).
EFFECTS OF SPATIAL RESOLUTION IN CARS MEASUREMENTS Final Report
P. Bouchardy, G. Collin, P. Magre, and M. Pealat May 1987

26 p In FRENCH Sponsored by Direction des Recherches, Etudes et Techniques, Paris, France
(PB88-121900; ONERA-RF-45/7131-PY) Avail: NTIS HC E04/MF E04 CSCL 07D

Spatial resolution in CARS temperature measurements was estimated experimentally and theoretically. Potential measurement biases in the case of temperature-heterogeneous measurement volumes were estimated by numeric simulation of the spectra created in the volume. Based on these estimates, the effects of inadequate spatial resolution were examined, using results previously obtained in various combustion flows (premixed laminar and turbulent flames, industrial combustion chamber). GRA

N88-24728 Northwestern Univ., Evanston, Ill.
ON THE STRUCTURE, PROPAGATION, EXTINCTION AND STABILITY OF LAMINAR PREMIXED FLAMES IN DISSOCIATION EQUILIBRIUM Ph.D. Thesis
Beei-Huan Chao 1987 244 p
Avail: Univ. Microfilms Order No. DA8728967

The effects of heat loss, preferential diffusion, and product dissociation on the propagation, extinction, stabilization and diffusional thermal stability of one dimensional freely propagating and burner stabilized laminar premixed flames were analytically studied using activation energy asymptotics. Results show that downstream heat loss is more destabilizing than upstream heat loss, that product dissociation cannot extinguish an adiabatic flame but does promote the extinction of a nonadiabatic flame, that high mobility of the dissociated products enhances the burning rate, that product dissociation has a stabilizing influence on the flame, and that previous experimental observations on the duality of the flame speed and flame location can also be successfully interpreted. The issue of the closure scheme in the asymptotic analysis of premixed flames was also investigated.
Dissert. Abstr.

N88-24729 Wichita State Univ., Kans.
COMPUTATION AND CHARACTERISTICS OF PULSATILE MULTI-BIFURCATION FLOW Ph.D. Thesis
Su Su Feng 1987 146 p
Avail: Univ. Microfilms Order No. DA8728503

A numerical calculation of pulsatile multi-bifurcation flow is made. From the Navier-Stokes equation and the continuity equation, two vorticity transport equations are derived. Using these equations, the stream function and vorticity fields are calculated at sequential times throughout the pulsatile period. Then the fields of velocity, pressure and shear stress can be calculated. The proper treatment of boundary conditions at both the entrance and the exit of the flow field is essential. At the entrance and exit, the flow is linear. The pulsatile flow under study results from the superposition of a steady flow and an oscillatory flow. The oscillatory pressure gradient term can be normalized and expressed in terms of a Karman number and a Stokes number, while the steady pressure gradient can be expressed simply by a Karman number. With these numbers, a normalized momentum equation at both the entrance and the exit can be derived. From this momentum equation, the stream function, vorticity, and velocity distribution at the entrance and exit can be obtained. Results of calculation can be presented in terms of contour plots of stream function, vorticity, shear stress and pressure. From these plots, the characteristics of pulsatile flow can be discussed. Dissert. Abstr.

N88-24730# Foreign Applied Sciences Assessment Center, La Jolla, Calif.
SOVIET COMBUSTION RESEARCH
W. J. McLean, C. A. Amann, C. T. Bowman, P. A. Libby, and R. E. Palmer Mar. 1987 299 p
(PB88-182324; FASAC-TAR-3120) Avail: NTIS HC A13/MF A01 CSCL 21B

The report is an assessment of Soviet basic and applied combustion research, prepared by a panel of seven U.S. combustion scientists and engineers who evaluated a large body of published Soviet scientific literature. The panel examined a broad selection of topics in Soviet combustion research, spanning the range from very applied to very fundamental. Soviet research related to combustion of energetic materials (e.g., propellants and explosives) was intentionally omitted from the assessment. Chapter headings include the following: Assessments, Solid fuels combustion; Heat-engine combustion; Practical combustion of gaseous and liquid fuels--Combustion and explosion safety; Theory of laminar and turbulent reacting flows; Combustion chemistry; Advanced combustion diagnostics and instrumentation. GRA

N88-24731# Oak Ridge National Lab., Tenn. Chemical Technology Div.
PHOTOSYNTHETIC WATER SPLITTING Annual Report, 1987
E. Greenbaum Jan. 1988 36 p
(Contracts GRI-5083-260-0880; DE-AC05-84OR-21400)
(PB88-188891; ORNL/TM-10704; GRI-88/0044) Avail: NTIS HC A03/MF A01 CSCL 07D

The annual report on basic physics and chemistry of photosynthetic water splitting for the production of hydrogen and oxygen is presented. Two key advances were made during the current reporting period. First, it was discovered that, contrary to conventional belief, unicellular green algae are capable of evolving molecular hydrogen in the presence of carbon dioxide. The controlling factors that determine hydrogen evolution are either temperature or light intensity. In addition, it was discovered that certain mutants of the green algae Chalmydomonas are capable of evolving hydrogen in the presence of carbon dioxide. The significance of these discoveries is that the presence of carbon dioxide (or bicarbonate) is a key factor in determining the activity of the Photosystem 2 water splitting complex. Second, an advance in oxygen sensor technology was made that, for the first time, allows the absolute measurement of photosynthetically evolved oxygen from a single colony of microalgae growing on a solidified agar medium. The key aspect of this electrochemical sensor is the utilization of ultra-pure potassium hydroxide as the electrolyte impurities play in contributing to base line noise. A tool that allows the absolute measurement of photosynthetic rates from single colonies will be extremely useful in applying the techniques of molecular biology and genetic engineering to the photosynthetic water splitting problems. GRA

N88-24732* National Aeronautics and Space Administration. Pasadena Office, Calif.
ISOTOPE SEPARATION USING TUNED LASER AND ELECTRON BEAM Patent
Sandor Trajmar, inventor (to NASA) (Jet Propulsion Lab., California Inst. of Tech., Pasadena.) 3 Nov. 1987 13 p Filed 13 Nov. 1986 Supersedes N87-18625 (25 - 11, p 1451)
(NASA-Case-NPO-16907-1-CU; US-Patent-4,704,197;
US-Patent-Appl-SN-930217; US-Patent-Class-204-157.22;
US-Patent-Class-250-423-P; US-Patent-Class-250-427) Avail: US Patent and Trademark Office CSCL 07D

The apparatus comprises means for producing an atomic beam containing the isotope of interest and other isotopes. Means are provided for producing a magnetic field traversing the path of the atomic beam of an intensity sufficient to broaden the energy domain of the various individual magnetic sublevels of the isotope of interest and having the atomic beam passing therethrough. A laser beam is produced of a frequency and polarization selected to maximize the activation of only individual magnetic sublevels of the isotope of interest with the portion of its broadened energy domain most removed from other isotopes with the stream. The laser beam is directed so as to strike the atomic beam within the magnetic field and traverse the path of the atomic beam whereby only the isotope of interest is activated by the laser beam. The apparatus further includes means for producing a collimated and high intensity beam of electrons of narrow energy distribution within the magnetic field which is aimed so as to strike the atomic beam while the atomic beam is simultaneously struck by the laser beam and at an energy level selected to ionize the activated isotope of interest but not ground state species included therewith. Deflection means are disposed in the usual manner to collect the ions.
Official Gazette of the U.S. Patent and Trademark Office

N88-24733# Technische Hogeschool, Delft (Netherlands). Dept. of Aerospace Engineering.
COMBUSTION OF PMMA, PE AND PS IN A RAMJET
C. W. M. vanderGeld, P. A. O. G. Korting, and T. Wijchers Apr. 1987 73 p Sponsored by the Netherlands Technology Foundation and the Management Office for Energy Research, The Netherlands Prepared in cooperation with Prins Maurits Lab. TNO, Rijswijk, The Netherlands
(VTH-LR-514; PML-1987-C18; SFCC-42; B8733275; ETN-88-92458) Avail: NTIS HC A04/MF A01

The combustion behavior of polymethyl methacrylate (PMMA), polyethylene (PE) and polystyrene (PS) was investigated in a connected pipe test facility, to study phenomena that control or emanate from the combustion of a cylindrical solid fuel with a rearward facing step, as in solid fuel ramjets, safe burning of toxic waste, and hot gas generators. Regression rate, efficiency, temperatures, and soot production were examined. At pressures between 0.6 and 1.1 MPa, radiative heat transfer from soot causes an increase of regression rate from PMMA and PE. At pressure below 0.5 MPa hardly any soot is observed during combustion of PMMA and PE; PS is already sooting. Combustion efficiency varies from 70 to 90 percent, and depends on oxygen content, fuel grain length, and fuel composition. The large vortex structure downstream of the sudden expansion at the inlet is shed at a regular rate. This phenomenon is essentially two-dimensional and corresponds to temperature fluctuations of 200 K in the downstream end of the chamber and of 600 K in the upstream end. ESA

N88-24734# Technische Hogeschool, Delft (Netherlands). Dept. of Aerospace Engineering.
COMBUSTION BEHAVIOR OF THE VITIATOR. EXPERIMENTAL RESULTS OF A SECOND TEST SERIES
P. A. O. G. Korting Nov. 1986 22 p Prepared in cooperation with the Prins Maurits Lab. TNO, Rijswijk, The Netherlands
(Contracts STW-DLR-15.0120; PBE-90743.140)
(VTH-LR-509; PML-1986-C105; SFCC-39; B8733273; ETN-88-92457) Avail: NTIS HC A03/MF A01

A solid fuel combustion chamber vitiator was tested. The results indicate that due to heat losses the amounts of methane to be used to obtain the required air temperature are considerably higher than the calculated values, and increase with increasing total mass flow and (to a lesser extent) pressure. From the findings it is possible to make a better estimate of the various mass flows to be used to obtain the required air temperature at a given total mass flow. ESA

N88-24735# IIT Research Inst., Bartlesville, Okla. National Inst. for Petroleum and Energy Research.
THE THERMODYNAMIC PROPERTIES OF QUINOLINE AND ISOQUINOLINE
W. V. Steele, D. G. Archer, R. D. Chirico, W. B. Collier, B. E. Gammon, I. A. Hossenloop, A. Nguyen, and N. K. Smith Mar. 1988 58 p
(Contract DE-FC22-83FE-60149)
(DE88-001218; NIPER-301) Avail: NTIS HC A04/MF A01

Measurements leading to the calculation of the ideal-gas thermodynamic properties for quinoline and isoquinoline are reported. Thermodynamic and thermophysical properties were determined by adiabatic heat-capacity calorimetry, comparative ebulliometry, densimetry, and combustion calorimetry. Vibrational spectra of quinoline and isoquinoline were assigned. Entropies and enthalpies for the ideal-gas state from the claorimetric measurements and from the vibrational assignments were derived and compared. Entropies, enthalpies, and Gibbs energies of formation were derived at selected temperatures between T yields o and 1000 K. new density measurements for benzene are reported. DOE

N88-25046# Pacific Northwest Labs., Richland, Wash.
RESEARCH ON HYDROTREATING CATALYSTS TO HYDRODEOXYGENATE BIOCRUDE OILS
Douglas C. Elliott and Eddie G. Baker *In its* Proceedings of the 1987 Biomass Thermochemical Conversion Contractors' Review Meeting Nov. 1987 p 81-9 (For primary document see N88-25041 18-44)
(Contract DE-AC06-76RL-01830)
Avail: NTIS HC A09/MF A01

26 METALLIC MATERIALS

Includes physical, chemical, and mechanical properties of metals, e.g., corrosion; and metallurgy.

N88-24736# Ames Lab., Iowa.
EFFECT OF HYDROGEN, DEUTERIUM AND OXYGEN ON THE ANELASTIC PROPERTIES OF REFRACTORY ALLOYS M.S. Thesis - Iowa State Univ., Ames
Lisa Hager Brasche Nov. 1987 107 p
(Contract W-7405-eng-82)
(DE88-007349; IS-T-1251) Avail: NTIS HC A06/MF A01

The effect of hydrogen, deuterium and oxygen on the anelastic properties of V, Nb and V-Nb alloys were examined. Activation parameters were obtained for the oxygen Snoek peak in V and Nb with various hydrogen concentrations. Hydrogen was found not to affect these oxygen relaxation parameters. Thus no interaction of oxygen with hydrogen occurs in the pure metals. Measurement of the hydrogen Snoek peak and the deuterium Snoek peak in V-Nb alloys also led to determination of activation parameters for these interstitials that are consistent with those found by diffusion measurements in this same alloy series. An isotope effect was observed. In addition, oxygen was found not to affect the relaxation of the hydrogen in the V-Nb alloys, indicating that the oxygen-hydrogen interaction in the alloys is also negligible. DOE

N88-24737# California Univ., Berkeley. Lawrence Berkeley Lab.
STRAIN HARDENING AT LARGE STRAINS IN ALUMINUM ALLOYS Ph.D. Thesis
Anthony David Rollett Mar. 1988 367 p
(Contract W-7405-eng-36)
(DE88-007415; LA-11202-T) Avail: NTIS HC A16/MF A01

The strain hardening properties of high purity Al, commercial purity Al, Al-Mn, Al-Mg and Al-Cu alloys have been investigated at large strains in the temperature range 77-473K. Torsion of short thin walled cylinders was chosen as the deformation method. Results indicated that te stage of strain hardening known as Stage 4 occurs even in pure face centered metals in torsion. Stage 4 is the nearly constant hardening rate observed at large strains. The hardening rate in Stage 4 is approximately 2.10/sup -4/ where the hardening rate has been reduced by the shear modulus and Taylor factor in factor in order to put it in terms of critical resolved shear stresses on a single slip system. A plot of hardening rate versus stress characteristically shows a sharp transition from steadily decreasing hardening rate in Stage 3 to constant Stage 4. Stage 4 does not appear at high homologous temperatures. Alloying generally extends the occurrence of Stage 4 to high temperatures than in pure metals. A model has been developed that is based on the accumulation of dislocation debris such as dipoles and prismatic loops. This model is able to account for the characteristics of Stage 4, such as the sharp transition observed on a plot of hardening rate versus stress. DOE

N88-24738*# Alabama Univ., Huntsville. Center for Applied Optics.
OPTICAL MONITORING OF PROTEIN CRYSTAL GROWTH Final Report
A. Choudry 30 May 1988 6 p
(Grant NAG8-599)
(NASA-CR-182869; NAS 1.26:182869) Avail: NTIS HC A02/MF A01 CSCL 20L

The possibility of using various optical techniques for detecting the onset of nucleation in protein crystal growth was investigated. Direct microscopy, general metrologic techniques, light scattering, ultraviolet absorption, and interferometry are addressed along with

techniques for determining pH value. The necessity for collecting basic data on the optical properties of the growth solution as a prerequisite to the evaluation of monitoring techniques is pointed out. Author

N88-24739# Lockheed-Georgia Co., Marietta.
PREDICTIVE CORROSION MODELING, VOLUME 1 Final Report, Sep. 1985 - Jul. 1987
Robert N. Miller 23 Nov. 1987 59 p
(Contract F33615-85-C-5058)
(AD-A191229; LG87ER0083-Vol-1; AFWAL-TR-87-4105-Vol-1)
Avail: NTIS HC A04/MF A01 CSCL 01C

This report for a program to develop a predictive corrosion model for aircraft summarizes the work completed in Task 3. The corrosion rate equations and models developed in Task 2 were converted into a VAX-11 FORTRAN program which enables the analysis of specific points on the C-5 aircraft and, utilizing environmental factors and the time periods an aircraft has been at various Air Force bases, gives recommended times for inspection and maintenance. The FORTRAN computer program includes a crack growth module which calculates the remaining flight hours until a theoretical crack grows to half its critical length, a corrosion module which calculates the remaining hours until exposed aircraft alloys corrode to a depth of 3 mils, and a coating degradation module which computes the optimum time remaining until the next paint renewal or complete repaint operation. Volume 1 describes the program effort. Volume 2 contains computer program printouts. GRA

N88-24740# Carnegie-Mellon Univ., Pittsburgh, Pa. Dept. of Metallurgical Engineering and Materials Science.
FUNDAMENTAL STUDIES OF BETA PHASE DECOMPOSITION MODES IN TITANIUM ALLOYS Annual Technical Report, 1 Oct. 1986 - 30 Sep. 1987
H. I. Aaronson, A. M. Dalley, T. Furuhara, and Y. Mou 31 Jan. 1988 30 p
(Grant AF-AFOSR-0303-84)
(AD-A191495; AFOSR-88-0021TR) Avail: NTIS HC A03/MF A01 CSCL 11F

An investigation of the interphase boundary structure of grain boundary alpha allotriomorphs in a Ti-7.15 W/O Cr alloy now in progress has established that complex, multiple sets of ledges are present at the interphase boundaries of allotriomorphs between not only the B grain with respect to which the allotriomorphs is Burgers oriented but also with respect to the adjacent B grain, with which the allotriomorph necessarily has a non-Burgers orientation relationship. Questions are arising, however, as to whether certain systems of ledges are (immobile) structural and growth ledges. Resolution of the misfit dislocations which must be present on the terraces of both types of ledges and distinguishing between misfit dislocations and ledges with short risers are important problems which have arisen in TEM studies of these interphase boundaries. GRA

N88-24741# California Univ., Davis. Dept. of Mechanical Engineering.
SUPERPLASTICITY: A FUNDAMENTAL INVESTIGATION ON DEFORMATION MECHANISM AND CAVITATION PHENOMENA Annual Technical Report, 1 Feb. 1987 - 31 Jan. 1988
A. H. Chokshi, T. Bieler, and A. K. Mukherjee 15 Feb. 1988 32 p
(Grant AF-AFOSR-00575-86)
(AD-A191548; AFOSR-88-0220TR) Avail: NTIS HC A03/MF A01 CSCL 11F

Al-Li alloy and the mechanically alloyed IN 91211 were investigated for superplasticity and enhanced plasticity. The deformation behavior of fine and coarse grains (coexisting in the same microstructure) was a function of strain rate. Both type of grains deformed in an intercrystalline manner in region 2. In region 3, only the fine grains deformed in this mode. The mechanically alloyed specimens revealed the high ductility of 500% elongation at the uncommonly high strain rate of 10 per sec. The stress exponent of strain rate for this alloy does not correlate with existing models for superplasticity. Additional mechanical and microstructural work underway are expected to shed more light on the micromechanism of deformation for this alloy. GRA

N88-24742# Virginia Univ., Charlottesville. Dept. of Chemical Engineering.
THE INFLUENCE OF CATHODIC PROTECTION ON EROSION-CORROSION OF METALS AND MODEL ALLOYS Annual Report, 1 Dec. 1986 - 1 Dec. 1987
M. E. Orazem 5 Feb. 1988 23 p
(Contract N00014-87-K-0042)
(AD-A191613; UVA/525418/CHE88/101) Avail: NTIS HC A03/MF A01 CSCL 11F

The object of this program is to develop a fundamental understanding of the influence of applied potential on mechanisms for erosion-corrosion as applied to copper and copper-based alloys. This work is intended to allow application of laboratory experiments to predict the onset of erosion-corrosion failure under field conditions and to guide development of workable strategies for prevention of erosion-corrosion. In the first year of the program, an electrochemical cell incorporating a scanning ellipsometer was designed and built. The cell uses a submerged electrolyte jet impinging on an electrode. The laser spot is around 25 x 70 micrometers and the position of the electrode-jet assembly relative to the laser spot can be controlled by stepping motor stages without altering the hydrodynamic environment. This system will be used to map local film thickness under well controlled fluid flow exhibiting high shear rates. The radial position at which the film thickness decreases can be related to a critical value for hydrodynamic shear required to remove the film, and the use of a well-characterized flow geometry allows separation of erosion-corrosion effects from corrosion enhancement associated with mass transfer. Experiments using this system will begin in the second year of the program. GRA

N88-24743# Lockheed Missiles and Space Co., Palo Alto, Calif. Research and Development Div.
EFFECT OF ALLOYING, RAPID SOLIDIFICATION, AND SURFACE KINETICS ON THE HIGH TEMPERATURE ENVIRONMENTAL RESISTANCE OF NIOBIUM Technical Report, Jan. 1987 - Jan. 1988
R. A. Perkins, G. H. Meier, R. A. Miller, and K. T. Chiang 8 Jan. 1988 49 p
(Contract F49620-86-C-0018)
(AD-A192093; LMSC-F24660; AFOSR-88-0088TR) Avail: NTIS HC A03/MF A01 CSCL 07B

An improved understanding of factors governing the selective oxidation of aluminum to form continuous alumina scales on modified niobium-aluminum alloys has been established. It has been demonstrated that highly protective alumina scales can be formed on niobium-titanium-chromium-vanadium-aluminum alloys without transient oxidation products at temperatures of 1400 to 1600 C in air. Aluminum content has been identified as the critical factor controlling single layer alumina formation. It also has been shown that the N sub Al(crit) for the formation of a continuous alumina scale is 0.375 - 0.38 at 1400 C, decreasing slightly with increased Nb-Ti ratio in the alloy. A fourth element must be added to niobium-titanium-aluminum for effective alumina formation. It has been established that this element should be from a group that can reduce the solubility-diffusivity at 1400 - 1600 C. Alumina can be formed at 1400 C by substituting V or Ti but a liquid transient oxide is produced. A high rate of transient oxidation relative to alumina formation in this range accelerated transient oxidation and precluded alumina growth instead. GRA

N88-24744# Lawrence Livermore National Lab., Calif.
DYNAMIC CONSOLIDATION OF METAL POWDERS Final Report
William H. Gourdin 25 Jan. 1988 4 p
(Contract MIPR-ARO-106-86)
(AD-A192126; ARO-18211.14-MS) Avail: NTIS HC A02/MF A01 CSCL 11F

We have studied the shock wave consolidation of copper,

4330 steel and aluminum+6% silicon powders. We measured the Hugoniots of the unsintered powders using piezoresistive pressure sensors as well as impedance matching techniques and found that they can be well described by available models for pore collapse. An elementary model for the surface heating was developed based on the flux of energy at the interfaces between powder particles during compaction. This model was found to agree quantitatively with observations of localized microstructural modifications in recovered specimens. We found that most of the energy of the compaction shock is deposited at the particle interfaces and that powder particle morphology and specific surface area are important variables. Localized thermal modifications can be either solid state transformations or surface melting and rapid cooling can produce metastable structures. Knowledge of the shock history is essential to the interpretation and control of the consolidated microstructure. We have produced and tested consolidated aluminum+6 percent silicon that has tensile properties comparable to those of wrought material. GRA

N88-24745# Advanced Research and Applications Corp., Sunnyvale, Calif.
THE INSPECTION OF ELECTRONIC METALLURGICAL BONDS Final Report
Bart Jackson, Jerel Smith, and James Stanley Feb. 1988 30 p
(Contract N00014-86-C-0860)
(AD-A192197; ARACOR-FR-563-88) Avail: NTIS HC A03/MF A01 CSCL 11F

The solder bonds in electronic assemblies are an area of increased Non-Destructive Evaluation interest as the number of bonds per assembly increases, the size of the bonds decreases, and the dependence on the bonds for electrical and mechanical performance increases. The current inspection techniques are not detecting many defects, and the inspection techniques are not adequate for the near-term Surface Mount Technology improvements. Computed Tomography is a new NDE technology that is beginning to find its place in industry. This project has surveyed the field of printed circuit board manufacturing to determine the types of flaws that need to be detected to improve the reliability of solder bonds in electronic systems. GRA

N88-24746*# Virginia Univ., Charlottesville. Dept. of Materials Science.
ENVIRONMENT ASSISTED DEGRADATION MECHANISMS IN ADVANCED LIGHT METALS Progress Report
Richard P. Gangloff, Glenn E. Stoner, and Robert E. Swanson Jun. 1988 119 p
(Grant NAG1-745)
(NASA-CR-182907; NAS 1.26:182907; UVA/528266/MS88/102) Avail: NTIS HC A06/MF A01 CSCL 11F

The general goals of the research program are to characterize alloy behavior quantitatively and to develop predictive mechanisms for environmental failure modes. Successes in this regard will provide the basis for metallurgical optimization of alloy performance, for chemical control of aggressive environments, and for engineering life prediction with damage tolerance and long term reliability. B.G.

N88-24747# Oak Ridge National Lab., Tenn.
MICROSTRUCTURAL CHARACTERIZATION AND PROPERTIES OF 3Cr-1.5Mo-O.1V THICK SECTION ELECTRON BEAM WELDS
S. A. David, J. F. King, and J. M. Vitek 1988 6 p Presented at the ASW/EWI Power Beam Conference, San Diego, Calif., 1 May 1988
(Contract DE-AC05-84OR-21400)
(DE88-004330; CONF-880547-1) Avail: NTIS HC A02/MF A01

Single pass, full penetration, thick-section (10 cm) electron beam weldments of high integrity were made of 3Cr-1.5Ml-0.1V steel using a 100 kW Sciaky electron beam welder. The weldment was characterized using microhardness measurements, Charpy V-notch impact, tensile, and guided bend tests. Microstructural characterization was done using both optical and electron microscopy. The mechanical properties results showed the electron beam weldments had properties that matched those of the base metal. A hardness minimum within the heat-affected zone (HAZ) was observed on either side of the fusion zone. Such a minimum is commonly observed in ferritic steel weldments, although this region was very narrow compared to the weldments made by other conventional processes. Microstructural characterization of the weld revealed that the fusion zone and immediately surrounding HAZ contained retained austenite between the bainite laths. Further away from the fusion zone, the HAZ structure consisted of bainite and proeutectoid ferrite, which corresponded to the drop in the microhardness, and resulted in a minimum. Tempered bainite was observed beyond this minimum in the HAZ. DOE

N88-24748# Pacific Northwest Labs., Richland, Wash.
IRRADIATION EFFECTS ON TUNGSTEN STABILIZED MARTENSITIC STEELS
D. S. Gelles, C. Y. Hsu, and T. A. Lechtenberg Aug. 1987 15 p Presented at the 3rd International Conference on Fusion Reactor Materials, Karlsruhe, Federal Republic of Germany, 4 Oct. 1987 Prepared in cooperation with General Atomics Co., San Diego, Calif.
(Contract DE-AC06-76RL-01830)
(DE88-007074; PNL-SA-15177; CONF-871036-34) Avail: NTIS HC A03/MF A01

Tungsten stabilized martensitic stainless steels are being developed for fusion reactor first wall application in order to lower retained radioactivity so as to permit shallow land burial after reactor decommissioning. Two such alloys have been designed, fabricated, and examined by transmission electron microscopy. The two compositions were Fe-7.5Cr-2.OW-.17C and Fe-10.2Cr-1.7W-.3V-.-2C. Conditions examined included irradiation temperatures of 365, 420, 520 and 600 C to doses as high as 34 dpa. Small amounts of void swelling are found at the two lowest temperatures. It is demonstrated that levels of tungsten on the order of 2 wt% do not result in excessive intermetallic precipitation under these irradiation conditions. DOE

N88-24749*# National Aeronautics and Space Administration. Lewis Research Center, Cleveland, Ohio.
STATUS AND PROGNOSIS FOR ALTERNATIVE ENGINE MATERIALS
Joseph R. Stephens and Michael V. Nathal 1988 16 p Proposed for presentation at the 6th International Symposium on Superalloys, Champion, Pa., 18-22 Sep. 1988; sponsored by TMS-AIME
(NASA-TM-100903; E-4154; NAS 1.15:100903) Avail: NTIS HC A03/MF A01 CSCL 11F

The current state of research and development of new materials for advanced aircraft engines is reviewed. The advantages and disadvantages of intermetallic compounds and refractory metals as replacements for today's nickel-base alloys are discussed along with some results of research directed at overcoming some of the problems which restrict their application. It is concluded that continuous fiber reinforced intermetallic matrix composites offer one of the best chances for success. However, major technical barriers still exist, especially in the development of suitable fibers. The introduction of these materials into aircraft engines is expected to take in excess of 5 to 10 years. Author

N88-24750# Societe Nationale Industrielle Aerospatiale, Suresnes (France). Direction de la Qualite.
IMPROVING KNOWLEDGE OF THE CORROSION BEHAVIOR OF ALUMINUM ALLOYS OF THE 7XXX SERIES [AMELIORATION DES CONNAISSANCES SUR LE COMPORTEMENT A LA CORROSION DES ALLIAGES D'ALUMINIUM DE LA SERIE 7XXX. PROCES-VERBAL 48-451/F]
J. Odorico and J. M. Cuntz 30 Jun. 1987 129 p In FRENCH
(Contract STPA-85-96-032)
(Rept-48-451/F; ETN-88-92148) Avail: NTIS HC A07/MF A01

Micrographic tests on 7XXX Al alloys were carried out for different norms and test conditions. A simple classification criterion of corrosion severity was adopted. A large variety of different

behaviors is observed. Even the T 73 alloys are in some cases sensitive to corrosion. Regarding the accelerated corrosion tests, it is found that a combination of the intercrystalline corrosion test and the EXCO tests allows to estimate the long term behavior. ESA

N88-24751# Societe Nationale Industrielle Aerospatiale, Suresnes (France). Direction Centrale de la Qualite.
CHARACTERIZATION OF THE 2219 CEGEDUR ALLOY. DATA ACQUISITION OF THE FRACTURE MECHANICS [CARACTERISATION DU 2219 CEGEDUR. ACQUISITION DE DONNEES DE MECANIQUE DE LA RUPTURE. PROCES-VERBAL 48-442/F]
J. Odorico and Y. Barbaux 28 Jul. 1987 36 p In FRENCH
(Contract STPA-85-96-032)
(Rept-48-442/F; ETN-88-92149) Avail: NTIS HC A03/MF A01

Tensile and fatigue tests were carried out using specimens from 5 mm thick plates. This copper-aluminum alloy shows breaking characteristics closer to a 7 x 75 T7 alloy than to a 2024 T3 alloy. Tensile tests carried out at minus 75 C confirm the good cryogenic behavior. ESA

N88-24752# Societe Nationale Industrielle Aerospatiale, Suresnes (France). Direction de la Qualite.
CHARACTERIZATION OF 7090 AND 7091 PROFILES MADE WITH CEGEDUR POWDER [CARACTERISATION DE PROFILES EN 7090 ET 7091 CEGEDUR. PROCES-VERBAL 48-441/F]
J. Odorico, Y. Barbaux, and M. Olechna 3 Aug. 1987 45 p In FRENCH
(Contract STPA-85-96-032)
(Rept-48-441/F; ETN-88-92158) Avail: NTIS HC A03/MF A01

Characterization tests of Airbus aircraft profiles obtained using cobalt-aluminum alloy powder metallurgy are described. The characterization includes mechanical and corrosion tests. The 7090 material is found to be a candidate for the substitution of Airbus components. It is particularly interesting regarding tensile strength, fatigue characteristics, and corrosion resistance. ESA

N88-24753*# National Aeronautics and Space Administration. Langley Research Center, Hampton, Va.
ALUMINUM ALLOY Patent Application
Linda B. Blackburn, inventor (to NASA) and Edgar A. Starke, Jr., inventor (to NASA) (Virginia Univ., Charlottesville.) 23 Mar. 1988 10 p
(NASA-Case-LAR-13924-1-CU; NAS 1.71:LAR-13924-1-CU; US-Patent-Appl-SN-172102) Avail: NTIS HC A02/MF A01 CSCL 11F

This invention relates to aluminum alloys, particularly to aluminum-copper-lithium alloys containing at least about 0.1 percent by weight of indium as an essential component, which are suitable for applications in aircraft and aerospace vehicles. At least about 0.1 percent by weight of indium is added as an essential component to an alloy which precipitates a T1 phase (Al2CuLi). This addition enhances the nucleation of the precipitate T1 phase, producing a microstructure which provides excellent strength as indicated by Rockwell hardness values and confirmed by standard tensile tests. NASA

N88-24754*# National Aeronautics and Space Administration. Lewis Research Center, Cleveland, Ohio.
ARC-TEXTURED METAL SURFACES FOR HIGH THERMAL EMITTANCE SPACE RADIATORS
Bruce A. Banks, Sharon K. Rutledge, Michael J. Mirtich, Tracy Behrend, Deborah Hotes, Michael Kussmaul, Jennifer Barry, Curtis Stidham, Thomas Stueber, and Frank DiFilippo (Case Western Reserve Univ., Cleveland, Ohio.) [1988] 11 p Presented at the International Conference on Metallurgical Coatings, San Diego, Calif., 11-15 Apr. 1988; sponsored by the American Vacuum Society
(NASA-TM-100894; E-4135; NAS 1.15:100894) Avail: NTIS HC A03/MF A01 CSCL 11F

Carbon arc electrical discharges struck across the surfaces of metals such as Nb-1 percent Zr, alter the morphology to produce a high thermal emittance surface. Metal from the surface and carbon from the arc electrode vaporize during arcing, and then condense on the metal surface to produce a microscopically rough surface having a high thermal emittance. Quantitative spectral reflectance measurements from 0.33 to 15 microns were made on metal surfaces which were carbon arc treated in an inert gas environment. The resulting spectral reflectance data were then used to calculate thermal emittance as a function of temperature for various methods of arc treatment. The results of arc treatment on various metals are presented for both ac and dc arcs. Surface characterization data, including thermal emittance as a function of temperature, scanning electron microscopy, and atomic oxygen durability, are also presented. The ac arc texturing was found to increase the thermal emittance at 800 K from 0.05 to 0.70. Author

N88-24755# Lawrence Livermore National Lab., Calif.
THE VARIATION OF TORSIONAL DUCTILITY OF HIGH-PURITY ALUMINUM WITH TEMPERATURE AND STRAIN RATE
M. E. Kassner, J. J. Oldani, and K. L. Cadwell 25 Jan. 1988 11 p Presented at the 22nd Associazione Italiana di Metallurgie Convention, Bologna, Italy, 17 May 1988
(Contract W-7405-eng-48)
(DE88-005618; UCRL-98000; CONF-880564-1) Avail: NTIS HC A03/MF A01

The torsional ductility of high-purity aluminum was measured over a wide temperature range (110-610 C and at three strain rates (5.1x 10 to the -4, 1.3 x 10 to the -2, and 5.1x 10 to the -1/s; several trends were noted that are only partially consistent with earlier work in this area. At each strain rate, the ductility or strain-to-failure first increases with increasing temperature, followed by decreases beyond a peak ductility at a peak temperature. The peak ductility and peak temperature appear to increase with strain rate. It appears that the lower-temperature ductility trends can be explained by increasing dynamic recovery processes that retard cracking and produce increasing ductility, while at higher temperature diffusive pore formation reduces the ductility. DOE

N88-24756# Cincinnati Univ., Ohio.
THE THEORY OF RANDOM ALLOYS
F. J. Pinski, D. M. Nicholson, G. M. Stocks, W. H. Butler, D. D. Johnson, and B. L. Gyorffy May 1988 11 p Presented at the 3rd International Conference on Supercomputing, Boston, Mass., 15 May 1988 Prepared in cooperation with ORNL, Tenn., NRL, Washington, D.C. and Bristol Univ., United Kingdom
(Contract DE-AC05-84OR-21400)
(DE88-006408; CONF-880567-1) Avail: NTIS HC A03/MF A01

We review the theory of random substitutional alloys which we have developed from microscopic quantum mechanics. This theory is based on the understanding of the electron glue which is responsible for cohension. We describe how many properties can be calculated from first-principles, i.e., only the atomic number sand concentrations are required inputs. These properties include the equilibrium volume, short-range order parameters, phase diagrams, magnetic properties, and the transport coefficients. Three types of mean-field approximation are used in these calculations. Density functional theory is used to reduce the many-electron problem to that of a single electron moving in mean field due to the other electrons, the coherent-potential approximation is used to replace the disordered potential field of the random alloy by an effective potential, and furthermore, the statistics of site occupation is treated in the mean field apponximation by the concentration functional theory (CFT) in the determination of short-range order. DOE

N88-24757# Oak Ridge Y-12 Plant, Tenn.
CALCULATION OF OXIDATION RATES FOR IRON IN CO-CO2

J. B. Condon Mar. 1988 16 p
(Contract DE-AC05-84OR-21400)
(DE88-007313; Y-2393) Avail: NTIS HC A03/MF A01

A new method is proposed for calculating the oxidation of iron in the presence of carbon monoxide and carbon dioxide. It is assumed that the oxidation is limited by an internal oxidation step. The calculational method, based on methods previously used to calculate the hydriding of uranium, uses no parameters for the calculation. The known oxygen solubility and diffusivity in iron along with the precipitation rate constants, all of which are obtainable from the literature, are used to make the calculation. The calculation is in good agreement with the rates of oxidation observed, which would seem to validate the method. DOE

N88-24758*# National Aeronautics and Space Administration, Washington, D.C.
THE PRECIPITATION PROCESSES OF Cu-Zr-Cr ALLOYS
Hisashi Suzuki and Motohiro Kanno Jun. 1988 17 p Transl. into ENGLISH from Nippon Kinzoku Gakkaishi (Japan), v. 36, no. 4, 1972 p 363-368 Transl. by SCITRAN, Inc., Santa Barbara, Calif.
(Contract NASw-4307)
(NASA-TT-20168; NAS 1.77:20168) Avail: NTIS HC A03/MF A01 CSCL 11F

Precipitation processes of a Cu-Zr-Cr ternary alloy were investigated by means of specific heat and electric resistance measurements, computing with those of Cu-Zr and Cu-Cr binary alloys. Specimens were solution treated at 950 C and quenched into iced water. Subsequently they were aged or cold rolled about 83 percent and then aged under various conditions. The precipitation processes during aging at temperatures elevated at a constant rate of 2 C min were examined in detail. The results obtained are detailed. Author

N88-24759*# National Aeronautics and Space Administration, Washington, D.C.
HIGH TEMPERATURE EMBRITTLENESS OF Cu-Cr ALLOY
Hisashi Suzuki, Motohiuro Kanno, and Hitoshi Kitano May 1988 17 p Transl. into ENGLISH from Nippon Kinzoku Gakkaishi (Japan), v. 34, 1970 p 497-501 Transl. by SCITRAN, Inc., Santa Barbara, Calif. Original document was prepared by Tokyo Univ.
(Contract NASw-4307)
(NASA-TT-20184; NAS 1.77:20184) Avail: NTIS HC A03/MF A01 CSCL 11F

The phenomenon and mechanism of high temperature embrittleness in Cu-Cr alloy were studied. Commercially available Cu-1.0 percent Cr alloys solution annealed, quenched, or subsequently cold worked were aged at various temperaturs up to 700 C. These specimens were tensile tested in the temperature range as above. As for the mechanism, the microstructures of tensile strained or fractured specimens were mainly examined by means of optical and electron microscopy, EMPA, etc. Results obtained were as follows: (1) the alloy except in the over-aged state always showed marked embrittleness at above 500 C; (2) although the phenomenon was associated with intergranular fracture, an abnormality at or near grain boundaries was never detected; (3) it was suggested from the microstructural studies that the embrittleness was due to the high stress concentration at the grain boundaries caused by blocking of the slip bands and the decrease in strength of the grain boundaries with rising temperatures. Author

N88-24760*# National Aeronautics and Space Administration, Washington, D.C.
CRITICAL COOLING RATES ON SOLUTION TREATMENT OF Cu-Cr AND Cu-Be ALLOYS
Tadatoshi Todi Jun. 1988 18 p Transl. into ENGLISH from Nippon Kinzoku Gakkaishi (Journal of Japan Inst. Metals) (Japan), v. 21, 1957 p 237-242 Transl. by SCITRAN, Inc., Santa Barbara, Calif.
(Contract NASw-4307)
(NASA-TT-20163; NAS 1.77:20163) Avail: NTIS HC A03/MF A01 CSCL 11F

It is shown that certain high strength and high electrical conductivity copper alloys, Cu-Cr and Cu-Be, do not undergo sufficent age hardening by slow quenching. This problem has been recently highlighted by the increasing demand for high strength alloys in the form of a large section. In order to find out the effect of the cooling rate on the formation of a supersaturated solid solution for Cu-Cr and Cu-Be alloys, the Jominy end quench tests and the isothermal treatment and aging tests were performed. A 25 diameter times 100 mm test bar similar to the standard bar for steel was used for the Jominy tests and the 1.0 mm diameter wire for the isothermal treatment and aging tests to determine the C-curve. The results obtained are detailed. It seems that the aging characteristics were particularly influenced by the cooling rate in the temperature range near the nose of the lower C-curve. It is concluded that the critical cooling rate on solution treatment of this alloy is 55 to 60 C/sec at about 500 C. Author

N88-24761*# National Aeronautics and Space Administration, Washington, D.C.
MARTENSITIC TRANSFORMATION AND MICROSTRUCTURES IN SINTERED NiAl ALLOYS
Shouichi Ochiai, Osamu Noguchi, and Manabu Ueno Jun. 1988 23 p Transl. into ENGLISH from Nippon Kinzoku Gakkaishi (Journal of the Japan Inst. of Metals) (Japan), v. 51, no. 7, Jul. 1987 p 686-693 Original language document was announced in IAA as A88-10603 Transl. by SCITRAN, Inc., Santa Barbara, Calif. Original document was prepared by the Technological Univ. of Nagaoka (Japan)
(Contract NASw-4307)
(NASA-TT-20178; NAS 1.77:20178) Avail: NTIS HC A03/MF A01 CSCL 11F

The characteristics of martensitic transformation and microstructures in sintered NiAl alloys manufactured by hot-pressed powder metallurgy were investigated. When presintering was followed by hot pressing in vacuum, alloys having a relative density higher than 99 percent of theroretical values were obtained. Sintered NiAl specimens quenched from 1573 K in ice brine had a complete martensitic structure. An increase in density of about 1 percent and a decrease in hardness of about 5 percent were observed in quenched specimens compared with prequenched ones. Both results can be explained qualitatively in terms of crystal structure change. All sintered NiAl alloys exhibited a good shape memory effect. The reverse transformation temperature decreased sharply with increasing Al content, with a slope of about 160 K at. percent Al. When the sintered specimens with martensite structure were bent with large deformation at room temperature, they tended to fail by cleavage fracture. Author

N88-24762*# National Aeronautics and Space Administration, Washington, D.C.
ON THE REVERSION PHENOMENA OF Cu-3 PERCENT Ti ALLOYS
K. Nagata, K. Umezu, and S. Nishikawa Jun. 1988 23 p Transl. into ENGLISH from Nippon Kinzoku Gakkaishi (Journal Japan Inst. Metals) (Japan), v. 34, 1970 p 1253-1259 Transl. by SCITRAN, Inc., Santa Barbara, Calif. Original document was prepared by Tokyo Univ.
(Contract NASw-4307)
(NASA-TT-20170; NAS 1.77:20170) Avail: NTIS HC A03/MF A01 CSCL 11F

The reversion phenomena of Cu-3 percent Ti alloys were investigated by measurements of electrical resistivity, hardness, 0.2 percent proof stress and tensile strength, and the X-ray method. Under constant aging conditions, the amount of reversion increases, and the time required for the maximum increment of electrical resistivity becomes shorter as the reversion temperature rises. Also, under the condition of a constant reversion temperature and a constant decrement of electrical resisitivity due to aging treatment, the amount of reversion is greater as the difference between aging and reversion temperature increases. Reversion phenomena of this alloy can be repeated many times almost completely when they are investigated by electrical resistivity 0.2 percent proof stress and tensile strength. However, this reversible

behavior is not complete in the case of hardness measurement. If it follows the spinodal decomposition, this reversion phenomena may be explained qualitatively by the temperature dependence of the critical wave length lambda sub c in the spinodal decomposition theory proposed by Cahn. Author

N88-24763*# National Aeronautics and Space Administration, Washington, D.C.
EFFECT OF SIZE OF PRECIPITATES ON RECRYSTALLIZATION TEMPERATURES IN Cu-Cr, Cu-Zr, AND Cu-Zr-Cr ALLOYS
Takeshi Nagai, Zenzo Henmi, Teruo Sakamoto, and Sigeyasu Koda Jun. 1988 20 p Transl. into ENGLISH from Nippon Kinzoku Gakkaishi (Journal Japan Inst. Metals) (Japan), v. 36, 1972 p 564-571 Transl. by SCITRAN, Inc., Santa Barbara, Calif.
(Contract NASw-4307)
(NASA-TT-20166; NAS 1.77:20166) Avail: NTIS HC A03/MF A01 CSCL 11F

In a previous paper, the reason for high recrystallization temperature in Cu-Cr, Cu-Zr, and Cu-Zr-Cr alloys was considered to be due to the formation of fine precipitates during recrystallization, which obstructed dislocation climbing or sliding and grain boundary migration. The recrystallization behaviors in Cu-Cr, Cu-Zr, and Cu-Zr-Cr alloys quenched, tempered (at 350, 450, 500, 550, and 700 C), heavily cold worked and annealed at various temperatures were studied by resistmetric method, measurements of mechanical properties, and transmission electron microscopy. No fine precipitates were detected at dislocations or sub-boundaries in the low temperature annealing stage, but fine precipitates, which retard recovery, must exist since electrical resistivity decreased by low temperature annealing. The mechanism of retardation of recovery is due to the binding of dislocation jogs and fine precipitates. In the high annealing temperature stage, the growth of precipitates and crystal grains was observed by transmission electron microscopy, and the effect of precipitates on retardation of recrystallization was also detected. The size of the precipitates by tempering before cold working did not affect the recrystallization temperature, because the precipitates were sheared by heavy cold working and became a constant size. Author

N88-24764*# National Aeronautics and Space Administration, Washington, D.C.
A STUDY ON THE PRECIPITATION AND REVERSION BEHAVIORS OF Cu-0.3 PERCENT Cr ALLOY BY THE STEP ANNEALING METHOD
K. Nagata and S. Nishikawa Jun. 1988 26 p Transl. into ENGLISH from Nippon Kinzoku Gakkaishi (Journal Japan Inst. Metal) (Japan), v. 37, 1973 p 1094-1100 Transl. by SCITRAN, Inc., Santa Barbara, Calif. Original document was prepared by Tokyo Univ.
(Contract NASw-4307)
(NASA-TT-20169; NAS 1.77:20169) Avail: NTIS HC A03/MF A01 CSCL 11F

The precipitation and reversion processes of Cu-0.28 wt percent Cr alloys were determined from the electrical resistivity change during step annealing of as-quenched and pre-aged samples. The results obtained are summarized as follows: (1) The precipitation process is separated into two parts by the reversion process taking place in the intermediate temperature range. (2) The activation energies of the two precipitation processes were nearly equal and 1.45 to 1.42 eV. (3) The reversion of low temperature precipitates is not complete but partial. (4) The apparent amount of reversion decreases rapidly as the pre-aging temperature rises. At a constant pre-aging temperature, it increases first with aging time and then decreases rapidly as the pre-aging temperature rises. (5) In the case of high temperature pre-aging for a short time, such as at 500 and 600 C for 2 mins, the reversion of low temperature precipitates is observed. (6) The activation energy obtained from the isothermal reversion curves is about 1.83 eV, and its process seems to be described by the first order equation. Author

N88-24765*# National Aeronautics and Space Administration, Washington, D.C.
ON QUENCH SENSITIVITY OF Cu-Cr ALLOYS
Shiro Sato and Koji Nagata May 1988 21 p Transl. into ENGLISH from Nippon Kinzoku Gakkaishi (Japan), v. 33, 1969 p 1155-1160 Transl. by Scientific Translation Service, Santa Barbara, Calif.
(Contract NASw-4307)
(NASA-TT-20174; NAS 1.77:20174) Avail: NTIS HC A03/MF A01 CSCL 11F

A study was made of the quench sensitivity of Cu-Cr-0.3 to 1.5 percent alloys. The time-temperature- precipitation (TTP) curve was drawn by plotting the electrical conductivity of the specimens which were solution treated and then directly quenched over the temperature range of isothermal head treatment. The quench sensitivity was established by measuring the electrical conductivity, hardness, and tensile strength. The TTP curve had noses at 800 to 850 C and 500 C. As the Cr content increased, the nose of the upper C-curve shifted to the left, but that of the lower C-curve shifted slightly to the right. The precipitations at the upper nose made no contribution to strengthening; those at the lower nose made a large contribution. It is considered that the appearance of two noses on the TTP curve is due to the difference of nucleating sites. That is, at the upper nose temperature Cr would precipitate at such crystal defects as boundaries and insoluble Cr, while at the lower nose temperature Cr would precipitate at such lattice defects as vacancy clusters formed by quenching. Author

N88-24766*# National Aeronautics and Space Administration. Lewis Research Center, Cleveland, Ohio.
ISOTHERMAL AND BITHERMAL THERMOMECHANICAL FATIGUE BEHAVIOR OF A NiCoCrAlY-COATED SINGLE CRYSTAL SUPERALLOY
J. Gayda, T. P. Gabb, and R. V. Miner [1988] 14 p Prepared for presentation at the 6th International Conference on Superalloys, Seven Springs, Pa., 18-22 Sep. 1988; sponsored by the American Inst. of Mining Metallurgical and Petroleum Engineers
(NASA-TM-100907; E-4077; NAS 1.15:100907) Avail: NTIS HC A03/MF A01 CSCL 11F

Specimens of single crystal PWA 1480 with group of zone axes (100) orientation, bare, or with NiCoCrAlY coating PWA 276, were tested in low cycle fatigue (LCF) at 650, 870, and 1050 C, and in simplified bithermal thermomechanical fatigue (TMF) tests between these temperatures. These tests were examined as a bridge between isothermal LCF and general TMF. In the bithermal test, an inelastic strain is applied at one temperature, T sub max, and reversed at T sub min. The out-of-phase (OP) test type imposing tension at T sub min and compression at T sub max received most study, since it was more damaging than the in-phase type. Specifically investigated were the effects of: inelastic strain range, the coating, delta T, T sub max, T sub min, and the environment. Author

27 NONMETALLIC MATERIALS

Includes physical, chemical, and mechanical properties of plastics, elastomers, lubricants, polymers, textiles, adhesives, and ceramic materials.

For composite materials see *24 Composite Materials.*

N88-24767# IKE Associates, Inc., Indianapolis, Ind.
DEVELOPMENT OF TEST METHODS FOR THE ELECTROSTATIC PROPERTIES OF NONHOMOGENEOUS FABRICS, PHASE 2 Final Report, 28 May 1986 - 7 Dec. 1987
Bader I. Rupe 7 Dec. 1987 79 p
(Contract DAAK60-85-C-0074)
(AD-A190853; Rept-22; NATICK-TR-88/010) Avail: NTIS HC A05/MF A01 CSCL 11E

This report covers phase 2 of a project initiated for the purpose of establishing the feasibility of testing for electrostatic charge decay rates, field suppression capabilities, and triboelectric charge generating properties of textiles which incorporate a small

percentage of conductive content, and to provide suitable test equipment and test methodology for determining these characteristics in laboratory situations. Commercially available instrumentation was modified and new equipment designed and fabricated as necessary to achieve the desired results. All modifications and the new equipment were thoroughly documented to facilitate possible later duplication with retention of critical parameters. This effort has resulted in the equipment and methodology necessary to determine the percentage of field suppression offered by the conductive content of a fabric, the charge decay rate of teh nonconductive content of the same fabric, and the triboelectric charge generating properties of any fabric. GRA

N88-24768# California Univ., Santa Barbara. Inst. for Polymers and Organic Solids.
TIME RESOLVED SPECTROSCOPY FACILITY FOR THE STUDY OF NONLINEAR OPTICAL PROPERTIES OF SEMICONDUCTING POLYMERS Final Report
A. J. Heeger 13 Nov. 1987 4 p
(Contract N00014-86-G-0216)
(AD-A191221) Avail: NTIS HC A02/MF A01 CSCL 20L

We have measured the third order susceptibility associated with frequency tripling the fundamental of a Nd:YAG laser in various samples of polyacetylene. By measurement of the amount of third harmonic power reflected from a trans-polyacetylene sample relative to that from a sample of intrinsic silicon, we have determined the magnitude of Xv(3) (all indices parallel to the chain direction) to be XII(3) = 9 + or - 5 x 10 to the -10th esu. Studies on oriented samples indicate that XII(3) dominates all other components of the XII(3) tensor, consistent with the large nonlinear susceptibility being due to the conjugated pi-electron backbone. We have also measured third harmonic generations in cis-rich polyacetylene samples. GRA

N88-24769# Connecticut Univ., Storrs.
PREFERENTIAL SURFACE ADSORPTION IN MISCIBLE BLENDS OF POLYSTYRENE AND POLY(VINYL METHYL ETHER)
Q. S. Bhatia, D. H. Pan, and J. T. Koberstein 2 Feb. 1988 50 p
(Contract DAAL03-86-K-0133)
(AD-A191451; TR-4; ARO-24165.4-MS) Avail: NTIS HC A03/MF A01 CSCL 07F

The surface structure and properties of miscible blends of polystyrene (PS) with poly(vinyl methyl ether) (PVME) have been studied as a function of the blend composition and constituent molecular weights. The lower surface tension of the PVME compared to that of PS results in preferential adsorption of PVME at the surface. The surface PVME enrichment is characterized by measurements of the surface tension as a function of the temperature, accomplished with an automated pendant drop apparatus, and by x-ray photoelectron spectroscopy (XPS). Angle-dependent XPS has been used to determine the surface concentration profiles of the blend constituents. GRA

N88-24770# Virginia Polytechnic Inst. and State Univ., Blacksburg. Dept. of Materials Engineering.
ROLE OF CRACKS IN THE CREEP OF STRUCTURAL POLYCRYSTALLINE CERAMICS Final Report, 15 Apr. 1985 - 30 Sep. 1987
D. P. Hasselman, Kimberly Y. Donaldson, and Anuradha Venkateswaran 15 Jan. 1988 122 p
(Contract DAAG29-85-K-0106)
(AD-A191485; ARO-21710.7-MS) Avail: NTIS HC A06/MF A01 CSCL 11B

A study was conducted of the role of crack formation in the non-linear stress-strain behavior of a fine-grained polycrystalline aluminum oxide at high temperature under conditions of displacement-rate-controlled mechanical loading. The observed deformation behavior could be divided into three regimes. At the lowest values of deformation rate the load levelled off to a constant value without crack formation, consistent with deformation by diffusional creep. Over a range of intermediate values of deformation considerable non-linear deformation took place, manifested by a decrease in stress with increasing strain as the result of strain-softening due to the formation and growth of cracks. At the highest rates of displacement, specimen fracture occurred by the formation of a single crack without significant non-linear deformation and without the formation of additional cracks. These results are discussed in terms of the general mechanisms and kinetics of the deformation of non-ductile solids. GRA

N88-24771# Texas Christian Univ., Fort Worth. Dept. of Chemistry.
SYNTHESIS AND CHARACTERIZATION OF NEW PHOSPHAZENE POLYMERS Final Report, 1984 - 1987
Robert H. Neilson and Patty Wisian-Neilson 21 Jan. 1988 22 p
(Contract DAAG29-84-K-0147)
(AD-A191508; ARO-24179.19-CH) Avail: NTIS HC A03/MF A01 CSCL 07F

We report here the results of our recent studies of poly(alkyl/arylphosphazenes) with particular emphasis on the following areas: (1) the overall scope of, and improvements in, the condensation polymerization method; (2) the characterization of a representative series of these polymers by dilute solution techniques (viscosity, membrane osmometry, light scattering, and size exclusion chromatography), thermal analysis (TGA and DSC), NMR spectroscopy, and X ray diffraction; (3) the preparation and preliminary thermolysis reactions of new, functionalized phosphoranimine monomers; (4) the mechanism of the polymerization reaction; and (5) the derivative chemistry of the preformed poly(alkyl/arylphosphazenes). GRA

N88-24772# Texas Univ., Arlington. Dept. of Chemistry.
ELECTRONIC AND IONIC TRANSPORT IN POLYMERS Quarterly Technical Report, No. 5, 1 Jan. - 31 Mar. 1988
Timothy D. Shaffer 6 Apr. 1988 5 p
(Contract N00014-86-K-0769)
(AD-A191642) Avail: NTIS HC A02/MF A01 CSCL 07F

Ethylmercapto-substituted polythiophenes have been studied and when doped, they show considerably lower conductivity than the parent polythiophene. Calculations have shown that a significant fraction of the positive charge resides on the sulfur of the side chain and this is consistent with the low conductivity. Mechanistic electrochemical studies on these systems have been completed. Studies have continued on the fluorescence modulation induced by the redox switching of polypyrrole. A pyrrole substituted at the 3-position with anthracene has been prepared and characterized. A new soluble, electroactive polymer poly(bis-oxystyryldithiolene nickel) has been prepared and is being studied. A quartz crystal microbalance study of the electropolymerization of pyrrole has been completed and shows that is a useful quantitative tool for polymer deposition studies. A PMO study of aromatic conducting hydrocarbon oligomers and polymers has been completed. GRA

N88-24773# Air Force Wright Aeronautical Labs., Wright-Patterson AFB, Ohio.
NEW POLYISOIMIDES: AN APPROACH TO IN SITU RIGID-ROD POLYIMIDE FORMATION Final Report, Mar. 1983 - Aug. 1985
J. S. Wallace, L. S. Tan, and F. E. Arnold Oct. 1987 53 p
(AD-A191665; AFWAL-TR-87-4071) Avail: NTIS HC A04/MF A01 CSCL 07F

In situ generation of rigid rod polymides was investigated by synthesizing a series of soluble (DMAC) benzidine and p-aminobenzene derivative based polyisoimides. The synthesis was carried out by reacting equimolar amounts of new and commercial diamines with pyro-mellitic dianhydride and then cyclodehydrating the resulting polyamic acids with DCC to give polyisoimides. The newly prepared polymers had I.V.'s ranging from 0.25 to 1.89. Neat and composite films of the polyisoimides were cast from DMAC and isomerized with heating to produce the rigid rod polyimides. The resulting cured films showed no visible signs of

phase separation. A study of the isomerization reaction (polyisoimide to polyimide) was conducted by FTIR. GRA

N88-24774# Air Force Wright Aeronautical Labs., Wright-Patterson AFB, Ohio.
HIGH STRENGTH/SIGH MODULUS AROMATIC HETEROCYCLIC ABA BLOCK COPOLYMERS Final 1 Mar. 1984 - 30 Mar. 1985
T. T. Tsai and F. E. Arnold May 1987 29 p
(AD-A191666; AFWAL-TR-87-4072) Avail: NTIS HC A03/MF A01 CSCL 07F

Described is research on the synthesis and properties of ABA block copolymers composed of a rigid-rod (B) block for reinforcement and a flexible coil (A) block as the matrix. In addition to better processability, it was anticipated that the block copolymer would have better mechanical strength than those from physical blends of the rigid-rod/flexible coil composition. In the block copolymer, the rigid-rod constituent would be chemically bonded to the flexible coil matrix, while in the physically blended molecular composite the reinforcing rigid-rod polymer is only physically entangled in the matrix. Hence, the translation of stress or strain from the reinforcing rigid-rod molecule in the matrix should be more efficient in the block copolymer than in the physical blend. This would not only provide higher tensile strength, but also fracture toughness and dimensional stability. GRA

N88-24775# Pratt and Whitney Aircraft, West Palm Beach, Fla. Government Products Div.
RAPIDLY SOLIDIFIED LIGHTWEIGHT DURABLE DISK MATERIAL Final Report, Jun. 1984 - Mar. 1987
C. C. Law and M. J. Blackburn 15 Dec. 1987 127 p
(Contract F33615-84-C-5067)
(AD-A191697; PW/GPD-FR-19875; AFWAL-TR-87-4102) Avail: NTIS HC A07/MF A01 CSCL 11F

A 2-year program was conducted to explore the potential of NiAl as a high temperature structural material with emphasis on overcoming the low temperature brittleness problem. The inherent ductility characteristics of binary alloys containing 29 a/o Al to 54 a/o Al were studied and it was observed that room temperature ductility was achieved only in alloys with lower amounts of Al. The highest Al level in which room temperature ductility was observed is process dependent, being 35 a/o in the case of the melt spun alloys and 29 a/o for the cast alloys. The brittle to ductile transition temperatures for the higher aluminum alloys (43 a/o - 52 a/o) were found to be in the range 375 c to 625 c, showing no clear trends in terms of the Al content and starting form (castings versus powder). Minor additions of boron significantly raised strength and the brittle to ductile transition temperature. An attempt to improve the ductility of NiAl through modification of the basic deformation behavior was made. GRA

N88-24776# Massachusetts Inst. of Tech., Cambridge.
LIQUID CARBON Report, 1 Sep. 1986 - 31 Aug. 1987
M. S. Dresselhaus and J. Steinbeck 30 Oct. 1987 31 p
(Contract F49629-85-C-0147)
(AD-A191707; AFOSR-88-0224TR) Avail: NTIS HC A03/MF A01 CSCL 07B

In this brief review article on liquid carbon, the following topics are considered: the phase diagram of carbon, methods for preparing and characterizing liquid carbon, a survey of what is known about the properties of liquid carbon, and models that have been used to account for the properties of liquid carbon. Special emphasis is given to experiments on carbon fibers relevant to determination of the electrical resistivity of liquid carbon. GRA

N88-24777# Massachusetts Inst. of Tech., Cambridge.
SIZE EFFECTS IN THE ELECTRICAL RESISTIVITY OF BENZENE-DERIVED CARBON FIBERS Report, 1 Sep. 1986 - 31 Aug. 1987
M. S. Dresselhaus and K. Sugihara 30 Oct. 1987 2 p
(Contract F49629-85-C-0147)
(AD-A191708; AFOSR-88-0232TR) Avail: NTIS HC A02/MF A01 CSCL 11B

Tahar and others in the Dresselhaus group previously reported a size effect in the electrical resistivity of benzene-derived carbon fibers with small diameters. A simple theory indicates that the resistivity has a linear dependence on the reciprocal diameter associated with boundary scattering together with a constant term due to a size-independent scattering process. The observed results are well represented by this relation if the diameter is large enough, while for samples with small diameter, the observed resistivity data are considerably smaller than the theoretical expectation. This discrepancy is removed by considering the correct boundary conditions and by solving the Boltzmann equation. GRA

N88-24778# Massachusetts Inst. of Tech., Cambridge.
RAMAN CHARACTERIZATION OF AsF5-INTERCALATED VAPOR GROWN GRAPHITE FIBERS Report, 1 Sep. 1986 - 31 Aug. 1987
I. Ohana, M. S. Dresselhaus, M. Endo, and Y. C. Liu 30 Oct. 1987 2 p
(Contract F49629-85-C-0147)
(AD-A191709; AFOSR-88-0233TR) Avail: NTIS HC A02/MF A01 CSCL 11B

A great deal of attention has recently been focussed on the very high electrical conductivity reported in arsenic penta fluoride intercalated vapor grown graphite fibers, previously heat treated to high temperatures. To characterize individual arsenic penta fluoride intercalated vapor grown fibers for stage index and staging fidelity along the fiber length, Raman scattering measurements have been carried out. These results are discussed in terms of their high electrical conductivity and structural features. GRA

N88-24779# Massachusetts Inst. of Tech., Cambridge.
STRESS MEASUREMENTS IN GRAPHITE FIBERS BY LASER RAMAN SPECTROSCOPY Report, 1 Sep. 1986 - 31 Aug. 1987
H. Sakata, G. Dresselhaus, and M. Endo 30 Oct. 1987 3 p
(Contract F49629-85-C-0147)
(AD-A191710; AFOSR-88-0234TR) Avail: NTIS HC A02/MF A01 CSCL 11B

Heat treated benzene derived graphite fibers have been characterized by Raman spectroscopy as a function of applied uniaxial tensile stress. Linear shifts are observed in the frequency of the Raman lines as a function of the applied stress. Thus it is shown that laser Raman spectroscopy provides a powerful nondestructive technique for monitoring the local stress variations near the surface of carbon fibers. The Raman microprobe used in this experiment provides approximately two micrometers spatial resolution within the optical skin depth. This spatial resolution is much higher than conventional techniques such as X-ray analysis which typically has a spatial resolution of several millimeters. Stress measurements in semiconductors such as Silicon, Germanium and Gallium Arsenide by Raman spectroscopy have been previously reported. Since benzene-derived graphite fibers are typically between ten and 20 micrometers in diameter, Raman spectroscopy has been used to examine the stress variation within the optical skin depth (approximately 600 Angstroms for light scattering at 4880 Angstroms) of single carbon fibers. GRA

N88-24780# Massachusetts Inst. of Tech., Cambridge.
ELECTRICAL CONDUCTION IN THIN FILM CARBONS Report, 1 Sep. 1986 - 31 Aug. 1987
K. Sugihara and M. S. Dresselhaus 30 Oct. 1987 3 p
(Contract F49629-85-C-0147)
(AD-A191726; AFOSR-88-0230TR) Avail: NTIS HC A02/MF A01 CSCL 07B

The interaction between electrons and phonons in a thin carbon film is investigated. Sound wave propagation in a thin carbon film has a small sound velocity and small damping. The scattering of electrons by phonons associated with the Rayleigh wave is found to be responsible for the anomalous temperature dependence of the resistivity and for the negative magnetoresistance of pregraphitic carbons at low temperatures. GRA

N88-24781# Massachusetts Inst. of Tech., Cambridge.
ELECTRON-RAYLEIGH WAVE INTERACTION IN THIN FILM CARBONS Report, 1 Sep. 1986 - 31 Aug. 1987
K. Sugihara 30 Oct. 1987 4 p
(Contract F49629-85-C-0147)
(AD-A191727; AFOSR-88-0229TR) Avail: NTIS HC A02/MF A01 CSCL 07B

Sound wave propagation in thin film carbon is investigated in the long wavelength approximation. Strain-free and stress-free boundary conditions lead to the same solution. The Rayleigh wave, with a small damping constant and with polarization perpendicular to the layer planes, has a small sound velocity. Since the long wavelength phonon energies associated with this wave are very small, these phonons are readily excited even at very low temperatures. Furthermore, those phonons strongly scatter carriers at low temperatures. Of particular interest for transport properties is the determination of the carrier relaxation time for very thin film thicknesses. These phonons are also responsible for the temperature dependence of the negative magnetoresistance of pregraphitic carbons at low temperatures. GRA

N88-24782# Massachusetts Inst. of Tech., Cambridge.
PHOTOCONDUCTIVITY IN CARBON FIBERS Report, 1 Sep. 1986 - 31 Aug. 1987
J. Steinbeck, F. Yu, G. Braunstein, G. Desselhaus, and M.S. Dresselhaus 30 Oct. 1987 13 p Prepared in cooperation with Bell Communications Research, Inc., Murray Hill, N.J.
(Contract F49629-85-C-0147)
(AD-A191728; AFOSR-88-0228TR) Avail: NTIS HC A03/MF A01 CSCL 11B

Photoconductivity has been observed in vapor grown graphite fibers with a high quantum efficiency of carriers generated by photons. The photocurrent varies approximately as the square root of the intensity of illumination. No change in the growth or decay time of the photocurrent is observed as a function of illumination intensity or of the temperature. The photocurrent observed in semi-metallic graphite fibers is attributed to transitions between localized defect states which act as traps for photo-excited carriers. As the heat treatment temperature is raised above 1500 Kelvin, vapor grown graphite fibers show a decrease in the photocurrent due to the annealing of defects and an increase in the electron-hole recombination time. GRA

N88-24783# Massachusetts Inst. of Tech., Cambridge.
EFFECT OF UNIAXIAL STRESS ON THE RAMAN SPECTRA OF GRAPHITE FIBERS Report, 1 Sep. 1986 - 31 Aug. 1987
H. Sakata, G. Dresselhaus, M. S. Dresselhaus, and M. Endo 30 Oct. 1987 16 p Prepared in cooperation with Shinshu Univ., Nagano Japan
(Contract F49629-85-C-0147)
(AD-A191730; AFOSR-88-0226TR) Avail: NTIS HC A03/MF A01 CSCL 11B

Measurements of the effect of uniaxial stress on the frequency of the zone center optical phonons in heat-treated benzene-derived graphite fibers have been performed using first-order Raman scattering. Application of uniaxial stress along the fiber axis was found to cause polarization-dependent splittings and shifts of the Raman peaks of the zone center doubly degenerate optical phonons. From these observed splittings and shifts, experimental values for the phenomenological coefficients which describe the changes in the elastic constant of these phonons with strain were determined. It is concluded that Raman spectroscopy can be used to characterize the local stress or strain conditions of graphite fibers nondestructively. GRA

N88-24784# Naval Ocean Systems Center, San Diego, Calif.
THERMAL CONDUCTIVITY OF HARD ANODIZED COATINGS ON ALUMINUM Professional Paper, period ending Jun. 1987
T. R. Ogden Nov. 1987 6 p Previously announced in IAA as A87-45388
(AD-A191755) Avail: NTIS HC A02/MF A01 CSCL 11C

Thermal conductivities of several commercial hard anodic coatings are measured using a transient heat-flow technique. These coatings were found to be effective heat insulators with thermal conductivities of the commercial coatings averaging 0.7 W/m/K. A laboratory anodization facility was assembled and the variation of thermal conductivity of the anodic coatings measured as a function of the anodization parameters. Preliminary results show that thermal conductivities as high as 1.3 W/m/K can be obtained in thick anodic coatings by optimizing the anodization parameters. GRA

N88-24785# Akron Univ., Ohio. Inst. of Polymer Science.
ADHESION BETWEEN POLYSTYRENE AND POLYMETHYLMETHACRYLATE
K. Cho and A. N. Gent Mar. 1988 31 p
(Contract N00014-85-K-0222)
(AD-A192050; TR-13) Avail: NTIS HC A03/MF A01 CSCL 11I

Measurements have been made of the energy required to break through unit area of polystyrene (PS), polymethylmethacrylate (PMMA), and joints prepared by molding the two polymers in contact. The interface was significantly weaker than either adherend, but surprisingly strong for two incompatible materials. Microscopy and selective dyeing revealed that fracture took place at the interface itself, with no appreciable transfer of material from one side to the other. It is concluded that van der Waals interactions are sufficient to create relatively strong bonds. GRA

N88-24786# Rockwell International Corp., Thousand Oaks, Calif. Science Center.
ENVIRONMENTAL INTEGRITY OF COATING/METAL INTERFACE Annual Progress Report No. 1, 1 Feb. 1987 - 31 Jan. 1988
M. Kendig, R. Addison, and S. Jeanjaquet Jan. 1988 32 p
(Contract N00014-87-C-0075)
(AD-A192184; SC5508-APR) Avail: NTIS HC A03/MF A01 CSCL 07F

Corrosion of polymer coated steel in neutral media entails the initiation of anodic dissolution of the metal at defects in the coating with the cathodic reduction of oxygen at the adjacent interface. The cathodic reduction of oxygen produces a buildup of NaOH at the interface which enhances adhesion loss which leads to the propagation of corrosion. In-situ acoustic microscopy of a coating undergoing cathodic disbonding at constant potential has allowed evaluation of both the kinetics and microscopic structure of the disbond front with detail not previously attained. Disbonding of a hydroxy-terminated polybutadiene coating from polished and degreased steel in 0.5 M NaCl has been examined in-situ as a function of applied potential. The results show that potentials more negative than -550 mV vs Ag/AgCl accelerate disbonding by the formation of a weak fluid boundary layer at the coating/metal interface just ahead of electroosmotically produced approximately 50 micro m blisters. Concentration of NaOH in the microblister weakens the polymer metal interface while the osmotic pressure in the microblisters provides the mechanical force necessary to rupture the coating/metal bond. GRA

N88-24787# Universite de Technologie de Compiegne (France). Dept. de Genie Mecanique.
INFLUENCE OF CARBON FIBER SURFACE TREATMENT Final Report [INFLUENCE DES TRAITEMENTS DE SURFACE DES FIBRES DE CARBONE]
A. Oberlin and M. Guigon 1987 41 p In FRENCH
(Contract DRET-84-011)
(ETN-88-92536) Avail: NTIS HC A03/MF A01

The effects of crystallinity, fiber orientation, and oxidation on polyacrylonitrile carbon fibers were tested by heating them in a nitrogen atmosphere at temperatures from 250 to 1000 C. Results show that the crystallographic state of the oxidized polymer is an important parameter in determining plasticity, time of fiber orientation, and homogeneity. Carbonization under stress is necessary to achieve a good orientation. Heating conditions during carbonization are vital in determining the final elementary composition of the fiber. ESA

N88-24788# Universite des Sciences et Techniques de Lille (France). Lab. de Structure et Proprietes de l'Etat Solide.
THE INFLUENCE OF THE CHEMICAL NATURE OF RESINS ON THEIR RETICULATION KINETICS AND THE CONSEQUENCES FOR THEIR NONELASTIC MECHANICAL PROPERTIES Final Report [INFLUENCE DE LA NATURE CHIMIQUE DES RESINES SUR LEUR CINETIQUE DE RETICULATION ET LES CONSEQUENCES SUR LEURS PROPRIETES MECANIQUES NON-ELASTIQUES]
B. Escaig, G. Coulon, and X. Caux 16 Mar. 1988 50 p In FRENCH
(Contract DRET-84-168)
(ETN-88-92539) Avail: NTIS HC A03/MF A01

The mechanical properties of polystyrylpyridine (PSP) and epoxy resins were related to their chemical structure. Reticulation kinetics and the local and global mechanical capacities of the materials were determined as a function of molecular and mechanical characteristics (dynamic and nonelastic). For epoxy resins, the effect of reticulation density on nonelastic mechanical properties (elastic limit, consolidation) is shown. It is shown that thermosetting resins can be studied using physical metallurgy concepts. The measurement of plastic consolidation for slight deformations and thermodynamic analysis at the threshold of plastic flow are very efficient ways to link fabrication conditions to mechanical behavior under slight and considerable plastic deformation. ESA

N88-24789# Virginia Polytechnic Inst. and State Univ., Blacksburg. Dept. of Mechanical Engineering.
CALCULATIONAL MODEL DEVELOPMENT FOR FIBROUS THERMAL INSULATION TRANSIENT TEST PROCEDURES
J. R. Thomas, Jr. Feb. 1988 68 p
(Contract DE-AC05-84OR-21400)
(DE88-007843; ORNL/Sub-85-27494/1) Avail: NTIS HC A04/MF A01

A new theoretical model of transient combined radiation and conduction heat transfer in fibrous insulations has been developed and tested by comparison to experimental data obtained with the ORNL flat screen tester. This model predicts results which agree with this data to within +/- 1.2 C for all of the transient test results available. Sensitivities of the model to the pertinent radiative transfer properties of the insulation have been determined, and are presented in this report. The most important findings are: (1) the extinction coefficient of SRM 1451 fiberglass insulation is approximately 650/m, and (2) the fiberglass used in the tests almost certainly contained sufficient moisture to significantly affect the test results. DOE

N88-24790# Oak Ridge National Lab., Tenn.
AN INVESTIGATION OF CERAMIC COATINGS FOR PROTECTION OF SiC FROM HIGH-TEMPERATURE CORROSION
J. I. Federer Feb. 1988 46 p
(Contract DE-AC05-84OR-21400)
(DE88-007873; ORNL/TM-10606) Avail: NTIS HC A03/MF A01

Silicon carbide (SiC) ceramics are susceptible to corrosion by certain industrial furnace environments. This behavior would limit the use of SiC components in ceramic heat exchangers. Because oxide ceramics corrode substantially less in the same environments, ceramic coatings have been investigated for corrosion protection. Coatings with Al sub 2 O sub 3, SiO sub 2, or ZrO sub 2 as the main constituent were applied to sintered alpha and recrystallized (CS101) SiC substrates. The coated specimens were thermally cycled between room temperature and 1200 C as a test of adherence. Some coatings adhered better to the inherently rougher CS101 SiC; however, most coatings did not adhere to either substrate. Two Al sub 2 O sub 3-based coatings developed cracks but remained intact during thermal cycling, and two ZrO sub 2-based coatings were adherent without cracks. These four coatings were subjected to corrosion testing at 1200 C in an oxidizing atmosphere containing Na sub 2CO sub 3. None of these four coatings exhibited the desired corrosion resistance in this test. Coated samples, however, corroded less than an uncoated sample, indicating that coatings can improve corrosion resistance. DOE

N88-24791*# National Aeronautics and Space Administration. Marshall Space Flight Center, Huntsville, Ala.
THE ELECTROKINETIC BEHAVIOR OF CALCIUM OXALATE MONOHYDRATE IN MACROMOLECULAR SOLUTIONS
P. A. Curreri, G. Y. Onoda, Jr., and B. Finlayson (Florida Univ., Gainesville.) [1988] 22 p Submitted for publication
(NASA-TM-101144; NAS 1.15:101144) Avail: NTIS HC A03/MF A01 CSCL 11B

Electrophoretic mobilities were measured for calcium oxalate monohydrate (COM) in solutions containing macromolecules. Two mucopolysaccharides (sodium heparin and chrondroitin sulfate) and two proteins (positively charged lysozyme and negatively charged bovine serum albumin) were studied as adsorbates. The effects of pH, calcium oxalate surface charge (varied by calcium or oxalate ion activity), and citrate concentration were investigated. All four macromolecules showed evidence for chemical adsorption. The macromolecule concentrations needed for reversing the surface charge indicated that the mucopopolysacchrides have greater affinity for the COM surface than the proteins. The amount of proteins that can chemically adsorb appears to be limited to approximately one monomolecular layer. When the surface charge is high, an insufficient number of proteins can chemically adsorb to neutralize or reverse the surface charge. The remaining surface charge is balanced by proteins held near the surface by longer range electrostatic forces only. Citrate ions at high concentrations appear to compete effectively with the negative protein for surface sites but show no evidence for competing with the positively charged protein. Author

N88-24792# Office National d'Etudes et de Recherches Aerospatiales, Paris (France). Direction Scientifique des Materiaux.
STRUCTURAL STUDY OF THE TGMDA-DDS SYSTEM [ETUDE STRUCTURALE DU SYSTEME TGMDA-DDS]
J. Ancelle, A. J. Attais, B. Bloch, and G. Gillmann Aug. 1986 137 p In FRENCH
(Contract DRET-85-34-001)
(ONERA-RT-4/3346-M; ETN-88-92143) Avail: NTIS HC A07/MF A01

A high resolution carbon 13 nuclear magnetic resonance solid state procedure was employed to characterize the formation and structure of the cross-linked network of an epoxy resin system. The resulting complex spectra were identified by reference to carbon 13 in a solution of model components. Cycling reactions are identified. The intermolecular ether forming reaction looks improbable. The plastic deformation behavior of hardened resin was also studied using the same method. ESA

N88-24793# Societe Nationale Industrielle Aerospatiale, Suresnes (France). Direction de la Qualite.
CALCULATION OF ASSEMBLIES BONDED WITH QUASI-ELASTIC ADHESIVES [CALCUL DES ASSEMBLAGES COLLES. ADHESIFS QUASI-ELASTIQUES. PROCES-VERBAL 47-632/F]
J. N. Dewas, J. P. Jeandreau, and J. Odorico 21 Aug. 1987 82 p In FRENCH
(Contract DRET-84-34-497-00-470-75-01)
(Rept-47-632/F; ETN-88-92146) Avail: NTIS HC A05/MF A01

A bibliographic study including analytic and finite element methods for calculating adhesive-bonded elements is presented. A finite element two dimensional code, CASTOR, was adapted to the analysis of structures in the elastic domain. Structural adhesives were studied to furnish the required mechanical characterization data. Strain measurements agree well with the model results. ESA

N88-24794# Sandia National Labs., Albuquerque, N. Mex.
DIFFUSION OF HOMOPOLYMERS INTO NONEQUILIBRUM DIBLOCK COPOLYMER STRUCTURES
P. F. Green, T. P. Russell, and R. Jerome 1988 9 p Presented at the International Symposium on New Trends in Physics and Physical Chemistry of Polymers, Toronto, Ontario, 5 Jun. 1988 Prepared in cooperation with IBM, San Jose, Calif. and Liege Univ., Belgium
(Contract DE-AC04-76DP-00789)
(DE88-005306; SAND-87-2509C; CONF-880660-1) Avail: NTIS HC A02/MF A01

Of concern in the present report is the diffusion of homopolmer chains into microphase separated symmetric diblock copolymer hosts. Forward recoil spectrometry was used to study the diffusion of deuterated PS (d-PS) and of d-PMMA into two symmetric diblock copolymer hosts comprised of polystyrene (PS) and polymethylmethacrylate (PMMA). The molecular weight and temperature dependence of diffusion are reported. DOE

N88-24795# Pacific Northwest Labs., Richland, Wash.
ENVIRONMENTAL EFFECTS ON SLOW CRACK GROWTH IN SILICON NITRIDE
C. H. Henager, Jr. and R. H. Jones Jan. 1988 13 p Presented at the 12th Annual Conference on Composites and Advanced Ceramics, Cocoa Beach, Fla., 20 Jan. 1988
(Contract DE-AC06-76RL-01830)
(DE88-007206; PNL-SA-15072; CONF-880118-3) Avail: NTIS HC A03/MF A01

Slow crack growth measurements are being conducted to determine crack velocity versus stress intensity as a function of chemical environment in advanced ceramic materials. Controlled, artificial flaws are placed in the flat tensile faces of hot pressed Si3N4 tensile specimens (2.3 x 2.3 x 21.6 mm gage) and oriented to open in mode 1 on tensile loading. Tests have been performed in air and without a coating of sodium sulfate at 1573 K. Results indicate that slow crack growth in the presence of sodium sulfate is about twice as fast as in air. DOE

N88-24796# Syracuse Univ., N. Y. Dept. of Chemical Engineering and Materials Science.
MECHANISMS OF GAS PERMEATION THROUGH POLYMER MEMBRANES: RENEWAL PROPOSAL FOR PERIOD DECEMBER 1, 1986 - NOVEMBER 30, 1989 Final Report
S. A. Stern 1988 82 p
(Contract DE-AC02-78ER-05015)
(DE88-007436; DOE/ER-05015/T5) Avail: NTIS HC A05/MF A01

The recent progress in membrane separation technology can be sustained only through the development of new types of polymer membranes with a higher intrinsic permeability and selectivity for specified gases. Objectives of this project are to investigate the mechanisms of transport of small molecules in and through nonporous polymers membranes, as well as the dependence of these mechanisms on polymer structure. Both experimental and theoretical studies will be conducted. DOE

N88-24797*# National Aeronautics and Space Administration, Washington, D.C.
DIFFERENTIAL TECHNOLOGY IN PLASTICS INDUSTRIES DIFFERENTIATION IN COMBINATION TECHNOLOGY NONFLAMMABILITY TECHNOLOGY
A. Taniuchi Jun. 1988 24 p Transl. into ENGLISH from Purasuchikkusu Eji (Japan), v. 33, no. 4, 1987 p 130-137 Transl. By SCITRAN, Inc., Santa Barbara, Calif. Original document was prepared by Daiichi Kogyo Seiyaku, Inc.
(Contract NASw-4307)
(NASA-TT-20256; NAS 1.77:20256) Avail: NTIS HC A03/MF A01 CSCL 11B

Flame-retardant techniques for plastics were reviewed. Flame retardants, mainly halogen or phosphate containing materials were summarized with their melting point and decomposition temperatures. Future trends in Western Europe and America are also discussed. Author

N88-24798*# National Aeronautics and Space Administration, Washington, D.C.
SAMPLE DECOMPOSITION IN SEALED TEFLON VESSELS
Tetsuo Uchida Jun. 1988 19 p Transl. into ENGLISH from Bunseki (Japan), v. 1, 1986 p 9-15 Transl. by SCITRAN, Inc., Santa Barbara, Calif.
(Contract NASw-4307)
(NASA-TT-20189; NAS 1.77:20189) Avail: NTIS HC A03/MF A01 CSCL 11B

A review is presented on the quality and structure of teflon vessels, and the merits, drawbacks and care needed for the decomposition of samples in them. Examples are given to illustrate the decomposition of organic and silicate samples in sealed teflon vessels. Author

N88-24699# Imperial Chemical Industries Ltd., Runcorn (England).
THE SYNTHESIS OF POLYPHENYLENE FROM A CIS-DIHYDROCATECHOL BIOLOGICALLY PRODUCED MONOMER
D. G. H. Ballard, A. Courtis, I. M. Shirley, and S. C. Taylor (ICI Biological Products Business, Billingham, England) *In* American Society for Composites, Proceedings of the American Society for Composites 1987 p 53-94 (For primary document see N88-24693 18-24)
Avail: NTIS HC A06/MF A01 CSCL 11B

28 PROPELLANTS AND FUELS

Includes rocket propellants, igniters, and oxidizers; their storage and handling procedures; and aircraft fuels.

For related information see also *07 Aircraft Propulsion and Power, 20 Spacecraft Propulsion and Power,* and *44 Energy Production and Conversion.*

N88-24799# Lockheed-California Co., Burbank.
FUEL CONTAINMENT CONCEPTS: TRANSPORT CATEGORY AIRPLANES Final Report, Jan. 1986 - Mar. 1987
Gil Wittlin Nov. 1987 214 p
(Contract DTFA03-86-C-00005)
(AD-A189818; LR-31216; DOT/FAA/CT-87/18) Avail: NTIS HC A10/MF A01 CSCL 01C

This report describes a four phase study to identify potential fuel containment concepts for transport category aircraft. A literature survey was performed and the relative contributions from 53 documents are noted. Transport airplane data are summarized including the results from full-scale airplane crash tests and section tests. Analyses results which depict dynamic pulses are presented. Several reports including the U.S. Army Crash Survival Design Guide and the Special Aviation Fire and Explosion Reduction (SAFER) Advisory Committee are discussed in detail. Several fuel containment structural design concepts are evaluated with regard to both wing and fuselage usage. The state-of-the-art technology is summarized in this report. Included in this summary is a priority ranking of approaches. A selection of approaches is described. The selected concepts are reviewed with regard to benefit and penalties. The concepts are prioritized in order of effectiveness. GRA

N88-24800# Sandia National Labs., Livermore, Calif. Combustion Research Facility.
THE BURNING OF HAN-BASED (HYDROXYLAMMONIUM NITRATE) LIQUID PROPELLANTS
Steven R. Vosen Feb. 1988 27 p Presented at the 22nd International Symposium on Combustion, Seattle, Wash., 14 Aug. 1988
(Contract DE-AC04-76DR-00789)
(DE88-006863; SAND-88-8600; CONF-880802-6) Avail: NTIS HC A03/MF A01

To improve the understanding of the physical processes which occur during the combustion of liquid propellants (LP), a strand burner was used to study hydroxylammonium nitrate-based LP

flames. By observing the combustion of LP in such an arrangement, much has been deduced of the physical processes that occur during LP ignition and combustion. Combustion experiments were performed in which mixtures of the salts hydroxylammonium nitrate (HAN) and triethanolammonium nitrate (TEAN) in water were ignited by an electric discharge in a vessel at pressures of up to 30 MPa. Results of experiments conducted during turbulent combustion are: (1) the combustion of HAN-based LP occurs in two stages in which the liquid phase decomposition of HAN is followed by the decomposition of TEAN, (2) the turbulent combustion rate of LP 1846 decreases with increasing pressure. This variation of apparent burning rate with pressure, a result which is not seen in single component propellant combustion, is attributed to changes in the stability of the liquid-gas interface with pressure, and (3) a model of the combustion of HAN-based liquid propellants as it occurs in bulk has been presented, showing the reaction sequence of the components of HAN-based liquid propellants. DOE

N88-24801# Fraunhofer Inst. fuer Kurzzeitdynamik, Freiburg im Breisgau (West Germany).
ELECTRICAL IGNITION OF HAN-BASED LIQUID PROPELLANTS Interim Reports Nos. 1-3, 1 Oct. 1986 - 1 Oct. 1987
G. Klingenberg 1 Oct. 1987 19 p
(Contract DAJA45-86-C-0029)
(AD-A191349) Avail: NTIS HC A03/MF A01 CSCL 19A

The scope of this study is to investigate and optimize the electrical ignition of hydroxyl-ammonium nitrate (HAN) based liquid monopropellants (LP) in conjunction with its use as a propellant charge in the regenerative liquid propellant gun (RLPG). In this research, the fundamentals of LP ignition will be investigated which will contribute to the design at electrical igniter devices suitable for large caliber RLPG systems. Specific goals are: to investigate various means of electrical ignition of LP, to develop quantitative ignition criteria, to achieve reproducible igniter output energies, to obtain igniter energy effluxes that are capable of starting the regenerative process and producing sustained ignition in the gun chamber, to scale the ignition requirements to large volumes. GRA

N88-24802# Colorado Univ., Boulder. Dept. of Mechanical Engineering.
CHEMICAL KINETICS OF NITRAMINE PROPELLANT COMBUSTION Interim Technical Report, 1, Oct. 1986 - 30 Sep. 1987
Melvyn C. Branch Nov. 1987 14 p
(Grant AF-AFOSR-00006-84)
(AD-A191556; AFOSR-88-0044TR) Avail: NTIS HC A03/MF A01 CSCL 19A

The decomposition of many solid reactants during combustion leads to the formation of gaseous hydrocarbons and oxides of nitrogen which can react to support a flame above the surface of the solid. These flames can provide heat which is fed back to the propellant surface and thereby influence the burning rate of the solid. In the case of nitramine based solid rocket propellants, the gas phase decomposition products include significant amounts of Formaldehyde. Nitrogen dioxide, Hydrogen Cyanide, Nitric oxide, Nitrous oxide, oxygen. This study is intended to provide experimental data on the structure of hydrocarbon flames supported by oxides of nitrogen in order to establish the reaction mechanism for such flames. Laminar, premixed, flat flames of methane/NO2/O2 and CH2O/NO2/O2 have been investigated and a reaction mechanism is suggested which accounts for all of the major observations in the data. GRA

N88-24803# Geo-Centers, Inc., Newton, Mass.
REFERENCE FILTERS FOR ELECTROSTATIC CHARGING TENDENCY MEASUREMENTS OF FUELS Final Report, Jul. 1986 - Jun. 1987
Wilbur A. Affens Sep. 1987 36 p
(Contract N00014-86-C-2288; Z08-38)
(AD-A191717; GC-TR-87-1628-F) Avail: NTIS HC A03/MF A01 CSCL 21D

A study has been made to determine whether laboratory filter papers might be suitable as reference filters for the determination of charging tendencies of jet fuels as measured in the EXXON Mini-Static Tester (MST). It was concluded that, compared to commercial fuel filters, these filters do not generate enough charge to afford repeatable and reliable measurements. Some correlation was observed between the polarity of the generated charges and the nature of the filter paper surfaces. However, attempts to repeat these experiments after a time period of about six to eight months were unsuccessful because of variations in the data, particularly that of polarity of the charge. It is suggested that the variations may have been due to relative humidity and temperature changes. Another possible explanation might be changes in fuel composition due to degradation. A few studies of some ion exchange resin coated filter papers suggest some tentative generalizations. It was observed that the flow rate of fuel through each type of filter was not constant for any given run. Since it was necessary to have accurate flow rate data for each filter to be able to calculate charging tendency from the measured streaming current, a method was devised to make this measurement. GRA

N88-24804# Pacific Northwest Labs., Richland, Wash.
PRODUCTION COSTS OF HYDROCARBON FUELS FROM BIOMASS
D. J. Stevens and E. I. Wan Feb. 1988 27 p Presented at the Energy from Biomass and Wastes, New Orleans, La., 15 Feb. 1988
(Contract DE-AC06-76RL-01830)
(DE88-006667; PNL-SA-15622; CONF-880215-3) Avail: NTIS HC A03/MF A01

Biomass is an important energy resource offering excellent potential for the future. This expected energy impact is to be achieved in part by liquid transportation fuels derived from biomass. Liquid fuels are more energy dense than biomass itself and more closely match existing end-use patterns. DOE's Biofuels and Municipal Waste Technology Division is sponsoring research on the production of liquid hydrocarbon fuels from biomass which are generated by first converting the biomass resource to biocrude oils and then upgrading those to hydrocarbon products. This paper presents an evaluation of production costs for hydrocarbon fuels from two advanced biomass-to-gasoline processes being sponsored by DOE. These include one conceptual process where biomass is rapidly pyrolyzed and the resulting biocrude oil is hydrotreated to gasoline hydrocarbons. A second conceptual process is also considered where biomass is pyrolyzed and the intermediate biocrude vapors are upgraded over zeolite catalysts. A technoeconomic analysis is performed for these two concepts based both on currently attainable experimental results as well as projected results assumed to be attainable with additional research. DOE

N88-24805# Sandia National Labs., Albuquerque, N. Mex.
THERMAL DECOMPOSITION STUDIES OF EXPLOSIVES FOR COMPONENT APPLICATIONS
R. G. Jungst 1988 39 p Presented at the Center for Explosives Technology Research Seminar Series, Socorro, N. Mex., 25 Mar. 1988
(Contract DE-AC04-76DP-00789)
(DE88-007201; SAND-88-0765C; CONF-880365-1) Avail: NTIS HC A03/MF A01

The explosives PETN and HNS are currently found in a variety of Sandia devices. We have carried out a number of special studies to measure decomposition rates of these materials in hardware at moderate temperatures. The goal of this work was to generate information to enable predictions of component lifetimes to be made. This presentation will discuss sampling and measurement techniques for decomposition products and show results of their application to components containing PETN and HNS. DOE

N88-24806# Sandia National Labs., Albuquerque, N. Mex.
A COMPATIBLE ENCAPSULANT FOR EXPLOSIVES

K. B. Wischmann 1988 10 p Presented at the SAMPE Electronic Materials and Processes Conference, Seattle, Wash., 14 Jun. 1988
(Contract DE-AC04-76DP-00789)
(DE88-007212; SAND-87-2087C; CONF-880690-1) Avail: NTIS HC A02/MF A01

Many epoxy resin encapsulants are amine cured; unfortunately, amine cured systems have long-term compatibility problems with certain explosives, i.e., HNS (hexanitrostilbene) and HNAB (hexanitroazobenzene). In response to this problem, an epoxy/anhydride encapsulant was developed that does not rely on amine catalysts. A new catalyst, an organochromium complex, was employed which was found to be compatible with the above explosives. This catalyst provided good cures at temperatures as low as 80 C; normally epoxy/anhydride systems require curing at temperatures well above 100 C. Our epoxy/anhydride formulation exhibits low exotherms, long pot life, and can be compounded with glass microballoons to attenuate shock and lower the encapsulant's coefficient of thermal expansion. This paper documents the formulation, physical property characterization, processing, and compatibility studies. DOE

N88-24807# Lockheed-California Co., Burbank.
FUEL CONTAINMENT CONCEPTS: TRANSPORT CATEGORY AIRPLANES Final Report, Jan. 1986 - Mar. 1987
G. Wittlin Nov. 1987 214 p
(Contract DTFA03-86-C-00005)
(DOT/FAA/CT-87/18; LR-31216) Avail: NTIS HC A10/MF A01

A four phase study to identify potential fuel containment concepts for transport category aircraft is described. The study includes a review and evaluation of: accident crash test and analyses data; design guidelines, specifications, and criteria; design procedures; state-of-the-art technology; and design studies and conclusions. A literature survey was performed and the relative contributions from 53 documents are noted. Transport airplane data are summarized including the results from full-scale airplane crash tests and section tests. Analyses results which depict dynamic pulses are presented. Several reports including the U.S. Army Crash Survival Design Guide and the Special Aviation Fire and Explosion Reduction (SAFER) Advisory Committee are discussed in detail. Several fuel containment structural design concepts are evaluated with regard to both wing and fuselage usage. The state-of-the-art technology is summarized. Included in this summary is a priority ranking of approaches. A selection of approaches is described. The selected concepts are reviewed with regard to benefit and penalties. The concepts are prioritized in order of effectiveness. Author

N88-24808*# National Aeronautics and Space Administration. Lewis Research Center, Cleveland, Ohio.
CHARACTERIZATION OF ALUMINUM/RP-1 GEL PROPELLANT PROPERTIES
Douglas C. Rapp (Sverdrup Technology, Inc., Cleveland, Ohio.) and Robert L. Zurawski 1988 23 p Presented at the 24th Joint Propulsion Conference, Boston, Mass., 11-13 Jul. 1988; sponsored by AIAA, ASME, SAE and ASEE
(NASA-TM-100951; E-4242; NAS 1.15:100951; AIAA-88-2821)
Avail: NTIS HC A03/MF A01 CSCL 21I

Research efforts are being conducted by the NASA Lewis Research Center to formulate and characterize the properties of Al/RP-1 and RP-1 gelled propellants for rocket propulsion systems. Twenty four different compositions of gelled fuels were formulated with 5 and 16 micron, atomized aluminum powder in RP-1. The total solids concentration in the propellant varied from 5 to 60 wt percent. Tests were conducted to evaluate the stability and rheological characteristics of the fuels. Physical separation of the solids occurred in fuels with less than 50 wt percent solids concentration. The rheological characteristics of the Al/RP-1 fuels varied with solids concentration. Both thixotropic and rheopectic gel behavior were observed. The unmetallized RP-1 gels, which were formulated by a different technique than the Al/RP-1 gels, were highly viscoelastic. A history of research efforts which were conducted to formulate and characterize the properties of metallized propellants for various applications is also given. Author

N88-25050# Aerospace Research Corp., Roanoke, Va.
EVALUATION OF MANURE AS A FEEDSTOCK FOR GAS TURBINES
Joseph T. Hamrick *In* Pacific Northwest Labs., Proceedings of the 1987 Biomass Thermochemical Conversion Contractors' Review Meeting Nov. 1987 p 151-169 Sponsored by DOE
(For primary document see N88-25041 18-44)
Avail: NTIS HC A09/MF A01

N88-25051# Aerospace Research Corp., Roanoke, Va.
A 3 MW WOOD FIRED GAS TURBINE AT RED BOILING SPRINGS, TENNESSEE
Joseph T. Hamrick *In* Pacific Northwest Labs., Proceedings of the 1987 Biomass Thermochemical Conversion Contractors' Review Meeting Nov. 1987 p 171-182 Sponsored by DOE
(For primary document see N88-25041 18-44)
Avail: NTIS HC A09/MF A01

29 MATERIALS PROCESSING

Includes space-based development of products and processes for commercial applications.
For biological materials see *55 Space Biology*.

N88-24809*# National Aeronautics and Space Administration. Marshall Space Flight Center, Huntsville, Ala.
DEMIXING OF AQUEOUS POLYMER TWO-PHASE SYSTEMS IN LOW GRAVITY
S. Bamberger, J. M. Harris, J. K. Baird, J. Boyce, J. M. VanAlstine, R. S. Snyder, and D. E. Brooks (British Columbia Univ., Vancouver.) [1986] 26 p Submitted for publication
(NASA-TM-101141; NAS 1.15:101141) Avail: NTIS HC A03/MF A01 CSCL 22A

When polymers such as dextran and poly(ethylene glycol) are mixed in aqueous solution biphasic systems often form. On Earth the emulsion formed by mixing the phases rapidly demixes because of phase density differences. Biological materials can be purified by selective partitioning between the phases. In the case of cells and other particulates the efficiency of these separations appears to be somewhat compromised by the demixing process. To modify this process and to evaluate the potential of two-phase partitioning in space, experiments on the effects of gravity on phase emulsion demixing were undertaken. The behavior of phase systems with essentially identical phase densities was studied at one-g and during low-g parabolic aircraft maneuvers. The results indicate the demixing can occur rather rapidly in space, although more slowly than on Earth. The demixing process was examined from a theoretical standpoint by applying the theory of Ostwald ripening. This theory predicts demizing rates many orders of magnitude lower than observed. Other possible demixing mechanisms are considered. Author

N88-24810# Erno Raumfahrttechnik G.m.b.H., Bremen (West Germany).
OPERATIONAL FACILITIES OF EURECA A1 MISSION [DIE NUTZLAST DER EURECA-A1 MISSION]
K. Sommer, W. Koehler-Naumann, and O. Pophanken Apr. 1987 56 p In GERMAN
(ETN-88-91939) Avail: NTIS HC A04/MF A01

The EURECA microgravitational facilities are reviewed: automatic mirror furnace, crystal growth solution, protein crystallization, multi-furnace assembly, exobiological radiation assembly, high precision thermostat, and surface forces adhesion experiment. Components described relative to aerospace sciences are: solar spectrum experiment, solar variation experiment, occultation radiometer, wide angle telescope for X-ray and timeband capture cell experiment. Demonstration technologies outlined are:

radio frequency ionization thruster assembly, interorbit communication experiment, and advanced solar gallium arsenide array. ESA

N88-24811*# National Aeronautics and Space Administration. Lewis Research Center, Cleveland, Ohio.
PREPARATION FOR MICROGRAVITY: THE ROLE OF THE MICROGRAVITY MATERIALS SCIENCE LABORATORY
J. Christopher Johnston, Bruce N. Rosenthal, MaryJo B. Meyer, and Thomas K. Glasgow [1988] 11 p Presented at the Space Programs and Technologies Conference, Houston, Tex., 21-24 Jun. 1988; sponsored by the AIAA
(NASA-TM-100906; E-4157; NAS 1.15:100906; AIAA-88-2645) Avail: NTIS HC A03/MF A01 CSCL 22A

A laboratory dedicated to ground based materials processing in preparation for space flight was established at the NASA Lewis Research Center. Experiments are performed to delineate the effects of gravity on processes of both scientific and commercial interest. Processes are modeled physically and mathematically. Transport model systems are used where possible to visually track convection, settling, crystal growth, phase separation, agglomeration, vapor transport, diffusive flow, and polymers reactions. The laboratory contains apparatus which functionally duplicates apparatus available for flight experiments and other pieces instrumented specifically to allow process characterization. Materials addressed include metals, alloys, salts, glasses, ceramics, and polymers. The Microgravity Materials Science Laboratory is staffed by engineers and technicians from a variety of disciplines and is open to users from industry and academia as well as the government. Examples will be given of the laboratory apparatus typical experiments and results. Author

31 ENGINEERING (GENERAL)

Includes vacuum technology; control engineering; display engineering; cryogenics; and fire prevention.

N88-24812# Edgerton, Germeshausen and Grier, Inc., Idaho Falls, Idaho.
LABORATORY SCALE INERT GAS ATOMIZER FOR PRODUCING RAPIDLY SOLIDIFIED POWDERS
G. E. Korth, V. W. Storhok, and J. V. Burch 1988 8 p Presented at the 2nd International Conference of Rapidly Solidified Materials, San Diego, Calif. 7 Mar. 1988
(Contract DE-AC07-76ID-01570)
(DE88-006734; EGG-M-12487; CONF-880358-2) Avail: NTIS HC A02/MF A01

An inert gas atomizer was constructed to produce rapidly solidified metal powders in batches of up to 3 kg. The atomizing tank assembly is 0.5 m in diameter x 1.8 m high. Various nozzle/crucible designs and processing parameters were evaluated for their effect on the powder product. The apparatus was used to produce tin, copper, and stainless steel powders with nozzle pressures no greater than 3 MPa and yielding spherical powders ranging from 200 to less than 1 micron. Various nozzle designs were evaluated and preliminary studies were initiated to investigate the process parameters as they pertain to the final powder product. DOE

N88-24813# Ballistic Research Labs., Aberdeen Proving Ground, Md.
AN EXTINGUISHER TO QUENCH PROPELLANT FIRES
Memorandum Report, Dec. 1982 - Sep. 1986
Anthony E. Finnerty Jan. 1988 28 p
(AD-A190785; BRL-MR-3645) Avail: NTIS HC A03/MF A01 CSCL 13L

Details are given on a novel fire extinguisher which has been used successfully to extinguish propellant fires. The extinguishing fluid is driven by an explosive charge. This allows complete quenching of propellant fires in as short a time as 5 milliseconds after activation of the extinguisher. The effect of certain variables on the success of the extinguishing experiments are reported. These variables are: volume of extinguishing agent; weight of explosive; time delay between start of fire and activation of the device; and the composition of the extinguishing fluid. GRA

N88-24814*# National Aeronautics and Space Administration. Pasadena Office, Calif.
ENERGY EFFICIENT CONTINUOUS FLOW ASH LOCKHOPPER Patent Application
Earl R. Collins, Jr., inventor (to NASA), Jerry W. Suitor, inventor (to NASA), and David Dubis, inventor (to NASA) (Jet Propulsion Lab., California Inst. of Tech., Pasadena.) 16 Mar. 1988 19 p Prepared in cooperation with Jet Propulsion Lab., California Inst. of Tech., Pasadena.
(Contract NAS7-918)
(NASA-Case-NPO-16985-1-CU; NAS 1.71:NPO-16985-1-CU; US-Patent-Appl-SN-195222) Avail: NTIS HC A03/MF A01 CSCL 13I

The invention relates to an energy efficient continuous flow ash lockhopper, or other lockhopper for reactor product or byproduct. The invention includes an ash hopper at the outlet of a high temperature, high pressure reactor vessel containing heated high pressure gas, a fluidics control chamber having an input port connected to the ash hopper's output port and an output port connected to the input port of a pressure letdown means, and a control fluid supply for regulating the pressure in the control chamber to be equal to or greater than the internal gas pressure of the reactor vessel, whereby the reactor gas is contained while ash is permitted to continuously flow from the ash hopper's output port, impelled by gravity. The main novelty resides in the use of a control chamber to so control pressure under the lockhopper that gases will not exit from the reactor vessel, and to also regulate the ash flow rate. There is also novelty in the design of the ash lockhopper shown in two figures. The novelty there is the use of annular passages of progressively greater diameter, and rotating the center parts on a shaft, with the center part of each slightly offset from adjacent ones to better assure ash flow through the opening. NASA

N88-24815*# National Aeronautics and Space Administration. Pasadena Office, Calif.
TOWER EVAPORATOR Patent Application
Eugene R. duFresne, inventor (to NASA) (Jet Propulsion Lab., California Inst. of Tech., Pasadena.) 19 Apr. 1983 28 p Prepared in cooperation with Jet Propulsion Lab., California Inst. of Tech., Pasadena.
(Contract NAS7-100)
(NASA-Case-NPO-15609-2; NAS 1.71:NPO-15609-2; US-Patent-Appl-SN-761310) Avail: NTIS HC A03/MF A01 CSCL 13B

Liquids, such as juices, milk, molten metal, and the like are concentrated by forming uniformly-sized small droplets in a precision droplet forming assembly and deploying the droplets in free fall downwardly as a central column within an evacuated tower having cool walls. A portion of the solvent evaporates. The vapor flows to the wall, condenses, and usually flows down the wall as a film to the condensate collector and drain. (In special cases, the condensate may be frozen on the wall, and stripped from it as a solid). The vertical column of freely-falling droplets enters the splash guard. The condensate can be collected, sent to other towers or recycled. NASA

N88-24816*# National Aeronautics and Space Administration. Langley Research Center, Hampton, Va.
STIFFENED TITANIUM PANELS Patent Application
Randall C. Davis, inventor (to NASA), Thomas T. Bales, inventor (to NASA), and Dick M. Royster, inventor (to NASA) 2 Feb. 1988 12 p
(NASA-Case-LAR-13814-1; NAS 1.71:LAR-13814-1; US-Patent-Appl-SN-151678) Avail: NTIS HC A03/MF A01 CSCL 13B

The invention is a reinforced, stiffened titanium panel having corrugations with beaded reinforcement in the corrugation sidewalls. The method for molding these complex structural shapes

is also a part of the invention. The technique developed to form the panels of this invention involve raising the temperature of the titanium plate to a temperature which permits plastic flow of the metal. The metal is then blown into a female mold using evacuation of the mold and overpressure on the opposite side of the titanium sheet. Using this method, the titanium can be stretched and elongated in much the same manner as glass is blown. Shapes which are impractical by conventional means can be easily achieved. The structural shapes formed in the present invention increase the structural efficiency of the panels. With no increase in weight, the stiffness and resistance of molding these shapes using superplastic forming techniques. NASA

N88-24817*# National Aeronautics and Space Administration. Marshall Space Flight Center, Huntsville, Ala.
LOW TEMPERATURE STORAGE CONTAINER FOR TRANSPORTING PERISHABLES TO SPACE STATION Patent Application
William G Dean, inventor (to NASA) (Lockheed Missiles and Space Co., Huntsville, Ala.) and James W. Owen, inventor (to NASA) 1 Apr. 1988 17 p
(NASA-Case-MFS-28248-1; NAS 1.71:MFS-28248-1; US-Patent-Appl-SN-176545) Avail: NTIS HC A03/MF A01 CSCL 13B

This invention is directed to the long term storage of frozen and refrigerated food and biological samples by the space shuttle to the space station. A storage container is utilized which has a passive system so that fluid/thermal and electrical interfaces with the logistics module is not required. The container for storage comprises two units, each having an inner storage shell and an outer shell receiving the inner shell and spaced about it. The novelty appears to lie in the integration of thermally efficient cryogenic storage techniques with phase change materials, including the multilayer metalized surface thin plastic film insulation and the vacuum between the shells. Additionally the fiberglass constructed shells having fiberglass honeycomb portions, and the lining of the space between the shells with foil combine to form a storage container which may keep food and biological samples at very low temperatures for very long periods of time utilizing a passive system. NASA

N88-24818*# National Aeronautics and Space Administration. Pasadena Office, Calif.
ACOUSTIC CONVECTIVE SYSTEM Patent Application
Eugene H. Trinh, inventor (to NASA) and Judith L. Robey, inventor (to NASA) (Jet Propulsion Lab., California Inst. of Tech., Pasadena.) 3 Feb. 1988 11 p Prepared in cooperation with Jet Propulsion Lab., California Inst. of Tech., Pasadena.
(Contract NAS7-918)
(NASA-Case-NPO-17278-1-CU; NAS 1.71:NPO-17278-1-CU; US-Patent-Appl-SN-172100) Avail: NTIS HC A03/MF A01 CSCL 13B

A small and simple system is provided for cooling or heating a small component by flowing air or other fluid over it, which does not require any macroscopic moving parts. The system includes a transducer and reflector that are spaced apart with the component between them, and with the transducer being operated at a frequency resonant to the spacing between it and the reflector. The resulting standing wave pattern produces acoustic streaming which results in the circulating of air or other fluid in the environment across the component. The system is especially useful in the reduced gravity environment of outer space because of the absence of any buoyancy-induced convection there. NASA

32 COMMUNICATIONS AND RADAR

Includes radar; land and global communications; communications theory; and optical communications.

For related information see also *04 Aircraft Communications and Navigation* and *17 Space Communications, Spacecraft Communications, Command and Tracking.* For search and rescue see *03 Air Transportation and Safety,* and *16 Space Transportation.*

N88-24819# Massachusetts Inst. of Tech., Cambridge. Artificial Intelligence Lab.
TIME-FREQUENCY REPRESENTATIONS FOR SPEECH SIGNALS Ph.D. Thesis
Michael D. Riley Jun. 1987 153 p
(Contract N00014-85-K-0124)
(AD-A188661; AI-TR-974) Avail: NTIS HC A08/MF A01 CSCL 25D

This work addresses two related questions. The first question is what joint time-frequency energy representations are most appropriate for auditory signals, in particular, for speech signals in sonorant regions. The quadratic transforms of the signal are examined, a large class that includes, for example, the spectrograms and the Wigner distribution. Quasi-stationarity is not assumed, since this would neglect dynamic regions. A set of desired properties is proposed for the representation: (1) shift-invariance, (2) positivity, (3) superposition, (4) locality, and (5) smoothness. The second question addressed is how to obtain a rich, symbolic description of the phonetically relevant features of these time-frequency energy surfaces, the so-called schematic spectrogram time-frequency ridges, the 2-D analog of spectral peaks, are one feature that is proposed. If non-oriented kernels are used for the energy representation, then the ridge tops can be identified with zero-crossings in the inner project of the gradient vector and the direction of greatest downward curvature. If oriented kernels are used, the method can be generalized to give better orientation selectivity (e.g., intersecting ridges) at the cost of poorer time-frequency locality. GRA

N88-24820# Chalmers Univ. of Technology, Goeteborg (Sweden). Space Observatory.
GEODESY BY RADIO INTERFEROMETRY: OPTIMIZATION OF WET PATH DELAY ALGORITHMS USING MICROWAVE RADIOMETER DATA
J. M. Johansson, G. Elgered, and J. L. Davis 1987 53 p Prepared in cooperation with Harvard-Smithsonian Center for Astrophysics, Cambridge, Mass. and Geological Survey, Menlo Park, Calif.
(PB88-167739; RR-152) Avail: NTIS HC A04/MF A01 CSCL 20N

The report deals with algorithms for estimating the excess propagation path of radio waves through the atmosphere using microwave radiometer data. The authors have used radiosonde data from different sites to study and evaluate the performance of such algorithms. The sites chosen represent climates similar to that of nearby currently existing or planned antennas for use in geodetic very-long-baseline interferometry experiments. They find that the accuracy of the algorithm, assuming noise-free measurements and error-free expressions for the atmospheric attenuation, is significantly improved if the algorithms are optimized for a given site. They present site-optimized algorithms, with and without using surface meteorological data, for the most common frequency pairs of existing microwave radiometers, namely 20.7 to 31.4 GHz and 21.0 to 31.4 GHz. GRA

N88-24821# Foerenade Fabriksverken, Linkoeping (Sweden).
HIGH RESOLUTION RADAR TECHNIQUES: FIVE CONTRIBUTIONS TO MILINF 86
B. Brusmark, A. Gustavsson, H. Hellsten, J. Kjellgren, and B. Larsson Jan. 1988 44 p In SWEDISH; ENGLISH summary
(PB88-172721; FOA-B-30120-3.2) Avail: NTIS HC A03/MF A01 CSCL 17I

The report consists of five contributions describing various methods of increasing the information contents of radar data, e.g.,

by a high spatial or temporal resolution, several dimensions of measurement, an increased accuracy or uniqueness of data. The first contribution describes how the aperture and hence the angular resolution may be increased synthetically in e.g., a common microwave radar by varying the geometry of measurement in a known way. The second contribution is applied in the radio band in order to push the resolution towards the size of the wavelength with the intention of increasing the uniqueness of the measurement data. The third contribution treats high resolution with respect to time variations of the measurement scene (Doppler technique). The fourth contribution gives a general treatment of the properties obtained by using multistatic radar concepts and departs from the conventional monostatic geometry of measurement. The last contribution, which relates to the potentially high spatial resolution of the mm-wave region, illustreates various aspects of importance when considering applications. GRA

N88-24822# Arizona Univ., Tucson. Optical Sciences Center.
NONLINEAR SURFACE POLARITONS Final Report, 15 Nov. 1984 - 14 Nov. 1987
G. I. Stegeman 15 Dec. 1987 12 p
(Contract DAAG29-85-K-0026)
(AD-A191046; ARO-22336.14PH) Avail: NTIS HC A03/MF A01 CSCL 20F

Analytical and numerical (the Beam Propagation Method) techniques were used to analyze a variety of nonlinear optics phenomena at surfaces and in thin film waveguides. A number of new device possibilities for all optical signal processing were identified. New nonlinear guided-wave phenomena have been predicted, of which many are of interest for potential experimental and device applications. The highlights are: (1) The analytical solutions for highly nonlinear waves guided by single interfaces and thin films extended to realistic media which exhibit saturation in the optically induced index change. (2) Beam propagation techniques used to find the stability of nonlinear guided waves for the first time. Furthermore, non-stationary nonlinear guided waves were found, also for the first time. (3) The generation of solitons predicted for nonlinear waveguides excited at high powers. Applications to optical limiters and optical logic via the exchange of solitons identified. The effects of non-ideal excitation conditions, waveguide absorption, and index saturation investigated. (4) Analytical and numerical solutions for nonlinear TM-polarized guided waves obtained for the first time. (5) The feasibility of light-by-light modulation using nonlinear guided waves of both polarizations predicted. (6) The origin of bistability in nonlinear prism couplers fully explained for the first time. (7) The response of nonlinear directional couplers to very high excitation calculated, resulting in unexpected steady state conditions. GRA

N88-24823# Pennsylvania State Univ., University Park. Lab. for Electromagnetic and Acoustic Research.
MULTIPLE SCATTERING OF WAVES IN DISCRETE RANDOM MEDIA Final Report, 1 Nov. 1984 - 14 Nov. 1987
Vijay K. Varadan, Vasundara V. Varadan, and Yushieh Ma 31 Dec. 1987 148 p
(Contract DAAG29-84-K-0187)
(AD-A191068; ARO-21825.17-GS) Avail: NTIS HC A07/MF A01 CSCL 20K

Multiple scattering of waves in discrete random media was investigated particularly in the scattered intensities (coherent and incoherent). The formalism was applied to examine the effective properties, which are frequency dependent, of either structural composites or wave absorbing composite materials (electronic, elastic and acoustic). The pair correlation function for hard disks was obtained using Monte Carlo simulation and later was used to compute the effective propagation constants for fiber reinforced composites. Nonspherical statistics was employed to study scattering from densely distributed nonspherical scatterers in host medium. The coherent as well as incoherent intensities were computed for spheroidal scatterers and spherical scatterers with different polarizations. The backscattered intensities obtained from our formalism which parallels the diagram method first proposed by Feynman compare favorably with those from optical experiments. GRA

N88-24824# Electrospace Systems, Inc., Arlington, Va.
WIPP (WAVE INDUCED PARTICLE PRECIPITATION) EXPERIMENT LOGISTIC SUPPORT Final Report, Jun. - Dec. 1987
E. A. Ray 31 Dec. 1987 31 p
(Contract N00014-87-C-0666)
(AD-A191184) Avail: NTIS HC A03/MF A01 CSCL 25B

The WIPP (Wave Induced Particle Precipitation) Program required that a series of unique modulation (keying) events be transmitted from the U.S. Navy Very Low Frequency (VLF) transmitter at Annapolis, Md. Support was provided in assisting the Scientific Officer (ONR Code 1114) in negotiations with the cognizant Navy Broadcast Control Authority, and the Operational COmmanders of the facility, for the cooperative use of the Annapolis VLF broadcast transmitter. Additionally, unique keyers, previously developed to support the Stimulated Emission of Energetic Particles (SEEP) experiment, which performed keying events similar to those needed by the WIPP program were tested, and repaired as required, and installed at Annapolis. Finally, Navy personnel at Annapolis were trained in the use of the keyers, and instructed in the provision of support to the WIPP experiment. GRA

N88-24825# Arizona Univ., Tucson. Optical Sciences Center.
SIGNAL PROCESSING WITH DEGENERATE FOUR-WAVE MIXING Final Report, 1 Sep. 1983 - 31 Aug. 1987
G. I. Stegeman and C. T. Seaton 7 Dec. 1987 10 p
(Grant AF-AFOSR-0277-84)
(AD-A191496; AFOSR-88-0050TR) Avail: NTIS HC A02/MF A01 CSCL 20F

The original goals of this program were: 1. To demonstrate degenerate four-wave mixing in planar waveguides, 2. To fabricate nonlinear organic waveguides using the Langmuir-Blodgett (L-B) technique, and 3. To demonstrate all-optical signal processing based on degenerate four-wave mixing. During the course of this program, it became clear that nonlinear organic waveguides based on L-B deposition techniques would never exhibit losses low enough for guided-wave degenerate four-wave mixing. As a result, it was decided: 4. To develop semiconductor-doped glass waveguides, 5. To demonstrate degenerate four-wave mixing in these waveguides, and 6. To demonstrate all-optical signal processing in semiconductor-doped waveguides. GRA

N88-24826# Washington Univ., St. Louis, Mo. Electronic Systems and Signals Research Lab.
DELAY-DOPPLER RADAR IMAGING Semiannual Progress Report, 1 Jun. - 30 Nov. 1987
Donald L. Snyder 30 Nov. 1987 47 p
(Contract N00014-86-K-0370)
(AD-A191509; ESSRL-88-1; SAPR-3) Avail: NTIS HC A03/MF A01 CSCL 17I

The goal of this project is to formulate and investigate new approaches for forming images of radar targets from spot-light-mode, delay-doppler mesurements. These measure-ments could be acquired with a high-resolution radar-imaging system operating with an optical- or radio-frequency carrier. Two approaches are under study. The first is motivated by an image-reconstruction algorithm used in radionuclide imaging called the confidence-weighted algorithm; here, we will refer to this approach as the chirp-rate modulation approach. The second approach is based on more fundamental principles which starts with a mathematical model that accurately describes the physics of an imaging radar-system and then uses statistical-estimation theory with this model to derive processing algorithms; we will refer to this as the estimation-theory approach. Spotlight-mode high-resolution radar-imaging relies upon the relative motion between the transmitter, target, and receiver. The target is illuminated by a series of transmitted pulses. The return for each pulse is a superposition of reflections from various locations on the target, with each location affecting the pulse by introducing a

time delay, doppler shift, and reflectance gain. The returns are processed to produce an image of the target. Two types of images are possible. One is a map in delay/doppler or range/cross-range coordinates of the target's complex-valued reflectivity, which indicates the amplitude-gain applied to the incident radar. GRA

N88-24827# Illinois Univ., Urbana.
MILLIMETER AND SUBMILLIMETER WAVES AND FREQUENCY SELECTIVE SURFACES Final Report, 21 Aug. 1985 - 31 Dec. 1987
R. Mittra Jan. 1988 6 p
(Contract DAAG29-85-K-0183)
(AD-A191511; ARO-22634.6-EL) Avail: NTIS HC A02/MF A01 CSCL 09A

We have investigated two different class of problems in this effort. The first of these falls in the category of microwave and millimeter wave integrated circuits and the second is concerned with frequency selective surfaces, or FSS. Our research in the millimeter wave area has focused on the development of analytical and numerical techniques for determining the characteristics of planar transmission lines, as well as circuit components and antennas that are compatible with these lines. As for frequency selective surfaces, our investigation of the FSS screens dealt with the development of methodologies for predicting the transmission and reflection properties of these screens as a function of the frequency. Both the free-standing screens and those with a dielectric substrate or superstate have been studied. In addition, curved and finite screens have also been investigated. GRA

N88-24828# Syracuse Univ., N. Y. Dept. of Electrical and Computer Engineering.
ELECTROMAGNETIC PENETRATION INTO A CONDUCTING CIRCULAR CYLINDER THROUGH A NARROW SLOT, TE CASE Interim Technical Report No. 8
Joseph R. Mautz and Roger F. Harrington Nov. 1987 56 p
(Contract DAAG29-84-K-0078)
(AD-A191602; SYRU/DECE/TR-87/4; ARO-21378.11-EL) Avail: NTIS HC A04/MF A01 CSCL 20C

A procedure is presented for calculating the electromagnetic field in the vicinity of an infinitesimally thin conducting circular cylindrical shell with an infinitely long slot illuminated by a TE plane wave. This field is the short-circuit field plus the field due to the slot. The shorter-circuit field is the field that would exist if there were no slot. The field due to the slot stems from the phi component of the electric field in the slot. Approximated by a linear combination of expansion functions that satisfy the edge conditions, this field component is determined by testing the equation of continuity of the axial magnetic field in the slot with non-negative powers of phi where phi is the angular distance from the center of the slot. Alternative expansion functions are introduced to preserve the accuracy of the solution in the vicinity of an internal resonance. Containing the resonant electric field, the first alternative expansion function is normalized so that its axial magnetic field remains finite as the resonant frequency is approached. The resonant electric field is that interior electric field whose phi component approaches zero on the closed surface consisting of the cylindrical shell and the slot as the frequency approaches the resonant frequency. The rest of the alternative expansion functions are orthogonal to the resonant electric field. GRA

N88-24829# Naval Research Lab., Washington, D.C.
AUTOMATED TEST DEVICE FOR FASR (FIXED ARRAY SURVEILLANCE RADAR) BEAM STEERING COMPONENTRY Interim Report
Russell A. Scott 10 Feb. 1988 14 p
(AD-A191650; NRL-MR-6143) Avail: NTIS HC A03/MF A01 CSCL 17I

The Fixed Array Surveillance Radar System uses an automated test device known as the Axis Box Tester. An axis box serves as a distribution point connecting the horizontal and vertical busses of the array and monitors the rf of phase shifters and aids with beam steering. The tester diagnoses axis boxes and verifies proper operation. All digital circuitry is tested, including all data flow paths to and from the phase shifters, all control line information, and all circuitry to select rows and columns. The tester attempts to provide information that will aid, if not solve problems. The software is parsed into modules that perform various tests upon the axis box. The hardware, which uses a single-board computer with an Intel 8086 microprocessor, provides the interface between the microprocessor and the axis box. The tester provides very accurate diagnostics and can reduce debugging time by a factor of 100. Some problems prevent the tester from doing more than guessing at possible causes of a problem. GRA

N88-24830# Naval Ocean Systems Center, San Diego, Calif.
A MININEC MODEL OF THE MINILOOP ANTENNA Report, period ending Mar. 1987
James C. Logan Oct. 1987 15 p
(AD-A191759) Avail: NTIS HC A03/MF A01 CSCL 09A

The Miniloop is an HF loop antenna, which has found use on U.S. Coast Guard vessels. The antenna is a large diameter loop mounted on a pedestal. It is tuned with a variable capacitor mounted in series at the top of the loop. Inductive coupling from a much smaller loop on the lower rim is used as a feed. MININEC (NOSC TD 938), The New MININEC Version 3); a Mini-Numerical Electromagnetics Code, by J. W. Rockway and J. C. Logan, September 1986, is used to represent the Miniloop antenna mounted over a perfectly conducting ground plane. The development and validation of the MININEC model of the Miniloop will be discussed. A sample method for determining radiation efficiency will also be presented. GRA

N88-24831# Naval Ocean Systems Center, San Diego, Calif.
PRACTICAL VLF/LF RADIO TEST SYSTEM
Paul A. Singer Feb. 1988 5 p
(AD-A191768) Avail: NTIS HC A02/MF A01 CSCL 25B

A practical VLF/LF radio test system designated as the AN/URM-212, Test Set, Radio is a recent development of the Naval Ocean Systems Center working in conjunction with industry. The mission of the AN/URM-212 is to verify the operational readiness of VLF/LF receive communication systems installed in submarines. Navy aircraft, and tenders from antenna to printer. The AN/URM-212 tests processor-controlled VLF/LF receive components (e.g., VERDIN), in a quantitative manner and tests non-processor controlled VLF/LF receive components (e.g., receivers, antennas and associated couplers) in a qualitative manner. The AN/URM-212 is used to test all receive components of the VLF/LF communications system by measuring small performance degradations not discovered by automated performance monitoring, self test or other preventive maintenance procedures. GRA

N88-24832# Ohio State Univ., Columbus. Electroscience Lab.
A METHOD FOR DISCRIMINATION OF RADAR TARGETS USING COMPLEX NATURAL RESONANCES
Eric P. Bohley Sep. 1987 82 p
(Contract N00014-86-K-0202)
(AD-A191848; ESL-718048-4) Avail: NTIS HC A05/MF A01 CSCL 17I

A prediction-correlation target discrimination algorithm using target complex natural resonances is investigated. The targets natural resonances are extracted from experimentally measured frequency domain scattering data. Scattering data were obtained from scale model targets measured in the ElectroScience Laboratory compact radar range facility. The targets used are models of three military ground vehicles. Signal processing required for the extraction of poles is described. The principles of the prediction-correlation algorithm are discussed and the algorithm is demonstrated for both noiseless data and data with additive white noise. Classification results are plotted for the targets at aspect angles of 0, 10, 20, 30, 60, and 90 degrees from nose on. GRA

N88-24833# Ohio State Univ., Columbus. Electroscience Lab.
NONPARAMETRIC DISCRIMINANT ANALYSIS APPLIED TO THE EXTRACTION AND SELECTION OF RADAR TARGET SIGNATURE FEATURES Final Report
O. Snorrason and F. D. Garber Dec. 1987 39 p
(Contract N00014-85-K-0321)
(AD-A191849; ESL-717220-7) Avail: NTIS HC A03/MF A01 CSCL 17I

A nonparametric criterion of discriminant analysis is applied to a large scale data set, of radar returns from aircrafts, for frequency selection. The performance of the optimum sets characterized is evaluated using Monte-Carlo simulation. The effect of the number of frequencies and the a priori information of the azimuth angle on the performance of the pattern recognition system is examined. Also the effect of multiple measurements is examined. GRA

N88-24834# City Coll. of the City Univ. of New York.
COMMUNICATIONS USING CHANNELS FORMED BY METEOR BURSTS Annual Technical Report, 1 Jan. - 31 Dec. 1987
Donald L. Schilling and Eliphaz Hibshoosh 31 Dec. 1987 177 p
(Grant AF AFOSr-0234-85)
(AD-A192088; AFOSR-88-0018TR) Avail: NTIS HC A09/MF A01 CSCL 25B

There is currently an urgent need for alternate channels for communication. The large variety and quantity of users throughout the world have caused all of the existing channels to become extremely congested. A world wide search for such alternate channels is now being conducted for both present day and future communication systems through the use of different types of channels such as optical, laser, cable, satellite, etc. The particular application of Beyond-Line-Of-Sight (BLOS) communications, which uses the High Frequency (HF) spectral band from 3 to 30 MHz, is very important to many current and potential users. However, HF is very sensitive to solar disturbances such as sunspot activity, solar storms and other galactic phenomena, as well as multipath returns from both ground and atmosphere, weather related attenuation, and other degrading factors. Because of these factors a channel for communication is needed which has low congestion, is robust and relatively indestructible, has very little outside interference and does not compete for bandwidth with existing communication systems. GRA

N88-24835# Clarkson Univ., Potsdam, N.Y. Dept. of Mathematics and Computer Science.
NONLINEAR WAVE PROPAGATION Final Technical Report, 1 Nov. 1986 - 31 Oct. 1987
Mark J. Ablowitz 23 Nov. 1987 171 p
(Grant AF AFOSR-0005-84)
(AD-A192104; AFOSR-88-0065TR) Avail: NTIS HC A08/MF A01 CSCL 12B

This year has been an active and productive period for the group at Clarkson involved with nonlinear wave propagation. We have continued to make progress in the study of nonlinear evolution equations, their properties and their solutions for both one plus one and multidimensional nonlinear evolution equations. We are continuing our studies of Painleve equations and nonlinear partial difference equations which can be used as numerical approximations to various soliton equations. GRA

N88-24836# Syracuse Univ., N. Y. Dept. of Electrical and Computer Engineering.
ELECTROMAGNETIC FIELD PENETRATION INTO STRUCTURES Final Report, 1 Jul. 1984 - 30 Dec. 1987
Roger F. Harrington 10 Mar. 1988 8 p
(Contract DAAG29-84-K-0078)
(AD-A192127; ARO-21378.13-EL) Avail: NTIS HC A02/MF A01 CSCL 20C

This report summarizes the work done on electromagnetic field penetration into structures. An introductory section states the purpose and general findings of the research. The next section lists the research reports issued, with the abstract of each report. The third section lists the papers published in journals, with the abstract or each paper. GRA

N88-24837# University Coll. of Wales, Aberystwyth. Dept. of Physics.
RADIO-WAVE SCINTILLATIONS AND IONOSPHERIC IRREGULARITIES AT HIGH LATITUDES Final Report, 1 Apr. 1986 - 31 Mar. 1987
L. Kersley, S. E. Pryse, and N. S. Wheadon 30 May 1987 46 p
(Grant AF AFOSR-0190-85)
(AD-A192140; AFGL-TR-87-0247) Avail: NTIS HC A03/MF A01 CSCL 20N

Results are presented of studies of ionospheric scintillation obtained by monitoring of transmissions from NNSS satellites at Kiruna, Northern Sweden during a two year period from September 1984 to September 1987. Attention is concentrated in this report on phase scintillation morphology. Also presented are results of model studies of the geometrical influences in amplitude and phase scintillations at a high-latitude site aimed at interpreting the observations and understanding the nature of the ionospheric irregularities responsible for the scintillations. Also discussed are results of two coordinated studies of ionospheric irregularities using scintillation observations and data from HF and VHF backscatter radar systems respectively. GRA

N88-24838# North Carolina Univ., Chapel Hill. Dept. of Statistics.
INFORMATION AND STOCHASTIC SYSTEMS Final Report, 1 Dec. 1986 - 30 Nov. 1987
Charles R. Baker 30 Nov. 1987 6 p
(Grant AF AFOSR-0106-87)
(AD-A192167; AFOSR-88-0051TR) Avail: NTIS HC A02/MF A01 CSCL 25B

Equipment was purchased to support research in two main areas: communication channels with memory and signal detection and classification problems involving non-Gaussian stochastic processes. The research on communication channels involves largely the study of channel capacity under various assumptions and constraints. The research in signal detection and classification includes modeling, data analysis, and the development and evaluation of detection algorithms. GRA

N88-24839# Research Inst. of National Defence, Linkoeping (Sweden).
THE RADAR CROSS SECTION OF SOME SIMPLE REFLECTORS AT SHORT WAVELENGTHS
Jan Kjellgren, Stefan Nilsson, and Ain Sume Sep. 1987 26 p In SWEDISH; ENGLISH summary
(FOA-C-30472-3.3; ISSN-0347-3708; ETN-88-91884) Avail: NTIS HC A03/MF A01; Research Institute of National Defence, Box 1165, S-581 11 Linkoping, Sweden, 50 Swedish crowns

Methods for evaluating the radar cross section of simple reflector types, in single or multiple reflection, are described. Formulas which can be used for magnitude calculations are outlined. Approximate expressions are presented for geometrically simple reflector types: flat plate, cylinder, cylinder on a circular plane, concave cylinder, and a corner reflector. ESA

N88-24840# Research Inst. of National Defence, Linkoeping (Sweden).
A DIFFERENTIAL PHASE SHIFT KEYING (DPSK) MODULATOR FOR A FREQUENCY HOPPING SHORT WAVE SYSTEM
Mats Eriksson and Gunnar Eriksson Jul. 1987 76 p In SWEDISH; ENGLISH summary
(FOA-C-30460-3.3; ISSN-0347-3708; ETN-88-92487) Avail: NTIS HC A05/MF A01; Research Institute of National Defence, Box 1165, S-581 11 Linkoping, Sweden, 50 Swedish crowns

The demodulator was designed as a part of an experimental system. The data rate used is 5 or 6 k bits/sec. System hop rate is 100 hop/sec. The function of the demodulator is described and the results of performance measurements are presented. The

results show a difference compared with the theoretical values, due to an electromagnetic noise component, in addition to the already prevailing noise at the entry of the receiver, and probably generated in the demodulator itself. ESA

N88-24841# MATRA Espace, Toulouse (France).
ASSESSMENT OF OPTICAL COMMUNICATIONS SYSTEMS FOR DATA RELAY SATELLITE. VOLUME 1: EXECUTIVE SUMMARY
Paris, France ESA 1988 119 p Prepared in cooperation with Battelle Inst., Frankfurt, Fed. Republic of Germany; CNES, Toulouse, France; Standard Telecommunications Labs. Ltd., Harlow, United Kingdom; and Societe Bertin et Cie, Plaisir, France
(Contract ESA-6392/85)
(ESA-CR(P)-2488-Vol-1; ETN-88-92550) Avail: NTIS HC A06/MF A01

The possibility, from the technical and planning viewpoints, of using optical technologies for supporting the high-data-rate (HDR) communication services of the European Data Relay Satellite (DRS) was assessed, and CO2 laser and semiconductor laser diode technologies were compared. It is concluded that optical communications using semiconductor laser diode technology is a promising candidate for DRS. However, system feasibility is not demonstrated yet, and significant development effort is necessary before delivery of flight-level hardware. For the 1991 experimental system, there is no alternative to the 0.8 micron GaAlAs technology. The only possibility concerning the 1.3 micron InGaAsP would be to add a reduced capacity channel to the GaAlAs-based system. The use of 0.8 micron for in-orbit demonstration does not preclude the possibility of switching to InGaAsP for the operational system; to compete with GaAlAs, the long wavelength technology should provide, by 1991, a transmitter laser, communication detectors, and PAT detectors. ESA

N88-24842# MATRA Espace, Toulouse (France).
ASSESSMENT OF OPTICAL COMMUNICATIONS SYSTEMS FOR THE DATA RELAY SATELLITE Final Report
Paris, France ESA 1988 151 p Prepared in cooperation with Teledix GmbH, Heidelberg, Fed. Republic of Germany
(Contract ESA-6392/85)
(ESA-CR(P)-2488-Vol-2; ETN-88-92551) Avail: NTIS HC A08/MF A01

The impact of reduced data rate on the high data rate link, at system level, of the European Data Relay Satellite; localization/orbit restitution from information provided by the tracking loop; and fine pointing mechanisms for a laser diode system were studied. ESA

N88-24843 New South Wales Univ., Kensington (Australia). Dept. of Electrical and Electronic Engineering.
PROPAGATION MANAGEMENT FOR NO-ACKNOWLEDGE HF COMMUNICATIONS LINKS M.S. Thesis Abstract Only
W. A. Parkins 1986 185 p
Avail: Issuing Activity

The problems in the engineering of no-acknowledge HF links are reviewed with particular application to Naval applications. Models for predicting the performance of the ionospheric path and techniques for measurement of channel quality are considered. Manual methods of propagation management are found to be limited by speed and accuracy in conducting measurements. Automation of the channel quality measurement process allowed observation of short term behavior of the link for comparison with predictions. Long term behavior tends toward the prediction but large deviations are found in the short term. Techniques for improving the estimates of the remote ionosphere were investigated. Updating predictions using a derived ionospheric index and the use of a backscatter sounder were attempted with limited success. Concepts for improvement in no-acknowledge links include networking between transmitting stations, modulation diversity and coding techniques, and development of intelligent receiving terminals with facilities for rapid selection of operating channels and overcoming unwanted signal interference. Recommendations for further work to investigate these concepts is presented. Author

N88-24844*# National Aeronautics and Space Administration. Goddard Space Flight Center, Greenbelt, Md.
THE ROLE OF SPACE BORNE IMAGING RADARS IN ENVIRONMENTAL MONITORING: SOME SHUTTLE IMAGING RADAR RESULTS IN ASIA
Marc L. Imhoff and C. H. Vermillion Nov. 1986 23 p
(NASA-TM-101178; NAS 1.15:101178) Avail: NTIS HC A03/MF A01 CSCL 17I

The synoptic view afforded by orbiting Earth sensors can be extremely valuable for resource evaluation, environmental monitoring and development planning. For many regions of the world, however, cloud cover has prevented the acquisition of remotely sensed data during the most environmentally stressful periods of the year. How synthetic aperture imaging radar can be used to provide valuable data about the condition of the Earth's surface during periods of bad weather is discussed. Examples are given of applications using data from the Shuttle Imaging Radars (SIR) A and B for agricultural land use and crop condition assessment, monsoon flood boundary and flood damage assessment, water resource monitoring and terrain modeling, coastal forest mapping and vegetation penetration, and coastal development monitoring. Recent SIR-B results in Bangladesh are emphasized, radar system basics are reviewed and future SAR systems are discussed. Author

N88-24845*# National Aeronautics and Space Administration. Langley Research Center, Hampton, Va.
ALMOND TEST BODY Patent Application
Allen K. Dominek, inventor (to NASA) (Ohio State Univ., Columbus.), Richard M. Wood, inventor (to NASA), and Melvin C. Gilreath, inventor (to NASA) 23 May 1988 9 p Prepared in cooperation with Ohio State Univ., Columbus
(NASA-Case-LAR-13747-1; NAS 1.71:LAR-13747-1; US-Patent-Appl-SN-197191) Avail: HC A02/MF A01 CSCL 20N

The invention is an almond shaped test body for use in measuring the performance characteristics of microwave anechoic chambers and for use as a support for components undergoing radar cross-section measurements. The novel aspect of this invention is its shape, which produces a large dynamic scattered field over large angular regions making the almond valuable for verifying the performance of microwave anechoic chambers. As a component mount, the almond exhibits a low return that does not perturb the measurement of the component and it simulates the backscatter characteristics of the component as if over an infinite ground plane. NASA

N88-24846*# National Aeronautics and Space Administration. Pasadena Office, Calif.
APPARATUS FOR USING A TIME INTERVAL COUNTER TO MEASURE FREQUENCY STABILITY Patent Application
Charles A. Greenhall, inventor (to NASA) (Jet Propulsion Lab., California Inst. of Tech., Pasadena.) 11 Feb. 1988 16 p Prepared in cooperation with Jet Propulsion Lab., California Inst. of Tech., Pasadena.
(Contract NAS7-918)
(NASA-Case-NPO-17325-1-CU; NAS 1.71:NPO-17325-1-CU; US-Patent-Appl-SN-184235) Avail: NTIS HC A03/MF A01 CSCL 20N

An apparatus for measuring the relative stability of two signals is disclosed comprising a means for mixing the two signals down to a beat note sine wave and for producing a beat note square wave whose upcrossings are the same as the sine wave. A source of reference frequency is supplied to a clock divider and interval counter to synchronize them and to generate a picket fence for providing a time reference grid of period shorter than the beat period. An interval counter is employed to make a preliminary measurement between successive upcrossings of the beat note square wave for providing an approximate time interval

therebetween as a reference. The beat note square wave and the picket fence are then provided to the interval counter to provide an output consisting of the time difference between the upcrossing of each beat note square wave cycle and the next picket fence pulse such that the counter is ready for each upcrossing and dead time is avoided. A computer containing an algorithm for calculating the exact times of the beat note upcrossings then computes the upcrossing times. NASA

N88-24847*# National Aeronautics and Space Administration. Marshall Space Flight Center, Huntsville, Ala.
CHARACTERIZATION OF A 30-GHz IMPATT SOLID STATE AMPLIFIER
Lawrence W. Wald Jul. 1988 16 p
(NASA-TM-100876; E-4110; NAS 1.15:100876) Avail: NTIS HC A03/MF A01 CSCL 09A

Described are the characterization and testing of a 20 W solid state amplifier operating in the Ka band to be used in low cost experimental ground terminals. The amplifier was developed by the TRW Electronic Systems Group under NASA Contract NAS3-23266 as a proof-of-concept (POC) device in support of the Advanced Communications Technology Satellite (ACTS) program. Additional goals were development of high-power IMPATT devices and circulators, and multistage diode circuits, which are an integral part of the amplifier. The amplifier underwent acceptance testing at the NASA Lewis Research Center, Cleveland, Ohio. Characteristics measured include the output power of 42 dB m, gain of 30 dB, an injection-locking RF bandwidth of 260 MHz, and an overall direct current-to-radiofrequency (dc-to-RF) efficiency of 6.7 percent. Author

N88-25118*# Massachusetts Inst. of Tech., Lexington.
THE FEDERAL AVIATION ADMINISTRATION/MASSACHUSETTS INSTITUTE OF TECHNOLOGY (FAA/MIT) LINCOLN LABORATORY DOPPLER WEATHER RADAR PROGRAM
James E. Evans *In* Tennessee Univ. Space Inst., Tullahoma. Meteorological and Environmental Inputs to Aviation Systems Jun. 1988 p 155-166 Sponsored by FAA (For primary document see N88-25105 18-47)
Avail: NTIS HC A11/MF A01 CSCL 20N

N88-25394*# Alabama Univ., Huntsville. Dept. of Electrical and Computer Engineering.
SPACE STATION INDUCED ELECTROMAGNETIC EFFECTS
N. Singh *In* NASA, Langley Research Center, A Study of Space Station Contamination Effects May 1988 p 31-42 (For primary document see N88-25390 18-88)
Avail: NTIS HC A07/MF A01 CSCL 20N

33 ELECTRONICS AND ELECTRICAL ENGINEERING

Includes test equipment and maintainability; components, e.g., tunnel diodes and transistors; microminiaturization; and integrated circuitry.

For related information see also *60 Computer Operations and Hardware* and *76 Solid-State Physics.*

N88-24848# Stanford Univ., Calif. Dept. of Electrical Engineering.
JOINT SERVICES ELECTRONICS PROGRAM Annual Report, 1 May 1986 - 30 Apr. 1987
James S. Harris, Jr. 30 Apr. 1987 63 p
(Contract DAAG29-85-K-0048)
(AD-A190239) Avail: NTIS HC A04/MF A01 CSCL 09A

Quantum well and reduced dimensional semiconductor systems, ultra-submicron devices, Ga/As silicon integrated circuits, the chemical and electronic structure of refractory metal GaAs interfaces, the study of crystal properties using channeling radiation, complementary MOS device and material physics at 77 degree K, real time statistical signal processing, and coding for spectrally constrained channels are discussed. GRA

N88-24849# Helsinki Univ. of Technology, Espoo (Finland). Circuit Theory Lab.
IDENTIFICATION OF CASCADED MICROWAVE CIRCUITS WITH MODERATE REFLECTIONS USING REFLECTIONS AND TRANSMISSION MEASUREMENTS
T. Veijola and M. Valtonen Nov. 1987 24 p
(PB88-171921; ISBN-951-754-312-3; CT-3) Avail: NTIS HC A03/MF A01 CSCL 09A

A method for identifying the component value of a cascaded microwave circuit with the aid of the time domain reflection and transmission coefficients is presented. The model proposed is composed of commensurate nondispersive transmission lines separated by either lumped series or shunt resistances. The line delays are equal to the sampling interval. The algorithm takes into account the third order multiple reflections thus allowing identification of circuits with moderate internal reflections (reflection coefficient smaller than about 0.2). The method is applicable, e.g., for modelling of connectors, discontinuities, transitions, jigs, and even impedance transformers. A numerical example is given to demonstrate the ability of the algorithm. GRA

N88-24850# Edgerton, Germeshausen and Grier, Inc., Salem, Mass.
TACTICAL RUBIDIUM FREQUENCY STANDARD (TRFS), VOLUME 2 Final Technical Report, Nov. 1983 - Dec. 1986
Thomas J. Lynch and William J. Riley Oct. 1987 209 p
(Contract F19628-83-C-0175)
(AD-A191190; RADC-TR-87-166-Vol-2) Avail: NTIS HC A10/MF A01 CSCL 14B

This report describes the accomplishments during a 3-year R&D program to design, develop, fabricate and evaluate two full scale engineering models of a Tactical Rubidium Frequency Standard (TRFS). The TRFS is a miniature atomic time and frequency source that is capable of operation in a harsh tactical military environment. In particular, it incorporates advances in miniaturization, ruggedness, fast warmup and high temperature operation that are required for aircraft applications. The report includes a detailed description of the TRFS design and the results of qualification tests on the two full scale engineering models. All program objectives were met. GRA

N88-24851# Technical Univ. of Istanbul (Turkey). Faculty of Aeronautics and Astronautics.
A DYNAMIC ANALYSIS OF PIEZOELECTRIC STRAINED ELEMENTS
M. C. Doekmeci Oct. 1987 15 p
(Contract DAJA45-86-C-0005)
(AD-A191478) Avail: NTIS HC A03/MF A01 CSCL 20B

In the first part of study, the existing work pertaining to the dynamic applications of piezoelectric crystals is reviewed with emphasis on the effect of initial stress. More than three hundred works are surveyed in the current literature concerned with the dynamic applications. Then, an update review article with two hundred and thirty three representative articles, entitled: Dynamic Applications of Piezoelectric Crystals, is submitted for publication in The Shock and Vibration Digest. The review article deals with the current literature that pertains to recent applications for waves and vibrations in piezoelectric crystals. Accordingly, it supplements the earlier review papers and should be considered in conjunction with them. The present compilation summarizes the rapid advancement of the subject due to the demand of both civil and military technology during the last three years. GRA

N88-24852# California Univ., San Diego, La Jolla. Dept. of Electrical Engineering and Computer Sciences.
COMPUTER AIDED DESIGN OF MONOLITHIC MICROWAVE AND MILLIMETER WAVE INTEGRATED CIRCUITS AND SUBSYSTEMS Annual Technical Report, 1 Sep. 1986 - 31 Aug. 1987
Walter H. Ku 31 Aug. 1987 54 p

(Grant AF AFOSR-0339-86)
(AD-A191593; AFOSR-88-0023TR) Avail: NTIS HC A04/MF A01 CSCL 09A

This interim technical report presents results of research on the computer aided design of monolithic microwave and millimeter wave integrated circuits and subsystems. A specific objective is to extend the state-of-the-art of the Computer Aided Design (CAD) of the monolithic microwave and millimeter wave integrated circuits (MIMIC). In this reporting period, we have derived a new model for the high electron mobility transistor (HEMT) based on a nonlinear charge control formulation which takes into consideration the variation of the 2DEG distance offset from the heterointerface as a function of bias. Pseudomorphic InGaAs/GaAs HEMT devices have been successfully fabricated at UCSD. For a 1 micron gate length, a maximum transconductance of 320 mS/mm was obtained. In cooperation with TRW, devices with 0.15 micron and 0.25 micron gate lengths have been successfully fabricated and tested. New results on the design of ultra-wideband distributed amplifiers using 0.15 micron pseudomorphic InGaAs/GaAs HEMT's have also been obtained. In addition, two-dimensional models of the submicron MESFET's, HEMT's and HBT's are currently being developed for the CRAY X-MP/48 supercomputer. Preliminary results obtained are also presented in this report. GRA

N88-24853# Ohio State Univ., Columbus. Electroscience Lab.
JOINT SERVICES ELECTRONICS PROGRAM Annual Report No. 10, Oct. 1986 - Sep. 1987
Dec. 1987 133 p
(Contract N00014-78-C-0049)
(AD-A191749; ESL-718109-2) Avail: NTIS HC A07/MF A01 CSCL 09A

This report represents the tenth annual summary of The Ohio State University Joint Services Program (JSEP). The transfer of the compact range technology initiated under JSEP support for time domain studies continues to make large advances. A new and yet improved design for the compact reflector has now been generated. As has been the case in recent years, the diffraction studies and the integral equation studies both continue to focus on the study of the interaction of electromagnetic energy with penetrable media. Progress can also be reported on several of the remaining very difficult diffraction processes for conducting bodies including that of corner and tip diffraction and edge wave contribution to scattered/radiated fields. The tip diffraction studies were highly successful and now a comparable advance is being made in the area of corner diffraction. The new Adaptive Array unit has shown substantial progress. JSEP support for the K-pulse studies for target identification terminated under the previous grant period. GRA

N88-24854# Naval Ocean Systems Center, San Diego, Calif.
SILICON-SAPPHIRE WAVEGUIDES Professional Paper, period ending Sep. 1986
D. J. Albares and R. A. Soref Nov. 1987 4 p
(AD-A191754) Avail: NTIS HC A02/MF A01 CSCL 09A

The first silicon-on-sapphire optical waveguides have been demonstrated. Waveguiding at lambda = 1.3 microns has been observed in silicon films 0.95 and 1.5 microns thick and in raised strip structures 1.5 microns thick. Previously, an epitaxial silicon-on-silicon technique was used to construct silicon waveguides for lambda = 1.3 or 1.55 microns, but the Si-on-Si technique allows guided light to spread evanescently into the lossy substrate because the refractive index step between substrate and guiding layer is approximately 0.01. However, tighter mode confinement is offered at these wavelengths by Silicon-On-Insulator (SOI) structures. This occurs because the Si-to-dielectric compositional change gives a larger index-step than the Si-to-Si doping profile change. Various SOI waveguide structures are possible including silicon-on-SiO, MBE-silicon-on-CAF and Silicon-On Sapphire (SOS). SOS is an attractive candidate structure because of sapphire's excellent mechanical, electrical and optical properties and of its development for the electronics industry. Electronic device fabrication on the same chip with the optical waveguide devices (optoelectronic integration) is possible. Waveguide theory predicts a single TE guided mode of 1.3 micron radiation in an SOS film below 0.22 microns in thickness. The ordinary refractive index of the sapphire substrate is 1.75 and the Si index is 3.50. We obtained SOS films of 0.3, 0.95 and 1.5 microns thickness and for these, theory predicts 2, 5, and 7 TE modes respectively. GRA

N88-24855# Aerospace Corp., El Segundo, Calif. Chemistry and Physics Lab.
NICKEL HYDROGEN LOW EARTH ORBIT LIFE TESTING
Charles C. Badcock and R. L. Haag 1 Feb. 1988 20 p
(Contract F04701-85-C-0086)
(AD-A191946; TR-0086(6909-05)-1; SD-TR-88-22) Avail: NTIS HC A03/MF A01 CSCL 09A

A program to demonstrate the long-term reliability of nickel hydrogen (NiH2) cells in low earth orbit (LEO) and support use in mid-altitude orbit (MAO) has been initiated. Both 3.5 and 4.5 in. diameter NiH2 cells are included in the test plan. Cells from all U.S. vendors are to be tested. The tests will be performed at -5 and 10 C at 40 and 60 percent depth of discharge (DOD) for LEO orbit and 10 C and 80 percent DOD for MAO orbit simulations. The goals of the testing are 20,000 cycles at 60 percent DOD and 30,000 cycles at 40 percent DOD. Cells are presently undergoing acceptance and characterization testing at Naval Weapons Support Center (NWSC), Crane, Indiana. Funding has been provided by the Air Force Space Technology Center (AFSTC) and two AF System Program Offices (SPO's) to initiate the testing, but additional funding must be acquired to complete the purchase of cells and to assure completion of the testing. GRA

N88-24856# Texas Univ., Austin. Electronics Research Center.
JOINT SERVICES ELECTRONICS PROGRAM Annual Report, 1 Jan. - 31 Dec. 1987
Edward J. Powers 31 Dec. 1987 59 p
(Contract F49620-86-C-0045)
(AD-A192076; AFOSR-88-0184TR) Avail: NTIS HC A04/MF A01 CSCL 09A

This Annual Report covers the twelve month period January 1, 1987 through December 31, 1987. The progress reported was accomplished during the second year of the current triennial technical program. Ten faculty members and approximately twenty graduate students from the Department of Electrical and Computer Engineering and the Department of Physics conducted the research. The University of Texas DoD JSEP program is a broad-based program with four research units in Solid State Electronics, two in Electromagnetics, two in Quantum Electronics, and two in Information Electronics. The Solid State Electronics program involves the fundamental issues in semiconductor physics and technology and addresses the basic problems to be solved for the development of the next generation of electronic and optical devices. In the following significant accomplishments section, we summarize recent advances in molecular beam epitaxy for ultra-high speed device applications and ion implantation of InP. In the Electromagnetics area several novel monolithic millimeter-wave integrated circuit structures are investigated for use as quasi-optical array elements. GRA

N88-24857# University of Southern California, Los Angeles. School of Engineering.
JOINT SERVICES ELECTRONICS PROGRAM RESEARCH IN ELECTRONICS Annual Technical Report, 1 Jan. - 31 Dec. 1987
31 Dec. 1987 36 p
(Contract F49620-85-C-0071)
(AD-A192206; AFOSR-88-0175TR) Avail: NTIS HC A03/MF A01 CSCL 09A

This program was designed to investigate the fundamental properties of ultrathin layers and the devices that would be fabricated from them. We have concentrated our investigations on the influence of growth conditions on the interfaces between AlGaAs and GaAs and the effect these properties have upon device performance. This has allowed us to optimize the techniques for interface formation to the point that low interface state densities

can be achieved for both normal and inverted heterojunctions. We have also determined the optimal conditions for the growth of quantum well structures and have achieved state of the art low temperature PL linewidths for metalorganic chemical vapor deposition (MOCVD) quantum wells (QW). We also investigated and analyzed the design of heterojunction bipolar transistors (HBT) during the course of this program. Our studies pointed out that a significant opportunity to increase the capabilities of bipolar circuits through the use of complementary device designs had been overlooked. We developed a methodology for device analysis that showed that Pnp HBT's could be designed that were comparable in performance to the Npn designs used by most workers. The realization of this analysis would allow designers to consider low power complementary bipolar circuits in GaAs for the first time. GRA

N88-24858# Texas Instruments, Inc., Dallas.
A MONOLITHIC REDUCED-SIZE Ku-BAND SPOT (SINGLE-POLE DOUBLE THROW) FET SWITCH
D. T. Bryant 1988 17 p Presented at the IEEE MTT-S International Microwave Symposium, New York, N.Y., 25 May 1988
(Contract DE-AC04-76DP-00789)
(DE88-006273; SAND-87-7172C; CONF-880565-2) Avail: NTIS HC A03/MF A01

A GaAs ku-band monolithic Single-Pole Double-Throw (SPDT) Field Effect Transistor (FET) switch has been designed and demonstrated. Small-signal insertion loss is less than 1.4 dB over a 14 GHz to 18 GHz band with a VSWR less than 1.5:1. The common terminal to off-channel isolation exceeds 18 dB. The switching is achieved with a -4.5 volt signal on the gate of the on-channel FET with the other gate at 0 volts. The switching current requirement is only the reverse bias gate leakage current (typically 3 uA). Large-signal performance is similar with a -10 volt control signal. The small chip size, 1.3 mm x 1.3 mm x 0.15 mm, permits more than 2300 monolithic switches to be fabricated on a single 3-inch GaAs wafer. DOE

N88-24859# General Electric Co., Schenectady, N.Y. Corporate Research and Development Center.
A MICROCOMPUTER-BASED CONTROL AND SIMULATION OF AN ADVANCED IPM (INTERIOR PERMANENT MAGNET) SYNCHRONOUS MACHINE DRIVE SYSTEM FOR ELECTRIC VEHICLE PROPULSION
B. K. Bose and P. M. Szczesny 1987 41 p Presented at the IECON Conference, Cambridge, Mass., 2 Nov. 1987
(Contracts DE-AC07-76ID01570; DE-AC07-85NV-10418)
(DE88-006735; EGG-M-12287; CONF-8711165-1) Avail: NTIS HC A03/MF A01

Advanced digital control and computer-aided control system design techniques are playing key roles in the complex drive system design and control implementation. The paper describes a high performance microcomputer-based control and digital simulation of an inverter-fed Interior Permanent Magnet (IPM) synchronous machine which uses a neodymium-iron-boron magnet. The fully operational four-quadrant drive system includes constant-torque region with zero speed operation and high speed field-weakening constant-power region. The control uses vector or field-oriented technique in constant-torque region with the direct axis aligned to the stator flux, whereas the constant-power region control is based on torque angle orientation of the impressed square-wave voltage. All the key feedback signals for the control are estimated with precision. The drive system is basically designed with an outer torque control loop for electric vehicle appliation, but speed and position control loops can be added for other industrial applications. The distributed microcomputer-based control system is based on Intel-8096 microcontroller and Texas Instruments TMS32010 type digital signal processor. The complete drive system has been simulated using the VAX-based simulation language SIMMON. DOE

N88-24860# Cooper Industries, Inc., Cannonsburg, Pa. Power Systems Div.
HARMONIC CONSIDERATIONS FOR ELECTRICAL DISTRIBUTION FEEDERS
Mar. 1988 147 p
(Contract DE-AC05-84OR-21400)
(DE88-007849; ORNL/Sub-81-95011/4) Avail: NTIS HC A07/MF A01

Harmonics on the electric power distribution system can cause motor overheating, capacitor failures,watt-hour meter error, and relay malfunctions. The degree of problems caused by harmonics is greatly dependent on the characteristics of the distribution feeder, which can absorb a considerable percentage of its capacity in harmonic currents without ill effects. However, power factor correction capacitors can cause resonances near harmonic voltages that can result in intolerable distortion. Both motor loads and resistive loads can decrease the effect of resonance significantly. This report describes useful techniques to analyze, suppress, and measure harmonics on distribution feeders. Applicable areas for manual analysis and computer analysis are explained. The basic formulae are presented as well as sophisticated computer methods. Emphasis is placed on the fundamental principle. Models of harmonic-producing devices are presented and their limitations discussed. Most distribution feeder harmonics analyses can be performed using simple current source models. Filtering of specific loads and general, dispersed load is discussed. The fundamental principle in filtering distribution feeders is to shorten the harmonic current path. 3-dimensional plots enhance the understanding of the filtering action. Equipment and procedures for making measurements are described. DOE

N88-24861*# Stanford Univ., Calif. Center for Space Science and Astrophysics.
THE OFF-AXIS CHANNEL MACROPLATE
J. Gethyn Timothy, Peter W. Graves, Thomas J. Loretz, and Raymond L. Roy (Detector Technology, Inc., Brookfield, Mass.) [1987] 5 p
(Contracts NASw-4093; NAS5-29274; Grant NAG5-622)
(NASA-CR-182938; NAS 1.26:182938) Avail: NTIS HC A02/MF A01 CSCL 09A

High-gain microchannel plates (MCPs) which utilize curvature of the channel to inhibit ion feedback (C-plate MCRs) have demonstrated excellent performance characteristics. However, C-plate MCPs are at present costly to fabricate, and the shearing process used to curve the channels produces a low device yield. Described here is a totally new type of high-gain MCP structure in which each channel has an axially symmetric curvature. Initial tests of proof-of-concept units of these MCPs with 75-micron-diameter channels (macroplates) suggest that their performance characteristics have the potential to be equal to those of a C-plate MCP while the fabrication process is no more complex than that of a conventional straight-channel MCP. Author

N88-24862* National Aeronautics and Space Administration. Pasadena Office, Calif.
MAGNETICALLY SWITCHED POWER SUPPLY SYSTEM FOR LASERS Patent
Thomas J. Pacala, inventor (to NASA) (Jet Propulsion Lab., California Inst. of Tech., Pasadena.) 6 Oct. 1987 12 p Filed 12 Feb. 1987 Continuation of US-Patent-Appl-SN-727931, Apr. 29, 1985, abandoned
(NASA-Case-NPO-16402-2; US-Patent-4,698,518; US-Patent-Appl-SN-013803; US-Patent-Class-307-106; US-Patent-Class-328-67; US-Patent-Class-315-172; US-Patent-Class-315-173; US-Patent-Appl-SN-727931) Avail: US Patent and Trademark Office CSCL 09A

A laser power supply system is described in which separate pulses are utilized to avalanche ionize the gas within the laser and then produce a sustained discharge to cause the gas to emit light energy. A pulsed voltage source is used to charge a storage device such as a distributed capacitance. A transmission line or other suitable electrical conductor connects the storage device to the laser. A saturable inductor switch is coupled in the transmission

line for containing the energy within the storage device until the voltage level across the storage device reaches a predetermined level, which level is less than that required to avalanche ionize the gas. An avalanche ionization pulse generating circuit is coupled to the laser for generating a high voltage pulse of sufficient amplitude to avalanche ionize the laser gas. Once the laser gas is avalanche ionized, the energy within the storage device is discharged through the saturable inductor switch into the laser to provide the sustained discharge. The avalanche ionization generating circuit may include a separate voltage source which is connected across the laser or may be in the form of a voltage multiplier circuit connected between the storage device and the laser. Official Gazette of the U.S. Patent and Trademark Office

N88-24863*# National Aeronautics and Space Administration. Pasadena Office, Calif.
TIMING CONTROL SYSTEM Patent Application
Gordon A. Wiker, inventor (to NASA) and George H. Wells, Jr., inventor (to NASA) (Jet Propulsion Lab., California Inst. of Tech., Pasadena.) 23 Sep. 1987 30 p Prepared in cooperation with Jet Propulsion Lab., California Inst. of Tech., Pasadena.
(Contract NAS7-918)
(NASA-Case-NPO-16882-1-CU; NAS 1.71:NPO-16882-1-CU; US-Patent-Appl-SN-154711) Avail: NTIS HC A03/MF A01 CSCL 09A

A timing control system is disclosed which is particularly useful in connection with simulated mortar shells. Special circuitry is provided to assure that the shell does not over shoot, but rather detonates early in case of an improper condition; this ensures that ground personnel will not be harmed by a delayed detonation. The system responds to an externally applied frequency control code which is configured to avoid any confusion between different control modes. A premature detonation routine is entered in case an improper time-setting signal is entered, or if the shell is launched before completion of the time-setting sequence. Special provisions are also made for very early launch situations and improper detonator connections. An alternate abort mode is provided to discharge the internal power supply without a detonation in a manner that can be externally monitored, thereby providing a mechanism for non-destructive testing. The abort mode also accelerates the timing function for rapid testing. NASA

N88-24864*# National Aeronautics and Space Administration. Pasadena Office, Calif.
A UNIVERSAL COMPUTER CONTROL SYSTEM FOR MOTORS Patent Application
Zoltan F. Szakaly, inventor (to NASA) (Jet Propulsion Lab., California Inst. of Tech., Pasadena.) 23 Mar. 1988 34 p Prepared in cooperation with Jet Propulsion Lab., California Inst. of Tech., Pasadena.
(Contract NAS7-918)
(NASA-Case-NPO-17134-1-CU; NAS 1.71:NPO-17134-1-CU; US-Patent-Appl-SN-172105) Avail: NTIS HC A03/MF A01 CSCL 09A

A control system for a multi-motor system such as a space telerobot, having a remote computational node and a local computational node interconnected with one another by a high speed data link is described. A Universal Computer Control System (UCCS) for the telerobot is located at each node. Each node is provided with a multibus computer system which is characterized by a plurality of processors with all processors being connected to a common bus, and including at least one command processor. The command processor communicates over the bus with a plurality of joint controller cards. A plurality of direct current torque motors, of the type used in telerobot joints and telerobot hand-held controllers, are connected to the controller cards and responds to digital control signals from the command processor. Essential motor operating parameters are sensed by analog sensing circuits and the sensed analog signals are converted to digital signals for storage at the controller cards where such signals can be read during an address read/write cycle of the command processing processor. NASA

N88-24865# Sandia National Labs., Albuquerque, N. Mex.
DESIGNING TO SAFE POWER LIMITS IN HYBRID CIRCUITS
D. Norwood 1988 10 p Presented at the 38th Electronics Components Conference, Los Angeles, Calif., 9 May 1988
(Contract DE-AC04-76DP-00789)
(DE88-005533; SAND-87-2768C; CONF-880554-1) Avail: NTIS HC A02/MF A01

Experiments are performed at two heat transfer conditions simulating minimum and maximum heat transfer. Since hybrid circuit heat dissipation is dependent on factors such as heat sinking, package design, substrate material, environment and other considerations, it was decided to bracket the extremes of power dissipation for hybrid circuits. Tests performed at these two heat transfer conditions yielded data which was used to form relationships between the hybrid variables of temperature, size, and power. To establish these relationships, the various sizes of resistors and hybrid substrates were accommodated by forming a ratio of resistor to substrate size; this ratio was then used to relate the variables of power density and temperature. Both resistor and substrate temperature were predictable within the desired temperature limits of 0 to 300 C using the relationships developed. Finally, the data and relationships shown graphically were converted to equation form making it possible to incorporate them into computer design programs. The power-temperature relationships developed make possible the predictions of both resistor and substrate temperatures at circuit design. This is both necessary and advantageous for design of hybrid circuits having increased power and circuit density. The work presented is not intended as a universal guide for designing circuits to safe power limits, rather, it should serve as an example or model for establishing power limits applicable to specific hybrid technologies. DOE

N88-24866# Sandia National Labs., Albuquerque, N. Mex.
MONOLITHIC GaAs Ku-BAND ONE WATT CONSTANT PHASE VARIABLE POWER AMPLIFIER
S. D. Pritchett May 1988 4 p Presented at the IEEE MTT-S International Microwave Symposium, New York, N.Y., 25 May 1988
(Contract DE-AC04-76DP-00789)
(DE88-006272; SAND-87-7173C; CONF-880565-1) Avail: NTIS HC A02/MF A01

A GaAs monolithic Ku-band 1.0 Watt constant phase variable power amplifer has been demonstated. Compressed gain is greater than 14 dB and 1.0 Watt output power over a 13.5 to 15.5 GHz band. More than 30 dB of gain control with less than + or - 10(degrees) of phase variation was demonstrated. DOE

N88-24867# Sandia National Labs., Albuquerque, N. Mex.
AN OVERVIEW OF ADVANCED BATTERY DEVELOPMENT AT SANDIA NATIONAL LABORATORIES
K. D. Murphy and R. B. Diegle Mar. 1988 24 p Presented at the 2nd International Rechargeable Battery Seminar, Deerfield Beach, Fla., 7 Mar. 1988
(Contract DE-AC04-76DP-00789)
(DE88-006823; SAND-88-0276C; CONF-880325-1) Avail: NTIS HC A03/MF A01

This paper contains a description of the activities of Sandia National Laboratories directed towards the development of electric battery technology. Batteries being developed have applications in electric powered vehicles, utility load leveling, and solar electric energy storage. General design points, recent achievements, and some applications of the work at Sandia are mentioned. DOE

N88-24868# Honeywell, Inc., Horsham, Pa. Power Sources Center.
OPTIMIZATION OF RESERVE LITHIUM THIONYL CHLORIDE BATTERY ELECTROCHEMICAL DESIGN PARAMETERS
N. Doddapaneni and N. A. Godshall 1987 13 p Presented at the 172nd Meeting of the Electrochemical Society, Honolulu, Hawaii, 18 Oct. 1987 Prepared in cooperation with Sandia National Labs., Albuquerque, N. Mex.

(Contract DE-AC04-76DP-00789)
(DE88-007109; SAND-87-1136C; CONF-871027-46) Avail: NTIS HC A03/MF A01

The performance of Reserve Lithium Thionyl Chloride (RLTC) batteries was optimized by conducting a parametric study of seven electrochemical parameters: electrode compression, carbon thickness, presence of catalyst, temperature, electrode limitation, discharge rate, and electrolyte acidity. Increasing electrode compression (from 0 to 15 percent) improved battery performance significantly (10 percent greater carbon capacity density). Although thinner carbon cathodes yielded less absolute capacity than did thicker cathodes, they did so with considerably higher volume efficiencies. The effect of these parameters, and their synergistic interactions, on electrochemical cell performance is illustrated. DOE

N88-24869*# National Aeronautics and Space Administration, Washington, D.C.
ON THE ABNORMAL PHENOMENA OBSERVED IN THE ELECTRICAL RESISTIVITY MEASUREMENT DURING THE DECOMPOSITION PROCESS OF SATURATED Cu-Fe ALLOYS
Kazuo Nagata and Seiichi Nishikawa Jun. 1988 13 p Transl. into ENGLISH from Cu-0.52 wt percent Fegokin Jiko Shoki ni Okeruhiteiko Zoka Oyobi Cu-Fe Gokin Jikozai no Sosei Kako ni Yoru Ijo Denki Teiko Zoka ni Tsuite, Seisan Kenkyu (Japan), v. 25, no. 7, 1973 p 288-293 Transl. by SCITRAN, Inc., Santa Barbara, Calif.
(Contract NASw-4307)
(NASA-TT-20183; NAS 1.77:20183) Avail: NTIS HC A03/MF A01 CSCL 09C

An anomalous increase of the electrical resistivity (p) in the initial period of aging of Cu-Fe (0.52 or 2.46 wt percent) alloys was ascribed to clustering of supersaturated Fe atoms in the process of quenching alloys and resolidifying of smaller clusters which were ones at higher temperatures. This anomalous increase of p(delta p) was observed when the aging temperature (T sub a) was greater than 550 deg, was more distinct at higher temperatures, was inversely proportioned to the cooling rate, and temperature in the quenching process. Typical values of delta p at T sub a = 600 and 700 deg were 0.1 and 0.2 microohms cm respectively. Delta p was also proportional to the specimen diameter. The anomalous delta p caused by plastic deformation of alloys (2.46 wt percent of Fe) was not explanable solely in terms of clustering and transformation of Fe atoms. Author

N88-24870*# National Aeronautics and Space Administration. Lewis Research Center, Cleveland, Ohio.
PROGRESS IN InP SOLAR CELL RESEARCH
Irving Weinberg and David J. Brinker 1988 16 p Presented at the 23rd Intersociety Energy Conversion Engineering Conference, Denver, Colo., 31 Jul. - 5 Aug. 1988; sponsored by ASME, AIAA, ANS, SAE, IEEE, ACS and AIChE
(NASA-TM-100914; E-4166; NAS 1.15:100914) Avail: NTIS HC A03/MF A01 CSCL 10A

Progress, in the past year, in InP solar cell research is reviewed. Small area cells with AMO, total area efficiencies of 18.8 percent were produced by OMCVD and Ion Implantation. Larger area cells (2 and 4 sq cm) were processed on a production basis. One thousand of the 2 sq cm cells will be used to supply power to a small piggyback lunar orbiter scheduled for launch in February 1990. Laboratory tests of ITO/InP cells, under 10 MeV proton irradiation, indicate radiation resistance comparable to InP n/p homojunction cells. Computer modeling studies indicate that, for identical geometries and dopant concentrations, InP solar cells are significantly more radiation resistant than GaAs under 1 MeV electron irradiation. Additional computer modeling calculations were used to produce rectangular and circular InP concentrator cell designs for both the low concentration SLATS and higher concentration Cassegrainian Concentrators. Author

N88-24871# Stanford Univ., Calif.
DEFECT DETECTION AND CLASSIFICATION IN VLSI PATTERN INSPECTION Ph.D. Thesis
Soo-Ik Chae 1987 122 p
Avail: Univ. Microfilms Order No. DA8800913

Inspection of VLSI circuit patterns is becoming increasingly important in maintaining high yields as the scale of integration in electronic circuits continues to increase. Most mask and wafer inspection systems compare a die image derived from the design database. In this approach, some form of alignment between the acquired image and reference data is required and the volume of the database becomes enormous as die complexity increases; in addition, defects cannot be classified. Alternative approaches studied detect and classify defects by employing the geometric properties of local images. In one approach, a local image is compared to template set representing both acceptable and defective patterns. In another approach, relevant topology can be obtained by determining the Euler number and its derivatives. In a third approach, a new chain coding scheme is developed from which the geometric properties can be obtained. Custom VLSI chips comprised of maskable content addressable memories were designed, fabricated and tested as an implementation of a high speed template matching system. New alternatives are provided for defect classification. Dissert. Abstr.

N88-24872# Helsinki Univ. Technology, Otaniemi (Finland). Digital Systems Lab.
SOME UNSOLVED PROBLEMS IN MODELLING SELF-TIMED CIRCUITS USING PETRI NETS, SERIES B, NUMBER 2
M. Tiusanen Jan. 1988 15 p
(PB88-181466; ISBN-951-754-344-1) Avail: NTIS HC A03/MF A01 CSCL 09C

Some open problems that have arisen in the context of using conflict free labelled Petri Nets to model so-called self-timed or self-synchronizing circuits are presented. These are circuits designed to operate correctly independently of the delays inherent in the components. The problems presented concern the concurrency of transitions in the marking class, formulation of a new concession rule for modelling mass phenomena, and modelling nondistributive Muller diagrams by Petri Nets. Author

34 FLUID MECHANICS AND HEAT TRANSFER

Includes boundary layers; hydrodynamics; fluidics; mass transfer; and ablation cooling.

For related information see also *02 Aerodynamics* and *77 Thermodynamics and Statistical Physics.*

N88-24873# Rutgers - The State Univ., New Brunswick, N. J.
HEAT TRANSFER FROM A NEGATIVELY BUOYANT WALL JET Annual Report
K. Kapoor and Y. Jaluria Feb. 1988 46 p
(Contract NB83-NADA-4047)
(PB88-181953; NBS/GCR-88/541) Avail: NTIS HC A03/MF A01 CSCL 20D

An experimental investigation, carried out on the heat transfer characteristics of a turbulent, negatively buoyant, two-dimensional wall jet. A jet of hot air is discharged adjacent to a water-cooled, isothermal surface in an extensive environment. The heat transfer to the surface from the elevated-temperature jet is measured along the isothermal surface for several values of wall, jet and ambient temperatures. Wide ranges of Grashof number and Reynolds number are investigated. The total heat transfer to the isothermal surface is obtained. GRA

N88-24874# Ballistic Research Labs., Aberdeen Proving Ground, Md.
INTERNAL FLUID DYNAMICS WITHIN A NONSPINNING PARTIALLY LIQUID-FILLED SHELL DUE TO BURSTER RUPTURE
Paul Weinacht and Charles J. Nietubicz Dec. 1987 47 p

(AD-A191055; BRL-TR-2880) Avail: NTIS HC A03/MF A01 CSCL 19J

This forced liquid projectile is being directed by the Munitions Branch of the U.S. Army Chemical Research, Development and Engineering Center (CRDEC). The Computational Aerodynamics Branch, Launch and Flight Division U.S. Army Ballistic Research Laboratory (BRL), has been tasked to determine the internal fluid dynamics within a partially liquid-filled shell subject to large rapidly applied pressures which result from internal burster tube rupture. The main area of concern is the determination of the time history of the internal pressure on the shell sidewalls and base. A numerical model has been developed to simulate the internal fluid dynamics of this partially liquid-filled configuration. This numerical model solves the quasi one-dimensional Euler equations and a equation of state for liquid using the explicit MacCormack numerical technique. Results have been generated for an internal shell geometry currently being tested by the Terminal Ballistics Division (TBD), BRL. Comparisons are made between the numerically predicted pressure levels and the pressure measurements performed by TBD. GRA

N88-24875# Cincinnati Univ., Ohio. Dept. of Aerospace Engineering and Engineering Mechanics.
COMPOSITE REDUCED NAVIER-STOKES PROCEDURES FOR FLOW PROBLEMS WITH STRONG PRESSURE INTERACTIONS Annual Report, 1 Feb. 1987 - 31 Jan. 1988
S. G. Rubin and P. K. Khosla 2 Feb. 1988 60 p
(Contract F49620-85-C-0027)
(AD-A191127; AFOSR-88-0296TR) Avail: NTIS HC A04/MF A01 CSCL 20D

A Reduced Navier Stokes (RNS) system is more computationally efficient than full Navier Stokes solvers and more accurate and less cumbersome than matched viscous and inviscid methods has been shown to apply to a significant class of aerodynamic problems. The RNS system is a composite of the full Euler and boundary layer equations and is discritized to optimize the numerical representation of viscous and inviscid regions, respectively. GRA

N88-24876# Douglas Aircraft Co., Inc., Long Beach, Calif.
INSTABILITY OF LAMINAR SEPARATION BUBBLES: CAUSES AND EFFECTS Technical Report, Mar. - Sep. 1987
Tuncer Cebeci Sep. 1987 16 p
(Contract F49620-84-C-0007)
(AD-A191168; MDC-K0534; AFOSR-88-0249TR) Avail: NTIS HC A03/MF A01 CSCL 01A

A combination of interactive boundary layer and stability theories has been used to investigate the reasons for the instability of laminar separation bubbles on the leading edge of thin airfoils. It is shown that transition plays an important role and is likely to preclude the existence of long separation bubbles and their supposed instability. GRA

N88-24877# Georgia Inst. of Tech., Atlanta. School of Aerospace Engineering.
STAGNATING TURBULENT REACTING FLOWS Final Report, 1 Oct. 1983 - 30 Nov. 1987
Warren C. Strahle 15 Jan. 1988 9 p
(Contract DAAG29-84-K-0143)
(AD-A191449; ARO-20658.5-EG) Avail: NTIS HC A02/MF A01 CSCL 20D

Theoretical and experimental results are reported concerning the problem of heat transfer to bodies when there is turbulence imbedded in the freestream. Both velocity and temperature turbulence are considered and a fully variable density theory is developed. Experiments were conducted in collaboration with NASA/Lewis. Excellent closure of theory and experiment was achieved for the case of no freestream temperature fluctuations. With no data available for comparison, no closure could be achieved for the case of temperature fluctuations, but the theory indicates that the heat transfer effect of this phenomenon is strong. GRA

N88-24878# California Univ., Irvine. Dept. of Mechanical Engineering.
STUDY OF MIXING AND REACTION IN THE FIELD OF A VORTEX Report, for Oct. 1986 - Oct. 1987
B. M. Cetegen and W. A. Sirignano 20 Nov. 1987 5 p
(Grant AF-AFOSR-0016-86)
(AD-A191489; AFOSR-88-0251TR) Avail: NTIS HC A02/MF A01 CSCL 20D

In turbulent reacting flows, completion of chemical reactions requires diffusion of reactive species at a molecular level. Eddies rich in one reactant can be present in many turbulent flows involving finite rate chemical reactions. Local species stratifications are dissipated by molecular diffusion and chemical reaction under the influence of the local flow field. In many turbulent flows, the local flow field has a strong rotational character. It is mostly this rotational motion which enhances mixing through flow stretch and convection leading to mixing at the molecular level. In this paper, molecular mixing and finite rate chemical reactions in a two dimensional viscous vortex are examined analytically. Two species initially separated across a plane are allowed to diffuse and react in the presence of a line vortex centered at this separation plane. GRA

N88-24879# University of Southern California, Los Angeles. School of Engineering.
DYNAMICS AND CONTROL OF TURBULENT SHEAR FLOWS Report, for 1 Oct. 1986 - 30 Sep. 1987
30 Sep. 1987 21 p
(Contract N00014-86-K-0679)
(AD-A191527) Avail: NTIS HC A03/MF A01 CSCL 20D

Some areas of research are: Dynamics and Control of Turbulent Shear Flows; Control of Bounded Shear Flows -- Experimental Flows; Control of the Large - Scale Features in Turbulent Mixing Layers; Direct Numerical Simulations of Flow Control; Control of Entrainment in Confined Shear Layers; Theoretical Underpinnings; Amplitude and Phase Descriptions of Coherent Structures; Phase Control of Vortex Structures in Shear Flows; and Invariant Manifold Theory for Hydrodynamic Transition. GRA

N88-24880# Washington State Univ., Pullman. Dept. of Mechanical Engineering.
TRANSIENT PARTICLE DEPOSITION IN A BOUNDARY LAYER OF IMPULSIVE FLOW OVER A FLAT PLATE Contractor Report, Jul. - Aug. 1985
Jacob N. Chung Nov. 1987 60 p
(DA Proj. 1L1-61102-AH-3)
(AD-A191537; BRL-CR-589) Avail: NTIS HC A04/MF A01 CSCL 20D

The transport and deposition of fine particles in a boundary layer of impulsive flow over a flat plate have been examined by numerical methods. The transient impulsive flow over a flat plate is solved by a vortex sheet method and the particle transport equation is numerically integrated by the Strongly Implicit Procedure. The transient solutions are preliminary because refinement of the computer program is needed. Some trends and interesting features may be drawn from the results. GRA

N88-24881# Naval Ship Research and Development Center, Bethesda, Md.
COMPUTATION OF THE TURBULENT BOUNDARY LAYER DOWNSTREAM OF VORTEX GENERATORS Final Report, Sep. 1986 - Sep. 1987
Paul K. Chang Dec. 1987 47 p
(AD-A191544; DTRC-87/054; DTRC/AERO-1302) Avail: NTIS HC A03/MF A01 CSCL 20D

The approximate analysis of three-dimensional incompressible turbulent boundary layer downstream of vortex generators is presented. Extensive numerical computations are carried out to assess the effectiveness of single-row, counter-rotating vane-type vortex generators to alleviate flow separation lines. Flow separation downstream of the vortex generators on a thick airfoil are determined in terms of size, location, and arrangement of the vortex generators. These lines are compared with the separation

line without the vortex generators. High efficiency is obtained with the moderately slender rectangular blade of the generator. The results indicate that separations is alleviated more effectively in the region closer to the symmetry axis of the generator than in the outer region of the symmetry axis. No optimum conditions for the alleviation of flow separation are established in this investigation, and no comparisons are made with other analytical results and experimental data. GRA

N88-24882# Rutgers - The State Univ., New Brunswick, N. J. Dept. of Mechanical and Aerospace Engineering.
THEORETICAL INVESTIGATION OF 3-D SHOCK WAVE-TURBULENT BOUNDARY LAYER INTERACTIONS, PART 6 Annual Report, 1 Oct. 1986 - 30 Sep. 1987
Doyle D. Knight Jan. 1988 48 p
(Grant AF-AFOSR-0266-86)
(AD-A191546; RU-TR-171-MAE-F; AFOSR-88-0127TR) Avail: NTIS HC A03/MF A01 CSCL 20D

The research concerns the understanding of 3-D shock wave-turbulent boundary layer interactions. The research activity has focused on several areas. First, the 3-D swept compression corner has been computed at Mach 3 for a sweep angle of 40 deg and compression angle of 24 deg. The calculated flows are in good agreement with experiment. Second, the flowfield structure of the 3-D swept compression corner is dominated by a large vortical structure. Third, the interaction has been found quantitatively to be dominated by inviscid effects except within a small fraction of the boundary layer. Fourth, the effect of boundary layer bleed has been examined for the 3-D shock wave-turbulent boundary layer interaction generated by a sharp fin. The effects of bleed are principally limited to the near surface region. The overall vortical structure is insensitive to surface bleed. GRA

N88-24883# Jet Propulsion Lab., California Inst. of Tech., Pasadena.
THE BEHAVIOR OF DROP-CONTAINING TURBULENT EDDIES Annual Report, 1 Oct. 1986 - 30 Sep. 1987
Josette Bellan 30 Nov. 1987 5 p
(Grant AF-AFOSR-ISSA-0025-87)
(AD-A191669; AFOSR-88-0252TR) Avail: NTIS HC A02/MF A01 CSCL 20D

The effect of turbulent entrainment and mixing at the boundary of a cluster of evaporating drops has been studied. The results obtained by solving the model equations show that for dense clusters turbulence exchange processes are crucial in determining the lifetime of the drops in the clusters. The results also show that turbulence helps evaporate larger clusters of drops faster when the clusters are dense. GRA

N88-24884# Aeronautical Research Associates of Princeton, Inc., N. J.
RESEARCH IN NONLINEAR WAVE MOTION Final Report, 15 Oct. 1984 - 30 Nov. 1987
Harvey Segur Jan. 1988 138 p
(Contract DAAG29-85-C-0001)
(AD-A191686; ARAP-617; ARO-21716.9-MA) Avail: NTIS HC A07/MF A01 CSCL 20D

An important result of this research is a new model of periodic waves of finite amplitude, propagating without change of form in shallow water. The model is analytic and deterministic, and it shows good agreement with laboratory experiments. A second important result is the development of a rigorous method to find exponentially small effects, which lie beyond all orders in conventional asymptotic expansion. GRA

N88-24885# Pennsylvania State Univ., University Park. Applied Research Lab.
AXISYMMETRIC VISCID-INVISCID INTERACTION BY A FROZEN VORTICITY APPROXIMATION
G. H. Hoffman 14 Jan. 1988 49 p
(Contract N00014-85-C-6041)
(AD-A191743; TM-88-12) Avail: NTIS HC A03/MF A01 CSCL 20D

A numerical solution procedure capable of a high degree of automation is presented for calculating the flow field associated with viscid-inviscid interaction on a body of revolution. The method makes use of ideas from asymptotic triple deck analysis of the trailing edge problem. A simpler problem is solved in which two layers are postulated, an outer inviscid, rotational layer (frozen vorticity) which largely governs the pressure in the trailing edge region, and an inner turbulent layer which is modeled in a simple manner. These two layers are patched at a fixed distance from the wall and wake centerline rather than asymptotically matched. The method allows the viscid-inviscid interaction solution to be computed in four interactions, none of which require any user intervention. A high degree of automation is achieved in the computer code because of three factors: (1) the solution cycle is very stable, (2) all calculations use a common streamwise grid, and (3) information is transferred to successive stages of the calculation by computer generated files. Numerical solutions are presented for three bodies and the results compared with published experimental data. GRA

N88-24886# Defence Research Establishment Atlantic, Dartmouth (Nova Scotia).
CROSS STREAM DIFFERENCING FOR INTEGRAL BOUNDARY LAYER EQUATIONS
David Hally Nov. 1987 25 p
(AD-A191744; DREA-TM-87/217) Avail: NTIS HC A03/MF A01 CSCL 20D

An efficient, stable, explicit, first-order cross-stream differencing scheme having low truncation error is derived and applied to three dimensional integral boundary layer equations. The analysis is considered in detail for the particular case of the momentum integral equations and Head's entrainment equation with power law profiles and Mager's cross flow assumption. In comparison with upwinding differencing, the new scheme has better stability properties, smaller truncation error, and smaller artificial viscosity. GRA

N88-24887# Dayton Univ., Ohio. Research Inst.
FAST ALGORITHM DEVELOPMENT FOR LARGE-EDDY SIMULATION OF CIRCULAR-JET TURBULENCE Final Technical Report, 15 Sep. 1985 - 14 Oct. 1987
L. Krishnamurthy, C. A. Hall, and T. A. Porsching Dec. 1987 30 p
(Contract F49620-85-C-0137)
(AD-A192044; UDR-TR-87-150; AFOSR-88-0091TR) Avail: NTIS HC A03/MF A01 CSCL 20D

The research addresses a single, free, round turbulent jet expanding into a quiescent environment, and deals with the large scale motions through large eddy simulation and the small scale motions through subgrid-scale turbulence modeling. The computational fluid dynamic investigation of the nearfield downstream of an axisymmetric nozzle is based on a two dimensional procedure involving a variable reduction method, with the farfield fully developed flow structure analyzed by matched asymptotic expansions for large Reynolds numbers. The numerical algorithm development examines vectorization, three dimensional flowfield, and the construction of weakly dissipative difference methods. GRA

N88-24888# Purdue Univ., West Lafayette, Ind. School of Mechanical Engineering.
INJECTION OF DRAG REDUCING ADDITIVES INTO TURBULENT WATER FLOWS Technical Report, 1 Mar. - 30 Nov. 1987
David T. Walker and William G. Tiederman Feb. 1988 38 p
(Contract N00014-83-K-0183)
(AD-A192072; PME-FM-88-1) Avail: NTIS HC A03/MF A01 CSCL 20D

The primary objective of this portion of the program is to build a data base that is sufficient to critically test models of the initial mixing between a polymer solution injected at the wall and a turbulent water flow. Time-resolved concentration measurements were made using a laser-induced fluorescence technique downstream of a flush mounted wall injector. The injected polymer

solution was a 700 ppm aqueous solution of SEPARAN AP-273. For comparison purposes, measurements were also made for a water injection at the same flow rate. The results for the instantaneous, mean and root-mean-square concentration profiles at positions 10, 25, 50 and 100 mm downstream of the injector show how the mixing decreases when the injectant is a polymer solution. GRA

N88-24889# Clarkson Univ., Potsdam, N.Y. Dept. of Mathematics and Computer Science.
NONLINEAR WAVES Final Report
Mark J. Ablowitz and Athanassios S. Fokas Feb. 1988 7 p
(Contract N00014-86-K-0603)
(AD-A192148) Avail: NTIS HC A02/MF A01 CSCL 12A

This work has important applications in fluid dynamics (e.g. long waves in stratified fluids, solitons generated by ships), nonlinear optics (e.g. self-induced transparence, and self-focussing of light), digital communications via solitons, inverse scattering in one and higher dimensions. Areas of Study Include: Solutions of nonlinear multidimensional systems arising in Physics, inverse problems, especially in multidimensions, and DBAR methodology; Riemann-Hilbert boundary value problems, and inverse problems; Solitons in multidimensional systems, solitons, generated by ships in narrow channels; Nonlinear systems with external focussing; Semi infinite boundary value problems; IST for nonlinear singular integro-differential equations; the Benjamin-Ono equation, the intermediate Long Wave Equation, the Sine-Hilbert equation, multidimensional generalizations; Discrete IST and numerical simulations; Painleve equations; Focussing singularities in nonlinear wave propagation; Applications to surface waves, internal waves, shear flows; nonlinear optics, S.I.T., relativity etc; Direct linearizing methods for nonlinear evolution equations; Multidimensional generalizations of the Sine-Gordon and wave equations arising in differential geometry; Algebraic methods and symmetries of multidimensional nonlinear evolution equations; and Solutions to semiperiodic multidimensional equations. GRA

N88-24890# Wyoming Univ., Laramie.
ADAPTIVE LOCAL GRID REFINEMENT IN COMPUTATIONAL FLUID MECHANICS Final Report, 1 Apr. 1985 - 30 Sep. 1987
Richard E. Ewing, Myron B. Allen, M. J. Djomehri, John H. George, and Eli L. Isaacson Nov. 1987 19 p
(Grant AF-AFOSR-0117-85)
(AD-A192215; AFOSR-87-1984TR) Avail: NTIS HC A03/MF A01 CSCL 20D

Several promising new techniques for efficient and accurate numerical solution of large-scale fluid flow problems have been developed. These methods include self-adaptive mesh modification techniques for applications requiring front-tracking and local grid refinement as well as new preconditioning ideas for efficient implementation. Properties of systems of hyperbolic conservation laws have been obtained which will aid in development of accurate front-tracking algorithms. Adaptive grid refinement techniques developed include moving grid methods, local, fixed refinement involving linked-list data structures, and certain local patch refinement ideas which have great potential for ease of implementation in existing large scale codes. Domain decomposition concepts for obtaining efficient preconditioners for iterative techniques have proved quite useful both for local patch refinement and for the solution of problems with rapidly varying coefficients. The fast adaptive algorithms being developed have high potential for both parallelization and vectorization. The algorithms have been designed to take advantage of the emerging parallel and vector-oriented computer architectures. Finally, the incorporation of these fast algorithms in accurate finite element, collocation, and finite difference methods is underway. GRA

N88-24891# Max-Planck-Institut fuer Stroemungsforschung, Goettingen (West Germany).
HYDROACOUSTIC PULSATING JET GENERATOR [EIN HYDROAKUSTISCHER PULSSTRAHLERZEUGER]
A. Unrau and G. E. A. Meier Apr. 1987 27 p In GERMAN
(MPIS-7/1987; ISSN-0436-1199; ETN-88-91928) Avail: NTIS HC A03/MF A01; Max-Planck-Institut fuer Stroemungsforschung, Boettinger Strasse 6-8, 3400 Goettingen, Federal Republic of Germany 15 Deutsche marks

A high pressure turbulent jet generator connected to a low pressure hydraulic tube is studied to investigate water hammer in tubes with fast flow variations, generating high pressure pulsating water jets. The pulsating jet generator consists of a tube, a hydraulic valve, a spring, and a water container. The jet is the effect of the combination of turbulent pipe flow with a valve for flow nozzle. The jet pressure depends on specific oscillation impedance and flow velocity variations. For inlet pressure of 0.5 to 2 bar the pressure rises to 40 bar. The described pulsating jet generator is more effective than the earlier model. A piezoelectric pressure controller is used to register pressure signals and high speed photos are made of the jet. Test results are consistent with theoretical calculation. ESA

N88-24892# Max-Planck-Institut fuer Stroemungsforschung, Goettingen (West Germany).
THEORETICAL INVESTIGATION OF THE DEVELOPMENT OF THE NORMAL FLUID AND SUPERFLUID VELOCITY DISTRIBUTIONS DURING SPIN-UP FOR A He2-FILLED CYLINDER
W. Poppe and D. W. Schmidt Mar. 1987 55 p Sponsored by Deutsche Forschungsgemeinschaft
(MPIS-6/1987; ISSN-0436-1199; ETN-88-91927) Avail: NTIS HC A04/MF A01; Max-Planck-Institut fuer Stroemungsforschung, Boettinger Strass 6-8, 3400 Goettingen, Federal Republic of Germany 33 Deutsche marks

The development of the normal and superfluid velocity distributions during spin-up for an He2-filled, abruptly accelerated rotating cylinder was analyzed. The one-dimensional nonstationary hydrodynamic equations of the Hall-Vinen-Bekarevich-Khalatnikov-theory for flows with high density of vortex lines was solved numerically. The calculations were carried out for the case of only dissipative spreading at normal fluid vorticity and for the case of dissipative as well as convective spreading of vorticity, in the course of which secondary flows were described with regard to the Wedemeyer-model for normal fluids. The boundary conditions for the superfluid component were modeled by the assumption of a certain flux of vortex lines through the wall of the cylinder. As the results of this theoretical analysis do not match those of experimental investigations in detail, calculations were also made for modifications of the model of secondary flow and the boundary conditions for the normal fluid component. ESA

N88-24893# Imperial Coll. of Science and Technology, London (England). Computational Fluid Dynamics Unit.
COMPUTATIONAL FLUID DYNAMICS APPLIED TO THE PREDICTION OF THE HEAT-TRANSFER, MECHANICAL AND THERMAL-STRESS BEHAVIOR OF HEAT EXCHANGERS
D. B. Spalding Aug. 1987 62 p Presented at a conference, Pune, India, Jun. 1986
(CFDU/87/7; ETN-88-92504) Avail: NTIS HC A04/MF A01

It is argued that it is easy to compute the flow patterns in heat-exchange equipment, (single or two-phase steady or transient) whether the geometry is simple or complex. The transition from the possible to the easy results from the development of user-friendly software used for a great variety of computational fluid dynamics applications, which transmit to the heat exchanger industry the benefits of research carried out on behalf of quite different communities. ESA

N88-24894# Imperial Coll. of Science and Technology, London (England). Computational Fluid Dynamics Unit.
CFD BENEFITS, GOALS, STEPPING-STONES AND TECHNIQUES. PROPOSALS FOR THE SCIENTIFIC PROGRAMME OF THE EUROPEAN RESERCH CENTRE ON FLOW, TURBULENCE AND COMBUSTION
D. Brian Spalding Jan. 1988 37 p
(CFDU/88/1; ETN-88-92507) Avail: NTIS HC A03/MF A01

The benefits of computerized simulation of flow, turbulence,

and combustion in the aerospace, automobile, power-generation, vehicular and aircraft-propulsion, chemical and process, nuclear, food-manufacturing, pharmaceutical, environmental, and biomedical domains are outlined. Industrially or socially useful goals which might reasonably be achieved by the end of the first decade of intensive collaborative work, and stepping-stone projects, i.e., those which need to be achieved first in order that the grander goals can be achieved later, are summarized. ESA

N88-24895# Imperial Coll. of Science and Technology, London (England). Computational Fluid Dynamics Unit.
NUMERICAL SIMULATIONS OF THE FLAT-PLATE LAMINAR BOUNDARY LAYER IN SUBSONIC AND SUPERSONIC FLOW
F. Villasenor and D. Radosavljevic Dec. 1987 36 p
(PDR/CFDU-IC/36; ETN-88-92508) Avail: NTIS HC A03/MF A01

Numerical predictions of the boundary-layer flow on plates made by the PHOENICS code were compared with published results. The study covers subsonic and supersonic laminar flow for compressible and incompressible fluids. Kinematic heating and variations of viscosity and density with temperature are taken into account, for finite and zero wall heat transfer. Velocity and temperature distributions, together with the local skin friction and local Nusselt numbers are provided. They show good agreement with previous solutions. ESA

N88-24896# Grenoble-1 Univ. (France). Inst. de Mecanique.
THREE DIMENSIONAL SPECTRAL ENERGY MEASUREMENT ON TURBULENCE SUBJECTED TO A HIGH DEGREE OF PLANE DEFORMATION Final Report [MESURES DES SPECTRES TRIDIMENSIONNELS D'ENERGIE D'UNE TURBULENCE SOUMISE A UN FORT TAUX DE DEFORMATION PLANE]
E. J. Hopfinger and Ph. Caperan May 1987 58 p In FRENCH
(Contract DRET-83-324)
(ETN-88-92537) Avail: NTIS HC A04/MF A01

The correlations and the three-dimensional spectra of an initially isotropic turbulence subjected to a large plane deformation were studied to determine nonlinear transfer mechanisms, particularly anisotropy mechanisms and the return to isotropy, and to produce reliable results for calibrating two-point closure models and numerical simulation at large scales. Wind tunnel tests were performed to acquire data. Results show good correlations in the isotropic zone. Bad convergence of the three-dimensional spectra prevents a detailed analysis of their structure. Data smoothing is required, but is impossible due to insufficient theoretical knowledge. ESA

N88-24897# Von Karman Inst. for Fluid Dynamics, Rhode-Saint-Genese (Belgium).
TWO DIMENSIONAL HYPERBOLIC GRID GENERATION
Zuheyr Alsalihi Oct. 1987 60 p
(VKI-TN-162; ETN-88-92482) Avail: NTIS HC A04/MF A01

A two dimensional body-fitted coordinate system was generated for use in solving the turbulent or laminar, (thin-layer) Navier-Stokes equations for transonic flow fields about airfoils. The technique employed is hyperbolic grid generation with the condition of orthogonality and cell area (inverse of the metric Jacobian) specification. Addition of fourth-order numerical dissipation terms in the streamwise direction has no detrimental effect on the orthogonality. Results indicate that the method is applicable to any kind of grid topology without modification if the outer boundary is not prescribed. However, incorporation of a shooting method or combination of the technique with another method (such as transfinite interpolation technique) can be utilized in cases where specification of points on the outer boundary is required. Extension of the technique to three space dimensions and incorporation of physical grid adaptivity (dynamic remeshing) making use of the gradients of physical quantities in the specification of the cell area is also possible. The listing and user instructions of a FORTRAN program written for the implementation of the technique are included. ESA

N88-24898# Sandia National Labs., Albuquerque, N. Mex. Fluid and Thermal Sciences Dept.
CONTINUUM THEORIES FOR FLUID-PARTICLE FLOWS: SOME ASPECTS OF LIFT FORCES AND TURBULENCE
David F. McTigue, Richard C. Givler, and Jace W. Nunziato 1988 17 p Presented at the Transport Processes in Dispersed Two-Phase Flows with Applications to Propulsion Systems Conference, Huntsville, Ala., 25 Feb. 1988
(Contract DE-AC04-76DP-00789)
(DE88-007038; SAND-88-0542C; CONF-880250-2) Avail: NTIS HC A03/MF A01

A general framework is outlined for the modeling of fluid particle flows. The momentum exchange between the constituents embodies both lift and drag forces, constitutive equations for which can be made explicit with reference to known single particle analyses. Relevant results for lift are reviewed, and invariant representations are posed. The fluid and particle velocities and the particle volume fraction are then decomposed into mean and fluctuating parts to characterize turbulent motions, and the equations of motion are averaged. In addition to the Reynolds stresses, further correlations between concentration and velocity fluctuations appear. These can be identified with turbulent transport processes such as eddy diffusion of the particles. When the drag force is dominant, the classical convection dispersion model for turbulent transport of particles is recovered. When other interaction forces enter, particle segregation effects can arise. This is illustrated qualitatively by consideration of turbulent channel flow with lift effects included. Author

N88-24899*# Lockheed Missiles and Space Co., Huntsville, Ala. Computational Mechanics Section.
DUCT FLOW NONUNIFORMITIES FOR SPACE SHUTTLE MAIN ENGINE (SSME) Final Report
30 Dec. 1987 129 p
(Contract NAS8-35592)
(NASA-CR-179338; NAS 1.26:179338; LMSC-HEC-TR-F225755)
Avail: NTIS HC A07/MF A01 CSCL 20D

A three-duct Space Shuttle Main Engine (SSME) Hot Gas Manifold geometry code was developed for use. The methodology of the program is described, recommendations on its implementation made, and an input guide, input deck listing, and a source code listing provided. The code listing is strewn with an abundance of comments to assist the user in following its development and logic. A working source deck will be provided. A thorough analysis was made of the proper boundary conditions and chemistry kinetics necessary for an accurate computational analysis of the flow environment in the SSME fuel side preburner chamber during the initial startup transient. Pertinent results were presented to facilitate incorporation of these findings into an appropriate CFD code. The computation must be a turbulent computation, since the flow field turbulent mixing will have a profound effect on the chemistry. Because of the additional equations demanded by the chemistry model it is recommended that for expediency a simple algebraic mixing length model be adopted. Performing this computation for all or selected time intervals of the startup time will require an abundance of computer CPU time regardless of the specific CFD code selected. Author

N88-24900*# National Aeronautics and Space Administration. Ames Research Center, Moffett Field, Calif.
CHARACTERISTICS OF MERGING SHEAR LAYERS AND TURBULENT WAKES OF A MULTI-ELEMENT AIRFOIL
Desmond Adair and W. Clifton Horne Feb. 1988 79 p
(NASA-TM-100053; A-88048; NAS 1.15:100053) Avail: NTIS HC A05/MF A01 CSCL 20D

Flow characteristics in the vicinity of the trailing edge of a single-slotted airfoil flap are presented and analyzed. The experimental arrangement consisted of a NACA 4412 airfoil equipped with a NACA 4415 flap whose angle of deflection was 21.8 deg. The flow remained attached over the model surfaces except in the vicinity of the flap trailing edge where a small region of boundary-layer separation extended over the aft 7 percent of flap chord. The flow was complicated by the presence of a strong,

initially inviscid jet emanating from the slot between airfoil and flap, and a gradual merging of the main airfoil wake and flap suction-side boundary layer. Downstream of the flap, the airfoil and flap wakes fully merged to form an asymmetrical curved wake. The airfoil configuration was tested at an angle of attack of 8.2 deg, at a Mach number of 0.09, and a chord based Reynolds number of 1.8 x 10 to the 6th power in the Ames Research Center 7- by 10-Foot Wind Tunnel. Surface pressure measurements were made on the airfoil and flap and on the wind tunnel roof and floor. It was estimated that the wall interference increased the C sub L by 7 percent and decreased the C sub M by 4.5 percent. Velocity characteristics were quantified using hot-wire anemometry in regions of flow with preferred direction and low turbulence intensity. A 3-D laser velocimeter was used in regions of flow recirculation and relatively high turbulence intensity.

Author

N88-24901 Yale Univ., New Haven, Conn.
MANIPULATION OF THE STRUCTURE OF A TURBULENT BOUNDARY LAYER Ph.D. Thesis
Theodore Brooks Lynn 1987 168 p
Avail: Univ. Microfilms Order No. DA8729107

The manipulation of a turbulent boundary layer for the purpose of net drag reduction is an attractive topic for research, because even modest success will result in large energy savings. The focus is on passive manipulation, one of the simplest manipulation techniques. The most promising manipulator is the so-called BLADE device, consisting of two thin ribbons or foils suspended in the outer portion of the boundary layer. When the research was begun, there was significant controversy over the magnitude of the net drag reduction possible (20 percent) and the maximum skin friction reduction obtainable (50 percent). Accurate local skin-friction measurements were made using sublayer fences in a perturbed boundary layer. By comparing the direct measurements with those obtained by indirect methods, it was determined that the degree of drag reduction obtained depends on the method used to calculate the combined device drag and skin friction drag. Using auto and two-point correlation measurements as well as space-time correlations, the effects of BLADE were investigated on the turbulent structures in the boundary layer, comparing them with wire devices, which are not known to produce a net reduction in drag. The space-time correlation revealed that the most significant effect of the BLADE device was on the large structures (the dominant structures in the outer region of the boundary layer). The inner layer devices consisting of sublayer wires were also investigated. The results from both the inner and outer layer manipulations suggest that the effective alteration of a turbulent boundary layer depends on the scaling of the device.

Dissert. Abstr.

N88-24902 Pennsylvania State Univ., University Park.
GAS DIFFUSION STUDIES IN STEADY AND NONSTEADY CAVITIES Ph.D. Thesis
Krishnaswamy Ravindra 1987 162 p
Avail: Univ. Microfilms Order No. DA8728068

Water-tunnel experiments for two-dimensional flows were conducted on cavities behind a stationary and oscillating flat plate hydrofoil. It is found that the steady cavity pressures were significantly higher than the vapor pressure of water and larger cavities tend to maintain higher cavity pressures. Unsteady cavity pressures were found to be significant only at low frequencies of profile oscillation. Downstream and upstream of the cavity, the oscillating cavity was observed to behave like a dipole source at low frequencies of oscillation and like a quadrupole source at high frequencies of foil oscillation. For sinusoidal motions of the foil, the first two harmonics of the cavity motions are significant. A mathematical model is then developed to estimate the nonsteady gaseous entrainment behind two-dimensional steady and oscillating cavities. It is found that gas pressure within the cavity affects the steady entrainment behind the cavity. The phase angle between the foil motion and cavity motion is determined by a physically driven argument that is seen to be consistent with experimental observations. The nonsteady gaseous entrainment behind the cavity is seen to depend only on the cavity volume fluctuations and cavity gas pressure fluctuations.

Dissert. Abstr.

N88-24903 Purdue Univ., West Lafayette, Ind.
FORCED RESPONSE UNSTEADY AERODYNAMICS IN A MULTISTAGE COMPRESSOR Ph.D. Thesis
Vincent Ralph Capece 1987 208 p
Avail: Univ. Microfilms Order No. DA8729723

The fundamental flow physics of the unsteady aerodynamics associated with forced vibrations in turbomachinery are investigated. Unique data are obtained through a series of experiments in a three stage axial flow research compressor which quantify the unsteady harmonic gust interaction phenomena over a range of operating and geometric conditions at high values of reduced frequency. In these experiments the effects of the following on the stator vane unsteady aerodynamics were quantified: (1) the steady aerodynamic loading, (2) the detailed waveform of the aerodynamic forcing function, including the chordwise and transverse gust components, (3) multistage blade row interactions, and (4) the solidity, ranging from a design value of 1.09 to an isolated airfoil. In addition, the effect of flow separation on the unsteady aerodynamics of an isolated airfoil was also investigated.

Dissert. Abstr.

N88-24904 Purdue Univ., West Lafayette, Ind.
A VARIATIONAL FINITE ELEMENT METHOD FOR THREE-DIMENSIONAL, STEADY, COMPRESSIBLE, VISCOUS FLOWS Ph.D. Thesis
Wen-Hann Sheu 1987 183 p
Avail: Univ. Microfilms Order No. DA8729795

A variational formulation is developed for three-dimensional steady, compressible and viscous flows starting with the Hamilton's principle. The Clebsch transformation of the velocity vector and a set of governing equations in terms of Lagrangian multipliers and entropy are derived. It is shown that these equations are equivalent to the Navier-Stokes equations written in terms of the velocity vector, pressure and density. The finite element approximation and a relaxation scheme are employed to obtain the steady state solution of these equations. This formulation provides a unified solution scheme for potential, Euler and Navier-Stokes equations. Developing channel flow is analyzed and compared with available theoretical results. Compressible viscous flow through a convergent channel is also investigated.

Dissert. Abstr.

N88-24905# Purdue Univ., West Lafayette, Ind. Heat Transfer Lab.
HEATING AND EVAPORATION OF TURBULENT LIQUID FILMS: MEASUREMENT OF FILM THICKNESS AND THE ONSET OF NUCLEATE BOILING Annual Progress Report
I. A. Mudawwar, W. G. Tiederman, J. E. Koskie, and W. J. Marsh Mar. 1988 202 p
(Contract DE-FG02-85ER-13398)
(DE88-006388; DOE/ER-13398/8) Avail: NTIS HC A10/MF A01

The hydrodynamics of liquid films has been a subject of intense interest in the design of process equipment. Many chemical reaction chambers introduce liquid reactants in the form of films on the walls of a vessel. Liquid films are also commonly encountered in heat exchangers. For example, in process condensers, a vapor condeses and forms a liquid film on a solid surface. Great interest has developed in recent years in plate type condensers and evaporators. These heat exchangers consist of a number of parallel vertical plates. The fluid to be heated and the liquid to be cooled flow in the form of liquid films in the spaces between alternating plates. Since the design is simple, these devices are efficient to construct; however, the thermal design of the equipment is still empirical. One special case of liquid films that is commonly encountered in industrial processes is the free-falling film on a vertical surface. This case is of interest not only because it is often used, but also because it is a limiting case of the much broader problem of shear driven film flows. A number of investigations of falling films have been conducted; however no

one has been able to model fully the interfacial disturbances. The general purpose of this study is to develop a better understanding of the fluid mechanics of falling liquid films. DOE

N88-24906# Lawrence Livermore National Lab., Calif.
LLNL GRANULAR SOLIDS FLOW PROJECT Quarterly Report, Jul. - Sep. 1987
O. R. Walton, ed. Oct. 1987 9 p
(Contract W-7405-eng-48)
(DE88-007492; UCID-20297-87-3) Avail: NTIS HC A02/MF A01

Research under this project has emphasized the study of rapid shearing flows of dry, cohesionless granular solids. This is a first step toward developing a more general understanding of multi-phase solids containing flows under a wide range of flow conditions. During this period we extended the range of parameters examined in our study of steady shearing flows of inelastic, frictional spheres, determining the effect of friction coefficient and particle stiffness on stresses at various solid packing fractions. We found that stresses for smooth (frictionless) spheres increased as the effective stiffness of the particles increased, while stresses in systems of frictional spheres decreased as the stiffness increased. Available volume and effective contact duration arguments appear to explain the observed effects. We also added an approximate air-drag algorithm to the 3DSHEAR model and performed further simulation calculations of previously described channel flow experiments. Inclusion of the air-drag term significantly improved the correlation between simulated and measured velocity profiles; however, some discrepancies remain. Further calculations are planned to examine sensitivity of the results to various parameters, including the friction coefficient of the glass side walls and the channel width. DOE

N88-24907# Paris-Sud Univ., Orsay (France). Lab. d'Analyse Numerique.
IMPROVING THE PERFORMANCE OF A FINITE ELEMENT METHOD USING VECTOR ANALYSIS ON CRAY 1 Final Report [AMELIORATION DES PERFORMANCES D'UNE METHODE D'ELEMENTS FINIS PAR VECTORISATION SUR CRAY 1]
C. H. Bruneau, J. Laminie, and R. Temam 30 Jan. 1987 29 p In FRENCH
(Contract DRET-84-023)
(ETN-88-92153) Avail: NTIS HC A03/MF A01

Vector analysis techniques were applied to a finite element method separated subsonic flow computed from steady Euler equations. The CPU time rate between the vector version and the sequential version for a 50,000 point grid is 5 times less. The original method is shown to be robust, but a three-dimensional computation for a fine grid is expensive, requiring 15 hr of CRAY time. ESA

N88-24908# Ecole Normale Superieure, Paris (France). Groupe de Physique des Solides.
NUMERICAL SIMULATION OF NONLINEAR STRUCTURAL DYNAMICS OF LARGE SCALE UNSTEADY FLOW Final Report [SIMULATION NUMERIQUE DIRECTE DE LA DYNAMIQUE NON-LINEAIRE ET DES STRUCTURES A GRANDE ECHELLE D'ECOULEMENTS INSTABLES]
1988 89 p Partly in ENGLISH and FRENCH
(Contract DRET-85-1378)
(ETN-88-92156) Avail: NTIS HC A05/MF A01

Large scale unsteady flow structures are studied by determining and integrating the phase equations. The domain of validity is obtained by comparison with the direct numerical simulation of the primitive equations. The analysis includes the discussion of Eckhaus instability, oscillation instabilities, and nonlinear waves. It is found that depending of the values of the Prandtl number and the basic roll pattern wavenumber, the oscillatory instability can be supercritical or subcritical. ESA

N88-24909# Technische Hogeschool, Delft (Netherlands). Dept. of Aerospace Engineering.
THEORETICAL ANALYSIS OF LAMINAR INCOMPRESSIBLE FLOW IN SLENDER CHANNELS
G. C. KleinLebbink Apr. 1987 161 p Prepared in cooperation with the Prins Maurits Lab. TNO, Rijswijk, The Netherlands
(VTH-LR-517; PML-1987-C31; SFCC-44; B8733278;
ETN-88-92460) Avail: NTIS HC A08/MF A01

Incompressible flow in a channel with mass injection is studied. Exact solutions are calculated for extremely small and large values of the Reynolds number of the injected flow. For intermediate values the dimensionless stream function is expanded in a power series of the nondimensional transverse coordinate, yielding Poiseuille like flow and a solution with a reversed flow region is studied. The magnitude of sine-like wall disturbances is such that the flow in these channels can be supposed to be a small perturbation of the flow in a channel with a constant cross section. The nondimensional perturbation stream function is separated into two functions, one depending on the transverse coordinate only and one depending on the axial coordinate only. The function depending on the transverse coordinate is expanded in a power series of this coordinate. For rapidly varying wall undulations there appears to be a small phase difference between the wall disturbances and the pressure field. ESA

N88-24910*# National Aeronautics and Space Administration. Langley Research Center, Hampton, Va.
METHOD AND APPARATUS FOR DETECTING LAMINAR FLOW SEPARATION AND REATTACHMENT Patent Application
John P. Stack, inventor (to NASA) and Sivaramakrishnan M. Mangalam, inventor (to NASA) (Analytical Services and Materials, Inc., Hampton, Va.) 7 Jun. 1988 22 p
(NASA-Case-LAR-13952-1-SB; NAS 1.71:LAR-13952-1-SB; US-Patent-Appl-SN-203178) Avail: NTIS HC A03/MF A01 CSCL 20D

The invention is a method and apparatus for detecting laminar flow separation and flow reattachment of a fluid stream by simultaneously sensing and comparing a plurality of output signals, each representing the dynamic shear stress at one of an equal number of sensors spaced along a straight line on the surface of an airfoil or the like that extends parallel to the fluid stream. The output signals are concurrently compared to detect the sensors across which a reversal in phase of said output signal occurs, said detected sensors being in the region of laminar separation or reattachment. The novelty in this invention is the discovery and use of the phase reversal phenomena to detect laminar separation and attachment of a fluid stream from any surface such as an airfoil supported therein. NASA

N88-24911*# Iowa State Univ. of Science and Technology, Ames. Engineering Research Inst.
SIMPLIFIED CURVE FITS FOR THE TRANSPORT PROPERTIES OF EQUILIBRIUM AIR Final Report
S. Srinivasan and J. C. Tannehill Dec. 1987 39 p
(Grant NAG1-313)
(NASA-CR-178411; NAS 1.26:178411; ISU-ERI-Ames-88405)
Avail: NTIS HC A03/MF A01 CSCL 20D

New, improved curve fits for the transport properties of equilibruim air have been developed. The curve fits are for viscosity and Prandtl number as functions of temperature and density, and viscosity and thermal conductivity as functions of internal energy and density. The curve fits were constructed using grabau-type transition functions to model the tranport properties of Peng and Pindroh. The resulting curve fits are sufficiently accurate and self-contained so that they can be readily incorporated into new or existing computational fluid dynamics codes. The range of validity of the new curve fits are temperatures up to 15,000 K densities from 10 to the -5 to 10 amagats (rho/rho sub o). Author

N88-24912# Los Alamos National Lab., N. Mex.
A SEMIGROUP FOR LAGRANGIAN 1D ISENTROPIC FLOW
G. H. Pimbley 1988 14 p Presented at the Conference on

Transport Theory, Invariant Imbedding and Integral Equations, Santa Fe, N. Mex., 20 Jan. 1988
(Contract W-7405-eng-36)
(DE88-006464; LA-UR-88-508; CONF-880123-1) Avail: NTIS HC A03/MF A01

This paper discusses a system of Lagrangian equations used to describe 1D isentropic flow. This paper covers the approximate differential equations, the Banach space re-metrization and semigroup generation. DOE

N88-24913# Los Alamos National Lab., N. Mex.
SOLA-DM: A NUMERICAL SOLUTION ALGORITHM FOR TRANSIENT THREE-DIMENSIONAL FLOWS
T. L. Wilson, B. D. Nichols, C. W. Hirt, and L. R. Stein Feb. 1988 88 p
(Contract W-7405-eng-36)
(DE88-007159; LA-11161-MS) Avail: NTIS HC A05/MF A01

SOLA-DM is a 3-D time-explicit, finite-difference, Eulerian, fluid-dynamics computer code for solving the time-dependent incompressible Navier-Stokes equations. The solution algorithm (SOLA) evolved from the marker-and-cell (MAC) method, and the code is highly vectorized for efficient performance on a Cray computer. The computational domain is discretized by a mesh of parallelepiped cells in either cartesian or cylindrical geometry. The primary hydrodynamic variables for approximating the solution of the momentum equations are cell-face-centered velocity components and cell-centered pressures. Spatial accuracy is selected by the user to be first or second order; the time differencing is first-order accurate. The incompressibility condition results in an elliptic equation for pressure that is solved by a conjugate gradient method. Boundary conditions of five general types may be chosen: free-slip, no-slip, continuative, periodic, and specified pressure. In addition, internal mesh specifications to model obstacles and walls are provided. SOLA-DM also solves the equations for discrete particle dynamics, permitting the transport of marker particles or other solid particles through the fluid to be modeled. DOE

N88-24914*# North Carolina State Univ., Raleigh. Dept. of Mechanical and Aerospace Engineering.
NUMERICAL SOLUTIONS OF THE COMPLETE NAVIER-STOKES EQUATIONS Progress Report, 1 Jan. - 30 Jun. 1988
H. A. Hassan 6 Jul. 1988 27 p
(Grant NAG1-244)
(NASA-CR-183023; NAS 1.26:183023; PR-13) Avail: NTIS HC A03/MF A01 CSCL 20D

The physical phenomena within supersonic flows that sustain chemical reactions are investigated. An earlier study to develop accurate physical models for supersonic reacting flowfields focused on 2-D laminar shear layers. The objective is to examine the mixing and subsequent combustion within turbulent reacting shear layers. To conduct this study, a computer program has been written to solve the axisymmetric Reynolds averaged Navier-Stokes equations. The numerical method uses a cell-centered finite volume approach and a Runge Kutta time stepping scheme. The Reynolds averaged equations are closed using the eddy viscosity concept. Several zero-equation models have been tested by making calculations for an H2-air nonreacting coaxial jet flow. Comparisons made with experimental data show that Cohen's eddy viscosity model provides best agreement. The finite rate chemistry model used in the study of 2-D laminar shear layers is incorporated into the computer program and data is compared from a recent experiment performed at NASA Langley. Author

N88-24915*# North Carolina State Univ., Raleigh. Dept. of Mechanical and Aerospace Engineering.
COMPUTATIONAL FLUID MECHANICS Progress Report, 15 Dec. 1987 - 14 Jun. 1988
H. A. Hassan 5 Jul. 1988 18 p
(Contract NCC1-22)
(NASA-CR-183022; NAS 1.26:183022; PR-18) Avail: NTIS HC A03/MF A01 CSCL 20D

A one-equation turbulence model based on the turbulent kinetic energy equation is presented. The model is motivated by the success of the Johnson-King model and incorporates a number of features uncovered by Simpson's experiments on separated flows. Based on the results obtained, the model duplicates the success of algebraic models in attached flow regions and outperforms the two-equation models in detached flow regions. Author

N88-24916*# National Aeronautics and Space Administration. Langley Research Center, Hampton, Va.
SPATIAL STABILITY OF A COMPRESSIBLE MIXING LAYER Final Report
T. L. Jackson and C. E. Grosch (Old Dominion Univ., Norfolk, Va.) Jun. 1988 55 p Submitted for publication
(Contract NAS1-18107)
(NASA-CR-181671; ICASE-88-33; NAS 1.26:181671) Avail: NTIS HC A04/MF A01 CSCL 20D

Presented are the results of a study of the inviscid spatial stability of a parallel compressible mixing layer. The parameters of this study are the Mach number of the moving stream, the ratio of the temperature of the stationary stream to that of the moving stream, the frequency and the direction of propagation of the disturbance wave. Stability characteristics of the flow as a function of these parameters are given. It is shown that if the Mach number exceeds a critical value there are always two groups of unstable waves. One of these groups is fast with phase speeds greater than 1/2, and the other is slow with speeds less than 1/2. Phase speeds for the neutral and unstable modes are given, as well as growth rates for the unstable modes. It is shown that three dimensional modes have the same general behavior as the two dimensional modes but with higher growth rates over some range of propagation direction. Finally, a group of very low frequency unstable modes was found for sufficiently large Mach numbers. These modes have very low phase speeds but large growth rates. Author

N88-24917*# Sverdrup Technology, Inc., Arnold Air Force Station, Tenn.
HYPERSONIC TURBULENT WALL BOUNDARY LAYER COMPUTATIONS Final Report
S. C. Kim and G. J. Harloff May 1988 9 p Presented at the 24th Joint Propulsion Conference, Boston, Mass., 11-13 Jul. 1988; sponsored in part by AIAA, ASEE, ASME, and SAE
(Contract NAS3-25266)
(NASA-CR-182147; E-4172; NAS 1.26:182147; AIAA-88-2829) Avail: NTIS HC A02/MF A01 CSCL 20D

The Baldwin-Lomax algebraic turbulence model was modified for hypersonic flow conditions. Two coefficients in the outer layer eddy viscosity model were determined as functions of Mach number and temperature ratio. By matching the solutions from the Baldwin-Lomax model to those from the Cebeci-Smith model for a flat plate at hypersonic speed, the new values of the coefficient were obtained. The results show that the values of C sub cp and C sub kleb are functions of both Mach number and wall temperature ratio. The C sub cp and C sub kleb variations with Mach number and wall temperature were used for the calculations of both a 4 deg wedge flow at Mach 18 and an axisymmetric Mach 20 nozzle flow. The Navier-Stokes equations with thin layer approximation were solved for the above hypersonic flow conditions and the results were compared with existing experimental data. The agreement between the numerical solutions and the existing experimental data were good. The modified Baldwin-Lomax model thus is useful in the computations of hypersonic flows. Author

N88-24918 Michigan Univ., Ann Arbor.
OPEN CHANNEL FLOW NEAR THE RESONANCE SPEED Ph.D. Thesis
Song-ping Zhu 1987 133 p
Avail: Univ. Microfilms Order No. DA8801456

Flows in an open channel with either corrugated side walls or a corrugated bottom, posses critical speeds at or near which the prediction of either the free surface wave or the internal wave by

linear approximation fails. However, if the nonlinear terms in Euler equation and boundary conditions are kept, a finite amplitude of the free surface wave or the internal wave can then be determined. Three different open channel flows of an inviscid liquid, which may be stratified, are studied, and the amplitude of either the free surface wave or the internal wave is successfully determined to be of the order of the 1/3 power of the amplitude of the corrugation of the side walls or of the bottom. Dissert. Abstr.

N88-24919 Virginia Polytechnic Inst. and State Univ., Blacksburg.
FINITE ELEMENT SOLUTION OF 3-D TURBULENT NAVIER-STOKES EQUATIONS FOR PROPELLER-DRIVEN SLENDER BODIES Ph.D. Thesis
Russell Hicks Thomas 1987 187 p
Avail: Univ. Microfilms Order No. DA8802739

Three-dimensional turbulent flow over the aft end of a slender propeller driven body with the wake from a slender, planar appendage was calculated for 4 configurations. The finite element method in the form of the weak Galerkin formulation with the penalty method was used to solve the Reynolds averaged Navier-Stokes equations. The actual code was FIDAP, modified with a propeller body force and turbulence model, used for the solution. The turbulence model included an Inner Layer Integrated TKE model, and Outer Layer mixing length model, and a Planar Wake model. No separate boundary layer method was used for the body, rather modifications to the Integrated TKE model were made to account for the primary effects of the surface boundary layer on the flow. The flow was calculated at two levels of thrust and corresponding swirl, selfpropelled and 100 percent overthrust, as well as with selfpropelled thrust but no torque simulating an ideal rotor stator combination. Also, the selfpropelled case was calculated with a simplified turbulence model using only the Inner Layer and Planar Wake model. The results compared favorably with experiments. Dissert. Abstr.

N88-24920 California Univ., Davis.
TURBULENT HEAT TRANSFER AND FLUID FLOW MEASUREMENTS DOWNSTREAM OF ABRUPT EXPANSIONS AND IN A CAVITY OF A CIRCULAR TUBE AT A UNIFORM WALL TEMPERATURE Ph.D. Thesis
Daehee Lee 1987 195 p
Avail: Univ. Microfilms Order No. DA8729952

An experimental investigation was made of the turbulent heat transfer and fluid flow in separated, recirculating and reattached regions created by an axisymmetric and asymmetric abrupt expansions and by an abrupt expansion followed by an abrupt contraction in a circular tube at a uniform wall temperature. The flow just upstream of the expansion was unheated and proved to be fully developed hydrodynamically at the entrance to the heated abrupt expansion region. Measurements were made with small to large diameter ratios of 0.4 and 0.533 and over the Reynolds numbers range of 4100 to 21900. The mean velocity and temperature profiles were measured downstream of an axisymmetric abrupt expansion. Heat transfer coefficients were determined both around the circumference of the tube and along its length. General results indicate a substantial augmentation in the heat transfer coefficients downstream of the flow separation caused by the high turbulence and mixing action, in spite of the mean velocity in the recirculating region being only a few percent of the downstream core flow velocity in the large tube.
Dissert. Abstr.

N88-24921 Harvard Univ., Cambridge, Mass.
A SINGLE STREAMWISE VORTICAL STRUCTURE AND ITS INSTABILITY IN SHEAR FLOWS Ph.D. Thesis
Zhongmin Yang 1987 143 p
Avail: Univ. Microfilms Order no. DA8800867

A single streamwise vortex structure is generated from the tip of an obstacle in a shear flow on a water table. Its streamwise velocity field is measured using a laser Doppler velocimetry system with small scattering volume. The strength of the vortex, the vortex Reynolds number, is estimated using Pearson and Abernathy's flow model. An improved flow model with a parabolic velocity distribution as a basic flow field is discussed. The vortex structure in shearing flows is considered as a fundamental flow structure for laminar-turbulent transition. Experiments on natural transition in subcritical flows show that instability of the flow depends on the vortex Reynolds number. By increasing the vortex strength, laminar-turbulent transition occurs at a fixed vortex Reynolds number, independent of the value of the conventional flow Reynolds number. In this manner, transition could always be induced at subcritical flow Reynolds number. Dissert. Abstr.

N88-24922*# Old Dominion Univ., Norfolk, Va. Dept. of Mechanical Engineering and Mechanics.
APPLICATION OF ADVANCED GRID GENERATION TECHNIQUES FOR FLOW FIELD COMPUTATIONS ABOUT COMPLEX CONFIGURATIONS Progress Report, period ended 31 Jul. 1988
Monchai Kathong and Surendra N. Tiwari Jul. 1988 202 p
(Contract NCC1-68)
(NASA-CR-183049; NAS 1.26:183049) Avail: NTIS HC A10/MF A01 CSCL 20D

In the computation of flowfields about complex configurations, it is very difficult to construct a boundary-fitted coordinate system. An alternative approach is to use several grids at once, each of which is generated independently. This procedure is called the multiple grids or zonal grids approach; its applications are investigated. The method conservative providing conservation of fluxes at grid interfaces. The Euler equations are solved numerically on such grids for various configurations. The numerical scheme used is the finite-volume technique with a three-stage Runge-Kutta time integration. The code is vectorized and programmed to run on the CDC VPS-32 computer. Steady state solutions of the Euler equations are presented and discussed. The solutions include: low speed flow over a sphere, high speed flow over a slender body, supersonic flow through a duct, and supersonic internal/external flow interaction for an aircraft configuration at various angles of attack. The results demonstrate that the multiple grids approach along with the conservative interfacing is capable of computing the flows about the complex configurations where the use of a single grid system is not possible. Author

35 INSTRUMENTATION AND PHOTOGRAPHY

Includes remote sensors; measuring instruments and gages; detectors; cameras and photographic supplies; and holography.

For aerial photography see *43 Earth Resources and Remote Sensing*. For related information see also *06 Aircraft Instrumentation*, and *19 Spacecraft Instrumentation*.

N88-24923# California Inst. of Tech., Pasadena. Graduate Aeronautical Labs.
INSTRUMENTATION FOR TURBULENT REACTING FLOWS Final Report, 1 Feb. 1985 - 30 Jun. 1987
P. E. Dimotakis, D. B. Lang, and R. C. Miake-Lye 23 Apr. 1987 22 p
(Grant AF AFOSR-0153-85)
(AD-A191671; AFOSR-88-0041TR) Avail: NTIS HC A03/MF A01 CSCL 14B

The design and technical capabilities of the following systems are described: (1) Copper Vapor Laser pulsed light source with spatial filter and collimator;(2) Proximity focussed diode intensified linear CCD camera; (3) High speed multiplexed Analog to Digital Conversion system; and (4) Monochromator system for point or line imaging of chemiluminescence. This instrumentation has been assembled to exploit several nonintrusive optical techniques to make measurements in a wide range of turbulent flows. The primary, but not exclusive, measurement technique to be implemented was Rayleigh scattering, imaged along a line as a function of time. A slightly modified version of the same apparatus was to be used in performing scattering measurements or

(liquid-phase) laser-induced fluorescence measurements with the same temporal and spatial resolution capabilities. A second technique was to make use of a monochromator to analyze, and possibly image, chemiluminescence in a reacting flow in a wavelength-specific fashion, either at a point or along a line. The light source, the detection systems, and the data acquisition systems assembled under this funding will each be described.
GRA

N88-24924 New South Wales Univ., Kensington (Australia).
AN INVESTIGATION OF A DISTRIBUTED CLOCK FOR LOCAL AREA NETWORKS WITH RING TOPOLOGY Abstract Only.
M.S. Thesis
Shih Zen Wang Mar. 1987 146 p
Avail: Issuing Activity

Synchronization methods for Local Area Networks (LANs) with ring topology are examined. The feasibility of a number of alterative methods were examined and a distributed clock system was studied in detail, by computer simulation, analytically, and using a laboratory model. Methods of implementation were also examined. The laboratory model consists of a number of Phase Locked Loops (PLLs) units connected by means of an optical fiber to form a ring. The analytical model assumes that the PLLs are operating the linear region and thus can only account for certain aspects of system operation. The computer model was used to study steady state stability, transient behavior, and synchronization problems. The computer modeling results are in close agreement with analytical results, which show that a system build up from first order PLLs is always stable while one built from second order PLLs is only conditionally stable. For LANs designed for mixed traffic, a strict control on the frequency of the distributed clock is required. Methods of achieving such a realization are also examined. The theoretical study of white Gaussian jitter in a ring of two first order PLLs shows that jitter characteristics are strongly affected by the phase detector parameters. It is concluded that a stable distributed ring clock is realizable, provided that stable low-gain PLLs with reasonably linear phase detector characteristics are used.
Author

N88-24925# Los Alamos National Lab., N. Mex.
REMOTE TEMPERATURE-MEASUREMENT INSTRUMENTATION FOR A HEATED ROTATING TURBINE DISK
S. S. Lutz, W. D. Turley, H. M. Borella, B. W. Noel, M. R. Cates, and M. R. Probert (Delco Electronics, Goleta, Calif.) 1988 20 p Presented at the 34th International Instrumentation Symposium, Alburquerque, N. Mex., 1 May 1988 Prepared in cooperation with Los Alamos National Lab., NM.;Oak Ridge Gaseous Diffusion Plant, TN.;Delco Electronics Corp., Goleta, CA.
(Contract W-7405-eng-36)
(DE88-006456; LA-UR-88-599; CONF-880548-2) Avail: NTIS HC A03/MF A01

Thermographic-Phosphor (TP) remote temperature sensors were installed on a turbine disk and subjected to thermal and centrifugal stresses in a spin-pit test. The sensors were placed at three different radii on the disk, which was run at 6600, 9330, 11400, and 13200 rpm at nominal temperatures of ambient, 300 F, 600 F, 900 F, and 1250 F. The paper gives details of the TP temperature-measurement method, phosphor bonding to the disk, calibration, optical-system design, and electronics instrumentation. The temperatures measured by the TP sensors were compared with those measured by thermocouples mounted on the disk. A number of the thermocouples behaved erratically after we operated the disk at 677 C for an extended period. Nevertheless, for those cases where they could be compared with confidence, the agreement between the TP sensors and the thermocouples was good.
DOE

N88-24926# Sandia National Labs., Albuquerque, N. Mex.
A MULTI-FRAME ION PINHOLE CAMERA FOR INTENSE ION BEAM TRANSPORT AND FOCUSING EXPERIMENTS
W. A. Stygar, R. J. Leeper, L. P. Mix, E. R. Brock, J. E. Bailey, D. E. Hebron, D. J. Johnson, T. R. Lockner, J. Maenchen, and T. A. Mehlhorn 1988 16 p Presented at the 7th Topical Conference on High Temperature Plasma Diagnostics, Napa, Calif., 13 Mar. 1988
(Contract DE-AC04-76DP-00789)
(DE88-007283; SAND-87-3136C; CONF-880364-5) Avail: NTIS HC A03/MF A01

We have developed a new ion pinhole camera to obtain energy density profiles of a focused multi-terawatt ion beam as a function of ion energy. Beam ions that are elastically scattered from a thin gold foil are imaged through six baffled pinholes onto six separate areas of a sheet of CR-39 nuclear track detector. Each of the areas is covered by an aluminum range filter and records an image with a different lower bound on the ion energy. Subtracting images with adjacent cutoff energies results in images with upper and lower bounds on the ion energy. Ion images are read from the CR-39 with VERA, a fully-automatic, image-processor-based nuclear-track-counting system. Images of the Particle Beam Fusion Accelerator-2 (PBFA-2) proton beam have been obtained and show that the beam has been focused to achieve a horizontal FWHM of 5.7 mm and has delivered 18 kJcm^2 to a target.
DOE

N88-24927* National Aeronautics and Space Administration. Lyndon B. Johnson Space Center, Houston, Tex.
LINEAR FORCE DEVICE Patent
John P. Clancy 12 Apr. 1988 8 p Filed 30 Apr. 1987 Continuation of US-Patent-Appl-SN-790596, Oct. 23, 1985, abandoned
(NASA-Case-MSC-20549-2; US-Patent-4,736,927; US-Patent-Appl-SN-045743; US-Patent-Class-254-93-R; US-Patent-Class-254-93-H; US-Patent-Class-72-750; US-Patent-Class-269-246; US-Patent-Class-269-147; US-Patent-Appl-SN-790596) Avail: US Patent and Trademark Office CSCL 14B

The object of the invention is to provide a mechanical force actuator which is lightweight and manipulatable and utilizes linear motion for push or pull forces while maintaining a constant overall length. The mechanical force producing mechanism comprises a linear actuator mechanism and a linear motion shaft mounted parallel to one another. The linear motion shaft is connected to a stationary or fixed housing and to a movable housing where the movable housing is mechanically actuated through actuator mechanism by either manual means or motor means. The housings are adapted to releasably receive a variety of jaw or pulling elements adapted for clamping or prying action. The stationary housing is adapted to be pivotally mounted to permit an angular position of the housing to allow the tool to adapt to skewed interfaces. The actuator mechanisms is operated by a gear train to obtain linear motion of the actuator mechanism.
Official Gazette of the U.S. Patent and Trademark Office

N88-24928# Deutsche Forschungs- und Versuchsanstalt fuer Luft- und Raumfahrt, Brunswick (West Germany). Inst. fuer Flugfuehrung.
OPTICS: PERSPECTIVES FOR MEASUREMENT TECHNIQUES AND SIGNAL PROCESSING FOR FLIGHT GUIDANCE
Aug. 1987 295 p Partly in ENGLISH and GERMAN Colloquium held in Brunswick, Fed. Republic of Germany, 21-22 May 1987 Report will also be announced as translation (ESA-TT-1112)
(DFVLR-Mitt-87-21; ISSN-0176-7739; ETN-88-92313) Avail: NTIS HC A13/MF A01; DFVLR, VB-PL-DO, 90 60 58, 5000 Cologne, Fed. Republic of Germany 88 Deutsche marks

Concepts for the improvement and stabilization of laser gyroscopes, and the use of rate-bias techniques for laser gyroscopes are presented. The development of mirrors for high-precision laser gyroscopes, and the use of laser gyroscopes in multifunction navigation and flight guidance systems are outlined. Navigation using fiber optic gyroscopes, and the limits of accuracy and range of laser radars are discussed. The optical accelerometer as a sensor for inertial flight guidance is presented. The status of development and the development potential of fiber optic gyroscopes and Global Positioning System receivers is described. Digital fiber-optic displacement sensors, and electro-optical multistability for signal processing were investigated. The status

of optical computers and optical methods for data processing is described. For individual titles, see N88-24929 through N88-24939.

N88-24929# Deutsche Forschungs- und Versuchsanstalt fuer Luft- und Raumfahrt, Brunswick (West Germany).
CONCEPTS FOR A LASER GYROSCOPE OF THE HIGHEST PRECISION [KONZEPTE FUER EINEN LASERKREISEL HOECHSTER PRAEZISION]
Ruediger Rodloff *In its* Optics: Perspectives for Measurement Techniques and Signal Processing for Flight Guidance Aug. 1987 p 9-60 In GERMAN (For primary document see N88-24928 18-35)
Avail: NTIS HC A13/MF A01; DFVLR, VB-PL-DO, 90 60 58, 5000 Cologne, Fed. Republic of Germany 88 Deutsche marks

Concepts for the improvement and stabilization of laser gyroscopes, are discussed: vertical beam stability (VBS) and lock-in stabilization (LIST). A beam-geometrical model for the description of the error behavior of laser gyroscopes was developed. The agreement with experimental results is so good that the knowledge can be transferred to commercial laser gyroscopes. The VSS-controller improves drift stability, optimizes the beam position, improves the stability against thermal and mechanical environmental effects, and reduces the requirements for the parallel control of the mirrors. The LIST-controller reduces the global backscatter to a reproducible, low level, and stabilizes the lock-in threshold for any effect at an extremely low level. The required amount of additional hardware for the realization of the proposed stabilization measures is very small. ESA

N88-24930# Deutsche Forschungs- und Versuchsanstalt fuer Luft- und Raumfahrt, Brunswick (West Germany).
LASER GYROSCOPES USING THE RATE-BIAS TECHNIQUE [LASERKREISEL MIT RATE-BIAS-TECHNIK]
Eberhard Handrich *In its* Optics: Perspectives for Measurement Techniques and Signal Processing for Flight Guidance Aug. 1987 p 61-80 In GERMAN (For primary document see N88-24928 18-35)
Avail: NTIS HC A13/MF A01; DFVLR, VB-PL-DO, 90 60 58, 5000 Cologne, Fed. Republic of Germany 88 Deutsche marks

The use of the rate-bias techniques for laser gyroscopes is discussed. The principle of the laser gyroscope and the status of the technique are described. The lock-in phenomenon and the dither method to overcome it, as well as the disadvantages of this method are explained. The rate-bias technique as an alternative solution is presented. The advantages of this technique as compared to the dither method are outlined. ESA

N88-24931# Deutsche Forschungs- und Versuchsanstalt fuer Luft- und Raumfahrt, Brunswick (West Germany).
DEVELOPMENT OF MIRRORS FOR HIGH-PRECISION LASER GYROSCOPES [ENTWICKLUNG VON SPIEGELN FUER HOCHGENAUE LASERKREISEL]
Dirk-Roger Schmitt *In its* Optics: Perspectives for Measurement Techniques and Signal Processing for Flight Guidance Aug. 1987 p 81-106 In GERMAN (For primary document see N88-24928 18-35)
Avail: NTIS HC A13/MF A01; DFVLR, VB-PL-DO, 90 60 58, 5000 Cologne, Fed. Republic of Germany 88 Deutsche marks

Methods for the production of laser mirrors with low scatter and loss levels were developed. Polishing processes for the production of optical surfaces were investigated with a view to the quality of the substrates which are the most important component of the laser mirror. The surfaces were evaluated using optical-microscope, differential-interference contrast, and integral scattering light measurement. Quartz substrates were used for the laser mirrors. The mirror layers were made of TiO2/SiO2 interference layer with silver layers. The maximum obtainable reflection of the produced laser mirrors is mainly determined by the backscatter properties. A better mirror quality requires a further reduction of the scattered light levels, imposing an improved substrate quality using optimized polishing methods. Ion beam methods can improve layer technology. ESA

N88-24932# Deutsche Forschungs- und Versuchsanstalt fuer Luft- und Raumfahrt, Brunswick (West Germany).
LABORATORY TESTS OF LASER GYROSCOPES FOR FUTURE UTILIZATION IN MULTIFUNCTION SYSTEMS FOR PRECISION NAVIGATION AND FLIGHT GUIDANCE [LABORTESTS VON LASERKREISELN FUER DEN ZUKUENFTIGEN EINSATZ IN MULTIFUNKTIONSSYSTEMEN ZUR PRAEZISIONSNAVIGATION UND ZUR FLUGREGELUNG]
H. Niederstrasser, V. Wetzig, and E. Luebeck *In its* Optics: Perspectives for Measurement Techniques and Signal Processing for Flight Guidance Aug. 1987 p 107-126 In GERMAN (For primary document see N88-24928 18-35)
Avail: NTIS HC A13/MF A01; DFVLR, VB-PL-DO, 90 60 58, 5000 Cologne, Fed. Republic of Germany 88 Deutsche marks

The use of laser gyroscopes in multifunction Inertial Reference Units was investigated in the laboratory using a single-axis revolving platform. The use of the laser gyroscope as sensor for inertial navigation shows a good reproducibility of the average slope of the characteristic (0.5 ppm). For the measurement of single angular shifts, the laser gyroscope shows a constant error of 2.9 sec and an error between 0.004 and 0.0016 deg/hr depending on the interval length. The dynamic investigation of the laser gyroscope as sensor for flight guidance shows an amplitude distortion below 1 percent and a phase shift below 0.4 mrad in the whole frequency range up to 100 Hz. ESA

N88-24933# Deutsche Forschungs- und Versuchsanstalt fuer Luft- und Raumfahrt, Brunswick (West Germany).
NAVIGATION USING THE TELDIX FIBER-OPTIC GYROSCOPE [NAVIGATION MIT TELDIX-FASERKREISELN]
Eberhard Kiesel *In its* Optics: Perspectives for Measurement Techniques and Signal Processing for Flight Guidance Aug. 1987 p 127-141 In GERMAN (For primary document see N88-24928 18-35)
Avail: NTIS HC A13/MF A01; DFVLR, VB-PL-DO, 90 60 58, 5000 Cologne, Fed. Republic of Germany 88 Deutsche marks

The status of components technology and detection methods in fiber optic gyroscopes is presented. The measurement of rotation rates using fiber optic gyroscopes is explained. The technical status of the different components used in the production of fiber optic gyroscopes (sensor coil, phase modulator, coupler, polarizer, depolarizer, light sources) is depicted. The signal detection method and the applied fiber-optic electronics are described. A system for the testing of fiber optic gyroscopes for surface navigation is presented. ESA

N88-24934# Deutsche Forschungs- und Versuchsanstalt fuer Luft- und Raumfahrt, Brunswick (West Germany).
LIMITS OF ACCURACY AND RANGE OF LASER RADARS [GRENZEN VON GENAUIGKEIT UND REICHWEITE BEIM LASERRADAR]
Kurt Fricke *In its* Optics: Perspectives for Measurement Techniques and Signal Processing for Flight Guidance Aug. 1987 p 143-158 In GERMAN (For primary document see N88-24928 18-35)
Avail: NTIS HC A13/MF A01; DFVLR, VB-PL-DO, 90 60 58, 5000 Cologne, Fed. Republic of Germany 88 Deutsche marks

The limitations and errors involved in laser range finding for flight guidance are treated. The measurement principle of the developed laser radar is explained. Limitation in laser power to protect humans is discussed. The laser power and the radiation noise level at the multiplier cathode, and the possible range were calculated. Errors of the range and angle measurements are discussed. The comparison between measured and calculated laser radar data shows that the range is 12 percent too small. The required measurement accuracy is outlined. Instrument errors are significantly smaller than those due to atmospheric effects. An optimized laser design, as well as a controlled beam shape and a postamplification of the laser pulse in the receiver can increase the range. ESA

N88-24935# Deutsche Forschungs- und Versuchsanstalt fuer Luft- und Raumfahrt, Brunswick (West Germany).
THE OPTICAL ACCELEROMETER: A NOVEL SENSOR FOR VERTICAL FLIGHT GUIDANCE [DER OPTISCHE BESCHLEUNIGUNGSMESSER - EIN NEUER SENSOR FUER DIE INERTIALE FLUGFUEHRUNG]
Wolfgang Holzapfel *In its* Optics: Perspectives for Measurement Techniques and Signal Processing for Flight Guidance Aug. 1987 p 159-192 In GERMAN (For primary document see N88-24928 18-35)
Avail: NTIS HC A13/MF A01; DFVLR, VB-PL-DO, 90 60 58, 5000 Cologne, Fed. Republic of Germany 88 Deutsche marks

Concepts for optical accelerometers, functioning according to the laser principle and using oscillator-internal conversion effects, are presented. The physical and measuring principles of these optical accelerometers are explained. The theoretical expected measurement range is between 100 g and 10 to the 8th power g. Seismic and photoelastic laser accelerometers are presented. Experimental results with both accelerometers show proportionality over almost 5 decades of the input signal. The resolution and estimated accuracies are of the order of 0.00001 g. ESA

N88-24936# Deutsche Forschungs- und Versuchsanstalt fuer Luft- und Raumfahrt, Brunswick (West Germany).
INERTIAL REFERENCE SYSTEM WITH GLOBAL POSITIONING SYSTEM (GPS) SUPPORT [INERTIALES REFERENZSYSTEM MIT GPS-STUETZUNG] **c04**
Eberhard Schlemper *In its* Optics: Perspectives for Measurement Techniques and Signal Processing for Flight Guidance Aug. 1987 p 193-220 In GERMAN (For primary document see N88-24928 18-35)
Avail: NTIS HC A13/MF A01; DFVLR, VB-PL-DO, 90 60 58, 5000 Cologne, Fed. Republic of Germany 88 Deutsche marks

The status of development and the development potential of fiber optic gyroscopes and GPS-receivers is described, with a view to airborne autonomous navigation. In fiber optic gyroscopes, frequency and phase modulation are compared; the error mechanisms in phase modulated gyroscopes are explained; the amplitude modulation of regularly gyrating light waves is discussed; the amplitude and phase modulation of the reflections and the stability of the scale factor are presented; and the frequency modulated gyroscope is discussed. The use of GPS is discussed with a view to the development of receivers and the capability of an integration with inertial sensors. The design of a cheap inertial reference system with GPS-support is presented. ESA

N88-24937# Deutsche Forschungs- und Versuchsanstalt fuer Luft- und Raumfahrt, Brunswick (West Germany).
DIGITAL FIBER OPTIC DISPLACEMENT SENSORS
Norbert Fuerstenau *In its* Optics: Perspectives for Measurement Techniques and Signal Processing for Flight Guidance Aug. 1987 p 221-242 (For primary document see N88-24928 18-35)
Avail: NTIS HC A13/MF A01; DFVLR, VB-PL-DO, 90 60 58, 5000 Cologne, Fed. Republic of Germany 88 Deutsche marks

A digital fiber optic displacement sensor using a Mach-Zehnder interferometer was tested. The theoretical sensitivity of digital interferometer displacement sensors, and the dual polarization method are presented. Experimental results show that interferometric displacement sensors with digital readout by fringe counting may be set up either by longitudinally straining the sensing fiber or by tension bending. In both cases the birefringence-induced phase shifts are low enough for the dual polarization approach to be applicable for the determination of the change of sign. The angular position may be measured employing a translation stage driven by a micrometer screw. The temperature sensitivity of two-beam interferometers can be minimized using balanced interferometer arms. ESA

N88-24938# Deutsche Forschungs- und Versuchsanstalt fuer Luft- und Raumfahrt, Brunswick (West Germany).
INVESTIGATIONS IN ELECTRO-OPTICAL MULTISTABILITY FOR SIGNAL PROCESSING **c74**
Christopher Watts and Norbert Fuerstenau *In its* Optics: Perspectives for Measurement Techniques and Signal Processing for Flight Guidance Aug. 1987 p 243-266 (For primary document see N88-24928 18-35)
Avail: NTIS HC A13/MF A01; DFVLR, VB-PL-DO, 90 60 58, 5000 Cologne, Fed. Republic of Germany 88 Deutsche marks

A Michelson interferometer with electro-optical feedback was investigated with respect to multistability. The systems behavior as a function of input power or feedback gain, modulation index, and signal bias is summarized. For the idealized case of a zero reaction time constant, a detailed linear stability analysis, employing the complete differential-difference equation of a realistic setup, shows that multistable solutions are to be expected if the quotient of feedback delay time and systems time constant is much smaller than one. This result is quantitatively verified by the numerical integration of the differential-difference equation. Experimental results agree with these predictions. ESA

N88-24939# Technische Univ., Brunswick (West Germany). Inst. fuer Hochfrequenztechnik.
OPTICAL COMPUTER AND OPTICAL METHODS FOR DATA PROCESSING [OPTISCHE RECHNER UND OPTISCHE METHODEN IN DER DATENVERARBEITUNG] **c60**
Karl-Joachim Ebeling *In* DFVLR, Optics: Perspectives for Measurement Techniques and Signal Processing for Flight Guidance Aug. 1987 p 267-294 In GERMAN (For primary document see N88-24928 18-35)
Avail: NTIS HC A13/MF A01; DFVLR, VB-PL-DO, 90 60 58, 5000 Cologne, Fed. Republic of Germany 88 Deutsche marks

The status of development of optical computers, as well as key problems are described. Concepts for optical computers, such as the optical analog computer, digital vector-matrix multiplication, and a purely optical parallel processor, are discussed. The decisive point for the efficiency of optical computers, namely the quality of the nonlinear switching elements, is considered (nonlinear Fabry-Perot resonators, absorptive nonlinearities, excitation nonlinearities). Hybrid opto-electronic techniques (optical couplings in electronic systems, combined modulator-detector elements) are presented. ESA

N88-24940# Max-Planck-Institut fuer Stroemungsforschung, Goettingen (West Germany).
SIMPLE HIGH SPEED CAMERA WITH CCD-SENSOR [EINE EINFACHE HOCHGESCHWINDIGKEITSKAMERA MIT CCD-SENSOR]
W. J. Hiller and T. A. Kowalewski Jun. 1987 17 p In GERMAN
(MPIS-8/1987; ISSN-0436-1199; ETN-88-92084) Avail: NTIS HC A03/MF A01; Max-Planck Institut fuer Stroemungsforschung, Boettinger Strasse 6-8, 3400 Goettingen, Fed. Republic of Germany 14 DM

Experience with a high speed video-camera including a semiconductor sensor, used to study disintegration of thin fluid beams in small droplets is described. Observations are made with a bright-field microscope; light source is a pulsed diode, exposure time is 200 sec. Video signals are treated by an image processor. Validity of the multiple exposure process is discussed on the example of an oscillating droplet with determination of its diameter and oscillation frequency. ESA

N88-24941*# National Aeronautics and Space Administration. Lyndon B. Johnson Space Center, Houston, Tex.
ELECTROSTATIC DISCHARGE TEST APPARATUS Patent Application
William Conrad Smith, inventor (to NASA) (Lockheed Engineering and Management Services Co., Inc., Houston, Tex.) 16 Feb. 1988 20 p
(NASA-Case-MSC-21094-1; NAS 1.71:MSC-21094-1; US-Patent-Appl-SN-156393) Avail: NTIS HC A03/MF A01 CSCL 14B

Electrostatic discharge properties of materials are quantitatively measured and ranked. Samples are rotated on a turntable beneath selectable, co-available electrostatic chargers, one being a corona

charging element and the other a sample-engaging triboelectric charging element. Samples then pass under a voltage meter to measure the amount of residual charge on the samples. After charging is discontinued, measurements are continued to record the charge decay history over time. NASA

N88-24942*# National Aeronautics and Space Administration. Langley Research Center, Hampton, Va.
THERMAL COMPENSATING MOUNT Patent Application
Antony Jalink, Jr., inventor (to NASA) and Scott R. Campbell, inventor (to NASA) (KEI Laser, Fla.) 14 Mar. 1988 9 p
(NASA-Case-LAR-13794-1; NAS 1.71:LAR-13794-1; US-Patent-Appl-SN-168065) Avail: NTIS HC A02/MF A01 CSCL 14B

This invention relates to a device for mounting an alignment sensitive component to provide stability during temperature fluctuations. Alignment sensitive components such as quartz prisms for lasers are often subjected to temperature changes which result in undesirable misalignment from thermal expansion. A thermal compensating mount is provided for an alignment sensitive component. The thermal compensating mount comprises a cylindrical extension which is formed integral to and has the same coefficient of thermal expansion as the alignment sensitive component. A cylindrical receptacle is formed into a mounting surface. The cylindrical extension is placed into the cylindrical receptacle and is secured by an adhesive. The difference between the diameter of the cylindrical and the cylindrical receptacle is such that the differential thermal expansion across the cylindrical extension and the edges of the cylindrical receptacle is exactly compensated for by the thermal expansion of the adhesive. The novelty of this invention resides in its selection of materials with compatible coefficients of thermal expansion to mount an alignment sensitive device. NASA

N88-24943*# National Aeronautics and Space Administration. Pasadena Office, Calif.
NONCONTACT TEMPERATURE PATTERN MEASURING DEVICE Patent Application
D. D. Elleman, inventor (to NASA), J. L. Allen, inventor (to NASA), and M. C. Lee, inventor (to NASA) (Jet Propulsion Lab., California Inst. of Tech., Pasadena.) 12 Nov. 1987 23 p Prepared in cooperation with Jet Propulsion Lab., California Inst. of Tech., Pasadena.
(Contract NAS7-918)
(NASA-Case-NPO-17024-1-CU; NAS 1.71:NPO-17024-1-CU; US-Patent-Appl-SN-159613) Avail: NTIS HC A03/MF A01 CSCL 14B

This invention relates to a noncontact imagine pyrometer system for obtaining the true temperature image of a given substance in a contactless fashion without making assumptions about localized emissivity of the substance or the uniformity of the temperature distribution. Such a contactless temperature imaging system has particular application in the study and production of many materials where the physical contact required to make a conventional temperature measurement drastically effects or contaminates the physical process being observed. Two examples where accurate temperature profiles are of critical interest are: (1) the solid-liquid phase change interface in the production of electronic materials and (2) metastable materials in the undercooling region. The apparent novelty resides in the recognition that an active pyrometer system may be advantageously adapted to perform contactless temperature imaging so that an accurate temperature profile can be obtained. NASA

N88-24944*# National Aeronautics and Space Administration. Pasadena Office, Calif.
ATMOSPHERIC AUTOROTATING IMAGING DEVICE Patent Application
James D. Burke, inventor (to NASA) (Jet Propulsion Lab., California Inst. of Tech., Pasadena.) 28 Mar. 1988 15 p Prepared in cooperation with Jet Propulsion Lab., California Inst. of Tech., Pasadena.
(Contract NAS7-918)
(NASA-Case-NPO-17390-1-CU; NAS 1.71:NPO-17390-1-CU; US-Patent-Appl-SN-205899) Avail: NTIS HC A03/MF A01 CSCL 14B

This invention relates to a scanning imaging device for deployment in either terrestrial or extraterrestrial atmospheres. An object of the present invention is to provide an extremely simple device that, upon deployment in an atmospheric environment, automatically rotates without the use of a propulsion system. An image detector appropriately disposed therein scans a panoramic view with each rotation of the device. Data gathered by the image detector may be transmitted to a remote receiver. The present invention may be particularly useful in the exploration of, for example, the Martian surface. The novelty of the present invention resides in the ability of the device to scan an image without the use of any moving parts or the expenditure of fuel energy. NASA

N88-24945# Sandia National Labs., Albuquerque, N. Mex.
ANALYSIS OF BINARIZED HARTLEY PHASE-ONLY FILTER PERFORMANCE WITH RESPECT TO STOCHASTIC NOISE
F. M. Dickey, J. J. Mason, and K. T. Stalker 1988 15 p Presented at the SPIE's Technical Symposium on Optics, Electro-optic and Sensors, Orlando, Fla., 4 Apr. 1988
(Contract DE-AC04-76DP-00789)
(DE88-007604; SAND-88-0669C; CONF-880462-4) Avail: NTIS HC A03/MF A01

Binary phase-only filters (BPOF) are a viable canidate for the replacement of matched filters in real-time image processing and pattern recognition applications. The original BPOFs were binarized versions of the real or imaginary parts of the Fourier transform. Recently, a filter has been proposed which is the binarized Hartley transform. In this paper, the noise performance of the binarized Hartley phase-only filter is analyzed and compared to other BPOFs as well as the phase-only and matched filter. It is well known that the matched filter optimizes signal-to-noise ratio. Further, it can be shown that the matched filter phase is the optimum phase-only filter. A bound on the BPOF signal-to- noise ration relative to that of the phase-only filter is derived. Finally, the analysis is applied to the generalized form of the binarized Hartley transform. DOE

N88-24946*# National Aeronautics and Space Administration. Ames Research Center, Moffett Field, Calif.
EXTREMA PRINCIPLES OF ENTROPHY PRODUCTION AND ENERGY DISSIPATION IN FLUID MECHANICS
W. Clifton Horne and Krishnamurty Karamcheti (Florida State Univ., Tallahassee.) May 1988 10 p
(NASA-TM-100992; A-88131; NAS 1.15:100992) Avail: NTIS HC A02/MF A01 CSCL 07D

A survey is presented of several extrema principles of energy dissipation as applied to problems in fluid mechanics. An exact equation is derived for the dissipation function of a homogeneous, isotropic, Newtonian fluid, with terms associated with irreversible compression or expansion, wave radiation, and the square of the vorticity. By using entropy extrema principles, simple flows such as the incompressible channel flow and the cylindrical vortex are identified as minimal dissipative distributions. The principal notions of stability of parallel shear flows appears to be associated with a maximum dissipation condition. These different conditions are consistent with Prigogine's classification of thermodynamic states into categories of equilibrium, linear nonequilibrium, and nonlinear nonequilibrium thermodynamics; vortices and acoustic waves appear as examples of dissipative structures. The measurements of a typical periodic shear flow, the rectangular wall jet, show that direct measurements of the dissipative terms are possible. Author

36 LASERS AND MASERS

Includes parametric amplifiers.
For related information see also *76 Solid-State Physics.*

N88-24947# Los Alamos National Lab., N. Mex.
LASER COUNTERMEASURE IMPACTS AND PENALTIES
G. H. Canavan Apr. 1988 23 p
(Contract W-7405-eng-36)
(DE88-006871; LA-11264-MS) Avail: NTIS HC A03/MF A01

Countermeasures could determine the ultimate effectiveness of directed energy weapons. This report discusses shielding and spinning boosters, the countermeasures specific to lasers, and provides an overall assessment of their impact, which is modest. DOE

N88-24948*# David Sarnoff Research Center, Princeton, N.J.
DISTRIBUTED FEEDBACK LASERS Final Report, 19 Jun. 1984 - 19 Jun. 1986
I. Ladany, J. T. Andrews, and G. A. Evans Washington NASA Jun. 1988 86 p
(Contract NAS1-17351)
(NASA-CR-4154; NAS 1.26:4154; RCA-PRRL-87-CR-3B) Avail: NTIS HC A05/MF A01 CSCL 20E

A ridge waveguide distributed feedback laser was developed in InGaAsP. These devices have demonstrated CW output powers over 7 mW with threshold currents as low as 60 mA at 25 C. Measurements of the frequency response of these devices show a 3 dB bandwidth of about 2 GHz, which may be limited by the mount. The best devices have a single mode spectra over the entire temperature range tested with a side mode suppression of about 20 dB in both CW and pulsed modes. The design of this device, including detailed modeling of the ridge guide structure, effective index calculations, and a discussion of the grating configuration are presented. Also, the fabrication of the devices is presented in some detail, especially the fabrication of and subsequent growth over the grating. In addition, a high frequency fiber pigtailed package was designed and tested, which is a suitable prototype for a commercial package. Author

N88-24949# Center for Night Vision and Electro-Optics, Fort Belvoir, Va.
AN OPTICAL PREAMPLIFIER FOR DETECTION OF CO2 LASER RADIATION Final Report, Mar. - Sep. 1987
Jay A. Fox and Cynthia R. Gautier Jan. 1988 26 p
(AD-A190790; AMSEL-NV-TR-0061) Avail: NTIS HC A03/MF A01 CSCL 17E

A tunable, low pressure CO2 transverse discharge system is described in order to test an optical preamplifier that can provide gain to incoming laser radiation in the 9-11 micrometer range without adding detectable noise. Especially high gains were observed on strong laser lines such as 10P20, suggesting the potential use of the preamplifier in certain applications including long-distance rangefinding. GRA

N88-24950# Defense Intelligence Agency, Washington, D.C. Directorate for Scientific and Technical Intelligence.
BIBLIOGRAPHY OF SOVIET LASER DEVELOPMENTS, NUMBER 83, MAY - JUNE 1986
Sep. 1987 133 p
(AD-A190969; DIA-DST-2700Z-007-87) Avail: NTIS HC A07/MF A01 CSCL 09C

This is the Soviet Laser Bibliography for May-June 1986, and is No. 83 in a continuing series on Soviet laser developments. The coverage includes basic research on solid state, liquid, gas, and chemical lasers; components; nonlinear optics; spectroscopy of laser materials; ultrashort pulse generation; theoretical aspects of advanced lasers; and general laser theory. Laser applications are listed under biological effects; communications systems; beam propagation; adaptive optics; computer technology; holography; laser-induced chemical reactions; measurement of laser parameters; laser measurement applications; laser-excited optical effects; laser spectroscopy; beam-target interaction; and plasma generation and diagnostics. GRA

N88-24951# University Coll., London (England). Dept. of Physics and Astronomy.
COMPONENTS OF AN ATMOSPHERIC LIDAR SYSTEM: DOPPLER WIND LIDAR Final Report, 1 Oct. 1986 - 30 Sep. 1987
David Rees 30 Nov. 1987 6 p
(Grant AF AFOSR-0198-85)
(AD-A191222; AFOSR-88-0039TR) Avail: NTIS HC A02/MF A01 CSCL 17I

Six papers have been published in the literature during the past two years related to the development and performance of the Doppler Lidar Detector System and its associated wavelength meters. The instrumentation and all of the necessary software is now available at University College London. Three complete Doppler Detector/Wavelength meter units have been fabricated. One of these has been delivered to AFGL, awaiting the completion of the Laser system. Another one of these combined units was integrated temporarily with the complete Lidar system of the Bonn University group at Andoya in August 1987, for proof of concept, and to demonstrate that all of the optical and electronic interfaces and software functioned correctly. Due to limited time in the field, and very poor weather, it was not possible to obtain direct data on the lower thermosphere, but the tests did prove that the entire system functioned as designed. Further tests with Bonn University are planned in 1988. GRA

N88-24952# New Mexico State Univ., Las Cruces. Dept. of Physics.
ATMOSPHERIC PROPAGATION OF LASER BEAMS Final Report, 1 Sep. 1984 - 31 Dec. 1987
Robert L. Armstrong and Leon J. Radziemski 8 Mar. 1988 14 p
(Contract DAAG29-84-K-0180)
(AD-A191447; ARO-21751.6-GS) Avail: NTIS HC A03/MF A01 CSCL 09C

This report describes work done under the cited ARO research grant. Experimental and theoretical results are described, papers and conference presentations resulting from this work are enumerated, and a list of personnel supported under this grant is provided. GRA

N88-24953# Los Alamos National Lab., N. Mex.
APPLICATION OF PARTICLE SIMULATIONS TO THE NRL LASER EXPERIMENT Technical Report, Oct. - Dec. 1987
Dan Winske 10 Dec. 1987 50 p Sponsored by Defense Nuclear Agency, Washington, D.C.
(AD-A191641; LA-UR-87-4072) Avail: NTIS HC A03/MF A01 CSCL 20I

Particle simulation methods are used to address issues related to recent results of the NRL laser experiment. The simulations, which include all the electron and ion scale lengths, examine dense plasma clouds expanding across a magnetic field into a vacuum under various conditions. The wavenumbers of the observed short wavelength instability, identified as the lower hybrid drift instability, are found to be independent of the magnetic field (in agreement with experiment) and the ion to electron mass ratio, consistent with a simple model for the expansion. In addition, differences in the instability due to the initial velocity distribution and the angular spread of the expansion are studied. Nonlinear phenomena, such as possible flute tip bifurcation, bending and separation, have also been observed in the calculations and are related to similar effects seen in the experiments. However, detailed analysis of the simulations show that there is no short wavelength cutoff to the instability, contrary to the predictions of linear theory, indicating that the wavelength scaling is spurious. Possible physical and numerical reasons for this behavior are examined, and it is shown that another instability, the electron cyclotron drift instability can still be excited at shorter wavelengths. The overall consequences of the results on the suitability of these methods for modeling the laser experiment are discussed. GRA

N88-24954# University Coll. of North Wales, Bangor. School of Electronic Engineering.
FAST ACTING OPTICAL BEAM DETECTION AND DEFLECTION SYSTEM Final Report, 1983 - 1987
D. K. Das-Gupta 7 Dec. 1987 57 p
(Contract DAJA45-83-C-0016; DA Proj. 1L1-61102-BH-57)
(AD-A192161; ARDG-R/D-4246-R-MS) Avail: NTIS HC A04/MF A01 CSCL 17E

The final report gives an account of progress made in the time period of January 1983 - December 1987 on Fast Acting Optical Beam Detection and Deflection System. It has been divided into two parts, each section being self-contained. Part 1 deals with the investigation of optical detection of coherent radiations of helium-neon laser of wavelength 0.6328 micrometers with corona poled polyvinylidene fluoride (PVDF) film using its pyroelectric property. The results show that a detection time of 0.56 microsec may be achieved with PVDF pyroelectric detectors. Part 2 reports the results of acousto-optic deflection of coherent He-Ne laser radiations using a water-cell which was energized by well-poled PVDF film in the frequency range of 10 MHz-70MHz 100% deflection efficiency of the primary beam energy has been achieved with this technique at a deflection angle of 1 deg. The water cell was then replaced with a Tellurium dioxide cell which provided 84% deflection efficiency at an angle of 3 deg. Finally, the report discusses a possible effective method of simultaneous deflection and deflection of coherent laser radiations with very high efficiency using blazed diffraction grating in the wavelength range of 0.4 - 1 micrometer at angles 18 deg or more. GRA

N88-24955# Los Alamos National Lab., N. Mex.
AURORA STATUS AND PLANS
R. Kristal, L. S. Blair, M. D. Burrows, D. C. Cartwright, P. D. Goldstone, D. P. Greene, J. A. Hanlon, A. Hauer, M. Kang, and B. L. Kortegaard Oct. 1987 27 p Presented at the 8th International Workshop on Laser Interaction and Related Plasma Phenomena, Monterey, Calif., 27 Oct. 1987
(Contract W-7405-eng-36)
(DE88-006476; LA-UR-88-409; CONF-871093-5) Avail: NTIS HC A03/MF A01

Aurora is a short wavelength (248 nm) 10 kJ KrF laser system in the ICF program at Los Alamos National Laboratory. It is both an experiment in driver technology and a means for studying target performance using KrF laser light. Both features will be used to help evaluate the uv excimer laser as a viable fusion driver. The system has been designed to employ several electron-beam pumped amplifiers in series, with a final aperture of one meter square, to amplify 96 angularly mulitplexed 5 ns beamlets to the 10 kJ level. In Phase 1, 48 of these beamlets are brought to target by demultiplexing and focusing with f26 optics. The beamlet ensemble, contained within an f1.9 bundle, is focused as a single beam; however, pointing is done individually. Spot size in the target plane is variable from 0.1-4 mm, with maximum averaged intensity of -4 times 10 to the 15th power W/square cm. The illumination geometry is designed specifically for several classes of important target physics experiments. These include: energy flow, symmetry and preheat studies related to indirectly driven targets; x-ray conversion and plasma coupling characterization on disc targets, and hydrodynamic instability studies in planar geometry. DOE

N88-24956# Brookhaven National Lab., Upton, N. Y.
INTEGRAL EQUATION FOR THE LASER FIELD: MULTIMODE DESCRIPTION OF A FREE-ELECTRON LASER OSCILLATOR
J. C. Gallardo, G. Dattoli, A. Renieri, and T. Hermsen 1987 15 p Presented at the 9th International Free-Electron Laser Conference, Williamsburg, Va., 14 Sep. 1987 Prepared in cooperation with ENEA, Frascati (Italy).
(Contract DE-AC02-76CH-00016)
(DE88-007050; BNL-40844; CONF-8709110-20) Avail: NTIS HC A03/MF A01

In the first part of this article we present a one-dimensional multimode theory of a free-electron laser. We show that the evolution of the laser field in a single pass through the undulator satisfies an integral equation. The formulation is exact, describing saturation and both low and high gain regime of a long-pulse free-electron laser. In the second part we derive the laser field evolution equation for an oscillator configuration in the small signal regime and the long pulse limit. The theory is based on the space-time approach that leads to a generalized Schroedinger-like equation for the laser radiation field. The explicit expressions for the solutions of the evolution equation and the gain coefficient of the system are presented. Some results have already been derived by some of the authors using a different approach. DOE

N88-24957# Los Alamos National Lab., N. Mex.
HIGH-ENERGY LASER-ASSISTED IMAGING THROUGH VAPORIZING AEROSOLS
A. Zardecki and S. A. W. Gerstl Feb. 1988 13 p Presented at the SPIE's Technical Symposium on Optics, Electro-optic and Sensors, Orlando, FLa., 4 Apr. 1988
(Contract W-7405-eng-36)
(DE88-007911; LA-UR-88-669; CONF-880462-6) Avail: NTIS HC A03/MF A01

The degradation of image quality due to multiple scattering in a turbid medium is analyzed under various conditions of illumination. The emphasis is on the forward-peaked multiple scattering effects, which can adequately be described by the small-angle approximation. In the case of incoherent illumination, the modulation transfer function (MTF) can be given explicity both in the low- and high-frequency limits. For scattering with smaller degree of anisotropy, the MTF should be imputed numerically by considering solutions to the equation of radiative transfer with a line or point source. As the beam power increases, the turbid medium becomes modified by its interactions with the beam, thus affecting the image resolution. In this nonlinear transport regime (flux levels of the order of 10^6 Wcm^3 and higher) the propagation leads actually to beam narrowing. In the context of the imaging problem, an apparent paradosical situation in which the image of a point source narrows down as the high-energy laser (HEL) beam propagates is discussed. DOE

N88-24958* National Aeronautics and Space Administration. Lyndon B. Johnson Space Center, Houston, Tex.
RANGE AND RANGE RATE SYSTEM Patent
Olin L. Graham, inventor (to NASA), Jim K. Russell, inventor (to NASA), and Walter L. Epperly, inventor (to NASA) (Westinghouse Electric Corp., Baltimore, Md.) 5 Apr. 1988 8 p Filed 4 May 1987 Supersedes N87-25570 (25 - 19, p 2614)
(NASA-Case-MSC-20867-1; US-Patent-4,736,247;
US-Patent-Appl-SN-045984; US-Patent-Class-358-107;
US-Patent-Class-356-1; US-Patent-Class-356-4;
US-Patent-Class-356-376; US-Patent-Class-364-561) Avail: US Patent and Trademark Office CSCL 20E

A video controlled solid state range finding system which requires no radar, high power laser, or sophisticated laser target is disclosed. The effective range of the system is from 1 to about 200 ft. The system includes an opto-electric camera such as a lens CCD array device. A helium neon laser produces a source beam of coherent light which is applied to a beam splitter. The beam splitter applies a reference beam to the camera and produces an outgoing beam applied to a first angularly variable reflector which directs the outgoing beam to the distant object. An incoming beam is reflected from the object to a second angularly variable reflector which reflects the incoming beam to the opto-electric camera via the beam splitter. The first reflector and the second reflector are configured so that the distance travelled by the outgoing beam from the beam splitter and the first reflector is the same as the distance travelled by the incoming beam from the second reflector to the beam splitter. The reference beam produces a reference signal in the geometric center of the camera. The incoming beam produces an object signal at the camera.
Official Gazette of the U.S. Patent and Trademark Office

N88-24959# Messer Griesheim G.m.b.H., Frankfurt am Main (West Germany).
HIGH POWER AXIAL FLOW CO2 LASER Final Report [AXIAL GESTROEMTER HOCHLEISTUNGS CO2-LASER]

L. Bakowsky Aug. 1987 94 p In GERMAN Prepared in cooperation with Technische Hochschule Darmstadt, Fed. Republic of Germany; Technische Hochschule, Aachen, Fed. Republic of Germany and Fraunhofer-Institut fuer Lasertechnik, Aachen, Fed. Republic of Germany
(Contract BMFT-13N-5284)
(ETN-88-91951) Avail: NTIS HC A05/MF A01

A carbon dioxide laser was improved by reduction of focus radius and appropriate beam modulation giving higher power densities in focus. Modulation of the resonator and of the power exciter enable the realization of a 1 kW system with one discharge tube and a 2.5 kW system with six discharge tubes. Higher performances in cutting and welding of metals are obtained. ESA

N88-24960# Lawrence Livermore National Lab., Calif.
REDUCING SENSITIVITY TO ERRORS IN FREE ELECTRON LASER AMPLIFIERS
H. D. Shay and E. T. Scharlemann 14 Jan. 1988 20 p Presented at the 9th International Free-Electron Laser Conference, Williamsburg, Va., 14 Sep. 1987
(Contract W-7405-eng-48)
(DE88-007017; UCRL-98103; CONF-8709110-22) Avail: NTIS HC A03/MF A01

Random errors that affect the transport of electron beams through long wigglers can degrade the performance of free-electron laser amplifiers. We describe the origin and magnitude of the degradation, and test (with simulations) possible ways to improve amplifier performance in the presence of errors. DOE

N88-24961# Lawrence Livermore National Lab., Calif.
FRACTURE OF SOLID STATE LASERS
J. E. Marion Aug. 1987 13 p Presented at the 31st SPIE Annual International Technical Symposium on Optical and Optoelectronic Applied Science and Engineering, San Diego, Calif., 16 Aug. 1987
(Contract W-7405-eng-48)
(DE88-007023; UCRL-95880-Rev-1; CONF-8708110-33-Rev-1)
Avail: NTIS HC A03/MF A01

The understanding of fracture in solid state lasers is reviewed, with an emphasis on fracture of high average power thin slabs. Methods for characterizing strength in the context of materials selection and device implementation are discussed. Progress in slab strengthening is analyzed; aggressive optical fabrication research (to give low damage surfaces), coupled with the implementation of existing schemes for placing the slab surfaces in compression, are recommended to reduce the problem of slab fracture. DOE

37 MECHANICAL ENGINEERING

Includes auxiliary systems (nonpower); machine elements and processes; and mechanical equipment.

N88-24962* Smithsonian Astrophysical Observatory, Cambridge, Mass.
UTILIZATION OF THE IR TELESCOPE GIMBALING SYSTEM AS A STABILIZED POINTING PLATFORM FOR BALLOON PAYLOADS. VOLUME 1: TECHNICAL RESULTS Final Report, 4 Feb. - 3 May 1988
George U. Nystrom May 1988 90 p
(Contract NAS8-37579)
(NASA-CR-179339; NAS 1.26:179339) Avail: Issuing Activity CSCL 13I

This report studies modification of existing balloon gimbal designs for use on the Gamma Ray Imaging device experiment. Improved bearings and brushless torque motors are required to lower bearing torque noise and meet stringent pointing requirements. Analytical results from a strawman gondola and control system design show that pointing requirements are satisfied. Author

N88-24963# Army Military Personnel Center, Alexandria, Va.
THE COORDINATION OF MULTIPLE ROBOTIC MANIPULATORS M.S. Thesis
Reed F. Young 11 Dec. 1987 176 p
(AD-A190869) Avail: NTIS HC A09/MF A01 CSCL 13H

In this thesis, the problem of the coordination of multiple robots is investigated at length. Included in the discussion are the position control, path planning, and collision avoidance strategies involved in the control of two robots mutually holding an object. The theories and algorithms presented in this thesis are tested and implemented in the computer simulation CoordSim. Major results from this thesis include a verification of the resolved position control theory as it drives the robots to any position and orientation. Also, a concatenation and adaption of various single robot theories is made and introduced as the Striving Technique. This solution is a complete movement algorithm which drives the two robots mutually holding an object through a field with obstacles. The algorithm also generates a path function given only the start and end positions and orientations. Finally, the concepts of the coordinated work envelope and twisting collision are derived and discussed. GRA

N88-24964# BKM, Inc., San Diego, Calif.
SERVOJET RETROFIT Final Report, Aug. 1986 - Jun. 1987
Robert L. Barkhimer and John Beck Jul. 1987 92 p
(Contract DAAE07-86-C-R069)
(AD-A191075; TACOM-TR-13301) Avail: NTIS HC A05/MF A01 CSCL 21G

A retrofit diesel engine fuel system of an advanced high-pressure concept is designed and demonstrated. By applying the principle of a spill port operated accumulator injector, the system is projected to enhance starting, as well as the idle and part-load operating characteristics of existing engines. The system has been given the model designation SR-1. GRA

N88-24965 Rensselaer Polytechnic Inst., Troy, N.Y.
THE FLYING CHARACTERISTICS OF THE MEMBRANE SLIDER BEARING Ph.D. Thesis
Cal Edward Hardie 1987 236 p
Avail: Univ. Microfilms Order No. DA8729307

The membrane slider bearing presents an alternate approach to the design of low clearance slider bearings used in direct access storage devices. The slider bearing serves to separate the read/write transducer and the disk surface. The thin air film provided between the slider and the disk surface eliminates contact and thereby prevents the damage and wear of the slider and recording medium. The slider bearing must have two important design characteristics: a low flying height in order to achieve a high storage data density; and a high fluid film stiffness to insure a nearly uniform air bearing clearance and thereby increase the reliability and efficiency of data storage and retrieval. The membrane slider bearing is analyzed with a view towards these design requirements. A steady state analysis will examine the overall feasibility of the membrane slider design. The effects on membrane shape of various physical parameters such as flexural stiffness, and surface tension will be explored. The steady-state elastohydrodynamics of the membrane slider will be compared to documented results for conventional foil bearings. A transient analysis will assess the fluid stiffness of the membrane slider bearing. The membrane slider bearing will be presented as a stiff air bearing that can achieve competitive flying heights with a stable dynamic response to disk runout or surface contaminants. Dissert. Abstr.

N88-24966 Purdue Univ., West Lafayette, Ind.
EFFECTS OF CORIOLIS ACCELERATION ON THE VIBRATIONS OF SPINNING STRUCTURES Ph.D. Thesis
Shyh-Chin Huang [1987] 164 p
Avail: Univ. Microfilms Order No. DA8729742

The vibration behavior of a rotating ring and a rotating cylindrical shell is investigated. The equations of motion for a rotating cylindrical shell are derived from Hamilton's principle. The initial tensions generated by the centrifugal forces due to rotation and internal pressure are taken into account in the equations of motion.

The equations are first specialized for the rotating ring problem. Bifurcations of natural frequencies and traveling modes due to Coriolis acceleration are discussed for the free vibration. A modal expansion technique follows to yield the solution for the forced vibration, where the so-called generalization coordinates characterize the solution. The extensional assumption further simplifies the solution such that closed form solutions are feasible for various loading conditions. A stationary ring subjected to traveling loads is also solved for so that the effect of the Coriolis component can be extracted through the comparison. The analysis is extented to a rotating cylindrical shell. Similar properties for the rotating ring problem are obtained for a rotating shell as far as the natural response is concerned. Corresponding traveling loads on a stationary shell case accompany each example to show the effect of Coriolis components on the steady state response. Dissert. Abstr.

N88-24967 West Virginia Univ., Morgantown.
KINEMATICS, DYNAMICS AND CONTROL OF A CLOSED CHAIN MECHANISM MANIPULATOR Ph.D. Thesis
Krit Kittiampon [1987] 219 p
Avail: Univ. Microfilms Order No. DA8729228

Three main areas of robots with closed kinematic chain mechanisms are examined: kinematics, dynamics, and control. In kinematic analysis, both direct and inverse kinematic solutions were discussed. Based on an algebraic approach to inverse kinematic problems, an inverse kinematic solution for a manipulator with closed kinematic chain mechanism, G.E. P-50 robot, was derived. A computer program using algebraic manipulation language REDUCE was writeen to generate symbolic closed-form dynamic equations for open-chain mechanism manipulator with as many as six degrees of freedom. This computer program utilized the recursive Newton-Euler formulation. By incorporating derived kinematic constraints in the REDUCE program, symbolic closed-form dynamic equations G.E. P-50 robot were generated. Based on these dynamic equations and actuator dynamics, an integrated joint dynamics model was developed. By applying the model reference adaptive control technique to the integrated joint dynamic model, an independent adaptive joint control scheme was derived. A computer simulation study, using G.E. P-50 robot model, was conducted to evaluate and compare the performance of the developed adaptive controller with the computer-torque controller. Simulation results showed that independent adaptive joint control scheme with feedforward compensation is effective for positioning control of the manipulator with closed kinematic chain mechanism and outperform the computed-torque method. Dissert. Abstr.

N88-24968*# National Aeronautics and Space Administration. Lewis Research Center, Cleveland, Ohio.
DEVELOPMENT OF A LIQUID-FED WATER RESISTOJET
W. Earl Morren and James R. Stone 1988 20 p Presented at the 24th Joint Propulsion Conference, Boston, Mass., 11-13 Jul. 1988; sponsored by AIAA, ASME, SAE and ASEE
(NASA-TM-100927; E-4192; NAS 1.15:100927; AIAA-88-3288)
Avail: NTIS HC A03/MF A01 CSCL 13I

A concept for a forced-flow once-through water vaporizer for application to resistojet thrusters was evaluated as an element of a laboratory model thruster and tested to investigate its operating characteristics. The vaporizer design concept employs flow swirling to attach the liquid flow to the boiler chamber wall, providing for separation of the two liquid phases. This vaporizer was modified with a nozzle and a centrally-located heater to facilitate vaporization, superheating, and expansion of the propellant, allowing it to function as a resistojet. Performance was measured at thrust levels ranging from 170 to 360 mN and at power levels ranging from 443 to 192 W. Maximum measured specific impulse was 192 sec. Author

N88-24969*# National Aeronautics and Space Administration. Lyndon B. Johnson Space Center, Houston, Tex.
TOGGLE RELEASE Patent Application
Thomas Joseph Graves, inventor (to NASA), Robert Alexander Yang, inventor (to NASA), and Christopher William Brown, inventor (to NASA) (Boeing Aerospace Co., Seattle, Wash.) 11 Feb. 1988 21 p
(NASA-Case-MSC-21354-1; NAS 1.71:MSC-21354-1; US-Patent-Appl-SN-154712) Avail: NTIS HC A03/MF A01 CSCL 13I

The invention relates to a pyrotechnic actuated release mechanism which is mechanically two fault tolerant for effecting release. It is particularly well suited for releasably connecting structures to be used in the space environment or in other aerospace applications. The device comprises a fastener plate and fastener body, each attachable to either one of a pair of structures to be joined. The fastener plate and the body are fastenable by a toggle supported at one end on the fastener plate and mounted for universal pivotal movement thereon. At its other end, which is received in a central opening in the fastener body and adapted for limited pivotal movement therein, the toggle is restrained by three retractable latching pins. Each pin is individually retractable by combustion of a pyrotechnic charge. While retraction of all three pins releases the toggle, the fastener is mechanically two fault tolerant since the failure of any single or pair of the latch pins to retract results in an asymmetrical loading on the toggle and its pivotal movement to effect a release. An annular bolt is mounted on the fastener plate as a support for the socket mounting of the toggle whereby its selective axial movement provides a means for pre-loading the toggle. NASA

N88-24970*# National Aeronautics and Space Administration. Langley Research Center, Hampton, Va.
STRUCTURALLY TAILORABLE NON-LINEAR SNAP-THROUGH SPRING SYSTEM Patent Application
Gary L. Farley, inventor (to NASA), James H. Starnes, Jr., inventor (to NASA), and Wayne R. Mantay, inventor (to NASA) (Army Aviation Systems Command, Hampton, Va.) 1 Apr. 1988 11 p
(NASA-Case-LAR-13729-1; NAS 1.71:LAR-13729-1; US-Patent-Appl-SN-176544) Avail: NTIS HC A03/MF A01 CSCL 13K

The invention relates to a structural, tailorable, nonlinear spring system which has a controllable, predictable and abrupt change in load-deflection response and which is readily adaptable to structural applications. In particular, the system can be employed to change the geometry of helicopter rotor blades as the aerodynamic and centrifugal forces acting upon the rotor blades change. The spring system comprises an external case containing a pin-connected two-bar linkage and a tension or compression spring. As a load is applied to the snap-through spring the linkage bars laterally deform until the bars collapse and snap-through. The stiffness as the load is applied is a function of the axial stiffness of the internal spring and bending stiffness of the pin-connected two-bar linkage. When the snap-through occurs, a large deformation occurs as a result of the small increase of applied load. The load-deflection response at this point is a function of the internal spring and the membrane stiffness of the bars. Additional stiffness can be provided to the post-snap-through response by including restraints that contact the external spring case. The load-deflection response of the system is tailorable by changing the size, stiffness and orientation of its various components. In addition, multiple devices can be put in parallel or series to produce an infinite number of different load-deflection responses. NASA

N88-24971*# National Aeronautics and Space Administration. Marshall Space Flight Center, Huntsville, Ala.
UNIVERSAL PRECISION SINE BAR ATTACHMENT Patent Application
Franklin D. Mann, inventor (to NASA) 9 Mar. 1988 17 p
(NASA-Case-MFS-28253-1; NAS 1.71:MFS-28253-1; US-Patent-Appl-SN-165943) Avail: NTIS HC A03/MF A01 CSCL 13H

This invention relates to an attachment for a sine bar which can be used to perform measurements during lathe operations or other types of machining operations. The attachment can be used for setting precision angles on vises, dividing heads, rotary tables and angle plates. It can also be used in the inspection of machined

parts, when close tolerances are required, and in the layout of precision hardware. The novelty of the invention is believed to reside in a specific versatile sine bar attachment for measuring a variety of angles on a number of different types of equipment.
NASA

N88-24972*# National Aeronautics and Space Administration. Marshall Space Flight Center, Huntsville, Ala.
TRAILER SHIELD ASSEMBLY FOR A WELDING TORCH Patent Application
Gerald E. Dyer, inventor (to NASA) (Rockwell International Corp., Huntsville, Ala.) 16 Feb. 1988 15 p
(NASA-Case-MFS-29260-1; NAS 1.71:MFS-29260-1; US-Patent-Appl-SN-156059) Avail: NTIS HC A03/MF A01 CSCL 13H

This invention relates generally to trailer shields for gas shielded arc welding torches, and more particularly to a trailer shield assembly provided with a shield gas manifold for providing an even dispersion of shield gas to the interior of the shield assembly, which generally encloses a joint being welded and a welding trailing portion of hot welded metal. The novelty of the invention lies in providing trailer shield with a manifold tube having a plurality of openings from which shield gas is distributed. A gas manifold region ahead of the torch is also provided with shield gas from a tube to protect metal preheated by the torch. Further novelty lies in constructing portions of sides and housing and portions of side walls of the guide of stainless steel screen having a tight mesh.
NASA

N88-24973*# National Aeronautics and Space Administration. Pasadena Office, Calif.
ARTICULATED SUSPENSION SYSTEM Patent Application
Donald B. Bickler, inventor (to NASA) (Jet Propulsion Lab., California Inst. of Tech., Pasadena.) 22 Mar. 1988 12 p Prepared in cooperation with Jet Propulsion Lab., California Inst. of Tech., Pasadena.
(Contract NAS7-918)
(NASA-Case-NPO-17354-1-CU; NAS 1.71:NPO-17354-1-CU; US-Patent-Appl-SN-184236) Avail: NTIS HC A03/MF A01 CSCL 13F

The invention provides a rough terrain vehicle which maintains a substantially constant weight, and therefore traction, on all wheels, despite one wheel moving considerably higher or lower than the others, while avoiding a very soft spring suspension. The vehicle includes a chassis or body to be supported and a pair of side suspensions at either side of the body. In a six wheel vehicle, each side suspension includes a middle wheel, and front and rear linkages respectively coupling the front and rear wheels to the middle wheel. A body link pivotally connects the front and rear linkages together, with the middle of the body link rising or falling by only a fraction of the rise or fall of any of the three wheels. The body link pivotally supports the middle of the length of the body. A transverse suspension for suspending the end of the body on the side suspensions includes a middle part pivotally connected to the body about a longitudinal axis and opposite ends each pivotally connected to one of the side suspensions along at least a longitudinal axis.
NASA

N88-24974# Oak Ridge National Lab., Tenn.
REAL-TIME IMPLEMENTATION OF A KINEMATIC OPTIMIZATION SCHEME FOR SEVEN-DEGREE-OF-FREEDOM REDUNDANT ROBOTS WITH SPHERICAL WRISTS
R. V. Dubey, J. A. Euler, S. M. Babcock, and R. L. Glassell 1988 4 p Presented at the American Control Conference, Atlanta, Ga., 15 Jun. 1988
(Contract DE-AC05-84OR-21400)
(DE88-006785; CONF-880685-1) Avail: NTIS HC A02/MF A01

A computationally efficient, kinematic optimization scheme is presented for seven-degree-of-freedom robots with spherical wrists. This scheme uses the gradient projection method, and it does not require the generalized inverse of the Jacobian. An efficient formulation for determining joint velocities is obtained. Thus, this control scheme is well-suited for real-time implementation, which is essential if the end-effector trajectory is continuously modified based on sensory feedback. A comparison of the computational complexity with previously available schemes is presented. Implementation of this scheme on a Motorola 68020 VMEbus-based controller of the seven-degree-of-freedom manipluator at the ORNL Center for Engineering Systems Advanced Research (CESAR) is described.
DOE

N88-24975*# Transmission Technology Co., Inc., Fairfield, N. J.
DESIGN, MANUFACTURE AND SPIN TEST OF HIGH CONTACT RATIO HELICOPTER TRANSMISSION UTILIZING SELF-ALIGNING BEARINGLESS PLANETARY (SABP) Final Contractor Report
Dezi Folenta and William Lebo Washington NASA Jun. 1988 112 p
(Contract NAS3-24539; DA Proj. 1L1-62209-AH-76)
(NASA-CR-4155; E-4049; NAS 1.26:4155; TTC-87-07R; AVSCOM-TR-88-C-009) Avail: NTIS HC A06/MF A01 CSCL 13I

A 450 hp high ratio Self-Aligning Bearingless Planetary (SABP) for a helicopter application was designed, manufactured, and spin tested under NASA contract NAS3-24539. The objective of the program was to conduct research and development work on a high contact ratio helical gear SABP to reduce weight and noise and to improve efficiency. The results accomplished include the design, manufacturing, and no-load spin testing of two prototype helicopter transmissions, rated at 450 hp with an input speed of 35,000 rpm and an output speed of 350 rpm. The weight power density ratio of these gear units is 0.33 lb hp. The measured airborne noise at 35,000 rpm input speed and light load is 94 dB at 5 ft. The high speed, high contact ratio SABP transmission appears to be significantly lighter and quieter than comtemporary helicopter transmissions. The concept of the SABP is applicable not only to high ratio helicopter type transmissions but also to other rotorcraft and aircraft propulsion systems.
Author

N88-24976*# Illinois Univ., Chicago.
DETERMINATION OF SETTINGS OF A TILTED HEAD-CUTTER FOR GENERATION OF HYPOID AND SPIRAL BEVEL GEARS Final Report
F. L. Litvin, Y. Zhang, M. Lundy, and C. Heine (Dana Corp., Fort Wayne, Ind.) Jun. 1988 27 p
(Grant NAG3-783)
(NASA-CR-182138; NAS 1.26:182138; AVSCOM-TR-88-C-016)
Avail: NTIS HC A03/MF A01 CSCL 13I

Kinematics of Gleason mechanisms of hypoid and spiral bevel cutting machines are considered. These mechanisms are designated to install the position and tilt of the head cutter. The tilt of the head cutter with standard blades provides the required pressure angle. The authors have developed the matrix presentation of kinematics of these meachanisms and basic equations for the required settings. An example is presented based on the developed computation procedure.
Author

38 QUALITY ASSURANCE AND RELIABILITY

Includes product sampling procedures and techniques; and quality control.

N88-24977# Oak Ridge Gaseous Diffusion Plant, Tenn.
A QUALITY PHILOSOPHY FOR RESEARCH AND DEVELOPMENT
G. J. Kidd, Jr. Feb. 1988 17 p
(Contract DE-AC05-84OT-21400)
(DE88-006512; K/QT-178) Avail: NTIS HC A03/MF A01

The application of traditional quality assurance techniques to research and development (R and D) has not been successful. This report presents some of the features that distinguish R and D from other industrial enterprises and suggests an approach for adapting existing standards to R and D.
DOE

N88-24978# Chemical Research and Development Center, Aberdeen Proving Ground, Md.
PROPOSED QUALITY ASSURANCE/QUALITY CONTROL PLAN Special Publication Oct. 1984 - Apr. 1985
Susan F. Hallowell, Emory W. Sarver, and Dennis J. Reutter Dec. 1987 27 p
(AD-A191490; CRDEC-SP-88007) Avail: NTIS HC A03/MF A01 CSCL 13H

Preparation of this report is a result of a mandate by Dr. Richardson, U.S. Army Chemical Research, Development and Engineering Center (CRDEC) Technical Director. The need to develop a quality assurance program for CRDEC was underscored by a review of the body protection group within the Physical Protection Directorate. This review indicated that there was a significant need to incorporate documented quality control (QC) and quality assurance (QA) procedures in the development and testing of individual protection items. This plan was our initial attempt to organize a QA mechanism into the infrastructure of CRDEC without interrupting mission objectives. It describes a 3-yr plan, which would ultimately result in the creation of a QA Office directly under the Commander with a QA/QC mechanism in place. All major portions of this plan were accepted with some modifications. An Agency Testing Task Force (ATTF) has been developed. The mission concerns the use and handling of chemical agents only. It has resulted in the formation of a program for users of Standard Analytical Reference Materials (SARMs) for the chemical agents (CASARMs). Also notable has been the formation of a subcommittee to develop user Standard Reference Material (SRMs) and the development of a standardized format for the documentation of Analytical Test Methodology. Two training courses in the areas of QC in the laboratory and experimental design strategy have been sponsored by the ATTF. GRA

N88-24979# North Carolina Univ., Chapel Hill. Dept. of Operations Research.
SENSITIVITY ANALYSIS FOR THE SYSTEM RELIABILITY FUNCTION Technical Report, Dec. 1986 - Dec. 1987
George S. Fishman Dec. 1987 50 p
(Grant AF AFOSR-0140-84)
(AD-A191648; UNC/OR/TR-87-6; AFOSR-88-0363TR) Avail: NTIS HC A03/MF A01 CSCL 12C

Sensitivity analysis, which represents an integral part of virtually every study of system reliability, measures variation in this quantity in response to changes in component reliabilities or in system design. Replacing old components with new ones with higher reliabilities affects system reliability. As time elapses, system reliability deteriorates when a non replacement policy for components all affect system reliability. Sampling variation in component reliability estimates induce sampling variation in the corresponding system reliability estimate. Having access to a model that accurately predicts these changes in system behavior allows one to make considerably more well informed decisions for maintaining or enhancing performance. This paper presents a method for estimating variation in system reliability in response to variation in component reliabilities. It describes a Monte Carlo sampling plan that on each of w sets of distinct component reliabilities. It describes a Monte Carlo sampling plan that on each replication provides sample data that contribute to the estimation of system reliability for each w sets of distinct component reliabilities. The sets may represent alternative component replacement plans, deteriorating component reliabilities at a succession of time points or extremal points of simultaneous component reliability interval estimates (Fishman 1987). GRA

N88-24980 Texas Univ., Austin.
ANALYSIS AND DESIGN OF DETECTION FILTERS WITHIN CLOSED-LOOP SYSTEMS Ph.D. Thesis
Shaul Attar 1987 248 p
Avail: Univ. Microfilms Order No. DA8728511

The detection and isolation of a failure is a key issue in the development of highly reliable fault-tolerant control systems. The design of detection filters is extended to include the augmented closed-loop feedback system. Since one of the primary uses of detection filters is to detect failures within critical closed-loop systems, the choice of the controller gains to enhance detection filter design is extremely advantageous. The spectral approach to detection filter design is taken and even further simplified. By including the feedback gains as part of the detection filter design, it is shown that for the case where the number of faults equals the number of measurements, the detection filter closed-loop eigenvalues can all be chosen generically. A formulation for the mutual detectability property is given in terms of the controllability with respect to the family of failures. A general method for optimizing the eigenvalues of a detection filter under stochastic inputs is developed. Practical design and analysis techniques are presented. Two major design approaches are derived for robust detection filters. Dissert. Abstr.

N88-24981# Pacific Northwest Labs., Richland, Wash.
KNOWLEDGE BASED SYSTEMS IN NONDESTRUCTIVE EVALUATION
R. B. Melton Aug. 1987 7 p Presented at the NATO Advanced Research Workshop on Signal Processing and Pattern Recognition in Nondestructive Evaluation of Materials, Lac Beauport, Quebec, 19 Aug. 1987
(Contract DE-AC06-76RL-01830)
(DE88-006653; PNL-SA-15670; CONF-8708225-1) Avail: NTIS HC A02/MF A01

This paper dicusses the application of knowledge based systems technology to problems in nondestructive evaluation (NDE). The Saft Image Interpretation Assistant (SIIA) is used as an illustrative example. SIIA is a prototype knowledge based system designed to assist in making the operation of the Synthetic Aperture Focusing Technique (SAFT) Ultrasonic Inspection System more reliable and efficient. The two primary motivations for developing SIIA were to insure that the SAFT system is used correctly and consistently and to assist in interpreting the results of a SAFT inspection. Our initial goal was to develop a system to assist in the interpretation of the images resulting from a SAFT inspection. As we started to identify the structure of the inspection problem, however, we realized knowledge based system technology could be more effectively applied to develop a system that is in essence an on-line procedure generator that guides a user through a SAFT inspection. When fully developed such a system could assist in proper setup of the inspection equipment for each of the steps in a SAFT inspection and in interpreting the inspection results for each step. DOE

N88-24982# Brookhaven National Lab., Upton, N. Y.
APPLICATIONS OF FAULT TREE ANALYSIS TO THE DESIGN PROCESS
R. W. Youngblood 1988 10 p Presented at the Photovoltaics Safety Conference, Denver, Colo., 19 Jan. 1988
(Contract DE-AC02-76CH-00016)
(DE88-007048; BNL-40839; CONF-880112-1) Avail: NTIS HC A02/MF A01

Fault tree analysis of a system can provide a complete characterization of system failure modes, i.e., what combinations of component failures can give rise to system failure. This can be applied to the design process at several levels: confirmatory analysis, in which a fault tree development is used to verify design adequacy, importance analysis, in which fault tree analysis is used to highlight system vulnerabilities, and design optimization, in which fault tree analysis is used to pick the least expensive configuration from a collection of possibilities satisfying a given constraint. Experience shows that the complexity of real systems warrants the systematic and structured development of fault trees for systems whose failure can have severe consequences. DOE

N88-24983*# United Technologies Corp., East Hartford, Conn.
QUALITY AND PRODUCTIVITY DRIVE INNOVATION AND IMPROVEMENT AT UNITED TECHNOLOGIES AEROSPACE OPERATIONS, INC.
L. G. Jamar 24 Nov. 1986 19 p Submitted for publication
(Contract NAS8-36300)

(NASA-CR-182944; NAS 1.26:182944) Avail: NTIS HC A03/MF A01 CSCL 14D

Quality and innovation are the hallmarks of the national space program. In programs that preceded the Shuttle Program the emphasis was on meeting the risks and technical challenges of space with safety, quality, reliability, and success. At United Technologies Aerospace Operations, Inc. (UTAO), the battle has developed along four primary fronts. These fronts include programs to motivate and reward people, development and construction of optimized processes and facilities, implementation of specifically tailored management systems, and the application of appropriate measurement and control systems. Each of these initiatives is described. However, to put this quality and productivity program in perspective, UTAO and its role in the Shuttle Program are described first. B.G.

N88-24984 Centre d'Etudes et de Recherches, Toulouse (France). Dept. d'Etudes et de Recherches en Micro-Ondes.
NONDESTRUCTIVE TESTING USING ULTRAHIGH FREQUENCIES Final Report [CONTROLE NON DESTRUCTIF PAR HYPERFREQUENCES]
Antoine Assice and Alain Priou Jul. 1986 52 p In FRENCH
(Contract DRET-85-002)
(CERT-5/1333-MO; ETN-88-92165) Avail: NTIS HC A04; Centre d'Etudes et de Recherches, 2 Avenue Edouard Belin, BP 4025, 31055 Toulouse Cedex

Theoretical models used in flaw detection, and detection of inhomogeneities and temperature gradients in composite materials were reviewed, and radiometric test procedures for nondestructive control were examined. Experiments show that inhomogeneity detection limits are of the order of defects of dimension lambda/2. The flaw could be an air bubble or a semiconductor flaw buried at least 4 cm down in a plastic material. ESA

N88-24985# Center for Mathematics and Computer Science, Amsterdam (Netherlands). Dept. of Applied Mathematics.
RELIABILITY OF STOCHASTICALLY FORCED SYSTEMS (EXTENDED VERSION)
H. N. M. Roozen Jan. 1988 30 p
(CWI-AM-R8801; B8805670; ETN-88-92584) Copyright Avail: NTIS HC A03/MF A01

The reliability of a mechanical system is related to a first passage problem in the theory of stochastic dynamical systems. The phenomenon of fatigue is modelled by allowing a slow change in time of the system parameters. The methods yield expressions for the lifetime on the basis of the dynamics of the mechanical system. For this reason it is expected that better predictions of the lifetime can be made, e.g., in case of accelerated life testing, than by pure statistical methods. ESA

39 STRUCTURAL MECHANICS

Includes structural element design and weight analysis; fatigue; and thermal stress.

For applications see *05 Aircraft Design, Testing and Performance* and *18 Spacecraft Design, Testing and Performance.*

N88-24986# Edgerton, Germeshausen and Grier, Inc., Idaho Falls, Idaho.
THEORETICAL AND EXPERIMENTAL DAMPING VALUES OF PIPING SYSTEMS AT HIGH DUCTILITIES
A. G. Ware 1987 10 p Presented at the 5th National Congress on Pressure Vessels and Piping, San Diego, Calif., 28 Jun. 1987
(Contract DE-AC07-76ID-01570)
(DE88-006717; EGG-M-31686; CONF-870636-15) Avail: NTIS HC A02/MF A01

This paper presents a simplified theoretical explanation and test data for piping system damping during post-yield dynamic behavior. The theoretical frequency and damping variations with material ductility are discussed. The results of high excitation level tests from seven sources are described and correlated on common bases. Starting with 0% of critical damping at a local ductility of 1 (yield strain), damping values of from 30 to 50% of critical are estimated at the time of piping system failure. Since 50% of critical damping corresponds to no dynamic amplification at resonance, it is concluded that the input energy is being continually and completely dissipated by the forcing function changing the plastic dynamic deflection shape, with no dynamic amplification of displacements. An experimental method for consistent estimation of damping values at elastoplastic response levels is recommended. DOE

N88-24987# Ballistic Research Labs., Aberdeen Proving Ground, Md.
PLATE RESPONSE ANALYSIS USING SHOCK TUBE Final Report
Joseph M. Santiago Nov. 1987 38 p
(AD-A190828; BRL-TR-2876) Avail: NTIS HC A03/MF A01 CSCL 11F

Rectangular aluminum plates, 0.508 and 0.813 mm thick, were subjected to increasingly higher levels of reflected shock pressures, ranging from 77 to 339 kPa, at the closed-off end of a shock tube. The resulting large transient deflections of the plates were measured optically and compared with counterpart finite difference code calculations. The incorporation of a simple piston theory model in the code to account for the fluid-plate interaction was found to improve correlation with test results. GRA

N88-24988# Brown Univ., Providence, R. I. Div. of Engineering.
DYNAMIC SHEAR BAND DEVELOPMENT IN PLANE STRAIN
Alan Needleman Nov. 1987 30 p
(Contract DAAG29-85-K-0003)
(AD-A190915; Rept-7; ARO-22306.11-EG) Avail: NTIS HC A03/MF A01 CSCL 20K

Plane strain compression of a rectangular block is used as a model problem to investigate the dynamics of shear band development from an internal inhomogeneity. The material is characterized as a von Mises elastic-viscoplastic solid, with a hardness function that exhibits a local maximum. Regardless of whether the material is hardening or softening, plastic strain development involves the evolution of finger-like contours emanating from the inhomogeneity at 45 degrees to the compression axis. Once a given strain contour crosses the specimen, it fans out about its initial direction of propagation. For a softening solid, this fanning out ceases for some strain level greater than the strain at the hardness maximum and further straining takes place in an ever narrowing band. Many of the qualitative features of shear band development under dynamic loading conditions are the same as under quasi-static loading conditions, but a significant retardation of shear band development due to inertial effects is found. GRA

N88-24989# Virginia Polytechnic Inst. and State Univ., Blacksburg. Dept. of Aerospace and Ocean Engineering.
EXPERIMENTAL STUDY OF ACTIVE VIBRATION CONTROL Final Technical Report, 30 Jan. 1986 - 31 Aug. 1987
William L. Hallauer, Jr 31 Aug. 1987 71 p
(Contract F49620-85-C-0024)
(AD-A191454; AFOSR-88-0060TR) Avail: NTIS HC A04/MF A01 CSCL 22B

Complementary experimental-theoretical studies were conducted on the following subjects related to the dynamics and control of flexible large spacecraft structures: 1) Transient wave propagation - Extensive results are presented for traveling waves in a laboratory structure excited by suddenly applied oscillatory point forces; 2) The dynamics of a thin-walled grid with a ridgid body slewing degree of freedom. The design, theoretical analysis, experimental testing, and experimental, and experimental-theoretical correlation are reported. Even after much refinement, the finite element model of the relatively simple structure did not satisfactorily predict the measured dynamic behavior; and 3) Active damping and control the slewing gird with the use of structure-borne accelerometers and reaction wheel actuators - The results of an active vibration damping experiment

are presented. Also discussed are the serious practical problems encountered in this research and the potential for future experiments with simultaneous control of maneuvering and vibration. GRA

N88-24990# Army Armament Research and Development Command, Watervliet, N. Y. Weapons Lab.
STRESS CORROSION CRACKING OF A723 STEEL PRESSURE VESSELS: TWO CASE STUDIES Final Report
J. H. Underwood and J. J. Miller Jan. 1988 40 p
(AD-A191741; ARCCB-TR-88002) Avail: NTIS HC A03/MF A01 CSCL 11F

Two separate investigations of apparent stress corrosion cracking of cannon tubes under field service conditions are described. The first investigation involved several tubes in which cracking initiated at the inner diameter surface due to the combination of cannon firing products and tensile residual stresses. Results of metallographic and fracture surface studies; residual stress measurements; fatigue life and material mechanical tests; and stress corrosion simulation tests of tube sections are presented and discussed. The second investigation involved two tubes in which apparent stress corrosion cracking occurred on the outer diameter surface due to the combination of an unknown substance, presumed to be a cleaning product, and tensile residual stress due to autofrettage of the tube. The critical requirements for stress corrosion cracking are discussed in general and in relation to the pressure vessels of the two investigations. Conclusions are drawn regarding design and service conditions for pressure vessels which will help prevent the occurrence of stress corrosion cracking. GRA

N88-24991# Florida Univ., Gainesville. Dept. of Civil Engineering.
FINITE ELEMENT ANALYSIS OF AN UNDERGROUND STRUCTURE Final Report, Sep. 1985 - Sep. 1986
M. C. McVay and S. Zalzman Jan. 1988 165 p
(Contract F08635-83-C-0136)
(AD-A191747; AFESC/ESL-TR-87-05) Avail: NTIS HC A08/MF A01 CSCL 13M

The evaluation and design of underground structures subjected to blast loads are presently based upon empirical correlations of field studies and numerical analysis of structural components. Recently, the United States Air Force initiated an investigation of the feasibility of implementing analytical procedures and computer models to evaluate the response of these structures. This study was concerned with the evaluation of the finite element program NONSAP-C (nonlinear elasto-dynamic finite element program) as a means to predict the response of a structure subjected to different loading conditions. The evaluation was made by comparing the predicted responses with the observed responses from laboratory tests. These tests were performed on laboratory scaled structures with simple geometry. Three types of tests were conducted on the scaled structures. The first two tests consisted of the application of static dynamic loads to a scaled concrete structure. The third test consisted of the application of an explosive load to a scaled concrete structure buried in dry sand and subjected to a high gravity environment. The three types of tests were simulated with the program NONSAP-C. GRA

N88-24992# United Technologies Corp., East Hartford, Conn.
FRACTURE MECHANICS ANALYSIS FOR SHORT CRACKS Annual Report, 1 Aug. 1986 - 31 Jul. 1987
B. S. Annigeri 27 Aug. 1987 22 p
(Contract F49620-86-C-0095)
(AD-A192002; UTRC/R87-957565-1; AFOSR-88-0195TR) Avail: NTIS HC A03/MF A01 CSCL 20K

This study addresses the development of the Surface-Integral and Finite Element ((SAFE) hybrid method for the analysis of short or physically small cracks. In this report, a brief review of representative research papers on fracture mechanics of short cracks is provided. The development of the SAFE hybrid method for materially nonlinear analysis is discussed. Motivation for the use of lumped plasticity models via modelling shear bands at the crack tip is given. Work in progress and future research tasks to be performed under this contract are outlined. GRA

N88-24993# Poitiers Univ. (France). Lab. de Mecanique des Solides.
DETERMINATION OF THE TOUGHNESS OF A BRITTLE MATERIAL USING STRAIN GAGES Final Report [DETERMINATION DE LA TENACITE SUR UN MATERIAU FRAGILE PAR EXTENSOMETRIE]
A. Lagarde and M. Cottron Nov. 1987 44 p In FRENCH
(Contract DRET-85-1209)
(ETN-88-92540) Avail: NTIS HC A03/MF A01

A method to determine the toughness of high strength materials by measuring strain at several points around crack tips was developed. Two techniques for obtaining the stress intensity factor are outlined (single and multipoint measurements). The techniques were applied to a brittle polymer and a brittle steel. The methods are both valid, but the advantage of using only one gage for the single point technique is outweighed by the precision required in orienting the gage and the fact that the position of the point of cracking must be known accurately before the rupture test. ESA

N88-24994# Office National d'Etudes et de Recherches Aerospatiales, Paris (France). Direction Scientifique de la Resistance des Structures.
INVESTIGATION OF THE EFFECT OF MINIMUM LOADS AND COMPRESSION OF LOAD SPECTRA ON THE PREDICTION CAPACITIES OF THE ONERA CRACK MODEL Final Report [ETUDE DE L'EFFET DES CHARGES MINIMALES ET DE COMPRESSION DES SPECTRES DE CHARGEMENT SUR LES CAPACITES DE PREVISION DU MODELE DE FISSURATION ONERA]
G. Baudin and M. Robert Oct. 1987 46 p In FRENCH
(Contract STPA-85-95-004)
(ONERA-RTS-33/7169-RY-064-R; ETN-88-92546) Avail: NTIS HC A03/MF A01

The ONERA fatigue crack prediction model was tested for the case of a wing with high compression loads. Results for various thicknesses are satisfactory (conservative in a ratio of 0.53 to 0.68). This type of load spectrum needs a simple adaptation of the model: cycles which are entirely compressive should be ignored when calculating the loading parameter. Another possible amelioration would be to widen the measuring domain of threshold functions towards negative R ratios and big thicknesses during model identification. ESA

N88-24995# Aeronautical Research Inst. of Sweden, Stockholm. Structures Dept.
SOME STRESS INTENSITY FACTOR EQUATIONS
Bjoern Palmberg Nov. 1987 109 p
(Contracts FMV-FFL-82250-85-076-73-001; FMV-FFL-82250-85-282-24-001)
(FFA-TN-1987-07; ETN-88-92492) Avail: NTIS HC A06/MF A01

Stress intensity factors available in the subroutine library of the crack growth prediction program LIFE, and a handbook for stress intensity factor equations are presented. All stress intensity factors are given as equations. Stress intensity factors which can be described by a single crack length measure, (stress intensity factors for through-the-thickness cracks; and stress intensity factors for which two crack length measures are required (typically, part-through cracks (elliptical, semielliptical, quarter-elliptical) but also nonsymmetric through-the-thickness cracks) are included. ESA

N88-24996# Aeronautical Research Inst. of Sweden, Stockholm. Structures Dept.
AUTOMATED ANALYSIS OF CRACK GROWTH RATE FOR OBTAINING da/dN VERSUS DELTA K RELATION
Bjoern Palmberg Nov. 1987 33 p Sponsored in cooperation with the Swedish Board for Technical Development

(Contract FMV-FFL-82250-85-273-25-001)
(FFA-TN-1987-70; ETN-88-92494) Avail: NTIS HC A03/MF A01

A computer program, called GROWFIT, which uses linear and nonlinear regression analyses with the crack closure concept to fit a stepwise linear relation (in a log-log scale) to experimental data on the crack growth rate versus stress intensity range was written. The program can take into account experimental data for several different stress ratios in a single run. A minimum of data have to be supplied by the user in addition to the experimental data sets (delta K, da/dN). The advantage of the program compared to normal procedures is that different users can obtain the same results based on the same experimental data. The disadvantage is that experimental data for different stress ratios may not be equally well fitted, since the stress ratio dependence is governed by the assumed crack closure formula. ESA

N88-24997*# Syracuse Univ., N. Y. Dept. of Mechanical and Aerospace Engineering.
RESOLVED SHEAR STRESS INTENSITY COEFFICIENT AND FATIGUE CRACK GROWTH IN LARGE CRYSTALS Final Contractor Report
Qi Chen and Hao-wen Liu Jun. 1988 56 p
(Grant NAG3-348)
(NASA-CR-182137; NAS 1.26:182137) Avail: NTIS HC A04/MF A01 CSCL 20K

Fatigue crack growth in large grain Al alloy was studied. Fatigue crack growth is caused primarily by shear decohesion due to dislocation motion in the crack tip region. The crack paths in the large crystals are very irregular and zigzag. The crack planes are often inclined to the loading axis both in the inplane direction and the thickness direction. The stress intensity factors of such inclined cracks are approximated from the two dimensional finite element calculations. The plastic deformation in a large crystal is highly anisotropic, and dislocation motion in such crystals are driven by the resolved shear stress. The resolved shear stress intensity coefficient in a crack solid, RSSIC, is defined, and the coefficients for the slip systems at a crack tip are evaluated from the calculated stress intensity factors. The orientations of the crack planes are closely related to the slip planes with the high RSSIC values. If a single slip system has a much higher RSSIC than all the others, the crack will follow the slip plane, and the slip plane becomes the crack plane. If two or more slip systems have a high RSSIC, the crack plane is the result of the decohesion processes on these active slip planes. Author

N88-24998 Universite de Technologie de Compiegne (France).
DAMAGE BY CREEP FATIGUE: INFLUENCE OF THE VISCO-ELASTICITY OF THE MATRIX
F. X. deCharentenay and J. R. Lee Nov. 1986 21 p In FRENCH Sponsored by Direction des Recherches, Etudes et Techniques, Paris, France
(PB88-124706) Avail: NTIS HC E03/MF E03 CSCL 20K

Under heavy loads, flow accelerates the degradative effect of creep fatigue on carbon-epoxy laminates (+ or - 45 deg)2S. Under light loads (which are normally encountered), flow decreases the degradative effect. In combined fatigue, a linear model of damage cumulation applies if one introduces terms for a first cycle dependent on maximum charge and a second cycle assumed to be constant for a given material. The study clearly confirms the general schema of how composites are damaged. The progressive evolution of damage, which spreads in a homogeneous manner beginning at a certain threshold, is followed by a rapid phase during which the damage concentrates in a catastrophic fashion at certain points. GRA

N88-24999 Chicago Univ., Ill.
SELF-CONSISTENT MODEL FOR THE BRITTLE RESPONSE OF SOLIDS Ph.D. Thesis
Dragoslav Sumarac 1987 144 p
Avail: Univ. Microfilms Order No. DA8728754

The formulation of a simple continuum damage model based on the geometry of the mesostructure and the principles of fracture mechanics are examined. At this stage, the study is limited to the weak interaction of cracks justifying the application of the self-consistent method. The kinetic equations, defining the pattern in which the cracks grow (change their length) is derived on the basis of fracture mechanics. Many simplifying assumptions (such as the one related to the size of initial cracks and distances separating energy barriers) are introduced purely for computational convenience. The suggestion regarding the ultimate failure criterion should be re-examined in light of other failure modes. The proposed model is characterized by a conceptually clear and computationally simple algorithm. The numerical results exhibit proper tendencies reinforcing the intuitive feeling related to the applicability of the Taylor's approximation in case of modest crack concentrations. It is finally important to notice that the results are obtained without introducing a single additional material parameter. Dissert. Abstr.

N88-25000 Purdue Univ., West Lafayette, Ind.
DYNAMIC RESPONSE OF PLATES TO MOVING LOADS: STRUCTURAL IMPEDANCE AND FINITE ELEMENT METHODS Ph.D. Thesis
Mohammad Reza Taheri 1987 184 p
Avail: Univ. Microfilms Order No. DA8729803

To study the transient response of plates with arbitrary boundary conditions to moving loads, two algorithms are developed. The first is based on a structural impedance approach and the second adopts a finite element approach. A thin plate theory is assumed for the plate model. General viscoelastic foundation support can be introduced as a series of springs and dashpots lumped at the nodes. The algorithms place no restrictions on the loading conditions. Two parallel moving loads with suspension systems are considered. Two general purpose codes PLATEIMP and PLATEFEM were developed. These are used to study the dynamic response of plates as they interact with the moving loads. Both programs account for the complete dynamic interactions between the moving loads and the plate structure. Thus the computer codes can be applied to the general moving mass problems and simplified moving force and static problems. The accuracy of the algorithms and the corresponding codes are verified by comparing the numerical results, in the case of moving force solutions, with the exact solutions and with other numerical results. A parametric study concerning the effects of speed, acceleration, damping and the suspension system is also presented. Dissert. Abstr.

N88-25001 State Univ. of New York, Buffalo.
VIBRATION PROTECTION OF INELASTIC STRUCTURES BY MEANS OF ACTIVE AND PASSIVE CONTROL Ph.D. Thesis
Chung-Yuan Wen 1987 158 p
Avail: Univ. Microfilms Order No. DA8727758

Modern methods of vibration protection, such as active, passive, and semi-active control were developed. The aim of these controls is to protect the structure and also to improve the serviceability. Three types of control are presented as protective systems for inelastic structures in which the structures can be designed inelastically or in which nonlinear media can be inserted in order to absorb the input energy. First, the Bounded State Active Control was developed. This scheme of control assures that the structural deformations remain below some assumed threshold limits. The method is based on application of external forces to the structure through cables, air jets, or other devices. Second, the passive Earthquake Barrier System (EBS), a sliding base system combined with external energy dissipation devices, is presented. Finally, three types of combined (hybrid) control systems were developed. Emphasis is on the development and verification of feasibility of bounded state control for response reduction of inelastic structures; the modeling of a sliding system coupled with a highly nonlinear medium (EBS) for response reduction of elastic superstructures; and the development of hybrid systems for response reduction of structures. Numerical examples are presented to illustrate the methods developed and modified.
Dissert. Abstr.

N88-25002 State Univ. of New York, Buffalo.
ADVANCED DEVELOPMENT OF THE BOUNDARY ELEMENT METHOD FOR ELASTIC AND INELASTIC THERMAL STRESS ANALYSIS Ph.D. Thesis
Donald P. Henry, Jr. 1987 265 p
Avail: Univ. Microfilms Order No. DA8727709

The focus is on advanced development of the boundary element method for elastic and inelastic thermal stress analysis. Formulations for the treatment of body forces and nonlinear effects are derived. These formulations, which are based on particular integral theory, eliminate the need for volume integrals or extra surface integrals to account for these effects. The formulations are presented for axisymmetric, two or three dimensional analysis. Also two dimensional and axisymmetric formulations for elastic and inelastic, inhomogeneous stress analysis are introduced. The derivations account for inhomogeneities due to spatially dependent material parameters, and thermally induced inhomogeneities. The nonlinear formulations are based on a incremental initial stress approach. Two inelastic solutions algorithms are implemented: an iterative; and a variable stiffness type approach. The Von Mises yield criterion with variable hardening and the associated flow rule are adopted in these algorithms. All formulations are implemented in a general purpose, multi-region computer code with the capability of local definition of boundary conditions. Quadratic, isoparametric shape functions are used to model the geometry and field variables of the boundary (and domain) of the problem. To test the program, results obtained for simple test cases are checked against their analytical solutions. Thereafter, a range of problems of practical interest are analyzed. Author

N88-25003 Purdue Univ., West Lafayette, Ind.
VIBRATIONS OF ROTATING THICK OR THIN RINGS Ph.D. Thesis
Jeong-Luh Lin 1987 262 p
Avail: Univ. Microfilms Order No. DA8729762

Complete sets of equations of motion for general in-plane vibrations of rotating thick and thin rings on elastic foundations are derived. This thick ring theory takes account of the effects of extensibility, transverse shear, rotatory inertia and rotation as well as the effects of initial stresses due to pressure loads and centrifugal force. Frequency predictions are very close to the experimental data for both nonrotating thick rings and rotating thin rings. It is argued that inextensional assumptions in thick ring theories are improper because extensional coupling effects are as important as shearing effects, especially for the rotating ring. The correct quadratic displacement terms in the strain-displacement relations, necessary for the complete description of initial stress effects, are also discussed. The dynamic response of a rotating thick ring is obtained, subjected to either force or displacememt excitation. The equations of motion are formulated in an inertial reference frame with structural damping of ring and foundation being considered. A receptance approach is utilized for obtaining the solutions. The effects which foundation stiffness, pressure loading, and structural damping have on the development of standing waves are investigated. A criterion for critical speed equivalent to the characteristic equation for zero eigenvalues is obtained and an explicit expression for critical speeds in extensible thin ring is derived. Responses of force and displacement actions which cause standing waves are analyzed and compared by using receptance methods. Dissert. Abstr.

N88-25004 Illinois Univ., Chicago.
THE STRESS ANALYSIS OF CERAMIC, POLYMERIC, AND METALLIC COMPOSITE SYSTEMS BY THE FINITE ELEMENT METHOD Ph.D. Thesis
Byung-Jin Min [1987] 300 p
Avail: Univ. Microfilms Order No. DA8726094

Residual stresses occur in various engineering fields. With the help of the finite element method based on the concept of the elasto-viscoplastic approach, the residual stresses in ceramic metal composite systems resulting from differences between the thermophysical and mechanical properties of the ceramic and metal components was analyzed. The inclusion of the variation of elastic properties of both metal and ceramics with temperature was examined. From the results of the studies the variation of material properties with temperature is found to produce higher tensile residual stresses in the ceramic as well as in the alloy. It was also observed that the inclusion of variation of the coefficient of thermal expansion (alpha) is more important for residual stress calculations than the effect of the variation of the modulus of elasticity (E) with temperature. The loss of the prosthesis and the successful replacement with restorative prosthetic crown is a problem which has intrigued dental researchers for decades. A finite element study was performed for cement bonded porcelain-fused-to-metal (PFM) restorative systems. It was found that the value of the stresses can be reduced significantly if the cement layer is considered. Instead of PFM restorations the all-ceramic prosthesis was recently introduced. The stresses in an all-ceramic restoration were also calculated. The results suggest that PFM systems are stronger than all-ceramic systems under given loading conditions and the model studied. Dissert. Abstr.

N88-25005 State Univ. of New York, Buffalo.
FORCED MOTION OF INITIALLY STRESSED SHELLS AND PLATES Ph.D. Thesis
Massood Omrani [1987] 181 p
Avail: Univ. Microfilms Order No. DA8727728

Equations of motion of thick cylindrical shells subjected to a general state of initial stresses are developed by application of Hamilton's Principle. Two types of thick cylindrical shells subjected to prestresses are considered: cylindrical shells with initial axial forces and cylindrical shells with initial bending moments. Analytical solutions are developed for a freely supported cylindrical shell under a local non-symmetric step force by application of separation of variable and double Fourier-series technique. The dynamic equations of shells are then reduced to equations for shallow shells under a general state of initial stress. These equations are solved for an axially stressed shallow shell under local step forces. The equations of motion of shallow shells are simplified to dynamic equations of plates under a general state of prestress. A plate under initial bending moment in the plane of the plate and subjected to local step forces is considered and solved in closed form. For each of the cases of shells and plates, magnitudes of the buckling stresses and natural frequencies with prestresses are computed. Forced motion solutions result in the study of deflections as a function of time with prestress as a parameter. Dissert. Abstr.

N88-25006 State Univ. of New York, Buffalo.
REDUCED ORDER MODELLING AND ANALYTICAL MODEL MODIFICATION FOR STRUCTURAL DYNAMICS AND CONTROL Ph.D. Thesis
Kwang Harold Yae [1987] 91 p
Avail: Univ. Microfilms Order No. DA8727759

Given the mass and stiffness matrices from the finite element method (FEM) and the modal data such as natural frequencies, damping ratios and mode shape vectors, an analytical model, which is expressed in terms of the mass and stiffness matrices derived through FEM and an estimated damping matrix, is converted into the state space representation and then reduced by the internal balancing method. The new states in the reduced model are a subset of the original states. Through the model modification the reduced model is constrained to satisfy the modal data. Thus the final analytical model is smaller than the original FEM model. The reduced model reflects not only the original FEM model but also the modal data. Each state in the reduced model preserves the original physical meaning very closely. Dissert. Abstr.

N88-25007 Rensselaer Polytechnic Inst., Troy, N.Y.
THEORY OF VISCOPLASTICITY BASED ON OVERSTRESS WITH APPLICATIONS Ph.D. Thesis
David Yao [1987] 242 p
Avail: Univ. Microfilms Order No. DA8729339

A phenomenological theory of viscoplasticity based on overstress with a differential growth law for the equilibrium stress is presented. It does not use yield and loading-unloading conditions, and considers creep and plasticity actions in a unified way. The

base model of the theory shows an isotropic cyclic neutral time-dependent material behavior. A modified theory which includes an extra growth law represents an isotropic time-dependent cyclic hardening, further hardening and partial fading memory in two amplitudes step-up and step-down tests, respectively, and additional hardening observed in 90 deg out-of-phase strain-controlled cyclic strainings. The theory is used to generate numerical simulations of several material behaviors including rate-dependent and nearly rate-independent ones. Compared with the available room temperature test data, the base model provides reasonable predictions for the uniaxial ratchetting tests of a Ti-alloy, and for monotonic and cyclic (both in-phase and out-of-phase) straining of an Al-alloy. For Type 304 Stainless Steel, the modified theory is used to simulate in-phase and 90 deg out-of-phase strain-controlled cyclic tests with emphasis on amplitude dependent hardening, further hardening, partial fading memory, and extra hardening observed in 90 deg out-of-phase loading. The theoretical calculations correlate closely with the experimental results.
Dissert. Abstr.

N88-25008# Technische Univ., Berlin (West Germany).
CALCULATION OF ROLLING CONTACT OF TWO VISCOELASTIC CYLINDERS WITH APPLICATION TO THE STEADY STATE NORMAL CONTACT PROBLEM [ZUR BERECHNUNG DES ROLLENDEN KONTAKTES ZWEIER VISKOELASTISCHER WALZEN MIT ANWENDUNG AUF DAS STATIONAERE NORMALKONTAKTPROBLEM]
Klaus Knothe and Guangqiu Wang Oct. 1987 77 p In GERMAN
(ILR-Mitt-188; ETN-88-91934) Avail: NTIS HC A05/MF A01

Mechanical models for linear viscoelastic materials are analyzed with Kelvin-Voigt, Maxwell, and Poynting theorems. Generalized Kelvin model is applied for the integral equation of stress-deformation. The basic equation of the linear viscoelastic theory is presented with an analogy between elastic and viscoelastic behavior. Constitutive equations and distortions in consequence of single and distributed normal loads are presented. Formulation and basic equation of the viscoelastic rolling contract problems, contact conditions, and kinetic equations for tangential problems are also reviewed. ESA

N88-25009# Fraunhofer Inst. fuer Werkstoffmechanik, Freiburg (West Germany).
ANALYSIS AND DEVELOPMENTS OF FAILURE CONCEPTS IN FRACTURE MECHANICS BASED ON RESEARCH RESULTS IN THE FIELD OF COMPONENT SAFETY TOPICS: J-INTEGRAL CONCEPT; CRACK RESISTANCE CURVES; DYNAMIC CRITERION Final Report [ANALYSE UND WEITERENTWICKLUNG BRUCHMECHANISCHER VERSAGENSKONZEPTE AUF DER GRUNDLAGE VON FORSCHUNGSERGEBNISSEN AUF DEM GEBIET DER KOMPONENTENSICHERHEIT SCHWERPUNKTE: J-INTEGRALKONZEPT RISSWIDERSTANDSKURVEN DYNAMISCHE KENNWERTE]
W. Schmitt Jun. 1986 99 p In GERMAN Sponsored by Bundesministerium fuer Forschung und Technologie, Fed. Republic of Germany
(V-19/86; ETN-88-91942) Avail: NTIS HC A05/MF A01

Results and data obtained in reactor safety research programs are applied for further development and application of failure concepts to study structural behavior of parts and components. Theoretical and numerical experimental tests are carried out for the determination of continuum resistance and failure concepts by using J-integrals and dynamical stress analysis. ESA

N88-25010*# Texas Univ., Austin. Center for Aeronautical Research.
MULTISHAKER MODAL TESTING Final Report Phase 2, Aug. 1985 - Aug. 1987
Roy R. Craig, Jr. Dec. 1987 45 p
(Contract NAS8-35338)
(NASA-CR-179355; NAS 1.26:179355; CAR-87-7) Avail: NTIS HC A03/MF A01 CSCL 20K

The major accomplishments of this research are: (1) the refinement and documentation of a multi-input, multi-output modal parameter estimation algorithm which is applicable to general linear, time-invariant dynamic systems; (2) the development and testing of an unsymmetric block-Lanzcos algorithm for reduced-order modeling of linear systems with arbitrary damping; and (3) the development of a control-structure-interaction (CSI) test facility.
J.P.B.

N88-25011*# National Aeronautics and Space Administration. Langley Research Center, Hampton, Va.
RADIO FREQUENCY (RF) STRAIN MONITOR Patent Application
Joseph S. Heyman, inventor (to NASA), Robert S. Rogowski, inventor (to NASA), and Milford S. Holben, Jr., inventor (to NASA) (PRC Kentron, Inc., Hampton, Va.) 7 Jun. 1988 14 p
(NASA-Case-LAR-13705-1; NAS 1.71:LAR-13705-1; US-Patent-Appl-SN-203177) Avail: NTIS HC A03/MF A01 CSCL 20K

This invention relates to an apparatus for measuring strain in a structure. In particular, the invention detects strain in parts per million to over ten percent along an entire length (or other dimension) of a structure measuring a few millimeters to several kilometers. By using a propagation path bonded to the structure, the invention is not limited by the signal attenuation characteristics of the structure and thus frequencies in the megahertz to gigahertz range may be used to detect strain in part per million to over ten percent with high precision. NASA

N88-25012# Sandia National Labs., Albuquerque. N. Mex.
ON THE BENDING RESPONSE OF KEVLAR 49/EPOXY BEAMS AND RINGS
E. D. Reedy, Jr. May 1988 15 p Presented at the ABAQUS User's Meeting, Newport, R.I., 31 May 1988
(Contract DE-AC04-76DP-00789)
(DE88-006824; SAND-88-0612C; CONF-880572-1) Avail: NTIS HC A03/MF A01

Kevlar 49/epoxy laminates often exhibit substantial material nonlinearity when subjected to bending. This is a consequence of the yield-like behavior of a Kevlar 49/epoxy lamina in fiber-directed compression. In this paper, analyses that utilize a simple idealization of compressive yielding are described and calculated results for Kevlar 49 reinforced beams and rings are compared with available data. First, results of a finite element analysis of a thin, unidirectionally reinforced ring subjected to diametral compression are presented. This analysis uses beam elements that incorporate linear tensile and elastic perfectly-plastic compressive behavior. Then a method used to analyze quasi-isotropic beams tested in four-point bending is discussed. This finite element analysis uses a layered shell element with a lamina constitutive model that permits elastic-perfectly plastic response to fiber-directed compression, but otherwise assumes linear elastic behavior. Comparison of calculated and experimental results corroborate the ability of analyses using a simple compressive yield model to account for much of the observed flexural nonlinearity in Kevlar 49/epoxy beams and rings. DOE

N88-25013*# National Aeronautics and Space Administration. Marshall Space Flight Center, Huntsville, Ala.
SRM PROPELLANT AND POLYMER MATERIALS STRUCTURAL TEST PROGRAM
Carleton J. Moore May 1988 16 p
(NASA-TP-2821; NAS 1.60:2821) Avail: NTIS HC A03/MF A01 CSCL 20K

The SRM propellant and polymer materials structural test program has potentially wide application to the testing and structural analysis of polymer materials and other materials generally characterized as being made of viscoelastic materials. The test program will provide a basis for characterization of the dynamic failure criteria for Solid Rocket Motor (SRM) propellant, insulation, inhibitor and liners. This experimental investigation will also endeavor to obtain a consistent complete set of materials test

data. This test will be used to improve and revise the presently used theoretical math models for SRM propellant, insulators, inhibitor, liners, and O-ring seals. Author

N88-25014*# Lehigh Univ., Bethlehem, Pa.
THE SURFACE CRACK PROBLEM IN AN ORTHOTROPIC PLATE UNDER BENDING AND TENSION
Bing-Hua Wu and F. Erdogan Apr. 1987 78 p
(Grant NGR-39-007-011)
(NASA-CR-178281; NAS 1.26:178281) Avail: NTIS HC A05/MF A01 CSCL 20K

The elasticity problem for an infinite orthotropic flat plate containing a series of through and part through cracks and subjected to bending and tension loads is considered. The problem is formulated by using Reissner's plate bending theory and considering three-dimensional material orthotropy. The Line-spring model developed by Rice and Levy is used to formulate the surface crack problem in which a total of nine material constants were used. The effects of material orthotropy on the stress intensity factors was determined, the interaction between two asymmetrically arranged collinear cracks was investigated, and extensive numerical results regarding the stress intensity factors are provided. The problem is reduced to a system of singular integral equations which is solved by using the Gauss-Chebyshev quadrature formulas. The calculated results show that the material orthotropy does have a significant effect on the stress intensity factor. Author

N88-25015# British Library Lending Div., Boston Spa (England).
CALCULATION OF ROOT-MEAN-SQUARE LOADS
V. F. Egorov, V. P. Prilukov, Sh. V. Khamitsev, and V. S. Chalkov [1987] 7 p Transl. into ENGLISH from Vysshikh Uchebnykh Zavedeniy Chernaya Metallurgiya (USSR), no. 10, 1987 p 108-111
(BLL-M-37776-(5828.4)) Avail: British Library Lending Div., Boston Spa, United Kingdom

The development of computer assisted engineering calculation of root-mean-square loads is described. Investigations were carried out for the characteristic forms of load charts with the attainable computational accuracy of equivalent loads on nonlinear sections, the coefficients of the approximating polynomials being selected with the aid of the method of least squares. Author

N88-25016*# Illinois Univ., Urbana. Dept. of Mechanical Engineering.
CYCLIC FATIGUE DAMAGE CHARACTERISTICS OBSERVED FOR SIMPLE LOADINGS EXTENDED TO MULTIAXIAL LIFE PREDICTION
David J. Jones and Peter Kurath Jun. 1988 100 p
(Grant NAG3-465)
(NASA-CR-182126; NAS 1.26:182126) Avail: NTIS HC A05/MF A01 CSCL 20K

Fully reversed uniaxial strain controlled fatigue tests were performed on smooth cylindrical specimens made of 304 stainless steel. Fatigue life data and cracking observations for uniaxial tests were compared with life data and cracking behavior observed in fully reversed torsional tests. It was determined that the product of maximum principle strain amplitude and maximum principle stress provided the best correlation of fatigue lives for these two loading conditions. Implementation of this parameter is in agreement with observed physical damage and it accounts for the variation of stress-strain response, which is unique to specific loading conditions. Biaxial fatigue tests were conducted on tubular specimens employing both in-phase and out-of-phase tension torsion cyclic strain paths. Cracking observations indicated that the physical damage which occurred in the biaxial tests was similar to the damage observed in uniaxial and torsional tests. The Smith, Watson, and Topper parameter was then extended to predict the fatigue lives resulting from the more complex loading conditions. Author

N88-25017 Stanford Univ., Calif.
FATIGUE CRACK GROWTH DUE TO RANDOM LOADING
Ph.D. Thesis
Paul Steven Veers 1987 163 p
Avail: Univ. Microfilms Order No. DA8801054

A new crack growth model provides a means of approximating load sequence effects by continuously updating the crack opening stress, accounting for both acceleration and retardation effects in a simplified manner. This model is shown to predict published test results and is used to investigate sequence effects due to random loading. Random load models are outlined ranging from simple random variable descriptions, for sequenceless applications, to random process simulations, for analyses that include load sequences. Practical methods for calculating crack growth life are presented by applying the load models to the crack growth model, and to an alternative model that neglects sequence effects. Inherent difficulties in the traditional, sample block load model are identified. Analytical estimates of crack growth life that include sequence effects are examined using scalar diffusion models. Dissert. Abstr.

42 GEOSCIENCES (GENERAL)

No abstracts in this category.

43 EARTH RESOURCES AND REMOTE SENSING

Includes remote sensing of earth resources by aircraft and spacecraft; photogrammetry; and aerial photography.

For instrumentation see *35 Instrumentation and Photography.*

N88-25018# Army Cold Regions Research and Engineering Lab., Hanover, N.H.
ICE CONDITIONS ALONG THE OHIO RIVER AS OBSERVED ON LANDSAT IMAGES, 1972-1985
Lawrence W. Gatto Jan. 1988 168 p
(AD-A191172; CRREL-SR-88-1) Avail: NTIS HC A08/MF A01 CSCL 08L

Lansat images were used to map ice distributions along the Ohio River. Ice conditions were inferred based on image grey tones interpreted using conventional photointerpretation techniques. Portions of the river that appeared black were considered ice-free. Grey tones were interpreted as ice that varied from patches of thin, snow-free solid or fragmented ice, sometimes with open areas, to floes, pans and slush. A white tone represented thick ice or snow-covered ice with few interspersed open areas. Ice that produced grey tones on the images occurred most frequently. Ice typically forms in late December or early January on the Ohio River and is gone by mid to late February. Ice was observed on the upstream section of the river from Pittsburgh to Greenup Dam during 7 of the 13 winters from 1972 to 1985, on the middle section from Greenup Dam to Cannelton Dam during 3 winters, and on the downstream section from Cannelton Dam to the Mississippi River during 4 winters. The most severe and long-lasting ice conditions occurred during the 1976-77 winter when ice covered 65 percent of the upstream section, 56 percent of the middle section, and 78 percent of the downstream section. GRA

N88-25019# Brigham Young Univ., Provo, Utah. Dept. of Civil Engineering.
EVALUATING EVAPORATION WITH SATELLITE THERMAL DATA Final Report, 1 Apr. - 1 Oct. 1987
A. W. Miller and Eric L. Mills Nov. 1987 116 p
(Grant AF AFOSR-0177-87)

(AD-A192042; AFOSR-88-0131TR) Avail: NTIS HC A06/MF A01 CSCL 08H

Water surface temperatures can be obtained from satellite thermal remote sensing. Landsat and other satellites sense emitted thermal infrared radiation on a regular basis over much of the earth's surface. Evaporation is accomplished by the net transport of mass from the water surface to the atmosphere. Energy for the change of state in part comes from the subsurface and passes through the surface conduction layer. The latent transfer (evaporation) predominantly determines the water surface temperature. There should be good correlations between evaporation and surface temperatures. Satellite thermal data and evaporation data from four different years were obtained for the Great Salt Lake and surrounding region. More than 350 correlation and linear regression analyses were performed on the temperature and evaporation data. These included daily, multiple-day, and monthly values from measurements and modeling for the whole lake and areas within the lake using both day and night observations. The lake salt concentrations were also factored into the analyses in several different ways. The correlation results were generally very good and a methodology for using satellite-derived water surface temperatures along with salt concentrations were developed to estimate evaporation. Continuing efforts now include acquiring thermal data at less cost, more frequently and more quickly in order to apply the temperature evaporation models in near real time to lakes and the ocean. GRA

N88-25020# Technische Hogeschool, Eindhoven (Netherlands).
THE APPLICATION OF SATELLITES IN CONNECTION WITH THE ENVIRONMENT
Hermann Bondi 1986 13 p Presented at the Holst Memorial Lecture, Eindhoven, Netherlands, 3 Dec. 1986
(ETN-88-92474) Avail: NTIS HC A03/MF A01

Satellite observation for geology, crop monitoring, environmental monitoring, resources management, pest control, and oceanography is discussed. ESA

N88-25021 Rensselaer Polytechnic Inst., Troy, N.Y.
AUTOMATED CARTOGRAPHIC GENERALIZATION FOR LINEAR MAP FEATURES Ph.D. Thesis
Bradford George Nickerson 1987 134 p
Avail: Univ. Microfilms Order No. DA8729315

Cartographic generalization is the task of making smaller-scale maps from larger-scale maps. An automated method is presented for generalization of linear features that are already in a topologically structured computer-readable form. The method consists of three stages: feature elimination, feature simplification, and interference detection and resolution. The first stage is implemented using English-like rules. These rules specify which map features are to be eliminated at the generalized map scale. The second stage consists of the simplification of linear map features. A procedure for polyline simplification is presented, along with algorithms for subdivision of linear features and riverbank combination. The third stage deals with interference and detection among linear map features. Interference may occur when a simplified feature is added to the generalized map. The algorithms used to detect feature interference and to perform the subsequent feature displacement propagation are described. A FORTRAN 77 computer program called MAPEX was written to perform automated generalization of linear map features. This program assumes a topologically structured input data file similar to the U.S. Geological Survey 1:24,000 scale Digital Line Graph map data files. To integrate the English-like rules with MAPEX, a rule compiler was written to translate the English-like rules to a FORTRAN 77 subroutine. The results of running MAPEX on a topologically structured test data file are given, along with the algorithmic details used in the implementation of MAPEX. Dissert. Abstr.

N88-25022 New South Wales Univ., Sydney (Australia). Faculty of Science.
INFORMATION ANALYSIS OF INTEGRAL EQUATIONS IN REMOTE SENSING OF ATMOSPHERIC AEROSOLS Ph.D. Thesis Abstract Only
G. Viera Feb. 1987 194 p
Avail: Issuing Activity

Some integral equations of the first kind that arise in the inverse problem of determining the size distribution of aerosol particles from forward scattering and multispectral extinction experiments are examined. In particular, the information content of these equations relative to typical size distributions is analyzed using the eigenfunction and singular function theories. The aerosols were assumed to be homogeneous dielectric spheres, thus allowing the use of Mie theory, and the final integral equations representing extinction and scattering from a polydispersion were obtained assuming independent and single scattering. The anomalous diffraction and Rayleigh-Gans approximations to the Mie theory resulted in integral equations that could be solved using an analytical eigenfunction theory. When using Mie theory kernels and finite patameter ranges it is necessary to use singular function theory to investigate the information content. Simulated numerical inversion showed that for extinction, the accumulation mode can be retrieved with the first three terms of the singular function expansion. The singular analysis for the scattering integral equation resulted in a slower eigenvalue decay when compared with extinction. The numerical inversions showed that scattering is more capable of reproducing the coarse mode and the multimodal nature of the distribution, in particular if the lower limit of angular measurement can be made approximately one degree. However, the extinction inversions were in general smoother. Author

N88-25023# Geoexplorers International, Inc., Denver, Colo.
GEOLOGICAL EVOLUTION AND ANALYSIS OF CONFIRMED OR SUSPECTED GAS HYDRATE LOCALITIES. VOLUME 2: BASIN ANALYSIS, FORMATION AND STABILITY OF GAS HYDRATES IN THE BLACK SEA
M. S. Ciesnik and J. Krason May 1987 107 p
(Contract DE-AC21-84MC-21181)
(DE88-001052; DOE/MC-21181/1950-Vol-11) Avail: NTIS HC A06/MF A01

This document is Volume 11 of a series of reports entitled Geological Evolution and Analysis Confirmed or Suspected Gas Hydrate Localities. Volume 11 provides an analysis of the Black Sea region. The report presents a geological description of the Black Sea region, including regional and local structural settings, geomorphology, geological history, stratigraphy, and physical properties. Included also is a discussion of bottom simulating acoustic reflectors, sediment acoustic properties, distribution of hydrates within the sediments, and the relation of hydrate distribution to other features such as salt dispirism. The formation and stabilization of gas hydrates in sediments are discussed in terms of phase relations, nucleation, and crystallization constraints, gas solubility, pore fluid chemistry, inorganic diagenesis, and sediment organic content. A depositional analysis of the areas is discussed in order to better understand the thermal evolution of the locality and to assess the potential for thermogenic hydrocarbon generation. DOE

N88-25024*# Colorado Univ., Boulder. Cooperative Inst. for Research in Environmental Sciences.
DMSP-SSM/1 NASA ALGORITHM VALIDATION USING PRIMARILY LANDSAT AND SECONDARILY DMSP AND/OR AVHRR VISIBLE AND THERMAL INFRARED SATELLITE IMAGERY Annual Progress Report
K. Steffen, R. Barry, and A. Schweiger Jun. 1988 108 p
(Grant NAG5-882)
(NASA-CR-182979; NAS 1.26:182979) Avail: NTIS HC A06/MF A01 CSCL 05B

The approach to the DMSP SSMI (Defense Meteorological Satellite Program; Special Sensor Microwave Imager) sea-ice validation effort is to demonstrate a quantitative relationship between the SSMI-derived sea ice parameters and those same parameters derived from other data sets including visible and infrared satellite imagery, aerial photographic and high-resolution microwave aircraft imagery. The question to be addressed is to what accuracy (relative to these other observations) can the

following ice parameters be determined: (1) position of the ice boundary; (2) total sea ice concentration; and (3) multiyear sea ice concentration. Specific tasks include: (1) a study of the interrelationship of surface information content and sensor spatial and spectral resolution in order to establish relationships between ice surface features and the manner in which they are expressed in the satellite observations; and (2) apply these relationships to map the sea ice features which can be used to evaluate NASA's proposed SSM/1 sea ice algorithms. Other key points to be addressed include the accuracy to which these parameters can be determined in different regions (marginal ice zone such as Bering Sea, Arctic ocean, such as Beaufort Sea); the accuracy of these parameters for different seasons; the accuracy of the algorithms weather filter under different weather conditions; and the effectiveness of the 85.5 GHz channels to locate the ice edge. Author

N88-25025# Institut fuer Angewandte Geodaesie, Frankfurt am Main (West Germany).
REPORTS ON CARTOGRAPHY AND GEODESY. SERIES 1, NO. 99 [NACHRICHTEN AUS DEM KARTEN- UND VERMESSUNGSWESSEN. REIHE 1, HEFT NR. 99]
1987 164 p In GERMAN; ENGLISH summary Original contains color illustrations
(ETN-88-92387; ISSN-0469-4236) Avail: NTIS HC A08/MF A01

Developments in computer aided topography and cartography mainly in the field of land management, cadastral mapping, urban traffic and relief mapping are reviewed. Techniques described are based on digitalization and vectorization of graphics, automatic pattern recognition, and data storage in data banks. Data structures and raster algorithms are outlined. For individual titles, see N88-25026 through N88-25040.

N88-25026# Institut fuer Angewandte Geodaesie, Frankfurt am Main (West Germany).
WEST GERMAN GEODETIC WORKING GROUP: OFFICIAL TOPOGRAPHIC-CARTOGRAPHIC INFORMATION SYSTEM (ATKIS), CONTENT DESCRIPTION [DAS ADV-VORHABEN: AMTLICHES TOPOGRAPHISCH-KARTOGRAPHICSCHES INFORMATIONSSYSTEM (ATKIS) - INHALTLICHE KONZEPTION]
Rolf Harbeck *In its* Reports on Cartography and Geodesy. Series 1, No. 99 1987 p 7-14 In GERMAN; ENGLISH summary (For primary document see N88-25025 18-43)
Avail: NTIS HC A08/MF A01

The statutory charge of the Surveying and Mapping Agencies in the Federal Republic of Germany consists of carrying out topographic surveys and of representing results in official topographic map series. Corresponding to the demands of users, it also includes the task of making available basic information of the surface of the Earth in a digital mode. Therefore the Surveying and Mapping Agencies decided to build an Information System. The primary model is that of the topographic landforms, the secondary describes the cartographic landforms models and tertiary model concerns the users' environment. Object and signature catalogs convert the digital landform models to digital cartographic models. ESA

N88-25027# Institut fuer Angewandte Geodaesie, Frankfurt am Main (West Germany).
WEST GERMAN GEODETIC WORKING GROUP: OFFICIAL TOPOGRAPHIC-CARTOGRAPHIC INFORMATION SYSTEM (ATKIS), TECHNICAL CONCEPTION [DAS ADV-VORHABEN: AMTLICHES TOPOGRAPHISCH-KARTOGRAPHISCHES INFORMATIONSSYSTEM (ATKIS) - TECHNISCHE KONZEPTION]
Gerfried Appelt *In its* Reports on Cartography and Geodesy. Series 1, No. 99 1987 p 15-22 In GERMAN; ENGLISH summary (For primary document see N88-25025 18-43)
Avail: NTIS HC A08/MF A01

The creation of an Official Topographic-Cartographic Information System (ATKIS) necessitates defining the underlying structures and the procedure. The logic design of the data structure and its implementation, the methods of data collection, data processing and output, as well as the steps toward a realization of ATKIS are described. Logical data structure comprises two data banks for vector and raster data storage, signature catalog with interactive data processing for editing and output recording. Object catalog includes the landforms elements like surfaces, lines, texts, objects names and coordinates. ESA

N88-25028# Institut fuer Angewandte Geodaesie, Frankfurt am Main (West Germany).
VECTOR GRAPHICS AND RASTER DATA PROCESSING FOR SPATIAL INFORMATION SYSTEMS [VEKTORGRAPHIK UND RASTERDATENVERARBEITUNG FUER RAUMBEZOGENE INFORMATIONSSYSTEME]
Klaus Benndorf *In its* Reports on Cartography and Geodesy. Series 1, No. 99 1987 p 23-35 In GERMAN; ENGLISH summary Original contains color illustrations (For primary document see N88-25025 18-43)
Avail: NTIS HC A08/MF A01

The image processing component of SICAD realizes the combination of vector graphics as well as raster graphics, transforms vector graphics into raster graphics and processes them on the display unit with array processor and optical disk. Deriving vector graphics out of raster images, in particular with regard to a fast and economic data collection by means of scanner technique is performed. Finally raster and vector structures, each structure being processed with its own technique, are superposed. ESA

N88-25029# Institut fuer Angewandte Geodaesie, Frankfurt am Main (West Germany).
DIGITIZING THE TRAFFIC NETWORK OF JOG 250 BY SCANNING [DIGITALISIERUNG DES VERKEHRSNETZES DER JOG 250 MIT EINEM SCANNER]
Juergen Brennecke *In its* Reports on Cartography and Geodesy. Series 1, No. 99 1987 p 37-56 In GERMAN; ENGLISH summary (For primary document see N88-25025 18-43)
Avail: NTIS HC A08/MF A01

A method of automatically digitizing the traffic network by scanning the map content was developed and tested on the example of the military map JOG 250. The basis of digitization are the road fills which exist in principle on separated plates according to the road type. The remaining feature separation is done partly by hand before the scanning (by covering the highway fills) and in part automatically after the scanning (by positioning the built-up areas). To the skeleton parts are assigned different color codes, depending on road type and priority, so that they can be stored later on together with the corresponding attributes. After the vectorization of the automatically retouched skelton parts, most parts of the typical and unavoidable faults of the skeleton formation are eliminated automatically. Highways are digitized interactively on the raster display by means of the scanned planimetric plate. ESA

N88-25030# Institut fuer Angewandte Geodaesie, Frankfurt am Main (West Germany).
TESTS FOR THE AUTOMATIC PATTERN RECOGNITION OF BUILDING SURFACES BY THE TK 50 [VERSUCHE ZUR AUTOMATISCHEN MUSTERERKENNUNG VON GEBAEUDEFLAECHEN DER TK 50]
Juergen Brennecke *In its* Reports on Cartography and Geodesy. Series 1, No. 99 1987 p 57-77 In GERMAN; ENGLISH summary (For primary document see N88-25025 18-43)
Avail: NTIS HC A08/MF A01

An essentially automatic procedure to separate features of built-up areas from the other planimetric features of the TK 50 map is presented. The features are classified by means of the object features width and area in a feature space, here two-dimensional. The procedure is based on simple raster operations: thinning, thickening, extending, and counting of pixels. The rate of wrong classifications amounts to only 3 percent. The total processing time required for 1/4 map sheet is 12 hr. The automatic vectorization of building outlines is described. ESA

N88-25031# Institut fuer Angewandte Geodaesie, Frankfurt am Main (West Germany).
CREATION OF DIGITAL TOPOGRAPHIC MODELS WITH THE ALK-GIAP. THE DLM 25 AS AN EXAMPLE [DER AUFBAU DIGITALER LANDSCHAFTSMODELLE MIT DEM ALK-GIAP - AM BEISPIEL DES DLM 25]
Heinz Brueggemann *In its* Reports on Cartography and Geodesy. Series 1, No. 99 1987 p 79-84 In GERMAN; ENGLISH summary (For primary document see N88-25025 18-43)
Avail: NTIS HC A08/MF A01

On the proposal of the Working Groups Technical Conception and Information Output, the AdV (Working Committee of the Survey Administrations of the States of the FRG) suggested to its member administrations the creation of an Official Topographic-Cartographic Information System (ATKIS). Contents and structure of ATKIS and ways of implementation are pointed out. The ALK planimetry data file is to serve for storage. The ALK-GIAP proved suitable for data collection, for structuring the data after the ATKIS model, and for graphic output, including the use of raster plotters. The content of DLM 25 (digital landforms models) is described in the objects catalog giving the names and attributes of objects like points, lines and surfaces and their relations. The ALK-GIAP is designed to provide an interactive aid for the automatic generation of surfaces and linear objects for the digital cartographic model with data issued from DLM 25. ESA

N88-25032# Institut fuer Angewandte Geodaesie, Frankfurt am Main (West Germany).
TOPOGRAPHIC DATA PROCESSING FOR ENVIRONMENTAL PLANNING [GELAENDEDATENVERARBEITUNG ZUR UMWELTPLANUNG]
Wolfhart Gillessen *In its* Reports on Cartography and Geodesy. Series 1, No. 99 1987 p 85-102 In GERMAN; ENGLISH summary (For primary document see N88-25025 18-43)
Avail: NTIS HC A08/MF A01

Methodology and possibilities of raster data processing, particularly with respect to equidistantly screened terrain/environmental data, are presented. Data sets and software modules are described using examples from environmental planning. Display of the original data and of the planning process on color monitors as well as representation of these data as a thematic map is illustrated. The inclusion of the possibilities of vectorization is discussed. ESA

N88-25033# Institut fuer Angewandte Geodaesie, Frankfurt am Main (West Germany).
DIGITAL MAPS FOR AN ELECTRONIC TRAFFIC GUIDE [DIGITALE KARTEN FUER EINEN VERKEHRSLOTSEN]
Wolfgang Hentschel *In its* Reports on Cartography and Geodesy. Series 1, No. 99 1987 p 103-108 In GERMAN; ENGLISH summary (For primary document see N88-25025 18-43)
Avail: NTIS HC A08/MF A01

An electronic guide for motorists comprising a digital map of the roads and streets including the attributes for the traffic is presented. The study reports kind and extent of data acquisition concerning the geometry of the streets network and their attributes. Data sources are German landmaps at 1:5000 where knots are digitized and visually displayed. A pilot project for Hannover-Hildesheim is carried out based on a topographic landmap at 1:25000. ESA

N88-25034# Institut fuer Angewandte Geodaesie, Frankfurt am Main (West Germany).
DEVELOPMENT IN DATA STRUCTURES IN PHOCUS FOR DIGITAL MAPPING [DIE DATENSTRUKTUREN IN PHOCUS ZUR DIGITALEN KARTENHERSTELLUNG UND-FORTFUEHRUNG]
Kurt Menke *In its* Reports on Cartography and Geodesy. Series 1, No. 99 1987 p 109-116 In GERMAN; ENGLISH summary (For primary document see N88-25025 18-43)
Avail: NTIS HC A08/MF A01

The PHOCUS is a universal photogrammetric-cartographic system. Two central features of PHOCUS are its object-oriented data structure allowing complex access techniques as well as exchangeable graphics codes for use in cadastral mapping and environment protection. ESA

N88-25035# Institut fuer Angewandte Geodaesie, Frankfurt am Main (West Germany).
STATE OF DEVELOPMENT OF ALK (OCTOBER 1986) [STAND DER ALK-ENTWICKLUNG (OKTOBER 1986)]
Gerhard Mittelstrass *In its* Reports on Cartography and Geodesy. Series 1, No, 99 1987 p 117-120 In GERMAN; ENGLISH summary (For primary document see N88-25025 18-43)
Avail: NTIS HC A08/MF A01

State of development related to ALK, e.g., maintenance agreement, administrative regulations for data collection and suitability of ALK for the organization of an Official Topographic and Cartographic Information System (ATKIS) are described. The ALK is a digital mapping system where logical data structures are provided for objects and geometric maps elements. These structures can be used for cadastral mapping and building design. The two main parts are a data bank and an interactive graphic workstation. Developments in user friendly applications program optimizations, implementation on various computers and elimination of errors are pursued. ESA

N88-25036# Institut fuer Angewandte Geodaesie, Frankfurt am Main (West Germany).
VECTORIZATION OF RASTER ALGORITHMS FOR ELEVATION DATA PROCESSING [VEKTORISIERTE RASTERALGORITHMEN ZUR VERABEITUNG VON HOEHENSCHICHTEN]
Detlef Niese and Wigand Weber *In its* Reports on Cartography and Geodesy. Series 1, No. 99 1987 p 121-142 In GERMAN; ENGLISH summary (For primary document see N88-25025 18-43)
Avail: NTIS HC A08/MF A01

The derivation of elevation lines in raster mode from contours as well as with different automatic evaluations, as e.g., pseudoplastic terrain representation, hill shading according to Tanaka, maps indicating slope, continuous hill shading and transformation of a digital elevation model with hypsometric layers into one with rectangular meshes are described. These evaluations constitute algorithms which are characterized by vectorization (also by hierarchization) and the predominance of logical instead of arithmetic principles. Such algorithms are particularly suited for modern vector processes. ESA

N88-25037# Institut fuer Angewandte Geodaesie, Frankfurt am Main (West Germany).
GEOMETRIC RECTANGULAR DATA FILE (GERD): AN AID TO THE RAPID ACCESS TO POSITION DATA [DIE GEOMETRISCHE RECHTECK-DATEI GERD - EIN HILFSMITTEL ZUM SCHNELLEN ZUGRIFF AUF LAGEBEZOGENE DATEN]
Hans-Gerd Reimer *In its* Reports on Cartography and Geodesy. Series 1, No. 99 1987 p 143-153 In GERMAN; ENGLISH summary (For primary document see N88-25025 18-43)
Avail: NTIS HC A08/MF A01

Universal cartographic automation system with complex geometric data bases on a large computer is described. Geometric access to the data stock of any area can be realized by means of a geometric directory which points to the specific features through the feature designations. The division of the directory consists in subdividing the entire area into regularly limited sections to access only the section to be searched. As to the formation of storage units, the different density of contents has to be considered as individually as possible, for which purpose the principle of successive cell quartering (Quadtree-Method) is applied. The program package GeRD (geometrische Rechteck-Datei) (Geometric rectangular file) was established in FORTRAN 77, in which the individual search fields are represented in the form of sets of a direct access on position as well as on identifier for the feature type. The GeRD can be integrated into existing programs of surveying. ESA

N88-25038# Institut fuer Angewandte Geodaesie, Frankfurt am Main (West Germany).
RECENT DEVELOPMENTS IN SOFTWARE AND HARDWARE BY SCITEX CO. [NEUENTWICKLUNGEN IM HARD- UND SOFTWAREBEREICH BEI FIRMA SCITEX]
Ferdinand Salomon *In its* Reports on Cartography and Geodesy. Series 1, No. 99 1987 p 157-165 In GERMAN; ENGLISH summary (For primary document see N88-25025 18-43)
Avail: NTIS HC A08/MF A01

The raster data processing applications offered by the Response 280 system of Scitex Company are being expanded in the field of user software by more sophisticated raster and vector processing modes, as interactive text positioning, DIANA (Digital Analysis) and DTM (Digital Terrain Modelling). Improved possibilities of communication achieved via direct connection of IBM/PC and or Microvax 2 of DEC are substantial hardware extensions. ESA

N88-25039# Institut fuer Angewandte Geodaesie, Frankfurt am Main (West Germany).
PERSONAL COMPUTER AS A WORKSTATION IN A CARTOGRAPHIC AUTOMATION SYSTEM? [DER PC - ARBEITSSTATION IN EINEM KARTOGRAPHISCHEN AUTOMATIONSSYSTEM?]
Gerhard Schweinfurth *In its* Reports on Cartography and Geodesy. Series 1, No. 99 1987 p 167-176 In GERMAN; ENGLISH summary (For primary document see N88-25025 18-43)
Avail: NTIS HC A08/MF A01

Personal computers as graphic workstations within a cartographic automation-system using typical paint-programs are outlined. The possibilities of layout-systems to manipulate digital maps are demonstrated. A way to configurate a cartographic automation-system and how to realize this concept are outlined. ESA

N88-25040# Institut fuer Angewandte Geodaesie, Frankfurt am Main (West Germany).
USE OF MODERN SCANNER TECHNIQUES IN CARTOGRAPHY [EINSATZ MODERNER SCANNER-TECHNIKEN IN DER KARTOGRAPHIE]
Wolfgang Voss *In its* Reports on Cartography and Geodesy. Series 1, No. 99 1987 p 177-180 In GERMAN; ENGLISH summary (For primary document see N88-25025 18-43)
Avail: NTIS HC A08/MF A01

The scanner/plotter-system INTERGRAPH CAD is designed to digitize maps, plans and graphs with all the software and hardware necessary to store the information in a data bank on a VAX computer. Integral parts are: scanner/plotter, graphics processor, scanned data capture software, and optronics plotter software. ESA

44 ENERGY PRODUCTION AND CONVERSION

Includes specific energy conversion systems, e.g., fuel cells; global sources of energy; geophysical conversion; and windpower.

For related information see also *07 Aircraft Propulsion and Power, 20 Spacecraft Propulsion and Power,* and *28 Propellants and Fuels.*

N88-25041# Pacific Northwest Labs., Richland, Wash.
PROCEEDINGS OF THE 1987 BIOMASS THERMOCHEMICAL CONVERSION CONTRACTORS' REVIEW MEETING
Nov. 1987 190 p Meeting held in Atlanta, Ga., 20-21 May 1987
(Contract DE-AC06-76RL-01830)
(DE88-006730; PNL-SA-15482; CONF-8705212) Avail: NTIS HC A09/MF A01

Thermochemical conversion technology issues were discussed. Biomass liquefaction, pyrolysis of biomass, mass spectroscopic studies of wood vapor, gasoline production from biomass and the use of manure as a feedstock for gas turbines are among the topics covered. For individual titles, see N88-25042 through N88-25051.

N88-25042# Arizona Univ., Tucson. Dept. of Chemical Engineering.
AN ADVANCED EXTRUDER-FEEDER BIOMASS LIQUEFACTION REACTOR SYSTEM
Don H. White, D. Wolf, G. Davenport, S. Mathews, M. Porter, and Y. Zhao *In* Pacific Northwest Labs., Proceedings of the 1987 Biomass Thermochemical Conversion Contractors' Review Meeting Nov. 1987 p 5-21 (For primary document see N88-25041 18-44)
(Contracts DE-AC06-76RL-01830; EW-78-S-05-5679)
Avail: NTIS HC A09/MF A01

A unique method of pumping concentrated, viscous biomass slurries that are characteristic of biomass direct liquefaction systems was developed. A modified single-screw extruder was shown to be capable of pumping solid slurries as high as 60 weight percent wood flour in wood oil derived vacuum bottoms, as compared to only 10 to 20 weight percent wood flour in wood oil in conventional systems. During the period August, 1985 to April, 1987, a total of 18 experimental continuous biomass liquefaction runs were made using white birch feedstock. Good operability with feed rates up to 30 lb/hr covering a range of carbon monoxide, sodium carbonate catalyst, pressures from 800 to 3000 psi and temperatures from 350 C to 430 C was achieved. Crude wood oils containing 6 to 10 weight percent residual oxygen were obtained. Other wood oil characteristics are reported. Author

N88-25043# Georgia Tech Research Inst., Atlanta.
LOW PRESSURE ENTRAINED FLOW PYROLYSIS OF BIOMASS TO PRODUCE LIQUID FUELS
R. J. Kovac, C. W. Gorton, D. J. ONeil, and C. J. Newman *In* Pacific Northwest Labs., Proceedings of the 1987 Biomass Thermochemical Conversion Contractors' Review Meeting Nov. 1987 p 23-39 Sponsored by DOE (For primary document see N88-25041 18-44)
Avail: NTIS HC A09/MF A01

The continuous research effort on the entrained flow pyrolysis of hardwoods is discussed. A brief description is given of the entrained flow pyrolysis system and its operation, experimental progress since October, 1985 and an indication of the status of the modeling effort. A total of 30 experimental runs have been made to date. The first ten of these were made using the eight inch reactor and the remaining using the six inch reactor. The eight inch reactor provided valuable operating experience and experimental data needed to modify the Process Research Unit (PRU) system to increase pyrolytic oil production. The tests on the six inch reactor have shown that dry oil yields over 50 percent can be obtained with the six inch reactor. The computer modeling effort indicates that oil yields up to 63 percent are possible using the present PRU system. Author

N88-25044# Midwest Research Inst., Golden, Colo. Solar Energy Research Inst.
MOLECULAR-BEAM, MASS-SPECTROMETRIC STUDIES OF WOOD VAPOR AND MODEL COMPOUNDS OVER HZSM-5 CATALYST
Robert J. Evans and Thomas A. Milne *In* Pacific Northwest Labs., Proceedings of the 1987 Biomass Thermochemical Conversion Contractors' Review Meeting Nov. 1987 p 41-60 Sponsored by DOE (For primary document see N88-25041 18-44)
Avail: NTIS HC A09/MF A01

The use of molecular beam mass spectrometry (MBMS) for the real time screening of wood pyrolysis product conversion over Mobil's HZSM-5 catalyst allows the evaluation of the performance of different catalysts, reaction conditions and feedstocks. This information can help guide more extensive testing at the bench scale level and provide insight into the chemistry of conversion. The following conclusions can be drawn from the work to date:

(1) there can be no breakthrough of primary wood vapor organics until the weight of wood/weight of the catalyst is 1; (2) there are few intermediates from wood on the way to alkenes, light aromatics, and naphthalenes; (3) the light aromatics/alkenes ration is 1 for the nonoptimized conditions studied to date; (4) much of the oxygen is favorably rejected as CO and CO sub 2; (5) the coke yield is about 10 percent in these experiments; and (6) methanol is a poor model for wood because the mechanism of hydrocarbon formation is apparently different. Author

N88-25045# Midwest Research Inst., Golden, Colo. Solar Energy Research Inst.
UPGRADING PYROLYSIS VAPORS TO AROMATIC GASOLINE WITH ZEOLITE CATALYSIS AT ATMOSPHERIC PRESSURE
James Diebold and John Scahill *In* Pacific Northwest Labs., Proceedings of the 1987 Biomass Thermochemical Conversion Contractors' Review Meeting Nov. 1987 p 61-80 Sponsored by DOE (For primary document see N88-25041 18-44)
Avail: NTIS HC A09/MF A01

The effect of different by-products on the theoretical gasoline yield is examined. Preliminary results, generated with a reactor having a fixed bed of 100 g of catalyst, are examined for the continuous feeding of never-condensed primary vapors and compared to feeding methanol in the same reactor. The conversion of primary pyrolysis vapors made from biomass is a relatively new research and development area which is showing early promise. The extent to which the product slate can be manipulated by process variables will impact heavily on the viability of this process. Author

N88-25046# Pacific Northwest Labs., Richland, Wash.
RESEARCH ON HYDROTREATING CATALYSTS TO HYDRODEOXYGENATE BIOCRUDE OILS **c25**
Douglas C. Elliott and Eddie G. Baker *In its* Proceedings of the 1987 Biomass Thermochemical Conversion Contractors' Review Meeting Nov. 1987 p 81-9 (For primary document see N88-25041 18-44)
(Contract DE-AC06-76RL-01830)
Avail: NTIS HC A09/MF A01

Catalytic hydrotreating of wood-derived liquids is being studied using a continuous-feed, fixed-bed reactor. Commercial hydrotreating catalysts and conditions are used to hydroeoxygenate and hydrocrack the biomass liquefaction products generated by high pressure processing. Biomass flash pyrolyzates require alternate processing to first stabilize the products prior to catalytic hydrotreating. Experiments are performed in an upflow reactor wherein both liquid phase and gas phase reactions are considered to be important. Although hydrocarbons are not produced in any significant amount by thermochemical direct liquefaction of wood, the use of a secondary hydrogenation step to treat the initial product can result in nearly pure hydrocarbons. These hydrocarbons are primarily cyclics and aromatics which would be useful in gasoline blending. Author

N88-25047# Pacific Northwest Labs., Richland, Wash.
LOW-TEMPERATURE THERMOCHEMICAL CONVERSION OF HIGH MOISTURE BIOMASS FEEDSTOCKS
R. S. Butner, Douglas C. Elliott, and L. J. Sealock, Jr. *In its* Proceedings of the 1987 Biomass Thermochemical Conversion Contractors' Review Meeting Nov. 1987 p 99-113 (For primary document see N88-25041 18-44)
(Contract DE-AC06-76RL-01830)
Avail: NTIS HC A09/MF A01

Pacific Northwest Laboratory has been developing a catalytic reactor for the thermochemical conversion of high moisture biomass feedstocks to higher valued energy products, including high-BTU gas and liquid fuels. The high moisture feedstocks which have been tested include many underutilized materials such as energy crops, agricultural residues, and food processing solid wastes. Recent progress towards developing this technology, including modifications to the experimental system and procedures and the design of a continuously-fed reactor which is scheduled for construction during late 1987 is described. Author

N88-25048# Science Applications International Corp., McLean, Va.
TECHNICAL AND ECONOMIC EVALUATION OF EMERGING BIOMASS PYROLYSIS PROCESSES FOR GASOLINE PRODUCTION
Edward I. Wan, Malcolm D. Fraser, and Isaac K. Kwarteng *In* Pacific Northwest Labs., Proceedings of the 1987 Biomass Thermochemical Conversion Contractors' Review Meeting Nov. 1987 p 115-139 (For primary document see N88-25041 18-44)
Avail: NTIS HC A09/MF A01

The technical and economic results are given of a recent evaluation of two advanced biomass-to-gasoline processes: a fast pyrolysis process in which wood pyrolyzate is upgraded via two-stage hydrotreating, and a flash ablative pyrolysis process in which pyrolyzate vapors are upgraded via deoxygenation over zeolite catalysts. The results indicate that gasoline can be produced from a 1000-tpd future biomass conversion plant via Georgia Tech's fast pyrolysis for about $0.86 to $1.07 per gallon of product at a potential yield of 91.6 gallons per ton (dry), and via SERI flash pyrolysis for about $0.94 to $1.13 per gallon at a yield of 65.5 gallons per ton (dry). Author

N88-25049# Pacific Northwest Labs., Richland, Wash.
BENCH-SCALE STUDIES ON FLUID-BED PYROLYSIS OF WOOD USING DIFFERENT CONTACT GASES
L. K. Mudge, M. D. Brown, and W. A. Wilcox *In its* Proceedings of the 1987 Biomass Thermochemical Conversion Contractors' Review Meeting Nov. 1987 p 141-150 (For primary document see N88-25041 18-44)
(Contract DE-AC06-76RL-01830)
Avail: NTIS HC A09/MF A01

Results of bench scale studies of fluid-bed pyrolysis of wood with carbon dioxide, methane and hydrogen contact gases are described. The objective was to determine the effect of thermal treatment with these gases on product yields, primarily yields and composition of condensible hydrocarbons. The effects of temperature, contact gas, wood feed rate, and gas contact time on the yields of gases, liquids and chars are discussed. Yields of condensible hydrocarbons with different contact gases are compared to yields from steam pyrolysis of wood. Author

N88-25050# Aerospace Research Corp., Roanoke, Va.
EVALUATION OF MANURE AS A FEEDSTOCK FOR GAS TURBINES **c28**
Joseph T. Hamrick *In* Pacific Northwest Labs., Proceedings of the 1987 Biomass Thermochemical Conversion Contractors' Review Meeting Nov. 1987 p 151-169 Sponsored by DOE (For primary document see N88-25041 18-44)
Avail: NTIS HC A09/MF A01

A preliminary program on evaluation of feedlot manure as a feedstock for gas turbines has been completed. It was determined that manure can be pulverized and fed into a gas turbine production system with the manure burning in much the same manner as a liquid or gaseous fuel. Ash and dirt in the manure did not appear to have a significant effect on combustion and were effectively removed by the cyclone filters. The exhaust gases varied from clear to a blue haze. Severe problems were encountered with slagging of the hot refractory walls of the combustor. Development of a suitable combustor will be required before a commercial size system can be designed. Author

N88-25051# Aerospace Research Corp., Roanoke, Va.
A 3 MW WOOD FIRED GAS TURBINE AT RED BOILING SPRINGS, TENNESSEE **c28**
Joseph T. Hamrick *In* Pacific Northwest Labs., Proceedings of the 1987 Biomass Thermochemical Conversion Contractors' Review Meeting Nov. 1987 p 171-182 Sponsored by DOE (For primary document see N88-25041 18-44)
Avail: NTIS HC A09/MF A01

Operation of a 3000 kW system at Red Boiling Springs, Tennessee has produced valuable information about operation with wood and limitations as to operating temperatures. Emission

measurements and analysis show that no significant problems exist with emissions from the system. After running for 481 hours, 62 percent of which were generating power, no turbine erosion has been detected. The major long term problem involves periodic cleaning of deposits from the turbine stators and blades, a problem that is manageable for operation at turbine inlet temperatures at or below 1450 F. Author

N88-25052# Technische Univ., Berlin (West Germany). Inst. fuer Luft- und Raumfahrt.

LIMITS OF DESIGN FEASIBILITY OF MULTIWING WIND TURBINES WITH INDIVIDUAL ARTICULATED WING STRUCTURE Interim Report, 1 Jan. - 31 Dec. 1986 [GRENZEN DER BAUBARKEIT VON MEHRFLUEGLIGEN WINDTURBINEN MIT INDIVIDUELLEM SCHLAGGELENK]

Joerg Maurer 1987 135 p In GERMAN

(ILR-Mitt-180; ETN-88-91932) Avail: NTIS HC A07/MF A01

Mechanical modeling for the feasibility study of a wind turbine with wing diameters from 3.5 to 35 m is described. Velocity and acceleration of a wing tip; calculation of the load forces on the blades; dimensional analysis of the wings; internal and external geometry of the wingforms; effect of construction size on mass distribution, rigidity, and strain of the structure are described. Results concern the design, profile, mass and dampings of the wind turbine system, effects of construction size on operating characteristics, and effect of gravity and rotating moments on loads. ESA

N88-25053# Instituto Nacional de Tecnica Aeroespacial, Esteban Terradas, Torrejon de Ardoz (Spain). Dept. of Motopropulsion y Energia.

EVALUATION OF THE CHROMIUM OXIDE ARC SPRAYING TREATMENT ON SOLAR ENERGY COLLECTORS [EVALUACION DE TRATAMIENTO DE OXIDO DE CROMO PARA ABSORBEDORES SOLARES APPLICADOS POR PROYECCION CON SOPLETES DE PLASMA]

Gloria FernandezArroyo, Antonio GonzalezGarcia-Conde, Francisco MoralesPoyato, Jose Maria ArreraJaraiz, Cristina BlancoTemprano, and Francisco CamonAlvarez 1988 9 p In SPANISH; ENGLISH summary

(ETN-88-92564) Avail: NTIS HC A02/MF A01

Accelerated aging tests were performed on steel specimens coated with plasma gun Cr2O3 arc sprays. The chromium oxide coating is attractive due to its radiation absorptance characteristic, especially for solar thermal energy absorption applications. The use of plasma blowpipes gives low porosity coatings. Collector efficiency curves were determined and compared to the curves of conventional black paint collectors. The efficiency is close to conventional painting. The excellent behavior at high temperatures makes this treatment applicable to concentrated radiation absorbers. ESA

N88-25054# Institute of Gas Technology, Chicago, Ill.

SULFUR-TOLERANT ANODE MATERIALS Annual Report, Sep. 1986 - Sep. 1987

R. J. Remick, T Osif,, and M. Lawson Sep. 1987 78 p

(Contract DE-AC21-86MC-23267)

(DE88-001034; DOE/MC-23267/2537) Avail: NTIS HC A05/MF A01

This report summarizes the results of the first year's technical effort performed on a program identifying and evaluating alternative anode materials for use in molten carbonate fuel cells (MCFC) operating with high levels of sulfur contaminants in the fuel. A literature survey was performed on materials for use in the MCFC and on materials exhibiting good electrical conductivity at high temperature. A list candidate materials having a reported electrical conductivity in excess of 0.1 (ohm-cm) sub -1 was compiled. 19 candidate materials were selected, and nine have been tested for electrical conductivity and for stability in the molten eletrolyte. To date, only cobalt metal has proved to be stable under all test conditions. Several water-gas shift catalysts were also evaluated for their catalytic activity and sulfur resistance under conditions prevailing in the MCFC anode. DOE

N88-25055# Utah Univ., Salt Lake City. Dept. of Mechanical Engineering.

YAW DYNAMICS OF HORIZONTAL AXIS WIND TURBINES Annual Report No. 1

C. Xudong, A. Hansen, and N. Siedschlag Feb. 1988 104 p

(Contract DE-AC02-83CH-10093)

(DE88-001137; SERI/STR-217-3309) Avail: NTIS HC A06/MF A01

Numerous problems associated with yaw exists on free-yaw and yaw-driven wind turbines. Yaw-driven machines experience failures in the yaw drive due to excessive loads, while free-yaw machines experience high yaw rates and frequent misalignment problems. This report describes a theoretical investigation of the yaw behavior of wind turbines, which was carried out by the University of Utah. The basic approach to this analysis was to develop a series of analytical and computer models such that each successive model added complexity and increased accuracy. These models are described and compared to results from other models and also to test data. Comments are made on the models' ability to predict yaw moments and response. Also, useful insight is presented regarding the free-yaw behavior of wind turbines as observed using these models. The most complex of these models is used to predict the coupled free-yaw and flap motions of a rotor. This model, YawDyn, is operational; however, experience with it is limited. Future plans, for further enhancing and validating this model, are also discussed. DOE

N88-25056# Midwest Research Inst., Golden, Colo. Solar Energy Research Inst.

PHOTOVOLTAIC ADVANCED RESEARCH AND DEVELOPMENT PROJECT, SOLAR RADIATION RESEARCH Annual Report, 1 Oct. 1986 - 30 Sep. 1987

R. L. Hulstrom, T. W. Cannon, and C. J. Riordan Mar. 1988 31 p

(Contract DE-AC02-83CH-10093)

(DE88-001143; SERI/PR-215-3297) Avail: NTIS HC A03/MF A01

This report summarizes work performed in FY 1987 by SERI's Resource Assessment and Instrumentation Branch, Solar Electric Research Division, under the Solar Radiation Research Task of the Photovoltaic Advanced Research and Development Project. The objectives of this task are to implement improved spectral solar radiation models and data bases, and to develop specialized instrumentation/ measurement techniques needed to help develop a technical understanding of the relationships between photovoltaic device performance and outdoor spectral solar radiation variations. DOE

N88-25057# Pacific Northwest Labs., Richland, Wash.

OVERVIEW OF WIND BEHAVIOR RESEARCH IN THE US WIND ENERGY PROGRAM

L. L. Wendell Oct. 1987 7 p Presented at Windpower '87, San Francisco, Calif., 5 Oct. 1987

(Contract DE-AC06-76RL-01830)

(DE88-005683; PNL-SA-15101; CONF-871062-13) Avail: NTIS HC A02/MF A01

The relevant behavior presently under investigation includes rotor-scale turbulence and wind variability on a scale applicable to wind farms caused by terrain complexity and turbine-generated wakes in the array. Results of rotor-scale turbulence experiments have demonstrated that the spatial variation of the flow across the rotor disk is critical in the type of forcing function experienced by a rotating blade. Rotor-scale turbulence models that approximate the effect of rotational sampling with spectral information from a single anemometer or time series data from several levels on a single tower have been developed and tested. A self-optimizing flow model has demonstrated the capability to produce wind speed estimates over a wind farm area in complex terrain generally to within a 5% root mean square error. Wind turbine wake field experiments have shown a strong site-dependence in the factors affecting wake behavior. Work has begun in the area of combining complex terrain flow models and wind turbine array models for micrositing applications. DOE

N88-25058# Pacific Northwest Labs., Richland, Wash.
FIELD EXPERIENCE WITH AQUIFER THERMAL ENERGY STORAGE
L. D. Kannberg Nov. 1987 15 p Presented at the 15th Annual Energy Technology Conference and Exposition, Washington, D.C., 17 Feb. 1988
(Contract DE-AC06-76RL-01830)
(DE88-007075; PNL-SA-15449; CONF-880212-6) Avail: NTIS HC A03/MF A01

Aquifer thermal energy storage (ATES) has the potential to provide storage for large-scale building heating and cooling at many sites in the US. However, implementation requires careful attention to site geohydraulic and geochemical characteristics. Field tests in the US have shown the over 60% of the heat injected at temperatures over 100 C can be recovered on a seasonal cycle. Similarly, aquifer storage of shilled ground water can provide building cooling with annual cooling electrical energy reductions of over 50% and a reduction in summer peak cooling electrical usage by as much as a factor of 20. A number of projects have been built and operated around the world. China has installed numerous ATES systems in many major cities. Installations in Europe and Scandinavia are almost exclusively low-temperature heat storage systems that use heat pumps. Two high-temperature systems (over 100 C) are in operation or undergoing preliminary testing: one in Denmark, the other in France. Heat ATES often requires water treatment to prevent precipitation of calcium and magnesium carbonates. At some sites, consideration of other geochemical and microbiological issues (such as iron bacteria) must be resolved. DOE

N88-25059*# National Aeronautics and Space Administration. Lewis Research Center, Cleveland, Ohio.
SMALL SCALE BIPOLAR NICKEL-HYDROGEN TESTING
Michelle A. Manzo 1988 10 p Presented at the 33rd International Power Sources Symposium, Cherry Hill, N.J., 13-16 Jun. 1988; sponsored by the Department of the Army
(NASA-TM-100936; E-4216; NAS 1.15:100936) Avail: NTIS HC A02/MF A01 CSCL 10C

Bipolar nickel-hydrogen batteries, ranging in capacity from 6 to 40 A-hr, have been tested at the NASA Lewis Research Center over the past six years. Small scale tests of 1 A-hr nickel-hydrogen stacks have been initiated as a means of screening design and component variations for bipolar nickel-hydrogen cells and batteries. Four small-scale batteries have been built and tested. Characterization and limited cycle testing were performed to establish the validity of test results in the scaled down hardware. The results show characterization test results to be valid. LEO test results in the small scale hardware have limited value.
Author

45 ENVIRONMENT POLLUTION

Includes atmospheric, noise, thermal, and water pollution.

N88-25060# General Accounting Office, Washington, D. C. Resources, Community and Economic Development Div.
AIR POLLUTION: OZONE ATTAINMENT REQUIRES LONG-TERM SOLUTIONS TO SOLVE COMPLEX PROBLEMS
Jan. 1988 63 p
(PB88-167275; GAO/RCED-88-40) Avail: NTIS HC A04/MF A01 CSCL 13B

The General Accounting Office reviewed the efforts of the Environmental Protection Agency (EPA) to reduce ozone levels to meet the national air quality ozone standard. The nation's progress is discussed in reducing ozone levels, the status of EPA's review of the latest scientific data on the health effects of ozone, problems three areas have had in implementing ozone programs, and EPA's oversight of state and local efforts to reduce ozone. Author

N88-25061# Imperial Coll. of Science and Technology, London (England). Computational Fluid Dynamics Unit.
REVIEW OF NUMERICAL METHODS FOR RADIONUCLIDE TRANSPORT IN THREE-DIMENSIONAL POROUS MEDIA, AT HIGH PECLET NUMBERS
D. B. Spalding and W. M. Pun 1987 74 p
(Contracts PECD-7/9/322; ICCFDU-4C.2)
(CFDU/87/10; ETN-88-92505) Avail: NTIS HC A04/MF A01

It is shown that computer simulation of radionuclide transport by groundwater flow can make a valuable contribution to the determination of what sites are safe, but only if the mathematical model employed is physically realistic, and the procedures for working out its implications are numerically accurate. Accuracy of alternative means of formulating the advection-diffusion equation, in three-dimensions, with the expenditure of a limited amount of computing resources, measured by the fineness of the computational grid and by the number of time steps, was assessed. Accuracy depends mainly on the formula used to compute the average value of the concentration of pollutant in fluid crossing the surface of a computational cell during a time step. A moving-grid formulation, which can be applied to many practical situations, performs best. It eliminates the source of the inaccuracy entirely by reducing the problem to one of diffusion alone. However, it must be ascertained if the adsorption-desorption processes between the radionuclides and the soil can be adequately represented by the use of a retardation factor, and if annual fluctuations in groundwater flow, which undoubtedly causes transported material to spread over a larger volume, can be adequately represented by the diffusion approximation. ESA

N88-25062*# Washington Univ., Seattle. School of Oceanography.
OXIDATION AND REDUCTION RATES FOR ORGANIC CARBON IN THE AMAZON MAINSTREAM TRIBUTARY AND FLOODPLAIN, INFERRED FROM DISTRIBUTIONS OF DISSOLVED GASES
Jeffrey E. Richey, Allan H. Devol, Steven C. Wofsy, Reynaldo Victoria, and Maria N. G. Riberio (Instituto Nacional de Pesquisas da Amazonia, Manaus, Brazil) [1986] 28 p
(Grant NAGw-711)
(NASA-CR-182943; NAS 1.26:182943) Avail: NTIS HC A03/MF A01 CSCL 13B

Concentrations of CO2, O2, CH4, and N2O in the Amazon River system reflect an oxidation-reduction sequence in combination with physical mixing between the floodplain and the mainstem. Concentrations of CO2 ranged from 150 microM in the Amazon mainstem to 200 to 300 microM in aerobic waters of the floodplain, and up to 1000 microM in oxygen-depleted environments. Apparent oxygen utilization (AOU) ranged from 80 to 250 microM. Methane was highly supersaturated, with concentrations ranging from 0.06 microM in the mainstem to 100 microM on the floodplain. Concentrations of N2O were slightly supersaturated in the mainstem, but were undersaturated on the floodplain. Fluxes calculated from these concentrations indicated decomposition of 1600 g C sq m y(-1) of organic carbon in Amazon floodplain waters. Analysis of relationships between CH4, O2, and CO2 concentrations indicated that approximately 50 percent of carbon mineralization on the floodplain is anaerobic, with 20 percent lost to the atmoshphere as CH4. The predominance of anaerobic metabolism leads to consumption of N2O on the flood plane. Elevated concentrations of CH4 in the mainstem probably reflect imput from the floodplain, while high levels of CO2 in the mainstem are derived from a combination of varzea drainage and in situ respiration. Author

N88-25063# Gesellschaft fuer Strahlen- und Umweltforschung m.b.H., Munich (West Germany).
WORKSHOP ON ATMOSPHERIC OH [ATMOSPHAERISCHES OH]
Franz Josef Comes, ed. (Johann-Wolfgang-Goethe-Univ., Frankfurt am Main, West Germany) and Klaus-Dieter Hoefken, ed. 1987 117 p Partly in ENGLISH and GERMAN Workshop held in

Frankfurt am Main, Fed. Republic of Germany, 18-19 May 1987 (BPT-7/87; ISSN-0176-0777; ETN-88-92337) Copyright Avail: NTIS HC A06/MF A01

Hydroxyl radical (OH) formation and concentration measurements in the troposphere are discussed. Laboratory and field equipments are presented with emphasis on present limitations of the methods and future developments. For concentration measurements of OH and atmospheric trace gases, the following methods are described: laser differential optical absorption spectroscopy, longpath absorption with rapid spectral concordance, double pulsed UV laser, laser induced fluorescence, tunable diode lasers, and continuous wave laser frequency modulation spectroscopy. For individual titles, see N88-25064 through N88-25073.

N88-25064# Max-Planck-Inst. fuer Aeronomie, Katlenburg-Lindau (West Germany).

OZONE IN THE ATMOSPHERE [OZON IN DER ATMOSPHAERE]

P. Fabian *In* Gesellschaft fuer Strahlen- und Umweltforschung GmbH, Workshop on Atmospheric OH 1987 p 3-11 In GERMAN (For primary document see N88-25063 18-45)

Copyright Avail: NTIS HC A06/MF A01

Chemical reactions for the formation of hydroxyl radicals (OH) by photolysis of ozone are given. The OH radicals by combination with methane, hydrogen, and carbon dioxide contribute to the formation of smog in urban regions where combustion products and automobile exhaust gases are present. Measurements carried out during the past 10 yr show an increase of ozone concentration from 25 ppb to 40 ppb in middle Europe leading to major smog periods. ESA

N88-25065# Fraunhofer-Inst. fuer Atmosphaerische Umweltforschung, Garmisch-Partenkirchen (West Germany).

ULTRAVIOLET MEASUREMENTS: MEASUREMENTS OF PHOTOLYSIS RATES [UV-MESSUNGEN - MESSUNGEN VON PHOTOLYSERATEN]

W. Junkermann *In* Gesellschaft fuer Strahlen- und Umweltforschung GmbH, Workshop on Atmospheric OH 1987 p 13-17 In GERMAN (For primary document see N88-25063 18-45)

Copyright Avail: NTIS HC A06/MF A01

Two methods for the determination of photolysis rates of ozone are considered. The conventional method using the chemical actionometer does not produce accurate and continuous measurement results. A photoelectric detector, simpler and cheaper, with interference filters for the elimination of the effects of waves length variations is proposed. Results indicate proportionality between OH-concentrations and photolysis rates. ESA

N88-25066# Gesamthochschule, Wuppertal (West Germany). Inst. fuer Physikalische Chemie.

LABORATORY EXPERIMENTS ON ATMOSPHERIC OH REACTIONS [LABORUNTERSUCHUNGEN UEBER ATMOSPHAERISCHE OH-REAKTIONEN]

K. H. Becker *In* Gesellschaft fuer Strahlen- und Umweltforschung GmbH, Workshop on Atmospheric OH 1987 p 19-30 In GERMAN (For primary document see N88-25063 18-45)

Copyright Avail: NTIS HC A06/MF A01

Laboratory experiments for the determination of the kinetic parameters of the chemical reactions of OH were carried out by simulation of atmospheric conditions. Environmental temperature, presence of various trace products, quantitative analysis of product output, reaction mechanisms, and rate constants are examined. Direct and indirect photolytic and chemical OH-sources are considered. A 6 m long and 0.5 m diameter photoreaction with UV and IR spectrometer is used. ESA

N88-25067# Goettingen Univ. (West Germany). Inst. fuer Physikalische Chemie.

EFFECT OF CARBOHYDRATE OXIDATION ON THE TROPOSPHERIC HOx-SYSTEM [DER EINFLUSS DER KOHLENWASSERSTOFF-OXIDATION AUF DAS HOX-SYSTEM DER TROPOSPHAERE]

R. Zellner, G. Weibring, and K. J. Niemitz *In* Gesellschaft fuer Strahlen- und Umweltforschung GmbH, Workshop on Atmospheric OH 1987 p 31-40 In GERMAN (For primary document see N88-25063 18-45)

Copyright Avail: NTIS HC A06/MF A01

The tropospheric oxidation cycle of the hydroxyl radicals HOx, HO, HO2 contributing to the chemical activity of the troposphere is studied. Of special importance are the variations of CH4-concentrations and its oxidation products. Runge-Kutta algorithms are used to study 25 carbohydrates reacting in 60 chemical reactions. Results in the absence and the presence of CH4 are given. ESA

N88-25068# Max-Planck-Inst. fuer Chemie, Mainz (West Germany). Abteilung Luftchemie.

MEASUREMENT OF ATMOSPHERIC OH WITH LASER DIFFERENTIAL OPTICAL ABSORPTION SPECTROSCOPY (LDOAS) [MESSUNG VON ATMOSPHAERISCHEM OH MIT DIFFERENTIELLER OPTISCHER ABSORPTIONSSPEKTROSKOPIE (LDOAS)]

D. Perner and U. Platt (Kernforschungsanlage, Juelich, West Germany) *In* Gesellschaft fuer Strahlen- und Umweltforschung GmbH, Workshop on Atmospheric OH 1987 p 41-55 In GERMAN (For primary document see N88-25063 18-45)

Copyright Avail: NTIS HC A06/MF A01

Direct absorption spectroscopy is used for the measurement of atmospheric OH; autocalibration is achieved by laser induced fluorescence. Measurements by optical absorption present problems concerning the selfproduction of OH, test sensitivity and interaction of several absorption products. With this method it is possible to obtain absorption spectra from SO2, CS2, CH2O, in addition to OH. ESA

N88-25069# Johann-Wolfgang-Goethe-Univ., Frankfurt am Main (West Germany). Inst. fuer Physikalische und Theoretische Chemie.

TROPOSPHERIC OH MEASUREMENTS BY LONG PATH ABSORPTION WITH RAPID SPECTRAL CONCORDANCE [TROPOSPHAERISCHE OH-MESSUNGEN DURCH LANGWEGABSORPTION MIT SCHNELLER SPEKTRENDURCHSTIMMUNG]

W. Armerding, A. Herbert, G. Mollekopf, M. Spahn, and F. J. Comes *In* Gesellschaft fuer Strahlen- und Umweltforschung GmbH, Workshop on Atmospheric OH 1987 p 57-72 In GERMAN (For primary document see N88-25063 18-45)

Copyright Avail: NTIS HC A06/MF A01

The development of a long path absorption spectroscope with test sensitivity of 100,000 OH/cc, test length of 1 km and integration time of 1 min is described. The method permits the elimination of atmospheric fluctuations, the use of one-beam device, and of laser as monochromator. This device is designed for field measurements by reflecting the light path (test length). Results of preliminary field tests indicate the suitability of this device for the measurements of 8 ppb SO2. ESA

N88-25070# Goettingen Univ. (West Germany). Inst. fuer Physikalische Chemie.

DETERMINATION OF TROPOSPHERIC H CONCENTRATIONS BY A DOUBLE-PULSED UV LASER METHOD [BESTIMMUNG DER TROPOSPHAERISCHEN OH-KONZENTRATION DURCH EIN UV-LASER-DOPPELPULS-VERFAHREN]

R. Zellner, R. Paschke, and J. Haegele *In* Gesellschaft fuer Strahlen- und Umweltforschung GmbH, Workshop on Atmospheric OH 1987 p 73-86 In GERMAN (For primary document see N88-25063 18-45)

Copyright Avail: NTIS HC A06/MF A01

The principle of double pulsed UV laser for the determination

of OH-concentrations is described and the main difficulties discussed. The test light beam is absorbed only by OH, the reference beam is not submitted to absorption. Measurements for the absorption spectra of SO2, CH2 and OH are presented. Statistical analysis of standard errors and reasons for signal instability are analyzed. ESA

N88-25071# Kernforschungsanlage, Juelich (West Germany). Inst. fuer Atmosphaerische Chemie.
TROPOSPHERIC OH MEASUREMENT BY LASER INDUCED FLUORESCENCE (LIF) [TROPOSPHAERISCHE OH-MESSUNGEN DURCH LASERINDUZIERTE FLUORESZENZ (LIF)]
A. Hofzumahaus *In* Gesellschaft fuer Strahlen- und Umweltforschung GmbH, Workshop on Atmospheric OH 1987 p 87-97 In GERMAN (For primary document see N88-25063 18-45)
Copyright Avail: NTIS HC A06/MF A01

Development of a laser induced fluorescence apparatus for field measurement of OH-concentrations with the advantage of eliminating the ozone/water interference in the testing zone is examined. The excitation wave length is 308 nm. This method is well adapted for field tests; it is more compact and mobile than the long path absorption spectroscopy. ESA

N88-25072# Max-Planck-Inst. fuer Chemie, Mainz (West Germany).
TRACE GAS MEASUREMENTS IN THE TROPOSPHERE USING TUNABLE DIODE LASERS
G. W. Harris *In* Gesellschaft fuer Strahlen- und Umweltforschung GmbH, Workshop on Atmospheric OH 1987 p 99-103 (For primary document see N88-25063 18-45)
Copyright Avail: NTIS HC A06/MF A01

Application of tunable diode laser absorption spectroscopy to the measurement of trace atmospheric gases is discussed. Factors limiting instrument performance are surveyed: effects due to laser wavelength fluctuations, etalon signal calibration, and random noise elimination. Measurement of atmospheric HOx radicals using infrared absorption spectrometry is considered. ESA

N88-25073# Fraunhofer-Inst. fuer Toxikologie und Aerosolforschung, Schmallenberg-Grafschaft (West Germany). Abteilung Physikalische Chemie.
DEVELOPMENT OF CONTINUOUS WAVE LASER FREQUENCY MODULATION OF OH IN TROPOSPHERIC CONCENTRATIONS RANGE [ENTWICKLUNG DER CW-LASER-FREQUENZMODULATIONS-SPEKTROSKOPIE ZU EINER METHODE ZUR MESSUNG VON OH IM TROPOSPHAERISCHEN KONZENTRATIONSBEREICH]
C. Leonard and C. Zetzsch *In* Gesellschaft fuer Strahlen- und Umweltforschung GmbH, Workshop on Atmospheric OH 1987 p 105-113 In GERMAN (For primary document see N88-25063 18-45)
Copyright Avail: NTIS HC A06/MF A01

High sensitivity laser spectroscopy is considered for the determination of tropospheric OH concentrations in the range of 1 million OH/cc. Experimental equipment design is described, including dye laser, frequency doubler, intensity stabilizer, electro-optical modulator, wavemeter, spectral analyzer, and long path absorption cell. Noise spectra of the measurement apparatus is established, permitting a more accurate determination of OH-radical concentration. ESA

N88-25074# Instituto Nacional de Tecnica Aeroespacial, Esteban Terradas, Torrejon de Ardoz (Spain). Grupo Atmosfera.
CHANGES IN THE ANTARCTIC ATMOSPHERE DUE TO THE REDUCTION OF STRATOSPHERIC OZONE [ALTERACIONES EN LA ATMOSFERA ANTARTICA COMO CONSECUENCIA DE LA REDUCCION DEL OZONO ESTRATOSFERICO]
Manuel GilOjeda, Ma Jesus SainzdeAja, and Javier CachoGomez 1988 18 p In SPANISH; ENGLISH summary
(ETN-88-92565) Avail: NTIS HC A03/MF A01

Energy disturbances in the stratosphere and modifications in spectral distribution of ultraviolet radiation on the terrestrial surface were calculated using a one dimensional radiative model for a number of different ozone concentrations. The study concerns the austral convergence area in spring when the measured ozone depletion is maximum. The results show considerable danger for the antarctic ecosystem. The UV radiation could go up to 10,000 percent for wavelengths below 295 nanometers. Related temperature changes are discussed. ESA

N88-25075# Eustance and Horowitz, Circleville, N.Y.
FLOTATION PROCESSES
Inder Jit Kumar, William E. Eustance, and Lawrence K. Wang, ed. (Lenox Inst. for Research, Inc., Mass.) Mar. 1988 69 p Sponsored by Lenox Inst. for Research, Inc., Mass.
(PB88-180302; LIR/03-88/284) Avail: NTIS HC A04/MF A01 CSCL 13B

The theory and various types of flotation processes are presented. The topics include: buoyancy, air solubility, bubble particle contact, pressure flotation, vacuum flotation, dispersed air flotation, electroflotation, plain flotation, oil-water separation, laboratory testing, pilot plants, chemical additives, chemical analysis and design examples. Author

N88-25076# Environmental Protection Agency, Research Triangle Park, N.C. Atmospheric Sciences Research Lab.
MOTOR VEHICLES AS SOURCES OF COMPOUNDS IMPORTANT TO TROPOSPHERIC AND STRATOSPHERIC OZONE
F. M. Black Apr. 1988 30 p
(PB88-195219; EPA/600/D-88/067) Avail: NTIS HC A03/MF A01 CSCL 13B

One of the most rapidly growing human activities in the U.S. of importance to atmospheric ozone is the use of highway motor vehicles. Transportation sources are estimated to have been responsible for about 34% of 1985 U.S. anthropogenic hydrocarbon emissions, 70% of carbon monoxide emissions, 45% of nitrogen oxide emissions, 24% of nonaerosol chlorofluorocarbon emissions, and 14% of carbon dioxide emissions. Data is presented describing possible uninventoried transportation hydrocarbon emissions that could increase their estimated contribution to 45 to 50% of the anthropogenic total. Data is also presented suggesting motor vehicles to be relatively insignificant sources of anthropogenic nitrous oxide, but noting that these emissions are increased by the control technologies used to reduce hydrocarbon, carbon monoxide, and nitrogen oxides emissions. The sensitivity of motor vehicle emission rates and compositions to such operating variables as ambient temperature, altitude, and average speed is discussed. Author

46 GEOPHYSICS

Includes aeronomy; upper and lower atmosphere studies; ionospheric and magnetospheric physics; and geomagnetism.

For space radiation see *93 Space Radiation.*

N88-25077# Riso National Lab., Roskilde (Denmark).
LOW FREQUENCY ELECTROSTATIC TURBULENCE IN THE POLAR CAP E-REGION
H. L. Pecseli, F. Primdahl, and A. Bahnsen [1988] 38 p
(DRI-3-88) Avail: NTIS HC A03/MF A01

Electrostatic turbulent fluctuations in a broad frequency band are detected in the polar cap E-region over Greenland by an instrumented rocket payload. The fluctuations were detected by potential-difference measurements on two sets of boom-mounted spherical probes. The direction and magnitude of the phase velocity of the fluctuations was determined by standard correlation techniques. The driving mechanism for the turbulence is identified as the Farley-Buneman instability. Deviations from the predictions of a linear stability analysis indicate the effect of nonlinear saturation mechanisms. A correlation time 20 to 150 ms along the rocket trajectory is determined, indicating that the fluctuations are

essentially statistically independent for altitude separations greater than 50 m. A conditional analysis of the signals indicate that a good approximation can be described by Gaussian statistics. The data exclude the possibility of wave steepening as a saturation mechanism for the linear instability. Author

N88-25078# Arizona State Univ., Tempe.
DRILLING INVESTIGATION OF A YOUNG MAGMATIC INTRUSION BENEATH THE INYO DOMES, LONG VALLEY, CALIFORNIA: STRUCTURAL AND TEXTURAL STUDIES
J. Fink Nov. 1987 11 p
(Contract DE-FG02-85ER-13320)
(DE88-006613; DOE/ER-13320/1) Avail: NTIS HC A03/MF A01

The purpose of this project was to characterize the geometry and emplacement mechanisms of silicic dikes beneath the Inyo Domes, California. The investigation involved surface structural and textural studies in the Inyo area, mapping projects in analogous areas that offered better controls on either the three-dimensional geometry or emplacement conditions of dikes, and analytical studies of drill core samples. Mapping of structures on and around the Domes suggested that they were fed by an echelon arrangement of rotated dike segments, as later confirmed by the drill cores, and that the dike propagated obliquely to the north. A model was derived relating dike segmentation to changes in host-rock rheology and fracture behavior, rather than to variations in principle stress orientations. Studies of eroded volcanoes showed that the rotation of segments and host-rock brecciation both increase as a dike approaches the surface. SEM and isotopic studies of drill cores led to a model for volatile migration within advancing silicic flows which predicts that explosive hazards associated with these flows may increase as the flow gets farther from its vent. A new model for selective withdrawal from a stratified dike explained observed compositional and textural variations within and among the three Inyo Domes. DOE

N88-25079# Catholic Univ., Santiago (Chile). Lab. de Neurofisiologia.
DEVELOPMENT AND VALIDATION OF TRANSMISSION MEASUREMENTS TECHNIQUES OF IMAGE CONTRAST, UTILIZING EXISTING IR IMAGERS
Ami Ben-Shalom, Adam D. Devir, and Leslie B. Salem Sep. 1987 35 p
(Contract DAJA45-86-C-0045)
(AD-A191471) Avail: NTIS HC A03/MF A01 CSCL 04A

This interim report summarizes the work done in the first two months of the contract period. The objective was to evaluate different methods proposed for the measurement of atmospheric transmittance with AGA 780 camera. Simultaneously, a computerized formulation was prepared for the data analysis of the output of the AGA system (the data link). A first field test was performed over a range of 400m. As a result of this experiment a calibration procedure, which is needed for the measurement of an absolute (integrated) atmospheric transmittance, was established. This procedure is needed to further evaluation of the measurement methods. GRA

N88-25080# Naval Oceanographic Office, Bay St. Louis, Miss.
DOD 1985 WORLD MAGNETIC MODEL: CHARTS AND GRID VALUES
Lana G. Cagle Nov. 1987 114 p
(AD-A191484; NOO-TN-8222-02-87) Avail: NTIS HC A06/MF A01 CSCL 08D

The new Department of Defense magnetic model, WC-85 has been adopted as the official model by United States and United Kingdom defense establishments, and by the International Hydrographic Bureau. Provided in this publication are a list of the WC-85 coefficients, 5 deg grid tables, and small-scale charts of main field and annual change values for the northward, eastward, and vertical components, total and horizontal intensities, declination and inclination of the geomagnetic field. GRA

N88-25081# Naval Research Lab., Washington, D.C.
THE EFFECT OF THE IONOSPHERE ON COMMUNICATION, NAVIGATION AND SURVEILLANCE SYSTEMS BASED ON IONOSPH ERIC EFFECTS SYMPOSIUM HELD ON 5-7 MAY 1987 IN SPRINGFIELD, VIRGINIA
John M. Goodman, John A. Klobuchar, R. G. Joiner, and Haim Soicher 1987 720 p Symposium held in Springfield, Va., 5-7 May 1987
(AD-A191855) Avail: NTIS HC A99/MF A02 CSCL 04A

Topics addressed include: wideband high frequency and longwave studies, tranionospheric propagation - total electron content, high frequency measurements, ionospheric modification, high frequency models, spacecraft glow, transionospheric propagation - scintillation, and high latitude ionospheric interaction. GRA

N88-25082# Smithsonian Astrophysical Observatory, Cambridge, Mass.
MOLECULAR SOURCES OF IONOSPHERIC HOLES Final Report, 1 Apr. 1984 - 30 Sep. 1987
Steven L. Guberman 19 Nov. 1987 50 p
(Grant AF AFOSR-0109-84)
(AD-A191857; AFOSR-88-0064TR) Avail: NTIS HC A03/MF A01 CSCL 20E

The dissociative recombination of molecular ions with electrons determines many of the properties of the Earth's ionosphere under both quiescent and disturbed conditions. However, in spite of its importance, there has never been an experimental measurement of dissociative recombination rates from individual excited ion vibrational levels. Completed are large scale ab initio calculations of cross sections and rates for the dissociative recombination of the molecular oxygen ion leading to excited oxygen atoms in the IS and ID states, the upper states of the well known green and red lines, respectively. A new method for calculating electronic autoionization widths using high Rydberg state wave functions to represent the inner part of the free electron wave function has been used and tested on the NO molecule where the widths can be calculated to an expected accuracy of about 15 percent. THe widths have been used to determine dissociative recombination cross sections as a function of electron energy. Large windows have been discovered in the cross sections from excited vibrational levels. The windows, at which the cross sections drop precipitously, are due to the overlap of the peak in the continuum vibrational wave functions. GRA

N88-25083# Aerospace Corp., El Segundo, Calif. Space Sciences Lab.
DEEP DIELECTRIC CHARGING EFFECTS DUE TO HIGH ENERGY ELECTRONS IN EARTH'S OUTER MAGNETOSPHERE
D. N. Baker, R. D. Belian, P. R. Higbie, R. W. Klebesadel, and J. B. Blake 5 Feb. 1988 33 p
(Contract F04701-85-C-0086)
(AD-A192154; TR-0086A(2940-05)-1; SD-TR-88-08) Avail: NTIS HC A03/MF A01 CSCL 04A

Many spacecraft operational problems in Earth's outer magnetosphere appear to be due to intense, transient radiation phenomena. Three types of naturally occurring, and highly variable, hostile particle radiation environments are encountered at, or near, the geostationary orbit: (1) high-energy protons due to solar flares; (2) energetic ions and electrons produced by magnetospheric substorms; and (3) very high energy electrons of uncertain origin. In this report, particular emphasis is given to highly relativistic electrons, (3 approximately 10 MeV). Electron fluxes and energy spectra are shown which were measured by two high-energy electron sensor systems at 6.6 RE from 1979 through 1984. Large, persistent increases in this population were found to be relatively infrequent and sporadic in 1979-81 around solar maximum. During the approach to solar minimum (1981 - present), it is observed that the highly relativistic electrons occur with a regular 27-day periodicity and are well associated with the re-established solar wind stream structures. Through a superposed epoch analysis technique, we show that an energetic electron enhancement typically rises on a 2- to 3-day time scale and decays on a 3- to

4-day time scale at essentially all energies above approximately 3 MeV. The present analysis suggests that these electrons have a very deleterious influence on spacecraft systems due to deep dielectric charging and low-dose susceptibility effects. GRA

N88-25084# Institut d'Aeronomie Spatiale de Belgique, Brussels.
STRATOSPHERIC POSITIVE ION COMPOSITION MEASUREMENTS AND ACETONITRILE DETECTION: A CONSISTENT PICTURE
E. Arijs, D. Nevejans, and J. Ingels 1988 33 p Submitted for publication
(Contract BNSF-2-0095-83)
(Aeronomica-Acta-A-326-1987; ISSN-0065-3713; ETN-88-92486)
Avail: NTIS HC A03/MF A01

Positive ion composition measurements performed with balloon-borne ion mass spectrometers in the Earth's atmosphere between 20 and 45 km are reviewed. The derivation of the acetonitrile volume mixing ratio profile is discussed. The results are compared with model calculations, data obtained with airplane-borne instruments, and ground level samplings. The consistency of the present picture is verified. Comparisons with results of laboratory experiments show that electric field induced collisional dissociation occurs in balloon-borne ion mass spectrometers. Probably, this is one of the major causes for the observed discrepancies between the data of airplane and balloon-borne instruments. ESA

N88-25085# Swedish Inst. of Space Physics, Kiruna.
OBSERVATIONS OF WAVE NUMBER DEPENDENT SPECTRAL LINE RATIO FLUCTUATIONS IN THE ATMOSPHERIC EMISSIONS
Bo Thelin Dec. 1987 22 p
(IRF-Preprint-101; ETN-88-92490) Avail: NTIS HC A03/MF A01

Observational results concerning wave-number dependent spectral line ratio fluctuations in atmospheric emissions are reported. Linear relationships are obtained when spectral line ratio fluctuations are plotted vs. the photon energies when studying Ba-release, nightglow, and auroral emissions. ESA

N88-25086 Cincinnati Univ., Ohio.
BRUNT-DOPPLER DUCTING OF BUOYANCY WAVES IN A TEMPERATURE- AND WIND-STRATIFIED ATMOSPHERE Ph.D. Thesis
Ding-Yi Wang 1987 157 p
Avail: Univ. Microfilms Order No. DA8729265

A Brunt-Doppler ducting mechanism for buoyancy waves is examined and linear modal solutions are obtained by full wave treatment for different inviscid temperature-stratified atmosphere models without or with wind profile including mean circulation and tidal components in zonal and meridional directions. Dispersion relations and directional filtering are discussed. The stability of the modes is investigated by the Richardson's number, and relative significance of the inertial, viscous, and nonlinear terms is estimated by the linear, inviscid solutions. The following represent selected findings: When the local Brunt period is greater than the intrinsic wave period, the wave propagation is prohibited. It, together with the rigid ground, can generate a set of discrete, fully ducted modes with energy density concentrated either near the ground or near the lower thermosphere. The thermospheric modes have properties very similar to the Lamb modes, and may more effectively produce density fluctuation. The windless modes with periods less than 9 min can be stable even when relative density fluctuation is 20 percent at 100 km. The winds, whose zonal component is more important even though the meridional has larger tidal wind in the upper region, strongly affect wave ducting, spectrum, energy distribution, and stability, which may vary with period and propagation direction. Dissert. Abstr.

N88-25087 New South Wales Univ., Kensington (Australia). Dept. of Applied Geology.
A SEDIMENTOLOGICAL AND MINERALOGICAL STUDY OF THE KOOGAH FORMATION, NEW SOUTH WALES Ph.D. Thesis Abstract Only
Douglas Nichol 21 Jun. 1986 255 p
Avail: Issuing Activity

A detailed sedimentological and mineralogical study was undertaken in the Early Permian Koogah Formation which is located a little to the northeast of Wingen in the Hunter Valley, NSW, with the principal objective being a better understanding of the conditions responsible for the development of this unusual sedimentary unit. From the outset it was realized that the formation comprises two distinctive and to some extent contrasting facies: that forming the lower part, consisting essentially of kaolinite clayrocks or flint clays up to 75 meters thick; and that constituting the upper section almost entirely of quartz-lithic sandstones and conglomerates. Nevertheless coal seams are generally lenticular and non-commercial are common to both facies. The Lower Koogah Formation is underlain by the Werrie Basalts, a two kilometer thick lava pile composed of fractionated alkaline basalt flows. The topmost flows are altered due to chemical weathering and several alteration profiles exist. Analysis of vertical sequences within the Lower Koogah Formation enabled four lithofacies to be identified. The Upper Koogah Formation consists of conglomerates, sandstones, siltstones, shales, and coals with minor interbeds of kaolinite clayrocks and are typical coal measures deposited in a floodplain setting. The body of evidence favors an allochthonous origin for the bulk of the kaolinite clayrocks. Author

N88-25088 Deutscher Wetterdienst, Hamburg (West Germany).
RESULTS OF RADIATION MEASUREMENTS IN WEST GERMANY AND FROM SPECIAL MEASUREMENT SERIES IN THE METEOROLOGICAL OBSERVATORY OF HAMBURG [ERGEBNISSE VON STRAHLUNGSMESSUNGEN IN DER BUNDESREPUBLIK DEUTSCHLAND SOWIE VON SPEZIELLEN MESSREIHEN AM METEOROLOGISCHEN OBSERVATORIUM, HAMBURG]
1987 134 p In GERMAN
(Rept-11; ETN-88-91952) Avail: Deutscher Wetterdienst, Frahmredder 95, D-2000 Hamburg 95, Fed. Republic of Germany

Results of radiation measurements carried out in West Germany during the year 1986 are given. The main parameters for short wave solar radiation and long wave terrestrial radiation presented are: global radiation, direct and diffuse solar radiation, terrestrial reflected radiation, atmospheric and terrestrial thermal radiation, and global radiation balance. ESA

N88-25089# Laboratoire de Meteorologie Dynamique, Paris (France). Groupe Analyse du Rayonnement Atmospherique.
THREE-DIMENSIONAL TEMPERATURE FIELDS IN THE ATMOSPHERE UP TO 50 km ALTITUDE Final Report [CHAMPS TRI-DIMENSIONNELS DE TEMPERATURE DE L'ATMOSPHERE TERRESTRE JUSQU'A 50 KM D'ALTITUDE]
A. Chedin and Melle Moine Jan. 1987 125 p In FRENCH
(Contract DRET-84-140)
(ETN-88-92150) Avail: NTIS HC A06/MF A01

Temperature profiles, atmospheric density, and geostrophic wind gradient were studied from TIROS-N series satellite observations. The analysis is based on the stratospheric sounding unit TIROS experiment. An algorithm to determine the three dimensional atmospheric temperature profile was developed. It is based on a multilinear regression estimating technique. The comparison of results with data from lidar and rocket sounding are satisfactory. ESA

N88-25090# Center for Mathematics and Computer Science, Amsterdam (Netherlands). Dept. of Applied Mathematics.
ANALYSIS OF A SIX-COMPONENT BAROTROPIC SPECTRAL MODEL: CHAOTIC MOTION, PREDICTABILITY AND VACILLATION
H. E. deSwart Dec. 1987 28 p

(CWI-AM-R8710; B8805669; ETN-88-92583) Copyright Avail: NTIS HC A03/MF A01

A low-order spectral model of the barotropic potential vorticity equation in a beta-plane channel is considered. Its physical and mathematical properties are investigated by a numerical bifurcation analysis of the steady states and periodic solutions. The two parameters varied are the external forcing and width-length ratio of the channel with which the topographic and barotropic instability mechanisms can be controlled, respectively. The existence of solutions describing a flow with a limited predictability and which can vacillate between different preferent regimes is considered. It appears that, depending on the parameter values and initial conditions, the long-term behavior of the flow can be either stationary, periodic, quasi-periodic or chaotic. An important scenario is found which leads to the generation of strange attractors. It includes the occurrence of homoclinic orbits for specific parameter values, which connect an unstable stationary point with itself. For nearby parameter values chaotic orbits exist which move in small tubes around the homoclinic orbits, in agreement with Silnikov's theory. The chaotic motion, characterized by a positive Lyapunov exponent, describes irregular flow predictable on a time scale given by the reciprocal of this exponent. However, despite its interesting properties the model cannot describe transitions between different preferent regimes. It is argued that this is due to the structure of the equations as well as to the severe truncation of the spectral expansions. ESA

N88-25091# Southwest Research Inst., San Antonio, Tex. Dept. of Space Sciences.

DYNAMICS EXPLORER-2 MEASUREMENTS DURING AN ISOLATED AURORAL SUBSTORM

J. R. Sharber and J. D. Winningham 18 Oct. 1987 17 p Presented at the 3rd Finnish-American Auroral Workshop, Sodankyla, Finland, 14-18 Oct. 1985

(Contract F49620-86-C-0029; Grant NSF INT-85-09939)

(AD-A191202; AFOSR-88-0112TR) Avail: NTIS HC A03/MF A01 CSCL 04A

On December 15, 1981 an isolated substorm, preceded by a clear southward turning of the Interplanetary Magnetic Field occurred over the Finland/Scandinavian sector. This paper uses particle and plasma flow measurements from the Dynamics Explorer-2 satellite to provide global information on the substorm development. GRA

N88-25092*# Massachusetts Inst. of Tech., Cambridge. Earth Resources Lab.

THE INTERPRETATION OF CRUSTAL DYNAMICS DATA IN TERMS OF PLATE INTERACTIONS AND ACTIVE TECTONICS OF THE ANATOLIAN PLATE AND SURROUNDING REGIONS IN THE MIDDLE EAST Semiannual Report, 15 Sep. 1987 - 14 Mar. 1988

M. Nafi Toksoz 8 Jul. 1988 4 p

(Grant NAG5-753)

(NASA-CR-183024; NAS 1.26:183024) Avail: NTIS HC A02/MF A01 CSCL 08G

The long-term objective of this project is to interpret NASA's Crustal Dynamics measurements (SLR) in the Eastern Mediterranean region in terms of relative plate movements and intraplate deformation. The approach is to combine realistic modeling studies with analysis of available geophysical and geological observations to provide a framework for interpreting NASA's measurements. This semi-annual report concentrates on recent results regarding the tectonics of Anatolia and surrounding regions from ground based observations. Also reported on briefly is progress in the use of the Global Positioning System to densify SLR observations in the Eastern Mediterranean. Reference is made to the previous annual report for a discussion of modeling results. Author

N88-25093*# California Inst. of Tech., Pasadena. Div. of Geological and Planetary Sciences.

PHOTOCHEMICAL AND THERMAL MODELING IN THE EARLY ATMOSPHERE OF THE EARTH Final Report, 1 Oct. 1981 - 31 Dec. 1987

Yuk L. Yung 12 Jul. 1988 3 p

(Grant NAGw-254)

(NASA-CR-183029; NAS 1.26:183029) Avail: NTIS HC A02/MF A01 CSCL 04A

The simplest carbon compounds, present in the terrestrial and planetary atmospheres, exhibit a wide range of oxidation states, carbon dioxide and methane being the most oxidized and the most reduced form of carbon, respectively. The question arises as to the origin and the interconversion among the carbon species. The chemical pathways for the conversion of CH4 to CO and CO2 are for the most part known. The reverse process, the reduction of CO to CH4 is however, poorly understood. A new reaction is proposed, H2CO + H + M yields CH3O + M, which might play a fundamental role in the reduction of CO or CH4. An update is presented of nitrile photochemistry on Titan. Author

N88-25094*# National Aeronautics and Space Administration. Langley Research Center, Hampton, Va.

SAM 2 DATA USER'S GUIDE

W. P. Chu, M. T. Osborn (ST Systems Corp., Hampton, Va.), and L. R. McMaster Jul. 1988 29 p

(NASA-RP-1200; L-16377; NAS 1.61:1200) Avail: NTIS HC A03/MF A01 CSCL 04A

This document is intended to serve as a guide to the use of the data products from the Stratospheric Aerosol Measurement (SAM) 2 experiment for scientific investigations of polar stratospheric aerosols. Included is a detailed description of the Beta and Aerosol Number Density Archive Tape (BANAT), which is the SAM 2 data product containing the aerosol extinction data available for these investigations. Also included are brief descriptions of the instrument operation, data collection, processing and validation, and some of the scientific analyses conducted to date. Author

N88-25095# Tokyo Univ. (Japan). Inst. of Space and Astronautical Science.

ELECTRIC FIELD MEASUREMENT BY S-520-9 SOUNDING ROCKET USING THE TIME OF FLIGHT TECHNIQUE OF LITHIUM ION BEAM

M. Nakamura, H. Hayakawa, and K. Tsuruda [1988] 142 p

(ISAS-RN-367) Avail: NTIS HC A07/MF A01

Electric field is a fundamental parameter to understand the phenomena in space plasma, however it is not measured sufficiently. A method of the electric field measurement using the time of flight technique was developed. Artificially ejected charged particles from a spacecraft or a sounding rocket into the space plasma return to the origin when the direction of the ejection is perpendicular to both the magnetic field and the electric field. The time of light of the return particles includes the information of the magnetic field and the electric field as the particles' motion is controlled by these quantities. Measurement of the time of flight of the particles gives the magnitudes of these fields. The direction of the electric field is derived from the return beam direction, so that the electric field is measured as a vector quantity. This method is applied to the electric field measurement in the ionosphere using the lithium ion as a tracer by the sounding rocket S-520-9 which was launched in January 1987, from Kagoshima Space Center. The experiment was carried out successfully and the electric field in the rocket frame was measured with the accuracy of 0.3 mV/m. The magnetic field was measured simultaneously with the accuracy of 2 nT. Author

47 METEOROLOGY AND CLIMATOLOGY

Includes weather forecasting and modification.

N88-25096# National Center for Atmospheric Research, Boulder, Colo.
EVALUATION OF NMC (NATIONAL METEOROLOGICAL CENTER) GLOBAL ANALYSES: 1979-1987
K. E. Trenberth and J. G. Olson Jan. 1988 87 p
(Grant NSF-ATM-87-09659)
(PB88-178157; NCAR/TN-299-STR) Avail: NTIS HC A05/MF A01 CSCL 04B

In order to make optimal use of the data set of global analyses from the U.S. National Meteorological Center (NMC), it is necessary to know of any problems that might exist and the effects of any changes in the operational system that produced the analyses. The researchers have summarized what is known about the analyses and produced under the Global Data Assimilation System (GDAS) and carried out a number of tests of their internal consistency. They have identified the missing analyses in the data and days where something clearly went wrong in the operational analysis and forecast cycle as revealed in the internal consistency checks. They recommend that such days should be omitted from all compilations of climatological statistics or in other uses of the data set such as forecasting experiments. A detailed chronology of the changes in GDAS has been compiled and they have identified the main impacts on the analyses. Discontinuities are found in certain characteristics of the analyses in most cases. These give rise to spurious trends in the data and can lead to false impressions as to what the real anomalies are. There is excessive noise in the tropics prior to May 1980 and the analyses south of 55 deg S are of very limited value for most of the record. GRA

N88-25097# National Oceanographic Data Center, Washington, D. C.
MARINERS WEATHER LOG, VOLUME 32, NUMBER 1, WINTER 1988 Quarterly Report
1988 75 p
(PB88-173869) Avail: NTIS HC A04/MF A01; also available SOD HC $3.50 as 703-029-00013-2 CSCL 04B

Various articles relating to meteorological data are reported. Some of the topics are: Surf out of the storm; Lightships; North Atlantic tropical cyclones, 1987; Anatomy of a monster; Beyond the rainbow; Marine observations program; PMO report; The mailbag; Tips to the radio officer; and Hurricane alley. Author

N88-25098# National Center for Atmospheric Research, Boulder, Colo.
TAIWAN AREA MESOSCALE EXPERIMENT: P-3 AIRCRAFT OPERATIONS SUMMARY
D. P. Jorgensen and M. A. LeMone Jan. 1988 77 p
(Grant NSF-ATM-87-09659)
(PB88-169073; NCAR/TN-304-STR) Avail: NTIS HC A05/MF A01 CSCL 04B

The P-3 Aircraft, operated by the Office of Aircraft Operations of the U.S. NOAA, was a vital part of the TAMEX data collections system. It provided data in the regions not accessible to the TAMEX ground-based observational network. This included badly needed data over the ocean which are already revealing more about the influence of the Taiwan land mass on the surrounding airflow and its embedded convection. Furthermore, unique data on mesoscale convective systems in this part of the world were collected on several occasions. On a few lucky occasions, the aircraft was able to fly in the vicinity of the ground-based Doppler radars, enabling further coverage of the precipitating convection in the area and perhaps providing an opportunity at last to compare fields retrieved from Doppler radar to those directly measured by the aircraft. Enroute to and from the missions, the P-3 also collected occasional vertical soundings of the wind and thermodynamic fields, which should improve the data set for observational case study analyses, and numerical model initialization and verification. GRA

N88-25099# Reading Univ. (England). Dept. of Meteorology.
REPORT ON PROJECT WIND: PRELIMINARY EXPERIMENTS W ITH THE UK METEOROLOGICAL OFFICE MESOSCALE MODEL, SEPTEMBER 1987 Interim Report No. 2
28 Oct. 1987 12 p
(Contract DAJA45-87-C-0035)
(AD-A191621) Avail: NTIS HC A03/MF A01 CSCL 04B

The Meteorological Office (MO) mesoscale model has been run for the simulation of the summer flow on 27 June 1985 in the Sacramento Valley, California. The purpose is to examine its predictive capability using the meso-Beta high resolution observations that were obtained during Phase I of U.S. Army Project WIND and compare with it similar runs made with the ASL SIGMET model. The simulated region is a 460 X 460 km area centered at (39.75 N, 121.8 W) as in the SIGMET simulation by Williams et al., (1986). Three simulations were performed with the same topography, horizontal grid spacing (Delta-x Delta-y = 20 km) and period of integration, and also the same radiosonde initialization (that for Orchard, 1700 GMT) as in the SIGMET run. Fig. 1 illustrates the topography of the region, which includes an artificial apron following the SIGMET run. Three simulations were performed and their characteristics are summarized in Table 1. In the first simulation, the MO model was modified to run with vertical levels as in the SIGMET run (36, 116, 213, 330, 471, 4779, 6219 m) while the other experiments, Numbers 2 and 3, were run with the vertical spacings and number of levels (16) used by the operational MO mesoscale model simulations. In the third run the evaporation resistance was increased from 100 to 500 s/m resulting in effectively reducing the evaporation to nearly zero. This reflects the relatively dry conditions over the Sacramento Valley at that time. GRA

N88-25100# Miami Univ., Fla. Div. of Meteorology and Physical Oceanography.
OBSERVATION OF STRATIFORM RAIN WITH 94 GHz AND s-B AND DOPPLER RADAR Scientific Report No. 1
Roger M. Lhermitte 30 Sep. 1987 23 p
(Contract F19628-87-C-0106)
(AD-A192013; AFOSR-87-0268TR) Avail: NTIS HC A03/MF A01 CSCL 17I

This is a report of a pilot experiment, which took place at the AFGL site in Sudbury, MA. This experiment was concerned with the testing and operation of a 94 GHz radar to be used in a project devoted to the study of stratiform rain characteristics and evolution. Some of the data collected during the test are presented. The main experiment involving several radars operating at different wavelengths is scheduled to take place in November 1987 at the same site. GRA

N88-25101# Stanford Univ., Calif. Center for Large Scale Scientific Computation.
ADAPTIVE GRID REFINEMENT FOR NUMERICAL WEATHER PREDICTION Ph.D. Thesis
William C. Skamarock Oct. 1987 137 p
(Contracts N00014-82-K-0335; N00014-84-K-0267)
(AD-A192172; CLASSIC-87-05) Avail: NTIS HC A07/MF A01 CSCL 04B

This dissertation describes the application of an adaptive solution technique to the dynamical equations used in numerical weather models. The adaptive technique employed is that of Berger and Oliger. It uses a finite difference method to integrate the dynamical equations first on a coarse grid and then on finer grids. The location of the fine grids is determined using a Richardson-type estimate of the truncation error in the coarse grid solution. By correctly coupling the integrations on the various grids, periodically re-estimating the error and recreating the finer grids, approximately uniformly accurate solutions are economically produced. GRA

N88-25102# Los Alamos National Lab., N. Mex.
THEORETICAL BASIS FOR AN EXPERIMENTAL TEST WITH REGARD TO THE ORIGIN OF VHF (VERY HIGH FREQUENCY) RADIATION FROM NATURAL LIGHTNING

J. P. Mondt May 1988 26 p
(Contract W-7405-eng-36)
(DE88-007535; LA-11276-MS) Avail: NTIS HC A03/MF A01

The VHF radiation from a return stroke is known to commence only several tens of microseconds after the electrostatic field change caused by the return stroke. One long-held interpretation of this delay restricts the emission to the in-cloud portion of the return stroke. This interpretation correlates positively with reports on laboratory observations of UHF and VHF radiation associated with corona breakdown of droplets. On the other hand, a recent study shows that an apparent delay of VHF radiation from return strokes should be expected on the basis of ground-wave attenuation. However, the study does not settle the question of the very existence of attenuated signals from low altitude commensurate with the source strength inferred from higher, i.e., unattenuated, portions of the return stroke. The purpose of this report is to provide the theoretical basis and motivation for a quantitative determination of VHF radiation from the lower portion of the return stroke. A conclusive experiment would reveal whether the VHF radiation from return strokes is primarily caused by corona breakdown of water droplets or by processes operative in dry air as well. DOE

N88-25103# Arizona Univ., Tucson. Inst. of Atmospheric Physics.
ANALYSIS OF LIGHTNING FIELD CHANGES DURING ACTIVE THUNDERSTORMS IN FLORIDA
William J. Koshak and E. Philip Krider 11 Feb. 1987 64 p Submitted for publication
Avail: NTIS HC A04/MF A01

Data from a ground-based network of electric field-mills at the NASA Kennedy Space Center were computer-analyzed to determine the parameters of the point-charge (Q) and point-dipole (P) models that describe large lightning-caused changes in thunderstorm electric fields. An algorithm that identifies the proper field-change values under active storm conditions will be described, and the data for portions of two active thunderstorms on July 6 and 31, 1978, will be presented. It was found that the altitudes, magnitudes, and time variations of the Q-parameters in the active storms are similar to those in small storms. In general, the Q-parameters appear to be independent of the overall time-development of the storm and the flashing rate. Conversely, the parameters of P-model solutions vary with time within a given storm interval and from storm to storm. In general, the P-vectors below 6 km all tend to point upward, and those at high altitude tend to point downward. When a P-solution is located in the altitude range corresponding to Q-altitudes, the direction of P tends to be horizontal. Since Q-solutions typically describe cloud-to-ground lightning and P-solutions cloud discharges, the altitude dependence of the P vectors charge at altitudes corresponding to the Q-altitudes. Author

N88-25104# Clermont-Ferrand Univ. (France). Lab. Associe de Meteorologique Physique.
ICE FORMATION ON AIRCRAFT Final Report [GIVRAGE DES AERONEFS]
J. F. Gayet Dec. 1986 15 p In FRENCH
(Contract DRET-85-34-016)
(ETN-88-92154) Avail: NTIS HC A03/MF A01

he in-flight icing measurements carried out onboard a Transall aircraft are discussed. A total of 50 flight hr for different meteorological conditions were included. The data acquisition system allowed the recording of one and two dimensional parameters, including microphysics, thermodynamic, dynamic, and electrical data with 10 min resolution. The interpretation of the results clarifies problems about the localization of icing zones and electric fields in highly convective clouds. ESA

N88-25105*# Tennessee Univ. Space Inst., Tullahoma.
METEOROLOGICAL AND ENVIRONMENTAL INPUTS TO AVIATION SYSTEMS
Dennis W. Camp, ed. and Walter Frost, ed. Jun. 1988 226 p Workshop held in Tullahoma, Tenn., 12-14 Mar. 1985; sponsored by NASA, Washington, NOAA, FAA, DOD, and Office of the Federal Coordinator for Meteorology
(NASA-CP-2498; L-16338; NAS 1.55:2498) Avail: NTIS HC A11/MF A01 CSCL 04B

Reports on aviation meteorology, most of them informal, are presented by representatives of the National Weather Service, the Bracknell (England) Meteorological Office, the NOAA Wave Propagation Lab., the Fleet Numerical Oceanography Center, and the Aircraft Owners and Pilots Association. Additional presentations are included on aircraft/lidar turbulence comparison, lightning detection and locating systems, objective detection and forecasting of clear air turbulence, comparative verification between the Generalized Exponential Markov (GEM) Model and official aviation terminal forecasts, the evaluation of the Prototype Regional Observation and Forecast System (PROFS) mesoscale weather products, and the FAA/MIT Lincoln Lab. Doppler Weather Radar Program. For individual titles, see N88-25106 through N88-25118.

N88-25106*# National Weather Service, Silver Spring, Md.
AUTOMATION OF SURFACE OBSERVATIONS PROGRAM
Steve E. Short *In* Tennessee Univ. Space Inst., Tullahoma. Meteorological and Environmental Inputs to Aviation Systems Jun. 1988 p 25-39 (For primary document see N88-25105 18-47)
Avail: NTIS HC A11/MF A01 CSCL 04B

At present, surface weather observing methods are still largely manual and labor intensive. Through the nationwide implementation of Automated Surface Observing Systems (ASOS), this situation can be improved. Two ASOS capability levels are planned. The first is a basic-level system which will automatically observe the weather parameters essential for aviation operations and will operate either with or without supplemental contributions by an observer. The second is a more fully automated, stand-alone system which will observe and report the full range of weather parameters and will operate primarily in the unattended mode. Approximately 250 systems are planned by the end of the decade. When deployed, these systems will generate the standard hourly and special long-line transmitted weather observations, as well as provide continuous weather information direct to airport users. Specific ASOS configurations will vary depending upon whether the operation is unattended, minimally attended, or fully attended. The major functions of ASOS are data collection, data processing, product distribution, and system control. The program phases of development, demonstration, production system acquisition, and operational implementation are described. J.P.B.

N88-25107*# Meteorological Office, Bracknell (England).
BRACKNELL METEOROLOGICAL OFFICE
Colin R. Flood *In* Tennessee Univ. Space Inst., Tullahoma. Meteorological and Environmental Inputs to Aviation Systems Jun. 1988 p 41-51 (For primary document see N88-25105 18-47)
Avail: NTIS HC A11/MF A01 CSCL 04B

The Bracknell (U.K.) Meteorological Office runs a global weather model twice a day, providing the following data: surface and radiosonde; aircraft reports; and satellite soundings and wind. A human forecast is made every six hours. The model runs on a 150 km grid with 15 levels, and takes about four minutes on a Cyber-205. The standard output from the global products are wind, temperature, height, tropopause, and maximum wind. Various experiments have been conducted to see if short-range forecasters could improve on the upper-wind forecasts over the numerical model; the numerical model remains of paramount importance. Small-scale models are being run in the U.S. and the U.K. A fine-mesh model covers Europe and the Atlantic. A mesoscale model is under development. A great deal of verification work is done to see how good the models are. J.P.B.

N88-25108*# National Oceanic and Atmospheric Administration, Boulder, Colo. Wave Propagation Lab.
SPECIAL OBSERVATIONS
Donald Beran *In* Tennessee Univ. Space Inst., Tullahoma. Meteorological and Environmental Inputs to Aviation Systems Jun. 1988 p 53-65 (For primary document see N88-25105 18-47)
Avail: NTIS HC A11/MF A01 CSCL 04B

The wind or temperature profiler is a new special observation device designed to supplement traditional atmospheric measurement and provide more accurate middle-range forecasts, including aviation and space applications. Radar is most useful in the short, nowcast time frame. Satellites and surface observations are also most useful for short-range forecasts but have less impact on the longer range. The radiosonde network, on the other hand, only starts to be very important after about six hours and has greatest impact at lead times of 12 hours or more. In the wind profiler, wind is measured by using clear-air Doppler radar principles, Two fixed beams, pointing 15 deg to the north and 15 deg to the east, sense the Doppler shift. The resulting wind vectors are then rotated to the horizontal and combined to give total wind. The temperature profiler measures temperature and humidity by using passive radiometers. Development on the profiler is 95 percent complete, and on the temperature profiler 75 percent complete. J.P.B.

N88-25109*# Fleet Numerical Oceanography Center, Monterey, Calif.
APPLICATIONS PRODUCTS OF AVIATION FORECAST MODELS
John P. Garthner *In* Tennessee Univ. Space Inst., Tullahoma. Meteorological and Environmental Inputs to Aviation Systems Jun. 1988 p 67-77 (For primary document see N88-25105 18-47)
Avail: NTIS HC A11/MF A01 CSCL 04B

A service called the Optimum Path Aircraft Routing System (OPARS) supplies products based on output data from the Naval Oceanographic Global Atmospheric Prediction System (NOGAPS), a model run on a Cyber-205 computer. Temperatures and winds are extracted from the surface to 100 mb, approximately 55,000 ft. Forecast winds are available in six-hour time steps. J.P.B.

N88-25110*# Aircraft Owners and Pilots Association, Frederick, Md.
GENERAL-AVIATION'S VIEW OF PROGRESS IN THE AVIATION WEATHER SYSTEM
Douglas J. Lundgren *In* Tennessee Univ. Space Inst., Tullahoma. Meteorological and Environmental Inputs to Aviation Systems Jun. 1988 p 79-85 (For primary document see N88-25105 18-47)
Avail: NTIS HC A11/MF A01 CSCL 04B

For all its activity statistics, general-aviation is the most vulnerable to hazardous weather. Of concern to the general aviation industry are: (1) the slow pace of getting units of the Automated Weather Observation System (AWOS) to the field; (2) the efforts of the National Weather Service to withdraw from both the observation and dissemination roles of the aviation weather system; (3) the need for more observation points to improve the accuracy of terminal and area forecasts; (4) the need for improvements in all area forecasts, terminal forecasts, and winds aloft forecasts; (5) slow progress in cockpit weather displays; (6) the erosion of transcribed weather broadcasts (TWEB) and other deficiencies in weather information dissemination; (7) the need to push to make the Direct User Access Terminal (DUAT) a reality; and (7) the need to improve severe weather (thunderstorm) warning systems. J.P.B.

N88-25111*# FWG Associates, Inc., Tullahoma, Tenn.
AIRCRAFT/LIDAR TURBULENCE COMPARISON
Kao-Huah Huang *In* Tennessee Univ. Space Inst., Tullahoma. Meteorological and Environmental Inputs to Aviation Systems Jun. 1988 p 103-113 (For primary document see N88-25105 18-47)
Avail: NTIS HC A11/MF A01 CSCL 04B

Very good agreement between remotely sensed winds using a ground-based Doppler lidar and in situ measurements with an instrumented aircraft is possible. Results show that turbulence intensities computed from time histories measured with the aircraft and time histories of the radial wind measured with lidar can be analyzed statistically to provide turbulence intensities and turbulence spectra which agree well with one another. The results further show that the second moment data, as presently compared with the NASA/MSFC algorithms, do not provide meaningful comparisons with turbulence intensities measured with the aircraft. This disagreement, however, must be investigated further in terms of the accuracy of the second moment data determined by both the lidar hardware and the algorithm for computing the second moment. Author

N88-25112*# Commerce Dept., Rockville, Md. Office of the Federal Coordinator for Meteorology.
LIGHTNING DETECTION AND LOCATING SYSTEMS
Russell L. Hovey *In* Tennessee Univ. Space Inst., Tullahoma. Meteorological and Environmental Inputs to Aviation Systems Jun. 1988 p 115-120 (For primary document see N88-25105 18-47)
Avail: NTIS HC A11/MF A01 CSCL 04B

U.S. agency and agency-sponsored programs for lightning detection are listed. Research and development in the area of lightning sensors is described. J.P.B.

N88-25113*# Analytic Sciences Corp., Reading, Mass.
NATIONAL PLANS FOR AIRCRAFT ICING AND IMPROVED AIRCRAFT ICING FORECASTS AND ASSOCIATED WARNING SERVICES
Ralph P. Pass *In* Tennessee Univ. Space Inst., Tullahoma. Meteorological and Environmental Inputs to Aviation Systems Jun. 1988 p 121-123 (For primary document see N88-25105 18-47)
Avail: NTIS HC A11/MF A01 CSCL 04B

Recently, the United States has increased its activities related to aircraft icing in numerous fields: ice phobics, revised characterization of icing conditions, instrument development/evaluation, de-ice/anti-ice devices, simulated supercooled clouds, computer simulation and flight tests. The Federal Coordinator for Meteorology is involved in two efforts, one a National Plan on Aircraft Icing and the other a plan for Improved Aircraft Icing Forecasts and Associated Warning Services. These two plans will provide an approved structure for future U.S. activities related to aircraft icing. The recommended activities will significantly improve the position of government agencies to perform mandated activities and to enable U.S. manufacturers to be competitive in the world market. J.P.B.

N88-25114*# Dayton Univ., Ohio.
OBJECTIVE DETECTION AND FORECASTING OF CLEAR-AIR TURBULENCE (CAT): A STATUS REPORT
John L. Keller *In* Tennessee Univ. Space Inst., Tullahoma. Meteorological and Environmental Inputs to Aviation Systems Jun. 1988 p 125-132 (For primary document see N88-25105 18-47)
Avail: NTIS HC A11/MF A01 CSCL 04B

Clear-air turbulence has become the largest single cause of weather-related injuries occurring in commercial carriers at cruising altitudes. A technique for objective operational CAT detection (the SCATR index) has been formulated. Its physical basis ties CAT to total energy dissipation as a response to meso- and synoptic-scale dynamical processes associated with upper-level jet stream/frontal zones. Early case studies using properly analyzed routine RAOB rawinsonde sounding data have shown promise. J.P.B.

N88-25115*# National Weather Service, Silver Spring, Md. Techniques Development Lab.
COMPARATIVE VERIFICATION BETWEEN GEM MODEL AND OFFICIAL AVIATION TERMINAL FORECASTS
Robert G. Miller *In* Tennessee Univ. Space Inst., Tullahoma. Meteorological and Environmental Inputs to Aviation Systems Jun. 1988 p 133-138 (For primary document see N88-25105 18-47)
Avail: NTIS HC A11/MF A01 CSCL 04B

The Generalized Exponential Markov (GEM) model uses the local standard airways observation (SAO) to predict hour-by-hour the following elements: temperature, pressure, dew point depression, first and second cloud-layer height and amount, ceiling, total cloud amount, visibility, wind, and present weather conditions. GEM is superior to persistence at all projections for all elements

in a large independent sample. A minute-by-minute GEM forecasting system utilizing the Automated Weather Observation System (AWOS) is under development. J.P.B.

N88-25116*# National Weather Service, Silver Spring, Md. Aviation Services Branch.
COMPUTER AND MODEL CHANGES AT NATIONAL METEOROLOGICAL CENTER (NWC) **c61**
Charles H. Sprinkle *In* Tennessee Univ. Space Inst., Tullahoma. Meteorological and Environmental Inputs to Aviation Systems Jun. 1988 p 139-143 (For primary document see N88-25105 18-47)
Avail: NTIS HC A11/MF A01 CSCL 09B

New models, hardware, and software packages in use at the National Meteorological Center (NMC) are described. J.P.B.

N88-25117*# National Oceanic and Atmospheric Administration, Boulder, Colo.
DENVER ARTCC EVALUATION OF PROFS (PROTOTYPE REGIONAL OBSERVATIONS AND FORECAST SYSTEM) MESOSCALE WEATHER PRODUCTS
John W. Hinkelman *In* Tennessee Univ. Space Inst., Tullahoma. Meteorological and Environmental Inputs to Aviation Systems Jun. 1988 p 145-153 (For primary document see N88-25105 18-47)
Avail: NTIS HC A11/MF A01 CSCL 04B

The Denver Air Traffic Control Center has had a Prototype Regional Observation and Forecast System (PROFS) display system since the spring of 1982. Outputs of the system are presented and explained. J.P.B.

N88-25118*# Massachusetts Inst. of Tech., Lexington.
THE FEDERAL AVIATION ADMINISTRATION/MASSACHUSETTS INSTITUTE OF TECHNOLOGY (FAA/MIT) LINCOLN LABORATORY DOPPLER WEATHER RADAR PROGRAM **c32**
James E. Evans *In* Tennessee Univ. Space Inst., Tullahoma. Meteorological and Environmental Inputs to Aviation Systems Jun. 1988 p 155-166 Sponsored by FAA (For primary document see N88-25105 18-47)
Avail: NTIS HC A11/MF A01 CSCL 20N

The program focuses on providing real-time information on hazardous aviation weather to end users such as air traffic control and pilots. Existing systems will soon be replaced by a Next Generation Weather Radar (NEXRAD), which will be concerned with detecting such hazards as heavy rain and hail, turbulence, low-altitude wind shear, and mesocyclones and tornadoes. Other systems in process are the Central Weather Processor (CWP), and the terminal Doppler weather radar (TDWR). Weather measurements near Memphis are central to ongoing work, especially in the area of microbursts and wind shear. J.P.B.

N88-25119# National Weather Service, Honolulu, Hawaii.
TROPICAL CYCLONES, 1987: CENTRAL NORTH PACIFIC
W. Au, A. Chun, and H. Rosendal Apr. 1988 45 p
(PB88-188081; NOAA-TM-NWSTM-PR-33) Avail: NTIS HC A03/MF A01 CSCL 04B

Tropical Storm FERNANDA crossed 140W and into the central Pacific Hurricane Center's area of responsibility on July 26 at 0000 UTC. FERNANDA developed about 48 hours earlier near 11N 130W as Tropical Depression NINE-E and subsequently attained tropical storm strength 24 hours later near 11N 136W. This system developed farther west than usually is the case for eastern Pacific tropical cyclones. Assuming the normal cycle of development, FERNANDA appeared to be in a location favorable for further intensification and movement toward the Hawaiian Islands. The unfavorable environment created by the closing upper trough began to have its effect on FERNANDA by the 26th when it was near 13N 142W. The storm failed to intensify and showed signs of becoming sheared and elongated in a northeast/southwest direction. Air Force reconnaissance into the storm of the 27th verified previous estimations of maximum winds using Dvorak classification techniques. Author

48 OCEANOGRAPHY

Includes biological, dynamic, and physical oceanography; and marine resources.

For related information see also *43 Earth Resources and Remote Sensing.*

N88-25120# Cornell Univ., Ithaca, N.Y. Dept. of Geological Sciences.
TO RELATE MEASUREMENTS OF GRAVITY AND GEOID ANOMALIES OVER THE OCEANS TO NEAR SURFACE DENSITY DISTRIBUTIONS Final Technical Report
Donald L. Turcotte 1987 2 p
(Contract N00014-85-K-0063)
(AD-A192168) Avail: NTIS HC A02/MF A01 CSCL 08E

One of the principal objectives of the research is to understand the relationship between the measured geoid and gravity anomalies and bathymetric anomalies. The principal approach was to use the Haxby-Ockendon-Turcotte (HOT) geoid formula to relate the oceanic geoid to the structure of the oceanic lithosphere. Significant progress has been made on correlating geoid spectra with bathymetry spectra. Various models for relating bathymetry to geoid have been applied to this problem from uncompensated topography to partial compensation at a variety of depths. A second objective of our research was to develop a fundamental understanding of the morphology of the sea floor. This research followed two lines, the first used synthetic stratigraphy in order to understand how continental margins evolved and the second used the fractal character of the spectrum of oceanic bathymetry and oceanic geoid in order to better understand fundamental origins of bathymetry and geoid anomalies. GRA

N88-25121# Sippican Ocean Systems, Inc., Marion, Mass.
EXPENDABLE CONDUCTIVITY, TEMPERATURE AND DEPTH SYSTEM (XCTD) DEVELOPMENT PROGRAM Final Report
Richard W. Lancaster 30 Jan. 1988 139 p
(Contract N00014-82-C-0579)
(AD-A192182; R-2119) Avail: NTIS HC A07/MF A01 CSCL 08C

It was the objective of the expendable conductivity, temperature and depth (XCTD) development program to develop and test an expendable instrument system capable of providing ocean salinity to an overall accuracy of 0.05 parts per thousand. Table 1.1 is a summary of the design goals. A workable XCTD system has emerged from the development work pursued to date. An XCTD probe subsystem design has been built and tested at sea that provides data from the surface to 1000 meters as required. A deck gear subsystem, with supporting host computer software has been demonstrated in the laboratory and at sea. The calibration techniques have been developed that permit accurate calibration of probes in prototype quantities. GRA

N88-25122# Science Applications International Corp., College Station, Tex.
HIGHER FREQUENCY AMBIENT NOISE IN THE ARCTIC OCEAN Technical Report, 1 Jan. - 31 Dec. 1987
James K. Lewis and Warren W. Denner Jan. 1988 28 p
(Contract N00014-87-C-0115)
(AD-A192203; SAIC-87/1868) Avail: NTIS HC A03/MF A01 CSCL 20A

Higher frequency (1000 Hz) arctic ambient noise episodes during non-summer months were used to study generating mechanisms. In most cases, thermal fracturing of sea ice was responsible. A suite of heating and cooling processes that relate to thermal fracturing of sea ice were considered. Numerical simulations with a daily heating cycle and no snow cover implied that maximum noise levels occurred at 1900 hrs local. Radiational heat balances are more important than sensible heat flux in producing fracturing of sea ice. With snow cover, the amount of ice fracturing is reduced. A daily heating cycle produces maximum fracturing at 0300 to 0800 hrs local, a common feature seen in observed noise data. Simulations were made using observed Arctic Ocean solar radiation, air temperature, wind speed, albedo, and cloud cover from the spring of 1976. The agreement between the

model ice fracturing parameter and the observed 1000 Hz noise levels was excellent. However, results indicate that blowing snow and ice fog may be additional factors in the heat flux balance of sea ice. The short space scales of higher frequency, arctic ambient noise are likely a result of spatial variations in snow cover. GRA

N88-25123# Science Applications International Corp., McLean, Va.
IDENTIFICATION AND ACOUSTIC CHARACTERIZATION OF SEAMOUNTS
A. I. Eller and L. Haines 30 Nov. 1987 75 p
(Contract N00014-86-D-0137)
(AD-A192204; SAIC-87/1722) Avail: NTIS HC A04/MF A01 CSCL 08C

The presence of seamounts introduces a discrimination problem between acoustic returns from these geological features and from targets. The returns from seamounts can be quite large and can extend over long periods of time. A process has been developed which will efficiently extract, identify and acoustically characterize seamounts. This process extracts seamounts from an area of ocean and estimates their location, height, base area and acoustic target strength. Separate treatment of seamounts is necessary because the baseline model, is likely to miss individual seamounts that lie between the radials. This report describes seamount statistics, origins and summarizes bathymetric processing approaches used to extract them. The performance of the extraction software is evaluated by comparing a digitally derived database to a manually derived one. Seamount reverberation papers and seamount size statistics are presented along with a first order approximation of seamount target strengths. GRA

N88-25124# Institute of Oceanographic Sciences, Wormley (England).
SEASOAR PROFILES IN THE ICELAND-SCOTLAND AREA, MAY 1987
W. J. Gould, J. F. Read, and J. Smithers 1987 47 p Sponsored in part by the United Kingdom Ministry of Defence
(IOS-253; ETN-88-92535) Avail: NTIS HC A03/MF A01; Institute of Oceanographic Sciences, Deacon Laboratory, Wormley, Godalming, Surrey GU8 5UB, United Kingdom 15 pounds

Sections of temperature, salinity, and derived parameters including sound speed were obtained using the SeaSoar towed CTD system in May in the Iceland-Faroes area, and include several crossings of the Iceland-Faroes Front. The data cover 1250 km of ship track and give information between the surface and 300 m depth. ESA

N88-25125 Miami Univ., Fla.
AN EXPERIMENTAL STUDY OF THE COHERENT UNDER-ICE REFLECTIVITY OF SOUND IN THE GREENLAND SEA MARGINAL ICE ZONE Ph.D. Thesis
Patricia L. Gruber 1987 162 p
Avail: Univ. Microfilms Order No. DA8729364

The coherent component of acoustic under-ice reflectivity was investigated as a function of frequency and grazing angle in the Marginal Ice Zone (MIZ). Measured reflectivity was compared with predictions by scattering theories to test the hypothesis of ridge scattering dominance in the MIZ. Explosive source acoustic signals were received on a vertical array during the Marginal Ice Zone Experiment (MIZEX 84), and deconvolved to separate the direct and surface-reflected arrivals. Data was available from multiple days and ranges, resulting in an ensemble of ice-scattered measurements. The surface arrivals were aligned in time and coherently averaged over grazing angle for frequency bins from 64 to 256 Hz. Coherent reflectivity decreased with grazing angle from 12 to 35 deg and with frequency from 64 to 256 Hz. Remote sensing data showed that the ice cover was primarily composed of small floes. Laser ice-surface height measurements were analyzed to infer a pressure ridge sail height distribution or surface rms roughness for input to corresponding scattering theories. The measured reflectivity was compared with reflectivity from smooth elastic plates theory, perturbation theory for a rough pressure release surface, perturbation theory for a rough elastic surface, and Burke-Twersky theory for hard and soft, infinite, semi-elliptical cylinders on a soft plane. The data-theory comparison suggests that under-ice scattering in the MIZ, at angles less than 30 deg, and frequencies less than 256, is dominated by ridge-like scattering which depends on the geometric rather than the physical properties of the ice. Dissert. Abstr.

N88-25126# Delaware Univ., Lewes. Sea Grant Coll. Program.
CONSTRUCTION OF APPROXIMATIONS TO ACOUSTIC GREEN'S FUNCTIONS FOR NONHOMOGENEOUS OCEANS USING TRANSMUTATION
R. P. Gilbert, Y. Xu, and D. H. Wood Feb. 1988 24 p Sponsored by Naval Underwater Systems Center, New London, Conn.
(PB88-185384; DEL-SG-02-88) Avail: NTIS HC A03/MF A01 CSCL 08C

Transmutation can map the solutions of one equation into solutions of another equation. Recent applications of transmutation in underwater acoustics have involved the Helmholtz equation that governs the propagation of sound in the ocean and the Sturm-Louiville problem that governs the depth dependent normal modes of the ocean. In all of these cases, the goal was to find solutions corresponding to depth dependent indices of refraction from knowing solutions for a constant index of refraction because the latter solutions are much easier to find. In the present paper the authors again use transmutation from constant to variable indices, but emphasize finding and using approximate solutions corresponding to variable indices of refraction. GRA

N88-25127# Kiel Univ. (West Germany). Inst. fuer Meereskunde.
DETERMINATION OF MESOSCALE VARIABILITY OF SEA SURFACE TEMPERATURE AND ATTENUATION IN THE NORTH ATLANTIC FROM SATELLITE MEASUREMENT Thesis [BESTIMMUNG MESOSKALIGER VARIABILITAETEN DER OBERFLAECHENTEMPERATUR UND DER ATTENUATION IM NORDATLANTIK AUS SATELLITENMESSUNGEN]
Thomas Viehoff 1987 219 p In GERMAN; ENGLISH summary
(Rept-162; ISSN-0341-8561; ETN-88-91946) Avail: NTIS HC A10/MF A01

Analyses of horizontal distributions of mesoscale variabilities and temperature were performed using data from the AVHRR and the CZCS during summer 1981 and 1983 in the area of the North Atlantic current. Sea surface temperature distributions at strong thermal fronts are comparable with the temperature of the diurnal mixed layer. At the polar front the thermal pattern is moving eastward with a relative persistence of mesoscale pattern of more than 14 days. The attenuation pattern shows a greater amount of versatility than the corresponding temperature distributions. The isotropic part of the scalar variance-spectra has a mean slope of -2.2 + or - 0.17 at scales of 10 to 100 km. Theoretically predicted spectral slopes for the temperature are -1 and -3. There are significant maxima in the variance-spectra of temperature and attenuation at scales between 50 and 250 km. ESA

51 LIFE SCIENCES (GENERAL)

N88-25128# School of Aerospace Medicine, Brooks AFB, Tex.
BEHAVIORAL RESPONSE OF RATS EXPOSED TO HIGH-POWER MICROWAVE RADIATION Interim Report, Sep. 1986 - Jan. 1987
Robert E. Cordts, James H. Merritt, David N. Erwin, Kenneth A. Hardy, and Michael G. Yochmowitz Feb. 1988 29 p
(AD-A192199; USAFSAM-TR-87-30) Avail: NTIS HC A03/MF A01 CSCL 06G

Emerging high-power microwave technologies require that bioeffects of exposure to this type of radiation be investigated for health and safety considerations. Disruption of animal behavior is reported to be a sensitive indicator of microwave exposure. Three

behavioral tasks were chosen for this initial investigation of exposure to U.S. Air Force high-power microwave emitters. The tasks were: (1) single trail avoidance, (2) water satiation, and (3) rotarod performance. Exposure to high-power microwave radiation from the USAFSAM peak power simulator significantly affected the single trial avoidance task. Neither the single trail avoidance task nor rotarod performance was affected by the Gypsy emitter. However, animals exposed to 9 kW and 11 kW outputs from the USAFSAM emitter spent significantly less time imbibing water postexposure than sham-exposed animals. The most consistent finding in the animals exposed to the Gypsy pulses was that those exposed at 4 m (13.1 ft) spent significantly less time drinking water than those exposed at 1 m (3.28 ft). This paradoxical result may be due to the complex shape of the Gypsy pulse. These data are from the first studies in a series of bioeffects studies of high-power microwave exposure. Other bioeffects investigations using these sources are under way. GRA

N88-25129*# Maryland Univ., Baltimore. Dept. of Neurology.
DEXAMETHASONE REGULATES GLUTAMINE SYNTHETASE EXPRESSION IN RAT SKELETAL MUSCLES
Stephen R. Max, Masaaki Konagaya, Yoko Konagaya, John W. Thomas, Carl Banner, and Ljubisa Vitkovic (National Inst. of Health, Bethesda, Md.) [1986] 23 p
(Grant NAG2-100)
(NASA-CR-182935; NAS 1.26:182935) Avail: NTIS HC A03/MF A01 CSCL 06B

The regulation of glutamine synthetase by glucocorticoids in rat skeletal muscles was studied. Administration of dexamethasone strikingly enhanced glutamine synthetase activity in plantaris and soleus muscles. The dexamethasone-mediated induction of glutamine synthetase activity was blocked to a significant extent by orally administered RU38486, a glucocorticoid antagonist, indicating the involvement of intracellular glucocorticoid receptors in the induction. Northern blot analysis revealed that dexamethasone-mediated enhancement of glutamine synthetase activity involves dramatically increased levels of glutamine synthetase mRNA. The induction of glutamine synthetase was selective in that glutaminase activity of soleus and plantaris muscles was not increased by dexamethasone. Furthermore, dexamethasone treatment resulted in only a small increase in glutamine synthetase activity in the heart. Accordingly, there was only a slight change in glutamine synthetase mRNA level in this tissue. Thus, glucocorticoids regulate glutamine synthetase gene expression in rat muscles at the transcriptional level via interaction with intracellular glutamine production by muscle and to mechanisms underlying glucocorticoid-induced muscle atrophy. Author

N88-25130# Rouen Univ. (France). Lab. de Toxicologie.
EVALUATION OF THE TOXICITY OF PRODUCTS FROM THE THERMAL DEGRADATION OF MATERIALS Final Report [EVALUATION DE LA TOXICITE DES PRODUITS DE DEGRADATION THERMIQUE DES MATERIAUX]
J. M. Jouany and M. Guerbet Feb. 1987 197 p In FRENCH
(Contract DRET-84-044)
(ETN-88-91995) Avail: NTIS HC A09/MF A01

Thermal decomposition risk on 15 materials selected using inflammability and toxicity criteria was studied. The experimental procedure included biological measurement on rats (mortality, injury). The results were treated using multivariate analysis in order to define categories of variables and materials. The analysis of ventilation effects shows that the concentration parameter (g/cu m) is a realistic parameter. ESA

N88-25131# Los Alamos National Lab., N. Mex.
THE HUMAN GENOME: COMPUTATIONAL CHALLENGES
G. I. Bell Feb. 1988 19 p Presented at the 3rd International Conference on Supercomputing, Boston, Mass., 15 May 1988
(Contract W-7405-eng-36)
(DE88-006465; LA-UR-88-450; CONF-880567-2) Avail: NTIS HC A03/MF A01

The deoxyribonucleic acid (DNA) of a human cell contains all the information required for specifying that cell, or indeed the whole person, and constitues the human genome. Programs are now under way to obtain genetic linkage maps and physical maps of human chromosomes containing the DNA, and large scale efforts will soon begin to provide detailed sequences. The challenges involved in assembling these data into a knowledge base are examined. Computations will play a key role in enabling the scientists to understand the information contained in sequence data. Pattern recognition and string matching algorithms will be of particular importance. Recent results in the use of adaptive networks for pattern detection will be presented. DOE

N88-25132# Oak Ridge National Lab., Tenn.
ECOLOGICAL RISK FACTORS RELATED TO ENVIRONMENTAL USES OF GENETICALLY ENGINEERED ORGANISMS
F. E. Sharples 1987 29 p Presented at the Meeting on Bioaugmentation as a Means to Enhanced Waste Treatment, New Orleans, La., 30 Aug. 1987
(Contract DE-AC05-84OR-21400)
(DE88-006674; CONF-8708224-1) Avail: NTIS HC A03/MF A01

The purpose of this paper is to discuss some of the ecological questions and conerns related to environmental applications of biotechnology. There are a number of uncertainties about the risks entailed in the use of such products. These uncertainties arise principally because of gaps in the knowledge bases in basic ecology, microbial biology and ecology, genetics, and risk assessment. The need to ensure that the benefits of biotechnology products are safely realized and that their environmental applications do not result in new sources of environmental degradation provides the fundamental rationale for systematic assessments of risk before field testing or commercial use. DOE

N88-25133*# National Aeronautics and Space Administration. John F. Kennedy Space Center, Cocoa Beach, Fla.
MONITORING BIOLOGICAL IMPACTS OF SPACE SHUTTLE LAUNCHES FROM VANDENBERG AIR FORCE BASE: ESTABLISHMENT OF BASELINE CONDITIONS
Paul A. Schmaizer and C. Ross Hinkle (Bionetics Corp., Cocoa Beach, Fla.) Dec. 1987 100 p
(NASA-TM-100982; NAS 1.15:100982) Avail: NTIS HC A05/MF A01 CSCL 06C

Space shuttle launches produce environmental impacts resulting from the formation of an exhaust cloud containing hydrogen chloride aerosols and aluminum oxide particulates. Studies have shown that most impacts occur near-field (within 1.5 km) of the launch site while deposition from launches occurs far-field (as distant as 22 km). In order to establish baseline conditions of vegetation and soils in the areas likely to be impacted by shuttle launches from Vandenberg Air Force Base (VAFB), vegetation and soils in the vicinity of Space Launch Complex-6 (SLC-6) were sampled and a vegetation map prepared. The areas likely to be impacted by launches were determined considering the structure of the launch complex, the prevailing winds, the terrain, and predictions of the Rocket Exhaust Effluent Diffusion Model (REEDM). Fifty vegetation transects were established and sampled in March 1986 and resampled in September 1986. A vegetation map was prepared for six Master Planning maps surrounding SLC-6 using LANDSAT Thematic Mapper imagery as well as color and color infrared aerial photography. Soil samples were collected form the 0 to 7.5 cm layer at all transects in the wet season and at a subsample of the transects in the dry season and analyzed for pH, organic matter, conductivity, cation exchange capacity, exchangeable Ca, Mg, Na, K, and Al, available NH3-N, PO4-P, Cu, Fe, Mn, Zn, and TKN. Author

N88-25134*# National Aeronautics and Space Administration. John F. Kennedy Space Center, Cocoa Beach, Fla.
HISTORY OF WILDLAND FIRES ON VANDENBERG AIR FORCE BASE, CALIFORNIA
Diana E. Hickson (Bionetics Corp., Cocoa Beach, Fla.) Mar. 1988 39 p

(Contract NAS10-10285)
(NASA-TM-100983; BIO-1; NAS 1.15:100983) Avail: NTIS HC A03/MF A01 CSCL 06C

The fire history of the past 50 years for Vandenberg AFB, California was determined using aerial photography, field investigation, and historical and current written records. This constitutes a record of the vegetation age classes for the entire base. The location, cause, and fuel type for sixty fires from this time period were determined. The fires were mapped and entered into a geographic infomation system (GIS) for Vandenberg. Fire history maps derived from this GIS were printed at 1:9600 scale and are on deposit at the Vandenberg Environmental Task Force Office. Although some ecologically significant plant communities on Vandenberg are adapted to fire, no natural fire frequency could be determined, since only one fire possibly caused by lightning occurred in the area now within the base since 1937. Observations made during this study suggest that burning may encourage the invasion of exotic species into chaparral, in particular Burton Mesa or sandhill chaparral, an unusual and geographically limited form of chaparral found on the base. Author

52 AEROSPACE MEDICINE

Includes physiological factors; biological effects of radiation; and effects of weightlessness on man and animals.

N88-25135# Aerospace Medical Research Labs., Wright-Patterson AFB, Ohio.
A SYSTEMS ENGINEERING BASED METHODOLOGY FOR ANALYZING HUMAN ELECTROCORTICAL RESPONSES Summary Report, Sep. 1983 - Dec. 1986
Andrew M. Junker, William H. Levison, and Richard T. Gill 20 Jul. 1987 199 p
(AD-A190809; AAMRL-TR-87-030) Avail: NTIS HC A09/MF A01 CSCL 06D

The objective of this work was to develop a systems engineering based methodology for quantifying and modeling effects of cognitive loading on human electrocortical responses in systems engineering terms. The visual-cortical response was selected as the input-output channel around which the methodology was developed. A steady-state input (a continuous sum of 10 sine waves) and a transient input (a train of pulses) were used for system stimulation. The human occipital EEG (surface electrodes at Oz and mastoids) was used as the cortical describing functions (gain and phase) and remnant spectra (background EEG). A stimulus parametric investigation indicated that sensitivity to stimulus modulation depth is unequal across frequencies, and that relatively low stimulus intensity and depth of modulation are desirable to reduce response saturation. Comparisons between transient and steady-state simulation revealed that both forms produced functionally related responses, suggesting that the visual-cortical response contains a measurable linear portion. Time domain amplitude changes corresponded to transient and steady-state gain changes. To investigate cognitive loading effects three tasks were utilized: manual tracking, grammatical reasoning, and supervisory control. Changes in visual-cortical response measures related to task loading were observed. With increased cognitive loading, alpha responders generally showed reductions in alpha band gain and remnant. GRA

N88-25136# Rockefeller Univ., New York.
MOTOR THEORY OF AUDITORY PERCEPTION Annual Technical Report, 1 Sep. 1986 - 31 Aug. 1987
Heather Williams 24 Sep. 1987 39 p
(Grant AF AFOSR-0336-86)
(AD-A192095; AFOSR-87-1563TR) Avail: NTIS HC A03/MF A01 CSCL 06C

The behavioral and neural substrate for motor processing of vocalizations exists in an animal model (the zebra finch). What had been considered a simple vocalization, learned from one model and carrying one message, proves to consist of compound sound units (syllables) arranged in a complex structure. The syllables in each vocalization are learned from several different sources or improvised, and are assembled to form a new vocalization. The vocal motor neurons have an auditory function (the muscles of the vocal organ contract slightly when the animal is presented with an auditory stimulus), the vocal motor neurons are spatially ordered according to their target muscle (and hence their vocal function), and vocal motor neurons in different pools have different auditory responses. Behavioral experiments to test whether the vocal motor system is involved in perception have been initiated. A new method for visual analysis of sounds is being tested. GRA

N88-25137 National Building Research Inst., Pretoria (South Africa).
EFFECTS OF MODERATE COLD AND HEAT STRESS ON THE POTENTIAL WORK PERFORMANCE OF INDUSTRIAL WORKERS. PART 6: THE EFFECTS OF INCREASING VAPOUR PRESSURE AT FOUR AIR TEMPERATURES ON THE PERFORMANCE AND PHYSIOLOGY OF WHITE FEMALES
R. Kok, G. B. Meese, and M. I. Lewis 1986 30 p
(PB88-124854; CSIR-RR-630-Pt-6; ISBN-0-7988-3289-4) Avail: NTIS HC E05/MF E05 CSCL 06S

Part six in the continuing series detailing the effects of moderate cold and heat stress on the potential work performance of industrial workers. The effects of increasing humidity at four air temperatures on the performance and physiology of white female workers are examined. Dissert. Abstr.

N88-25138 New South Wales Univ., Kensington (Australia). School of Biochemistry.
A CARDIOSTIMULANT PROTEIN FROM THE AUSTRALIAN RED WARATAH SEA ANEMONE, ACTINIA TENEBROSA Abstract Only. M.S. Thesis
Murray Thomson Jan. 1987 78 p
Avail: Issuing Activity

Toxic polypeptides from coelenterates can be differentiated on the basis of size into three groups, one of 2,000 to 3,000, a second with 4,000 to 6,000 and a third having molecular weights over 10,000. The first two groups of sea anemone toxins act on excitable membranes and affect mainly the fast sodium channel. At high doses members of the first group are cardio- and neurotoxins but at low doses they are useful cardiostimulants. Members of the third group are sometimes cardioactive and generally cytolytic. A cardiostimulant protein was purified to electrophoretic homogeneity from the Australian Red Waratah sea anemone Actinia tenebrosa by subjecting sulphate precipitates of A. tenebrosa extracts to gel filtration, ion exchange, and adsorption chromatography. The resulting protein Tenebrosin-I, was found to be hemolytic and have a molecular weight of 20,000. It can be classified as a group 3 sea anemone toxin. Preliminary pharmacological characterization of tenebrosin-I suggests that the molecule may exert its biological effects by forming channels in cell membranes. Additional characterization of the proteins mode of action forms the basis of this study. Author

N88-25139# Army Research Inst. of Environmental Medicine, Natick, Mass.
PHYSIOLOGICAL AND HEMATOLOGICAL RESPONSES OF MATCHED OLDER AND YOUNGER MEN DURING DRY-HEAT ACCLIMATION
Kent B. Pandolf, Bruce S. Cadarette, Michael N. Sawka, Andrew J. Young, and Ralph P. Francesconi Jun. 1987 27 p
(AD-A186450) Avail: NTIS HC A03/MF A01 CSCL 06P

Nine younger and nine older men were matched for body weight, surface area, surface area-to-weight ratio, percent body fat, and maximal aerobic power, but differed in age by 25 years and regular weekly aerobic activity. After evaluaton in a comfortable environment (22 C, 50 percent rh), these subjects were concurrently heat acclimated by treadmill walking for two to 50 min exercise bouts separated by, 10 min rest for 10 consecutive days in a hot-dry environment. During the first day of exposure, performance time was 27 min longer for the older men while final rectal and skin temperatures and heart rate were lower, and final total body

sweat loss higher when compared to younger men. These physiological advantages for the older men persisted for the first few days of exercise-heat acclimation. By the end of acclimation, no physiological or performance time differences were observed between groups. Final rated perceived exertion was generally higher for the younger men throughout the acclimation period while final thermal sensation was higher only on the first acclimation day. Sweating sensitivity, esophageal temperature at sweating onset, and the sweating onset time did not differ between groups either pre- or post-acclimation. GRA

N88-25140*# National Aeronautics and Space Administration. Ames Research Center, Moffett Field, Calif.
CARDIOVASCULAR EFFECTS OF WEIGHTLESSNESS AND GROUND-BASED SIMULATION
Harold Sandler Jun. 1988 103 p
(NASA-TM-88314; A-86284; NAS 1.15:88314) Avail: NTIS HC A06/MF A01 CSCL 06P

A large number of animal and human flight and ground-based studies were conducted to uncover the cardiovascular effects of weightlessness. Findings indicate changes in cardiovascular function during simulations and with spaceflight that lead to compromised function on reambulation and/or return to earth. This altered state termed cardiovascular deconditioning is most clearly manifest when in an erect body state. Hemodynamic parameters inidicate the presence of excessive tachnycardia, hypotension (leading to presyncope in one-third of the subjects), decreased heart volume, decreased plasma and circulating blood volumes and loss of skeletal muscle mass, particularly in the lower limbs. No clinically harmful effects were observed to date, but in-depth follow-ups were limited, as was available physiologic information. Available data concerning the causes for the observed changes indicate significant roles for mechanisms involved with body fluid-volume regulation, altered cardiac function, and the neurohumoral control of the control of the peripheral circulation. Satisfactory measures are not found. Return to preflight state was variable and only slightly dependent on flight duration. Future progress awaits availability of flight durations longer than several weeks. Author

N88-25141* NASA Scientific and Technical Information Facility, Baltimore/Washington International Airport, Md. 21240.
AEROSPACE MEDICINE AND BIOLOGY: A CONTINUING BIBLIOGRAPHY WITH INDEXES (SUPPLEMENT 312)
Jul. 1988 99 p
(NASA-SP-7011(312); NAS 1.21:7011(312)) Avail: NTIS HC A06; NTIS standing order as PB88-912300, $9.00 domestic, $18.00 foreign CSCL 06E

This bibliography lists 300 reports, articles, and other documents introduced into the NASA scientific and technical information system in June, 1988. Author

53 BEHAVIORAL SCIENCES

Includes psychological factors; individual and group behavior; crew training and evaluation; and psychiatric research.

N88-25142# Georgia Inst. of Tech., Atlanta. Center for Man-Machine Systems Research.
HUMAN PROBLEM SOLVING IN COMPLEX DYNAMIC ENVIRONMENTS Interim Report, Jun. 1984 - May 1985
William B. Rouse and Richard L. Henneman Dec. 1987 65 p
(Contract MDA903-82-C-0145; DA Proj. 2Q1-61102-B-74-F)
(AD-A190788; ARI-RN-87-84) Avail: NTIS HC A04/MF A01 CSCL 23B

This research note summarizes three years of a four year contract to study ways of improving human performance in highly integrated systems in such areas as communications, transportation, manufacturing, etc. Rule-based computer models of human performance (CAIN) are discussed, as are methods from measuring the complexity of the task of monitoring these large-scale systems. Finally, the development of a computer model (MABEL) which requires subjects to monitor a large-scale communications network is described. GRA

N88-25143# Aerospace Medical Research Labs., Wright-Patterson AFB, Ohio.
EYE AND HEAD RESPONSE TO AN ATTENTION CUE IN A DUAL TASK PARADIGM Final Report, Apr. - Dec. 1984
Gloria L. Calhoun Jul. 1987 49 p
(AD-A191052; AAMRL-TR-87-033) Avail: NTIS HC A03/MF A01 CSCL 05H

Eight subjects were used to characterize eye and head movements in response to a cue to refixate in a dual task paradigm. The subject's tasks were complete a centrally located pursuit tracking task and identify targets which were vertically displaced from the normal line-of-sight. Reaction time and movement pattern of the eye and head were recorded as well as conventional performance measures for the following: 1) two difficulty levels of the tracking task; 2) presence and absence of an attention cue prior to target presentation; and 3) two target locations which were vertically displaced from the centrally located task. The results indicated that eye and manual reaction time increase the farther a target is vertically displaced from the centrally located task and head reaction time decreases with the presence of a verbal cue prior to target presentation. Since the experimental conditions examined in the present study affected these measures differently, eye, head, and manual reaction times should be examined further. The differences found in eye and head response as a function of information location and presence of an attention cue suggest that such unobtrusive measures may be valuable in the design of multifunction display symbology and attention cueing systems. GRA

N88-25144# Bolt, Beranek, and Newman, Inc., Cambridge, Mass.
A FRAMEWORK FOR A THEORY OF MAPPING Interim Report, Mar. 1986 - Mar. 1987
Allan Collins and Mark Burstein Dec. 1987 27 p
(Contract MDA903-85-C-0411; DA Proj. 2Q1-61102-B-74-F)
(AD-A191071; ARI-RN-87-64) Avail: NTIS HC A03/MF A01 CSCL 05H

The literature on similarity, analogy, and metaphor ranges over many different kinds of mappings. Some of the disagreements arise because researchers are talking about different kinds of mappings or the different contexts in which mappings are made. Our goal is to clarify the issues being addressed and the critical distinctions that need to be made. We will attempt to consider the entire territory over which the discussion of mapping arises, but no doubt we will miss some of the critical distinctions and issues. We have divided the paper into three main sections. The first section distinguishes the different kinds of entities that are related by analogy and similarity mappings, some of their more salient properties. The second section discusses the different contexts or tasks that give rise to mappings. The third section catalogues the set of issues we have identified in the literature, and identifies some of the different solutions proposed or possible for each issue. In a concluding section we briefly discuss the implications of this framework for research. GRA

N88-25145# Illinois Univ., Urbana.
PERFORMANCE EFFECTIVENESS AND THE WORK/REST CYCLE Final Report, 1 Oct. 1983 - 31 Dec. 1987
David Birch 1 Feb. 1988 17 p
(Contract DAAG29-83-K-0138)
(AD-A191448; ARO-21059.6-LS) Avail: NTIS HC A03/MF A01 CSCL 06D

The supervisor-monitor of a modern automated system is called upon to perform continuously a variety of cognitive tasks over prolonged periods of time. Such work is structured by the characteristics of the system, by the particular requirements of the individual tasks to be carried out, and by the motivational and cognitive processes that take place as the work goes on. It is useful to refer to the scheduling of these events and to inquire

about the structure of work that emerges as a consequence of this scheduling. Six new studies directed to the understanding of how scheduling of events occurs in continuous work have resulted in significant progress theoretically on problems of scheduling and in applications of the theory. New models and extensions of existing models to the continuous behavioral situation are reported. Three other studies, each addressed to different aspects of the structure of tasks as determined by motivation and cognition, provide new information about continuous work in three different settings: during single-task and dual-task tracking, while making predictions of system criterion values from multiple cue values that differ in validity and redundancy, and while judging similarities of visual inputs from symbolic representations of the stimuli. GRA

N88-25146# California Univ., Los Angeles. Motor Control Lab.
OPTIMIZING FEEDBACK UTILIZATION IN MOTOR SKILL TRAINING Interim Report, Jun. 1985 - Jun. 1986
Richard A. Schmidt and Diane C. Shapiro Feb. 1988 38 p
(Contract MDA903-85-K-0225; DA Proj. 2Q1-61102-B-74-F)
(AD-A191559; ARI-RN-88-05) Avail: NTIS HC A03/MF A01 CSCL 05I

This research note deals with the acquisition of motor skills, specifically with the optimal use of feedback on goal achievement (termed Knowledge of Results, KR) for the maximization of learning and retention. A great deal of evidence suggests that enhancing the amount or quality of KR can improve performance in a session where KR is present, but limited evidence suggests that this might not be effective on a delayed criterion test when KR is removed -- a typical goal of many Army training settings. Two variations of KR were studied: relative frequency - the proportion of trials receiving KR, and summary KR - where KR is given about an entire set of trials. In each case, alterations in KR which degraded training performance (relative to a condition with KR on each trial) actually produced enhanced performance on a delayed no-KR retention test. A third paradigm examined the learning of error-detection capabilities as a basis for these effects. Overall, six experiments suggest that enhancing KR in acquisition may generate KR overreliance, preventing the learning of important features of the task which are critical for retention of performance when feedback is removed or degraded (e.g. in markmanship), Our results have implications for improved feedback in training. GRA

N88-25147# California Univ., Irvine. Dept. of Information and Computer Science.
MODELS OF INCREMENTAL CONCEPT FORMATION Interim Report, Mar. 1986 - Mar. 1987
John H. Gennari, Pat Langley, and Doug Fisher Feb. 1988 33 p
(Contract MDA903-85-C-0324; DA Proj. 2Q1-61102-B-74-F)
(AD-A191597; ARI-RN-88-06) Avail: NTIS HC A03/MF A01 CSCL 05H

This document reviews three previous models of incremental concept formation and presents a model, CLASSIT, that extends these earlier systems. All of the models integrate the process of recognition and learning, and all can be viewed as carrying out a search through the space of possible concept hierarchies. In an attempt to show that CLASSIT is a robust model of concept formation, empirical studies of the system's behavior under a variety of conditions are also presented. GRA

N88-25148# California Univ., Berkeley. Dept. of Psychology.
VISUAL INFORMATION PROCESSING IN THE PERCEPTION OF FEATURES AND OBJECTS Annual Technical Report No. 1, 1 Jan. - 31 Dec. 1987
Anne Treisman 22 Jan. 1988 23 p
(Grant AF AFOSR-0125-87)
(AD-A192026; AFOSR-88-0215TR) Avail: NTIS HC A03/MF A01 CSCL 17K

The first year of the grant was spent in setting up the laboratory, and in starting research on a number of different projects. All are concerned with the visual processing of information in the perception of objects. A series of experiments has explored the perception of conjunctions of features, attempting to determine what makes this difficult or easy. A new method (detection of apparent motion) was tested and a modification of feature-integration theory was developed to accommodate the new results. Other projects have been concerned with coding of features, finding evidence for modularity, testing the level of abstraction at which features (such as orientation) are coded, the different media which support the coding of shape, and the space in which they are represented (retinal or three-dimensional). Another project has probed the effects of perceptual learning with extended practice at detecting particular sets of targets; the results suggest that automatization in search is highly specific to the practiced task and has little effect on other perceptual tests. GRA

54 MAN/SYSTEM TECHNOLOGY AND LIFE SUPPORT

Includes human engineering; biotechnology; and space suits and protective clothing.

For related information see also *16 Space Transportation.*

N88-25149# Applications Research Corp., Dayton, Ohio.
AN ADVANCED PROTOTYPING TOOL FOR HUMAN FACTORS DESIGN Final Report
Thomas V. Brown Mar. 1987 81 p
(Contract DAAA15-86-C-0063)
(AD-A187290; ARC-TR-8782) Avail: NTIS HC A05/MF A01 CSCL 23B

Modern equipment has placed new demands on human factors because of more complex machine/computer functions and increased speed demands. The human operator must interface with mechanical systems, computer software, artificial feedback effects, and other humans. There is a need for a formal, explicitly defined methodology that can be used to model all of these interfaces within one context. This report describes a methodology that satisfies this need. This is a decompositional methodology that is general enough to include all system interactions, including machine effects and psychological characteristics of a human operator. The methodology is also rigorous enough to identify gaps and inadequacies to the user. Its foundation is the USE.IT methodology which was not created under this effort, but the application of which to human factors problems did originate here. An interactive intercom system, a body motion modeling task involving walking and lifting, and a human operator interacting with a radio to keep it tuned are included as examples. GRA

N88-25150*# Purdue Univ., West Lafayette, Ind. Dept. of Psychological Sciences.
TIMESHARING PERFORMANCE AS AN INDICATOR OF PILOT MENTAL WORKLOAD Final Report
Patricia A. Casper 31 May 1988 103 p
(Contract NCC2-349)
(NASA-CR-182807; NAS 1.26:182807) Avail: NTIS HC A06/MF A01 CSCL 05H

The research was performed in two simultaneous phases, each intended to identify and manipulate factors related to operator mental workload. The first phase concerned evaluation of attentional deficits (workloads) in a timesharing task. Work in the second phase involved incorporating the results from these and other experiments into an expert system designed to provide workload metric selection advice to nonexperts in the field interested in operator workload. The results of the experiments conducted are summarized. B.G.

N88-25151# Army Natick Research and Development Command, Mass.
THE EFFECTS OF DIFFERENT COMBINATIONS OF INLET AIR CONDITIONS USED FOR COOLING AS MEASURED ON A HEATED MANIKIN Final Report, Dec. 1986 - Jan. 1987
Barry DeCristofano and Joseph Cohen Oct. 1987 28 p

(AD-A191116; NATICK/TR-88/002) Avail: NTIS HC A03/MF A01 CSCL 05H

The effects of using different inlet air conditions on the cooling performance of the Army's microclimate air vest were studied. A significant difference was found between the use of a 75 F dew point, and either a 60, 65, or 70 F dew point. The interaction between dew point and flow rate was also found to be significant. The testing was done on a sectionalized heated manikin featuring a sweating skin. The results may provide some preliminary guidelines for the development of microclimate cooling equipment. The findings also suggest courses of investigation that future studies should be directed towards. GRA

N88-25152# California Univ., Irvine. Dept. of Information and Computer Science.

A COMPUTATIONAL MODEL OF MOTOR BEHAVIOR Interim Report, Mar. 1986 - Mar. 1987

Wayne Iba and Pat Langley Dec. 1987 13 p

(Contract MDA903-85-C-0324; DA Proj. 2Q1-61102-B-74-F)

(AD-A191179; ARI-RN-87-72) Avail: NTIS HC A03/MF A01 CSCL 12I

Generating even simple motor behavior using artificial manipulators has proven to be a very difficult task. A computational model of motor behavior is presented that assumes three inputs: a limb to carry out motor commands, a viewer-centered schema describing the desired behavior, and a sensory-motor interface allowing two-way communication between the agent and the environment. A motor schema is defined as a memory structure containing a few positions from the trace of a movement. The model then produces intervening points between those in the schema. A viewer-centered schema is transformed into its dual representation, facilitating execution of the desired movement on the limb. These two forms of a schema represent the same points in three-dimensional space, but behave in ways which have important differences when they are acted upon by the model. Our model accounts for a number of phenomena from the literature, including the speed/accuracy tradeoff, and the closed and open loop distinction. The model suggests directions for further experimentation. GRA

N88-25153# Army Aeromedical Research Lab., Fort Rucker, Ala.

SIMULTANEOUS MULTIPLE CONTROL FORCE EXERTION CAPABILITIES OF MALES AND FEMALES VERSUS HELICOPTER CONTROL FORCE DESIGN LIMITS

Aaron W. Schopper and George R. Mastroianni Sep. 1987 43 p

(AD-A191653; USAARL-87-14) Avail: NTIS HC A03/MF A01 CSCL 01D

Military standards and design guidelines do not consider the potential for degradation in the magnitude of force which can be applied by a crewmember or operator as the result of having to perform more than one control input at the same time. In assessing helicopter-control referenced strength capabilities as a part of an overall program to update medical standards for US Army flying duty, 130 subjects performed maximal voluntary exertions on each of the three primary helicopter controls (cyclic, collective, and pedals). These exertions were undertaken both as separate inputs to single controls and as simultaneously executed inputs to all three controls. The findings revealed substantial and significant force degradation occurred during simultaneously executed exertions (relative to the magnitudes of single control exertions). Cyclic inputs were affected least. The degree of force degradation associated with collective and pedal inputs varied with the particular combinations of direction-of-exertion employed. The resulting patterns for force degradation were similar for the collective and pedal with the extent of degradation being larger for the pedal inputs (typically 40-50 percent) than for collective inputs (typically 20-35 percent). Substantial proportions of the subjects (approximately 50 percent of the males and more than 90 percent of the females) were unable to consistently attain design-guide force levels (MIL-H-8501A, 1961) on all three controls during all of the 16 simultaneously executed exertions. GRA

N88-25154# Ballistic Research Labs., Aberdeen Proving Ground, Md.

PERFORMANCE ESTIMATES FOR OPERATIONS CONDUCTED WHILE WEARING INDIVIDUAL PROTECTIVE EQUIPMENT: USER MANUAL Final Report

Charles H. Wick Jan. 1988 57 p

(AD-A191871; BRL-MR-3647) Avail: NTIS HC A04/MF A01 CSCL 05H

The purpose of this publication is to describe the procedures which may be used to determine the individual performance decrement resulting from wearing Individual Protective Equipment (IPE) for exercise and training purposes only. Further, it describes the procedure for using the Force-on-Force algorithm for predicting additional required battalion sized units for exercises simulating combat operations while wearing IPE. Although actual operations are not explicity described, it is believed that results using the Dbase and procedures of this publication will provide commanders and staff a realistic appreciation of the performance decrement which results from the wearing of IPE. The numerical results should be applied in training and exercise situations. Section 2 is an introduction to the use of the Performance Dbase System. Section 3 is the methodologies which constituted the Dbase, the type of procedures used and the methodology for extracting information from the Dbase. Section 4 introduces the user to the Force-on-Force algorithm and the hypothetical estimations for additional required battalion sized units during simulated combat operations while wearing IPE. GRA

N88-25155*# Maryland Univ., College Park. Biomechanics Lab.

THE EFFICACY OF USING HUMAN MYOELECTRIC SIGNALS TO CONTROL THE LIMBS OF ROBOTS IN SPACE Final Report, 15 Apr. 1987-1988

Jane E. Clark and Sally J. Phillips 20 Jun. 1988 289 p

(Grant NAG5-895)

(NASA-CR-182901; NAS 1.26:182901) Avail: NTIS HC A13/MF A01 CSCL 05H

This project was designed to investigate the usefulness of the myoelectric signal as a control in robotics applications. More specifically, the neural patterns associated with human arm and hand actions were studied to determine the efficacy of using these myoelectric signals to control the manipulator arm of a robot. The advantage of this approach to robotic control was the use of well-defined and well-practiced neural patterns already available to the system, as opposed to requiring the human operator to learn new tasks and establish new neural patterns in learning to control a joystick or mechanical coupling device. Author

N88-25156*# McDonnell-Douglas Astronautics Co., Huntington Beach, Calif.

HUMAN PERFORMANCE ISSUES ARISING FROM MANNED SPACE STATION MISSIONS

William K. Douglas Washington NASA Oct. 1986 61 p

(Contract NAS2-11723)

(NASA-CR-3942; NAS 1.26:3942; MDC-H1363) Avail: NTIS HC A04/MF A01 CSCL 05H

Ten former NASA astronauts were interviewed using a set of 51 questions developed to encourage the contacts to discuss any thoughts, opinions, conclusions, or suggestions which might have evolved since they left the astronaut program. Strict confidentiality was maintained. At least one astronaut from each of the NASA manned space flight programs, excluding the Space Transportation System (Shuttle), was interviewed. The report records the answers to the questions asked, spontaneous comments, and the investigator's own personal evaluations of the material obtained. No statistical analysis of the material was attempted. The professional opinions of these ten experienced astronauts will be of value to persons concerned with the design and operation of manned spacecraft and manned space stations. Author

55 SPACE BIOLOGY

Includes exobiology; planetary biology; and extraterrestrial life.

No abstracts in this category.

59 MATHEMATICAL AND COMPUTER SCIENCES (GENERAL)

No abstracts in this category.

60 COMPUTER OPERATIONS AND HARDWARE

Includes hardware for computer graphics, firmware, and data processing.

For components see *33 Electronics and Electrical Engineering.*

N88-25157# Oak Ridge National Lab., Tenn.
TUTORIAL ON COMPUTER CONTROL
R. C. Juras Sep. 1987 25 p Presented at the SNEAP Conference, Tallahassee, Fla., 27 Sep. 1987
(Contract DE-AC05-84OR-21400)
(DE88-006185; CONF-8709217-4) Avail: NTIS HC A03/MF A01

This paper discusses computer architecture modfications and development used to control particle accelerators. DOE

N88-25158# Duke Univ., Durham, N. C. Dept. of Computer Science.
EFFECTIVENESS EVALUATION OF FAULT-TOLERANT MULTIPROCESSOR SYSTEMS Final Report, 1 Oct. 1983 - 30 Aug. 1987
Kishor S. Trivedi 27 Jan. 1988 5 p
(Contract DAAG29-84-K-0045)
(AD-A191688) Avail: NTIS HC A02/MF A01 CSCL 12E

An important area of research is in the analysis of the coverage of a fault tolerant system, that is, the probability that the system can recover from a fault. A variety of models, from simple phase-type models to very complex stochastic Petri net models is studied, and solution techniques investigated for each model type. The methodology allows consideration of external events that can interfere with recovery, such as a hard limit on recovery time, or the occurrence of a second near-coincident fault. It was discovered that a policy of attempting transient recovery upon detection of an error (as opposed to automatically reconfiguring the affected component out of the system) may actually increase the unreliability of the system. This result holds if the error detectability is not nearly perfect, so that the risk of producing an undetectable error (if the transient error is present) is greater than the benefit gained by not discarding the component. GRA

N88-25159# Virginia Polytechnic Inst. and State Univ., Blacksburg. Human Factors Lab.
DESIGN AND TESTING OF A LUMINANCE AND CHROMINANCE STABILIZATION SYSTEM FOR A COMPUTER-CONTROLLED COLOR DISPLAY Final Report, Mar. 1984 - Jul. 1987
Willard W. Farley Jul. 1987 147 p
(Contract F33615-84-C-0510)
(AD-A191922; VPI/HFL-86-1; AAMRL-TR-87-027) Avail: NTIS HC A07/MF A01 CSCL 12F

The improvements in computer display technology have made it possible for researchers in color vision to make use of this technology to generate stimuli for color research. The early research has shown the tremendous advantages of this technique in the large number of different stimuli that can be presented in a single experiment. Unfortunately, the early research also highlighted several problems with the computer display system. One of the major problems is the computer display is not constant over time. This report outlines a Feedback Control System that may be connected to any computer display system whose video bandwidth is lower than 50 MHz. The system receives light from a red, green and blue area of the screen that is always commanded to the same intensity level via three detectors. The signal from the detectors is used as the reference signal and in a feedback control system such that the luminance of each of three guns of the display is made to have a constant output. A single-channel version can also be constructed to stabilize the luminance of a monochrome CRT. GRA

N88-25160 Maryland Univ., College Park.
SYMBL: A NEW BOOLEAN COMPILER Ph.D. Thesis
Sau-Mou Wu 1987 134 p
Avail: Univ. Microfilms Order No. DA8725591

A novel approach is presented to lay out Boolean functions, along with the software (SYMBL) based on it. Taking advantage of the symmetric properties inherent in the given functions, the approach tries to manipulate the Boolean functions into a symmetric cover consisting of a sum of product terms of some totally symmetric functions. A symmetric cover can be easily realized in such a way that the complexity of the corresponding circuit is dependent on the number of the product terms. It is shown that if the functions have a reasonable degree of symmetry, the size of the minimum symmetric cover will be substantially smaller than that of the minimum sum-of-product cover. The bounds on the area are established to realize such circuits in the grid model of VLSI; the results show that these layouts will be considerably smaller than that of the corresponding programmable logic arrays (PLAs) for partially symmetric functions. SYMBL first partitions the set of input variables into equivalence classes so that the functions are symmetric with respect to each equivalence class. A heuristic minimizer then finds a near optimal symmetric cover for the functions. Finally, the last phase performs the placement and routing procedures to optimize the layout structure consisting of a combination of Weinberger arrays, PLAs, and special tree blocks. Dissert. Abstr.

N88-25161# Sandia National Labs., Albuquerque, N. Mex.
A MULTIPROCESSOR DATA FLOW ACCELERATOR MODULE
G. S. Davidson and P. E. Pierce 1988 9 p Presented at the Military Computing Conference, Anaheim, Calif., 3 May 1988
(Contract DE-AC04-76DP-00789)
(DE88-007587; SAND-88-0622C; CONF-880577-2) Avail: NTIS HC A02/MF A01

Real-time controllers often need to minimize the latency between the arrival of a stimulus and the delivery of a control signal. Using multiprocessors to compute the control algorithm is appealing for these applications, but problem decomposition and load leveling are not straightforward. The data flow model of computation offers a solution which can be implemented for shared memory, parallel processors by the addition of a single circuit board. A typical parallel processor, the data flow model, and several versions of the Data Flow Accelerator Module (DFAM) are presented together with some preliminary results. DOE

N88-25162# Oak Ridge National Lab., Tenn.
MULTI-SENSOR INTEGRATION ON THE NCUBE HYPERCUBE COMPUTER
C. W. Glover 1988 12 p Presented at the 3rd Conference on Hypercube Concurrent Computers and Applications, Pasadena, Calif., 19 Jan. 1988
(Contract DE-AC05-84OR-21400)
(DE88-007472; CONF-880117-4) Avail: NTIS HC A03/MF A01

This paper presents the quantitative performance results

obtained from converting a large sequential Multi-Sensor Integration (MSI) program into aconcurrent form, and executing the program on an NCUBE hypercube computer for several test case scenarios. Each sensor track was assigned to a different node of the hypercube where computationally intensive calculations were performed. A 4-mode hypercube was found to be the optimal size for the test case scenario discussed here, where speed-up factors of 1.5 to 1.7 were obtained. A completely concurrent MSI algorithm is also presented. DOE

N88-25163# Transportation Systems Center, Cambridge, Mass.
COMPUTER RESOURCE MANAGEMENT TECHNOLOGY PROGRAM (PE 64740F). TASK NO. 9: ADVANCED USER AUTHENTICATION Final Report, May - Nov. 1987
L. Watson and W. Barron Mar. 1988 125 p Sponsored by the Air Force, Hanscom AFB, Mass.
(PB88-183066; DOT-TSC-RSPA-88-1; DOT-VA846-88-1) Avail: NTIS HC A06/MF A01 CSCL 09B

The various technologies which can be used to perform user authentication are examined with an emphasis on biometric techniques. The methods by which each device performs the authentication of users are examined individually, and their suitability for a multilevel computer environment is assessed. The status and direction of computer user authentication devices and techniques, in general, are evaluated. Included are independent testing results, government requirements, selection considerations, and a glossary of computer security and user authentication terminology. Author

N88-24939# Technische Univ., Brunswick (West Germany). Inst. fuer Hochfrequenztechnik.
OPTICAL COMPUTER AND OPTICAL METHODS FOR DATA PROCESSING [OPTISCHE RECHNER UND OPTISCHE METHODEN IN DER DATENVERARBEITUNG]
Karl-Joachim Ebeling *In* DFVLR, Optics: Perspectives for Measurement Techniques and Signal Processing for Flight Guidance Aug. 1987 p 267-294 In GERMAN (For primary document see N88-24928 18-35)
Avail: NTIS HC A13/MF A01; DFVLR, VB-PL-DO, 90 60 58, 5000 Cologne, Fed. Republic of Germany 88 Deutsche marks

61 COMPUTER PROGRAMMING AND SOFTWARE

Includes computer programs, routines, alogorithms, and specific applications, e.g., CAD/CAM.

N88-25164# JAYCOR, Vienna, Va.
KNOWLEDGE ACQUISITION TOOL IMPLEMENTATION
16 Jun. 1987 13 p
(Contract N00014-86-C-2352)
(AD-A190415) Avail: NTIS HC A03/MF A01 CSCL 23B

The Knowledge Acquisition Tool is a graphics oriented user interfaces to the system under development. It provides a pictorial representation of the network and allows the user to add information in a much simplified manner. The tool does error checking for simple errors and has a facility for specifying dependency relations. These relations are graphically displayed as a set of nodes and edges. The interface to the underlying Bayesian Reasoning Tool is actually spread throughout the code, hence is somewhat inseparable from it. However, enclosed is the source code for the major functions used by the KA Tool for much of the graphics, etc. At this writing, this code is, and will continue to be, quite dynamic in structure as new ideas/different approaches are tried. The code is self-documenting. It also responds to the describe function available on the LISP machines. GRA

N88-25165# Air Force Inst. of Tech., Wright-Patterson AFB, Ohio. School of Engineering.
FEATURE EXTRACTION USING THE HOUGH TRANSFORM M.S. Thesis
Marvin L. Hill Dec. 1987 110 p
(AD-A190679; AFIT/GE/ENG/87D-24) Avail: NTIS HC A06/MF A01 CSCL 12F

This thesis applied the normal straight line parameterization of the Hough transform to a variety of images using the accumulator method. Simple inputs were used initially to illustrate the distortion characteristics of the Hough transform due to rotations, scales and translations of an input. Making use of work performed by D. Casasent and R. Krishnapuram of Carnegie-Mellon University, the Hough transform was then applied to segmented and edged doppler images. A distort-and-compare routine, which makes use of the Hough space distortion characteristics, was implemented in the Hough transform domain to estimate input space characteristics of an object. Next, the Hough transform, generated using Fourier transform techniques, was applied to some of the same inputs to demonstrate that the accumulator method is actually a discrete version of the continuous Hough transform. An unsuccessful attempt at implementing the continuous Hough transform using computer-generated interferograms was outlined. A method of implementing the continuous Hough transform and its inverse using phase filters was presented as a suggestion for further research. GRA

N88-25166# Oak Ridge National Lab., Tenn.
THE DEVELOPMENT OF KENO AND THE CALCULATION OF DIFFERENTIAL PARAMETERS WITH KENO
G. E. Whitesides 1987 6 p Presented at the Workshop on the Influence of Neutron Spectra on Experimental Measurements, Tucson, Ariz., 23 Mar. 1987
(Contract DE-AC05-84OR-21400)
(DE88-006176; CONF-8703156-2) Avail: NTIS HC A02/MF A01

This paper is designed to review the origin of the KENO program, to discuss its development, to explain some reasons for its form and capabilities, and lastly, to comment on the codes capability relative to the subject of this meeting, namely neutron spectra. The original programming, which was later to become KENO, was nothing more than a few energy groups, fixed-source calculation of neutron leakage, and absorption in a right circular cylinder. Its sole purpose initially was to be used to evaluate the capabilities of several computers with regard to performing Monte-Carlo-type calculations. This original program grew to a fission source iteration that was used to evaluate single, cylindrical uranium metal units being studied by J.T. Thomas. This development was followed by providing the capability to treat arrays of cylindrical units, which was also a part of the Thomas' experimental studies. DOE

N88-25167# Cornell Univ., Ithaca, N.Y. Mathematical Sciences Inst.
ANNOTATED COMPUTER OUTPUT FOR SPLIT PLOT DESIGN: SAS GLM Interim Technical Report
W. T. Federer, Z. D. Feng, M. P. Meredith, and N. J. Miles-McDermott 4 Nov. 1987 46 p
(Contract DAAG29-85-C-0018)
(AD-A190800; ARO-23306.133-MA) Avail: NTIS HC A03/MF A01 CSCL 12C

The analysis of covariance for split plot designs is not always straightforward when using a statistical software package such as SAS PROC GLM. In order to demonstrate correct analyses several data sets are examined and annotated SAS output is given. Hypothetical data are analyzed first without and then with the covariate included. The whole plots are arranged in a RCBD and the covariate is measured on the subplot experimental units. A second example has whole plots arranged in a CRD and the covariate measured only on the whole plot experimental units. Complete ANOVA tables for both examples may be computed in a single procedural call to SAS PROC GLM. Both Type 1 and Type 3 sums of squares are necessary to construct the proper

ANOVA table. A commonly employed approach requiring two separate procedural calls to GLM is also demonstrated. Formulae for the standard errors of the difference between adjusted whole plot and subplot means are reported. This is part of a continuing project that produces annotated computer output for the analysis of balanced split plot experiments with covariates. The complete project will involve processing three examples on SAS/GLM, BMDP/2V, SPSS-X/MANOVA, GENSTAT/ANOVA, and SYSTAT/MGLH. GRA

N88-25168# Massachusetts Inst. of Tech., Cambridge. Lab. for Computer Science.
A MIXED-INTEGER LINEAR PROGRAMMING PROBLEM WHICH IS EFFICIENTLY SOLVABLE
Charles Leiserson and James B. Saxe Oct. 1987 13 p
(Contracts N00014-80-C-0622; N00014-76-C-0370)
(AD-A191028; MIT/LCS/TM-343) Avail: NTIS HC A02/MF A01 CSCL 12D

Much research has centered on the problem of finding shortest paths in graphs. It is well known that there is a direct correspondence between the single source shortest-paths problem and the following simple linear programming problems: Let S be a set of linear inequalities of the form x sub j - x sub i < or = (a sub ij, where the x sub i are unknowns and the a sub ij are given real constants. Determine a set of values for the x sub i such that the inequalities in S are satisfied, or determine that no such values exist. This paper considers the mixed-integer linear programming variant of this problem in which some (but not necessarily all) of the x sub i are required to be integers. The problem arises in the context of synchronous circuit optimization but it has applications to PERT scheduling and VLSI layout compaction as well. GRA

N88-25169# Rensselaer Polytechnic Inst., Troy, N.Y. Dept. of Computer Science.
EPL (EQUATIONAL PROGRAMING LANGUAGE) SYSTEM DESIGN: INTERMEDIATE PROCESSING STEPS
Duncan E. Clarke Dec. 1987 176 p
(Contracts N00014-86-K-0042; DAAL03-86-K-0112)
(AD-A191203; RPI-TR-87-33) Avail: NTIS HC A09/MF A01 CSCL 12E

A detailed design is presented for the intermediate processing steps of a compiler, written in C for UNIX based systems, for translating an equational programming language into a high level sequential programming language. Detailed discussions of the design and implementation of algorithms for performing in-depth semantic checking, data type propagation, range propagation, and graph-theoretic based scheduling are presented with numerous examples throughout. GRA

N88-25170# Army Stategic Defense Command, Huntsville, Ala. Advanced Technology Directorate.
A GENERAL APPROACH FOR AUTOMATING SOURCE CODE VERIFICATION Summary Report
James H. Cordle 2 Dec. 1987 72 p
(AD-A191461; ATD-88-1) Avail: NTIS HC A04/MF A01 CSCL 12E

Conventional debugger systems rely on user guidance to conduct error localization procedures. System procedures are typically time consuming and inefficient due in part to the human factor. In addition, compatability is limited among different hardware and software systems. These factors inhibit program design and development while increasing system cost. A prototype software system has been developed that automates the debugging process. The system uses automation as an alternative technique for improving current debugger designs. Problem areas associated with typical debugger systems are presented. Concepts employing automation are supplied to remedy these deficiencies. Validation of these concepts are demonstrated by the prototype system. The prototype system exploits automation concepts through test case verification and provides the framework for an automated debugger system. GRA

N88-25171# California Univ., San Diego, La Jolla. Dept. of Mathematics.
RESEARCH IN ENUMERATION AND GRAPH THEORY WITH APPLICATIONS TO COMPUTER SCIENCE Final Report
Edward A. Bender 26 Feb. 1988 4 p
(Contract N00014-85-K-0495)
(AD-A191567) Avail: NTIS HC A02/MF A01 CSCL 12B

During the contract, almost half of the author's effort has been directed toward studying maps on surfaces other than the sphere. Other completed research was on convex polyhedra, and the size of PLA's. At present, research is underway on three problems in graph theory. GRA

N88-25172# California Univ., Irvine. Dept. of Information and Computer Science.
LispSEI: THE PROGRAMMER'S MANUAL Interim Report, Jan. 1986 - Jan. 1987
Hans Tallis Jan. 1988 20 p
(Contract MDA903-85-C-0324; DA Proj. 2Q1-61102-B-74-F)
(AD-A191632; ARI-RN-88-01) Avail: NTIS HC A03/MF A01 CSCL 12E

The purpose of LispSEI and this document is to: 1) Hide, once and for all, all C code within the SEI; 2) Provide a convenient listing of lowest level Lisp functions accessing and changing state in the SEI; 3) Provide a more precise definition of the capabilities of the different layers of the SEI. Currently the functions provided via FRANZSELL (for example) represent a mix of simple data copying operations (for example, passing the list of world objects on up to the organism) as well as more intelligent operations (the multi-step implementation of turn for example). LispSEI will provide only the simple data passing and control operations defined below, with the more complex operations being defined elsewhere in the SEI; 4) Separate out filtering operations from the basic copying of the world state. The filtering/massaging will be taking place in a number of library modules discusses elsewhere; and 5) Clean up some other unnecessary hair present in the current SEI implementation. GRA

N88-25173# Tennessee Univ., Knoxville. Management Science Program.
DECOMPOSITION OF LINEAR PROGRAMS USING PARALLEL COMPUTATION
James K. Ho, Tak C. Lee, and R. P. Sundarraj Jul. 1987 23 p
(Contract N00014-87-K-0163)
(AD-A191718; MSP-87-4) Avail: NTIS HC A03/MF A01 CSCL 12F

This paper describes DECOMPAR: an implementation of the Dantzig-Wolfe decomposition algorithm for block-angular linear programs using parallel processing of the subproblems. The software is based on a robust experimental code for LP decomposition and runs on the CRYSTAL multi-computer at the University of Wisconsin-Madison. Initial computational experience is reported. Promising directions in future development of this approach are discussed. GRA

N88-25174# Naval Ocean Systems Center, San Diego, Calif.
IGUANA: INTERACTIVE GRAPHICS UTILITY FOR AUTOMATED NEC ANALYSIS Report, period ending Mar. 1987
James C. Logan and John Strauch Oct. 1987 2 p
(AD-A191760) Avail: NTIS HC A02/MF A01 CSCL 12F

The Interactive Graphics Utility for Automated NEC Analysis (IGUANA) is a computer program designed to reduce the time for antenna model evaluation by providing partial automation to both the data entry process and the data display process. IGUANA is an aid to NEC input data preparation and NEC output data display: IGUANA performs no antenna evaluations itself. IGUANA resides on a microcomputer (an IBM XT or compatible) and is independent of the main frame on which NEC resides. IGUANA is a composite of independently developed but fully integrated subprograms designed to aid in preparation and display of NEC related data sets. The effort required for NEC model composition and data entry is significantly reduced by the use of IGUANA; hence the

time required to prepare an error free data set constituting a valid NEC model may be significantly reduced (from weeks to a matter of hours in some cases involving very complex models). GRA

N88-25175# Ohio State Univ., Columbus. Electroscience Lab.
CIMAG2: THE COMPUTER PROGRAM TO GENERATE COLOR IMAGES
G. Dural, S. Smithberger, and J. D. Young Nov. 1987 107 p
(Contract N00014-86-K-0202)
(AD-A191847; ESL-718048-7) Avail: NTIS HC A06/MF A01 CSCL 12E

This report describes a user interactive FORTRAN program, CIMAG2, to be used to produce color images using either measured for calculated scattered field data. The program provides the processing of either the frequency or time domain data, and produces a 2-D image of the target of interest. Color plots of the images are done by another program called CLRPL which can also be accessed while running CIMAG2. The report includes the user's and programming manuals, a listing of the commands in the HELP library and all the FORTRAN subroutines. GRA

N88-25176# Rensselaer Polytechnic Inst., Troy, N.Y. Dept. of Computer Science.
BEYOND Ada: GENERATING Ada CODE FROM EQUATIONAL SPECIFICATIONS
Boleslaw K. Szymanski 1987 6 p
(Contract N00014-86-K-0442)
(AD-A191866) Avail: NTIS HC A02/MF A01 CSCL 12E

Real time mission-oriented embedded systems are much more difficult to design than ordinary software systems. They require highly reliable and efficient implementations to satisfy mission and time constraints imposed by the applications. The Ada language has been design to facilitate real time system software development. However, for many programmers the size and complexity of Ada itself are of concern. In the assertive programming paradigm, computations are specified as sets of assertions about properties of the solution, and not as a sequence of procedural steps. Solving procedures are automatically generated from the assertive description. Real time programming for mission-oriented systems is supported by equational languages in which assertions are expressed as algebraic equations. Programs written in equational languages are concise, free from implementation details, and easily amenable to verification and parallel processing. The level of programming expertise required to program in an equational language is much lower than the level that is needed by Ada programmers. The paper describes an implementation of an equational language system which generates highly efficient distributed code in Ada. It also demonstrates how the equational language system can be used in real time software development. GRA

N88-25177# Florida Univ., Gainesville.
AN ELECTROSTATIC POTENTIAL COMPARATOR Contractor Report, Jul. 1983 - Mar. 1984
George D. Purvis, III and James W. King Feb. 1988 35 p Prepared in cooperation with Battelle, Research Triangle Park, N.C.
(Contract DAAG29-81-D—0100)
(AD-A192051; CRDEC-CR-88038) Avail: NTIS HC A03/MF A01 CSCL 15F

A program called ELESTA for computing, displaying, and comparing electrostatic potentials from semiempirical INDO wavefunctions and from ad initio Gaussian-type wavefunctions has been developed. Electrostatic potentials for DFP (diisopropyl phosphorofluoridate), GB (isopropyl methylphosphonofluoridate), 4,5-dichloro 2,3-difluoro-1,3-dioxolane, and GABA (gamma-aminobutyric acid) zwitterion are reported. GRA

N88-25178# Yale Univ., New Haven, Conn. Foundation for Research in Economics.
A CENTERED PROJECTIVE ALGORITHM FOR LINEAR PROGRAMMING
Michael J. Todd and Yinyu Ye Feb. 1988 43 p Prepared in cooperation with Stanford Univ., Calif.
(Contract N00014-87-K-0212; Grant NSF ECS-86-02534)
(AD-A192100; DISCUSSION PAPER-861) Avail: NTIS HC A03/MF A01 CSCL 12A

We describe a projective algorithm for linear programming that shares features with Karmarkar's projective algorithm and its variants and with the path-following methods of Gonzaga, Kojima-Mizuno-Yoshise, Monteiro-Adler, Renegar, Vaidya and Ye. It operates in a primal-dual setting, stays close to the central trajectories, and converges in O the square root of n x L iterations like the latter methods. (Here n is the number of variables and L the input size of the problem.) However, it is motivated by seeking reductions in a suitable potential function as in projective algorithms, and the approximate centering is an automatic byproduct of our choice of potential function. GRA

N88-25179# Research Inst. of National Defence, Linkoeping (Sweden).
SYSTEM OVERVIEW: TERAGON 4000, AN IMAGE PROCESSING EQUIPMENT AT FOA 3
Olof Berglund, Mats Ekman, Hans-Ake Olsson, and Bjoern Starkenberg Oct. 1987 45 p In SWEDISH; ENGLISH summary
(FOA-C-30465-3.3; ISSN-0347-3708; ETN-88-91883) Avail: NTIS HC A03/MF A01; Research Institute of National Defence, Box 1165, S-581 11 Linkoping, Sweden, 50 Swedish crowns

A display processor, general image processor, filter processor, resampling processor, video input-processor, and video disks are described. The equipment is connected to a VAX computer via a direct memory access. A videoprint of high resolution for black and white and color films is used. The application support package, image processing package, dialog, operator assembler, image base routiner, spider interface, and security programs are outlined. ESA

N88-25180# Ecole Nationale Superieure des Telecommunications, Paris (France). Dept. d'Images.
APPLICATION OF DYNAMIC PROGRAMMING TO IMAGE REGISTRATION Ph.D. Thesis [APPLICATION DE LA PROGRAMMATION DYNAMIQUE AU RECALAGE D'IMAGES]
Yifeng Wu Oct. 1987 141 p In FRENCH; ENGLISH summary
(ENST-87E022; ISSN-0751-1353; ETN-88-92181) Avail: NTIS HC A07/MF A01

A dynamic programming (DP) approach to image registration is presented. A picture is paired with a reference map. In order to achieve registration, an ordered sequence of primitive patterns is formed from the map. An attempt is made to locate a similar sequence from the picture using classical picture processing methods. This yields a distorted and unordered sequence marked by noise. Dynamic programming is used to search for a common match to the two sequences. The initial and final registration states are, however, unknown. Moreover, the continuity of the path is frequently interrupted, due to shortcomings in detection, or perhaps occlusions. The concept of virtual state, kept in memory, suspends broken paths until they can be reconnected, thus bridging gaps between the different parts of the path. The proposed algorithm was applied to satellite images with their contours sectioned by clouds. Results show very good registration, in spite of image contours badly hampered by noise and or clouds. For images subjected to parametric deformations, DP is used to estimate the parameters of the transformation. For nonparametric distortion, DP is used with autoregressive models. ESA

N88-25181# Los Alamos National Lab., N. Mex.
A GRAPHICAL, INTELLIGENT INTERFACE FOR DISCRETE-EVENT SIMULATIONS
C. Michelsen, J. Dreicer, and D. Morgeson 1988 8 p Presented at the Computer Human Interaction Conference, Washington, D.C., 15 May 1988
(Contract W-7405-eng-36)
(DE88-000522; LA-UR-87-3090; CONF-880516-2) Avail: NTIS HC A02/MF A01

This paper will present a prototype of an engagement analysis

simulation tool. This simulation environment is to assist a user (analyst) in performing sensitivity analysis via the repeated execution of user-specified engagement scenarios. This analysis tool provides an intelligent front-end which is easy to use and modify. The intelligent front-end provides the capabilities to assist the use in the selection of appropriate scenario value. The incorporated graphics capabilities also provide additional insight into the simulation events as they are unfolding. DOE

N88-25182# Stanford Univ., Calif. Systems Optimization Lab.
MAKING PROGRESS DURING A STALL IN THE SIMPLEX ALGORITHM
G. B. Dantzig Feb. 1988 9 p
(Contract DE-FG03-87ER-25028)
(DE88-007120; SOL-88-5) Avail: NTIS HC A02/MF A01

All the standard methods for avoiding cycling in the simplex algorithm set up a subprogram related to the blocking rows in the canonical form and look for an improving homogeneous solution. The method proposed in this paper does not. Instead, the Gass-Saaty parametric method applied to the objective (cost) form is used to choose the incoming column. The pivot-row choice among blocking rows, i.e., those tied for pivot, is arbitrary. A simple anti-cycling device is used which avoids dual degeneracy of the parameterized objective with probability one. Tests were run on nine highly degenerate practical test problems ranging in size from small to large. Using MINOS software, the standard simplex method required 31195 iterations of which 20504 (or 66%) were blocked pivots. Using the parametic scheme required 14379 iterations, of which 9481 or 66% were also blocked. The reduction in the number of interactions for this set of highly degenerate test problems is over 50%. CPU time reduction under the current way of implementation is 40%. DOE

N88-25183*# Illinois Univ., Urbana-Champaign. Computer Systems Group.
AN IMPROVED SIMULATED ANNEALING ALGORITHM FOR STANDARD CELL PLACEMENT
Mark Jones and Prithviraj Banerjee [1988] 9 p Presented at the International Conference on Computer Design, New York, N.Y., 2-4 Oct. 1987
(Grant NAG1-613)
(NASA-CR-182952; NAS 1.26:182952) Avail: NTIS HC A02/MF A01 CSCL 09B

Simulated annealing is a general purpose Monte Carlo optimization technique that was applied to the problem of placing standard logic cells in a VLSI ship so that the total interconnection wire length is minimized. An improved standard cell placement algorithm that takes advantage of the performance enhancements that appear to come from parallelizing the uniprocessor simulated annealing algorithm is presented. An outline of this algorithm is given. B.G.

N88-25184*# National Aeronautics and Space Administration. Langley Research Center, Hampton, Va.
THE ENVIRONMENT FOR APPLICATION SOFTWARE INTEGRATION AND EXECUTION (EASIE), VERSION 1.0. VOLUME 3: PROGRAM EXECUTION GUIDE
James L. Schwing, Lawrence F. Rowell, and Russell E. Criste (Computer Sciences Corp., Hampton, Va.) Apr. 1988 124 p
(NASA-TM-100575; NAS 1.15:100575) Avail: NTIS HC A06/MF A01 CSCL 09B

The Environment for Application Software Integration and Execution, EASIE, provides a methodology and a set of software utility programs to ease the task of coordinating engineering design and analysis codes. EASIE was designed to meet the needs of conceptual design engineers that face the task of integrating the results of many stand-alone engineering analysis programs. EASIE provides access to these programs via a quick, uniform, user-friendly interface. In addition, EASIE provides utilities which aid in the execution of the following tasks: selection of application programs, modification and review of program data, automatic definition and coordination of data files during program execution and a logging of steps executed throughout a design study. Volume 3, the Program Execution Guide, describes the executive capabilities provided by EASIE and defines the command language and menus available under Version 1.0. EASIE provides users with two basic modes of operation. One is the Application-Derived Executive (ADE) which provides users with sufficient guidance to quickly review data, select menu action items, and execute application programs. The second is the Complete Control Executive (CCE), which provides a full executive interface allowing users in-depth control of the design process. Author

N88-25185*# California Univ., San Diego. Dept. of Applied Mechanics and Engineering Sciences.
DESIGN OF CATALYTIC MONOLITHS FOR CLOSED-CYCLE CARBON DIOXIDE LASERS Progress Report
Richard K. Herz 30 Jun. 1988 30 p
(Grant NAG1-823)
(NASA-CR-182983; NAS 1.26:182983; UCSD-88-5205) Avail: NTIS HC A03/MF A01 CSCL 09B

A computer program was written that allows the design of catalytic monoliths for closed-cycle carbon dioxide lasers. Using design parameters obtained from workers at NASA Langley Research Center and from the literature, several specific monoliths were designed and the results were communicated to the research group working on this project at Langley. Two oral presentations were made at NASA-sponsored workshops - at Langley in January 1988 and in Gainesville, Florida in May 1988. Author

N88-25186# Karlsruhe Univ. (West Germany). Inst. fuer Informatik.
KA-PROLOG. KAP-COMPUTER: COMPUTER MODEL AND INSTRUCTIONS SET [KA-PROLOG. KAP-MASCHINE: MASCHINENMODELL UND INSTRUKTIONSSATZ]
Burkhard Neidecker 1987 33 p In GERMAN
(ETN-88-91948) Avail: NTIS HC A03/MF A01

The Karlsruher Prolog Project was initiated for the efficient use of the Prolog programming language in artificial intelligence research. Developments and improvements achieved concern the main programmed instructions, structure of register, representation of data and query procedures, help procedures, unify, input, and index instructions. ESA

N88-25187# Center for Mathematics and Computer Science, Amsterdam (Netherlands). Dept. of Numerical Mathematics.
SOLVING BIDIAGONAL SYSTEMS OF LINEAR EQUATIONS ON THE CDC CYBER 205
J. J. F. M. Schlichting and H. A. vanderVorst Nov. 1987 49 p
(CWI-NM-R8725; B8805676; ETN-88-92596) Copyright Avail: NTIS HC A03/MF A01

Algorithms for the solution of a bidiagonal system of linear equations on a Cyber 205 are analyzed and tested and the estimated and actual execution times are found to be in good accordance. Unrolling, statement sequencing, and other well known optimization techniques are applied to the straightforward solution of the problem, coded in standard FORTRAN. The performance improvements obtainable by hand optimization and compiler optimization options are measured. Cyclic reduction allows the solution algorithm to be at least partly vectorized. The so-called stride problem may be mitigated by the compress and sparse vector instructions or by the application of a folding technique allowing fast compactification of sparse data, but with increased computational complexity. In scalar algorithms for recursive problems cyclic reduction allows the computational parallelism in the scalar processor to be exploited. The swap instruction exchanges data between register file and memory up to four times faster than load and store instructions. A simple algorithm by which the ratio of equations, that must be reduced to obtain the fastest scalar code, can be computed was developed. On a Cyber 205 with a single vector pipe, the fastest algorithm is fully scalar. For two pipes a partial vectorization gives the best results and on a four-pipe Cyber 205 a fully vectorized algorithm is required to obtain optimal performance. In half precision mode the highest performance is achieved by partial vectorization for a one-pipe

Cyber and by full vectorization on a two or four-pipe Cyber 205.
ESA

N88-25188# Los Alamos National Lab., N. Mex.
THE -MDOC MACRO PACKAGE: A SOFTWARE TOOL TO SUPPORT COMPUTER DOCUMENTATION STANDARDS
C. E. Sanders 16 Sep. 1987 13 p Presented at the 35th Annual International Technical Communication Conference, Philadelphia, Pa., 10 May 1988
(Contract W-7405-eng-36)
(DE88-000500; LA-UR-87-3129; CONF-880528-1) Avail: NTIS HC A03/MF A01

At Los Alamos National Laboratory a small staff of writers and word processors in the Computer Documentation Group is responsible for producing computer documentation for the over 8000 users of the laboratory's computer network. The -mdoc macro package was developed as a software tool to support that effort. The -mdoc macro package is used with the NROFF/TROFF document preparation system on the UNIX operating system. The -mdoc macro package incorporates the standards for computer documentation at Los Alamos established by the writers. Use of the -mdoc macro package has freed the staff of programming format details, allowing writers to concentrate on content of documents and word processors to produce documents in a timely manner. It is an easy-to-use software tool that adapts to changing skills, needs, and technology.
DOE

N88-25189# Sandia National Labs., Albuquerque, N. Mex.
CONSIDERATIONS INVOLVED IN THE DISPLAY OF FINITE ELEMENT RESULTS USING ANIMATION
K. W. Gwinn and J. R. Koteras 1988 6 p Presented at the ASME Pressure Vessel and Piping Conference, Pittsburgh, Pa., 19 Jun. 1988
(Contract DE-AC04-76DP-00789)
(DE88-007581; SAND-87-2552C; CONF-880661-4) Avail: NTIS HC A02/MF A01

The presentation of results from complicated finite element analyses is as important and sometimes as difficult as the analysis itself. As the analyses become more systematically and physically complicated the presentation of vast quantities of data has become the limiting factor for understanding the results. This is due to limitations in the available display media with the additional difficulty of data transmission to the media itself. The use of high-end graphics devices is one useful means of interpreting the complex results from numerical analyses. Generation of animation sequences is another useful tool for examining results. In the past, movie film has served as the basis for generation of animation sequences. Processing and editing of film has proved to be a cumbersome process. Video is an alternative which eliminates some of the problems of film. However, computer animation and video must be carefully integrated if the high quality of the computer animation is to be preserved. The various considerations are discussed which are to be made when video is used as a basis for generation of animation sequences for numerical analysis.
DOE

N88-25190*# National Aeronautics and Space Administration. Langley Research Center, Hampton, Va.
THE SIZING AND OPTIMIZATION LANGUAGE, (SOL): COMPUTER LANGUAGE FOR DESIGN PROBLEMS
Stephen H. Lucas (Vigyan Research Associates, Inc., Hampton, Va.) and Stephen J. Scotti Apr. 1988 44 p Presented at the 29th Structures, Structural Dynamics and Materials Conference, Williamsburg, Va., 18-20 Apr. 1988
(NASA-TM-100565; NAS 1.15:100565) Avail: NTIS HC A03/MF A01 CSCL 09B

The Sizing and Optimization Language, (SOL), a new high level, special purpose computer language was developed to expedite application of numerical optimization to design problems and to make the process less error prone. SOL utilizes the ADS optimization software and provides a clear, concise syntax for describing an optimization problem, the OPTIMIZE description, which closely parallels the mathematical description of the problem. SOL offers language statements which can be used to model a design mathematically, with subroutines or code logic, and with existing FORTRAN routines. In addition, SOL provides error checking and clear output of the optimization results. Because of these language features, SOL is best suited to model and optimize a design concept when the model consits of mathematical expressions written in SOL. For such cases, SOL's unique syntax and error checking can be fully utilized. SOL is presently available for DEC VAX/VMS systems. A SOL package is available which includes the SOL compiler, runtime library routines, and a SOL reference manual.
Author

N88-25191*# Tennessee Univ., Knoxville. Dept. of Computer Science.
ALGORITHMS AND SOFTWARE FOR SOLVING FINITE ELEMENT EQUATIONS ON SERIAL AND PARALLEL ARCHITECTURES Final Report
Eleanor Chu and Alan George 22 Jun. 1988 135 p
(Grant NAG1-803)
(NASA-CR-183027; NAS 1.26:183027) Avail: NTIS HC A07/MF A01 CSCL 09B

The primary objective was to compare the performance of state-of-the-art techniques for solving sparse systems with those that are currently available in the Computational Structural Mechanics (MSC) testbed. One of the first tasks was to become familiar with the structure of the testbed, and to install some or all of the SPARSPAK package in the testbed. A brief overview of the CSM Testbed software and its usage is presented. An overview of the sparse matrix research for the Testbed currently employed in the CSM Testbed is given. An interface which was designed and implemented as a research tool for installing and appraising new matrix processors in the CSM Testbed is described. The results of numerical experiments performed in solving a set of testbed demonstration problems using the processor SPK and other experimental processors are contained.
Author

N88-25192*# National Aeronautics and Space Administration. Ames Research Center, Moffett Field, Calif.
SIMULATING FUTURES IN EXTENDED COMMON LISP
Philip R. Nachtsheim Jun. 1988 11 p
(NASA-TM-101000; A-88176; NAS 1.15:101000) Avail: NTIS HC A03/MF A01 CSCL 09B

Stack-groups comprise the mechanism underlying implementation of multiprocessing in Extended Common LISP, i.e., running multiple quasi-simultaneous processes within a single LISP address space. On the other hand, the future construct of MULTILISP, an extension of the LISP dialect scheme, deals with parallel execution. The source of concurrency that future exploits is the overlap between computation of a value and use of the value. Described is a simulation of the future construct by an interpreter utilizing stack-group extensions to common LISP.
Author

N88-25116*# National Weather Service, Silver Spring, Md. Aviation Services Branch.
COMPUTER AND MODEL CHANGES AT NATIONAL METEOROLOGICAL CENTER (NWC)
Charles H. Sprinkle *In* Tennessee Univ. Space Inst., Tullahoma. Meteorological and Environmental Inputs to Aviation Systems Jun. 1988 p 139-143 (For primary document see N88-25105 18-47)
Avail: NTIS HC A11/MF A01 CSCL 09B

62 COMPUTER SYSTEMS

Includes computer networks and special application computer systems.

N88-25193# Naval Postgraduate School, Monterey, Calif.
DESIGN, IMPLEMENTATION AND EVALUATION OF AN OPERATING SYSTEM FOR A NETWORK OF TRANSPUTERS

M.S. Thesis
Mauricio deMenezesCordeiro Jun. 1987 163 p
(AD-A186593) Avail: NTIS HC A08/MF A01 CSCL 09B

This thesis presents the Design, Implementation and Evaluation of an Operating System for a Network of Transputers, with main focus on the Communiation Subsystem. It also introdues the novice to the Transputer Development System (TDS), and suggests a sequence for developing applications. All the programs and examples presented in this thesis were implemented in the OCCAM1 Programming Language, and using the Transputer Development System (TDS-D600), running under the VAX/VMS Operating System at the Naval Postgraduate School (NPS).
GRA

N88-25194# Oak Ridge National Lab., Tenn.
NETWORK ARCHITECTURE FOR OPS5
P. L. Butler, J. D. Allen, and D. W. Bouldin 1988 14 p Presented at the 15th Annual International Symposium on Computer Architecture, Hawaii, 30 May 1988
(Contract DE-AC05-84OR-21400)
(DE88-002802; CONF-880540-1) Avail: NTIS HC A03/MF A01

The design and implementation of a non-Rete based architecture which captures some of the inherent parallelism in the OPS5 expert system language are discussed. A central feature of the architecture is a network bus over which a single host processor broadcasts messages to a set of parallel rule processors. This transmit-only bus is implented by a memory-mapped scheme which permits the rule processors to be decoded in parallel. All OPS5 rule matching processes and most of those associated with conflict resolution are executed by the parallel rule processors. The host performs the tasks associated with the firing of a selected rule. Performance data are presented for the prototype system which comprise a hot processor and 64 parallel rule processors, each embodying a Motorola MC68000 microprocessor and 512 kbytes of unshared memory.
DOE

N88-25195# Lawrence Livermore National Lab., Calif.
EFFECTIVE USE OF SHARED MEMORY MULTIPROCESSORS
E. D. Brooks, III 16 Feb. 1988 16 p Presented at the 3rd International Conference on Supercomputing, Boston, Mass., 15 May 1988
(Contract W-7405-eng-48)
(DE88-007019; UCRL-98211; CONF-880567-3) Avail: NTIS HC A03/MF A01

Two application codes are considered as case studies for the performance of shared memory multiprocessors. The first code is a packet switched network simulator, the second implements a new Monte Carlo algorithm for line transport. The codes are written in a portable parallel extension of the C programming language that can be compiled and executed on several shared memory multiprocessors, and that can be compiled into efficient serial code on any uniprocessor. We find that the latest crop of cost effective shared memory multiprocessors, when effectively used as multiprocessors on a single application, can exceed the performance of a well known supercomputer.
DOE

N88-25196*# National Aeronautics and Space Administration. Ames Research Center, Moffett Field, Calif.
NAS: THE FIRST YEAR
F. R. Bailey and Paul Kutler Jun. 1988 17 p
(NASA-TM-101006; A-88187; NAS 1.15:101006) Avail: NTIS HC A03/MF A01 CSCL 09B

Discussed are the capabilities of NASA's Numerical Aerodynamic Simulation (NAS) Program and its application as an advanced supercomputing system for computational fluid dynamics (CFD) research. First, the paper describes the NAS computational system, called the NAS Processing System Network, and the advanced computational capabilities it offers as a consequence of carrying out the NAS pathfinder objective. Second, it presents examples of pioneering CFD research accomplished during NAS's first operational year. Examples are included which illustrate CFD applications for predicting fluid phenomena, complementing and supplementing experimentation, and aiding in design. Finally, pacing elements and future directions for CFD and NAS are discussed.
Author

63 CYBERNETICS

Includes feedback and control theory, artificial intelligence, robotics and expert systems.

For related information see also *54 Man/System Technology and Life Support.*

N88-25197# Duke Univ., Durham, N. C. Dept. of Computer Science.
REPRESENTATION AND DECISION MECHANISMS IN ARTIFICIAL INTELLIGENCE Final Report, May 1984 - Sep. 1987
Donald W. Loveland and Alan W. Biermann 28 Dec. 1987 13 p
(Contract DAAG29-84-K-0072)
(AD-A191083; ARO-21213.7-MA) Avail: NTIS HC A03/MF A01 CSCL 12I

During the period of this grant, six subprojects were investigated and five subprojects have reports and/or publications at present. The sixth area is the subject of a Ph.D. dissertation expected to be completed in 1988. The areas include: Automatic selection of most efficient programs, determination of confidence factors in expert systems, analysis of errors that learning machines make, real time program synthesis through graph factorization, an extension to Prolog, and finding efficient test-and-treatment procedures.
GRA

N88-25198# Naval Research Lab., Washington, D.C.
GRAM-SCHMIDT IMPLEMENTATION OF A LINEARLY CONSTRAINED ADAPTIVE ARRAY Interim Report
Karl Gerlach 26 Feb. 1988 24 p
(AD-A191651; NRL-9056) Avail: NTIS HC A03/MF A01 CSCL 09A

A Gram-Schmidt (GS) implementation of the linearly constrained adaptive algorithm proposed by Frost is developed. This implementation is shown to be equivalent to the technique developed by Jim, Griffiths, and Buckley whereby the constrained problem is reduced to an unconstrained problem. In addition, analytical, results are presented for the convergence rate when the Sampled Matrix Inversion (SMI) algorithm is employed. It had been previously shown that the steady state solution for the optimal weights is identical for both constrained and reduced unconstrained problems. In this report, it is shown that if the SMI or GS algorithms are employed, then the transient weighting vector solution for the constrained problem is identical to equivalent transient weighting vector solution for the reduced unconstrained implementation.
GRA

N88-25199# Scientific Systems, Inc., Cambridge, Mass.
ADAPTIVE TIME SERIES ANALYSIS USING PREDICTIVE INFERENCE AND ENTROPY Annual Report, Dec. 1986 - Dec. 1987
Donald E. Dustafson Dec. 1987 85 p
(Contract F49620-87-C-0026)
(AD-A191858; AFOSR-88-0032TR) Avail: NTIS HC A05/MF A01 CSCL 12A

Research is being conducted on adaptive time series methods for detecting and tracking both abrupt and slow changes in both structure and parameters. The methods are based on a unified statistical frame work which is motivated by statistical inference and entropy arguments. The method yields estimates of input/output dynamics and noise statistics. An integrated approach which combines canonical variates analysis and maximum likelihood estimation has been developed and tested. Specific attention is given to the problem of parameter truncation in both a linear predictor and Kalman filter framework.
GRA

N88-25200# University of Southern California, Marina del Rey. Information Sciences Inst.
THE ISI (INFORMATION SCIENCES INSTITUTE) GRAPHER MANUAL
Gabriel Robins Feb. 1988 105 p
(Contract MDA903-81-C-0335)
(AD-A192198; ISI/TM-88-197) Avail: NTIS HC A06/MF A01 CSCL 12E

This document describes the implementation and usage of the Information Sciences Institute (ISI) Grapher, a portable software package that allows graphs to be displayed pictorially. The salient features of the ISI Grapher are its speed, portability, extensibility, and versatility. The ISI Grapher currently runs on several different kinds of workstations (including Symbolics, TI Explorers, SUNS, and Macintosh 2), and is available commercially. GRA

N88-25201# Institut National Polytechnique, Grenoble (France).
INTRODUCTION TO COMPLIANCE IN PROGRAMMING OF ROBOTS Ph.D. Thesis [INTRODUCTION DE LA COMPLIANCE DANS LA PROGRAMMATION DES ROBOTS]
Christian Gandon 1987 141 p In FRENCH
(ETN-88-92189) Avail: NTIS HC A07/MF A01

The interaction of a robot manipulator with its environment was studied. Approaches to compliance were reviewed. The definition and interpretation of compliant movements allowing force and position control of robots are outlined. A methodological approach to robot programming which takes into account the material possibilities of the robot manipulator to interact with its environment is presented. ESA

N88-25202# Institut National Polytechnique, Grenoble (France).
MODELING OF GEOMETRIC REASONING FOR ROBOT PROGRAMMING Ph.D. Thesis [MODELISATION DU RAISONNEMENT GEOMETRIQUE POUR LA PROGRAMMATION DES ROBOTS]
Jocelyne Pertin-Troccaz 1987 193 p In FRENCH; ENGLISH summary
(ETN-88-92290) Avail: NTIS HC A09/MF A01

The geometric modeling requirements of robotics are analyzed, and a model (multiple representation, spatial evolution modeling, uncertainty modeling) is proposed. A method for dealing with purposive automatic grasping is described. The general architecture of a system for automatic robot programming is proposed. ESA

N88-25203# Tennessee Univ., Knoxville.
ROBOT NAVIGATION USING SIMPLE SENSOR FUSION
D. M. Jollay and R. E. Ricks 1988 22 p Presented at the Spring Decus, Cincinnati, Ohio, 16 May 1988 Prepared in cooperation with Tennessee Univ., Chattanooga.
(Contract DE-AC05-84OR-21400)
(DE88-006184; CONF-880569-1) Avail: NTIS HC A03/MF A01

Sensors on an autonomous mobile system are essential in enviornment determination for navigation purposes. As is well documented in previous publications, sonar sensors are inadequate in providing a depiction of a real world environment and therefore do not provide accurate information for navigation, if not used in conjunction with another type of sensor. This paper describes a simple, inexpensive, and relatively fast navigation algorithm involving vision and sonar sensor fusion for use in navigating an autonomous robot in an unknown and potentially dynamic environment. Navigation of the mobile robot was accomplished by use of a TV camera as the primary sensor. Input data received from the camera were digitized through a video module and then processed using a dedicated vision system to enable detection of obstacles and to determine edge positions relative to the robot. Since 3D vision was not attempted due to its complex and time consuming nature, sonar sensors were then used as secondary sensors in order to determine the proximity of detected obstacles. By then fusing the sensor data, the robot was able to navigate (quickly and collision free) to a given goal, achieving obstacle avoidance in real-time. DOE

N88-25204*# National Aeronautics and Space Administration. Langley Research Center, Hampton, Va.
ROBUST ADAPTIVE REGULATION WITHOUT PERSISTENT EXCITATION
Rogelio Lozano-Leal May 1988 34 p
(NASA-TM-100571; NAS 1.15:100571) Avail: NTIS HC A03/MF A01 CSCL 09B

A globally convergent adaptive regulator for minimum or nonminimum phase systems subject to bounded distrubances and unmodeled dynamics is presented. The control strategy is designed for a particular input-output representation obtained from the state space representation of the system. The leading coefficient of the new representation is the product of the observability and controllability matrices of the system. The controller scheme uses a Least Squares identification algorithm with a dead zone. The dead zone is chosen to obtain convergence properties on the estimates and on the covariance matrix as well. This allows the definition of modified estimates which secure well-conditioned matrices in the adaptive control law. Explicit bounds on the plant output are given. Author

N88-25205*# National Aeronautics and Space Administration, Washington, D.C.
STATE OF TUNING
Shigenori Okubo Jun. 1988 22 p Transl. into ENGLISH from Journal of the Society of Instrument and Control Engineers, (Japan), v. 25, no. 9, Sep. 1986 p 832-839 Transl. by SCITRAN, Inc., Santa Barbara, Calif.
(Contract NASw-4307)
(NASA-TT-20195; NAS 1.77:20195) Avail: NTIS HC A03/MF A01 CSCL 09B

The trend of today's tuning is changing from the off-line type of Ziegler-Nichols to the on-line; however, we are still far away from complete auto-tuning. Discussed are some aspects of tuning. Author

N88-25206*# Catholic Univ. of America, Washington, D.C. Dept. of Electrical Engineering.
ANALYSIS OF A CLOSED-KINEMATIC CHAIN ROBOT MANIPULATOR Semiannual Report
Charles C. Nguyen and Farhad J. Pooran Jul. 1988 20 p
(Grant NAG5-780)
(NASA-CR-183031; NAS 1.26:183031) Avail: NTIS HC A03/MF A01 CSCL 09B

Presented are the research results from the research grant entitled: Active Control of Robot Manipulators, sponsored by the Goddard Space Flight Center (NASA) under grant number NAG-780. This report considers a class of robot manipulators based on the closed-kinematic chain mechanism (CKCM). This type of robot manipulators mainly consists of two platforms, one is stationary and the other moving, and they are coupled together through a number of in-parallel actuators. Using spatial geometry and homogeneous transformation, a closed-form solution is derived for the inverse kinematic problem of the six-degree-of-freedom manipulator, built to study robotic assembly in space. Iterative Newton Raphson method is employed to solve the forward kinematic problem. Finally, the equations of motion of the above manipulators are obtained by employing the Lagrangian method. Study of the manipulator dynamics is performed using computer simulation whose results show that the robot actuating forces are strongly dependent on the mass and centroid locations of the robot links. Author

N88-25207*# National Aeronautics and Space Administration. Hugh L. Dryden Flight Research Center, Edwards, Calif.
APPLICATION OF FLIGHT SYSTEMS METHODOLOGIES TO THE VALIDATION OF KNOWLEDGE-BASED SYSTEMS
Eugene L. Duke Jul. 1988 19 p Presented at the Space Operations Automation and Robotics (SOAR) Workshop, Dayton, Ohio, 20-23 Jul. 1988
(NASA-TM-100442; H-1493; NAS 1.15:100442) Avail: NTIS HC A03/MF A01 CSCL 09B

Flight and mission-critical systems are verified, qualified for

flight, and validated using well-known and well-established techniques. These techniques define the validation methodology used for such systems. In order to verify, qualify, and validate knowledge-based systems (KBS's), the methodology used for conventional systems must be addressed, and the applicability and limitations of that methodology to KBS's must be identified. The author presents an outline of how this approach to the validation of KBS's is being developed and used at the Dryden Flight Research Facility of the NASA Ames Research Center.
Author

64 NUMERICAL ANALYSIS

Includes iteration, difference equations, and numerical approximation.

N88-25208# Oak Ridge National Lab., Tenn.
A CONCURRENT NEURAL NETWORK ALGORITHM FOR THE TRAVELING SALESMAN PROBLEM
N. Toomarian 1988 9 p Presented at the 3rd Conference on Hypercube Concurrent Computers and Applications, Pasadena, Calif., 19 Jan. 1988
(Contract DE-AC05-84OR-21400)
(DE88-006981; CONF-880117-2) Avail: NTIS HC A02/MF A01

A binary neuromorphic data structure is used to encode the N-city Traveling Salesman Problem (TSP). In this representation the computational complexity, in terms of number of neurons, is reduced from Hopfield and Tank's 0(N sup 2) to 0(N log sub 2 N). A continuous synchronous neural network algorithm in conjunction with the Lagrange multiplier, is used to solve the problem. The algorithm has been implemented on the NCUBE hypercube multiprocessor. This algorithm converges faster and has a higher probability to reach a valid tour than previously available results.
DOE

N88-25209# Aeronautical Research Labs., Melbourne (Australia).
PAFEC LEVEL 6.2 APPLICATION PROGRAM
J. Paul Dec. 1987 15 p
(AD-A191037; ARL-STRUC-TM-475; DODA-AR-004-568) Avail: NTIS HC A03/MF A01 CSCL 12E

Finite element programs such as PAFEC often produce vast quantities of data which need to be processed. For analysis purposes only certain information is required and the rest is often discarded. However, the massive amounts of output generated sometimes makes it difficult to locate the relevant information. This report provides a brief outline of a suite of programs which have been developed for use with PAFEC to enable easier processing of the relevant data.
GRA

N88-25210# Florida State Univ., Tallahassee. Dept. of Statistics.
ASYMPTOTIC THEORY FOR WEIGHTED LEAST SQUARES ESTIMATORS IN AALEN'S ADDITIVE RISK MODEL
Ian W. McKeague Nov. 1987 16 p
(Contract DAAL03-86-K-0094)
(AD-A191085; FSU-TR-M-774; TR-D-100-ARO; ARO-23699.15-MA) Avail: NTIS HC A03/MF A01 CSCL 12C

Let h(t/Z sub i) be the conditional hazard function for the survival time of an individual sub i given the p-dimensional covariate process Z sub i(t). This document inference for Aalen's additive risk model h(t/Z sub i)=Z sub i(t) alpha (t), where alpha is a p-vector of unknown hazard functions. The theory of counting processes is used to obtain weak convergence results for weighted least squares estimators of the hazard functions and the cumulative hazard functions based on continuous data. Results for weighted least squares estimators based on grouped data are also described.
GRA

N88-25211# Prometheus, Inc., Sharon, Mass.
NULL STEERING APPLICATIONS OF POLYNOMIALS WITH UNIMODULAR COEFFICIENTS Final Report, 1 Aug. 1986 - 28 Feb. 1987
James S. Byrnes, Donald J. Newman, and Martin Goldstein 23 Mar. 1987 76 p
(Contract F49620-86-C-0088)
(AD-A191087; Rept-87-01; AFOSR-87-2014TR) Avail: NTIS HC A05/MF A01 CSCL 12A

Concerning adaptive array and null steering applications of polynomials with restricted coefficients, the basic mathematical question to consider in electronic beam steering, with a discrete array consisting of omnidirectional elements spaced at equal increments along a straight line, is how coefficients of a polynomial may be chosen in a robust yet computationally efficient manner so as to arrive at a desired beam pattern. In numerous applications, these coefficients are required to satisfy certain restrictions, such as a bound on their dynamic range. Thus, particularly in null steering, it is often advantageous, or even necessary, for the shading coefficients to all have the same magnitude. Basic properties of such polynomials and their applications to beamforming are described.
GRA

N88-25212# Arizona State Univ., Tempe.
MATHEMATICAL MODELS FOR VLSI DEVICE SIMULATION Final Report
Christian Ringhofer 24 Nov. 1987 9 p
(Grant AF AFOSR-0240-85)
(AD-A191125; AFOSR-88-0346TR) Avail: NTIS HC A02/MF A01 CSCL 20L

The research supported under this grant was concerned with analytical and numerical simulation aspects of the basic semiconductor equations. The research focused on an analysis of the mathematical structure of solutions via a singular perturbation approach, and the development of numerical methods for the transient problem.
GRA

N88-25213# Rochester Univ., N. Y. Dept. of Computer Science.
ALGORITHMS AND DATA STRUCTURES FOR AN EXPANDED FAMILY OF MATROID INTERSECTION PROBLEMS
Greg N. Frederickson and Mandayam A. Srinivas Sep. 1987 55 p
(Contracts N00014-86-K-0689; N00014-82-K-0193; Grant NSF DCR-83-20124)
(AD-A191482; TR-227) Avail: NTIS HC A04/MF A01 CSCL 12B

Matroids are discrete mathematical structures that appear in a variety of applications. They are structures for which greedy algorithm gives an optimal solution, and when interested characterize such problems as minimum weight maximum cardinality bipartite matching. In this paper we study a class of combinatorial problems from a matroid point of view. Consider a matroid of rank n in which each element has a real-valued cost and one of d > 1 colors. A class of matroid intersection problems is studied in which one of the matroids is a partition matroid that specifies that base have 9 sub k elements of color j, for j = 12 =1, 2, ..., d. Relationships are characterized among the solutions to the family of problems generated when the vector (q sub 1, q sub,... q sub d) is allowed to range over all values that sum to n. A fast algorithm is given for solving such matroid intersection problems when d is small. A characterization is presented for how the solution changes when one element changes in cost. Data structures are given for updating the solution on-line each time the cost of an arbitrary matroid element is modified. Efficient update algorithms are given for maintaining a color-constrained minimum spanning tree in either a general or a planar graph. An application for the techniques to finding a minimum spanning tree with several degree-constrained vertices is described.
GRA

N88-25214# California Inst. of Tech., Pasadena. Dept. of Electrical Engineering.
THEORETICAL INVESTIGATION OF OPTICAL COMPUTING BASED ON NEURAL NETWORK MODELS Annual Report, 30 Sep. 1986 - 29 Sep. 1987
Yaser Abu-Mostafa and Demetri Psaltis 29 Sep. 1987 84 p (Grant AF AFOSR-0296-86)
(AD-A191668; AFOSR-88-0025TR) Avail: NTIS HC A05/MF A01 CSCL 23C

It is difficult to find good mathematical models for many natural problems such as pattern recognition. Not only does this difficulty preclude finding good solutions for these problems, but it also precludes estimating their complexity using the standard tools of the theory oc computational complexity (Traub, 1985). Part of the difficulty can be traced to symptoms such as ill-definition, fuzziness, and inexactness. However, the difficulty of modeling these problems may be inherent in some cases. GRA

N88-25215# Pittsburgh Univ., Pa. Inst. for Computational Mathematics and Applications.
NFEARS: A NONLINEAR ADAPTIVE FINITE ELEMENT SOLVER, PART 1
Charles K. Mesztenyi and Werner C. Rheinboldt Dec. 1987 50 p Prepared in cooperation with Maryland Univ., College Park (Contracts N00014-80-C-0455; N00014-85-K-0169; Grant NSF DCR-83-09926)
(AD-A191823; ICMA-87-113-Pt-1) Avail: NTIS HC A03/MF A01 CSCL 12A

The two parts of this report present an introduction to the design and usage of the NFEARS system developed jointly at the Universities of Maryland and Pittsburgh. The acronym stands for Nonlinear Finite Element Adaptive Research Solver and refers to an experimental software system for the solution of a class of nonlinear, stationary boundary value problems in two space dimensions involving two real parameters. The overall concept of the system is similar to that of the earlier system FEARS for linear elliptic problems and retains many of the features of that system. The eight sections of Part 1 describe the mathematical background of the processes incorporated into NFEARS, and the six sections of Part 2 serve as User's Manual for the program. As the earlier program, NFEARS was developed strictly as a research tool and is expected to be subject to continual modifications. GRA

N88-25216# American Mathematical Society, New York, N.Y.
INFINITE DIMENSIONAL DYNAMICAL SYSTEMS AND THEIR FINITE DIMENSIONAL ANALOGUES Final Report, 15 Jul. - 14 Sep. 1987
Maxwell 1987 34 p
(Grant AF AFOSR-0279-87)
(AD-A192041; AFOSR-88-0186TR) Avail: NTIS HC A03/MF A01 CSCL 12A

Reports are given research to-date concerning nonlinear Partial Differential Equations and possible systems of Ordinary Differential Equations which faithfully capture their essential behavior, particularly in terms of chaotic behavior. GRA

N88-25217# Grenoble-1 Univ., Saint Martin d'Heres (France). Techniques de l'Informatique, des Mathematiques, de la Microelectronique et de la Microscopie Quanti
A PRIMAL-DUAL ALGORITHM FOR THE COMPUTATION OF THE MINIMUM OF A CONVEX FUNCTION ON THE INTERSECTION OF CONVEX FUNCTIONS, AND ITS APPLICATION IN DATA ANALYSIS [UN ALGORITHME PRIMAL-DUAL POUR LE CALCUL DU MINIMUM D'UNE FONCTION CONVEXE SUR UNE INTERSECTION DE CONVEXES ET SES APPLICATIONS EN ANALYSE DES DONNEES]
Mohamed Boughazi and Dinh Tao Pham Jan. 1987 51 p In FRENCH; ENGLISH summary
(RR-638-M; ETN-88-92280) Avail: NTIS HC A04/MF A01

An algorithm for computation of the minimum of a convex function over the intersection of closed, convex sets is presented. The algorithm, derived from the partial inverse method developed by Spingarn (1983), simultaneously generates two sequences globally converging respectively to a primal and a dual solution. As applications, two problems from data analysis (isotonic regression and convex regression) are shown. ESA

N88-25218# Grenoble-1 Univ., Saint Martin d'Heres (France). Techniques de l'Informatique, des Mathematiques, de la Microelectronique et de la Microscopie Quanti
OPEN OR CLOSED CURVES BY REGULARIZED B-SPLINES
Pierre-Jean Laurent Mar. 1987 26 p In FRENCH; ENGLISH summary
(RR-652-M; ETN-88-92282) Avail: NTIS HC A03/MF A01

Regularized least squares PASCAL procedures based on B-splines are given for the representation of open curves and of closed curves (periodicity constraints). They are applied to cases where data are missing in places. ESA

N88-25219# Grenoble-1 Univ., Saint Martin d'Heres (France). Techniques de l'Informatique, des Mathematiques, de la Microelectronique et de la Microscopie Quanti
VARIANCES AND HIGHER ORDER CORRELATION COEFFICIENTS: CONTINUED [VARIANCES ET COEFFICIENTS DE CORRELATION D'ORDRE SUPERIEUR: SUITE]
R. Blacher Apr. 1987 208 p In FRENCH; ENGLISH summary
(RR-655-M; ETN-88-92283) Avail: NTIS HC A10/MF A01

Correlation coefficients of order (i,j) and variances of order i are studied. The asymptotic distribution of empirical correlation coefficient of order (i,j) and the asymptotic distribution of empirical variance of order i are obtained. The type of dependence which is measured by these coefficients is investigated. Applications to conditional probability are proposed. ESA

N88-25220# Grenoble-1 Univ., Saint Martin d'Heres (France). Techniques de l'Informatique, des Mathematiques, de la Microelectronique et de la Microscopie Quanti
A FAST AND EFFICIENT PROCEDURE FOR GENERALIZED CROSS-VALIDATION WITH LARGE DATA SETS. APPLICATION TO IMAGE RECONSTRUCTION
Didier Girard May 1987 35 p In FRENCH; ENGLISH summary
(RR-669-M; ETN-88-92289) Avail: NTIS HC A03/MF A01

A fast Monte-Carlo algorithm is proposed for calculating reliable estimates of the trace of the influence matrix At involved in regularization of integral equations or data smoothing problems, where t is the regularization or smoothing parameter. It is shown by theoretical bounds and by numerical simulations on typical problems, that the expected relative precision of the estimates is good when the number of data points (n) is large enough and so they can be used in the minimization with respect to t of the Generalized Cross-Validation (GCV) function. This permits the use of (approximate) GCV on large data sets, with the same work as the standard residual method. Numerical application of this method to optimal spline smoothing in one- and two-dimensions (on this second problem with n of the order of 1000 and a conjugate gradient method for the computation of Aty, given y, the existing methods for GCV are impractical) show its efficiency. ESA

N88-25221# Sheffield Univ. (England). Dept. of Control Engineering.
ON FREQUENCY RESPONSE FOR NONLINEAR SYSTEMS
S. P. Banks and B. Chanane Dec. 1987 14 p
(RR-323; ETN-88-92523) Avail: NTIS HC A03/MF A01

The idea of a generalized frequency response for a nonlinear system is presented. The theory is illustrated in the linear and bilinear cases, and realization results are obtained. Sufficient conditions for L sq-stability of bilinear systems are derived. For simplicity, single input-single output systems are considered. ESA

N88-25222 Texas Univ., Austin.
OPTIMAL A PRIORI COVARIANCE SELECTION FOR THE SOLUTION OF ILL-CONDITIONED NONLINEAR INVERSE PROBLEMS Ph.D. Thesis
David Allen Cicci 1987 262 p
Avail: Univ. Microfilms Order No. DA8728534

The method of data augmentation, in the form of a priori convariance information concerning the reference solution, as a means to overcome the effects of ill-conditioning is a class of nonlinear inverse problems was investigated. Specifically, for the case when the ill-conditioning results in an unobserved problem and the a priori covariance is unknown, methods by which the a priori covariance is optimally chosen are presented. These solution techniques, which are based upon the theory of ridge regression, choose the augmenting data set by minimizing the mean square error of the solution. This criterion uses the notion of adding a small amount of bias to the solution while substantially reducing the variance. The ridge-type solution methods are demonstrated by their application to two unobservable gravity field recovery simulations. The first simulation consists of a perfectly modeled dynamical system, while the second consists of a case where imperfections exist in the dynamical model. Results of the simulations are compared to results obtained by the conventionally used technique of assigning preprescribed values for the a priori covariance. Algorithms which allow the ridge-type methods to be implemented using orthogonal transformations in place of direct normal matrix solution techniques are presented. The ridge-type solution methods presented are applicale to observable problems as well as the unobservable problems directly addressed.
Dissert. Abstr.

N88-25223 Northwestern Univ., Evanston, Ill.
PROBABILISTIC FINITE ELEMENT METHODS Ph.D. Thesis
Ayyakannu Mani 1987 180 p
Avail: Univ. Microfilms Order No. DA8729019

Probabilistic finite element methods (PFEM), synthesizing the power of finite element methods with second moment techniques, are formulated for various classes of problems in structural and solid mechanics. Time invariant random materials, geometric properties and loads are incorporated in terms of their fundamental statistics viz. second moments. Analogous to the discretization of the displacement field in finite element methods, the random fields are also discretized. Preserving the conceptual simplicity, the response moments are calculated with minimal computations. By incorporating certain computational techniques, these methods are shown to be capable of handling large systems with many sources of uncertainties. By construction, these methods are applicable when the scale of randomness is not very large and when the probabilistic density functions have decaying tails. The accuracy and efficiency of these methods, along with their limitations, are demonstrated by various applications. Results obtained are compared with those of Monte Carlo simulation. The methods are amenable to implementation in deterministic FEM based computer codes.
Dissert. Abstr.

N88-25224 New South Wales Univ., Kensington (Australia). School of Mathematics.
SOME PROPERTIES OF MODULAR EQUATIONS AND THE PARTITION FUNCTION M.S. Thesis Abstract Only
Barry Flynn 13 Mar. 1987 82 p
Avail: Issuing Activity

In 1919 Ramanujan conjectured that if a is greater than or = to 1, and mu(a) is the reciprocal modulo 11(a) of 24, then p(11(a)sub n + mu(a)) is identical to 0 mod 11(a). The main objective of this study was to prove this conjecture using elementary techniques similar to those of Hirschhorn and Hunt and Garvan. In the process, some of the results they obtained have been generalized and simplified, and some new results were obtained. In particular, a more generalized modular equation of the nth order was established. However, we have not been able to conclusively prove enough of the properties of the equation to prove Ramanujan's conjecture. In an attempt to determine what results we should be trying to prove, a 1000 line FORTRAN computer program was written to try and spot some patterns. As a result we have been able to state some interesting conjectures. If some of these conjectures are true, then Ramanujan's conjecture can be proven using elementary techniques.
Author

N88-25225# Vrije Universiteit, Amsterdam (Netherlands). Subfaculteit Wiskunde en Informatica.
LINEAR SPACES, ABSOLUTE RETRACTS AND THE COMPACT EXTENSION PROPERTY
J. vanderBijl and J. vanMill Oct. 1987 17 p
(PB88-181110; WS-333) Avail: NTIS HC A03/MF A01 CSCL 12A

The authors formulate a partial realization property and prove that this property is equivalent to the compact extension property. In addition, they prove that a linear space L has the compact extension property if and only if L is admissible if and only if L has the sigma-compact extension property. This implies that for a sigma-compact linear space L, the following statements are equivalent: (1) L is an absolute retract; (2) L has the compact extension property; and (3) L is admissible. Finally, it is proven that if there exists a linear space which is not an absolute retract, then there is an admissible linear space which is not an absolute retract.
GRA

N88-25226# Atlanta Univ., Ga. Dept. of Physics.
COMPUTATIONAL SCIENCES Final Report, 1 Jul. 1985 - 30 Sep. 1987
Kofi B. Bota Nov. 1987 37 p
(Grant DAAG29-85-G-0109)
(AD-A190826; ARO-23145-MA-H) Avail: NTIS HC A03/MF A01 CSCL 12A

Topics addressed include: stochastic difference equations; random differential equations; random Volterra integral equations; optimal processes; random Love integral equation; mixed Min-Max optimization problems; and mixed Min-Max control problems. For individual titles, see N88-25227 through N88-25237.

N88-25227# Atlanta Univ., Ga. Dept. of Mathematics and Computer Science.
NUMERICAL SOLUTION OF A SYSTEM OF RANDOM VOLTERRA INTEGRAL EQUATIONS. 1: SUCCESSIVE APPROXIMATION METHOD Abstract Only
Negash G. Medhin and M. Sambandham *In its* Computational Sciences Nov. 1987 1 p Prepared in cooperation with Morehouse Coll., Atlanta, Ga. (For primary document see N88-25226 18-64)
Avail: NTIS HC A03/MF A01 CSCL 12A

The successive approximation method for a system of random Volterra integral equations is discussed. An example is presented to implement the theory. Kolmogorov-Smirnov test is used to fit a distribution of the solutions.
Author

N88-25228# Atlanta Univ., Ga. Dept. of Mathematics and Computer Science.
A MIXED MIN-MAX CONTROL PROBLEM GOVERNED BY INTEGRAL EQUATIONS Abstract Only
Negash G. Medhin *In its* Computational Sciences Nov. 1987 1 p (For primary document see N88-25226 18-64)
Avail: NTIS HC A03/MF A01 CSCL 12A

A mixed min-max control problem is considered using relaxed controls. Mixed min-max problems govered by differential equations were considered using Dubovitskii and Milyutin Theory and Convex Analysis. Relaxed controls and penalization were used to deal with a process governed by integral equations. The technique was employed to deal with control problems governed by integral equations.
Author

N88-25229# Texas Univ., Arlington. Dept. of Mathematics.
NUMERICAL SOLUTIONS TO STOCHASTIC DIFFERENCE EQUATIONS Abstract Only **c65**
G. S. Ladde and M. Sambandham (Atlanta Univ., Ga.) *In* Atlanta Univ., Computational Sciences Nov. 1987 1 p Prepared in cooperation with Morehouse Coll., Atlanta, Ga. (For primary

document see N88-25226 18-64)
(Grant DAAG29-84-G-0060)
Avail: NTIS HC A03/MF A01 CSCL 12A

Statistical properties of the numerical solutions of random difference equations are estimated. By an application of variation of constant formula, error estimates between random solutions and smooth solutions (deterministic solution) are discussed.

Author

N88-25230# Atlanta Univ., Ga. Dept. of Mathematics and Computer Science.

NUMERICAL SOLUTION TO A SYSTEM OF RANDOM VOLTERRA INTEGRAL EQUATIONS Abstract Only

Negash G. Medhin, M. Sambandham, and C. K. Zoltani (Ballistic Research Labs., Aberdeen Proving Ground, Md.) *In its* Computational Sciences Nov. 1987 1 p Prepared in cooperation with Morehouse Coll., Atlanta, Ga. (For primary document see N88-25226 18-64)
Avail: NTIS HC A03/MF A01 CSCL 12A

A brief summary of the numerical solution of a system of random Volterra integral equations is presented. The methods used are: Newton's method and successive approximation method. Based on the simulation, the mean and variance of the solution of a system of random Volterra integral equations is discussed.

Author

N88-25231# Atlanta Univ., Ga.

OPTIMAL PROCESSES GOVERNED BY INTEGRAL EQUATIONS WITH UNILATERAL CONSTRAINT Abstract Only

Negash G. Medhin *In its* Computational Sciences Nov. 1987 1 p (For primary document see N88-25226 18-64)
Avail: NTIS HC A03/MF A01 CSCL 12A

An optimal process with unilateral constraint is considered using relaxed controls. Existence of optimal control is automatic. Further, problems with linear and certain quadratic cost functions with linear integral and state constraints are such that the controls are actually ordinary, i.e., bounded measurable functions. In addition, if the control set is a convex polyhedron the optimal controls take their values in the vertices of the polyhedron. Control processes governed by integral equations were considered. However, existence is not shown for the general problem and optimality conditions are not available for the problem when state constraints are presented.

Author

N88-25232# Atlanta Univ., Ga. Dept. of Mathematics and Computer Science.

MIXED MIN-MAX OPTIMIZATION PROBLEM WITH RESTRICTIONS Abstract Only

Negash G. Medhin and M. Sambandham *In its* Computational Sciences Nov. 1987 1 p Prepared in cooperation with Morehouse Coll., Atlanta, Ga. (For primary document see N88-25226 18-64)
Avail: NTIS HC A03/MF A01 CSCL 12A

A min-max optimization problem was considered using relaxed controls. Such problems were considered using Dubovitskii and Milyutin Theory and convex analysis. The problem was reformulated where a unilateral constraint is added. The reformulated problem was dealt with using penalization. The procedure produces more optimality conditions than convex analysis and also more insight into convex analysis. In the special case where the controls appear linearly and the control sets are convex polyhedra the relaxed controls are ordinary controls taking values in the vertices of the polyhedra. Finally, examples are presented where it was demonstrated how the optimal controls and trajectories could be calculated and some worked out numerically.

Author

N88-25233# Morehouse Coll., Atlanta, Ga. Dept. of Mathematics.

APPROXIMATE SOLUTION OF RANDOM DIFFERENTIAL EQUATION Abstract Only

M. Sambandham and Negash G. Medhin *In* Atlanta Univ., Computational Sciences Nov. 1987 1 p Prepared in cooperation with Atlanta Univ., Ga. (For primary document see N88-25226 18-64)
Avail: NTIS HC A03/MF A01 CSCL 12A

The Chebyshev method for solving random differential equations is presented. The convergence of the random coefficients of the Chebyshev series is established. Statistical properties of the random coefficients are discussed.

Author

N88-25234# Atlanta Univ., Ga. Dept. of Mathematics.

A METHOD FOR THE NUMERICAL SOLUTION OF RANDOM CAUCHY SINGULAR INTEGRAL EQUATION

M. Sambandham, T. S. Srivatsan (Georgia Inst. of Tech., Atlanta.), and K. B. Bota *In its* Computational Sciences Nov. 1987 22 p Prepared in cooperation with Morehouse Coll., Atlanta, Ga. (For primary document see N88-25226 18-64)
(Grant NSF PRM-82-15949)
Avail: NTIS HC A03/MF A01 CSCL 12A

The solution of several elasticity problems, and particularly crack problems, can be reduced to the solution of one-dimensional singular integral equations with a Cauchy-type kernel. A method for the numerical solution of a random singular integral solution of the Cauchy-type is presented. To illustrate this method, it is applied to the random singular integral equation that arises in the problem of periodic array of straight cracks inside an infinite isotropic elastic medium and subjected to random pressure distribution along the crack edges. The statistical properties of the random solution are evaluated numerically, and used to determine the stress intensity factor at the crack tips. Results of this study highlight the advantage of using this method to solve a random Cauchy-type singular integral equation. The method is applied to the crack problem suggested to different forcing functions.

Author

N88-25235# Morehouse Coll., Atlanta, Ga. Dept. of Mathematics.

NUMERICAL SOLUTION OF RANDOM LOVE'S INTEGRAL EQUATION Abstract Only

M. Sambandham, V. Thangaraj (Madras Univ., India), and K. B. Bota *In* Atlanta Univ., Computational Sciences Nov. 1987 2 p Prepared in cooperation with Atlanta Univ., Ga. (For primary document see N88-25226 18-64)
Avail: NTIS HC A03/MF A01 CSCL 12A

A method is presented for the numerical solution of random Love's integral equation. The technique involves a Chebyshev series approximation, the coefficients of which are the solution of a system of random linear equations. The statistical properties of the random solution are evaluated numerically and used to determine the distribution of the random coefficients. These distributions are expressed in histograms.

Author

N88-25236# Atlanta Univ., Ga.

THE USE OF LAGRANGE MULTIPLIERS AND KUHN-TUCKER'S THEORY IN OPTIMIZATION PROBLEMS Abstract Only. M.S. Thesis

Joseph T. Seko *In its* Computational Sciences Nov. 1987 1 p (For primary document see N88-25226 18-64)
Avail: NTIS HC A03/MF A01 CSCL 12A

Lagrange multipliers, penalty methods, and Kuhn-Tucker's theory are some important mathematical tools used in optimization problems. These tools are discussed so that one can appreciate the current areas of optimization research. Moreover, since extensive research work exists for linear optimization problems, only nonlinear applications are discussed.

Author

N88-25237# Morehouse Coll., Atlanta, Ga.

NUMERICAL SOLUTION OF LINEAR INTEGRAL EQUATIONS WITH RANDOM FORCING TERMS Abstract Only. B.S. Thesis

Daniel Ephraim *In* Atlanta Univ., Computational Sciences Nov. 1987 1 p (For primary document see N88-25226 18-64)
Avail: NTIS HC A03/MF A01 CSCL 12A

The Fredholm integral equations of the second kind, Volterra integral equations of the second kind, are defined and differentiated. Why integral equations are so important is explained. Numerical

procedures to integral equations are discussed. The equations used are of two types: Fredholm equations and Volterra. The methods used for the Fredholm equations are: Simpson's rule, Trapezoidal rule, Weddle's rule; the Collocation method, and the Galerkin method. For Volterra equations the successive approximation method was used with Simpson's rule, Trapezoidal rule, and Weddle's rule to evaluate the integrals. In both Fredholm and Volterra integral equations the forcing term is random. The simulation results are presented in tables and graphs. Author

N88-25238*# National Aeronautics and Space Administration. Ames Research Center, Moffett Field, Calif.
AUTOMATIC DISCOVERY OF OPTIMAL CLASSES
Peter Cheeseman, John Stutz, Don Freeman, and Matthew Self [1986] 17 p
(NASA-TM-101174; NAS 1.15:101174) Avail: NTIS HC A03/MF A01 CSCL 12A

A criterion, based on Bayes' theorem, is described that defines the optimal set of classes (a classification) for a given set of examples. This criterion is transformed into an equivalent minimum message length criterion with an intuitive information interpretation. This criterion does not require that the number of classes be specified in advance, this is determined by the data. The minimum message length criterion includes the message length required to describe the classes, so there is a built in bias against adding new classes unless they lead to a reduction in the message length required to describe the data. Unfortunately, the search space of possible classifications is too large to search exhaustively, so heuristic search methods, such as simulated annealing, are applied. Tutored learning and probabilistic prediction in particular cases are an important indirect result of optimal class discovery. Extensions to the basic class induction program include the ability to combine category and real value data, hierarchical classes, independent classifications and deciding for each class which attributes are relevant. Author

N88-25239*# National Aeronautics and Space Administration. Lewis Research Center, Cleveland, Ohio.
SOLVING TIME-DEPENDENT TWO-DIMENSIONAL EDDY CURRENT PROBLEMS
Min Eig Lee, S. I. Hariharan, and Nathan Ida (Akron Univ., Ohio.) Jun. 1988 32 p
(Grant NSF DMS-86-04047)
(NASA-TM-100875; E-4106; NAS 1.15:100875) Avail: NTIS HC A03/MF A01 CSCL 12A

Results of transient eddy current calculations are reported. For simplicity, a two-dimensional transverse magnetic field which is incident on an infinitely long conductor is considered. The conductor is assumed to be a good but not perfect conductor. The resulting problem is an interface initial boundary value problem with the boundary of the conductor being the interface. A finite difference method is used to march the solution explicitly in time. The method is shown. Treatment of appropriate radiation conditions is given special consideration. Results are validated with approximate analytic solutions. Two stringent test cases of high and low frequency incident waves are considered to validate the results. Author

N88-25240# Center for Mathematics and Computer Science, Amsterdam (Netherlands). Dept. of Applied Mathematics.
ON A BIORTHOGONAL SYSTEM ASSOCIATED WITH UNIFORM ASYMPTOTIC EXPANSIONS
K. Soni and N. M. Temme Nov. 1987 25 p
(CWI-AM-R8709; B8805668; ETN-88-92582) Copyright Avail: NTIS HC A03/MF A01

The Soni and Sleeman (1987) family of polynomials which are related to the coefficients in a uniform asymptotic expansion of a class of integrals is introduced. In this expansion parabolic cylinder functions (Weber functions) occur as basic approximants and the resulting series is of Bleistein type. A family of rational functions is introduced, and the two families form a biorthogonal system on a contour in the complex plane. The system can be viewed as a generalization of the families (z to the n) and (z to the -n-1) which occur in Taylor expansions and the Cauchy integrals of analytic functions. Explicit representations of the rational functions are given together with rigorous estimates. These results are used to establish convergence of expansions of certain functions in terms of the polynomials and the rational functions. The main motivation to study this system stems from the problem on the asymptotic expansion of a class of integrals. It is shown how to use the system in order to construct bounds for the remainders in the asymptotic expansion. An example is worked out. ESA

N88-25241# Center for Mathematics and Computer Science, Amsterdam (Netherlands). Dept. of Applied Mathematics.
MATHEMATICAL MORPHOLOGY FOR STRUCTURES WITHOUT TRANSLATION SYMMETRY
J. B. T. M. Roerdink and H. J. A. M. Heijmans Jan. 1988 11 p Presented at the IEEE-ASSP and EURASIP 5th Workshop on Multidimensional Signal Processing, Noordwijkerhout, The Netherlands, 14-16 Sep. 1987
(CWI-AM-R8803; B8805672; ETN-88-92586) Copyright Avail: NTIS HC A03/MF A01

Euclidean mathematical morphology based on the use of translation-invariant transformations of the Boolean lattice of all subsets of the Euclidean space as used in image analysis is introduced. It is shown how the theory can be generalized to arbitrary complete atomic Boolean lattices with a commutative group structure on the set of atoms. Simple examples are given. ESA

N88-25242# Center for Mathematics and Computer Science, Amsterdam (Netherlands). Dept. of Numerical Mathematics.
MULTIGRID METHODS FOR ELLIPTIC PARTIAL DIFFERENTIAL EQUATIONS (PDEs)
W. M. Lioen Nov. 1987 18 p Submitted for publication
(CWI-NM-R8722; B8805673; ETN-88-92593) Copyright Avail: NTIS HC A03/MF A01

Multigrid methods are introduced, and algorithmic choices in the NUMVEC Library routine MGZEB (a highly vectorized multigrid code for the solution of linear systems resulting from the 7-point discretization of general linear 2nd order elliptic PDEs in two dimensions), are discussed. Since the relaxation process is the most expensive part of a multigrid iteration cycle, the data structure was adapted to avoid Cyber 205 stride-problems when executing zebra relaxation. The effects of vectorization/choosing another data structure are considered, and large problems on the Cyber 205 are mentioned. ESA

N88-25243# Center for Mathematics and Computer Science, Amsterdam (Netherlands). Dept. of Numerical Mathematics.
STABILITY AND CONVERGENCE OF THE PEACEMAN-RACHFORD ADI METHOD FOR INITIAL-BOUNDARY VALUE PROBLEMS
W. H. Hundsdorfer and J. G. Verwer Nov. 1987 31 p Submitted for publication
(CWI-NM-R8724; B8805675; ETN-88-92595) Copyright Avail: NTIS HC A03/MF A01

The alternating direction implicit method of Peaceman and Rachford applied to initial-boundary value problems for partial differential equations in two space dimensions is analyzed using the method of lines approach. Motivated by developments in the field of stiff nonlinear ordinary differential equations, the analysis focuses on problems where the semidiscrete system, obtained after discretization in space, satisfies a one sided Lipschitz condition with a constant independent of the grid spacing. For such problems unconditional stability and convergence results are derived. ESA

N88-25244*# Old Dominion Univ., Norfolk, Va. Dept. of Mechanical Engineering and Mechanics.
SINGLE-MODE PROJECTION FILTERS FOR MODAL PARAMETER IDENTIFICATION FOR FLEXIBLE STRUCTURES
Final Report, for period ending 31 Dec. 1987
Jen-Kuang Huang and Chung-Wen Chen Feb. 1988 73 p

(Grant NAG1-655)
(NASA-CR-182680; NAS 1.26:182680) Avail: NTIS HC A04/MF A01 CSCL 12A

Single-mode projection filters are developed for eigensystem parameter identification from both analytical results and test data. Explicit formulations of these projection filters are derived using the orthogonal matrices of the controllability and observability matrices in the general sense. A global minimum optimization algorithm is applied to update the filter parameters by using the interval analysis method. The updated modal parameters represent the characteristics of the test data. For illustration of this new approach, a numerical simulation for the MAST beam structure is shown by using a one-dimensional global optimization algorithm to identify modal frequencies and damping. Another numerical simulation of a ten-mode structure is also presented by using a two-dimensional global optimization algorithm to illustrate the feasibility of the new method. The projection filters are practical for parallel processing implementation. Author

N88-25245# Oak Ridge National Lab., Tenn.
SIMILARITY SOLUTIONS OF NONLINEAR PARTIAL DIFFERENTIAL EQUATIONS INVARIANT TO A FAMILY OF AFFINE GROUPS
L. Dresner Aug. 1987 13 p Presented at the 6th International Conference on Mathematical Modelling, St. Louis, Mo., 4 Aug. 1987
(Contract DE-AC05-84OR-21400)
(DE88-003404; CONF-870860-1) Avail: NTIS HC A03/MF A01

Problems of technological interest can very often be described by partial differential equations (PDEs) with one dependent and two independent variables (call them c, z, and t, respectively). Many such PDEs are invariant to one-parameter families of one-parameter affine groups. Similarity solutions are solutions of the PDE that are invariant to one group of the family. The great utility of similarity solutions is that they may be calculated by solving an ordinary differential equation (ODE) rather than a PDE and are thus much more easily accessible than other solutions. The form of the principal ODE depends, of course, on the form of the PDE, but it can be proved quite generally that the principal ODE is itself invarient to the one-parameter affine group or associated group. Because of the invariance of the principal ODE to the associated group, the dependence on the boundary and initial conditions of certain special values of the function y(x), e.g., y(O), y(infinity), y(O), ets., may be predicted a priori without solving the principal ODE. The nonlinear PDE of heat transport in superfluid He-2, is used as an illustration of these ideas in this review. DOE

N88-25246*# National Aeronautics and Space Administration. Langley Research Center, Hampton, Va.
GALERKIN APPROXIMATION FOR INVERSE PROBLEMS FOR NONAUTONOMOUS NONLINEAR DISTRIBUTED SYSTEMS Final Report
H. T. Banks, Simeon Reich, and I. G. Rosen (University of Southern California, Los Angeles.) Jun. 1988 22 p Submitted for publication Sponsored in part by Technion - Israel Inst. of Tech., Haifa
(Contract NAS1-18107; Grant NAG1-517)
(NASA-CR-181676; ICASE-88-38; NAS 1.26:181676) Avail: NTIS HC A03/MF A01 CSCL 12A

An abstract framework and convergence theory is developed for Galerkin approximation for inverse problems involving the identification of nonautonomous nonlinear distributed parameter systems. A set of relatively easily verified conditions is provided which are sufficient to guarantee the existence of optimal solutions and their approximation by a sequence of solutions to a sequence of approximating finite dimensional identification problems. The approach is based on the theory of monotone operators in Banach spaces and is applicable to a reasonably broad class of nonlinear distributed systems. Operator theoretic and variational techniques are used to establish a fundamental convergence result. An example involving evolution systems with dynamics described by nonstationary quasilinear elliptic operators along with some applications are presented and discussed. Author

N88-25247*# National Aeronautics and Space Administration. Langley Research Center, Hampton, Va.
OPTIMAL DISCRETE-TIME LQR PROBLEMS FOR PARABOLIC SYSTEMS WITH UNBOUNDED INPUT: APPROXIMATION AND CONVERGENCE Final Report
I. G. Rosen (University of Southern California, Los Angeles.) Jun. 1988 31 p Submitted for publication
(Contract NAS1-18107)
(NASA-CR-181673; ICASE-88-35; NAS 1.26:181673) Avail: NTIS HC A03/MF A01 CSCL 12A

An abstract approximation and convergence theory for the closed-loop solution of discrete-time linear-quadratic regulator problems for parabolic systems with unbounded input is developed. Under relatively mild stabilizability and detectability assumptions, functional analytic, operator techniques are used to demonstrate the norm convergence of Galerkin-based approximations to the optimal feedback control gains. The application of the general theory to a class of abstract boundary control systems is considered. Two examples, one involving the Neumann boundary control of a one-dimensional heat equation, and the other, the vibration control of a cantilevered viscoelastic beam via shear input at the free end, are discussed. Author

N88-25248 Stanford Univ., Calif.
NEW MIXED FINITE ELEMENT METHODS Ph.D. Thesis
Leopoldo Penna Franca 1987 179 p
Avail: Univ. Microfilms Order No. DA8800934

New finite element methods are proposed for mixed variational formulations. The methods are constructed by adding to the classical Galerkin method various least squares like terms. The additional terms involve integrals over element interiors, and include mesh parameter dependent coefficients. The methods are designed to enhance stability. Consistency is achieved in the sense that exact solutions identically satisfy the variational equations. Applied to several problems, simple finite element interpolations are rendered convergent, including convenient equal order interpolations which are generally unstable within the Galerkin approach. The methods are subdivided into two classes according to the manner in which stability is attained: (1) Circumventing Babuska-Brezzi condition methods; (2) Satisfying Bubuska-Brezzi condition methods. Convergence is established for each class of methods. Applications of the first class of methods to Stokes flow and compressible linear elasticity are presented. The second class is applied to the Poisson, Timoshenko beam and incompressible elasticity problems. Numerical results demonstrate the good stability and accuracy of the methods. Dissert. Abstr.

N88-25249*# Brown Univ., Providence, R. I.
HIGH DEGREE INTERPOLATION POLYNOMIAL IN NEWTON FORM Final Report
Hillel Tal-Ezer (Brown Univ., Providence, R. I.) 1988 24 p Submitted for publication
(Contract NAS1-18107)
(NASA-CR-181677; ICASE-88-39; NAS 1.26:181677) Avail: NTIS HC A03/MF A01 CSCL 12A

Polynomial interpolation is an essential subject in numerical analysis. Dealing with a real interval, it is well known that even if f(x) is an analytic function, interpolating at equally spaced points can diverge. On the other hand, interpolating at the zeroes of the corresponding Chebyshev polynomial will converge. Using the Newton formula, this result of convergence is true only on the theoretical level. It is shown that the algorithm which computes the divided differences is numerically stable only if: (1) the interpolating points are arranged in a different order, and (2) the size of the interval is 4. Author

65 STATISTICS AND PROBABILITY

Includes data sampling and smoothing; Monte Carlo method; and stochastic processes.

N88-25250# Vrije Universiteit, Amsterdam (Netherlands). Subfaculteit Wiskunde en Informatica.
ADDITIVE PROPHET INEQUALITIES FOR TRANSFORMS OF UNIFORMLY BOUNDED PAIRWISE INDEPENDENT RANDOM VARIABLES
F. A. Boshuizen Sep. 1987 22 p
(PB88-173513; Rept-331) Avail: NTIS HC A03/MF A01 CSCL 12A

E(Summation of i = I to i = n) of (x(i)-x(i-l)) sup + and E(Summation of i = I to i = n), of (EX(i)-X((il))+ are the maximal expected returns of pairwise independent uniformly bounded random variables X(0)...X(n) transformed respectively by random variables taking values in (0,1) and predictable random variables taking values in (0,1). Probabilistically, these quantities are respectively the maximal gain of a prophet (player with complete foresight) and the maximal gain of a gambler (player who knows only the past and the present). Best possible upperbounds are given for the difference ((Summation of i = 1 to i = n) of (X9i) - x(i-1))sup + E(Summation of i = 1 to i = n), of (EX(i) - X(i - 1)) + in the identically distributed case and the case of nonincreasing expectations. Also, a best possible implicity defined upperbound is given in the general case. GRA

N88-25251# Edgerton, Germeshausen and Grier, Inc., Idaho Falls, Idaho.
A PERSPECTIVE OF PC-BASED PROBABILISTIC RISK ASSESSMENT
M. B. Sattison, D. M. Rasmuson, R. C. Robinson, K. D. Russell, and V. S. VanSicien 1987 9 p Presented at the ASME Winter Meeting, Boston, Mass., 13 Dec. 1987 Prepared in cooperation with Nuclear Regulatory Commission, Washington, D.C.
(Contract DE-AC07-76ID-01570)
(DE88-006715; EGG-M-33687; CONF-871234-14) Avail: NTIS HC A02/MF A01

Probabilistic risk assessment (PRA) information has been under-utilized in the past due to the large effort required to input the PRA data and the large expense of the computers needed to run PRA codes. The microcomputer-based Integrated Reliability and Risk Analysis System (IRRAS) and the System Analysis and Risk Assessment (SARA) System, under development at the Idaho National Engineering Laboratory, have greatly enhanced the ability of managers to use PRA techniques in their decision-making. IRRAS is a tool that allows an analyst to create, modify, update, and reanalyze a plant PRA to keep the risk assessment current with the plant's configuration and operation. The SARA system is used to perform sensitivity studies on the results of a PRA. This type of analysis can be used to evaluate proposed changes to a plant or its operation. The success of these two software projects demonstrate that risk information can be made readily available to those that need it. This is the first step in the development of a true risk management capability. DOE

N88-25252# North Carolina Univ., Chapel Hill.
POISSON FUNCTIONALS OF MARKOV PROCESSES AND QUEUEING NETWORKS Interim Report, 1 Oct. 1986 - 25 Dec. 1987
Richard F. Serfozo 25 Dec. 1987 26 p Prepared in cooperation with Georgia Inst. of Tech., Atlanta
(Contract F49620-85-C-0144; Grant AF AFOSR-0367-84)
(AD-A191217; AFOSR-88-0335TR) Avail: NTIS HC A03/MF A01 CSCL 12C

We present conditions under which a point process of certain jump times of a Markov process is a Poisson process. One result is that if the Markov process is stationary and the compensator of the point process in reverse time has a constant intensity a, then the point process is Poisson with rate a. A classical example is that the output flow from a M/M/1 queueing system is Poisson. We also present similar Poisson Characterizations of more general marked point process functionals of a Markov process. These results yield easy-to-use criteria for a collection of such processes to be multi-variate Poisson or marked Poisson with a specified dependence or independence. We give several applications of queueing systems, and indicate how our results extend of functionals of non-Markovian processes. GRA

N88-25253# Florida Univ., Gainesville. Dept. of Statistics.
EXACT TESTS FOR VARIANCE COMPONENT MODELS WITH UNEQUAL CELL FREQUENCIES IN THE LAST STAGE
A. I. Khuri Jan. 1988 23 p
(Contract N00014-86-K-0059)
(AD-A191645; TR-296) Avail: NTIS HC A03/MF A01 CSCL 12C

This paper presents a method to construct exact tests for the variance components in a general unbalanced random model. It is assumed that the imbalance affects only the last stage of the design with no missing cells. GRA

N88-25254# North Carolina Univ., Chapel Hill. Dept. of Statistics.
SYMMETRIZED NEAREST NEIGHBOR REGRESSION ESTIMATES
R. J. Carroll and W. Hardle Dec. 1987 9 p
(Contract F49620-85-C-0144)
(AD-A191998; MMS-1742; AFOSR-88-0201TR) Avail: NTIS HC A02/MF A01 CSCL 12C

The authors consider univariate nonparametric regression. Two standard nonparametric regression function estimates are kernel estimates and nearest neighbor estimates. Mack noted that both methods can be defined with respect to a kernel or weighting function, and that for a given kernel and a suitable choice of bandwidth, the optimal mean squared error is the same asymptotically for kernel and nearest neighbor estimates. Yang defined a new type of nearest neighbor regression estimate using the empirical distribution function of the predictors to define the window over which to average. This has the effect of forcing the number of neighbors to be the same both above and below the value of the predictor of interest; we call these symmetrized nearest neighbor estimates. The estimate is a kernel regression estimate with predictors given by the empirical distribution function of the true predictors. We show that for estimating the regression function at a point, the optimum mean squared error of this estimate differs from that of the optimum mean squared error for kernel and ordinary nearest neighbor estimates. No estimate dominates the others. They are asymptotically equivalent with respect to mean squared error if one is estimating the regression function at a mode of the predictor. GRA

N88-25255# Tennessee Univ., Knoxville. Dept. of Mathematics.
ON PATH PROPERTIES OF CERTAIN INFINITELY DIVISIBLE PROCESSES Report, Apr. - Nov. 1987
Jan Rosinski Nov. 1987 19 p
(Contract F49620-85-C-0144; Grant AF AFOSR-0136-87)
(AD-A192016; AFOSR-88-0203TR) Avail: NTIS HC A03/MF A01 CSCL 12C

Sample path properties of Poissonian type stochastic integral processes are studied. It is proven that various properties of the sections of the deterministic kernel (as, for example, unboundedness, discontinuity, etc.) are inherited by the sample paths of the corresponding stochastic integral process. An analogous statement for Gaussian processes is false. As a main tool, a series representation of stochastic integral processes is fully developed and this may be of independent interest. GRA

N88-25256# Flow Research, Inc., Kent, Wash.
DIRECT NUMERICAL SIMULATIONS OF THE PDF'S (PROBABILITY DENSITY FUNCTIONS) OF A PASSIVE SCALAR IN A FORCED MIXING LAYER
P. Givi and P. A. McMurtry Sep. 1987 16 p Prepared in cooperation with Washington Univ., Seattle
(Contract F49620-85-C-0067)

(AD-A192134; AFOSR-88-0268TR) Avail: NTIS HC A03/MF A01 CSCL 08C

The probability density functions of a passive scalar quantity are calculated in a perturbed mixing layer by means of direct numerical simulations. The results indicate that the two-dimensional rollup of the unsteady shear layer, and the pairing process in particular, contributes greatly to the generation of the predominant peak of the PDF's within the mixing region. GRA

N88-25257# Sheffield Univ. (England). Dept. of Control Engineering.
RECURSIVE MAXIMUM LIKELIHOOD IDENTIFICATION OF A NONLINEAR OUTPUT-AFFINE MODEL
S. Chen and S. A. Billings Dec. 1987 30 p
(Grant SERC-GR/D/30587)
(RR-322; ETN-88-92521) Avail: NTIS HC A03/MF A01

On-line identification of the parameters in a nonlinear output-affine model is considered. A recursive maximum likelihood estimator derived for linear systems is extended to work for nonlinear systems which can be described by a stochastic form of Sontag's output-affine model. Numerical implementation aspects are discussed, a convergence analysis is given, and a computer simulation study is included. ESA

N88-25229# Texas Univ., Arlington. Dept. of Mathematics.
NUMERICAL SOLUTIONS TO STOCHASTIC DIFFERENCE EQUATIONS Abstract Only
G. S. Ladde and M. Sambandham (Atlanta Univ., Ga.) *In* Atlanta Univ., Computational Sciences Nov. 1987 1 p Prepared in cooperation with Morehouse Coll., Atlanta, Ga. (For primary document see N88-25226 18-64)
(Grant DAAG29-84-G-0060)
Avail: NTIS HC A03/MF A01 CSCL 12A

66 SYSTEMS ANALYSIS

Includes mathematical modeling; network analysis; and operations research.

No abstracts in this category.

67 THEORETICAL MATHEMATICS

Includes topology and number theory.

N88-25258# Center for Mathematics and Computer Science, Amsterdam (Netherlands). Dept. of Applied Mathematics.
PERTURBATION THEORY FOR DUAL SEMIGROUPS. PART 4: THE INTERTWINING FORMULA AND THE CANONICAL PAIRING
Ph. Clement, O. Diekmann, M. Gyllenberg, H. J. A. M. Heijmans (Heidelberg Univ., West Germany), and H. R. Thieme Jan. 1988 19 p Presented at the Meeting on Trends in Semigroup Theory and Applications, Trieste, Italy, 28 Sep. - 20 Oct. 1987 Submitted for publication
(CWI-AM-R8802-Pt-4; B8805671-Pt-4; ETN-88-92585) Copyright Avail: NTIS HC A03/MF A01

The theory of dual semigroups of bounded linear operators on nonreflexive Banach spaces is used to give a natural generalization of the notion of a bounded perturbation of the generator and a version of the variation-of-constants formula. In order to handle the general (i.e., not necessarily sun-reflexive) case an intertwining formula extends the semigroup from the closure of the domain of the generator to the whole space and, a duality pairing between the second semigroup-dual space and X sup asterisk describes the duality relations. Results pertinent to inhomogenous linear problems, semilinear problems, compactness, positivity, and irreducibility are reviewed. ESA

N88-25259# Center for Mathematics and Computer Science, Amsterdam (Netherlands). Dept. of Numerical Mathematics.
A COMPARATIVE STUDY OF CHEBYSHEV ACCELERATION AND RESIDUE SMOOTHING IN THE SOLUTION OF NONLINEAR ELLIPTIC DIFFERENCE EQUATIONS
P. J. vanderHouwen, B. P. Sommeijer, and G. Pontrelli Nov. 1987 26 p Sponsored by the CNR, Italy
(CWI-NM-R8723; B8805674; ETN-88-92594) Copyright Avail: NTIS HC A03/MF A01

Chebyshev acceleration is compared with an acceleration technique based on residue smoothing. The effect of residue smoothing is that the spectral radius of the Jacobian matrix associated with the system of equations can be reduced substantially, so that the eigenvalues of the iteration matrix of the iteration method used are considerably decreased. Comparative experiments clearly indicate that residue smoothing is superior to Chebyshev acceleration. A model problem shows that the rate of convergence of the smoothed Jacobi process is comparable with that of ADI methods. The smoothing matrices by which the residue smoothing is achieved allow for a very efficient implementation, thus hardly increasing the computational effort of the iteration process. Residue smoothing is directly applicable to nonlinear problems without affecting the algorithmic complexity. The simplicity of the method offers excellent prospects for execution on vector and parallel computers. ESA

70 PHYSICS (GENERAL)

For precision time and time interval (PTTI) see *35 Instrumentation and Photography;* for geophysics, astrophysics or solar physics see *46 Geophysics, 90 Astrophysics,* or *92 Solar Physics.*

N88-25260*# National Aeronautics and Space Administration. Lewis Research Center, Cleveland, Ohio.
RECENT ADVANCES IN LOW-THRUST PROPULSION TECHNOLOGY
James R. Stone [1988] 27 p Presented at the 24th Joint Propulsion Conference, Boston, Mass., 11-13 Jul. 1988; sponsored by AIAA, ASME, SAE, and ASEE
(NASA-TM-100959; E-4245; NAS 1.15:100959; AIAA-88-3283)
Avail: NTIS HC A03/MF A01 CSCL 20C

The NASA low-thrust propulsion technology program is aimed at providing high performance options to a broad class of near-term and future missions. Major emphases of the program are on storable and hydrogen/oxygen low-thrust chemical, low-power (auxiliary) electrothermal, and high-power electric propulsion. This paper represents the major accomplishments of the program and discusses their impact. Author

N88-25261# Technische Hogeschool, Delft (Netherlands). Afd. der Elektrotechniek.
BORN-TYPE RECONSTRUCTION OF MATERIAL PARAMETERS OF AN INHOMOGENEOUS, LOSSY DIELECTRIC SLAB FROM REFLECTED-FIELD DATA
A. G. Tijhuis Jan. 1988 48 p
(PB88-188958; Rept-1988-02) Avail: NTIS HC A03/MF A01 CSCL 20C

Several Born-type techniques for reconstructing the permittivity and/or the conductivity profiles of a one-dimensionally inhomogeneous, lossy dielectric slab from reflected field data are considered. Traditionally, the properties of such techniques have been found mainly by numerical experimentation. A closed form analysis is given that explains these properties. It is argued that there exists only one version of the Born-type scheme that leads to a fully detailed reconstruction of the unknown profiles. All other versions suffer from an inherent band limitation. Conclusions are confirmed numerically as well as by using alternative inversion techniques. Author

71 ACOUSTICS

Includes sound generation, transmission and attenuation. For noise pollution see *45 Environmental Pollution*.

N88-25262# Haut Commissariat a la Recherche, Algiers (Algeria). Centre d'Etudes Nucleaires et Solaires.
FREQUENCY ANALYSIS OF ACOUSTIC EMISSION - APPLICATION TO MACHINING AND WELDING M.S. Thesis
A. Snoussi Jan. 1987 115 p In FRENCH; ENGLISH summary
(DE88-701478; INIS-mf-11087) Avail: NTIS (US Sales Only) HC A06/MF A01

Ultrasonic acoustic waves were seized and exploited within a bandwidth ranging from 30 kHz to 55 kHz for non-destructive control when boring three kinds of steel with a digitally programmed drill. In addition, these waves were considered in soldering two steels and one aluminum using T.I.G. process. Spectrum analysis of acoustic emissions produced during the drill is closely related to the extraction of turnings from the metal. Because of the wick's progressive wearing out, the spectrum tends to be close to the machine's own noise spectrum. Meanwhile in the soldering operation of test-tubes of 2 mm thickness, the frequency analysis shows a particular frequency called signature corresponding to the flow of protection gas. Other frequencies associated to some internal defects in the soldering process as a delay in the fissure and a lack in the fusion were detected. DOE

N88-25263# Army Construction Engineering Research Lab., Champaign, Ill.
OPERATIONAL NOISE DATA FOR CH-47D AND AH-64 ARMY HELICOPTERS Final Report
Paul D. Schomer, Aaron J. Averbuch, Richard Raspet, and Richard K. Wolf Mar. 1988 44 p
(AD-A191059; CERL-TR-N-88/04) Avail: NTIS HC A03/MF A01 CSCL 01C

The objectives of this study were to develop sound exposure level (SEL) versus distance curves for flight operations and time-average sound level (LEQ) contours versus distance for static operations for two new Army aircraft. Sound levels produced by the helicopters were measured for the aircraft both hovering and traveling at various speeds. The CH-47D was operated in both a heavily and a lightly loaded configuration; the heavy load was achieved by sling-loading a 10-ton Army truck. The data show that the aircraft are quieter than the types they are replacing; the CH-47C and the AH-1G. Except at the highest speeds, sound variation with speed is not a large factor. In terms of sound variation with load, the CH-47D actually made less sound during level flight at full load than it did lightly loaded, although the sound did increase with load during takeoff and landing. As with other aircraft, the CH-47D makes more sound during landing than it does during level flight or takeoff, but the sound levels for the AH-64 are virtually independent of operation. Only two of each aircraft were supplied. Both types of aircraft exhibited sound levels which were a little higher than expected, and more aircraft would have enhanced the statistical reliability of the data. In the future, a minimum of four aircraft of any type should be supplied. They should be measured in two groups of two, separated by at least 1 month in time to better insure the statistical reliability of the data. GRA

N88-25264# Science Applications International Corp., San Francisco, Calif.
TRANSMITTING BOUNDARY FOR FINITE-DIFFERENCE CALCULATIONS WITH FINITE MODELING OF AN INFINITE MEDIUM Final Report, 1 Dec. 1984 - 30 Apr. 1986
William Yeung and Michael B. Gross 20 Nov. 1987 50 p
(Grant AF-AFOSR-0023-85)
(AD-A191441; AFOSR-87-1754TR) Avail: NTIS HC A03/MF A01 CSCL 20A

The purpose of this effort was to study the construction of novel energy absorbing boundary conditions for use at the artificial far field boundaries of exterior wave problems. One approach was pursued which involves the superposition of the solutions for a fixed boundary and for a free boundary. An analytic model was used to identify the cause of the small errors that result in the cancellation process of this approach. This model showed that the appropriate velocity at the free boundary has to be modified when the computational time step is less than the maximum stable time step. First and second order corrections have been developed. GRA

N88-25265# Texas Univ., Austin. Applied Research Lab.
EVALUATION OF THE BIOT COEFFICIENTS Final Technical Report
B. Yavari and A. Bedford 1987 30 p
(Contract N00014-86-K-0387)
(AD-A191643) Avail: NTIS HC A03/MF A01 CSCL 20A

The Biot equations are the most promising approach for modeling the propagation of acoustic waves in ocean sediments. A method has been developed to determine the drag and virtual mass coefficients in Biot's equations as functions of frequency. The method requires solving for the motion of the fluid in the pores when the pore walls are subjected to a spatially uniform, oscillatory motion. In this project, a finite element algorithm has been developed to determine the fluid motion. The accuracy of the model has been verified using a model problem for which exact results could be obtained. The drag and virtual mass coefficients have been determined for several two-dimensional pore spaces. It has been determined that the drag coefficient is insensitive to the pore geometry while the virtual mass coefficient is very sensitive to the pore geometry. It has also been shown that the coefficients can be expressed in nondimensional forms which permit their values to be scaled for different values of a characteristic linear dimension of the pore space. This project has established a firm basis for proceeding to determine the coefficients for three-dimensional pore spaces. GRA

N88-25266# Army Armament Research and Development Command, Watervliet, N. Y. Weapons Lab.
THE HIGH PRESSURE SOUND VELOCITY AND EQUATION OF STATE OF AQUEOUS SOLUTIONS OF HYDROXYLAMMONIUM NITRATE AND TRIETHANOLAMMONIUM NITRATE Final Report
J. Frankel and M. Doxbeck Jan. 1988 25 p
(AD-A191740; ARCCB-TR-88001) Avail: NTIS HC A03/MF A01 CSCL 21I

A cell for high pressure sound velocity measurements of liquids was designed and used in a Birch-Bridgman high pressure system with a liquid propellant specimen. The dependence of the sound velocity on pressure to 4.2 kbar (4200 atmospheres) was measured at room temperature and on temperatures between 220 and 293 K at room pressure. These data, together with the temperature dependence of the specific heat which was also measured and some thermodynamic arguments, were used to obtain the full equation of state with temperature and the pressure dependence of the specific heat and of the volume expansitivity at room temperature. We compare our results with data obtained by volumetric and other ultrasonic measurements. GRA

N88-25267# Washington Univ., Seattle. Applied Physics Lab.
REMOTE SENSING OF ACOUSTIC PROPERTIES OF SHALLOW WATER SEDIMENTS: A REVIEW
M. Schulkin Sep. 1987 56 p
(Contract N00014-84-K-0646)
(AD-A192107; APL-UW-8711) Avail: NTIS HC A04/MF A01 CSCL 08C

A review is presented of remote sensing methods and associated inverse procedures for obtaining the acoustic properties of sediments in shallow water. The properties of interest are the vertical profiles of density, compressional wave velocity and attenuation, and shear wave velocity and attenuation. For compressional waves, the remotely sensed information required is the modal reflection coefficient of the seabed, usually expressed in terms of the depth-dependent Green's function at specific locations in the water column. For shear waves, information about the Scholte and Rayleigh interface waves on the seabed is

necessary. Also reviewed are methods for remote sensing of the Biot geophysical parameters, shear modulus, permeability, and porosity, from which geoacoustic properties can be derived.
GRA

N88-25268*# Akron Univ., Ohio. Dept. of Mathematical Sciences.
LINEAR AND NONLINEAR ACOUSTIC WAVE PROPAGATION IN THE ATMOSPHERE
S. I. Hariharan and Ping Yu Washington NASA Jun. 1988 38 p
(Grant NAG1-624)
(NASA-CR-4157; NAS 1.26:4157) Avail: NTIS HC A03/MF A01 CSCL 20A

The investigation of the acoustic wave propagation theory and numerical implementation for the situation of an isothermal atmosphere is described. A one-dimensional model to validate an asymptotic theory and a 3-D situation to relate to a realistic situation are considered. In addition, nonlinear wave propagation and the numerical treatment are included. It is known that the gravitational effects play a crucial role in the low frequency acoustic wave propagation. They propagate large distances and, as such, the numerical treatment of those problems become difficult in terms of posing boundary conditions which are valid for all frequencies.
Author

N88-25269# Massachusetts Inst. of Tech., Cambridge. Artificial Intelligence Lab.
SHAPE FROM SHADING, OCCLUSION AND TEXTURE
A. L. Yuille May 1987 56 p
(Contract N00014-85-K-0124)
(AD-A184840; AI-M-885) Copyright Avail: NTIS HC A04/MF A01 CSCL 20A

Shape from shading, occlusion and texture are three important sources of depth information. Work done on these modules is reviewed and summarized.
GRA

72 ATOMIC AND MOLECULAR PHYSICS

Includes atomic structure, electron properties, and molecular spectra.

N88-25270# Michigan Univ., Ann Arbor. Dept. of Atmospheric and Oceanic Science.
BIMOLECULAR REACTIONS AND ENERGY-TRANSFER PROCESSES OF HIGHLY VIBRATIONALLY EXCITED MOLECULES RELATED TO ENERGETIC MATERIALS Final Report, 1 Jul. 1985 - 30 Sep. 1987
John R. Barker Dec. 1987 49 p
(Contract DAAG29-85-K-0193)
(AD-A189013; ARO-23199.6-CH) Avail: NTIS HC A03/MF A01 CSCL 07C

Infrared Multiphoton Absorption (IRMPA) was used to produce populations of vibrationally excited 1,1,2-trifluoroethane, which were characterized by optoacoustic measurements of absorbed laser power and collision free decomposition yields. The measurements were accurately fitted with a Master Equation that included Quack's theory of IRMPA, three RKM unimolecular reaction channels, and collisional energy transfer. The highly constrained adjustable parameters indicate that the optical coupling matrix elements are dramatically reduced in magnitude near reaction threshold energies where vibrational anharmonicity becomes important. Observed infrared fluorescence from the excited molecules is in excellent agreement with Master Equation predictions and it was used to monitor collisional deactivation of the excited molecules. The energy transfer exhibits a weak vibrational energy on bimolecular reactions of 1,1 2-trifluorethane (TFE), but no such effects have yet been observed. A Monte Carlo method is described for efficient multidimensional integration not restricted to hyper-dimensional rectangles, but applied to more complicated domains. When known, the boundaries of a arbitrary integration region can be used to define the sampling domain, resulting in sampling with unit efficiency.
GRA

N88-25271# Minnesota Univ., Minneapolis. School of Physics and Astronomy.
NUCLEAR STRUCTURE STUDIES AT INTERMEDIATE ENERGIES
N. M. Hintz 31 Dec. 1987 30 p
(Contract DE-AC02-77ER-04215)
(DE88-006683; DOE/ER-04215/T4) Avail: NTIS HC A03/MF A01

This paper discusses progress on studies on nuclear structure at the University of Minnesota. Some of the topics discussed are: nucleon-nucleon interactions, high spin stretched states, deformed and transition nuclei, giant resonances, measurement of spin observables, pion scattering, delta resonances, and electron scattering.
DOE

N88-25272# Michigan Univ., Ann Arbor. Dept. of Atmospheric, Oceanic and Space Science.
ENERGY-TRANSFER PROPERTIES AND MECHANISMS Progress Report, 1 Mar. 1987 - 31 Mar. 1988
John R. Barker Feb. 1988 18 p
(Contract DE-FG02-85ER-13442)
(DE88-007107; DOE/ER-13442/T1) Avail: NTIS HC A03/MF A01

This project continues the research on vibrational energy transfer involving large molecules. The motivation of the research is to advance knowledge concerning molecular energy in the electronic ground state so that meaningful predictions can be made. The experimental program will use several techniques on several different molecules with the aim of eliminating experimental artifacts and gaining more insight into energy transfer processes. The theoretical effort will be directed toward assessing the validity of the Biased Random Walk theory and toward developing simpler models that adequately describe the energy transfer process.
DOE

N88-25273# Lawrence Livermore National Lab., Calif.
HIGH-ORDER MULTIPHOTON IONIZATION OF THE NOBLE GASES Ph.D. Thesis
Michael Dale Perry Nov. 1987 293 p
(Contract W-7405-eng-48)
(DE88-007489; UCRL-53852) Avail: NTIS HC A13/MF A01

Ionization of an atom by the absorption of several photons from a strong electromagnetic field is considered. Specifically, the absolute yield of multiply charged ions of the noble gases, argon, krypton, and xenon produced using a well-characterized, tunable picosecond dye laser is reported as a function of both laser intensity and frequency. Theoretical models are developed to provide a quantitative interpretation of the data. The experiments were designed to investigate the influence of intermediate atomic states on the multiphoton ionization probability at intensities such that the strength of the applied field approached that of the internal atomic field. This was accomplished by measuring the ion yield over a broad range of laser intensity, 10 to the 12th less than or equal to 1 less than or equal to 4 x 10 to the 14th W/sq cm and frequency. The laser wavelength was varied between 570 and 620 nm and the second harmonic, 285 to 310 nm. Enhancement of the yield of singly-charged krypton ions by two orders of magnitude by three-photon resonant, four-photon ionization was observed at intensities nearly two orders of magnitude above previous results. A model which considers only two atomic levels coupled by the strong field is presented and is found to be in good agreement with the experimental results. Measured values of the three-photon Rabi rate to, and the photoionization cross sections of, several excited states of Kr 1 are reported. In addition, even at intensities exceeding 10 to the 13th W/sq cm, it was to find frequencies at which no resonant enhancement of the ionization probability could be observed. Charge states as high as Ar(4+), Kr(5+), and Xe(5+) produced by this non-resonant multiphoton ionization were observed at the highest intensities.
DOE

N88-25274# Arizona Univ., Tucson.
EXPERIMENTAL ELEMENTARY PARTICLE PHYSICS Final Report
M. W. Arenton and K.-W. Lai Mar. 1988 6 p
(Contract DE-AC02-80ER-10663)
(DE88-007510; DOE/ER-10663/T3) Avail: NTIS HC A02/MF A01

The activities of the experimental elementary particle physics group at the University of Arizona are described. These encompass a series of experiments at Fermilab on the subjects of hadronic production of heavy flavor states and on high transverse momentum phenomena. DOE

N88-25275# Ministere des Armees, Saint-Cloud (France).
CONTRIBUTIONS OF AUTOIONIZING RESONANCES TO THE ELECTRON COLLISIONAL EXCITATION RATES FOR Be-LIKE IONS
Mau H. Chen and Bernd Crasemann 22 Sep. 1987 28 p
(Grant AF AFOSR-0026-87)
(AD-A190924; AFOSR-87-1994TR) Avail: NTIS HC A03/MF A01 CSCL 20E

The contributions of autoionizing resonances to the electron-impact excitation-rate coefficients for the n = 2 to n = 2 transitions in Be-like ions have been evaluated for six ions with atomic numbers Z = 30, 34, 36, 42, 47, and 54. The calculations were carried out in the isolated-resonance approximation. Interference between direct and resonance channels was neglected. The detailed Auger and radiative rates were computed using the multiconfiguration Dirac-Fock model. Results for 45 transitions among 10 states from 1s2 2l 2l configurations are listed. For electric dipole allowed transitions, the contributions from the autoionizing resonance are quite small. However, the autoionizing resonances can enhance the excitation rates by a factor of 2-4 dipole forbidden transitions. GRA

N88-25276# California Univ., San Diego.
A NEW APPROACH TO GENERATING NEGATIVE ION BEAMS Final Report, 1 Jul. 1986 - 30 Sep. 1987
Roy H. Neynaber and Sheng Y. Tang 2 Nov. 1987 4 p
(Contract F49620-86-C-0085)
(AD-A191119; AFOSR-87-1791TR) Avail: NTIS HC A02/MF A01 CSCL 20E

The report describes measurements of ion-pair production cross sections for He*(2(1,3)S)-Li, Li-Cs, Li-Na, and Li-Na*(3p) collisions at energies of several keV. Measurements of chemi-ionization cross sections for He*(2(1,3)S)-Li collisions are also mentioned. A method is described for exciting a fraction of the atoms in a Li vapor to the 2p resonance state using a dye laser. The fraction is determined by observing with the laser on and off the ion-pair production of Cl- when a fast Cl beam collides with the vapor. GRA

N88-25277# Naval Research Lab., Washington, D.C.
A CONSTRAINT ALGORITHM FOR MAINTAINING RIGID BONDS IN MOLECULAR DYNAMICS SIMULATIONS OF LARGE MOLECULES
S. G. Lambrakos, J. P. Boris, E. S. Oran, I. Chandrasekhar, and M. Nagumo 4 Mar. 1988 39 p
(AD-A191663; NRL-MR-6174) Avail: NTIS HC A03/MF A01 CSCL 07D

We present an efficient new algorithm, the Multiple Constraint Force (MCF) algorithm, for maintaining fixed distances in molecular dynamics simulations of polyatomic molecules. A reversible leapfrog integration scheme is modified to calculate the constraint forces required to maintain fixed interparticle distances (usually corresponding to chemical bonds). The procedure is exact for diatomic systems. It converges in a small number of iterations for polyatomic molecules and scales linearly with the number of bonds to be kept rigid. The MCF algorithm, like the SHAKE algorithm, iteratively corrects the constrained equations of motion. Rather than successively correcting particle positions or inverting a matrix, however, the MCF algorithm iteratively correct the constraint forces required to maintain the fixed distances. GRA

N88-25278# Brookhaven National Lab., Upton, N. Y.
AN OPTICAL TECHNIQUE FOR MEASURING DIVERGENCE, BEAM PROFILE, AND AIMING DIRECTION, OF RELATIVISTIC NEGATIVE HYDROGEN IONS
A. Hershcovitch Feb. 1988 4 p Presented at the 3rd European Workshop Production and Applications of Light Negative Ions, Amersfoort, Netherlands, 17 Feb. 1988
(Contract DE-AC02-76CH-00016)
(DE88-007049; BNL-40784; CONF-880256-1) Avail: NTIS HC A02/MF A01

A novel, nonobstructive diagnostic technique for high energy H sup minus D sup minus ion beams is described. This scheme employs spectroscopic techniques designed to measure beam profile, perpendicular velocity spread (i.e., divergence), and orientation of multiMeV H sup minus beams. The basic principle of this method is to photoneutralize a small portion of the H sup minus beam in a way such that the photodetachment process results in the formation of excited hydrogen atoms in the n = 2 levels. Observation of fluorescence from spontaneous decay of H(sp) and/or induced decay of H(2s) can be readily used to determine beam profile. Doppler broadening measurements can be used to determine velocity spread from which beam emittance is calculated. For photodetachment, the best commercially available laser is found to be ArF eximer laser. The analysis is performed for the 200 MEV BNL Linac. The process under consideration has a resonance known as the shape resonance. As the following literature review indicates, the total cross section is known and there is a reasonable agreement between theory and experiment. DOE

N88-25279# California Univ., Berkeley. Lawrence Berkeley Lab.
NUCLEAR AND ASTROPHYSICAL EVIDENCE ON THE EQUATION OF STATE
N. K. Glendenning Jan. 1988 9 p Presented at the 16th International Workshop on Gross Properties of Nuclei and Nuclear Excitations, Hirschegg, Austria, 18 Jan. 1988
(Contract DE-AC03-76SF-00098)
(DE88-007397; LBL-24649; CONF-880161-2) Avail: NTIS HC A02/MF A01

Data on the nuclear equation of state from a number of different sources, from nuclei, high energy nuclear collisions, supernova and neutron stars is analyzed. The current situation concerning supernova simulations is critically appraised. It is found that simualtions that have achieved a prompt ejection do so with an equation of state that is too soft to support the measured masses of several known neutron stars. It is concluded that supernova explosions have not been proven to provide a significant constraint on the nuclear equation of state. Additionally it is concluded that the theoretical bias used to interpret data on neutron star masses as if they belonged to a population all having the same mass is unjustified. Evidence from the various nuclear data and neutron star masses favor a high compression modulus, K approx. 300 MeV. No definitive statement can be made about the equation of state at higher density, save that the neutron star equation of state must be moderately stiff to accommodate neutron stars of mass approx. 1.85M. DOE

N88-25280# Nationaal Inst. voor Kernfysica en Hoge Energiefysica, Amsterdam (Netherlands).
RIGID SYMMETRIES AND BRST-INVARIANCE IN GAUGE THEORIES
J. W. vanHolten Sep. 1987 9 p
(PB88-180948; NIKHEF-H-87/17) Avail: NTIS HC A02/MF A01 CSCL 20H

The structure of the symmetry algebra of theories with simultaneous local and rigid symmetries is analyzed. BRST-invariant Faddeev-Popov gauge-fixing in such theories is discussed, and it is proven that the BRST-transformations can always be made to commute with the rigid symmetries by assigning specific transformation rules to the ghosts. The problem of keeping the rigid symmetries manifest in the quantum theory is shown to reduce

to the problem of finding covariant gauge conditions. Such covariant gauges exist only if the algebra of local and rigid symmetries has a semi-direct product structure. GRA

N88-25281*# National Aeronautics and Space Administration. Pasadena Office, Calif.
TROCHOIDAL ANALYSIS OF SCATTERED ELECTRONS IN A MERGED ELECTRON-ION BEAM Patent Application
Ara Chutjian, inventor (to NASA) (Jet Propulsion Lab., California Inst. of Tech., Pasadena.) 4 Sep. 1987 19 p Prepared in cooperation with Jet Propulsion Lab., California Inst. of Tech., Pasadena.
(Contract NAS7-918)
(NASA-Case-NPO-16789-1-CU; NAS 1.71:NPO-16789-1-CU; US-Patent-Appl-SN-154713) Avail: NTIS HC A03/MF A01 CSCL 20H

The method and apparatus of this invention provides a plurality of measurements indicative of the absolute cross section for excitation of an ion beam. The ion beam is merged for excitation by specific energies of electrons in an electron beam. Both beams are merged in an evacuated enclosure having a longitudinal magnetic field and a crossed uniform electric field. The ions and electrons interact over a known merged longitudinal length in a merged beam area. After collision, the electron and ion beams are demerged. Forward and backward-scattered electrons are collected and position-detected by a pair of microchannel plate arrays located at opposite ends of said longitudinal beam-merging area. A series of electron and ion primary current measurements are taken at full ion and electron beam strength. Measurements are also taken at greatly reduced beam strength to obtain a beam overlap profile. NASA

N88-25282# Oak Ridge National Lab., Tenn.
CALORIMETRY APPLIED TO NUCLEUS-NUCLEUS COLLISIONS AT ULTRARELATIVISTIC ENERGIES
F. Plasil 1988 45 p Presented at the Miniworkshop on Experimental Techniques in Relativistic Heavy-ion Experiments, Bombay, India, 13 Feb. 1988
(Contract DE-AC05-84OR-21400)
(DE88-006173; CONF-880244-1) Avail: NTIS HC A03/MF A01

A general introduction to high-energy calorimetry is presented, together with brief descriptions of the two types of cascades relevant to calorimetric measurements. This is followed by a discussion of compensation and of the e/h ratio. A detailed description of two calorimeters designed and constructed for the CERN WA80 experiment are also given. DOE

N88-25283# Oak Ridge National Lab., Tenn.
ENERGY MEASUREMENTS IN OXYGEN-INDUCED REACTIONS AT 60 A GeV AND 200 A GeV
T. C. Awes, R. Albrecht, C. Baktash, P. Beckmann, F. Berger, R. Bock, G. Claesson, L. Dragon, R. L. Ferguson, and A. Franz et al. 1988 17 p Presented at the 16th International Workshop on Gross Properties of Nuclei and Nuclear Excitations, Hirschegg, Austria, 18 Jan. 1988 Prepared in cooperation with Gesellschaft fuer Schwerionenforschung m.b.H., Darmstadt and Muenster Univ., Fed. Republic of Germany, California Univ., Berkeley, Lawrence Berkeley Lab. and Lund Univ., Sweden
(Contract DE-AC05-84OR-21400)
(DE88-006420; CONF-880161-1) Avail: NTIS HC A03/MF A01

In an effort to isolate characteristic features of nucleus-nucleus collisions (e.g., collective phenomena) from those that may be expected on the basis of a linear superposition of nuelceon-nucleon collisions, we will compare measured quantities with calculations that reproduce data from nucleon-induced reactions and that make predictions for nucleus-nucleus reactions. While several models are available for this procedure, none has yet been demonstrated to have clear advantages over the others. Consequently, we have chosen to make comparisons with the LUND model for high-energy nucleus-nucleus interactions (FRITIOF). Effects of detector acceptance and of trigger bias have been included in all FRITIOF simulations shown in this work. In describing the nuclear density, the radius parameter r/sub O/ = 1.10 fm has been used for the Woods-Saxon distributions. This results in somewhat larger sizes of the light nuclei as compared to the standard FRITIOF parameter selection, but is in better agreement with results for the nuclear density distribution from electron scattering. DOE

N88-25284# Brookhaven National Lab., Upton, N. Y.
THE MULTISTRING MODEL VENUS FOR ULTRARELATIVISTIC HEAVY ION COLLISIONS
K. Werner Feb. 1988 7 p Presented at the 5th Winter Workshop on Nuclear Dynamics, Sun Valley, Idaho, 22 Feb. 1988
(Contract DE-AC02-76CH-00016)
(DE88-007666; BNL-40999; CONF-880260-1) Avail: NTIS HC A02/MF A01

The event generator VENUS is based on a multistring model for heavy ion collisions at ultrarelativistic energies. The model is a straightforward extension of a successful model for soft proton-proton scattering, the latter one being consistent with e(sup +-) e(sup -) annihilation and deep inelastic lepton scattering. Comparisons of VENUS results with pA and recent AA data alow some statements about intranuclear cascading. DOE

N88-25285*# National Aeronautics and Space Administration, Washington, D.C.
COMPUTER SIMULATION OF UPHILL DIFFUSION IN TERNARY IONIC SYSTEM
Takashi Yamagishi, Kiyosumi Fujii, and Shigeo Kitsutaka Jun. 1988 16 p Transl. into ENGLISH from Yogyo Kyokai Shi (Japan) no. 94(12), 1986 p 1206-1212 Transl. by SCITRAN, Inc., Santa Barbara, Calif. Original document was prepared by Nippon Sheet Glass Co., Ltd., Kaidoshita (Japan)
(Contract NASw-4307)
(NASA-TT-20194; NAS 1.77:20194) Avail: NTIS HC A03/MF A01 CSCL 20H

In mutli-component ionic diffusion systems, uphill diffusion is frequently observed. The conditions for the development of uphill diffusion were investigated by computerized simulation of ion exchange between a glass containing two cations (A,B) and a molten salt containing the third cation (C). The following conclusions were obtained. The uphill diffusion of B ion is observed when D sub A is greater than D sub B is greater than D sub C or D sub A is greater than D sub C is greater than D sub B, if all diffusion coefficients of D are independent of concentration. This uphill diffusion behavior is affected by the molar ratio of A to B in a mother glass. In the simulated ion exchange systems that were investigated, the uphill diffusion was prominent when the mother fraction of B ion is around 0.25. The concentration dependence of D does influence the distribution of ions, however, the relationship between three diffusion coefficients is a more important condition for the development for uphill diffusion. Ion exchange experiments in (Na,Rb) glass/(K) salt and (Na, K) glass/(Tl) salt systems were performed to confirm the results of the simulation. The uphill diffusion of Rb and K ions was observed as predicted by the simulation. The diffusion behavior of ions in glass during the ion exchanging process for the fabrication of gradient index lens was also investigated by computerized simulation. The progression of ion concentration profiles during this ion exchange process, especially the development of the uphill diffusion of Tl ions in the initial stage of this process, was well reproduced.
Author

N88-25286# Tokyo Univ. (Japan). Inst. of Space and Astronautical Science.
PARA-ORTHO ABUNDANCE RATIO OF MOLECULAR HYDROGEN IN NGC2023
K. Takayanagi, K. Sakimoto, and K. Onda Sep. 1986 25 p Submitted for publication
(ISAS-RN-352) Avail: NTIS HC A03/MF A01

Recent infrared emission line observation by Hasegawa clearly indicated that the para-ortho abundance ratio of H2 in the reflection nebula NGC2023 is quite different from 1:3. A simplified steady state problem is solved to determine the vibrational-rotational level population. In addition to radiative processes, the H2 formation on grains and the gas-phase para-ortho conversion processes are

taken into account. A good fit to the observed line intensity ratio can be obtained if the rotational Boltzmann distribution with temperature T sub f = 60 to approximately 70 K is assumed for H2 formed on grain surface. Author

73 NUCLEAR AND HIGH-ENERGY PHYSICS

Includes elementary and nuclear particles; and reactor theory.

For space radiation see *93 Space Radiation.*

N88-25287# Brookhaven National Lab., Upton, N. Y.
EXPERIMENTS WITH HIGH ENERGY NUCLEAR BEAMS AT BROOKHAVEN: FROM AGS TO RHIC (RELATIVISTIC HEAVY ION COLLIDER)
T. W. Ludlam 1987 14 p Presented at the International Symposium on Position Detectors for High Energy Physics, Dubna, USSR, 22 Sep. 1987
(Contract DE-AC02-76CH-00016)
(DE88-007042; BNL-40884; CONF-8709252-1) Avail: NTIS HC A03/MF A01

We have now seen the first results from experiments with high energy nuclear beams at Brookhaven and CERN. These experiments, which began about a year ago, use fixed targets at the AGS and SPS. These programs have begun with relatively light ions (A less than or equal to 32 amu) to explore states of compressed nuclear matter in which high energy density is achieved in an environment of high baryon density at energies near the maximum for nuclear stopping. These experiments are providing the first glimpse of what is expected to be an entire new regime of physical phenomena. These experiments will be followed in the near future by measurements with much higher beam masses and much higher collision energies. This is the mission of the Relativistic Heavy Ion Collider (RHIC) project now being prepared for construction at Brookhaven. In this presentation the author briefly describes the experiments which are now being carried out with ions accelerated in the AGS and the plans for heavier beams in the near future with the completion of the AGS Booster Synchrotron, which is now under construction. DOE

N88-25288# Brookhaven National Lab., Upton, N. Y. National Synchrotron Light Source Dept.
ON BUNCH LENGTHENING USING THE FOURTH HARMONIC CAVITY IN THE NSLS VUV RING
J. M. Wachtel Feb. 1988 21 p
(Contract DE-AC02-76CH-00016)
(DE88-007392; BNL-40929) Avail: NTIS HC A03/MF A01

It has been suggested that the phase of the beam excited voltage in the harmonic cavity can be controlled by detuning its resonant frequency from the beam current harmonic. Unfortunately the detuning needed to flatten the acceleration waveform also corresponds to the region of Robinson instability for the harmonic cavity. Therefore, lengthening the bunch may be followed by large amplitude synchrotron oscillation of the bunch center of mass. Bunch lengthening is discussed in this note from several points of view. There follows a simple review of single electron oscillations in a quartic potential. Then equations are developed for the coupled oscillations of a cavity and a rigid bunch as a fully nonlinear, time dependent initial value problem. Next, a computer program that solves these equations for one, two or more cavities, with and without externally driven fields, is described and some simulations of the harmonic cavity interaction are shown. Finally, the fully nonlinear equations are linearized to derive a dispersion relation for the case of beam excitation in the harmonic cavity. DOE

N88-25289# California Univ., Irvine. Dept. of Physics.
PROPAGATION OF NEUTRALIZED ION BEAMS Final Technical Report, 1 Oct. 1985 - 31 Dec. 1987
Amnon Fisher and Norman Rostoker Dec. 1987 13 p
(Contract F49620-86-K-0004)
(AD-A191599; AFOSR-88-0053TR) Avail: NTIS HC A03/MF A01 CSCL 20G

The propagation of plasmoids (neutralized beams) in a vacuum transverse magnetic field has been studied in the UCI laboratory for several years. The most recent experiments are aimed at studying the plasmoid propagation dynamics and losses in the presence of a background, magnetized plasma which is intended to short the induced polarization electric field and stop the beam. Preliminary results indicate that the beam propagation losses increase with the background plasma density. Principal diagnostics include: magnetically insulated Faraday cups, floating potential probes, calorimeters, microwave interferometer, and thermal-witness paper. Experiments in the near future will use an improved accelerator and transverse-field coil system which allows higher energy, 500 keV, higher current density plasmoids to be studied; this generator will improve the beam uniformity and angular divergence to allow beam propagation for up to five meters and permit study of losses from surface erosion. GRA

N88-25290# Maryland Univ., College Park.
ACCELERATOR RESEARCH STUDIES Annual Progress Report
Mar. 1988 62 p
(Contract DE-AC05-85ER-40216)
(DE88-007124; DOE/ER-40216/5) Avail: NTIS HC A04/MF A01

Our major goal in this experiment is to study the physics of a space-charge dominated beam propagating through a long, periodic transport channel consisting in our case of 38 solenoid lenses two of which are being used to match the beam from the gun into the periodic lattice. In addition, a small separate test stand gives us the capability of studying different electron gun designs including measurements of beam perveance and emittance, beam propagation in drift space and through a single solenoid lens. Most of our transport studies in the periodic channel have been conducted with a 5 keV, 200 mA electron beam from a gun with a 1-inch diameter thermionic cathode. The beam physics phenomena of greatest interest are instabilities due to resonant interaction between the beam and the periodic lattice, non-linear effects due to external forces (e.g., spherical lens aberrations) or due to nonuniform charge distributions, beam off-centering and misalignments which also include the effects of image forces. In principle, all of these effects may lead to emittance growth and beam loss. An important question is whether there exists a window of 100 percent transmission and minimal emittance growth in such a long periodic channel. DOE

N88-25291# Continuous Electron Beam Accelerator Facility, Newport New, Va.
THE LOSS PARAMETERS FOR VERY SHORT BUNCHES
J. J. Bisognano, S. A. Heifets, and B. C. Yunn [1987] 24 p
(Contract DE-AC05-84ER-40150)
(CEBAF-PR-88-005) Avail: NTIS HC A03/MF A01

Semi-empirical formulas for the transverse and longitudinal loss factors generated by cavity and step discontinuities are given in the limit of short bunch length. The parametric transition between the cavity and step approximations is considered. The differences between the impedances offered by periodic structures and isolated single cavities are also discussed. Author

74 OPTICS

Includes light phenomena; and optical devices.

For lasers see *36 Lasers and Masers.*

N88-25292# Gosudarstvennyj Komitet po Ispolzovaniyu Atomnoi Energii, Serpukhov (USSR). Inst. Fiziki Vysokikh Ehnergij.
STUDY OF LIGHT TRANSMISSION METHODS FROM SCINTILLATORS TO OPTICAL FIBER WITH WAVE LENGTH SHIFTER
V. I. Kryshkin and A. I. Ronzhin 1987 8 p In RUSSIAN;

ENGLISH summary
(DE88-701587; IFVE-OEF-87-22) Avail: NTIS (US Sales Only) HC A02/MF A01

Efficiency of light transmission and its transport from plastic scintillators to optical fiber with a wave length shifter has been investigated. Results of measuring the amount of photoelectrons for different geometrics of a wave length shifter and a light pipe are presented. Analysis of the results obtained has shown that to increase the light collection, use of multilayer optical fibers similar in structure is optimal. The best results on light collection are given with scintillator plates produced with the casting technique in which two-layer optical fiber is baked inside a scintillator. The count of electrons of 0.7 has been produced from each of two fiber edges. Inhomogeneity of response on plate dimensions (97x94x5 mm) constitutes plus or minus 0.7 percent. Results of investigation into light transmission methods have shown the advantage of optical-fiber light extraction in laminated calorimeters as compared with use of plate-wave length shifters. DOE

N88-25293# Pennsylvania Univ., Philadelphia. Electrowave-Optics Lab.
OPTICAL COMPUTING BASED ON NEURONAL MODELS Final Report, 16 Feb. 1986 - 15 Feb. 1987
Nabil H. Farhat Oct. 1987 65 p
(Contract N00014-85-K-2036)
(AD-A191481; EO/MO-12) Avail: NTIS HC A04/MF A01 CSCL 23C

Ever since the fit between what neural net models can offer (collective, iterative, nonlinear, robust, and fault-tolerant approach to information processing) and the inherent capabilities of optics (parallelism and massive interconnectivity) was first pointed out and the first optical associative memory demonstrated in 1985, work and interest in neuromorphic optical signal processing has been growing steadily. For example, work in optical associative memories is currently being conducted at several academic institutions (e.g., California Institute of Technology, University of Colorado, University of California-San Diego, Stanford University, University of Rochester, and the author's own institution the University of Pennsylvania) and at several industrial and governmental laboratories (e.g., Hughes Research Laboratories - Malibu, the Naval Research Laboratory, and the Jet Propulsion Laboratory). In these efforts, in addition to the vector matrix multiplication with thresholding and feedback scheme utilized in early implementations, an arsenal of sophisticated optical tools such as holographic storage, phase conjugate optics, and wavefront modulation and mixing are being drawn on to realize associative memory functions. GRA

N88-25294# Brown Univ., Providence, R. I. Div. of Engineering.
NOVEL FIBER PREFORMS: RARE EARTH DOPING Final Technical Report, 1 Nov. 1986 - 30 Nov. 1987
T. F. Morse 21 Jan. 1988 43 p
(Grant AF-AFOSR-0058-87)
(AD-A191549; AFOSR-88-0221TR) Avail: NTIS HC A03/MF A01 CSCL 07B

Rare earth glasses have been studied with emphasis on those characteristics related to rare earth doping of optical fiber preforms for fiber sensor applications. Progress has been made in the following areas: further experience with the Modified Chemical Vapor Deposition (MCVD) preform facility, and the establishment of an optical draw tower provides the ability to create state-of-the-art fibers with a host of novel dopants. We will continue to concentrate on fibers doped with rare earth elements by several techniques, and to continue studies of bulk formation of rare earth glasses, and to study certain aspects of second harmonic generation in rare earth doped silica based fibers. GRA

N88-25295# Rockwell International Corp., Thousand Oaks, Calif. Science Center.
STUDIES OF OPTICAL MATRIX MULTIPLICATION AND RECONFIGURABLE OPTICAL INTERCONNECT CONCEPTS Annual Report No. 1, 1 Nov. 1986 - 31 Oct. 1987
Pochi Yeh Jan. 1988 37 p
(Contract F49620-87-C-0015; ARPA Order 5884)
(AD-A191635; SC5502.AR; AFOSR-88-0094TR) Avail: NTIS HC A03/MF A01 CSCL 20F

In the first year of the program, we studied a number of concepts on matrix multiplication and reconfigurable optical interconnection using photorefractive materials such as BaTiO3. We have conceived several new concepts in the same area. The results are documented in three technical paper/presentations and four patent disclosures. GRA

N88-25296# Honeywell, Inc., Bloomington, Minn. Physical Sciences Center.
OPTICAL SYMBOLIC PROCESSOR FOR EXPERT SYSTEM EXECUTION Quarterly Technical Report, 1 Sep. - 30 Nov. 1987
Aloke Guha 30 Nov. 1987 13 p
(Contract F49620-86-C-0082; ARPA Order 5794)
(AD-A192005; AFOSR-88-0022TR) Avail: NTIS HC A03/MF A01 CSCL 20F

The goal of this program is to develop a concept for an optical computer architecture for symbolic computing by defining a computation model of a high level language, examining the possible devices for the ultimate construction of a processor, and by defining required optical operations. This quarter we investigated the implementation alternatives for an optical shuffle exchange network (SEN). Work in previous quarter had led to the conclusion that the SEN was most appropriate optical interconnection network topology for the symbolic processing architecture (SPARO). A more detailed analysis was therefore conducted to examine implementation possibilities. It was determined that while the shuffle connection of the SEN was very feasible in optics using passive devices, a full-scale exchange switch which handles conflict resolution among competing messages is much more difficult. More emphasis was therefore given to the exchange switch design. The functionalities required for the exchange switch and its controls were analyzed. These functionalities were then assessed for optical implementation. It is clear that even the basic exchange switch, that is, an exchange without the controls for conflict resolution, delivery, etc..., is quite a difficult problem in optics. We have proposed a number of optical techniques that appear to be good candidates for realizing the basic exchange switch. A reasonable approach appears to be to evaluate these techniques. GRA

N88-25297# Arizona Univ., Tucson. Optical Sciences Center.
RESEARCH IN THE OPTICAL SCIENCES Final Report, 1 Oct. 1984 - 30 Sep. 1987
Robert R. Shannon 15 Dec. 1987 172 p
(Contracts F49620-85-C-0039; MIPR-ARO-101-86)
(AD-A192175; ARO-22288.64-PH) Avail: NTIS HC A08/MF A01 CSCL 20F

Various topics in optical sciences research are given. The titles of that research are: Research in the Optical Sciences; Nonlinear Dynamics and Chaos in intracavity Quantum Electrodynamics; Generation and Application of Femtosecond Laser Pulses; Optical Studies of Metallic Superlattices; Study of Optical Interconnects using Nonlinear Surface Interactions; Long-Rage Surface Plasmons; Physics and Applications of Surface Guided Fields; Optical Elements for Extreme Ultraviolet; Production of High Reflectivity Mirrors; Novel Ion-beam Milling Techniques for Integrated Optics; Optical Properties of Inhomogeneous Media; Quantum Theory of Multiwave Mixing; Etalon Logic and Two Dimensional Arrays; Optical Nonlinearities of Thin Evaporated Films and Color Filters; Ultrasound Assisted Deposition of Dielectric Films Wavefront Sensing and Adaptive Optics; Development of an Electrical Readout X ray Imaging System; Surface Figure Probe; Guided Wave Optical Limiters; Room Temperature CW Operation of a Bistable GaAs Etalon using a Laser Diode Light Source; Ion Beam Processing for Optical Coatings on Plastics; Aberrated Gaussian Beams; and Modulated Emittance Spectroscopy. GRA

N88-25298# Indiana Univ., Bloomington. Dept. of Chemistry.
A DISPOSABLE LIQUID MICROCELL FOR NEAR-INFRARED REFLECTANCE ANALYSIS

Robert A. Lodder and Gary M. Hieftje 22 Feb. 1988 12 p
(Contract N00014-86-K-0366; Grant NSF-CHE-83-20053)
(AD-A192190; INDU/DC/GMH/TR-88-22) Avail: NTIS HC A03/MF A01 CSCL 20F

A disposable, 70 microliter, liquid analysis transmission cell is described for use in near infrared reflectance instruments. The small sample volume relative to the overall cell size allows many analyses to be performed without a thermostatically controlled heating cycle. Complex purge/fill and wash cycles are also necessary. The cell is ideally suited for the analysis of potentially hazardous liquid samples. GRA

N88-25299# Research Inst. of National Defence, Linkoeping (Sweden). Div. of Optical Technology.
[ACTIVITIES REPORT OF THE DIVISION OF OPTICAL TECHNOLOGY] Annual Report, 1986-1987
Dietmar Letalick Dec. 1987 19 p In SWEDISH; ENGLISH summary
(FOA-C-30477-3; ISSN-0347-3708; ETN-88-92488) Avail: NTIS HC A03/MF A01; Research Institute of National Defence, Box 1165, 5-581 11 Linkoping, Sweden, 50 Swedish crowns

Research concerning hydrooptics; remote sensing with lasers; coherent CO2 laser radar; optical signatures; atmospheric transmission; ionizing radiation effects on electronics; fiber optics; optical processing; and simulation in terrain models is summarized. ESA

N88-25300*# Ohio State Univ., Columbus. ElectroScience Lab.
CURVATURE OF BLENDED ROLLED EDGE REFLECTORS AT THE SHADOW BOUNDARY CONTOUR
S. W. Ellingson Apr. 1988 63 p
(Grant NsG-1613)
(NASA-CR-182974; NAS 1.26:182974; ESL-TR-716148-29)
Avail: NTIS HC A04/MF A01 CSCL 20F

A technique is advanced for computing the radius of curvature of blended rolled edge reflector surfaces at the shadow boundary, in the plane perpendicular to the shadow boundary contour. This curvature must be known in order to compute the spurious endpoint contributions in the physical optics (PO) solution for the scattering from reflectors with rolled edges. The technique is applicable to reflectors with radially-defined rim-shapes and rolled edge terminations. The radius of curvature for several basic reflector systems is computed, and it is shown that this curvature can vary greatly along the shadow boundary contour. Finally, the total PO field in the target zone of a sample compact range system is computed and corrected using the shadow boundary radius of curvature, obtained using the technique. It is shown that the fields obtained are a better approximation to the true scattered fields. Author

N88-25301*# National Aeronautics and Space Administration. Pasadena Office, Calif.
REAL-TIME OPTICAL MULTIPLE OBJECT RECOGNITION AND TRACKING SYSTEM AND METHOD Patent Application
Tien-Hsin Chao, inventor (to NASA) and Hua Kuang Liu, inventor (to NASA) (Jet Propulsion Lab., California Inst. of Tech., Pasadena.) 10 Dec. 1987 18 p Prepared in cooperation with Jet Propulsion Lab., California Inst. of Tech., Pasadena.
(Contract NAS7-918)
(NASA-Case-NPO-17139-1-CU; NAS 1.71:NPO-17139-1-CU; US-Patent-Appl-SN-154718) Avail: NTIS HC A03/MF A01 CSCL 20A

The invention relates to an apparatus and associated methods for the optical recognition and tracking of multiple objects in real time. Multiple point spatial filters are employed that pre-define the objects to be recognized at run-time. The system takes the basic technology of a Vander Lugt filter and adds a hololens. The technique replaces time, space and cost-intensive digital techniques. In place of multiple objects, the system can also recognize multiple orientations of a single object. This later capability has potential for space applications where space and weight are at a premium. NASA

N88-25302*# National Aeronautics and Space Administration. Langley Research Center, Hampton, Va.
PHASE LENGTH OPTICAL PHASE-LOCKED-LOOP SENSOR Patent Application
Joseph S. Heyman, inventor (to NASA) 11 Feb. 1988 12 p
(NASA-Case-LAR-13387-1; NAS 1.71:LAR-13387-1; US-Patent-Appl-SN-154716) Avail: NTIS HC A03/MF A01 CSCL 20F

The invention is a device that provides a high resolution measurement of the change in optical phase length from the device optical system source to an optical reflector. The invention consists of a optical phase locked loop that uses a laser beam as a carrier of an intensity modulated energy source. The novelty of the invention appears to lie in the overall combination of elements which provide high resolution without loss of wide dynamic range. The invention does not depend on coherent reflection from a target, and thus can measure targets that do not have special preparation or corner reflectors. The use of carrier modulation achieves high resolution without the problems of high speed pulse duration systems. Thus the invention has the advantages of simplicity, low cost, and small size without sacrificing resolution. NASA

N88-25303*# National Aeronautics and Space Administration. Marshall Space Flight Center, Huntsville, Ala.
OPTICAL PRESSURE SEALING COUPING (LIGHT JOINT) Patent Application
Timothy Irvin, inventor (to NASA) and Richard French, inventor (to NASA) (Rockwell International Corp., Canoga Park, Calif.) 16 Feb. 1988 14 p
(NASA-Case-MFS-29348-1; NAS 1.71:MFS-29348-1; US-Patent-Appl-SN-156518) Avail: NTIS HC A03/MF A01 CSCL 20F

The invention is directed toward an optical pressure sealing coupling providing pressure sealing feed through a fiber optic probe used as a monitoring device. The invention is primarily adapted for feeding optical signals from one section of a probe under high pressure cryogenic conditions to another section of the probe at ambient pressure. The novelty of the convention is in the combination of optically coupling and sealing the probe against the high pressure differential while maintaining discrete optical send/receive channels through the connection despite vibration. The advantages appear to be a rugged coupling having sensitive optics contained internally and eliminates the requirement of independently sealing the probe itself. NASA

N88-25304*# National Aeronautics and Space Administration. Pasadena Office, Calif.
LOW-LOSS, HIGH-ISOLATION, FIBER-OPTIC ISOLATOR Patent Application
George F. Lutes, inventor (to NASA) (Jet Propulsion Lab., California Inst. of Tech., Pasadena.) 31 Mar. 1988 11 p Prepared in cooperation with Jet Propulsion Lab., California Inst. of Tech., Pasadena.
(Contract NAS7-918)
(NASA-Case-NPO-17207-1-CU; NAS 1.71:NPO-17207-1-CU; US-Patent Appl-SN-190185) Avail: NTIS HC A03/MF A01 CSCL 20F

A low-loss, high-isolation, fiber-optic isolator for use in single-mode fiber systems utilizes a Faraday rotator and two polarizers, one at each end angularly oriented from each other at the angle of rotation for isolation, and two aspheric lens connectors to couple optical fibers to the Faraday isolator to reduce forward loss to about 2.5 dB and improve isolation to greater than 70 dB. NASA

N88-25305*# National Aeronautics and Space Administration. Pasadena Office, Calif.
REAL-TIME IMAGE DIFFERENCE DETECTION USING A POLARIZATION ROTATION SPACIAL LIGHT MODULATOR Patent Application
Tien-hsin Chao, inventor (to NASA) and Hua-Kuang Liu, inventor (to NASA) (Jet Propulsion Lab., California Inst. of Tech.,

Pasadena.) 18 Apr. 1988 16 p Prepared in cooperation with Jet propulsion Lab., California Inst. of Tech., Pasadena.
(Contract NAS7-918)
(NASA-Case-NPO-17144-1-CU; NAS 1.71:NPO-17144-1-CU; US-Patent-Appl-SN-187716) Avail: NTIS HC A03/MF A01 CSCL 20F

An image difference detection system is described, of the type wherein two created image representations such as transparencies representing the images to be compared lie coplanar, while light passes through the two transparencies and is formed into coincident images at the image plane for comparison. The two transparencies are formed by portions of a polarization-rotation spatial light modulator display such as a multi-pixel liquid crystal display or a magnetooptical rotation type display. In a system where light passing through the two transparencies is polarized in transverse directions to enable the use of a Wollaston prism to bring the images into coincidence, a liquid crystal display can be used which is devoid of polarizing sheets that would interfere with transverse polarizing of the light passing through the two transparencies. NASA

N88-25306# Joint Inst. for Nuclear Research, Dubna (USSR). Lab. of Nuclear Problems.
OPTICAL SYSTEM OF LASER ILLUMINATED STREAMER CHAMBER
Eh. Sodnomyn, Ban Khe Sok, and N. K. Ilieva-Sokolinova et al. 1987 9 p In RUSSIAN
(DE88-702127; JINR-13-87-312) Avail: NTIS (US Sales Only) HC A02/MF A01

An optical system of the laser-illuminated streamer chamber is described. Characteristics of the optical system elements are given. Photographs of particle tracks were obtained for the first time. The photographs were taken with bright-field and dark-field techniques. The results obtained in the course of experiments and opportunities of using the laser-illuminated streamer chamber in physics are discussed. DOE

N88-25307# Stanford Univ., Calif.
LIGHT PROPAGATION THROUGH GRAVITATIONALLY PERTURBED FRIEDMANN UNIVERSES Ph.D. Thesis
Eric V. Linder 1987 162 p
Avail: Univ. Microfilms Order No. DA8800976

The vast majority of the knowledge of the universe arises from measurement of electromagnetic radiation emitted from astrophysical process. To what extent these observations faithfully represent the sources rather than characteristics induced in propagation is therefore a question of great interest. Light propagation is determined by the metric of spacetime and so is sensitive to the physical inhomogeneities that perturb the idealized smooth cosmology. Two varieties of metric perturbations are analyzed: gravitational waves and gravitational lenses. Some possible methods for including their properties within a unified formalism dealing with light propagation through gravitationally perturbed cosmologies are discussed. In addition to investigating the astrophysical effects of these inhomogeneities (redshift, position, and luminosity fluctuations), upper limits are derived on the energy density in gravitational waves by examining cosmic microwave background anisotropies and galaxy clustering correlations. Constraints were also calculated on the mass and number density of compact objects acting as gravitational lenses by examining supernova amplification probabilities.
Dissert. Abstr.

N88-24938# Deutsche Forschungs- und Versuchsanstalt fuer Luft- und Raumfahrt, Brunswick (West Germany).
INVESTIGATIONS IN ELECTRO-OPTICAL MULTISTABILITY FOR SIGNAL PROCESSING
Christopher Watts and Norbert Fuerstenau *In its* Optics: Perspectives for Measurement Techniques and Signal Processing for Flight Guidance Aug. 1987 p 243-266 (For primary document see N88-24928 18-35)
Avail: NTIS HC A13/MF A01; DFVLR, VB-PL-DO, 90 60 58, 5000 Cologne, Fed. Republic of Germany 88 Deutsche marks

75 PLASMA PHYSICS

Includes magnetohydrodynamics and plasma fusion.
For ionospheric plasmas see *46 Geophysics*. For space plasmas see *90 Astrophysics*.

N88-25308# Sandia National Labs., Albuquerque, N. Mex.
INTENSE ION BEAM DIAGNOSTICS FOR PARTICLE BEAM FUSION EXPERIMENTS ON PBFA 2
R. J. Leeper, W. A. Stygar, J. Maenchen, C. L. Ruiz, R. P. Kensek, D. J. Johnson, T. R. Lockner, J. Bailey, G. Cooper, and J. R. Lee et al. 1988 29 p Presented at the 7th Topical Conference on High Temperature Plasma Diagnostics, Napa, Calif., 13 Mar. 1988
(Contract DE-AC04-76DP-00789)
(DE88-007279; SAND-88-0426C; CONF-880364-4) Avail: NTIS HC A03/MF A01

A review of diagnostics used at Sandia National Laboratories to measure the parameters of intense proton and lithium beams generated on the PBFA-2 accelerator will be presented. These diagnostics consist of several types, namely: K gamma x-ray pinhole cameras, a multi-frame dE/dx ion pinhole camera, a p-i-n array ion pinhole camera, Thomson parabola spectrographs, a Rutherford magnetic spectrograph, plasma visible spectroscopy and several nuclear activation diagnostics. These components when taken together enable a rather thorough description of the 5-MW, 10-TW ion beams presently being produced. A unique feature of these diagnostics is that they are capable of operating in hard (several MeV) x-ray bremsstrahlung backgrounds of some 10 to the 9th to 10 to the 10th power Rad/sec. Details of each diagnostic, its integration, data reduction procedures, and recent PBFA-2 data will be discussed. DOE

N88-25309# New York Univ., New York. Inst. of Mathematical Sciences.
THEORETICAL PLASMA PHYSICS RESEARCH OF ACTIVE SPACE EXPERIMENTS Final Report, 1 Jul. - 31 Dec. 1986
Grossman 1987 8 p
(Contract F49620-86-C-0086)
(AD-A192075; AFOSR-88-0191TR) Avail: NTIS HC A02/MF A01 CSCL 20H

The following report describes our present understanding and recent results from an analysis of the effects of elastic scattering on neutral beam penetration. The important factors affecting neutral beam propagation in the upper atmosphere at altitudes of 200-250 km are discussed. Two primary factors affecting the beam quality are the accuracy of beam collimation and the effect of collisions between the beam particles and the background atmospheric particles. A further factor is ionization of the beam particles in terms of radiation or waves and instabilities that may result from the collective interaction between the ionized beam particles and the charged particles in the background atmosphere. GRA

N88-25310# Stuttgart Univ. (West Germany). Inst. fuer Raumfahrtsysteme.
BASIC PROCESSES OF PLASMA PROPULSION Annual Scientific Report, 1 Aug. 1986 - 31 Jul. 1987
Herbert O. Schrade Aug. 1987 78 p
(Grant AF AFOSR-0337-86)
(AD-A192117; AFOSR-88-0135TR) Avail: NTIS HC A05/MF A01 CSCL 20I

This report describes the research work on cathode phenomena and presents the development work and the results of several model calculations by means of which the performance of coaxial magnetoplasmadynamic (MPD) thrusters can be predicted. Electrode effects like spot formation and spot motion can cause high erosion on the cathode and backplate of an MPD thruster. These effects are qualitatively and partially quantitatively explained by means of a unique theoretical approach. By means of these performance calculations the onset conditions were calculated based on the fact that due to magnetic contraction (pinch effect) the plasma density becomes zero at the anode (onset theory of Hugel). The results of these calculations are in excellent agreement with those of the experiments. GRA

N88-25311# Swedish Inst. of Space Physics, Kiruna.
STUDIES OF SPECTRAL LINE RATIO FLUCTUATIONS USING INDUCTIVELY COUPLED PLASMA (ICP) LIGHT
Bo Thelin Dec. 1987 27 p
(IRF-Preprint-100; ISSN-0284-1711; ETN-88-92489) Avail: NTIS HC A03/MF A01

An analysis method of organizing spectral line intensity ratio fluctuations for different elements was used with inductively coupled plasmas, mounted end-on and side-on. Linear graphs are obtained for various iron lines when the spectral line ratio fluctuations are plotted versus the photon energies of these lines at different salt concentrations. Similar linear relationships are obtained from different elements when the spectral line ratio fluctuations are plotted versus the photon energies and the ionization energies of these lines. When these fluctuations are plotted versus the upper level energies instead of the conventional intensity equation, no linear structure is obtained. This analysis method was improved mathematically by using absolute differentials. The analyses were carried out by using a computerized image dissector echelle spectrometer system. ESA

N88-25312 Missouri Univ., Columbia.
THEORETICAL INVESTIGATIONS OF DRIFT WAVES IN A MAGNETIC QUADRUPOLE Ph.D. Thesis
Yildirim Aktas 1987 102 p
Avail: Univ. Microfilms Order No. DA8728783

A linear theory is developed for drift waves with frequencies between the electron and ion bounce frequencies in a collisionless plasma confined to a magnetic quadrupole. An integro-differential eigenvalue equation which allows for large ion-Larmor-radius effect, temperature gradients, and radial variation of the eigenfunction is derived from the linearized Vlasov equation. The drift wave instability is studied. Formulas are derived for the growth rate due to a dissipative trapped-electron mechanism and the damping rate due to ion viscosity. A numerical study is made of the drift waves which occur spontaneously in the shared flux region of the UMIST quadrupole. The effects of electron-neutral collisions on drift waves are investigated. A new formula for the growth rate is derived which includes nondetrapping as well as detrapping collisions and is not based on the small ion-Larmor-radius approximation. A numerical study has been made of the fundamental drift mode and the next harmonic which has two full wavelengths around a closed magnetic field line. The damping rates of electrostatic waves due to ion-ion and ion-neutral collisions are investigated. Finally, a numerical method of solving the integro-differential eigenvalue equation is presented. Dissert. Abstr.

N88-25313 State Univ. of New York, Buffalo.
OPTICAL INVESTIGATIONS OF THE THERMAL BOUNDARY LAYER IN ARC PLASMAS Ph.D. Thesis
Nanu Brates [1987] 404 p
Avail: Univ. Microfilms Order No. DA8727671

Experimental studies were conducted to determine the temporal and radial distributions of temperature within the thermal boundary layer of a pulsed, high pressure air arc discharge. Additionally, timewise distribution of the arc size and of the thermal boundary layer thickness were determined. The effects of upstream electrode geometry and of electrode material vapor upon the plasma discharge and flow pattern were also investigated. Differential interferometry was employed to study the thermal boundary layer in a single flow experiment. Results presented include radial distribution of the temperauture within the boundary layer, timewise distributions of arc size and thickness of the mantle and radial distribution of air particle and copper density within the thermal boundary layer. The spatial resolution achieved for these experiments was 0.1 mm, much higher than the typical spatial resolution reported in the literature. Dissert. Abstr.

N88-25314 Minnesota Univ., Minneapolis.
MODELLING OF THERMAL PLASMA SYSTEMS Ph.D. Thesis
Yau-Pin Chyou [1987] 397 p
Avail: Univ. Microfilms Order No. DA8727408

Thermal plasma systems, comprising two different states of matter, plasma and particles, for thermal plasma processing were studied. The primary objective of is to develop computational models for thermal plasma systems and to extent the knowledge of thermal plasma processing through theoretical considerations. The thermal plasma is regarded as a continuum fluid, and the global governing equations can be derived in Eulerian coordinates. A two-dimensional theoretical model for turbulent swirling plasma jets is established. The turbulence model used incorporates multiple time scales for velocity and temperature fluctuations, and a density-weighted averaging for the density fluctuation effect. Finite difference numerical schemes are implemented to solve the aforementioned problem. An iterative solution procedure is applied to general, elliptic type flows which may have recirculations, induced by strongly swirling flows. A modified marching procedure for parabolic type flows is also developed because in a plasma jet with weak or moderate swirl, there is no reverse flow in the predominant flow direction. Parametric investigations of the effect of swirls on flow fields for confined and free jets are also included. In addition, the characteristics of plasma flow compared to its counterparts of cold flow are also investigated. A modified approach for investigating non-continuum effects on plasma-particle heat transfer is proposed. Comparisons of theoretical predictions based on the present model with available experimental data are, in general, in reasonable agreement. Dissert. Abstr.

N88-25315 California Univ., Irvine.
STOCHASTICITY IN A Q-MACHINE PLASMA Ph.D. Thesis
Rezwanul Karim [1987] 165 p
Avail: Univ. Microfilms Order No. DA8727950

Experiments were designed to show the development of stochasticity in a Q-machine plasma. A resonance-overlap criterion developed by Chirikov and the Hamiltonian-stochasticity formalism developed by Escande and Doveil were used in the calculations. The verifiable signatures of the changes of measureable plasma transport properties, due to transition of the plasma into stochasticity, are not well established in the literature. The additional changes of plasma transport properties due to the simultaneous action of two waves individually, are correlated with the calculated stochasticity parameter. The development of broadband noise spectra due to the presence of two instabilites is also correlated with the calculated stochasticity parameter. Results from four different experiments are presented. Experimental observations of the change of the plasma transport properties and observed development of broadband noise spectra in these experiments agrees with theoretical predictions of the transition as expected from the calculation of the stochasticity parameter. In the experiments, it was observed that, as the potentials of the waves were slowly increased, the system gradually developed global stochasticity. The change of plasma transport properties and development of broadband noise were also gradual. As the strengths of the potential of the two waves are increased, the Kolmogorov-Arnold-Moser (KAM) surfaces are destroyed, and a few particles will behave chaotically. A further increase of the potentials will force more KAM surface destruction, forcing more particle motions to become stochastic. Dissert. Abstr.

N88-25316# Oak Ridge National Lab., Tenn.
SYSTEMS ANALYSIS OF INTOR-LIKE DESIGNS
C. A. Flanagan and J. D. Galambos Nov. 1987 72 p Presented at the International Tokamak Reactor Workshop, Vienna, Austria, 13 Jul. 1987
(Contract DE-AC05-84OR-21400)
(DE88-004422; FEDC-R-87-INTOR-1; CONF-8707106-5-Draft)
Avail: NTIS HC A04/MF A01

A systems analysis of the five INTOR-like designs was performed. This study was established to evaluate and determine the specific impact produced in a given design by making a specific change in that design. Such a quantitative analysis of the impact of various changes can provide evaluable insights as to how different choices affect a given design. The results of this analytic comparative study of the five INTOR-like designs should allow the fusion community to factor such design impacts into the development of the next generation of tokamak designs. DOE

N88-25317# Brookhaven National Lab., Upton, N. Y. AGS Dept.
PLASMA NEUTRALIZER WORK AT BNL (BROOKHAVEN NATIONAL LABORATORY)
A. Hershcovitch, V. Kovarik, and K. Prelec 1988 6 p Presented at the 3rd European Workshop Production and Applications of Light Negative Ions, Amersfoort, Netherlands, 17 Feb. 1988
(Contract DE-AC02-76CH-00016)
(DE88-007046; BNL-40856; CONF-880256-2) Avail: NTIS HC A02/MF A01

Conversion of high energy light negative ions into neutrals due to collisions with plasma electrons and ions can be very efficient (85 percent for H sup minus D sup minus and > 60 percent for Li sup minus). For negative ions above 1 MeV, the presence of gases and ions heavier than protons in a neutralizer dramatically reduces neutralization efficiencies, especially those of heavier negative ions (e.g., Li sup minus, C sup minus, Si sup minus). Consequently, our neutralizer studies were focused on generation of hydrogen plasma targets. As a plasma source, the hollow cathode discharge (HCD) proved to be optimal due to its flexibility and steady-state generation of a high density, highly ionized plasma. Plasma targets in a number of configurations were generated with a power consumption well over an order of magnitude lower than other plasma targets. A full-scale plasma neutralizer was successfully built and deployed in a beam line of the BNL Tandem Van de Graaff to neutralize multi-MeV beams of Li sup minus, C sup minus, and Si sup minus. Another plasma neutralizer was designed for the 1-2 A, 160 keV steady state D sup minus LBL (National Plan) beam line. Preliminary experiments to generate field-free plasma targets were performed. DOE

N88-25318# Texas Univ., Austin.
SELF SHIELDING OF SURFACES IRRADIATED BY INTENSE ENERGY FLUXES Progress Report, 1 Jun. 1987 - 31 May 1988
J. R. Howell and P. L. Varghese Feb. 1988 17 p
(Contract DE-FG05-87ER-13735)
(DE88-007094; DOE/ER-13735/1) Avail: NTIS HC A03/MF A01

This report summarizes work completed to date on the study of the effects of the impingement of a very high fluence plasma onto a target surface. Particular emphasis is placed on self-shielding of the target surface caused by initial surface erosion and the resulting presence of heavy metal ions in an ionsized shield layer near the surface. A high energy hydrogen plasma will be produced by a rail gun coupled to high-current sources (capacitor banks or high-current pulse homoplar generators developed at the University of Texas at Austin). Because of the extremely fast transients present in the experiments, considerable instrumentation development is necessary to provide the diagnostic tools for characterizing the incident plasma as well as the transient development of the vapor layer. The experimental results will be used to verify and/or modifify the dimensional transient computer code that models the complete plasma-surface interaction history. The model includes the effects of evaporated and sputtered wall material and its interaction with the incident plasma. DOE

N88-25319# Texas Univ., Austin. Inst. for Fusion Studies.
A STUDY OF RUNAWAY ELECTRON CONFINEMENT IN THE ASDEX TOKAMAK
O. J. Kwon, P. H. Diamond, F. Wagner, and G. Fussmann (Max-Planck-Inst. fuer Plasmaphysik, Garching, West Germany) Mar. 1988 38 p
(Contract DE-FG05-80ET-53088)
(DE88-007327; DOE/ET-53088/316; IFSR-316) Avail: NTIS HC A03/MF A01

The results of runaway electron confinement experiments from ASDEX are analyzed to elucidate the structure of electromagnetic turbulence that causes anomalous electron heat transport in the L-mode confinement regime. From a simple model, the radial correlation length (W) of the magnetic turbulence is determined to be about 1 mm. Using this value and that of the experimentally deduced electron thermal diffusivity, we determine the radial magnetic fluctuation level at the plasma edge in the L-mode to be (B tilde sub r/B sub 0 similar to 2 x 10 to the -4 power. Scalings of W and B tilde sub r/B sub 0 are deduced from parameter scans. From a comparison of these results with the predictions of various theoretical models, it is concluded that skin-depth turbulence, electromagnetic drift wave turbulence, rippling modes, and microtearing modes are inferior candidates and that resistive-ballooning modes offer the best possibility for a consistent interpretation of the data. DOE

N88-25320# Auburn Univ., Ala. Dept. of Physics.
DESIGN STUDIES OF LOW ASPECT-RATIO TORSATRONS Annual Progress Report, 1 Jun. 1987 - 1 Mar. 1988
J. D. Hanson 1 Mar. 1988 13 p
(Contract DE-FG05-87ER-53245)
(DE88-007562; DOE/ER-53245/1) Avail: NTIS HC A03/MF A01

Low aspect ratio is one of many design criteria for torsatrons. A new magnetic field design technique based on the Hamiltonian structure of magnetic field line flow is used to investigate feasible torsatron configurations. Significant improvements have been made in the computer code IFS. The problem of too large a magnetic axis wobble has been solved with the addition of an l = 1 m = 6 helical coil. DOE

N88-25321# Oak Ridge National Lab., Tenn.
A TWO-WAVELENGTH INFRARED INTERFEROMETER/POLARIMETER SYSTEM FOR CIT (COMPACT IGNITION TOKAMAK)
C. H. Ma, D. P. Hutchinson, and K. L. VanderSluis 1988 12 p Presented at the 7th Topical Conference on High Temperature Plasma Diagnostics, Napa, Calif., 13 Mar. 1988
(Contract DE-AC05-84OR-21400)
(DE88-007681; CONF-880364-12) Avail: NTIS HC A03/MF A01

The results of a feasibility study of a two-wavelength infrared interferometer-polarimeter system for measurements of electron density and plasma current profiles in the Compact Ignition Tokamak (CIT) are presented. The system utilizes CO sub 2 lasers at a wavelength of 10.6 microns, and water-vapor lasers at 28 microns. Both magneto-optic and electro-optic polarization-modulation techniques have been used to determine the sensitivity and time response of the polarimetry at 10.6 microns. Measurement of a simulated plasma Faraday rotation demonstrated a sensitivity of approximately 0.01 (o) for a CO sub 2 laser polarimeter with an electrooptic CdTe crystal modulator. DOE

N88-25322# Los Alamos National Lab., N. Mex.
OPTICAL DIAGNOSTICS FOR A HIGH POWER, RF-INDUCTIVELY COUPLED PLASMA
N. S. Nogar, G. L. Keaton, J. E. Anderson, and M. Trkula 1988 7 p Presented at the Spring Meeting of the Materials Research Society, Reno, Nev., 4 Apr. 1988
(Contract W-7405-eng-36)
(DE88-007822; LA-UR-88-1025; CONF-880408-7) Avail: NTIS HC A02/MF A01

Emission spectroscopy and laser-induced fluorescence have been used to monitor the field and tail-flame regions of a Hull-design inductively coupled plasma. This plasma is used for a variety of syntheses including SiC, TiC, BN, A1N and diamond. Temporally- and spatially-resolved spectra of both pure Ar and Ar/gas mixtures have been studied as a function of RF power, pressure and flow rate. Preliminary data suggest that the system is far from local thermodynamic equilibrium. DOE

N88-25323*# National Aeronautics and Space Administration. Marshall Space Flight Center, Huntsville, Ala.
MHD BENDING WAVES IN A CURRENT SHEET
Z. E. Musielak and S. T. Suess [1988] 36 p Submitted for publication
(NASA-TM-101149; NAS 1.15:101149) Avail: NTIS HC A03/MF A01 CSCL 20I

Transverse MHD bending waves are considered in an isothermal

and compressible two-dimensional current sheet of finite thickness in which the magnetic field changes direction and strength. The general form of the wave equation is obtained. It is shown that rotation of the magnetic field across the current sheet prevents the existence of singular points so that continuous spectrum solutions and the concomitant wave decay disappear. Instead, normal modes exist and closed integral solution for arbitrary current sheet structure are found. The results are discussed in terms of small-scale waves on the heliospheric current sheet. Author

N88-25324# FOM-Inst. voor Plasmafysica, Rijnhuizen, Jutphaas (Netherlands).
[ACTIVITIES REPORT IN PLASMA PHYSICS] Annual Report, 31 Dec. 1986
1986 91 p Sponsored by Euratom and the Netherlands Organization for the Advancement of Pure Research
(ETN-88-92221) Avail: NTIS HC A05/MF A01

Experiments on plasma pinches; turbulent heating in TORTUR and diagnostical studies; electron cyclotron resonance heating; and low-temperature plasma are described. Analyses concerning magnetohydrodynamics, wave dynamics, and transport problems are summarized. ESA

N88-25325 California Univ., Davis.
QN3D: A 3-DIMENSIONAL QUASI-NEUTRAL HYBRID PARTICLE-IN-CELL CODE WITH APPLICATIONS TO THE TILT MODE INSTABILITY IN FIELD REVERSED CONFIGURATIONS Ph.D. Thesis
Eric Jack Horowitz 1987 138 p
Avail: Univ. Microfilms Order No. DA8729949

The tilt mode instability of a field reversed configuration (FRC) is discussed. Current numerical models do not properly explain the behavior of this mode. A particle-in-cell (PIC) model in cartesian coordinates is introduced with an explanation as to why it represents the physics of FRCs more closely. The model is presented by first simplifying Maxwell's equations using the Darwin limit. A final set of equations are derived by assuming the electrons to be an inertialess fluid with zero temperature. The model is implemented in a FORTRAN code, QN3D. The major elements of this code are presented indicating the many techniques required for its optimization. Testing of the code is presented in three phases. First, single particle motion is analyzed. Next, the normal modes are calculated and simulated. Finally, QN3D is applied to the rigid rotor problem. These tests indicate that the code is suited to model plasma phenomena in the parameter regimes of interest. Dissert. Abstr.

76 SOLID-STATE PHYSICS

Includes superconductivity.

For related information, see also *33 Electronics and Electrical Engineering* and *36 Lasers and Masers.*

N88-25326# Joint Inst. for Nuclear Research, Dubna (USSR). Lab. of Neutron Physics.
NEUTRON DIFFRACTION REFINEMENT OF CsHSO4 SUPERIONIC PHASE STRUCTURE
A. M. Balagurov, A. I. Beskrovnyj, V. I. Gordelij, S. Vratislav, M. Dlouga, I. D. Datt, Z. Irak, and L. A. Shuvalov 1987 5 p In RUSSIAN; ENGLISH summary
(DE88-701496; JINR-14-87-353) Avail: NTIS (US Sales Only) HC A02/MF A01

The supersonic phase structure of the crystal CsHSO4 (T sub c approx = 414 K) was determined from neutron diffraction data. The volume centered tetragonal structure (sp.gr. I4(sub 1) and, a=5.718 A, c=14.232 A) is in the state of dynamical disorder: the tetrahedron SO4 occupies two positions with a tilting of + or - 20 deg around the c axis, the hydrogen atoms connect the tetrahedrons in the chain the direction of the (111) type. The proton conductivity proceeds by jump diffusion for the distances of 2.85 A, and 3.60 A along the (100) and (001) directions, respectively. With reducing temperature the subgroup phase transition occurs with one of the states being being frozen. DOE

N88-25327*# Princeton Univ., N. J. Dept. of Chemical Engineering.
NASA RESEARCH PROGRAM: THE ROLES OF FLUID MOTION AND OTHER TRANSPORT PHENOMENA IN THE MORPHOLOGY OF MATERIALS Final Report, Jul. 1983 - Oct. 1987
D. A. Saville May 1988 208 p
(Grant NAG3-447)
(NASA-CR-182801; NAS 1.26:182801) Avail: NTIS HC A10/MF A01 CSCL 20L

The influence of transport phenomena on the morphology of crystalline materials was investigated. Two problems were studied: the effects of convection on the crystallization of pure materials, and the crystallization of proteins from solution. For individual titles, see N88-25328 through N88-25329.

N88-25328*# Princeton Univ., N. J. Dept. of Chemical Engineering.
DENDRITIC GROWTH IN THE PRESENCE OF CONVECTION Ph.D. Thesis
Pantelis John Beaghton *In its* NASA Research Program: The Roles of Fluid Motion and other Transport Phenomena in the Morphology of Materials May 1988 151 p (For primary document see N88-25327 18-76)
Avail: NTIS HC A10/MF A01 CSCL 20L

The motion of the freezing front between a dendritic crystal and a supercooled liquid is studied using an interface evolution equation derived from a boundary integral transformation of the transient convective-diffusion equation. A new steady-state theory is introduced that incorporates the effects of convection in dendritic growth. It is shown that in the absence of capillary effects the shape of the crystal-melt interface is a paraboloid of revolution, similar to that found in situations where diffusion is the sole heat transfer mechanism. A relation between the supercooling, the product of the tip velocity and tip radius, and the strength of the flow is derived which reduces to the well-known Ivantsov theory in the absence of convection. A non-linear interface-tracking algorithm is developed and used to study the temporal and spatial evolution of the dendritic interface. The important role of capillarity and convection on the interface dynamics is established and the response of the interface to finite amplitude disturbances is examined for the first time. Tip splitting is identified as the dominant destabilization mechanism in the limit of zero surface tension. Finite surface tension leads to interface stabilization, irrespective of the magnitude and structure of the external perturbations. Finally, convection significantly decreases the magnitude of the freezing velocity. Author

N88-25329*# Princeton Univ., N. J. Dept. of Chemical Engineering.
TWO PUZZLING ASPECTS OF PROTEIN CRYSTAL GROWTH
M. L. Grant and D. A. Saville *In its* NASA Research Program: The Roles of Fluid Motion and other Transport Phenomena in the Morphology of Materials May 1988 34 p (For primary document see N88-25327 18-76)
Avail: NTIS HC A10/MF A01 CSCL 20L

A study is presented of several mechanisms which may reduce crystal growth rates and or terminate crystal growth. It is found that salt gradients which change the local chemical potential of the protein are insufficient to account for the slow crystal growth rates which have been reported. Contaminants which adsorb protein from solution may reduce the effective protein concentration, but the impurity's concentration and its affinity for protein are unknown. Association of protein molecules in bulk solution can reduce the monomer concentration significantly, but extant theory and experiment are not sensitive enough to determine the actual concentration of aggregates in solution. For systems of interest, shear-induced effects were found to be too weak to interfere with normal binding of incoming protein molecules. Although we found that most crystal growth occurs in a regime

where both interfacial kinetics and diffusion influence crystal growth, the role of mass transfer rates on the terminal size of crystals is unknown, primarily because no data exist which cover the size range of interest (0.1 mm to 1 mm in length). Author

N88-25330# Sandia National Labs., Albuquerque, N. Mex.
STRUCTURAL STUDIES ON La/SUB 2/CuO/SUB 4+DELTA/
B. Morosin, J. D. Jorgensen, J. E. Schirber, E. L. Venturini, and D. S. Ginley 1988 4 p Presented at the Spring Meeting of the Materials Research Society, Reno, Nev., 4 Apr. 1988 Prepared in cooperation with Argonne National Lab., Ill.
(Contract DE-AC04-76DP-00789)
(DE88-006828; SAND-88-0047C; CONF-880408-1) Avail: NTIS HC A02/MF A01

This preliminary study reports on detailed diffraction investigations underway to establish the structural properties of La2CuO4. Though not completely analyzed, these spectra illustrate changes in the apparent cell dimension with oxygen treatment and show the lattice symmetry changes must be small and subtle. DOE

N88-25331# Polytechnic Inst. of New York, Brooklyn.
PHYSICAL PROPERTIES OF f ELECTRON SYSTEMS Progress Report, Feb. 1987 - Jan. 1988
P. S. Riseborough 1988 9 p
(Contract DE-FG02-84ER-45127)
(DE88-006886; DOE/ER-45127/3) Avail: NTIS HC A02/MF A01

This paper discusses the progress in research on f electron systems. The major properties discussed in this paper are: magnetic properties, transport properties, heavy fermion superconductivity, and photo-emission spectroscopy. DOE

N88-25332# Georgia Inst. of Tech., Atlanta. School of Physics.
CRYSTALLINE METAL-SEMICONDUCTOR SUPERLATTICES Progress Report, 1 Jul. 1986 - 31 Dec. 1987
Ahmet Erbil 1988 13 p
(Contract DE-FG05-86ER-45266)
(DE88-007063; DOE/ER-45266/1) Avail: NTIS HC A03/MF A01

The focus of the program in the Phase 1 period has been the development of underlying science and technology for the fabrication of LaTe/PbTe metal-semiconductor superlattices. The major motivation for this work was to search for excitonic superconductivity in these structures as predicted by theory. Despite recent breakthroughs in the discovery of high-T superconductors, there are still many outstanding problems remaining. Some of the outstanding issues are lack of understanding of the mechanism of high-T superconductivity, difficulty in preparing materials with reproducible properties, requirement for cryogenic cooling, etc. We propose to address these issues. We have discovered a new Y-Ba-Cu-O compound with a transition temperature above 500 K. DOE

N88-25333# Brown Univ., Providence, R. I.
ELECTRONIC STRUCTURE, ELEMENTARY EXCITATIONS, OPTICAL AND TRANSPORT PROPERTIES OF SEMICONDUCTOR SUPERLATTICES Final Report, 1 Aug. 1984 - 31 Oct. 1987
John J. Quinn Dec. 1987 10 p
(Contract DAAG29-84-K-0008)
(AD-A190795; ARO-20428.1-PH) Avail: NTIS HC A02/MF A01 CSCL 20L

The following areas have been studied: (1) Collective Charge Density Excitation in Artificially Structures Materials; (a) Intra-and Intersubband Excitations of a Semiconductor Superlattice; (b) Plasmon Bands of Periodic Metallic Heterostructures; (c) Surface Plasmons in Artificially Structured Solids; (d) Raman and Inelastic Electron Energy Loss Spectroscopy due to Collective Charge Density Excitation; (e) Plasmon in Quasi Periodic Layered Electron Gas Systems; (2) Impurity Levels, Excitons, Phonons, and Magnetic Polarons in Quantum Well Structures; (3) The Single Particle Self-Energy in Layered Electron Gas Systems; (4) The Quantum Hall Effect. The results appear in 58 publications. GRA

N88-25334# Colorado Univ., Colorado Springs.
MAGNETIC SUPERLATTICES Final Report, 17 Sep. 1984 - 16 Sep. 1987
R. E. Camley 13 Jan. 1988 10 p
(Contract DAAG29-84-K-0201)
(AD-A191450; ARO-21558.20-PH) Avail: NTIS HC A02/MF A01 CSCL 20L

This project involved a general theoretical study of magnetic properties of layered systems. Three major areas were: (1) Phase transitions in magnetic superlattices. (2) The excitations in thin films and layered structures and the connection to optical properties. (3) Nonlinear optical properties of thin films and layered structures. GRA

N88-25335# Massachusetts Inst. of Tech., Cambridge.
OPTICAL PROPERTIES OF HETEROSTRUCTURES AND SUPERLATTICES Final Report, 15 Jun. 1984 - 31 Dec. 1986
Benjamin Lax Mar. 1988 24 p
(Contract N00014-84-K-0431)
(AD-A191542) Avail: NTIS HC A03/MF A01 CSCL 20L

The project for the study of the optical properties of single and multiple quantum wells involved both experimental and theoretical studies of such heterostructures. This study has utilized a variety of optical techniques such as laser excited luminescence, photoreflectance, laser emission with and without magnetic fields. The initial experiments which were conducted on a single quantum well of GaAs/GaAlAs structure led to an interesting discovery and explanation of exciton transport at low excitation intensities at a critical range of temperatures. The second class of experiments involved high intensity laser excitation which led to the discovery of a new lower high density excitonic state below the lowest exciton when under moderate excitation. The identification of this new state was facilitated by the use of high magnetic fields. A corollary to this experiment was the observation of the electron-hole plasma state at the highest intensities. This occurs at still a lower energy and was shown to be the source of stimulated emission in a quantum well. GRA

N88-25336# Jet Propulsion Lab., California Inst. of Tech., Pasadena.
AN INVESTIGATION OF 2-6 SUPERLATTICE DEPOSITION BY LASER PHOTOCHEMICAL TECHNIQUES Annual Report, 26 Nov. 1986 - 24 Nov. 1987
Richard J. Stirn, Akbar Nouhi, and Gouri Radhakrishnan Jan. 1988 34 p
(Grant AF-AFOSR-ISSA-0032-87)
(AD-A191547; AFOSR-88-0222TR) Avail: NTIS HC A03/MF A01 CSCL 07B

The objectives of this research program are to develop metalorganic chemical vapor deposition (MOCVD) techniques for Manganese-bearing 2-6 ternary compounds epitaxially grown on Gallium Arsenide substrates, and to explore the usefulness of UV laser assist for deposition for superlattice structures of wider bandgap 2-6 binary compounds. For the first time, high quality single-crystal (111) Cd1-xMnxTe was grown by conventional MOCVD on (100) GaAs wafers with high resolution cross-selectional transmission electron microscopy was used for structural characterization, showing atomically abrupt interfaces, but different microstructures within the epi-film depending on growth temperature. UV adsorption spectra of a number of metalalkyl sources for Cadmium, Zinc, Selenium, and Tellurium were measured and optical adsorption cross sections calculated. Preliminary depositions of Cadmium Telluride and Zinc telluride films on glass substrates were made at 200 C with UV excitation provided by an excimer gas laser operating at 193 nm and by using a parallel beam geometry. Some optical and X-ray diffraction data are presented as well as a description of the low pressure laser photochemical deposition system. GRA

N88-25337# University of Southern California, Los Angeles. Dept. of Electrical Engineering.
OPTICAL NONLINEARITIES IN GaAs/GaAlAs MULTIPLE QUANTUM WELLS FABRICATED BY METALORGANIC CHEMICAL VAPOR DEPOSITION FOR USE IN OPTICAL SIGNAL PROCESSING Final Report, 8 Jan. 1985 - 6 Jan. 1987
E. Garmire and P. D. Dapkus Dec. 1987 75 p
(Grant AF-AFOSR-0297-85)
(AD-A191558; AFOSR-88-0130TR) Avail: NTIS HC A04/MF A01 CSCL 20L

Preparation of high quality GaAs/GaA1As Multiple Quantum Wells (MQW) grown by Metalorganic Chemical Vapor Deposition on GaAs substrates and measurement of nonlinear saturation has been completed in this 18 month contract. The results show materials which rivals the highest quality MQW's grown by any technique. Preparation of GaAs/GaA1As MQW's on GaP substrates and measurement of nonlinear saturation has been completed. It was shown that this material has high cw saturation intensity and, if used in a nonlinear Fabry-Perot, would be useful only in pulsed experiments. The material looks ideal for hybrid devices. GRA

N88-25338# Naval Ocean Systems Center, San Diego, Calif.
PLANAR FULLY ION-IMPLANTED HIGH POWER InP MISFETs Professional Paper, period ending Aug. 1987
L. J. Messick, R. Nguyen, and D. A. Collins Dec. 1987 11 p
(AD-A191589) Avail: NTIS HC A03/MF A01 CSCL 09A

Planar fully ion-implanted InP power MISFETs using SiO2 as the gate insulator have been fabricated. At 9.7 GHz CW with 3.7 dB gain 800 micron gate width devices exhibited power per unit gate width as high as 2.9 W/mm, more than twice the highest value ever reported for GaAs FETs. For comparison at the same CW frequency and 4 dB gain our 1 mm gate width mesa-type epitaxial InP power MISFETs have demonstrated power per unit gate width as high as 4.5 W/mm, more than three times the highest GaAs value. GRA

N88-25339# American Society for Engineering Education, Washington, D. C.
[RESEARCH WORK COMPLETED AT THE NAVAL SURFACE WARFARE CENTER SOLID STATE GROUP OF THE RADIATION DIVISION] Final Technical Report, period ending 1 Nov. 1987
Joseph P. Teter 9 Feb. 1988 28 p
(Contract N00014-83-D-0689)
(AD-A191627) Avail: NTIS HC A03/MF A01 CSCL 20C

The two man-years worth of my Post-doctoral appointment to the Solid State group of the Radiation Division of NSWC has produced major advances in the understanding of the phenomenon of magnetostriction as evidenced by the 4 papers published in scientific journals. An appendix lists these papers plus 1 other paper that has been published in collaboration with numerous scientists at various institutions such as the Applied Physics Lab of the John Hopkins University and the University of Salford in England. There are three papers yet to be written for which I have contributed small portions of experimental datas. The two most recent papers listed in the appendix have not been included in previous quarterly reports and are, therefore, attached to this final report for completeness. GRA

N88-25340# Naval Ocean Systems Center, San Diego, Calif.
RECENT DATA ON Si:As IMPURITY BAND CONDUCTION MULTIPLEXED ARRAYS Report, period ending Mar. 1987
J. D. Merriam and R. K. Bentley Nov. 1987 6 p
(AD-A191752) Avail: NTIS HC A02/MF A01 CSCL 20L

Data is presented from recent measurements of two Si:As impurity band conduction multiplexed arrays. The devices were produced by different manufacturers. The devices were measured at a temperature of 12 K, and at a background of 1.5x10 to the 12th power Photons/sec. sq cm. Both devices show high responsivity and excellent uniformity. The development of impurity band conduction detectors offers the opportunity for high responsivity, uniform, multiplexed arrays for imaging applications. This paper presents data from recent measurements on two Si:As impurity band conduction multiplexed arrays. The arrays were manufactured by Hughes Aircraft Company and Rockwell International. Both arrays were operated at a background photon flux density of 1.5x10 to the 12th power Photons/sec. sq cm. and at a temperature of 12 K. The spectral response curves of the two devices are presented. Both devices exhibit a spectral peak near 24 micrometers. Note the extended long wavelength response of these two detectors. This long wavelength response is bias voltage dependent, the response extending the longer wavelengths at higher bias voltages. These spectral data were obtained at a bias of 1.5 volts. GRA

N88-25341# Office of the Under Secretary of Defense (Acquisitions), Washington, D.C. Research and Advanced Technology.
DEPARTMENT OF DEFENSE STATEMENT ON THE X-RAY LITHOGRAPHY PROGRAM TO THE RESEARCH AND DEVELOPMENT SUBCOMMITTEE OF THE HOUSE ARMED SERVICES COMMITTEE OF 100TH CONGRESS, SECOND SESSION
E. D. Maynard, Jr. 17 Mar. 1988 7 p
(AD-A191854) Avail: NTIS HC A02/MF A01 CSCL 09A

The Department has a broad and necessarily diverse program in semiconductor science and technology. The three principal goals of that effort are: Reduce the gap between commercial integrated circuit usage and its deployment in military systems, assure a healthy on-shore industrial base to support our defense needs, enhance the producibility of specialized military semiconductor products. The major effort to achieve the first of these objectives is the Very High Speed Integrated Circuits (VHSIC) Program which is nearing completion. The Microwave/millimeter wave Monolithic Integrated Circuit (MIMIC) program has just completed a study program to define the product mix needed to meet military system requirements for radar, electronic warfare, smart weapons and telecommunications. We are bringing together the system requirements of all DoD with the device fabrication and product delivery capabilities of industry in an Infrared Focal Plane Array (IRFPA) program. The goal of the Software Initiative is to enhance our warfighting capability through development of efficient software generation technology and products plus the creation of a technology infusion infrastructure to couple the technology and products to system applications. The X-Ray Lithography Program will begin to establish the industrial base which will be required to sustain U.S. leadership in the semiconductor industry for the late 1990s. GRA

N88-25342# Army Lab. Command, Watertown, Mass. Material Technology Lab.
CHARACTERIZATION OF YTTRIUM ALUMINUM GARNET/YAG/USING 14 MeV NEUTRON ACTIVATION
Forrest Burns, Michaeline F. Chen, and Jaroslav L. Caslavsky Dec. 1987 21 p
(AD-A191925; MTL-TR-87-2) Avail: NTIS HC A03/MF A01 CSCL 07B

A non-destructive method for the analysis of yttrium, aluminum and oxygen in Yttrium Aluminum Garnet /YAG/ by 14 MeV neutron activation analysis had been developed and evaluated. The fast neutron induces primarily /n,2n/, /n,p/ or /n, alpha/ reactions with yttrium, aluminum, and oxygen to produce isotopes with measurable characteristic gamma-ray spectra. Concentrations of Y, Al and O were determined on the basis of calibrated nuclear decay emission spectra recorded on selected standards. After each analysis the crystal was returned to the furnace for further adjustments of the growth parameters, and any resultant elemental variations were observed in the next analysis. The accuracy of this method was determined by repeated analyses with various YAG crystals from a series of separate furnace runs. GRA

N88-25343# Advanced Research and Applications Corp., Sunnyvale, Calif.
THE INSPECTION OF METALLURGICAL BOUNDS IN ELECTRONIC SYSTEMS

Jerel A. Smith and James H. Stanley Feb. 1988 3 p
(Contract N00014-86-C-0860)
(AD-A192064) Avail: NTIS HC A02/MF A01 CSCL 12B

Electronic subassemblies are getting more and more difficult to inspect. Integrated Circuits (IC's) are being designed with more input/output (I/O) connections spaced closer together. These new designs make the solder-joint inspections more difficult at the same time that joints are being relied upon to accommodate more demanding mechanical requirements. The higher I/O pin count has forced the adoption of Surface Mount Technology (SMT) which places higher demands on the mechanical strength of the solder bonds due to the shorter and less compliant leads, or the elimination of the leads altogether, on the IC package. In addition the high I/O count is leading to IC package designs with pins or pads in the interior as well as around the package perimeter. There is no inspection technique that is currently capable of inspecting solder joint integrity beneath an IC package. Functional testing of an assembly can detect shorts or opens but cannot detect the many flaws that can cause premature failure of the solder bonds. GRA

N88-25344# Illinois Inst. of Tech., Chicago.
SPECTROSCOPY AND ENERGY TRANSFER KINETICS OF THE INTERHALOGENS Final Report, 18 Jun. 1985 - 14 Nov. 1987
Michael C. Heaven 8 Feb. 1988 41 p
(Grant AF-AFOSR-0210-85)
(AD-A192103; AFOSR-88-0128TR) Avail: NTIS HC A03/MF A01 CSCL 07B

The electronic spectra and energy transfer pathways of matrix isolated iodine monofluride and diatomic iodine have been investigated. Laser excitation of matrix isolated IF revealed the presence of three electronic states which had not been observed previously. The lowest energy state was identified as A(3)pi(2). Determination of the position and lifetime of this state has provided a means for assessing its role in the chemical excitation of the B state. The higher energy states have been tentatively assigned to a doubly excited electronic configuration. The I2 A yields X system was studied in Argon, Krypton, and Xenon matrices. Analyses of the emission spectra showed that previous vibrational assignments were in error. The A state lifetime was found to be 50 + or - 15 microseconds in all three matrix hosts. Continuous wave excitation and wavelength-resolved flourescence techniques were used to study the self-quenching and energy transfer kinetics of diatomic bromine (B). GRA

N88-25345# Harry Diamond Labs., Adelphi, Md.
DEVELOPMENT OF THE FIELD-INDUCED ELECTRON INJECTION AND IMPACT IONIZATION (F4I) TECHNIQUE FOR RADIATION HARDNESS TESTING OF MOS (METAL-OXIDE-SEMICONDUCTOR) GATE INSULATORS Final Report, 1980 - 1983
Harold E. Boesch, Jr. Mar. 1988 59 p Sponsored by Defense Nuclear Agency, Washington, D.C.
(AD-A192114; HDL-TR-2137) Avail: NTIS HC A04/MF A01 CSCL 09A

Results are presented of an effort to develop an all-electrical means for simulating the effects of ionizing radiation on the radiation-sensitive oxide layers of metal-oxide-semiconductor (MOS) microelectronic devices. The report describes the field-induced electron injection and impact ionization (F4I) technique, its successful demonstration, and successful correlation of F4I test results with conventional radiation hardness tests using an ionizing radiation source (60Co). Also described are the development and operation of a microcomputer-controlled test system that permits semiautomatic application of the F4I test to circuit test structures. GRA

N88-25346*# Westinghouse Research and Development Center, Pittsburgh, Pa.
ADVANCED DEVELOPMENT OF DOUBLE-INJECTION, DEEP-IMPURITY SEMICONDUCTOR SWITCHES Final Report, 13 Jun. 1985 - 15 Dec. 1987
M. H. Hanes 7 Dec. 1987 143 p
(Contract NAS3-24637)
(NASA-CR-182118; NAS 1.26:182118) Avail: NTIS HC A07/MF A01 CSCL 20L

Deep-impurity, double-injection devices, commonly refered to as (DI) squared devices, represent a class of semiconductor switches possessing a very high degree of tolerance to electron and neutron irradiation and to elevated temperature operation. These properties have caused them to be considered as attractive candidates for space power applications. The design, fabrication, and testing of several varieties of (DI) squared devices intended for power switching are described. All of these designs were based upon gold-doped silicon material. Test results, along with results of computer simulations of device operation, other calculations based upon the assumed mode of operation of (DI) squared devices, and empirical information regarding power semiconductor device operation and limitations, have led to the conculsion that these devices are not well suited to high-power applications. When operated in power circuitry configurations, they exhibit high-power losses in both the off-state and on-state modes. These losses are caused by phenomena inherent to the physics and material of the devices and cannot be much reduced by device design optimizations. The (DI) squared technology may, however, find application in low-power functions such as sensing, logic, and memory, when tolerance to radiation and temperature are desirable (especially is device performance is improved by incorporation of deep-level impurities other than gold. Author

N88-25347 New South Wales Univ., Kensington (Australia).
DETERMINATION OF DOPING PROFILES IN SILICON FROM RESISTIVITY MEASUREMENTS VIA THE FOUR-POINT PROBE IN COMBINATION WITH LAYER STRIPPINGS VIA ANODIC OXIDATION M.S. Thesis Abstract Only
Brian H. Lis Aug. 1987 124 p
Avail: Issuing Activity

The performance of resistivity measurements using the four-point probe in combination with layer strippings using anodic oxidation, is a well-known and useful method for profiling doped layers of silicon. The method is implemented and critically assessed. This method uses a technique for forming silicon dioxide on the surface of silicon wafers at room temperature. By performing four-point probe resistivity measurements both before and after the process, the differential resistivity is calculated and converted to an electrically active dopant concentration for the average depth of the layer removed. Repeating this process until the opposite conductivity type silicon is reached, yields the series of points quantifying the dopant concentration at specific depths into the silicon. Anodic oxidation is used to form the silicon dioxide. This technique is discussed and a critical review of the literature presented. Precautions and general considerations for measuring resistivity via the four-point probe are also given. An error analysis is undertaken to determine the source of some of the observed experimental error. The project report details all aspects of the method, offers techniques for improved accuracy and repeatability, looks into surface effects, critiques the method, and explores further areas for work. The experimental doping profiles obtained are compared with profiles obtained from four other methods (two experimental and two theoretical). Author

N88-25348# California Univ., Berkeley. Lawrence Berkeley Lab. Materials and Chemical Sciences Div.
VACANCY ORDERING IN THE BASAL PLANE OF YBa2Cu3O(SUB)z
L. T. Wille, A. Berera, D. deFontaine, and S. C. Moss (Houston Univ., Tex.) Nov. 1987 5 p Presented at the Fall Meeting of the Materials Research Society, Boston, Mass., 30 Nov. 1987
(Contract DE-AC03-76SF-00098)
(DE88-004572; LBL-24263; CONF-871124-94) Avail: NTIS HC A02/MF A01

The ordering in the Cu-O basal plane of the high T sub c superconductor YBa sub 2 Cu sub 3 O sub z is investigated. Asymmetric pairwise interactions between nearest and next nearest neighbors are assumed. Ordering instabilities in two-dimensional

k-space are mapped out as a function of the interactions and the ordered ground state superstructures consisting of occupied and empty oxygen sites are determined. A temperature-composition phase diagram is calculated by means of the Cluster Variation Method. The thermodynamic behavior of the superconducting compound is discussed in the light of these results. DOE

N88-25349# Los Alamos National Lab., N. Mex.
INTRODUCTION TO LATTICE GAUGE THEORY
R. Gupta 1987 47 p Presented at the Theoretical Advanced Summer Institute, Santa Fe, N. Mex., 6 Jul. 1987
(Contract W-7405-eng-36)
(DE88-006073; LA-UR-88-629; CONF-8707141-5) Avail: NTIS HC A03/MF A01

The lattice formulation of Quantum Field Theory (QFT) can be exploited in many ways. We can derive the lattice Feynman rules and carry out weak coupling perturbation expansions. The lattice then serves as a manifestly gauge invariant regularization scheme, albeit one that is more complicated than standard continuum schemes. Strong coupling expansions: these give us useful qualitative information, but unfortunately no hard numbers. The lattice theory is amenable to numerical simulations by which one calculates the long distance properties of a strongly interacting theory from first principles. The observables are measured as a function of the bare coupling g and a gauge invariant cut-off approx. = 1/alpha, where alpha is the lattice spacing. The continuum (physical) behavior is recovered in the limit alpha yields 0, at which point the lattice artifacts go to zero. This is the more powerful use of lattice formulation, so in these lectures the author focuses on setting up the theory for the purpose of numerical simulations to get hard numbers. The numerical techniques used in Lattice Gauge Theories have their roots in statistical mechanics, so it is important to develop an intuition for the interconnection between quantum mechanics and statistical mechanics. DOE

N88-25350# California Univ., Berkeley. Lawrence Berkeley Lab.
THE MORPHOLOGICAL STABILITY OF CONTINUOUS INTERGRANULAR PHASES: THERMODYNAMIC CONSIDERATIONS Ph.D. Thesis
W. C. Carter Dec. 1987 46 p
(Contract DE-AC03-76SF-00098)
(DE88-006328; LBL-24695) Avail: NTIS HC A03/MF A01

A complete analysis of morphological instability has two components: a thermodynamic analysis identifying the smallest wavelength (infinitesimal amplitude) perturbation for which the amplitude will increase, and a kinetic analysis determining the particular wavelength for which perturbation growth is most rapid. A thermodynamic analysis for nonfaceting surfaces with single-valued interfacial tensions is presented. Possible modifications resulting from surface faceting and the implications of the analysis to the kinetics of phase breakdown have been discussed elsewhere. DOE

N88-25351# Pacific Northwest Labs., Richland, Wash.
MOLECULAR CHARACTERIZATION OF STRUCTURE AND BONDING IN THIN FILM MATERIALS
G. J. Exarhos Dec. 1987 17 p Presented at the National Meeting of the Society of Optoelectronics and Laser Applications in Science and Engineering, Los Angeles, Calif., 10 Jan. 1988
(Contract DE-AC06-76RL-01830)
(DE88-006811; PNL-SA-15049; CONF-880110-23) Avail: NTIS HC A03/MF A01

The application of Raman spectroscopy to the analysis of dielectric films with respect to phase composition and homogeneity has been reported during the past several years. Interfacial strain at the film-substrate interface, which influences chemical bonding, also perturbs the vibrational spectrum and can be quantified from measured frequency shifts. Recent work has shown that this inelastic light scattering technique can be used as an in situ probe of chemical bonding during film deposition and under conditions where the film undergoes catastrophic degradation caused by high energy particle or high pulse energy laser irradiation. Examples are presented in this review which demonstrate the utility of this technique for understanding molecular structural changes which result during sol-gel or plasma processing of films. Real-time measurements of thin films subjected to high temperature and pressure environments also emphasized. DOE

N88-25352# Helsinki Univ. of Technology, Espoo (Finland). Dept. of Technical Physics.
INFLUENCE OF ALTERNATING MAGNETIC FIELDS ON Zn-67 MOESSBAUER RESONANCE IN ZnO
E. Ikonen, J. Hietaniemi, and T. Katila 1987 44 p
(PB88-186432; TKK-F-A618; ISBN-951-754-284-4) Avail: NTIS HC A03/MF A01 CSCL 20L

A phase-modulation theory was developed to describe the influence of alternating magnetic fields on the Mossbauer resonance of (67)Zn in ZnO. Results of the low- and high-frequency Zeeman scanning experiments were in accordance with the theoretical predictions. The transient oscillations observed were used to evaluate the amplitude of phase modulation and the gyromagnetic ratio of the 93-keV state of (67)Zn. The advantages of the time-domain approach combined with the use of the high-resolution resonance of (67)Zn were discussed. GRA

N88-25353*# SRI International Corp., Menlo Park, Calif. Molecular Physics Dept.
TRANSITION PROBABILITIES IN OH A 2 SIGMA + - X 2 PI I: BANDS WITH V PRIME = 0 AND 1, V DOUBLE PRIME = 0 TO 4
Richard A. Copeland, Jay B. Jeffries, and David R. Crosley 4 Nov. 1986 17 p Submitted for publication
(Contract NAS1-16956)
(NASA-CR-182946; NAS 1.26:182946; MP-86-234) Avail: NTIS HC A03/MF A01 CSCL 20L

Experimental results for relative vibrational band transition probabilities for v prime = 0 and 1, and v double prime = 0 to 4 in the A-X electronic system of OH are presented. The measurements, part of a larger set involving v prime = 0 to 4 and v double prime = 0 to 6, were made using spectrally dispersed laser-induced fluorescence (LIF) in the burnt gases of a flame. These Einstein coefficients will be useful in dynamics experiments for quantitative LIF determinations of OH radical concentrations in high v double prime. Author

N88-25354*# National Aeronautics and Space Administration. Marshall Space Flight Center, Huntsville, Ala.
ELECTRONIC CONTROLLER FOR RECIPROCATING ROTARY CRYSTALLIZER
Roger L. Kroes, Donald A. Reiss, and Howard B. Hester [1988] 9 p Submitted for publication
(NASA-TM-101140; NAS 1.15:101140) Avail: NTIS HC A02/MF A01 CSCL 20L

An electronic controller for a reciprocating rotary crystallizer is described. The heart of this system is the electronic timer circuit. A schematic along with a detailed description of its operation is given. Author

N88-25355*# National Aeronautics and Space Administration. Langley Research Center, Hampton, Va.
METHOD OF FORMING A MULTIPLE LAYER DIELECTRIC AND A HOT FILM SENSOR THEREWITH Patent Application
Purnell Hopson, Jr., inventor (to NASA) and Sang Q. Tran, inventor (to NASA) 1 Apr. 1988 18 p
(NASA-Case-LAR-13678-1; NAS 1.71:LAR-13678-1; US-Patent-Appl-SN-176547) Avail: NTIS HC A03/MF A01 CSCL 20L

The invention is a method of forming a multiple layer dielectric for use in a hot-film laminar separation sensor. The multiple layer dielectric substrate is formed by depositing a first layer of a thermoelastic polymer such as on an electrically conductive substrate such as the metal surface of a model to be tested under cryogenic conditions and high Reynolds numbers. Next, a second dielectric layer of fused silica is formed on the first dielectric layer of thermoplastic polymer. A resistive metal film is deposited

on selected areas of the multiple layer dielectric substrate to form one or more hot-film sensor elements to which aluminum electrical circuits deposited upon the multiple layered dielectric substrate are connected. NASA

N88-25356*# National Aeronautics and Space Administration. Marshall Space Flight Center, Huntsville, Ala.
HANGING DROP CRYSTAL GROWTH APPARATUS AND METHOD Patent Application
Daniel C. Carter, inventor (to NASA) and Robbie Smith, inventor (to NASA) (Tennessee Scientific Glass Co.) 23 Mar. 1988 20 p
(NASA-Case-MFS-28206-1-SB; NAS 1.71:MFS-28206-1-SB; US-Patent-Appl-SN-172101) Avail: NTIS HC A03/MF A01 CSCL 20B

This invention relates generally to hanging drop crystal growth devices and methods, and more particularly to such a device wherein the drop containing protein to be crystallized is exposed to vapor from a flow of control fluid, with this control fluid having a vapor pressure which varies as solvent is drawn from the drop. A hanging drop apparatus is constructed having a cylindrical enclosure, with a wicking element or disc constructed of sintered glass and being mounted in an upper portion thereof. A well or recess is cut into an upper side of the disc. A cover slip or plate having a protein drop disposed thereon is sealably positioned on the disc, with the drop being positioned in the well. A flow of control fluid is generated by a programmable gradient former, with this flow being coupled to the disc. The vapor pressure of the control fluid is initially selected to be considerably lower than that of the drop, causing solvent in the drop to readily evaporate. As evaporation progresses, the vapor pressure of the control fluid is adjusted to slow the rate of evaporation from the drop, allowing a slow approach to the critical supersaturation point of the protein to be crystallized. The novelty of this invention particularly lies in exposing the drop to a control fluid having a variable pressure. Further novelty lies in the particular apparatuses and methods by which this is accomplished. NASA

N88-25357*# National Aeronautics and Space Administration. Marshall Space Flight Center, Huntsville, Ala.
CRYSTAL GROWTH APPARATUS Patent Application
Fred Herrmann, inventor (to NASA) and Blair Herren, inventor (to NASA) 29 Feb. 1988 17 p
(NASA-Case-MFS-28182-1; NAS 1.71:MFS-28182-1; US-Patent-Appl-SN-161681) Avail: NTIS HC A03/MF A01 CSCL 20L

This invention relates generally to crystal growth devices, and more particularly to a device in which protein crystals are grown in a hanging drop. The drop is suspended from a surface positioned in the interior of an enclosure which is sealably coupled via a valve to a vessel containing solvent used in the drop. A second opening in the enclosure is coupled via a valve to a vessel containing a selected desiccant material. The valve may be fully or partially opened to add a selected quantity of solvent in a vapor phase to the drop, and the valve may be fully or partially opened to cause a selected quantity of solvent to evaporate from the drop. The process is monitored by a camera, and in conjunction with a graduated pattern superimposed over the drop, relative volumes of the drop are determined. Alternately, the process may be automated by using a computer coupled to servo motors, which in turn are coupled to and operate a cap and valves, respectively. The computer is responsive to a detection device which detects changes of light passing through the drop from the light source. NASA

N88-25358*# National Aeronautics and Space Administration. Pasadena Office, Calif.
IMPROVED PROPERTIES OF SiGe/GaP ALLOYS Patent Application
Jan W. VanderSande, inventor (to NASA), Charles Wood, inventor (to NASA), and Susan L. Draper, inventor (to NASA) (Jet Propulsion Lab., California Inst. of Tech., Pasadena.) 20 Apr. 1988 16 p Prepared in cooperation with Jet Propulsion Lab., California Inst. of Tech., Pasadena.
(Contract NAS7-918)
(NASA-Case-NPO-17259-1-CU; NAS 1.71:NPO-17259-1-CU; US-Patent-Appl-SN-184234) Avail: NTIS HC A03/MF A01 CSCL 20L

The thermoelectric conversion efficiency of a GaP doped SiGe alloy is improved about 30 percent by annealing the alloy at a temperature above the melting point of the alloy, preferably stepwise from 1200 C to 1275 C in air to form large grains having a size over 50 microns and to form a GeGaP rich phase and a silicon rich phase containing SiP and SiO2 particles. NASA

N88-25359# Oak Ridge National Lab., Tenn.
QUENCH DETECTION BY FLUID DYNAMIC MEANS IN CABLE-IN-CONDUIT SUPERCONDUCTORS
L. Dresner Jun. 1987 5 p Presented at the Cryogenic Engineering Conference, St. Charles, Ill., 14 Jun. 1987
(Contract DE-AC05-84OR-21400)
(DE88-007269; CONF-8706125-27) Avail: NTIS HC A02

The tight confinement of the helium in cable-in-conduit superconductors creates protection problems because of the substantial pressure rise that can occur during a quench. But the same pressure rise offers the useful possibility of a non-electrical means of detecting incipient quenches by monitoring the outflow from the various hydraulic paths of the magnet. If the method is to work, the signal must be large enough to be detected unambiguously at an early enough time, and the signal must not depend too strongly on the length, Joule power density, or rate of growth of the initial normal zone (because these things are not entirely within our control). This paper explores by calculation the degree to which these conditions can be met. The Westinghouse coil for the Large Coil Task (LCT) is used as the basis for illustrative examples. DOE

N88-25360# Oak Ridge National Lab., Tenn.
GROUND STATE PROPERTIES AND ELECTRONIC STRUCTURE OF HIGH T SUB c SUPERCONDUCTORS
G. M. Stocks, W. M. Temmerman, Z. Szotek, G. Y. Guo, and P. J. Durham 1988 3 p Presented at the International Conference on High Temperature Superconductors and Materials and Mechanisms of Superconductivity, Interlaken, Switzerland, 29 Feb. 1988 Prepared in cooperation with Daresbury Nuclear Physics Lab., United Kingdom
(Contract DE-AC05-84OR-21400)
(DE88-007485; CONF-880206-3) Avail: NTIS HC A02/MF A01

We report the results of calculations of the ground state properties (equibrium volume, bulk modulus and antiferromagnetism) and the electronic structure of a number of high T sub c superconductors and related materials. The calculations are based on the local density approximation and were performed using the ASA-LMTO method. DOE

N88-25361# Sandia National Labs., Albuquerque, N. Mex.
METASTABILITY IN SiGe/Si STRAINED-LAYER STRUCTURES
B. W. Dodson 1988 17 p Presented at the Spring Meeting of the Materials Research Society, Reno, Nev., 4 Apr. 1988
(Contract DE-AC04-76DP-00789)
(DE88-007603; SAND-88-0033C; CONF-880408-5) Avail: NTIS HC A03/MF A01

The physics governing growth and stability properties in SiGe/Si strained-layer structures is reviewed. The role of metastability in crystal growth is outlined. Experimental data on stability limits and rates of strain relaxation are examined. It is concluded that essentially all observations on relaxation of semiconductor strained-layer structures can be explained by standard models of plastic deformation adapted to the special conditions controlling dislocation dynamics in these structures. DOE

N88-25362# California Univ., Berkeley. Lawrence Berkeley Lab.
ON THE USE OF CONVERGENT BEAM ELECTRON DIFFRACTION FOR IDENTIFICATION OF ANTIPHASE BOUNDARIES IN GaAs GROWN ON Si

Z. Liliental-Weber, L. Parechanian-Allen, and J. Washburn Jan. 1988 13 p Presented at the Arizona State University Winter Workshop on Electron Diffraction and Channeling At Kilovolt Energies, Wickenburg, Ariz., 11 Jan. 1988 Prepared in cooperation with California Univ., Berkeley and Kopin Corp., Taunton, Mass.
(Contract DE-AC03-76SF-00098)
(DE88-008220; LBL-24749; CONF-880174-1) Avail: NTIS HC A03/MF A01

This study shows that dynamical coupling effects in convergent beam electron diffraction (CBED) patterns can be unambiguously used to detect antiphase boundaries (APBs). A high density of APBs can be present in GaAs grown by MOCVD (metalorganic chemical vapor deposition) on Si (100) surfaces. APB formation is promoted by surface contamination and irregularities. APBs act as natural obstacles for the propagation of twins and stacking faults into the growing epitaxial layer. Faceting of APBs is probably connected with anisotropy of the interfacial energy of APBs. In most cases extended surface areas of APBs were observed to lie on the energetically favorable (110) planes. This observation is in agreement with earlier theoretical calculations. DOE

77 THERMODYNAMICS AND STATISTICAL PHYSICS

Includes quantum mechanics; theoretical physics; and Bose and Fermi statistics.

For related information see also *25 Inorganic and Physical Chemistry* and *34 Fluid Mechanics and Heat Transfer.*

N88-25363# Hiroshima Univ., Takehara (Japan). Research Inst. for Theoretical Physics.
INTRODUCTION TO COVARIANT FORMULATION OF SUPERSTRING (FIELD) THEORY
S. Uehara Sep. 1986 16 p
(DE87-703038; RRK-86-38) Avail: NTIS (US Sales Only) HC A03/MF A01

The present paper briefly discusses covariant formulation of superstring theories based on BRS invariance. First, the Neveu-Schwarz-Ramond (NSR) model is outlined. This model describes a string on which fermions are living. Those fermions are described by two dimensional Majorana spinors, since a string spans a two-dimensional surface, i.e., world sheet in the D-dimensional space-time. The relations between space-time bosons and fermions, super Virasoro algebra, no-ghost theorem, BRS charge and supersymmetry in the NSR model are then discussed. Another section is devoted to describing covariant (free) field theory of superstring using the first-quantized BRS charges. Discussions are presented on field theories of point particle, bosonic string and superstring, as well as space-time supersymmetry. It is concluded that field theories of closed strings including the heterotic string can be considered in similar ways. Interaction terms are constructed according to the BRS invariance of the total actions. Two kinds of them have been proposed, though the relation between them has not been clarified. Furthermore, covariant gauge fixing of interacting string field theories and, or covariant quantization have some difficulties and have not been clarified. It is also pointed out that the space-time supersymmetry would come from the two-dimensional gauge symmetries, or could be regarded as a part of the original string gauge symmetries. DOE

N88-25364# Council for Mineral Technology, Randburg (South Africa).
PHASE DIAGRAMS IN MATERIALS SCIENCE AND THE USE OF THE COMPUTER IN THEIR CALCULATION
Robert Paton Oct. 1987 42 p
(PB88-155262; MINTEK-M318; ISBN-0-86999-799-8) Avail: NTIS HC A03/MF A01 CSCL 20M

The use of the computer for the calculation of available thermodynamic data is discussed with particular reference to the FACT (Facility for the Analysis of Chemical Thermodynamics) system, an on-line scientific numeric data base located in Montreal, Canada. The calculation of the binary system nickel-titanium and of the ternary system iron-chromium-vanadium are explained. Some views are expressed concerning the usefulness of the method. GRA

N88-25365*# National Aeronautics and Space Administration. Marshall Space Flight Center, Huntsville, Ala.
INEVITABLE INFLATION IN EINSTEIN-CARTAN THEORY WITH IMPROVED ENERGY-MOMENTUM TENSOR WITH SPIN
A. J. Fennelly, James C. Bradas (Alabama Univ., Huntsville.), and Larry L. Smalley [1988] 13 p Prepared in cooperation with Army Missile Command, Redstone Arsenal, Ala. Submitted for publication
(NASA-TM-101146; NAS 1.15:101146) Avail: NTIS HC A03/MF A01 CSCL 20C

Generalized, or power-law, inflation is shown to necessarily exist for a simple, anisotropic, (Bianchi Type-1) cosmology in the Einstein-Cartan gravitational theory with the Ray-Smalley improved energy momentum tensor with spin. Formal solution of the EC field equations with the fluid equations of motion explicitly shows inflation caused by the RS spin angular kinetic energy density. Shear is not effective in preventing inflation in the ECRS model. The relation between fluid vorticity, torsion, reference axis rotation, and shear ellipsoid precession shows through clearly. Author

N88-25366# California Univ., Berkeley. Lawrence Berkeley Lab.
THE GEOMETRY OF THE VIRASORO GROUP FOR PHYSICISTS
B. Zumino Nov. 1987 19 p Presented at the NATO Advanced Studies Institute Summer School on Particle Physics, Cargese, France, 3 Aug. 1987
(Contract DE-AC03-76SF-00098)
(DE88-007374; LBL-24319; CONF-8708230-1) Avail: NTIS HC A03/MF A01

Diff(S sup 1), the group of reparametrizations of the circle, is known as the Virasoro group in string theory. Reparametrizations keeping fixed a point of the circle form the quotient space Diff(S sup 1)/S sup 1. The geometry of this space is relevant for string theory and string field theory. We describe this space as an infinite dimensional complex manifold with a Kaehler metric and compute ist Riemann tensor and its Ricci tensor. DOE

N88-25367# Hiroshima Univ., Takehara (Japan). Research Inst. for Theoretical Physics.
COMMENT ON NON-RENORMALIZATION THEOREM IN THE FOUR DIMENSIONAL SUPERSTRINGS
Jiro Soda, Naohito Nakazawa, Kenji Sakai, and Shuichi Ojima Oct. 1987 10 p
(DE88-752551; RRK-87-26) Avail: NTIS (US Sales Only) HC A02/MF A01

We discuss non-renormalization theorem in the context of the four-dimensional superstrings. We explicitly demonstrate that the graviton 3-point one-loop amplitude does not vanish in contrast to the ten-dimensional superstring theories. DOE

N88-25368# British Library Lending Div., Boston Spa (England).
CERTAIN QUESTIONS OF THERMODYNAMIC THEORY OF WEAK SOLUTIONS
D. M. Laptev [1987] 12 p Transl. into ENGLISH from Vysshikh Uchebnykh Zavedeniy Chernaya Metallurgiya (USSR), no. 10, 1987 p 9-13
Avail: British Library Lending Div., Boston Spa, United Kingdom

Questions such as the standard states and the difference and similarity of the thermodynamic properties of a component in the limiting concentration regions, the additive constants in thermodynamic expressions and their interpretation, and the activity and coefficient of activity for different standard states are examined on the basis of the thermodynamic theory of weak solutions as constructed by Gibb's method. The states of the pure component according to Raoult's law and Henry's law are introduced on the basis of the determining laws of weak solutions. Author

N88-25369 California Univ., Santa Barbara.
FROM GENERAL RELATIVITY TO THE THEORY OF SUPERSTRINGS Ph.D. Thesis
Sigurd Sannan 1987 81 p
Avail: Univ. Microfilms Order No. DA8729689

Some classical and quantum effects of Einstein's theory of gravity are investigated. Within the context of classical general relativity, the Hawking definition of mass in a Tolman-Bondi model that asymptotically approaches the open Friedmann universe is tested. An expanding universe filled with dustlike matter of zero pressure is considered. The matter distribution is spherically symmetric but nonhomogeneous. With appropriate boundary conditions, the calculation yields a finite and nonzero value for the Hawking mass, measured as a deviation from a renormalized zero mass in the unperturbed Friedmann model. These boundary conditions are more restrictive than those found for a model with gravitational radiation. The tree amplitude was next calculated for graviton-graviton scattering of the Einstein theory of gravity in D dimensions. It is shown that in ten dimensions this agrees completely with the zero-slope limit of the four particle tree amplitude given by the type-II superstring theory. When six of the spatial dimensions are compactified, it is shown that the four particle string amplitude agrees with the helicity amplitudes obtained from general relativity in four dimensions. Dissert. Abstr.

N88-25370# Idaho Univ., Moscow. Center for Applied Thermodynamic Studies.
STUDY OF DATA DISTRIBUTIONS AND FUNCTIONS FOR THE DEVELOPMENT OF THERMODYNAMIC EQUATIONS OF STATE Annual Report, Jun. 1986 - May 1987
R. T. Jacobsen, W. P. Clarke, K. D. Braven, and K. R. Bjornn Jun. 1987 85 p Sponsored by Gas Research Inst.
Chicago, Ill.
(Contract GRI-5086-260-1421)
(PB88-196365; GRI-87/0206) Avail: NTIS HC A05/MF A01 CSCL 20M

The principle objective of the project is to evaluate current techniques of data analysis and correlation used to develop wide range thermodynamic property formulations. The knowledge gained from the evaluation should provide experimenters with advice concerning the amount and type of data needed to develop an accurate model for the properties of a fluid and should provide correlators with better overall understanding of the data analysis and correlation process. Author

80 SOCIAL SCIENCES (GENERAL)

Includes educational matters.

N88-25371*# Taylor and Associates, Inc., Wrightwood, Calif.
SPACE STATION ARCHITECTURAL ELEMENTS AND ISSUES DEFINITION STUDY
T. C. Taylor, J. S. Spencer, and C. J. Rocha May 1986 78 p
(NASA Order A-16516-C)
(NASA-CR-3941; NAS 1.26:3941) Avail: NTIS HC A05/MF A01 CSCL 22B

A study was conducted to define the architectural elements and issues of the Space Station. The objective of the study was to identify those questions which require further research and suggest ways in which the research can be undertaken. The study examined five primary topics, asked salient questions and described the merits of alternative solutions. Author

N88-25372*# Anacapa Sciences, Inc., Santa Barbara, Calif.
SPACE STATION HABITABILITY RECOMMENDATIONS BASED ON A SYSTEMATIC COMPARATIVE ANALYSIS OF ANALOGOUS CONDITIONS
Jack W. Stuster Washington NASA Sep. 1986 209 p
(Contract NAS2-11690)
(NASA-CR-3943; NAS 1.26:3943) Avail: NTIS HC A10/MF A01 CSCL 06K

Conditions analogous to the proposed NASA Space Station are systematically analyzed in order to extrapolate design guidelines and recommendations concerning habitability and crew productivity. Analogous environments studied included Skylab, Sealab, Tektite, submarines, Antarctic stations and oil drilling platforms, among others. These analogues were compared and rated for size and composition of group, social organization, preparedness for mission, duration of tour, types of tasks, physical and psychological isolation, personal motivation, perceived risk, and quality of habitat and life support conditions. One-hundred design recommendations concerning, sleep, clothing, exercise, medical support, personal hygiene, food preparation, group interaction, habitat aesthetics, outside communications, recreational opportunities, privacy and personal space, waste disposal, onboard training, simulation and task preparation, and behavioral and physiological requirements associated with a microgravity environment, are provided. Author

81 ADMINISTRATION AND MANAGEMENT

Includes management planning and research.

N88-25373# General Accounting Office, Washington, D. C. Accounting and Financial Management Div.
FINANCIAL REPORTING: NASA (NATIONAL AERONAUTICS AND SPACE ADMINISTRATION) CAN IMPROVE COMPLIANCE WITH GAO (GENERAL ACCOUNTING OFFICE) STANDARDS AND TREASURY REQUIREMENTS
Feb. 1988 18 p
(PB88-172523; GAO/AFMD-88-21) Avail: NTIS HC A03/MF A01 CSCL 05A

The results are presented of the authors review of the National Aeronautics and Space Administration's preparation of its fiscal year 1986 Report on Financial Position, commonly referred to as a balance sheet. The review, one segment of a government wide effort, was performed to determine the extent of compliance with the General Accounting Office's and the Department of the Treasury's annual financial reporting requirements. Author

N88-25374# Pentagon Library, Washington, D.C.
MANAGEMENT AND THE EXECUTIVE Final Report, 1 Jan. 1982 - 31 Dec. 1987
1 Jan. 1988 44 p
(AD-A190778) Avail: NTIS HC A03/MF A01 CSCL 05A

This bibliography lists books and periodical articles covering such topics as personnel management, corporate planning, decision-making, executive training, leadership, management information systems, and organizational behavior. In addition, it highlights some special interest areas: women executives, chief executive officers, job stress, and ethics. An index of management topics is appended to assist readers in finding related items. GRA

N88-25375# Northwest Regional Educational Lab., Portland, Oreg.
SELECTION AND EFFECTS OF CHANNELS IN DISTRIBUTED COMMUNICATION AND DECISION MAKING TASKS: A THEORETICAL REVIEW AND A PROPOSED RESEARCH PARADIGM Interim Report, May 1986 - May 1987
Stephen M. Reder and Nancy F. Conklin Feb. 1988 43 p
(Contract MDA903-86-C-0171; DA Proj. 2Q1-61102-B-74-F)
(AD-A191807; ARI-RN-88-04) Avail: NTIS HC A03/MF A01 CSCL 05A

This research note examines the relationships between the communication patterns of decision groups and the nature and results of their decision processes. It looks at the selection of particular channels and channel effects, as well. A review of research indicates that no satisfactory theoretical framework has yet been developed which accounts for the often strategic and tactical nature of communication channel selection. An initial theory is outlined, establishing quantifiable relationships among causally linked sets of variables: 1) characteristics of the decision group (size, structure, and spatial dispersion), 2) characteristics of the

decision task (nature of the decision, perceived organizational significance, time available, and available communication channels), 3) channel selection(s) made by the group, 4) structural and content characteristics of the messages produced, 5) decisions reached, and 6) perceived characteristics of the decision process. GRA

N88-25376# Office of the Director of Defense Research and Engineering, Washington, D. C.
DEPARTMENT OF DEFENSE STATEMENT ON THE TECHNOLOGY BASE TO THE SUBCOMMITTEE ON DEFENSE INDUSTRY AND TECHNOLOGY OF THE COMMITTEE ON ARMED SERVICES, UNITED STATES SENATE, 100TH CONGRESS, SECOND SESSION
Robert C. Duncan 18 Mar. 1988 19 p
(AD-A191839) Avail: NTIS HC A03/MF A01 CSCL 05A

The prime functions is to ensure coordination of technology programs of the Services and the Defense Agencies. Every scientist, engineer and R&D manager has, as part of his normal duties, the responsibility for assuring that his work is in harmony with other work in his field or technical interest area. The data bands, documentation centers, analysis centers, professional societies and literature are tools to assist individuals and organizations in accomplishing this important task. Within DDR&E, special procedures are undertaken to enhance technology coordination. The second important subject addressed in the summer study was improving the transition of technology from the laboratory to new or existing weapon systems. GRA

N88-25377# Office of the Director of Defense Research and Engineering, Washington, D. C.
DEPARTMENT OF DEFENSE STATEMENT ON DEFENSE AGENCY RESEARCH AND DEVELOPMENT TO THE SUBCOMMITTEE ON DEFENSE OF THE COMMITTEE ON APPROPRIATIONS, UNITED STATES HOUSE OF REPRESENTATIVES, 100TH CONGRESS, SECOND SESSION
Robert C. Duncan 22 Mar. 1988 15 p
(AD-A191840) Avail: NTIS HC A03/MF A01 CSCL 05A

As requested by the Committee of Appropriations of the U.S. House of Representatives, the Director of Defense Research and Engineering reported on the functions and accomplishments of DDR&E. Topics covered include: Organizational Effectiveness; Balanced Technology Initiative; Air Defense Initiative; Semiconductor Manufacturing; Software Engineering; Microwave and Millimeter Wave Monolithic Integrated Circuits; Joint Remotely Piloted Vehicles; Budget Summary. GRA

N88-25378# Office of the Director of Defense Research and Engineering, Washington, D. C.
DEPARTMENT OF DEFENSE STATEMENT ON THE BALANCED TECHNOLOGY INITIATIVE TO THE COMMITTEE ON ARMED SERVICES, UNITED STATES SENATE, 100TH CONGRESS, SECOND SESSION
Robert C. Duncan 11 Apr. 1988 42 p
(AD-A191841) Avail: NTIS HC A03/MF A01 CSCL 05A

Strong support is stated for the Balanced Technology Initiative and its objectives. The program has special importance in view of the recent INF Treaty and the growing need to improve the defensive capabilities of US and Allied conventional forces in Europe. The technology development and demonstration program implemented is a sound and responsive one that properly addresses both near-term and longer-term conventional defense needs. Continuing effective development and management of the program will be provided to assure that its objectives and full potential will be realized. Maintaining a strong and balanced defense program is of critical importance for assuring the national security of the United States and the well being of our Allies now and into the future. Program categories: Smart Weapons Technology; RSTA/BMC3 Technology; Armor/Anti-Armor Technology; High Power Microwaves; and Special Technology Opportunities. GRA

N88-25379# Department of Defense, Washington, D. C.
THE DEPARTMENT OF DEFENSE REPORT ON THE MERIT REVIEW PROCESS FOR COMPETITIVE SELECTION OF UNIVERSITY RESEARCH PROJECTS AND AN ANALYSIS OF THE POTENTIAL FOR EXPANDING THE GEOGRAPHIC DISTRIBUTION OF RESEARCH FOR THE COMMITTEES ON APPROPRIATIONS, UNITED STATES CONGRESS
Apr. 1987 33 p
(AD-A191842) Avail: NTIS HC A03/MF A01 CSCL 05A

This report responds to the Committee on Conference request, DoD Appropriations Act, 1987 as set forth in the following. With the establishment of the University Research Initiative in fiscal year 1986 and rising funds for the Strategic Defense Initiative, the Department of Defense's investment in university-based research is increasing. Consequently, the appropriations Committees need to ensure that the peer review process for the allocation of university funding is working effectively, and that mechanisms are in place to broaden the base of DoD university research commensurate with these increasing resources. Therefore, the conferees direct the Department of Defense to submit a report to the Appropriations Committees by March 1, 1987, which (1) explains in detail the current peer review process in a step-by-step fashion; (2) explains current participants in this process, including peer review panels, boards, or conferences, and how such peer reviewers are evaluated and chosen; and (3) an analysis of the potential for expanding the research base into geographical areas which at the present time receive little defense-related university funding. This report explains DoD's merit review process and the participants in that process and also describes the current distribution of DoD research funding to universities and the potential for geographic expansion. GRA

N88-25380# Office of the Deputy Under Secretary of Defense for Research and Development (Research and Advanced Technology), Washington, D.C.
THE FY 1989 DEPARTMENT OF DEFENSE STATEMENT ON THE SCIENCE AND TECHNOLOGY PROGRAM TO 100TH CONGRESS, SECOND SESSION
George P. Millburn Mar. 1988 37 p
(AD-A191843) Avail: NTIS HC A03/MF A01 CSCL 05B

The military strength of the nation is often evaluated in the number of tanks, ships, aircraft and personnel that can be brought to bear on national security objectives. Certainly these are factors that must be present if our military goals are to be achieved. However, sheer dependence upon numbers is a difficult strategy for the US to pursue. The build-up of Soviet nuclear and conventional forces places great pressure on the US and its Allies and threatens international security. This build-up is based in large measure on fielding military forces that vastly outnumber their opponents. The nature of our society and our economy precludes matching the Soviets tank-for-tank, aircraft-for-aircraft, satellite-for-satellite or man-for-man to provide a viable deterrent to their global ambitions. In order to preserve our common defense and our future security, prudent improvements must be made to our forces as further threats to our national posture and readiness arise. GRA

N88-25381# Massachusetts Inst. of Tech., Cambridge. Lab. for Information and Decision Systems.
MODELING AND EVALUATION OF VARIABLE STRUCTURE ORGANIZATIONS M.S. Thesis
Jean-Marc Monguillet Dec. 1987 150 p
(Contract N00014-84-K-0519)
(AD-A191947; LIDS-TH-1730) Avail: NTIS HC A07/MF A01 CSCL 05A

Variable structure organizations are defined as decision making organizations in which the pattern of interactions between decision makers can vary. A quantitative methodology is developed to evaluate their effectiveness in the achievement of their mission. A model of these organizations using Predicate Transition Nets is presented, in which the decision makers are treated as an ordinary resource. The decision makers are modeled by tokens that move from one pattern of interactions to the other, depending on designer

defined protocols. An example of a three member variable structure organization carrying out an air defense task is presented. In that organization, the headquarters sets the pattern of interactions of the field units according to the characteristics of the incoming signals. Ranges of mission requirements are computed in which this variable organization is the most effective, when compared to corresponding organizations with a fixed structure of interactions. GRA

82 DOCUMENTATION AND INFORMATION SCIENCE

Includes information management; information storage and retrieval technology; technical writing; graphic arts; and micrography.

For computer documentation see *61 Computer Programming and Software.*

N88-25382# Defense Technical Information Center, Alexandria, Va.
DEFENSE TECHNICAL INFORMATION CENTER CATALOGING GUIDELINES
Apr. 1988 78 p Supersedes DTIC/TR-87/4
(AD-A192200; DTIC/TR-88/4; DTIC/TR-87/4) Avail: NTIS HC A05/MF A01 CSCL 05B

The guidelines for descriptive cataloging is a procedure manual published by the Defense Technical Information Center. It outlines the cataloging information to be included in the data fields for online input of technical publications. The text is arranged numerically, by field number, and includes Appendices A through O, with separate sections on special handling and search procedures for duplicate checking. Changes to the security classification fields have been added to implement DoD 5200.1-R, Information Security Program Regulation. An enhanced version of this guideline for remote input is available as the Shared Bibliographic Input Manual. GRA

N88-25383 Iowa Univ., Iowa City.
DESIGN OF PARTIALLY REPLICATED DISTRIBUTED DATABASE SYSTEMS: AN INTEGRATED METHODOLOGY Ph.D. Thesis
Ravi Mukkamala 1987 279 p
Avail: Univ. Microfilms Order No. DA8729494

The process of designing a partially replicated distributed database system involves solving a number of interrelated and complex problems. Relation partitioning, fragment allocation, and distributed query processing are some of the key issues involved in this design. A number of techniques, optimal as well as heuristic, currently exist to solve these individual problems. Almost all these techniques have two common drawbacks: a restrictive transaction model and an inability to handle large size problems. Fragment allocation algorithms that overcome these drawbacks are proposed and evaluated. These algorithms utilize data interaction information to reduce the size of the allocation problem. Load balancing in a distributed database system may significantly improve the performance of such a system. An efficient method is proposed for static load distribution during the design of partially replicated distributed database systems. The prime contribution is the development of an integrated methodology to design partially replicated distributed database systems. Due to the computational intractability of the combined problem, an iterative solution technique is proposed. A set of heuristic algorithms to determine a minimal set of participating nodes for a transaction execution are developed and evaluated. The performance of these algorithms is compared with optimal, as well as other heuristic algorithms. Dissert. Abstr.

N88-25384*# NASA Scientific and Technical Information Facility, Baltimore/Washington International Airport, Md. 21240.
NASA COMBINED FILE POSTINGS STATISTICS BASED ON NASA THESAURUS, JAN. 1968 - JULY 1988
[1988] 345 p
(NASA-CR-182985; NAS 1.26:182985) Avail: NTIS HC A15/MF A01 CSCL 05B

The NASA Combined File Postings Statistics is published semiannually (January and July). This alphabetical listing of postable subject terms contained in the NASA Thesaurus is used to display the numbers of postings (documents) indexed by each subject term from 1968 to date. The postings total per term are separated by announcement or other media into STAR, IAA, NLN, and OTHER columnar entries covering the NASA document collection (1968 to date). Nearly 594,000 book postings for NALNET Books held by NASA libraries are now included under the NLN column. CSTAR postings as well as some previously unreported series are now listed under the other column. File postings statistics for the Alternate Data Base covering the NASA collection from 1962 through 1967 were published on a one-time basis in September 1975. Subject terms for the Alternate Data Base are derived from the Subject Authority List, reprinted in 1985, which is available on request. The distribution of 16,919,195 postings among the 17,105 Thesaurus terms is tabulated on the last page of Combined File Postings Statistics. Author

N88-25385# Oak Ridge National Lab., Tenn.
THE ATF (ADVANCED TOROIDAL FACILITY) DATA M MANAGEMENT SYSTEM Final Report
K. L. Kannan and L. R. Baylor 1987 3 p Presented at the 5th Conference on Real-Time Computer Applications in Nuclear, Particle and Plasma Physics, San Francisco, Calif., 12 May 1987
(Contract DE-AC05-84OR-21400)
(DE88-007265; CONF-870552-31) Avail: NTIS HC A02/MF A01

The Advanced Toroidal Facility (ATF) Data Management System (DMG) is a VAX-based software system that provides unified data access for ATF data acquisition and analysis. The system was designed with user accessibility, software maintainability, and extensibility as primary goals. This paper describes the layered architecture of the system design, the system implementation, use, and the data file structure. DOE

N88-25386# Oak Ridge National Lab., Tenn.
SAMS: THE SYNCHRONIZATION AND MONITORING SYSTEM FOR ATF (ADVANCED TOROIDAL FACILITY) DATA ACQUISITION PROVIDES UNIFIED DATA ACCESS FOR ATF DATA ACQUISITION
D. E. Greenwood 1987 2 p Presented at the 5th Conference on Real Time Computer Applications in Nuclear, Particle and Plasma Physics, San Francisco, Calif., 12 May 1987
(Contract DE-AC05-84OR-21400)
(DE88-007268; CONF-870552-29) Avail: NTIS HC A02/MF A01

SAMS performs much of the synchronization of the distributed data acquisition system for the Advanced Toroidal Facility (ATF). SAMS is responsible for propagating shot information and managing data system directories and logical names. This paper describes how SAMS communicates with other processes, both within the VAX cluster that supports most of the ATF data acquisition and on VAXes that are connected to the cluster via DECnet. DOE

N88-25387# Sandia National Labs., Albuquerque, N. Mex.
ENGINEERING DRAWINGS AND CHANGES: STORING AND CONTROLLING BY THE TENS OF TERRABYTES
J. D. Stauffer 1988 8 p Presented at the 10th Annual Ideas in Science and Electronics Exposition, Albuquerque, N. Mex., 10 May 1988
(Contract DE-AC04-76DP-00789)
(DE88-007605; SAND-87-2862C; CONF-880579-1) Avail: NTIS HC A02/MF A01

This talk presents an overview of the equipment and methods being installed at Sandia National Laboratories, Albuquerque, to manage information in a digital form. To store and access this data, the Design Information Management Department is planning a network of Write-Once-Read-Many (WORM) optical disk storage, image management workstations in centralized locations and

across the laboratories, compression and conversion software, and access and database software interfaces to traditional engineering data processing. Computer-aided design data will be transmitted directly to the centralized storage area, and paper and microfilm documents will be entered through scanning, which will allow drawing restoration, modification, and general editing. DOE

N88-25388* National Aeronautics and Space Administration, Washington, D.C.
NASA PATENT ABSTRACTS BIBLIOGRAPHY: A CONTINUING BIBLIOGRAPHY. SECTION 1: ABSTRACTS
Jul. 1988 25 p
(NASA-SP-7039(33); NAS 1.21:7039(33)) Avail: NTIS HC A03 CSCL 05B

Abstracts are provided for 16 patents and patent applications entered into the NASA scientific and technical information systems during the period January 1988 through June 1988. Each entry consists of a citation, an abstract, and in most cases, a key illustration selected from the patent or patent application. Author

83 ECONOMICS AND COST ANALYSIS

Includes cost effectiveness studies.

No abstracts in this category.

84 LAW, POLITICAL SCIENCE AND SPACE POLICY

Includes NASA appropriation hearings; aviation law; space law and policy; international law; international cooperation; and patent policy.

N88-25389# Technische Hogeschool, Delft (Netherlands).
CENTRE FOR INTERNATIONAL CO-OPERATION AND APPRORIATE TECHNOLOGY (CICAT) Annual Report, 1986
1986 47 p
(PB88-165501) Avail: NTIS HC A03/MF A01 CSCL 05A

Included are: actual work in 1986 in view of the policy intentions; finished jobs and new plans; micro-projects; inter-institutional linkages; ecological building technology; re-use of old surveying equipment (Rose); research; education; documentation center; organization; and composition of council, board, and bureau. GRA

85 URBAN TECHNOLOGY AND TRANSPORTATION

Includes applications of space technology to urban problems; technology transfer; technology assessment; and surface and mass transportation.

For related information see also *03 Air Transportation and Safety, 16 Space Transportation,* and *44 Energy Production and Conversion.*

No abstracts in this category.

88 SPACE SCIENCES (GENERAL)

N88-25390*# National Aeronautics and Space Administration. Langley Research Center, Hampton, Va.
A STUDY OF SPACE STATION CONTAMINATION EFFECTS
M. R. Torr, ed., J. F. Spann, ed., and T. W. Moorehead, ed.
May 1988 141 p Workshop held in Hilton Head Island, S.C., 29-30 Oct. 1987 Sponsored by NASA, Washington
(NASA-CP-3002; M-586; NAS 1.55:3002) Avail: NTIS HC A07/MF A01 CSCL 22B

A workshop was held with the specific objective of reviewing the state-of-knowledge regarding Space Station contamination, the extent to which the various categories of contamination can be predicted, and the extent to which the predicted levels would interfere with onboard scientific investigations or space station functions. The papers presented at the workshop are compiled and address the following topics: natural environment, plasma electromagnetic environment, optical environment, particulate environment, spacecraft contamination, surface physics processes, laboratory experiments and vented chemicals/contaminants. For individual titles, see N88-25391 through N88-25403.

N88-25391*# Science and Engineering Associates, Inc., Englewood, Colo.
NEUTRAL ENVIRONMENT FOR SPACE STATION **c18**
R. O. Rantanen *In* NASA, Langley Research Center, A Study of Space Space Station Contamination Effects May 1988 p 1-9 (For primary document see N88-25390 18-88)
Avail: NTIS HC A07/MF A01 CSCL 22B

The results of studies to determine the contamination compatibility of the cross boom and dual keel Space Station configurations with attached payloads are presented. The approach was to define the 3-D configuration of the Space Station and calculate surface-to-surface view factors and solid angles between surfaces and points in an extensive point matrix around the Space Station via a modified TRASYS model. The molecular number column densities along specific experiment lines-of-sight on the cross boom generally meet JSC 30426 requirements. The deposition of contaminants on payload surfaces exceeds the JSC 30426 requirements. These model predictions require updating because of the impact on background brightness predictions. An increase of a factor of 2 to 10 in column densities would result in an unacceptable optical background. Author

N88-25392*# National Aeronautics and Space Administration. Lyndon B. Johnson Space Center, Houston, Tex.
SPACE STATION NEUTRAL EXTERNAL ENVIRONMENT **c18**
H. Ehlers and L. Leger *In* NASA, Langley Research Center, A Study of Space Station Contamination Effects May 1988 p 11-17 (For primary document see N88-25390 18-88)
Avail: NTIS HC A07/MF A01 CSCL 22B

Molecular contamination levels arising from the external induced neutral environment of the Space Station (Phase 1 configuration) were calculated using the MOLFLUX model. Predicted molecular column densities and deposition rates generally meet the Space Station contamination requirements. In the doubtful cases of deposition due to materials outgassing, proper material selection, generally excluding organic products exposed to the external environment, must be considered to meet contamination requirements. It is important that the Space Station configuration, once defined, is not significantly modified to avoid introducing new unacceptable contamination sources. Author

N88-25393*# Iowa Univ., Iowa City. Dept. of Physics and Astronomy.
CONTAMINANT IONS AND WAVES IN THE SPACE STATION ENVIRONMENT **c18**
G. B. Murphy *In* NASA, Langley Research Center, A Study of Space Space Station Contamination Effects May 1988 p 19-29 (For primary document see N88-25390 18-88)
Avail: NTIS HC A07/MF A01 CSCL 22B

The probable plasma (ions and electrons) and plasma wave environment that will exist in the vicinity of the Space Station and how this environment may affect the operation of proposed experiments are discussed. Differences between quiescent operational periods and non-operational periods are also addressed. Areas which need further work are identified and a course of action suggested. Author

N88-25394*# Alabama Univ., Huntsville. Dept. of Electrical and Computer Engineering.
SPACE STATION INDUCED ELECTROMAGNETIC EFFECTS c32

N. Singh *In* NASA, Langley Research Center, A Study of Space Station Contamination Effects May 1988 p 31-42 (For primary document see N88-25390 18-88)
Avail: NTIS HC A07/MF A01 CSCL 20N

Several mechanisms which can cause electric (E) and magnetic (B) field contaminations of the Space Station environment are identified. The level of E and B fields generated by some of them such as the motion of the vehicle across the ambient magnetic field B(0) and the 20-kHz leakage currents and charges can be controlled by proper design considerations. On the other hand, there are some mechanisms which are inherent to the interaction of large vehicles with the plasma and probably their contributions to E and B fields cannot be controlled; these include plasma waves in the wake and ram directions and the effects of the volume current generated by the ionization of neutrals. The interaction of high-voltage solar arrays with plasma is yet another rich source of E and B fields and it is probably uncontrollable. Wherever possible, quantitative estimates of E and B are given. A set of recommendations is included for further study in areas where indepth knowledge is seriously lacking. Author

N88-25395*# Alabama Univ., Huntsville. Center for Space Plasma and Aeronomic Research.
SPACE STATION CONTAMINATION STUDY: ASSESSMENT OF CONTAMINANT SPECTRAL BRIGHTNESS c18

D. G. Torr *In* NASA, Langley Research Center, A Study of Space Station Contamination Effects May 1988 p 43-59 (For primary document see N88-25390 18-88)
Avail: NTIS HC A07/MF A01 CSCL 22B

The assessment of spectral brightness resulting from the ambient-contaminant interaction requires a knowledge of the details of cross sections and excitation mechanisms. The approach adopted was to utilize the spectral brightness measurements made on Spacelab 1 and on the S3-4 spacecraft to identify source mechanisms, key cross sections and hence, the abundance of contaminant species. These inferred abundances were then used to update the composition comprising the total column concentrations predicted by the Science and Engineering Associates' configuration contamination model for the Space Station and to scale the irradiances to four altitudes: 300, 350, 400, and 463 km. The concentration irradiances are compared with zodiacal natural background levels. The results demonstrate that emissive contamination is significantly more severe than anticipated. It is shown that spectral emissions can become competitive with the zodiacal background up to altitudes as high as 400 km for the vacuum ultraviolet and visible emissions. M.G.

N88-25396*# Physical Sciences, Inc., Andover, Mass.
CALCULATION OF SPACE STATION INFRARED IRRADIANCE FROM ATMOSPHERE-INDUCED EMISSIONS c18

M. E. Fraser, A. Gelb, B. D. Green, and D. G. Torr (Alabama Univ., Huntsville.) *In* NASA, Langley Research Center, A Study of Space Station Contamination Effects May 1988 p 61-69 (For primary document see N88-25390 18-88)
(Grant NAGw-922)
Avail: NTIS HC A07/MF A01 CSCL 22B

The excitation mechanisms and radiance estimates over the 1 to 10 micron region for CO2(v), H2O(v), CO(v), OH(v), NO2(2B-2A) and N2(B3 pi - A3 sigma) are discussed. The infrared irradiance of the Space Station at an altitude of 460 km was estimated. The surface material was presumed to be non-carbonaceous and inert. The determined number densities of the various gases relevant to the Space Station from both ambient and outgassing sources are presented. A model for the production of and emission from the infrared active molecules was constructed that considers two classes of production processes: (1) gas phase excitation of molecules in the near Station environment by collision with ambient flux; and (2) surface processes that lead to molecular excitation. A composite spectrum of all major emitting species shows that the observed irradiance is non-uniform over the 1 to 8 micron region. The comparison of predicted irradiance with the zodiacal background indicates that the Space Station infrared background from atmosphere-induced emissions may be a problem of consequence. Author

N88-25397*# National Aeronautics and Space Administration. Marshall Space Flight Center, Huntsville, Ala.
SPACE STATION PARTICULATE CONTAMINATION ENVIRONMENT c18

E. R. Miller and K. S. Clifton *In* NASA, Langley Research Center, A Study of Space Station Contamination Effects May 1988 p 71-77 (For primary document see N88-25390 18-88)
Avail: NTIS HC A07/MF A01 CSCL 22B

The origin of particulate contamination on the Space Station will mostly be from pre-launch operations. The adherence and subsequent release of these particles during space flight are discussed. Particle size, release velocity, and release direction are important in determining particle behavior in the vicinity of the vehicle. The particulate environment at the principal science instrument locations is compared to the space shuttle bay environment. Recommendations for possibly decreasing the particulate contamination are presented. Author

N88-25398*# Physical Sciences, Inc., Andover, Mass.
THE PARTICULATE ENVIRONMENT SURROUNDING THE SPACE STATION: ESTIMATES FROM THE PACS DATA c18

Byron David Green *In* NASA, Langley Research Center, A Study of Space Station Contamination Effects May 1988 p 79-90 (For primary document see N88-25390 18-88)
Avail: NTIS HC A07/MF A01 CSCL 22B

The objectives of the Particle Analysis Cameras for Shuttle (PACS) experiment (flown on STS-61C) are described and the experiment results are discussed in reference to the expected Space Station environment. Estimates of the sources of particulates surrounding the Space Station were made based on the existing orbital observations data base. Particulates surrounding the shuttle are mostly event related or from the residual release of mass (dust) brought to orbit from the ground. The particulates surrounding the Space Station are likely to arise from additional sources such as operations, docking, erosion, and abrasion. Thus, scaling of the existing data base to long-duration missions in low-Earth orbit requires analysis, modeling, and simulation testing. Author

N88-25399*# Science and Engineering Associates, Inc., Englewood, Colo.
EFFECTS OF METEOROIDS AND SPACE DEBRIS ON THE PARTICULATE ENVIRONMENT FOR SPACE STATION c18

W. R. Seebaugh *In* NASA, Langley Research Center, A Study of Space Station Contamination Effects May 1988 p 91-99 (For primary document see N88-25390 18-88)
Avail: NTIS HC A07/MF A01 CSCL 22B

A large orbiting platform such as Space Station will be subjected to numerous impacts by meteoroids and space debris fragments. These hypervelocity impacts will produce clouds of ejected structural material in the vicinity of the Station. The development of a preliminary model for impact-generated ejecta production which combines the fluxes of meteoroids and space debris fragments with a description of the number of ejecta particles produced by hypervelocity impacts is reported. Modeling results give mean ejecta densities from 30 to 100 percent of the present particulate background limitation of 1 particle 5 microns and larger per orbit per 1 x 10(-5) sr field-of-view as seen by a 1-m-diameter aperture telescope in the 1990's time frame. Projected increases in the space debris flux raise this density to 300 percent of this limitation after 2010. The model is also applied to estimate the vulnerability of metallic claddings on composite structural members to penetration by hypervelocity projectiles, thereby exposing the substrate to atomic oxygen. The estimated annual number of penetrations is from 4 to 8 per square meter of cross-sectional area in the mid 1990's, increasing to more than 40 penetrations per square meter after 2010. Author

N88-25400*# Aerospace Corp., Los Angeles, Calif. Chemistry and Physics Lab.
CONTAMINATION OF OPTICAL SURFACES **c18**
Graham S. Arnold and David F. Hall *In* NASA, Langley Research Center, A Study of Space Station Contamination Effects May 1988 p 101-108 (For primary document see N88-25390 18-88)
Avail: NTIS HC A07/MF A01 CSCL 22B

The effect of molecular contamination on Space Station optical surfaces is examined. In particular, contamination of solar voltaic power sources and optical solar reflectors for thermal control or solar dynamic power generation is addressed. The published Space Station requirements for molecular contamination accretion and for the monitoring of such accretion is discussed in the context of the historical performance of space systems. Specific reference is made to the results from the Spacecraft Charging at High Altitudes (SCATHA) ML12 experiment. Author

N88-25401*# Washington State Univ., Pullman. Dept. of Physics.
SURFACE INTERACTIONS RELEVANT TO SPACE STATION CONTAMINATION PROBLEMS **c18**
J. T. Dickinson *In* NASA, Langley Research Center, A Study of Space Station Contamination Effects May 1988 p 109-121 (For primary document see N88-25390 18-88)
(Grant NSF DMR-86-01281)
Avail: NTIS HC A07/MF A01 CSCL 22B

The physical and chemical processes at solid surfaces which can contribute to Space Station contamination problems are reviewed. Suggested areas for experimental studies to provide data to improve contamination modeling efforts are presented. Author

N88-25402*# Physical Sciences, Inc., Andover, Mass.
LABORATORY EXPERIMENTS OF RELEVANCE TO THE SPACE STATION ENVIRONMENT **c18**
G. E. Caledonia *In* NASA, Langley Research Center, A Study of Space Station Contamination Effects May 1988 p 123-130 (For primary document see N88-25390 18-88)
Avail: NTIS HC A07/MF A01 CSCL 22B

It has been found that the interaction between orbital vehicles and the ambient environment produces a contaminant cloud which can cause deletrious effects to spacecraft materials and equipment, create increased radiative backgrounds that would interfere with observational instrumentation, and enhance surface charging. A brief overview of the phenomena that produce the contaminant cloud is presented along with a review of physical data required to characterize it. Laboratory techniques which can be utilized to provide the required data are described. In particular, several oxygen beam apparati are discussed. Author

N88-25403*# Naval Research Lab., Washington, D.C. Geophysical and Plasma Dynamics Branch.
CONTAMINATION OF THE SPACE STATION ENVIRONMENT BY VENTED CHEMICALS **c18**
Paul A. Bernhardt *In* NASA, Langley Research Center, A Study of Space Station Contamination Effects May 1988 p 131-140 (For primary document see N88-25390 18-88)
Avail: NTIS HC A07/MF A01 CSCL 22B

Gaseous materials vented from materials and life science experiments on the Space Station may have noticeable effects on the optical or plasma environment. The magnitude of the effects depends on: (1) rarefied gas dynamics; (2) photochemical reactions; and (3) airglow excitation mechanisms. In general, the effects from atomic species can be mitigated, but the disturbances resulting from venting of molecules like SF6, CO2 and C2H2 can be significant. The interaction of molecules with ambient plasma at orbital velocities should be studied with laboratory or space experiments. Author

89 ASTRONOMY

Includes radio, gamma-ray, and infrared astronomy, and astrometry.

N88-25404# Virginia Univ., Charlottesville. Dept. of Astronomy.
INFRARED ASTRONOMY AT EXTREMELY FAINT LIGHT LEVELS IN SUPPORT OF THE LAIRTS PROGRAM Final Technical Report, 1 Feb. 1985 - 30 Sep. 1987
Trinh X. Thuan Sep. 1987 4 p
(Grant AF-AFOSR-0125-85)
(AD-A191497; AFOSR-88-0040TR) Avail: NTIS HC A02/MF A01 CSCL 03A

Near infrared observations have been obtained for a large sample of dwarf irregular galaxies, dwarf elliptical and blue compact dwarf galaxies. Near infrared photometry was obtained for radio sources discovered in a deep VLA radio survey. Near infrared observations were also obtained for the first brightest galaxy in a sample of nearby clusters. A large redshift survey, using the 21-cm hydrogen line, of dwarf galaxies in the northern hemisphere has been completed. Work has been done to understand the stellar populations and star formation are presently occurring. GRA

N88-25405# Geneva Observatory (Switzerland).
DUPLICITY IN THE SOLAR NEIGHBORHOOD. PART 3: NEW SPECTROSCOPIC ELEMENTS FOR NINE SOLAR-TYPE BINARY STARS
A. Duquennoy and M. Mayor 1987 19 p Submitted for publication Sponsored by the Swiss National Foundation for Scientific Research
(Ser-C-Prepubl-Fasc-18-Pt-3; ETN-88-92498) Avail: NTIS HC A03/MF A01

Measurements and spectroscopic elements of nine solar-type binary stars in the solar neighborhood are presented. Seven are resolved into double-lined binaries; HD 16620, HD 64096 and HD 81809 are known visual binaries and spectroscopically resolved. Orbital elements are given for the known variables HD 17433 and HD 66751, and for those previously unknown, HD 61994 and HD 153631. The first elements for the secondary component of the star HD 13974, and an orbit of the so-called standard binary star HD 202275 are given. Results suggest that the stars HD 61994, HD 66751 and HD 153631 could be resolved by speckle interferometric observations. The nine binaries are part of a radial velocity survey of F-G dwarfs in the solar vicinity. ESA

N88-25406*# Dartmouth Coll., Hanover, N.H. Dept. of Physics and Astronomy.
ULTRAVIOLET SPECTRA OF SUBLUMINOUS OBJECTS FOUND IN THE KISO SCHMIDT SURVEY AND SYSTEMATIC REANALYSIS OF THE ARCHIVED ULTRAVIOLET SPECTRA OF WHITE DWARFS OBSERVED WITH THE IUE SATELLITE UNDER THE ASTROPHYSICS DATA PROGRAM (ADP) Semiannual Report
Gary A. Wegner 30 Jun. 1988 8 p
(Grant NAG5-971)
(NASA-CR-182976; NAS 1.26:182976) Avail: NTIS HC A02/MF A01 CSCL 03A

Recent research under NASA grant NAG5-971 consisted of the performance of two projects in conjunction with the International Ultraviolet Explorer (IUE) satellites. These are: (1) to look at the ultraviolet spectra of subluminous stars identified from visual wavelength spectroscopy that had been originally discovered from the Kiso Schmidt survey for ultraviolet excess stars and (2) to carry out a systematic reanalysis of the archived IUE spectra of white dwarfs. This report presents information on the progress of the re-reduction of over 600 IUE white dwarf spectra and their subsequent analysis employing model atmospheres and the observation of the Kiso ultraviolet excess stars. Author

N88-25407 Harvard Univ., Cambridge, Mass.
SPECKLE IMAGING OF ACTIVE GALACTIC NUCLEI: NGC 1068 AND NGC 4151 Ph.D. Thesis
Steven Michael Ebstein 1987 72 p
Avail: Univ. Microfilms Order No. DA8800770

High resolution images of NGC 1068 and NGC 4151 in the 5007 A line and the nearby continuum produced from data taken with the PAPA photon counting imaging detector using the technique of speckle imaging are presented. The images show an unresolved core of 5007 A emission in the middle of an extended emission region. The extended emission tends to lie alongside the subarcsecond radio structure. In NGC 4151, the extended emission comes from a nearly linear structure extending on both sides of the unresolved core. In NGC 1068, the extended emission is concentrated in lobes lying to the unresolved core but the emission is concentrated in lobes lying to either side of the major axis. The continuum of NGC 4151 is spatially unresolved. The continuum of NGC 1068 is extended approx. 1 in to the SW of the center of the 5007 A emission. Certain aspects of the PAPA detector are discussed, including the variable threshold discriminators that track the image intensifier pulse height and the camera artifacts. The data processing is described in detail.
Dissert. Abstr.

N88-25408*# Dartmouth Coll., Hanover, N.H. Dept. of Physics and Astronomy.
ULTRAVIOLET SPECTRA OF TWO MAGNETIC WHITE DWARFS AND ULTRAVIOLET SPECTRA OF SUBLUMINOUS OBJECTS FOUND IN THE KISO SCHMIDT SURVEY Final Technical Report, 1 Jan. - 31 Dec. 1987
Gary A. Wegner 12 Jul. 1988 22 p
(Grant NAG5-287)
(NASA-CR-183051; NAS 1.26:183051) Avail: NTIS HC A03/MF A01 CSCL 03A

Research under NASA Grant NAG5-287 has carried out a number of projects in conjunction with the International Ultraviolet Explorer (IUE) satellite. These include: (1) studies of the UV spectra of DA white dwarfs which show quasi-molecular bands of H2 and H2(+); (2) the peculiar star HR6560; (3) the UV spectra of two magnetic white dwarfs that also show the quasi-molecular features; (4) investigations of the UV spectra of subluminous stars, primarily identified from visual wavelength spectroscopy in the Kiso survey of UV excess stars, some of which show interesting metal lines in their UV spectra; and (5) completion of studies of UV spectra of DB stars. The main result of this research has been to further knowledge of the structure and compositions of subluminous stars which helps cast light on their formation and evolution. Author

90 ASTROPHYSICS

Includes cosmology; celestial mechanics; space plasmas; and interstellar and interplanetary gases and dust.
For related information see also *75 Plasma Physics*.

N88-25409# Geneva Observatory (Switzerland).
PRE-SUPERNOVA EVOLUTION OF SN 1987A
Andre Maeder 1987 11 p Presented at the ESO Workshop on SN 1987A, Jul. 1987 Submitted for publication
(Ser-C-Prepubl-Fasc-15; ETN-88-92497) Avail: NTIS HC A03/MF A01

Stellar evolution with a moderate overshooting and a substantial mass loss, such that the progenitor of SN 1987A lost half its initial mass in a previous red supergiant stage, is proposed to account for observational properties of SN 1987A as well as of massive stars. The blue progenitor of SN 1987A; the large N/C and N/O ratios in the ejecta of SN 1987A; the very low frequency of supernovae like SN 1987A occurring from blue progenitors; supernovae statistics, i.e., the relative ratio of SNII and SNIb or equivalently the initial mass limit separating the evolution towards the two kinds of SN types; the relative frequency of red supergiants in the Large Magellanic Cloud (LMC); metallicity dependence of the red supergiant frequencies in different galaxies; and the lowest possible mass limit for WR stars are accounted for. The models imply that at a given L and Teff the mass loss rates for an LMC star are equal to 40 percent of the values for a star in the solar neighborhood. ESA

N88-25410# Geneva Observatory (Switzerland).
RADIAL VELOCITIES MONITORING OF A SAMPLE OF BARIUM AND S STARS USING CORAVEL: TOWARDS AN EVOLUTIONARY LINK BETWEEN BARIUM AND S STARS?
A. Jorissen (Vrije Universiteit, Brussels, Belgium) and M. Mayor 1987 17 p Submitted for publication Sponsored by the Institut pour l'Encouragement de la Recherche Scientifique dans l'Industrie et l'Agriculture, Brussels, Belgium and the Swiss National Foundation for Scientific Research
(Ser-C-Prepubl-Fasc-19; ETN-88-92499) Avail: NTIS HC A03/MF A01

A sample of 27 southern Ball and nine northern S stars was observed with the radial velocity spectrometer CORAVEL during three seasons. A high proportion (89 percent) of stars with variable (either well above or just at the three sigma level) radial velocities is found in both samples. Concerning Ball stars, there is no doubt about the orbital origin of the observed radial velocity variations. At least five S stars show velocity variations originating in orbital motions, while Mira-type pulsations of small amplitude cannot be firmly excluded for more S stars displaying velocity variations with dispersions in the interval 1.0 to 1.5 km sec. Observations support the Ball-S evolutionary scheme, although a review of other observational data shows that it is probably not possible to totally rule out the M-S-C sequence. A binary scenario involving mass transfer and accounting for this dual origin of S stars is proposed. This scenario could also account for the rather wide range of stellar populations in which S stars are found. ESA

N88-25411# Geneva Observatory (Switzerland).
REVIEW OF THE THEORETICAL CHANGES OF SURFACE CHEMISTRY DURING MASSIVE STAR EVOLUTION
Andre Maeder 1987 5 p Submitted for publication
(Ser-C-Prepubl-Fasc-17; ETN-88-92500) Avail: NTIS HC A02/MF A01

It is suggested that for main sequence stars, central nuclear processing generally has no effect on surface abundances. Later in the evolution, the newly synthetized elements may be revealed at the stellar surface by processes such as mass loss, convective dredge-up, overshooting, diffusion, and rotational and tidal mixing. Changes of CNO abundances are the most conspicuous and the easiest to observe spectroscopically; abundance ratios like C/N, O/N may undergo changes by more than 100. Surface chemistry is thus a most powerful diagnostics of stellar evolution, model assumptions, and nuclear cross sections. ESA

N88-25412 New Hampshire Univ., Durham.
ROCKET-BORNE LOW ENERGY ION MEASUREMENTS IN SPACE Ph.D. Thesis
Craig James Pollock 1987 262 p
Avail: Univ. Microfilms Order No. DA8800187

A capped hemisphere electrostatic analyzer has been developed for the purpose of performing detailed studies of charged particle distributions in space from sounding rocket platforms. This instrument employs micro channel plate detectors in conjunction with a linear resistive anode to carry out angular imaging, by resistive charge division, of particle arrivals. Two such instruments, capable of supplying 64 by 32 angle-energy positive ion distributions about every 1 second were flown on two separate high latitude sounding rockets in February 1985 from Sondre Stromfjord, Greenland. One of these rockets featured an active ion beam experiment whereby 200 eV/q Ar(+) ions were injected into the ionospheric plasma from a separated sub payload in broad (approx. 60 deg FWHM) beams directed alternately either parallel to or perpendicular to the geomagnetic field. Ion fluxes associated with beam operations were observed on the main payload out to a main sub payload separation distance of nearly 1 km. Several distinct ion populations are identified based on their energy pitch angle characteristics, and the existence of ion fluxes at unexpected energies and pitch angles is demonstrated and discussed in light of current understanding of these types of beam-plasma systems. The ion flux signatures of parallel versus perpendicular beam injections are compared and contrasted. Dissert. Abstr.

N88-25413 Harvard Univ., Cambridge, Mass.
MICROWAVE SPECTROSCOPY AND GRAVITATIONAL COLLAPSE Ph.D. Thesis
Eric Ravinen Keto 1987 192 p
Avail: Univ. Microfilms Order No. DA8800800

High resolution observations of NH3 in the molecular cloud cores surrounding five ultracompact HII regions are reported. Three of the sources show velocity structure consistent with gravitational collapse of the core onto the central HII region. One which was extensively observed, shows a hot centrally condensed core with temperature scaling as r sup -1/2 and density as approx. r sup -2. The temperature and density maps show strong velocity gradients consistent with rotational and infall motions. At a spatial resolution of better than 0.014 pc, the accretion flow onto the HII region is resolved and can be characterized by differential rotation and accelerating collapse. The projected angular velocity was determined at 4 different radii from the central source. Less detailed observations of the other two of the three sources show velocity structure similar to that seen in the above source, suggesting that the molecular cloud cores in these sources may also be in gravitational collapse. The other two sources in the survey show evidence that the molecular gas surrounding the HII region is driven by strong outflow from the central stars. Dissert. Abstr.

91 LUNAR AND PLANETARY EXPLORATION

Includes planetology; and manned and unmanned flights. For spacecraft design or space stations see *18 Spacecraft Design, Testing and Performance.*

N88-25414*# Eagle Engineering, Inc., Webster, Tex.
MARS ROVER/SAMPLE RETURN MISSION REQUIREMENTS AFFECTING SPACE STATION
31 Mar. 1988 117 p
(Contract NAS9-17878)
(NASA-CR-172048; NAS 1.26:172048; EEI-88-183) Avail: NTIS HC A06/MF A01 CSCL 03B

The possible interfaces between the Space Station and the Mars Rover/Sample Return (MRSR) mission are defined. In order to constrain the scope of the report a series of seven design reference missions divided into three major types were assumed. These missions were defined to span the probable range of Space Station-MRSR interactions. The options were reduced, the MRSR sample handling requirements and baseline assumptions about the MRSR hardware and the key design features and requirements of the Space Station are summarized. Only the aspects of the design reference missions necessary to define the interfaces, hooks and scars, and other provisions on the Space Station are considered. An analysis of each of the three major design reference missions, is reported, presenting conceptual designs of key hardware to be mounted on the Space Station, a definition of weights, interfaces, and required hooks and scars. Author

N88-25415*# Eagle Engineering, Inc., Houston, Tex.
LUNAR BASE SURFACE MISSION OPERATIONS. LUNAR BASE SYSTEMS STUDY (LBSS) TASK 4.1
1 Dec. 1987 161 p
(Contract NAS9-17878; EAGLE-TO-87-57)
(NASA-CR-172050; NAS 1.26:172050; EEI-87-172) Avail: NTIS HC A08/MF A01 CSCL 03B

The purpose was to perform an analysis of the surface operations associated with a human-tended lunar base. Specifically, the study defined surface elements and developed mission manifests for a selected base scenario, determined the nature of surface operations associated with this scenario, generated a preliminary crew extravehicular and intravehicular activity (EVA/IVA) time resource schedule for conducting the missions, and proposed concepts for utilizing remotely operated equipment to perform repetitious or hazardous surface tasks. The operations analysis was performed on a 6 year period of human-tended lunar base operation prior to permanent occupancy. The baseline scenario was derived from a modified version of the civil needs database (CNDB) scenario. This scenario emphasizes achievement of a limited set of science and exploration objectives while emplacing the minimum habitability elements required for a permanent base. Author

N88-25416 Hawaii Univ., Honolulu.
THE EVOLUTION OF COMETARY ACTIVITY Ph.D. Thesis
Alexander David Storrs 1987 95 p
Avail: Univ. Microfilms Order No. DA8729424

First, all major silicate mineral classes are tested, and the effects of organic materials on the formation of filamentary sublimate residues (FSR), silicates resembling those formed from subliming dirty ice in comets, are investigated. Organic FSR resembles the structure observed to cover most of the nucleus of Halley's comet. Second, the morphology of the outflow of the OH radical in the inner coma of Halley's comet is investigated. When a ratio is made of images of the comet in the OH (1-1) and (00) bands (around 3100 A), the resulting image maps the projection along the line of sight of the sunward velocity of the gas in the coma. Qualitative interpretation of these images shows that, although constant velocity, spherically symmetric outflow is usually observed, gas jets and other asymmetries are not uncommon. Poor quantitative agreement with the theory (Schleicher and A'Hearn 1982) suggests either gas outflows on the order of 4 km sec, or fine structure in the ratio which was not modeled in the theory. Dissert. Abstr.

N88-25417*# National Aeronautics and Space Administration. Marshall Space Flight Center, Huntsville, Ala.
SUPERTHERMAL ELECTRON PROCESSES IN THE UPPER ATMOSPHERE OF URANUS: AURORA AND ELECTROGLOW
J. H. Waite, Jr., M. O. Chandler, R. V. Yelle, and B. R. Sandel (Arizona Univ., Tucson.) [1987] 51 p Submitted for publication
(NASA-TM-101150; NAS 1.15:101150) Avail: NTIS HC A04/MF A01 CSCL 03B

Strong ultraviolet emissions from the upper atmosphere of Uranus suggest that both auroral and electroglow phenomena are of significant aeronomical consequences in the structure of the upper atmosphere. Combined modeling and data analysis were performed to determine the effect of electroglow and auroral phenomena on the global heat and atomic hydrogen budgets in the Uranus upper atmosphere. The results indicate that the auroral and electroglow heat sources are not adequate to explain the high exospheric temperature observed at Uranus, but that the atomic hydrogen supplied by these processes is more than sufficient to explain the observations. The various superthermal electron distributions modeled have significantly different efficiencies for the various processes such as UV emission, heating, ionization, and atomic hydrogen production, and produce quite different H2 band spectra. However, additional information on the UV spectra and global parameters is needed before modeling can be used to distinguish between the possible mechanisms for electroglow. Author

N88-25418*# National Meteorological Center, Washington, D.C.
CLUSTER ANALYSIS OF MULTIPLE PLANETARY FLOW REGIMES
Kingtse Mo and Michael Ghil (California Univ., Los Angeles.) Mar. 1987 86 p
(Grant NAG5-713)
(NASA-CR-182931; NAS 1.26:182931) Avail: NTIS HC A05/MF A01 CSCL 03B

A modified cluster analysis method was developed to identify spatial patterns of planetary flow regimes, and to study transitions between them. This method was applied first to a simple deterministic model and second to Northern Hemisphere (NH) 500 mb data. The dynamical model is governed by the fully-nonlinear, equivalent-barotropic vorticity equation on the sphere. Clusters of point in the model's phase space are associated with either a few persistent or with many transient events. Two stationary clusters have patterns similar to unstable stationary model

solutions, zonal, or blocked. Transient clusters of wave trains serve as way stations between the stationary ones. For the NH data, cluster analysis was performed in the subspace of the first seven empirical orthogonal functions (EOFs). Stationary clusters are found in the low-frequency band of more than 10 days, and transient clusters in the bandpass frequency window between 2.5 and 6 days. In the low-frequency band three pairs of clusters determine, respectively, EOFs 1, 2, and 3. They exhibit well-known regional features, such as blocking, the Pacific/North American (PNA) pattern and wave trains. Both model and low-pass data show strong bimodality. Clusters in the bandpass window show wave-train patterns in the two jet exit regions. They are related, as in the model, to transitions between stationary clusters. Author

N88-25419*# National Aeronautics and Space Administration. Goddard Space Flight Center, Greenbelt, Md.
THE Io SULFUR TORUS IN 1981
Ronald J. Oliversen, Frank Scherb, and Fred L. Roesler (Wisconsin Univ., Madison.) Sep. 1986 21 p Prepared in cooperation with Kitt Peak National Observatory, Tucson, Ariz.
(Grants NGL50-002-162; NAGw-695; NSF ATM-80-21064)
(NASA-TM-101139; NAS 1.15:101139; WU-249) Avail: NTIS HC A03/MF A01 CSCL 03B

A Fabry-Perot spectrometer was used to obtain images of the Io torus in emission lines of S II (wavelength 6716 and 6731) and S III (wavelength 9531) in February and March 1981, on the 2.1 meter telescope at KPNO. The S II and S III images showed a large variation in brightness and radial extent. There is an indication the S II and S III emissions in the warm torus are correlated. The S II and S III emissions in the warm torus also have similar scale heights along the magnetic field lines of approximately 0.6 to 0.72 R sub J. The east-west asymmetry in the S II images taken at similar magnetic longitudes, but 2.5 Jovian rotations apart, supports the theory of convective motions suggested by others. In addition to the images, simultaneous measurements of the S II (6731 wavelength) line profile were also made on one night using a Fabry-Perot scanning spectrometer on the 4 meter at KPNO. The S II spectral scans implied ion temperatures of 52 (+ or - 10) x 10 to the 3rd at 5.2 to 5.6 R sub J from Jupiter and a minimum temperature of at least 3 x 10 to the 5th K at 6 R sub J from Jupiter. Author

N88-25420*# National Aeronautics and Space Administration. Ames Research Center, Moffett Field, Calif.
DIURNAL VARIATIONS IN OPTICAL DEPTH AT MARS: OBSERVATIONS AND INTERPRETATIONS
D. S. Colburn, J. B. Pollack, and R. M. Haberle May 1988 73 p
(NASA-TM-100057; A-88067; NAS 1.15:100057) Avail: NTIS HC A04/MF A01 CSCL 03B

Viking lander camera images of the Sun were used to compute atmospheric optical depth at two sites over a period of 1 to 1/3 martian years. The complete set of 1044 optical depth determinations is presented in graphical and tabular form. Error estimates are presented in detail. Optical depths in the morning (AM) are generally larger than in the afternoon (PM). The AM-PM differences are ascribed to condensation of water vapor into atmospheric ice aerosols at night and their evaporation in midday. A smoothed time series of these differences shows several seasonal peaks. These are simulated using a one-dimensional radiative convective model which predicts martial atmospheric temperature profiles. A calculation combining these profiles with water vapor measurements from the Mars Atmospheric Water Detector is used to predict when the diurnal variations of water condensation should occur. The model reproduces a majority of the observed peaks and shows the factors influencing the process. Diurnal variation of condensation is shown to peak when the latitude and season combine to warm the atmosphere to the optimum temperature, cool enough to condense vapor at night and warm enough to cause evaporation at midday. Author

92 SOLAR PHYSICS

Includes solar activity, solar flares, solar radiation and sunspots.

For related information see *93 Space Radiation.*

N88-25421# California Inst. of Tech., Pasadena.
AN IMAGE PROCESSING SYSTEM FOR RESEARCH IN SOLAR PHYSICS Final Technical Report, 15 Aug. 1986 - 14 Aug. 1987
Harold Zirin 1 Dec. 1987 3 p
(Grant AF AFOSR-0300-86)
(AD-A191673; AFOSR-88-0188TR) Avail: NTIS HC A02/MF A01 CSCL 12I

A powerful new image processing system consisting of a MicroVAX 2 and a Megavision image processor was purchased by the Big Bear Solar Observatory. The system has been immensely successful, and a number of important research projects have already been carried out with it. GRA

N88-25422# Institut d'Aeronomie Spatiale de Belgique, Brussels.
INTERPRETATION OF THE NORTHWARD B SUB Z (NBZ) BIRKELAND CURRENT SYSTEM AND POLAR CAP CONVECTION PATTERNS IN TERMS OF THE IMPULSIVE PENETRATION MODEL
J. Lemaire 1987 32 p Presented at the Chapman Conference on Magnetotail Physics, Laurel, Md., 28-31 Oct. 1985 Submitted for publication
(Aeronomica-Acta-A-321-1987; ISSN-0065-3713; ETN-88-92483)
Avail: NTIS HC A03/MF A01

Impulsive penetration theory is used to show that in the Northern Hemisphere, the region of preferred penetration of solar wind plasmoids into the magnetotail is shifted toward dusk for a positive By, and toward dawn for By less than 0. The direction of these shifts is reversed in the Southern Hemisphere. The polar cap convection pattern associated with impulsive penetration of solar wind plasma irregularities is therefore also shifted toward dusk or dawn, according to the value of By. The northward Bz (NBZ) Birkeland currents driven at the interfaces between the penetrating plasmoids and the ambiant geomagnetic field are downward (upwards) in the dusk (dawn) side for both hemispheres. The amplitudes of NBZ currents are expected to be larger when Bz is larger (and positive). The region of reversal of the NBZ currents is also shifted toward dawn or dusk depending on the sign of By. These transient field aligned currents, driven upwards and downwards, are associated with the nonzero field aligned component of curl B sub bar (i.e., with magnetic shears) in the vicinity of the penetrating diamagnetic plasmoids. ESA

N88-25423*# National Aeronautics and Space Administration. Marshall Space Flight Center, Huntsville, Ala.
THE 2-D MAGNETOHYDROSTATIC CONFIGURATIONS LEADING TO FLARES OR QUIESCENT FILAMENT ERUPTIONS
C.-H. An, S. T. Suess, and R. L. Moore [1988] 39 p Submitted for publication
(NASA-TM-101147; NAS 1.15:101147) Avail: NTIS HC A03/MF A01 CSCL 03B

To investigate the cause of flares and quiescent filament eruptions the quasi-static evolution of a magnetohydrostatic (MHS) model was studied. The results lead to a proposal that: the sudden disruption of an active-region filament field configuration and the accompanying flare result from the lack of a neighboring equilibrium state as magnetic shear is increased above the critical value; and a quiescent filament eruption is due to an ideal MHD kink instability of a highly twisted detached flux tube formed by the increase of plasma current flowing along the length of the filament. A numerical solution was developed for the 2-D MHS equation for the self-consistent equilibrium of a filament and overlying coronal magnetic field. Increase of the poloidal current causes increase of magnetic shear. As shear increases past a critical point, there is a discontinuous topological change in the equilibrium configuration. It was proposed that the lack of a neighboring equilibrium triggers a flare. Increase of the axial current results in

a detached tube with enough helical twist to be unstable to ideal MHD kink modes. It was proposed that this is the condition for the eruption of a quiescent filament. Author

N88-25424*# National Aeronautics and Space Administration. Marshall Space Flight Center, Huntsville, Ala.
THE SAMEX VECTOR MAGNETOGRAPH: A DESIGN STUDY FOR A SPACE-BASED SOLAR VECTOR MAGNETOGRAPH
M. J. Hagyard, G. A. Gary, and E. A. West Jun. 1988 437 p
(NASA-TM-4048; NAS 1.15:4048) Avail: NTIS HC A19/MF A01 CSCL 03B

This report presents the results of a pre-phase A study performed by the Marshall Space Flight Center (MSFC) for the Air Force Geophysics Laboratory (AFGL) to develop a design concept for a space-based solar vector magnetograph and hydrogen-alpha telescope. These are two of the core instruments for a proposed Air Force mission, the Solar Activities Measurement Experiments (SAMEX). This mission is designed to study the processes which give rise to activity in the solar atmosphere and to develop techniques for predicting solar activity and its effects on the terrestrial environment. Author

93 SPACE RADIATION

Includes cosmic radiation; and inner and outer earth's radiation belts.

For biological effects of radiation see *52 Aerospace Medicine*. For theory see *73 Nuclear and High-Energy Physics*.

N88-25425*# California Univ., San Diego, La Jolla. Center for Astrophysics and Space Sciences.
OBSERVATIONS OF COSMIC RAYS IN THE OUTER HELIOSPHERE
Walker Fillius [1986] 4 p
(Grant NGL-05-005-007)
(NASA-CR-182942; NAS 1.26:182942) Avail: NTIS HC A02/MF A01 CSCL 03B

Outward propagating cosmic ray modulation features seen in the outer heliosphere include Forbush decreases, the minimum of the 11 year cycle, and intervals of set recovery rate. The best theoretical model may not be the same for all these features. Some modulation features have been modified or have disappeared between Pioneer 11 and Pioneer 10 as if by the action of an interpalnetary low-pass filter. Azimuthal symmetry still applies, and the radial gradient for nucleons is greater than approximately 500 MeV nucleon is approximately 1 percent AU. Author

N88-25426# Lawrence Livermore National Lab., Calif.
GAMMA RAYS FROM CYGNUS X-1: MODELING AND NONTHERMAL PAIR PRODUCTION
C. D. Dermer and E. P. Liang Feb. 1988 7 p Presented at the Workshop on Nuclear Spectroscopy of Astrophysical Sources, Washington, D.C., 14 Dec. 1987
(Contract W-7405-eng-48)
(DE88-006830; UCRL-98253; CONF-871245-3) Avail: NTIS HC A02/MF A01

The gamma-ray bump observed between 0.5 and 2 MeV in the spectrum of Cygnus X-1 can be interpreted as the thermal emissions from a hot (kT approximately 400 keV) pair-dominated cloud. We argue that the X-rays and gamma rays are produced in separate emission regions, and calculate the photon-photon pair production rate from X-ray and gamma-ray interactions in the vicinity of Cyg X-1 by employing a simplified geometry for the two emitting regions. DOE

N88-25427*# National Aeronautics and Space Administration. Langley Research Center, Hampton, Va.
PRELIMINARY ESTIMATES OF RADIATION EXPOSURES FOR MANNED INTERPLANETARY MISSIONS FROM ANOMALOUSLY LARGE SOLAR FLARE EVENTS
Lawrence W. Townsend, John E. Nealy, and John W. Wilson May 1988 16 p
(NASA-TM-100620; NAS 1.15:100620) Avail: NTIS HC A03/MF A01 CSCL 03B

Preliminary estimates of radiation exposures for manned interplanetary missions resulting from anomalously large solar flare events are presented. The calculations use integral particle fluences for the February 1956, November 1960, and August 1972 events as inputs into the Langley Research Center nucleon transport code BRYNTRN. This deterministic code transports primary and secondary nucleons (protons and neutrons) through any number of layers of target material of arbitrary thickness and composition. Contributions from target nucleus fragmentation and recoil are also included. Estimates of 5 cm depth doses and dose equivalents in tissue are presented behind various thicknesses of aluminum, water, and composite aluminum/water shields for each of the three solar flare events. Author

99 GENERAL

N88-25428*# National Aeronautics and Space Administration, Washington, D.C.
NASA HISTORY DATA BOOK. VOLUME 1: NASA RESOURCES 1958-1968
Jane VanNimmen, Leonard C. Bruno, and Robert L. Rosholt [1988] 639 p
(Contract NASw-3597)
(NASA-SP-4012-Vol-1; NAS 1.21:4012-Vol-1; LC-74-600126)
Avail: NTIS MF A01; SOD HC $57.00 in set of 3 as 033-000-01017-6 CSCL 05D

This is Volume 1, NASA Resources 1958-1968, of a three-volume series providing a 20-year compilation of summary statistical and other data descriptive of NASA's programs in aeronautics and manned and unmanned spaceflight. This series is an important component of NASA published historical reference works, used by NASA personnel, managers, external researchers, and other government agencies. Author

N88-25429*# National Aeronautics and Space Administration, Washington, D.C.
NASA HISTORICAL DATA BOOK. VOLUME 2: PROGRAMS AND PROJECTS 1958-1968
Linda Neuman Ezell [1988] 652 p
(Contract NASw-3597)
(NASA-SP-4012-Vol-2; NAS 1.21:4012-Vol-2; LC-74-600126)
Avail: NTIS MF A01; SOD HC $57.00 in set of 3 as 033-000-01017-6 CSCL 05D

This is Volume 2, Programs and Projects 1958-1968, of a three-volume series providing a 20-year compilation of summary statistical and other data descriptive of NASA's programs in aeronautics and manned and unmanned spaceflight. This series is an important component of NASA published historical reference works, used by NASA personnel, managers, external researchers, and other government agencies. Author

N88-25430*# National Aeronautics and Space Administration, Washington, D.C.
NASA HISTORICAL DATA BOOK. VOLUME 3: PROGRAMS AND PROJECTS 1969-1978
Linda Neuman Ezell [1988] 492 p
(Contract NASw-3597)
(NASA-SP-4012-Vol-3; NAS 1.21:4012-Vol-3; LC-74-600126)
Avail: NTIS MF A01; SOD HC $57.00 in set of 3 as 033-000-01017-6 CSCL 05D

This is Volume 3, Programs and Projects 1969-1978, of a three-volume series providing a 20-year compilation of summary statistical and other data descriptive of NASA's programs in aeronautics and manned and unmanned spaceflight. This series is an important component of NASA published historical reference works, used by NASA personnel, managers, external researchers, and other government agencies. Author

Typical Subject Index Listing

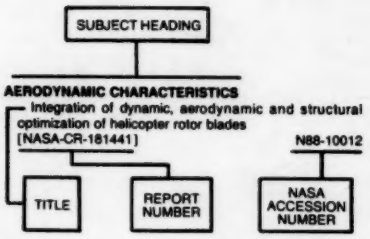

The subject heading is the key to the subject content of the document. Titles, report numbers, and accession numbers of pertinent documents are provided under each subject heading. When the title is insufficiently descriptive of the document content, a title extension has been added, separated from the title by three hyphens. The report number helps to indicate the type of document cited (e.g., NASA report, NASA translation, NASA contractor report). The NASA accession number is the number by which the document abstracts are arranged in this journal and by which the document is sold or requested. The titles, with title extensions if present, are arranged under each subject heading in ascending accession number order. The subject headings have been selected from the latest revision of the *NASA Thesaurus* (NASA SP-7053).

A

ABILITIES
Optimizing feedback utilization in motor skill training [AD-A191559] N88-25146

ABLATION
Use of a two-stage light-gas gun as an injector for electromagnetic railguns [DE88-007200] N88-24857

ABLATIVE NOSE CONES
Experimental investigation of hypersonic aerodynamics [NASA-CR-182973] N88-24591

ABSORPTION CROSS SECTIONS
Temperature dependence of ultraviolet absorption cross sections of chlorofluoroethanes [AERONOMICA-ACTA-A-325-1987] N88-24726

ABSORPTION SPECTROSCOPY
Measurement of atmospheric OH with laser differential optical absorption spectroscopy (LDOAS) N88-25066
Tropospheric OH measurements by long path absorption with rapid spectral concordance N88-25069

ABSTRACTS
Infinite dimensional dynamical systems and their finite dimensional analogues [AD-A192041] N88-25216

ABUNDANCE
Para-ortho abundance ratio of molecular hydrogen in NGC2023 [ISAS-RN-352] N88-25286
Review of the theoretical changes of surface chemistry during massive star evolution [SER-C-PREPUBL-FASC-17] N88-25411

ACCELERATION (PHYSICS)
Effects of Coriolis acceleration on the vibrations of spinning structures N88-24966

ACCELEROMETERS
The optical accelerometer: A novel sensor for vertical flight guidance N88-24935

ACCESS CONTROL
Computer resource management technology program (PE 64740F). Task no. 9: Advanced user authentication [PB88-183066] N88-25163

ACCIDENT PREVENTION
Rotorcraft TCAS (traffic alert and collision avoidance system) evaluation: Group 3 results [AD-A191719] N88-24814

ACCOUNTING
Financial reporting: NASA (National Aeronautics and Space Administration) can improve compliance with GAO (General Accounting Office) standards and treasury requirements [PB88-172523] N88-25373

ACCURACY
Limits of accuracy and range of laser radars N88-24934
DMSP-SSM/1 NASA algorithm validation using primarily LANDSAT and secondarily DMSP and/or AVHRR visible and thermal infrared satellite imagery [NASA-CR-182979] N88-25024

ACETONITRILE
Electrochemistry in near-critical and supercritical fluids. 6: The electrochemistry of ferrocene and phenazine in acetonitrile between 25C and 300C [AD-A192171] N88-24723

ACOUSTIC EMISSION
Frequency Analysis of Acoustic Emission - Application to machining and welding [DE88-701478] N88-25262

ACOUSTIC PROPAGATION
Linear and nonlinear acoustic wave propagation in the atmosphere [NASA-CR-4157] N88-25268

ACOUSTIC PROPERTIES
Remote sensing of acoustic properties of shallow water sediments: A review [AD-A192107] N88-25267

ACOUSTIC VELOCITY
Operational noise data for CH-47D and AH-64 army helicopters [AD-A191059] N88-25263
Evaluation of the biot coefficients [AD-A191643] N88-25265
The high pressure sound velocity and equation of state of aqueous solutions of hydroxylammonium nitrate and triethanolammonium nitrate [AD-A191740] N88-25266

ACOUSTICS
Acoustic convective system [NASA-CASE-NPO-17278-1-CU] N88-24818
Identification and acoustic characterization of seamounts [AD-A192204] N88-25123
Remote sensing of acoustic properties of shallow water sediments: A review [AD-A192107] N88-25267

ACOUSTO-OPTICS
Fast acting optical beam detection and deflection system [AD-A192161] N88-24954

ACTIVE CONTROL
Low authority control of large space structures using a constrained threshold control formulation N88-24667
Experimental study of active vibration control [AD-A191454] N88-24989
Vibration protection of inelastic structures by means of active and passive control N88-25001
Analysis of a closed-kinematic chain robot manipulator [NASA-CR-183031] N88-25206

ACTIVE GALACTIC NUCLEI
Speckle imaging of active galactic nuclei: NGC 1068 and NGC 4151 N88-25407

ACTS
Service offerings and interfaces for the ACTS network of Earth stations [NASA-TM-100809] N88-24663

ACTUATORS
Linear force device [NASA-CASE-MSC-20549-2] N88-24927
Toggle release [NASA-CASE-MSC-21354-1] N88-24969

ADA (PROGRAMMING LANGUAGE)
New York TRACON demonstration of program recoding requirements analysis document [DOT/FAA/CT-87/34] N88-24822
Beyond Ada: Generating Ada code from equational specifications [AD-A191866] N88-25176

ADAPTATION
Adaptive local grid refinement in computational fluid mechanics [AD-A192215] N88-24890

ADAPTIVE CONTROL
Accurate multigrid solution of the Euler equations on unstructured and adaptive meshes [NASA-CR-181679] N88-24808
Parameter-adaptive model-following for in-flight simulation [AD-A190567] N88-24845
Kinematics, dynamics and control of a closed chain mechanism manipulator N88-24967
Robust adaptive regulation without persistent excitation [NASA-TM-100571] N88-25204

ADAPTIVE OPTICS
Research in the optical sciences [AD-A192175] N88-25297

ADDITIVES
Improved properties of SiGe/GaP alloys [NASA-CASE-NPO-17259-1-CU] N88-25358

ADHESION
Adhesion between polystyrene and polymethylmethacrylate [AD-A192050] N88-24785
Environmental integrity of coating/metal interface [AD-A192184] N88-24786

ADHESIVE BONDING
Thermographic detection of buried debonds [AD-A192115] N88-24880
Calculation of assemblies bonded with quasi-elastic adhesives [REPT-47-632/F] N88-24793

ADSORPTION
Preferential surface adsorption in miscible blends of polystyrene and poly(vinyl methyl ether) [AD-A191451] N88-24789
The electrokinetic behavior of calcium oxalate monohydrate in macromolecular solutions [NASA-TM-101144] N88-24791

AEROCAPTURE
A design study of onboard navigation and guidance during aerocapture at Mars [NASA-CR-172053] N88-24854

AERODYNAMIC CHARACTERISTICS
Experiment investigation on longitudinal characteristics of the forward swept wing [AD-A191553] N88-24582
High speed and high angle of attack aerodynamic characteristics of winged space vehicle [ISSN-0285-6808] N88-24599

AERODYNAMIC CONFIGURATIONS
An analytic model for aerodynamic shapes [AD-A191573] N88-24583
Wind tunnel investigation of wing and control panel loads at transonic and supersonic speeds on some schematic cruciform missile configurations [FFA-TN-1986-43] N88-24585
Incompressible Euler solution on a multiblock grid around a car configuration [FFA-TN-1987-65] N88-24586
Summary of low-speed wind tunnel results of several high-speed counterrotation propeller configurations [NASA-TM-100945] N88-24597
High speed and high angle of attack aerodynamic characteristics of winged space vehicle [ISSN-0285-6808] N88-24599
Actuated forebody strakes [NASA-CASE-LAR-13983-1] N88-24628
Application of advanced grid generation techniques for flow field computations about complex configurations [NASA-CR-183049] N88-24922

AERODYNAMIC FORCES
Nonlinear programming extensions to rational function approximation methods for unsteady aerodynamic forces
[NASA-TP-2776] N88-24623
AERODYNAMIC STABILITY
Actuated forebody strakes
[NASA-CASE-LAR-13983-1] N88-24628
AERODYNAMICS
Aeronautical engineering: A continuing bibliography with indexes (supplement 227)
[NASA-SP-7037(227)] N88-24578
Some rotorcraft applications of computational fluid dynamics
[NASA-TM-100066] N88-24601
A decade of computer simulations for space shuttle aerodynamics
[NASA-TM-100990] N88-24603
Nonlinear programming extensions to rational function approximation methods for unsteady aerodynamic forces
[NASA-TP-2776] N88-24623
Nonlinear flying quality parameters based on dynamic inversion
[AD-A192146] N88-24627
Internal fluid dynamics within a nonspinning partially liquid-filled shell due to burster rupture
[AD-A191055] N88-24874
NAS: The first year
[NASA-TM-101006] N88-25196
AEROELASTICITY
Aircraft aeroelasticity and structural dynamics research at the NASA Langley Research Center: Some illustrative results
[NASA-TM-100627] N88-24598
AERONAUTICAL ENGINEERING
Aeronautical engineering: A continuing bibliography with indexes (supplement 227)
[NASA-SP-7037(227)] N88-24578
NASA history data book. Volume 1: NASA resources 1958-1968
[NASA-SP-4012-VOL-1] N88-25428
AERONAUTICS
NASA historical data book. Volume 2: Programs and projects 1958-1968
[NASA-SP-4012-VOL-2] N88-25429
NASA historical data book. Volume 3: Programs and projects 1969-1978
[NASA-SP-4012-VOL-3] N88-25430
AEROSOLS
High-energy laser-assisted imaging through vaporizing aerosols
[DE88-007911] N88-24957
Information analysis of integral equations in remote sensing of atmospheric aerosols N88-25022
SAM 2 data user's guide
[NASA-RP-1200] N88-25094
AEROSPACE ENGINEERING
Effects of spatial resolution in CARS measurements
[PB88-121900] N88-24727
AEROSPACE ENVIRONMENTS
Electromagnetic damping and vibration isolation of space structures
[AD-A191492] N88-24665
AEROSPACE INDUSTRY
Quality and productivity drive innovation and improvement at United Technologies Aerospace Operations, Inc.
[NASA-CR-182944] N88-24983
AEROSPACE MEDICINE
Aerospace medicine and biology: A continuing bibliography with indexes (supplement 312)
[NASA-SP-7011(312)] N88-25141
AEROSPACE PLANES
A system status monitor for the National Aerospace Plane
[AD-A190681] N88-24624
Guidance and control strategies for aerospace vehicles
[NASA-CR-183032] N88-24644
AEROSPACE SAFETY
Parachute for in-flight training on parachute ejection
[REPT-87-11] N88-24593
AGING (MATERIALS)
Aging of carbon fibers
[SNPE-NT-10/86/CRB/NP] N88-24707
Evaluation of the chromium oxide arc spraying treatment on solar energy collectors
[ETN-88-92564] N88-25053
AGING (METALLURGY)
On the reversion phenomena of Cu-3 percent Ti alloys
[NASA-TT-20170] N88-24762
On the abnormal phenomena observed in the electrical resistivity measurement during the decomposition process of saturated Cu-Fe alloys
[NASA-TT-20183] N88-24869
AGREEMENTS
Department of Defense Statement on the Balanced Technology Initiative to the Committee on Armed Services, United States Senate, 100th Congress, second session
[AD-A191841] N88-25378
AH-64 HELICOPTER
Operational noise data for CH-47D and AH-64 army helicopters
[AD-A191059] N88-25263
AIR
Simplified curve fits for the transport properties of equilibrium air
[NASA-CR-178411] N88-24911
AIR CONDITIONING EQUIPMENT
The effects of different combinations of inlet air conditions used for cooling as measured on a heated manikin
[AD-A191116] N88-25151
AIR COOLING
Acoustic convective system
[NASA-CASE-NPO-17278-1-CU] N88-24818
The effects of different combinations of inlet air conditions used for cooling as measured on a heated manikin
[AD-A191116] N88-25151
AIR DEFENSE
Modeling and evaluation of variable structure organizations
[AD-A191947] N88-25381
AIR FLOW
Acoustic convective system
[NASA-CASE-NPO-17278-1-CU] N88-24818
AIR POLLUTION
Air pollution: Ozone attainment requires long-term solutions to solve complex problems
[PB88-167275] N88-25060
Ozone in the atmosphere N88-25064
Motor vehicles as sources of compounds important to tropospheric and stratospheric ozone
[PB88-195219] N88-25076
AIR QUALITY
Air pollution: Ozone attainment requires long-term solutions to solve complex problems
[PB88-167275] N88-25060
AIR SAMPLING
Aircraft emissions characterization: TF41-A2, TF30-P103 and TF30-P109 engines
[AD-A192053] N88-24638
AIR TRAFFIC
FAA (Federal Aviation Administration) technical center: Mission and role in natinal airspace system plan implementation
[PB88-169818] N88-24609
AIR TRAFFIC CONTROL
FAA (Federal Aviation Administration) technical center: Mission and role in natinal airspace system plan implementation
[PB88-169818] N88-24609
Optimization of the dilation characteristic on the control jurisdiction of an area control facility
[AD-A191720] N88-24615
AIR TRANSPORTATION
FAA aviation forecasts fiscal years 1988-1999
[AD-A191711] N88-24576
AIRCRAFT ACCIDENT INVESTIGATION
Aircraft accident/incident, Copperhill, Tennessee, February 22, 1986
[PB88-910407] N88-24612
AIRCRAFT ACCIDENTS
Peak Acceleration Device (PAD)
[AD-A191639] N88-24611
Fuel containment concepts: Transport category airplanes
[DOT/FAA/CT-87/18] N88-24807
AIRCRAFT CARRIERS
Simulator evaluation of lineup visual landing aids for night carrier landing
[AD-A191212] N88-24648
AIRCRAFT CONFIGURATIONS
Aircraft aeroelasticity and structural dynamics research at the NASA Langley Research Center: Some illustrative results
[NASA-TM-100627] N88-24598
Applications of the Navier-Stokes equations to wings and complex configurations using a zonal approach
[NASA-TM-100080] N88-24602
Actuated forebody strakes
[NASA-CASE-LAR-13983-1] N88-24628
Computational design of low aspect ratio wing-winglet configurations for transonic wind-tunnel tests
[NASA-CR-183021] N88-24630
Application of advanced grid generation techniques for flow field computations about complex configurations
[NASA-CR-183049] N88-24922
AIRCRAFT CONSTRUCTION MATERIALS
Characterization of the 2219 Cegedur alloy. Data acquisition of the fracture mechanics — aircraft construction materials
[REPT-48-442/F] N88-24751
Characterization of 7090 and 7091 profiles made with Cegedur powder — powder metallurgy, aircraft construction materials
[REPT-48-441/F] N88-24752
Aluminum alloy
[NASA-CASE-LAR-13924-1-CU] N88-24753
AIRCRAFT CONTROL
Optimization of the dilation characteristic on the control jurisdiction of an area control facility
[AD-A191720] N88-24615
Actuated forebody strakes
[NASA-CASE-LAR-13983-1] N88-24628
AIRCRAFT DESIGN
Acta aeronautica et astronautica sinica (selected articles)
[AD-A191552] N88-24575
A transonic small disturbance wing design methodology N88-24590
Class 2 design update for the family of commuter airplanes
[NASA-CR-182681] N88-24629
AIRCRAFT DETECTION
Acta aeronautica et astronautica sinica (selected articles)
[AD-A191552] N88-24575
AIRCRAFT FUELS
Fuel containment concepts: Transport category airplanes
[DOT/FAA/CT-87/18] N88-24807
AIRCRAFT GUIDANCE
Optics: Perspectives for Measurement Techniques and Signal Processing for Flight Guidance — conference
[DFVLR-MITT-87-21] N88-24928
Laboratory tests of laser gyroscopes for future utilization in multifunction systems for precision navigation and flight guidance N88-24932
Limits of accuracy and range of laser radars N88-24934
The optical accelerometer: A novel sensor for vertical flight guidance N88-24935
AIRCRAFT HAZARDS
National plans for aircraft icing and improved aircraft icing forecasts and associated warning services N88-25113
AIRCRAFT INDUSTRY
FAA aviation forecasts fiscal years 1988-1999
[AD-A191711] N88-24576
Class 2 design update for the family of commuter airplanes
[NASA-CR-182681] N88-24629
AIRCRAFT LANDING
Simulator evaluation of lineup visual landing aids for night carrier landing
[AD-A191212] N88-24648
AIRCRAFT MAINTENANCE
Composite repair of cracked aluminum alloy aircraft structure
[AD-A190514] N88-24573
Predictive corrosion modeling, volume 1
[AD-A191229] N88-24739
AIRCRAFT MODELS
Nonlinear flying quality parameters based on dynamic inversion
[AD-A192146] N88-24627
AIRCRAFT PERFORMANCE
Airplane runway performance monitoring system
[NASA-CASE-LAR-13854-1-CU] N88-24621
Method for prediction and determination of takeoff performance for vectored thrust vehicles
[AD-A191809] N88-24626
AIRCRAFT SAFETY
Study of benefits of passenger protective breathing equipment from analysis of past accidents
[DOT/FAA/CT-88/03] N88-24610
Development of a multipurpose smart recorder for general aviation aircraft
[NASA-CR-168353] N88-24637
AIRFOILS
Passive shock wave-boundary layer control for the Boll FX69-H-098 airfoil N88-24588
Prediction of laminar and turbulent flows past single and twin airfoils N88-24589
Two dimensional hyperbolic grid generation
[VKI-TN-162] N88-24897
Characteristics of merging shear layers and turbulent wakes of a multi-element airfoil
[NASA-TM-100053] N88-24900
Manipulation of the structure of a turbulent boundary layer N88-24901
Computational Fluid Mechanics
[NASA-CR-183022] N88-24915

AIRPORT PLANNING
FAA aviation forecasts fiscal years 1988-1999
[AD-A191711] N88-24576
AIRPORTS
Microwave landing system mathematical modeling study for Midway Airport Runway 22L, Chicago, Illinois
[AD-A191721] N88-24616
ALBEDO
Higher frequency ambient noise in the arctic ocean
[AD-A192203] N88-25122
ALGAE
Photosynthetic water splitting
[PB88-188891] N88-24731
ALGORITHMS
A feedback linearization approach to spacecraft control using momentum exchange devices
[NASA-CR-172057] N88-24668
Dynamics of a flexible orbiting platform with MRMS
[ISSN-0285-6808] N88-24673
Geodesy by radio interferometry: Optimization of wet path delay algorithms using microwave radiometer data
[PB88-187739] N88-24820
Delay-doppler radar imaging
[AD-A191509] N88-24826
A method for discrimination of radar targets using complex natural resonances
[AD-A191848] N88-24832
Information and stochastic systems
[AD-A192167] N88-24838
Identification of cascaded microwave circuits with moderate reflections using reflections and transmission measurements
[PB88-171921] N88-24849
Fast algorithm development for large-eddy simulation of circular-jet turbulence
[AD-A192044] N88-24867
SOLA-DM: A numerical solution algorithm for transient three-dimensional flows
[DE88-007159] N88-24913
The coordination of multiple robotic manipulators
[AD-A190869] N88-24963
Dynamic response of plates to moving loads: Structural impedance and finite element methods N88-25000
Advanced development of the boundary element method for elastic and inelastic thermal stress analysis N88-25002
Multishaker modal testing
[NASA-CR-179355] N88-25010
DMSP-SSM/1 NASA algorithm validation using primarily LANDSAT and secondarily DMSP and/or AVHRR visible and thermal infrared satellite imagery
[NASA-CR-182979] N88-25024
Analysis of lightning field changes during active thunderstorms in Florida N88-25103
A multiprocessor data flow accelerator module
[DE88-007587] N88-25161
Multi-sensor integration on the NCUBE hypercube computer
[DE88-007472] N88-25162
A mixed-integer linear programming problem which is efficiently solvable
[AD-A191028] N88-25168
Decomposition of linear programs using parallel computation
[AD-A191718] N88-25173
An electrostatic potential comparator
[AD-A192051] N88-25177
A centered projective algorithm for linear programming
[AD-A192100] N88-25178
Making progress during a stall in the simplex algorithm
[DE88-007120] N88-25182
An improved simulated annealing algorithm for standard cell placement
[NASA-CR-182952] N88-25183
Algorithms and software for solving finite element equations on serial and parallel architectures
[NASA-CR-183027] N88-25191
Gram-Schmidt implementation of a linearly constrained adaptive array
[AD-A191651] N88-25198
Robot navigation using simple sensor fusion
[DE88-006184] N88-25203
A concurrent neural network algorithm for the traveling salesman problem
[DE88-006961] N88-25208
Algorithms and data structures for an expanded family of matroid intersection problems
[AD-A191482] N88-25213
A primal-dual algorithm for the computation of the minimum of a convex function on the intersection of convex functions, and its application in data analysis
[RR-638-M] N88-25217
Multigrid methods for elliptic Partial Differential Equations (PDEs)
[CWI-NM-R8722] N88-25242
A constraint algorithm for maintaining rigid bonds in molecular dynamics simulations of large molecules
[AD-A191663] N88-25277
Dendritic growth in the presence of convection N88-25328
ALIGNMENT
Thermal compensating mount
[NASA-CASE-LAR-13794-1] N88-24942
ALLOYS
Predictive corrosion modeling, volume 1
[AD-A191229] N88-24739
Effect of size of precipitates on recrystallization temperatures in Cu-Cr, Cu-Zr, and Cu-Zr-Cr alloys
[NASA-TT-20166] N88-24763
On quench sensitivity of Cu-Cr alloys
[NASA-TT-20174] N88-24765
ALUMINIDES
Chemical compatibility between silicon carbide and a nickel aluminide
[DE88-006188] N88-24708
ALUMINUM
The variation of torsional ductility of high-purity aluminum with temperature and strain rate
[DE88-005818] N88-24755
Plate response analysis using shock tube
[AD-A190828] N88-24987
ALUMINUM ALLOYS
Strain hardening at large strains in aluminum alloys
[DE88-007415] N88-24737
Improving knowledge of the corrosion behavior of aluminum alloys of the 7XXX series
[REPT-48-451/F] N88-24750
Characterization of the 2219 Cegedur alloy. Data acquisition of the fracture mechanics — aircraft construction materials
[REPT-48-442/F] N88-24751
Aluminum alloy
[NASA-CASE-LAR-13924-1-CU] N88-24753
Martensitic transformation and microstructures in sintered NiAl alloys
[NASA-TT-20178] N88-24761
Rapidly solidified lightweight durable disk material
[AD-A191697] N88-24775
ALUMINUM GALLIUM ARSENIDES
Optical nonlinearities in GaAs/GaAlAs multiple quantum wells fabricated by metalorganic chemical vapor deposition for use in optical signal processing
[AD-A191558] N88-25337
ALUMINUM OXIDES
Thermal conductivity of hard anodized coatings on aluminum
[AD-A191755] N88-24784
AMAZON REGION (SOUTH AMERICA)
Oxidation and reduction rates for organic carbon in the Amazon mainstream tributary and floodplain, inferred from distributions of dissolved gases
[NASA-CR-182943] N88-25062
AMINES
Aromatic cyclotriphosphazenes
[NASA-CASE-ARC-11428-3] N88-24692
AMMONIA
Microwave spectroscopy and gravitational collapse N88-25413
AMMONIUM NITRATES
The burning of HAN-based (hydroxylammonium nitrate) liquid propellants
[DE88-006863] N88-24800
Electrical ignition of HAN-based liquid propellants
[AD-A191349] N88-24801
The high pressure sound velocity and equation of state of aqueous solutions of hydroxylammonium nitrate and triethanolammonium nitrate
[AD-A191740] N88-25266
AMPLIFIERS
Characterization of a 30-GHz IMPATT solid state amplifier
[NASA-TM-100876] N88-24847
Aurora status and plans
[DE88-006476] N88-24955
Reducing sensitivity to errors in free electron laser amplifiers
[DE88-007017] N88-24960
ANALOG TO DIGITAL CONVERTERS
Digitizing the traffic network of JOG 250 by scanning — JOG 250 map N88-25029
Tests for the automatic pattern recognition of building surfaces by the TK 50 N88-25030
ANALOGS
Infinite dimensional dynamical systems and their finite dimensional analogues
[AD-A192041] N88-25216
Space station habitability recommendations based on a systematic comparative analysis of analogous conditions
[NASA-CR-3943] N88-25372
ANALYSIS OF VARIANCE
Exact tests for variance component models with unequal cell frequencies in the last stage
[AD-A191645] N88-25253
ANECHOIC CHAMBERS
Almond test body — for microwave anechoic chambers
[NASA-CASE-LAR-13747-1] N88-24845
ANELASTICITY
Effect of hydrogen, deuterium and oxygen on the anelastic properties of refractory alloys
[DE88-007349] N88-24736
ANGLES (GEOMETRY)
Universal precision sine bar attachment
[NASA-CASE-MFS-28253-1] N88-24971
ANGULAR ACCELERATION
Laser gyroscopes using the rate-bias technique N88-24930
ANGULAR VELOCITY
Automatic feedback control of a rigid body for finite displacements N88-24674
ANIMALS
A cardiostimulant protein from the Australian Red Waratah Sea anemone, Actinia tenebrosa N88-25138
ANISOTROPY
Shape stability in composites N88-24706
ANNEALING
A study on the precipitation and reversion behaviors of Cu-0.3 percent Cr alloy by the step annealing method
[NASA-TT-20169] N88-24764
An improved simulated annealing algorithm for standard cell placement
[NASA-CR-182952] N88-25183
ANODES
Sulfur-tolerant anode materials
[DE88-001034] N88-25054
ANODIC COATINGS
Thermal conductivity of hard anodized coatings on aluminum
[AD-A191755] N88-24784
ANOMALIES
Electrical conduction in thin film carbons
[AD-A191726] N88-24780
ANTARCTIC REGIONS
Changes in the Antarctic atmosphere due to the reduction of stratospheric ozone
[ETN-88-92565] N88-25074
ANTENNA ARRAYS
Gram-Schmidt implementation of a linearly constrained adaptive array
[AD-A191651] N88-25198
ANTENNA FEEDS
A MININEC model of the miniloop antenna
[AD-A191759] N88-24830
ANTENNA RADIATION PATTERNS
A MININEC model of the miniloop antenna
[AD-A191759] N88-24830
ANTENNAS
Practical VLF/LF radio test system
[AD-A191768] N88-24831
IGUANA: Interactive graphics utility for automated NEC analysis
[AD-A191760] N88-25174
ANTHRACENE
Electronic and ionic transport in polymers
[AD-A191642] N88-24772
ANTIFERROMAGNETISM
Ground state properties and electronic structure of high T sub c superconductors
[DE88-007485] N88-25360
APPLICATIONS PROGRAMS (COMPUTERS)
Prediction of laminar and turbulent flows past single and twin airfoils N88-24589
Dynamics of a flexible orbiting platform with MRMS
[ISSN-0285-6808] N88-24673
Shape stability in composites N88-24706
Kinematics, dynamics and control of a closed chain mechanism manipulator N88-24967
Dynamic response of plates to moving loads: Structural impedance and finite element methods N88-25000
Advanced development of the boundary element method for elastic and inelastic thermal stress analysis N88-25002
Automated cartographic generalization for linear map features N88-25021
Computer and model changes at National Meteorological Center (NWC) N88-25116
SYMBL: A new Boolean compiler N88-25160
The Environment for Application Software Integration and Execution (EASIE), version 1.0. Volume 3: Program execution guide
[NASA-TM-100575] N88-25184
Phase diagrams in materials science and the use of the computer in their calculation
[PB88-155262] N88-25364

APPROPRIATIONS
Department of Defense statement on defense agency research and development to the Subcommittee on Defense of the Committee on Appropriations, United States House of Representatives, 100th Congress, second session
[AD-A191840] N88-25377
The Department of Defense report on the merit review process for competitive selection of university research projects and an analysis of the potential for expanding the geographic distribution of research for the Committees on Appropriations, United States Congress
[AD-A191842] N88-25379

APPROXIMATION
Nonlinear programming extensions to rational function approximation methods for unsteady aerodynamic forces
[NASA-TP-2776] N88-24623
A feedback linearization approach to spacecraft control using momentum exchange devices
[NASA-CR-172057] N88-24668
Axisymmetric viscid-inviscid interaction by a frozen vorticity approximation
[AD-A191743] N88-24885
Construction of approximations to acoustic Green's functions for nonhomogeneous oceans using transmutation
[PB88-185384] N88-25126
Open or closed curves by regularized B-splines
[RR-652-M] N88-25218
A mixed min-max control problem governed by integral equations N88-25228
Numerical solution of linear integral equations with random forcing terms N88-25237
On a biorthogonal system associated with uniform asymptotic expansions
[CWI-AM-R8709] N88-25240
Galerkin approximation for inverse problems for nonautonomous nonlinear distributed systems
[NASA-CR-181676] N88-25246
Optimal discrete-time LQR problems for parabolic systems with unbounded input: Approximation and convergence
[NASA-CR-181673] N88-25247
Curvature of blended rolled edge reflectors at the shadow boundary contour
[NASA-CR-182974] N88-25300

AQUEOUS SOLUTIONS
The high pressure sound velocity and equation of state of aqueous solutions of hydroxylammonium nitrate and triethanolammonium nitrate
[AD-A191740] N88-25266

AQUIFERS
Field experience with aquifer thermal energy storage
[DE88-007075] N88-25058

ARC DISCHARGES
Arcing and rf signal generation during target irradiation by a high-energy, pulsed neutral particle beam
[DE88-007169] N88-24864

ARC JET ENGINES
Performance and long duration test of a 30 kw thermal arcjet engine
[AD-A190962] N88-24677
Evaluation of the communications impact of a low power arcjet thruster
[NASA-TM-100926] N88-24682
An extended life and performance test of a low-power arcjet
[NASA-TM-100942] N88-24687

ARC SPRAYING
Evaluation of the chromium oxide arc spraying treatment on solar energy collectors
[ETN-88-92564] N88-25053

ARC WELDING
Trailer shield assembly for a welding torch
[NASA-CASE-MFS-29260-1] N88-24972

ARCHITECTURE
Space station architectural elements and issues definition study
[NASA-CR-3941] N88-25371

ARCHITECTURE (COMPUTERS)
Adaptive local grid refinement in computational fluid mechanics
[AD-A192215] N88-24890
Tutorial on computer control
[DE88-006185] N88-25157
The -mdoc macro package: A software tool to support computer documentation standards
[DE88-000500] N88-25188
Algorithms and software for solving finite element equations on serial and parallel architectures
[NASA-CR-183027] N88-25191
Network architecture for OPS5
[DE88-002802] N88-25194
The ATF (Advanced Toroidal Facility) Data M Management System
[DE88-007265] N88-25385
SAMS: The synchronization and monitoring system for ATF (Advanced Toroidal Facility) data acquisition provides unified data access for ATF data acquisition
[DE88-007268] N88-25386

ARCTIC OCEAN
Higher frequency ambient noise in the arctic ocean
[AD-A192203] N88-25122

ARCTIC REGIONS
Higher frequency ambient noise in the arctic ocean
[AD-A192203] N88-25122

ARMATURES
Fundamental limits to the velocity of solid armatures in railguns N88-24856

ARMED FORCES (UNITED STATES)
Management and the executive
[AD-A190778] N88-25374
Department of Defense Statement on the Technology Base to the Subcommittee on Defense Industry and Technology of the Committee on Armed Services, United States Senate, 100th Congress, second session
[AD-A191839] N88-25376

ARRAYS
Joint services electronics program
[AD-A191749] N88-24853
Null steering applications of polynomials with unimodular coefficients
[AD-A191087] N88-25211

ARSENIC
Raman characterization of AsF5-intercalated vapor grown graphite fibers
[AD-A191709] N88-24778

ARSENIDES
Recent data on Si:As impurity band conduction multiplexed arrays
[AD-A191752] N88-25340

ARTIFICIAL INTELLIGENCE
A system status monitor for the National Aerospace Plane
[AD-A190681] N88-24824
Timesharing performance as an indicator of pilot mental workload
[NASA-CR-182807] N88-25150
A computational model of motor behavior
[AD-A191179] N88-25152
LispSEI: The programmer's manual
[AD-A191632] N88-25172
Representation and decision mechanisms in artificial intelligence
[AD-A191083] N88-25197
The ISI (Information Sciences Institute) grapher manual
[AD-A192198] N88-25200
Modeling of geometric reasoning for robot programming
[ETN-88-92290] N88-25202
Robot navigation using simple sensor fusion
[DE88-006184] N88-25203
Application of flight systems methodologies to the validation of knowledge-based systems
[NASA-TM-100442] N88-25207
Automatic discovery of optimal classes
[NASA-TM-101174] N88-25238

ASHES
Energy efficient continuous flow ash lockhopper
[NASA-CASE-NPO-16985-1-CU] N88-24814

ASSOCIATIVE PROCESSING (COMPUTERS)
Optical computing based on neuronal models
[AD-A191481] N88-25293

ASTRONAUTS
Human performance issues arising from manned space station missions
[NASA-CR-3942] N88-25156

ASTRONOMICAL SPECTROSCOPY
Radial velocities monitoring of a sample of barium and S stars using CORAVEL: Towards an evolutionary link between barium and S stars?
[SER-C-PREPUBL-FASC-19] N88-25410

ASYMPTOTIC SERIES
Asymptotic theory for weighted least squares estimators in Aalen's additive risk model
[AD-A191085] N88-25210
On a biorthogonal system associated with uniform asymptotic expansions
[CWI-AM-R8709] N88-25240

ATLANTIC OCEAN
SeaSoar profiles in the Iceland-Scotland area, May 1987
[IOS-253] N88-25124
Determination of mesoscale variability of sea surface temperature and attenuation in the North Atlantic from satellite measurement
[REPT-162] N88-25127

ATMOSPHERIC ATTENUATION
Atmospheric propagation of laser beams
[AD-A191447] N88-24952
Development and validation of transmission measurements techniques of image contrast, utilizing existing IR imagers
[AD-A191471] N88-25079

ATMOSPHERIC CHEMISTRY
Ozone in the atmosphere N88-25064
Laboratory experiments on atmospheric OH reactions N88-25066
Effect of carbohydrate oxidation on the tropospheric HOx-system N88-25067
Measurement of atmospheric OH with laser differential optical absorption spectroscopy (LDOAS) N88-25068
Tropospheric OH measurements by long path absorption with rapid spectral concordance N88-25069
Determination of tropospheric H concentrations by a double-pulsed UV laser method N88-25070
Tropospheric OH measurement by Laser Induced Fluorescence (LIF) N88-25071
Development of continuous wave laser frequency modulation of OH in tropospheric concentrations range N88-25073

ATMOSPHERIC CIRCULATION
Analysis of a six-component barotropic spectral model: Chaotic motion, predictability and vacillation — atmospheric circulation
[CWI-AM-R8710] N88-25090
Cluster analysis of multiple planetary flow regimes
[NASA-CR-182931] N88-25418

ATMOSPHERIC COMPOSITION
Information analysis of integral equations in remote sensing of atmospheric aerosols N88-25022
Oxidation and reduction rates for organic carbon in the Amazon mainstream tributary and floodplain, inferred from distributions of dissolved gases
[NASA-CR-182943] N88-25062
Trace gas measurements in the troposphere using tunable diode lasers N88-25072
Stratospheric positive ion composition measurements and acetonitrile detection: A consistent picture
[AERONOMICA-ACTA-A-326-1987] N88-25084

ATMOSPHERIC DENSITY
Three-dimensional temperature fields in the atmosphere up to 50 km altitude
[ETN-88-92150] N88-25089

ATMOSPHERIC ENTRY
Guidance and control strategies for aerospace vehicles
[NASA-CR-183032] N88-24644
A design study of onboard navigation and guidance during aerocapture at Mars
[NASA-CR-172053] N88-24654

ATMOSPHERIC IONIZATION
Theoretical plasma physics research of active space experiments
[AD-A192075] N88-25309

ATMOSPHERIC LASERS
Atmospheric propagation of laser beams
[AD-A191447] N88-24952

ATMOSPHERIC MODELS
Changes in the Antarctic atmosphere due to the reduction of stratospheric ozone
[ETN-88-92565] N88-25074
Brunt-Doppler ducting of buoyancy waves in a temperature- and wind-stratified atmosphere N88-25086
Analysis of a six-component barotropic spectral model: Chaotic motion, predictability and vacillation — atmospheric circulation
[CWI-AM-R8710] N88-25090
Photochemical and thermal modeling in the early atmosphere of the earth
[NASA-CR-183029] N88-25093
Adaptive grid refinement for numerical weather prediction
[AD-A192172] N88-25101
Bracknell Meteorological Office N88-25107
Applications products of aviation forecast models N88-25109
Comparative verification between GEM model and official aviation terminal forecasts N88-25115
Computer and model changes at National Meteorological Center (NWC) N88-25116

ATMOSPHERIC OPTICS
Activities report of the Division of Optical Technology
[FOA-C-30477-3] N88-25299

ATMOSPHERIC PHYSICS
Theoretical plasma physics research of active space experiments
[AD-A192075] N88-25309

ATMOSPHERIC RADIATION
Observations of wave number dependent spectral line ratio fluctuations in the atmospheric emissions
[IRF-PREPRINT-101] N88-25085

ATMOSPHERIC SOUNDING
Stratospheric positive ion composition measurements and acetonitrile detection: A consistent picture
[AERONOMICA-ACTA-A-326-1987] N88-25084
ATMOSPHERIC TEMPERATURE
Three-dimensional temperature fields in the atmosphere up to 50 km altitude
[ETN-88-92150] N88-25089
Effects of moderate cold and heat stress on the potential work performance of industrial workers. Part 6: The effects of increasing vapour pressure at four air temperatures on the performance and physiology of white females
[PB88-124854] N88-25137
ATMOSPHERIC TURBULENCE
Aircraft/lidar turbulence comparison N88-25111
ATOMIC BEAMS
Laboratory experiments of relevance to the space station environment N88-25402
ATOMIC CLOCKS
Tactical Rubidium Frequency Standard (TRFS), volume 2
[AD-A191190] N88-24850
ATOMIC STRUCTURE
The theory of random alloys
[DE88-006408] N88-24756
Silicon-sapphire waveguides
[AD-A191754] N88-24854
Electronic structure, elementary excitations, optical and transport properties of semiconductor superlattices
[AD-A190795] N88-25333
Transition probabilities in OH A 2 sigma + - X 2 pi i: Bands with v prime = 0 and 1, v double prime = 0 to 4
[NASA-CR-182946] N88-25353
Ground state properties and electronic structure of high T sub c superconductors
[DE88-007485] N88-25360
ATOMIZERS
Laboratory scale inert gas atomizer for producing rapidly solidified powders
[DE88-006734] N88-24812
ATTENTION
Eye and head response to an attention cue in a dual task paradigm
[AD-A191052] N88-25143
ATTENUATION
Theoretical basis for an experimental test with regard to the origin of VHF (Very High Frequency) radiation from natural lightning
[DE88-007535] N88-25102
Determination of mesoscale variability of sea surface temperature and attenuation in the North Atlantic from satellite measurement
[REPT-162] N88-25127
ATTENUATION COEFFICIENTS
Remote sensing of acoustic properties of shallow water sediments: A review
[AD-A192107] N88-25267
ATTITUDE CONTROL
Attitude control laws for gas-jet spacecraft N88-24643
AUDITORY PERCEPTION
Motor theory of auditory perception
[AD-A192095] N88-25136
AUDITORY SIGNALS
Time-frequency representations for speech signals
[AD-A188661] N88-24819
Motor theory of auditory perception
[AD-A192095] N88-25136
AUDITORY STIMULI
Motor theory of auditory perception
[AD-A192095] N88-25136
AURORAS
Dynamics Explorer-2 measurements during an isolated auroral substorm
[AD-A191202] N88-25091
Superthermal electron processes in the upper atmosphere of Uranus: Aurora and electroglow
[NASA-TM-101150] N88-25417
AUTOCLAVES
The 700 F properties of autoclave cured PMR-2 composites
[NASA-TM-100923] N88-24712
AUTOIONIZATION
Contributions of autoionizing resonances to the electron collisional excitation rates for Be-like ions
[AD-A190924] N88-25275
AUTOMATIC CONTROL
A general approach for automating source code verification
[AD-A191461] N88-25170
Development of the field-induced electron injection and impact ionization (F4I) technique for radiation hardness testing of MOS (Metal-Oxide-Semiconductor) gate insulators
[AD-A192114] N88-25345
AUTOMATIC FREQUENCY CONTROL
State of tuning
[NASA-TT-20195] N88-25205
AUTOMATION
Automation of surface observations program N88-25106
AUTOMOBILE ENGINES
Motor vehicles as sources of compounds important to tropospheric and stratospheric ozone
[PB88-195219] N88-25076
AUTOMOBILES
Incompressible Euler solution on a multiblock grid around a car configuration
[FFA-TN-1987-65] N88-24586
Navigation system for land vehicles
[NASA-CASE-LAR-13322-1] N88-24620
Digital maps for an electronic traffic guide N88-25033
AVALANCHE DIODES
Characterization of a 30-GHz IMPATT solid state amplifier
[NASA-TM-100876] N88-24847
AVIATION METEOROLOGY
Meteorological and Environmental Inputs to Aviation Systems
[NASA-CP-2498] N88-25105
Automation of surface observations program N88-25106
Bracknell Meteorological Office N88-25107
Special observations N88-25108
Applications products of aviation forecast models N88-25109
General-aviation's view of progress in the aviation weather system N88-25110
Objective detection and forecasting of Clear-Air Turbulence (CAT): A status report N88-25114
Comparative verification between GEM model and official aviation terminal forecasts N88-25115
Denver ARTCC evaluation of PROFS (Prototype Regional Observations and Forecast System) mesoscale weather products N88-25117
The Federal Aviation Administration/Massachusetts Institute of Technology (FAA/MIT) Lincoln Laboratory Doppler weather radar program N88-25118
AVIONICS
User's guide to the Fault Inferring Nonlinear Detection System (FINDS) computer program
[NASA-CR-178410] N88-24619
AXIAL COMPRESSION LOADS
Local delamination buckling in layered structures N88-24711
AXIAL FLOW
Solid rocket motor aft field joint flow field analysis
[NASA-CR-179288] N88-24675
AXIAL FLOW TURBINES
Experimental vibration damping characteristics of the third-stage rotor of a three-stage transonic axial-flow compressor
[NASA-TM-100948] N88-24642
AXIAL STRAIN
Effect of uniaxial stress on the Raman spectra of graphite fibers
[AD-A191730] N88-24783
AXISYMMETRIC FLOW
Solid rocket motor aft field joint flow field analysis
[NASA-CR-179288] N88-24675

B

BACKSCATTERING
Multiple scattering of waves in discrete random media
[AD-A191068] N88-24823
Radio-wave scintillations and ionospheric irregularities at high latitudes
[AD-A192140] N88-24837
BACTERIA
The synthesis of polyphenylene from a CIS-dihydrocatechol biologically produced monomer N88-24699
BALLISTICS
Experimental investigation of hypersonic aerodynamics
[NASA-CR-182973] N88-24591
BALLOON SOUNDING
Stratospheric positive ion composition measurements and acetonitrile detection: A consistent picture
[AERONOMICA-ACTA-A-326-1987] N88-25084
BALLOON-BORNE INSTRUMENTS
Utilization of the IR telescope gimbaling system as a stabilized pointing platform for balloon payloads. Volume 1: Technical results
[NASA-CR-179339] N88-24962
BALLOONS
Utilization of the IR telescope gimbaling system as a stabilized pointing platform for balloon payloads. Volume 1: Technical results
[NASA-CR-179339] N88-24962
BARIUM
Radial velocities monitoring of a sample of barium and S stars using CORAVEL: Towards an evolutionary link between barium and S stars?
[SER-C-PREPUBL-FASC-19] N88-25410
BARIUM OXIDES
Vacancy ordering in the basal plane of YBa2Cu3O(sub)z
[DE88-004572] N88-25348
BAROTROPIC FLOW
Analysis of a six-component barotropic spectral model: Chaotic motion, predictability and vacillation — atmospheric circulation
[CWI-AM-R8710] N88-25090
Cluster analysis of multiple planetary flow regimes
[NASA-CR-182931] N88-25418
BATHYMETERS
To relate measurements of gravity and geoid anomalies over the oceans to near surface density distributions
[AD-A192166] N88-25120
Identification and acoustic characterization of seamounts
[AD-A192204] N88-25123
BATHYTHERMOGRAPHS
Expendable conductivity, temperature and depth system (XCTD) development program
[AD-A192182] N88-25121
BAYES THEOREM
Knowledge acquisition tool implementation
[AD-A190415] N88-25164
Automatic discovery of optimal classes
[NASA-TM-101174] N88-25238
BEAM INTERACTIONS
Gamma rays from Cygnus X-1: Modeling and nonthermal pair production
[DE88-006830] N88-25426
BEAMS (RADIATION)
Fast acting optical beam detection and deflection system
[AD-A192161] N88-24954
BEAMS (SUPPORTS)
Space station architectural elements model study
[NASA-CR-4027] N88-24632
Estimation and control of distributed models for certain elastic systems arising in large space structures
[AD-A192120] N88-24666
On the bending response of Kevlar 49/epoxy beams and rings
[DE88-006824] N88-25012
BEARINGLESS ROTORS
Design, manufacture and spin test of high contact ratio helicopter transmission utilizing Self-Aligning Bearingless Planetary (SABP)
[NASA-CR-4155] N88-24975
BEARINGS
The flying characteristics of the membrane slider bearing N88-24965
BEHAVIOR
The behavior of drop-containing turbulent eddies
[AD-A191669] N88-24883
Behavioral response of rats exposed to high-power microwave radiation
[AD-A192199] N88-25128
Motor theory of auditory perception
[AD-A192095] N88-25136
Modeling and evaluation of variable structure organizations
[AD-A191947] N88-25381
BENDING
On the bending response of Kevlar 49/epoxy beams and rings
[DE88-006824] N88-25012
MHD bending waves in a current sheet
[NASA-TM-101149] N88-25323
BENZENE
Size effects in the electrical resistivity of benzene-derived carbon fibers
[AD-A191708] N88-24777
BERYLLIUM
Contributions of autoionizing resonances to the electron collisional excitation rates for Be-like ions
[AD-A190924] N88-25275
BIBLIOGRAPHIES
Aeronautical engineering: A continuing bibliography with indexes (supplement 227)
[NASA-SP-7037(227)] N88-24578
Electromagnetic field penetration into structures
[AD-A192127] N88-24836
Bibliography of Soviet laser developments, number 83, May - June 1986
[AD-A190969] N88-24950

Aerospace medicine and biology: A continuing bibliography with indexes (supplement 312) [NASA-SP-7011(312)] N88-25141
Management and the executive [AD-A190778] N88-25374
NASA patent abstracts bibliography: A continuing bibliography. Section 1: Abstracts [NASA-SP-7039(33)] N88-25388

BINARY INTEGRATION
Analysis of binarized Hartley phase-only filter performance with respect to stochastic noise [DE88-007604] N88-24945

BINARY STARS
Duplicity in the solar neighborhood. Part 3: New spectroscopic elements for nine solar-type binary stars [SER-C-PREPUBL-FASC-18-PT-3] N88-25405

BINARY SYSTEMS (MATERIALS)
Demixing of aqueous polymer two-phase systems in low gravity [NASA-TM-101141] N88-24809

BIOLOGICAL EFFECTS
A cardiostimulant protein from the Australian Red Waratah Sea anemone, Actinia tenebrosa N88-25138
Aerospace medicine and biology: A continuing bibliography with indexes (supplement 312) [NASA-SP-7011(312)] N88-25141

BIOMASS
Production costs of hydrocarbon fuels from biomass [DE88-006687] N88-24804
Proceedings of the 1987 Biomass Thermochemical Conversion Contractors' Review Meeting [DE88-006730] N88-25041
An advanced extruder-feeder biomass liquefaction reactor system N88-25042
Molecular-beam, mass-spectrometric studies of wood vapor and model compounds over HZSM-5 catalyst N88-25044
Low-temperature thermochemical conversion of high moisture biomass feedstocks N88-25047

BIOMASS ENERGY PRODUCTION
Proceedings of the 1987 Biomass Thermochemical Conversion Contractors' Review Meeting [DE88-006730] N88-25041
An advanced extruder-feeder biomass liquefaction reactor system N88-25042
Low pressure entrained flow pyrolysis of biomass to produce liquid fuels N88-25043
Molecular-beam, mass-spectrometric studies of wood vapor and model compounds over HZSM-5 catalyst N88-25044
Upgrading pyrolysis vapors to aromatic gasoline with zeolite catalysis at atmospheric pressure N88-25045
Low-temperature thermochemical conversion of high moisture biomass feedstocks N88-25047
Technical and economic evaluation of emerging biomass pyrolysis processes for gasoline production N88-25048
Bench-scale studies on fluid-bed pyrolysis of wood using different contact gases N88-25049

BIOMETRICS
Computer resource management technology program (PE 64740F). Task no. 9: Advanced user authentication [PB88-183066] N88-25163

BIOT METHOD
Evaluation of the biot coefficients [AD-A191643] N88-25265

BIOTECHNOLOGY
Proceedings of the American Society for Composites [AD-A189661] N88-24693
Carbon matrix composites prospective roles for biotechnology N88-24694
Current and future molecular structures of aerospace organic matrix resins N88-24695
Industrial perspective on current and future needs in aerospace matrix resin chemistry N88-24696
Applications of biotechnology to synthetic chemistry for aerospace matrix resins development N88-24697
The application of hydrocarbon bioconversion technology to aerospace materials production N88-24698
Ecological risk factors related to environmental uses of genetically engineered organisms [DE88-006674] N88-25132

BIPOLAR TRANSISTORS
Joint services electronics program research in electronics [AD-A192206] N88-24857

BIPOLARITY
Small scale bipolar nickel-hydrogen testing [NASA-TM-100936] N88-25059

BIRDS
Motor theory of auditory perception [AD-A192095] N88-25136

BLACK SEA
Geological evolution and analysis of confirmed or suspected gas hydrate localities. Volume 2: Basin analysis, formation and stability of gas hydrates in the Black Sea [DE88-001052] N88-25023

BLUFF BODIES
Incompressible Euler solution on a multiblock grid around a car configuration [FFA-TN-1987-65] N88-24566

BODY-WING CONFIGURATIONS
A transonic small disturbance wing design methodology N88-24590

BOLTZMANN DISTRIBUTION
Para-ortho abundance ratio of molecular hydrogen in NGC2023 [ISAS-RN-352] N88-25286

BOLTZMANN TRANSPORT EQUATION
The development of KENO and the calculation of differential parameters with KENO [DE88-006176] N88-25166

BONDING
The inspection of electronic metallurgical bonds [AD-A192197] N88-24745
Molecular characterization of structure and bonding in thin film materials [DE88-006811] N88-25351

BOOLEAN FUNCTIONS
SYMBL: A new Boolean compiler N88-25160

BORN APPROXIMATION
Born-type reconstruction of material parameters of an inhomogeneous, lossy dielectric slab from reflected-field data [PB88-188958] N88-25261

BORON-EPOXY COMPOSITES
Composite repair of cracked aluminum alloy aircraft structure [AD-A190514] N88-24573

BOUNDARIES
Transmitting boundary for finite-difference calculations with finite modeling of an infinite medium [AD-A191441] N88-25264
Curvature of blended rolled edge reflectors at the shadow boundary contour [NASA-CR-182974] N88-25300
On the use of convergent beam electron diffraction for identification of antiphase boundaries in GaAs grown on Si [DE88-008220] N88-25362

BOUNDARY LAYER CONTROL
Passive shock wave-boundary layer control for the Bell FX69-H-098 airfoil N88-24588

BOUNDARY LAYER EQUATIONS
Composite reduced Navier-Stokes procedures for flow problems with strong pressure interactions [AD-A191127] N88-24875
Transient particle deposition in a boundary layer of impulsive flow over a flat plate [AD-A191537] N88-24880
Cross stream differencing for integral boundary layer equations [AD-A191744] N88-24886

BOUNDARY LAYER FLOW
Transient particle deposition in a boundary layer of impulsive flow over a flat plate [AD-A191537] N88-24880
Hypersonic turbulent wall boundary layer computations [NASA-CR-182147] N88-24917

BOUNDARY LAYER SEPARATION
Instability of laminar separation bubbles: Causes and effects [AD-A191188] N88-24876
Computation of the turbulent boundary layer downstream of vortex generators [AD-A191544] N88-24881

BOUNDARY LAYER STABILITY
Cross stream differencing for integral boundary layer equations [AD-A191744] N88-24886

BOUNDARY LAYER TRANSITION
Boundary layer transition [CERT-OA-37/5018-AYD] N88-24595

BOUNDARY LAYERS
A formulation for the boundary-layer equations in general coordinates [NASA-TM-100079] N88-24600

BOUNDARY VALUE PROBLEMS
The calculation of transonic flow over the shuttle orbiter using slender body theory N88-24606
Computation and characteristics of pulsatile multi-bifurcation flow N88-24729
Nonlinear waves [AD-A192148] N88-24889
Duct flow nonuniformities for Space Shuttle Main Engine (SSME) [NASA-CR-179338] N88-24899
Advanced development of the boundary element method for elastic and inelastic thermal stress analysis N88-25002
NFEARS: A nonlinear adaptive finite element solver, part 1 [AD-A191823] N88-25215
Solving time-dependent two-dimensional eddy current problems [NASA-TM-100875] N88-25239
Stability and convergence of the Peaceman-Rachford ADI method for initial-boundary value problems [CWI-NM-R8724] N88-25243
On bunch lengthening using the fourth harmonic cavity in the NSLS VUV ring [DE88-007392] N88-25288

BREATHING APPARATUS
Study of benefits of passenger protective breathing equipment from analysis of past accidents [DOT/FAA/CT-88/03] N88-24810

BREMSSTRAHLUNG
Intense ion beam diagnostics for particle beam fusion experiments on PBFA 2 [DE88-007279] N88-25308

BRIGHTNESS
Space station contamination study: Assessment of contaminant spectral brightness N88-25395

BRITTLENESS
Rapidly solidified lightweight durable disk material [AD-A191697] N88-24775
Self-consistent model for the brittle response of solids N88-24999

BUBBLE CHAMBERS
Optical system of laser illuminated streamer chamber [DE88-702127] N88-25306

BUBBLES
Instability of laminar separation bubbles: Causes and effects [AD-A191188] N88-24876

BUCKLING
Forced motion of initially stressed shells and plates N88-25005

BUDGETING
Department of Defense statement on defense agency research and development to the Subcommittee on Defense of the Committee on Appropriations, United States House of Representatives, 100th Congress, second session [AD-A191840] N88-25377
Department of Defense Statement on the Balanced Technology Initiative to the Committee on Armed Services, United States Senate, 100th Congress, second session [AD-A191841] N88-25378

BULK MODULUS
Ground state properties and electronic structure of high T sub c superconductors [DE88-007485] N88-25360

BUOYANCY
Brunt-Doppler ducting of buoyancy waves in a temperature- and wind-stratified atmosphere N88-25066

BUOYS
Descriptions of HF and VHF Loran-C buoys and evaluations as potential datum marker buoys [AD-A192069] N88-24618

BURNING RATE
Chemical kinetics of nitramine propellant combustion [AD-A191556] N88-24802

BY-PRODUCTS
Upgrading pyrolysis vapors to aromatic gasoline with zeolite catalysis at atmospheric pressure N88-25045

C

CADASTRAL MAPPING
Tests for the automatic pattern recognition of building surfaces by the TK 50 N88-25030
Recent developments in software and hardware by Scitex Co. — computer aided mapping N88-25038

CALIBRATING
Expendable conductivity, temperature and depth system (XCTD) development program [AD-A192182] N88-25121

CALORIMETERS
Calorimetry applied to nucleus-nucleus collisions at ultrarelativistic energies [DE88-006173] N88-25282

CANONICAL FORMS
Perturbation theory for dual semigroups. Part 4: The intertwining formula and the canonical pairing [CWI-AM-R8802-PT-4] N88-25258

CANOPIES (VEGETATION)
History of wildland fires on Vandenberg Air Force Base, California [NASA-TM-100983] N88-25134

CARBOHYDRATES
Workshop on Atmospheric OH
[BPT-7/87] N88-25063
Effect of carbohydrate oxidation on the tropospheric HOx-system N88-25067
CARBON
Liquid carbon
[AD-A191707] N88-24776
Electrical conduction in thin film carbons
[AD-A191726] N88-24780
Electron-Rayleigh wave interaction in thin film carbons
[AD-A191727] N88-24781
CARBON DIOXIDE LASERS
An optical preamplifier for detection of CO2 laser radiation
[AD-A190790] N88-24949
High power axial flow CO2 laser
[ETN-88-91951] N88-24959
Design of catalytic monoliths for closed-cycle carbon dioxide lasers
[NASA-CR-182983] N88-25185
A two-wavelength infrared interferometer/polarimeter system for CIT (Compact Ignition Tokamak)
[DE88-007681] N88-25321
CARBON FIBER REINFORCED PLASTICS
Elementary characterization of preimpregnated carbon epoxy T400H/DA0506 from STRUCTIL. Test report M6-577100
[CEAT-047426] N88-24703
Detecting delaminations in CFRP specimens using X-ray techniques
[FFA-TN-1988-04] N88-24704
CARBON FIBERS
Aging of carbon fibers
[SNPE-NT-10/86/CRB/NP] N88-24707
Size effects in the electrical resistivity of benzene-derived carbon fibers
[AD-A191708] N88-24777
Photoconductivity in carbon fibers
[AD-A191728] N88-24782
Effect of uniaxial stress on the Raman spectra of graphite fibers
[AD-A191730] N88-24783
Influence of carbon fiber surface treatment
[ETN-88-92536] N88-24787
CARBON STEELS
Environmental integrity of coating/metal interface
[AD-A192184] N88-24786
CARBONIZATION
Influence of carbon fiber surface treatment
[ETN-88-92536] N88-24787
CARDIOVASCULAR SYSTEM
Cardiovascular effects of weightlessness and ground-based simulation
[NASA-TM-88314] N88-25140
CARTAN SPACE
Inevitable inflation in Einstein-Cartan theory with improved energy-momentum tensor with spin
[NASA-TM-101146] N88-25365
CARTESIAN COORDINATES
A formulation for the boundary-layer equations in general coordinates
[NASA-TM-100079] N88-24600
QN3D: A 3-dimensional quasi-neutral hybrid particle-in-cell code with applications to the tilt mode instability in field reversed configurations N88-25325
CASES (CONTAINERS)
Low temperature storage container for transporting perishables to space station
[NASA-CASE-MFS-28248-1] N88-24817
CATALYSIS
A scientific basis for an alternate cathode architecture
[AD-A191498] N88-24717
CATALYSTS
Catalytic ignition of hydrogen and oxygen propellants
[NASA-TM-100957] N88-24689
Surface composition-reactivity relationships in heterogeneous catalysis
[DE88-006679] N88-24714
Update of low temperature catalyst development
[DE88-007032] N88-24715
Molecular-beam, mass-spectrometric studies of wood vapor and model compounds over HZSM-5 catalyst N88-25044
Upgrading pyrolysis vapors to aromatic gasoline with zeolite catalysis at atmospheric pressure N88-25045
Research on hydrotreating catalysts to hydrodeoxygenate biocrude oils N88-25046
Sulfur-tolerant anode materials
[DE88-001034] N88-25054
CATALYTIC ACTIVITY
Design of catalytic monoliths for closed-cycle carbon dioxide lasers
[NASA-CR-182983] N88-25185
CATHODE RAY TUBES
Design and testing of a luminance and chrominance stabilization system for a computer-controlled color display
[AD-A191922] N88-25159
CATHODES
A scientific basis for an alternate cathode architecture
[AD-A191498] N88-24717
Basic processes of plasma propulsion
[AD-A192117] N88-25310
CATHODIC COATINGS
The influence of cathodic protection on erosion-corrosion of metals and model alloys
[AD-A191613] N88-24742
CATIONS
Computer simulation of uphill diffusion in ternary ionic system
[NASA-TT-20194] N88-25285
CAUCHY INTEGRAL FORMULA
A method for the numerical solution of random Cauchy singular integral equation N88-25234
CAVITATION FLOW
Superplasticity: A fundamental investigation on deformation mechanism and cavitation phenomena
[AD-A191548] N88-24741
Gas diffusion studies in steady and nonsteady cavities N88-24902
CAVITY RESONATORS
On bunch lengthening using the fourth harmonic cavity in the NSLS VUV ring
[DE88-007392] N88-25288
CDC CYBER 205 COMPUTER
Solving bidiagonal systems of linear equations on the CDC CYBER 205
[CWI-NM-R8725] N88-25187
CERAMIC COATINGS
An investigation of ceramic coatings for protection of SiC from high-temperature corrosion
[DE88-007873] N88-24790
CERAMIC MATRIX COMPOSITES
Carbon matrix composites prospective roles for biotechnology N88-24694
CERAMICS
Thrust chamber thermal barrier coating techniques
[NASA-TM-100933] N88-24690
Role of cracks in the creep of structural polycrystalline ceramics
[AD-A191485] N88-24770
Environmental effects on slow crack growth in silicon nitride
[DE88-007206] N88-24795
The stress analysis of ceramic, polymeric, and metallic composite systems by the finite element method N88-25004
CEREBRAL CORTEX
A systems engineering based methodology for analyzing human electrocortical responses
[AD-A190809] N88-25135
CERTIFICATION
US civil airmen statistics, 1987
[AD-A191714] N88-24577
CHAINS
Kinematics, dynamics and control of a closed chain mechanism manipulator N88-24967
Analysis of a closed-kinematic chain robot manipulator
[NASA-CR-183031] N88-25206
CHANGE DETECTION
Real-time image difference detection using a polarization rotation special light modulator
[NASA-CASE-NPO-17144-1-CU] N88-25305
CHANNEL CAPACITY
Communications using channels formed by meteor bursts
[AD-A192088] N88-24834
Information and stochastic systems
[AD-A192167] N88-24838
CHANNEL FLOW
A variational finite element method for three-dimensional, steady, compressible, viscous flows N88-24904
Theoretical analysis of laminar incompressible flow in slender channels
[VTH-LR-517] N88-24909
CHANNELS (DATA TRANSMISSION)
Communications using channels formed by meteor bursts
[AD-A192088] N88-24834
Selection and effects of channels in distributed communication and decision making tasks: A theoretical review and a proposed research paradigm
[AD-A191807] N88-25375
CHARACTERIZATION
Aircraft emissions characterization: TF41-A2, TF30-P103 and TF30-P109 engines
[AD-A192053] N88-24838
Elementary characterization of preimpregnated carbon epoxy T400H/DA0506 from STRUCTIL. Test report M6-577100
[CEAT-047426] N88-24703
Characterization of a 30-GHz IMPATT solid state amplifier
[NASA-TM-100878] N88-24847
CHARGE COUPLED DEVICES
Simple high speed camera with CCD-sensor
[MPIS-8/1987] N88-24940
CHARGE DISTRIBUTION
The electrokinetic behavior of calcium oxalate monohydrate in macromolecular solutions
[NASA-TM-101144] N88-24791
Analysis of lightning field changes during active thunderstorms in Florida N88-25103
CHASSIS
Articulated suspension system
[NASA-CASE-NPO-17354-1-CU] N88-24973
CHEBYSHEV APPROXIMATION
Approximate solution of random differential equation N88-25233
A comparative study of Chebyshev acceleration and residue smoothing in the solution of nonlinear elliptic difference equations
[CWI-NM-R8723] N88-25259
CHEMICAL ANALYSIS
Selective detection in gas chromatography
[AD-A191499] N88-24718
Synthesis and characterization of new phosphazene polymers
[AD-A191508] N88-24771
Geological evolution and analysis of confirmed or suspected gas hydrate localities. Volume 2: Basin analysis, formation and stability of gas hydrates in the Black Sea
[DE88-001052] N88-25023
CHEMICAL BONDS
Liquid carbon
[AD-A191707] N88-24776
A constraint algorithm for maintaining rigid bonds in molecular dynamics simulations of large molecules
[AD-A191663] N88-25277
CHEMICAL COMPOSITION
Aging of carbon fibers
[SNPE-NT-10/86/CRB/NP] N88-24707
Surface composition-reactivity relationships in heterogeneous catalysis
[DE88-006679] N88-24714
Rapidly solidified lightweight durable disk material
[AD-A191697] N88-24775
Geological evolution and analysis of confirmed or suspected gas hydrate localities. Volume 2: Basin analysis, formation and stability of gas hydrates in the Black Sea
[DE88-001052] N88-25023
CHEMICAL PROPERTIES
Chemical compatibility between silicon carbide and a nickel aluminide
[DE88-006188] N88-24706
CHEMICAL PROPULSION
Recent advances in low-thrust propulsion technology
[NASA-TM-100959] N88-25260
CHEMICÁ .. REACTIONS
Chemical compatibility between silicon carbide and a nickel aluminide
[DE88-006188] N88-24706
Electrochemistry in liquid crystals
[AD-A191554] N88-24719
Analysis of molecular mixing and chemical reaction in mixing layer
[AD-A191600] N88-24721
Structural study of the TGMDA-DDS system — epoxy system
[ONERA-RT-4/3346-M] N88-24792
Study of mixing and reaction in the field of a vortex
[AD-A191489] N88-24878
Numerical solutions of the complete Navier-Stokes equations
[NASA-CR-183023] N88-24914
Workshop on Atmospheric OH
[BPT-7/87] N88-25063
Ozone in the atmosphere N88-25064
Laboratory experiments on atmospheric OH reactions N88-25066
Characterization of yttrium aluminum garnet/YAG/using 14 MeV neutron activation
[AD-A191925] N88-25342
Surface interactions relevant to space station contamination problems N88-25401
CHEMICAL REACTORS
Research on hydrotreating catalysts to hydrodeoxygenate biocrude oils N88-25046
Low-temperature thermochemical conversion of high moisture biomass feedstocks N88-25047
CHIPS (ELECTRONICS)
Defect detection and classification in VLSI pattern inspection N88-24871

An improved simulated annealing algorithm for standard cell placement
[NASA-CR-182952] N88-25183
CHLORINE FLUORIDES
Temperature dependence of ultraviolet absorption cross sections of chlorofluoroethanes
[AERONOMICA-ACTA-A-325-1987] N88-24726
CHROMIUM
On quench sensitivity of Cu-Cr alloys
[NASA-TT-20174] N88-24765
CHROMIUM ALLOYS
Fundamental studies of beta phase decomposition modes in titanium alloys
[AD-A191495] N88-24740
The precipitation processes of Cu-Zr-Cr alloys
[NASA-TT-20166] N88-24758
High temperature embrittleness of Cu-Cr alloy
[NASA-TT-20184] N88-24759
CHROMIUM OXIDES
Evaluation of the chromium oxide arc spraying treatment on solar energy collectors
[ETN-88-92564] N88-25053
CIRCUIT BOARDS
The inspection of electronic metallurgical bonds
[AD-A192197] N88-24745
CIRCUIT DIAGRAMS
Defect detection and classification in VLSI pattern inspection N88-24871
CIVIL AVIATION
Competitive assessment of the U.S. civil helicopter industry
[PB88-186325] N88-24574
FAA aviation forecasts fiscal years 1988-1999
[AD-A191711] N88-24576
US civil airmen statistics, 1987
[AD-A191714] N88-24577
General-aviation's view of progress in the aviation weather system N88-25110
CLASSIFICATIONS
A method for discrimination of radar targets using complex natural resonances
[AD-A191848] N88-24832
Automatic discovery of optimal classes
[NASA-TM-101174] N88-25238
CLEAR AIR TURBULENCE
Objective detection and forecasting of Clear-Air Turbulence (CAT): A status report N88-25114
CLOCKS
An investigation of a distributed clock for local area networks with ring topology N88-24924
CLOSED CYCLES
Design of catalytic monoliths for closed-cycle carbon dioxide lasers
[NASA-CR-182963] N88-25185
Analysis of a closed-kinematic chain robot manipulator
[NASA-CR-183031] N88-25206
CLOUDS
SAM 2 data user's guide
[NASA-RP-1200] N88-25094
CLUSTER ANALYSIS
Cluster analysis of multiple planetary flow regimes
[NASA-CR-182931] N88-25418
CMOS
Joint services electronics program
[AD-A190239] N88-24848
COATINGS
Predictive corrosion modeling, volume 1
[AD-A191229] N88-24739
Environmental integrity of coating/metal interface
[AD-A192184] N88-24788
COAXIAL FLOW
Numerical solutions of the complete Navier-Stokes equations
[NASA-CR-183023] N88-24914
COCKPIT SIMULATORS
An enumeration of research to determine the optimal design and use of Army flight training simulators
[AD-A191242] N88-24849
CODING
Analytic and numerical modeling of heat and material transport in electrical hypervelocity guns
[AD-A192178] N88-24655
Joint services electronics program
[AD-A190239] N88-24848
Adaptive local grid refinement in computational fluid mechanics
[AD-A192215] N88-24890
Duct flow nonuniformities for Space Shuttle Main Engine (SSME)
[NASA-CR-179338] N88-24899
COEFFICIENTS
Evaluation of the biot coefficients
[AD-A191643] N88-25265
COGNITION
A systems engineering based methodology for analyzing human electrocortical responses
[AD-A190809] N88-25135
Performance effectiveness and the work/rest cycle
[AD-A191448] N88-25145
Models of incremental concept formation
[AD-A191597] N88-25147
A computational model of motor behavior
[AD-A191179] N88-25152
Selection and effects of channels in distributed communication and decision making tasks: A theoretical review and a proposed research paradigm
[AD-A191807] N88-25375
COHERENT RADIATION
Fast acting optical beam detection and deflection system
[AD-A192161] N88-24954
COINCIDENCE CIRCUITS
Some unsolved problems in modelling self-timed circuits using Petri Nets, series B, number 2
[PB88-181466] N88-24872
COLD ACCLIMATIZATION
Effects of moderate cold and heat stress on the potential work performance of industrial workers. Part 6: The effects of increasing vapour pressure at four air temperatures on the performance and physiology of white females
[PB88-124854] N88-25137
COLLISION AVOIDANCE
Rotorcraft TCAS (traffic alert and collision avoidance system) evaluation: Group 3 results
[AD-A191719] N88-24814
COLLISION RATES
Contributions of autoionizing resonances to the electron collisional excitation rates for Be-like ions
[AD-A190924] N88-25275
COLLISIONS
The multistring model VENUS for ultrarelativistic heavy ion collisions
[DE88-007666] N88-25284
COLOR
CIMAG2: The computer program to generate color images
[AD-A191847] N88-25175
COLOR VISION
Design and testing of a luminance and chrominance stabilization system for a computer-controlled color display
[AD-A191922] N88-25159
COMBINATORIAL ANALYSIS
Algorithms and data structures for an expanded family of matroid intersection problems
[AD-A191482] N88-25213
COMBUSTION
Soviet combustion research
[PB88-182324] N88-24730
The thermodynamic properties of quinoline and isoquinoline
[DE88-001218] N88-24735
Evaluation of manure as a feedstock for gas turbines N88-25050
COMBUSTION CHAMBERS
An empirical model of the effects of curvature and convergence on dilution jet mixing
[NASA-TM-100896] N88-24640
Thrust chamber thermal barrier coating techniques
[NASA-TM-100933] N88-24690
Combustion behavior of the vitiator. Experimental results of a second test series
[VTH-LR-509] N88-24734
Evaluation of manure as a feedstock for gas turbines N88-25050
COMBUSTION PHYSICS
On the structure, propagation, extinction and stability of laminar premixed flames in dissociation equilibrium N88-24728
Combustion of PMMA, PE and PS in a ramjet
[VTH-LR-514] N88-24733
CFD benefits, goals, stepping-stones and techniques. Proposals for the scientific programme of the European Research Centre on flow, turbulence and combustion — computational fluid dynamics
[CFDU/88/1] N88-24894
COMBUSTION PRODUCTS
Evaluation of manure as a feedstock for gas turbines N88-25050
COMET NUCLEI
The evolution of cometary activity N88-25416
COMETS
The evolution of cometary activity N88-25416
COMMONALITY
Class 2 design update for the family of commuter airplanes
[NASA-CR-182681] N88-24629
COMMUNICATION
Evaluation of the communications impact of a low power arcjet thruster
[NASA-TM-100926] N88-24882
COMMUNICATION EQUIPMENT
Information and stochastic systems
[AD-A192167] N88-24838
COMMUNICATION NETWORKS
Propagation management for no-acknowledge HF communications links N88-24843
Human problem solving in complex dynamic environments
[AD-A190788] N88-25142
COMMUNICATION SATELLITES
Experimental radio frequency link for Ka-band communications applications
[NASA-TM-100824] N88-24859
Simulations of the electrostatic charging of ESA communications satellites
[ESA-STM-239] N88-24870
COMPACTING
Dynamic consolidation of metal powders
[AD-A192126] N88-24744
COMPARATORS
An electrostatic potential comparator
[AD-A192051] N88-25177
COMPARISON
Space station habitability recommendations based on a systematic comparative analysis of analogous conditions
[NASA-CR-3943] N88-25372
COMPATIBILITY
Chemical compatibility between silicon carbide and a nickel aluminide
[DE88-006188] N88-24708
A compatible encapsulant for explosives
[DE88-007212] N88-24806
Sulfur-tolerant anode materials
[DE88-001034] N88-25054
COMPILERS
EPL (Equational Programing Language) system design: Intermediate processing steps
[AD-A191203] N88-25169
COMPLEX SYSTEMS
Accurate multigrid solution of the Euler equations on unstructured and adaptive meshes
[NASA-CR-181679] N88-24808
Application of advanced grid generation techniques for flow field computations about complex configurations
[NASA-CR-183049] N88-24922
Human problem solving in complex dynamic environments
[AD-A190788] N88-25142
COMPONENT RELIABILITY
Small scale bipolar nickel-hydrogen testing
[NASA-TM-100936] N88-25059
COMPOSITE MATERIALS
Mixed-mode fracture of uniaxial fiber reinforced composites
[AD-A191629] N88-24700
Interfacial shear phenomena in graphite epoxy composites under impact loading using dynamic moire interferometry
[DE88-006773] N88-24709
Functional and mechanical analysis of continuous media-application to the study of elastic composites with periodic structure: Homogenization
[NASA-TT-20188] N88-24710
The 700 F properties of autoclave cured PMR-2 composites
[NASA-TM-100923] N88-24712
Status and prognosis for alternative engine materials
[NASA-TM-100903] N88-24749
New polyisoimides: An approach to in situ rigid-rod polyimide formation
[AD-A191665] N88-24773
High strength/sigh modulus aromatic heterocyclic ABA block copolymers
[AD-A191666] N88-24774
Nondestructive testing using ultrahigh frequencies
[CERT-5/1333-MO] N88-24984
COMPOSITE STRUCTURES
Interaction of ultrasonic waves with composite plates
[AD-A191879] N88-24702
Shape stability in composites N88-24706
The stress analysis of ceramic, polymeric, and metallic composite systems by the finite element method N88-25004
COMPRESSIBLE BOUNDARY LAYER
Theoretical investigation of 3-D shock wave-turbulent boundary layer interactions, part 6
[AD-A191546] N88-24882
Spatial stability of a compressible mixing layer
[NASA-CR-181671] N88-24916

COMPRESSIBLE FLOW
Boundary layer transition
[CERT-OA-37/5018-AYD] N88-24595
Compressible flow in a pie-shaped cylinder rotating about the vertex N88-24604
Accurate multigrid solution of the Euler equations on unstructured and adaptive meshes
[NASA-CR-181679] N88-24606
Internal fluid dynamics within a nonspinning partially liquid-filled shell due to burster rupture
[AD-A191055] N88-24874
A variational finite element method for three-dimensional, steady, compressible, viscous flows N88-24904
COMPRESSING
Dynamic shear band development in plane strain
[AD-A190915] N88-24988
COMPRESSION LOADS
Investigation of the effect of minimum loads and compression of load spectra on the prediction capacities of the ONERA crack model — wings
[ONERA-RTS-33/7169-RY-064-R] N88-24994
COMPRESSIVE STRENGTH
High strength/sigh modulus aromatic heterocyclic ABA block copolymers
[AD-A191666] N88-24774
COMPRESSOR BLADES
Research on aero-thermodynamic distortion induced structural dynamic response of multi-stage compressor blading
[AD-A192169] N88-24584
COMPRESSORS
Experimental vibration damping characteristics of the third-stage rotor of a three-stage transonic axial-flow compressor
[NASA-TM-100948] N88-24642
Forced response unsteady aerodynamics in a multistage compressor N88-24903
COMPUTATION
Quench detection by fluid dynamic means in cable-in-conduit superconductors
[DE88-007269] N88-25359
Comment on non-renormalization theorem in the four dimensional superstrings
[DE88-752551] N88-25367
COMPUTATIONAL FLUID DYNAMICS
Progress and future directions in computational fluid dynamics
[NASA-TM-100091] N88-24579
Prediction of laminar and turbulent flows past single and twin airfoils N88-24589
A transonic small disturbance wing design methodology N88-24590
A formulation for the boundary-layer equations in general coordinates
[NASA-TM-100079] N88-24600
Some rotorcraft applications of computational fluid dynamics
[NASA-TM-100066] N88-24601
Applications of the Navier-Stokes equations to wings and complex configurations using a zonal approach
[NASA-TM-100080] N88-24602
A decade of computer simulations for space shuttle aerodynamics
[NASA-TM-100990] N88-24603
Simulations of a missile with liquid payload under launch conditions
[AD-A191479] N88-24625
Internal fluid dynamics within a nonspinning partially liquid-filled shell due to burster rupture
[AD-A191055] N88-24874
Adaptive local grid refinement in computational fluid mechanics
[AD-A192215] N88-24890
Computational fluid dynamics applied to the prediction of the heat-transfer, mechanical and thermal-stress behavior of heat exchangers
[CFDU/87/7] N88-24893
CFD benefits, goals, stepping-stones and techniques. Proposals for the scientific programme of the European Reserch Centre on flow, turbulence and combustion — computational fluid dynamics
[CFDU/88/1] N88-24894
Three dimensional spectral energy measurement on turbulence subjected to a high degree of plane deformation
[ETN-88-92537] N88-24896
Two dimensional hyperbolic grid generation
[VKI-TN-162] N88-24897
Duct flow nonuniformities for Space Shuttle Main Engine (SSME)
[NASA-CR-179336] N88-24899
Improving the performance of a finite element method using vector analysis on CRAY 1
[ETN-88-92153] N88-24907
Theoretical analysis of laminar incompressible flow in slender channels
[VTH-LR-517] N88-24909
Review of numerical methods for radionuclide transport in three-dimensional porous media, at high Peclet numbers
[CFDU/87/10] N88-25061
NAS: The first year
[NASA-TM-101006] N88-25196
COMPUTATIONAL GRIDS
Incompressible Euler solution on a multiblock grid around a car configuration
[FFA-TN-1987-65] N88-24586
Accurate multigrid solution of the Euler equations on unstructured and adaptive meshes
[NASA-CR-181679] N88-24606
Adaptive local grid refinement in computational fluid mechanics
[AD-A192215] N88-24890
Two dimensional hyperbolic grid generation
[VKI-TN-162] N88-24897
Application of advanced grid generation techniques for flow field computations about complex configurations
[NASA-CR-183049] N88-24922
DOD 1985 world magnetic model: Charts and grid values
[AD-A191484] N88-25080
Adaptive grid refinement for numerical weather prediction
[AD-A192172] N88-25101
Multigrid methods for elliptic Partial Differential Equations (PDEs)
[CWI-NM-R8722] N88-25242
COMPUTER AIDED DESIGN
An OOD (Object-Oriented Design) paradigm for flight simulators
[AD-A191097] N88-24647
Computer aided design of monolithic microwave and millimeter wave integrated circuits and subsystems
[AD-A191593] N88-24852
Calculation of root-mean-square loads
[BLL-M-37776-(5828.4)] N88-25015
The Environment for Application Software Integration and Execution (EASIE), version 1.0. Volume 3: Program execution guide
[NASA-TM-100575] N88-25184
The Sizing and Optimization Language, (SOL): Computer language for design problems
[NASA-TM-100565] N88-25190
COMPUTER AIDED MAPPING
Reports on cartography and geodesy. Series 1, no. 99
[ETN-88-92387] N88-25025
West German Geodetic Working Group: Official topographic-cartographic information system (ATKIS), content description N88-25026
West German Geodetic Working Group: Official topographic-cartographic information system (ATKIS), technical conception N88-25027
Vector graphics and raster data processing for spatial information systems N88-25028
Digitizing the traffic network of JOG 250 by scanning — JOG 250 map N88-25029
Tests for the automatic pattern recognition of building surfaces by the TK 50 N88-25030
Creation of digital topographic models with the ALK-GIAP. The DLM 25 as an example N88-25031
Topographic data processing for environmental planning N88-25032
Digital maps for an electronic traffic guide N88-25033
Development in data structures in PHOCUS for digital mapping N88-25034
State of development of ALK (October 1986) N88-25035
Vectorization of raster algorithms for elevation data processing N88-25036
Geometric rectangular data file (GERD): An aid to the rapid access to position data N88-25037
Recent developments in software and hardware by Scitex Co. — computer aided mapping N88-25038
Personal computer as a workstation in a cartographic automation system? N88-25039
Use of modern scanner techniques in cartography N88-25040
COMPUTER DESIGN
Optical computer and optical methods for data processing N88-24939
COMPUTER GRAPHICS
An analytic model for aerodynamic shapes
[AD-A191573] N88-24583
Airplane runway performance monitoring system
[NASA-CASE-LAR-13854-1-CU] N88-24621
The coordination of multiple robotic manipulators
[AD-A190869] N88-24963
Vector graphics and raster data processing for spatial information systems N88-25028
Personal computer as a workstation in a cartographic automation system? N88-25039
Knowledge acquisition tool implementation
[AD-A190415] N88-25164
IGUANA: Interactive graphics utility for automated NEC analysis
[AD-A191760] N88-25174
A graphical, intelligent interface for discrete-event simulations
[DE88-000522] N88-25181
Considerations involved in the display of finite element results using animation
[DE88-007561] N88-25189
The ISI (Information Sciences Institute) grapher manual
[AD-A192198] N88-25200
Engineering drawings and changes: Storing and controlling by the tens of terrabytes
[DE88-007605] N88-25387
COMPUTER INFORMATION SECURITY
Computer resource management technology program (PE 64740F). Task no. 9: Advanced user authentication
[PB88-183066] N88-25163
COMPUTER NETWORKS
Network architecture for OPS5
[DE88-002602] N88-25194
COMPUTER PROGRAMMING
An OOD (Object-Oriented Design) paradigm for flight simulators
[AD-A191097] N88-24647
Calculation of assemblies bonded with quasi-elastic adhesives
[REPT-47-632/F] N88-24793
Automated cartographic generalization for linear map features N88-25021
LispSEI: The programmer's manual
[AD-A191632] N88-25172
CIMAG2: The computer program to generate color images
[AD-A191847] N88-25175
Beyond Ada: Generating Ada code from equational specifications
[AD-A191866] N88-25176
System overview: Teragon 4000, an image processing equipment at FOA 3
[FOA-C-30465-3.3] N88-25179
KA-PROLOG. KAP-computer: Computer model and instructions set
[ETN-88-91948] N88-25186
The Sizing and Optimization Language, (SOL): Computer language for design problems
[NASA-TM-100565] N88-25190
Introduction to compliance in programming of robots
[ETN-88-92189] N88-25201
Modeling of geometric reasoning for robot programming
[ETN-88-92290] N88-25202
Design of partially replicated distributed database systems: An integrated methodology N88-25363
COMPUTER PROGRAMS
A system status monitor for the National Aerospace Plane
[AD-A190681] N88-24624
An OOD (Object-Oriented Design) paradigm for flight simulators
[AD-A191097] N88-24647
Automated test device for FASR (Fixed Array Surveillance Radar) beam steering componentry
[AD-A191650] N88-24829
Practical VLF/LF radio test system
[AD-A191768] N88-24831
Transient particle deposition in a boundary layer of impulsive flow over a flat plate
[AD-A191537] N88-24880
SOLA-DM: A numerical solution algorithm for transient three-dimensional flows
[DE88-007159] N88-24913
The development of KENO and the calculation of differential parameters with KENO
[DE88-006176] N88-25166
Annotated computer output for split plot design: SAS GLM
[AD-A190800] N88-25167
A general approach for automating source code verification
[AD-A191461] N88-25170
Research in enumeration and graph theory with applications to computer science
[AD-A191567] N88-25171
IGUANA: Interactive graphics utility for automated NEC analysis
[AD-A191760] N88-25174
CIMAG2: The computer program to generate color images
[AD-A191847] N88-25175

An electrostatic potential comparator
[AD-A192051] N88-25177
Design of catalytic monoliths for closed-cycle carbon dioxide lasers
[NASA-CR-182983] N88-25185
KA-PROLOG. KAP-computer: Computer model and instructions set
[ETN-88-91948] N88-25186
The ISI (Information Sciences Institute) grapher manual
[AD-A192198] N88-25200
State of tuning
[NASA-TT-20195] N88-25205
PAFEC level 6.2 application program
[AD-A191037] N88-25209
NFEARS: A nonlinear adaptive finite element solver, part 1
[AD-A191823] N88-25215
A perspective of PC-based probabilistic risk assessment
[DE88-006715] N88-25251
QN3D: A 3-dimensional quasi-neutral hybrid particle-in-cell code with applications to the tilt mode instability in field reversed configurations N88-25325
Department of Defense statement on the X-ray Lithography Program to the Research and Development Subcommittee of the House Armed Services Committee of 100th Congress, second session
[AD-A191854] N88-25341
Defense Technical Information Center cataloging guidelines
[AD-A192200] N88-25382

COMPUTER STORAGE DEVICES

A computational model of motor behavior
[AD-A191179] N88-25152

COMPUTER SYSTEMS PERFORMANCE

Beyond Ada: Generating Ada code from equational specifications
[AD-A191866] N88-25176
Solving bidiagonal systems of linear equations on the CDC CYBER 205
[CWI-NM-R8725] N88-25187

COMPUTER SYSTEMS PROGRAMS

Automated analysis of crack growth rate for obtaining da/dN versus delta K relation
[FFA-TN-1987-70] N88-24996

COMPUTER TECHNIQUES

Effectiveness evaluation of fault-tolerant multiprocessor systems
[AD-A191688] N88-25158
A multiprocessor data flow accelerator module
[DE88-007587] N88-25161
Feature extraction using the Hough transform
[AD-A190679] N88-25165
Optical symbolic processor for expert system execution
[AD-A192005] N88-25296

COMPUTERIZED SIMULATION

A decade of computer simulations for space shuttle aerodynamics
[NASA-TM-100990] N88-24603
Simulations of a missile with liquid payload under launch conditions
[AD-A191479] N88-24825
Computational design of low aspect ratio wing-winglet configurations for transonic wind-tunnel tests
[NASA-CR-183021] N88-24830
Analytic and numerical modeling of heat and material transport in electrical hypervelocity guns
[AD-A192178] N88-24655
Use of a two-stage light-gas gun as an injector for electromagnetic railguns
[DE88-007200] N88-24657
Simulations of the electrostatic charging of ESA communications satellites
[ESA-STM-239] N88-24670
Computer simulation of turbulent combustion in reciprocating engines
[CFDU/87/11] N88-24725
Calculation of assemblies bonded with quasi-elastic adhesives
[REPT-47-832/F] N88-24793
Numerical simulations of the flat-plate laminar boundary layer in subsonic and supersonic flow
[PDR/CFDU-IC/36] N88-24895
Numerical simulation of nonlinear structural dynamics of large scale unsteady flow
[ETN-88-92156] N88-24908
An investigation of a distributed clock for local area networks with ring topology N88-24924
Finite element analysis of an underground structure
[AD-A191747] N88-24991
Yaw dynamics of horizontal axis wind turbines
[DE88-001137] N88-25055
Report on project WIND: Preliminary experiments w ith the UK Meteorological Office mesoscale model, September 1987
[AD-A191821] N88-25099
Analysis of lightning field changes during active thunderstorms in Florida N88-25103
LispSEI: The programmer's manual
[AD-A191632] N88-25172
A graphical, intelligent interface for discrete-event simulations
[DE88-000522] N88-25181
Computer simulation of uphill diffusion in ternary ionic system
[NASA-TT-20194] N88-25285
Accelerator research studies
[DE88-007124] N88-25290
Determination of doping profiles in silicon from resistivity measurements via the four-point probe in combination with layer strippings via anodic oxidation N88-25347

COMPUTERS

Computer and model changes at National Meteorological Center (NWC) N88-25116

CONCENTRATION (COMPOSITION)

Selective detection in gas chromatography
[AD-A191499] N88-24718
Preferential surface adsorption in miscible blends of polystyrene and poly(vinyl methyl ether)
[AD-A191451] N88-24789
Workshop on Atmospheric OH
[BPT-7/87] N88-25063
Measurement of atmospheric OH with laser differential optical absorption spectroscopy (LDOAS) N88-25068
Tropospheric OH measurements by long path absorption with rapid spectral concordance N88-25069
Determination of tropospheric H concentrations by a double-pulsed UV laser method N88-25070
Development of continuous wave laser frequency modulation of OH in tropospheric concentrations range N88-25073
Evaluation of the toxicity of products from the thermal degradation of materials
[ETN-88-91995] N88-25130
Characterization of yttrium aluminum garnet/YAG/using 14 MeV neutron activation
[AD-A191925] N88-25342

CONCRETES

Design of overlays for rigid airport pavements
[DOT/FAA/PM-87/19] N88-24652

CONCURRENT PROCESSING

Design, implementation and evaluation of an operating system for a network of transputers
[AD-A186593] N88-25193

CONDENSERS (LIQUEFIERS)

Tower evaporator
[NASA-CASE-NPO-15609-2] N88-24815

CONDUCTION BANDS

Recent data on Si:As impurity band conduction multiplexed arrays
[AD-A191752] N88-25340

CONFERENCES

Proceedings of the American Society for Composites
[AD-A189661] N88-24693
High resolution radar techniques: Five contributions to MILINF 86
[PB88-172721] N88-24821
Optics: Perspectives for Measurement Techniques and Signal Processing for Flight Guidance — conference
[DFVLR-MITT-87-21] N88-24928
Proceedings of the 1987 Biomass Thermochemical Conversion Contractors' Review Meeting
[DE88-006730] N88-25041
Workshop on Atmospheric OH
[BPT-7/87] N88-25063
The Effect of the Ionosphere on Communication, Navigation and Surveillance Systems Based on Ionosph eric Effects Symposium held on 5-7 May 1987 in Springfield, Virginia
[AD-A191855] N88-25081
Dynamics Explorer-2 measurements during an isolated auroral substorm
[AD-A191202] N88-25091
Infinite dimensional dynamical systems and their finite dimensional analogues
[AD-A192041] N88-25216
A Study of Space Station Contamination Effects — conference
[NASA-CP-3002] N88-25390

CONFINEMENT

A study of runaway electron confinement in the ASDEX tokamak
[DE88-007327] N88-25319

CONGESTION

Communications using channels formed by meteor bursts
[AD-A192088] N88-24834

CONGRESSIONAL REPORTS

Department of Defense Statement on the Technology Base to the Subcommittee on Defense Industry and Technology of the Committee on Armed Services, United States Senate, 100th Congress, second session
[AD-A191839] N88-25376
Department of Defense statement on defense agency research and development to the Subcommittee on Defense of the Committee on Appropriations, United States House of Representatives, 100th Congress, second session
[AD-A191840] N88-25377
Department of Defense Statement on the Balanced Technology Initiative to the Committee on Armed Services, United States Senate, 100th Congress, second session
[AD-A191841] N88-25378
The FY 1989 Department of Defense statement on the Science and Technology Program to 100th Congress, second session
[AD-A191843] N88-25380

CONICAL BODIES

Almond test body — for microwave anechoic chambers
[NASA-CASE-LAR-13747-1] N88-24845

CONNECTORS

Toggle release
[NASA-CASE-MSC-21354-1] N88-24969

CONSTRAINTS

A constraint algorithm for maintaining rigid bonds in molecular dynamics simulations of large molecules
[AD-A191663] N88-25277

CONTAINERS

Sample decomposition in sealed teflon vessels
[NASA-TT-20189] N88-24798

CONTAINMENT

Fuel containment concepts: Transport category airplanes
[DOT/FAA/CT-87/18] N88-24807

CONTAMINANTS

A Study of Space Station Contamination Effects — conference
[NASA-CP-3002] N88-25390
Neutral environment for space station N88-25391
Space station neutral external environment N88-25392
Contaminant ions and waves in the space station environment N88-25393
Space station particulate contamination environment N88-25397
The particulate environment surrounding the space station: Estimates from the PACS data N88-25398
Effects of meteoroids and space debris on the particulate environment for space station N88-25399
Contamination of optical surfaces — Space Station N88-25400
Surface interactions relevant to space station contamination problems N88-25401
Contamination of the space station environment by vented chemicals N88-25403

CONTINUITY (MATHEMATICS)

Computation and characteristics of pulsatile multi-bifurcation flow N88-24729

CONTINUOUS RADIATION

The loss parameters for very short bunches
[CEBAF-PR-88-005] N88-25291

CONTINUOUS WAVE LASERS

Distributed feedback lasers
[NASA-CR-4154] N88-24948

CONTINUUM FLOW

Energy efficient continuous flow ash lockhopper
[NASA-CASE-NPO-16985-1-CU] N88-24814

CONTINUUMS

Continuum theories for fluid-particle flows: Some aspects of lift forces and turbulence
[DE88-007038] N88-24898

CONTRAROTATING PROPELLERS

Summary of low-speed wind tunnel results of several high-speed counterrotation propeller configurations
[NASA-TM-100945] N88-24597

CONTROL SYSTEMS DESIGN

Analysis and design of detection filters within closed-loop systems N88-24980
Vibration protection of inelastic structures by means of active and passive control N88-25001
The efficacy of using human myoelectric signals to control the limbs of robots in space
[NASA-CR-182901] N88-25155
Electronic controller for reciprocating rotary crystallizer
[NASA-TM-101140] N88-25354

CONTROL THEORY

Attitude control laws for gas-jet spacecraft N88-24643
Estimation and control of distributed models for certain elastic systems arising in large space structures
[AD-A192120] N88-24666

A feedback linearization approach to spacecraft control using momentum exchange devices
[NASA-CR-172057] N88-24668
Dynamics of a flexible orbiting platform with MRMS
[ISSN-0285-6808] N88-24673
Automatic feedback control of a rigid body for finite displacements N88-24674
The coordination of multiple robotic manipulators
[AD-A190869] N88-24963
Real-time implementation of a kinematic optimization scheme for seven-degree-of-freedom redundant robots with spherical wrists
[DE88-006785] N88-24974
Mixed min-max optimization problem with restrictions N88-25232

CONTROL UNITS (COMPUTERS)
Design and testing of a luminance and chrominance stabilization system for a computer-controlled color display
[AD-A191922] N88-25159

CONTROLLERS
A universal computer control system for motors
[NASA-CASE-NPO-17134-1-CU] N88-24864
Electronic controller for reciprocating rotary crystallizer
[NASA-TM-101140] N88-25354

CONVECTION
Taiwan area mesoscale experiment: P-3 aircraft operations summary
[PB88-169073] N88-25098
Dendritic growth in the presence of convection N88-25328

CONVECTION CLOUDS
Ice formation on aircraft
[ETN-88-92154] N88-25104

CONVECTIVE FLOW
Acoustic convective system
[NASA-CASE-NPO-17278-1-CU] N88-24818
Dendritic growth in the presence of convection N88-25328

CONVECTIVE HEAT TRANSFER
Acoustic convective system
[NASA-CASE-NPO-17278-1-CU] N88-24818

CONVERGENCE
An empirical model of the effects of curvature and convergence on dilution jet mixing
[NASA-TM-100896] N88-24640
Gram-Schmidt implementation of a linearly constrained adaptive array
[AD-A191651] N88-25198
A concurrent neural network algorithm for the traveling salesman problem
[DE88-006981] N88-25208
Stability and convergence of the Peaceman-Rachford ADI method for initial-boundary value problems
[CWI-NM-R8724] N88-25243
Optimal discrete-time LQR problems for parabolic systems with unbounded input: Approximation and convergence
[NASA-CR-181673] N88-25247
On the use of convergent beam electron diffraction for identification of antiphase boundaries in GaAs grown on Si
[DE88-008220] N88-25382

CONVERGENT-DIVERGENT NOZZLES
Nozzle fabrication technique
[NASA-CASE-MSC-21299-1] N88-24684

CONVEXITY
A primal-dual algorithm for the computation of the minimum of a convex function on the intersection of convex functions, and its application in data analysis
[RR-638-M] N88-25217

COPOLYMERS
High strength/sigh modulus aromatic heterocyclic ABA block copolymers
[AD-A191666] N88-24774
Diffusion of homopolymers into nonequilibrum diblock copolymer structures
[DE88-005306] N88-24794

COPPER
On quench sensitivity of Cu-Cr alloys
[NASA-TT-20174] N88-24765

COPPER ALLOYS
Strain hardening at large strains in aluminum alloys
[DE88-007415] N88-24737
Characterization of the 2219 Cegedur alloy. Data acquisition of the fracture mechanics — aircraft construction materials
[REPT-48-442/F] N88-24751
Aluminum alloy
[NASA-CASE-LAR-13924-1-CU] N88-24753
The precipitation processes of Cu-Zr-Cr alloys
[NASA-TT-20168] N88-24758
High temperature embrittleness of Cu-Cr alloy
[NASA-TT-20184] N88-24759
Critical cooling rates on solution treatment of Cu-Cr and Cu-Be alloys
[NASA-TT-20163] N88-24760
On the reversion phenomena of Cu-3 percent Ti alloys
[NASA-TT-20170] N88-24762
On the abnormal phenomena observed in the electrical resistivity measurement during the decomposition process of saturated Cu-Fe alloys
[NASA-TT-20183] N88-24869

COPPER OXIDES
Vacancy ordering in the basal plane of YBa2Cu3O(sub)z
[DE88-004572] N88-25348

CORIOLIS EFFECT
Effects of Coriolis acceleration on the vibrations of spinning structures N88-24966

CORRELATION COEFFICIENTS
Variances and higher order correlation coefficients: Continued
[RR-655-M] N88-25219

CORROSION
Predictive corrosion modeling, volume 1
[AD-A191229] N88-24739
Environmental integrity of coating/metal interface
[AD-A192184] N88-24786

CORROSION PREVENTION
The influence of cathodic protection on erosion-corrosion of metals and model alloys
[AD-A191613] N88-24742
An investigation of ceramic coatings for protection of SiC from high-temperature corrosion
[DE88-007873] N88-24790

CORROSION RESISTANCE
Improving knowledge of the corrosion behavior of aluminum alloys of the 7XXX series
[REPT-48-451/F] N88-24750
Characterization of 7090 and 7091 profiles made with Cegedur powder — powder metallurgy, aircraft construction materials
[REPT-48-441/F] N88-24752

CORROSION TESTS
Improving knowledge of the corrosion behavior of aluminum alloys of the 7XXX series
[REPT-48-451/F] N88-24750

CORRUGATED PLATES
Stiffened titanium panels
[NASA-CASE-LAR-13814-1] N88-24816

COSMIC RAYS
Observations of cosmic rays in the outer heliosphere
[NASA-CR-182942] N88-25425

COSMOLOGY
Light propagation through gravitationally perturbed Friedmann universes N88-25307
Inevitable inflation in Einstein-Cartan theory with improved energy-momentum tensor with spin
[NASA-TM-101146] N88-25365
The geometry of the Virasoro group for physicists
[DE88-007374] N88-25366

COUNTERMEASURES
Laser countermeasure impacts and penalties
[DE88-006871] N88-24947

COUPLED MODES
Studies of spectral line ratio fluctuations using Inductively Coupled Plasma (ICP) light
[IRF-PREPRINT-100] N88-25311

COUPLING
Optical pressure sealing couping (light joint)
[NASA-CASE-MFS-29348-1] N88-25303

COVARIANCE
Annotated computer output for split plot design: SAS GLM
[AD-A190800] N88-25167
Optimal a priori covariance selection for the solution of ill-conditioned nonlinear inverse problems N88-25222

COVERINGS
Hatch cover
[NASA-CASE-MSC-21356-1] N88-24671

CRACK INITIATION
Investigation of the effect of minimum loads and compression of load spectra on the prediction capacities of the ONERA crack model — wings
[ONERA-RTS-33/7169-RY-064-R] N88-24994
Cyclic fatigue damage characteristics observed for simple loadings extended to multiaxial life prediction
[NASA-CR-182126] N88-25016

CRACK PROPAGATION
Composite repair of cracked aluminum alloy aircraft structure
[AD-A190514] N88-24573
Mixed-mode fracture of uniaxial fiber reinforced composites
[AD-A191629] N88-24700
Predictive corrosion modeling, volume 1
[AD-A191229] N88-24739
Role of cracks in the creep of structural polycrystalline ceramics
[AD-A191485] N88-24770
Environmental effects on slow crack growth in silicon nitride
[DE88-007206] N88-24795
Fracture mechanics analysis for short cracks
[AD-A192002] N88-24992
Some stress intensity factor equations
[FFA-TN-1987-07] N88-24995
Automated analysis of crack growth rate for obtaining da/dN versus delta K relation
[FFA-TN-1987-70] N88-24996
Resolved shear stress intensity coefficient and fatigue crack growth in large crystals
[NASA-CR-182137] N88-24997
Self-consistent model for the brittle response of solids N88-24999
Fatigue crack growth due to random loading N88-25017

CRACK TIPS
Determination of the toughness of a brittle material using strain gages
[ETN-88-92540] N88-24993

CRACKING (FRACTURING)
Analysis and developments of failure concepts in fracture mechanics based on research results in the field of component safety topics: J-integral concept; crack resistance curves; dynamic criterion
[V-19/86] N88-25009
Higher frequency ambient noise in the arctic ocean
[AD-A192203] N88-25122

CRACKS
A method for the numerical solution of random Cauchy singular integral equation N88-25234

CRASHWORTHINESS
Peak Acceleration Device (PAD)
[AD-A191639] N88-24611
Fuel containment concepts: Transport category airplanes
[AD-A189818] N88-24799
Fuel containment concepts: Transport category airplanes
[DOT/FAA/CT-87/18] N88-24807

CREEP PROPERTIES
Role of cracks in the creep of structural polycrystalline ceramics
[AD-A191485] N88-24770
Damage by creep fatigue: Influence of the visco-elasticity of the matrix
[PB88-124706] N88-24998

CREW PROCEDURES (INFLIGHT)
Parameter-adaptive model-following for in-flight simulation
[AD-A190567] N88-24645

CREW WORKSTATIONS
Space station architectural elements model study
[NASA-CR-4027] N88-24632

CRITICAL VELOCITY
Open channel flow near the resonance speed N88-24918

CROSS FLOW
The calculation of transonic flow over the shuttle orbiter using slender body theory N88-24606
Cross stream differencing for integral boundary layer equations
[AD-A191744] N88-24688

CRUISING FLIGHT
Inflow measurements made with a laser velocimeter on a helicopter model in forward flight. Volume 1: Rectangular planform blades at an advance ration of 0.15
[NASA-TM-100541] N88-24607
Periodic solutions in aircraft cruise-dash optimization N88-24631

CRUSTAL FRACTURES
Drilling investigation of a young magmatic intrusion beneath the Inyo Domes, Long Valley, California: Structural and textural studies
[DE88-006613] N88-25078

CRYOGENIC EQUIPMENT
Low temperature storage container for transporting perishables to space station
[NASA-CASE-MFS-28248-1] N88-24817

CRYOGENIC WIND TUNNELS
Aerodynamic performance and pressure distributions for a NASA SC(2)-0714 airfoil tested in the Langley 0.3-meter transonic cryogenic tunnel
[NASA-TM-4044] N88-24580
Design study. Manipulator systems for model handling in European transonic wind tunnels
[ETN-88-91944] N88-24651
Method of forming a multiple layer dielectric and a hot film sensor therewith
[NASA-CASE-LAR-13678-1] N88-25355

CRYOGENICS
Thermodynamic modeling of the no-vent fill methodology for transferring cryogens in low gravity
[NASA-TM-100932] N88-24686
CRYSTAL DEFECTS
On the use of convergent beam electron diffraction for identification of antiphase boundaries in GaAs grown on Si
[DE88-008220] N88-25362
CRYSTAL GROWTH
Optical monitoring of protein crystal growth
[NASA-CR-182669] N88-24736
Preparation for microgravity: The role of the microgravity materials science laboratory
[NASA-TM-100906] N88-24811
Joint services electronics program research in electronics
[AD-A192206] N88-24857
Dendritic growth in the presence of convection N88-25328
Two puzzling aspects of protein crystal growth N88-25329
The morphological stability of continuous intergranular phases: Thermodynamic considerations
[DE88-006326] N88-25350
Electronic controller for reciprocating rotary crystallizer
[NASA-TM-101140] N88-25354
Hanging drop crystal growth apparatus and method
[NASA-CASE-MFS-28206-1-SB] N88-25356
Crystal growth apparatus
[NASA-CASE-MFS-28182-1] N88-25357
CRYSTAL LATTICES
Structural studies on La/sub 2/CuO/sub 4+delta/
[DE88-006826] N88-25330
CRYSTAL STRUCTURE
Fundamental studies of beta phase decomposition modes in titanium alloys
[AD-A191495] N88-24740
Superplasticity: A fundamental investigation on deformation mechanism and cavitation phenomena
[AD-A191548] N88-24741
Liquid carbon
[AD-A191707] N88-24776
Raman characterization of AsF5-intercalated vapor grown graphite fibers
[AD-A191709] N88-24778
Structural studies on La/sub 2/CuO/sub 4+delta/
[DE88-006826] N88-25330
Magnetic superlattices
[AD-A191450] N88-25334
CRYSTAL SURFACES
A scientific basis for an alternate cathode architecture
[AD-A191498] N88-24717
CRYSTALLIZATION
Effect of size of precipitates on recrystallization temperatures in Cu-Cr, Cu-Zr, and Cu-Zr-Cr alloys
[NASA-TT-20166] N88-24763
NASA research Program: The roles of fluid motion and other transport phenomena in the morphology of materials
[NASA-CR-182801] N88-25327
Electronic controller for reciprocating rotary crystallizer
[NASA-TM-101140] N88-25354
CRYSTALLOGRAPHY
Influence of carbon fiber surface treatment
[ETN-88-92536] N88-24787
Dendritic growth in the presence of convection N88-25328
CRYSTALS
Joint services electronics program
[AD-A190239] N88-24848
NASA research Program: The roles of fluid motion and other transport phenomena in the morphology of materials
[NASA-CR-182801] N88-25327
CUES
Analysis procedures and subjective flight results of a simulator validation and cue fidelity experiment
[NASA-TM-88270] N88-24834
Eye and head response to an attention cue in a dual task paradigm
[AD-A191052] N88-25143
CURING
Current and future molecular structures of aerospace organic matrix resins N88-24695
The 700 F properties of autoclave cured PMR-2 composites
[NASA-TM-100923] N88-24712
A compatible encapsulant for explosives
[DE88-007212] N88-24806
CURVATURE
An empirical model of the effects of curvature and convergence on dilution jet mixing
[NASA-TM-100898] N88-24840
CURVE FITTING
Simplified curve fits for the transport properties of equilibrium air
[NASA-CR-178411] N88-24911
CURVES (GEOMETRY)
Open or closed curves by regularized B-splines
[RR-652-M] N88-25218
CUTTING
High power axial flow CO2 laser
[ETN-88-91951] N88-24959
CYCLIC COMPOUNDS
Aromatic cyclotriphosphazenes
[NASA-CASE-ARC-11428-3] N88-24892
Structural study of the TGMDA-DDS system — epoxy system
[ONERA-RT-4/3348-M] N88-24792
CYCLIC LOADS
An extended life and performance test of a low-power arcjet
[NASA-TM-100942] N88-24687
Cyclic fatigue damage characteristics observed for simple loadings extended to multiaxial life prediction
[NASA-CR-182126] N88-25016
CYCLOGENESIS
Tropical cyclones, 1987: Central North Pacific
[PB88-188081] N88-25119
CYCLONES
Mariners weather log, volume 32, number 1, Winter 1988
[PB88-173869] N88-25097
CYGNUS CONSTELLATION
Gamma rays from Cygnus X-1: Modeling and nonthermal pair production
[DE88-006830] N88-25426
CYLINDRICAL SHELLS
Forced motion of initially stressed shells and plates N88-25005

D

DAMAGE
Damage by creep fatigue: Influence of the visco-elasticity of the matrix
[PB88-124706] N88-24998
DATA ACQUISITION
Cessna 172 MLS (Microwave Landing System) terminal instrument procedures (TERPS) approach data collection and processing data report
[AD-A191241] N88-24613
Adaptive data acquisition multiplexing system and method
[NASA-CASE-MSC-21170-1] N88-24662
Taiwan area mesoscale experiment: P-3 aircraft operations summary
[PB88-169073] N88-25098
Knowledge acquisition tool implementation
[AD-A190415] N88-25164
SAMS: The synchronization and monitoring system for ATF (Advanced Toroidal Facility) data acquisition provides unified data access for ATF data acquisition
[DE88-007268] N88-25386
DATA BASE MANAGEMENT SYSTEMS
Reports on cartography and geodesy. Series 1, no. 99
[ETN-88-92367] N88-25025
West German Geodetic Working Group: Official topographic-cartographic information system (ATKIS), content description N88-25026
West German Geodetic Working Group: Official topographic-cartographic information system (ATKIS), technical conception N88-25027
Creation of digital topographic models with the ALK-GIAP. The DLM 25 as an example N88-25031
Topographic data processing for environmental planning N88-25032
State of development of ALK (October 1986) N88-25035
Geometric rectangular data file (GERD): An aid to the rapid access to position data N88-25037
Photovoltaic Advanced Research and Development Project, solar radiation research
[DE88-001143] N88-25056
The human genome: Computational challenges
[DE88-006465] N88-25131
The ATF (Advanced Toroidal Facility) Data M Management System
[DE88-007265] N88-25385
DATA BASES
Cessna 172 MLS (Microwave Landing System) terminal instrument procedures (TERPS) approach data collection and processing data report
[AD-A191241] N88-24613
Evaluation of NMC (National Meteorological Center) global analyses: 1979-1987
[PB88-178157] N88-25096
Identification and acoustic characterization of seamounts
[AD-A192204] N88-25123
EPL (Equational Programing Language) system design: Intermediate processing steps
[AD-A191203] N88-25169
Phase diagrams in materials science and the use of the computer in their calculation
[PB88-155262] N88-25364
Defense Technical Information Center cataloging guidelines
[AD-A192200] N88-25382
Design of partially replicated distributed database systems: An integrated methodology N88-25383
DATA CORRELATION
Study of data distributions and functions for the development of thermodynamic equations of state
[PB88-196365] N88-25370
DATA LINKS
Development and validation of transmission measurements techniques of image contrast, utilizing existing IR imagers
[AD-A191471] N88-25079
DATA MANAGEMENT
The ATF (Advanced Toroidal Facility) Data M Management System
[DE88-007265] N88-25385
DATA PROCESSING
Western Pacific Omega validation: Project description
[AD-A191753] N88-24617
Automated test device for FASR (Fixed Array Surveillance Radar) beam steering componentry
[AD-A191650] N88-24829
Information and stochastic systems
[AD-A192167] N88-24838
Optical computer and optical methods for data processing N88-24939
Vectorization of raster algorithms for elevation data processing N88-25036
Development and validation of transmission measurements techniques of image contrast, utilizing existing IR imagers
[AD-A191471] N88-25079
Evaluation of NMC (National Meteorological Center) global analyses: 1979-1987
[PB88-178157] N88-25096
Visual information processing in the perception of features and objects
[AD-A192026] N88-25148
LispSEI: The programmer's manual
[AD-A191632] N88-25172
IGUANA: Interactive graphics utility for automated NEC analysis
[AD-A191760] N88-25174
PAFEC level 6.2 application program
[AD-A191037] N88-25209
Phase diagrams in materials science and the use of the computer in their calculation
[PB88-155262] N88-25364
Defense Technical Information Center cataloging guidelines
[AD-A192200] N88-25382
The ATF (Advanced Toroidal Facility) Data M Management System
[DE88-007265] N88-25385
SAMS: The synchronization and monitoring system for ATF (Advanced Toroidal Facility) data acquisition provides unified data access for ATF data acquisition
[DE88-007268] N88-25386
DATA PROCESSING TERMINALS
Adaptive data acquisition multiplexing system and method
[NASA-CASE-MSC-21170-1] N88-24662
DATA SMOOTHING
A fast and efficient procedure for generalized cross-validation with large data sets. Application to image reconstruction
[RR-669-M] N88-25220
DATA STORAGE
The flying characteristics of the membrane slider bearing N88-24965
DATA STRUCTURES
Development in data structures in PHOCUS for digital mapping N88-25034
EPL (Equational Programing Language) system design: Intermediate processing steps
[AD-A191203] N88-25169
Algorithms and data structures for an expanded family of matroid intersection problems
[AD-A191482] N88-25213
DATA TRANSMISSION
Automated test device for FASR (Fixed Array Surveillance Radar) beam steering componentry
[AD-A191650] N88-24829

DECISION MAKING
Timesharing performance as an indicator of pilot mental workload
[NASA-CR-182807] N88-25150
Representation and decision mechanisms in artificial intelligence
[AD-A191063] N88-25197
A perspective of PC-based probabilistic risk assessment
[DE88-006715] N88-25251
Selection and effects of channels in distributed communication and decision making tasks: A theoretical review and a proposed research paradigm
[AD-A191807] N88-25375
Modeling and evaluation of variable structure organizations
[AD-A191947] N88-25381
DECOMPOSITION
Fundamental studies of beta phase decomposition modes in titanium alloys
[AD-A191495] N88-24740
Sample decomposition in sealed teflon vessels
[NASA-TT-20189] N88-24798
DEFECTS
Harmfulness of defects: Behaviour in service of a delamination in a composite containing many differently oriented layers
[PB88-124714] N88-24705
DEFENSE INDUSTRY
Department of Defense Statement on the Technology Base to the Subcommittee on Defense Industry and Technology of the Committee on Armed Services, United States Senate, 100th Congress, second session
[AD-A191839] N88-25376
DEFENSE PROGRAM
Department of Defense statement on the X-ray Lithography Program to the Research and Development Subcommittee of the House Armed Services Committee of 100th Congress, second session
[AD-A191854] N88-25341
Department of Defense Statement on the Technology Base to the Subcommittee on Defense Industry and Technology of the Committee on Armed Services, United States Senate, 100th Congress, second session
[AD-A191839] N88-25376
Department of Defense statement on defense agency research and development to the Subcommittee on Defense of the Committee on Appropriations, United States House of Representatives, 100th Congress, second session
[AD-A191840] N88-25377
Department of Defense Statement on the Balanced Technology Initiative to the Committee on Armed Services, United States Senate, 100th Congress, second session
[AD-A191841] N88-25378
The Department of Defense report on the merit review process for competitive selection of university research projects and an analysis of the potential for expanding the geographic distribution of research for the Committees on Appropriations, United States Congress
[AD-A191842] N88-25379
The FY 1989 Department of Defense statement on the Science and Technology Program to 100th Congress, second session
[AD-A191843] N88-25380
DEFLECTION
Fast acting optical beam detection and deflection system
[AD-A192161] N88-24954
Plate response analysis using shock tube
[AD-A190828] N88-24987
DEFORMATION
Superplasticity: A fundamental investigation on deformation mechanism and cavitation phenomena
[AD-A191548] N88-24741
Role of cracks in the creep of structural polycrystalline ceramics
[AD-A191485] N88-24770
DEGENERATION
Signal processing with degenerate four-wave mixing
[AD-A191496] N88-24825
DEGRADATION
Shape stability in composites N88-24706
Predictive corrosion modeling, volume 1
[AD-A191229] N88-24739
Environment assisted degradation mechanisms in advanced light metals
[NASA-CR-182907] N88-24746
Evaluation of the toxicity of products from the thermal degradation of materials
[ETN-88-91995] N88-25130
Molecular characterization of structure and bonding in thin film materials
[DE88-006811] N88-25351
DELAMINATING
Thermographic detection of buried debonds
[AD-A192115] N88-24880
Detecting delaminations in CFRP specimens using X-ray techniques
[FFA-TN-1988-04] N88-24704
Harmfulness of defects: Behaviour in service of a delamination in a composite containing many differently oriented layers
[PB88-124714] N88-24705
Local delamination buckling in layered structures N88-24711
DEMODULATORS
A Differential Phase Shift Keying (DPSK) modulator for a frequency hopping short wave system
[FOA-C-30460-3.3] N88-24840
DENDRITIC CRYSTALS
Dendritic growth in the presence of convection N88-25328
DENSE PLASMAS
Application of particle simulations to the NRL laser experiment
[AD-A191641] N88-24953
DENSITY DISTRIBUTION
To relate measurements of gravity and geoid anomalies over the oceans to near surface density distributions
[AD-A192168] N88-25120
DEPLOYMENT
Payload deployment method and system
[NASA-CASE-MSC-21330-1] N88-24660
DEPTH
Construction of approximations to acoustic Green's functions for nonhomogeneous oceans using transmutation
[PB88-185384] N88-25126
DESIGN ANALYSIS
Computational design of low aspect ratio wing-winglet configurations for transonic wind-tunnel tests
[NASA-CR-183021] N88-24830
Design study. Manipulator systems for model handling in European transonic wind tunnels
[ETN-88-91944] N88-24851
A design study of onboard navigation and guidance during aerocapture at Mars
[NASA-CR-172053] N88-24854
Fuel containment concepts: Transport category airplanes
[DOT/FAA/CT-87/18] N88-24807
Designing to safe power limits in hybrid circuits
[DE88-005533] N88-24865
Optimization of reserve lithium thionyl chloride battery electrochemical design parameters
[DE88-007109] N88-24868
Aurora status and plans
[DE88-006476] N88-24955
Applications of fault tree analysis to the design process
[DE88-007048] N88-24982
Limits of design feasibility of multiwing wind turbines with individual articulated wing structure
[ILR-MITT-180] N88-25052
Systems analysis of INTOR-like designs
[DE88-004422] N88-25316
Design studies of low aspect-ratio torsatrons
[DE88-007562] N88-25320
Space station architectural elements and issues definition study
[NASA-CR-3941] N88-25371
DETECTION
User's guide to the Fault Inferring Nonlinear Detection System (FINDS) computer program
[NASA-CR-178410] N88-24819
Fast acting optical beam detection and deflection system
[AD-A192161] N88-24954
Analysis and design of detection filters within closed-loop systems N88-24980
Lightning detection and locating systems N88-25112
Effectiveness evaluation of fault-tolerant multiprocessor systems
[AD-A191688] N88-25158
Quench detection by fluid dynamic means in cable-in-conduit superconductors
[DE88-007269] N88-25359
DETONATION
Timing control system
[NASA-CASE-NPO-16882-1-CU] N88-24863
DEUTERIUM
Effect of hydrogen, deuterium and oxygen on the anelastic properties of refractory alloys
[DE88-007349] N88-24736
DEVELOPING NATIONS
Centre for International Co-Operation and Approriate Technology (CICAT)
[PB88-165501] N88-25389
DIAGNOSIS
Optical diagnostics for a high power, rf-inductively coupled plasma
[DE88-007822] N88-25322
DIATOMIC MOLECULES
A constraint algorithm for maintaining rigid bonds in molecular dynamics simulations of large molecules
[AD-A191663] N88-25277
DICTIONARIES
NASA combined file postings statistics based on NASA thesaurus, Jan. 1988 - July 1988
[NASA-CR-182965] N88-25384
DIELECTRIC PROPERTIES
Deep dielectric charging effects due to high energy electrons in earth's outer magnetosphere
[AD-A192154] N88-25083
Theoretical basis for an experimental test with regard to the origin of VHF (Very High Frequency) radiation from natural lightning
[DE88-007535] N88-25102
DIELECTRICS
Arcing and rf signal generation during target irradiation by a high-energy, pulsed neutral particle beam
[DE88-007169] N88-24864
Born-type reconstruction of material parameters of an inhomogeneous, lossy dielectric slab from reflected-field data
[PB88-188958] N88-25261
Molecular characterization of structure and bonding in thin film materials
[DE88-006811] N88-25351
Method of forming a multiple layer dielectric and a hot film sensor therewith
[NASA-CASE-LAR-13678-1] N88-25355
DIESEL ENGINES
Servojet retrofit
[AD-A191075] N88-24964
DIFFERENCE EQUATIONS
A comparative study of Chebyshev acceleration and residue smoothing in the solution of nonlinear elliptic difference equations
[CWI-NM-R8723] N88-25259
DIFFERENTIAL EQUATIONS
Computational sciences
[AD-A190826] N88-25226
Numerical solutions to stochastic difference equations N88-25229
Approximate solution of random differential equation N88-25233
DIFFRACTION
Joint services electronics program
[AD-A191749] N88-24853
DIFFUSION
Chemical compatibility between silicon carbide and a nickel aluminide
[DE88-006188] N88-24708
Diffusion of homopolymers into nonequilibrum diblock copolymer structures
[DE88-005306] N88-24794
DIFFUSIVITY
Calculation of oxidation rates for iron in CO-CO2
[DE88-007313] N88-24757
DIGITAL DATA
Reports on cartography and geodesy. Series 1, no. 99
[ETN-88-92387] N88-25025
Digital maps for an electronic traffic guide N88-25033
Development in data structures in PHOCUS for digital mapping N88-25034
DIGITAL NAVIGATION
Digital fiber optic displacement sensors N88-24937
DIGITAL SIMULATION
CFD benefits, goals, stepping-stones and techniques. Proposals for the scientific programme of the European Reserch Centre on flow, turbulence and combustion --- computational fluid dynamics
[CFDU/88/1] N88-24894
Direct numerical simulations of the PDF's (Probability Density Functions) of a passive scalar in a forced mixing layer
[AD-A192134] N88-25256
DIGITAL SYSTEMS
Automated test device for FASR (Fixed Array Surveillance Radar) beam steering componentry
[AD-A191650] N88-24829
Some unsolved problems in modelling self-timed circuits using Petri Nets, series B, number 2
[PB88-181466] N88-24872
DILUTION
An empirical model of the effects of curvature and convergence on dilution jet mixing
[NASA-TM-100896] N88-24640
DIMENSIONS
Solving time-dependent two-dimensional eddy current problems
[NASA-TM-100875] N88-25239

DISCONNECT DEVICES
Toggle release
[NASA-CASE-MSC-21354-1] N88-24969
DISCRETE FUNCTIONS
Optimal discrete-time LQR problems for parabolic systems with unbounded input: Approximation and convergence
[NASA-CR-181673] N88-25247
DISCRIMINANT ANALYSIS (STATISTICS)
Nonparametric discriminant analysis applied to the extraction and selection of radar target signature features
[AD-A191849] N88-24833
DISCRIMINATION
A method for discrimination of radar targets using complex natural resonances
[AD-A191848] N88-24832
DISPENSERS
A scientific basis for an alternate cathode architecture
[AD-A191496] N88-24717
DISPLACEMENT
Automatic feedback control of a rigid body for finite displacements N88-24874
DISPLACEMENT MEASUREMENT
Digital fiber optic displacement sensors N88-24937
DISPLAY DEVICES
Denver ARTCC evaluation of PROFS (Prototype Regional Observations and Forecast System) mesoscale weather products N88-25117
Eye and head response to an attention cue in a dual task paradigm
[AD-A191052] N88-25143
Design and testing of a luminance and chrominance stabilization system for a computer-controlled color display
[AD-A191922] N88-25159
IGUANA: Interactive graphics utility for automated NEC analysis
[AD-A191760] N88-25174
Considerations involved in the display of finite element results using animation
[DE88-007581] N88-25189
DISSOCIATION
Molecular sources of ionospheric holes
[AD-A191857] N88-25082
DISTRIBUTED FEEDBACK LASERS
Distributed feedback lasers
[NASA-CR-4154] N88-24948
DISTRIBUTED PARAMETER SYSTEMS
Galerkin approximation for inverse problems for nonautonomous nonlinear distributed systems
[NASA-CR-181676] N88-25246
DISTRIBUTED PROCESSING
Low authority control of large space structures using a constrained threshold control formulation N88-24867
Design, implementation and evaluation of an operating system for a network of transputers
[AD-A186593] N88-25193
Design of partially replicated distributed database systems: An integrated methodology N88-25383
DISTRIBUTION (PROPERTY)
Rocket-borne low energy ion measurements in space N88-25412
DISTRIBUTION FUNCTIONS
Symmetrized nearest neighbor regression estimates
[AD-A191998] N88-25254
DISTRIBUTION MOMENTS
Variances and higher order correlation coefficients: Continued
[RR-855-M] N88-25219
DISTRIBUTORS
Harmonic considerations for electrical distribution feeders
[DE88-007849] N88-24880
DIURNAL VARIATIONS
Diurnal variations in optical depth at Mars: Observations and interpretations
[NASA-TM-100057] N88-25420
Interpretation of the northward B sub z (NBZ) Birkeland current system and polar cap convection patterns in terms of the impulsive penetration model
[AERONOMICA-ACTA-A-321-1987] N88-25422
DIVERGENCE
Current flight test experience related to structural divergence of forward-swept wings
[NASA-TM-100445] N88-24633
DMSP SATELLITES
DMSP-SSM/1 NASA algorithm validation using primarily LANDSAT and secondarily DMSP and/or AVHRR visible and thermal infrared satellite imagery
[NASA-CR-182979] N88-25024
DOCUMENTATION
The -mdoc macro package: A software tool to support computer documentation standards
[DE88-000500] N88-25188
DOPED CRYSTALS
Determination of doping profiles in silicon from resistivity measurements via the four-point probe in combination with layer strippings via anodic oxidation N88-25347
DOPPLER EFFECT
Delay-doppler radar imaging
[AD-A191509] N88-24826
Feature extraction using the Hough transform
[AD-A190679] N88-25165
DOPPLER RADAR
Components of an atmospheric lidar system: Doppler wind lidar
[AD-A191222] N88-24951
Observation of stratiform rain with 94 GHz and s-b and Doppler radar
[AD-A192013] N88-25100
Aircraft/lidar turbulence comparison N88-25111
The Federal Aviation Administration/Massachusetts Institute of Technology (FAA/MIT) Lincoln Laboratory Doppler weather radar program N88-25118
DRAG
Experimental investigation of hypersonic aerodynamics
[NASA-CR-182973] N88-24591
Continuum theories for fluid-particle flows: Some aspects of lift forces and turbulence
[DE88-007038] N88-24898
DRAG REDUCTION
Injection of drag reducing additives into turbulent water flows
[AD-A192072] N88-24888
Manipulation of the structure of a turbulent boundary layer N88-24901
DRIFT
Theoretical investigations of drift waves in a magnetic quadrupole N88-25312
DRILLS
Frequency Analysis of Acoustic Emission - Application to machining and welding
[DE88-701478] N88-25262
DROPS (LIQUIDS)
Tower evaporator
[NASA-CASE-NPO-15609-2] N88-24815
The behavior of drop-containing turbulent eddies
[AD-A191669] N88-24883
Simple high speed camera with CCD-sensor
[MPIS-8/1987] N88-24940
Hanging drop crystal growth apparatus and method
[NASA-CASE-MFS-28206-1-SB] N88-25356
Crystal growth apparatus
[NASA-CASE-MFS-28182-1] N88-25357
DRUGS
A cardiostimulant protein from the Australian Red Waratah Sea anemone, Actinia tenebrosa N88-25138
DUCTILITY
The variation of torsional ductility of high-purity aluminum with temperature and strain rate
[DE88-005618] N88-24755
Theoretical and experimental damping values of piping systems at high ductilities
[DE88-006717] N88-24986
DWARF STARS
Duplicity in the solar neighborhood. Part 3: New spectroscopic elements for nine solar-type binary stars
[SER-C-PREPUBL-FASC-18-PT-3] N88-25405
DYNAMIC CHARACTERISTICS
Time-frequency representations for speech signals
[AD-A188661] N88-24819
A dynamic analysis of piezoelectric strained elements
[AD-A191478] N88-24851
Infinite dimensional dynamical systems and their finite dimensional analogues
[AD-A192041] N88-25216
A constraint algorithm for maintaining rigid bonds in molecular dynamics simulations of large molecules
[AD-A191663] N88-25277
DYNAMIC CONTROL
Dynamics and control of turbulent shear flows
[AD-A191527] N88-24879
DYNAMIC LOADS
Dynamic shear band development in plane strain
[AD-A190915] N88-24988
Finite element analysis of an underground structure
[AD-A191747] N88-24991
Dynamic response of plates to moving loads: Structural impedance and finite element methods N88-25000
DYNAMIC MODELS
Nonlinear flying quality parameters based on dynamic inversion
[AD-A192146] N88-24627
DYNAMIC PROGRAMMING
Application of dynamic programming to image registration
[ENST-87E022] N88-25180
DYNAMIC RESPONSE
Research on aero-thermodynamic distortion induced structural dynamic response of multi-stage compressor blading
[AD-A192189] N88-24584
The flying characteristics of the membrane slider bearing N88-24965
Theoretical and experimental damping values of piping systems at high ductilities
[DE88-006717] N88-24986
Dynamic response of plates to moving loads: Structural impedance and finite element methods N88-25000
DYNAMIC STRUCTURAL ANALYSIS
Aircraft aeroelasticity and structural dynamics research at the NASA Langley Research Center: Some illustrative results
[NASA-TM-100627] N88-24598
Current flight test experience related to structural divergence of forward-swept wings
[NASA-TM-100445] N88-24633
Experimental study of active vibration control
[AD-A191454] N88-24989
Dynamic response of plates to moving loads: Structural impedance and finite element methods N88-25000
Reduced order modelling and analytical model modification for structural dynamics and control N88-25006
Analysis and developments of failure concepts in fracture mechanics based on research results in the field of component safety topics: J-integral concept; crack resistance curves; dynamic criterion
[V-19/86] N88-25009
Multishaker modal testing
[NASA-CR-179355] N88-25010
SRM propellant and polymer materials structural test program
[NASA-TP-2821] N88-25013
Single-mode projection filters for modal parameter identification for flexible structures
[NASA-CR-182680] N88-25244
DYNAMICAL SYSTEMS
Reliability of stochastically forced systems (extended version)
[CWI-AM-R8801] N88-24985
Infinite dimensional dynamical systems and their finite dimensional analogues
[AD-A192041] N88-25216

E

E REGION
Low frequency electrostatic turbulence in the polar cap E-region
[DRI-3-88] N88-25077
EARTH ATMOSPHERE
Ozone in the atmosphere N88-25064
Brunt-Doppler ducting of buoyancy waves in a temperature- and wind-stratified atmosphere N88-25086
Linear and nonlinear acoustic wave propagation in the atmosphere
[NASA-CR-4157] N88-25268
EARTH CRUST
The interpretation of crustal dynamics data in terms of plate interactions and active tectonics of the Anatolian Plate and surrounding regions in the Middle East
[NASA-CR-183024] N88-25092
EARTH IONOSPHERE
The Effect of the Ionosphere on Communication, Navigation and Surveillance Systems Based on Ionospheric Effects Symposium held on 5-7 May 1987 in Springfield, Virginia
[AD-A191855] N88-25081
Rocket-borne low energy ion measurements in space N88-25412
EARTH OBSERVATIONS (FROM SPACE)
The role of space borne imaging radars in environmental monitoring: Some shuttle imaging radar results in Asia
[NASA-TM-101178] N88-24844
EARTH ORBITAL ENVIRONMENTS
A Study of Space Station Contamination Effects — conference
[NASA-CP-3002] N88-25390
Neutral environment for space station N88-25391
Space station neutral external environment N88-25392
Contaminant ions and waves in the space station environment N88-25393
Space station induced electromagnetic effects N88-25394
Space station contamination study: Assessment of contaminant spectral brightness N88-25395
Calculation of space station infrared irradiance from atmosphere-induced emissions N88-25396

Space station particulate contamination environment N88-25397
The particulate environment surrounding the space station: Estimates from the PACS data N88-25398
Effects of meteoroids and space debris on the particulate environment for space station N88-25399
Contamination of optical surfaces — Space Station N88-25400
Surface interactions relevant to space station contamination problems N88-25401
Laboratory experiments of relevance to the space station environment N88-25402
Contamination of the space station environment by vented chemicals N88-25403

EARTH ORBITS
Advanced nuclear rocket engine mission analysis
[DE88-006797] N88-24681

EARTH PLANETARY STRUCTURE
DOD 1985 world magnetic model: Charts and grid values
[AD-A191484] N88-25080

EARTH RESOURCES
The application of satellites in connection with the environment
[ETN-88-92474] N88-25020

ECOLOGY
Changes in the Antarctic atmosphere due to the reduction of stratospheric ozone
[ETN-88-92565] N88-25074
Ecological risk factors related to environmental uses of genetically engineered organisms
[DE88-006674] N88-25132

ECONOMIC ANALYSIS
Production costs of hydrocarbon fuels from biomass
[DE88-006667] N88-24804
Technical and economic evaluation of emerging biomass pyrolysis processes for gasoline production N88-25048

EDDY CURRENTS
Solving time-dependent two-dimensional eddy current problems
[NASA-TM-100875] N88-25239

EDGES
Curvature of blended rolled edge reflectors at the shadow boundary contour
[NASA-CR-182974] N88-25300

EFFECTIVENESS
Effectiveness evaluation of fault-tolerant multiprocessor systems
[AD-A191686] N88-25158

EFFICIENCY
Study of light transmission methods from scintillators to optical fiber with wave length shifter
[DE88-701587] N88-25292

EIGENVALUES
Theoretical investigations of drift waves in a magnetic quadrupole N88-25312

EINSTEIN EQUATIONS
Inevitable inflation in Einstein-Cartan theory with improved energy-momentum tensor with spin
[NASA-TM-101146] N88-25365

EJECTA
Effects of meteoroids and space debris on the particulate environment for space station N88-25399

ELASTIC BENDING
The surface crack problem in an orthotropic plate under bending and tension
[NASA-CR-178281] N88-25014

ELASTIC BUCKLING
Local delamination buckling in layered structures N88-24711

ELASTIC DAMPING
Theoretical and experimental damping values of piping systems at high ductilities
[DE88-006717] N88-24986

ELASTIC MEDIA
Functional and mechanical analysis of continuous media-application to the study of elastic composites with periodic structure: Homogenization
[NASA-TT-20188] N88-24710

ELASTIC PLATES
Estimation and control of distributed models for certain elastic systems arising in large space structures
[AD-A192120] N88-24666

ELASTIC PROPERTIES
Mixed-mode fracture of uniaxial fiber reinforced composites
[AD-A191629] N88-24700
Vibration protection of inelastic structures by means of active and passive control N88-25001
Vibrations of rotating thick or thin rings N88-25003

ELASTIC SCATTERING
Nuclear structure studies at intermediate energies
[DE88-006663] N88-25271

ELASTIC WAVES
Remote sensing of acoustic properties of shallow water sediments: A review
[AD-A192107] N88-25267

ELASTOPLASTICITY
Theoretical and experimental damping values of piping systems at high ductilities
[DE88-006717] N88-24986

ELECTRIC ARCS
Arc-textured metal surfaces for high thermal emittance space radiators
[NASA-TM-100894] N88-24754

ELECTRIC BATTERIES
An overview of advanced battery development at Sandia National Laboratories
[DE88-006823] N88-24867
Optimization of reserve lithium thionyl chloride battery electrochemical design parameters
[DE88-007109] N88-24868

ELECTRIC CHARGE
The theory of random alloys
[DE88-006408] N88-24756
Development of test methods for the electrostatic properties of nonhomogeneous fabrics, phase 2
[AD-A190853] N88-24767
Electronic and ionic transport in polymers
[AD-A191642] N88-24772

ELECTRIC CONNECTORS
Studies of optical matrix multiplication and reconfigurable optical interconnect concepts
[AD-A191635] N88-25295

ELECTRIC CORONA
Theoretical basis for an experimental test with regard to the origin of VHF (Very High Frequency) radiation from natural lightning
[DE88-007535] N88-25102

ELECTRIC DISCHARGES
Electrostatic discharge test apparatus
[NASA-CASE-MSC-21094-1] N88-24941
Deep dielectric charging effects due to high energy electrons in earth's outer magnetosphere
[AD-A192154] N88-25083
Theoretical basis for an experimental test with regard to the origin of VHF (Very High Frequency) radiation from natural lightning
[DE88-007535] N88-25102
Plasma neutralizer work at BNL (Brookhaven National Laboratory)
[DE88-007046] N88-25317

ELECTRIC FIELDS
Electromagnetic penetration into a conducting circular cylinder through a narrow slot, TE case
[AD-A191602] N88-24828
Electric field measurement by S-520-9 sounding rocket using the time of flight technique of lithium ion beam
[ISAS-RN-367] N88-25095
Space station induced electromagnetic effects N88-25394

ELECTRIC IGNITION
Electrical ignition of HAN-based liquid propellants
[AD-A191349] N88-24801

ELECTRIC MOTOR VEHICLES
A microcomputer-based control and simulation of an advanced IPM (Interior Permanent Magnet) synchronous machine drive system for electric vehicle propulsion
[DE88-006735] N88-24859

ELECTRIC MOTORS
A microcomputer-based control and simulation of an advanced IPM (Interior Permanent Magnet) synchronous machine drive system for electric vehicle propulsion
[DE88-006735] N88-24859

ELECTRIC POTENTIAL
An electrostatic potential comparator
[AD-A192051] N88-25177

ELECTRIC POWER SUPPLIES
Magnetically switched power supply system for lasers
[NASA-CASE-NPO-16402-2] N88-24862

ELECTRIC POWER TRANSMISSION
Harmonic considerations for electrical distribution feeders
[DE88-007849] N88-24860

ELECTRIC PROPULSION
Performance and long duration test of a 30 kw thermal arcjet engine
[AD-A190962] N88-24677
Performance of a hydrogen pulsed electrothermal thruster. Strategic defense initiative organization innovative science and technology. SBIR, phase 1
[AD-A191999] N88-24679

ELECTRICAL MEASUREMENT
Electrochemistry in near-critical and supercritical fluids. 6: The electrochemistry of ferrocene and phenazine in acetonitrile between 25C and 300C
[AD-A192171] N88-24723

ELECTRICAL PROPERTIES
The inspection of electronic metallurgical bonds
[AD-A192197] N88-24745

ELECTRICAL RESISTANCE
Liquid carbon
[AD-A191707] N88-24776

ELECTRICAL RESISTIVITY
The precipitation processes of Cu-Zr-Cr alloys
[NASA-TT-20168] N88-24758
On the reversion phenomena of Cu-3 percent Ti alloys
[NASA-TT-20170] N88-24762
Size effects in the electrical resistivity of benzene-derived carbon fibers
[AD-A191708] N88-24777
Raman characterization of AsF5-intercalated vapor grown graphite fibers
[AD-A191709] N88-24778
Electrical conduction in thin film carbons
[AD-A191726] N88-24780
On the abnormal phenomena observed in the electrical resistivity measurement during the decomposition process of saturated Cu-Fe alloys
[NASA-TT-20183] N88-24869
Sulfur-tolerant anode materials
[DE88-001034] N88-25054
Determination of doping profiles in silicon from resistivity measurements via the four-point probe in combination with layer strippings via anodic oxidation N88-25347

ELECTRO-OPTICS
Topological stereochemistry
[AD-A191867] N88-24691
Silicon-sapphire waveguides
[AD-A191754] N88-24854
Investigations in electro-optical multistability for signal processing N88-24938

ELECTROCHEMICAL CELLS
Optimization of reserve lithium thionyl chloride battery electrochemical design parameters
[DE88-007109] N88-24868

ELECTROCHEMICAL CORROSION
The influence of cathodic protection on erosion-corrosion of metals and model alloys
[AD-A191613] N88-24742

ELECTROCHEMICAL OXIDATION
Electrochemistry in near-critical and supercritical fluids. 6: The electrochemistry of ferrocene and phenazine in acetonitrile between 25C and 300C
[AD-A192171] N88-24723

ELECTROCHEMISTRY
Electrochemistry in liquid crystals
[AD-A191554] N88-24719
Electrochemistry in near-critical and supercritical fluids. 6: The electrochemistry of ferrocene and phenazine in acetonitrile between 25C and 300C
[AD-A192171] N88-24723
Photosynthetic water splitting
[PB88-188891] N88-24731

ELECTRODES
Electrochemistry in liquid crystals
[AD-A191554] N88-24719
Optical investigations of the thermal boundary layer in arc plasmas N88-25313

ELECTROKINETICS
The electrokinetic behavior of calcium oxalate monohydrate in macromolecular solutions
[NASA-TM-101144] N88-24791

ELECTROMAGNETIC FIELDS
Electromagnetic penetration into a conducting circular cylinder through a narrow slot, TE case
[AD-A191602] N88-24828
Electromagnetic field penetration into structures
[AD-A192127] N88-24836
Space station induced electromagnetic effects N88-25394

ELECTROMAGNETIC NOISE
A Differential Phase Shift Keying (DPSK) modulator for a frequency hopping short wave system
[FOA-C-30480-3.3] N88-24840

ELECTROMAGNETIC PROPULSION
Fabrication issues and technology development for HELEOS (Hypervelocity Electromagnetic Launcher for Equation Of State)
[DE88-007419] N88-24858

ELECTROMAGNETIC PULSES
Arcing and rf signal generation during target irradiation by a high-energy, pulsed neutral particle beam
[DE88-007169] N88-24864

ELECTROMAGNETIC RADIATION
Electromagnetic penetration into a conducting circular cylinder through a narrow slot, TE case
[AD-A191602] N88-24828
Electromagnetic field penetration into structures
[AD-A192127] N88-24836
Joint services electronics program
[AD-A191749] N88-24853

Theoretical basis for an experimental test with regard to the origin of VHF (Very High Frequency) radiation from natural lightning
[DE88-007535] N88-25102

ELECTROMAGNETIC SCATTERING
Born-type reconstruction of material parameters of an inhomogeneous, lossy dielectric slab from reflected-field data
[PB88-188958] N88-25261
Curvature of blended rolled edge reflectors at the shadow boundary contour
[NASA-CR-182974] N88-25300

ELECTROMAGNETIC SHIELDING
Electromagnetic field penetration into structures
[AD-A192127] N88-24836

ELECTROMAGNETIC WAVE TRANSMISSION
Propagation of neutralized ion beams
[AD-A191599] N88-25289
Theoretical plasma physics research of active space experiments
[AD-A192075] N88-25309

ELECTROMAGNETISM
Electromagnetic damping and vibration isolation of space structures
[AD-A191492] N88-24865

ELECTRON ACCELERATORS
The loss parameters for very short bunches
[CEBAF-PR-88-005] N88-25291

ELECTRON BEAM WELDING
Microstructural characterization and properties of 3Cr-1.5Mo-0.1V thick section electron beam welds
[DE88-004330] N88-24747

ELECTRON BEAMS
Isotope separation using tuned laser and electron beam
[NASA-CASE-NPO-16907-1-CU] N88-24732
Microstructural characterization and properties of 3Cr-1.5Mo-0.1V thick section electron beam welds
[DE88-004330] N88-24747
Integral equation for the laser field: Multimode description of a free-electron laser oscillator
[DE88-007050] N88-24956
Null steering applications of polynomials with unimodular coefficients
[AD-A191087] N88-25211
Trochoidal analysis of scattered electrons in a merged electron-ion beam
[NASA-CASE-NPO-16789-1-CU] N88-25281
Accelerator research studies
[DE88-007124] N88-25290
The loss parameters for very short bunches
[CEBAF-PR-88-005] N88-25291

ELECTRON CAPTURE
Selective detection in gas chromatography
[AD-A191499] N88-24718

ELECTRON DENSITY (CONCENTRATION)
The theory of random alloys
[DE88-006408] N88-24756
A two-wavelength infrared interferometer/polarimeter system for CIT (Compact Ignition Tokamak)
[DE88-007681] N88-25321
Superthermal electron processes in the upper atmosphere of Uranus: Aurora and electroglow
[NASA-TM-101150] N88-25417

ELECTRON DIFFRACTION
On the use of convergent beam electron diffraction for identification of antiphase boundaries in GaAs grown on Si
[DE88-006220] N88-25362

ELECTRON DISTRIBUTION
Application of particle simulations to the NRL laser experiment
[AD-A191641] N88-24953

ELECTRON ENERGY
The Io sulfur torus in 1981
[NASA-TM-101139] N88-25419

ELECTRON IMPACT
Contributions of autoionizing resonances to the electron collisional excitation rates for Be-like ions
[AD-A190924] N88-25275
Development of the field-induced electron injection and impact ionization (F4I) technique for radiation hardness testing of MOS (Metal-Oxide-Semiconductor) gate insulators
[AD-A192114] N88-25345

ELECTRON MICROSCOPY
SHaRE: Collaborative materials science research
[DE88-007175] N88-24848

ELECTRON PHONON INTERACTIONS
Electron-Rayleigh wave interaction in thin film carbons
[AD-A191727] N88-24781

ELECTRON SCATTERING
Trochoidal analysis of scattered electrons in a merged electron-ion beam
[NASA-CASE-NPO-16789-1-CU] N88-25281

ELECTRON TRANSITIONS
Transition probabilities in OH A 2 sigma + - X 2 pi i: Bands with v prime = 0 and 1, v double prime = 0 to 4
[NASA-CR-182946] N88-25353

ELECTRON-ION RECOMBINATION
Molecular sources of ionospheric holes
[AD-A191857] N88-25062

ELECTRONIC COUNTERMEASURES
Acta aeronautica et astronautica sinica (selected articles)
[AD-A191552] N88-24575

ELECTRONIC EQUIPMENT
Joint services electronics program
[AD-A192076] N88-24856
The inspection of metallurgical bounds in electronic systems
[AD-A192064] N88-25343
Electronic controller for reciprocating rotary crystallizer
[NASA-TM-101140] N88-25354

ELECTRONIC SPECTRA
Contributions of autoionizing resonances to the electron collisional excitation rates for Be-like ions
[AD-A190924] N88-25275

ELECTRONS
Contributions of autoionizing resonances to the electron collisional excitation rates for Be-like ions
[AD-A190924] N88-25275
A study of runaway electron confinement in the ASDEX tokamak
[DE88-007327] N88-25319
Physical properties of f electron systems
[DE88-006886] N88-25331
Contaminant ions and waves in the space station environment N88-25393

ELECTROPHYSICS
Joint services electronics program
[AD-A190239] N88-24848
Joint services electronics program
[AD-A192076] N88-24856

ELECTROSTATIC CHARGE
Simulations of the electrostatic charging of ESA communications satellites
[ESA-STM-239] N88-24670
Reference filters for electrostatic charging tendency measurements of fuels
[AD-A191717] N88-24803
An electrostatic potential comparator
[AD-A192051] N88-25177

ELECTROSTATIC PROBES
Rocket-borne low energy ion measurements in space N88-25412

ELECTROSTATIC WAVES
Theoretical investigations of drift waves in a magnetic quadrupole N88-25312

ELECTROSTATICS
Development of test methods for the electrostatic properties of nonhomogeneous fabrics, phase 2
[AD-A190853] N88-24767
Demixing of aqueous polymer two-phase systems in low gravity
[NASA-TM-101141] N88-24809
Electrostatic discharge test apparatus
[NASA-CASE-MSC-21094-1] N88-24941
Low frequency electrostatic turbulence in the polar cap E-region
[DRI-3-88] N88-25077

ELECTROTHERMAL ENGINES
Performance of a hydrogen pulsed electrothermal thruster. Strategic defense initiative organization innovative science and technology. SBIR, phase 1
[AD-A191999] N88-24679

ELEMENTARY EXCITATIONS
Electronic structure, elementary excitations, optical and transport properties of semiconductor superlattices
[AD-A190795] N88-25333

ELEVATION
Vectorization of raster algorithms for elevation data processing N88-25036

ELLIPTIC DIFFERENTIAL EQUATIONS
Multigrid methods for elliptic Partial Differential Equations (PDEs)
[CWI-NM-R8722] N88-25242
A comparative study of Chebyshev acceleration and residue smoothing in the solution of nonlinear elliptic difference equations
[CWI-NM-R8723] N88-25259

ELONGATION
Superplasticity: A fundamental investigation on deformation mechanism and cavitation phenomena
[AD-A191548] N88-24741

EMBRITTLEMENT
High temperature embrittleness of Cu-Cr alloy
[NASA-TT-20184] N88-24759

EMISSION SPECTRA
Molecular sources of ionospheric holes
[AD-A191857] N88-25062
Optical diagnostics for a high power, rf-inductively coupled plasma
[DE88-007822] N88-25322

ENCAPSULATING
A compatible encapsulant for explosives
[DE88-007212] N88-24806

ENERGY ABSORPTION
Transmitting boundary for finite-difference calculations with finite modeling of an infinite medium
[AD-A191441] N88-25264

ENERGY BUDGETS
Low authority control of large space structures using a constrained threshold control formulation N88-24867

ENERGY CONSERVATION
NASA/industry advanced turboprop technology program
[NASA-TM-100929] N88-24841

ENERGY CONVERSION EFFICIENCY
Progress in InP solar cell research
[NASA-TM-100914] N88-24870

ENERGY DISSIPATION
Electromagnetic damping and vibration isolation of space structures
[AD-A191492] N88-24865
Extrema principles of entrophy production and energy dissipation in fluid mechanics
[NASA-TM-100992] N88-24946

ENERGY LEVELS
Optical properties of heterostructures and superlattices
[AD-A191542] N88-25335

ENERGY SPECTRA
Time-frequency representations for speech signals
[AD-A188661] N88-24819

ENERGY TRANSFER
Bimolecular reactions and energy-transfer processes of highly vibrationally excited molecules related to energetic materials
[AD-A189013] N88-25270
Energy-transfer properties and mechanisms
[DE88-007107] N88-25272
Spectroscopy and energy transfer kinetics of the interhalogens
[AD-A192103] N88-25344
Transition probabilities in OH A 2 sigma + - X 2 pi i: Bands with v prime = 0 and 1, v double prime = 0 to 4
[NASA-CR-182946] N88-25353

ENGINE DESIGN
Status and prognosis for alternative engine materials
[NASA-TM-100903] N88-24749
Design, manufacture and spin test of high contact ratio helicopter transmission utilizing Self-Aligning Bearingless Planetary (SABP)
[NASA-CR-4155] N88-24975

ENGINE PARTS
Status and prognosis for alternative engine materials
[NASA-TM-100903] N88-24749

ENGINE TESTS
Aircraft emissions characterization: TF41-A2, TF30-P103 and TF30-P109 engines
[AD-A192053] N88-24638

ENGINEERING DRAWINGS
Engineering drawings and changes: Storing and controlling by the tens of terrabytes
[DE88-007605] N88-25387

ENGINEERING MANAGEMENT
A perspective of PC-based probabilistic risk assessment
[DE88-006715] N88-25251

ENTHALPY
The thermodynamic properties of quinoline and isoquinoline
[DE88-001218] N88-24735

ENTRAINMENT
Gas diffusion studies in steady and nonsteady cavities N88-24902
Direct numerical simulations of the PDF's (Probability Density Functions) of a passive scalar in a forced mixing layer
[AD-A192134] N88-25256

ENTROPY
Extrema principles of entrophy production and energy dissipation in fluid mechanics
[NASA-TM-100992] N88-24946

ENTROPY (STATISTICS)
Adaptive time series analysis using predictive inference and entropy
[AD-A191858] N88-25199

ENVIRONMENT EFFECTS
Environmental effects on slow crack growth in silicon nitride
[DE88-007206] N88-24795
Changes in the Antarctic atmosphere due to the reduction of stratospheric ozone
[ETN-88-92565] N88-25074

Monitoring biological impacts of space shuttle launches from Vandenberg Air Force Base: Establishment of baseline conditions
[NASA-TM-100982] N88-25133

ENVIRONMENTAL CHEMISTRY
Workshop on Atmospheric OH
[BPT-7/87] N88-25063

ENVIRONMENTAL MONITORING
The role of space borne imaging radars in environmental monitoring: Some shuttle imaging radar results in Asia
[NASA-TM-101178] N88-24844
The application of satellites in connection with the environment
[ETN-88-92474] N88-25020
Monitoring biological impacts of space shuttle launches from Vandenberg Air Force Base: Establishment of baseline conditions
[NASA-TM-100982] N88-25133

ENZYME ACTIVITY
Dexamethasone regulates glutamine synthetase expression in rat skeletal muscles
[NASA-CR-182935] N88-25129

EPOXY MATRIX COMPOSITES
Elementary characterization of preimpregnated carbon epoxy T400H/DA0506 from STRUCTIL. Test report M6-577100
[CEAT-047426] N88-24703

EPOXY RESINS
Interfacial shear phenomena in graphite epoxy composites under impact loading using dynamic moire interferometry
[DE88-006773] N88-24709
High strength/sigh modulus aromatic heterocyclic ABA block copolymers
[AD-A191666] N88-24774
The influence of the chemical nature of resins on their reticulation kinetics and the consequences for their nonelastic mechanical properties
[ETN-88-92539] N88-24788
Structural study of the TGMDA-DDS system — epoxy system
[ONERA-RT-4/3346-M] N88-24792
Research work completed at the Naval Surface Warfare Center Solid State Group of the Radiation Division
[AD-A191627] N88-25339

EQUATIONS OF MOTION
Nonlinear programming extensions to rational function approximation methods for unsteady aerodynamic forces
[NASA-TP-2776] N88-24623
Particle-laden weakly swirling free jets: Measurements and predictions
[NASA-TM-100920] N88-24639
Effects of Coriolis acceleration on the vibrations of spinning structures N88-24966
Vibrations of rotating thick or thin rings N88-25003
Forced motion of initially stressed shells and plates N88-25005
A constraint algorithm for maintaining rigid bonds in molecular dynamics simulations of large molecules
[AD-A191663] N88-25277

EQUATIONS OF STATE
Use of a two-stage light-gas gun as an injector for electromagnetic railguns
[DE88-007200] N88-24657
Fabrication issues and technology development for HELEOS (Hypervelocity Electromagnetic Launcher for Equation Of State)
[DE88-007419] N88-24658
The high pressure sound velocity and equation of state of aqueous solutions of hydroxylammonium nitrate and triethanolammonium nitrate
[AD-A191740] N88-25266
Nuclear and astrophysical evidence on the equation of state
[DE88-007397] N88-25279
Study of data distributions and functions for the development of thermodynamic equations of state
[PB88-196365] N88-25370

EQUILIBRIUM FLOW
Simplified curve fits for the transport properties of equilibrium air
[NASA-CR-178411] N88-24911

EQUIPMENT SPECIFICATIONS
Tower evaporator
[NASA-CASE-NPO-15609-2] N88-24815
Electrostatic discharge test apparatus
[NASA-CASE-MSC-21094-1] N88-24941
Mars rover/sample return mission requirements affecting space station
[NASA-CR-172048] N88-25414

EROSION
Analytic and numerical modeling of heat and material transport in electrical hypervelocity guns
[AD-A192178] N88-24655
Internal erosion rates of a 10-kW xenon ion thruster
[NASA-TM-100954] N88-24688
The influence of cathodic protection on erosion-corrosion of metals and model alloys
[AD-A191613] N88-24742
A 3 MW wood fired gas turbine at Red Boiling Springs, Tennessee N88-25051

ERROR ANALYSIS
Determination of doping profiles in silicon from resistivity measurements via the four-point probe in combination with layer strippings via anodic oxidation N88-25347

ERROR CORRECTING CODES
A general approach for automating source code verification
[AD-A191461] N88-25170

ERRORS
Reducing sensitivity to errors in free electron laser amplifiers
[DE88-007017] N88-24980
Effectiveness evaluation of fault-tolerant multiprocessor systems
[AD-A191688] N88-25158

ESA SATELLITES
Assessment of optical communications systems for Data Relay Satellite. Volume 1: Executive summary
[ESA-CR(P)-2488-VOL-1] N88-24841
Assessment of optical communications systems for the Data Relay Satellite
[ESA-CR(P)-2488-VOL-2] N88-24842

ESTIMATES
Performance estimates for operations conducted while wearing individual protective equipment: User manual
[AD-A191871] N88-25154
Symmetrized nearest neighbor regression estimates
[AD-A191998] N88-25254
Preliminary estimates of radiation exposures for manned interplanetary missions from anomalously large solar flare events
[NASA-TM-100620] N88-25427

ESTIMATING
Asymptotic theory for weighted least squares estimators in Aalen's additive risk model
[AD-A191085] N88-25210

ETHANE
Temperature dependence of ultraviolet absorption cross sections of chlorofluoroethanes
[AERONOMICA-ACTA-A-325-1987] N88-24726

ETHERS
Preferential surface adsorption in miscible blends of polystyrene and poly(vinyl methyl ether)
[AD-A191451] N88-24769

EUCLIDEAN GEOMETRY
Mathematical morphology for structures without translation symmetry
[CWI-AM-R8803] N88-25241

EULER EQUATIONS OF MOTION
Incompressible Euler solution on a multiblock grid around a car configuration
[FFA-TN-1987-65] N88-24586
Applications of the Navier-Stokes equations to wings and complex configurations using a zonal approach
[NASA-TM-100080] N88-24602
Accurate multigrid solution of the Euler equations on unstructured and adaptive meshes
[NASA-CR-181679] N88-24608
Composite reduced Navier-Stokes procedures for flow problems with strong pressure interactions
[AD-A191127] N88-24675

EULER-LAGRANGE EQUATION
A semigroup for Lagrangian 1D isentropic flow
[DE88-006464] N88-24912

EURECA (ESA)
Operational facilities of EURECA A1 mission
[ETN-88-91939] N88-24810

EVALUATION
Evaluation of the communications impact of a low power arcjet thruster
[NASA-TM-100926] N88-24682
Evaluating evaporation with satellite thermal data
[AD-A192042] N88-25019
Effectiveness evaluation of fault-tolerant multiprocessor systems
[AD-A191688] N88-25158
Multi-sensor integration on the NCUBE hypercube computer
[DE88-007472] N88-25162

EVAPORATION
Heating and evaporation of turbulent liquid films: Measurement of film thickness and the onset of nucleate boiling
[DE88-006388] N88-24905
Evaluating evaporation with satellite thermal data
[AD-A192042] N88-25019
Report on project WIND: Preliminary experiments w ith the UK Meteorological Office mesoscale model, September 1987
[AD-A191621] N88-25099

EVAPORATORS
Tower evaporator
[NASA-CASE-NPO-15609-2] N88-24815

EVOKED RESPONSE (PSYCHOPHYSIOLOGY)
Eye and head response to an attention cue in a dual task paradigm
[AD-A191052] N88-25143

EXCIMER LASERS
Aurora status and plans
[DE88-006476] N88-24955

EXCITATION
Robust adaptive regulation without persistent excitation
[NASA-TM-100571] N88-25204
Trochoidal analysis of scattered electrons in a merged electron-ion beam
[NASA-CASE-NPO-16789-1-CU] N88-25281
Optical properties of heterostructures and superlattices
[AD-A191542] N88-25335

EXHAUST EMISSION
Aircraft emissions characterization: TF41-A2, TF30-P103 and TF30-P109 engines
[AD-A192053] N88-24838
A 3 MW wood fired gas turbine at Red Boiling Springs, Tennessee N88-25051
Motor vehicles as sources of compounds important to tropospheric and stratospheric ozone
[PB88-195219] N88-25076

EXHAUST GASES
Aircraft emissions characterization: TF41-A2, TF30-P103 and TF30-P109 engines
[AD-A192053] N88-24838

EXOBIOLOGY
Aerospace medicine and biology: A continuing bibliography with indexes (supplement 312)
[NASA-SP-7011(312)] N88-25141

EXPANSION
Turbulent heat transfer and fluid flow measurements downstream of abrupt expansions and in a cavity of a circular tube at a uniform wall temperature N88-24920
The Department of Defense report on the merit review process for competitive selection of university research projects and an analysis of the potential for expanding the geographic distribution of research for the Committees on Appropriations, United States Congress
[AD-A191842] N88-25379

EXPERIMENT DESIGN
Operational facilities of EURECA A1 mission
[ETN-88-91939] N88-24810

EXPERT SYSTEMS
Knowledge based systems in nondestructive evaluation
[DE88-006653] N88-24981
Timesharing performance as an indicator of pilot mental workload
[NASA-CR-182807] N88-25150
Application of flight systems methodologies to the validation of knowledge-based systems
[NASA-TM-100442] N88-25207
Optical symbolic processor for expert system execution
[AD-A192005] N88-25296

EXPLOSIONS
Nuclear and astrophysical evidence on the equation of state
[DE88-007397] N88-25279

EXPLOSIVE DEVICES
Toggle release
[NASA-CASE-MSC-21354-1] N88-24969

EXPLOSIVES
Thermal decomposition studies of explosives for component applications
[DE88-007201] N88-24805
A compatible encapsulant for explosives
[DE88-007212] N88-24806
An extinguisher to quench propellant fires
[AD-A190785] N88-24813

EXTINGUISHING
An extinguisher to quench propellant fires
[AD-A190785] N88-24813

EXTRATERRESTRIAL RADIATION
From general relativity to the theory of superstrings N88-25369

EXTREMELY HIGH FREQUENCIES
Experimental radio frequency link for Ka-band communications applications
[NASA-TM-100624] N88-24659

EYE MOVEMENTS
Eye and head response to an attention cue in a dual task paradigm
[AD-A191052] N88-25143

F

FABRICATION
Nozzle fabrication technique
[NASA-CASE-MSC-21299-1] N88-24684
Sol/gel processing techniques for glass matrix composites
[AD-A191748] N88-24701
FAILURE ANALYSIS
User's guide to the Fault Inferring Nonlinear Detection System (FINDS) computer program
[NASA-CR-178410] N88-24619
Internal erosion rates of a 10-kW xenon ion thruster
[NASA-TM-100954] N88-24688
Environment assisted degradation mechanisms in advanced light metals
[NASA-CR-182907] N88-24746
Analysis and design of detection filters within closed-loop systems N88-24980
FAILURE MODES
Analysis of notched metal matrix composites under tension loading
[NASA-TM-100629] N88-24713
Applications of fault tree analysis to the design process
[DE88-007048] N88-24982
FAINT OBJECTS
Ultraviolet spectra of two magnetic white dwarfs and ultraviolet spectra of subluminous objects found in the Kiso Schmidt survey
[NASA-CR-183051] N88-25408
FAR FIELDS
Transmitting boundary for finite-difference calculations with finite modeling of an infinite medium
[AD-A191441] N88-25264
FARM CROPS
Low-temperature thermochemical conversion of high moisture biomass feedstocks N88-25047
FASTENERS
Toggle release
[NASA-CASE-MSC-21354-1] N88-24969
FATIGUE (MATERIALS)
Design of overlays for rigid airport pavements
[DOT/FAA/PM-87/19] N88-24652
Predictive corrosion modeling, volume 1
[AD-A191229] N88-24739
Resolved shear stress intensity coefficient and fatigue crack growth in large crystals
[NASA-CR-182137] N88-24997
Fatigue crack growth due to random loading N88-25017
FATIGUE LIFE
Damage by creep fatigue: Influence of the visco-elasticity of the matrix
[PB88-124706] N88-24998
Cyclic fatigue damage characteristics observed for simple loadings extended to multiaxial life prediction
[NASA-CR-182126] N88-25016
FATIGUE TESTS
Detecting delaminations in CFRP specimens using X-ray techniques
[FFA-TN-1988-04] N88-24704
Predictive corrosion modeling, volume 1
[AD-A191229] N88-24739
FAULT TOLERANCE
Toggle release
[NASA-CASE-MSC-21354-1] N88-24969
Analysis and design of detection filters within closed-loop systems N88-24980
Effectiveness evaluation of fault-tolerant multiprocessor systems
[AD-A191688] N88-25158
FAULT TREES
Applications of fault tree analysis to the design process
[DE88-007048] N88-24982
FEASIBILITY ANALYSIS
Search and rescue satellite system (SERES), phase A0
[ETN-88-92335] N88-24669
The efficacy of using human myoelectric signals to control the limbs of robots in space
[NASA-CR-182901] N88-25155
FEDERAL BUDGETS
The Department of Defense report on the merit review process for competitive selection of university research projects and an analysis of the potential for expanding the geographic distribution of research for the Committees on Appropriations, United States Congress
[AD-A191642] N88-25379
FEED SYSTEMS
An advanced extruder-feeder biomass liquefaction reactor system N88-25042
FEEDBACK
Optimizing feedback utilization in motor skill training
[AD-A191559] N88-25146
FEEDBACK CONTROL
Automatic feedback control of a rigid body for finite displacements N88-24674
Analysis and design of detection filters within closed-loop systems N88-24980
Multishaker modal testing
[NASA-CR-179355] N88-25010
Design and testing of a luminance and chrominance stabilization system for a computer-controlled color display
[AD-A191922] N88-25150
Frequency Analysis of Acoustic Emission - Application to machining and welding
[DE88-701478] N88-25262
FEEDERS
Harmonic considerations for electrical distribution feeders
[DE88-007849] N88-24860
FERMIONS
Introduction to covariant formulation of superstring (field) theory
[DE87-703038] N88-25363
FERROELECTRICITY
Topological stereochemistry
[AD-A191867] N88-24691
FIBER COMPOSITES
Carbon matrix composites prospective roles for biotechnology N88-24694
Mixed-mode fracture of uniaxial fiber reinforced composites
[AD-A191629] N88-24700
Sol/gel processing techniques for glass matrix composites
[AD-A191748] N88-24701
Interaction of ultrasonic waves with composite plates
[AD-A191879] N88-24702
Analysis of notched metal matrix composites under tension loading
[NASA-TM-100629] N88-24713
Multiple scattering of waves in discrete random media
[AD-A191068] N88-24823
FIBER OPTICS
Optics: Perspectives for Measurement Techniques and Signal Processing for Flight Guidance — conference
[DFVLR-MITT-87-21] N88-24928
Navigation using the Teldix fiber-optic gyroscope N88-24933
Digital fiber optic displacement sensors N88-24937
Activities report of the Division of Optical Technology
[FOA-C-30477-3] N88-25299
Optical pressure sealing couping (light joint)
[NASA-CASE-MFS-29348-1] N88-25303
Low-loss, high-isolation, fiber-optic isolator
[NASA-CASE-NPO-17207-1-CU] N88-25304
FIBERS
Raman characterization of AsF5-intercalated vapor grown graphite fibers
[AD-A191709] N88-24778
Stress measurements in graphite fibers by laser raman spectroscopy
[AD-A191710] N88-24779
FIELD EFFECT TRANSISTORS
A monolithic reduced-size Ku-Band SPOT (Single-Pole Double Throw) FET switch
[DE88-006273] N88-24858
Planar fully ion-implanted high power InP MISFETs
[AD-A191589] N88-25336
FIELD THEORY (PHYSICS)
Introduction to covariant formulation of superstring (field) theory
[DE87-703038] N88-25363
FILTERS
Single-mode projection filters for modal parameter identification for flexible structures
[NASA-CR-182680] N88-25244
FILTRATION
Reference filters for electrostatic charging tendency measurements of fuels
[AD-A191717] N88-24803
FINANCIAL MANAGEMENT
Financial reporting: NASA (National Aeronautics and Space Administration) can improve compliance with GAO (General Accounting Office) standards and treasury requirements
[PB88-172523] N88-25373
FINE STRUCTURE
Functional and mechanical analysis of continuous media-application to the study of elastic composites with periodic structure: Homogenization
[NASA-TT-20188] N88-24710
FINITE DIFFERENCE THEORY
Fundamental limits to the velocity of solid armatures in railguns N88-24658
Cross stream differencing for integral boundary layer equations
[AD-A191744] N88-24886
Adaptive local grid refinement in computational fluid mechanics
[AD-A192215] N88-24890
Adaptive grid refinement for numerical weather prediction
[AD-A192172] N88-25101
Transmitting boundary for finite-difference calculations with finite modeling of an infinite medium
[AD-A191441] N88-25264
Modelling of thermal plasma systems N88-25314
FINITE ELEMENT METHOD
Simulations of a missile with liquid payload under launch conditions
[AD-A191479] N88-24825
Fundamental limits to the velocity of solid armatures in railguns N88-24658
Mixed-mode fracture of uniaxial fiber reinforced composites
[AD-A191629] N88-24700
Adaptive local grid refinement in computational fluid mechanics
[AD-A192215] N88-24890
A variational finite element method for three-dimensional, steady, compressible, viscous flows N88-24904
Improving the performance of a finite element method using vector analysis on CRAY 1
[ETN-88-92153] N88-24907
Finite element solution of 3-D turbulent Navier-Stokes equations for propeller-driven slender bodies N88-24919
Finite element analysis of an underground structure
[AD-A191747] N88-24991
Fracture mechanics analysis for short cracks
[AD-A192002] N88-24992
Dynamic response of plates to moving loads: Structural impedance and finite element methods N88-25000
The stress analysis of ceramic, polymeric, and metallic composite systems by the finite element method N88-25004
Reduced order modelling and analytical model modification for structural dynamics and control N88-25006
Considerations involved in the display of finite element results using animation
[DE88-007581] N88-25189
Algorithms and software for solving finite element equations on serial and parallel architectures
[NASA-CR-183027] N88-25191
PAFEC level 6.2 application program
[AD-A191037] N88-25209
NFEARS: A nonlinear adaptive finite element solver, part 1
[AD-A191823] N88-25215
Probabilistic finite element methods N88-25223
New mixed finite element methods N88-25248
FIRE EXTINGUISHERS
An extinguisher to quench propellant fires
[AD-A190785] N88-24813
FIRE PREVENTION
Study of benefits of passenger protective breathing equipment from analysis of past accidents
[DOT/FAA/CT-88/03] N88-24810
FIRES
An extinguisher to quench propellant fires
[AD-A190785] N88-24813
FITTING
Evaluation of the US Army fitting program for the integrated helmet unit of the integrated helmet and display sighting system
[AD-A191616] N88-24835
FIXED WINGS
Aircraft aeroelasticity and structural dynamics research at the NASA Langley Research Center: Some illustrative results
[NASA-TM-100627] N88-24598
FLAME IONIZATION
Selective detection in gas chromatography
[AD-A191499] N88-24718
FLAME PROPAGATION
On the structure, propagation, extinction and stability of laminar premixed flames in dissociation equilibrium N88-24728
FLAME RETARDANTS
Differential technology in plastics industries differentiation in combination technology nonflammability technology
[NASA-TT-20256] N88-24797
FLAME STABILITY
On the structure, propagation, extinction and stability of laminar premixed flames in dissociation equilibrium N88-24728

FLAMEOUT
On the structure, propagation, extinction and stability of laminar premixed flames in dissociation equilibrium
N88-24728
FLAMES
Application of Rayleigh scattering to turbulent flow with heat transfer and combustion
[AD-A191565] N88-24720
FLAPS (CONTROL SURFACES)
Characteristics of merging shear layers and turbulent wakes of a multi-element airfoil
[NASA-TM-100053] N88-24900
FLAT PLATES
Numerical simulations of the flat-plate laminar boundary layer in subsonic and supersonic flow
[PDR/CFDU-IC/36] N88-24895
Forced motion of initially stressed shells and plates
N88-25005
FLAVOR (PARTICLE PHYSICS)
Experimental elementary particle physics
[DE88-007510] N88-25274
FLEXIBILITY
Single-mode projection filters for modal parameter identification for flexible structures
[NASA-CR-182680] N88-25244
FLEXIBLE BODIES
Nonlinear programming extensions to rational function approximation methods for unsteady aerodynamic forces
[NASA-TP-2776] N88-24623
Experimental study of active vibration control
[AD-A191454] N88-24989
FLIGHT CONTROL
Parameter-adaptive model-following for in-flight simulation
[AD-A190567] N88-24645
Simultaneous multiple control force exertion capabilities of males and females versus helicopter control force design limits
[AD-A191653] N88-25153
FLIGHT ENVELOPES
Current flight test experience related to structural divergence of forward-swept wings
[NASA-TM-100445] N88-24633
FLIGHT HAZARDS
Ice formation on aircraft
[ETN-88-92154] N88-25104
FLIGHT MANAGEMENT SYSTEMS
Application of flight systems methodologies to the validation of knowledge-based systems
[NASA-TM-100442] N88-25207
FLIGHT OPTIMIZATION
Periodic solutions in aircraft cruise-dash optimization
N88-24631
FLIGHT PATHS
Method for prediction and determination of takeoff performance for vectored thrust vehicles
[AD-A191809] N88-24626
Periodic solutions in aircraft cruise-dash optimization
N88-24631
FLIGHT RECORDERS
Development of a multipurpose smart recorder for general aviation aircraft
[NASA-CR-168353] N88-24637
FLIGHT SAFETY
Meteorological and Environmental Inputs to Aviation Systems
[NASA-CP-2498] N88-25105
General-aviation's view of progress in the aviation weather system N88-25110
FLIGHT SIMULATION
Wind tunnel investigation of wing and control panel loads at transonic and supersonic speeds on some schematic cruciform missile configurations
[FFA-TN-1986-43] N88-24585
Parameter-adaptive model-following for in-flight simulation
[AD-A190567] N88-24645
Simulator evaluation of lineup visual landing aids for night carrier landing
[AD-A191212] N88-24648
FLIGHT SIMULATORS
Analysis procedures and subjective flight results of a simulator validation and cue fidelity experiment
[NASA-TM-88270] N88-24634
An OOD (Object-Oriented Design) paradigm for flight simulators
[AD-A191097] N88-24647
FLIGHT TESTS
Rotorcraft TCAS (traffic alert and collision avoidance system) evaluation: Group 3 results
[AD-A191719] N88-24614
Western Pacific Omega validation: Project description
[AD-A191753] N88-24617
Method for prediction and determination of takeoff performance for vectored thrust vehicles
[AD-A191809] N88-24626
Current flight test experience related to structural divergence of forward-swept wings
[NASA-TM-100445] N88-24633
Analysis procedures and subjective flight results of a simulator validation and cue fidelity experiment
[NASA-TM-88270] N88-24634
FLIGHT TRAINING
An enumeration of research to determine the optimal design and use of Army flight training simulators
[AD-A191242] N88-24649
FLOATING
Flotation processes
[PB88-180302] N88-25075
FLOOD PLAINS
Oxidation and reduction rates for organic carbon in the Amazon mainstream tributary and floodplain, inferred from distributions of dissolved gases
[NASA-CR-182943] N88-25062
FLOTATION
Flotation processes
[PB88-180302] N88-25075
FLOW CHARACTERISTICS
Forced response unsteady aerodynamics in a multistage compressor N88-24903
FLOW DISTRIBUTION
Experiment investigation on longitudinal characteristics of the forward swept wing
[AD-A191553] N88-24582
Supplements to the study of the wake of a Mirage G8 model at F2 — wind tunnel
[CERT-RT-OA-20/5025-AYD] N88-24596
A decade of computer simulations for space shuttle aerodynamics
[NASA-TM-100990] N88-24603
Solid rocket motor aft field joint flow field analysis
[NASA-CR-179288] N88-24675
Research study: Space shuttle main engine plume flowfield model
[NASA-CR-179336] N88-24676
Analysis of molecular mixing and chemical reaction in mixing layer
[AD-A191600] N88-24721
Computation and characteristics of pulsatile multi-bifurcation flow N88-24729
Joint services electronics program
[AD-A191749] N88-24853
Transient particle deposition in a boundary layer of impulsive flow over a flat plate
[AD-A191537] N88-24880
Theoretical investigation of 3-D shock wave-turbulent boundary layer interactions, part 6
[AD-A191546] N88-24882
Axisymmetric viscid-inviscid interaction by a frozen vorticity approximation
[AD-A191743] N88-24885
Fast algorithm development for large-eddy simulation of circular-jet turbulence
[AD-A192044] N88-24887
Two dimensional hyperbolic grid generation
[VKI-TN-162] N88-24897
Characteristics of merging shear layers and turbulent wakes of a multi-element airfoil
[NASA-TM-100053] N88-24900
A single streamwise vortical structure and its instability in shear flows N88-24921
Application of advanced grid generation techniques for flow field computations about complex configurations
[NASA-CR-183049] N88-24922
FLOW EQUATIONS
Analysis of molecular mixing and chemical reaction in mixing layer
[AD-A191600] N88-24721
Transient particle deposition in a boundary layer of impulsive flow over a flat plate
[AD-A191537] N88-24880
Numerical simulation of nonlinear structural dynamics of large scale unsteady flow
[ETN-88-92156] N88-24908
FLOW GEOMETRY
Three dimensional spectral energy measurement on turbulence subjected to a high degree of plane deformation
[ETN-88-92537] N88-24896
FLOW MEASUREMENT
Supplements to the study of the wake of a Mirage G8 model at F2 — wind tunnel
[CERT-RT-OA-20/5025-AYD] N88-24596
Inflow measurements made with a laser velocimeter on a helicopter model in forward flight. Volume 1: Rectangular planform blades at an advance ration of 0.15
[NASA-TM-100541] N88-24607
Method of forming a multiple layer dielectric and a hot film sensor therewith
[NASA-CASE-LAR-13678-1] N88-25355
FLOW REGULATORS
Energy efficient continuous flow ash lockhopper
[NASA-CASE-NPO-16985-1-CU] N88-24814
FLOW STABILITY
Numerical simulation of nonlinear structural dynamics of large scale unsteady flow
[ETN-88-92156] N88-24908
A single streamwise vortical structure and its instability in shear flows N88-24921
FLOW VELOCITY
Reference filters for electrostatic charging tendency measurements of fuels
[AD-A191717] N88-24803
FLOW VISUALIZATION
Unsteady flow around a profile subjected to pulsed motions
[ETN-88-92151] N88-24594
FLUID DYNAMICS
Dynamics and control of turbulent shear flows
[AD-A191527] N88-24879
Nonlinear waves
[AD-A192148] N88-24889
Gas diffusion studies in steady and nonsteady cavities
N88-24902
FLUID FILMS
Heating and evaporation of turbulent liquid films: Measurement of film thickness and the onset of nucleate boiling
[DE88-006388] N88-24905
FLUID FILTERS
Reference filters for electrostatic charging tendency measurements of fuels
[AD-A191717] N88-24803
FLUID FLOW
Simulations of a missile with liquid payload under launch conditions
[AD-A191479] N88-24625
Adaptive local grid refinement in computational fluid mechanics
[AD-A192215] N88-24890
A semigroup for Lagrangian 1D isentropic flow
[DE88-006464] N88-24912
NASA research Program: The roles of fluid motion and other transport phenomena in the morphology of materials
[NASA-CR-182801] N88-25327
FLUID MECHANICS
Fundamental aspects of the structure of supersonic turbulent boundary layers
[AD-A191494] N88-24581
Internal fluid dynamics within a nonspinning partially liquid-filled shell due to burster rupture
[AD-A191055] N88-24874
Heating and evaporation of turbulent liquid films: Measurement of film thickness and the onset of nucleate boiling
[DE88-006388] N88-24905
Extreme principles of entrophy production and energy dissipation in fluid mechanics
[NASA-TM-100992] N88-24948
FLUIDICS
Dynamics and control of turbulent shear flows
[AD-A191527] N88-24879
FLUORESCENCE
Optical diagnostics for a high power, rf-inductively coupled plasma
[DE88-007822] N88-25322
FOCUSING
A multi-frame ion pinhole camera for intense ion beam transport and focusing experiments
[DE88-007283] N88-24926
Aurora status and plans
[DE88-006476] N88-24955
Aurora status and plans
[DE88-006476] N88-24955
FORCE DISTRIBUTION
Linear force device
[NASA-CASE-MSC-20549-2] N88-24927
FORCED VIBRATION
Forced response unsteady aerodynamics in a multistage compressor N88-24903
FOREBODIES
Actuated forebody strakes
[NASA-CASE-LAR-13983-1] N88-24628
FORECASTING
FAA aviation forecasts fiscal years 1988-1999
[AD-A191711] N88-24576
FOREIGN POLICY
Department of Defense Statement on the Balanced Technology Initiative to the Committee on Armed Services, United States Senate, 100th Congress, second session
[AD-A191841] N88-25378
FOREST FIRES
History of wildland fires on Vandenberg Air Force Base, California
[NASA-TM-100983] N88-25134

FORMALISM
Stochasticity in a Q-machine plasma N88-25315
FORTRAN
CIMAG2: The computer program to generate color images
[AD-A191847] N88-25175
FOURIER TRANSFORMATION
Analysis of binarized Hartley phase-only filter performance with respect to stochastic noise
[DE88-007604] N88-24945
Integral equation for the laser field: Multimode description of a free-electron laser oscillator
[DE88-007050] N88-24956
Feature extraction using the Hough transform
[AD-A190679] N88-25165
On frequency response for nonlinear systems
[RR-323] N88-25221
FRACTURE MECHANICS
Design of overlays for rigid airport pavements
[DOT/FAA/PM-87/19] N88-24852
Mixed-mode fracture of uniaxial fiber reinforced composites
[AD-A191629] N88-24700
Local delamination buckling in layered structures N88-24711
Characterization of the 2219 Cegedur alloy. Data acquisition of the fracture mechanics — aircraft construction materials
[REPT-48-442/F] N88-24751
Isothermal and bithermal thermomechanical fatigue behavior of a NiCoCrAlY-coated single crystal superalloy
[NASA-TM-100907] N88-24766
Fracture of solid state lasers
[DE88-007023] N88-24961
Stress corrosion cracking of A723 steel pressure vessels: Two case studies
[AD-A191741] N88-24990
Fracture mechanics analysis for short cracks
[AD-A192002] N88-24992
Investigation of the effect of minimum loads and compression of load spectra on the prediction capacities of the ONERA crack model — wings
[ONERA-RTS-33/7169-RY-064-R] N88-24994
Self-consistent model for the brittle response of solids N88-24999
Analysis and developments of failure concepts in fracture mechanics based on research results in the field of component safety topics: J-integral concept; crack resistance curves; dynamic criterion
[V-19/86] N88-25009
FRACTURE STRENGTH
High strength/sigh modulus aromatic heterocyclic ABA block copolymers
[AD-A191666] N88-24774
FRACTURES (MATERIALS)
Mixed-mode fracture of uniaxial fiber reinforced composites
[AD-A191629] N88-24700
FRACTURING
Fracture of solid state lasers
[DE88-007023] N88-24961
FREDHOLM EQUATIONS
Numerical solution of linear integral equations with random forcing terms N88-25237
FREE ELECTRON LASERS
Integral equation for the laser field: Multimode description of a free-electron laser oscillator
[DE88-007050] N88-24956
Reducing sensitivity to errors in free electron laser amplifiers
[DE88-007017] N88-24960
FREE FLOW
Stagnating turbulent reacting flows
[AD-A191449] N88-24877
FREE JETS
Effect of initial tangential velocity distribution on the mean evolution of a swirling turbulent free jet
[NASA-TM-100934] N88-24592
Particle-laden weakly swirling free jets: Measurements and predictions
[NASA-TM-100920] N88-24639
FREEZING
Dendritic growth in the presence of convection N88-25328
FREQUENCIES
Time-frequency representations for speech signals
[AD-A188661] N88-24819
Exact tests for variance component models with unequal cell frequencies in the last stage
[AD-A191645] N88-25253
Frequency Analysis of Acoustic Emission - Application to machining and welding
[DE88-701478] N88-25262
FREQUENCY HOPPING
A Differential Phase Shift Keying (DPSK) modulator for a frequency hopping short wave system
[FOA-C-30460-3.3] N88-24840
FREQUENCY MEASUREMENT
Apparatus for using a time interval counter to measure frequency stability
[NASA-CASE-NPO-17325-1-CU] N88-24846
FREQUENCY RESPONSE
On frequency response for nonlinear systems
[RR-323] N88-25221
FREQUENCY SHIFT KEYING
An FSK (Frequency Shift Keying) telemetry module for vector measuring current meters
[AD-A192142] N88-24661
FREQUENCY STABILITY
Apparatus for using a time interval counter to measure frequency stability
[NASA-CASE-NPO-17325-1-CU] N88-24846
FREQUENCY STANDARDS
Tactical Rubidium Frequency Standard (TRFS), volume 2
[AD-A191190] N88-24850
FRICTION
LLNL granular solids flow project
[DE88-007492] N88-24906
FROZEN FOODS
Low temperature storage container for transporting perishables to space station
[NASA-CASE-MFS-28248-1] N88-24817
FUEL CELLS
Sulfur-tolerant anode materials
[DE88-001034] N88-25054
FUEL CONSUMPTION
NASA/industry advanced turboprop technology program
[NASA-TM-100929] N88-24641
Computer simulation of turbulent combustion in reciprocating engines
[CFDU/87/11] N88-24725
FUEL CONTAMINATION
Fuel containment concepts: Transport category airplanes
[AD-A189618] N88-24799
FUEL SYSTEMS
Fuel containment concepts: Transport category airplanes
[AD-A189618] N88-24799
Servojet retrofit
[AD-A191075] N88-24964
FUEL TESTS
Aircraft emissions characterization: TF41-A2, TF30-P103 and TF30-P109 engines
[AD-A192053] N88-24638
FUELS
History of wildland fires on Vandenberg Air Force Base, California
[NASA-TM-100983] N88-25134
FUNCTION SPACE
Linear spaces, absolute retracts and the compact extension property
[PB88-181110] N88-25225
FUNCTIONAL DESIGN SPECIFICATIONS
Parachute for in-flight training on parachute ejection
[REPT-87-11] N88-24593
Preparation for microgravity: The role of the microgravity materials science laboratory
[NASA-TM-100906] N88-24811
FUSION REACTORS
Design studies of low aspect-ratio torsatrons
[DE88-007562] N88-25320

G

GALERIKIN METHOD
Numerical solution of linear integral equations with random forcing terms N88-25237
Galerkin approximation for inverse problems for nonautonomous nonlinear distributed systems
[NASA-CR-181676] N88-25246
New mixed finite element methods N88-25248
GALILEO SPACECRAFT
Experimental investigation of hypersonic aerodynamics
[NASA-CR-182973] N88-24591
GALLIUM ARSENIDES
Joint services electronics program research in electronics
[AD-A192206] N88-24857
A monolithic reduced-size Ku-Band SPOT (Single-Pole Double Throw) FET switch
[DE88-006273] N88-24858
Monolithic GaAs Ku-band one watt constant phase variable power amplifier
[DE88-006272] N88-24866
Optical nonlinearities in GaAs/GaAlAs multiple quantum wells fabricated by metalorganic chemical vapor deposition for use in optical signal processing
[AD-A191558] N88-25337
On the use of convergent beam electron diffraction for identification of antiphase boundaries in GaAs grown on Si
[DE88-008220] N88-25362
GALLIUM PHOSPHIDES
Improved properties of SiGe/GaP alloys
[NASA-CASE-NPO-17259-1-CU] N88-25358
GAMMA RAY SPECTRA
Characterization of yttrium aluminum garnet/YAG/using 14 MeV neutron activation
[AD-A191925] N88-25342
GAMMA RAYS
Utilization of the IR telescope gimbaling system as a stabilized pointing platform for balloon payloads. Volume 1: Technical results
[NASA-CR-179339] N88-24962
Gamma rays from Cygnus X-1: Modeling and nonthermal pair production
[DE88-006830] N88-25426
GAS ANALYSIS
Structure/property/reactivity relations among nitramine and other energetic materials
[AD-A190878] N88-24716
Geological evolution and analysis of confirmed or suspected gas hydrate localities. Volume 2: Basin analysis, formation and stability of gas hydrates in the Black Sea
[DE88-001052] N88-25023
GAS ATOMIZATION
Laboratory scale inert gas atomizer for producing rapidly solidified powders
[DE88-006734] N88-24812
GAS CHROMATOGRAPHY
Selective detection in gas chromatography
[AD-A191499] N88-24718
Thermal decomposition studies of explosives for component applications
[DE88-007201] N88-24805
GAS FLOW
Compressible flow in a pie-shaped cylinder rotating about the vertex N88-24604
GAS GUNS
Use of a two-stage light-gas gun as an injector for electromagnetic railguns
[DE88-007200] N88-24657
GAS IONIZATION
High-order multiphoton ionization of the noble gases
[DE88-007489] N88-25273
GAS LASERS
High power axial flow CO2 laser
[ETN-88-91951] N88-24959
GAS MIXTURES
Trace gas measurements in the troposphere using tunable diode lasers N88-25072
GAS PIPES
Trailer shield assembly for a welding torch
[NASA-CASE-MFS-29260-1] N88-24972
GAS PRESSURE
Gas diffusion studies in steady and nonsteady cavities N88-24902
GAS TURBINES
Research on aero-thermodynamic distortion induced structural dynamic response of multi-stage compressor blading
[AD-A192169] N88-24584
An empirical model of the effects of curvature and convergence on dilution jet mixing
[NASA-TM-100896] N88-24640
Evaluation of manure as a feedstock for gas turbines N88-25050
A 3 MW wood fired gas turbine at Red Boiling Springs, Tennessee N88-25051
GASEOUS DIFFUSION
Mechanisms of gas permeation through polymer membranes: Renewal proposal for period December 1, 1986 - November 30, 1989
[DE88-007436] N88-24796
Gas diffusion studies in steady and nonsteady cavities N88-24902
GASES
Heating and evaporation of turbulent liquid films: Measurement of film thickness and the onset of nucleate boiling
[DE88-006388] N88-24905
GASIFICATION
Bench-scale studies on fluid-bed pyrolysis of wood using different contact gases N88-25049
GASOLINE
Upgrading pyrolysis vapors to aromatic gasoline with zeolite catalysis at atmospheric pressure N88-25045
Research on hydrotreating catalysts to hydrodeoxygenate biocrude oils N88-25048

Technical and economic evaluation of emerging biomass pyrolysis processes for gasoline production N88-25048
GATES (CIRCUITS)
Planar fully ion-implanted high power InP MISFETs [AD-A191589] N88-25338
Development of the field-induced electron injection and impact ionization (F4I) technique for radiation hardness testing of MOS (Metal-Oxide-Semiconductor) gate insulators [AD-A192114] N88-25345
GAUGE THEORY
Rigid symmetries and BRST-invariance in gauge theories [PB88-180948] N88-25280
Introduction to lattice gauge theory [DE88-006073] N88-25349
GEARS
Linear force device [NASA-CASE-MSC-20549-2] N88-24927
Design, manufacture and spin test of high contact ratio helicopter transmission utilizing Self-Aligning Bearingless Planetary (SABP) [NASA-CR-4155] N88-24975
Determination of settings of a tilted head-cutter for generation of hypoid and spiral bevel gears [NASA-CR-182138] N88-24976
GELLED PROPELLANTS
Characterization of aluminum/RP-1 gel propellant properties [NASA-TM-100951] N88-24806
GENERAL AVIATION AIRCRAFT
Development of a multipurpose smart recorder for general aviation aircraft [NASA-CR-168353] N88-24637
GENETIC CODE
The human genome: Computational challenges [DE88-006465] N88-25131
GENETIC ENGINEERING
The human genome: Computational challenges [DE88-006465] N88-25131
Ecological risk factors related to environmental uses of genetically engineered organisms [DE88-006674] N88-25132
GEOCHEMISTRY
A sedimentological and mineralogical study of the Koogah Formation, New South Wales N88-25087
GEODESY
Geodesy by radio interferometry: Optimization of wet path delay algorithms using microwave radiometer data [PB88-167730] N88-24820
GEODYNAMICS
Drilling investigation of a young magmatic intrusion beneath the Inyo Domes, Long Valley, California: Structural and textural studies [DE88-006613] N88-25078
The interpretation of crustal dynamics data in terms of plate interactions and active tectonics of the Anatolian Plate and surrounding regions in the Middle East [NASA-CR-183024] N88-25092
GEOGRAPHY
The Department of Defense report on the merit review process for competitive selection of university research projects and an analysis of the potential for expanding the geographic distribution of research for the Committees on Appropriations, United States Congress [AD-A191842] N88-25379
GEOIDS
To relate measurements of gravity and geoid anomalies over the oceans to near surface density distributions [AD-A192168] N88-25120
GEOLOGY
Geological evolution and analysis of confirmed or suspected gas hydrate localities. Volume 2: Basin analysis, formation and stability of gas hydrates in the Black Sea [DE88-001052] N88-25023
GEOMAGNETIC TAIL
Interpretation of the northward B sub z (NBZ) Birkeland current system and polar cap convection patterns in terms of the impulsive penetration model [AERONOMICA-ACTA-A-321-1987] N88-25422
GEOMAGNETISM
DOD 1985 world magnetic model: Charts and grid values [AD-A191484] N88-25080
GEOMETRY
Internal fluid dynamics within a nonspinning partially liquid-filled shell due to burster rupture [AD-A191055] N88-24874
Modeling of geometric reasoning for robot programming [ETN-88-92290] N88-25202
Optical investigations of the thermal boundary layer in arc plasmas N88-25313
The geometry of the Virasoro group for physicists [DE88-007374] N88-25366
GEOMORPHOLOGY
Geological evolution and analysis of confirmed or suspected gas hydrate localities. Volume 2: Basin analysis, formation and stability of gas hydrates in the Black Sea [DE88-001052] N88-25023
GEOPHYSICS
Remote sensing of acoustic properties of shallow water sediments: A review [AD-A192107] N88-25267
GEOSTROPHIC WIND
Three-dimensional temperature fields in the atmosphere up to 50 km altitude [ETN-88-92150] N88-25089
GERMANIUM ALLOYS
Improved properties of SiGe/GaP alloys [NASA-CASE-NPO-17259-1-CU] N88-25358
Metastability in SiGe/Si strained-layer structures [DE88-007603] N88-25361
GIANT STARS
Review of the theoretical changes of surface chemistry during massive star evolution [SER-C-PREPUBL-FASC-17] N88-25411
GIBBS FREE ENERGY
Certain questions of thermodynamic theory of weak solutions N88-25368
GIMBALS
Utilization of the IR telescope gimbaling system as a stabilized pointing platform for balloon payloads. Volume 1: Technical results [NASA-CR-179339] N88-24962
GLASS FIBERS
Sol/gel processing techniques for glass matrix composites [AD-A191748] N88-24701
Calculational model development for fibrous thermal insulation transient test procedures [DE88-007843] N88-24789
Novel fiber preforms: Rare earth doping [AD-A191549] N88-25294
GLOBAL POSITIONING SYSTEM
Inertial reference system with Global Positioning System (GPS) support N88-24936
GLUTAMINE
Dexamethasone regulates glutamine synthetase expression in rat skeletal muscles [NASA-CR-182935] N88-25129
GOALS
Advanced development of double-injection, deep-impurity semiconductor switches [NASA-CR-182118] N88-25346
GONDOLAS
Utilization of the IR telescope gimbaling system as a stabilized pointing platform for balloon payloads. Volume 1: Technical results [NASA-CR-179339] N88-24962
GOVERNMENT PROCUREMENT
Department of Defense Statement on the Technology Base to the Subcommittee on Defense Industry and Technology of the Committee on Armed Services, United States Senate, 100th Congress, second session [AD-A191839] N88-25376
GOVERNMENT/INDUSTRY RELATIONS
Class 2 design update for the family of commuter airplanes [NASA-CR-182681] N88-24629
The Department of Defense report on the merit review process for competitive selection of university research projects and an analysis of the potential for expanding the geographic distribution of research for the Committees on Appropriations, United States Congress [AD-A191842] N88-25379
GRAIN BOUNDARIES
The morphological stability of continuous intergranular phases: Thermodynamic considerations [DE88-006328] N88-25350
GRANULAR MATERIALS
LLNL granular solids flow project [DE88-007492] N88-24906
GRAPH THEORY
A mixed-integer linear programming problem which is efficiently solvable [AD-A191028] N88-25168
Research in enumeration and graph theory with applications to computer science [AD-A191567] N88-25171
GRAPHIC ARTS
The ISI (Information Sciences Institute) grapher manual [AD-A192198] N88-25200
GRAPHITE
Interfacial shear phenomena in graphite epoxy composites under impact loading using dynamic moire interferometry [DE88-006773] N88-24709
Raman characterization of AsF5-intercalated vapor grown graphite fibers [AD-A191709] N88-24778
Stress measurements in graphite fibers by laser raman spectroscopy [AD-A191710] N88-24779
Electron-Rayleigh wave interaction in thin film carbons [AD-A191727] N88-24781
Photoconductivity in carbon fibers [AD-A191728] N88-24782
Effect of uniaxial stress on the Raman spectra of graphite fibers [AD-A191730] N88-24783
GRAPHITE-POLYIMIDE COMPOSITES
The 700 F properties of autoclave cured PMR-2 composites [NASA-TM-100923] N88-24712
GRAVITATION THEORY
Inevitable inflation in Einstein-Cartan theory with improved energy-momentum tensor with spin [NASA-TM-101146] N88-25365
From general relativity to the theory of superstrings N88-25369
GRAVITATIONAL COLLAPSE
Microwave spectroscopy and gravitational collapse N88-25413
GRAVITATIONAL EFFECTS
Flotation processes [PB88-180302] N88-25075
Cardiovascular effects of weightlessness and ground-based simulation [NASA-TM-88314] N88-25140
GRAVITATIONAL LENSES
Light propagation through gravitationally perturbed Friedmann universes N88-25307
GRAVITATIONAL WAVES
Light propagation through gravitationally perturbed Friedmann universes N88-25307
GRAVITONS
Comment on non-renormalization theorem in the four dimensional superstrings [DE88-752551] N88-25367
GRAVITY ANOMALIES
To relate measurements of gravity and geoid anomalies over the oceans to near surface density distributions [AD-A192168] N88-25120
GRAZING INCIDENCE
An experimental study of the coherent under-ice reflectivity of sound in the Greenland Sea Marginal Ice Zone N88-25125
GREEN'S FUNCTIONS
Construction of approximations to acoustic Green's functions for nonhomogeneous oceans using transmutation [PB88-185384] N88-25126
GROUND BASED CONTROL
Optimization of the dilation characteristic on the control jurisdiction of an area control facility [AD-A191720] N88-24615
GROUND STATE
Energy-transfer properties and mechanisms [DE88-007107] N88-25272
Ground state properties and electronic structure of high T sub c superconductors [DE88-007485] N88-25360
GROUND STATIONS
Service offerings and interfaces for the ACTS network of Earth stations [NASA-TM-100809] N88-24663
GROUP THEORY
Perturbation theory for dual semigroups. Part 4: The intertwining formula and the canonical pairing [CWI-AM-R8802-PT-4] N88-25258
GUARDS (SHIELDS)
Trailer shield assembly for a welding torch [NASA-CASE-MFS-29260-1] N88-24972
GUIDANCE SENSORS
The optical accelerometer: A novel sensor for vertical flight guidance N88-24935
GUN PROPELLANTS
Electrical ignition of HAN-based liquid propellants [AD-A191349] N88-24801

H

HABITABILITY
Space station habitability recommendations based on a systematic comparative analysis of analogous conditions [NASA-CR-3943] N88-25372
HADRONS
Experimental elementary particle physics [DE88-007510] N88-25274
HALLEY'S COMET
The evolution of cometary activity N88-25416

HALOGEN COMPOUNDS
Spectroscopy and energy transfer kinetics of the interhalogens
[AD-A192103] N88-25344
HARDENING (MATERIALS)
Theory of viscoplasticity based on overstress with applications N88-25007
HARDNESS TESTS
Critical cooling rates on solution treatment of Cu-Cr and Cu-Be alloys
[NASA-TT-20163] N88-24760
HARMONICS
Harmonic considerations for electrical distribution feeders
[DE88-007849] N88-24860
Motor theory of auditory perception
[AD-A192095] N88-25136
HATCHES
Hatch cover
[NASA-CASE-MSC-21356-1] N88-24871
HEAD DOWN TILT
Determination of settings of a tilted head-cutter for generation of hypoid and spiral bevel gears
[NASA-CR-182138] N88-24976
HEAD-UP DISPLAYS
An evaluation of three linear scale radar altimeter displays
[AD-A192173] N88-24636
HEAT ACCLIMATIZATION
Physiological and hematological responses of matched older and younger men during dry-heat acclimation
[AD-A186450] N88-25139
HEAT EXCHANGERS
Computational fluid dynamics applied to the prediction of the heat-transfer, mechanical and thermal-stress behavior of heat exchangers
[CFDU/87/7] N88-24893
HEAT MEASUREMENT
Calorimetry applied to nucleus-nucleus collisions at ultrarelativistic energies
[DE88-006173] N88-25262
HEAT OF COMBUSTION
Application of Rayleigh scattering to turbulent flow with heat transfer and combustion
[AD-A191565] N88-24720
HEAT RESISTANT ALLOYS
Effect of alloying, rapid solidification, and surface kinetics on the high temperature environmental resistance of niobium
[AD-A192093] N88-24743
Isothermal and bithermal thermomechanical fatigue behavior of a NiCoCrAlY-coated single crystal superalloy
[NASA-TM-100907] N88-24766
HEAT STORAGE
Field experience with aquifer thermal energy storage
[DE88-007075] N88-25058
HEAT TOLERANCE
Effects of moderate cold and heat stress on the potential work performance of industrial workers. Part 6: The effects of increasing vapour pressure at four air temperatures on the performance and physiology of white females
[PB88-124854] N88-25137
HEAT TRANSFER
Analytic and numerical modeling of heat and material transport in electrical hypervelocity guns
[AD-A192178] N88-24655
Designing to safe power limits in hybrid circuits
[DE88-005533] N88-24865
Heat transfer from a negatively buoyant wall jet
[PB88-181953] N88-24873
Computational fluid dynamics applied to the prediction of the heat-transfer, mechanical and thermal-stress behavior of heat exchangers
[CFDU/87/7] N88-24893
Similarity solutions of nonlinear partial differential equations invariant to a family of affine groups
[DE88-003404] N88-25245
Modelling of thermal plasma systems N88-25314
HEAT TREATMENT
A study on the precipitation and reversion behaviors of Cu-0.3 percent Cr alloy by the step annealing method
[NASA-TT-20169] N88-24764
HEATING
Acoustic convective system
[NASA-CASE-NPO-17278-1-CU] N88-24818
Heating and evaporation of turbulent liquid films: Measurement of film thickness and the onset of nucleate boiling
[DE88-006388] N88-24905
HEAVY IONS
The multistring model VENUS for ultrarelativistic heavy ion collisions
[DE88-007666] N88-25284
Experiments with high energy nuclear beams at Brookhaven: From AGS to RHIC (Relativistic Heavy Ion Collider)
[DE88-007042] N88-25287
HELICOPTER CONTROL
Simultaneous multiple control force exertion capabilities of males and females versus helicopter control force design limits
[AD-A191653] N88-25153
HELICOPTER DESIGN
Structurally tailorable non-linear snap-through spring system
[NASA-CASE-LAR-13729-1] N88-24970
HELICOPTERS
Competitive assessment of the U.S. civil helicopter industry
[PB88-186325] N88-24574
Passive shock wave-boundary layer control for the Bell FX69-H-096 airfoil N88-24588
Some rotorcraft applications of computational fluid dynamics
[NASA-TM-100066] N88-24801
Inflow measurements made with a laser velocimeter on a helicopter model in forward flight. Volume 1: Rectangular planform blades at an advance ration of 0.15
[NASA-TM-100541] N88-24607
Rotorcraft TCAS (traffic alert and collision avoidance system) evaluation: Group 3 results
[AD-A191719] N88-24814
An enumeration of research to determine the optimal design and use of Army flight training simulators
[AD-A191242] N88-24649
Design, manufacture and spin test of high contact ratio helicopter transmission utilizing Self-Aligning Bearingless Planetary (SABP)
[NASA-CR-4155] N88-24975
HELIOSPHERE
Observations of cosmic rays in the outer heliosphere
[NASA-CR-182942] N88-25425
HELIUM-NEON LASERS
Fast acting optical beam detection and deflection system
[AD-A192161] N88-24954
HELMET MOUNTED DISPLAYS
Evaluation of the US Army fitting program for the integrated helmet unit of the integrated helmet and display sighting system
[AD-A191616] N88-24835
HEMATOLOGY
Physiological and hematological responses of matched older and younger men during dry-heat acclimation
[AD-A186450] N88-25139
HENRY LAW
Certain questions of thermodynamic theory of weak solutions N88-25368
HETEROCYCLIC COMPOUNDS
High strength/sigh modulus aromatic heterocyclic ABA block copolymers
[AD-A191686] N88-24774
HETEROJUNCTIONS
Joint services electronics program research in electronics
[AD-A192206] N88-24857
Optical properties of heterostructures and superlattices
[AD-A191542] N88-25335
HEURISTIC METHODS
Design of partially replicated distributed database systems: An integrated methodology N88-25383
HIGH ELECTRON MOBILITY TRANSISTORS
Computer aided design of monolithic microwave and millimeter wave integrated circuits and subsystems
[AD-A191593] N88-24852
HIGH ENERGY ELECTRONS
Deep dielectric charging effects due to high energy electrons in earth's outer magnetosphere
[AD-A192154] N88-25083
HIGH ENERGY INTERACTIONS
Energy measurements in oxygen-induced reactions at 60 A GeV and 200 A GeV
[DE88-006420] N88-25283
HIGH FREQUENCIES
Communications using channels formed by meteor bursts
[AD-A192068] N88-24834
Radio-wave scintillations and ionospheric irregularities at high latitudes
[AD-A192140] N88-24837
HIGH GAIN
The off-axis channel macroplate
[NASA-CR-182936] N88-24861
HIGH LEVEL LANGUAGES
New York TRACON demonstration of program recoding requirements analysis document
[DOT/FAA/CT-87/34] N88-24822
EPL (Equational Programing Language) system design: Intermediate processing steps
[AD-A191203] N88-25169
HIGH POWER LASERS
High power axial flow CO2 laser
[ETN-88-91951] N88-24959
HIGH PRESSURE
The high pressure sound velocity and equation of state of aqueous solutions of hydroxylammonium nitrate and triethanolammonium nitrate
[AD-A191740] N88-25266
HIGH RESOLUTION
High resolution radar techniques: Five contributions to MILINF 86
[PB88-172721] N88-24821
DMSP-SSM/1 NASA algorithm validation using primarily LANDSAT and secondarily DMSP and/or AVHRR visible and thermal infrared satellite imagery
[NASA-CR-182979] N88-25024
HIGH SPEED CAMERAS
Simple high speed camera with CCD-sensor
[MPIS-8/1987] N88-24940
HIGH TEMPERATURE
The variation of torsional ductility of high-purity aluminum with temperature and strain rate
[DE88-005618] N88-24755
HIGH TEMPERATURE ENVIRONMENTS
Effect of alloying, rapid solidification, and surface kinetics on the high temperature environmental resistance of niobium
[AD-A192093] N88-24743
HIGH TEMPERATURE SUPERCONDUCTORS
Crystalline metal-semiconductor superlattices
[DE88-007063] N88-25332
Ground state properties and electronic structure of high T sub c superconductors
[DE88-007485] N88-25360
HIGH TEMPERATURE TESTS
Combustion behavior of the vitiator. Experimental results of a second test series
[VTH-LR-509] N88-24734
HINGES
Payload deployment method and system
[NASA-CASE-MSC-21330-1] N88-24660
HISTORIES
The application of hydrocarbon bioconversion technology to aerospace materials production N88-24698
History of wildland fires on Vandenberg Air Force Base, California
[NASA-TM-100963] N88-25134
NASA history data book. Volume 1: NASA resources 1958-1968
[NASA-SP-4012-VOL-1] N88-25428
NASA historical data book. Volume 2: Programs and projects 1958-1968
[NASA-SP-4012-VOL-2] N88-25429
NASA historical data book. Volume 3: Programs and projects 1969-1978
[NASA-SP-4012-VOL-3] N88-25430
HOMOGENIZING
Functional and mechanical analysis of continuous media-application to the study of elastic composites with periodic structure: Homogenization
[NASA-TT-20188] N88-24710
HOPPERS
Energy efficient continuous flow ash lockhopper
[NASA-CASE-NPO-18985-1-CU] N88-24814
HOT PRESSING
Martensitic transformation and microstructures in sintered NiAl alloys
[NASA-TT-20178] N88-24761
HOT-FILM ANEMOMETERS
Method of forming a multiple layer dielectric and a hot film sensor therewith
[NASA-CASE-LAR-13678-1] N88-25355
HOVERING
Method for prediction and determination of takeoff performance for vectored thrust vehicles
[AD-A191809] N88-24626
Operational noise data for CH-47D and AH-64 army helicopters
[AD-A191059] N88-25263
HUMAN BEHAVIOR
Performance effectiveness and the work/rest cycle
[AD-A191448] N88-25145
HUMAN FACTORS ENGINEERING
Space station architectural elements model study
[NASA-CR-4027] N88-24632
Evaluation of the US Army fitting program for the integrated helmet unit of the integrated helmet and display sighting system
[AD-A191616] N88-24635
Human problem solving in complex dynamic environments
[AD-A190788] N88-25142

An advanced prototyping tool for human factors design
[AD-A187290] N88-25149
Human performance issues arising from manned space station missions
[NASA-CR-3942] N88-25156
Space station habitability recommendations based on a systematic comparative analysis of analogous conditions
[NASA-CR-3943] N88-25372

HUMAN PERFORMANCE
Effects of moderate cold and heat stress on the potential work performance of industrial workers. Part 6: The effects of increasing vapour pressure at four air temperatures on the performance and physiology of white females
[PB88-124854] N88-25137
Eye and head response to an attention cue in a dual task paradigm
[AD-A191052] N88-25143
Optimizing feedback utilization in motor skill training
[AD-A191559] N88-25146
Performance estimates for operations conducted while wearing individual protective equipment: User manual
[AD-A191871] N88-25154
Modeling and evaluation of variable structure organizations
[AD-A191947] N88-25361

HYBRID CIRCUITS
Designing to safe power limits in hybrid circuits
[DE88-005533] N88-24885

HYDRATES
Geological evolution and analysis of confirmed or suspected gas hydrate localities. Volume 2: Basin analysis, formation and stability of gas hydrates in the Black Sea
[DE88-001052] N88-25023

HYDRAULIC JETS
Hydroacoustic pulsating jet generator
[MPIS-7/1987] N88-24891

HYDROCARBON COMBUSTION
Chemical kinetics of nitramine propellant combustion
[AD-A191556] N88-24802

HYDROCARBON FUEL PRODUCTION
Research on hydrotreating catalysts to hydrodeoxygenate biocrude oils N88-25046

HYDROCARBON FUELS
Dual-fuel, dual-mode rocket engine
[NASA-CASE-LAR-13773-1] N88-24685
Production costs of hydrocarbon fuels from biomass
[DE88-006667] N88-24804
Motor vehicles as sources of compounds important to tropospheric and stratospheric ozone
[PB88-195219] N88-25076

HYDROCARBONS
The application of hydrocarbon bioconversion technology to aerospace materials production N88-24898

HYDROCHLORIC ACID
Monitoring biological impacts of space shuttle launches from Vandenberg Air Force Base: Establishment of baseline conditions
[NASA-TM-100982] N88-25133

HYDROCRACKING
Research on hydrotreating catalysts to hydrodeoxygenate biocrude oils N88-25046

HYDRODYNAMICS
The influence of cathodic protection on erosion-corrosion of metals and model alloys
[AD-A191613] N88-24742
Dynamics and control of turbulent shear flows
[AD-A191527] N88-24879
Heating and evaporation of turbulent liquid films: Measurement of film thickness and the onset of nucleate boiling
[DE88-006388] N88-24905
LLNL granular solids flow project
[DE88-007492] N88-24906

HYDROGEN
Effect of hydrogen, deuterium and oxygen on the anelastic properties of refractory alloys
[DE88-007349] N88-24736

HYDROGEN FUELS
Performance of a hydrogen pulsed electrothermal thruster. Strategic defense initiative organization innovative science and technology. SBIR, phase 1
[AD-A191999] N88-24679
Dual-fuel, dual-mode rocket engine
[NASA-CASE-LAR-13773-1] N88-24685
Catalytic ignition of hydrogen and oxygen propellants
[NASA-TM-100957] N88-24689

HYDROGEN IONS
An optical technique for measuring divergence, beam profile, and aiming direction, of relativistic negative hydrogen ions
[DE88-007049] N88-25278

HYDROGEN OXYGEN ENGINES
Recent advances in low-thrust propulsion technology
[NASA-TM-100959] N88-25260

HYDROGENATION
Surface composition-reactivity relationships in heterogeneous catalysis
[DE88-006679] N88-24714
Research on hydrotreating catalysts to hydrodeoxygenate biocrude oils N88-25046

HYDROPHONES
Remote sensing of acoustic properties of shallow water sediments: A review
[AD-A192107] N88-25267

HYDROXIDES
Transition probabilities in OH A 2 sigma + - X 2 pi i Bands with v prime = 0 and 1, v double prime = 0 to 4
[NASA-CR-182946] N88-25353

HYDROXYL COMPOUNDS
The burning of HAN-based (hydroxylammonium nitrate) liquid propellants
[DE88-006863] N88-24800

HYDROXYL RADICALS
Ultraviolet measurements: Measurements of photolysis rates N88-25065
Laboratory experiments on atmospheric OH reactions N88-25066
Effect of carbohydrate oxidation on the tropospheric HOx-system N88-25067
Measurement of atmospheric OH with laser differential optical absorption spectroscopy (LDOAS) N88-25068
Tropospheric OH measurements by long path absorption with rapid spectral concordance N88-25069
Determination of tropospheric H concentrations by a double-pulsed UV laser method N88-25070
Tropospheric OH measurement by Laser Induced Fluorescence (LIF) N88-25071
Development of continuous wave laser frequency modulation of OH in tropospheric concentrations range N88-25073
The evolution of cometary activity N88-25416

HYPERBOLIC COORDINATES
Two dimensional hyperbolic grid generation
[VKI-TN-162] N88-24897

HYPERCUBE MULTIPROCESSORS
Multi-sensor integration on the NCUBE hypercube computer
[DE88-007472] N88-25162

HYPERSONIC BOUNDARY LAYER
Hypersonic turbulent wall boundary layer computations
[NASA-CR-182147] N88-24917

HYPERSONIC FLOW
Boundary layer transition
[CERT-OA-37/5018-AYD] N88-24595
Hypersonic turbulent wall boundary layer computations
[NASA-CR-182147] N88-24917

HYPERSONIC WIND TUNNELS
The performance of the VKI longshot hypersonic wind tunnel
[VKI-TN-161] N88-24650

HYPERVELOCITY GUNS
Analytic and numerical modeling of heat and material transport in electrical hypervelocity guns
[AD-A192178] N88-24655

HYPERVELOCITY IMPACT
Effects of meteoroids and space debris on the particulate environment for space station N88-25399

HYPERVELOCITY LAUNCHERS
Fabrication issues and technology development for HELEOS (Hypervelocity Electromagnetic Launcher for Equation Of State)
[DE88-007419] N88-24658

HYPSOGRAPHY
Vectorization of raster algorithms for elevation data processing N88-25036

I

ICE FORMATION
Ice formation on aircraft
[ETN-88-92154] N88-25104
National plans for aircraft icing and improved aircraft icing forecasts and associated warning services N88-25113

ICE REPORTING
Ice conditions along the Ohio River as observed on LANDSAT images, 1972-1985
[AD-A191172] N88-25018
An experimental study of the coherent under-ice reflectivity of sound in the Greenland Sea Marginal Ice Zone N88-25125

ICELAND
SeaSoar profiles in the Iceland-Scotland area, May 1987
[IOS-253] N88-25124

IGNITERS
Catalytic ignition of hydrogen and oxygen propellants
[NASA-TM-100957] N88-24689

IGNITION
Catalytic ignition of hydrogen and oxygen propellants
[NASA-TM-100957] N88-24689
The burning of HAN-based (hydroxylammonium nitrate) liquid propellants
[DE88-006863] N88-24800

ILLUMINATING
Optical system of laser illuminated streamer chamber
[DE88-702127] N88-25306

IMAGE ANALYSIS
Mathematical morphology for structures without translation symmetry
[CWI-AM-R8803] N88-25241
Real-time image difference detection using a polarization rotation special light modulator
[NASA-CASE-NPO-17144-1-CU] N88-25305

IMAGE CONTRAST
Development and validation of transmission measurements techniques of image contrast, utilizing existing IR imagers
[AD-A191471] N88-25079

IMAGE PROCESSING
Analysis of binarized Hartley phase-only filter performance with respect to stochastic noise
[DE88-007604] N88-24945
High-energy laser-assisted imaging through vaporizing aerosols
[DE88-007911] N88-24957
Visual information processing in the perception of features and objects
[AD-A192026] N88-25148
CIMAG2: The computer program to generate color images
[AD-A191847] N88-25175
System overview: Teragon 4000, an image processing equipment at FOA 3
[FOA-C-30465-3.3] N88-25179
Shape from shading, occlusion and texture
[AD-A184840] N88-25269
Optical system of laser illuminated streamer chamber
[DE88-702127] N88-25306
An image processing system for research in solar physics
[AD-A191673] N88-25421

IMAGE RECONSTRUCTION
Application of dynamic programming to image registration
[ENST-87E022] N88-25180
A fast and efficient procedure for generalized cross-validation with large data sets. Application to image reconstruction
[RR-669-M] N88-25220

IMAGE RESOLUTION
Instrumentation for turbulent reacting flows
[AD-A191671] N88-24923

IMAGERY
Atmospheric autorotating imaging device
[NASA-CASE-NPO-17390-1-CU] N88-24944

IMAGING RADAR
The role of space borne imaging radars in environmental monitoring: Some shuttle imaging radar results in Asia
[NASA-TM-101178] N88-24844

IMAGING TECHNIQUES
Delay-doppler radar imaging
[AD-A191509] N88-24826
High-energy laser-assisted imaging through vaporizing aerosols
[DE88-007911] N88-24957
Utilization of the IR telescope gimbaling system as a stabilized pointing platform for balloon payloads. Volume 1: Technical results
[NASA-CR-179339] N88-24962

IMIDES
Aromatic cyclotriphosphazenes
[NASA-CASE-ARC-11428-3] N88-24892

IMPACT ACCELERATION
Peak Acceleration Device (PAD)
[AD-A191639] N88-24611

IMPACT LOADS
Interfacial shear phenomena in graphite epoxy composites under impact loading using dynamic moire interferometry
[DE88-006773] N88-24709

IMPACT RESISTANCE
Evaluation of the US Army fitting program for the integrated helmet unit of the integrated helmet and display sighting system
[AD-A191616] N88-24635

IMPACT TESTS
Peak Acceleration Device (PAD)
[AD-A191639] N88-24611

IMPURITIES
Recent data on Si:As impurity band conduction multiplexed arrays
[AD-A191752] N88-25340
Advanced development of double-injection, deep-impurity semiconductor switches
[NASA-CR-182118] N88-25346
IN-FLIGHT MONITORING
A system status monitor for the National Aerospace Plane
[AD-A190661] N88-24824
INCIDENCE
Curvature of blended rolled edge reflectors at the shadow boundary contour
[NASA-CR-182974] N88-25300
INCOHERENT SCATTERING
Multiple scattering of waves in discrete random media
[AD-A191068] N88-24823
INCOMPRESSIBLE FLOW
Incompressible Euler solution on a multiblock grid around a car configuration
[FFA-TN-1987-65] N88-24586
Prediction of laminar and turbulent flows past single and twin airfoils N88-24589
Continuum theories for fluid-particle flows: Some aspects of lift forces and turbulence
[DE88-007038] N88-24896
Theoretical analysis of laminar incompressible flow in slender channels
[VTH-LR-517] N88-24909
INDEXES (DOCUMENTATION)
NASA combined file postings statistics based on NASA thesaurus, Jan. 1968 - July 1988
[NASA-CR-182985] N88-25384
INDIUM ALLOYS
Aluminum alloy
[NASA-CASE-LAR-13924-1-CU] N88-24753
INDIUM PHOSPHIDES
Progress in InP solar cell research
[NASA-TM-100914] N88-24870
Planar fully ion-implanted high power InP MISFETs
[AD-A191589] N88-25338
INDUSTRIES
Competitive assessment of the U.S. civil helicopter industry
[PB88-186325] N88-24574
The application of hydrocarbon bioconversion technology to aerospace materials production N88-24898
INELASTIC SCATTERING
Nuclear structure studies at intermediate energies
[DE88-006683] N88-25271
INEQUALITIES
Additive prophet inequalities for transforms of uniformly bounded pairwise independent random variables
[PB88-173513] N88-25250
INERTIAL GUIDANCE
Inertial reference system with Global Positioning System (GPS) support N88-24936
INERTIAL NAVIGATION
Optics: Perspectives for Measurement Techniques and Signal Processing for Flight Guidance — conference
[DFVLR-MITT-87-21] N88-24928
Laboratory tests of laser gyroscopes for future utilization in multifunction systems for precision navigation and flight guidance N88-24932
The optical accelerometer: A novel sensor for vertical flight guidance N88-24935
INERTIAL REFERENCE SYSTEMS
Laboratory tests of laser gyroscopes for future utilization in multifunction systems for precision navigation and flight guidance N88-24932
Inertial reference system with Global Positioning System (GPS) support N88-24936
INFERENCE
User's guide to the Fault Inferring Nonlinear Detection System (FINDS) computer program
[NASA-CR-178410] N88-24819
Adaptive time series analysis using predictive inference and entropy
[AD-A191858] N88-25199
INFORMATION DISSEMINATION
Computer resource management technology program (PE 64740F). Task no. 9: Advanced user authentication
[PB88-183066] N88-25163
INFORMATION FLOW
A multiprocessor data flow accelerator module
[DE88-007587] N88-25161
INFORMATION RETRIEVAL
Defense Technical Information Center cataloging guidelines
[AD-A192200] N88-25382
Engineering drawings and changes: Storing and controlling by the tens of terrabytes
[DE88-007605] N88-25387
INFORMATION SYSTEMS
Information and stochastic systems
[AD-A192167] N88-24838
The human genome: Computational challenges
[DE88-006465] N88-25131
INFRARED ASTRONOMY
Infrared astronomy at extremely faint light levels in support of the LAIRTS program
[AD-A191497] N88-25404
INFRARED IMAGERY
Thermographic detection of buried debonds
[AD-A192115] N88-24680
INFRARED INSTRUMENTS
A disposable liquid microcell for near-infrared reflectance analysis
[AD-A192190] N88-25298
INFRARED INTERFEROMETERS
A two-wavelength infrared interferometer/polarimeter system for CIT (Compact Ignition Tokamak)
[DE88-007681] N88-25321
INFRARED RADIATION
Bimolecular reactions and energy-transfer processes of highly vibrationally excited molecules related to energetic materials
[AD-A189013] N88-25270
Calculation of space station infrared irradiance from atmosphere-induced emissions N88-25396
INFRARED SPECTRA
Optical constants of minerals and other materials from the millimeter to the ultraviolet
[AD-A192210] N88-24724
INFRARED TELESCOPES
Utilization of the IR telescope gimbaling system as a stabilized pointing platform for balloon payloads. Volume 1: Technical results
[NASA-CR-179339] N88-24962
INSPECTION
Knowledge based systems in nondestructive evaluation
[DE88-006653] N88-24981
The inspection of metallurgical bounds in electronic systems
[AD-A192064] N88-25343
INSTRUCTORS
US civil airmen statistics, 1987
[AD-A191714] N88-24577
INSTRUMENT APPROACH
Cessna 172 MLS (Microwave Landing System) terminal instrument procedures (TERPS) approach data collection and processing data report
[AD-A191241] N88-24613
INSTRUMENT FLIGHT RULES
Aircraft accident/incident, Copperhill, Tennessee, February 22, 1986
[PB88-910407] N88-24612
INSULATORS
Development of the field-induced electron injection and impact ionization (F4I) technique for radiation hardness testing of MOS (Metal-Oxide-Semiconductor) gate insulators
[AD-A192114] N88-25345
INTAKE SYSTEMS
Inflow measurements made with a laser velocimeter on a helicopter model in forward flight. Volume 1: Rectangular planform blades at an advance ration of 0.15
[NASA-TM-100541] N88-24607
The effects of different combinations of inlet air conditions used for cooling as measured on a heated manikin
[AD-A191116] N88-25151
INTEGERS
A mixed-integer linear programming problem which is efficiently solvable
[AD-A191028] N88-25168
INTEGRAL EQUATIONS
Joint services electronics program
[AD-A191749] N88-24853
Cross stream differencing for integral boundary layer equations
[AD-A191744] N88-24886
Integral equation for the laser field: Multimode description of a free-electron laser oscillator
[DE88-007050] N88-24956
Fracture mechanics analysis for short cracks
[AD-A192002] N88-24992
Information analysis of integral equations in remote sensing of atmospheric aerosols N88-25022
A mixed min-max control problem governed by integral equations N88-25228
Optimal processes governed by integral equations with unilateral constraint N88-25231
Numerical solution of random Love's integral equation N88-25235
INTEGRATED CIRCUITS
Millimeter and submillimeter waves and frequency selective surfaces
[AD-A191511] N88-24827
Joint services electronics program
[AD-A190239] N88-24848
Computer aided design of monolithic microwave and millimeter wave integrated circuits and subsystems
[AD-A191593] N88-24852
The inspection of metallurgical bounds in electronic systems
[AD-A192064] N88-25343
INTEGRATED MISSION CONTROL CENTER
Optimization of the dilation characteristic on the control jurisdiction of an area control facility
[AD-A191720] N88-24615
INTEGRATED OPTICS
Nonlinear surface polaritons
[AD-A191046] N88-24822
Research in the optical sciences
[AD-A192175] N88-25297
INTERACTIONAL AERODYNAMICS
Forced response unsteady aerodynamics in a multistage compressor N88-24903
INTERFACE STABILITY
The morphological stability of continuous intergranular phases: Thermodynamic considerations
[DE88-006328] N88-25350
INTERFACES
Service offerings and interfaces for the ACTS network of Earth stations
[NASA-TM-100809] N88-24663
Interfacial shear phenomena in graphite epoxy composites under impact loading using dynamic moire interferometry
[DE88-006773] N88-24709
INTERFACIAL TENSION
Dendritic growth in the presence of convection N88-25328
INTERFEROMETRY
Geodesy by radio interferometry: Optimization of wet path delay algorithms using microwave radiometer data
[PB88-167739] N88-24820
INTERMETALLICS
Chemical compatibility between silicon carbide and a nickel aluminide
[DE88-006188] N88-24708
Martensitic transformation and microstructures in sintered NiAl alloys
[NASA-TT-20178] N88-24761
INTERNATIONAL COOPERATION
CFD benefits, goals, stepping-stones and techniques. Proposals for the scientific programme of the European Reserch Centre on flow, turbulence and combustion — computational fluid dynamics
[CFDU/88/1] N88-24894
Centre for International Co-Operation and Approriate Technology (CICAT)
[PB88-165501] N88-25389
INTERNATIONAL TRADE
Competitive assessment of the U.S. civil helicopter industry
[PB88-186325] N88-24574
INTERPLANETARY FLIGHT
Preliminary estimates of radiation exposures for manned interplanetary missions from anomalously large solar flare events
[NASA-TM-100620] N88-25427
INTERPLANETARY MAGNETIC FIELDS
Dynamics Explorer-2 measurements during an isolated auroral substorm
[AD-A191202] N88-25091
INTERPOLATION
High degree interpolation polynomial in Newton form
[NASA-CR-181677] N88-25249
INVARIANCE
Similarity solutions of nonlinear partial differential equations invariant to a family of affine groups
[DE88-003404] N88-25245
Rigid symmetries and BRST-invariance in gauge theories
[PB88-180948] N88-25280
INVERSE SCATTERING
Born-type reconstruction of material parameters of an inhomogeneous, lossy dielectric slab from reflected-field data
[PB88-188958] N88-25261
INVERTERS
A microcomputer-based control and simulation of an advanced IPM (Interior Permanent Magnet) synchronous machine drive system for electric vehicle propulsion
[DE88-006735] N88-24859
INVISCID FLOW
Accurate multigrid solution of the Euler equations on unstructured and adaptive meshes
[NASA-CR-181679] N88-24608

Composite reduced Navier-Stokes procedures for flow problems with strong pressure interactions
[AD-A191127] N88-24875
Theoretical investigation of 3-D shock wave-turbulent boundary layer interactions, part 6
[AD-A191546] N88-24882
Axisymmetric viscid-inviscid interaction by a frozen vorticity approximation
[AD-A191743] N88-24885
Open channel flow near the resonance speed
N88-24918

IO
The Io sulfur torus in 1981
[NASA-TM-101139] N88-25419

ION BEAMS
A multi-frame ion pinhole camera for intense ion beam transport and focusing experiments
[DE88-007283] N88-24926
A new approach to generating negative ion beams
[AD-A191119] N88-25276
An optical technique for measuring divergence, beam profile, and aiming direction, of relativistic negative hydrogen ions
[DE88-007049] N88-25278
Trochoidal analysis of scattered electrons in a merged electron-ion beam
[NASA-CASE-NPO-16789-1-CU] N88-25281
Experiments with high energy nuclear beams at Brookhaven: From AGS to RHIC (Relativistic Heavy Ion Collider)
[DE88-007042] N88-25287
Propagation of neutralized ion beams
[AD-A191599] N88-25289
Intense ion beam diagnostics for particle beam fusion experiments on PBFA 2
[DE88-007279] N88-25308

ION CURRENTS
Internal erosion rates of a 10-kW xenon ion thruster
[NASA-TM-100954] N88-24688

ION ENGINES
Internal erosion rates of a 10-kW xenon ion thruster
[NASA-TM-100954] N88-24688

ION EXCHANGING
Computer simulation of uphill diffusion in ternary ionic system
[NASA-TT-20194] N88-25285

ION IMPLANTATION
Planar fully ion-implanted high power InP MISFETs
[AD-A191589] N88-25338

ION MICROSCOPES
SHaRE: Collaborative materials science research
[DE88-007175] N88-24646

IONIC COLLISIONS
Plasma neutralizer work at BNL (Brookhaven National Laboratory)
[DE88-007046] N88-25317

IONIC DIFFUSION
Computer simulation of uphill diffusion in ternary ionic system
[NASA-TT-20194] N88-25285

IONIZATION
Contributions of autoionizing resonances to the electron collisional excitation rates for Be-like ions
[AD-A190924] N88-25275

IONIZATION CROSS SECTIONS
Photoionization dynamics and abundance patterns in laser vaporized tin and lead clusters
[AD-A191604] N88-24722
Molecular sources of ionospheric holes
[AD-A191857] N88-25082
High-order multiphoton ionization of the noble gases
[DE88-007489] N88-25273
A new approach to generating negative ion beams
[AD-A191119] N88-25276
Trochoidal analysis of scattered electrons in a merged electron-ion beam
[NASA-CASE-NPO-16789-1-CU] N88-25281

IONIZATION FREQUENCIES
Photoionization dynamics and abundance patterns in laser vaporized tin and lead clusters
[AD-A191604] N88-24722

IONOSPHERIC DISTURBANCES
Radio-wave scintillations and ionospheric irregularities at high latitudes
[AD-A192140] N88-24837
The Effect of the Ionosphere on Communication, Navigation and Surveillance Systems Based on Ionospheric Effects Symposium held on 5-7 May 1987 in Springfield, Virginia
[AD-A191855] N88-25081

IONOSPHERIC ION DENSITY
Rocket-borne low energy ion measurements in space
N88-25412

IONOSPHERIC PROPAGATION
The Effect of the Ionosphere on Communication, Navigation and Surveillance Systems Based on Ionospheric Effects Symposium held on 5-7 May 1987 in Springfield, Virginia
[AD-A191855] N88-25081

IONS
Contributions of autoionizing resonances to the electron collisional excitation rates for Be-like ions
[AD-A190924] N88-25275
Contaminant ions and waves in the space station environment N88-25393
Rocket-borne low energy ion measurements in space
N88-25412

IRON
Calculation of oxidation rates for iron in CO-CO2
[DE88-007313] N88-24757

IRON ALLOYS
On the abnormal phenomena observed in the electrical resistivity measurement during the decomposition process of saturated Cu-Fe alloys
[NASA-TT-20183] N88-24869

IRRADIANCE
Calculation of space station infrared irradiance from atmosphere-induced emissions N88-25396

IRRADIATION
Arcing and rf signal generation during target irradiation by a high-energy, pulsed neutral particle beam
[DE88-007169] N88-24664
Behavioral response of rats exposed to high-power microwave radiation
[AD-A192199] N88-25128
Self shielding of surfaces irradiated by intense energy fluxes
[DE88-007094] N88-25318
Molecular characterization of structure and bonding in thin film materials
[DE88-006811] N88-25351

IRREGULAR GALAXIES
Infrared astronomy at extremely faint light levels in support of the LAIRTS program
[AD-A191497] N88-25404

ISENTROPIC PROCESSES
A semigroup for Lagrangian 1D isentropic flow
[DE88-006464] N88-24912

ISOLATORS
Low-loss, high-isolation, fiber-optic isolator
[NASA-CASE-NPO-17207-1-CU] N88-25304

ISOMERIZATION
New polyisoimides: An approach to in situ rigid-rod polyimide formation
[AD-A191665] N88-24773

ISOTHERMAL FLOW
Heat transfer from a negatively buoyant wall jet
[PB88-181953] N88-24873

ISOTHERMAL PROCESSES
Isothermal and bithermal thermomechanical fatigue behavior of a NiCoCrAlY-coated single crystal superalloy
[NASA-TM-100907] N88-24766

ISOTOPE SEPARATION
Isotope separation using tuned laser and electron beam
[NASA-CASE-NPO-16907-1-CU] N88-24732

ITERATIVE SOLUTION
Adaptive local grid refinement in computational fluid mechanics
[AD-A192215] N88-24890

J

J INTEGRAL
Analysis and developments of failure concepts in fracture mechanics based on research results in the field of component safety topics: J-integral concept; crack resistance curves; dynamic criterion
[V-19/86] N88-25009

JET ENGINE FUELS
Selective detection in gas chromatography
[AD-A191499] N88-24718
Reference filters for electrostatic charging tendency measurements of fuels
[AD-A191717] N88-24803

JET FLOW
Heat transfer from a negatively buoyant wall jet
[PB88-181953] N88-24873
Hydroacoustic pulsating jet generator
[MPIS-7/1987] N88-24891
Numerical solutions of the complete Navier-Stokes equations
[NASA-CR-183023] N88-24914

JET MIXING FLOW
Effect of initial tangential velocity distribution on the mean evolution of a swirling turbulent free jet
[NASA-TM-100934] N88-24592
An empirical model of the effects of curvature and convergence on dilution jet mixing
[NASA-TM-100896] N88-24640

JET VANES
TVC (Thrust Vector Control) jet vane thermal modeling using parametric system identification
[AD-A191518] N88-24678

JOINTS (JUNCTIONS)
The inspection of metallurgical bounds in electronic systems
[AD-A192064] N88-25343

JUDGMENTS
A framework for a theory of mapping
[AD-A191071] N88-25144

K

KERNEL FUNCTIONS
Symmetrized nearest neighbor regression estimates
[AD-A191998] N88-25254

KEVLAR (TRADEMARK)
On the bending response of Kevlar 49/epoxy beams and rings
[DE88-006824] N88-25012

KEYING
WIPP (Waste Induced Particle Precipitation) experiment logistic support
[AD-A191184] N88-24824

KINEMATICS
Kinematics, dynamics and control of a closed chain mechanism manipulator N88-24967
Real-time implementation of a kinematic optimization scheme for seven-degree-of-freedom redundant robots with spherical wrists
[DE88-006785] N88-24974
Determination of settings of a tilted head-cutter for generation of hypoid and spiral bevel gears
[NASA-CR-182138] N88-24978
MHD bending waves in a current sheet
[NASA-TM-101149] N88-25323

KINETIC ENERGY
Inevitable inflation in Einstein-Cartan theory with improved energy-momentum tensor with spin
[NASA-TM-101146] N88-25365

KINETICS
Effect of alloying, rapid solidification, and surface kinetics on the high temperature environmental resistance of niobium
[AD-A192093] N88-24743

KNOWLEDGE REPRESENTATION
Representation and decision mechanisms in artificial intelligence
[AD-A191083] N88-25197
Application of flight systems methodologies to the validation of knowledge-based systems
[NASA-TM-100442] N88-25207

KRAMERS-KRONIG FORMULA
Optical constants of minerals and other materials from the millimeter to the ultraviolet
[AD-A192210] N88-24724

KRYPTON FLUORIDE LASERS
Aurora status and plans
[DE88-006476] N88-24955

L

LABORATORIES
An overview of advanced battery development at Sandia National Laboratories
[DE88-006823] N88-24867

LABORATORY EQUIPMENT
SHaRE: Collaborative materials science research
[DE88-007175] N88-24646
Laboratory experiments on atmospheric OH reactions
N88-25068
Hanging drop crystal growth apparatus and method
[NASA-CASE-MFS-28206-1-SB] N88-25356

LAGRANGE MULTIPLIERS
A concurrent neural network algorithm for the traveling salesman problem
[DE88-006981] N88-25208
The use of Lagrange multipliers and Kuhn-Tucker's theory in optimization problems N88-25236

LAMINAR BOUNDARY LAYER
Numerical simulations of the flat-plate laminar boundary layer in subsonic and supersonic flow
[PDR/CFDU-IC/36] N88-24895

LAMINAR FLOW
Wave growth associated with turbulent spots in plane Poiseuille flow
[FFA-TN-1988-08] N88-24587
Prediction of laminar and turbulent flows past single and twin airfoils N88-24589

Theoretical analysis of laminar incompressible flow in slender channels
[VTH-LR-517] N88-24909
Method and apparatus for detecting laminar flow separation and reattachment
[NASA-CASE-LAR-13952-1-SB] N88-24910
Method of forming a multiple layer dielectric and a hot film sensor therewith
[NASA-CASE-LAR-13678-1] N88-25355

LAMINAR FLOW AIRFOILS
Instability of laminar separation bubbles: Causes and effects
[AD-A191166] N88-24876

LAMINATES
Local delamination buckling in layered structures N88-24711
Damage by creep fatigue: Influence of the visco-elasticity of the matrix
[PB88-124706] N88-24998
On the bending response of Kevlar 49/epoxy beams and rings
[DE88-006824] N88-25012
Method of forming a multiple layer dielectric and a hot film sensor therewith
[NASA-CASE-LAR-13678-1] N88-25355
Metastability in SiGe/Si strained-layer structures
[DE88-007603] N88-25361

LANDING AIDS
Cessna 172 MLS (Microwave Landing System) terminal instrument procedures (TERPS) approach data collection and processing data report
[AD-A191241] N88-24613
Microwave landing system mathematical modeling study for Midway Airport Runway 22L, Chicago, Illinois
[AD-A191721] N88-24616
Simulator evaluation of lineup visual landing aids for night carrier landing
[AD-A191212] N88-24648

LANDSAT SATELLITES
DMSP-SSM/1 NASA algorithm validation using primarily LANDSAT and secondarily DMSP and/or AVHRR visible and thermal infrared satellite imagery
[NASA-CR-182979] N88-25024

LANTHANUM TELLURIDES
Crystalline metal-semiconductor superlattices
[DE88-007063] N88-25332

LAPLACE EQUATION
The calculation of transonic flow over the shuttle orbiter using slender body theory N88-24606

LARGE SPACE STRUCTURES
Electromagnetic damping and vibration isolation of space structures
[AD-A191492] N88-24665
Estimation and control of distributed models for certain elastic systems arising in large space structures
[AD-A192120] N88-24666
Low authority control of large space structures using a constrained threshold control formulation N88-24667
Experimental study of active vibration control
[AD-A191454] N88-24969

LASER APPLICATIONS
Isotope separation using tuned laser and electron beam
[NASA-CASE-NPO-16907-1-CU] N88-24732
Bibliography of Soviet laser developments, number 83, May - June 1986
[AD-A190969] N88-24950
Optical diagnostics for a high power, rf-inductively coupled plasma
[DE88-007822] N88-25322

LASER DOPPLER VELOCIMETERS
Inflow measurements made with a laser velocimeter on a helicopter model in forward flight. Volume 1: Rectangular planform blades at an advance ration of 0.15
[NASA-TM-100541] N88-24607

LASER GUIDANCE
Optics: Perspectives for Measurement Techniques and Signal Processing for Flight Guidance — conference
[DFVLR-MITT-87-21] N88-24928

LASER GYROSCOPES
Concepts for a laser gyroscope of the highest precision N88-24929
Laser gyroscopes using the rate-bias technique N88-24930
Development of mirrors for high-precision laser gyroscopes N88-24931
Laboratory tests of laser gyroscopes for future utilization in multifunction systems for precision navigation and flight guidance N88-24932

LASER INDUCED FLUORESCENCE
Instrumentation for turbulent reacting flows
[AD-A191671] N88-24923
Tropospheric OH measurement by Laser Induced Fluorescence (LIF) N88-25071

LASER MATERIALS
Fracture of solid state lasers
[DE88-007023] N88-24961

LASER MODE LOCKING
Laser gyroscopes using the rate-bias technique N88-24930

LASER MODES
Distributed feedback lasers
[NASA-CR-4154] N88-24948

LASER OUTPUTS
Magnetically switched power supply system for lasers
[NASA-CASE-NPO-16402-2] N88-24862
Distributed feedback lasers
[NASA-CR-4154] N88-24948
An optical preamplifier for detection of CO2 laser radiation
[AD-A190790] N88-24949
Atmospheric propagation of laser beams
[AD-A191447] N88-24952
Fast acting optical beam detection and deflection system
[AD-A192161] N88-24954
Integral equation for the laser field: Multimode description of a free-electron laser oscillator
[DE88-007050] N88-24956
An optical technique for measuring divergence, beam profile, and aiming direction, of relativistic negative hydrogen ions
[DE88-007049] N88-25278
Optical system of laser illuminated streamer chamber
[DE88-702127] N88-25306

LASER PROPULSION
Possibilities and limits for use of laser propulsion systems in interorbital space flight
[ILR-MITT-185] N88-24683

LASER PUMPING
Application of particle simulations to the NRL laser experiment
[AD-A191641] N88-24953

LASER RANGE FINDERS
Limits of accuracy and range of laser radars N88-24934
Range and range rate system
[NASA-CASE-MSC-20867-1] N88-24958

LASER SPECTROSCOPY
Time resolved spectroscopy facility for the study of nonlinear optical properties of semiconducting polymers
[AD-A191221] N88-24768
Stress measurements in graphite fibers by laser raman spectroscopy
[AD-A191710] N88-24779
Workshop on Atmospheric OH
[BPT-7/87] N88-25063
Determination of tropospheric H concentrations by a double-pulsed UV laser method N88-25070
Tropospheric OH measurement by Laser Induced Fluorescence (LIF) N88-25071
Trace gas measurements in the troposphere using tunable diode lasers N88-25072
Development of continuous wave laser frequency modulation of OH in tropospheric concentrations range N88-25073

LASER TARGETS
Aurora status and plans
[DE88-006476] N88-24955

LASER WEAPONS
Laser countermeasure impacts and penalties
[DE88-006871] N88-24947

LASERS
Magnetically switched power supply system for lasers
[NASA-CASE-NPO-16402-2] N88-24862
Bibliography of Soviet laser developments, number 83, May - June 1986
[AD-A190969] N88-24950
Components of an atmospheric lidar system: Doppler wind lidar
[AD-A191222] N88-24951

LASING
Isotope separation using tuned laser and electron beam
[NASA-CASE-NPO-16907-1-CU] N88-24732

LATCHES
Toggle release
[NASA-CASE-MSC-21354-1] N88-24969

LATE STARS
Duplicity in the solar neighborhood. Part 3: New spectroscopic elements for nine solar-type binary stars
[SER-C-PREPUBL-FASC-18-PT-3] N88-25405

LATHES
Universal precision sine bar attachment
[NASA-CASE-MFS-28253-1] N88-24971

LATTICE PARAMETERS
Structural studies on La/sub 2/CuO/sub 4+delta/
[DE88-006828] N88-25330

LAUNCHING
Simulations of a missile with liquid payload under launch conditions
[AD-A191479] N88-24625

LEAD (METAL)
Photoionization dynamics and abundance patterns in laser vaporized tin and lead clusters
[AD-A191604] N88-24722

LEAD TELLURIDES
Crystalline metal-semiconductor superlattices
[DE88-007063] N88-25332

LEADERSHIP
Management and the executive
[AD-A190778] N88-25374

LEARNING
Optimizing feedback utilization in motor skill training
[AD-A191559] N88-25146
Models of incremental concept formation
[AD-A191597] N88-25147
Visual information processing in the perception of features and objects
[AD-A192026] N88-25148
Representation and decision mechanisms in artificial intelligence
[AD-A191083] N88-25197

LEAST SQUARES METHOD
Calculation of root-mean-square loads
[BLL-M-37776-(5828.4)] N88-25015
Asymptotic theory for weighted least squares estimators in Aalen's additive risk model
[AD-A191085] N88-25210
New mixed finite element methods N88-25248

LIFE (DURABILITY)
Internal erosion rates of a 10-kW xenon ion thruster
[NASA-TM-100954] N88-24688
Environment assisted degradation mechanisms in advanced light metals
[NASA-CR-182907] N88-24746

LIFT
Continuum theories for fluid-particle flows: Some aspects of lift forces and turbulence
[DE88-007036] N88-24898

LIGHT (VISIBLE RADIATION)
Light propagation through gravitationally perturbed Friedmann universes N88-25307

LIGHT BEAMS
An optical technique for measuring divergence, beam profile, and aiming direction, of relativistic negative hydrogen ions
[DE88-007049] N88-25278

LIGHT SCATTERING
Molecular characterization of structure and bonding in thin film materials
[DE88-006811] N88-25351

LIGHT TRANSMISSION
Atmospheric propagation of laser beams
[AD-A191447] N88-24952
Study of light transmission methods from scintillators to optical fiber with wave length shifter
[DE88-701587] N88-25292
Low-loss, high-isolation, fiber-optic isolator
[NASA-CASE-NPO-17207-1-CU] N88-25304

LIGHTNING
Theoretical basis for an experimental test with regard to the origin of VHF (Very High Frequency) radiation from natural lightning
[DE88-007535] N88-25102
Analysis of lightning field changes during active thunderstorms in Florida N88-25103
Lightning detection and locating systems N88-25112

LINE SPECTRA
An optical preamplifier for detection of CO2 laser radiation
[AD-A190790] N88-24949
Observations of wave number dependent spectral line ratio fluctuations in the atmospheric emissions
[IRF-PREPRINT-101] N88-25085
Studies of spectral line ratio fluctuations using Inductively Coupled Plasma (ICP) light
[IRF-PREPRINT-100] N88-25311
Recent data on Si:As impurity band conduction multiplexed arrays
[AD-A191752] N88-25340

LINEAR EQUATIONS
Solving bidiagonal systems of linear equations on the CDC CYBER 205
[CWI-NM-R8725] N88-25187

LINEAR PROGRAMMING
A mixed-integer linear programming problem which is efficiently solvable
[AD-A191028] N88-25168
Decomposition of linear programs using parallel computation
[AD-A191718] N88-25173
A centered projective algorithm for linear programming
[AD-A192100] N88-25178

LINEAR QUADRATIC REGULATOR
Optimal discrete-time LQR problems for parabolic systems with unbounded input: Approximation and convergence
[NASA-CR-181673] N88-25247
LINEAR SYSTEMS
Robust adaptive regulation without persistent excitation
[NASA-TM-100571] N88-25204
Linear and nonlinear acoustic wave propagation in the atmosphere
[NASA-CR-4157] N88-25268
LINEARITY
Automated cartographic generalization for linear map features N88-25021
Linear spaces, absolute retracts and the compact extension property
[PB88-181110] N88-25225
LINKAGES
Payload deployment method and system
[NASA-CASE-MSC-21330-1] N88-24680
LIQUEFACTION
Proceedings of the 1987 Biomass Thermochemical Conversion Contractors' Review Meeting
[DE88-006730] N88-25041
An advanced extruder-feeder biomass liquefaction reactor system N88-25042
LIQUID CRYSTALS
Electrochemistry in liquid crystals
[AD-A191554] N88-24719
LIQUID FILLED SHELLS
Internal fluid dynamics within a nonspinning partially liquid-filled shell due to burster rupture
[AD-A191055] N88-24874
Theoretical investigation of the development of the normal fluid and superfluid velocity distributions during spin-up for a He2-filled cylinder
[MPIS-6/1987] N88-24892
LIQUID FLOW
Development of a liquid-fed water resistojet
[NASA-TM-100927] N88-24968
LIQUID FUELS
The burning of HAN-based (hydroxylammonium nitrate) liquid propellants
[DE88-006863] N88-24800
Electrical ignition of HAN-based liquid propellants
[AD-A191349] N88-24801
Low pressure entrained flow pyrolysis of biomass to produce liquid fuels N88-25043
Low-temperature thermochemical conversion of high moisture biomass feedstocks N88-25047
LIQUID HELIUM 2
Theoretical investigation of the development of the normal fluid and superfluid velocity distributions during spin-up for a He2-filled cylinder
[MPIS-6/1987] N88-24892
LIQUID ROCKET PROPELLANTS
Performance of a hydrogen pulsed electrothermal thruster. Strategic defense initiative organization innovative science and technology. SBIR, phase 1
[AD-A191999] N88-24679
LIQUIDS
Liquid carbon
[AD-A191707] N88-24776
LISP (PROGRAMMING LANGUAGE)
Simulating futures in extended common LISP
[NASA-TM-101000] N88-25192
LITHIUM ALLOYS
Aluminum alloy
[NASA-CASE-LAR-13924-1-CU] N88-24753
LITHIUM CHLORIDES
Optimization of reserve lithium thionyl chloride battery electrochemical design parameters
[DE88-007109] N88-24868
LITHOGRAPHY
Department of Defense statement on the X-ray Lithography Program to the Research and Development Subcommittee of the House Armed Services Committee of 100th Congress, second session
[AD-A191854] N88-25341
LITHOLOGY
A sedimentological and mineralogical study of the Koogah Formation, New South Wales N88-25087
LOADS (FORCES)
Calculation of root-mean-square loads
[BLL-M-37776-(5828.4)] N88-25015
LOCAL AREA NETWORKS
An investigation of a distributed clock for local area networks with ring topology N88-24924
LOCAL GROUP (ASTRONOMY)
Duplicity in the solar neighborhood. Part 3: New spectroscopic elements for nine solar-type binary stars
[SER-C-PREPUBL-FASC-18-PT-3] N88-25405
LOGIC CIRCUITS
Joint services electronics program research in electronics
[AD-A192206] N88-24857
SYMBL: A new Boolean compiler N88-25160
LOGIC DESIGN
SYMBL: A new Boolean compiler N88-25160
LOGISTICS
Lunar base surface mission operations. Lunar Base Systems Study (LBSS) task 4.1
[NASA-CR-172050] N88-25415
LONG TERM EFFECTS
Environment assisted degradation mechanisms in advanced light metals
[NASA-CR-182907] N88-24746
LONG WAVE RADIATION
Nonlinear waves
[AD-A192148] N88-24889
LONGITUDINAL STABILITY
Experiment investigation on longitudinal characteristics of the forward swept wing
[AD-A191553] N88-24582
LOOP ANTENNAS
A MININEC model of the miniloop antenna
[AD-A191759] N88-24830
LOOPS
Phase length optical phase-locked-loop sensor
[NASA-CASE-LAR-13387-1] N88-25302
LORAN C
Descriptions of HF and VHF Loran-C buoys and evaluations as potential datum marker buoys
[AD-A192069] N88-24618
LOSSES
The loss parameters for very short bunches
[CEBAF-PR-88-005] N88-25291
LOSSY MEDIA
Born-type reconstruction of material parameters of an inhomogeneous, lossy dielectric slab from reflected-field data
[PB88-188958] N88-25261
LOW ASPECT RATIO
Computational design of low aspect ratio wing-winglet configurations for transonic wind-tunnel tests
[NASA-CR-183021] N88-24830
Design studies of low aspect-ratio torsatrons
[DE88-007562] N88-25320
LOW FREQUENCIES
Practical VLF/LF radio test system
[AD-A191768] N88-24831
LOW GRAVITY MANUFACTURING
Preparation for microgravity: The role of the microgravity materials science laboratory
[NASA-TM-100906] N88-24811
LOW PRESSURE
Low pressure entrained flow pyrolysis of biomass to produce liquid fuels N88-25043
LOW SPEED WIND TUNNELS
Summary of low-speed wind tunnel results of several high-speed counterrotation propeller configurations
[NASA-TM-100945] N88-24597
LOW TEMPERATURE
Update of low temperature catalyst development
[DE88-007032] N88-24715
LOW THRUST PROPULSION
Recent advances in low-thrust propulsion technology
[NASA-TM-100959] N88-25260
LUMINANCE
Design and testing of a luminance and chrominance stabilization system for a computer-controlled color display
[AD-A191922] N88-25159
LUMINESCENCE
Superthermal electron processes in the upper atmosphere of Uranus: Aurora and electroglow
[NASA-TM-101150] N88-25417
LUNAR BASES
Lunar base surface mission operations. Lunar Base Systems Study (LBSS) task 4.1
[NASA-CR-172050] N88-25415

M

MACH NUMBER
Spatial stability of a compressible mixing layer
[NASA-CR-181671] N88-24916
MACHINE TOOLS
Determination of settings of a tilted head-cutter for generation of hypoid and spiral bevel gears
[NASA-CR-182138] N88-24976
MACHINING
Frequency Analysis of Acoustic Emission - Application to machining and welding
[DE88-701478] N88-25262
MAGNESIUM ALLOYS
Strain hardening at large strains in aluminum alloys
[DE88-007415] N88-24737
MAGNET COILS
Quench detection by fluid dynamic means in cable-in-conduit superconductors
[DE88-007269] N88-25359
MAGNETIC FIELDS
Electromagnetic penetration into a conducting circular cylinder through a narrow slot, TE case
[AD-A191602] N88-24828
Application of particle simulations to the NRL laser experiment
[AD-A191641] N88-24953
Solving time-dependent two-dimensional eddy current problems
[NASA-TM-100875] N88-25239
Propagation of neutralized ion beams
[AD-A191599] N88-25289
Basic processes of plasma propulsion
[AD-A192117] N88-25310
Design studies of low aspect-ratio torsatrons
[DE88-007562] N88-25320
Influence of alternating magnetic fields on Zn-67 Moessbauer resonance in ZnO
[PB88-186432] N88-25352
Space station induced electromagnetic effects N88-25394
MAGNETIC MATERIALS
Magnetic superlattices
[AD-A191450] N88-25334
MAGNETIC MEASUREMENT
The SAMEX vector magnetograph: A design study for a space-based solar vector magnetograph
[NASA-TM-4048] N88-25424
MAGNETIC POLES
Theoretical investigations of drift waves in a magnetic quadrupole N88-25312
MAGNETIC PROPERTIES
Electromagnetic damping and vibration isolation of space structures
[AD-A191492] N88-24685
The theory of random alloys
[DE88-006408] N88-24756
Physical properties of f electron systems
[DE88-006886] N88-25331
Magnetic superlattices
[AD-A191450] N88-25334
MAGNETIC STARS
Ultraviolet spectra of two magnetic white dwarfs and ultraviolet spectra of subluminous objects found in the Kiso Schmidt survey
[NASA-CR-183051] N88-25408
MAGNETIC STORMS
Dynamics Explorer-2 measurements during an isolated auroral substorm
[AD-A191202] N88-25091
MAGNETIC SWITCHING
Magnetically switched power supply system for lasers
[NASA-CASE-NPO-16402-2] N88-24862
MAGNETIC VARIATIONS
DOD 1985 world magnetic model: Charts and grid values
[AD-A191484] N88-25080
MAGNETOHYDRODYNAMIC FLOW
Basic processes of plasma propulsion
[AD-A192117] N88-25310
MAGNETOHYDRODYNAMIC STABILITY
The 2-D magnetohydrostatic configurations leading to flares or quiescent filament eruptions
[NASA-TM-101147] N88-25423
MAGNETOHYDRODYNAMIC WAVES
MHD bending waves in a current sheet
[NASA-TM-101149] N88-25323
MAGNETOPLASMADYNAMICS
Basic processes of plasma propulsion
[AD-A192117] N88-25310
MAGNETORESISTIVITY
Electrical conduction in thin film carbons
[AD-A191726] N88-24780
Electron-Rayleigh wave interaction in thin film carbons
[AD-A191727] N88-24781
MAGNETOSTRICTION
Research work completed at the Naval Surface Warfare Center Solid State Group of the Radiation Division
[AD-A191627] N88-25339
MAINTENANCE
Predictive corrosion modeling, volume 1
[AD-A191229] N88-24739
A perspective of PC-based probabilistic risk assessment
[DE88-006715] N88-25251
MAN MACHINE SYSTEMS
Human problem solving in complex dynamic environments
[AD-A190788] N88-25142

Eye and head response to an attention cue in a dual task paradigm
[AD-A191052] N88-25143
An advanced prototyping tool for human factors design
[AD-A187290] N88-25149
A graphical, intelligent interface for discrete-event simulations
[DE88-000522] N88-25181

MAN-COMPUTER INTERFACE
An advanced prototyping tool for human factors design
[AD-A187290] N88-25149
Knowledge acquisition tool implementation
[AD-A190415] N88-25164

MANAGEMENT
Management and the executive
[AD-A190778] N88-25374
Department of Defense Statement on the Balanced Technology Initiative to the Committee on Armed Services, United States Senate, 100th Congress, second session
[AD-A191841] N88-25378

MANAGEMENT INFORMATION SYSTEMS
Management and the executive
[AD-A190778] N88-25374

MANAGEMENT METHODS
Propagation management for no-acknowledge HF communications links N88-24843
Management and the executive
[AD-A190778] N88-25374

MANEUVERS
Nonlinear flying quality parameters based on dynamic inversion
[AD-A192146] N88-24627

MANGANESE ALLOYS
Strain hardening at large strains in aluminum alloys
[DE88-007415] N88-24737

MANIPULATORS
The coordination of multiple robotic manipulators
[AD-A190869] N88-24963
Kinematics, dynamics and control of a closed chain mechanism manipulator N88-24967
Real-time implementation of a kinematic optimization scheme for seven-degree-of-freedom redundant robots with spherical wrists
[DE88-006785] N88-24974
A computational model of motor behavior
[AD-A191179] N88-25152
The efficacy of using human myoelectric signals to control the limbs of robots in space
[NASA-CR-182901] N88-25155
Introduction to compliance in programming of robots
[ETN-88-92189] N88-25201
Analysis of a closed-kinematic chain robot manipulator
[NASA-CR-183031] N88-25206

MANNED SPACE FLIGHT
Human performance issues arising from manned space station missions
[NASA-CR-3942] N88-25156
Preliminary estimates of radiation exposures for manned interplanetary missions from anomalously large solar flare events
[NASA-TM-100620] N88-25427

MANNED SPACECRAFT
Hatch cover
[NASA-CASE-MSC-21356-1] N88-24671

MANUALS
Defense Technical Information Center cataloging guidelines
[AD-A192200] N88-25382

MANURES
Evaluation of manure as a feedstock for gas turbines N88-25050

MAPPING
Automated cartographic generalization for linear map features N88-25021
Drilling investigation of a young magmatic intrusion beneath the Inyo Domes, Long Valley, California: Structural and textural studies
[DE88-006613] N88-25078
A framework for a theory of mapping
[AD-A191071] N88-25144

MAPS
Research in enumeration and graph theory with applications to computer science
[AD-A191567] N88-25171

MARINE METEOROLOGY
Mariners weather log, volume 32, number 1, Winter 1988
[PB88-173669] N88-25097

MARKERS
Descriptions of HF and VHF Loran-C buoys and evaluations as potential datum marker buoys
[AD-A192069] N88-24618

MARKOV PROCESSES
Poisson functionals of Markov processes and queuing networks
[AD-A191217] N88-25252

MARS (PLANET)
A design study of onboard navigation and guidance during aerocapture at Mars
[NASA-CR-172053] N88-24654

MARS ATMOSPHERE
Diurnal variations in optical depth at Mars: Observations and interpretations
[NASA-TM-100057] N88-25420

MARS PROBES
Mars rover/sample return mission requirements affecting space station
[NASA-CR-172048] N88-25414

MARTENSITE
Irradiation effects on tungsten stabilized martensitic steels
[DE88-007074] N88-24748

MARTENSITIC TRANSFORMATION
Martensitic transformation and microstructures in sintered NiAl alloys
[NASA-TT-20178] N88-24761

MASS SPECTROMETERS
Stratospheric positive ion composition measurements and acetonitrile detection: A consistent picture
[AERONOMICA-ACTA-A-326-1987] N88-25084

MASS SPECTROSCOPY
Molecular-beam, mass-spectrometric studies of wood vapor and model compounds over HZSM-5 catalyst N88-25044

MATERIAL ABSORPTION
Bimolecular reactions and energy-transfer processes of highly vibrationally excited molecules related to energetic materials
[AD-A189013] N88-25270

MATERIALS HANDLING
Proposed quality assurance/quality control plan
[AD-A191490] N88-24978

MATHEMATICAL MODELS
An analytic model for aerodynamic shapes
[AD-A191573] N88-24583
Compressible flow in a pie-shaped cylinder rotating about the vertex N88-24604
Microwave landing system mathematical modeling study for Midway Airport Runway 22L, Chicago, Illinois
[AD-A191721] N88-24616
Nonlinear flying quality parameters based on dynamic inversion
[AD-A192146] N88-24627
Particle-laden weakly swirling free jets: Measurements and predictions
[NASA-TM-100920] N88-24639
An enumeration of research to determine the optimal design and use of Army flight training simulators
[AD-A191242] N88-24649
Analytic and numerical modeling of heat and material transport in electrical hypervelocity guns
[AD-A192178] N88-24655
Fundamental limits to the velocity of solid armatures in railguns N88-24656
Thermodynamic modeling of the no-vent fill methodology for transferring cryogens in low gravity
[NASA-TM-100932] N88-24686
Interaction of ultrasonic waves with composite plates
[AD-A191879] N88-24702
Shape stability in composites N88-24706
The influence of cathodic protection on erosion-corrosion of metals and model alloys
[AD-A191613] N88-24742
Delay-doppler radar imaging
[AD-A191509] N88-24826
Internal fluid dynamics within a nonspinning partially liquid-filled shell due to burster rupture
[AD-A191055] N88-24874
Transient particle deposition in a boundary layer of impulsive flow over a flat plate
[AD-A191537] N88-24880
Research in nonlinear wave motion
[AD-A191686] N88-24884
Gas diffusion studies in steady and nonsteady cavities N88-24902
Numerical solutions of the complete Navier-Stokes equations
[NASA-CR-183023] N88-24914
Experimental study of active vibration control
[AD-A191454] N88-24989
Self-consistent model for the brittle response of solids N88-24999
Reduced order modelling and analytical model modification for structural dynamics and control N88-25006
Theory of viscoplasticity based on overstress with applications N88-25007
Multishaker modal testing
[NASA-CR-179355] N88-25010
Fatigue crack growth due to random loading N88-25017
Yaw dynamics of horizontal axis wind turbines
[DE88-001137] N88-25055
Photovoltaic Advanced Research and Development Project, solar radiation research
[DE88-001143] N88-25056
Drilling investigation of a young magmatic intrusion beneath the Inyo Domes, Long Valley, California: Structural and textural studies
[DE88-006613] N88-25078
DOD 1985 world magnetic model: Charts and grid values
[AD-A191484] N88-25080
Report on project WIND: Preliminary experiments w ith the UK Meteorological Office mesoscale model, September 1987
[AD-A191621] N88-25099
Analysis of lightning field changes during active thunderstorms in Florida N88-25103
A computational model of motor behavior
[AD-A191179] N88-25152
A concurrent neural network algorithm for the traveling salesman problem
[DE88-006981] N88-25208
Mathematical models for VLSI device simulation
[AD-A191125] N88-25212
Theoretical investigation of optical computing based on neural network models
[AD-A191668] N88-25214
Direct numerical simulations of the PDF's (Probability Density Functions) of a passive scalar in a forced mixing layer
[AD-A192134] N88-25256
Tranamitting boundary for finite-difference calculations with finite modeling of an infinite medium
[AD-A191441] N88-25264
Computer simulation of uphill diffusion in ternary ionic system
[NASA-TT-20194] N88-25285
Para-ortho abundance ratio of molecular hydrogen in NGC2023
[ISAS-RN-352] N88-25286
Modelling of thermal plasma systems N88-25314
Study of data distributions and functions for the development of thermodynamic equations of state
[PB88-196365] N88-25370
Superthermal electron processes in the upper atmosphere of Uranus: Aurora and electroglow
[NASA-TM-101150] N88-25417
Cluster analysis of multiple planetary flow regimes
[NASA-CR-182931] N88-25418
Diurnal variations in optical depth at Mars: Observations and interpretations
[NASA-TM-100057] N88-25420

MATRIX MATERIALS
Carbon matrix composites prospective roles for biotechnology N88-24694
Sol/gel processing techniques for glass matrix composites
[AD-A191748] N88-24701

MAXIMUM LIKELIHOOD ESTIMATES
Adaptive time series analysis using predictive inference and entropy
[AD-A191858] N88-25199
Recursive maximum likelihood identification of a nonlinear output-affine model
[RR-322] N88-25257

MEASURING INSTRUMENTS
Electrostatic discharge test apparatus
[NASA-CASE-MSC-21094-1] N88-24941
Universal precision sine bar attachment
[NASA-CASE-MFS-28253-1] N88-24971

MECHANICAL DRIVES
A microcomputer-based control and simulation of an advanced IPM (interior Permanent Magnet) synchronous machine drive system for electric vehicle propulsion
[DE88-006735] N88-24859

MECHANICAL IMPEDANCE
Dynamic response of plates to moving loads: Structural impedance and finite element methods N88-25000

MECHANICAL PROPERTIES
Carbon matrix composites prospective roles for biotechnology N88-24694
Interaction of ultrasonic waves with composite plates
[AD-A191879] N88-24702
Fundamental studies of beta phase decomposition modes in titanium alloys
[AD-A191495] N88-24740
Environment assisted degradation mechanisms in advanced light metals
[NASA-CR-182907] N88-24748

Characterization of 7090 and 7091 profiles made with Cegedur powder — powder metallurgy, aircraft construction materials
[REPT-48-441/F] N88-24752
Effect of size of precipitates on recrystallization temperatures in Cu-Cr, Cu-Zr, and Cu-Zr-Cr alloys
[NASA-TT-20166] N88-24763
Stress measurements in graphite fibers by laser raman spectroscopy
[AD-A191710] N88-24779
The influence of the chemical nature of resins on their reticulation kinetics and the consequences for their nonelastic mechanical properties
[ETN-88-92539] N88-24788
Characterization of aluminum/RP-1 gel propellant properties
[NASA-TM-100951] N88-24808

MECHANICAL SHOCK
Peak Acceleration Device (PAD)
[AD-A191639] N88-24611

MEDITERRANEAN SEA
The interpretation of crustal dynamics data in terms of plate interactions and active tectonics of the Anatolian Plate and surrounding regions in the Middle East
[NASA-CR-183024] N88-25092

MEMBRANES
Mechanisms of gas permeation through polymer membranes: Renewal proposal for period December 1, 1986 - November 30, 1989
[DE88-007436] N88-24796
The flying characteristics of the membrane slider bearing N88-24965

MEMORY (COMPUTERS)
Effective use of shared memory multiprocessors
[DE88-007019] N88-25195

MENTAL PERFORMANCE
A framework for a theory of mapping
[AD-A191071] N88-25144

MESOSCALE PHENOMENA
Taiwan area mesoscale experiment: P-3 aircraft operations summary
[PB88-169073] N88-25098
Report on project WIND: Preliminary experiments w ith the UK Meteorological Office mesoscale model, September 1987
[AD-A191621] N88-25099
Determination of mesoscale variability of sea surface temperature and attenuation in the North Atlantic from satellite measurement
[REPT-162] N88-25127

MESSAGE PROCESSING
Motor theory of auditory perception
[AD-A192095] N88-25136
Automatic discovery of optimal classes
[NASA-TM-101174] N88-25238

METAL BONDING
Composite repair of cracked aluminum alloy aircraft structure
[AD-A190514] N88-24573
A scientific basis for an alternate cathode architecture
[AD-A191498] N88-24717
Environmental integrity of coating/metal interface
[AD-A192184] N88-24786

METAL FATIGUE
Environment assisted degradation mechanisms in advanced light metals
[NASA-CR-182907] N88-24746
Isothermal and bithermal thermomechanical fatigue behavior of a NiCoCrAlY-coated single crystal superalloy
[NASA-TM-100907] N88-24766
Cyclic fatigue damage characteristics observed for simple loadings extended to multiaxial life prediction
[NASA-CR-182126] N88-25016

METAL IONS
Self shielding of surfaces irradiated by intense energy fluxes
[DE88-007094] N88-25318

METAL MATRIX COMPOSITES
Analysis of notched metal matrix composites under tension loading
[NASA-TM-100629] N88-24713
Research work completed at the Naval Surface Warfare Center Solid State Group of the Radiation Division
[AD-A191627] N88-25339

METAL OXIDE SEMICONDUCTORS
Development of the field-induced electron injection and impact ionization (F4I) technique for radiation hardness testing of MOS (Metal-Oxide-Semiconductor) gate insulators
[AD-A192114] N88-25345

METAL PLATES
Plate response analysis using shock tube
[AD-A190828] N88-24987

METAL POWDER
Laboratory scale inert gas atomizer for producing rapidly solidified powders
[DE88-006734] N88-24812

METAL PROPELLANTS
Characterization of aluminum/RP-1 gel propellant properties
[NASA-TM-100951] N88-24808

METALS
The influence of cathodic protection on erosion-corrosion of metals and model alloys
[AD-A191613] N88-24742
Arc-textured metal surfaces for high thermal emittance space radiators
[NASA-TM-100894] N88-24754
The stress analysis of ceramic, polymeric, and metallic composite systems by the finite element method N88-25004

METASTABLE STATE
Metastability in SiGe/Si strained-layer structures
[DE88-007603] N88-25361

METEOROID SHOWERS
Communications using channels formed by meteor bursts
[AD-A192088] N88-24834

METEOROIDS
Effects of meteoroids and space debris on the particulate environment for space station N88-25399

METEOROLOGICAL PARAMETERS
Ice formation on aircraft
[ETN-88-92154] N88-25104

METEOROLOGICAL RADAR
Observation of stratiform rain with 94 GHz and s-b and Doppler radar
[AD-A192013] N88-25100

METEOROLOGY
Evaluation of NMC (National Meteorological Center) global analyses: 1979-1987
[PB88-178157] N88-25096
Taiwan area mesoscale experiment: P-3 aircraft operations summary
[PB88-169073] N88-25098

METHYL ALCOHOL
Update of low temperature catalyst development
[DE88-007032] N88-24715

METHYL COMPOUNDS
Preferential surface adsorption in miscible blends of polystyrene and poly(vinyl methyl ether)
[AD-A191451] N88-24769
Stratospheric positive ion composition measurements and acetonitrile detection: A consistent picture
[AERONOMICA-ACTA-A-326-1987] N88-25084

MICHELSON INTERFEROMETERS
Investigations in electro-optical multistability for signal processing N88-24938

MICROBURSTS (METEOROLOGY)
The Federal Aviation Administration/Massachusetts Institute of Technology (FAA/MIT) Lincoln Laboratory Doppler weather radar program N88-25118

MICROCHANNEL PLATES
The off-axis channel macroplate
[NASA-CR-182938] N88-24861

MICROCLIMATOLOGY
The effects of different combinations of inlet air conditions used for cooling as measured on a heated manikin
[AD-A191116] N88-25151

MICROHARDNESS
Microstructural characterization and properties of 3Cr-1.5Mo-O.1V thick section electron beam welds
[DE88-004330] N88-24747

MICROORGANISMS
Ecological risk factors related to environmental uses of genetically engineered organisms
[DE88-006674] N88-25132

MICROSTRUCTURE
Chemical compatibility between silicon carbide and a nickel aluminide
[DE88-006188] N88-24708
Superplasticity: A fundamental investigation on deformation mechanism and cavitation phenomena
[AD-A191548] N88-24741
Dynamic consolidation of metal powders
[AD-A192128] N88-24744
Microstructural characterization and properties of 3Cr-1.5Mo-O.1V thick section electron beam welds
[DE88-004330] N88-24747
High temperature embrittleness of Cu-Cr alloy
[NASA-TT-20184] N88-24759
An investigation of 2-6 superlattice deposition by laser photochemical techniques
[AD-A191547] N88-25336

MICROWAVE AMPLIFIERS
Monolithic GaAs Ku-band one watt constant phase variable power amplifier
[DE88-006272] N88-24866

MICROWAVE CIRCUITS
Identification of cascaded microwave circuits with moderate reflections using reflections and transmission measurements
[PB88-171921] N88-24849
Computer aided design of monolithic microwave and millimeter wave integrated circuits and subsystems
[AD-A191593] N88-24852

MICROWAVE EQUIPMENT
The off-axis channel macroplate
[NASA-CR-182938] N88-24861

MICROWAVE INTERFEROMETERS
Geodesy by radio interferometry: Optimization of wet path delay algorithms using microwave radiometer data
[PB88-167739] N88-24820

MICROWAVE LANDING SYSTEMS
Cessna 172 MLS (Microwave Landing System) terminal instrument procedures (TERPS) approach data collection and processing data report
[AD-A191241] N88-24813
Microwave landing system mathematical modeling study for Midway Airport Runway 22L, Chicago, Illinois
[AD-A191721] N88-24816

MICROWAVE SCATTERING
Almond test body — for microwave anechoic chambers
[NASA-CASE-LAR-13747-1] N88-24845

MICROWAVE SPECTRA
Microwave spectroscopy and gravitational collapse N88-25413

MICROWAVE TRANSMISSION
Identification of cascaded microwave circuits with moderate reflections using reflections and transmission measurements
[PB88-171921] N88-24849

MICROWAVES
The radar cross section of some simple reflectors at short wavelengths
[FOA-C-30472-3.3] N88-24839
Behavioral response of rats exposed to high-power microwave radiation
[AD-A192199] N88-25128

MILITARY HELICOPTERS
Operational noise data for CH-47D and AH-64 army helicopters
[AD-A191059] N88-25263

MILITARY OPERATIONS
Department of Defense statement on the X-ray Lithography Program to the Research and Development Subcommittee of the House Armed Services Committee of 100th Congress, second session
[AD-A191854] N88-25341

MILITARY TECHNOLOGY
Department of Defense statement on defense agency research and development to the Subcommittee on Defense of the Committee on Appropriations, United States House of Representatives, 100th Congress, second session
[AD-A191840] N88-25377
The FY 1989 Department of Defense statement on the Science and Technology Program to 100th Congress, second session
[AD-A191843] N88-25380

MILLIMETER WAVES
Optical constants of minerals and other materials from the millimeter to the ultraviolet
[AD-A192210] N88-24724
Millimeter and submillimeter waves and frequency selective surfaces
[AD-A191511] N88-24827
Computer aided design of monolithic microwave and millimeter wave integrated circuits and subsystems
[AD-A191593] N88-24852

MINERALOGY
A sedimentological and mineralogical study of the Koogah Formation, New South Wales N88-25087

MINERALS
Optical constants of minerals and other materials from the millimeter to the ultraviolet
[AD-A192210] N88-24724

MINIATURE ELECTRONIC EQUIPMENT
Development of the field-induced electron injection and impact ionization (F4I) technique for radiation hardness testing of MOS (Metal-Oxide-Semiconductor) gate insulators
[AD-A192114] N88-25345

MINIATURIZATION
Tactical Rubidium Frequency Standard (TRFS), volume 2
[AD-A191190] N88-24850

MINIMAX TECHNIQUE
A mixed min-max control problem governed by integral equations N88-25228
Mixed min-max optimization problem with restrictions N88-25232

MINING
Lunar base surface mission operations. Lunar Base Systems Study (LBSS) task 4.1
[NASA-CR-172050] N88-25415
MIRAGE AIRCRAFT
Supplements to the study of the wake of a Mirage G8 model at F2 — wind tunnel
[CERT-RT-OA-20/5025-AYD] N88-24596
MIRRORS
Development of mirrors for high-precision laser gyroscopes N88-24931
MISSILES
Wind tunnel investigation of wing and control panel loads at transonic and supersonic speeds on some schematic cruciform missile configurations
[FFA-TN-1986-43] N88-24585
MISSION PLANNING
Human performance issues arising from manned space station missions
[NASA-CR-3942] N88-25156
Modeling and evaluation of variable structure organizations
[AD-A191947] N88-25381
Mars rover/sample return mission requirements affecting space station
[NASA-CR-172048] N88-25414
Lunar base surface mission operations. Lunar Base Systems Study (LBSS) task 4.1
[NASA-CR-172050] N88-25415
MIXERS
Dual-fuel, dual-mode rocket engine
[NASA-CASE-LAR-13773-1] N88-24685
MIXING
Analysis of molecular mixing and chemical reaction in mixing layer
[AD-A191600] N88-24721
Signal processing with degenerate four-wave mixing
[AD-A191496] N88-24825
Spatial stability of a compressible mixing layer
[NASA-CR-181671] N88-24916
Direct numerical simulations of the PDF's (Probability Density Functions) of a passive scalar in a forced mixing layer
[AD-A192134] N88-25256
MODAL RESPONSE
Reduced order modelling and analytical model modification for structural dynamics and control N88-25006
Multishaker modal testing
[NASA-CR-179355] N88-25010
MODELS
Dynamic consolidation of metal powders
[AD-A192126] N88-24744
Computational Fluid Mechanics
[NASA-CR-183022] N88-24915
An investigation of a distributed clock for local area networks with ring topology N88-24924
The Effect of the Ionosphere on Communication, Navigation and Surveillance Systems Based on Ionospheric Effects Symposium held on 5-7 May 1987 in Springfield, Virginia
[AD-A191855] N88-25081
Energy measurements in oxygen-induced reactions at 60 A GeV and 200 A GeV
[DE88-006420] N88-25283
Modeling and evaluation of variable structure organizations
[AD-A191947] N88-25381
MODULATION TRANSFER FUNCTION
High-energy laser-assisted imaging through vaporizing aerosols
[DE88-007911] N88-24957
MOIRE INTERFEROMETRY
Interfacial shear phenomena in graphite epoxy composites under impact loading using dynamic moire interferometry
[DE88-006773] N88-24709
MOISTURE CONTENT
Low-temperature thermochemical conversion of high moisture biomass feedstocks N88-25047
MOLECULAR BEAMS
Molecular-beam, mass-spectrometric studies of wood vapor and model compounds over HZSM-5 catalyst N88-25044
MOLECULAR CLOUDS
Microwave spectroscopy and gravitational collapse N88-25413
MOLECULAR COLLISIONS
Bimolecular reactions and energy-transfer processes of highly vibrationally excited molecules related to energetic materials
[AD-A189013] N88-25270
Energy-transfer properties and mechanisms
[DE88-007107] N88-25272
MOLECULAR DIFFUSION
Mechanisms of gas permeation through polymer membranes: Renewal proposal for period December 1, 1986 - November 30, 1989
[DE88-007436] N88-24796
Study of mixing and reaction in the field of a vortex
[AD-A191489] N88-24878
MOLECULAR ENERGY LEVELS
Energy-transfer properties and mechanisms
[DE88-007107] N88-25272
MOLECULAR FLOW
Analysis of molecular mixing and chemical reaction in mixing layer
[AD-A191600] N88-24721
MOLECULAR STRUCTURE
Topological stereochemistry
[AD-A191867] N88-24691
Structural study of the TGMDA-DDS system — epoxy system
[ONERA-RT-4/3348-M] N88-24792
A compatible encapsulant for explosives
[DE88-007212] N88-24806
A constraint algorithm for maintaining rigid bonds in molecular dynamics simulations of large molecules
[AD-A191663] N88-25277
Neutron diffraction refinement of CsHSO4 superionic phase structure
[DE88-701496] N88-25326
Molecular characterization of structure and bonding in thin film materials
[DE88-006811] N88-25351
MOLECULES
New polyisoimides: An approach to in situ rigid-rod polyimide formation
[AD-A191665] N88-24773
Bimolecular reactions and energy-transfer processes of highly vibrationally excited molecules related to energetic materials
[AD-A189013] N88-25270
MOMENTUM TRANSFER
Continuum theories for fluid-particle flows: Some aspects of lift forces and turbulence
[DE88-007036] N88-24898
MONITORS
Airplane runway performance monitoring system
[NASA-CASE-LAR-13854-1-CU] N88-24621
Aircraft emissions characterization: TF41-A2, TF30-P103 and TF30-P109 engines
[AD-A192053] N88-24838
Automated test device for FASR (Fixed Array Surveillance Radar) beam steering componentry
[AD-A191650] N88-24829
Radio Frequency (RF) strain monitor
[NASA-CASE-LAR-13705-1] N88-25011
MONOCHROMATORS
Instrumentation for turbulent reacting flows
[AD-A191671] N88-24923
MONOMERS
Synthesis and characterization of new phosphazene polymers
[AD-A191508] N88-24771
MONOPROPELLANTS
Electrical ignition of HAN-based liquid propellants
[AD-A191349] N88-24801
MONTE CARLO METHOD
Multiple scattering of waves in discrete random media
[AD-A191068] N88-24823
Sensitivity analysis for the system reliability function
[AD-A191648] N88-24979
The development of KENO and the calculation of differential parameters with KENO
[DE88-006176] N88-25166
A fast and efficient procedure for generalized cross-validation with large data sets. Application to image reconstruction
[RR-669-M] N88-25220
Introduction to lattice gauge theory
[DE88-006073] N88-25349
MOORING
An FSK (Frequency Shift Keying) telemetry module for vector measuring current meters
[AD-A192142] N88-24661
MORPHOLOGY
Dynamic consolidation of metal powders
[AD-A192126] N88-24744
Mathematical morphology for structures without translation symmetry
[CWI-AM-R8803] N88-25241
NASA research Program: The roles of fluid motion and other transport phenomena in the morphology of materials
[NASA-CR-182801] N88-25327
The morphological stability of continuous intergranular phases: Thermodynamic considerations
[DE88-006328] N88-25350
The Io sulfur torus in 1981
[NASA-TM-101139] N88-25419
MOSSBAUER EFFECT
A scientific basis for an alternate cathode architecture
[AD-A191498] N88-24717
Influence of alternating magnetic fields on Zn-67 Moessbauer resonance in ZnO
[PB88-186432] N88-25352
MOTION PERCEPTION
Visual information processing in the perception of features and objects
[AD-A192026] N88-25148
MOTION SIMULATION
Fast algorithm development for large-eddy simulation of circular-jet turbulence
[AD-A192044] N88-24887
MOTORS
A universal computer control system for motors
[NASA-CASE-NPO-17134-1-CU] N88-24864
MOUNTING
Almond test body — for microwave anechoic chambers
[NASA-CASE-LAR-13747-1] N88-24845
Thermal compensating mount
[NASA-CASE-LAR-13794-1] N88-24942
MULTIPHOTON ABSORPTION
High-order multiphoton ionization of the noble gases
[DE88-007489] N88-25273
MULTIPLEXING
Adaptive data acquisition multiplexing system and method
[NASA-CASE-MSC-21170-1] N88-24662
MULTIPROCESSING (COMPUTERS)
A multiprocessor data flow accelerator module
[DE88-007587] N88-25161
Decomposition of linear programs using parallel computation
[AD-A191718] N88-25173
Effective use of shared memory multiprocessors
[DE88-007019] N88-25195
MULTISENSOR APPLICATIONS
Multi-sensor integration on the NCUBE hypercube computer
[DE88-007472] N88-25162
MULTIVARIATE STATISTICAL ANALYSIS
Parameter-adaptive model-following for in-flight simulation
[AD-A190567] N88-24845
Poisson functionals of Markov processes and queueing networks
[AD-A191217] N88-25252
MUSCLES
Dexamethasone regulates glutamine synthetase expression in rat skeletal muscles
[NASA-CR-182935] N88-25129
MUSCULAR FUNCTION
Motor theory of auditory perception
[AD-A192095] N88-25136
MYOELECTRICITY
The efficacy of using human myoelectric signals to control the limbs of robots in space
[NASA-CR-182901] N88-25155

N

NASA PROGRAMS
NAS: The first year
[NASA-TM-101006] N88-25196
Financial reporting: NASA (National Aeronautics and Space Administration) can improve compliance with GAO (General Accounting Office) standards and treasury requirements
[PB88-172523] N88-25373
NASA combined file postings statistics based on NASA thesaurus, Jan. 1968 - July 1988
[NASA-CR-182985] N88-25384
NASA patent abstracts bibliography: A continuing bibliography. Section 1: Abstracts
[NASA-SP-7039(33)] N88-25388
NASA history data book. Volume 1: NASA resources 1958-1968
[NASA-SP-4012-VOL-1] N88-25428
NASA historical data book. Volume 2: Programs and projects 1958-1968
[NASA-SP-4012-VOL-2] N88-25429
NASA historical data book. Volume 3: Programs and projects 1969-1978
[NASA-SP-4012-VOL-3] N88-25430
NATIONAL AIRSPACE SYSTEM
FAA (Federal Aviation Administration) technical center: Mission and role in natinal airspace system plan implementation
[PB88-169818] N88-24809

NAVIER-STOKES EQUATION
Prediction of laminar and turbulent flows past single and twin airfoils N88-24589
Some rotorcraft applications of computational fluid dynamics
[NASA-TM-100066] N88-24601
Applications of the Navier-Stokes equations to wings and complex configurations using a zonal approach
[NASA-TM-100060] N88-24602
Computation and characteristics of pulsatile multi-bifurcation flow N88-24729
Composite reduced Navier-Stokes procedures for flow problems with strong pressure interactions
[AD-A191127] N88-24875
Two dimensional hyperbolic grid generation
[VKI-TN-162] N88-24897
Finite element solution of 3-D turbulent Navier-Stokes equations for propeller-driven slender bodies N88-24919

NAVIGATION
A design study of onboard navigation and guidance during aerocapture at Mars
[NASA-CR-172053] N88-24654
Ice conditions along the Ohio River as observed on LANDSAT images, 1972-1985
[AD-A191172] N88-25018
Robot navigation using simple sensor fusion
[DE88-006184] N88-25203

NAVIGATION AIDS
Search and rescue satellite system (SERES), phase A0
[ETN-88-92335] N88-24669
Digital maps for an electronic traffic guide N88-25033

NAVIGATORS
US civil airmen statistics, 1987
[AD-A191714] N88-24577

NEAR FIELDS
Fast algorithm development for large-eddy simulation of circular-jet turbulence
[AD-A192044] N88-24887

NEAR INFRARED RADIATION
A disposable liquid microcell for near-infrared reflectance analysis
[AD-A192190] N88-25296
Infrared astronomy at extremely faint light levels in support of the LAIRTS program
[AD-A191497] N88-25404

NEBULAE
Para-ortho abundance ratio of molecular hydrogen in NGC2023
[ISAS-RN-352] N88-25286

NEGATIVE IONS
A new approach to generating negative ion beams
[AD-A191119] N88-25276
An optical technique for measuring divergence, beam profile, and aiming direction, of relativistic negative hydrogen ions
[DE88-007049] N88-25278
Plasma neutralizer work at BNL (Brookhaven National Laboratory)
[DE88-007046] N88-25317

NEURAL NETS
The efficacy of using human myoelectric signals to control the limbs of robots in space
[NASA-CR-182901] N88-25155
A concurrent neural network algorithm for the traveling salesman problem
[DE88-006981] N88-25206
Theoretical investigation of optical computing based on neural network models
[AD-A191668] N88-25214
Optical computing based on neuronal models
[AD-A191481] N88-25293

NEUROMUSCULAR TRANSMISSION
A systems engineering based methodology for analyzing human electrocortical responses
[AD-A190809] N88-25135

NEUTRAL BEAMS
Arcing and rf signal generation during target irradiation by a high-energy, pulsed neutral particle beam
[DE88-007169] N88-24884
Propagation of neutralized ion beams
[AD-A191599] N88-25289

NEUTRAL PARTICLES
Neutral environment for space station N88-25391
Space station neutral external environment N88-25392

NEUTRALIZERS
Plasma neutralizer work at BNL (Brookhaven National Laboratory)
[DE88-007046] N88-25317

NEUTRON ACTIVATION ANALYSIS
Characterization of yttrium aluminum garnet/YAG/using 14 MeV neutron activation
[AD-A191925] N88-25342

NEUTRON DIFFRACTION
Neutron diffraction refinement of CsHSO4 superionic phase structure
[DE88-701496] N88-25326
Structural studies on La/sub 2/CuO/sub 4+delta/
[DE88-006828] N88-25330

NEUTRON SPECTRA
The development of KENO and the calculation of differential parameters with KENO
[DE88-006176] N88-25186

NEUTRON STARS
Nuclear and astrophysical evidence on the equation of state
[DE88-007397] N88-25279

NEW YORK
New York TRACON demonstration of program recoding requirements analysis document
[DOT/FAA/CT-87/34] N88-24622

NEWTON METHODS
High degree interpolation polynomial in Newton form
[NASA-CR-181677] N88-25249

NEWTONIAN FLUIDS
Extrema principles of entrophy production and energy dissipation in fluid mechanics
[NASA-TM-100992] N88-24946

NICKEL ALLOYS
Martensitic transformation and microstructures in sintered NiAl alloys
[NASA-TT-20178] N88-24761
Rapidly solidified lightweight durable disk material
[AD-A191697] N88-24775

NICKEL HYDROGEN BATTERIES
Nickel hydrogen low earth orbit life testing
[AD-A191946] N88-24855
Small scale bipolar nickel-hydrogen testing
[NASA-TM-100936] N88-25059

NIGHT FLIGHTS (AIRCRAFT)
Simulator evaluation of lineup visual landing aids for night carrier landing
[AD-A191212] N88-24648

NIOBIUM
Effect of alloying, rapid solidification, and surface kinetics on the high temperature environmental resistance of niobium
[AD-A192093] N88-24743

NITRAMINE PROPELLANTS
Structure/property/reactivity relations among nitramine and other energetic materials
[AD-A190878] N88-24716
Chemical kinetics of nitramine propellant combustion
[AD-A191556] N88-24802

NOISE (SOUND)
Higher frequency ambient noise in the arctic ocean
[AD-A192203] N88-25122

NOISE GENERATORS
Higher frequency ambient noise in the arctic ocean
[AD-A192203] N88-25122

NOISE INTENSITY
Operational noise data for CH-47D and AH-64 army helicopters
[AD-A191059] N88-25263

NOISE REDUCTION
Evaluation of the US Army fitting program for the integrated helmet unit of the integrated helmet and display sighting system
[AD-A191616] N88-24635

NONDESTRUCTIVE TESTS
Stress measurements in graphite fibers by laser raman spectroscopy
[AD-A191710] N88-24779
Defect detection and classification in VLSI pattern inspection N88-24871
Knowledge based systems in nondestructive evaluation
[DE88-006853] N88-24981
Nondestructive testing using ultrahigh frequencies
[CERT-5/1333-MO] N88-24984

NONLINEAR EQUATIONS
Similarity solutions of nonlinear partial differential equations invariant to a family of affine groups
[DE88-003404] N88-25245

NONLINEAR EVOLUTION EQUATIONS
Nonlinear wave propagation
[AD-A192104] N88-24835
Nonlinear waves
[AD-A192148] N88-24889

NONLINEAR FEEDBACK
A feedback linearization approach to spacecraft control using momentum exchange devices
[NASA-CR-172057] N88-24868

NONLINEAR OPTICS
Nonlinear surface polaritons
[AD-A191046] N88-24822
Nonlinear waves
[AD-A192148] N88-24889
Research in the optical sciences
[AD-A192175] N88-25297

NONLINEAR PROGRAMMING
Nonlinear programming extensions to rational function approximation methods for unsteady aerodynamic forces
[NASA-TP-2776] N88-24623
The Sizing and Optimization Language, (SOL): Computer language for design problems
[NASA-TM-100565] N88-25190

NONLINEAR SYSTEMS
User's guide to the Fault Inferring Nonlinear Detection System (FINDS) computer program
[NASA-CR-178410] N88-24619
Signal processing with degenerate four-wave mixing
[AD-A191496] N88-24825
Research in nonlinear wave motion
[AD-A191686] N88-24884
Calculation of root-mean-square loads
[BLL-M-37776-(5828.4)] N88-25015
On frequency response for nonlinear systems
[RR-323] N88-25221
Galerkin approximation for inverse problems for nonautonomous nonlinear distributed systems
[NASA-CR-181676] N88-25246
Linear and nonlinear acoustic wave propagation in the atmosphere
[NASA-CR-4157] N88-25268

NONPARAMETRIC STATISTICS
Nonparametric discriminant analysis applied to the extraction and selection of radar target signature features
[AD-A191849] N88-24833
Symmetrized nearest neighbor regression estimates
[AD-A191998] N88-25254

NOTCH TESTS
Analysis of notched metal matrix composites under tension loading
[NASA-TM-100629] N88-24713

NOZZLE FLOW
Fast algorithm development for large-eddy simulation of circular-jet turbulence
[AD-A192044] N88-24887

NOZZLE GEOMETRY
Nozzle fabrication technique
[NASA-CASE-MSC-21299-1] N88-24884

NUCLEAR FUSION
Intense ion beam diagnostics for particle beam fusion experiments on PBFA 2
[DE88-007279] N88-25308

NUCLEAR MAGNETIC RESONANCE
Structural study of the TGMDA-DDS system — epoxy system
[ONERA-RT-4/3346-M] N88-24792

NUCLEAR PHYSICS
Experimental elementary particle physics
[DE88-007510] N88-25274

NUCLEAR POWER PLANTS
Knowledge based systems in nondestructive evaluation
[DE88-006853] N88-24981

NUCLEAR REACTIONS
Nuclear and astrophysical evidence on the equation of state
[DE88-007397] N88-25279

NUCLEAR ROCKET ENGINES
Advanced nuclear rocket engine mission analysis
[DE88-006797] N88-24681

NUCLEAR STRUCTURE
Nuclear structure studies at intermediate energies
[DE88-006883] N88-25271

NUCLEATE BOILING
Heating and evaporation of turbulent liquid films: Measurement of film thickness and the onset of nucleate boiling
[DE88-006388] N88-24905

NUCLEATION
Optical monitoring of protein crystal growth
[NASA-CR-182869] N88-24736

NUCLEON-NUCLEON INTERACTIONS
Nuclear structure studies at intermediate energies
[DE88-006883] N88-25271
Energy measurements in oxygen-induced reactions at 60 A GeV and 200 A GeV
[DE88-006420] N88-25263

NULL ZONES
Null steering applications of polynomials with unimodular coefficients
[AD-A191067] N88-25211

NUMBER THEORY
Some properties of modular equations and the partition function N88-25224

NUMERICAL ANALYSIS
Dynamics of a flexible orbiting platform with MRMS
[ISSN-0285-6808] N88-24673

Internal fluid dynamics within a nonspinning partially liquid-filled shell due to burster rupture
[AD-A191055] N88-24874
SOLA-DM: A numerical solution algorithm for transient three-dimensional flows
[DE88-007159] N88-24913
NAS: The first year
[NASA-TM-101006] N88-25196
Mathematical models for VLSI device simulation
[AD-A191125] N88-25212
Computational sciences
[AD-A190826] N88-25226
Numerical solution of a system of random Volterra integral equations. 1: Successive approximation method N88-25227
Numerical solutions to stochastic difference equations N88-25229
Numerical solution to a system of random Volterra integral equations N88-25230
A method for the numerical solution of random Cauchy singular integral equation N88-25234
Numerical solution of random Love's integral equation N88-25235
High degree interpolation polynomial in Newton form
[NASA-CR-181677] N88-25249
The 2-D magnetohydrostatic configurations leading to flares or quiescent filament eruptions
[NASA-TM-101147] N88-25423

NUMERICAL CONTROL
A universal computer control system for motors
[NASA-CASE-NPO-17134-1-CU] N88-24864
Design and testing of a luminance and chrominance stabilization system for a computer-controlled color display
[AD-A191922] N88-25159

NUMERICAL INTEGRATION
Vibration protection of inelastic structures by means of active and passive control N88-25001

NUMERICAL STABILITY
Stability and convergence of the Peaceman-Rachford ADI method for initial-boundary value problems
[CWI-NM-R8724] N88-25243
New mixed finite element methods N88-25248
CN3D: A 3-dimensional quasi-neutral hybrid particle-in-cell code with applications to the tilt mode instability in field reversed configurations N88-25325

NUMERICAL WEATHER FORECASTING
Analysis of a six-component barotropic spectral model: Chaotic motion, predictability and vacillation — atmospheric circulation
[CWI-AM-R8710] N88-25000
Adaptive grid refinement for numerical weather prediction
[AD-A192172] N88-25101
Bracknell Meteorological Office N88-25107
Applications products of aviation forecast models N88-25109
Computer and model changes at National Meteorological Center (NWC) N88-25116
The Federal Aviation Administration/Massachusetts Institute of Technology (FAA/MIT) Lincoln Laboratory Doppler weather radar program N88-25118

O

OCCLUSION
Shape from shading, occlusion and texture
[AD-A184840] N88-25269

OCEAN BOTTOM
To relate measurements of gravity and geoid anomalies over the oceans to near surface density distributions
[AD-A192168] N88-25120
Evaluation of the biot coefficients
[AD-A191643] N88-25265
Remote sensing of acoustic properties of shallow water sediments: A review
[AD-A192107] N88-25267

OCEAN TEMPERATURE
Evaluating evaporation with satellite thermal data
[AD-A192042] N88-25019

OCEANOGRAPHIC PARAMETERS
SeaSoar profiles in the Iceland-Scotland area, May 1987
[IOS-253] N88-25124

OCEANOGRAPHY
Mariners weather log, volume 32, number 1, Winter 1988
[PB88-173869] N88-25097

OCEANS
Identification and acoustic characterization of seamounts
[AD-A192204] N88-25123
Construction of approximations to acoustic Green's functions for nonhomogeneous oceans using transmutation
[PB88-185364] N88-25126

OHIO RIVER (US)
Ice conditions along the Ohio River as observed on LANDSAT images, 1972-1985
[AD-A191172] N88-25018

OILS
Low pressure entrained flow pyrolysis of biomass to produce liquid fuels N88-25043
Research on hydrotreating catalysts to hydrodeoxygenate biocrude oils N88-25046

OMEGA NAVIGATION SYSTEM
Western Pacific Omega validation: Project description
[AD-A191753] N88-24817

ONBOARD EQUIPMENT
Digital maps for an electronic traffic guide N88-25033

OPEN CHANNEL FLOW
Open channel flow near the resonance speed N88-24918

OPERATING SYSTEMS (COMPUTERS)
Design, implementation and evaluation of an operating system for a network of transputers
[AD-A186593] N88-25193

OPERATIONS RESEARCH
Optical symbolic processor for expert system execution
[AD-A192005] N88-25296

OPERATOR PERFORMANCE
An advanced prototyping tool for human factors design
[AD-A187290] N88-25149

OPTICAL COMMUNICATION
Assessment of optical communications systems for Data Relay Satellite. Volume 1: Executive summary
[ESA-CR(P)-2488-VOL-1] N88-24841
Assessment of optical communications systems for the Data Relay Satellite
[ESA-CR(P)-2488-VOL-2] N88-24842
Activities report of the Division of Optical Technology
[FOA-C-30477-3] N88-25299

OPTICAL COMPUTERS
Optical computer and optical methods for data processing N88-24939
Theoretical investigation of optical computing based on neural network models
[AD-A191668] N88-25214
Optical computing based on neuronal models
[AD-A191481] N88-25293
Optical symbolic processor for expert system execution
[AD-A192005] N88-25296

OPTICAL DATA PROCESSING
Nonlinear surface polaritons
[AD-A191046] N88-24822
Theoretical investigation of optical computing based on neural network models
[AD-A191668] N88-25214
Optical computing based on neuronal models
[AD-A191481] N88-25293
Activities report of the Division of Optical Technology
[FOA-C-30477-3] N88-25299
Optical nonlinearities in GaAs/GaAlAs multiple quantum wells fabricated by metalorganic chemical vapor deposition for use in optical signal processing
[AD-A191558] N88-25337

OPTICAL EQUIPMENT
Joint services electronics program
[AD-A192078] N88-24856
Optical symbolic processor for expert system execution
[AD-A192005] N88-25296
Research in the optical sciences
[AD-A192175] N88-25297

OPTICAL FIBERS
Study of light transmission methods from scintillators to optical fiber with wave length shifter
[DE88-701587] N88-25292
Novel fiber preforms: Rare earth doping
[AD-A191549] N88-25294

OPTICAL FILTERS
Analysis of binarized Hartley phase-only filter performance with respect to stochastic noise
[DE88-007604] N88-24945

OPTICAL GYROSCOPES
Navigation using the Teldix fiber-optic gyroscope N88-24933

OPTICAL MEASUREMENT
Optical monitoring of protein crystal growth
[NASA-CR-182669] N88-24738
Instrumentation for turbulent reacting flows
[AD-A191671] N88-24923
An optical preamplifier for detection of CO2 laser radiation
[AD-A190790] N88-24949
An optical technique for measuring divergence, beam profile, and aiming direction, of relativistic negative hydrogen ions
[DE88-007049] N88-25278

OPTICAL MEASURING INSTRUMENTS
Phase length optical phase-locked-loop sensor
[NASA-CASE-LAR-13387-1] N88-25302

OPTICAL MEMORY (DATA STORAGE)
Optical computing based on neuronal models
[AD-A191481] N88-25293

OPTICAL PATHS
Phase length optical phase-locked-loop sensor
[NASA-CASE-LAR-13387-1] N88-25302

OPTICAL POLARIZATION
Real-time image difference detection using a polarization rotation spacial light modulator
[NASA-CASE-NPO-17144-1-CU] N88-25305

OPTICAL PROPERTIES
Time resolved spectroscopy facility for the study of nonlinear optical properties of semiconducting polymers
[AD-A191221] N88-24788
Stress measurements in graphite fibers by laser raman spectroscopy
[AD-A191710] N88-24779
Studies of optical matrix multiplication and reconfigurable optical interconnect concepts
[AD-A191635] N88-25295
Research in the optical sciences
[AD-A192175] N88-25297
Electronic structure, elementary excitations, optical and transport properties of semiconductor superlattices
[AD-A190795] N88-25333
Optical properties of heterostructures and superlattices
[AD-A191542] N88-25335

OPTICAL RADAR
Optics: Perspectives for Measurement Techniques and Signal Processing for Flight Guidance — conference
[DFVLR-MITT-87-21] N88-24928
Limits of accuracy and range of laser radars N88-24934
Components of an atmospheric lidar system: Doppler wind lidar
[AD-A191222] N88-24951
Aircraft/lidar turbulence comparison N88-25111

OPTICAL REFLECTION
Phase length optical phase-locked-loop sensor
[NASA-CASE-LAR-13387-1] N88-25302

OPTICAL RESONATORS
High power axial flow CO2 laser
[ETN-88-91951] N88-24959

OPTICAL THICKNESS
Diurnal variations in optical depth at Mars: Observations and interpretations
[NASA-TM-100057] N88-25420

OPTICAL TRACKING
Real-time optical multiple object recognition and tracking system and method
[NASA-CASE-NPO-17139-1-CU] N88-25301

OPTICAL WAVEGUIDES
Silicon-sapphire waveguides
[AD-A191754] N88-24854

OPTIMAL CONTROL
Estimation and control of distributed models for certain elastic systems arising in large space structures
[AD-A192120] N88-24866
Low authority control of large space structures using a constrained threshold control formulation N88-24867
Optimal processes governed by integral equations with unilateral constraint N88-25231

OPTIMIZATION
Nonlinear programming extensions to rational function approximation methods for unsteady aerodynamic forces
[NASA-TP-2776] N88-24823
Guidance and control strategies for aerospace vehicles
[NASA-CR-183032] N88-24844
A feedback linearization approach to spacecraft control using momentum exchange devices
[NASA-CR-172057] N88-24868
Optimization of reserve lithium thionyl chloride battery electrochemical design parameters
[DE88-007109] N88-24868
Applications of fault tree analysis to the design process
[DE88-007048] N88-24982
A mixed-integer linear programming problem which is efficiently solvable
[AD-A191026] N88-25188
Solving bidiagonal systems of linear equations on the CDC CYBER 205
[CWI-NM-R8725] N88-25187

The Sizing and Optimization Language, (SOL): Computer language for design problems
[NASA-TM-100565] N88-25190
Gram-Schmidt implementation of a linearly constrained adaptive array
[AD-A191651] N88-25198
Mixed min-max optimization problem with restrictions N88-25232
The use of Lagrange multipliers and Kuhn-Tucker's theory in optimization problems N88-25236
Optimal discrete-time LQR problems for parabolic systems with unbounded input: Approximation and convergence
[NASA-CR-181673] N88-25247

ORBIT TRANSFER VEHICLES
Advanced nuclear rocket engine mission analysis
[DE88-006797] N88-24681

ORBITAL LIFETIME
An extended life and performance test of a low-power arcjet
[NASA-TM-100942] N88-24687

ORDER-DISORDER TRANSFORMATIONS
The theory of random alloys
[DE88-006408] N88-24756

ORDNANCE
Timing control system
[NASA-CASE-NPO-16882-1-CU] N88-24863

ORGANIC MATERIALS
The evolution of cometary activity N88-25416

ORTHOGONAL FUNCTIONS
Optimal a priori covariance selection for the solution of ill-conditioned nonlinear inverse problems N88-25222
On a biorthogonal system associated with uniform asymptotic expansions
[CWI-AM-R8709] N88-25240

ORTHOTROPIC PLATES
The surface crack problem in an orthotropic plate under bending and tension
[NASA-CR-178261] N88-25014

OSCILLATORS
Integral equation for the laser field: Multimode description of a free-electron laser oscillator
[DE88-007050] N88-24956

OUTGASSING
Neutral environment for space station N88-25391
Space station neutral external environment N88-25392
The evolution of cometary activity N88-25416

OXIDATION
Surface composition-reactivity relationships in heterogeneous catalysis
[DE88-006679] N88-24714
Calculation of oxidation rates for iron in CO-CO2
[DE88-007313] N88-24757
Effect of carbohydrate oxidation on the tropospheric HOx-system N88-25087

OXIDATION-REDUCTION REACTIONS
Oxidation and reduction rates for organic carbon in the Amazon mainstream tributary and floodplain, inferred from distributions of dissolved gases
[NASA-CR-182943] N88-25062
Photochemical and thermal modeling in the early atmosphere of the earth
[NASA-CR-183029] N88-25093

OXYGEN
Catalytic ignition of hydrogen and oxygen propellants
[NASA-TM-100957] N88-24689
Effect of hydrogen, deuterium and oxygen on the anelastic properties of refractory alloys
[DE88-007349] N88-24736

OXYGEN ATOMS
Laboratory experiments of relevance to the space station environment N88-25402

OXYGEN RECOMBINATION
Molecular sources of ionospheric holes
[AD-A191857] N88-25082

OXYGEN SPECTRA
Structural studies on La/sub 2/CuO/sub 4+delta/
[DE88-006828] N88-25330

OZONE
Air pollution: Ozone attainment requires long-term solutions to solve complex problems
[PB88-167275] N88-25060
Workshop on Atmospheric OH
[BPT-7/87] N88-25063
Ozone in the atmosphere N88-25064
Ultraviolet measurements: Measurements of photolysis rates N88-25065
Motor vehicles as sources of compounds important to tropospheric and stratospheric ozone
[PB88-195219] N88-25076

OZONE DEPLETION
Changes in the Antarctic atmosphere due to the reduction of stratospheric ozone
[ETN-88-92565] N88-25074

OZONOMETRY
Workshop on Atmospheric OH
[BPT-7/87] N88-25063
Ozone in the atmosphere N88-25064
Ultraviolet measurements: Measurements of photolysis rates N88-25065
Changes in the Antarctic atmosphere due to the reduction of stratospheric ozone
[ETN-88-92565] N88-25074

P

P-N-P JUNCTIONS
Joint services electronics program research in electronics
[AD-A192206] N88-24857

P-3 AIRCRAFT
Taiwan area mesoscale experiment: P-3 aircraft operations summary
[PB88-169073] N88-25098

PAINTS
Predictive corrosion modeling, volume 1
[AD-A191229] N88-24739

PAIR PRODUCTION
A new approach to generating negative ion beams
[AD-A191119] N88-25276
Gamma rays from Cygnus X-1: Modeling and nonthermal pair production
[DE88-006830] N88-25426

PANELS
Stiffened titanium panels
[NASA-CASE-LAR-13814-1] N88-24816

PANORAMIC SCANNING
Atmospheric autorotating imaging device
[NASA-CASE-NPO-17390-1-CU] N88-24944

PAPER (MATERIAL)
Reference filters for electrostatic charging tendency measurements of fuels
[AD-A191717] N88-24803

PARABOLIC DIFFERENTIAL EQUATIONS
Optimal discrete-time LQR problems for parabolic systems with unbounded input: Approximation and convergence
[NASA-CR-181673] N88-25247

PARACHUTE DESCENT
Parachute for in-flight training on parachute ejection
[REPT-87-11] N88-24593

PARACHUTES
Parachute for in-flight training on parachute ejection
[REPT-87-11] N88-24593

PARALLEL PROCESSING (COMPUTERS)
Decomposition of linear programs using parallel computation
[AD-A191718] N88-25173
An improved simulated annealing algorithm for standard cell placement
[NASA-CR-182952] N88-25183
Algorithms and software for solving finite element equations on serial and parallel architectures
[NASA-CR-183027] N88-25191
Network architecture for OPS5
[DE88-002802] N88-25194

PARALLEL PROGRAMMING
Beyond Ada: Generating Ada code from equational specifications
[AD-A191866] N88-25176

PARAMETER IDENTIFICATION
TVC (Thrust Vector Control) jet vane thermal modeling using parametric system identification
[AD-A191518] N88-24678
A fast and efficient procedure for generalized cross-validation with large data sets. Application to image reconstruction
[RR-869-M] N88-25220
Single-mode projection filters for modal parameter identification for flexible structures
[NASA-CR-182660] N88-25244
Recursive maximum likelihood identification of a nonlinear output-affine model
[RR-322] N88-25257

PARAMETERIZATION
Analysis of lightning field changes during active thunderstorms in Florida N88-25103
Making progress during a stall in the simplex algorithm
[DE88-007120] N88-25182

PARTIAL DIFFERENTIAL EQUATIONS
Similarity solutions of nonlinear partial differential equations invariant to a family of affine groups
[DE88-003404] N88-25245

PARTICLE ACCELERATORS
Tutorial on computer control
[DE88-006185] N88-25157

PARTICLE COLLISIONS
A new approach to generating negative ion beams
[AD-A191119] N88-25276
Calorimetry applied to nucleus-nucleus collisions at ultrarelativistic energies
[DE88-006173] N88-25282
Theoretical investigations of drift waves in a magnetic quadrupole N88-25312

PARTICLE EMISSION
WIPP (Wave Induced Particle Precipitation) experiment logistic support
[AD-A191184] N88-24824

PARTICLE IN CELL TECHNIQUE
QN3D: A 3-dimensional quasi-neutral hybrid particle-in-cell code with applications to the tilt mode instability in field reversed configurations N88-25325

PARTICLE INTERACTIONS
Calorimetry applied to nucleus-nucleus collisions at ultrarelativistic energies
[DE88-006173] N88-25282

PARTICLE PRECIPITATION
WIPP (Wave Induced Particle Precipitation) experiment logistic support
[AD-A191184] N88-24824

PARTICLE PRODUCTION
Experimental elementary particle physics
[DE88-007510] N88-25274

PARTICLE SIZE DISTRIBUTION
Transient particle deposition in a boundary layer of impulsive flow over a flat plate
[AD-A191537] N88-24880

PARTICLE TRACKS
Optical system of laser illuminated streamer chamber
[DE88-702127] N88-25306

PARTICLES
Particle-laden weakly swirling free jets: Measurements and predictions
[NASA-TM-100920] N88-24639
Application of particle simulations to the NRL laser experiment
[AD-A191641] N88-24953
Modelling of thermal plasma systems N88-25314

PARTICULATES
Space station particulate contamination environment N88-25397
The particulate environment surrounding the space station: Estimates from the PACS data N88-25398
Effects of meteoroids and space debris on the particulate environment for space station N88-25399

PARTITIONS (MATHEMATICS)
Some properties of modular equations and the partition function N88-25224

PASSENGER AIRCRAFT
Class 2 design update for the family of commuter airplanes
[NASA-CR-182681] N88-24629

PATENT APPLICATIONS
Navigation system for land vehicles
[NASA-CASE-LAR-13322-1] N88-24620
Airplane runway performance monitoring system
[NASA-CASE-LAR-13854-1-CU] N88-24621
Nozzle fabrication technique
[NASA-CASE-MSC-21299-1] N88-24684
Dual-fuel, dual-mode rocket engine
[NASA-CASE-LAR-13773-1] N88-24685
Energy efficient continuous flow ash lockhopper
[NASA-CASE-NPO-16985-1-CU] N88-24814
Low temperature storage container for transporting perishables to space station
[NASA-CASE-MFS-28248-1] N88-24817
Noncontact temperature pattern measuring device
[NASA-CASE-NPO-17024-1-CU] N88-24943
Atmospheric autorotating imaging device
[NASA-CASE-NPO-17390-1-CU] N88-24944
Universal precision sine bar attachment
[NASA-CASE-MFS-28253-1] N88-24971
Trailer shield assembly for a welding torch
[NASA-CASE-MFS-29260-1] N88-24972
Radio Frequency (RF) strain monitor
[NASA-CASE-LAR-13705-1] N88-25011
Optical pressure sealing couping (light joint)
[NASA-CASE-MFS-29348-1] N88-25303
Crystal growth apparatus
[NASA-CASE-MFS-28182-1] N88-25357

PATENT POLICY
NASA patent abstracts bibliography: A continuing bibliography. Section 1: Abstracts
[NASA-SP-7039(33)] N88-25388

PATENTS
Magnetically switched power supply system for lasers
[NASA-CASE-NPO-16402-2] N88-24662
Linear force device
[NASA-CASE-MSC-20549-2] N88-24927
Range and range rate system
[NASA-CASE-MSC-20867-1] N88-24958

PATTERN RECOGNITION
Nonparametric discriminant analysis applied to the extraction and selection of radar target signature features
[AD-A191849] N88-24833
Tests for the automatic pattern recognition of building surfaces by the TK 50 N88-25030
Feature extraction using the Hough transform
[AD-A190679] N88-25165
Real-time optical multiple object recognition and tracking system and method
[NASA-CASE-NPO-17139-1-CU] N88-25301
Cluster analysis of multiple planetary flow regimes
[NASA-CR-182931] N88-25418
PATTERN REGISTRATION
Application of dynamic programming to image registration
[ENST-87E022] N88-25180
PAVEMENTS
Design of overlays for rigid airport pavements
[DOT/FAA/PM-87/19] N88-24652
PAYLOAD DEPLOYMENT & RETRIEVAL SYSTEM
Payload deployment method and system
[NASA-CASE-MSC-21330-1] N88-24660
PAYLOADS
Lunar base surface mission operations. Lunar Base Systems Study (LBSS) task 4.1
[NASA-CR-172050] N88-25415
PECLET NUMBER
Review of numerical methods for radionuclide transport in three-dimensional porous media, at high Peclet numbers
[CFDU/87/10] N88-25061
PERFORMANCE PREDICTION
The performance of the VKI longshot hypersonic wind tunnel
[VKI-TN-161] N88-24650
Propagation management for no-acknowledge HF communications links N88-24843
Performance estimates for operations conducted while wearing individual protective equipment: User manual
[AD-A191871] N88-25154
PERFORMANCE TESTS
Performance and long duration test of a 30 kw thermal arcjet engine
[AD-A190962] N88-24677
An extended life and performance test of a low-power arcjet
[NASA-TM-100942] N88-24887
Laboratory tests of laser gyroscopes for future utilization in multifunction systems for precision navigation and flight guidance N88-24932
SRM propellant and polymer materials structural test program
[NASA-TP-2821] N88-25013
Small scale bipolar nickel-hydrogen testing
[NASA-TM-100936] N88-25059
PERMANENT MAGNETS
A microcomputer-based control and simulation of an advanced IPM (Interior Permanent Magnet) synchronous machine drive system for electric vehicle propulsion
[DE88-006735] N88-24859
PERMEATING
Mechanisms of gas permeation through polymer membranes: Renewal proposal for period December 1, 1986 - November 30, 1989
[DE88-007436] N88-24796
PERSONAL COMPUTERS
Personal computer as a workstation in a cartographic automation system? N88-25039
PERSONNEL
US civil airmen statistics, 1987
[AD-A191714] N88-24577
PERSONNEL MANAGEMENT
Management and the executive
[AD-A190778] N88-25374
PERSPIRATION
Physiological and hematological responses of matched older and younger men during dry-heat acclimation
[AD-A186450] N88-25139
PERTURBATION THEORY
An experimental study of the coherent under-ice reflectivity of sound in the Greenland Sea Marginal Ice Zone N88-25125
Perturbation theory for dual semigroups. Part 4: The intertwining formula and the canonical pairing
[CWI-AM-R8802-PT-4] N88-25258
PETN
Thermal decomposition studies of explosives for component applications
[DE88-007201] N88-24805
PETRI NETS
Some unsolved problems in modelling self-timed circuits using Petri Nets, series B, number 2
[PB88-181466] N88-24872
PETROGRAPHY
A sedimentological and mineralogical study of the Koogah Formation, New South Wales N88-25067
PHASE CHANGE MATERIALS
The morphological stability of continuous intergranular phases: Thermodynamic considerations
[DE88-006328] N88-25350
PHASE DIAGRAMS
Vacancy ordering in the basal plane of YBa2Cu3O(sub)z
[DE88-004572] N88-25348
PHASE LOCKED SYSTEMS
An investigation of a distributed clock for local area networks with ring topology N88-24924
Phase length optical phase-locked-loop sensor
[NASA-CASE-LAR-13387-1] N88-25302
PHASE MODULATION
Influence of alternating magnetic fields on Zn-67 Moessbauer resonance in ZnO
[PB88-186432] N88-25352
PHASE SHIFT KEYING
A Differential Phase Shift Keying (DPSK) modulator for a frequency hopping short wave system
[FOA-C-30460-3.3] N88-24840
PHASE TRANSFORMATIONS
The thermodynamic properties of quinoline and isoquinoline
[DE88-001218] N88-24735
Dynamic consolidation of metal powders
[AD-A192126] N88-24744
On the abnormal phenomena observed in the electrical resistivity measurement during the decomposition process of saturated Cu-Fe alloys
[NASA-TT-20183] N88-24869
PHASED ARRAYS
Automated test device for FASR (Fixed Array Surveillance Radar) beam steering componentry
[AD-A191650] N88-24829
PHONETICS
Time-frequency representations for speech signals
[AD-A186661] N88-24819
PHOSPHAZENE
Aromatic cyclotriphosphazenes
[NASA-CASE-ARC-11428-3] N88-24692
Synthesis and characterization of new phosphazene polymers
[AD-A191508] N88-24771
PHOSPHORS
Remote temperature-measurement instrumentation for a heated rotating turbine disk
[DE88-006456] N88-24925
PHOTOCHEMICAL REACTIONS
Photochemical and thermal modeling in the early atmosphere of the earth
[NASA-CR-183029] N88-25093
PHOTOCONDUCTIVITY
Liquid carbon
[AD-A191707] N88-24776
Photoconductivity in carbon fibers
[AD-A191726] N88-24782
PHOTOELECTRIC EMISSION
Physical properties of f electron systems
[DE88-006886] N88-25331
PHOTOGRAMMETRY
Development in data structures in PHOCUS for digital mapping N88-25034
PHOTOIONIZATION
Selective detection in gas chromatography
[AD-A191499] N88-24718
Photoionization dynamics and abundance patterns in laser vaporized tin and lead clusters
[AD-A191604] N88-24722
High-order multiphoton ionization of the noble gases
[DE88-007489] N88-25273
PHOTOLYSIS
Ultraviolet measurements: Measurements of photolysis rates N88-25065
An investigation of 2-6 superlattice deposition by laser photochemical techniques
[AD-A191547] N88-25336
PHOTOMICROGRAPHY
Improving knowledge of the corrosion behavior of aluminum alloys of the 7XXX series
[REPT-48-451/F] N88-24750
PHOTOMULTIPLIER TUBES
The off-axis channel macroplate
[NASA-CR-182938] N88-24861
PHOTONS
Bimolecular reactions and energy-transfer processes of highly vibrationally excited molecules related to energetic materials
[AD-A189013] N88-25270
PHOTOSYNTHESIS
Photosynthetic water splitting
[PB88-186891] N88-24731
PHOTOTHERMAL CONVERSION
Photochemical and thermal modeling in the early atmosphere of the earth
[NASA-CR-183029] N88-25093
PHOTOVOLTAIC CELLS
Photovoltaic Advanced Research and Development Project, solar radiation research
[DE88-001143] N88-25056
PHYSICAL EXAMINATIONS
US civil airmen statistics, 1987
[AD-A191714] N88-24577
PHYSICAL OPTICS
Curvature of blended rolled edge reflectors at the shadow boundary contour
[NASA-CR-182974] N88-25300
PHYSICAL WORK
Simultaneous multiple control force exertion capabilities of males and females versus helicopter control force design limits
[AD-A191653] N88-25153
PHYSIOLOGICAL EFFECTS
Effects of moderate cold and heat stress on the potential work performance of industrial workers. Part 6: The effects of increasing vapour pressure at four air temperatures on the performance and physiology of white females
[PB88-124854] N88-25137
Physiological and hematological responses of matched older and younger men during dry-heat acclimation
[AD-A186450] N88-25139
PHYSIOLOGICAL RESPONSES
Behavioral response of rats exposed to high-power microwave radiation
[AD-A192199] N88-25128
A systems engineering based methodology for analyzing human electrocortical responses
[AD-A190809] N88-25135
PIEZOELECTRIC CRYSTALS
A dynamic analysis of piezoelectric strained elements
[AD-A191478] N88-24851
PIEZOELECTRICITY
Dynamic consolidation of metal powders
[AD-A192126] N88-24744
PILOT PERFORMANCE
Aircraft accident/incident, Copperhill, Tennessee, February 22, 1986
[PB88-910407] N88-24612
Analysis procedures and subjective flight results of a simulator validation and cue fidelity experiment
[NASA-TM-88270] N88-24634
An evaluation of three linear scale radar altimeter displays
[AD-A192173] N88-24636
PILOT TRAINING
An enumeration of research to determine the optimal design and use of Army flight training simulators
[AD-A191242] N88-24649
PILOTS (PERSONNEL)
US civil airmen statistics, 1987
[AD-A191714] N88-24577
PINHOLE CAMERAS
A multi-frame ion pinhole camera for intense ion beam transport and focusing experiments
[DE88-007283] N88-24926
Intense ion beam diagnostics for particle beam fusion experiments on PBFA 2
[DE88-007279] N88-25308
PIPE FLOW
Energy efficient continuous flow ash lockhopper
[NASA-CASE-NPO-16985-1-CU] N88-24814
Hydroacoustic pulsating jet generator
[MPIS-7/1987] N88-24891
Turbulent heat transfer and fluid flow measurements downstream of abrupt expansions and in a cavity of a circular tube at a uniform wall temperature N88-24920
PIPES (TUBES)
Theoretical and experimental damping values of piping systems at high ductilities
[DE88-006717] N88-24966
PISTON ENGINES
Computer simulation of turbulent combustion in reciprocating engines
[CFDU/87/11] N88-24725
PISTON THEORY
The performance of the VKI longshot hypersonic wind tunnel
[VKI-TN-161] N88-24650
PLANE STRAIN
Dynamic shear band development in plane strain
[AD-A190915] N88-24968
PLANETARY ATMOSPHERES
A design study of onboard navigation and guidance during aerocapture at Mars
[NASA-CR-172053] N88-24654
PLANNING
Sensitivity analysis for the system reliability function
[AD-A191648] N88-24979

Management and the executive
[AD-A190778] N88-25374
Department of Defense statement on defense agency research and development to the Subcommittee on Defense of the Committee on Appropriations, United States House of Representatives, 100th Congress, second session
[AD-A191840] N88-25377
Department of Defense Statement on the Balanced Technology Initiative to the Committee on Armed Services, United States Senate, 100th Congress, second session
[AD-A191841] N88-25378
Centre for International Co-Operation and Approriate Technology (CICAT)
[PB88-165501] N88-25389

PLASMA CLOUDS
Application of particle simulations to the NRL laser experiment
[AD-A191641] N88-24953

PLASMA CURRENTS
Interpretation of the northward B sub z (NBZ) Birkeland current system and polar cap convection patterns in terms of the impulsive penetration model
[AERONOMICA-ACTA-A-321-1987] N88-25422

PLASMA DENSITY
Low frequency electrostatic turbulence in the polar cap E-region
[DRI-3-88] N88-25077
Plasma neutralizer work at BNL (Brookhaven National Laboratory)
[DE88-007046] N88-25317

PLASMA DIAGNOSTICS
Trochoidal analysis of scattered electrons in a merged electron-ion beam
[NASA-CASE-NPO-16789-1-CU] N88-25281
Intense ion beam diagnostics for particle beam fusion experiments on PBFA 2
[DE88-007279] N88-25306
A two-wavelength infrared interferometer/polarimeter system for CIT (Compact Ignition Tokamak)
[DE88-007681] N88-25321
Optical diagnostics for a high power, rf-inductively coupled plasma
[DE88-007822] N88-25322
Activities report in plasma physics
[ETN-88-92221] N88-25324

PLASMA DRIFT
Application of particle simulations to the NRL laser experiment
[AD-A191641] N88-24953

PLASMA ELECTRODES
Basic processes of plasma propulsion
[AD-A192117] N88-25310

PLASMA GUNS
Evaluation of the chromium oxide arc spraying treatment on solar energy collectors
[ETN-88-92564] N88-25053

PLASMA HEATING
Activities report in plasma physics
[ETN-88-92221] N88-25324

PLASMA INTERACTIONS
Theoretical plasma physics research of active space experiments
[AD-A192075] N88-25309

PLASMA JETS
Optical investigations of the thermal boundary layer in arc plasmas N88-25313
Modelling of thermal plasma systems N88-25314
Plasma neutralizer work at BNL (Brookhaven National Laboratory)
[DE88-007046] N88-25317

PLASMA PHYSICS
Theoretical plasma physics research of active space experiments
[AD-A192075] N88-25309
Activities report in plasma physics
[ETN-88-92221] N88-25324

PLASMA PINCH
Activities report in plasma physics
[ETN-88-92221] N88-25324

PLASMA PROPULSION
Basic processes of plasma propulsion
[AD-A192117] N88-25310

PLASMA RADIATION
Studies of spectral line ratio fluctuations using Inductively Coupled Plasma (ICP) light
[IRF-PREPRINT-100] N88-25311

PLASMA WAVES
Activities report in plasma physics
[ETN-88-92221] N88-25324
Contaminant ions and waves in the space station environment N88-25393

PLASMAS (PHYSICS)
Theoretical plasma physics research of active space experiments
[AD-A192075] N88-25309
Theoretical investigations of drift waves in a magnetic quadrupole N88-25312
Stochasticity in a Q-machine plasma N88-25315
Plasma neutralizer work at BNL (Brookhaven National Laboratory)
[DE88-007046] N88-25317
Self shielding of surfaces irradiated by intense energy fluxes
[DE88-007094] N88-25318
Optical diagnostics for a high power, rf-inductively coupled plasma
[DE88-007822] N88-25322

PLASTIC DEFORMATION
The influence of the chemical nature of resins on their reticulation kinetics and the consequences for their nonelastic mechanical properties
[ETN-88-92539] N88-24788
On the abnormal phenomena observed in the electrical resistivity measurement during the decomposition process of saturated Cu-Fe alloys
[NASA-TT-20183] N88-24869
Dynamic shear band development in plane strain
[AD-A190915] N88-24988

PLASTICS
Differential technology in plastics industries differentiation in combination technology nonflammability technology
[NASA-TT-20256] N88-24797

PLATES (TECTONICS)
The interpretation of crustal dynamics data in terms of plate interactions and active tectonics of the Anatolian Plate and surrounding regions in the Middle East
[NASA-CR-183024] N88-25092

PLOTTERS
Use of modern scanner techniques in cartography N88-25040

PLUMES
Research study: Space shuttle main engine plume flowfield model
[NASA-CR-179336] N88-24676
Evaluation of the communications impact of a low power arcjet thruster
[NASA-TM-100926] N88-24682

PLY ORIENTATION
Harmfulness of defects: Behaviour in service of a delamination in a composite containing many differently oriented layers
[PB88-124714] N88-24705

POINTING CONTROL SYSTEMS
Utilization of the IR telescope gimbaling system as a stabilized pointing platform for balloon payloads. Volume 1: Technical results
[NASA-CR-179339] N88-24962

POISSON DENSITY FUNCTIONS
Poisson functionals of Markov processes and queueing networks
[AD-A191217] N88-25252
On path properties of certain infinitely divisible processes
[AD-A192016] N88-25255

POLAR REGIONS
Low frequency electrostatic turbulence in the polar cap E-region
[DRI-3-88] N88-25077
SAM 2 data user's guide
[NASA-RP-1200] N88-25094

POLARIMETERS
A two-wavelength infrared interferometer/polarimeter system for CIT (Compact Ignition Tokamak)
[DE88-007681] N88-25321

POLARITONS
Nonlinear surface polaritons
[AD-A191046] N88-24822

POLICIES
Sensitivity analysis for the system reliability function
[AD-A191648] N88-24979
Centre for International Co-Operation and Approriate Technology (CICAT)
[PB88-165501] N88-25389

POLLUTION TRANSPORT
Review of numerical methods for radionuclide transport in three-dimensional porous media, at high Peclet numbers
[CFDU/87/10] N88-25061

POLOIDAL FLUX
The 2-D magnetohydrostatic configurations leading to flares or quiescent filament eruptions
[NASA-TM-101147] N88-25423

POLYACETYLENE
Time resolved spectroscopy facility for the study of nonlinear optical properties of semiconducting polymers
[AD-A191221] N88-24768

POLYBUTADIENE
Environmental integrity of coating/metal interface
[AD-A192184] N88-24786

POLYCRYSTALS
Role of cracks in the creep of structural polycrystalline ceramics
[AD-A191485] N88-24770

POLYESTERS
Combustion of PMMA, PE and PS in a ramjet
[VTH-LR-514] N88-24733

POLYETHYLENES
Combustion of PMMA, PE and PS in a ramjet
[VTH-LR-514] N88-24733

POLYIMIDE RESINS
New polyisoimides: An approach to in situ rigid-rod polyimide formation
[AD-A191665] N88-24773

POLYMER CHEMISTRY
Synthesis and characterization of new phosphazene polymers
[AD-A191508] N88-24771
Electronic and ionic transport in polymers
[AD-A191642] N88-24772

POLYMERIC FILMS
Mechanisms of gas permeation through polymer membranes: Renewal proposal for period December 1, 1986 - November 30, 1989
[DE88-007436] N88-24796

POLYMERIZATION
Aromatic cyclotriphosphazenes
[NASA-CASE-ARC-11428-3] N88-24692
Current and future molecular structures of aerospace organic matrix resins N88-24695
Synthesis and characterization of new phosphazene polymers
[AD-A191508] N88-24771
Electronic and ionic transport in polymers
[AD-A191642] N88-24772
Demixing of aqueous polymer two-phase systems in low gravity
[NASA-TM-101141] N88-24809

POLYMETHYL METHACRYLATE
Combustion of PMMA, PE and PS in a ramjet
[VTH-LR-514] N88-24733
Adhesion between polystyrene and polymethylmethacrylate
[AD-A192050] N88-24785

POLYNOMIALS
Sensitivity analysis for the system reliability function
[AD-A191648] N88-24979
Null steering applications of polynomials with unimodular coefficients
[AD-A191087] N88-25211
On a biorthogonal system associated with uniform asymptotic expansions
[CWI-AM-R8709] N88-25240
High degree interpolation polynomial in Newton form
[NASA-CR-181677] N88-25249

POLYPHENYLS
The synthesis of polyphenylene from a CIS-dihydrocatechol biologically produced monomer N88-24699

POLYSTYRENE
Preferential surface adsorption in miscible blends of polystyrene and poly(vinyl methyl ether)
[AD-A191451] N88-24769
Adhesion between polystyrene and polymethylmethacrylate
[AD-A192050] N88-24785
Diffusion of homopolymers into nonequilibrum diblock copolymer structures
[DE88-005306] N88-24794

POROUS MATERIALS
Review of numerical methods for radionuclide transport in three-dimensional porous media, at high Peclet numbers
[CFDU/87/10] N88-25061

POSITION (LOCATION)
Search and rescue satellite system (SERES), phase A0
[ETN-88-92335] N88-24689
Geometric rectangular data file (GERD): An aid to the rapid access to position data N88-25037

POSITIVE IONS
Stratospheric positive ion composition measurements and acetonitrile detection: A consistent picture
[AERONOMICA-ACTA-A-326-1987] N88-25084

POWDER METALLURGY
Characterization of 7090 and 7091 profiles made with Cegedur powder — powder metallurgy, aircraft construction materials
[REPT-48-441/F] N88-24752
Laboratory scale inert gas atomizer for producing rapidly solidified powders
[DE88-006734] N88-24812

POWDERED ALUMINUM
Dynamic consolidation of metal powders
[AD-A192126] N88-24744

PREAMPLIFIERS
An optical preamplifier for detection of CO2 laser radiation
[AD-A190790] N88-24949
PREBURNERS
Duct flow nonuniformities for Space Shuttle Main Engine (SSME)
[NASA-CR-179336] N88-24899
PRECIPITATION (CHEMISTRY)
Effect of size of precipitates on recrystallization temperatures in Cu-Cr, Cu-Zr, and Cu-Zr-Cr alloys
[NASA-TT-20166] N88-24763
A study on the precipitation and reversion behaviors of Cu-0.3 percent Cr alloy by the step annealing method
[NASA-TT-20169] N88-24764
PRECIPITATION HARDENING
The precipitation processes of Cu-Zr-Cr alloys
[NASA-TT-20168] N88-24758
Critical cooling rates on solution treatment of Cu-Cr and Cu-Be alloys
[NASA-TT-20163] N88-24760
PRECISION
Development of mirrors for high-precision laser gyroscopes N88-24931
PREDICTION ANALYSIS TECHNIQUES
Particle-laden weakly swirling free jets: Measurements and predictions
[NASA-TM-100920] N88-24839
Design of overlays for rigid airport pavements
[DOT/FAA/PM-87/19] N88-24852
Research study: Space shuttle main engine plume flowfield model
[NASA-CR-179336] N88-24676
Predictive corrosion modeling, volume 1
[AD-A191229] N88-24739
Environment assisted degradation mechanisms in advanced light metals
[NASA-CR-182907] N88-24746
Investigation of the effect of minimum loads and compression of load spectra on the prediction capacities of the ONERA crack model — wings
[ONERA-RTS-33/7169-RY-064-R] N88-24994
Some stress intensity factor equations
[FFA-TN-1987-07] N88-24995
Automated analysis of crack growth rate for obtaining da/dN versus delta K relation
[FFA-TN-1987-70] N88-24996
Adaptive grid refinement for numerical weather prediction
[AD-A192172] N88-25101
Adaptive time series analysis using predictive inference and entropy
[AD-A191858] N88-25199
PREDICTIONS
Progress and future directions in computational fluid dynamics
[NASA-TM-100091] N88-24579
Prediction of laminar and turbulent flows past single and twin airfoils N88-24589
Simulating futures in extended common LISP
[NASA-TM-101000] N88-25192
Automatic discovery of optimal classes
[NASA-TM-101174] N88-25238
Single-mode projection filters for modal parameter identification for flexible structures
[NASA-CR-182680] N88-25244
Energy measurements in oxygen-induced reactions at 60 A GeV and 200 A GeV
[DE88-006420] N88-25283
PREFORMS
Novel fiber preforms: Rare earth doping
[AD-A191549] N88-25294
PREIMPREGNATION
Elementary characterization of preimpregnated carbon epoxy T400H/DA0506 from STRUCTIL. Test report M6-577100
[CEAT-047426] N88-24703
PREMIXED FLAMES
On the structure, propagation, extinction and stability of laminar premixed flames in dissociation equilibrium N88-24728
PRESSURE EFFECTS
Unsteady flow in a supercritical supersonic inlet N88-24605
Structure/property/reactivity relations among nitramine and other energetic materials
[AD-A190878] N88-24716
Optical pressure sealing couping (light joint)
[NASA-CASE-MFS-29348-1] N88-25303
PRESSURE REDUCTION
Composite reduced Navier-Stokes procedures for flow problems with strong pressure interactions
[AD-A191127] N88-24875
PRESSURE VESSELS
Stress corrosion cracking of A723 steel pressure vessels: Two case studies
[AD-A191741] N88-24990
PRESTRESSING
Forced motion of initially stressed shells and plates N88-25005
PRIMITIVE EARTH ATMOSPHERE
Photochemical and thermal modeling in the early atmosphere of the earth
[NASA-CR-183029] N88-25093
PRINTED CIRCUITS
The inspection of electronic metallurgical bonds
[AD-A192197] N88-24745
PRIVACY
Computer resource management technology program (PE 64740F). Task no. 9: Advanced user authentication
[PB88-183066] N88-25163
PROBABILITY DENSITY FUNCTIONS
Probabilistic finite element methods N88-25223
Direct numerical simulations of the PDF's (Probability Density Functions) of a passive scalar in a forced mixing layer
[AD-A192134] N88-25256
Cluster analysis of multiple planetary flow regimes
[NASA-CR-182931] N88-25418
PROBABILITY THEORY
Additive prophet inequalities for transforms of uniformly bounded pairwise independent random variables
[PB88-173513] N88-25250
A perspective of PC-based probabilistic risk assessment
[DE88-006715] N88-25251
Transition probabilities in OH A 2 sigma + - X 2 pi i: Bands with v prime = 0 and 1, v double prime = 0 to 4
[NASA-CR-182946] N88-25353
PROBLEM SOLVING
Human problem solving in complex dynamic environments
[AD-A190788] N88-25142
A mixed-integer linear programming problem which is efficiently solvable
[AD-A191028] N88-25168
Algorithms and software for solving finite element equations on serial and parallel architectures
[NASA-CR-183027] N88-25191
Optimal a priori covariance selection for the solution of ill-conditioned nonlinear inverse problems N88-25222
Mixed min-max optimization problem with restrictions N88-25232
Multigrid methods for elliptic Partial Differential Equations (PDEs)
[CWI-NM-R8722] N88-25242
Similarity solutions of nonlinear partial differential equations invariant to a family of affine groups
[DE88-003404] N88-25245
PRODUCT DEVELOPMENT
P-Plus: Polar Platform utilization study, executive summary
[BAE-TP-8391] N88-24653
Development of mirrors for high-precision laser gyroscopes N88-24931
Navigation using the Teldix fiber-optic gyroscope N88-24933
PRODUCTION COSTS
Production costs of hydrocarbon fuels from biomass
[DE88-006667] N88-24804
PRODUCTIVITY
Quality and productivity drive innovation and improvement at United Technologies Aerospace Operations, Inc.
[NASA-CR-182944] N88-24983
PROGRAM VERIFICATION (COMPUTERS)
Automated test device for FASR (Fixed Array Surveillance Radar) beam steering componentry
[AD-A191650] N88-24829
Advanced development of the boundary element method for elastic and inelastic thermal stress analysis N88-25002
A general approach for automating source code verification
[AD-A191461] N88-25170
PROGRAMMED INSTRUCTION
KA-PROLOG. KAP-computer: Computer model and instructions set
[ETN-88-91948] N88-25186
PROGRAMMING LANGUAGES
KA-PROLOG. KAP-computer: Computer model and instructions set
[ETN-88-91948] N88-25186
The Sizing and Optimization Language, (SOL): Computer language for design problems
[NASA-TM-100565] N88-25190
Design, implementation and evaluation of an operating system for a network of transputers
[AD-A186593] N88-25193
PROGRESS
Progress and future directions in computational fluid dynamics
[NASA-TM-100091] N88-24579
PROJECTILES
Use of a two-stage light-gas gun as an injector for electromagnetic railguns
[DE88-007200] N88-24657
PROPELLANT COMBUSTION
Catalytic ignition of hydrogen and oxygen propellants
[NASA-TM-100957] N88-24689
The burning of HAN-based (hydroxylammonium nitrate) liquid propellants
[DE88-006863] N88-24800
Electrical ignition of HAN-based liquid propellants
[AD-A191349] N88-24801
Chemical kinetics of nitramine propellant combustion
[AD-A191556] N88-24802
PROPELLANT DECOMPOSITION
Chemical kinetics of nitramine propellant combustion
[AD-A191556] N88-24802
PROPELLANT SENSITIVITY
Structure/property/reactivity relations among nitramine and other energetic materials
[AD-A190878] N88-24716
PROPELLANTS
An extinguisher to quench propellant fires
[AD-A190785] N88-24813
PROPELLER EFFICIENCY
Summary of low-speed wind tunnel results of several high-speed counterrotation propeller configurations
[NASA-TM-100945] N88-24597
Finite element solution of 3-D turbulent Navier-Stokes equations for propeller-driven slender bodies N88-24919
PROPELLERS
NASA/industry advanced turboprop technology program
[NASA-TM-100929] N88-24641
PROPULSION SYSTEM CONFIGURATIONS
Recent advances in low-thrust propulsion technology
[NASA-TM-100959] N88-25260
PROSTHETIC DEVICES
The stress analysis of ceramic, polymeric, and metallic composite systems by the finite element method N88-25004
PROTECTION
Proposed quality assurance/quality control plan
[AD-A191490] N88-24978
Vibration protection of inelastic structures by means of active and passive control N88-25001
PROTECTIVE CLOTHING
Study of benefits of passenger protective breathing equipment from analysis of past accidents
[DOT/FAA/CT-88/03] N88-24810
The effects of different combinations of inlet air conditions used for cooling as measured on a heated manikin
[AD-A191116] N88-25151
Performance estimates for operations conducted while wearing individual protective equipment: User manual
[AD-A191871] N88-25154
PROTECTIVE COATINGS
Thrust chamber thermal barrier coating techniques
[NASA-TM-100933] N88-24690
Isothermal and bithermal thermomechanical fatigue behavior of a NiCoCrAlY-coated single crystal superalloy
[NASA-TM-100907] N88-24768
An investigation of ceramic coatings for protection of SiC from high-temperature corrosion
[DE88-007873] N88-24790
PROTECTORS
Performance estimates for operations conducted while wearing individual protective equipment: User manual
[AD-A191871] N88-25154
PROTEINS
Optical monitoring of protein crystal growth
[NASA-CR-182869] N88-24738
The electrokinetic behavior of calcium oxalate monohydrate in macromolecular solutions
[NASA-TM-101144] N88-24791
A cardiostimulant protein from the Australian Red Waratah Sea anemone, Actinia tenebrosa N88-25138
Two puzzling aspects of protein crystal growth N88-25329
Hanging drop crystal growth apparatus and method
[NASA-CASE-MFS-28206-1-SB] N88-25356
Crystal growth apparatus
[NASA-CASE-MFS-28182-1] N88-25357
PROTON BEAMS
A multi-frame ion pinhole camera for intense ion beam transport and focusing experiments
[DE88-007263] N88-24926

Intense ion beam diagnostics for particle beam fusion experiments on PBFA 2
[DE88-007279] N88-25308

PROVING
Analysis procedures and subjective flight results of a simulator validation and cue fidelity experiment
[NASA-TM-88270] N88-24634
Structural margins assessment approach
[NASA-TM-100332] N88-24672
Computer resource management technology program (PE 64740F). Task no. 9: Advanced user authentication
[PB88-183066] N88-25163
Application of flight systems methodologies to the validation of knowledge-based systems
[NASA-TM-100442] N88-25207

PSYCHOLOGICAL FACTORS
A framework for a theory of mapping
[AD-A191071] N88-25144

PSYCHOLOGY
Models of incremental concept formation
[AD-A191597] N88-25147

PULSED LASERS
Determination of tropospheric H concentrations by a double-pulsed UV laser method N88-25070

PUMPING
An advanced extruder-feeder biomass liquefaction reactor system N88-25042

PURITY
The variation of torsional ductility of high-purity aluminum with temperature and strain rate
[DE88-005616] N88-24755

PURSUIT TRACKING
Eye and head response to an attention cue in a dual task paradigm
[AD-A191052] N88-25143

PYROELECTRICITY
Fast acting optical beam detection and deflection system
[AD-A192161] N88-24954

PYROLYSIS
Proceedings of the 1987 Biomass Thermochemical Conversion Contractors' Review Meeting
[DE88-006730] N88-25041
Low pressure entrained flow pyrolysis of biomass to produce liquid fuels N88-25043
Molecular-beam, mass-spectrometric studies of wood vapor and model compounds over HZSM-5 catalyst N88-25044
Upgrading pyrolysis vapors to aromatic gasoline with zeolite catalysis at atmospheric pressure N88-25045
Technical and economic evaluation of emerging biomass pyrolysis processes for gasoline production N88-25048
Bench-scale studies on fluid-bed pyrolysis of wood using different contact gases N88-25049
Evaluation of the toxicity of products from the thermal degradation of materials
[ETN-88-91995] N88-25130

PYROMETERS
Noncontact temperature pattern measuring device
[NASA-CASE-NPO-17024-1-CU] N88-24943

Q

QUADRUPOLES
Theoretical investigations of drift waves in a magnetic quadrupole N88-25312

QUALITY CONTROL
A quality philosophy for research and development
[DE88-006512] N88-24977
Proposed quality assurance/quality control plan
[AD-A191490] N88-24978
Quality and productivity drive innovation and improvement at United Technologies Aerospace Operations, Inc.
[NASA-CR-182944] N88-24983

QUANTUM ELECTRODYNAMICS
Research in the optical sciences
[AD-A192175] N88-25297

QUANTUM ELECTRONICS
Joint services electronics program
[AD-A192076] N88-24856
Joint services electronics program research in electronics
[AD-A192206] N88-24857

QUANTUM THEORY
Joint services electronics program
[AD-A190239] N88-24848

QUANTUM WELLS
Optical properties of heterostructures and superlattices
[AD-A191542] N88-25335
Optical nonlinearities in GaAs/GaAlAs multiple quantum wells fabricated by metalorganic chemical vapor deposition for use in optical signal processing
[AD-A191558] N88-25337

QUENCHING
On quench sensitivity of Cu-Cr alloys
[NASA-TT-20174] N88-24765

QUENCHING (COOLING)
Critical cooling rates on solution treatment of Cu-Cr and Cu-Be alloys
[NASA-TT-20163] N88-24760

QUEUEING THEORY
Poisson functionals of Markov processes and queueing networks
[AD-A191217] N88-25252

QUINOLINE
The thermodynamic properties of quinoline and isoquinoline
[DE88-001218] N88-24735

R

RADAR
High resolution radar techniques: Five contributions to MILINF 86
[PB88-172721] N88-24821
Radio-wave scintillations and ionospheric irregularities at high latitudes
[AD-A192140] N88-24837

RADAR BEAMS
Automated test device for FASR (Fixed Array Surveillance Radar) beam steering componentry
[AD-A191650] N88-24829

RADAR CROSS SECTIONS
The radar cross section of some simple reflectors at short wavelengths
[FOA-C-30472-3.3] N88-24839
Almond test body — for microwave anechoic chambers
[NASA-CASE-LAR-13747-1] N88-24845

RADAR DETECTION
Acta aeronautica et astronautica sinica (selected articles)
[AD-A191552] N88-24575

RADAR IMAGERY
Delay-doppler radar imaging
[AD-A191509] N88-24826
Observation of stratiform rain with 94 GHz and s-b and Doppler radar
[AD-A192013] N88-25100

RADAR MEASUREMENT
Nonparametric discriminant analysis applied to the extraction and selection of radar target signature features
[AD-A191849] N88-24833

RADAR RESOLUTION
High resolution radar techniques: Five contributions to MILINF 86
[PB88-172721] N88-24821

RADAR SIGNATURES
Nonparametric discriminant analysis applied to the extraction and selection of radar target signature features
[AD-A191849] N88-24833

RADAR TARGETS
A method for discrimination of radar targets using complex natural resonances
[AD-A191848] N88-24832
Nonparametric discriminant analysis applied to the extraction and selection of radar target signature features
[AD-A191849] N88-24833

RADAR TRACKING
A method for discrimination of radar targets using complex natural resonances
[AD-A191848] N88-24832

RADIAL VELOCITY
Radial velocities monitoring of a sample of barium and S stars using CORAVEL: Towards an evolutionary link between barium and S stars?
[SER-C-PREPUBL-FASC-19] N88-25410

RADIATION DAMAGE
Molecular characterization of structure and bonding in thin film materials
[DE88-006811] N88-25351

RADIATION DOSAGE
Preliminary estimates of radiation exposures for manned interplanetary missions from anomalously large solar flare events
[NASA-TM-100620] N88-25427

RADIATION EFFECTS
Irradiation effects on tungsten stabilized martensitic steels
[DE88-007074] N88-24748
Behavioral response of rats exposed to high-power microwave radiation
[AD-A192199] N88-25128

RADIATION HARDENING
Development of the field-induced electron injection and impact ionization (F4I) technique for radiation hardness testing of MOS (Metal-Oxide-Semiconductor) gate insulators
[AD-A192114] N88-25345

RADIATION MEASUREMENT
Results of radiation measurements in West Germany and from special measurement series in the Meteorological Observatory of Hamburg
[REPT-11] N88-25088

RADIATION MEASURING INSTRUMENTS
Ultraviolet measurements: Measurements of photolysis rates N88-25065

RADIATION TRANSPORT
High-energy laser-assisted imaging through vaporizing aerosols
[DE88-007911] N88-24957

RADIATIVE TRANSFER
Analytic and numerical modeling of heat and material transport in electrical hypervelocity guns
[AD-A192178] N88-24855

RADIO ALTIMETERS
An evaluation of three linear scale radar altimeter displays
[AD-A192173] N88-24836

RADIO CONTROL
Timing control system
[NASA-CASE-NPO-16882-1-CU] N88-24883

RADIO EQUIPMENT
Practical VLF/LF radio test system
[AD-A191768] N88-24831

RADIO FREQUENCIES
Experimental radio frequency link for Ka-band communications applications
[NASA-TM-100824] N88-24859
Arcing and rf signal generation during target irradiation by a high-energy, pulsed neutral particle beam
[DE88-007189] N88-24864
Radio Frequency (RF) strain monitor
[NASA-CASE-LAR-13705-1] N88-25011
Optical diagnostics for a high power, rf-inductively coupled plasma
[DE88-007822] N88-25322

RADIO FREQUENCY INTERFERENCE
Evaluation of the communications impact of a low power arcjet thruster
[NASA-TM-100926] N88-24882
Propagation management for no-acknowledge HF communications links N88-24843

RADIO GALAXIES
Infrared astronomy at extremely faint light levels in support of the LAIRTS program
[AD-A191497] N88-25404

RADIO STARS
Infrared astronomy at extremely faint light levels in support of the LAIRTS program
[AD-A191497] N88-25404

RADIO TRANSMISSION
WIPP (Wave Induced Particle Precipitation) experiment logistic support
[AD-A191184] N88-24824

RADIOACTIVE WASTES
Review of numerical methods for radionuclide transport in three-dimensional porous media, at high Peclet numbers
[CFDU/87/10] N88-25061

RADIOMETERS
DMSP-SSM/1 NASA algorithm validation using primarily LANDSAT and secondarily DMSP and/or AVHRR visible and thermal infrared satellite imagery
[NASA-CR-182979] N88-25024

RAILGUN ACCELERATORS
Fundamental limits to the velocity of solid armatures in railguns N88-24856

RAIN
Observation of stratiform rain with 94 GHz and s-b and Doppler radar
[AD-A192013] N88-25100

RAMAN SPECTRA
Effect of uniaxial stress on the Raman spectra of graphite fibers
[AD-A191730] N88-24783
Atmospheric propagation of laser beams
[AD-A191447] N88-24952

RAMAN SPECTROSCOPY
Molecular characterization of structure and bonding in thin film materials
[DE88-006811] N88-25351

RANDOM LOADS
Fatigue crack growth due to random loading N88-25017

RANDOM PROCESSES
Computational sciences
[AD-A190826] N88-25226

Numerical solution of a system of random Volterra integral equations. 1: Successive approximation method N88-25227
Numerical solutions to stochastic difference equations N88-25229
Numerical solution to a system of random Volterra integral equations N88-25230
Approximate solution of random differential equation N88-25233
A method for the numerical solution of random Cauchy singular integral equation N88-25234
Numerical solution of random Love's integral equation N88-25235

RANDOM VARIABLES
Additive prophet inequalities for transforms of uniformly bounded pairwise independent random variables
[PB88-173513] N88-25250
Exact tests for variance component models with unequal cell frequencies in the last stage
[AD-A191645] N88-25253

RANGE (EXTREMES)
Extreme principles of entrophy production and energy dissipation in fluid mechanics
[NASA-TM-100992] N88-24946

RANGE AND RANGE RATE TRACKING
Range and range rate system
[NASA-CASE-MSC-20867-1] N88-24958

RANGEFINDING
An optical preamplifier for detection of CO2 laser radiation
[AD-A190790] N88-24949

RAOULT LAW
Certain questions of thermodynamic theory of weak solutions N88-25368

RAPID QUENCHING (METALLURGY)
Effect of alloying, rapid solidification, and surface kinetics on the high temperature environmental resistance of niobium
[AD-A192093] N88-24743
Laboratory scale inert gas atomizer for producing rapidly solidified powders
[DE88-006734] N88-24812

RARE EARTH COMPOUNDS
Novel fiber preforms: Rare earth doping
[AD-A191549] N88-25294

RARE GASES
High-order multiphoton ionization of the noble gases
[DE88-007489] N88-25273

RATES (PER TIME)
Two puzzling aspects of protein crystal growth N88-25329

RATS
Behavioral response of rats exposed to high-power microwave radiation
[AD-A192199] N88-25128
Dexamethasone regulates glutamine synthetase expression in rat skeletal muscles
[NASA-CR-182935] N88-25129

RAYLEIGH SCATTERING
Application of Rayleigh scattering to turbulent flow with heat transfer and combustion
[AD-A191565] N88-24720
Instrumentation for turbulent reacting flows
[AD-A191671] N88-24923

RAYLEIGH WAVES
Electron-Rayleigh wave interaction in thin film carbons
[AD-A191727] N88-24781

REACTION KINETICS
Calculation of oxidation rates for iron in CO-CO2
[DE88-007313] N88-24757
The influence of the chemical nature of resins on their reticulation kinetics and the consequences for their nonelastic mechanical properties
[ETN-88-92539] N88-24788
The burning of HAN-based (hydroxylammonium nitrate) liquid propellants
[DE88-006863] N88-24800
Chemical kinetics of nitramine propellant combustion
[AD-A191556] N88-24802
Laboratory experiments on atmospheric OH reactions N88-25066
Bimolecular reactions and energy-transfer processes of highly vibrationally excited molecules related to energetic materials
[AD-A188013] N88-25270
A new approach to generating negative ion beams
[AD-A191119] N88-25276
Spectroscopy and energy transfer kinetics of the interhalogens
[AD-A192103] N88-25344

REACTION PRODUCTS
The synthesis of polyphenylene from a CIS-dihydrocatechol biologically produced monomer N88-24699
Photosynthetic water splitting
[PB88-186891] N88-24731

REACTIVITY
Surface composition-reactivity relationships in heterogeneous catalysis
[DE88-006679] N88-24714
Structure/property/reactivity relations among nitramine and other energetic materials
[AD-A190878] N88-24716

REACTOR MATERIALS
Irradiation effects on tungsten stabilized martensitic steels
[DE88-007074] N88-24748

REACTOR SAFETY
Analysis and developments of failure concepts in fracture mechanics based on research results in the field of component safety topics: J-integral concept; crack resistance curves; dynamic criterion
[V-19/88] N88-25009

REACTOR TECHNOLOGY
Systems analysis of INTOR-like designs
[DE88-004422] N88-25316

REAGENTS
Proposed quality assurance/quality control plan
[AD-A191490] N88-24978

REAL TIME OPERATION
Evaluating evaporation with satellite thermal data
[AD-A192042] N88-25019
Beyond Ada: Generating Ada code from equational specifications
[AD-A191866] N88-25176
Representation and decision mechanisms in artificial intelligence
[AD-A191083] N88-25197
Real-time optical multiple object recognition and tracking system and method
[NASA-CASE-NPO-17139-1-CU] N88-25301
Real-time image difference detection using a polarization rotation spacial light modulator
[NASA-CASE-NPO-17144-1-CU] N88-25305

REATTACHED FLOW
Method and apparatus for detecting laminar flow separation and reattachment
[NASA-CASE-LAR-13952-1-SB] N88-24910

RECOGNITION
Models of incremental concept formation
[AD-A191597] N88-25147

RECURSIVE FUNCTIONS
Recursive maximum likelihood identification of a nonlinear output-affine model
[RR-322] N88-25257

REDUCED GRAVITY
Thermodynamic modeling of the no-vent fill methodology for transferring cryogens in low gravity
[NASA-TM-100932] N88-24686
Operational facilities of EURECA A1 mission
[ETN-88-91939] N88-24810
Acoustic convective system
[NASA-CASE-NPO-17278-1-CU] N88-24818

REENTRY VEHICLES
Experimental investigation of hypersonic aerodynamics
[NASA-CR-182973] N88-24591

REFLECTANCE
An experimental study of the coherent under-ice reflectivity of sound in the Greenland Sea Marginal Ice Zone N88-25125
Remote sensing of acoustic properties of shallow water sediments: A review
[AD-A192107] N88-25267
A disposable liquid microcell for near-infrared reflectance analysis
[AD-A192190] N88-25298

REFLECTION
Millimeter and submillimeter waves and frequency selective surfaces
[AD-A191511] N88-24827
Identification of cascaded microwave circuits with moderate reflections using reflections and transmission measurements
[PB88-171921] N88-24849

REFLECTORS
The radar cross section of some simple reflectors at short wavelengths
[FOA-C-30472-3.3] N88-24839
Joint services electronics program
[AD-A191749] N88-24853

REFRACTIVITY
Silicon-sapphire waveguides
[AD-A191754] N88-24854
Construction of approximations to acoustic Green's functions for nonhomogeneous oceans using transmutation
[PB88-185384] N88-25126
Determination of doping profiles in silicon from resistivity measurements via the four-point probe in combination with layer strippings via anodic oxidation N88-25347

REFRACTORY METAL ALLOYS
Effect of hydrogen, deuterium and oxygen on the anelastic properties of refractory alloys
[DE88-007349] N88-24736

REFUELING
Thermodynamic modeling of the no-vent fill methodology for transferring cryogens in low gravity
[NASA-TM-100932] N88-24686

REGIONAL PLANNING
Topographic data processing for environmental planning N88-25032

REGRESSION ANALYSIS
Automated analysis of crack growth rate for obtaining da/dN versus delta K relation
[FFA-TN-1987-70] N88-24996
Asymptotic theory for weighted least squares estimators in Aalen's additive risk model
[AD-A191085] N88-25210
Symmetrized nearest neighbor regression estimates
[AD-A191998] N88-25254

REGULATORY MECHANISMS (BIOLOGY)
Dexamethasone regulates glutamine synthetase expression in rat skeletal muscles
[NASA-CR-182935] N88-25129

REINFORCED PLATES
Interaction of ultrasonic waves with composite plates
[AD-A191879] N88-24702

REINFORCEMENT (STRUCTURES)
Stiffened titanium panels
[NASA-CASE-LAR-13814-1] N88-24816

RELATIVISTIC ELECTRON BEAMS
Deep dielectric charging effects due to high energy electrons in earth's outer magnetosphere
[AD-A192154] N88-25083

RELATIVISTIC PARTICLES
The multistring model VENUS for ultrarelativistic heavy ion collisions
[DE88-007666] N88-25284
Experiments with high energy nuclear beams at Brookhaven: From AGS to RHIC (Relativistic Heavy Ion Collider)
[DE88-007042] N88-25287

RELATIVISTIC VELOCITY
The multistring model VENUS for ultrarelativistic heavy ion collisions
[DE88-007666] N88-25284

RELATIVITY
From general relativity to the theory of superstrings N88-25369

RELIABILITY
Descriptions of HF and VHF Loran-C buoys and evaluations as potential datum marker buoys
[AD-A192069] N88-24818
An extended life and performance test of a low-power arcjet
[NASA-TM-100942] N88-24687
Sensitivity analysis for the system reliability function
[AD-A191648] N88-24979

RELIABILITY ANALYSIS
Reliability of stochastically forced systems (extended version)
[CWI-AM-R8801] N88-24985

RELIEF MAPS
Topographic data processing for environmental planning N88-25032

REMOTE HANDLING
Design study. Manipulator systems for model handling in European transonic wind tunnels
[ETN-88-91944] N88-24851

REMOTE MANIPULATOR SYSTEM
Design study. Manipulator systems for model handling in European transonic wind tunnels
[ETN-88-91944] N88-24851
Dynamics of a flexible orbiting platform with MRMS
[ISSN-0285-6808] N88-24673

REMOTE SENSING
Evaluating evaporation with satellite thermal data
[AD-A192042] N88-25019
The application of satellites in connection with the environment
[ETN-88-92474] N88-25020
Information analysis of integral equations in remote sensing of atmospheric aerosols N88-25022
DMSP-SSM/1 NASA algorithm validation using primarily LANDSAT and secondarily DMSP and/or AVHRR visible and thermal infrared satellite imagery
[NASA-CR-182979] N88-25024
Aircraft/lidar turbulence comparison N88-25111
Remote sensing of acoustic properties of shallow water sediments: A review
[AD-A192107] N88-25267
Activities report of the Division of Optical Technology
[FOA-C-30477-3] N88-25299

REMOTE SENSORS
Remote sensing of acoustic properties of shallow water sediments: A review
[AD-A192107] N88-25267
RESEARCH
Soviet combustion research
[PB88-182324] N88-24730
RESEARCH AIRCRAFT
Taiwan area mesoscale experiment: P-3 aircraft operations summary
[PB88-169073] N88-25098
RESEARCH AND DEVELOPMENT
The application of hydrocarbon bioconversion technology to aerospace materials production N88-24698
A quality philosophy for research and development
[DE88-006512] N88-24977
Department of Defense statement on defense agency research and development to the Subcommittee on Defense of the Committee on Appropriations, United States House of Representatives, 100th Congress, second session
[AD-A191840] N88-25377
The FY 1989 Department of Defense statement on the Science and Technology Program to 100th Congress, second session
[AD-A191843] N88-25380
Centre for International Co-Operation and Appropriate Technology (CICAT)
[PB88-165501] N88-25389
RESEARCH FACILITIES
Analysis procedures and subjective flight results of a simulator validation and cue fidelity experiment
[NASA-TM-88270] N88-24634
SHaRE: Collaborative materials science research
[DE88-007175] N88-24646
Preparation for microgravity: The role of the microgravity materials science laboratory
[NASA-TM-100906] N88-24811
RESEARCH MANAGEMENT
An overview of advanced battery development at Sandia National Laboratories
[DE88-006823] N88-24867
Space station architectural elements and issues definition study
[NASA-CR-3941] N88-25371
The Department of Defense report on the merit review process for competitive selection of university research projects and an analysis of the potential for expanding the geographic distribution of research for the Committees on Appropriations, United States Congress
[AD-A191842] N88-25379
NASA history data book. Volume 1: NASA resources 1958-1968
[NASA-SP-4012-VOL-1] N88-25428
NASA historical data book. Volume 2: Programs and projects 1958-1968
[NASA-SP-4012-VOL-2] N88-25429
NASA historical data book. Volume 3: Programs and projects 1969-1978
[NASA-SP-4012-VOL-3] N88-25430
RESIDUAL STRESS
Stress corrosion cracking of A723 steel pressure vessels: Two case studies
[AD-A191741] N88-24990
The stress analysis of ceramic, polymeric, and metallic composite systems by the finite element method N88-25004
RESIN BONDING
Adhesion between polystyrene and polymethylmethacrylate
[AD-A192050] N88-24785
RESIN MATRIX COMPOSITES
Proceedings of the American Society for Composites
[AD-A189861] N88-24693
Current and future molecular structures of aerospace organic matrix resins N88-24695
Industrial perspective on current and future needs in aerospace matrix resin chemistry N88-24696
Applications of biotechnology to synthetic chemistry for aerospace matrix resins development N88-24697
The 700 F properties of autoclave cured PMR-2 composites
[NASA-TM-100923] N88-24712
RESINS
Influence of carbon fiber surface treatment
[ETN-88-92536] N88-24787
RESISTOJET ENGINES
Development of a liquid-fed water resistojet
[NASA-TM-100927] N88-24968
RESONANCE
Harmonic considerations for electrical distribution feeders
[DE88-007849] N88-24860
Contributions of autoionizing resonances to the electron collisional excitation rates for Be-like ions
[AD-A190924] N88-25275
RESONANT FREQUENCIES
Open channel flow near the resonance speed N88-24918
RESONANT VIBRATION
Theoretical and experimental damping values of piping systems at high ductilities
[DE88-006717] N88-24986
RESOURCES MANAGEMENT
Department of Defense Statement on the Technology Base to the Subcommittee on Defense Industry and Technology of the Committee on Armed Services, United States Senate, 100th Congress, second session
[AD-A191839] N88-25376
RETROFITTING
Servojet retrofit
[AD-A191075] N88-24984
REVERSE FIELD PINCH
QN3D: A 3-dimensional quasi-neutral hybrid particle-in-cell code with applications to the tilt mode instability in field reversed configurations N88-25325
REVERSING
A study on the precipitation and reversion behaviors of Cu-0.3 percent Cr alloy by the step annealing method
[NASA-TT-20169] N88-24784
RHEOLOGY
Characterization of aluminum/RP-1 gel propellant properties
[NASA-TM-100951] N88-24808
RIGID STRUCTURES
Automatic feedback control of a rigid body for finite displacements N88-24674
RING STRUCTURES
Vibrations of rotating thick or thin rings N88-25003
RINGS
On the bending response of Kevlar 49/epoxy beams and rings
[DE88-006824] N88-25012
RISK
Asymptotic theory for weighted least squares estimators in Aalen's additive risk model
[AD-A191085] N88-25210
A perspective of PC-based probabilistic risk assessment
[DE88-006715] N88-25251
RIVER BASINS
Oxidation and reduction rates for organic carbon in the Amazon mainstream tributary and floodplain, inferred from distributions of dissolved gases
[NASA-CR-182943] N88-25062
ROADS
Digitizing the traffic network of JOG 250 by scanning — JOG 250 map N88-25029
ROBOTICS
A universal computer control system for motors
[NASA-CASE-NPO-17134-1-CU] N88-24864
The coordination of multiple robotic manipulators
[AD-A190869] N88-24963
The efficacy of using human myoelectric signals to control the limbs of robots in space
[NASA-CR-182901] N88-25155
Introduction to compliance in programming of robots
[ETN-88-92189] N88-25201
Modeling of geometric reasoning for robot programming
[ETN-88-92290] N88-25202
Analysis of a closed-kinematic chain robot manipulator
[NASA-CR-183031] N88-25206
Lunar base surface mission operations. Lunar Base Systems Study (LBSS) task 4.1
[NASA-CR-172050] N88-25415
ROBOTS
Kinematics, dynamics and control of a closed chain mechanism manipulator N88-24967
Real-time implementation of a kinematic optimization scheme for seven-degree-of-freedom redundant robots with spherical wrists
[DE88-006785] N88-24974
Robot navigation using simple sensor fusion
[DE88-006184] N88-25203
ROBUSTNESS (MATHEMATICS)
Robust adaptive regulation without persistent excitation
[NASA-TM-100571] N88-25204
ROCK INTRUSIONS
Drilling investigation of a young magmatic intrusion beneath the Inyo Domes, Long Valley, California: Structural and textural studies
[DE88-006613] N88-25078
ROCKET ENGINE DESIGN
Dual-fuel, dual-mode rocket engine
[NASA-CASE-LAR-13773-1] N88-24685
ROCKET ENGINES
Thrust chamber thermal barrier coating techniques
[NASA-TM-100933] N88-24690
ROCKET FLIGHT
Wind tunnel investigation of wing and control panel loads at transonic and supersonic speeds on some schematic cruciform missile configurations
[FFA-TN-1986-43] N88-24585
ROCKET NOZZLES
Nozzle fabrication technique
[NASA-CASE-MSC-21299-1] N88-24684
ROLLING CONTACT LOADS
Calculation of rolling contact of two viscoelastic cylinders with application to the steady state normal contact problem
[ILR-MITT-188] N88-25008
ROOT-MEAN-SQUARE ERRORS
Calculation of root-mean-square loads
[BLL-M-37776-(5828.4)] N88-25015
ROOTS OF EQUATIONS
A primal-dual algorithm for the computation of the minimum of a convex function on the intersection of convex functions, and its application in data analysis
[RR-638-M] N88-25217
ROTARY WING AIRCRAFT
Some rotorcraft applications of computational fluid dynamics
[NASA-TM-100066] N88-24801
Rotorcraft TCAS (traffic alert and collision avoidance system) evaluation: Group 3 results
[AD-A191719] N88-24814
ROTARY WINGS
Structurally tailorable non-linear snap-through spring system
[NASA-CASE-LAR-13729-1] N88-24970
Limits of design feasibility of multiwing wind turbines with individual articulated wing structure
[ILR-MITT-180] N88-25052
ROTATING BODIES
The calculation of transonic flow over the shuttle orbiter using slender body theory N88-24606
Effects of Coriolis acceleration on the vibrations of spinning structures N88-24966
ROTATING CYLINDERS
Compressible flow in a pie-shaped cylinder rotating about the vertex N88-24604
ROTATING DISKS
Remote temperature-measurement instrumentation for a heated rotating turbine disk
[DE88-006456] N88-24925
ROTATING FLUIDS
Simulations of a missile with liquid payload under launch conditions
[AD-A191479] N88-24625
ROTATION
Atmospheric autorotating imaging device
[NASA-CASE-NPO-17300-1-CU] N88-24944
Para-ortho abundance ratio of molecular hydrogen in NGC2023
[ISAS-RN-352] N88-25286
ROTOR BLADES (TURBOMACHINERY)
Experimental vibration damping characteristics of the third-stage rotor of a three-stage transonic axial-flow compressor
[NASA-TM-100948] N88-24642
ROTORS
Inflow measurements made with a laser velocimeter on a helicopter model in forward flight. Volume 1: Rectangular planform blades at an advance ration of 0.15
[NASA-TM-100541] N88-24607
RP-1 ROCKET PROPELLANTS
Characterization of aluminum/RP-1 gel propellant properties
[NASA-TM-100951] N88-24808
RUBIDIUM
Tactical Rubidium Frequency Standard (TRFS), volume 2
[AD-A191190] N88-24850
RUNWAY CONDITIONS
Airplane runway performance monitoring system
[NASA-CASE-LAR-13854-1-CU] N88-24621
RUNWAYS
Microwave landing system mathematical modeling study for Midway Airport Runway 22L, Chicago, Illinois
[AD-A191721] N88-24616
Airplane runway performance monitoring system
[NASA-CASE-LAR-13854-1-CU] N88-24621
RUPTURING
Internal fluid dynamics within a nonspinning partially liquid-filled shell due to burster rupture
[AD-A191055] N88-24874

S

S STARS
Radial velocities monitoring of a sample of barium and S stars using CORAVEL: Towards an evolutionary link between barium and S stars?
[SER-C-PREPUBL-FASC-19] N88-25410

S-N DIAGRAMS
Cyclic fatigue damage characteristics observed for simple loadings extended to multiaxial life prediction
[NASA-CR-182126] N88-25016

SAFETY
Designing to safe power limits in hybrid circuits
[DE88-005533] N88-24865
Quality and productivity drive innovation and improvement at United Technologies Aerospace Operations, Inc.
[NASA-CR-182944] N88-24963

SAFETY DEVICES
Timing control system
[NASA-CASE-NPO-16882-1-CU] N88-24883

SALINITY
Expendable conductivity, temperature and depth system (XCTD) development program
[AD-A192182] N88-25121

SAMPLING
A disposable liquid microcell for near-infrared reflectance analysis
[AD-A192190] N88-25296

SARSAT
Search and rescue satellite system (SERES), phase A0
[ETN-88-92335] N88-24669

SATELLITE IMAGERY
Ice conditions along the Ohio River as observed on LANDSAT images, 1972-1985
[AD-A191172] N88-25018
DMSP-SSM/1 NASA algorithm validation using primarily LANDSAT and secondarily DMSP and/or AVHRR visible and thermal infrared satellite imagery
[NASA-CR-182979] N88-25024
Monitoring biological impacts of space shuttle launches from Vandenberg Air Force Base: Establishment of baseline conditions
[NASA-TM-100982] N88-25133
Application of dynamic programming to image registration
[ENST-87E022] N88-25180
The Io sulfur torus in 1981
[NASA-TM-101139] N88-25419

SATELLITE OBSERVATION
The application of satellites in connection with the environment
[ETN-88-92474] N88-25020

SCALARS
Direct numerical simulations of the PDF's (Probability Density Functions) of a passive scalar in a forced mixing layer
[AD-A192134] N88-25256

SCALE MODELS
Limits of design feasibility of multiwing wind turbines with individual articulated wing structure
[ILR-MITT-180] N88-25052

SCANNERS
Atmospheric autorotating imaging device
[NASA-CASE-NPO-17390-1-CU] N88-24944
Use of modern scanner techniques in cartography N88-25040

SCANNING
Digitizing the traffic network of JOG 250 by scanning --- JOG 250 map N88-25029

SCATTER PROPAGATION
Multiple scattering of waves in discrete random media
[AD-A191068] N88-24823

SCATTERING
An experimental study of the coherent under-ice reflectivity of sound in the Greenland Sea Marginal Ice Zone N88-25125

SCHEDULING
Performance effectiveness and the work/rest cycle
[AD-A191448] N88-25145
A mixed-integer linear programming problem which is efficiently solvable
[AD-A191026] N88-25168

SCIENTIFIC SATELLITES
Evaluating evaporation with satellite thermal data
[AD-A192042] N88-25019

SCINTILLATION
Radio-wave scintillations and ionospheric irregularities at high latitudes
[AD-A192140] N88-24837

SCINTILLATION COUNTERS
Study of light transmission methods from scintillators to optical fiber with wave length shifter
[DE88-701587] N88-25292

SCOTLAND
SeaSoar profiles in the Iceland-Scotland area, May 1987
[IOS-253] N88-25124

SCREWS
An advanced extruder-feeder biomass liquefaction reactor system N88-25042

SEA ICE
DMSP-SSM/1 NASA algorithm validation using primarily LANDSAT and secondarily DMSP and/or AVHRR visible and thermal infrared satellite imagery
[NASA-CR-182979] N88-25024
Higher frequency ambient noise in the arctic ocean
[AD-A192203] N88-25122

SEA SURFACE TEMPERATURE
Determination of mesoscale variability of sea surface temperature and attenuation in the North Atlantic from satellite measurement
[REPT-162] N88-25127

SEALING
Composite repair of cracked aluminum alloy aircraft structure
[AD-A190514] N88-24573
Sample decomposition in sealed teflon vessels
[NASA-TT-20189] N88-24798
Optical pressure sealing couping (light joint)
[NASA-CASE-MFS-29348-1] N88-25303

SEAMOUNTS
Identification and acoustic characterization of seamounts
[AD-A192204] N88-25123

SEARCH RADAR
Automated test device for FASR (Fixed Array Surveillance Radar) beam steering componentry
[AD-A191650] N88-24829

SEDIMENTS
Geological evolution and analysis of confirmed or suspected gas hydrate localities. Volume 2: Basin analysis, formation and stability of gas hydrates in the Black Sea
[DE88-001052] N88-25023
Evaluation of the biot coefficients
[AD-A191643] N88-25265
Remote sensing of acoustic properties of shallow water sediments: A review
[AD-A192107] N88-25267

SEISMIC WAVES
Remote sensing of acoustic properties of shallow water sediments: A review
[AD-A192107] N88-25267

SELECTIVE SURFACES
Millimeter and submillimeter waves and frequency selective surfaces
[AD-A191511] N88-24827

SELECTORS
Selection and effects of channels in distributed communication and decision making tasks: A theoretical review and a proposed research paradigm
[AD-A191807] N88-25375

SELF ALIGNMENT
Design, manufacture and spin test of high contact ratio helicopter transmission utilizing Self-Aligning Bearingless Planetary (SABP)
[NASA-CR-4155] N88-24975

SEMICONDUCTOR DEVICES
Simple high speed camera with CCD-sensor
[MPIS-8/1987] N88-24940
Advanced development of double-injection, deep-impurity semiconductor switches
[NASA-CR-182118] N88-25346

SEMICONDUCTOR LASERS
Distributed feedback lasers
[NASA-CR-4154] N88-24948

SEMICONDUCTORS (MATERIALS)
Time resolved spectroscopy facility for the study of nonlinear optical properties of semiconducting polymers
[AD-A191221] N88-24768
Stress measurements in graphite fibers by laser raman spectroscopy
[AD-A191710] N88-24779
Joint services electronics program
[AD-A190239] N88-24848
Mathematical models for VLSI device simulation
[AD-A191125] N88-25212
Electronic structure, elementary excitations, optical and transport properties of semiconductor superlattices
[AD-A190795] N88-25333
An investigation of 2-6 superlattice deposition by laser photochemical techniques
[AD-A191547] N88-25336
Recent data on Si:As impurity band conduction multiplexed arrays
[AD-A191752] N88-25340

SENSITIVITY
On quench sensitivity of Cu-Cr alloys
[NASA-TT-20174] N88-24765
A multi-frame ion pinhole camera for intense ion beam transport and focusing experiments
[DE88-007283] N88-24926
Reducing sensitivity to errors in free electron laser amplifiers
[DE88-007017] N88-24960
Sensitivity analysis for the system reliability function
[AD-A191648] N88-24979

SENSORS
User's guide to the Fault Inferring Nonlinear Detection System (FINDS) computer program
[NASA-CR-178410] N88-24619

SEPARATED FLOW
Unsteady flow in a supercritical supersonic inlet N88-24605
Instability of laminar separation bubbles: Causes and effects
[AD-A191168] N88-24876
Computation of the turbulent boundary layer downstream of vortex generators
[AD-A191544] N88-24881
Improving the performance of a finite element method using vector analysis on CRAY 1
[ETN-88-92153] N88-24907
Method and apparatus for detecting laminar flow separation and reattachment
[NASA-CASE-LAR-13952-1-SB] N88-24910
Turbulent heat transfer and fluid flow measurements downstream of abrupt expansions and in a cavity of a circular tube at a uniform wall temperature N88-24920
Method of forming a multiple layer dielectric and a hot film sensor therewith
[NASA-CASE-LAR-13678-1] N88-25355

SEPARATORS
Flotation processes
[PB88-180302] N88-25075

SERIES EXPANSION
On a biorthogonal system associated with uniform asymptotic expansions
[CWI-AM-R8709] N88-25240

SERVICE LIFE
Performance and long duration test of a 30 kw thermal arcjet engine
[AD-A190962] N88-24677
An extended life and performance test of a low-power arcjet
[NASA-TM-100942] N88-24687
Harmfulness of defects: Behaviour in service of a delamination in a composite containing many differently oriented layers
[PB88-124714] N88-24705
Nickel hydrogen low earth orbit life testing
[AD-A191946] N88-24855

SET THEORY
Algorithms and data structures for an expanded family of matroid intersection problems
[AD-A191482] N88-25213
A primal-dual algorithm for the computation of the minimum of a convex function on the intersection of convex functions, and its application in data analysis
[RR-638-M] N88-25217

SHADOWS
Shape from shading, occlusion and texture
[AD-A184840] N88-25269
Curvature of blended rolled edge reflectors at the shadow boundary contour
[NASA-CR-182974] N88-25300

SHALLOW SHELL EQUATIONS
Forced motion of initially stressed shells and plates N88-25005

SHALLOW WATER
Remote sensing of acoustic properties of shallow water sediments: A review
[AD-A192107] N88-25267

SHAPES
An analytic model for aerodynamic shapes
[AD-A191573] N88-24583
Shape stability in composites N88-24706
Stiffened titanium panels
[NASA-CASE-LAR-13814-1] N88-24816
Shape from shading, occlusion and texture
[AD-A184840] N88-25269

SHEAR FLOW
Dynamics and control of turbulent shear flows
[AD-A191527] N88-24879
LLNL granular solids flow project
[DE88-007492] N88-24906
A single streamwise vortical structure and its instability in shear flows N88-24921

SHEAR LAYERS
Dynamics and control of turbulent shear flows
[AD-A191527] N88-24879
Characteristics of merging shear layers and turbulent wakes of a multi-element airfoil
[NASA-TM-100053] N88-24900

SHEAR PROPERTIES
The influence of cathodic protection on erosion-corrosion of metals and model alloys
[AD-A191613] N88-24742
SHEAR STRAIN
Dynamic shear band development in plane strain
[AD-A190915] N88-24988
SHEAR STRESS
Computation and characteristics of pulsatile multi-bifurcation flow N88-24729
Method and apparatus for detecting laminar flow separation and reattachment
[NASA-CASE-LAR-13952-1-SB] N88-24910
Resolved shear stress intensity coefficient and fatigue crack growth in large crystals
[NASA-CR-182137] N88-24997
SHIELDING
Laser countermeasure impacts and penalties
[DE88-006871] N88-24947
Trailer shield assembly for a welding torch
[NASA-CASE-MFS-29260-1] N88-24972
Systems analysis of INTOR-like designs
[DE88-004422] N88-25316
Self shielding of surfaces irradiated by intense energy fluxes
[DE88-007094] N88-25318
SHOCK TUBES
Plate response analysis using shock tube
[AD-A190828] N88-24987
SHOCK WAVE INTERACTION
Theoretical investigation of 3-D shock wave-turbulent boundary layer interactions, part 6
[AD-A191546] N88-24882
SHOCK WAVES
Passive shock wave-boundary layer control for the Bell FX69-H-098 airfoil N88-24588
SHORT CRACKS
Fracture mechanics analysis for short cracks
[AD-A192002] N88-24992
SHORT TAKEOFF AIRCRAFT
Method for prediction and determination of takeoff performance for vectored thrust vehicles
[AD-A191809] N88-24626
SHORT WAVE RADIATION
A MININEC model of the miniloop antenna
[AD-A191759] N88-24830
SHUTTLE IMAGING RADAR
The role of space borne imaging radars in environmental monitoring: Some shuttle imaging radar results in Asia
[NASA-TM-101178] N88-24844
SIGNAL ANALYSIS
Evaluation of the communications impact of a low power arcjet thruster
[NASA-TM-100926] N88-24682
SIGNAL DETECTION
Information and stochastic systems
[AD-A192167] N88-24838
Identification and acoustic characterization of seamounts
[AD-A192204] N88-25123
SIGNAL DETECTORS
Method and apparatus for detecting laminar flow separation and reattachment
[NASA-CASE-LAR-13952-1-SB] N88-24910
Design and testing of a luminance and chrominance stabilization system for a computer-controlled color display
[AD-A191922] N88-25159
SIGNAL PROCESSING
Time-frequency representations for speech signals
[AD-A188661] N88-24819
Signal processing with degenerate four-wave mixing
[AD-A191496] N88-24825
A method for discrimination of radar targets using complex natural resonances
[AD-A191848] N88-24832
Propagation management for no-acknowledge HF communications links N88-24843
Optics: Perspectives for Measurement Techniques and Signal Processing for Flight Guidance — conference
[DFVLR-MITT-87-21] N88-24928
Investigations in electro-optical multistability for signal processing N88-24938
Low frequency electrostatic turbulence in the polar cap E-region
[DRI-3-88] N88-25077
An experimental study of the coherent under-ice reflectivity of sound in the Greenland Sea Marginal Ice Zone N88-25125
Optical computing based on neuronal models
[AD-A191481] N88-25293
Optical nonlinearities in GaAs/GaAlAs multiple quantum wells fabricated by metalorganic chemical vapor depoeition for use in optical signal processing
[AD-A191556] N88-25337
SIGNAL TO NOISE RATIOS
Analysis of binarized Hartley phase-only filter performance with respect to stochastic noise
[DE88-007604] N88-24945
SILICA GLASS
Novel fiber preforms: Rare earth doping
[AD-A191549] N88-25294
SILICATES
The evolution of cometary activity N88-25416
SILICON
Metastability in SiGe/Si strained-layer structures
[DE88-007603] N88-25361
On the use of convergent beam electron diffraction for identification of antiphase boundaries in GaAs grown on Si
[DE88-008220] N88-25362
SILICON ALLOYS
Improved properties of SiGe/GaP alloys
[NASA-CASE-NPO-17259-1-CU] N88-25358
SILICON CARBIDES
An investigation of ceramic coatings for protection of SiC from high-temperature corrosion
[DE88-007873] N88-24790
SILICON COMPOUNDS
Recent data on SiAs impurity band conduction multiplexed arrays
[AD-A191752] N88-25340
SILICON NITRIDES
Environmental effects on slow crack growth in silicon nitride
[DE88-007206] N88-24795
SIMPLEX METHOD
Making progress during a stall in the simplex algorithm
[DE88-007120] N88-25182
SIMULATION
Simulating futures in extended common LISP
[NASA-TM-101000] N88-25192
NAS: The first year
[NASA-TM-101006] N88-25196
A constraint algorithm for maintaining rigid bonds in molecular dynamics simulations of large molecules
[AD-A191663] N88-25277
SINGLE CRYSTALS
Isothermal and bithermal thermomechanical fatigue behavior of a NiCoCrAlY-coated single crystal superalloy
[NASA-TM-100907] N88-24766
Resolved shear stress intensity coefficient and fatigue crack growth in large crystals
[NASA-CR-182137] N88-24997
Electronic controller for reciprocating rotary crystallizer
[NASA-TM-101140] N88-25354
SINTERED ALUMINUM POWDER
Characterization of 7090 and 7091 profiles made with Cegedur powder — powder metallurgy, aircraft construction materials
[REPT-48-441/F] N88-24752
SINTERING
Martensitic transformation and microstructures in sintered NiAl alloys
[NASA-TT-20178] N88-24761
SITE SELECTION
Review of numerical methods for radionuclide transport in three-dimensional porous media, at high Peclet numbers
[CFDU/87/10] N88-25061
SIZE DISTRIBUTION
Information analysis of integral equations in remote sensing of atmospheric aerosols N88-25022
SKIN FRICTION
Manipulation of the structure of a turbulent boundary layer N88-24901
SKY SURVEYS (ASTRONOMY)
Ultraviolet spectra of subluminous objects found in the Kiso Schmidt survey and systematic reanalysis of the archived ultraviolet spectra of white dwarfs observed with the IUE satellite under the Astrophysics Data Program (ADP)
[NASA-CR-182976] N88-25406
SLENDER BODIES
The calculation of transonic flow over the shuttle orbiter using slender body theory N88-24606
Finite element solution of 3-D turbulent Navier-Stokes equations for propeller-driven slender bodies N88-24919
SLIDING
The flying characteristics of the membrane slider bearing N88-24965
SLOTS
Solid rocket motor aft field joint flow field analysis
[NASA-CR-179288] N88-24675
Electromagnetic penetration into a conducting circular cylinder through a narrow slot, TE case
[AD-A191602] N88-24828
Characteristics of merging shear layers and turbulent wakes of a multi-element airfoil
[NASA-TM-100053] N88-24900
SLURRIES
An advanced extruder-feeder biomass liquefaction reactor system N88-25042
SMOG
Ozone in the atmosphere N88-25084
SMOOTHING
A comparative study of Chebyshev acceleration and residue smoothing in the solution of nonlinear elliptic difference equations
[CWI-NM-R8723] N88-25259
SNOW COVER
Ice conditions along the Ohio River as observed on LANDSAT images, 1972-1985
[AD-A191172] N88-25018
Higher frequency ambient noise in the arctic ocean
[AD-A192203] N88-25122
SOFTWARE ENGINEERING
An OOD (Object-Oriented Design) paradigm for flight simulators
[AD-A191097] N88-24847
The Environment for Application Software Integration and Execution (EASIE), version 1.0. Volume 3: Program execution guide
[NASA-TM-100575] N88-25184
Algorithms and software for solving finite element equations on serial and parallel architectures
[NASA-CR-183027] N88-25191
SOFTWARE TOOLS
New York TRACON demonstration of program recoding requirements analysis document
[DOT/FAA/CT-87/34] N88-24822
The Environment for Application Software Integration and Execution (EASIE), version 1.0. Volume 3: Program execution guide
[NASA-TM-100575] N88-25184
The -mdoc macro package: A software tool to support computer documentation standards
[DE88-000500] N88-25188
NFEARS: A nonlinear adaptive finite element solver, part 1
[AD-A191823] N88-25215
SOILS
Monitoring biological impacts of space shuttle launches from Vandenberg Air Force Base: Establishment of baseline conditions
[NASA-TM-100982] N88-25133
SOL-GEL PROCESSES
Sol/gel processing techniques for glass matrix composites
[AD-A191748] N88-24701
SOLAR ACTIVITY
The SAMEX vector magnetograph: A design study for a space-based solar vector magnetograph
[NASA-TM-4048] N88-25424
SOLAR ARRAYS
Contamination of optical surfaces — Space Station N88-25400
SOLAR ATMOSPHERE
The SAMEX vector magnetograph: A design study for a space-based solar vector magnetograph
[NASA-TM-4048] N88-25424
SOLAR CELLS
Progress in InP solar cell research
[NASA-TM-100914] N88-24870
SOLAR COLLECTORS
Progress in InP solar cell research
[NASA-TM-100914] N88-24870
Evaluation of the chromium oxide arc spraying treatment on solar energy collectors
[ETN-88-92564] N88-25053
SOLAR FLARES
The 2-D magnetohydrostatic configurations leading to flares or quiescent filament eruptions
[NASA-TM-101147] N88-25423
Preliminary estimates of radiation exposures for manned interplanetary missions from anomalously large solar flare events
[NASA-TM-100820] N88-25427
SOLAR MAGNETIC FIELD
The SAMEX vector magnetograph: A design study for a space-based solar vector magnetograph
[NASA-TM-4048] N88-25424
SOLAR PHYSICS
An image processing system for research in solar physics
[AD-A191673] N88-25421
SOLAR RADIATION
Photovoltaic Advanced Research and Development Project, solar radiation research
[DE88-001143] N88-25056
Results of radiation measurements in West Germany and from special measurement series in the Meteorological Observatory of Hamburg
[REPT-11] N88-25088
Observations of cosmic rays in the outer heliosphere
[NASA-CR-182942] N88-25425

Preliminary estimates of radiation exposures for manned interplanetary missions from anomalously large solar flare events
[NASA-TM-100620] N88-25427

SOLAR REFLECTORS
Contamination of optical surfaces --- Space Station N88-25400

SOLAR TERRESTRIAL INTERACTIONS
Interpretation of the northward B sub z (NBZ) Birkeland current system and polar cap convection patterns in terms of the impulsive penetration model
[AERONOMICA-ACTA-A-321-1987] N88-25422

SOLAR WIND
Interpretation of the northward B sub z (NBZ) Birkeland current system and polar cap convection patterns in terms of the impulsive penetration model
[AERONOMICA-ACTA-A-321-1987] N88-25422

SOLDERED JOINTS
The inspection of metallurgical bounds in electronic systems
[AD-A192064] N88-25343

SOLDERING
The inspection of electronic metallurgical bonds
[AD-A192197] N88-24745

SOLID MECHANICS
Probabilistic finite element methods N88-25223

SOLID PROPELLANT COMBUSTION
Combustion behavior of the vitiator. Experimental results of a second test series
[VTH-LR-509] N88-24734

SOLID PROPELLANT ROCKET ENGINES
Solid rocket motor aft field joint flow field analysis
[NASA-CR-179288] N88-24675
SRM propellant and polymer materials structural test program
[NASA-TP-2821] N88-25013

SOLID STATE DEVICES
Characterization of a 30-GHz IMPATT solid state amplifier
[NASA-TM-100878] N88-24847
Joint services electronics program
[AD-A192076] N88-24856

SOLID STATE LASERS
Fracture of solid state lasers
[DE88-007023] N88-24961

SOLIDIFICATION
Effect of alloying, rapid solidification, and surface kinetics on the high temperature environmental resistance of niobium
[AD-A192093] N88-24743
Laboratory scale inert gas atomizer for producing rapidly solidified powders
[DE88-006734] N88-24812

SOLIDS
Self-consistent model for the brittle response of solids N88-24999

SOLIDS FLOW
LLNL granular solids flow project
[DE88-007492] N88-24906

SOLITARY WAVES
Nonlinear surface polaritons
[AD-A191046] N88-24822

SOLUTIONS
Certain questions of thermodynamic theory of weak solutions N88-25368

SONAR
Robot navigation using simple sensor fusion
[DE88-006184] N88-25203

SOS (SEMICONDUCTORS)
Silicon-sapphire waveguides
[AD-A191754] N88-24854

SOUND PROPAGATION
Construction of approximations to acoustic Green's functions for nonhomogeneous oceans using transmutation
[PB88-185384] N88-25126
Linear and nonlinear acoustic wave propagation in the atmosphere
[NASA-CR-4157] N88-25268

SOUND WAVES
Evaluation of the biot coefficients
[AD-A191643] N88-25265

SOUNDING ROCKETS
Electric field measurement by S-520-9 sounding rocket using the time of flight technique of lithium ion beam
[ISAS-RN-367] N88-25095
Rocket-borne low energy ion measurements in space N88-25412

SPACE BASED RADAR
The role of space borne imaging radars in environmental monitoring: Some shuttle imaging radar results in Asia
[NASA-TM-101178] N88-24844

SPACE CHARGE
Deep dielectric charging effects due to high energy electrons in earth's outer magnetosphere
[AD-A192154] N88-25083
Accelerator research studies
[DE88-007124] N88-25290

SPACE COMMERCIALIZATION
Preparation for microgravity: The role of the microgravity materials science laboratory
[NASA-TM-100906] N88-24811

SPACE COMMUNICATION
Service offerings and interfaces for the ACTS network of Earth stations
[NASA-TM-100809] N88-24863

SPACE COOLING (BUILDINGS)
Field experience with aquifer thermal energy storage
[DE88-007075] N88-25058

SPACE DEBRIS
Effects of meteoroids and space debris on the particulate environment for space station N88-25399

SPACE FLIGHT
Possibilities and limits for use of laser propulsion systems in interorbital space flight
[ILR-MITT-185] N88-24683

SPACE HEATING (BUILDINGS)
Field experience with aquifer thermal energy storage
[DE88-007075] N88-25058

SPACE PLASMAS
Electric field measurement by S-520-9 sounding rocket using the time of flight technique of lithium ion beam
[ISAS-RN-367] N88-25095
Contaminant ions and waves in the space station environment N88-25393

SPACE PROCESSING
Preparation for microgravity: The role of the microgravity materials science laboratory
[NASA-TM-100906] N88-24811

SPACE SHUTTLE BOOSTERS
Quality and productivity drive innovation and improvement at United Technologies Aerospace Operations, Inc.
[NASA-CR-182944] N88-24983
SRM propellant and polymer materials structural test program
[NASA-TP-2821] N88-25013

SPACE SHUTTLE MAIN ENGINE
Research study: Space shuttle main engine plume flowfield model
[NASA-CR-179336] N88-24676
Duct flow nonuniformities for Space Shuttle Main Engine (SSME)
[NASA-CR-179338] N88-24899

SPACE SHUTTLE PAYLOADS
Payload deployment method and system
[NASA-CASE-MSC-21330-1] N88-24660

SPACE SHUTTLES
A decade of computer simulations for space shuttle aerodynamics
[NASA-TM-100990] N88-24603
Structural margins assessment approach
[NASA-TM-100332] N88-24672

SPACE STATION PAYLOADS
Mars rover/sample return mission requirements affecting space station
[NASA-CR-172048] N88-25414

SPACE STATION POLAR PLATFORMS
P-Plus: Polar Platform utilization study, executive summary
[BAE-TP-8391] N88-24653

SPACE STATIONS
Space station architectural elements model study
[NASA-CR-4027] N88-24632
Possibilities and limits for use of laser propulsion systems in interorbital space flight
[ILR-MITT-185] N88-24683
Human performance issues arising from manned space station missions
[NASA-CR-3942] N88-25156
Space station architectural elements and issues definition study
[NASA-CR-3941] N88-25371
Space station habitability recommendations based on a systematic comparative analysis of analogous conditions
[NASA-CR-3943] N88-25372
A Study of Space Station Contamination Effects --- conference
[NASA-CP-3002] N88-25390
Neutral environment for space station N88-25391
Space station neutral external environment N88-25392
Contaminant ions and waves in the space station environment N88-25393
Space station induced electromagnetic effects N88-25394
Space station contamination study: Assessment of contaminant spectral brightness N88-25395
Calculation of space station infrared irradiance from atmosphere-induced emissions N88-25396
Space station particulate contamination environment N88-25397
The particulate environment surrounding the space station: Estimates from the PACS data N88-25398
Effects of meteoroids and space debris on the particulate environment for space station N88-25399
Contamination of optical surfaces --- Space Station N88-25400
Surface interactions relevant to space station contamination problems N88-25401
Laboratory experiments of relevance to the space station environment N88-25402
Contamination of the space station environment by vented chemicals N88-25403

SPACEBORNE EXPERIMENTS
Theoretical plasma physics research of active space experiments
[AD-A192075] N88-25309
Contamination of the space station environment by vented chemicals N88-25403

SPACECRAFT CHARGING
Simulations of the electrostatic charging of ESA communications satellites
[ESA-STM-239] N88-24670
Deep dielectric charging effects due to high energy electrons in earth's outer magnetosphere
[AD-A192154] N88-25083

SPACECRAFT COMMUNICATION
Assessment of optical communications systems for the Data Relay Satellite
[ESA-CR(P)-2488-VOL-2] N88-24842

SPACECRAFT CONSTRUCTION MATERIALS
Aluminum alloy
[NASA-CASE-LAR-13924-1-CU] N88-24753

SPACECRAFT CONTAMINATION
A Study of Space Station Contamination Effects --- conference
[NASA-CP-3002] N88-25390
Neutral environment for space station N88-25391
Space station neutral external environment N88-25392
Contaminant ions and waves in the space station environment N88-25393
Space station induced electromagnetic effects N88-25394
Space station contamination study: Assessment of contaminant spectral brightness N88-25395
Space station particulate contamination environment N88-25397
The particulate environment surrounding the space station: Estimates from the PACS data N88-25398
Effects of meteoroids and space debris on the particulate environment for space station N88-25399
Contamination of optical surfaces --- Space Station N88-25400
Surface interactions relevant to space station contamination problems N88-25401
Laboratory experiments of relevance to the space station environment N88-25402
Contamination of the space station environment by vented chemicals N88-25403

SPACECRAFT CONTROL
Guidance and control strategies for aerospace vehicles
[NASA-CR-183032] N88-24644
Low authority control of large space structures using a constrained threshold control formulation N88-24667
A feedback linearization approach to spacecraft control using momentum exchange devices
[NASA-CR-172057] N88-24668

SPACECRAFT DESIGN
Progress and future directions in computational fluid dynamics
[NASA-TM-100091] N88-24579
High speed and high angle of attack aerodynamic characteristics of winged space vehicle
[ISSN-0265-6808] N88-24599
Attitude control laws for gas-jet spacecraft N88-24643
Structural margins assessment approach
[NASA-TM-100332] N88-24672
Mars rover/sample return mission requirements affecting space station
[NASA-CR-172048] N88-25414

SPACECRAFT DOCKING
Range and range rate system
[NASA-CASE-MSC-20867-1] N88-24958

SPACECRAFT EQUIPMENT
Acoustic convective system
[NASA-CASE-NPO-17278-1-CU] N88-24818
Range and range rate system
[NASA-CASE-MSC-20867-1] N88-24958

SPACECRAFT GLOW
Space station contamination study: Assessment of contaminant spectral brightness N88-25395

Calculation of space station infrared irradiance from atmosphere-induced emissions N88-25396

SPACECRAFT GUIDANCE
Guidance and control strategies for aerospace vehicles
[NASA-CR-183032] N88-24644
A design study of onboard navigation and guidance during aerocapture at Mars
[NASA-CR-172053] N88-24654

SPACECRAFT LAUNCHING
Monitoring biological impacts of space shuttle launches from Vandenberg Air Force Base: Establishment of baseline conditions
[NASA-TM-100982] N88-25133

SPACECRAFT MODULES
Space station architectural elements model study
[NASA-CR-4027] N88-24632

SPACECRAFT PROPULSION
Performance and long duration test of a 30 kw thermal arcjet engine
[AD-A190962] N88-24677
Development of a liquid-fed water resistojet
[NASA-TM-100927] N88-24968

SPACECRAFT RADIATORS
Arc-textured metal surfaces for high thermal emittance space radiators
[NASA-TM-100894] N88-24754

SPACECRAFT STRUCTURES
Progress and future directions in computational fluid dynamics
[NASA-TM-100091] N88-24579

SPACECREWS
Space station habitability recommendations based on a systematic comparative analysis of analogous conditions
[NASA-CR-3943] N88-25372

SPATIAL FILTERING
Real-time optical multiple object recognition and tracking system and method
[NASA-CASE-NPO-17139-1-CU] N88-25301

SPATIAL RESOLUTION
Effects of spatial resolution in CARS measurements
[PB88-121900] N88-24727
Spatial stability of a compressible mixing layer
[NASA-CR-181671] N88-24916

SPECIFIC HEAT
The thermodynamic properties of quinoline and isoquinoline
[DE88-001218] N88-24735
The precipitation processes of Cu-Zr-Cr alloys
[NASA-TT-20168] N88-24758

SPECIFIC IMPULSE
Performance of a hydrogen pulsed electrothermal thruster. Strategic defense initiative organization innovative science and technology. SBIR, phase 1
[AD-A191999] N88-24679

SPECIFICATIONS
Nonlinear flying quality parameters based on dynamic inversion
[AD-A192146] N88-24627
Use of a two-stage light-gas gun as an injector for electromagnetic railguns
[DE88-007200] N88-24657
The -mdoc macro package: A software tool to support computer documentation standards
[DE88-000500] N88-25188

SPECIMENS
Sample decomposition in sealed teflon vessels
[NASA-TT-20189] N88-24798
Low temperature storage container for transporting perishables to space station
[NASA-CASE-MFS-26248-1] N88-24817

SPECKLE INTERFEROMETRY
Speckle imaging of active galactic nuclei: NGC 1068 and NGC 4151 N88-25407

SPECKLE PATTERNS
Speckle imaging of active galactic nuclei: NGC 1068 and NGC 4151 N88-25407

SPECTRA
Time-frequency representations for speech signals
[AD-A188661] N88-24819
Molecular-beam, mass-spectrometric studies of wood vapor and model compounds over HZSM-5 catalyst N88-25044

SPECTRAL EMISSION
Space station contamination study: Assessment of contaminant spectral brightness N88-25395
Calculation of space station infrared irradiance from atmosphere-induced emissions N88-25396
Speckle imaging of active galactic nuclei: NGC 1068 and NGC 4151 N88-25407

SPECTRAL ENERGY DISTRIBUTION
Three dimensional spectral energy measurement on turbulence subjected to a high degree of plane deformation
[ETN-88-92537] N88-24896

SPECTRAL LINE WIDTH
Studies of spectral line ratio fluctuations using Inductively Coupled Plasma (ICP) light
[IRF-PREPRINT-100] N88-25311

SPECTRAL METHODS
Effects of spatial resolution in CARS measurements
[PB88-121900] N88-24727
Analysis of a six-component barotropic spectral model: Chaotic motion, predictability and vacillation — atmospheric circulation
[CWI-AM-R8710] N88-25090

SPECTRAL REFLECTANCE
Optical constants of minerals and other materials from the millimeter to the ultraviolet
[AD-A192210] N88-24724

SPECTROSCOPY
Optical diagnostics for a high power, rf-inductively coupled plasma
[DE88-007822] N88-25322
Spectroscopy and energy transfer kinetics of the interhalogens
[AD-A192103] N88-25344

SPECTRUM ANALYSIS
Studies of spectral line ratio fluctuations using Inductively Coupled Plasma (ICP) light
[IRF-PREPRINT-100] N88-25311

SPEECH
Time-frequency representations for speech signals
[AD-A188661] N88-24819

SPHERICAL COORDINATES
A formulation for the boundary-layer equations in general coordinates
[NASA-TM-100079] N88-24800

SPIN DYNAMICS
A scientific basis for an alternate cathode architecture
[AD-A191498] N88-24717
Theoretical investigation of the development of the normal fluid and superfluid velocity distributions during spin-up for a He2-filled cylinder
[MPIS-6/1987] N88-24892

SPIN RESONANCE
Nuclear structure studies at intermediate energies
[DE88-006683] N88-25271

SPLINE FUNCTIONS
Open or closed curves by regularized B-splines
[RR-652-M] N88-25218

SPLITTING
Photosynthetic water splitting
[PB88-188891] N88-24731

SPRINGS (ELASTIC)
Structurally tailorable non-linear snap-through spring system
[NASA-CASE-LAR-13729-1] N88-24970

STABILITY
Shape stability in composites N88-24706
Spatial stability of a compressible mixing layer
[NASA-CR-181671] N88-24916
Investigations in electro-optical multistability for signal processing N88-24938
Theoretical investigations of drift waves in a magnetic quadrupole N88-25312

STABILIZATION
Concepts for a laser gyroscope of the highest precision N88-24929

STAGNATION POINT
Stagnating turbulent reacting flows
[AD-A191449] N88-24877

STAR FORMATION
Infrared astronomy at extremely faint light levels in support of the LAIRTS program
[AD-A191497] N88-25404

STARK EFFECT
High-order multiphoton ionization of the noble gases
[DE88-007489] N88-25273

STATE VECTORS
A design study of onboard navigation and guidance during aerocapture at Mars
[NASA-CR-172053] N88-24654

STATIC ELECTRICITY
Development of test methods for the electrostatic properties of nonhomogeneous fabrics, phase 2
[AD-A190853] N88-24767

STATISTICAL ANALYSIS
Performance estimates for operations conducted while wearing individual protective equipment: User manual
[AD-A191871] N88-25154
Annotated computer output for split plot design: SAS GLM
[AD-A190800] N88-25167
A method for the numerical solution of random Cauchy singular integral equation N88-25234
Exact tests for variance component models with unequal cell frequencies in the last stage
[AD-A191645] N88-25253
On path properties of certain infinitely divisible processes
[AD-A192016] N88-25255

STATISTICAL DISTRIBUTIONS
The theory of random alloys
[DE88-006408] N88-24756

STATISTICAL MECHANICS
Introduction to lattice gauge theory
[DE88-006073] N88-25349

STATISTICAL WEATHER FORECASTING
Comparative verification between GEM model and official aviation terminal forecasts N88-25115

STEADY FLOW
A variational finite element method for three-dimensional, steady, compressible, viscous flows N88-24904

STEADY STATE
Periodic solutions in aircraft cruise-dash optimization N88-24631

STEELS
Irradiation effects on tungsten stabilized martensitic steels
[DE88-007074] N88-24748
Stress corrosion cracking of A723 steel pressure vessels: Two case studies
[AD-A191741] N88-24990

STEERING
Null steering applications of polynomials with unimodular coefficients
[AD-A191067] N88-25211

STELLAR CORES
Speckle imaging of active galactic nuclei: NGC 1068 and NGC 4151 N88-25407
Microwave spectroscopy and gravitational collapse N88-25413

STELLAR EVOLUTION
Pre-supernova evolution of SN 1987A
[SER-C-PREPUBL-FASC-15] N88-25409
Radial velocities monitoring of a sample of barium and S stars using CORAVEL: Towards an evolutionary link between barium and S stars?
[SER-C-PREPUBL-FASC-19] N88-25410
Review of the theoretical changes of surface chemistry during massive star evolution
[SER-C-PREPUBL-FASC-17] N88-25411

STELLAR LUMINOSITY
Ultraviolet spectra of subluminous objects found in the Kiso Schmidt survey and systematic reanalysis of the archived ultraviolet spectra of white dwarfs observed with the IUE satellite under the Astrophysics Data Program (ADP)
[NASA-CR-182976] N88-25406

STELLAR MODELS
Pre-supernova evolution of SN 1987A
[SER-C-PREPUBL-FASC-15] N88-25409

STELLAR SPECTRA
Duplicity in the solar neighborhood. Part 3: New spectroscopic elements for nine solar-type binary stars
[SER-C-PREPUBL-FASC-18-PT-3] N88-25405

STEREOCHEMISTRY
Topological stereochemistry
[AD-A191867] N88-24691

STIFFENING
Stiffened titanium panels
[NASA-CASE-LAR-13614-1] N88-24816

STIMULATED EMISSION DEVICES
Laser countermeasure impacts and penalties
[DE88-006871] N88-24947

STOCHASTIC PROCESSES
Information and stochastic systems
[AD-A192167] N88-24838
Analysis of binarized Hartley phase-only filter performance with respect to stochastic noise
[DE88-007604] N88-24945
Reliability of stochastically forced systems (extended version)
[CWI-AM-R8801] N88-24985
Computational sciences
[AD-A190826] N88-25226
Numerical solutions to stochastic difference equations N88-25229
On path properties of certain infinitely divisible processes
[AD-A192016] N88-25255
Stochasticity in a Q-machine plasma N88-25315

STOKES FLOW
New mixed finite element methods N88-25248

STORAGE BATTERIES
Small scale bipolar nickel-hydrogen testing
[NASA-TM-100936] N88-25059

STORAGE RINGS (PARTICLE ACCELERATORS)
On bunch lengthening using the fourth harmonic cavity in the NSLS VUV ring
[DE88-007392] N88-25288

STORM ENHANCEMENT
Tropical cyclones, 1987: Central North Pacific
[PB88-186081] N88-25119
STRAIN GAGES
Determination of the toughness of a brittle material using strain gages
[ETN-88-92540] N88-24993
STRAIN HARDENING
Strain hardening at large strains in aluminum alloys
[DE88-007415] N88-24737
STRAIN MEASUREMENT
Radio Frequency (RF) strain monitor
[NASA-CASE-LAR-13705-1] N88-25011
STRAIN RATE
Superplasticity: A fundamental investigation on deformation mechanism and cavitation phenomena
[AD-A191548] N88-24741
The variation of torsional ductility of high-purity aluminum with temperature and strain rate
[DE88-005618] N88-24755
Metastability in SiGe/Si strained-layer structures
[DE88-007603] N88-25361
STRAKES
Actuated forebody strakes
[NASA-CASE-LAR-13983-1] N88-24628
STRATIGRAPHY
Geological evolution and analysis of confirmed or suspected gas hydrate localities. Volume 2: Basin analysis, formation and stability of gas hydrates in the Black Sea
[DE88-001052] N88-25023
STRATOSPHERE
Stratospheric positive ion composition measurements and acetonitrile detection: A consistent picture
[AERONOMICA-ACTA-A-326-1987] N88-25084
Three-dimensional temperature fields in the atmosphere up to 50 km altitude
[ETN-88-92150] N88-25089
SAM 2 data user's guide
[NASA-RP-1200] N88-25094
STRESS ANALYSIS
Analysis of notched metal matrix composites under tension loading
[NASA-TM-100629] N88-24713
On the reversion phenomena of Cu-3 percent Ti alloys
[NASA-TT-20170] N88-24762
Stress measurements in graphite fibers by laser raman spectroscopy
[AD-A191710] N88-24779
Effect of uniaxial stress on the Raman spectra of graphite fibers
[AD-A191730] N88-24783
Computational fluid dynamics applied to the prediction of the heat-transfer, mechanical and thermal-stress behavior of heat exchangers
[CFDU/87/7] N88-24893
Plate response analysis using shock tube
[AD-A190826] N88-24967
Advanced development of the boundary element method for elastic and inelastic thermal stress analysis N88-25002
Forced motion of initially stressed shells and plates N88-25005
Fatigue crack growth due to random loading N88-25017
STRESS CORROSION CRACKING
Stress corrosion cracking of A723 steel pressure vessels: Two case studies
[AD-A191741] N88-24990
STRESS CYCLES
Theory of viscoplasticity based on overstress with applications N88-25007
STRESS FUNCTIONS
Dynamic shear band development in plane strain
[AD-A190915] N88-24988
STRESS INTENSITY FACTORS
Determination of the toughness of a brittle material using strain gages
[ETN-88-92540] N88-24993
Some stress intensity factor equations
[FFA-TN-1987-07] N88-24995
Automated analysis of crack growth rate for obtaining da/dN versus delta K relation
[FFA-TN-1987-70] N88-24996
Resolved shear stress intensity coefficient and fatigue crack growth in large crystals
[NASA-CR-182137] N88-24997
The surface crack problem in an orthotropic plate under bending and tension
[NASA-CR-178281] N88-25014
A method for the numerical solution of random Cauchy singular integral equation N88-25234
STRESS MEASUREMENT
Stress measurements in graphite fibers by laser raman spectroscopy
[AD-A191710] N88-24779
STRESS-STRAIN RELATIONSHIPS
Analysis of notched metal matrix composites under tension loading
[NASA-TM-100629] N88-24713
Role of cracks in the creep of structural polycrystalline ceramics
[AD-A191485] N88-24770
STRESSES
A dynamic analysis of piezoelectric strained elements
[AD-A191478] N88-24851
Theory of viscoplasticity based on overstress with applications N88-25007
STRING THEORY
Introduction to covariant formulation of superstring (field) theory
[DE87-703038] N88-25363
The geometry of the Virasoro group for physicists
[DE88-007374] N88-25366
Comment on non-renormalization theorem in the four dimensional superstrings
[DE88-752551] N88-25367
From general relativity to the theory of superstrings N88-25369
STRUCTURAL ANALYSIS
Research on aero-thermodynamic distortion induced structural dynamic response of multi-stage compressor blading
[AD-A192169] N88-24584
Electromagnetic damping and vibration isolation of space structures
[AD-A191492] N88-24685
Fundamental studies of beta phase decomposition modes in titanium alloys
[AD-A191495] N88-24740
Calculation of rolling contact of two viscoelastic cylinders with application to the steady state normal contact problem
[ILR-MITT-188] N88-25006
Probabilistic finite element methods N88-25223
STRUCTURAL DESIGN
Experimental vibration damping characteristics of the third-stage rotor of a three-stage transonic axial-flow compressor
[NASA-TM-100948] N88-24642
Design of overlays for rigid airport pavements
[DOT/FAA/PM-87/19] N88-24652
Fundamental limits to the velocity of solid armatures in railguns N88-24656
Use of a two-stage light-gas gun as an injector for electromagnetic railguns
[DE88-007200] N88-24657
Structural margins assessment approach
[NASA-TM-100332] N88-24672
Dynamics of a flexible orbiting platform with MRMS
[ISSN-0265-6808] N88-24673
Internal erosion rates of a 10-kW xenon ion thruster
[NASA-TM-100954] N88-24688
Calculation of assemblies bonded with quasi-elastic adhesives
[REPT-47-632/F] N88-24793
Fuel containment concepts: Transport category airplanes
[DOT/FAA/CT-87/18] N88-24807
Space station architectural elements and issues definition study
[NASA-CR-3941] N88-25371
STRUCTURAL FAILURE
Analysis and developments of failure concepts in fracture mechanics based on research results in the field of component safety topics: J-integral concept; crack resistance curves; dynamic criterion
[V-19/86] N88-25009
STRUCTURAL PROPERTIES (GEOLOGY)
A sedimentological and mineralogical study of the Koogah Formation, New South Wales N88-25087
SUBLIMATION
The evolution of cometary activity N88-25416
SUBMILLIMETER WAVES
Millimeter and submillimeter waves and frequency selective surfaces
[AD-A191511] N88-24827
SUBROUTINES
CIMAG2: The computer program to generate color images
[AD-A191847] N88-25175
SUBSONIC FLOW
Numerical simulations of the flat-plate laminar boundary layer in subsonic and supersonic flow
[PDR/CFDU-IC/36] N88-24895
SUBSTRATES
On the use of convergent beam electron diffraction for identification of antiphase boundaries in GaAs grown on Si
[DE88-008220] N88-25362
SULFUR
The io sulfur torus in 1981
[NASA-TM-101139] N88-25419
SULFUR COMPOUNDS
Electronic and ionic transport in polymers
[AD-A191642] N88-24772
SUMMER
Report on project WIND: Preliminary experiments w ith the UK Meteorological Office mesoscale model, September 1987
[AD-A191621] N88-25099
SUN
MHD bending waves in a current sheet
[NASA-TM-101149] N88-25323
SUPERCHARGERS
Servojet retrofit
[AD-A191075] N88-24964
SUPERCOMPUTERS
Effective use of shared memory multiprocessors
[DE88-007019] N88-25195
SUPERCONDUCTIVITY
Crystalline metal-semiconductor superlattices
[DE88-007063] N88-25332
SUPERCONDUCTORS
Research work completed at the Naval Surface Warfare Center Solid State Group of the Radiation Division
[AD-A191627] N88-25339
Vacancy ordering in the basal plane of YBa2Cu3O(sub)z
[DE88-004572] N88-25348
Quench detection by fluid dynamic means in cable-in-conduit superconductors
[DE88-007269] N88-25359
SUPERCRITICAL AIRFOILS
Aerodynamic performance and pressure distributions for a NASA SC(2)-0714 airfoil tested in the Langley 0.3-meter transonic cryogenic tunnel
[NASA-TM-4044] N88-24580
SUPERCRITICAL FLOW
Unsteady flow in a supercritical supersonic inlet N88-24805
Electrochemistry in near-critical and supercritical fluids. 6: The electrochemistry of ferrocene and phenazine in acetonitrile between 25C and 300C
[AD-A192171] N88-24723
SUPERCRITICAL FLUIDS
Electrochemistry in near-critical and supercritical fluids. 6: The electrochemistry of ferrocene and phenazine in acetonitrile between 25C and 300C
[AD-A192171] N88-24723
SUPERFLUIDITY
Theoretical investigation of the development of the normal fluid and superfluid velocity distributions during spin-up for a He2-filled cylinder
[MPIS-6/1987] N88-24892
SUPERHIGH FREQUENCIES
Monolithic GaAs Ku-band one watt constant phase variable power amplifier
[DE88-006272] N88-24866
SUPERLATTICES
Neutron diffraction refinement of CsHSO4 superionic phase structure
[DE88-701496] N88-25326
Crystalline metal-semiconductor superlattices
[DE88-007063] N88-25332
Electronic structure, elementary excitations, optical and transport properties of semiconductor superlattices
[AD-A190795] N88-25333
Magnetic superlattices
[AD-A191450] N88-25334
Optical properties of heterostructures and superlattices
[AD-A191542] N88-25335
An investigation of 2-6 superlattice deposition by laser photochemical techniques
[AD-A191547] N88-25336
SUPERNOVAE
Nuclear and astrophysical evidence on the equation of state
[DE88-007397] N88-25279
Pre-supernova evolution of SN 1987A
[SER-C-PREPUBL-FASC-15] N88-25409
SUPERPLASTICITY
Superplasticity: A fundamental investigation on deformation mechanism and cavitation phenomena
[AD-A191548] N88-24741
SUPERSONIC BOUNDARY LAYERS
Fundamental aspects of the structure of supersonic turbulent boundary layers
[AD-A191494] N88-24581
SUPERSONIC FLIGHT
Wind tunnel investigation of wing and control panel loads at transonic and supersonic speeds on some schematic cruciform missile configurations
[FFA-TN-1986-43] N88-24585

SUPERSONIC FLOW
Fundamental aspects of the structure of supersonic turbulent boundary layers
[AD-A191494] N88-24581
Numerical simulations of the flat-plate laminar boundary layer in subsonic and supersonic flow
[PDR/CFDU-IC/36] N88-24895
Numerical solutions of the complete Navier-Stokes equations
[NASA-CR-183023] N88-24914
SUPERSONIC INLETS
Unsteady flow in a supercritical supersonic inlet N88-24605
SUPERSYMMETRY
Introduction to covariant formulation of superstring (field) theory
[DE87-703038] N88-25363
Comment on non-renormalization theorem in the four dimensional superstrings
[DE88-752551] N88-25367
SUPPORTS
Almond test body — for microwave anechoic chambers
[NASA-CASE-LAR-13747-1] N88-24845
Thermal compensating mount
[NASA-CASE-LAR-13794-1] N88-24842
SURFACE CRACKS
The surface crack problem in an orthotropic plate under bending and tension
[NASA-CR-178281] N88-25014
SURFACE FINISHING
Influence of carbon fiber surface treatment
[ETN-88-92536] N88-24787
Evaluation of the chromium oxide arc spraying treatment on solar energy collectors
[ETN-88-92564] N88-25053
SURFACE LAYERS
Evaluating evaporation with satellite thermal data
[AD-A192042] N88-25019
SURFACE NAVIGATION
Navigation system for land vehicles
[NASA-CASE-LAR-13322-1] N88-24620
Navigation using the Teldix fiber-optic gyroscope N88-24933
SURFACE PROPERTIES
Arc-textured metal surfaces for high thermal emittance space radiators
[NASA-TM-100894] N88-24754
The electrokinetic behavior of calcium oxalate monohydrate in macromolecular solutions
[NASA-TM-101144] N88-24791
SURFACE REACTIONS
Surface interactions relevant to space station contamination problems N88-25401
SURFACE ROUGHNESS
An experimental study of the coherent under-ice reflectivity of sound in the Greenland Sea Marginal Ice Zone N88-25125
SURFACE TEMPERATURE
Evaluating evaporation with satellite thermal data
[AD-A192042] N88-25019
SURFACE VEHICLES
Articulated suspension system
[NASA-CASE-NPO-17354-1-CU] N88-24973
SURVEILLANCE
The Effect of the Ionosphere on Communication, Navigation and Surveillance Systems Based on Ionospheric Effects Symposium held on 5-7 May 1987 in Springfield, Virginia
[AD-A191655] N88-25081
SURVEILLANCE RADAR
Automated test device for FASR (Fixed Array Surveillance Radar) beam steering componentry
[AD-A191650] N88-24829
SURVEYS
Human performance issues arising from manned space station missions
[NASA-CR-3942] N88-25156
SUSPENSION SYSTEMS (VEHICLES)
Articulated suspension system
[NASA-CASE-NPO-17354-1-CU] N88-24973
SWEAT COOLING
The effects of different combinations of inlet air conditions used for cooling as measured on a heated manikin
[AD-A191116] N88-25151
SWEPT FORWARD WINGS
Experiment investigation on longitudinal characteristics of the forward swept wing
[AD-A191553] N88-24582
Current flight test experience related to structural divergence of forward-swept wings
[NASA-TM-100445] N88-24633
SWIRLING
Effect of initial tangential velocity distribution on the mean evolution of a swirling turbulent free jet
[NASA-TM-100934] N88-24592
Development of a liquid-fed water resistojet
[NASA-TM-100927] N88-24968
SWITCHES
A monolithic reduced-size Ku-Band SPOT (Single-Pole Double Throw) FET switch
[DE88-006273] N88-24858
SYLLABLES
Motor theory of auditory perception
[AD-A192095] N88-25136
SYMBOLS
Optical symbolic processor for expert system execution
[AD-A192005] N88-25296
SYMMETRY
Rigid symmetries and BRST-invariance in gauge theories
[PB88-180948] N88-25280
SYNCHROTRON RADIATION
On bunch lengthening using the fourth harmonic cavity in the NSLS VUV ring
[DE88-007392] N88-25288
SYNCHROTRONS
A two-wavelength infrared interferometer/polarimeter system for CIT (Compact Ignition Tokamak)
[DE88-007681] N88-25321
SYNOPTIC METEOROLOGY
Analysis of a six-component barotropic spectral model: Chaotic motion, predictability and vacillation — atmospheric circulation
[CWI-AM-R8710] N88-25090
SYNTHESIS (CHEMISTRY)
Topological stereochemistry
[AD-A191667] N88-24691
Aromatic cyclotriphosphazenes
[NASA-CASE-ARC-11428-3] N88-24692
Proceedings of the American Society for Composites
[AD-A189861] N88-24693
Current and future molecular structures of aerospace organic matrix resins N88-24695
Industrial perspective on current and future needs in aerospace matrix resin chemistry N88-24696
Applications of biotechnology to synthetic chemistry for aerospace matrix resins development N88-24697
The application of hydrocarbon bioconversion technology to aerospace materials production N88-24698
The synthesis of polyphenylene from a CIS-dihydrocatechol biologically produced monomer N88-24699
Update of low temperature catalyst development
[DE88-007032] N88-24715
Synthesis and characterization of new phosphazene polymers
[AD-A191508] N88-24771
High strength/sigh modulus aromatic heterocyclic ABA block copolymers
[AD-A191666] N88-24774
A cardiostimulant protein from the Australian Red Waratah Sea anemone, Actinia tenebrosa N88-25138
SYNTHETIC APERTURE RADAR
The role of space borne imaging radars in environmental monitoring: Some shuttle imaging radar results in Asia
[NASA-TM-101178] N88-24844
SYNTHETIC FIBERS
Development of test methods for the electrostatic properties of nonhomogeneous fabrics, phase 2
[AD-A190853] N88-24767
SYNTHETIC FUELS
Production costs of hydrocarbon fuels from biomass
[DE88-006667] N88-24804
SYSTEM EFFECTIVENESS
An enumeration of research to determine the optimal design and use of Army flight training simulators
[AD-A191242] N88-24649
SYSTEM FAILURES
Applications of fault tree analysis to the design process
[DE88-007048] N88-24982
SYSTEM IDENTIFICATION
TVC (Thrust Vector Control) jet vane thermal modeling using parametric system identification
[AD-A191518] N88-24678
SYSTEMS ANALYSIS
Possibilities and limits for use of laser propulsion systems in interorbital space flight
[ILR-MITT-185] N88-24683
Reliability of stochastically forced systems (extended version)
[CWI-AM-R8801] N88-24985
Systems analysis of INTOR-like designs
[DE88-004422] N88-25316
SYSTEMS ENGINEERING
Concepts for a laser gyroscope of the highest precision N88-24929
A systems engineering based methodology for analyzing human electrocortical responses
[AD-A190809] N88-25135
The ATF (Advanced Toroidal Facility) Data M Management System
[DE88-007265] N88-25385
SYSTEMS SIMULATION
Recursive maximum likelihood identification of a nonlinear output-affine model
[RR-322] N88-25257

T

TAIWAN
Taiwan area mesoscale experiment: P-3 aircraft operations summary
[PB88-169073] N88-25098
TARGET RECOGNITION
Joint services electronics program
[AD-A191749] N88-24853
Real-time optical multiple object recognition and tracking system and method
[NASA-CASE-NPO-17139-1-CU] N88-25301
TARGETS
Self shielding of surfaces irradiated by intense energy fluxes
[DE88-007084] N88-25318
TASK COMPLEXITY
Simultaneous multiple control force exertion capabilities of males and females versus helicopter control force design limits
[AD-A191653] N88-25153
TASKS
Performance estimates for operations conducted while wearing individual protective equipment: User manual
[AD-A191871] N88-25154
Lunar base surface mission operations. Lunar Base Systems Study (LBSS) task 4.1
[NASA-CR-172050] N88-25415
TDR SATELLITES
Assessment of optical communications systems for Data Relay Satellite. Volume 1: Executive summary
[ESA-CR(P)-2488-VOL-1] N88-24841
Assessment of optical communications systems for the Data Relay Satellite
[ESA-CR(P)-2488-VOL-2] N88-24842
TECHNOLOGICAL FORECASTING
Possibilities and limits for use of laser propulsion systems in interorbital space flight
[ILR-MITT-185] N88-24683
TECHNOLOGY ASSESSMENT
Proceedings of the American Society for Composites
[AD-A189861] N88-24693
Industrial perspective on current and future needs in aerospace matrix resin chemistry N88-24696
Differential technology in plastics industries differentiation in combination technology nonflammability technology
[NASA-TT-20256] N88-24797
Fuel containment concepts: Transport category airplanes
[DOT/FAA/CT-87/18] N88-24807
Assessment of optical communications systems for Data Relay Satellite. Volume 1: Executive summary
[ESA-CR(P)-2488-VOL-1] N88-24841
Assessment of optical communications systems for the Data Relay Satellite
[ESA-CR(P)-2488-VOL-2] N88-24842
Technical and economic evaluation of emerging biomass pyrolysis processes for gasoline production N88-25048
Recent advances in low-thrust propulsion technology
[NASA-TM-100959] N88-25260
TECHNOLOGY UTILIZATION
P-Plus: Polar Platform utilization study, executive summary
[BAE-TP-8391] N88-24653
Personal computer as a workstation in a cartographic automation system? N88-25039
TEFLON (TRADEMARK)
Sample decomposition in sealed teflon vessels
[NASA-TT-20189] N88-24798
TELECOMMUNICATION
An FSK (Frequency Shift Keying) telemetry module for vector measuring current meters
[AD-A192142] N88-24661
Practical VLF/LF radio test system
[AD-A191768] N88-24831
Information and stochastic systems
[AD-A192167] N88-24838

The Effect of the Ionosphere on Communication, Navigation and Surveillance Systems Based on Ionospheric Effects Symposium held on 5-7 May 1987 in Springfield, Virginia
[AD-A191855] N88-25081
Design, implementation and evaluation of an operating system for a network of transputers
[AD-A186593] N88-25193
Selection and effects of channels in distributed communication and decision making tasks: A theoretical review and a proposed research paradigm
[AD-A191807] N88-25375

TELEMETRY
An FSK (Frequency Shift Keying) telemetry module for vector measuring current meters
[AD-A192142] N88-24661
Adaptive data acquisition multiplexing system and method
[NASA-CASE-MSC-21170-1] N88-24662

TELEOPERATORS
A universal computer control system for motors
[NASA-CASE-NPO-17134-1-CU] N88-24664

TEMPERATURE COMPENSATION
Thermal compensating mount
[NASA-CASE-LAR-13794-1] N88-24942

TEMPERATURE CONTROL
Field experience with aquifer thermal energy storage
[DE88-007075] N88-25058

TEMPERATURE DEPENDENCE
Temperature dependence of ultraviolet absorption cross sections of chlorofluoroethanes
[AERONOMICA-ACTA-A-325-1987] N88-24726

TEMPERATURE DISTRIBUTION
Noncontact temperature pattern measuring device
[NASA-CASE-NPO-17024-1-CU] N88-24943
Optical investigations of the thermal boundary layer in arc plasmas N88-25313

TEMPERATURE EFFECTS
Effect of alloying, rapid solidification, and surface kinetics on the high temperature environmental resistance of niobium
[AD-A192093] N88-24743
High temperature embrittleness of Cu-Cr alloy
[NASA-TT-20184] N88-24759
Critical cooling rates on solution treatment of Cu-Cr and Cu-Be alloys
[NASA-TT-20183] N88-24760
On the reversion phenomena of Cu-3 percent Ti alloys
[NASA-TT-20170] N88-24762
Effect of size of precipitates on recrystallization temperatures in Cu-Cr, Cu-Zr, and Cu-Zr-Cr alloys
[NASA-TT-20186] N88-24763
Rapidly solidified lightweight durable disk material
[AD-A191697] N88-24775

TEMPERATURE MEASUREMENT
Effects of spatial resolution in CARS measurements
[PB88-121900] N88-24727
Remote temperature-measurement instrumentation for a heated rotating turbine disk
[DE88-006456] N88-24925
Special observations N88-25106

TEMPERATURE PROFILES
Three-dimensional temperature fields in the atmosphere up to 50 km altitude
[ETN-88-92150] N88-25089
Superthermal electron processes in the upper atmosphere of Uranus: Aurora and electroglow
[NASA-TM-101150] N88-25417
Diurnal variations in optical depth at Mars: Observations and interpretations
[NASA-TM-100057] N88-25420

TEMPLATES
Defect detection and classification in VLSI pattern inspection N88-24871

TENDENCIES
Reference filters for electrostatic charging tendency measurements of fuels
[AD-A191717] N88-24803

TENSILE PROPERTIES
Dynamic consolidation of metal powders
[AD-A192126] N88-24744

TENSILE STRENGTH
High strength/high modulus aromatic heterocyclic ABA block copolymers
[AD-A191686] N88-24774

TENSILE STRESS
Peak Acceleration Device (PAD)
[AD-A191639] N88-24811
Stress corrosion cracking of A723 steel pressure vessels: Two case studies
[AD-A191741] N88-24990
The surface crack problem in an orthotropic plate under bending and tension
[NASA-CR-178261] N88-25014

TENSORS
Inevitable inflation in Einstein-Cartan theory with improved energy-momentum tensor with spin
[NASA-TM-101146] N88-25365

TERMINOLOGY
NASA combined file postings statistics based on NASA thesaurus, Jan. 1988 - July 1988
[NASA-CR-182985] N88-25384

TERRESTRIAL RADIATION
Results of radiation measurements in West Germany and from special measurement series in the Meteorological Observatory of Hamburg
[REPT-11] N88-25088

TEST EQUIPMENT
Almond test body — for microwave anechoic chambers
[NASA-CASE-LAR-13747-1] N88-24845

TEST FACILITIES
SHaRE: Collaborative materials science research
[DE88-007175] N88-24646

TEXTURES
Shape from shading, occlusion and texture
[AD-A184840] N88-25289

THEORETICAL PHYSICS
Theoretical plasma physics research of active space experiments
[AD-A192075] N88-25309

THERMAL ANALYSIS
A scientific basis for an alternate cathode architecture
[AD-A191498] N88-24717
Evaluating evaporation with satellite thermal data
[AD-A192042] N88-25019

THERMAL BARRIERS (PLASMA CONTROL)
Thrust chamber thermal barrier coating technique
[NASA-TM-100933] N88-24690

THERMAL BOUNDARY LAYER
Optical investigations of the thermal boundary layer in arc plasmas N88-25313

THERMAL CONDUCTIVITY
Analytic and numerical modeling of heat and material transport in electrical hypervelocity guns
[AD-A192178] N88-24655
Thermal conductivity of hard anodized coatings on aluminum
[AD-A191755] N88-24784

THERMAL DECOMPOSITION
Thermal decomposition studies of explosives for component applications
[DE88-007201] N88-24805

THERMAL EMISSION
Arc-textured metal surfaces for high thermal emittance space radiators
[NASA-TM-100894] N88-24754
Gamma rays from Cygnus X-1: Modeling and nonthermal pair production
[DE88-006830] N88-25426

THERMAL EXPANSION
Thermal compensating mount
[NASA-CASE-LAR-13794-1] N88-24942

THERMAL INSULATION
Thermal conductivity of hard anodized coatings on aluminum
[AD-A191755] N88-24784
Calculational model development for fibrous thermal insulation transient test procedures
[DE88-007843] N88-24789

THERMAL MAPPING
Noncontact temperature pattern measuring device
[NASA-CASE-NPO-17024-1-CU] N88-24943

THERMAL PLASMAS
Modelling of thermal plasma systems N88-25314

THERMAL STABILITY
Current and future molecular structures of aerospace organic matrix resins N88-24695

THERMAL STRESSES
Computational fluid dynamics applied to the prediction of the heat-transfer, mechanical and thermal-stress behavior of heat exchangers
[CFDU/87/7] N88-24893
Advanced development of the boundary element method for elastic and inelastic thermal stress analysis N88-25002

THERMIONIC EMISSION
A scientific basis for an alternate cathode architecture
[AD-A191498] N88-24717

THERMOCHEMICAL PROPERTIES
Phase diagrams in materials science and the use of the computer in their calculation
[PB88-155262] N88-25364

THERMOCHEMISTRY
Structure/property/reactivity relations among nitramine and other energetic materials
[AD-A190878] N88-24716
Proceedings of the 1987 Biomass Thermochemical Conversion Contractors' Review Meeting
[DE88-006730] N88-25041
Low-temperature thermochemical conversion of high moisture biomass feedstocks N88-25047

THERMODYNAMIC PROPERTIES
TVC (Thrust Vector Control) jet vane thermal modeling using parametric system identification
[AD-A191518] N88-24678
The thermodynamic properties of quinoline and isoquinoline
[DE88-001218] N88-24735
Dynamic consolidation of metal powders
[AD-A192126] N88-24744

THERMODYNAMICS
Thermodynamic modeling of the no-vent fill methodology for transferring cryogens in low gravity
[NASA-TM-100932] N88-24686
Isothermal and bithermal thermomechanical fatigue behavior of a NiCoCrAlY-coated single crystal superalloy
[NASA-TM-100907] N88-24766
Advanced development of double-injection, deep-impurity semiconductor switches
[NASA-CR-182118] N88-25346
Vacancy ordering in the basal plane of YBa2Cu3O(sub)z
[DE88-004572] N88-25348
The morphological stability of continuous intergranular phases: Thermodynamic considerations
[DE88-006328] N88-25350
Phase diagrams in materials science and the use of the computer in their calculation
[PB88-155262] N88-25364
Study of data distributions and functions for the development of thermodynamic equations of state
[PB88-196365] N88-25370

THERMOELECTRICITY
Improved properties of SiGe/GaP alloys
[NASA-CASE-NPO-17259-1-CU] N88-25358

THERMOGRAPHY
Thermographic detection of buried debonds
[AD-A192115] N88-24680
Nondestructive testing using ultrahigh frequencies
[CERT-5/1333-MO] N88-24984

THERMOSPHERE
Components of an atmospheric lidar system: Doppler wind lidar
[AD-A191222] N88-24951

THESAURI
NASA combined file postings statistics based on NASA thesaurus, Jan. 1988 - July 1988
[NASA-CR-182985] N88-25384

THICKNESS
Thermal conductivity of hard anodized coatings on aluminum
[AD-A191755] N88-24784
Heating and evaporation of turbulent liquid films: Measurement of film thickness and the onset of nucleate boiling
[DE88-006388] N88-24905
Vibrations of rotating thick or thin rings N88-25003
Forced motion of initially stressed shells and plates N88-25005

THIN FILMS
Electrical conduction in thin film carbons
[AD-A191726] N88-24780
Electron-Rayleigh wave interaction in thin film carbons
[AD-A191727] N88-24781
Joint services electronics program research in electronics
[AD-A192206] N88-24857
Magnetic superlattices
[AD-A191450] N88-25334
Molecular characterization of structure and bonding in thin film materials
[DE88-006811] N88-25351

THIN PLATES
Dynamic response of plates to moving loads: Structural impedance and finite element methods N88-25000

THREE DIMENSIONAL BOUNDARY LAYER
Boundary layer transition
[CERT-OA-37/5018-AYD] N88-24595

THREE DIMENSIONAL FLOW
A variational finite element method for three-dimensional, steady, compressible, viscous flows N88-24904
SOLA-DM: A numerical solution algorithm for transient three-dimensional flows
[DE88-007159] N88-24913
Finite element solution of 3-D turbulent Navier-Stokes equations for propeller-driven slender bodies N88-24919
Review of numerical methods for radionuclide transport in three-dimensional porous media, at high Peclet numbers
[CFDU/87/10] N88-25061

THRUST
Development of a liquid-fed water resistojet
[NASA-TM-100927] N88-24968

THRUST VECTOR CONTROL
Method for prediction and determination of takeoff performance for vectored thrust vehicles
[AD-A191809] N88-24626
Attitude control laws for gas-jet spacecraft
N88-24643
TVC (Thrust Vector Control) jet vane thermal modeling using parametric system identification
[AD-A191518] N88-24678
THUNDERSTORMS
Analysis of lightning field changes during active thunderstorms in Florida N88-25103
TIME
Optimal discrete-time LQR problems for parabolic systems with unbounded input: Approximation and convergence
[NASA-CR-181673] N88-25247
TIME DEPENDENCE
Solving time-dependent two-dimensional eddy current problems
[NASA-TM-100875] N88-25239
TIME SERIES ANALYSIS
Adaptive time series analysis using predictive inference and entropy
[AD-A191858] N88-25199
TIME SHARING
Timesharing performance as an indicator of pilot mental workload
[NASA-CR-182807] N88-25150
TIMING DEVICES
Timing control system
[NASA-CASE-NPO-16882-1-CU] N88-24863
TIN
Photoionization dynamics and abundance patterns in laser vaporized tin and lead clusters
[AD-A191604] N88-24722
TITANIUM
Stiffened titanium panels
[NASA-CASE-LAR-13814-1] N88-24816
TITANIUM ALLOYS
Fundamental studies of beta phase decomposition modes in titanium alloys
[AD-A191495] N88-24740
On the reversion phenomena of Cu-3 percent Ti alloys
[NASA-TT-20170] N88-24762
TOKAMAK DEVICES
Systems analysis of INTOR-like designs
[DE88-004422] N88-25316
A study of runaway electron confinement in the ASDEX tokamak
[DE88-007327] N88-25319
A two-wavelength infrared interferometer/polarimeter system for CIT (Compact Ignition Tokamak)
[DE88-007681] N88-25321
TOLERANCES (PHYSIOLOGY)
Behavioral response of rats exposed to high-power microwave radiation
[AD-A192199] N88-25128
TOPOGRAPHY
Reports on cartography and geodesy. Series 1, no. 99
[ETN-88-92387] N88-25025
West German Geodetic Working Group: Official topographic-cartographic information system (ATKIS), content description N88-25026
West German Geodetic Working Group: Official topographic-cartographic information system (ATKIS), technical conception N88-25027
Creation of digital topographic models with the ALK-GIAP. The DLM 25 as an example N88-25031
Topographic data processing for environmental planning N88-25032
State of development of ALK (October 1986)
N88-25035
Vectorization of raster algorithms for elevation data processing N88-25036
Recent developments in software and hardware by Scitex Co. — computer aided mapping N88-25038
TOPOLOGY
Topological stereochemistry
[AD-A191867] N88-24691
TORSION
Strain hardening at large strains in aluminum alloys
[DE88-007415] N88-24737
The variation of torsional ductility of high-purity aluminum with temperature and strain rate
[DE88-005618] N88-24755
TOUGHNESS
Determination of the toughness of a brittle material using strain gages
[ETN-88-92540] N88-24993
TOXICITY
Evaluation of the toxicity of products from the thermal degradation of materials
[ETN-88-91995] N88-25130
TRACE ELEMENTS
Trace gas measurements in the troposphere using tunable diode lasers N88-25072
TRACKING (POSITION)
Descriptions of HF and VHF Loran-C buoys and evaluations as potential datum marker buoys
[AD-A192069] N88-24618
TRAFFIC
Digital maps for an electronic traffic guide
N88-25033
TRAILING EDGES
Axisymmetric viscid-inviscid interaction by a frozen vorticity approximation
[AD-A191743] N88-24885
Characteristics of merging shear layers and turbulent wakes of a multi-element airfoil
[NASA-TM-100053] N88-24900
TRAINING DEVICES
Parachute for in-flight training on parachute ejection
[REPT-87-11] N88-24593
TRAINING SIMULATORS
An enumeration of research to determine the optimal design and use of Army flight training simulators
[AD-A191242] N88-24649
TRAJECTORIES
A centered projective algorithm for linear programming
[AD-A192100] N88-25178
Accelerator research studies
[DE88-007124] N88-25290
TRAJECTORY OPTIMIZATION
Periodic solutions in aircraft cruise-dash optimization
N88-24631
TRANSDUCERS
Navigation system for land vehicles
[NASA-CASE-LAR-13322-1] N88-24620
TRANSFORMATIONS (MATHEMATICS)
An analytic model for aerodynamic shapes
[AD-A191573] N88-24583
Additive prophet inequalities for transforms of uniformly bounded pairwise independent random variables
[PB88-173513] N88-25250
TRANSIENT HEATING
Calculational model development for fibrous thermal insulation transient test procedures
[DE88-007843] N88-24789
TRANSIENT RESPONSE
SOLA-DM: A numerical solution algorithm for transient three-dimensional flows
[DE88-007159] N88-24913
TRANSITION FLOW
Prediction of laminar and turbulent flows past single and twin airfoils N88-24589
TRANSITION TEMPERATURE
Crystalline metal-semiconductor superlattices
[DE88-007063] N88-25332
TRANSMISSION LOSS
Low-loss, high-isolation, fiber-optic isolator
[NASA-CASE-NPO-17207-1-CU] N88-25304
TRANSMISSIONS (MACHINE ELEMENTS)
Design, manufacture and spin test of high contact ratio helicopter transmission utilizing Self-Aligning Bearingless Planetary (SABP)
[NASA-CR-4155] N88-24975
TRANSMITTANCE
Optical constants of minerals and other materials from the millimeter to the ultraviolet
[AD-A192210] N88-24724
Development and validation of transmission measurements techniques of image contrast, utilizing existing IR imagers
[AD-A191471] N88-25079
TRANSMITTERS
WIPP (Wave Induced Particle Precipitation) experiment logistic support
[AD-A191184] N88-24824
TRANSMUTATION
Construction of approximations to acoustic Green's functions for nonhomogeneous oceans using transmutation
[PB88-185384] N88-25128
TRANSONIC FLIGHT
Wind tunnel investigation of wing and control panel loads at transonic and supersonic speeds on some schematic cruciform missile configurations
[FFA-TN-1988-43] N88-24585
TRANSONIC FLOW
A transonic small disturbance wing design methodology N88-24590
The calculation of transonic flow over the shuttle orbiter using slender body theory N88-24606
Computational Fluid Mechanics
[NASA-CR-183022] N88-24915
TRANSONIC WIND TUNNELS
Design study. Manipulator systems for model handling in European transonic wind tunnels
[ETN-88-91944] N88-24651
TRANSPORT AIRCRAFT
Fuel containment concepts: Transport category airplanes
[AD-A189818] N88-24799
TRANSPORT PROPERTIES
Simplified curve fits for the transport properties of equilibrium air
[NASA-CR-178411] N88-24911
Stochasticity in a Q-machine plasma N88-25315
NASA research Program: The roles of fluid motion and other transport phenomena in the morphology of materials
[NASA-CR-182801] N88-25327
Electronic structure, elementary excitations, optical and transport properties of semiconductor superlattices
[AD-A190795] N88-25333
TRANSPORT THEORY
Physical properties of f electron systems
[DE88-006886] N88-25331
TRAVELING SALESMAN PROBLEM
A concurrent neural network algorithm for the traveling salesman problem
[DE88-006981] N88-25208
TRENDS
Development of a multipurpose smart recorder for general aviation aircraft
[NASA-CR-188353] N88-24837
The application of hydrocarbon bioconversion technology to aerospace materials production
N88-24898
TRIBOLOGY
Development of test methods for the electrostatic properties of nonhomogeneous fabrics, phase 2
[AD-A190853] N88-24767
TROPICAL STORMS
Tropical cyclones, 1987: Central North Pacific
[PB88-188081] N88-25119
TROPOSPHERE
Workshop on Atmospheric OH
[BPT-7/87] N88-25083
Effect of carbohydrate oxidation on the tropospheric HOx-system N88-25087
Trace gas measurements in the troposphere using tunable diode lasers N88-25072
Development of continuous wave laser frequency modulation of OH in tropospheric concentrations range
N88-25073
TUNABLE LASERS
Isotope separation using tuned laser and electron beam
[NASA-CASE-NPO-16907-1-CU] N88-24732
TUNGSTEN
Irradiation effects on tungsten stabilized martensitic steels
[DE88-007074] N88-24748
TUNGSTEN ALLOYS
Irradiation effects on tungsten stabilized martensitic steels
[DE88-007074] N88-24748
TUNING
State of tuning
[NASA-TT-20195] N88-25205
TURBINE BLADES
A 3 MW wood fired gas turbine at Red Boiling Springs, Tennessee N88-25051
TURBINES
Remote temperature-measurement instrumentation for a heated rotating turbine disk
[DE88-006456] N88-24925
TURBOCOMPRESSORS
Research on aero-thermodynamic distortion induced structural dynamic response of multi-stage compressor blading
[AD-A192189] N88-24584
Servojet retrofit
[AD-A191075] N88-24964
TURBOJET ENGINES
Aircraft emissions characterization: TF41-A2, TF30-P103 and TF30-P109 engines
[AD-A192053] N88-24638
TURBOMACHINERY
Forced response unsteady aerodynamics in a multistage compressor N88-24903
TURBOPROP AIRCRAFT
NASA/Industry advanced turboprop technology program
[NASA-TM-100929] N88-24641
TURBULENCE
Prediction of laminar and turbulent flows past single and twin airfoils N88-24589
Cross stream differencing for integral boundary layer equations
[AD-A191744] N88-24886
Fast algorithm development for large-eddy simulation of circular-jet turbulence
[AD-A192044] N88-24887

Three dimensional spectral energy measurement on turbulence subjected to a high degree of plane deformation
[ETN-88-92537] N88-24896
Computational Fluid Mechanics
[NASA-CR-183022] N88-24915
Modelling of thermal plasma systems N88-25314

TURBULENT BOUNDARY LAYER
Fundamental aspects of the structure of supersonic turbulent boundary layers
[AD-A191494] N88-24581
Computation of the turbulent boundary layer downstream of vortex generators
[AD-A191544] N88-24881
Theoretical investigation of 3-D shock wave-turbulent boundary layer interactions, part 6
[AD-A191546] N88-24882
The behavior of drop-containing turbulent eddies
[AD-A191669] N88-24883
Manipulation of the structure of a turbulent boundary layer N88-24901
Hypersonic turbulent wall boundary layer computations
[NASA-CR-182147] N88-24917

TURBULENT DIFFUSION
Continuum theories for fluid-particle flows: Some aspects of lift forces and turbulence
[DE88-007038] N88-24808

TURBULENT FLOW
Fundamental aspects of the structure of supersonic turbulent boundary layers
[AD-A191494] N88-24581
Wave growth associated with turbulent spots in plane Poiseuille flow
[FFA-TN-1988-08] N88-24567
Application of Rayleigh scattering to turbulent flow with heat transfer and combustion
[AD-A191565] N88-24720
Analysis of molecular mixing and chemical reaction in mixing layer
[AD-A191600] N88-24721
Stagnating turbulent reacting flows
[AD-A191449] N88-24877
Study of mixing and reaction in the field of a vortex
[AD-A191489] N88-24878
Dynamics and control of turbulent shear flows
[AD-A191527] N88-24879
Injection of drag reducing additives into turbulent water flows
[AD-A192072] N88-24888
CFD benefits, goals, stepping-stones and techniques. Proposals for the scientific programme of the European Research Centre on flow, turbulence and combustion — computational fluid dynamics
[CFDU/88/1] N88-24894
Duct flow nonuniformities for Space Shuttle Main Engine (SSME)
[NASA-CR-179338] N88-24899
Numerical solutions of the complete Navier-Stokes equations
[NASA-CR-183023] N88-24914
Finite element solution of 3-D turbulent Navier-Stokes equations for propeller-driven slender bodies N88-24919
Instrumentation for turbulent reacting flows
[AD-A191671] N88-24923
Low frequency electrostatic turbulence in the polar cap E-region
[DRI-3-88] N88-25077

TURBULENT HEAT TRANSFER
Application of Rayleigh scattering to turbulent flow with heat transfer and combustion
[AD-A191565] N88-24720
Stagnating turbulent reacting flows
[AD-A191449] N88-24877
Turbulent heat transfer and fluid flow measurements downstream of abrupt expansions and in a cavity of a circular tube at a uniform wall temperature N88-24920

TURBULENT JETS
Effect of initial tangential velocity distribution on the mean evolution of a swirling turbulent free jet
[NASA-TM-100934] N88-24592
Particle-laden weakly swirling free jets: Measurements and predictions
[NASA-TM-100920] N88-24639
Hydroacoustic pulsating jet generator
[MPIS-7/1987] N88-24891

TURBULENT MIXING
Study of mixing and reaction in the field of a vortex
[AD-A191489] N88-24878

TURBULENT WAKES
Characteristics of merging shear layers and turbulent wakes of a multi-element airfoil
[NASA-TM-100053] N88-24900

TWO DIMENSIONAL FLOW
Prediction of laminar and turbulent flows past single and twin airfoils N88-24589
Gas diffusion studies in steady and nonsteady cavities N88-24902

TWO FLUID MODELS
Computer simulation of turbulent combustion in reciprocating engines
[CFDU/87/11] N88-24725

U

U.S.S.R.
Bibliography of Soviet laser developments, number 83, May - June 1986
[AD-A190969] N88-24950

ULTRASONIC FLAW DETECTION
Nondestructive testing using ultrahigh frequencies
[CERT-5/1333-MO] N88-24984

ULTRASONIC TESTS
Interaction of ultrasonic waves with composite plates
[AD-A191879] N88-24702
Knowledge based systems in nondestructive evaluation
[DE88-006853] N88-24981

ULTRAVIOLET ABSORPTION
Temperature dependence of ultraviolet absorption cross sections of chlorofluoroethanes
[AERONOMICA-ACTA-A-325-1987] N88-24726

ULTRAVIOLET LASERS
An investigation of 2-6 superlattice deposition by laser photochemical techniques
[AD-A191547] N88-25336

ULTRAVIOLET RADIATION
Determination of tropospheric H concentrations by a double-pulsed UV laser method N88-25070

ULTRAVIOLET SPECTRA
Optical constants of minerals and other materials from the millimeter to the ultraviolet
[AD-A192210] N88-24724
An investigation of 2-6 superlattice deposition by laser photochemical techniques
[AD-A191547] N88-25336
Ultraviolet spectra of subluminous objects found in the Kiso Schmidt survey and systematic reanalysis of the archived ultraviolet spectra of white dwarfs observed with the IUE satellite under the Astrophysics Data Program (ADP)
[NASA-CR-182976] N88-25406
Ultraviolet spectra of two magnetic white dwarfs and ultraviolet spectra of subluminous objects found in the Kiso Schmidt survey
[NASA-CR-183051] N88-25408

UNDERGROUND STRUCTURES
Finite element analysis of an underground structure
[AD-A191747] N88-24991

UNDERWATER ACOUSTICS
Construction of approximations to acoustic Green's functions for nonhomogeneous oceans using transmutation
[PB88-185364] N88-25126
Evaluation of the biot coefficients
[AD-A191643] N88-25265

UNDERWATER OPTICS
Activities report of the Division of Optical Technology
[FOA-C-30477-3] N88-25299

UNSTEADY FLOW
Research on aero-thermodynamic distortion induced structural dynamic response of multi-stage compressor blading
[AD-A192169] N88-24584
Unsteady flow in a supercritical supersonic inlet N88-24605
Forced response unsteady aerodynamics in a multistage compressor N88-24903
Numerical simulation of nonlinear structural dynamics of large scale unsteady flow
[ETN-88-92156] N88-24908

UPLINKING
Experimental radio frequency link for Ka-band communications applications
[NASA-TM-100824] N88-24859

UPPER ATMOSPHERE
Observations of wave number dependent spectral line ratio fluctuations in the atmospheric emissions
[IRF-PREPRINT-101] N88-25085

URANUS ATMOSPHERE
Superthermal electron processes in the upper atmosphere of Uranus: Aurora and electroglow
[NASA-TM-101150] N88-25417

URBAN TRANSPORTATION
Digital maps for an electronic traffic guide N88-25033

USER MANUALS (COMPUTER PROGRAMS)
User's guide to the Fault Inferring Nonlinear Detection System (FINDS) computer program
[NASA-CR-178410] N88-24619
SAM 2 data user's guide
[NASA-RP-1200] N88-25094

USER REQUIREMENTS
P-Plus: Polar Platform utilization study, executive summary
[BAE-TP-8391] N88-24853
CIMAG2: The computer program to generate color images
[AD-A191847] N88-25175
Department of Defense statement on the X-ray Lithography Program to the Research and Development Subcommittee of the House Armed Services Committee of 100th Congress, second session
[AD-A191854] N88-25341
Advanced development of double-injection, deep-impurity semiconductor switches
[NASA-CR-182118] N88-25348
Mars rover/sample return mission requirements affecting space station
[NASA-CR-172048] N88-25414

V

VACUUM
Propagation of neutralized ion beams
[AD-A191599] N88-25289

VACUUM APPARATUS
Low temperature storage container for transporting perishables to space station
[NASA-CASE-MFS-28248-1] N88-24817

VACUUM SYSTEMS
Flotation processes
[PB88-180302] N88-25075

VANADIUM ALLOYS
Effect of hydrogen, deuterium and oxygen on the anelastic properties of refractory alloys
[DE88-007349] N88-24736

VAPOR DEPOSITION
Joint services electronics program research in electronics
[AD-A192206] N88-24857
An investigation of 2-6 superlattice deposition by laser photochemical techniques
[AD-A191547] N88-25336
Optical nonlinearities in GaAs/GaAlAs multiple quantum wells fabricated by metalorganic chemical vapor deposition for use in optical signal processing
[AD-A191558] N88-25337

VAPOR PRESSURE
Effects of moderate cold and heat stress on the potential work performance of industrial workers. Part 6: The effects of increasing vapour pressure at four air temperatures on the performance and physiology of white females
[PB88-124854] N88-25137

VAPORIZERS
Development of a liquid-fed water resistojet
[NASA-TM-100927] N88-24988

VAPORIZING
Photoionization dynamics and abundance patterns in laser vaporized tin and lead clusters
[AD-A191604] N88-24722
High-energy laser-assisted imaging through vaporizing aerosols
[DE88-007911] N88-24957

VAPORS
Photoconductivity in carbon fibers
[AD-A191728] N88-24782
Molecular-beam, mass-spectrometric studies of wood vapor and model compounds over HZSM-5 catalyst N88-25044
Upgrading pyrolysis vapors to aromatic gasoline with zeolite catalysis at atmospheric pressure N88-25045

VARIABLE GEOMETRY STRUCTURES
Structurally tailorable non-linear snap-through spring system
[NASA-CASE-LAR-13729-1] N88-24970

VARIABLE PITCH PROPELLERS
Structurally tailorable non-linear snap-through spring system
[NASA-CASE-LAR-13729-1] N88-24970

VARIANCE (STATISTICS)
Variances and higher order correlation coefficients: Continued
[RR-655-M] N88-25219
Operational noise data for CH-47D and AH-64 army helicopters
[AD-A191059] N88-25263

VAX COMPUTERS
SAMS: The synchronization and monitoring system for ATF (Advanced Toroidal Facility) data acquisition provides unified data access for ATF data acquisition
[DE88-007268] N88-25386

VECTOR ANALYSIS
An FSK (Frequency Shift Keying) telemetry module for vector measuring current meters
[AD-A192142] N88-24661
Improving the performance of a finite element method using vector analysis on CRAY 1
[ETN-88-92153] N88-24907
Gram-Schmidt implementation of a linearly constrained adaptive array
[AD-A191651] N88-25198
VECTOR CURRENTS
An FSK (Frequency Shift Keying) telemetry module for vector measuring current meters
[AD-A192142] N88-24661
VECTORS (MATHEMATICS)
Vector graphics and raster data processing for spatial information systems N88-25028
Electric field measurement by S-520-9 sounding rocket using the time of flight technique of lithium ion beam
[ISAS-RN-367] N88-25095
VEGETATION
Monitoring biological impacts of space shuttle launches from Vandenberg Air Force Base: Establishment of baseline conditions
[NASA-TM-100982] N88-25133
VELOCITY DISTRIBUTION
Effect of initial tangential velocity distribution on the mean evolution of a swirling turbulent free jet
[NASA-TM-100934] N88-24592
Theoretical investigation of the development of the normal fluid and superfluid velocity distributions during spin-up for a He2-filled cylinder
[MPIS-6/1987] N88-24892
A single streamwise vortical structure and its instability in shear flows N88-24921
VENTILATION
Evaluation of the toxicity of products from the thermal degradation of materials
[ETN-88-91995] N88-25130
VERY HIGH FREQUENCIES
Descriptions of HF and VHF Loran-C buoys and evaluations as potential datum marker buoys
[AD-A192069] N88-24618
Theoretical basis for an experimental test with regard to the origin of VHF (Very High Frequency) radiation from natural lightning
[DE88-007535] N88-25102
VERY LARGE SCALE INTEGRATION
Defect detection and classification in VLSI pattern inspection N88-24871
Some unsolved problems in modelling self-timed circuits using Petri Nets, series B, number 2
[PB88-181466] N88-24872
SYMBL: A new Boolean compiler N88-25160
An improved simulated annealing algorithm for standard cell placement
[NASA-CR-182952] N88-25183
Mathematical models for VLSI device simulation
[AD-A191125] N88-25212
VERY LOW FREQUENCIES
WIPP (Wave Induced Particle Precipitation) experiment logistic support
[AD-A191184] N88-24824
VIBRATION
Low authority control of large space structures using a constrained threshold control formulation N88-24667
A dynamic analysis of piezoelectric strained elements
[AD-A191478] N88-24851
Effects of Coriolis acceleration on the vibrations of spinning structures N88-24966
Vibration protection of inelastic structures by means of active and passive control N88-25001
Vibrations of rotating thick or thin rings N88-25003
Bimolecular reactions and energy-transfer processes of highly vibrationally excited molecules related to energetic materials
[AD-A189013] N88-25270
Para-ortho abundance ratio of molecular hydrogen in NGC2023
[ISAS-RN-352] N88-25286
Spectroscopy and energy transfer kinetics of the interhalogens
[AD-A192103] N88-25344
VIBRATION DAMPING
Experimental vibration damping characteristics of the third-stage rotor of a three-stage transonic axial-flow compressor
[NASA-TM-100948] N88-24642
Electromagnetic damping and vibration isolation of space structures
[AD-A191492] N88-24665
Experimental study of active vibration control
[AD-A191454] N88-24989
VIBRATIONAL SPECTRA
Energy-transfer properties and mechanisms
[DE88-007107] N88-25272
Molecular characterization of structure and bonding in thin film materials
[DE88-006811] N88-25351
VIDEO EQUIPMENT
System overview: Teragon 4000, an image processing equipment at FOA 3
[FOA-C-30465-3.3] N88-25179
VIDEO SIGNALS
Simple high speed camera with CCD-sensor
[MPIS-8/1987] N88-24940
Design and testing of a luminance and chrominance stabilization system for a computer-controlled color display
[AD-A191922] N88-25159
VINYL POLYMERS
Preferential surface adsorption in miscible blends of polystyrene and poly(vinyl methyl ether)
[AD-A191451] N88-24769
VISCOELASTIC CYLINDERS
Calculation of rolling contact of two viscoelastic cylinders with application to the steady state normal contact problem
[ILR-MITT-188] N88-25008
VISCOELASTICITY
Damage by creep fatigue: Influence of the visco-elasticity of the matrix
[PB88-124706] N88-24998
VISCOPLASTICITY
Theory of viscoplasticity based on overstress with applications N88-25007
VISCOUS FLOW
Composite reduced Navier-Stokes procedures for flow problems with strong pressure interactions
[AD-A191127] N88-24875
Theoretical investigation of 3-D shock wave-turbulent boundary layer interactions, part 6
[AD-A191546] N88-24882
Axisymmetric viscid-inviscid interaction by a frozen vorticity approximation
[AD-A191743] N88-24885
A variational finite element method for three-dimensional, steady, compressible, viscous flows N88-24904
VISUAL AIDS
Simulator evaluation of lineup visual landing aids for night carrier landing
[AD-A191212] N88-24648
VISUAL PERCEPTION
Visual information processing in the perception of features and objects
[AD-A192026] N88-25148
Shape from shading, occlusion and texture
[AD-A184840] N88-25269
VISUAL SIGNALS
Analysis procedures and subjective flight results of a simulator validation and cue fidelity experiment
[NASA-TM-88270] N88-24634
VISUAL STIMULI
A systems engineering based methodology for analyzing human electrocortical responses
[AD-A190809] N88-25135
VOICE COMMUNICATION
Time-frequency representations for speech signals
[AD-A188661] N88-24819
VOIDS
Vacancy ordering in the basal plane of YBa2Cu3O(sub)z
[DE88-004572] N88-25348
VOLTAGE CONTROLLED OSCILLATORS
Radio Frequency (RF) strain monitor
[NASA-CASE-LAR-13705-1] N88-25011
VOLTERRA EQUATIONS
Computational sciences
[AD-A190826] N88-25226
Numerical solution of a system of random Volterra integral equations. 1: Successive approximation method N88-25227
Numerical solution to a system of random Volterra integral equations N88-25230
Numerical solution of linear integral equations with random forcing terms N88-25237
VORTEX ALLEVIATION
Computation of the turbulent boundary layer downstream of vortex generators
[AD-A191544] N88-24881
VORTEX GENERATORS
Computation of the turbulent boundary layer downstream of vortex generators
[AD-A191544] N88-24881
VORTICES
Unsteady flow around a profile subjected to pulsed motions
[ETN-88-92151] N88-24594
Study of mixing and reaction in the field of a vortex
[AD-A191489] N88-24878
The behavior of drop-containing turbulent eddies
[AD-A191689] N88-24883
Fast algorithm development for large-eddy simulation of circular-jet turbulence
[AD-A192044] N88-24887
VORTICITY
Computation and characteristics of pulsatile multi-bifurcation flow N88-24729
Axisymmetric viscid-inviscid interaction by a frozen vorticity approximation
[AD-A191743] N88-24885
A single streamwise vortical structure and its instability in shear flows N88-24921

W

WAFERS
A monolithic reduced-size Ku-Band SPOT (Single-Pole Double Throw) FET switch
[DE88-006273] N88-24858
Determination of doping profiles in silicon from resistivity measurements via the four-point probe in combination with layer strippings via anodic oxidation N88-25347
WAKES
Unsteady flow around a profile subjected to pulsed motions
[ETN-88-92151] N88-24594
Supplements to the study of the wake of a Mirage G8 model at F2 — wind tunnel
[CERT-RT-OA-20/5025-AYD] N88-24596
WALL FLOW
Heat transfer from a negatively buoyant wall jet
[PB88-181953] N88-24873
Hypersonic turbulent wall boundary layer computations
[NASA-CR-182147] N88-24917
WALL TEMPERATURE
Turbulent heat transfer and fluid flow measurements downstream of abrupt expansions and in a cavity of a circular tube at a uniform wall temperature N88-24920
WARFARE
Acta aeronautica et astronautica sinica (selected articles)
[AD-A191552] N88-24575
WARNING SYSTEMS
Rotorcraft TCAS (traffic alert and collision avoidance system) evaluation: Group 3 results
[AD-A191719] N88-24614
WASTE DISPOSAL
Review of numerical methods for radionuclide transport in three-dimensional porous media, at high Peclet numbers
[CFDU/87/10] N88-25061
WATER
Photosynthetic water splitting
[PB88-188891] N88-24731
Development of a liquid-fed water resistojet
[NASA-TM-100927] N88-24968
WATER FLOW
Injection of drag reducing additives into turbulent water flows
[AD-A192072] N88-24888
WATER HAMMER
Hydroacoustic pulsating jet generator
[MPIS-7/1987] N88-24891
WATER TEMPERATURE
Evaluating evaporation with satellite thermal data
[AD-A192042] N88-25019
WATER WAVES
Research in nonlinear wave motion
[AD-A191686] N88-24884
WAVE EQUATIONS
Nonlinear waves
[AD-A192148] N88-24889
MHD bending waves in a current sheet
[NASA-TM-101149] N88-25323
WAVE INTERACTION
Electron-Rayleigh wave interaction in thin film carbons
[AD-A191727] N88-24781
WAVE PROPAGATION
Wave growth associated with turbulent spots in plane Poiseuille flow
[FFA-TN-1988-08] N88-24587
Nonlinear wave propagation
[AD-A192104] N88-24835
Research in nonlinear wave motion
[AD-A191686] N88-24884
Nonlinear waves
[AD-A192148] N88-24889
Atmospheric propagation of laser beams
[AD-A191447] N88-24952
Evaluation of the biot coefficients
[AD-A191643] N88-25265
Light propagation through gravitationally perturbed Friedmann universes N88-25307

WAVE SCATTERING
Multiple scattering of waves in discrete random media
[AD-A191068] N88-24823
WAVEGUIDE LASERS
Distributed feedback lasers
[NASA-CR-4154] N88-24948
WAVEGUIDES
Nonlinear surface polaritons
[AD-A191046] N88-24822
Signal processing with degenerate four-wave mixing
[AD-A191496] N88-24825
WAVES
Brunt-Doppler ducting of buoyancy waves in a temperature- and wind-stratified atmosphere N88-25086
WEATHER
Components of an atmospheric lidar system: Doppler wind lidar
[AD-A191222] N88-24951
Mariners weather log, volume 32, number 1, Winter 1988
[PB88-173889] N88-25097
Meteorological and Environmental Inputs to Aviation Systems
[NASA-CP-2498] N88-25105
WEATHER FORECASTING
Adaptive grid refinement for numerical weather prediction
[AD-A192172] N88-25101
Automation of surface observations program N88-25106
Special observations N88-25108
General-aviation's view of progress in the aviation weather system N88-25110
National plans for aircraft icing and improved aircraft icing forecasts and associated warning services N88-25113
Objective detection and forecasting of Clear-Air Turbulence (CAT): A status report N88-25114
Denver ARTCC evaluation of PROFS (Prototype Regional Observations and Forecast System) mesoscale weather products N88-25117
WEATHER MODIFICATION
The Effect of the Ionosphere on Communication, Navigation and Surveillance Systems Based on Ionosph eric Effects Symposium held on 5-7 May 1987 in Springfield, Virginia
[AD-A191855] N88-25081
WEATHERING
A sedimentological and mineralogical study of the Koogah Formation, New South Wales N88-25087
WEDGE FLOW
Compressible flow in a pie-shaped cylinder rotating about the vertex N88-24604
WEIGHTING FUNCTIONS
Asymptotic theory for weighted least squares estimators in Aalen's additive risk model
[AD-A191085] N88-25210
WEIGHTLESSNESS
Cardiovascular effects of weightlessness and ground-based simulation
[NASA-TM-98314] N88-25140
WELDED JOINTS
Microstructural characterization and properties of 3Cr-1.5Mo-0.1V thick section electron beam welds
[DE88-004330] N88-24747
WELDING
Frequency Analysis of Acoustic Emission - Application to machining and welding
[DE88-701478] N88-25262
WEST GERMANY
West German Geodetic Working Group: Official topographic-cartographic information system (ATKIS), content description N88-25026
West German Geodetic Working Group: Official topographic-cartographic information system (ATKIS), technical conception N88-25027
Creation of digital topographic models with the ALK-GIAP. The DLM 25 as an example N88-25031
State of development of ALK (October 1986) N88-25035
Results of radiation measurements in West Germany and from special measurement series in the Meteorological Observatory of Hamburg
[REPT-11] N88-25066
WHITE DWARF STARS
Ultraviolet spectra of subluminous objects found in the Kiso Schmidt survey and systematic reanalysis of the archived ultraviolet spectra of white dwarfs observed with the IUE satellite under the Astrophysics Data Program (ADP)
[NASA-CR-182976] N88-25406
Ultraviolet spectra of two magnetic white dwarfs and ultraviolet spectra of subluminous objects found in the Kiso Schmidt survey
[NASA-CR-183051] N88-25408
WIDEBAND COMMUNICATION
The Effect of the Ionosphere on Communication, Navigation and Surveillance Systems Based on Ionosph eric Effects Symposium held on 5-7 May 1987 in Springfield, Virginia
[AD-A191855] N88-25081
WILDERNESS
History of wildland fires on Vandenberg Air Force Base, California
[NASA-TM-100983] N88-25134
WIND (METEOROLOGY)
Report on project WIND: Preliminary experiments w ith the UK Meteorological Office mesoscale model, September 1987
[AD-A191621] N88-25099
WIND MEASUREMENT
Overview of wind behavior research in the US Wind Energy Program
[DE88-005683] N88-25057
Special observations N88-25108
Aircraft/lidar turbulence comparison N88-25111
WIND PROFILES
Special observations N88-25108
WIND SHEAR
The Federal Aviation Administration/Massachusetts Institute of Technology (FAA/MIT) Lincoln Laboratory Doppler weather radar program N88-25118
WIND TUNNEL MODELS
Inflow measurements made with a laser velocimeter on a helicopter model in forward flight. Volume 1: Rectangular planform blades at an advance ration of 0.15
[NASA-TM-100541] N88-24607
WIND TUNNEL TESTS
Aerodynamic performance and pressure distributions for a NASA SC(2)-0714 airfoil tested in the Langley 0.3-meter transonic cryogenic tunnel
[NASA-TM-4044] N88-24580
Experiment investigation on longitudinal characteristics of the forward swept wing
[AD-A191553] N88-24582
Passive shock wave-boundary layer control for the Bell FX89-H-098 airfoil N88-24588
Unsteady flow around a profile subjected to pulsed motions
[ETN-88-92151] N88-24594
Supplements to the study of the wake of a Mirage G8 model at F2 — wind tunnel
[CERT-RT-OA-20/5025-AYD] N88-24596
Summary of low-speed wind tunnel results of several high-speed counterrotation propeller configurations
[NASA-TM-100945] N88-24597
High speed and high angle of attack aerodynamic characteristics of winged space vehicle
[ISSN-0285-6808] N88-24599
WIND TURBINES
Yaw dynamics of horizontal axis wind turbines
[DE88-001137] N88-25055
WIND VELOCITY
Overview of wind behavior research in the US Wind Energy Program
[DE88-005683] N88-25057
WINDPOWER UTILIZATION
Overview of wind behavior research in the US Wind Energy Program
[DE88-005683] N88-25057
WINDPOWERED GENERATORS
Overview of wind behavior research in the US Wind Energy Program
[DE88-005683] N88-25057
WING PLANFORMS
Computational design of low aspect ratio wing-winglet configurations for transonic wind-tunnel tests
[NASA-CR-183021] N88-24630
WING TIP VORTICES
Wave growth associated with turbulent spots in plane Poiseuille flow
[FFA-TN-1988-08] N88-24587
WINGLETS
Computational design of low aspect ratio wing-winglet configurations for transonic wind-tunnel tests
[NASA-CR-183021] N88-24630
WINGS
High speed and high angle of attack aerodynamic characteristics of winged space vehicle
[ISSN-0285-6808] N88-24599
Applications of the Navier-Stokes equations to wings and complex configurations using a zonal approach
[NASA-TM-100080] N88-24602
Investigation of the effect of minimum loads and compression of load spectra on the prediction capacities of the ONERA crack model — wings
[ONERA-RTS-33/7169-RY-064-R] N88-24994
WIRING
An improved simulated annealing algorithm for standard cell placement
[NASA-CR-182952] N88-25183
WOLF-RAYET STARS
Review of the theoretical changes of surface chemistry during massive star evolution
[SER-C-PREPUBL-FASC-17] N88-25411
WOOD
Proceedings of the 1987 Biomass Thermochemical Conversion Contractors' Review Meeting
[DE88-006730] N88-25041
An advanced extruder-feeder biomass liquefaction reactor system N88-25042
Low pressure entrained flow pyrolysis of biomass to produce liquid fuels N88-25043
Molecular-beam, mass-spectrometric studies of wood vapor and model compounds over HZSM-5 catalyst N88-25044
Research on hydrotreating catalysts to hydrodeoxygenate biocrude oils N88-25046
Bench-scale studies on fluid-bed pyrolysis of wood using different contact gases N88-25049
A 3 MW wood fired gas turbine at Red Boiling Springs, Tennessee N88-25051
WORK-REST CYCLE
Performance effectiveness and the work/rest cycle
[AD-A191448] N88-25145
WORKLOADS (PSYCHOPHYSIOLOGY)
An evaluation of three linear scale radar altimeter displays
[AD-A192173] N88-24636
Timesharing performance as an indicator of pilot mental workload
[NASA-CR-182807] N88-25150
Simultaneous multiple control force exertion capabilities of males and females versus helicopter control force design limits
[AD-A191653] N88-25153
WRIST
Real-time implementation of a kinematic optimization scheme for seven-degree-of-freedom redundant robots with spherical wrists
[DE88-006785] N88-24974

X

X RAY ANALYSIS
Detecting delaminations in CFRP specimens using X-ray techniques
[FFA-TN-1988-04] N88-24704
Electrochemistry in liquid crystals
[AD-A191554] N88-24719
On the reversion phenomena of Cu-3 percent Ti alloys
[NASA-TT-20170] N88-24762

Y

YAW
Actuated forebody strakes
[NASA-CASE-LAR-13983-1] N88-24628
Yaw dynamics of horizontal axis wind turbines
[DE88-001137] N88-25055
YIELD STRENGTH
Rapidly solidified lightweight durable disk material
[AD-A191697] N88-24775
YTTRIUM OXIDES
Vacancy ordering in the basal plane of YBa2Cu3O(sub)z
[DE88-004572] N88-25348
YTTRIUM-ALUMINUM GARNET
Characterization of yttrium aluminum garnet/YAG/using 14 MeV neutron activation
[AD-A191925] N88-25342

Z

ZEOLITES
Upgrading pyrolysis vapors to aromatic gasoline with zeolite catalysis at atmospheric pressure N88-25045
ZINC
Influence of alternating magnetic fields on Zn-67 Moessbauer resonance in ZnO
[PB88-186432] N88-25352
ZINC OXIDES
Influence of alternating magnetic fields on Zn-67 Moessbauer resonance in ZnO
[PB88-186432] N88-25352
ZIRCONIUM ALLOYS
The precipitation processes of Cu-Zr-Cr alloys
[NASA-TT-20168] N88-24758

Typical Personal Author Index Listing

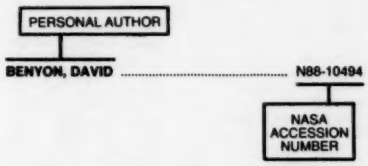

Listings in this index are arranged alphabetically by personal author. The NASA accession number denotes the number by which the citation is identified.

A

AARONSON, H. I. N88-24740
ABDALLAH, M. N88-24709
ABLOWITZ, MARK J. N88-24835
N88-24889
ABRUNA, HECTOR D. N88-24719
ABU-MOSTAFA, YASER N88-25214
ADAIR, DESMOND N88-24900
ADAMS, WILLIAM M., JR. N88-24623
ADDISON, R. N88-24786
AFFENS, WILBUR A. N88-24803
AKTAS, YILDIRIM N88-25312
ALBARES, D. J. N88-24854
ALBRECHT, R. N88-25283
ALLEN, ARTHUR A. N88-24618
ALLEN, J. D. N88-25194
ALLEN, J. L. N88-24943
ALLEN, MYRON B. N88-24890
ALLTON, CHARLES N88-24671
ALSALIHI, ZUHEYR N88-24897
ALTHOFF, SUSAN L. N88-24607
AMANN, C. A. N88-24730
AN, C.-H. N88-25423
ANCELLE, J. N88-24792
ANDERSON, J. E. N88-25322
ANDREWS, J. T. N88-24948
ANNIGERI, B. S. N88-24992
APPELT, GERFRIED N88-25027
ARCHER, D. G. N88-24735
ARENTON, M. W. N88-25274
ARIJS, E. N88-25084
ARMERDING, W. N88-25069
ARMSTRONG, ROBERT L. N88-24952
ARNAL, D. N88-24595
ARNOLD, F. E. N88-24773
N88-24774
ARNOLD, FRED E. N88-24695
ARNOLD, GRAHAM S. N88-25400
ARRERAJARAIZ, JOSE MARIA N88-25053
ASAY, J. R. N88-24657
ASSICE, ANTOINE N88-24984
ATTAIS, A. J. N88-24792
ATTAR, SHAUL N88-24980
AU, W. N88-25119
AVERBUCH, AARON J. N88-25263
AVILA, EDWARD RAYMOND N88-24643
AWES, T. C. N88-25283

B

BABARSKY, RICHARD JOSEPH N88-24604
BABCOCK, S. M. N88-24974
BADCOCK, CHARLES C. N88-24855
BAHNSEN, A. N88-25077
BAILEY, F. R. N88-25196
BAILEY, J. N88-25308
BAILEY, J. E. N88-24926
BAIRD, J. K. N88-24809
BAKER, CHARLES R. N88-24838
BAKER, D. N. N88-25083
BAKER, EDDIE G. N88-25046
BAKOWSKY, L. N88-24959
BAKTASH, C. N88-25283
BALAGUROV, A. M. N88-25326
BALES, THOMAS T. N88-24816
BALK, J. K. N88-24658
BALLARD, D. G. H. N88-24699
BAMBERGER, S. N88-24809
BANERJEE, PRITHVIRAJ N88-25183
BANKS, BRUCE A. N88-24754
BANKS, H. T. N88-25246
BANKS, S. P. N88-25221
BANNER, CARL N88-25129
BARBAUX, Y. N88-24751
N88-24752
BARD, ALLEN J. N88-24723
BARKER, JOHN R. N88-25270
N88-25272
BARKHIMER, ROBERT L. N88-24964
BARNETT, CLIFFORD J. N88-24660
BARRON, W. N88-25163
BARRY, JENNIFER N88-24754
BARRY, R. N88-25024
BARSON, JOHN V. N88-24835
BAUDIN, G. N88-24994
BAUER, RONALD S. N88-24696
BAUMANN, JAMES M. N88-24624
BAYLOR, L. R. N88-25385
BEAGHTON, PANTELIS JOHN N88-25328
BECK, JOHN N88-24964
BECKER, K. H. N88-25066
BECKMANN, P. N88-25283
BEDFORD, A. N88-25265
BEHREND, TRACY N88-24754
BELIAN, R. D. N88-25063
BELL, G. I. N88-25131
BELLAN, JOSETTE N88-24883
BEN-SHALOM, AMI N88-25079
BENDER, EDWARD A. N88-25171
BENDER, ROBERT L. N88-24676
BENNDORF, KLAUS N88-25028
BENTLEY, R. K. N88-25340
BERAN, DONALD N88-25106
BERERA, A. N88-25348
BERGER, F. N88-25283
BERGLIND, TORSTEN N88-24586
BERGLUND, OLOF N88-25179
BERNHARDT, PAUL A. N88-25403
BESKROVNYJ, A. I. N88-25326
BHATIA, Q. S. N88-24769
BICKLER, DONALD B. N88-24973
BIDLACK, TIMOTHY JOHN N88-24588
BIEDRON, ROBERT THOMAS N88-24605
BIELER, T. N88-24741
BIERMANN, ALAN W. N88-25197
BIGELOW, C. A. N88-24713
BILLINGS, S. A. N88-25257
BINIENDA, W. N88-24700
BIRCH, DAVID N88-25145
BISOGNANO, J. J. N88-25291
BJORNN, K. R. N88-25370
BLACHER, R. N88-25219
BLACK, F. M. N88-25076
BLACKBURN, LINDA B. N88-24753
BLACKBURN, M. J. N88-24775
BLAIR, L. S. N88-24955
BLAKE, J. B. N88-25083
BLANCOTEMPRANO, CRISTINA N88-25053
BLOCH, B. N88-24792
BLOCHER, REINER N88-24651
BOCK, R. N88-25283
BOESCH, HAROLD E., JR. N88-25345
BOHLEY, ERIC P. N88-24832
BONDI, HERMANN N88-25020
BORELLA, H. M. N88-24925
BORIS, J. P. N88-25277
BOSE, B. K. N88-24859
BOSHUIZEN, F. A. N88-25250
BOTA, K. B. N88-25234
N88-25235
BOTA, KOFI B. N88-25226
BOUCHARDY, P. N88-24727
BOUGHAZI, MOHAMED N88-25217
BOULDIN, D. W. N88-25194
BOWMAN, C. T. N88-24730
BOYCE, J. N88-24809
BRADAS, JAMES C. N88-25365
BRANCH, MELVYN C. N88-24802
BRASCHE, LISA HAGER N88-24736
BRATES, NANU N88-25313
BRAUNSTEIN, G. N88-24782
BRAVEN, K. D. N88-25370
BREMNECKE, JUERGEN N88-25029
N88-25030
BRENNER, A. N88-24714
BRILL, THOMAS B. N88-24716
BRINKER, DAVID J. N88-24870
BROCK, E. R. N88-24926
BROOKS, D. E. N88-24809
BROOKS, E. D., III N88-25195
BROPHY, J. R. N88-24677
BROWN, CHRISTOPHER K. N88-24630
BROWN, CHRISTOPHER WILLIAM N88-24969
BROWN, M. D. N88-25049
BROWN, THOMAS V. N88-25149
BRUEGGEMANN, HEINZ N88-25031
BRUNEAU, C. H. N88-24907
BRUNO, LEONARD C. N88-25428
BRUSMARK, B. N88-24821
BRYANT, D. T. N88-24858
BUDEN, D. N88-24661
BULZAN, DANIEL L. N88-24639
BURCH, J. V. N88-24812
BURKE, JAMES D. N88-24944
BURKE, W. R. N88-24670
BURNS, FORREST N88-25342
BURROWS, M. D. N88-24955
BURSTEIN, MARK N88-25144
BURTON, RODNEY L. N88-24679
BUTLER, P. L. N88-25194
BUTLER, W. H. N88-24756
BUTNER, R. S. N88-25047
BYRNES, JAMES S. N88-25211

C

CACHOGOMEZ, JAVIER N88-25074
CADARETTE, BRUCE S. N88-25139
CADWELL, K. L. N88-24755
CAGLAYAN, A. K. N88-24619
CAGLE, LANA G. N88-25080
CALEDONIA, G. E. N88-25402
CALHOUN, GLORIA L. N88-25143
CALVERT, J. F. N88-24626
CAMLEY, R. E. N88-25334
CAMONALVAREZ, FRANCISCO N88-25053
CAMP, DENNIS W. N88-25105
CAMPBELL, SCOTT R. N88-24942
CANAVAN, G. H. N88-24947
CANNON, RAYMOND K. N88-24573
CANNON, T. W. N88-25056
CAPECE, VINCENT RALPH N88-24903
CAPERAN, PH. N88-24896
CARLSSON, LEIF N88-24704
CARNEY, LYNNETTE M. N88-24682
CAROL, M. N88-24593
CARR, C. N88-24632
CARR, LARRY A. N88-24636
CARR, PETER C. N88-24634
CARROLL, R. J. N88-25254
CARTER, DANIEL C. N88-25356
CARTER, PATRICIA W. N88-24577
CARTER, W. C. N88-25350
CARTWRIGHT, D. C. N88-24955
CASLAVSKY, JAROSLAV L. N88-25342
CASPER, PATRICIA A. N88-25150
CATES, M. R. N88-24925
CAUX, X. N88-24788
CAZIER, F. W., JR. N88-24596
CEBECI, TUNCER N88-24876
CETEGEN, B. M. N88-24721
N88-24878
CHAE, SOO-IK N88-24871
CHALKOV, V. S. N88-25015
CHANANE, B. N88-25221

CHANDLER, M. O. N88-25417
CHANDRASEKHAR, I. N88-25277
CHANG, PAUL K. N88-24881
CHAO, BEEI-HUAN N88-24728
CHAO, TIEN-HSIN N88-25301
N88-25305
CHATO, DAVID J. N88-24666
CHEDIN, A. N88-25069
CHEESEMAN, PETER N88-25236
CHEN, CHUNG-WEN N88-25244
CHEN, MAU H. N88-25275
CHEN, MICHAELINE F. N88-25342
CHEN, QI N88-24997
CHEN, S. N88-25257
CHIANG, K. T. N88-24743
CHIRICO, R. D. N88-24735
CHO, K. N88-24785
CHOKSHI, A. H. N88-24741
CHOUDRY, A. N88-24738
CHU, ELEANOR N88-25191
CHU, W. P. N88-25094
CHUN, A. N88-25119
CHUNG, JACOB N. N88-24860
CHUTJIAN, ARA N88-25281
CHYOU, YAU-PIN N88-25314
CICCI, DAVID ALLEN N88-25222
CIESNIK, M. S. N88-25023
CIFANI, DIANE N88-24712
CLAESSON, G. N88-25283
CLANCY, JOHN P. N88-24927
CLARK, JANE E. N88-25155
CLARKE, DUNCAN E. N88-25169
CLARKE, W. P. N88-25370
CLEMENT, PH. N88-25258
CLIFFTON, E. N88-24632
CLIFTON, K. S. N88-25397
COHEN, JOSEPH N88-25151
COLBURN, D. S. N88-25420
COLLIER, W. B. N88-24735
COLLIN, G. N88-24727
COLLINS, ALLAN N88-25144
COLLINS, D. A. N88-25338
COLLINS, EARL R., JR. N88-24814
COMES, F. J. N88-25069
COMES, FRANZ JOSEF N88-25063
CONDON, J. B. N88-24757
CONEY, THOM A. N88-24663
CONKLIN, NANCY F. N88-25375
CONRAY, MARTIN J. N88-24659
COOPER, G. N88-25308
COPELAND, RICHARD A. N88-25353
CORDLE, JAMES H. N88-25170
CORDTS, ROBERT E. N88-25126
COTTRON, M. N88-24993
COULON, G. N88-24788
COURTIS, A. N88-24699
COUTANCEAU, MADELEINE N88-24594
CRAIG, ROY R., JR. N88-25010
CRASEMANN, BERND N88-25275
CREIGHTON, THOMAS R. N88-24629
CRISTE, RUSSELL E. N88-25184
CROOKS, RICHARD M. N88-24723
CROSLEY, DAVID R. N88-25353
CROSS, KENNETH D. N88-24649
CUNTZ, J. M. N88-24750
CURRAN, FRANCIS M. N88-24687
CURRERI, P. A. N88-24791

D

DALLEY, A. M. N88-24740
DALY, E. J. N88-24670
DANISZEWSKI, E. J. N88-24717
DANTZIG, G. B. N88-25182
DAPKUS, P. D. N88-25337
DARTYGE, JEAN MARCEL N88-24707
DAS-GUPTA, D. K. N88-24954
DATT, I. D. N88-25326
DATTOLI, G. N88-24956
DAUBE, OLIVIER N88-24594
DAVENPORT, G. N88-25042
DAVID, S. A. N88-24747
DAVIDSON, G. S. N88-25181
DAVIS, J. L. N88-24820
DAVIS, RANDALL C. N88-24816
DEAN, WILLIAM G N88-24817
DEASON, V. A. N88-24709
DECHARENTENAY, F. X. N88-24998
DECRISTOFANO, BARRY N88-25151
DEFONTAINE, D. N88-25348
DEININGER, W. D. N88-24677
DEMENEZESCORDEIRO, MAURICIO N88-25193
DENNER, WARREN W. N88-25122
DERMER, C. D. N88-25426
DESSELHAUS, G. N88-24782
DESWART, H. E. N88-25090
DEVIR, ADAM D. N88-25079
DEVOL, ALLAN H. N88-25062
DEWAS, J. N. N88-24793
DIAMOND, P. H. N88-25319
DICKEY, F. M. N88-24945
DICKINSON, J. T. N88-25401
DIEBOLD, JAMES N88-25045
DIEGLE, R. B. N88-24867
DIEKMANN, O. N88-25258
DIFILIPPO, FRANK N88-24754
DIMOTAKIS, P. E. N88-24923
DIPPOLITO, RICHARD N88-24647
DJOMEHRI, M. J. N88-24890
DLOUGA, M. N88-25326
DODDAPANENI, N. N88-24868
DODSON, B. W. N88-25361
DOEKMECI, M. C. N88-24351
DOGGETT, ROBERT V., JR. N88-24598
DOMINEK, ALLEN K. N88-24845
DONALDSON, KIMBERLY Y. N88-24770
DOUGLAS, WILLIAM K. N88-25156
DOXBECK, M. N88-25266
DRAGON, L. N88-25283
DRAPER, SUSAN L. N88-25358
DREICER, J. N88-25181
DRESNER, L. N88-25245
N88-25359
DRESSELHAUS, G. N88-24779
N88-24783
DRESSELHAUS, M. S. N88-24776
N88-24777
N88-24778
N88-24780
N88-24783
DRESSELHAUS, M.S. N88-24782
DUBEY, R. V. N88-24974
DUBIS, DAVID N88-24814
DUCAN, M. A. N88-24722
DUFRESNE, EUGENE R. N88-24815
DUKE, EUGENE L. N88-25207
DULIEU, ANNIE N88-24594
DUNCAN, ROBERT C. N88-25376
N88-25377
N88-25378
DUQUENNOY, A. N88-25405
DURAL, G. N88-25175
DURHAM, P. J. N88-25360
DUSTAFSON, DONALD E. N88-25199
DUVAUT, G. N88-24710
DYER, GERALD E. N88-24972
DZIELSKI, JOHN EDWARD N88-24668

E

EBELING, KARL-JOACHIM N88-24939
EBSTEIN, STEVEN MICHAEL N88-25407
EGOROV, V. F. N88-25015
EHLERS, H. N88-25392
EKMAN, MATS N88-25179
ELGERED, G. N88-24820
ELGERSMA, M. R. N88-24627
ELLEMAN, D. D. N88-24943
ELLER, A. I. N88-25123
ELLINGSON, S. W. N88-25300
ELLIOTT, DOUGLAS C. N88-25046
N88-25047
ELLIOTT, JOE W. N88-24607
ENDO, M. N88-24778
N88-24779
N88-24783
EPHRAIM, DANIEL N88-25237
EPPERLY, WALTER L. N88-24958
EPSTEIN, J. S. N88-24709
EPSTEIN, LINDA N88-24616
ERBIL, AHMET N88-25332
ERDOGAN, F. N88-25014
ERIKSSON, GUNNAR N88-24840
ERIKSSON, MATS N88-24840
ERWIN, DAVID H. N88-25128
ESCAIG, B. N88-24788
EULER, J. A. N88-24974
EUSTANCE, WILLIAM E. N88-25075
EVANS, G. A. N88-24948
EVANS, JAMES E. N88-25118
EVANS, ROBERT J. N88-25044
EWING, RICHARD E. N88-24890
EXARHOS, G. J. N88-25351
EYNON, SANDRA L. N88-24618
EZELL, LINDA NEUMAN N88-25429
N88-25430

F

FABIAN, P. N88-25084
FAETH, GERARD M. N88-24639
FARBMAN, G. N88-24681
FARHAT, NABIL H. N88-25293
FARLEY, GARY L. N88-24970
FARLEY, WILLARD W. N88-25159
FAROKHI, S. N88-24592
FEDERER, J. I. N88-24790
FEDERER, W. T. N88-25167
FENG, SU SU N88-24729
FENG, Z. D. N88-25167
FENNELLY, A. J. N88-25365
FERGUSON, R. L. N88-25283
FERNANDEZARROYO, GLORIA N88-25053
FILLIUS, WALKER N88-25425
FINGER, J. F. N88-24637
FINK, J. N88-25078
FINLAYSON, B. N88-24791
FINNERTY, ANTHONY E. N88-24813
FISHER, AMNON N88-25289
FISHER, DOUG N88-25147
FISHMAN, GEORGE S. N88-24979
FLANAGAN, C. A. N88-25316
FLEETER, SANFORD N88-24584
FLOOD, COLIN R. N88-25107
FLORES, JOLEN N88-24602
FLYNN, BARRY N88-25224
FOHLEN, GEORGE M. N88-24692
FOKAS, ATHANASSIOS S. N88-24889
FOLENTA, DEZI N88-24975
FOX, JAY A. N88-24949
FRANCA, LEOPOLDO PENNA N88-25248
FRANCESCONI, RALPH P. N88-25139
FRANKEL, J. N88-25266
FRANZ, A. N88-25283
FRASER, M. E. N88-25306
FRASER, MALCOLM D. N88-25048
FREDERICKSON, GREG N. N88-25213
FREEMAN, DON N88-25238
FRENCH, RICHARD N88-25303
FRICKE, KURT N88-24934
FROST, WALTER N88-25105
FUCILE, PAUL D. N88-24661
FUERSTENAU, NORBERT N88-24937
N88-24938
FUHRY, DOUGLAS PAUL N88-24654
FUJII, KIYOSUMI N88-25285
FUJIKAWA, GENE N88-24659
FURUHARA, T. N88-24740
FUSSMANN, G. N88-25319

G

GABB, T. P. N88-24766
GAINER, CHARLES A. N88-24649
GALAMBOS, J. D. N88-25316
GALLARDO, J. C. N88-24956
GAMIRE, E. N88-25337
GAMMON, B. E. N88-24735
GANDON, CHRISTIAN N88-25201
GANGLOFF, RICHARD P. N88-24746
GARBER, F. D. N88-24833
GARNER, H. DOUGLAS N88-24620
GARTHNER, JOHN P. N88-25109
GARY, G. A. N88-25424
GATTO, LAWRENCE W. N88-25018
GAUTIER, CYNTHIA R. N88-24949
GAYDA, J. N88-24766
GAYET, J. F. N88-25104
GAZZANIGA, JOHN A. N88-24597
GELB, A. N88-25396
GELLES, D. S. N88-24748
GENNARI, JOHN H. N88-25147
GENT, A. N. N88-24785
GEORGE, ALAN N88-25191
GEORGE, JOHN H. N88-24890
GERLACH, KARL N88-25198
GERSTL, S. A. W. N88-24957
GHIL, MICHAEL N88-25418
GIBELING, EDWARD J. N88-24675
GILBERT, R. P. N88-25126
GILL, RICHARD T. N88-25135
GILLESSEN, WOLFHART N88-25032
GILLMANN, G. N88-24792
GILLOTAY, D. N88-24726
GILOJEDA, MANUEL N88-25074
GILREATH, MELVIN C. N88-24845
GINLEY, D. S. N88-25330
GIRARD, DIDIER N88-25220
GIVI, P. N88-25256
GIVLER, RICHARD C. N88-24898
GLASGOW, THOMAS K. N88-24811

GLASSELL, R. L. N88-24974
GLENDENNING, N. K. N88-25279
GLEYZES, C. N88-24596
GLOVER, C. W. N88-25162
GODIWALA, P. M. N88-24619
GODSHALL, N. A. N88-24868
GOLDSTEIN, MARTIN N88-25211
GOLDSTEIN, SHYKE A. N88-24679
GOLDSTONE, P. D. N88-24955
GONZALEZGARCIA-CONDE, ANTONIO N88-25053
GOODMAN, JOHN M. N88-25081
GORDELIJ, V. I. N88-25326
GORTON, C. W. N88-25043
GOULD, W. J. N88-25124
GOURDIN, CHRISTIANE N88-24707
GOURDIN, WILLIAM H. N88-24744
GOWER, DANIEL W., JR. N88-24835
GRAHAM, OLIN L. N88-24958
GRANT, M. L. N88-25329
GRAVES, PETER W. N88-24861
GRAVES, THOMAS JOSEPH N88-24969
GRAY, JOHN F. N88-24611
GREEN, B. D. N88-25396
GREEN, BYRON DAVID N88-25398
GREEN, JAMES M. N88-24669
GREEN, P. F. N88-24794
GREENBAUM, E. N88-24731
GREENE, D. P. N88-24955
GREENHALL, CHARLES A. N88-24846
GREENWOOD, D. E. N88-25388
GREENWOOD, JOHN E. N88-24660
GROSCH, C. E. N88-24916
GROSS, ANTHONY R. N88-24579
GROSS, MICHAEL B. N88-25264
GROSSMAN, ... N88-25309
GRUBER, PATRICIA L. N88-25125
GUBERMAN, STEVEN L. N88-25082
GUDMUNDSON, SVEN ERIK N88-24585
GUERBET, M. N88-25130
GUHA, ALOKE N88-25296
GUIGON, M. N88-24787
GUO, G. Y. N88-25360
GUO, YAOBIN N88-24582
GUPTA, R. N88-25349
GUSTAVSSON, A. N88-24821
GWINN, K. W. N88-25189
GYLLENBERG, M. N88-25258
GYORFFY, B. L. N88-24756

H

HAAG, R. L. N88-24855
HAAG, THOMAS W. N88-24687
HABERLE, R. M. N88-25420
HADDICK, C. M., JR. N88-24662
HAEGELE, J. N88-25070
HAGYARD, M. J. N88-25424
HAINES, L. N88-25123
HALL, C. A. N88-24657
N88-24658
N88-24687
HALL, DAVID F. N88-25400
HALLAUER, WILLIAM L., JR N88-24989
HALLOWELL, SUSAN F. N88-24978
HALLY, DAVID N88-24886
HAMRICK, JOSEPH T. N88-25050
N88-25051
HANDRICH, EBERHARD N88-24930
HANES, M. H. N88-25346
HANLON, J. A. N88-24955
HANSEN, A. N88-25055
HANSON, J. D. N88-25320
HARBECK, ROLF N88-25026
HARDIE, CAL EDWARD N88-24965
HARDLE, W. N88-25254
HARDY, KENNETH A. N88-25128
HARIHARAN, S. I. N88-25239
N88-25268
HARLOFF, G. J. N88-24917
HARRINGTON, ROGER F. N88-24828
N88-24836
HARRIS, G. W. N88-25072
HARRIS, J. M. N88-24809
HARRIS, JAMES S., JR. N88-24848
HARRIS, P. N88-24681
HARVEY, C. A. N88-24627
HASSAN, H. A. N88-24914
N88-24915
HASSELMAN, D. P. N88-24770
HAUER, A. N88-24955
HAWKE, R. S. N88-24658
HAWKINS, GARY F. N88-24680
HAYAKAWA, H. N88-25095
HEAVEN, MICHAEL C. N88-25344
HEBRON, D. E. N88-24926
HEEGER, A. J. N88-24768
HEIFETS, S. A. N88-25291
HEIJMANS, H. J. A. M. N88-25241
N88-25258
HEINE, C. N88-24976
HELLSTEN, H. N88-24821
HENAGER, C. H., JR. N88-24795
HENDRICH, LOUIS J. N88-24629
HENNI, ZENZO N88-24783
HENNEMAN, RICHARD L. N88-25142
HENNINGSON, DAN S. N88-24587
HENRY, DONALD P., JR. N88-25002
HENTSCHEL, WOLFGANG N88-25033
HERBERT, A. N88-25089
HERMSEN, T. N88-24956
HERREN, BLAIR N88-25357
HERRMANN, FRED N88-25357
HERSHCOVITCH, A. N88-25278
N88-25317
HERZ, RICHARD K. N88-25185
HESTER, HOWARD B. N88-25354
HETTINGER, LAWRENCE J. N88-24648
HEYMAN, JOSEPH S. N88-25011
N88-25302
HIBEY, JOSEPH L. N88-24644
HIBSHOOSH, ELIPHAZ N88-24834
HICKSON, DIANA E. N88-25134
HIEFTJE, GARY M. N88-25298
HIETANIEMI, J. N88-25352
HIGBIE, P. R. N88-25083
HILL, ACQUILLA S. N88-24580
HILL, MARVIN L. N88-25165
HILL, RICHARD G. N88-24610
HILLER, W. J. N88-24940
HINES, G. N88-24627
HINKELMAN, JOHN W. N88-25117
HINKLE, C. ROSS N88-25133
HINTZ, N. M. N88-25271
HIRT, C. W. N88-24913
HO, JAMES K. N88-25173
HOEFKEN, KLAUS-DIETER N88-25063
HOFFMAN, G. H. N88-24885
HOFZUMAHAUS, A. N88-25071
HOLBEN, MILFORD S., JR. N88-25011
HOLDEMAN, JAMES D. N88-24640
HOLDREN, M. W. N88-24638
HOLMAN, EARL V. N88-24660
HOLZAPFEL, WOLFGANG N88-24935
HOPFINGER, E. J. N88-24896
HOPSON, PURNELL, JR. N88-25355
HORNE, W. CLIFTON N88-24900
N88-24946
HOROWITZ, ERIC JACK N88-25325
HOSSENLOOP, I. A. N88-24735
HOTES, DEBORAH N88-24754
HOVEY, RUSSELL L. N88-25112
HOWELL, J. R. N88-25318
HRIBAR, JOHN R. N88-24680
HSU, C. Y. N88-24748
HUANG, JEN-KUANG N88-25244
HUANG, KAO-HUAH N88-25111
HUANG, SHYH-CHIN N88-24966
HUGHES, CHRISTOPHER E. N88-24597
HULBERT, J. K. N88-24665
HULSTROM, R. L. N88-25056
HUNDSDORFER, W. H. N88-25243
HUSS, RONALD J. N88-24698
HUTCHINSON, D. P. N88-25321

I

IBA, WAYNE N88-25152
IBANEZ, PAUL N88-24611
IDA, NATHAN N88-25239
IKONEN, E. N88-25352
ILIEVA-SOKOLINOVA, N. K. N88-25306
IMHOFF, MARC L. N88-24844
INATANI, YOSHIFUMI N88-24599
INGELS, J. N88-25084
INOUYE, MAMORU N88-24603
INTRIERI, PETER F. N88-24591
IRAK, Z. N88-25326
IRVIN, TIMOTHY N88-25303
ISAACSON, ELI L. N88-24890

J

JACKSON, BART N88-24745
JACKSON, T. L. N88-24916
JACOBSEN, R. T. N88-25370
JALINK, ANTONY, JR. N88-24942
JALURIA, Y. N88-24873
JAMAR, L. G. N88-24983
JEANDREAU, J. P. N88-24793
JEANJAQUET, S. N88-24786
JEFFRIES, JAY B. N88-25353
JENKINS, RENALDO V. N88-24580
JEROME, R. N88-24794
JOHANSSON, J. M. N88-24820
JOHNSON, D. D. N88-24756
JOHNSON, D. J. N88-24926
N88-25308
JOHNSTON, J. CHRISTOPHER N88-24811
JOINER, R. G. N88-25081
JOLLAY, D. M. N88-25203
JONES, DAVID J. N88-25016
JONES, JESSE D. N88-24616
JONES, MARK N88-25183
JONES, R. H. N88-24795
JONES, SHERRIE A. N88-24648
JORGENSEN, D. P. N88-25096
JORGENSEN, J. D. N88-25330
JORISSEN, A. N88-25410
JOUANY, J. M. N88-25130
JUNGST, R. G. N88-24805
JUNKER, ANDREW M. N88-25135
JUNKERMANN, W. N88-25065
JURAS, R. C. N88-25157

K

KAHN, E. N88-24632
KAMAR, DEVENDRA N88-24692
KANG, M. N88-24955
KANNAN, K. L. N88-25385
KANNBERG, L. D. N88-25058
KANNO, MOTOHIRO N88-24758
KANNO, MOTOHIURO N88-24759
KAPOOR, K. N88-24873
KARAMCHETI, KRISHNAMURTY N88-24946
KARIM, REZWANUL N88-25315
KASSNER, M. E. N88-24755
KATHONG, MONCHAI N88-24922
KATILA, T. N88-25352
KEATON, G. L. N88-25322
KELLER, JOHN L. N88-25114
KENDIG, M. N88-24786
KENIK, EDWARD A N88-24646
KENSEK, R. P. N88-25308
KERSLEY, L. N88-24837
KETO, ERIC RAVINEN N88-25413
KHAMITSEV, SH. V. N88-25015
KHOSLA, P. K. N88-24875
KHURI, A. I. N88-25253
KIDD, G. J., JR. N88-24977
KIESEL, EBERHARD N88-24933
KIM, S. C. N88-24917
KING, D. Q. N88-24677
KING, J. F. N88-24747
KING, JAMES W. N88-25177
KITANO, HITOSHI N88-24759
KITSUTAKA, SHIGEO N88-25285
KITTIAMPON, KRIT N88-24967
KJELLGREN, J. N88-24821
KJELLGREN, JAN N88-24839
KLEBESADEL, R. W. N88-25083
KLEINLEBBINK, G. C. N88-24909
KLINGENBERG, G. N88-24801
KLOBUCHAR, JOHN A. N88-25081
KNIGHT, DOYLE D. N88-24882
KNOTHE, KLAUS N88-25008
KOBERSTEIN, J. T. N88-24769
KODA, SIGEYASU N88-24763
KOEHLER-NAUMANN, W. N88-24810
KOK, R. N88-25137
KONAGAYA, MASAAKI N88-25129
KONAGAYA, YOKO N88-25129
KONRAD, C. H. N88-24657
KORTEGAARD, B. L. N88-24955
KORTH, G. E. N88-24812
KORTING, P. A. O. G. N88-24733
N88-24734
KOSHAK, WILLIAM J. N88-25103
KOSKIE, J. E. N88-24905
KOTERAS, J. R. N88-25189
KOVAC, R. J. N88-25043
KOVARIK, V. N88-25317
KOWALEWSKI, T. A. N88-24940
KRASON, J. N88-25023
KRIDER, E. PHILIP N88-25103
KRISHNAMURTHY, L. N88-24887
KRISTAL, R. N88-24955
KROES, ROGER L. N88-25354
KRYSHKIN, V. I. N88-25292
KU, WALTER H. N88-24852
KUGEL, CARL P. N88-24617
KUHLMAN, JOHN M. N88-24630
KULKARNI, SUNIL SHRIKRISHNA N88-24674
KUMAR, INDER JIT N88-25075

KURATH, PETER N88-25016
KUSSMAUL, MICHAEL N88-24754
KUTLER, PAUL N88-24579
N88-25196
KWARTENG, ISAAC K. N88-25048
KWON, O. J. N88-25319

L

LADANY, I. N88-24948
LADDE, G. S. N88-25229
LAGARDE, A. N88-24993
LAI, K.-W. N88-25274
LAIHING, K. N88-24722
LAMBRAKOS, S. G. N88-25277
LAMINIE, J. N88-24907
LANCASTER, RICHARD W. N88-25121
LANG, D. N88-24705
LANG, D. B. N88-24923
LANGLEY, PAT N88-25147
N88-25152
LAPTEV, D. M. N88-25368
LARSSON, B. N88-24821
LAURENT, PIERRE-JEAN N88-25218
LAW, C. C. N88-24775
LAWSON, M. N88-25054
LAX, BENJAMIN N88-25335
LEBO, WILLIAM N88-24975
LECHTENBERG, T. A. N88-24748
LEE, C. P. N88-24653
LEE, DAEHEE N88-24920
LEE, J. R. N88-24998
N88-25308
LEE, KENNETH J. N88-24647
LEE, M. C. N88-24943
LEE, MIN EIG N88-25239
LEE, TAK C. N88-25173
LEEPER, R. J. N88-24926
N88-25308
LEGER, L. N88-25392
LEISERSON, CHARLES N88-25168
LEMAIRE, J. N88-25422
LEMONE, M. A. N88-25098
LEONARD, C. N88-25073
LETALICK, DIETMAR N88-25299
LEVISON, WILLIAM H. N88-25135
LEWIS, JAMES K. N88-25122
LEWIS, M. I. N88-25137
LHERMITTE, ROGER M. N88-25100
LIANG, E. P. N88-25426
LIBBY, P. A. N88-24730
LICINA, JOSEPH R. N88-24635
LILIENTAL-WEBER, Z. N88-25362
LIN, JEONG-LUH N88-25003
LINDENTHAL, ANDREAS N88-24683
LINDER, ERIC V. N88-25307
LIOEN, W. M. N88-25242
LIS, BRIAN H. N88-25347
LITVIN, F. L. N88-24976
LIU, C. T. N88-24708
LIU, HAO-WEN N88-24997
LIU, HUA KUANG N88-25301
LIU, HUA-KUANG N88-25305
LIU, Y. C. N88-24778
LOC, TA PHUOC N88-24594
LOCKNER, T. R. N88-24926
N88-25308
LODDER, ROBERT A. N88-25296
LOGAN, JAMES C. N88-24830
N88-25174
LOKOS, WILLIAM A. N88-24833
LONG, GLEN CARL, JR. N88-24656
LORETZ, THOMAS J. N88-24861
LORIOT, M. N88-24703
LOVELAND, DONALD W. N88-25197
LOZANO-LEAL, ROGELIO N88-25204
LUCAS, STEPHEN H. N88-25190
LUDLAM, T. W. N88-25287
LUEBECK, E. N88-24932
LUNDGREN, DOUGLAS J. N88-25110
LUNDY, M. N88-24976
LUTES, GEORGE F. N88-25304
LUTZ, S. S. N88-24925
LYNCH, THOMAS J. N88-24850
LYNN, THEODORE BROOKS N88-24901

M

MA, C. H. N88-25321
MA, YUSHIEH N88-24823
MADENCI, ERDOGAN N88-24711
MAEDER, ANDRE N88-25409
N88-25411
MAENCHEN, J. N88-24926
N88-25308
MAGRE, P. N88-24727
MAHAJAN, D. N88-24715
MANGALAM, SIVARAMAKRISHNAN M. N88-24910
MANI, AYYAKANNU N88-25223
MANN, FRANKLIN D. N88-24971
MANTAY, WAYNE R. N88-24970
MANZO, MICHELLE A. N88-25059
MARION, J. E. N88-24961
MARSH, W. J. N88-24905
MARTIN, JAMES A. N88-24685
MARTIN, JOHN S. N88-24635
MASON, J. J. N88-24945
MASTROIANNI, GEORGE R. N88-25153
MATHEWS, S. N88-25042
MAURER, JOERG N88-25052
MAUTZ, JOSEPH R. N88-24828
MAVRIPLIS, DIMITRI J. N88-24608
MAX, STEPHEN R. N88-25129
MAXFIELD, BRUCE W. N88-24665
MAXWELL N88-25216
MAYNARD, E. D., JR. N88-25341
MAYOR, M. N88-25405
N88-25410
MCCROSKEY, W. J. N88-24801
MCDONALD, HENRY N88-24675
MCDONALD, M. J. N88-24658
MCKEAGUE, IAN W. N88-25210
MCKISSICK, BURNELL T. N88-24634
MCLEAN, W. J. N88-24730
MCMASTER, L. R. N88-25094
MCMURTRY, P. A. N88-25256
MCTIGUE, DAVID F. N88-24898
MCVAY, M. C. N88-24991
MEDHIN, NEGASH G. N88-25227
N88-25228
N88-25230
N88-25231
N88-25232
N88-25233
MEESE, G. B. N88-25137
MEHLHORN, T. A. N88-24926
MEIER, G. E. A. N88-24891
MEIER, G. H. N88-24743
MELTON, R. B. N88-24981
MENKE, KURT N88-25034
MEREDITH, M. P. N88-25167
MERRIAM, J. D. N88-25340
MERRITT, JAMES H. N88-25128
MESSICK, L. J. N88-25338
MESSING, G. L. N88-24701
MESZTENYI, CHARLES K. N88-25215
MEYER, MARYJO B. N88-24811
MIAKE-LYE, R. C. N88-24923
MICHELSEN, C. N88-25181
MIDDLETON, DAVID B. N88-24621
MILES-MCDERMOTT, N. J. N88-25167
MILLBURN, GEORGE P. N88-25380
MILLER, A. W. N88-25019
MILLER, E. R. N88-25397
MILLER, J. J. N88-24990
MILLER, R. A. N88-24743
MILLER, ROBERT G. N88-25115
MILLER, ROBERT H. N88-24739
MILLER, S. E. N88-24638
MILLS, ERIC L. N88-25019
MILNE, THOMAS A. N88-25044
MIN, BYUNG-JIN N88-25004
MINEHAN, W. N88-24701
MINER, R. V. N88-24766
MIRTICH, MICHAEL J. N88-24754
MITTELSTRASS, GERHARD N88-25035
MITTRA, R. N88-24827
MIX, L. P. N88-24926
MO, KINGTSE N88-25418
MODI, VINOD J. N88-24673
MOINE, MELLE N88-25069
MOLLEKOPF, G. N88-25069
MONDT, J. P. N88-25102
MONGUILLET, JEAN-MARC N88-25381
MOORE, CARLETON J. N88-25013
MOORE, R. L. N88-25423
MOOREHEAD, T. W. N88-25390
MORALESPOYATO, FRANCISCO N88-25053
MORE, KARREN L. N88-24646
MORGESON, D. N88-25181
MORITA, YASUHIRO N88-24673
MOROSIN, B. N88-25330
MORREN, W. EARL N88-24968
MORSE, T. F. N88-25294
MORTON, B. G. N88-24827
MOSS, S. C. N88-25348
MOU, Y. N88-24740
MUDAWWAR, I. A. N88-24905
MUDGE, L. K. N88-25049
MUKHERJEE, A. K. N88-24741
MUKKAMALA, RAVI N88-25383
MULHOLLAND, ROBERT G. N88-24615
MURPHY, G. B. N88-25393
MURPHY, K. D. N88-24867
MURRI, DANIEL G. N88-24628
MUSIELAK, Z. E. N88-25323

N

NACHTSHEIM, PHILIP R. N88-25192
NAGAI, TAKESHI N88-24763
NAGATA, K. N88-24762
N88-24764
NAGATA, KAZUO N88-24869
NAGATA, KOJI N88-24765
NAGUMO, M. N88-25277
NAIDU, DESINENI S. N88-24844
NAKAMURA, M. N88-25095
NAKAZAWA, NAOHITO N88-25367
NATHAL, MICHAEL V. N88-24749
NAYFEH, ADNAN H. N88-24702
NEALY, JOHN E. N88-25427
NEEDLEMAN, ALAN N88-24988
NEIDECKER, BURKHARD N88-25186
NEILSON, ROBERT H. N88-24771
NEVEJANS, D. N88-25084
NEWMAN, C. J. N88-25043
NEWMAN, DONALD J. N88-25211
NEWMAN, FREDERICK A. N88-24642
NEYHABER, ROY H. N88-25276
NGUYEN, A. N88-24735
NGUYEN, CHARLES C. N88-25206
NGUYEN, R. N88-25338
NICHOL, DOUGLAS N88-25087
NICHOLS, B. D. N88-24913
NICHOLSON, D. M. N88-24756
NICKERSON, BRADFORD GEORGE N88-25021
NIEDERSTRASSER, H. N88-24932
NIEH, T. G. N88-24708
NIEMITZ, K. J. N88-25067
NIESE, DETLEF N88-25036
NIETUBICZ, CHARLES J. N88-24874
NILSSON, STEFAN N88-24839
NISHIKAWA, S. N88-24762
N88-24764
NISHIKAWA, SEIICHI N88-24869
NOEL, B. W. N88-24925
NOGAR, N. S. N88-25322
NOGUCHI, OSAMU N88-24761
NORWOOD, D. N88-24865
NOUHI, AKBAR N88-25336
NUNN, ROBERT H. N88-24678
NUNZIATO, JACE W. N88-24898
NYSTROM, GEORGE U. N88-24962

O

OBASIH, KEMAKOLAM M. N88-24589
OBERLIN, A. N88-24787
OCHIAI, SHOUICHI N88-24761
ODORICO, J. N88-24705
N88-24750
N88-24751
N88-24752
N88-24793
OGDEN, T. R. N88-24784
OHANA, I. N88-24778
OHARE, T. E. N88-24715
OHMI, KAZUO N88-24594
OJIMA, SHUICHI N88-25367
OKANE, JAMES H. N88-24671
OKUBO, SHIGENORI N88-25205
OLDANI, J. J. N88-24755
OLECHNA, M. N88-24752
OLIVERSEN, RONALD J. N88-25419
OLSON, J. G. N88-25096
OLSSON, HANS-AKE N88-25179
OMRANI, MASSOOD N88-25005
ONDA, K. N88-25286
ONEIL, D. J. N88-25043
ONODA, G. Y., JR. N88-24791
ORAN, E. S. N88-25277
ORAZEM, M. E. N88-24742
OSBORN, M. T. N88-25094
OSIF, T. N88-25054
OWEN, JAMES W. N88-24817

P

PACALA, THOMAS J. N88-24862
PAILHAS, G. N88-24596
PALMBERG, BJOERN N88-24995
N88-24996
PALMER, R. E. N88-24730
PAN, D. H. N88-24769

PANARAS, ARGYRIS G. N88-24600
PANDOLF, KENT B. N88-25139
PANTANO, C. G. N88-24701
PARECHANIAN-ALLEN, L. N88-25362
PARKER, JOHN A. N88-24692
PARKINS, W. A. N88-24843
PASCHKE, R. N88-25070
PASS, RALPH P. N88-25113
PATON, ROBERT N88-25364
PAUL, J. N88-25209
PEALAT, M. N88-24727
PECSELI, H. L. N88-25077
PERKINS, R. A. N88-24743
PERNER, D. N88-25068
PERRY, MICHAEL DALE N88-25273
PERSON, LEE H., JR. N88-24621
PERTIN-TROCCAZ, JOCELYNE N88-25202
PHAM, DINH TAO N88-25217
PHILLIPS, PAMELA SUSAN N88-24590
PHILLIPS, SALLY J. N88-25155
PIERCE, P. E. N88-25161
PIMBLEY, G. H. N88-24912
PINEIRO, LUIS A. N88-24645
PINSKI, F. J. N88-24756
PITZER, EDWARD W. N88-24718
PIVIROTTO, T. J. N88-24677
PLASIL, F. N88-25282
PLATT, U. N88-25068
PLINTA, CHARLES N88-24647
POLLACK, J. B. N88-25420
POLLOCK, CRAIG JAMES N88-25412
PONTRELLI, G. N88-25259
POORAN, FARHAD J. N88-25206
POPE, DALE E. N88-24659
POPHANKEN, O. N88-24810
POPPE, W. N88-24892
PORSCHING, T. A. N88-24887
PORTER, M. N88-25042
POWERS, EDWARD J. N88-24856
PRELEC, K. N88-25317
PRILUKOV, V. P. N88-25015
PRIMDAHL, F. N88-25077
PRIOU, ALAIN N88-24984
PRITCHETT, S. D. N88-24866
PROBERT, M. R. N88-24925
PRYSE, S. E. N88-24837
PSALTIS, DEMETRI N88-25214
PUGACZ, EDWARD J. N88-24613
PUN, W. M. N88-25061
PURVIS, GEORGE D., III N88-25177

Q

QI, D. N88-24701
QUENTMEYER, RICHARD J. N88-24690
QUERRY, MARVIN N88-24724
QUINN, JOHN J. N88-25333
QUINN, MARY T. N88-24680

R

RADFORD, DONALD W. N88-24706
RADHAKRISHNAN, GOURI N88-25336
RADOSAVLJEVIC, D. N88-24895
RADZIEMSKI, LEON J. N88-24952
RAJAGOPAL, KARUNAMURTHY N88-24606
RAMSTHALER, J. N88-24681
RANTANEN, R. O. N88-25391
RAO, K. V. N88-24800
RAPP, DOUGLAS C. N88-24808
RASH, CLARENCE E. N88-24635
RASMUSON, D. M. N88-25251
RASPET, RICHARD N88-25263
RAVINDRA, KRISHNASWAMY N88-24902
RAWLIN, VINCENT K. N88-24688
RAY, E. A. N88-24824
RAY, EDWARD J. N88-24580
READ, J. F. N88-25124
REDDY, E. S. N88-24700
REDER, STEPHEN M. N88-25375
REEDY, E. D., JR. N88-25012
REES, DAVID N88-24951
REHMANN, ALBERT J. N88-24614
REICH, SIMEON N88-25246
REIMER, HANS-GERD N88-25037
REISS, DONALD A. N88-25354
REMICK, R. J. N88-25054
RENIERI, A. N88-24956
REUTTER, DENNIS J. N88-24978
RHEINBOLDT, WERNER C. N88-25215
RIBERIO, MARIA N. G. N88-25062
RICE, E. J. N88-24592
RICHEY, JEFFREY E. N88-25062
RICKS, R. E. N88-25203
RILEY, MICHAEL D. N88-24819
RILEY, WILLIAM J. N88-24850
RINGHOFER, CHRISTIAN N88-25212
RIORDAN, C. J. N88-25056
RISEBOROUGH, P. S. N88-25331
RISSMAN, MICHAEL S. N88-24647
ROBE, R. Q. N88-24618
ROBERT, M. N88-24994
ROBEY, JUDITH L. N88-24818
ROBINS, GABRIEL N88-25200
ROBINSON, R. C. N88-25251
ROBISCOE, R. T. N88-24664
ROCHA, C. J. N88-24632
N88-25371
RODLOFF, RUEDIGER N88-24929
ROERDINK, J. B. T. M. N88-25241
ROESLER, FRED L. N88-25419
ROGOWSKI, ROBERT S. N88-25011
ROLLETT, ANTHONY DAVID N88-24737
ROLLINGS, RAYMOND S. N88-24652
RONZHIN, A. I. N88-25292
ROOZEN, H. N. M. N88-24985
ROSEN, I. G. N88-25246
N88-25247
ROSENBLAT, SIMON N88-24625
ROSENDAL, H. N88-25119
ROSENTHAL, BRUCE N. N88-24811
ROSHOLT, ROBERT L. N88-25428
ROSINSKI, JAN N88-25255
ROSTOKER, NORMAN N88-25289
ROUSE, WILLIAM B. N88-25142
ROWELL, LAWRENCE F. N88-25184
ROY, RAYMOND L. N88-24861
ROYSTER, DICK M. N88-24616
RUBIN, S. G. N88-24875
RUIZ, C. L. N88-25306
RUIZ, RAYMOND L. N88-24680
RUPE, BADER I. N88-24767
RUSSELL, JIM K. N88-24958
RUSSELL, K. D. N88-25251
RUSSELL, T. P. N88-24794
RUTLEDGE, SHARON K. N88-24754
RYAN, ROBERT S. N88-24672

S

SABNIS, JAYANT S. N88-24675
SAILEY, RICHARD H. N88-24607
SAINZDEAJA, MA JESUS N88-25074
SAKAI, KENJI N88-25367
SAKAMOTO, TERUO N88-24763
SAKATA, H. N88-24779
N88-24783
SAKIMOTO, K. N88-25286
SALAZAR, G. A. N88-24662
SALEM, LESLIE B. N88-25079
SALOMON, FERDINAND N88-25036
SAMBANDHAM, M. N88-25227
N88-25229
N88-25230
N88-25232
N88-25233
N88-25234
N88-25235
SANDEL, B. R. N88-25417
SANDERS, C. E. N88-25188
SANDLER, HAROLD N88-25140
SANDOW, FORREST A. N88-24573
SANNAN, SIGURD N88-25369
SANTIAGO, JOSEPH M. N88-24987
SAPIENZA, R. S. N88-24715
SARVER, EMORY W. N88-24978
SATO, SHIRO N88-24765
SATTISON, M. B. N88-25251
SATZ, H. S. N88-24619
SAUNDERS, ALAN L. N88-24659
SAVILLE, D. A. N88-25327
N88-25329
SAWKA, MICHAEL N. N88-25139
SAXE, JAMES B. N88-25168
SCAHILL, JOHN N88-25045
SCHARLEMANN, E. T. N88-24960
SCHERB, FRANK N88-25419
SCHILLING, DONALD L. N88-24834
SCHIRBER, J. E. N88-25330
SCHLEMPER, EBERHARD N88-24936
SCHLICHTING, J. J. F. M. N88-25187
SCHMAIZER, PAUL A. N88-25133
SCHMIDT, D. W. N88-24892
SCHMIDT, DON L. N88-24694
SCHMIDT, RICHARD A. N88-25146
SCHMITT, DIRK-ROGER N88-24931
SCHMITT, W. N88-25009
SCHOMER, PAUL D. N88-25263
SCHOPPER, AARON W. N88-25153
SCHRADE, HERBERT O. N88-25310
SCHULKIN, M. N88-25267
SCHUSTER, LAWRENCE S. N88-24633
SCHWEIGER, A. N88-25024
SCHWEINFURTH, GERHARD N88-25039
SCHWING, JAMES L. N88-25184
SCOTT, RUSSELL A. N88-24829
SCOTTI, STEPHEN J. N88-25190
SEALOCK, L. J., JR. N88-25047
SEATON, C. T. N88-24825
SEEBAUGH, W. R. N88-25399
SEGUR, HARVEY N88-24884
SEKO, JOSEPH T. N88-25236
SELF, MATTHEW N88-25238
SERFOZO, RICHARD F. N88-25252
SHAFFER, TIMOTHY D. N88-24772
SHAHINPOOR, M. N88-24657
SHANKAR, UDAY J. N88-24631
SHANNON, ROBERT R. N88-25297
SHAPIRO, DIANE C. N88-25146
SHARBER, J. R. N88-25091
SHARPLES, F. E. N88-25132
SHAY, H. D. N88-24960
SHEPPARD, DANIEL J. N88-24648
SHEU, WEN-HANN N88-24904
SHIRLEY, I. M. N88-24699
SHORT, STEVE E. N88-25106
SHUEN, JIAN-SHUN N88-24639
SHUVALOV, L. A. N88-25326
SIEDSCHLAG, N. N88-25055
SIMEONIDES, G. N88-24650
SIMON, P. C. N88-24726
SINDERSON, R. L. N88-24662
SINGER, PAUL A. N88-24831
SINGH, N. N88-25394
SIRIGNANO, W. A. N88-24721
N88-24878
SKAMAROCK, WILLIAM C. N88-25101
SKAPERDAS, G. T. N88-24715
SMALLEY, LARRY L. N88-25365
SMITH, D. L. N88-24638
SMITH, JEREL N88-24745
SMITH, JEREL A. N88-25343
SMITH, N. K. N88-24735
SMITH, R. N. N88-24638
SMITH, ROBBIE N88-25356
SMITH, WILLIAM CONRAD N88-24941
SMITHBERGER, S. N88-25175
SMITHERS, J. N88-25124
SMITS, A. J. N88-24581
SNORRASON, O. N88-24833
SNOUSSI, A. N88-25262
SNYDER, DONALD L. N88-24826
SNYDER, R. S. N88-24809
SODA, JIRO N88-25367
SODNOMYN, EH. N88-25306
SOICHER, HAIM N88-25081
SOK, BAN KHE N88-25306
SOMMEIJER, B. P. N88-25259
SOMMER, K. N88-24810
SONI, K. N88-25240
SOREF, R. A. N88-24854
SPAHN, C. J. N88-24662
SPAHN, M. N88-25069
SPALDING, D. B. N88-24893
N88-25061
SPALDING, D. BRIAN N88-24725
N88-24894
SPANN, J. F. N88-25390
SPEITEL, LOUISE N88-24610
SPENCER, J. S. N88-24632
N88-25371
SPICER, C. W. N88-24638
SPRINKLE, CHARLES H. N88-25116
SRINIVAS, MANDAYAM A. N88-25213
SRINIVASAN, RAM N88-24640
SRINIVASAN, S. N88-24911
SRIVATSAN, RAGHAVACHARI N88-24821
SRIVATSAN, T. S. N88-25234
STACK, JOHN P. N88-24910
STALKER, K. T. N88-24945
STANLEY, JAMES N88-24745
STANLEY, JAMES H. N88-25343
STARKE, EDGAR A., JR. N88-24753
STARKENBERG, BJOERN N88-25179
STARNES, JAMES H., JR. N88-24970
STAUFFER, J. D. N88-25387
STEELE, W. V. N88-24735
STEFFEN, K. N88-25024
STEGEMAN, G. I. N88-24822
N88-24825
STEGER, JOSEPH L. N88-24600
STEIN, L. R. N88-24913
STEINBECK, J. N88-24778
N88-24782
STEPHENS, J. J. N88-24708

STEPHENS, JOSEPH R. N88-24749
STERN, S. A. N88-24796
STEVENS, D. J. N88-24804
STIDHAM, CURTIS N88-24754
STIRN, RICHARD J. N88-25336
STOCKS, G. M. N88-24756
N88-25360
STONE, JAMES R. N88-24966
N88-25260
STONER, GLENN E. N88-24746
STORHOK, V. W. N88-24812
STORRS, ALEXANDER DAVID N88-25416
STRAHLE, WARREN C. N88-24877
STRAUCH, JOHN N88-25174
STUEBER, THOMAS N88-24754
STUSTER, JACK W. N88-25372
STUTZ, JOHN N88-25238
STYGAR, W. A. N88-24926
N88-25306
SUESS, S. T. N88-25323
N88-25423
SUGIHARA, K. N88-24777
N88-24780
N88-24781
SUITOR, JERRY W. N88-24814
SULMEISTERS, T. N88-24681
SUMARAC, DRAGOSLAV N88-24999
SUME, AIN N88-24839
SUNDARRAJ, R. P. N88-25173
SUSOEFF, A. R. N88-24658
SUZUKI, HISASHI N88-24758
N88-24759
SWANSON, PAUL E. N88-24698
SWANSON, ROBERT E. N88-24746
SZAKALY, ZOLTAN F. N88-24864
SZCZESNY, P. M. N88-24859
SZOTEK, Z. N88-25360
SZYMANSKI, BOLESLAW K. N88-25176

T

TAGHAVI, R. N88-24592
TAHERI, MOHAMMAD REZA N88-25000
TAKAYANAGI, K. N88-25286
TAL-EZER, HILLEL N88-25249
TALBOT, L. N88-24720
TALLIS, HANS N88-25172
TAN, L. S. N88-24773
TANABE, MASATO N88-24697
TANG, SHENG Y. N88-25276
TANIUCHI, A. N88-24797
TANNEHILL, J. C. N88-24911
TAYLOR, S. C. N88-24699
TAYLOR, T. C. N88-24632
N88-25371
TEMAM, R. N88-24907
TEMME, N. M. N88-25240
TEMMERMAN, W. M. N88-25360
TETER, JOSEPH P. N88-25339
TEXIER, ALAIN N88-24594
THANGARAJ, V. N88-25235
THEIBERT, L. SCOTT N88-24694
THELIN, BO N88-25065
N88-25311
THIEME, H. R. N88-25258
THOMAS, J. R., JR. N88-24789
THOMAS, JOHN W. N88-25129
THOMAS, RUSSELL HICKS N88-24919
THOMSON, MURRAY N88-25138
THUAN, TRINH X. N88-25404
TIEDERMAN, W. G. N88-24905
TIEDERMAN, WILLIAM G. N88-24888
TIFFANY, SHERWOOD H. N88-24823
TIJHUIS, A. G. N88-25261
TIMOTHY, J. GETHYN N88-24861
TIUSANEN, M. N88-24872
TIWARI, SURENDRA N. N88-24922
TODD, MICHAEL J. N88-25178
TODI, TADATOSHI N88-24760
TOKSOZ, M. NAFI N88-25092
TOOMARIAN, N. N88-25208
TORNGREN, LARS N88-24585
TORR, D. G. N88-25395
N88-25396
TORR, M. R. N88-25390
TOWNSEND, LAWRENCE W. N88-25427
TRAJMAR, SANDOR N88-24732
TRAN, SANG Q. N88-25355
TREISMAN, ANNE N88-25148
TRENBERTH, K. E. N88-25096
TRINH, EUGENE H. N88-24818
TRIVEDI, KISHOR S. N88-25158
TRIKULA, M. N88-25322
TSAI, T. T. N88-24774
TSURUDA, K. N88-25095
TURCOTTE, DONALD L. N88-25120
TURLEY, W. D. N88-24925

U

UCHIDA, TETSUO N88-24798
UEHARA, S. N88-25363
UENO, MANABU N88-24761
UMEZU, K. N88-24762
UNDERWOOD, J. H. N88-24990
UNRAU, A. N88-24891

V

VALDES, JAMES R. N88-24661
VALTONEN, M. N88-24849
VANALSTINE, J. M. N88-24809
VANDALSEM, WILLIAM R. N88-24600
VANDERBIJL, J. N88-25225
VANDERGELD, C. W. M. N88-24733
VANDERHOUWEN, P. J. N88-25259
VANDERSANDE, JAN W. N88-25358
VANDERSLUIS, K. L. N88-25321
VANDERVORST, H. A. N88-25187
VANHOLTEN, J. W. N88-25280
VANLAETHEM-MEUREE, N. N88-24726
VANMILL, J. N88-25225
VANNIMMEN, JANE N88-25426
VANNUCCI, RAYMOND D. N88-24712
VANSCOY, ROGER N88-24647
VANSICLEN, V. S. N88-25251
VARADAN, VASUNDARA V. N88-24823
VARADAN, VIJAY K. N88-24823
VARGHESE, P. L. N88-25318
VEERS, PAUL STEVEN N88-25017
VEIJOLA, T. N88-24849
VENKATESH, C. N. N88-24662
VENKATESWARAN, ANURADHA N88-24770
VENTURINI, E. L. N88-25330
VERMILLION, C. H. N88-24844
VERWER, J. G. N88-25243
VICTORIA, REYNALDO N88-25062
VIEHOFF, THOMAS N88-25127
VIERA, G. N88-25022
VILLASENOR, F. N88-24895
VITEK, J. M. N88-24747
VITKOVIC, LJUBISA N88-25129
VOSEN, STEVEN R. N88-24800
VOSS, WOLFGANG N88-25040
VRABEL, MICHAEL J. N88-24583
VRATISLAV, S. N88-25326

W

WACHTEL, J. M. N88-25288
WADSWORTH, J. N88-24708
WAGNER, F. N88-25319
WAITE, J. H., JR. N88-25417
WALBA, DAVID M. N88-24691
WALD, LAWRENCE W. N88-24847
WALKER, DAVID T. N88-24886
WALLACE, J. S. N88-24773
WALTON, O. R. N88-24906
WAN, E. I. N88-24804
WAN, EDWARD I. N88-25048
WANG, A. S. N88-24700
WANG, DING-YI N88-25086
WANG, GUANGQIU N88-25008
WANG, LAWRENCE K. N88-25075
WANG, SHIH ZEN N88-24924
WANG, SHIH-YING N88-24679
WANG, XUEJIAN N88-24582
WARE, A. G. N88-24986
WASHBURN, J. N88-25362
WATSON, L. N88-25163
WATTS, CHRISTOPHER N88-24938
WEBER, WIGAND N88-25036
WEGNER, GARY A. N88-25406
N88-25408
WEIBRING, G. N88-25067
WEINACHT, PAUL N88-24874
WEINBERG, IRVING N88-24870
WEISS, EBERHARD N88-24651
WELLS, DENNIS L. N88-24684
WELLS, GEORGE H., JR. N88-24863
WEN, CHUNG-YUAN N88-25001
WENDELL, L. L. N88-25057
WERNER, K. N88-25284
WEST, E. A. N88-25424
WESTRA, DANIEL P. N88-24648
WETZIG, V. N88-24932
WHEADON, N. S. N88-24837
WHEELER, R. G. N88-24722
WHITE, CRAIG D. N88-24640
WHITE, DON H. N88-25042
WHITE, J. H. N88-24637
WHITE, LUTHER W. N88-24666
WHITESIDES, G. E. N88-25166
WHITLOW, JOHN B., JR. N88-24641
WICK, CHARLES H. N88-25154
WIJCHERS, T. N88-24733
WIKER, GORDON A. N88-24863
WILCOX, W. A. N88-25049
WILLE, L. T. N88-25348
WILLIAMS, HEATHER N88-25136
WILSON, JOHN W. N88-25427
WILSON, T. L. N88-24913
WILSON, W. L. N88-24722
WINNINGHAM, J. D. N88-25091
WINSKE, DAN N88-24953
WINSOR, NIELS K. N88-24655
WISCHMANN, K. B. N88-24808
WISEMBERG, J. N88-24726
WISIAN-NEILSON, PATTY N88-24771
WITTLIN, G. N88-24807
WITTLIN, GR. N88-24799
WOFSY, STEVEN C. N88-25062
WOLF, D. N88-25042
WOLF, RICHARD K. N88-25263
WOOD, CHARLES N88-25358
WOOD, D. H. N88-25126
WOOD, RICHARD M. N88-24845
WU, BING-HUA N88-25014
WU, SAU-MOU N88-25160
WU, YIFENG N88-25180

X

XU, Y. N88-25126
XUDONG, C. N88-25055

Y

YAE, KWANG HAROLD N88-25006
YAMAGISHI, TAKASHI N88-25285
YANG, ROBERT ALEXANDER N88-24969
YANG, ZHONGMIN N88-24921
YAO, DAVID N88-25007
YAVARI, B. N88-25265
YE, YINYU N88-25178
YEH, POCHI N88-25295
YELLE, R. V. N88-25417
YEUNG, WILLIAM N88-25264
YOCHMOWITZ, MICHAEL G. N88-25128
YOUNG, ANDREW J. N88-25139
YOUNG, J. D. N88-25175
YOUNG, REED F. N88-24963
YOUNGBLOOD, R. W. N88-24982
YU, F. N88-24782
YU, PING N88-25268
YUILLE, A. L. N88-25269
YUNG, YUK L. N88-25093
YUNN, B. C. N88-25291

Z

ZALZMAN, S. N88-24991
ZARDECKI, A. N88-24957
ZEILNER, R. N88-25070
ZELLNER, R. N88-25067
ZETZSCH, C. N88-25073
ZHANG, BINJIANG N88-24582
ZHANG, Y. N88-24976
ZHAO, Y. N88-25042
ZHONG, Y. N88-24700
ZHU, SONG-PING N88-24918
ZIEMIANSKI, JOSEPH A. N88-24641
ZIMMERMAN, DAVID C. N88-24667
ZIRIN, HAROLD N88-25421
ZOLTANI, C. K. N88-25230
ZUMINO, B. N88-25366
ZURAWSKI, ROBERT L. N88-24689
N88-24808

Typical Corporate Source Index Listing

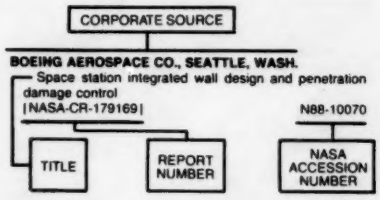

Listings in this index are arranged alphabetically by corporate source. The title of the document provides the user with a brief description of the subject matter. The report number helps to indicate the type of document cited (e.g., NASA report, translation, NASA contractor report). The NASA accession number denotes the number by which the citation is identified. The titles are arranged under each corporate source in ascending accession number order.

A

ADVANCED RESEARCH AND APPLICATIONS CORP., SUNNYVALE, CALIF.
The inspection of electronic metallurgical bonds
[AD-A192197] N88-24745
The inspection of metallurgical bounds in electronic systems
[AD-A192064] N88-25343

AERONAUTICAL RESEARCH ASSOCIATES OF PRINCETON, INC., N. J.
Research in nonlinear wave motion
[AD-A191686] N88-24884

AERONAUTICAL RESEARCH INST. OF SWEDEN, STOCKHOLM.
Wind tunnel investigation of wing and control panel loads at transonic and supersonic speeds on some schematic cruciform missile configurations
[FFA-TN-1988-43] N88-24585
Incompressible Euler solution on a multiblock grid around a car configuration
[FFA-TN-1987-65] N88-24586
Wave growth associated with turbulent spots in plane Poiseuille flow
[FFA-TN-1988-08] N88-24587
Detecting delaminations in CFRP specimens using X-ray techniques
[FFA-TN-1988-04] N88-24704
Some stress intensity factor equations
[FFA-TN-1987-07] N88-24995
Automated analysis of crack growth rate for obtaining da/dN versus delta K relation
[FFA-TN-1987-70] N88-24996

AERONAUTICAL RESEARCH LABS., MELBOURNE (AUSTRALIA).
PAFEC level 6.2 application program
[AD-A191037] N88-25209

AERONAUTICAL SYSTEMS DIV., WRIGHT-PATTERSON AFB, OHIO.
An evaluation of three linear scale radar altimeter displays
[AD-A192173] N88-24636

AEROSPACE CORP., EL SEGUNDO, CALIF.
Thermographic detection of buried debonds
[AD-A192115] N88-24680
Nickel hydrogen low earth orbit life testing
[AD-A191946] N88-24855
Deep dielectric charging effects due to high energy electrons in earth's outer magnetosphere
[AD-A192154] N88-25083

AEROSPACE CORP., LOS ANGELES, CALIF.
Contamination of optical surfaces N88-25400

AEROSPACE MEDICAL RESEARCH LABS., WRIGHT-PATTERSON AFB, OHIO.
A systems engineering based methodology for analyzing human electrocortical responses
[AD-A190809] N88-25135
Eye and head response to an attention cue in a dual task paradigm
[AD-A191052] N88-25143

AEROSPACE RESEARCH CORP., ROANOKE, VA.
Evaluation of manure as a feedstock for gas turbines N88-25050
A 3 MW wood fired gas turbine at Red Boiling Springs, Tennessee N88-25051

AIR FORCE INST. OF TECH., WRIGHT-PATTERSON AFB, OHIO.
A system status monitor for the National Aerospace Plane
[AD-A190681] N88-24624
Parameter-adaptive model-following for in-flight simulation
[AD-A190567] N88-24645
Feature extraction using the Hough transform
[AD-A190679] N88-25185

AIR FORCE SYSTEMS COMMAND, WRIGHT-PATTERSON AFB, OHIO.
Acta aeronautica et astronautica sinica (selected articles)
[AD-A191552] N88-24575
Experiment investigation on longitudinal characteristics of the forward swept wing
[AD-A191553] N88-24582

AIR FORCE WRIGHT AERONAUTICAL LABS., WRIGHT-PATTERSON AFB, OHIO.
Composite repair of cracked aluminum alloy aircraft structure
[AD-A190514] N88-24573
Carbon matrix composites prospective roles for biotechnology N88-24694
Current and future molecular structures of aerospace organic matrix resins N88-24695
Selective detection in gas chromatography
[AD-A191499] N88-24718
New polyisoimides: An approach to in situ rigid-rod polyimide formation
[AD-A191665] N88-24773
High strength/sigh modulus aromatic heterocyclic ABA block copolymers
[AD-A191666] N88-24774

AIRCRAFT OWNERS AND PILOTS ASSOCIATION, FREDERICK, MD.
General-aviation's view of progress in the aviation weather system N88-25110

AKRON UNIV., OHIO.
Adhesion between polystyrene and polymethylmethacrylate
[AD-A192050] N88-24785
Linear and nonlinear acoustic wave propagation in the atmosphere
[NASA-CR-4157] N88-25268

ALABAMA UNIV., HUNTSVILLE.
Optical monitoring of protein crystal growth
[NASA-CR-182869] N88-24738
Space station induced electromagnetic effects N88-25394
Space station contamination study: Assessment of contaminant spectral brightness N88-25395

AMERICAN MATHEMATICAL SOCIETY, NEW YORK, N.Y.
Infinite dimensional dynamical systems and their finite dimensional analogues
[AD-A192041] N88-25216

AMERICAN SOCIETY FOR COMPOSITES, DAYTON, OHIO.
Proceedings of the American Society for Composites
[AD-A189861] N88-24693

AMERICAN SOCIETY FOR ENGINEERING EDUCATION, WASHINGTON, D. C.
Research work completed at the Naval Surface Warfare Center Solid State Group of the Radiation Division
[AD-A191627] N88-25339

AMES LAB., IOWA.
Effect of hydrogen, deuterium and oxygen on the anelastic properties of refractory alloys
[DE88-007349] N88-24736

ANACAPA SCIENCES, INC., FORT RUCKER, ALA.
An enumeration of research to determine the optimal design and use of Army flight training simulators
[AD-A191242] N88-24649

ANACAPA SCIENCES, INC., SANTA BARBARA, CALIF.
Space station habitability recommendations based on a systematic comparative analysis of analogous conditions
[NASA-CR-3943] N88-25372

ANALYTIC SCIENCES CORP., READING, MASS.
National plans for aircraft icing and improved aircraft icing forecasts and associated warning services N88-25113

ANCO ENGINEERS, INC., CULVER CITY, CALIF.
Peak Acceleration Device (PAD)
[AD-A191639] N88-24611

ANT NACHRICHTENTECHNIK, BACKNANG (WEST GERMANY).
Search and rescue satellite system (SERES), phase A0
[ETN-88-92335] N88-24689

APPLICATIONS RESEARCH CORP., DAYTON, OHIO.
An advanced prototyping tool for human factors design
[AD-A187290] N88-25149

ARGONNE NATIONAL LAB., ILL.
Structural studies on La/sub 2/CuO/sub 4+delta/
[DE88-006828] N88-25330

ARIZONA STATE UNIV., TEMPE.
Drilling investigation of a young magmatic intrusion beneath the Inyo Domes, Long Valley, California: Structural and textural studies
[DE88-006813] N88-25078
Mathematical models for VLSI device simulation
[AD-A191125] N88-25212

ARIZONA UNIV., TUCSON.
Nonlinear surface polaritons
[AD-A191048] N88-24822
Signal processing with degenerate four-wave mixing
[AD-A191496] N88-24825
An advanced extruder-feeder biomass liquefaction reactor system N88-25042
Analysis of lightning field changes during active thunderstorms in Florida N88-25103
Experimental elementary particle physics
[DE88-007510] N88-25274
Research in the optical sciences
[AD-A192175] N88-25297

ARMY AEROMEDICAL RESEARCH LAB., FORT RUCKER, ALA.
Evaluation of the US Army fitting program for the integrated helmet unit of the integrated helmet and display sighting system
[AD-A191616] N88-24635
Simultaneous multiple control force exertion capabilities of males and females versus helicopter control force design limits
[AD-A191653] N88-25153

ARMY ARMAMENT RESEARCH AND DEVELOPMENT COMMAND, WATERVLIET, N. Y.
Stress corrosion cracking of A723 steel pressure vessels: Two case studies
[AD-A191741] N88-24990
The high pressure sound velocity and equation of state of aqueous solutions of hydroxylammonium nitrate and triethanolammonium nitrate
[AD-A191740] N88-25266

ARMY AVIATION RESEARCH AND DEVELOPMENT COMMAND, MOFFETT FIELD, CALIF.
Some rotorcraft applications of computational fluid dynamics
[NASA-TM-100086] N88-24601

ARMY AVIATION SYSTEMS COMMAND, HAMPTON, VA.
Inflow measurements made with a laser velocimeter on a helicopter model in forward flight. Volume 1: Rectangular planform blades at an advance ration of 0.15
[NASA-TM-100541] N88-24607

ARMY COLD REGIONS RESEARCH AND ENGINEERING LAB., HANOVER, N.H.
Ice conditions along the Ohio River as observed on LANDSAT images, 1972-1985
[AD-A191172] N88-25018
ARMY CONSTRUCTION ENGINEERING RESEARCH LAB., CHAMPAIGN, ILL.
Operational noise data for CH-47D and AH-64 army helicopters
[AD-A191059] N88-25263
ARMY ENGINEER WATERWAYS EXPERIMENT STATION, VICKSBURG, MISS.
Design of overlays for rigid airport pavements
[DOT/FAA/PM-87/19] N88-24652
ARMY LAB. COMMAND, WATERTOWN, MASS.
Characterization of yttrium aluminum garnet/YAG/using 14 MeV neutron activation
[AD-A191925] N88-25342
ARMY MILITARY PERSONNEL CENTER, ALEXANDRIA, VA.
The coordination of multiple robotic manipulators
[AD-A190869] N88-24963
ARMY MISSILE COMMAND, REDSTONE ARSENAL, ALA.
Inevitable inflation in Einstein-Cartan theory with improved energy-momentum tensor with spin
[NASA-TM-101146] N88-25365
ARMY NATICK RESEARCH AND DEVELOPMENT COMMAND, MASS.
The effects of different combinations of inlet air conditions used for cooling as measured on a heated manikin
[AD-A191116] N88-25151
ARMY RESEARCH INST. OF ENVIRONMENTAL MEDICINE, NATICK, MASS.
Physiological and hematological responses of matched older and younger men during dry-heat acclimation
[AD-A186450] N88-25139
ARMY STATEGIC DEFENSE COMMAND, HUNTSVILLE, ALA.
A general approach for automating source code verification
[AD-A191461] N88-25170
ATLANTA UNIV., GA.
Computational sciences
[AD-A190826] N88-25226
Numerical solution of a system of random Volterra integral equations. 1: Successive approximation method N88-25227
A mixed min-max control problem governed by integral equations N88-25228
Numerical solution to a system of random Volterra integral equations N88-25230
Optimal processes governed by integral equations with unilateral constraint N88-25231
Mixed min-max optimization problem with restrictions N88-25232
Approximate solution of random differential equation N88-25233
A method for the numerical solution of random Cauchy singular integral equation N88-25234
Numerical solution of random Love's integral equation N88-25235
The use of Lagrange multipliers and Kuhn-Tucker's theory in optimization problems N88-25236
AUBURN UNIV., ALA.
Design studies of low aspect-ratio torsatrons
[DE88-007562] N88-25320

B

BALLISTIC RESEARCH LABS., ABERDEEN PROVING GROUND, MD.
An extinguisher to quench propellant fires
[AD-A190785] N88-24813
Internal fluid dynamics within a nonspinning partially liquid-filled shell due to burster rupture
[AD-A191055] N88-24874
Plate response analysis using shock tube
[AD-A190828] N88-24967
Performance estimates for operations conducted while wearing individual protective equipment: User manual
[AD-A191871] N88-25154
BATTELLE COLUMBUS LABS., RESEARCH TRIANGLE PARK, N.C.
An electrostatic potential comparator
[AD-A192051] N88-25177
BATTELLE COLUMBUS LABS., OHIO.
Aircraft emissions characterization: TF41-A2, TF30-P103 and TF30-P109 engines
[AD-A192053] N88-24638
BATTELLE INST., FRANKFURT AM MAIN (WEST GERMANY).
Assessment of optical communications systems for Data Relay Satellite. Volume 1: Executive summary
[ESA-CR(P)-2488-VOL-1] N88-24841
BELL COMMUNICATIONS RESEARCH, INC., MURRAY HILL, N.J.
Photoconductivity in carbon fibers
[AD-A191728] N88-24782
BIO-TECHNICAL RESOURCES, INC., MANITOWOC, WISC.
The application of hydrocarbon bioconversion technology to aerospace materials production N88-24698
BKM, INC., SAN DIEGO, CALIF.
Servojet retrofit
[AD-A191075] N88-24964
BLOCHER-MOTOR G.M.B.H. AND CO. K.G., METZINGEN (WEST GERMANY).
Design study. Manipulator systems for model handling in European transonic wind tunnels
[ETN-88-91944] N88-24851
BOLT, BERANEK, AND NEWMAN, INC., CAMBRIDGE, MASS.
A framework for a theory of mapping
[AD-A191071] N88-25144
BRIGHAM YOUNG UNIV., PROVO, UTAH.
Evaluating evaporation with satellite thermal data
[AD-A192042] N88-25019
BRISTOL UNIV. (ENGLAND).
The theory of random alloys
[DE88-006408] N88-24758
BRITISH AEROSPACE PUBLIC LTD. CO., BRISTOL (ENGLAND).
P-Plus: Polar Platform utilization study, executive summary
[BAE-TP-8391] N88-24853
BRITISH LIBRARY LENDING DIV., BOSTON SPA (ENGLAND).
Calculation of root-mean-square loads
[BLL-M-37776-(5828.4)] N88-25015
Certain questions of thermodynamic theory of weak solutions N88-25368
BROOKHAVEN NATIONAL LAB., UPTON, N. Y.
Update of low temperature catalyst development
[DE88-007032] N88-24715
Integral equation for the laser field: Multimode description of a free-electron laser oscillator
[DE88-007050] N88-24956
Applications of fault tree analysis to the design process
[DE88-007048] N88-24982
An optical technique for measuring divergence, beam profile, and aiming direction, of relativistic negative hydrogen ions
[DE88-007049] N88-25278
The multistring model VENUS for ultrarelativistic heavy ion collisions
[DE88-007666] N88-25284
Experiments with high energy nuclear beams at Brookhaven: From AGS to RHIC (Relativistic Heavy Ion Collider)
[DE88-007042] N88-25287
On bunch lengthening using the fourth harmonic cavity in the NSLS VUV ring
[DE88-007392] N88-25288
Plasma neutralizer work at BNL (Brookhaven National Laboratory)
[DE88-007046] N88-25317
BROWN UNIV., PROVIDENCE, R. I.
Dynamic shear band development in plane strain
[AD-A190915] N88-24988
High degree interpolation polynomial in Newton form
[NASA-CR-181677] N88-25249
Novel fiber preforms: Rare earth doping
[AD-A191549] N88-25294
Electronic structure, elementary excitations, optical and transport properties of semiconductor superlattices
[AD-A190795] N88-25333

C

CALIFORNIA INST. OF TECH., PASADENA.
Instrumentation for turbulent reacting flows
[AD-A191671] N88-24923
Photochemical and thermal modeling in the early atmosphere of the earth
[NASA-CR-183029] N88-25093
Theoretical investigation of optical computing based on neural network models
[AD-A191668] N88-25214
An image processing system for research in solar physics
[AD-A191673] N88-25421
CALIFORNIA UNIV., BERKELEY.
Application of Rayleigh scattering to turbulent flow with heat transfer and combustion
[AD-A191565] N88-24720
Visual information processing in the perception of features and objects
[AD-A192026] N88-25148
On the use of convergent beam electron diffraction for identification of antiphase boundaries in GaAs grown on Si
[DE88-006220] N88-25362
CALIFORNIA UNIV., BERKELEY. LAWRENCE BERKELEY LAB.
Strain hardening at large strains in aluminum alloys
[DE88-007415] N88-24737
Nuclear and astrophysical evidence on the equation of state
[DE88-007397] N88-25279
Energy measurements in oxygen-induced reactions at 60 A GeV and 200 A GeV
[DE88-006420] N88-25283
Vacancy ordering in the basal plane of YBa2Cu3O(sub)z
[DE88-004572] N88-25348
The morphological stability of continuous intergranular phases: Thermodynamic considerations
[DE88-006328] N88-25350
On the use of convergent beam electron diffraction for identification of antiphase boundaries in GaAs grown on Si
[DE88-006220] N88-25362
The geometry of the Virasoro group for physicists
[DE88-007374] N88-25366
CALIFORNIA UNIV., DAVIS.
Superplasticity: A fundamental investigation on deformation mechanism and cavitation phenomena
[AD-A191548] N88-24741
Turbulent heat transfer and fluid flow measurements downstream of abrupt expansions and in a cavity of a circular tube at a uniform wall temperature N88-24920
QN3D: A 3-dimensional quasi-neutral hybrid particle-in-cell code with applications to the tilt mode instability in field reversed configurations N88-25325
CALIFORNIA UNIV., IRVINE.
Analysis of molecular mixing and chemical reaction in mixing layer
[AD-A191600] N88-24721
Study of mixing and reaction in the field of a vortex
[AD-A191489] N88-24878
Models of incremental concept formation
[AD-A191597] N88-25147
A computational model of motor behavior
[AD-A191179] N88-25152
LispSEI: The programmer's manual
[AD-A191632] N88-25172
Propagation of neutralized ion beams
[AD-A191599] N88-25289
Stochasticity in a Q-machine plasma N88-25315
CALIFORNIA UNIV., LOS ANGELES.
Local delamination buckling in layered structures N88-24711
Optimizing feedback utilization in motor skill training
[AD-A191559] N88-25146
CALIFORNIA UNIV., SAN DIEGO.
Design of catalytic monoliths for closed-cycle carbon dioxide lasers
[NASA-CR-182983] N88-25185
A new approach to generating negative ion beams
[AD-A191119] N88-25276
CALIFORNIA UNIV., SAN DIEGO, LA JOLLA.
Computer aided design of monolithic microwave and millimeter wave integrated circuits and subsystems
[AD-A191593] N88-24852
Research in enumeration and graph theory with applications to computer science
[AD-A191567] N88-25171
Observations of cosmic rays in the outer heliosphere
[NASA-CR-182942] N88-25425
CALIFORNIA UNIV., SANTA BARBARA.
The calculation of transonic flow over the shuttle orbiter using slender body theory N88-24606
Time resolved spectroscopy facility for the study of nonlinear optical properties of semiconducting polymers
[AD-A191221] N88-24768
From general relativity to the theory of superstrings N88-25369
CARNEGIE-MELLON UNIV., PITTSBURGH, PA.
An OOD (Object-Oriented Design) paradigm for flight simulators
[AD-A191097] N88-24647
Fundamental studies of beta phase decomposition modes in titanium alloys
[AD-A191495] N88-24740

CATHOLIC UNIV., SANTIAGO (CHILE).
Development and validation of transmission measurements techniques of image contrast, utilizing existing IR imagers
[AD-A191471] N88-25079

CATHOLIC UNIV. OF AMERICA, WASHINGTON, D.C.
Analysis of a closed-kinematic chain robot manipulator
[NASA-CR-183031] N88-25206

CENTER FOR MATHEMATICS AND COMPUTER SCIENCE, AMSTERDAM (NETHERLANDS).
Reliability of stochastically forced systems (extended version)
[CWI-AM-R8801] N88-24985
Analysis of a six-component barotropic spectral model: Chaotic motion, predictability and vacillation
[CWI-AM-R8710] N88-25090
Solving bidiagonal systems of linear equations on the CDC CYBER 205
[CWI-NM-R8725] N88-25187
On a biorthogonal system associated with uniform asymptotic expansions
[CWI-AM-R8709] N88-25240
Mathematical morphology for structures without translation symmetry
[CWI-AM-R8803] N88-25241
Multigrid methods for elliptic Partial Differential Equations (PDEs)
[CWI-NM-R8722] N88-25242
Stability and convergence of the Peaceman-Rachford ADI method for initial-boundary value problems
[CWI-NM-R8724] N88-25243
Perturbation theory for dual semigroups. Part 4: The intertwining formula and the canonical pairing
[CWI-AM-R8802-PT-4] N88-25258
A comparative study of Chebyshev acceleration and residue smoothing in the solution of nonlinear elliptic difference equations
[CWI-NM-R8723] N88-25259

CENTER FOR NIGHT VISION AND ELECTRO-OPTICS, FORT BELVOIR, VA.
An optical preamplifier for detection of CO2 laser radiation
[AD-A190790] N88-24949

CENTRE D'ESSAIS AERONAUTIQUE TOULOUSE (FRANCE).
Elementary characterization of preimpregnated carbon epoxy T400H/DA0506 from STRUCTIL. Test report M6-577100
[CEAT-047426] N88-24703

CENTRE D'ETUDES ET DE RECHERCHES, TOULOUSE (FRANCE).
Boundary layer transition
[CERT-OA-37/5018-AYD] N88-24595
Supplements to the study of the wake of a Mirage G8 model at F2
[CERT-RT-OA-20/5025-AYD] N88-24596
Nondestructive testing using ultrahigh frequencies
[CERT-5/1333-MO] N88-24984

CENTRE NATIONAL D'ETUDES SPATIALES, TOULOUSE (FRANCE).
Assessment of optical communications systems for Data Relay Satellite. Volume 1: Executive summary
[ESA-CR(P)-2468-VOL-1] N88-24841

CHALMERS UNIV. OF TECHNOLOGY, GOETEBORG (SWEDEN).
Geodesy by radio interferometry: Optimization of wet path delay algorithms using microwave radiometer data
[PB88-167739] N88-24820

CHARLES RIVER ANALYTICS, INC., CAMBRIDGE, MASS.
User's guide to the Fault Inferring Nonlinear Detection System (FINDS) computer program
[NASA-CR-178410] N88-24619

CHEMICAL RESEARCH AND DEVELOPMENT CENTER, ABERDEEN PROVING GROUND, MD.
Optical constants of minerals and other materials from the millimeter to the ultraviolet
[AD-A192210] N88-24724
Proposed quality assurance/quality control plan
[AD-A191490] N88-24978

CHICAGO UNIV., ILL.
Self-consistent model for the brittle response of solids N88-24999

CINCINNATI UNIV., OHIO.
Interaction of ultrasonic waves with composite plates
[AD-A191879] N88-24702
The theory of random alloys
[DE88-006408] N88-24756
Composite reduced Navier-Stokes procedures for flow problems with strong pressure interactions
[AD-A191127] N88-24875
Brunt-Doppler ducting of buoyancy waves in a temperature- and wind-stratified atmosphere N88-25086

CITY COLL. OF THE CITY UNIV. OF NEW YORK.
Communications using channels formed by meteor bursts
[AD-A192088] N88-24834

CLARKSON UNIV., POTSDAM, N.Y.
Nonlinear wave propagation
[AD-A192104] N88-24835
Nonlinear waves
[AD-A192148] N88-24889

CLERMONT-FERRAND UNIV. (FRANCE).
Ice formation on aircraft
[ETN-88-92154] N88-25104

COAST GUARD RESEARCH AND DEVELOPMENT CENTER, GROTON, CONN.
Descriptions of HF and VHF Loran-C buoys and evaluations as potential datum marker buoys
[AD-A192069] N88-24618

COLORADO UNIV., BOULDER.
Topological stereochemistry
[AD-A191867] N88-24691
Chemical kinetics of nitramine propellant combustion
[AD-A191556] N88-24802
DMSP-SSM/1 NASA algorithm validation using primarily LANDSAT and secondarily DMSP and/or AVHRR visible and thermal infrared satellite imagery
[NASA-CR-182979] N88-25024

COLORADO UNIV., COLORADO SPRINGS.
Magnetic superlattices
[AD-A191450] N88-25334

COMMERCE DEPT., ROCKVILLE, MD.
Lightning detection and locating systems N88-25112

CONNECTICUT UNIV., STORRS.
Preferential surface adsorption in miscible blends of polystyrene and poly(vinyl methyl ether)
[AD-A191451] N88-24769

CONTINUOUS ELECTRON BEAM ACCELERATOR FACILITY, NEWPORT NEW, VA.
The loss parameters for very short bunches
[CEBAF-PR-88-005] N88-25291

COOPER INDUSTRIES, INC., CANNONSBURG, PA.
Harmonic considerations for electrical distribution feeders
[DE88-007849] N88-24860

CORNELL UNIV., ITHACA, N.Y.
Electrochemistry in liquid crystals
[AD-A191554] N88-24719
To relate measurements of gravity and geoid anomalies over the oceans to near surface density distributions
[AD-A192168] N88-25120
Annotated computer output for split plot design: SAS GLM
[AD-A190800] N88-25167

COUNCIL FOR MINERAL TECHNOLOGY, RANDBURG (SOUTH AFRICA).
Phase diagrams in materials science and the use of the computer in their calculation
[PB88-155262] N88-25364

D

DARESBURY NUCLEAR PHYSICS LAB. (ENGLAND).
Ground state properties and electronic structure of high T sub c superconductors
[DE88-007485] N88-25360

DARTMOUTH COLL., HANOVER, N.H.
Ultraviolet spectra of subluminous objects found in the Kiso Schmidt survey and systematic reanalysis of the archived ultraviolet spectra of white dwarfs observed with the IUE satellite under the Astrophysics Data Program (ADP)
[NASA-CR-182976] N88-25406
Ultraviolet spectra of two magnetic white dwarfs and ultraviolet spectra of subluminous objects found in the Kiso Schmidt survey
[NASA-CR-183051] N88-25408

DATA TRANSFORMATION CORP., SILVER SPRING, MD.
New York TRACON demonstration of program recoding requirements analysis document
[DOT/FAA/CT-87/34] N88-24622

DAVID SARNOFF RESEARCH CENTER, PRINCETON, N.J.
Distributed feedback lasers
[NASA-CR-4154] N88-24948

DAYTON UNIV., OHIO.
Fast algorithm development for large-eddy simulation of circular-jet turbulence
[AD-A192044] N88-24887
Objective detection and forecasting of Clear-Air Turbulence (CAT): A status report N88-25114

DEFENCE RESEARCH ESTABLISHMENT ATLANTIC, DARTMOUTH (NOVA SCOTIA).
Cross stream differencing for integral boundary layer equations
[AD-A191744] N88-24886

DEFENSE INTELLIGENCE AGENCY, WASHINGTON, D.C.
Bibliography of Soviet laser developments, number 83, May - June 1986
[AD-A190969] N88-24950

DEFENSE TECHNICAL INFORMATION CENTER, ALEXANDRIA, VA.
Defense Technical Information Center cataloging guidelines
[AD-A192200] N88-25382

DELAWARE UNIV., LEWES.
Construction of approximations to acoustic Green's functions for nonhomogeneous oceans using transmutation
[PB88-185384] N88-25126

DELAWARE UNIV., NEWARK.
Structure/property/reactivity relations among nitramine and other energetic materials
[AD-A190878] N88-24716

DEPARTMENT OF DEFENSE, WASHINGTON, D. C.
The Department of Defense report on the merit review process for competitive selection of university research projects and an analysis of the potential for expanding the geographic distribution of research for the Committees on Appropriations, United States Congress
[AD-A191842] N88-25379

DEUTSCHE FORSCHUNGS- UND VERSUCHSANSTALT FUER LUFT- UND RAUMFAHRT, BRUNSWICK (WEST GERMANY).
Optics: Perspectives for Measurement Techniques and Signal Processing for Flight Guidance
[DFVLR-MITT-87-21] N88-24928
Concepts for a laser gyroscope of the highest precision N88-24929
Laser gyroscopes using the rate-bias technique N88-24930
Development of mirrors for high-precision laser gyroscopes N88-24931
Laboratory tests of laser gyroscopes for future utilization in multifunction systems for precision navigation and flight guidance N88-24932
Navigation using the Teldix fiber-optic gyroscope N88-24933
Limits of accuracy and range of laser radars N88-24934
The optical accelerometer: A novel sensor for vertical flight guidance N88-24935
Inertial reference system with Global Positioning System (GPS) support N88-24936
Digital fiber optic displacement sensors N88-24937
Investigations in electro-optical multistability for signal processing N88-24938

DEUTSCHER WETTERDIENST, HAMBURG (WEST GERMANY).
Results of radiation measurements in West Germany and from special measurement series in the Meteorological Observatory of Hamburg
[REPT-11] N88-25088

DIRECTION DES ARMEMENTS TERRESTRES, TOULOUSE (FRANCE).
Parachute for in-flight training on parachute ejection
[REPT-87-11] N88-24593

DORNIER-WERKE G.M.B.H., FRIEDRICHSHAFEN (WEST GERMANY).
P-Plus: Polar Platform utilization study, executive summary
[BAE-TP-8391] N88-24653
Search and rescue satellite system (SERES), phase A0
[ETN-88-92335] N88-24660

DOUGLAS AIRCRAFT CO., INC., LONG BEACH, CALIF.
Instability of laminar separation bubbles: Causes and effects
[AD-A191168] N88-24876

DRAPER (CHARLES STARK) LAB., INC., CAMBRIDGE, MASS.
A design study of onboard navigation and guidance during aerocapture at Mars
[NASA-CR-172053] N88-24654
A feedback linearization approach to spacecraft control using momentum exchange devices
[NASA-CR-172057] N88-24668

DREXEL UNIV., PHILADELPHIA, PA.
Mixed-mode fracture of uniaxial fiber reinforced composites
[AD-A191629] N88-24700

DUKE UNIV., DURHAM, N. C.
Effectiveness evaluation of fault-tolerant multiprocessor systems
[AD-A191688] N88-25158
Representation and decision mechanisms in artificial intelligence
[AD-A191083] N88-25197

E

EAGLE ENGINEERING, INC., HOUSTON, TEX.
Lunar base surface mission operations. Lunar Base Systems Study (LBSS) task 4.1
[NASA-CR-172050] N88-25415

EAGLE ENGINEERING, INC., WEBSTER, TEX.
Mars rover/sample return mission requirements affecting space station
[NASA-CR-172048] N88-25414

ECOLE NATIONALE SUPERIEURE DES TELECOMMUNICATIONS, PARIS (FRANCE).
Application of dynamic programming to image registration
[ENST-87E022] N88-25180

ECOLE NORMALE SUPERIEURE, PARIS (FRANCE).
Numerical simulation of nonlinear structural dynamics of large scale unsteady flow
[ETN-88-92156] N88-24906

EDGERTON, GERMESHAUSEN AND GRIER, INC., IDAHO FALLS, IDAHO.
Advanced nuclear rocket engine mission analysis
[DE88-006797] N88-24881
Interfacial shear phenomena in graphite epoxy composites under impact loading using dynamic moire interferometry
[DE88-006773] N88-24709
Laboratory scale inert gas atomizer for producing rapidly solidified powders
[DE88-006734] N88-24812
Theoretical and experimental damping values of piping systems at high ductilities
[DE88-006717] N88-24986
A perspective of PC-based probabilistic risk assessment
[DE88-006715] N88-25251

EDGERTON, GERMESHAUSEN AND GRIER, INC., SALEM, MASS.
Tactical Rubidium Frequency Standard (TRFS), volume 2
[AD-A191190] N88-24850

ELECTROSPACE SYSTEMS, INC., ARLINGTON, VA.
WIPP (Wave Induced Particle Precipitation) experiment logistic support
[AD-A191184] N88-24824

ELORET CORP., SUNNYVALE, CALIF.
Experimental investigation of hypersonic serodynamics
[NASA-CR-182973] N88-24591

ENVIRONMENTAL PROTECTION AGENCY, RESEARCH TRIANGLE PARK, N.C.
Motor vehicles as sources of compounds important to tropospheric and stratospheric ozone
[PB88-195219] N88-25076

ERNO RAUMFAHRTTECHNIK G.M.B.H., BREMEN (WEST GERMANY).
Search and rescue satellite system (SERES), phase A0
[ETN-88-92335] N88-24689
Operational facilities of EURECA A1 mission
[ETN-88-91939] N88-24810

ESSEX CORP., ORLANDO, FLA.
Simulator evaluation of lineup visual landing aids for night carrier landing
[AD-A191212] N88-24648

EUROPEAN NUCLEAR ENERGY AGENCY, FRASCATI (ITALY).
Integral equation for the laser field: Multimode description of a free-electron laser oscillator
[DE88-007050] N88-24956

EUROPEAN SPACE AGENCY. EUROPEAN SPACE RESEARCH AND TECHNOLOGY CENTER, ESTEC, NOORDWIJK (NETHERLANDS).
Simulations of the electrostatic charging of ESA communications satellites
[ESA-STM-239] N88-24670

EUSTANCE AND HOROWITZ, CIRCLEVILLE, N.Y.
Flotation processes
[PB88-180302] N88-25075

F

FEDERAL AVIATION ADMINISTRATION, ATLANTIC CITY, N.J.
FAA aviation forecasts fiscal years 1988-1999
[AD-A191711] N88-24576
Rotorcraft TCAS (traffic alert and collision avoidance system) evaluation: Group 3 results
[AD-A191719] N88-24614
Optimization of the dilation characteristic on the control jurisdiction of an area control facility
[AD-A191720] N88-24615
Microwave landing system mathematical modeling study for Midway Airport Runway 22L, Chicago, Illinois
[AD-A191721] N88-24616

FEDERAL AVIATION ADMINISTRATION, WASHINGTON, D.C.
US civil airmen statistics, 1987
[AD-A191714] N88-24577
Cessna 172 MLS (Microwave Landing System) terminal instrument procedures (TERPS) approach data collection and processing data report
[AD-A191241] N88-24613

FEDERAL AVIATION AGENCY, ATLANTIC CITY, N.J.
Study of benefits of passenger protective breathing equipment from analysis of past accidents
[DOT/FAA/CT-88/03] N88-24610

FLEET NUMERICAL OCEANOGRAPHY CENTER, MONTEREY, CALIF.
Applications products of aviation forecast models
N88-25109

FLORIDA STATE UNIV., TALLAHASSEE.
Asymptotic theory for weighted least squares estimators in Aalen's additive risk model
[AD-A191085] N88-25210

FLORIDA UNIV., GAINESVILLE.
Finite element analysis of an underground structure
[AD-A191747] N88-24991
An electrostatic potential comparator
[AD-A192051] N88-25117
Exact tests for variance component models with unequal cell frequencies in the last stage
[AD-A191645] N88-25253

FLOW RESEARCH, INC., KENT, WASH.
Direct numerical simulations of the PDF's (Probability Density Functions) of a passive scalar in a forced mixing layer
[AD-A192134] N88-25256

FLUID DYNAMICS INTERNATIONAL, INC., EVANSTON, ILL.
Simulations of a missile with liquid payload under launch conditions
[AD-A191479] N88-24825

FOERENADE FABRIKSVERKEN, LINKOEPING (SWEDEN).
High resolution radar techniques: Five contributions to MILINF 86
[PB88-172721] N88-24821

FOM-INST. VOOR PLASMAFYSICA, RIJNHUIZEN, JUTPHAAS (NETHERLANDS).
Activities report in plasma physics
[ETN-88-92221] N88-25324

FOREIGN APPLIED SCIENCES ASSESSMENT CENTER, LA JOLLA, CALIF.
Soviet combustion research
[PB88-182324] N88-24730

FRAUNHOFER-INST. FUER ATMOSPHAERISCHE UMWELTFORSCHUNG, GARMISCH-PARTENKIRCHEN (WEST GERMANY).
Ultraviolet measurements: Measurements of photolysis rates N88-25065

FRAUNHOFER INST. FUER KURZZEITDYNAMIK, FREIBURG IM BREISGAU (WEST GERMANY).
Electrical ignition of HAN-based liquid propellants
[AD-A191349] N88-24801

FRAUNHOFER-INST. FUER LASERTECHNIK, AACHEN (WEST GERMANY).
High power axial flow CO2 laser
[ETN-88-91951] N88-24959

FRAUNHOFER-INST. FUER TOXIKOLOGIE UND AEROSOLFORSCHUNG, SCHMALLENBERG-GRAFSCHAFT (WEST GERMANY).
Development of continuous wave laser frequency modulation of OH in tropospheric concentrations range N88-25073

FRAUNHOFER INST. FUER WERKSTOFFMECHANIK, FREIBURG (WEST GERMANY).
Analysis and developments of failure concepts in fracture mechanics based on research results in the field of component safety topics: J-integral concept; crack resistance curves; dynamic criterion
[V-19/86] N88-25009

FWG ASSOCIATES, INC., TULLAHOMA, TENN.
Aircraft/lidar turbulence comparison N88-25111

G

GENERAL ACCOUNTING OFFICE, WASHINGTON, D. C.
FAA (Federal Aviation Administration) technical center: Mission and role in natinal airspace system plan implementation
[PB88-169818] N88-24609
Air pollution: Ozone attainment requires long-term solutions to solve complex problems
[PB88-167275] N88-25060
Financial reporting: NASA (National Aeronautics and Space Administration) can improve compliance with GAO (General Accounting Office) standards and treasury requirements
[PB88-172523] N88-25373

GENERAL ATOMIC CO., SAN DIEGO, CALIF.
Irradiation effects on tungsten stabilized martensitic steels
[DE88-007074] N88-24748

GENERAL ELECTRIC CO., SCHENECTADY, N.Y.
A microcomputer-based control and simulation of an advanced IPM (Interior Permanent Magnet) synchronous machine drive system for electric vehicle propulsion
[DE88-006735] N88-24859

GENEVA OBSERVATORY (SWITZERLAND).
Duplicity in the solar neighborhood. Part 3: New spectroscopic elements for nine solar-type binary stars
[SER-C-PREPUBL-FASC-18-PT-3] N88-25405
Pre-supernova evolution of SN 1987A
[SER-C-PREPUBL-FASC-15] N88-25409
Radial velocities monitoring of a sample of barium and S stars using CORAVEL: Towards an evolutionary link between barium and S stars?
[SER-C-PREPUBL-FASC-19] N88-25410
Review of the theoretical changes of surface chemistry during massive star evolution
[SER-C-PREPUBL-FASC-17] N88-25411

GEO-CENTERS, INC., NEWTON, MASS.
Reference filters for electrostatic charging tendency measurements of fuels
[AD-A191717] N88-24803

GEOEXPLORERS INTERNATIONAL, INC., DENVER, COLO.
Geological evolution and analysis of confirmed or suspected gas hydrate localities. Volume 2: Basin analysis, formation and stability of gas hydrates in the Black Sea
[DE88-001052] N88-25023

GEOLOGICAL SURVEY, MENLO PARK, CALIF.
Geodesy by radio interferometry: Optimization of wet path delay algorithms using microwave radiometer data
[PB88-167739] N88-24820

GEORGE WASHINGTON UNIV., WASHINGTON, D.C.
A transonic small disturbance wing design methodology N88-24590

GEORGIA INST. OF TECH., ATLANTA.
Stagnating turbulent reacting flows
[AD-A191449] N88-24877
Human problem solving in complex dynamic environments
[AD-A190788] N88-25142
Poisson functionals of Markov processes and queueing networks
[AD-A191217] N88-25252
Crystalline metal-semiconductor superlattices
[DE88-007063] N88-25332

GEORGIA TECH RESEARCH INST., ATLANTA.
Low pressure entrained flow pyrolysis of biomass to produce liquid fuels N88-25043

GEORGIA UNIV., ATHENS.
Photoionization dynamics and abundance patterns in laser vaporized tin and lead clusters
[AD-A191604] N88-24722

GESAMTHOCHSCHULE, WUPPERTAL (WEST GERMANY).
Laboratory experiments on atmospheric OH reactions N88-25066

GESELLSCHAFT FUER SCHWERIONENFORSCHUNG M.B.H., DARMSTADT (WEST GERMANY).
Energy measurements in oxygen-induced reactions at 60 A GeV and 200 A GeV
[DE88-006420] N88-25283

GESELLSCHAFT FUER STRAHLEN- UND UMWELTFORSCHUNG M.B.H., MUNICH (WEST GERMANY).
Workshop on Atmospheric OH
[BPT-7/87] N88-25063

GOETTINGEN UNIV. (WEST GERMANY).
Effect of carbohydrate oxidation on the tropospheric HOx-system N88-25067
Determination of tropospheric H concentrations by a double-pulsed UV laser method N88-25070

GOSUDARSTVENNYJ KOMITET PO ISPOLZOVANIYU ATOMNOI ENERGII, SERPUKHOV (USSR).
Study of light transmission methods from scintillators to optical fiber with wave length shifter
[DE88-701587] N88-25292

GRENOBLE-1 UNIV. (FRANCE).
Three dimensional spectral energy measurement on turbulence subjected to a high degree of plane deformation
[ETN-88-92537] N88-24896

GRENOBLE-1 UNIV., SAINT MARTIN D'HERES (FRANCE).
A primal-dual algorithm for the computation of the minimum of a convex function on the intersection of convex functions, and its application in data analysis
[RR-638-M] N88-25217
Open or closed curves by regularized B-splines
[RR-652-M] N88-25218
Variances and higher order correlation coefficients: Continued
[RR-655-M] N88-25219
A fast and efficient procedure for generalized cross-validation with large data sets. Application to image reconstruction
[RR-669-M] N88-25220
GT-DEVICES, ALEXANDRIA, VA.
Analytic and numerical modeling of heat and material transport in electrical hypervelocity guns
[AD-A192178] N88-24655
Performance of a hydrogen pulsed electrothermal thruster. Strategic defense initiative organization innovative science and technology. SBIR, phase 1
[AD-A191999] N88-24679

H

HARRY DIAMOND LABS., ADELPHI, MD.
An analytic model for aerodynamic shapes
[AD-A191573] N88-24583
Development of the field-induced electron injection and impact ionization (F4I) technique for radiation hardness testing of MOS (Metal-Oxide-Semiconductor) gate insulators
[AD-A192114] N88-25345
HARVARD-SMITHSONIAN CENTER FOR ASTROPHYSICS, CAMBRIDGE, MASS.
Geodesy by radio interferometry: Optimization of wet path delay algorithms using microwave radiometer data
[PB86-167739] N88-24820
HARVARD UNIV., CAMBRIDGE, MASS.
A single streamwise vortical structure and its instability in shear flows N88-24921
Speckle imaging of active galactic nuclei: NGC 1068 and NGC 4151 N88-25407
Microwave spectroscopy and gravitational collapse N88-25413
HAUT COMMISSARIAT A LA RECHERCHE, ALGIERS (ALGERIA).
Frequency Analysis of Acoustic Emission - Application to machining and welding
[DE88-701478] N88-25262
HAWAII UNIV., HONOLULU.
The evolution of cometary activity N88-25416
HELSINKI UNIV. OF TECHNOLOGY, ESPOO (FINLAND).
Identification of cascaded microwave circuits with moderate reflections using reflections and transmission measurements
[PB88-171921] N88-24849
Influence of alternating magnetic fields on Zn-67 Moessbauer resonance in ZnO
[PB88-186432] N88-25352
HELSINKI UNIV. TECHNOLOGY, OTANIEMI (FINLAND).
Some unsolved problems in modelling self-timed circuits using Petri Nets, series B, number 2
[PB88-181466] N88-24872
HERCULES AEROSPACE CO., MAGNA, UTAH.
Interfacial shear phenomena in graphite epoxy composites under impact loading using dynamic moire interferometry
[DE88-006773] N88-24709
HIROSHIMA UNIV., TAKEHARA (JAPAN).
Introduction to covariant formulation of superstring (field) theory
[DE87-703038] N88-25363
Comment on non-renormalization theorem in the four dimensional superstrings
[DE88-752551] N88-25367
HONEYWELL, INC., BLOOMINGTON, MINN.
Optical symbolic processor for expert system execution
[AD-A192005] N88-25296
HONEYWELL, INC., HORSHAM, PA.
Optimization of reserve lithium thionyl chloride battery electrochemical design parameters
[DE88-007109] N88-24868
HONEYWELL SYSTEMS AND RESEARCH CENTER, MINNEAPOLIS, MINN.
Nonlinear flying quality parameters based on dynamic inversion
[AD-A192146] N88-24627

I

IDAHO UNIV., MOSCOW.
Study of data distributions and functions for the development of thermodynamic equations of state
[PB86-196365] N88-25370
IIT RESEARCH INST., BARTLESVILLE, OKLA.
The thermodynamic properties of quinoline and isoquinoline
[DE88-001218] N88-24735
IKE ASSOCIATES, INC., INDIANAPOLIS, IND.
Development of test methods for the electrostatic properties of nonhomogeneous fabrics, phase 2
[AD-A190853] N88-24767
ILLINOIS INST. OF TECH., CHICAGO.
Spectroscopy and energy transfer kinetics of the interhalogens
[AD-A192103] N88-25344
ILLINOIS UNIV., CHICAGO.
Determination of settings of a tilted head-cutter for generation of hypoid and spiral bevel gears
[NASA-CR-182138] N88-24976
The stress analysis of ceramic, polymeric, and metallic composite systems by the finite element method N88-25004
ILLINOIS UNIV., URBANA.
Millimeter and submillimeter waves and frequency selective surfaces
[AD-A191511] N88-24827
Cyclic fatigue damage characteristics observed for simple loadings extended to multiaxial life prediction
[NASA-CR-182126] N88-25016
Performance effectiveness and the work/rest cycle
[AD-A191448] N88-25145
ILLINOIS UNIV., URBANA-CHAMPAIGN.
An improved simulated annealing algorithm for standard cell placement
[NASA-CR-182952] N88-25183
IMPERIAL CHEMICAL INDUSTRIES LTD., RUNCORN (ENGLAND).
The synthesis of polyphenylene from a CIS-dihydrocatechol biologically produced monomer N88-24699
IMPERIAL COLL. OF SCIENCE AND TECHNOLOGY, LONDON (ENGLAND).
Computer simulation of turbulent combustion in reciprocating engines
[CFDU/87/11] N88-24725
Computational fluid dynamics applied to the prediction of the heat-transfer, mechanical and thermal-stress behavior of heat exchangers
[CFDU/87/7] N88-24893
CFD benefits, goals, stepping-stones and techniques. Proposals for the scientific programme of the European Reserch Centre on flow, turbulence and combustion
[CFDU/88/1] N88-24894
Numerical simulations of the flat-plate laminar boundary layer in subsonic and supersonic flow
[PDR/CFDU-IC/36] N88-24895
Review of numerical methods for radionuclide transport in three-dimensional porous media, at high Peclet numbers
[CFDU/87/10] N88-25061
INDIANA UNIV., BLOOMINGTON.
A disposable liquid microcell for near-infrared reflectance analysis
[AD-A192190] N88-25298
INNOVATIVE SCIENCES, INC., SAN LEANDRO, CALIF.
Electromagnetic damping and vibration isolation of space structures
[AD-A191492] N88-24665
INSTITUT D'AERONOMIE SPATIALE DE BELGIQUE, BRUSSELS.
Temperature dependence of ultraviolet absorption cross sections of chlorofluoroethanes
[AERONOMICA-ACTA-A-325-1987] N88-24726
Stratospheric positive ion composition measurements and acetonitrile detection: A consistent picture
[AERONOMICA-ACTA-A-326-1987] N88-25084
Interpretation of the northward B sub z (NBZ) Birkeland current system and polar cap convection patterns in terms of the impulsive penetration model
[AERONOMICA-ACTA-A-321-1987] N88-25422
INSTITUT FUER ANGEWANDTE GEODAESIE, FRANKFURT AM MAIN (WEST GERMANY).
Reports on cartography and geodesy. Series 1, no. 99
[ETN-88-92387] N88-25025
West German Geodetic Working Group: Official topographic-cartographic information system (ATKIS), content description N88-25026
West German Geodetic Working Group: Official topographic-cartographic information system (ATKIS), technical conception N88-25027
Vector graphics and raster data processing for spatial information systems N88-25028
Digitizing the traffic network of JOG 250 by scanning N88-25029
Tests for the automatic pattern recognition of building surfaces by the TK 50 N88-25030
Creation of digital topographic models with the ALK-GIAP. The DLM 25 as an example N88-25031
Topographic data processing for environmental planning N88-25032
Digital maps for an electronic traffic guide N88-25033
Development in data structures in PHOCUS for digital mapping N88-25034
State of development of ALK (October 1986) N88-25035
Vectorization of raster algorithms for elevation data processing N88-25036
Geometric rectangular data file (GERD): An aid to the rapid access to position data N88-25037
Recent developments in software and hardware by Scitex Co. N88-25038
Personal computer as a workstation in a cartographic automation system? N88-25039
Use of modern scanner techniques in cartography N88-25040
INSTITUT NATIONAL POLYTECHNIQUE, GRENOBLE (FRANCE).
Introduction to compliance in programming of robots
[ETN-88-92189] N88-25201
Modeling of geometric reasoning for robot programming
[ETN-88-92290] N88-25202
INSTITUTE OF GAS TECHNOLOGY, CHICAGO, ILL.
Sulfur-tolerant anode materials
[DE88-001034] N88-25054
INSTITUTE OF OCEANOGRAPHIC SCIENCES, WORMLEY (ENGLAND).
SeaSoar profiles in the Iceland-Scotland area, May 1987
[IOS-253] N88-25124
INSTITUTO NACIONAL DE TECNICA AEROESPACIAL, ESTEBAN TERRADAS, TORREJON DE ARDOZ (SPAIN).
Evaluation of the chromium oxide arc spraying treatment on solar energy collectors
[ETN-88-92564] N88-25053
Changes in the Antarctic atmosphere due to the reduction of stratospheric ozone
[ETN-88-92565] N88-25074
INTERNATIONAL BUSINESS MACHINES CORP., SAN JOSE, CALIF.
Diffusion of homopolymers into nonequilibrum diblock copolymer structures
[DE88-005306] N88-24794
INTERNATIONAL TRADE ADMINISTRATION, WASHINGTON, D.C.
Competitive assessment of the U.S. civil helicopter industry
[PB88-186325] N88-24574
IOWA STATE UNIV. OF SCIENCE AND TECHNOLOGY, AMES.
Simplified curve fits for the transport properties of equilibrium air
[NASA-CR-178411] N88-24911
IOWA UNIV., IOWA CITY.
Prediction of laminar and turbulent flows past single and twin airfoils N88-24589
Design of partially replicated distributed database systems: An integrated methodology N88-25383
Contaminant ions and waves in the space station environment N88-25393

J

JAYCOR, VIENNA, VA.
Knowledge acquisition tool implementation
[AD-A190415] N88-25164
JET PROPULSION LAB., CALIFORNIA INST. OF TECH., PASADENA.
Performance and long duration test of a 30 kw thermal arcjet engine
[AD-A190962] N88-24677
Energy efficient continuous flow ash lockhopper
[NASA-CASE-NPO-18985-1-CU] N88-24814
Tower evaporator
[NASA-CASE-NPO-15809-2] N88-24815
Acoustic convective system
[NASA-CASE-NPO-17278-1-CU] N88-24818
Apparatus for using a time interval counter to measure frequency stability
[NASA-CASE-NPO-17325-1-CU] N88-24846
Timing control system
[NASA-CASE-NPO-16882-1-CU] N88-24863
A universal computer control system for motors
[NASA-CASE-NPO-17134-1-CU] N88-24864

The behavior of drop-containing turbulent eddies
[AD-A191669] N88-24883
Noncontact temperature pattern measuring device
[NASA-CASE-NPO-17024-1-CU] N88-24943
Atmospheric autorotating imaging device
[NASA-CASE-NPO-17390-1-CU] N88-24944
Articulated suspension system
[NASA-CASE-NPO-17354-1-CU] N88-24973
Trochoidal analysis of scattered electrons in a merged electron-ion beam
[NASA-CASE-NPO-16789-1-CU] N88-25281
Real-time optical multiple object recognition and tracking system and method
[NASA-CASE-NPO-17139-1-CU] N88-25301
Low-loss, high-isolation, fiber-optic isolator
[NASA-CASE-NPO-17207-1-CU] N88-25304
Real-time image difference detection using a polarization rotation spacial light modulator
[NASA-CASE-NPO-17144-1-CU] N88-25305
An investigation of 2-6 superlattice deposition by laser photochemical techniques
[AD-A191547] N88-25336
Improved properties of SiGe/GaP alloys
[NASA-CASE-NPO-17259-1-CU] N88-25358

JOHANN-WOLFGANG-GOETHE-UNIV., FRANKFURT AM MAIN (WEST GERMANY).
Tropospheric OH measurements by long path absorption with rapid spectral concordance N88-25069

JOINT INST. FOR NUCLEAR RESEARCH, DUBNA (USSR).
Optical system of laser illuminated streamer chamber
[DE88-702127] N88-25306
Neutron diffraction refinement of CsHSO4 superionic phase structure
[DE88-701496] N88-25326

K

KANSAS UNIV., LAWRENCE.
Class 2 design update for the family of commuter airplanes
[NASA-CR-182681] N88-24629

KARLSRUHE UNIV. (WEST GERMANY).
KA-PROLOG. KAP-computer: Computer model and instructions set
[ETN-88-91948] N88-25186

KERNFORSCHUNGSANLAGE, JUELICH (WEST GERMANY).
Tropospheric OH measurement by Laser Induced Fluorescence (LIF) N88-25071

KIEL UNIV. (WEST GERMANY).
Determination of mesoscale variability of sea surface temperature and attenuation in the North Atlantic from satellite measurement
[REPT-162] N88-25127

KITT PEAK NATIONAL OBSERVATORY, TUCSON, ARIZ.
The Io sulfur torus in 1981
[NASA-TM-101139] N88-25419

KOPIN CORP., TAUNTON, MASS.
On the use of convergent beam electron diffraction for identification of antiphase boundaries in GaAs grown on Si
[DE88-008220] N88-25362

L

LABEN SPACE INSTRUMENTATION AND SYSTEMS, MILAN (ITALY).
P-Plus: Polar Platform utilization study, executive summary
[BAE-TP-8391] N88-24653

LABORATOIRE DE METEOROLOGIE DYNAMIQUE, PARIS (FRANCE).
Three-dimensional temperature fields in the atmosphere up to 50 km altitude
[ETN-88-92150] N88-25089

LAWRENCE LIVERMORE NATIONAL LAB., CALIF.
Fabrication issues and technology development for HELEOS (Hypervelocity Electromagnetic Launcher for Equation Of State)
[DE88-007419] N88-24858
Dynamic consolidation of metal powders
[AD-A192126] N88-24744
The variation of torsional ductility of high-purity aluminum with temperature and strain rate
[DE88-005618] N88-24755
LLNL granular solids flow project
[DE88-007492] N88-24906
Reducing sensitivity to errors in free electron laser amplifiers
[DE88-007017] N88-24960
Fracture of solid state lasers
[DE88-007023] N88-24961
Effective use of shared memory multiprocessors
[DE88-007019] N88-25195
High-order multiphoton ionization of the noble gases
[DE88-007489] N88-25273
Gamma rays from Cygnus X-1: Modeling and nonthermal pair production
[DE88-006830] N88-25426

LEHIGH UNIV., BETHLEHEM, PA.
The surface crack problem in an orthotropic plate under bending and tension
[NASA-CR-178281] N88-25014

LIEGE UNIV. (BELGIUM).
Diffusion of homopolymers into nonequilibrum diblock copolymer structures
[DE88-005306] N88-24794

LOCKHEED-CALIFORNIA CO., BURBANK.
Fuel containment concepts: Transport category airplanes
[AD-A189818] N88-24799
Fuel containment concepts: Transport category airplanes
[DOT/FAA/CT-87/18] N88-24807

LOCKHEED-GEORGIA CO., MARIETTA.
Predictive corrosion modeling, volume 1
[AD-A191229] N88-24739

LOCKHEED MISSILES AND SPACE CO., HUNTSVILLE, ALA.
Duct flow nonuniformities for Space Shuttle Main Engine (SSME)
[NASA-CR-179338] N88-24899

LOCKHEED MISSILES AND SPACE CO., PALO ALTO, CALIF.
Chemical compatibility between silicon carbide and a nickel aluminide
[DE88-006188] N88-24708
Effect of alloying, rapid solidification, and surface kinetics on the high temperature environmental resistance of niobium
[AD-A192093] N88-24743

LOGICA LTD., LONDON (ENGLAND).
P-Plus: Polar Platform utilization study, executive summary
[BAE-TP-8391] N88-24653

LOS ALAMOS NATIONAL LAB., N. MEX.
Arcing and rf signal generation during target irradiation by a high-energy, pulsed neutral particle beam
[DE88-007169] N88-24664
A semigroup for Lagrangian 1D isentropic flow
[DE88-006464] N88-24912
SOLA-DM: A numerical solution algorithm for transient three-dimensional flows
[DE88-007159] N88-24913
Remote temperature-measurement instrumentation for a heated rotating turbine disk
[DE88-006456] N88-24925
Laser countermeasure impacts and penalties
[DE88-006871] N88-24947
Application of particle simulations to the NRL laser experiment
[AD-A191641] N88-24953
Aurora status and plans
[DE88-006476] N88-24955
High-energy laser-assisted imaging through vaporizing aerosols
[DE88-007911] N88-24957
Theoretical basis for an experimental test with regard to the origin of VHF (Very High Frequency) radiation from natural lightning
[DE88-007535] N88-25102
The human genome: Computational challenges
[DE88-006465] N88-25131
A graphical, intelligent interface for discrete-event simulations
[DE88-000522] N88-25181
The -mdoc macro package: A software tool to support computer documentation standards
[DE88-000500] N88-25188
Optical diagnostics for a high power, rf-inductively coupled plasma
[DE88-007822] N88-25322
Introduction to lattice gauge theory
[DE88-006073] N88-25349

LUND UNIV. (SWEDEN).
Energy measurements in oxygen-induced reactions at 60 A GeV and 200 A GeV
[DE88-006420] N88-25283

M

MARYLAND UNIV., BALTIMORE.
Dexamethasone regulates glutamine synthetase expression in rat skeletal muscles
[NASA-CR-182935] N88-25129

MARYLAND UNIV., COLLEGE PARK.
The efficacy of using human myoelectric signals to control the limbs of robots in space
[NASA-CR-182901] N88-25155
SYMBL: A new Boolean compiler N88-25160
NFEARS: A nonlinear adaptive finite element solver, part 1
[AD-A191823] N88-25215
Accelerator research studies
[DE88-007124] N88-25290

MASSACHUSETTS INST. OF TECH., CAMBRIDGE.
Liquid carbon
[AD-A191707] N88-24776
Size effects in the electrical resistivity of benzene-derived carbon fibers
[AD-A191708] N88-24777
Raman characterization of AsF5-intercalated vapor grown graphite fibers
[AD-A191709] N88-24778
Stress measurements in graphite fibers by laser raman spectroscopy
[AD-A191710] N88-24779
Electrical conduction in thin film carbons
[AD-A191726] N88-24780
Electron-Rayleigh wave interaction in thin film carbons
[AD-A191727] N88-24781
Photoconductivity in carbon fibers
[AD-A191728] N88-24782
Effect of uniaxial stress on the Raman spectra of graphite fibers
[AD-A191730] N88-24783
Time-frequency representations for speech signals
[AD-A188661] N88-24819
The interpretation of crustal dynamics data in terms of plate interactions and active tectonics of the Anatolian Plate and surrounding regions in the Middle East
[NASA-CR-183024] N88-25092
A mixed-integer linear programming problem which is efficiently solvable
[AD-A191028] N88-25168
Shape from shading, occlusion and texture
[AD-A184640] N88-25269
Optical properties of heterostructures and superlattices
[AD-A191542] N88-25335
Modeling and evaluation of variable structure organizations
[AD-A191947] N88-25381

MASSACHUSETTS INST. OF TECH., LEXINGTON.
The Federal Aviation Administration/Massachusetts Institute of Technology (FAA/MIT) Lincoln Laboratory Doppler weather radar program N88-25118

MATRA ESPACE, TOULOUSE (FRANCE).
P-Plus: Polar Platform utilization study, executive summary
[BAE-TP-8391] N88-24653
Assessment of optical communications systems for Data Relay Satellite. Volume 1: Executive summary
[ESA-CR(P)-2488-VOL-1] N88-24841
Assessment of optical communications systems for the Data Relay Satellite
[ESA-CR(P)-2488-VOL-2] N88-24842

MAX-PLANCK-INST. FUER AERONOMIE, KATLENBURG-LINDAU (WEST GERMANY).
Ozone in the atmosphere N88-25064

MAX-PLANCK-INST. FUER CHEMIE, MAINZ (WEST GERMANY).
Measurement of atmospheric OH with laser differential optical absorption spectroscopy (LDOAS) N88-25068
Trace gas measurements in the troposphere using tunable diode lasers N88-25072

MAX-PLANCK-INSTITUT FUER STROEMUNGSFORSCHUNG, GOETTINGEN (WEST GERMANY).
Hydroacoustic pulsating jet generator
[MPIS-7/1987] N88-24891
Theoretical investigation of the development of the normal fluid and superfluid velocity distributions during spin-up for a He2-filled cylinder
[MPIS-6/1987] N88-24892
Simple high speed camera with CCD-sensor
[MPIS-8/1987] N88-24940

MCDONNELL-DOUGLAS ASTRONAUTICS CO., HUNTINGTON BEACH, CALIF.
Human performance issues arising from manned space station missions
[NASA-CR-3942] N88-25156

MESSER GRIESHEIM G.M.B.H., FRANKFURT AM MAIN (WEST GERMANY).
High power axial flow CO2 laser
[ETN-88-91951] N88-24959

METEOROLOGICAL OFFICE, BRACKNELL (ENGLAND).
Bracknell Meteorological Office N88-25107

MIAMI UNIV., FLA.
Observation of stratiform rain with 94 GHz and s-b and Doppler radar
[AD-A192013] N88-25100
An experimental study of the coherent under-ice reflectivity of sound in the Greenland Sea Marginal Ice Zone N88-25125
MICHIGAN UNIV., ANN ARBOR.
Unsteady flow in a supercritical supersonic inlet N88-24605
Open channel flow near the resonance speed N88-24918
Bimolecular reactions and energy-transfer processes of highly vibrationally excited molecules related to energetic materials
[AD-A189013] N88-25270
Energy-transfer properties and mechanisms
[DE88-007107] N88-25272
MIDWEST RESEARCH INST., GOLDEN, COLO.
Molecular-beam, mass-spectrometric studies of wood vapor and model compounds over HZSM-5 catalyst N88-25044
Upgrading pyrolysis vapors to aromatic gasoline with zeolite catalysis at atmospheric pressure N88-25045
Photovoltaic Advanced Research and Development Project, solar radiation research
[DE88-001143] N88-25056
MINISTERE DES ARMEES, SAINT-CLOUD (FRANCE).
Contributions of autoionizing resonances to the electron collisional excitation rates for Be-like ions
[AD-A190924] N88-25275
MINNESOTA UNIV., MINNEAPOLIS.
Nuclear structure studies at intermediate energies
[DE88-006683] N88-25271
Modelling of thermal plasma systems N88-25314
MISSOURI UNIV., COLUMBIA.
Theoretical investigations of drift waves in a magnetic quadrupole N88-25312
MOREHOUSE COLL., ATLANTA, GA.
Numerical solution of a system of random Volterra integral equations. 1: Successive approximation method N88-25227
Numerical solutions to stochastic difference equations N88-25229
Numerical solution to a system of random Volterra integral equations N88-25230
Mixed min-max optimization problem with restrictions N88-25232
Approximate solution of random differential equation N88-25233
A method for the numerical solution of random Cauchy singular integral equation N88-25234
Numerical solution of random Love's integral equation N88-25235
Numerical solution of linear integral equations with random forcing terms N88-25237
MUENSTER UNIV. (WEST GERMANY).
Energy measurements in oxygen-induced reactions at 60 A GeV and 200 A GeV
[DE88-006420] N88-25283

N

NASA SCIENTIFIC AND TECHNICAL INFORMATION FACILITY, BALTIMORE/WASHINGTON INTERNATIONAL AIRPORT, MD. 21240.
Aerospace medicine and biology: A continuing bibliography with indexes (supplement 312)
[NASA-SP-7011(312)] N88-25141
NASA combined file postings statistics based on NASA thesaurus, Jan. 1988 - July 1988
[NASA-CR-182985] N88-25384
NATIONAAL INST. VOOR KERNFYSICA EN HOGE ENERGIEFYSICA, AMSTERDAM (NETHERLANDS).
Rigid symmetries and BRST-invariance in gauge theories
[PB88-180948] N88-25280
NATIONAL AERONAUTICS AND SPACE ADMINISTRATION, WASHINGTON, D.C.
Aeronautical engineering: A continuing bibliography with indexes (supplement 227)
[NASA-SP-7037(227)] N88-24578
Functional and mechanical analysis of continuous media-application to the study of elastic composites with periodic structure: Homogenization
[NASA-TT-20188] N88-24710
The precipitation processes of Cu-Zr-Cr alloys
[NASA-TT-20168] N88-24758
High temperature embrittleness of Cu-Cr alloy
[NASA-TT-20184] N88-24759
Critical cooling rates on solution treatment of Cu-Cr and Cu-Be alloys
[NASA-TT-20163] N88-24760
Martensitic transformation and microstructures in sintered NiAl alloys
[NASA-TT-20178] N88-24761
On the reversion phenomena of Cu-3 percent Ti alloys
[NASA-TT-20170] N88-24762
Effect of size of precipitates on recrystallization temperatures in Cu-Cr, Cu-Zr, and Cu-Zr-Cr alloys
[NASA-TT-20166] N88-24763
A study on the precipitation and reversion behaviors of Cu-0.3 percent Cr alloy by the step annealing method
[NASA-TT-20169] N88-24764
On quench sensitivity of Cu-Cr alloys
[NASA-TT-20174] N88-24765
Differential technology in plastics industries differentiation in combination technology nonflammability technology
[NASA-TT-20256] N88-24797
Sample decomposition in sealed teflon vessels
[NASA-TT-20189] N88-24798
On the abnormal phenomena observed in the electrical resistivity measurement during the decomposition process of saturated Cu-Fe alloys
[NASA-TT-20183] N88-24869
State of tuning
[NASA-TT-20195] N88-25205
Computer simulation of uphill diffusion in ternary ionic system
[NASA-TT-20194] N88-25285
NASA patent abstracts bibliography: A continuing bibliography. Section 1: Abstracts
[NASA-SP-7039(33)] N88-25388
NASA history data book. Volume 1: NASA resources 1958-1968
[NASA-SP-4012-VOL-1] N88-25428
NASA historical data book. Volume 2: Programs and projects 1958-1968
[NASA-SP-4012-VOL-2] N88-25429
NASA historical data book. Volume 3: Programs and projects 1969-1978
[NASA-SP-4012-VOL-3] N88-25430
NATIONAL AERONAUTICS AND SPACE ADMINISTRATION. AMES RESEARCH CENTER, MOFFETT FIELD, CALIF.
Progress and future directions in computational fluid dynamics
[NASA-TM-100091] N88-24579
A formulation for the boundary-layer equations in general coordinates
[NASA-TM-100079] N88-24600
Some rotorcraft applications of computational fluid dynamics
[NASA-TM-100066] N88-24601
Applications of the Navier-Stokes equations to wings and complex configurations using a zonal approach
[NASA-TM-100080] N88-24602
A decade of computer simulations for space shuttle aerodynamics
[NASA-TM-100990] N88-24603
Analysis procedures and subjective flight results of a simulator validation and cue fidelity experiment
[NASA-TM-88270] N88-24634
Aromatic cyclotriphosphazenes
[NASA-CASE-ARC-11428-3] N88-24692
Characteristics of merging shear layers and turbulent wakes of a multi-element airfoil
[NASA-TM-100053] N88-24900
Extrema principles of entrophy production and energy dissipation in fluid mechanics
[NASA-TM-100992] N88-24946
Cardiovascular effects of weightlessness and ground-based simulation
[NASA-TM-88314] N88-25140
Simulating futures in extended common LISP
[NASA-TM-101000] N88-25192
NAS: The first year
[NASA-TM-101006] N88-25196
Automatic discovery of optimal classes
[NASA-TM-101174] N88-25238
Diurnal variations in optical depth at Mars: Observations and interpretations
[NASA-TM-100057] N88-25420
NATIONAL AERONAUTICS AND SPACE ADMINISTRATION. GODDARD SPACE FLIGHT CENTER, GREENBELT, MD.
The role of space borne imaging radars in environmental monitoring: Some shuttle imaging radar results in Asia
[NASA-TM-101178] N88-24844
The Io sulfur torus in 1981
[NASA-TM-101139] N88-25419
NATIONAL AERONAUTICS AND SPACE ADMINISTRATION. HUGH L. DRYDEN FLIGHT RESEARCH CENTER, EDWARDS, CALIF.
Current flight test experience related to structural divergence of forward-swept wings
[NASA-TM-100445] N88-24633
Application of flight systems methodologies to the validation of knowledge-based systems
[NASA-TM-100442] N88-25207
NATIONAL AERONAUTICS AND SPACE ADMINISTRATION. JOHN F. KENNEDY SPACE CENTER, COCOA BEACH, FLA.
Monitoring biological impacts of space shuttle launches from Vandenberg Air Force Base: Establishment of baseline conditions
[NASA-TM-100982] N88-25133
History of wildland fires on Vandenberg Air Force Base, California
[NASA-TM-100983] N88-25134
NATIONAL AERONAUTICS AND SPACE ADMINISTRATION. LYNDON B. JOHNSON SPACE CENTER, HOUSTON, TEX.
Payload deployment method and system
[NASA-CASE-MSC-21330-1] N88-24660
Adaptive data acquisition multiplexing system and method
[NASA-CASE-MSC-21170-1] N88-24662
Hatch cover
[NASA-CASE-MSC-21356-1] N88-24671
Nozzle fabrication technique
[NASA-CASE-MSC-21299-1] N88-24684
Linear force device
[NASA-CASE-MSC-20549-2] N88-24927
Electrostatic discharge test apparatus
[NASA-CASE-MSC-21094-1] N88-24941
Range and range rate system
[NASA-CASE-MSC-20867-1] N88-24958
Toggle release
[NASA-CASE-MSC-21354-1] N88-24969
Space station neutral external environment N88-25392
NATIONAL AERONAUTICS AND SPACE ADMINISTRATION. LANGLEY RESEARCH CENTER, HAMPTON, VA.
Aerodynamic performance and pressure distributions for a NASA SC(2)-0714 airfoil tested in the Langley 0.3-meter transonic cryogenic tunnel
[NASA-TM-4044] N88-24580
Aircraft aeroelasticity and structural dynamics research at the NASA Langley Research Center: Some illustrative results
[NASA-TM-100627] N88-24598
Accurate multigrid solution of the Euler equations on unstructured and adaptive meshes
[NASA-CR-181679] N88-24608
Navigation system for land vehicles
[NASA-CASE-LAR-13322-1] N88-24620
Airplane runway performance monitoring system
[NASA-CASE-LAR-13854-1-CU] N88-24621
Nonlinear programming extensions to rational function approximation methods for unsteady aerodynamic forces
[NASA-TP-2776] N88-24623
Actuated forebody strakes
[NASA-CASE-LAR-13983-1] N88-24628
Dual-fuel, dual-mode rocket engine
[NASA-CASE-LAR-13773-1] N88-24685
Analysis of notched metal matrix composites under tension loading
[NASA-TM-100629] N88-24713
Aluminum alloy
[NASA-CASE-LAR-13824-1-CU] N88-24753
Stiffened titanium panels
[NASA-CASE-LAR-13814-1] N88-24816
Almond test body
[NASA-CASE-LAR-13747-1] N88-24845
Method and apparatus for detecting laminar flow separation and reattachment
[NASA-CASE-LAR-13952-1-SB] N88-24910
Spatial stability of a compressible mixing layer
[NASA-CR-181671] N88-24916
Thermal compensating mount
[NASA-CASE-LAR-13794-1] N88-24942
Structurally tailorable non-linear snap-through spring system
[NASA-CASE-LAR-13729-1] N88-24970
Radio Frequency (RF) strain monitor
[NASA-CASE-LAR-13705-1] N88-25011
SAM 2 data user's guide
[NASA-RP-1200] N88-25094
The Environment for Application Software Integration and Execution (EASIE), version 1.0. Volume 3: Program execution guide
[NASA-TM-100575] N88-25184
The Sizing and Optimization Language, (SOL): Computer language for design problems
[NASA-TM-100565] N88-25190
Robust adaptive regulation without persistent excitation
[NASA-TM-100571] N88-25204
Galerkin approximation for inverse problems for nonautonomous nonlinear distributed systems
[NASA-CR-181676] N88-25246

Optimal discrete-time LQR problems for parabolic systems with unbounded input: Approximation and convergence
[NASA-CR-181673] N88-25247
Phase length optical phase-locked-loop sensor
[NASA-CASE-LAR-13387-1] N88-25302
Method of forming a multiple layer dielectric and a hot film sensor therewith
[NASA-CASE-LAR-13678-1] N88-25355
A Study of Space Station Contamination Effects
[NASA-CP-3002] N88-25390
Preliminary estimates of radiation exposures for manned interplanetary missions from anomalously large solar flare events
[NASA-TM-100620] N88-25427

NATIONAL AERONAUTICS AND SPACE ADMINISTRATION. LEWIS RESEARCH CENTER, CLEVELAND, OHIO.

Effect of initial tangential velocity distribution on the mean evolution of a swirling turbulent free jet
[NASA-TM-100934] N88-24592
Summary of low-speed wind tunnel results of several high-speed counterrotation propeller configurations
[NASA-TM-100945] N88-24597
Particle-laden weakly swirling free jets: Measurements and predictions
[NASA-TM-100920] N88-24639
An empirical model of the effects of curvature and convergence on dilution jet mixing
[NASA-TM-100896] N88-24640
NASA/industry advanced turboprop technology program
[NASA-TM-100929] N88-24641
Experimental vibration damping characteristics of the third-stage rotor of a three-stage transonic axial-flow compressor
[NASA-TM-100948] N88-24642
Experimental radio frequency link for Ka-band communications applications
[NASA-TM-100824] N88-24659
Service offerings and interfaces for the ACTS network of Earth stations
[NASA-TM-100809] N88-24663
Evaluation of the communications impact of a low power arcjet thruster
[NASA-TM-100926] N88-24682
Thermodynamic modeling of the no-vent fill methodology for transferring cryogens in low gravity
[NASA-TM-100932] N88-24686
An extended life and performance test of a low-power arcjet
[NASA-TM-100942] N88-24687
Internal erosion rates of a 10-kW xenon ion thruster
[NASA-TM-100954] N88-24688
Catalytic ignition of hydrogen and oxygen propellants
[NASA-TM-100957] N88-24689
Thrust chamber thermal barrier coating techniques
[NASA-TM-100933] N88-24690
The 700 F properties of autoclave cured PMR-2 composites
[NASA-TM-100923] N88-24712
Status and prognosis for alternative engine materials
[NASA-TM-100903] N88-24749
Arc-textured metal surfaces for high thermal emittance space radiators
[NASA-TM-100894] N88-24754
Isothermal and bithermal thermomechanical fatigue behavior of a NiCoCrAlY-coated single crystal superalloy
[NASA-TM-100907] N88-24766
Characterization of aluminum/RP-1 gel propellant properties
[NASA-TM-100951] N88-24808
Preparation for microgravity: The role of the microgravity materials science laboratory
[NASA-TM-100906] N88-24811
Progress in InP solar cell research
[NASA-TM-100914] N88-24870
Development of a liquid-fed water resistojet
[NASA-TM-100927] N88-24968
Small scale bipolar nickel-hydrogen testing
[NASA-TM-100936] N88-25059
Solving time-dependent two-dimensional eddy current problems
[NASA-TM-100875] N88-25239
Recent advances in low-thrust propulsion technology
[NASA-TM-100959] N88-25260

NATIONAL AERONAUTICS AND SPACE ADMINISTRATION. MARSHALL SPACE FLIGHT CENTER, HUNTSVILLE, ALA.

Structural margins assessment approach
[NASA-TM-100332] N88-24672
The electrokinetic behavior of calcium oxalate monohydrate in macromolecular solutions
[NASA-TM-101144] N88-24791
Demixing of aqueous polymer two-phase systems in low gravity
[NASA-TM-101141] N88-24809
Low temperature storage container for transporting perishables to space station
[NASA-CASE-MFS-28248-1] N88-24817
Characterization of a 30-GHz IMPATT solid state amplifier
[NASA-TM-100876] N88-24847
Universal precision sine bar attachment
[NASA-CASE-MFS-28253-1] N88-24971
Trailer shield assembly for a welding torch
[NASA-CASE-MFS-29260-1] N88-24972
SRM propellant and polymer materials structural test program
[NASA-TP-2821] N88-25013
Optical pressure sealing couping (light joint)
[NASA-CASE-MFS-29348-1] N88-25303
MHD bending waves in a current sheet
[NASA-TM-101149] N88-25323
Electronic controller for reciprocating rotary crystallizer
[NASA-TM-101140] N88-25354
Hanging drop crystal growth apparatus and method
[NASA-CASE-MFS-28206-1-SB] N88-25356
Crystal growth apparatus
[NASA-CASE-MFS-28182-1] N88-25357
Inevitable inflation in Einstein-Cartan theory with improved energy-momentum tensor with spin
[NASA-TM-101146] N88-25365
Space station particulate contamination environment N88-25397
Superthermal electron processes in the upper atmosphere of Uranus: Aurora and electroglow
[NASA-TM-101150] N88-25417
The 2-D magnetohydrostatic configurations leading to flares or quiescent filament eruptions
[NASA-TM-101147] N88-25423
The SAMEX vector magnetograph: A design study for a space-based solar vector magnetograph
[NASA-TM-4048] N88-25424

NATIONAL AERONAUTICS AND SPACE ADMINISTRATION. PASADENA OFFICE, CALIF.

Isotope separation using tuned laser and electron beam
[NASA-CASE-NPO-16907-1-CU] N88-24732
Energy efficient continuous flow ash lockhopper
[NASA-CASE-NPO-16985-1-CU] N88-24814
Tower evaporator
[NASA-CASE-NPO-15609-2] N88-24815
Acoustic convective system
[NASA-CASE-NPO-17278-1-CU] N88-24818
Apparatus for using a time interval counter to measure frequency stability
[NASA-CASE-NPO-17325-1-CU] N88-24846
Magnetically switched power supply system for lasers
[NASA-CASE-NPO-16402-2] N88-24862
Timing control system
[NASA-CASE-NPO-16882-1-CU] N88-24863
A universal computer control system for motors
[NASA-CASE-NPO-17134-1-CU] N88-24864
Noncontact temperature pattern measuring device
[NASA-CASE-NPO-17024-1-CU] N88-24943
Atmospheric autorotating imaging device
[NASA-CASE-NPO-17390-1-CU] N88-24944
Articulated suspension system
[NASA-CASE-NPO-17354-1-CU] N88-24973
Trochoidal analysis of scattered electrons in a merged electron-ion beam
[NASA-CASE-NPO-16789-1-CU] N88-25281
Real-time optical multiple object recognition and tracking system and method
[NASA-CASE-NPO-17139-1-CU] N88-25301
Low-loss, high-isolation, fiber-optic isolator
[NASA-CASE-NPO-17207-1-CU] N88-25304
Real-time image difference detection using a polarization rotation spacial light modulator
[NASA-CASE-NPO-17144-1-CU] N88-25305
Improved properties of SiGe/GaP alloys
[NASA-CASE-NPO-17259-1-CU] N88-25358

NATIONAL BUILDING RESEARCH INST., PRETORIA (SOUTH AFRICA).

Effects of moderate cold and heat stress on the potential work performance of industrial workers. Part 6: The effects of increasing vapour pressure at four air temperatures on the performance and physiology of white females
[PB88-124854] N88-25137

NATIONAL CENTER FOR ATMOSPHERIC RESEARCH, BOULDER, COLO.

Evaluation of NMC (National Meteorological Center) global analyses: 1979-1987
[PB88-178157] N88-25096
Taiwan area mesoscale experiment: P-3 aircraft operations summary
[PB88-169073] N88-25098

NATIONAL METEOROLOGICAL CENTER, WASHINGTON, D.C.

Cluster analysis of multiple planetary flow regimes
[NASA-CR-182931] N88-25418

NATIONAL OCEANIC AND ATMOSPHERIC ADMINISTRATION, BOULDER, COLO.

Special observations N88-25108
Denver ARTCC evaluation of PROFS (Prototype Regional Observations and Forecast System) mesoscale weather products N88-25117

NATIONAL OCEANOGRAPHIC DATA CENTER, WASHINGTON, D. C.

Mariners weather log, volume 32, number 1, Winter 1988
[PB88-173869] N88-25097

NATIONAL TRANSPORTATION SAFETY BOARD, WASHINGTON, D. C.

Aircraft accident/incident, Copperhill, Tennessee, February 22, 1986
[PB88-910407] N88-24812

NATIONAL WEATHER SERVICE, HONOLULU, HAWAII.

Tropical cyclones, 1987: Central North Pacific
[PB88-188081] N88-25119

NATIONAL WEATHER SERVICE, SILVER SPRING, MD.

Automation of surface observations program N88-25106
Comparative verification between GEM model and official aviation terminal forecasts N88-25115
Computer and model changes at National Meteorological Center (NWC) N88-25116

NAVAL AIR TEST CENTER, PATUXENT RIVER, MD.

Method for prediction and determination of takeoff performance for vectored thrust vehicles
[AD-A191809] N88-24626

NAVAL OCEAN SYSTEMS CENTER, SAN DIEGO, CALIF.

Western Pacific Omega validation: Project description
[AD-A191753] N88-24617
Thermal conductivity of hard anodized coatings on aluminum
[AD-A191755] N88-24784
A MININEC model of the miniloop antenna
[AD-A191759] N88-24830
Practical VLF/LF radio test system
[AD-A191768] N88-24831
Silicon-sapphire waveguides
[AD-A191754] N88-24854
IGUANA: Interactive graphics utility for automated NEC analysis
[AD-A191760] N88-25174
Planar fully ion-implanted high power InP MISFETs
[AD-A191589] N88-25338
Recent data on Si:As impurity band conduction multiplexed arrays
[AD-A191752] N88-25340

NAVAL OCEANOGRAPHIC OFFICE, BAY ST. LOUIS, MISS.

DOD 1985 world magnetic model: Charts and grid values
[AD-A191484] N88-25060

NAVAL POSTGRADUATE SCHOOL, MONTEREY, CALIF.

TVC (Thrust Vector Control) jet vane thermal modeling using parametric system identification
[AD-A191518] N88-24678
Design, implementation and evaluation of an operating system for a network of transputers
[AD-A186593] N88-25193

NAVAL RESEARCH LAB., WASHINGTON, D.C.

The theory of random alloys
[DE88-006408] N88-24756
Automated test device for FASR (Fixed Array Surveillance Radar) beam steering componentry
[AD-A191650] N88-24829
The Effect of the Ionosphere on Communication, Navigation and Surveillance Systems Based on Ionosph eric Effects Symposium held on 5-7 May 1987 in Springfield, Virginia
[AD-A191855] N88-25061
Gram-Schmidt implementation of a linearly constrained adaptive array
[AD-A191651] N88-25198
A constraint algorithm for maintaining rigid bonds in molecular dynamics simulations of large molecules
[AD-A191663] N88-25277
Contamination of the space station environment by vented chemicals N88-25403

NAVAL SHIP RESEARCH AND DEVELOPMENT CENTER, BETHESDA, MD.

Computation of the turbulent boundary layer downstream of vortex generators
[AD-A191544] N88-24881

NEW HAMPSHIRE UNIV., DURHAM.

Rocket-borne low energy ion measurements in space N88-25412

NEW MEXICO STATE UNIV., LAS CRUCES.
Atmospheric propagation of laser beams
[AD-A191447] N88-24952
NEW MEXICO UNIV., ALBUQUERQUE.
Use of a two-stage light-gas gun as an injector for electromagnetic railguns
[DE88-007200] N88-24657
NEW SOUTH WALES UNIV., KENSINGTON (AUSTRALIA).
Propagation management for no-acknowledge HF communications links N88-24843
An investigation of a distributed clock for local area networks with ring topology N88-24924
A sedimentological and mineralogical study of the Koogah Formation, New South Wales N88-25087
A cardiostimulant protein from the Australian Red Waratah Sea anemone, Actinia tenebrosa N88-25138
Some properties of modular equations and the partition function N88-25224
Determination of doping profiles in silicon from resistivity measurements via the four-point probe in combination with layer strippings via anodic oxidation N88-25347
NEW SOUTH WALES UNIV., SYDNEY (AUSTRALIA).
Information analysis of integral equations in remote sensing of atmospheric aerosols N88-25022
NEW YORK UNIV., NEW YORK.
Theoretical plasma physics research of active space experiments
[AD-A192075] N88-25309
NORTH CAROLINA STATE UNIV., RALEIGH.
Automatic feedback control of a rigid body for finite displacements N88-24674
Numerical solutions of the complete Navier-Stokes equations
[NASA-CR-183023] N88-24914
Computational Fluid Mechanics
[...SA-CR-183022] N88-24915
NORTH CAROLINA UNIV., CHAPEL HILL.
Information and stochastic systems
[AD-A192167] N88-24838
Sensitivity analysis for the system reliability function
[AD-A191648] N88-24979
Poisson functionals of Markov processes and queueing networks
[AD-A191217] N88-25252
Symmetrized nearest neighbor regression estimates
[AD-A191998] N88-25254
NORTHWEST REGIONAL EDUCATIONAL LAB., PORTLAND, OREG.
Selection and effects of channels in distributed communication and decision making tasks: A theoretical review and a proposed research paradigm
[AD-A191607] N88-25375
NORTHWESTERN UNIV., EVANSTON, ILL.
On the structure, propagation, extinction and stability of laminar premixed flames in dissociation equilibrium N88-24728
Probabilistic finite element methods N88-25223
NUCLEAR REGULATORY COMMISSION, WASHINGTON, D. C.
A perspective of PC-based probabilistic risk assessment
[DE88-006715] N88-25251

O

OAK RIDGE GASEOUS DIFFUSION PLANT, TENN.
A quality philosophy for research and development
[DE88-006512] N88-24977
OAK RIDGE NATIONAL LAB., TENN.
SHaRE: Collaborative materials science research
[DE88-007175] N88-24846
Chemical compatibility between silicon carbide and a nickel aluminide
[DE88-006188] N88-24708
Photosynthetic water splitting
[PB88-188891] N88-24731
Microstructural characterization and properties of 3Cr-1.5Mo-O.1V thick section electron beam welds
[DE88-004330] N88-24747
The theory of random alloys
[DE88-006408] N88-24756
An investigation of ceramic coatings for protection of SiC from high-temperature corrosion
[DE88-007873] N88-24790
Real-time implementation of a kinematic optimization scheme for seven-degree-of-freedom redundant robots with spherical wrists
[DE88-006785] N88-24974
Ecological risk factors related to environmental uses of genetically engineered organisms
[DE88-006674] N88-25132
Tutorial on computer control
[DE88-006185] N88-25157
Multi-sensor integration on the NCUBE hypercube computer
[DE88-007472] N88-25162
The development of KENO and the calculation of differential parameters with KENO
[DE88-006176] N88-25186
Network architecture for OPS5
[DE88-002802] N88-25194
A concurrent neural network algorithm for the traveling salesman problem
[DE88-006981] N88-25208
Similarity solutions of nonlinear partial differential equations invariant to a family of affine groups
[DE88-003404] N88-25245
Calorimetry applied to nucleus-nucleus collisions at ultrarelativistic energies
[DE88-006173] N88-25282
Energy measurements in oxygen-induced reactions at 60 A GeV and 200 A GeV
[DE88-006420] N88-25283
Systems analysis of INTOR-like designs
[DE88-004422] N88-25316
A two-wavelength infrared interferometer/polarimeter system for CIT (Compact Ignition Tokamak)
[DE88-007681] N88-25321
Quench detection by fluid dynamic means in cable-in-conduit superconductors
[DE88-007269] N88-25359
Ground state properties and electronic structure of high T sub c superconductors
[DE88-007485] N88-25360
The ATF (Advanced Toroidal Facility) Data M Management System
[DE88-007265] N88-25385
SAMS: The synchronization and monitoring system for ATF (Advanced Toroidal Facility) data acquisition provides unified data access for ATF data acquisition
[DE88-007268] N88-25386
OAK RIDGE Y-12 PLANT, TENN.
Calculation of oxidation rates for iron in CO-CO2
[DE88-007313] N88-24757
OFFICE NATIONAL D'ETUDES ET DE RECHERCHES AEROSPATIALES, PARIS (FRANCE).
Effects of spatial resolution in CARS measurements
[PB88-121900] N88-24727
Structural study of the TGMDA-DDS system
[ONERA-RT-4/3346-M] N88-24792
Investigation of the effect of minimum loads and compression of load spectra on the prediction capacities of the ONERA crack model
[ONERA-RTS-33/7169-RY-064-R] N88-24994
OFFICE OF THE DEPUTY UNDER SECRETARY OF DEFENSE FOR RESEARCH AND DEVELOPMENT (RESEARCH AND ADVANCED TECHNOLOGY), WASHINGTON, D.C.
The FY 1989 Department of Defense statement on the Science and Technology Program to 100th Congress, second session
[AD-A191843] N88-25380
OFFICE OF THE DIRECTOR OF DEFENSE RESEARCH AND ENGINEERING, WASHINGTON, D. C.
Department of Defense Statement on the Technology Base to the Subcommittee on Defense Industry and Technology of the Committee on Armed Services, United States Senate, 100th Congress, second session
[AD-A191839] N88-25376
Department of Defense statement on defense agency research and development to the Subcommittee on Defense of the Committee on Appropriations, United States House of Representatives, 100th Congress, second session
[AD-A191840] N88-25377
Department of Defense Statement on the Balanced Technology Initiative to the Committee on Armed Services, United States Senate, 100th Congress, second session
[AD-A191841] N88-25378
OFFICE OF THE UNDER SECRETARY OF DEFENSE (ACQUISITIONS), WASHINGTON, D.C.
Department of Defense statement on the X-ray Lithography Program to the Research and Development Subcommittee of the House Armed Services Committee of 100th Congress, second session
[AD-A191854] N88-25341
OHIO STATE UNIV., COLUMBUS.
A method for discrimination of radar targets using complex natural resonances
[AD-A191848] N88-24832
Nonparametric discriminant analysis applied to the extraction and selection of radar target signature features
[AD-A191849] N88-24833
Almond test body
[NASA-CASE-LAR-13747-1] N88-24845
Joint services electronics program
[AD-A191749] N88-24853
CIMAG2: The computer program to generate color images
[AD-A191847] N88-25175
Curvature of blended rolled edge reflectors at the shadow boundary contour
[NASA-CR-182974] N88-25300
OKLAHOMA UNIV., NORMAN.
Estimation and control of distributed models for certain elastic systems arising in large space structures
[AD-A192120] N88-24666
OLD DOMINION UNIV., NORFOLK, VA.
Guidance and control strategies for aerospace vehicles
[NASA-CR-183032] N88-24644
Application of advanced grid generation techniques for flow field computations about complex configurations
[NASA-CR-183049] N88-24922
Single-mode projection filters for modal parameter identification for flexible structures
[NASA-CR-182680] N88-25244

P

PACIFIC NORTHWEST LABS., RICHLAND, WASH.
Irradiation effects on tungsten stabilized martensitic steels
[DE88-007074] N88-24748
Environmental effects on slow crack growth in silicon nitride
[DE88-007206] N88-24795
Production costs of hydrocarbon fuels from biomass
[DE88-006667] N88-24804
Knowledge based systems in nondestructive evaluation
[DE88-006653] N88-24981
Proceedings of the 1987 Biomass Thermochemical Conversion Contractors' Review Meeting
[DE88-006730] N88-25041
Research on hydrotreating catalysts to hydrodeoxygenate biocrude oils N88-25046
Low-temperature thermochemical conversion of high moisture biomass feedstocks N88-25047
Bench-scale studies on fluid-bed pyrolysis of wood using different contact gases N88-25049
Overview of wind behavior research in the US Wind Energy Program
[DE88-005683] N88-25057
Field experience with aquifer thermal energy storage
[DE88-007075] N88-25058
Molecular characterization of structure and bonding in thin film materials
[DE88-006811] N88-25351
PARIS-SUD UNIV., ORSAY (FRANCE).
Improving the performance of a finite element method using vector analysis on CRAY 1
[ETN-88-92153] N88-24907
PENNSYLVANIA STATE UNIV., UNIVERSITY PARK.
Sol/gel processing techniques for glass matrix composites
[AD-A191748] N88-24701
Multiple scattering of waves in discrete random media
[AD-A191068] N88-24823
Axisymmetric viscid-inviscid interaction by a frozen vorticity approximation
[AD-A191743] N88-24885
Gas diffusion studies in steady and nonsteady cavities N88-24902
PENNSYLVANIA UNIV., PHILADELPHIA.
Optical computing based on neuronal models
[AD-A191481] N88-25293
PENTAGON LIBRARY, WASHINGTON, D.C.
Management and the executive
[AD-A190778] N88-25374
PHYSICAL SCIENCES, INC., ANDOVER, MASS.
Calculation of space station infrared irradiance from atmosphere-induced emissions N88-25396
The particulate environment surrounding the space station: Estimates from the PACS data N88-25398
Laboratory experiments of relevance to the space station environment N88-25402
PITTSBURGH UNIV., PA.
NFEARS: A nonlinear adaptive finite element solver, part 1
[AD-A191823] N88-25215
POITIERS UNIV. (FRANCE).
Unsteady flow around a profile subjected to pulsed motions
[ETN-88-92151] N88-24594
Determination of the toughness of a brittle material using strain gages
[ETN-88-92540] N88-24993
POLYTECHNIC INST. OF NEW YORK, BROOKLYN.
Physical properties of f electron systems
[DE88-006886] N88-25331

PRATT AND WHITNEY AIRCRAFT, WEST PALM BEACH, FLA.
Rapidly solidified lightweight durable disk material
[AD-A191697] N88-24775
PRINCETON UNIV., N. J.
Fundamental aspects of the structure of supersonic turbulent boundary layers
[AD-A191494] N88-24581
NASA research Program: The roles of fluid motion and other transport phenomena in the morphology of materials
[NASA-CR-182601] N88-25327
Dendritic growth in the presence of convection N88-25328
Two puzzling aspects of protein crystal growth N88-25329
PRINS MAURITS LAB. TNO, RIJSWIJK (NETHERLANDS).
Combustion of PMMA, PE and PS in a ramjet
[VTH-LR-514] N88-24733
Combustion behavior of the vitiator. Experimental results of a second test series
[VTH-LR-509] N88-24734
Theoretical analysis of laminar incompressible flow in slender channels
[VTH-LR-517] N88-24909
PROMETHEUS, INC., SHARON, MASS.
Null steering applications of polynomials with unimodular coefficients
[AD-A191087] N88-25211
PURDUE UNIV., WEST LAFAYETTE, IND.
Research on aero-thermodynamic distortion induced structural dynamic response of multi-stage compressor blading
[AD-A192169] N88-24584
Injection of drag reducing additives into turbulent water flows
[AD-A192072] N88-24888
Forced response unsteady aerodynamics in a multistage compressor N88-24903
A variational finite element method for three-dimensional, steady, compressible, viscous flows N88-24904
Heating and evaporation of turbulent liquid films: Measurement of film thickness and the onset of nucleate boiling
[DE88-006388] N88-24905
Effects of Coriolis acceleration on the vibrations of spinning structures N88-24966
Dynamic response of plates to moving loads: Structural impedance and finite element methods N88-25000
Vibrations of rotating thick or thin rings N88-25003
Timesharing performance as an indicator of pilot mental workload
[NASA-CR-182807] N88-25150

R

READING UNIV. (ENGLAND).
Report on project WIND: Preliminary experiments w ith the UK Meteorological Office mesoscale model, September 1987
[AD-A191621] N88-25099
REMTECH, INC., HUNTSVILLE, ALA.
Research study: Space shuttle main engine plume flowfield model
[NASA-CR-179336] N88-24676
RENSSELAER POLYTECHNIC INST., TROY, N.Y.
Passive shock wave-boundary layer control for the Bell FX69-H-098 airfoil N88-24588
Shape stability in composites N88-24706
The flying characteristics of the membrane slider bearing N88-24965
Theory of viscoplasticity based on overstress with applications N88-25007
Automated cartographic generalization for linear map features N88-25021
EPL (Equational Programing Language) system design: Intermediate processing steps
[AD-A191203] N88-25169
Beyond Ada: Generating Ada code from equational specifications
[AD-A191866] N88-25176
RESEARCH INST. OF NATIONAL DEFENCE, LINKOEPING (SWEDEN).
The radar cross section of some simple reflectors at short wavelengths
[FOA-C-30472-3.3] N88-24839
A Differential Phase Shift Keying (DPSK) modulator for a frequency hopping short wave system
[FOA-C-30460-3.3] N88-24840
System overview: Teragon 4000, an image processing equipment at FOA 3
[FOA-C-30465-3.3] N88-25179
Activities report of the Division of Optical Technology
[FOA-C-30477-3] N88-25299
RESEARCH TRIANGLE INST., RESEARCH TRIANGLE PARK, N.C.
Development of a multipurpose smart recorder for general aviation aircraft
[NASA-CR-168353] N88-24637
RISO NATIONAL LAB., ROSKILDE (DENMARK).
Low frequency electrostatic turbulence in the polar cap E-region
[DRI-3-88] N88-25077
ROCHESTER UNIV., N. Y.
Algorithms and data structures for an expanded family of matroid intersection problems
[AD-A191482] N88-25213
ROCKEFELLER UNIV., NEW YORK.
Motor theory of auditory perception
[AD-A192095] N88-25136
ROCKWELL INTERNATIONAL CORP., THOUSAND OAKS, CALIF.
Environmental integrity of coating/metal interface
[AD-A192184] N88-24786
Studies of optical matrix multiplication and reconfigurable optical interconnect concepts
[AD-A191635] N88-25295
ROME AIR DEVELOPMENT CENTER, GRIFFISS AFB, N.Y.
A scientific basis for an alternate cathode architecture
[AD-A191498] N88-24717
ROUEN UNIV. (FRANCE).
Evaluation of the toxicity of products from the thermal degradation of materials
[ETN-88-91995] N88-25130
RUTGERS - THE STATE UNIV., NEW BRUNSWICK, N. J.
Heat transfer from a negatively buoyant wall jet
[PB88-181953] N88-24873
Theoretical investigation of 3-D shock wave-turbulent boundary layer interactions, part 6
[AD-A191546] N88-24882

S

SANDIA NATIONAL LABS., ALBUQUERQUE, N. MEX.
Use of a two-stage light-gas gun as an injector for electromagnetic railguns
[DE88-007200] N88-24857
Diffusion of homopolymers into nonequilibrum diblock copolymer structures
[DE88-005306] N88-24794
Thermal decomposition studies of explosives for component applications
[DE88-007201] N88-24805
A compatible encapsulant for explosives
[DE88-007212] N88-24806
Designing to safe power limits in hybrid circuits
[DE88-005533] N88-24865
Monolithic GaAs Ku-band one watt constant phase variable power amplifier
[DE88-006272] N88-24866
An overview of advanced battery development at Sandia National Laboratories
[DE88-006823] N88-24867
Optimization of reserve lithium thionyl chloride battery electrochemical design parameters
[DE88-007109] N88-24868
Continuum theories for fluid-particle flows: Some aspects of lift forces and turbulence
[DE88-007038] N88-24898
A multi-frame ion pinhole camera for intense ion beam transport and focusing experiments
[DE88-007283] N88-24926
Analysis of binarized Hartley phase-only filter performance with respect to stochastic noise
[DE88-007604] N88-24945
On the bending response of Kevlar 49/epoxy beams and rings
[DE88-006824] N88-25012
A multiprocessor data flow accelerator module
[DE88-007567] N88-25161
Considerations involved in the display of finite element results using animation
[DE88-007561] N88-25189
Intense ion beam diagnostics for particle beam fusion experiments on PBFA 2
[DE88-007279] N88-25308
Structural studies on La/sub 2/CuO/sub 4+delta/
[DE88-006828] N88-25330
Metastability in SiGe/Si strained-layer structures
[DE88-007603] N88-25361
Engineering drawings and changes: Storing and controlling by the tens of terrabytes
[DE88-007605] N88-25387
SANDIA NATIONAL LABS., LIVERMORE, CALIF.
The burning of HAN-based (hydroxylammonium nitrate) liquid propellants
[DE88-006863] N88-24800
SCHOOL OF AEROSPACE MEDICINE, BROOKS AFB, TEX.
Behavioral response of rats exposed to high-power microwave radiation
[AD-A192199] N88-25128
SCIENCE AND ENGINEERING ASSOCIATES, INC., ENGLEWOOD, COLO.
Neutral environment for space station N88-25391
Effects of meteoroids and apece debris on the particulate environment for space station N88-25399
SCIENCE APPLICATIONS INTERNATIONAL CORP., COLLEGE STATION, TEX.
Higher frequency ambient noise in the arctic ocean
[AD-A192203] N88-25122
SCIENCE APPLICATIONS INTERNATIONAL CORP., MCLEAN, VA.
Technical and economic evaluation of emerging biomass pyrolysis processes for gasoline production N88-25048
Identification and acoustic characterization of seamounts
[AD-A192204] N88-25123
SCIENCE APPLICATIONS INTERNATIONAL CORP., SAN FRANCISCO, CALIF.
Transmitting boundary for finite-difference calculations with finite modeling of an infinite medium
[AD-A191441] N88-25264
SCIENTIFIC RESEARCH ASSOCIATES, INC., GLASTONBURY, CONN.
Solid rocket motor aft field joint flow field analysis
[NASA-CR-179288] N88-24675
SCIENTIFIC SYSTEMS, INC., CAMBRIDGE, MASS.
Adaptive time series analysis using predictive inference and entropy
[AD-A191858] N88-25199
SHEFFIELD UNIV. (ENGLAND).
On frequency response for nonlinear systems
[RR-323] N88-25221
Recursive maximum likelihood identification of a nonlinear output-affine model
[RR-322] N88-25257
SHELL DEVELOPMENT CO., HOUSTON, TEX.
Industrial perspective on current and future needs in aerospace matrix resin chemistry N88-24696
SHINSHU UNIV., NAGANO (JAPAN).
Effect of uniaxial stress on the Raman spectra of graphite fibers
[AD-A191730] N88-24783
SIPPICAN OCEAN SYSTEMS, INC., MARION, MASS.
Expendable conductivity, temperature and depth system (XCTD) development program
[AD-A192182] N88-25121
SMITHSONIAN ASTROPHYSICAL OBSERVATORY, CAMBRIDGE, MASS.
Utilization of the IR telescope gimbaling system as a stabilized pointing platform for balloon payloads. Volume 1: Technical results
[NASA-CR-179339] N88-24962
Molecular sources of ionospheric holes
[AD-A191857] N88-25082
SOCIETE NATIONALE DES POUDRES ET EXPLOSIFS, VERT-LE-PETIT (FRANCE).
Aging of carbon fibers
[SNPE-NT-10/86/CRB/NP] N88-24707
SOCIETE NATIONALE INDUSTRIELLE AEROSPATIALE, SURESNES (FRANCE).
Harmfulness of defects: Behaviour in service of a delamination in a composite containing many differently oriented layers
[PB88-124714] N88-24705
Improving knowledge of the corrosion behavior of aluminum alloys of the 7XXX series
[REPT-48-451/F] N88-24750
Characterization of the 2219 Cegedur alloy. Data acquisition of the fracture mechanics
[REPT-48-442/F] N88-24751
Characterization of 7090 and 7091 profiles made with Cegedur powder
[REPT-48-441/F] N88-24752
Calculation of assemblies bonded with quasi-elastic adhesives
[REPT-47-632/F] N88-24793
SOUTHWEST RESEARCH INST., SAN ANTONIO, TEX.
Dynamics Explorer-2 measurements during an isolated auroral substorm
[AD-A191202] N88-25091
SRI INTERNATIONAL CORP., MENLO PARK, CALIF.
Applications of biotechnology to synthetic chemistry for aerospace matrix resins development N88-24697
Transition probabilities in OH A 2 sigma + - X 2 pi i: Bands with v prime = 0 and 1, v double prime = 0 to 4
[NASA-CR-182946] N88-25353

STANDARD TELECOMMUNICATION LABS. LTD., HARLOW (ENGLAND).
Assessment of optical communications systems for Data Relay Satellite. Volume 1: Executive summary
[ESA-CR(P)-2488-VOL-1] N88-24841
STANFORD UNIV., CALIF.
Joint services electronics program
[AD-A190239] N88-24848
The off-axis channel macroplate
[NASA-CR-182938] N88-24861
Defect detection and classification in VLSI pattern inspection N88-24871
Fatigue crack growth due to random loading N88-25017
Adaptive grid refinement for numerical weather prediction
[AD-A192172] N88-25101
A centered projective algorithm for linear programming
[AD-A192100] N88-25176
Making progress during a stall in the simplex algorithm
[DE88-007120] N88-25182
New mixed finite element methods N88-25248
Light propagation through gravitationally perturbed Friedmann universes N88-25307
STATE UNIV. OF NEW YORK, BUFFALO.
Low authority control of large space structures using a constrained threshold control formulation N88-24667
Vibration protection of inelastic structures by means of active and passive control N88-25001
Advanced development of the boundary element method for elastic and inelastic thermal stress analysis N88-25002
Forced motion of initially stressed shells and plates N88-25005
Reduced order modelling and analytical model modification for structural dynamics and control N88-25006
Optical investigations of the thermal boundary layer in arc plasmas N88-25313
STUTTGART UNIV. (WEST GERMANY).
Basic processes of plasma propulsion
[AD-A192117] N88-25310
SVERDRUP TECHNOLOGY, INC., ARNOLD AIR FORCE STATION, TENN.
Hypersonic turbulent wall boundary layer computations
[NASA-CR-182147] N88-24917
SWEDISH INST. OF SPACE PHYSICS, KIRUNA.
Observations of wave number dependent spectral line ratio fluctuations in the atmospheric emissions
[IRF-PREPRINT-101] N88-25085
Studies of spectral line ratio fluctuations using Inductively Coupled Plasma (ICP) light
[IRF-PREPRINT-100] N88-25311
SYRACUSE UNIV., N. Y.
Mechanisms of gas permeation through polymer membranes: Renewal proposal for period December 1, 1986 - November 30, 1989
[DE88-007436] N88-24796
Electromagnetic penetration into a conducting circular cylinder through a narrow slot, TE case
[AD-A191602] N88-24826
Electromagnetic field penetration into structures
[AD-A192127] N88-24836
Resolved shear stress intensity coefficient and fatigue crack growth in large crystals
[NASA-CR-182137] N88-24997

T

TAYLOR AND ASSOCIATES, INC., WRIGHTWOOD, CALIF.
Space station architectural elements model study
[NASA-CR-4027] N88-24632
Space station architectural elements and issues definition study
[NASA-CR-3941] N88-25371
TECHNICAL UNIV. OF ISTANBUL (TURKEY).
A dynamic analysis of piezoelectric strained elements
[AD-A191478] N88-24851
TECHNION - ISRAEL INST. OF TECH., HAIFA.
Galerkin approximation for inverse problems for nonautonomous nonlinear distributed systems
[NASA-CR-181676] N88-25246
TECHNISCHE HOCHSCHULE, AACHEN (WEST GERMANY).
High power axial flow CO2 laser
[ETN-88-91951] N88-24959
TECHNISCHE HOCHSCHULE, DARMSTADT (WEST GERMANY).
High power axial flow CO2 laser
[ETN-88-91951] N88-24959
TECHNISCHE HOGESCHOOL, DELFT (NETHERLANDS).
Combustion of PMMA, PE and PS in a ramjet
[VTH-LR-514] N88-24733
Combustion behavior of the vitiator. Experimental results of a second test series
[VTH-LR-509] N88-24734
Theoretical analysis of laminar incompressible flow in slender channels
[VTH-LR-517] N88-24909
Born-type reconstruction of material parameters of an inhomogeneous, lossy dielectric slab from reflected-field data
[PB88-188958] N88-25261
Centre for International Co-Operation and Approriate Technology (CICAT)
[PB88-165501] N88-25389
TECHNISCHE HOGESCHOOL, EINDHOVEN (NETHERLANDS).
The application of satellites in connection with the environment
[ETN-88-92474] N88-25020
TECHNISCHE UNIV., BERLIN (WEST GERMANY).
Possibilities and limits for use of laser propulsion systems in interorbital space flight
[ILR-MITT-185] N88-24683
Calculation of rolling contact of two viscoelastic cylinders with application to the steady state normal contact problem
[ILR-MITT-188] N88-25008
Limits of design feasibility of multiwing wind turbines with individual articulated wing structure
[ILR-MITT-180] N88-25052
TECHNISCHE UNIV., BRUNSWICK (WEST GERMANY).
Optical computer and optical methods for data processing N88-24939
TELDIX LUFTFAHRT-AUSRUESTUNGS G.M.B.H., HEIDELBERG (WEST GERMANY).
Assessment of optical communications systems for the Data Relay Satellite
[ESA-CR(P)-2488-VOL-2] N88-24842
TELESPAZIO, S.P.A., ROME (ITALY).
P-Plus: Polar Platform utilization study, executive summary
[BAE-TP-8391] N88-24853
TENNESSEE UNIV., CHATTANOOGA.
Robot navigation using simple sensor fusion
[DE88-006184] N88-25203
TENNESSEE UNIV., KNOXVILLE.
Decomposition of linear programs using parallel computation
[AD-A191718] N88-25173
Algorithms and software for solving finite element equations on serial and parallel architectures
[NASA-CR-183027] N88-25191
Robot navigation using simple sensor fusion
[DE88-006184] N88-25203
On path properties of certain infinitely divisible processes
[AD-A192016] N88-25255
TENNESSEE UNIV. SPACE INST., TULLAHOMA.
Meteorological and Environmental Inputs to Aviation Systems
[NASA-CP-2498] N88-25105
TEXAS CHRISTIAN UNIV., FORT WORTH.
Synthesis and characterization of new phosphazene polymers
[AD-A191508] N88-24771
TEXAS INSTRUMENTS, INC., DALLAS.
A monolithic reduced-size Ku-Band SPOT (Single-Pole Double Throw) FET switch
[DE88-006273] N88-24858
TEXAS UNIV., ARLINGTON.
Electronic and ionic transport in polymers
[AD-A191642] N88-24772
Numerical solutions to stochastic difference equations N88-25229
TEXAS UNIV., AUSTIN.
Attitude control laws for gas-jet spacecraft N88-24643
Fundamental limits to the velocity of solid armatures in railguns N88-24656
Electrochemistry in near-critical and supercritical fluids. 6: The electrochemistry of ferrocene and phenazine in acetonitrile between 25C and 300C
[AD-A192171] N88-24723
Joint services electronics program
[AD-A192076] N88-24856
Analysis and design of detection filters within closed-loop systems N88-24960
Multishaker modal testing
[NASA-CR-179355] N88-25010
Optimal a priori covariance selection for the solution of ill-conditioned nonlinear inverse problems N88-25222
Evaluation of the biot coefficients
[AD-A191643] N88-25265
Self shielding of surfaces irradiated by intense energy fluxes
[DE88-007094] N88-25318
A study of runaway electron confinement in the ASDEX tokamak
[DE88-007327] N88-25319
TOKYO UNIV. (JAPAN).
High speed and high angle of attack aerodynamic characteristics of winged space vehicle
[ISSN-0285-6808] N88-24599
Dynamics of a flexible orbiting platform with MRMS
[ISSN-0285-6808] N88-24673
Electric field measurement by S-520-9 sounding rocket using the time of flight technique of lithium ion beam
[ISAS-RN-367] N88-25095
Para-ortho abundance ratio of molecular hydrogen in NGC2023
[ISAS-RN-352] N88-25286
TRANSMISSION TECHNOLOGY CO., INC., FAIRFIELD, N. J.
Design, manufacture and spin test of high contact ratio helicopter transmission utilizing Self-Aligning Bearingless Planetary (SABP)
[NASA-CR-4155] N88-24975
TRANSPORTATION SYSTEMS CENTER, CAMBRIDGE, MASS.
Computer resource management technology program (PE 64740F). Task no. 9: Advanced user authentication
[PB88-183066] N88-25163

U

UNITED TECHNOLOGIES CORP., EAST HARTFORD, CONN.
Quality and productivity drive innovation and improvement at United Technologies Aerospace Operations, Inc.
[NASA-CR-182944] N88-24983
Fracture mechanics analysis for short cracks
[AD-A192002] N88-24992
UNIVERSITE DE TECHNOLOGIE DE COMPIEGNE (FRANCE).
Influence of carbon fiber surface treatment
[ETN-88-92536] N88-24787
Damage by creep fatigue: Influence of the visco-elasticity of the matrix
[PB88-124706] N88-24998
UNIVERSITE DES SCIENCES ET TECHNIQUES DE LILLE (FRANCE).
The influence of the chemical nature of resins on their reticulation kinetics and the consequences for their nonelastic mechanical properties
[ETN-88-92539] N88-24788
UNIVERSITY COLL., LONDON (ENGLAND).
Components of an atmospheric lidar system: Doppler wind lidar
[AD-A191222] N88-24951
UNIVERSITY COLL. OF NORTH WALES, BANGOR.
Fast acting optical beam detection and deflection system
[AD-A192161] N88-24954
UNIVERSITY COLL. OF WALES, ABERYSTWYTH.
Radio-wave scintillations and ionospheric irregularities at high latitudes
[AD-A192140] N88-24837
UNIVERSITY OF SOUTHERN CALIFORNIA, LOS ANGELES.
Joint services electronics program research in electronics
[AD-A192206] N88-24857
Dynamics and control of turbulent shear flows
[AD-A191527] N88-24879
Optical nonlinearities in GaAs/GaAlAs multiple quantum wells fabricated by metalorganic chemical vapor deposition for use in optical signal processing
[AD-A191558] N88-25337
UNIVERSITY OF SOUTHERN CALIFORNIA, MARINA DEL REY.
The ISI (Information Sciences Institute) grapher manual
[AD-A192198] N88-25200
UTAH UNIV., SALT LAKE CITY.
Yaw dynamics of horizontal axis wind turbines
[DE88-001137] N88-25055

V

VIRGINIA POLYTECHNIC INST. AND STATE UNIV., BLACKSBURG.
Periodic solutions in aircraft cruise-dash optimization N88-24631
Role of cracks in the creep of structural polycrystalline ceramics
[AD-A191485] N88-24770
Calculational model development for fibrous thermal insulation transient test procedures
[DE88-007843] N88-24789

Finite element solution of 3-D turbulent Navier-Stokes equations for propeller-driven slender bodies N88-24019
Experimental study of active vibration control [AD-A191454] N88-24969
Design and testing of a luminance and chrominance stabilization system for a computer-controlled color display [AD-A191922] N88-25159

VIRGINIA UNIV., CHARLOTTESVILLE.
Compressible flow in a pie-shaped cylinder rotating about the vertex N88-24804
The influence of cathodic protection on erosion-corrosion of metals and model alloys [AD-A191613] N88-24742
Environment assisted degradation mechanisms in advanced light metals [NASA-CR-182907] N88-24746
Infrared astronomy at extremely faint light levels in support of the LAIRTS program [AD-A191497] N88-25404

VON KARMAN INST. FOR FLUID DYNAMICS, RHODE-SAINT-GENESE (BELGIUM).
The performance of the VKI longshot hypersonic wind tunnel [VKI-TN-161] N88-24850
Two dimensional hyperbolic grid generation [VKI-TN-162] N88-24897

VRIJE UNIVERSITEIT, AMSTERDAM (NETHERLANDS).
Linear spaces, absolute retracts and the compact extension property [PB88-181110] N88-25225
Additive prophet inequalities for transforms of uniformly bounded pairwise independent random variables [PB88-173513] N88-25250

W

WASHINGTON STATE UNIV., PULLMAN.
Transient particle deposition in a boundary layer of impulsive flow over a flat plate [AD-A191537] N88-24880
Surface interactions relevant to space station contamination problems N88-25401

WASHINGTON UNIV., SEATTLE.
Oxidation and reduction rates for organic carbon in the Amazon mainstream tributary and floodplain, inferred from distributions of dissolved gases [NASA-CR-182943] N88-25062
Direct numerical simulations of the PDF's (Probability Density Functions) of a passive scalar in a forced mixing layer [AD-A192134] N88-25256
Remote sensing of acoustic properties of shallow water sediments: A review [AD-A192107] N88-25267

WASHINGTON UNIV., ST. LOUIS, MO.
Delay-doppler radar imaging [AD-A191509] N88-24826

WAYNE STATE UNIV., DETROIT, MICH.
Surface composition-reactivity relationships in heterogeneous catalysis [DE88-006679] N88-24714

WEST VIRGINIA UNIV., MORGANTOWN.
Computational design of low aspect ratio wing-winglet configurations for transonic wind-tunnel tests [NASA-CR-183021] N88-24830
Kinematics, dynamics and control of a closed chain mechanism manipulator N88-24967

WESTINGHOUSE RESEARCH AND DEVELOPMENT CENTER, PITTSBURGH, PA.
Advanced development of double-injection, deep-impurity semiconductor switches [NASA-CR-182118] N88-25346

WICHITA STATE UNIV., KANS.
Computation and characteristics of pulsatile multi-bifurcation flow N88-24729

WOODS HOLE OCEANOGRAPHIC INSTITUTION, MASS.
An FSK (Frequency Shift Keying) telemetry module for vector measuring current meters [AD-A192142] N88-24661

WYOMING UNIV., LARAMIE.
Adaptive local grid refinement in computational fluid mechanics [AD-A192215] N88-24890

Y

YALE UNIV., NEW HAVEN, CONN.
Manipulation of the structure of a turbulent boundary layer N88-24901
A centered projective algorithm for linear programming [AD-A192100] N88-25178

Typical Contract Number Index Listing

Listings in this index are arranged alphanumerically by contract number. Under each contract number the NASA accession numbers denoting documents that have been produced as a result of research done under that contract are arranged in ascending order. The NASA accession number denotes the number by which the citation is identified.

AF AFOSR-0005-84 ..... N88-24835
AF AFOSR-0018-86 ..... N88-24721
AF AFOSR-0026-87 ..... N88-25275
AF AFOSR-0039-87 ..... N88-24716
AF AFOSR-0052-86 ..... N88-24702
AF AFOSR-0108-87 ..... N88-24838
AF AFOSR-0109-84 ..... N88-25082
AF AFOSR-0124-84 ..... N88-24720
AF AFOSR-0125-87 ..... N88-25148
AF AFOSR-0138-87 ..... N88-25255
AF AFOSR-0140-84 ..... N88-24979
AF AFOSR-0153-85 ..... N88-24923
AF AFOSR-0177-87 ..... N88-25019
AF AFOSR-0190-85 ..... N88-24837
AF AFOSR-0196-85 ..... N88-24951
AF AFOSR-0234-85 ..... N88-24834
AF AFOSR-0240-85 ..... N88-25212
AF AFOSR-0271-84 ..... N88-24666
AF AFOSR-0279-87 ..... N88-25216
AF AFOSR-0296-86 ..... N88-25214
AF AFOSR-0300-86 ..... N88-25421
AF AFOSR-0336-86 ..... N88-25136
AF AFOSR-0337-86 ..... N88-25310
AF AFOSR-0339-86 ..... N88-24852
AF AFOSR-0367-84 ..... N88-25252
AF PROJ. 3058 ..... N88-24677
AF-AFOSR-ISSA-0025-87 ..... N88-24883
AF-AFOSR-ISSA-0032-87 ..... N88-25336
AF-AFOSR-0016-86 ..... N88-24878
AF-AFOSR-0023-85 ..... N88-25264
AF-AFOSR-0058-87 ..... N88-25294
AF-AFOSR-0117-85 ..... N88-24890
AF-AFOSR-0125-85 ..... N88-25404
AF-AFOSR-0126-85 ..... N88-24581
AF-AFOSR-0210-85 ..... N88-25344
AF-AFOSR-0245-87 ..... N88-24693
AF-AFOSR-0266-86 ..... N88-24882
AF-AFOSR-0277-84 ..... N88-24825
AF-AFOSR-0297-85 ..... N88-25337
AF-AFOSR-0303-84 ..... N88-24740
AF-AFOSR-00006-84 ..... N88-24802
AF-AFOSR-00575-86 ..... N88-24741
ARPA ORDER 5794 ..... N88-25296
ARPA ORDER 5884 ..... N88-25295
BMFT-01-YY-043-3 ..... N88-24869
BMFT-13N-5284 ..... N88-24959
BNSF-2-0095-83 ..... N88-25084
DA PROJ. 1L1-61102-AH-3 ..... N88-24880
DA PROJ. 1L1-61102-BH-57 ..... N88-24954
DA PROJ. 1L1-62209-AH-76 ..... N88-24975
DA PROJ. 1L6-65502-MM-40 ..... N88-24611
DA PROJ. 2Q1-61102-B-74-F N88-25142
N88-25144
N88-25148
N88-25147
N88-25152
N88-25172
N88-25375
DA PROJ. 2Q2-63744-A-795 ..... N88-24649
DAAA15-85-K-0004 ..... N88-24724
DAAA15-86-C-0063 ..... N88-25149
DAAD05-86-M-0985 ..... N88-24625
DAAE07-86-C-R069 ..... N88-24964
DAAG29-81-D—0100 ..... N88-25177
DAAG29-83-K-0138 ..... N88-25145
DAAG29-84-G-0060 ..... N88-25229
DAAG29-84-K-0008 ..... N88-25333
DAAG29-84-K-0045 ..... N88-25158
DAAG29-84-K-0072 ..... N88-25197
DAAG29-84-K-0078 ..... N88-24828
N88-24836
DAAG29-84-K-0143 ..... N88-24877
DAAG29-84-K-0147 ..... N88-24771
DAAG29-84-K-0180 ..... N88-24952
DAAG29-84-K-0187 ..... N88-24823
DAAG29-84-K-0201 ..... N88-25334
DAAG29-85-C-0001 ..... N88-24884
DAAG29-85-C-0018 ..... N88-25167
DAAG29-85-G-0109 ..... N88-25226
DAAG29-85-K-0003 ..... N88-24968
DAAG29-85-K-0026 ..... N88-24822
DAAG29-85-K-0040 ..... N88-24722
DAAG29-85-K-0048 ..... N88-24848
DAAG29-85-K-0106 ..... N88-24770
DAAG29-85-K-0183 ..... N88-24827
DAAG29-85-K-0193 ..... N88-25270
DAAK51-85-C-0009 ..... N88-24611
DAAK80-85-C-0074 ..... N88-24787
DAAL03-86-K-0094 ..... N88-25210
DAAL03-86-K-0112 ..... N88-25189
DAAL03-86-K-0133 ..... N88-24789
DAJA45-83-C-0018 ..... N88-24954
DAJA45-86-C-0005 ..... N88-24851
DAJA45-86-C-0029 ..... N88-24801
DAJA45-86-C-0045 ..... N88-25079
DAJA45-87-C-0035 ..... N88-25099
DE-AC02-76CH-00016 ..... N88-24715
N88-24956
N88-24982
N88-25278
N88-25284
N88-25287
N88-25288
N88-25317
DE-AC02-77ER-04215 ..... N88-25271
DE-AC02-78ER-05015 ..... N88-24796
DE-AC02-79ER-10381 ..... N88-24714
DE-AC02-80ER-10663 ..... N88-25274
DE-AC02-83CH-10093 ..... N88-25055
N88-25056
DE-AC03-76SF-00098 ..... N88-25279
N88-25348
N88-25350
N88-25362
N88-25366
DE-AC04-76DP-00789 ..... N88-24657
N88-24658
N88-24794
N88-24805
N88-24806
N88-24858
N88-24865
N88-24866
N88-24867
N88-24868
N88-24898
N88-24926
N88-24945
N88-25012
N88-25161
N88-25189
N88-25308
N88-25330
N88-25361
N88-25387
DE-AC04-78DR-00789 ..... N88-24800
DE-AC05-76OR-00033 ..... N88-24648
DE-AC05-84ER-40150 ..... N88-25291
DE-AC05-84OR-21400 ..... N88-24646
N88-24708
N88-24731
N88-24747
N88-24756
N88-24757
N88-24789
N88-24790
N88-24860
N88-24974
N88-25132
N88-25157
N88-25162
N88-25166
N88-25194
N88-25203
N88-25208
N88-25245
N88-25282
N88-25283
N88-25316
N88-25321
N88-25359
N88-25360
N88-25385
N88-25386
DE-AC05-84OT-21400 ..... N88-24977
DE-AC05-85ER-40216 ..... N88-25290
DE-AC06-76RL-01830 ..... N88-24748
N88-24795
N88-24804
N88-24981
N88-25041
N88-25042
N88-25046
N88-25047
N88-25049
N88-25057
N88-25058
N88-25351
DE-AC07-76ID-01570 ..... N88-24681
N88-24709
N88-24812
N88-24966
N88-25251
DE-AC07-76ID01570 ..... N88-24859
DE-AC07-85NV-10418 ..... N88-24859
DE-AC21-84MC-21181 ..... N88-25023
DE-AC21-86MC-23267 ..... N88-25054
DE-FC22-83FE-60149 ..... N88-24735
DE-FG02-84ER-45127 ..... N88-25331
DE-FG02-85ER-13320 ..... N88-25078
DE-FG02-85ER-13396 ..... N88-24905
DE-FG02-85ER-13442 ..... N88-25272
DE-FG03-87ER-25028 ..... N88-25182
DE-FG05-80ET-53088 ..... N88-25319
DE-FG05-86ER-45266 ..... N88-25332
DE-FG05-87ER-13735 ..... N88-25318
DE-FG05-87ER-53245 ..... N88-25320
DRET-83-324 ..... N88-24896
DRET-84-34-302 ..... N88-24707
DRET-84-34-497-00-470-75-01 ..... N88-24793
DRET-84-011 ..... N88-24787
DRET-84-020 ..... N88-24594
DRET-84-023 ..... N88-24907
DRET-84-044 ..... N88-25130
DRET-84-140 ..... N88-25089
DRET-84-168 ..... N88-24788
DRET-85-34-001 ..... N88-24792
DRET-85-34-016 ..... N88-25104
DRET-85-002 ..... N88-24984
DRET-85-1206 ..... N88-24993
DRET-85-1378 ..... N88-24908
DRET-86-002 ..... N88-24595
DTFA01-81-Y-10523 ..... N88-24652
DTFA03-85-C-0058 ..... N88-24622
DTFA03-86-C-00005 ..... N88-24799
N88-24807
EAGLE-TO-87-57 ..... N88-25415
EEC-303-78-1 ..... N88-24726
ESA-6392/85 ..... N88-24841
N88-24842
ESA-6608/85 ..... N88-24653
EW-78-S-05-5679 ..... N88-25042
FMV-FFL-82223-80-183-21-001 ..... N88-24704
FMV-FFL-82250-85-078-73-001 ..... N88-24995
FMV-FFL-82250-85-273-25-001 ..... N88-24996
FMV-FFL-82250-85-282-24-001 ..... N88-24995
FMV-FLYGFL-82223-74-001-07-001 ..... N88-24585

FMV-FLYGFL-82223-75-007-07-001 ..... N88-24585
F04701-85-C-0066 ..... N88-24680
N88-24855
N88-25063
F08635-83-C-0136 ..... N88-24991
F08635-85-C-0122 ..... N88-24638
F19628-83-C-0175 ..... N88-24850
F19628-85-C-0003 ..... N88-24647
F19628-87-C-0106 ..... N88-25100
F29601-85-C-0056 ..... N88-24701
F33615-84-C-0510 ..... N88-25159
F33615-84-C-5067 ..... N88-24775
F33615-85-C-5058 ..... N88-24739
F33615-86-C-3612 ..... N88-24627
F49620-83-K-0029 ..... N88-24584
F49620-84-C-0007 ..... N88-24876
F49620-85-C-0024 ..... N88-24989
F49620-85-C-0027 ..... N88-24875
F49620-85-C-0039 ..... N88-25297
F49620-85-C-0067 ..... N88-25256
F49620-85-C-0071 ..... N88-24857
F49620-85-C-0134 ..... N88-24855
F49620-85-C-0137 ..... N88-24887
F49620-85-C-0144 ..... N88-25252
N88-25254
N88-25255
F49620-86-C-0018 ..... N88-24743
F49620-86-C-0029 ..... N88-25091
F49620-86-C-0045 ..... N88-24856
F49620-86-C-0062 ..... N88-25296
F49620-86-C-0085 ..... N88-25276
F49620-86-C-0086 ..... N88-25309
F49620-86-C-0088 ..... N88-25211
F49620-86-C-0095 ..... N88-24992
F49620-86-K-0004 ..... N88-25289
F49620-87-C-0015 ..... N88-25295
F49620-87-C-0026 ..... N88-25199
F49620-87-C-0028 ..... N88-24679
F49620-87-C-0029 ..... N88-24665
F49629-85-C-0147 ..... N88-24776
N88-24777
N88-24778
N88-24779
N88-24780
N88-24781
N88-24782
N88-24783
GRI-5083-260-0960 ..... N88-24731
GRI-5086-260-1421 ..... N88-25370
ICCFDU-4C.2 ..... N88-25061
MDA903-81-C-0335 ..... N88-25200
MDA903-81-C-0504 ..... N88-24649
MDA903-82-C-0145 ..... N88-25142
MDA903-85-C-0324 ..... N88-25147
N88-25152
N88-25172
MDA903-86-C-0411 ..... N88-25144
MDA903-86-K-0225 ..... N88-25146
MDA903-88-C-0171 ..... N88-25375
MIPR-ARO-101-86 ..... N88-25297
MIPR-ARO-106-86 ..... N88-24744
MOD-NSN/13A/1A-90762 ..... N88-24725
NAGW-254 ..... N88-25093
NAGW-696 ..... N88-25419
NAGW-711 ..... N88-25062
NAGW-922 ..... N88-25396
NAG1-244 ..... N88-24914
NAG1-313 ..... N88-24911
NAG1-517 ..... N88-25246
NAG1-613 ..... N88-25183
NAG1-624 ..... N88-25268
NAG1-625 ..... N88-24630
NAG1-655 ..... N88-25244
NAG1-736 ..... N88-24644
NAG1-745 ..... N88-24748
NAG1-803 ..... N88-25191
NAG1-823 ..... N88-25185
NAG2-100 ..... N88-25129
NAG3-348 ..... N88-24997
NAG3-447 ..... N88-25327
NAG3-466 ..... N88-25016
NAG3-783 ..... N88-24976
NAG5-287 ..... N88-25408
NAG5-622 ..... N88-24861
NAG5-713 ..... N88-25418
NAG5-753 ..... N88-25092
NAG5-780 ..... N88-25206
NAG5-882 ..... N88-25024
NAG5-895 ..... N88-25155
NAG5-971 ..... N88-25408
NAG8-599 ..... N88-24738
NASA ORDER A-16516-C N88-25371
NASW-3597 ..... N88-25428
N88-25429
N88-25430
NASW-4093 ..... N88-24861
NASW-4307 ..... N88-24710
N88-24758
N88-24759
N88-24760
N88-24761
N88-24762
N88-24763
N88-24764
N88-24765
N88-24797
N88-24798
N88-24869
N88-25205
N88-25285
NAS1-18099 ..... N88-24637
NAS1-18956 ..... N88-25353
NAS1-17351 ..... N88-24948
NAS1-17719 ..... N88-24619
NAS1-18107 ..... N88-24608
N88-24916
N88-25246
N88-25247
N88-25249
NAS2-11690 ..... N88-25372
NAS2-11723 ..... N88-25156
NAS3-24539 ..... N88-24975
NAS3-24637 ..... N88-25346
NAS3-25266 ..... N88-24917
NAS5-29274 ..... N88-24861
NAS7-100 ..... N88-24815
NAS7-918 ..... N88-24814
N88-24818
N88-24846
N88-24863
N88-24864
N88-24943
N88-24944
N88-24973
N88-25281
N88-25301
N88-25304
N88-25305
N88-25358
NAS8-34135 ..... N88-24676
NAS8-35338 ..... N88-25010
NAS8-35592 ..... N88-24899
NAS8-36185 ..... N88-24675
NAS8-36300 ..... N88-24983
NAS8-37579 ..... N88-24962
NAS9-17560 ..... N88-24654
N88-24668
NAS9-17878 ..... N88-25414
N88-25415
NAS10-10285 ..... N88-25134
NB83-NADA-4047 ..... N88-24873
NCC1-22 ..... N88-24915
NCC1-68 ..... N88-24922
NCC2-349 ..... N88-25150
NCC2-475 ..... N88-24591
NCC3-56 ..... N88-24592
NGL-05-005-007 ..... N88-25425
NGL50-002-162 ..... N88-25419
NGR-39-007-011 ..... N88-25014
NGT-8001 ..... N88-24629
NSF ATM-80-21064 ..... N88-25419
NSF DCR-83-09926 ..... N88-25215
NSF DCR-83-20124 ..... N88-25213
NSF DMR-86-01281 ..... N88-25401
NSF DMS-86-04047 ..... N88-25239
NSF ECS-86-02534 ..... N88-25178
NSF INT-85-09939 ..... N88-25091
NSF PRM-82-15949 ..... N88-25234
NSF-ATM-87-09659 ..... N88-25096
N88-25098
NSF-CHE-83-20053 ..... N88-25296
NSG-1613 ..... N88-25300
N00014-76-C-0370 ..... N88-25168
N00014-78-C-0049 ..... N88-24853
N00014-80-C-0455 ..... N88-25215
N00014-80-C-0622 ..... N88-25168
N00014-82-C-0579 ..... N88-25121
N00014-82-K-0193 ..... N88-25213
N00014-82-K-0335 ..... N88-25101
N00014-83-D-0689 ..... N88-25339
N00014-83-K-0183 ..... N88-24888
N00014-84-C-0134 ..... N88-24661
N00014-84-K-0267 ..... N88-25101
N00014-84-K-0428 ..... N88-24723
N00014-84-K-0431 ..... N88-25335
N00014-84-K-0519 ..... N88-25381
N00014-84-K-0646 ..... N88-25267
N00014-84-K-0656 ..... N88-24719
N00014-85-C-6041 ..... N88-24885
N00014-85-K-0063 ..... N88-25120
N00014-85-K-0124 ..... N88-24819
N88-25269
N00014-85-K-0169 ..... N88-25215
N00014-85-K-0222 ..... N88-24785
N00014-85-K-0228 ..... N88-24691
N00014-85-K-0321 ..... N88-24833
N00014-85-K-0495 ..... N88-25171
N00014-85-K-2036 ..... N88-25293
N00014-86-C-0860 ..... N88-24745
N88-25343
N00014-86-C-2288 ..... N88-24803
N00014-86-C-2352 ..... N88-25164
N00014-86-D-0137 ..... N88-25123
N00014-86-G-0216 ..... N88-24768
N00014-86-K-0042 ..... N88-25169
N00014-86-K-0059 ..... N88-25253
N00014-86-K-0202 ..... N88-24832
N88-25175
N00014-86-K-0366 ..... N88-25298
N00014-86-K-0370 ..... N88-24826
N00014-86-K-0387 ..... N88-25265
N00014-86-K-0442 ..... N88-25176
N00014-86-K-0603 ..... N88-24889
N00014-86-K-0679 ..... N88-24879
N00014-86-K-0689 ..... N88-25213
N00014-86-K-0769 ..... N88-24772
N00014-87-C-0075 ..... N88-24766
N00014-87-C-0115 ..... N88-25122
N00014-87-C-0666 ..... N88-24824
N00014-87-K-0042 ..... N88-24742
N00014-87-K-0163 ..... N88-25173
N00014-87-K-0212 ..... N88-25178
N62269-85-C-0246 ..... N88-24700
N613339-85-D-0026 ..... N88-24648
PBE-90743.140 ..... N88-24734
PECD-7/9/322 ..... N88-25061
RDMFE-7/87 ..... N88-24725
SERC-GR/D/24371 ..... N88-24725
SERC-GR/D/30587 ..... N88-25257
SERC-GR/D/68139 ..... N88-24725
STPA-85-95-004 ..... N88-24596
N88-24994
STPA-85-96-032 ..... N88-24750
N88-24751
N88-24752
STU-87-0472 ..... N88-24586
STW-DLR-15.0120 ..... N88-24734
W-7405-ENG-36 ..... N88-24664
N88-24737
N88-24912
N88-24913
N88-24925
N88-24947
N88-24955
N88-24957
N88-25102
N88-25131
N88-25181
N88-25188
N88-25322
N88-25349
W-7405-ENG-48 ..... N88-24658
N88-24755
N88-24906
N88-24960
N88-24961
N88-25195
N88-25273
N88-25426
W-7405-ENG-82 ..... N88-24736
Z08-38 ..... N88-24803
154-20-80-16 ..... N88-25420
175-16-57-50 ..... N88-25105
199-21-12 ..... N88-25140
199-22-76-01 ..... N88-25427
505-07-01 ..... N88-24712
505-60-01 ..... N88-24579
N88-24603
505-60-21 ..... N88-24900
505-61-01 ..... N88-24946
505-61-01-02 ..... N88-24580
505-61-11-02 ..... N88-25268
505-61-51-10 ..... N88-24607
505-62-21 ..... N88-24592
N88-24639
N88-24640
N88-24917
N88-25239
505-63-1B N88-24997
505-63-01-05 ..... N88-24713
505-63-02 ..... N88-24833
505-63-11 ..... N88-24766
505-63-21 ..... N88-24598
505-63-21-04 ..... N88-24623
505-63-31-03 ..... N88-25190
505-63-51 ..... N88-24975
N88-24976
505-66-11 ..... N88-25207

505-66-41-04	N88-24619
505-90-21-01	N88-24608
	N88-24916
	N88-25246
	N88-25247
	N88-25249
506-40-31-01	N88-24911
506-41-11	N88-24870
506-41-21	N88-25059
506-41-41	N88-25346
506-42-11	N88-24806
506-42-21	N88-24689
506-42-31	N88-24682
	N88-24688
	N88-24968
	N88-25260
506-42-32	N88-24687
506-44-21-01	N88-24948
506-45-11-01	N88-25204
506-48-21	N88-24686
506-49-31-01	N88-25184
506-60-12	N88-25016
510-01-01	N88-24749
533-02-30	N88-24634
535-03-01	N88-24597
	N88-24641
535-05-01	N88-24642
536-01-11	N88-25196
549-03-31	N88-25192
582-01-11	N88-24690
586-01-11	N88-24754
650-60-23	N88-24847
665-10-40-04	N88-25094
674-27-05	N88-24811
679-10-00	N88-24663
992-21-01	N88-24601

Typical Report Number Index Listing

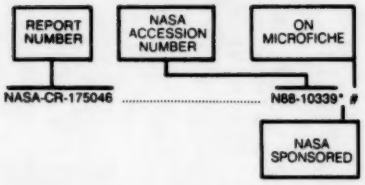

Listings in this index are arranged alphanumerically by report number. The NASA accession number denotes the number by which the citation is identified. An asterisk (*) indicates that the item is a NASA report. A pound sign (#) indicates that the item is available on microfiche.

A-86284 ..... N88-25140* #
A-88048 ..... N88-24900* #
A-88067 ..... N88-25420* #
A-88094 ..... N88-24601* #
A-88114 ..... N88-24600* #
A-88115 ..... N88-24602* #
A-88128 ..... N88-24579* #
A-88131 ..... N88-24946* #
A-88150 ..... N88-24603* #
A-88176 ..... N88-25192* #
A-88187 ..... N88-25196* #

AAMRL-TR-87-027 ..... N88-25159 #
AAMRL-TR-87-030 ..... N88-25135 #
AAMRL-TR-87-033 ..... N88-25143 #

AD-A184840 ..... N88-25269 #
AD-A186450 ..... N88-25139 #
AD-A186593 ..... N88-25193 #
AD-A187290 ..... N88-25149 #
AD-A188661 ..... N88-24819 #
AD-A189013 ..... N88-25270 #
AD-A189818 ..... N88-24799 #
AD-A189861 ..... N88-24693 #
AD-A190239 ..... N88-24848 #
AD-A190415 ..... N88-25164 #
AD-A190514 ..... N88-24573 #
AD-A190567 ..... N88-24645 #
AD-A190679 ..... N88-25165 #
AD-A190681 ..... N88-24624 #
AD-A190778 ..... N88-25374 #
AD-A190785 ..... N88-24813 #
AD-A190788 ..... N88-25142 #
AD-A190790 ..... N88-24949 #
AD-A190795 ..... N88-25333 #
AD-A190800 ..... N88-25167 #
AD-A190809 ..... N88-25135 #
AD-A190826 ..... N88-25226 #
AD-A190828 ..... N88-24987 #
AD-A190853 ..... N88-24767 #
AD-A190869 ..... N88-24963 #
AD-A190878 ..... N88-24716 #
AD-A190915 ..... N88-24988 #
AD-A190924 ..... N88-25275 #
AD-A190962 ..... N88-24677 #
AD-A190969 ..... N88-24950 #
AD-A191028 ..... N88-25166 #
AD-A191037 ..... N88-25209 #
AD-A191046 ..... N88-24822 #
AD-A191052 ..... N88-25143 #
AD-A191055 ..... N88-24874 #
AD-A191059 ..... N88-25263 #
AD-A191068 ..... N88-24823 #
AD-A191071 ..... N88-25144 #
AD-A191075 ..... N88-24964 #
AD-A191083 ..... N88-25197 #
AD-A191085 ..... N88-25210 #
AD-A191087 ..... N88-25211 #
AD-A191097 ..... N88-24647 #
AD-A191116 ..... N88-25151 #
AD-A191119 ..... N88-25276 #
AD-A191125 ..... N88-25212 #
AD-A191127 ..... N88-24875 #
AD-A191168 ..... N88-24876 * #
AD-A191172 ..... N88-25018 #
AD-A191179 ..... N88-25152 #
AD-A191184 ..... N88-24824 #
AD-A191190 ..... N88-24850 #
AD-A191202 ..... N88-25091 #
AD-A191203 ..... N88-25169 #
AD-A191212 ..... N88-24648 #
AD-A191217 ..... N88-25252 #
AD-A191221 ..... N88-24788 #
AD-A191222 ..... N88-24951 #
AD-A191229 ..... N88-24739 #
AD-A191241 ..... N88-24613 #
AD-A191242 ..... N88-24849 #
AD-A191349 ..... N88-24801 #
AD-A191441 ..... N88-25264 #
AD-A191447 ..... N88-24952 #
AD-A191448 ..... N88-25145 #
AD-A191449 ..... N88-24877 #
AD-A191450 ..... N88-25334 #
AD-A191451 ..... N88-24769 #
AD-A191454 ..... N88-24989 #
AD-A191461 ..... N88-25170 #
AD-A191471 ..... N88-25079 #
AD-A191478 ..... N88-24851 #
AD-A191479 ..... N88-24625 #
AD-A191481 ..... N88-25293 #
AD-A191482 ..... N88-25213 #
AD-A191484 ..... N88-25080 #
AD-A191485 ..... N88-24770 #
AD-A191489 ..... N88-24878 #
AD-A191490 ..... N88-24978 #
AD-A191492 ..... N88-24665 #
AD-A191494 ..... N88-24581 #
AD-A191495 ..... N88-24740 #
AD-A191496 ..... N88-24825 #
AD-A191497 ..... N88-25404 #
AD-A191498 ..... N88-24717 #
AD-A191499 ..... N88-24718 #
AD-A191508 ..... N88-24771 #
AD-A191509 ..... N88-24826 #
AD-A191511 ..... N88-24827 #
AD-A191518 ..... N88-24678 #
AD-A191527 ..... N88-24879 #
AD-A191537 ..... N88-24880 #
AD-A191542 ..... N88-25335 #
AD-A191544 ..... N88-24881 #
AD-A191546 ..... N88-24882 #
AD-A191547 ..... N88-25336 #
AD-A191548 ..... N88-24741 #
AD-A191549 ..... N88-25294 #
AD-A191552 ..... N88-24575 #
AD-A191553 ..... N88-24582 #
AD-A191554 ..... N88-24719 #
AD-A191556 ..... N88-24802 #
AD-A191558 ..... N88-25337 #
AD-A191559 ..... N88-25146 #
AD-A191565 ..... N88-24720 #
AD-A191567 ..... N88-25171 #
AD-A191573 ..... N88-24583 #
AD-A191589 ..... N88-25338 #
AD-A191593 ..... N88-24852 #
AD-A191597 ..... N88-25147 #
AD-A191599 ..... N88-25289 #
AD-A191600 ..... N88-24721 #
AD-A191602 ..... N88-24828 #
AD-A191604 ..... N88-24722 #
AD-A191613 ..... N88-24742 #
AD-A191616 ..... N88-24635 #
AD-A191621 ..... N88-25099 #
AD-A191627 ..... N88-25339 #
AD-A191629 ..... N88-24700 #
AD-A191632 ..... N88-25172 #
AD-A191635 ..... N88-25295 #
AD-A191639 ..... N88-24611 #
AD-A191641 ..... N88-24953 #
AD-A191642 ..... N88-24772 #
AD-A191643 ..... N88-25265 #
AD-A191645 ..... N88-25253 #
AD-A191648 ..... N88-24979 #
AD-A191650 ..... N88-24829 #
AD-A191651 ..... N88-25198 #
AD-A191653 ..... N88-25153 #
AD-A191663 ..... N88-25277 #
AD-A191665 ..... N88-24773 #
AD-A191666 ..... N88-24774 #
AD-A191668 ..... N88-25214 #
AD-A191669 ..... N88-24883 #
AD-A191671 ..... N88-24923 #
AD-A191673 ..... N88-25421 #
AD-A191686 ..... N88-24884 #
AD-A191688 ..... N88-25158 #
AD-A191697 ..... N88-24775 #
AD-A191707 ..... N88-24776 #
AD-A191708 ..... N88-24777 #
AD-A191709 ..... N88-24778 #
AD-A191710 ..... N88-24779 #
AD-A191711 ..... N88-24576 #
AD-A191714 ..... N88-24577 #
AD-A191717 ..... N88-24803 #
AD-A191718 ..... N88-25173 #
AD-A191719 ..... N88-24614 #
AD-A191720 ..... N88-24615 #
AD-A191721 ..... N88-24616 #
AD-A191726 ..... N88-24780 #
AD-A191727 ..... N88-24781 #
AD-A191728 ..... N88-24782 #
AD-A191730 ..... N88-24783 #
AD-A191740 ..... N88-25266 #
AD-A191741 ..... N88-24990 #
AD-A191743 ..... N88-24885 #
AD-A191744 ..... N88-24886 #
AD-A191747 ..... N88-24991 #
AD-A191748 ..... N88-24701 #
AD-A191749 ..... N88-24853 #
AD-A191752 ..... N88-25340 #
AD-A191753 ..... N88-24617 #
AD-A191754 ..... N88-24854 #
AD-A191755 ..... N88-24784 #
AD-A191759 ..... N88-24830 #
AD-A191760 ..... N88-25174 #
AD-A191768 ..... N88-24831 #
AD-A191807 ..... N88-25375 #
AD-A191809 ..... N88-24626 #
AD-A191823 ..... N88-25215 #
AD-A191839 ..... N88-25376 #
AD-A191840 ..... N88-25377 #
AD-A191841 ..... N88-25378 #
AD-A191842 ..... N88-25379 #
AD-A191843 ..... N88-25380 #
AD-A191847 ..... N88-25175 #
AD-A191848 ..... N88-24832 #
AD-A191849 ..... N88-24833 #
AD-A191854 ..... N88-25341 #
AD-A191855 ..... N88-25081 #
AD-A191857 ..... N88-25082 #
AD-A191858 ..... N88-25199 #
AD-A191866 ..... N88-25176 #
AD-A191867 ..... N88-24691 #
AD-A191871 ..... N88-25154 #
AD-A191879 ..... N88-24702 #
AD-A191922 ..... N88-25159 #
AD-A191925 ..... N88-25342 #
AD-A191946 ..... N88-24855 #
AD-A191947 ..... N88-25381 #
AD-A191998 ..... N88-25254 #
AD-A191999 ..... N88-24679 #
AD-A192002 ..... N88-24992 #
AD-A192005 ..... N88-25206 #
AD-A192013 ..... N88-25100 #
AD-A192016 ..... N88-25255 #
AD-A192026 ..... N88-25148 #
AD-A192041 ..... N88-25216 #
AD-A192042 ..... N88-25019 #
AD-A192044 ..... N88-24887 #
AD-A192050 ..... N88-24785 #
AD-A192051 ..... N88-25177 #
AD-A192053 ..... N88-24638 #
AD-A192064 ..... N88-25343 #
AD-A192069 ..... N88-24618 #
AD-A192072 ..... N88-24888 #
AD-A192075 ..... N88-25309 #
AD-A192076 ..... N88-24856 #
AD-A192088 ..... N88-24834 #

AD-A192093 ..... N88-24743 #
AD-A192095 ..... N88-25136 #
AD-A192100 ..... N88-25178 #
AD-A192103 ..... N88-25344 #
AD-A192104 ..... N88-24835 #
AD-A192107 ..... N88-25267 #
AD-A192114 ..... N88-25345 #
AD-A192115 ..... N88-24680 #
AD-A192117 ..... N88-25310 #
AD-A192120 ..... N88-24666 #
AD-A192126 ..... N88-24744 #
AD-A192127 ..... N88-24836 #
AD-A192134 ..... N88-25256 #
AD-A192140 ..... N88-24837 #
AD-A192142 ..... N88-24661 #
AD-A192146 ..... N88-24627 #
AD-A192148 ..... N88-24689 #
AD-A192154 ..... N88-25083 #
AD-A192161 ..... N88-24954 #
AD-A192167 ..... N88-24838 #
AD-A192168 ..... N88-25120 #
AD-A192169 ..... N88-24584 #
AD-A192171 ..... N88-24723 #
AD-A192172 ..... N88-25101 #
AD-A192173 ..... N88-24636 #
AD-A192175 ..... N88-25297 #
AD-A192178 ..... N88-24655 #
AD-A192182 ..... N88-25121 #
AD-A192184 ..... N88-24786 #
AD-A192190 ..... N88-25298 #
AD-A192197 ..... N88-24745 #
AD-A192198 ..... N88-25200 #
AD-A192199 ..... N88-25128 #
AD-A192200 ..... N88-25382 #
AD-A192203 ..... N88-25122 #
AD-A192204 ..... N88-25123 #
AD-A192206 ..... N88-24857 #
AD-A192210 ..... N88-24724 #
AD-A192215 ..... N88-24890 #

AD-E500953 ..... N88-24678 #

AD-F800025 ..... N88-24611 #

AERONOMICA-ACTA-A-321-1987 ..... N88-25422 #
AERONOMICA-ACTA-A-325-1987 ..... N88-24726 #
AERONOMICA-ACTA-A-326-1987 ..... N88-25084 #

AFAL-TR-87-010 ..... N88-24677 #

AFESC/ESL-TR-87-05 ..... N88-24991 #
AFESC/ESL-TR-87-27 ..... N88-24636 #

AFGL-TR-87-0247 ..... N88-24837 #

AFIT/GCE/ENG/87D-1 ..... N88-24624 #

AFIT/GE/ENG/87D-24 ..... N88-25165 #
AFIT/GE/ENG/87D-74 ..... N88-24645 #

AFOSR-87-0268TR ..... N88-25100 #
AFOSR-87-1563TR ..... N88-25136 #
AFOSR-87-1754TR ..... N88-25264 #
AFOSR-87-1791TR ..... N88-25276 #
AFOSR-87-1884TR ..... N88-24693 #
AFOSR-87-1984TR ..... N88-24890 #
AFOSR-87-1994TR ..... N88-25275 #
AFOSR-87-2014TR ..... N88-25211 #
AFOSR-88-0018TR ..... N88-24834 #
AFOSR-88-0021TR ..... N88-24740 #
AFOSR-88-0022TR ..... N88-25296 #
AFOSR-88-0023TR ..... N88-24852 #
AFOSR-88-0025TR ..... N88-25214 #
AFOSR-88-0028TR ..... N88-24581 #
AFOSR-88-0032TR ..... N88-25199 #
AFOSR-88-0039TR ..... N88-24951 #
AFOSR-88-0040TR ..... N88-25404 #
AFOSR-88-0041TR ..... N88-24923 #
AFOSR-88-0044TR ..... N88-24802 #
AFOSR-88-0045TR ..... N88-24584 #
AFOSR-88-0050TR ..... N88-24825 #
AFOSR-88-0051TR ..... N88-24838 #
AFOSR-88-0053TR ..... N88-25289 #
AFOSR-88-0060TR ..... N88-24989 #
AFOSR-88-0063TR ..... N88-24665 #
AFOSR-88-0064TR ..... N88-25082 #
AFOSR-88-0065TR ..... N88-24835 #
AFOSR-88-0068TR ..... N88-24743 #
AFOSR-88-0091TR ..... N88-24887 #
AFOSR-88-0094TR ..... N88-25295 #
AFOSR-88-0112TR ..... N88-25091 #
AFOSR-88-0127TR ..... N88-24882 #
AFOSR-88-0128TR ..... N88-25344 #
AFOSR-88-0130TR ..... N88-25337 #
AFOSR-88-0131TR ..... N88-25019 #
AFOSR-88-0135TR ..... N88-25310 #
AFOSR-88-0169TR ..... N88-24716 #
AFOSR-88-0175TR ..... N88-24857 #
AFOSR-88-0184TR ..... N88-24856 #
AFOSR-88-0186TR ..... N88-25216 #
AFOSR-88-0188TR ..... N88-25421 #
AFOSR-88-0191TR ..... N88-25309 #
AFOSR-88-0195TR ..... N88-24992 #
AFOSR-88-0196TR ..... N88-24679 #
AFOSR-88-0201TR ..... N88-25254 #
AFOSR-88-0203TR ..... N88-25255 #
AFOSR-88-0215TR ..... N88-25148 #
AFOSR-88-0220TR ..... N88-24741 #
AFOSR-88-0221TR ..... N88-25294 #
AFOSR-88-0222TR ..... N88-25336 #
AFOSR-88-0224TR ..... N88-24776 #
AFOSR-88-0226TR ..... N88-24783 #
AFOSR-88-0228TR ..... N88-24782 #
AFOSR-88-0229TR ..... N88-24781 #
AFOSR-88-0230TR ..... N88-24780 #
AFOSR-88-0232TR ..... N88-24777 #
AFOSR-88-0233TR ..... N88-24778 #
AFOSR-88-0234TR ..... N88-24779 #
AFOSR-88-0242TR ..... N88-24721 #
AFOSR-88-0245TR ..... N88-24666 #
AFOSR-88-0249TR ..... N88-24876 #
AFOSR-88-0251TR ..... N88-24878 #
AFOSR-88-0252TR ..... N88-24883 #
AFOSR-88-0257TR ..... N88-24655 #
AFOSR-88-0259TR ..... N88-24702 #
AFOSR-88-0268TR ..... N88-25256 #
AFOSR-88-0270TR ..... N88-24720 #
AFOSR-88-0296TR ..... N88-24875 #
AFOSR-88-0335TR ..... N88-25252 #
AFOSR-88-0346TR ..... N88-25212 #
AFOSR-88-0363TR ..... N88-24979 #

AFWAL-TR-86-2039 ..... N88-24718 #
AFWAL-TR-87-3072 ..... N88-24573 #
AFWAL-TR-87-3079 ..... N88-24627 #
AFWAL-TR-87-4071 ..... N88-24773 #
AFWAL-TR-87-4072 ..... N88-24774 #
AFWAL-TR-87-4102 ..... N88-24775 #
AFWAL-TR-87-4105-VOL-1 ..... N88-24739 #

AFWL-TN-86-59 ..... N88-24701 #

AF060722A.DOC ..... N88-24665 #

AI-M-885 ..... N88-25269 #

AI-TR-974 ..... N88-24819 #

AIAA-88-2645 ..... N88-24811* #
AIAA-88-2821 ..... N88-24808* #
AIAA-88-2829 ..... N88-24917* #
AIAA-88-2912 ..... N88-24688* #
AIAA-88-3105 ..... N88-24682* #
AIAA-88-3106 ..... N88-24687* #
AIAA-88-3138 ..... N88-24639* #
AIAA-88-3149 ..... N88-24597* #
AIAA-88-3180 ..... N88-24640* #
AIAA-88-3229 ..... N88-24642* #
AIAA-88-3283 ..... N88-25260* #
AIAA-88-3288 ..... N88-24968* #
AIAA-88-3300 ..... N88-24689* #
AIAA-88-3403 ..... N88-24686* #

AMSEL-NV-TR-0061 ..... N88-24949 #

ANCO-1663.11 ..... N88-24611 #

APL-UW-8711 ..... N88-25267 #

ARACOR-FR-563-88 ..... N88-24745 #

ARAP-617 ..... N88-24884 #

ARC-TR-8782 ..... N88-25149 #

ARCCB-TR-88001 ..... N88-25266 #
ARCCB-TR-88002 ..... N88-24990 #

ARDG-R/D-4246-R-MS ..... N88-24954 #

ARI-RN-87-64 ..... N88-25144 #
ARI-RN-87-72 ..... N88-25152 #
ARI-RN-87-84 ..... N88-25142 #
ARI-RN-88-01 ..... N88-25172 #
ARI-RN-88-04 ..... N88-25375 #
ARI-RN-88-05 ..... N88-25146 #
ARI-RN-88-06 ..... N88-25147 #

ARI-TR-763 ..... N88-24649 #

ARL-STRUC-TM-475 ..... N88-25209 #
ARO-18211.14-MS ..... N88-24744 #
ARO-20428.1-PH ..... N88-25333 #
ARO-20658.5-EG ..... N88-24877 #
ARO-21059.6-LS ..... N88-25145 #
ARO-21213.7-MA ..... N88-25197 #
ARO-21378.11-EL ..... N88-24828 #
ARO-21378.13-EL ..... N88-24836 #
ARO-21558.20-PH ..... N88-25334 #
ARO-21710.7-MS ..... N88-24770 #
ARO-21716.9-MA ..... N88-24884 #
ARO-21751.6-GS ..... N88-24952 #
ARO-21783.6-CH ..... N88-24722 #
ARO-21825.17-GS ..... N88-24823 #
ARO-22288.64-PH ..... N88-25297 #
ARO-22306.11-EG ..... N88-24988 #
ARO-22336.14PH ..... N88-24822 #
ARO-22634.6-EL ..... N88-24827 #
ARO-23145-MA-H ..... N88-25226 #
ARO-23199.6-CH ..... N88-25270 #
ARO-23306.133-MA ..... N88-25167 #
ARO-23699.15-MA ..... N88-25210 #
ARO-24165.4-MS ..... N88-24769 #
ARO-24179.19-CH ..... N88-24771 #

ASD-TR-87-5005 ..... N88-24636 #

ASI479-066-85 ..... N88-24649 #

ATD-88-1 ..... N88-25170 #

AVSCOM-TM-88-B-004 ..... N88-24607* #

AVSCOM-TR-88-C-009 ..... N88-24975* #
AVSCOM-TR-88-C-016 ..... N88-24976* #

BAE-TP-8391 ..... N88-24653 #

BIO-1 ..... N88-25134* #

BLL-M-37776-(5828.4) ..... N88-25015 #

BNL-40685 ..... N88-24715 #
BNL-40784 ..... N88-25278 #
BNL-40839 ..... N88-24982 #
BNL-40844 ..... N88-24956 #
BNL-40856 ..... N88-25317 #
BNL-40884 ..... N88-25287 #
BNL-40929 ..... N88-25288 #
BNL-40999 ..... N88-25284 #

BPT-7/87 ..... N88-25063 #

BRL-CR-589 ..... N88-24880 #

BRL-MR-3645 ..... N88-24813 #
BRL-MR-3647 ..... N88-25154 #

BRL-TR-2876 ..... N88-24987 #
BRL-TR-2880 ..... N88-24874 #

B8733273 ..... N88-24734 #
B8733275 ..... N88-24733 #
B8733278 ..... N88-24909 #
B8805668 ..... N88-25240 #
B8805669 ..... N88-25090 #
B8805670 ..... N88-24985 #
B8805671-PT-4 ..... N88-25258 #
B8805672 ..... N88-25241 #
B8805673 ..... N88-25242 #
B8805674 ..... N88-25259 #
B8805675 ..... N88-25243 #
B8805676 ..... N88-25187 #

CAR-87-7 ..... N88-25010* #

CEAT-047426 ..... N88-24703 #

CEBAF-PR-88-005 ..... N88-25291 #

CERL-TR-N-88/04 ..... N88-25263 #

CERT-OA-37/5018-AYD ..... N88-24595 #

CERT-RT-OA-20/5025-AYD ..... N88-24596 #

CERT-5/1333-MO N88-24984

CFDU/87/7 ..... N88-24893 #
CFDU/87/10 ..... N88-25061 #
CFDU/87/11 ..... N88-24725 #
CFDU/88/1 ..... N88-24894 #

CGR/DC-09/87 ..... N88-24618 #

CLASSIC-87-05 ..... N88-25101 #

CMU/SEI-87-TR-43 ..... N88-24647 #

CONF-870552-29 ..... N88-25386 #
CONF-870552-31 ..... N88-25385 #
CONF-870636-15 ..... N88-24986 #
CONF-870860-1 ..... N88-25245 #
CONF-871027-46 ..... N88-24868 #
CONF-871036-34 ..... N88-24748 #
CONF-871062-13 ..... N88-25057 #
CONF-871093-5 ..... N88-24955 #
CONF-871124-94 ..... N88-25348 #
CONF-871234-14 ..... N88-25251 #
CONF-871245-3 ..... N88-25426 #
CONF-871274-1 ..... N88-24681 #
CONF-880110-23 ..... N88-25351 #
CONF-880112-1 ..... N88-24982 #
CONF-880117-2 ..... N88-25208 #
CONF-880117-4 ..... N88-25162 #
CONF-880118-3 ..... N88-24795 #
CONF-880123-1 ..... N88-24912 #
CONF-880161-1 ..... N88-25283 #
CONF-880161-2 ..... N88-25279 #
CONF-880174-1 ..... N88-25362 #
CONF-880206-3 ..... N88-25360 #
CONF-880212-6 ..... N88-25058 #
CONF-880215-3 ..... N88-24804 #
CONF-880244-1 ..... N88-25282 #
CONF-880250-2 ..... N88-24898 #
CONF-880256-1 ..... N88-25278 #
CONF-880256-2 ..... N88-25317 #
CONF-880260-1 ..... N88-25284 #
CONF-880325-1 ..... N88-24867 #
CONF-880358-2 ..... N88-24812 #
CONF-880364-4 ..... N88-25306 #
CONF-880364-5 ..... N88-24926 #
CONF-880364-12 ..... N88-25321 #
CONF-880365-1 ..... N88-24805 #
CONF-880408-1 ..... N88-25330 #
CONF-880408-5 ..... N88-25361 #
CONF-880408-7 ..... N88-25322 #
CONF-880462-4 ..... N88-24945 #
CONF-880462-6 ..... N88-24957 #
CONF-880478-5 ..... N88-24657 #
CONF-880478-6 ..... N88-24658 #
CONF-880516-2 ..... N88-25181 #
CONF-880528-1 ..... N88-25188 #
CONF-880540-1 ..... N88-25194 #
CONF-880547-1 ..... N88-24747 #
CONF-880548-2 ..... N88-24925 #
CONF-880554-1 ..... N88-24865 #
CONF-880564-1 ..... N88-24755 #
CONF-880565-1 ..... N88-24866 #
CONF-880565-2 ..... N88-24858 #
CONF-880567-1 ..... N88-24756 #
CONF-880567-2 ..... N88-25131 #
CONF-880567-3 ..... N88-25195 #
CONF-880569-1 ..... N88-25203 #
CONF-880572-1 ..... N88-25012 #
CONF-880577-2 ..... N88-25161 #
CONF-880579-1 ..... N88-25387 #
CONF-880660-1 ..... N88-24794 #
CONF-880661-4 ..... N88-25189 #
CONF-880671-1 ..... N88-24706 #
CONF-880685-1 ..... N88-24974 #
CONF-880690-1 ..... N88-24806 #
CONF-880802-6 ..... N88-24800 #
CONF-880841-2 ..... N88-24646 #
CONF-8703156-2 ..... N88-25166 #
CONF-8705212 ..... N88-25041 #
CONF-8705261-1 ..... N88-24715 #
CONF-8706125-27 ..... N88-25359 #
CONF-8707106-5-DRAFT ..... N88-25316 #
CONF-8707141-5 ..... N88-25349 #
CONF-8708110-33-REV-1 ..... N88-24961 #
CONF-8708213-4 ..... N88-24709 #
CONF-8708224-1 ..... N88-25132 #
CONF-8708225-1 ..... N88-24981 #
CONF-8708230-1 ..... N88-25366 #
CONF-8709110-20 ..... N88-24956 #
CONF-8709110-22 ..... N88-24960 #
CONF-8709217-4 ..... N88-25157 #
CONF-8709252-1 ..... N88-25287 #
CONF-8711165-1 ..... N88-24859 #

CPR-93-13-203.00 ..... N88-24707 #

CRDEC-CR-88009 ..... N88-24724 #
CRDEC-CR-88020 ..... N88-24625 #
CRDEC-CR-88038 ..... N88-25177 #

CRDEC-SP-88007 ..... N88-24978 #

CRREL-SR-88-1 ..... N88-25018 #

CSDL-T-977 ..... N88-24668* #
CSDL-T-986 ..... N88-24654* #

CSIR-RR-630-PT-6 ..... N88-25137

CT-3 ..... N88-24849 #

CWI-AM-R8709 ..... N88-25240 #
CWI-AM-R8710 ..... N88-25090 #
CWI-AM-R8801 ..... N88-24985 #
CWI-AM-R8802-PT-4 ..... N88-25258 #
CWI-AM-R8803 ..... N88-25241 #

CWI-NM-R8722 ..... N88-25242 #
CWI-NM-R8723 ..... N88-25259 #
CWI-NM-R8724 ..... N88-25243 #
CWI-NM-R8725 ..... N88-25187 #

DEL-SG-02-88 ..... N88-25126 #

DERAT-37/5018-DY ..... N88-24595 #

DE87-709038 ..... N88-25363 #
DE88-000500 ..... N88-25188 #
DE88-000522 ..... N88-25181 #
DE88-001034 ..... N88-25054 #
DE88-001052 ..... N88-25023 #
DE88-001137 ..... N88-25055 #
DE88-001143 ..... N88-25056 #
DE88-001218 ..... N88-24735 #
DE88-002802 ..... N88-25194 #
DE88-003404 ..... N88-25245 #
DE88-004330 ..... N88-24747 #
DE88-004422 ..... N88-25316 #
DE88-004572 ..... N88-25348 #
DE88-005306 ..... N88-24794 #
DE88-005533 ..... N88-24865 #
DE88-005618 ..... N88-24755 #
DE88-005683 ..... N88-25057 #
DE88-006073 ..... N88-25349 #
DE88-006173 ..... N88-25282 #
DE88-006176 ..... N88-25166 #
DE88-006184 ..... N88-25203 #
DE88-006185 ..... N88-25157 #
DE88-006188 ..... N88-24708 #
DE88-006272 ..... N88-24866 #
DE88-006273 ..... N88-24858 #
DE88-006328 ..... N88-25350 #
DE88-006386 ..... N88-24905 #
DE88-006408 ..... N88-24756 #
DE88-006420 ..... N88-25283 #
DE88-006456 ..... N88-24925 #
DE88-006464 ..... N88-24912 #
DE88-006465 ..... N88-25131 #
DE88-006476 ..... N88-24955 #
DE88-006512 ..... N88-24977 #
DE88-006613 ..... N88-25078 #
DE88-006653 ..... N88-24981 #
DE88-006667 ..... N88-24804 #
DE88-006674 ..... N88-25132 #
DE88-006679 ..... N88-24714 #
DE88-006683 ..... N88-25271 #
DE88-006715 ..... N88-25251 #
DE88-006717 ..... N88-24966 #
DE88-006730 ..... N88-25041 #
DE88-006734 ..... N88-24812 #
DE88-006735 ..... N88-24859 #
DE88-006773 ..... N88-24709 #
DE88-006785 ..... N88-24974 #
DE88-006797 ..... N88-24681 #
DE88-006811 ..... N88-25351 #
DE88-006823 ..... N88-24867 #
DE88-006824 ..... N88-25012 #
DE88-006828 ..... N88-25330 #
DE88-006830 ..... N88-25426 #
DE88-006863 ..... N88-24800 #
DE88-006871 ..... N88-24947 #
DE88-006886 ..... N88-25331 #
DE88-006981 ..... N88-25208 #
DE88-007017 ..... N88-24960 #
DE88-007019 ..... N88-25195 #
DE88-007023 ..... N88-24961 #
DE88-007032 ..... N88-24715 #
DE88-007038 ..... N88-24898 #
DE88-007042 ..... N88-25287 #
DE88-007046 ..... N88-25317 #
DE88-007048 ..... N88-24982 #
DE88-007049 ..... N88-25276 #
DE88-007050 ..... N88-24956 #
DE88-007063 ..... N88-25332 #
DE88-007074 ..... N88-24748 #
DE88-007075 ..... N88-25058 #
DE88-007094 ..... N88-25318 #
DE88-007107 ..... N88-25272 #
DE88-007109 ..... N88-24868 #
DE88-007120 ..... N88-25182 #
DE88-007124 ..... N88-25290 #
DE88-007159 ..... N88-24913 #
DE88-007169 ..... N88-24664 #

DE88-007175 ..... N88-24646 #
DE88-007200 ..... N88-24657 #
DE88-007201 ..... N88-24805 #
DE88-007206 ..... N88-24795 #
DE88-007212 ..... N88-24806 #
DE88-007265 ..... N88-25365 #
DE88-007268 ..... N88-25366 #
DE88-007269 ..... N88-25359 #
DE88-007279 ..... N88-25308 #
DE88-007283 ..... N88-24926 #
DE88-007313 ..... N88-24757 #
DE88-007327 ..... N88-25319 #
DE88-007349 ..... N88-24736 #
DE88-007374 ..... N88-25366 #
DE88-007392 ..... N88-25288 #
DE88-007397 ..... N88-25279 #
DE88-007415 ..... N88-24737 #
DE88-007419 ..... N88-24658 #
DE88-007436 ..... N88-24796 #
DE88-007472 ..... N88-25162 #
DE88-007485 ..... N88-25360 #
DE88-007489 ..... N88-25273 #
DE88-007492 ..... N88-24906 #
DE88-007510 ..... N88-25274 #
DE88-007535 ..... N88-25102 #
DE88-007562 ..... N88-25320 #
DE88-007581 ..... N88-25189 #
DE88-007587 ..... N88-25161 #
DE88-007603 ..... N88-25361 #
DE88-007604 ..... N88-24945 #
DE88-007605 ..... N88-25387 #
DE88-007666 ..... N88-25284 #
DE88-007681 ..... N88-25321 #
DE88-007822 ..... N88-25322 #
DE88-007843 ..... N88-24789 #
DE88-007849 ..... N88-24860 #
DE88-007873 ..... N88-24790 #
DE88-007911 ..... N88-24957 #
DE88-008220 ..... N88-25362 #
DE88-701478 ..... N88-25262 #
DE88-701496 ..... N88-25326 #
DE88-701587 ..... N88-25292 #
DE88-702127 ..... N88-25306 #
DE88-752551 ..... N88-25367 #

DFVLR-MITT-87-21 ..... N88-24928 #

DIA-DST-2700Z-007-87 ..... N88-24950 #

DISCUSSION PAPER-861 ..... N88-25178 #

DODA-AR-004-588 ..... N88-25209 #

DOE/ER-04215/T4 ..... N88-25271 #
DOE/ER-05015/T5 ..... N88-24796 #
DOE/ER-10381/9 ..... N88-24714 #
DOE/ER-10663/T3 ..... N88-25274 #
DOE/ER-13320/1 ..... N88-25078 #
DOE/ER-13398/8 ..... N88-24905 #
DOE/ER-13442/T1 ..... N88-25272 #
DOE/ER-13735/1 ..... N88-25318 #
DOE/ER-40216/5 ..... N88-25290 #
DOE/ER-45127/3 ..... N88-25331 #
DOE/ER-45266/1 ..... N88-25332 #
DOE/ER-53245/1 ..... N88-25320 #

DOE/ET-53088/316 ..... N88-25319 #

DOE/MC-21181/1950-VOL-11 ..... N88-25023 #
DOE/MC-23267/2537 ..... N88-25054 #

DOT-TSC-RSPA-88-1 ..... N88-25163 #

DOT-VA846-88-1 ..... N88-25163 #

DOT/FAA/CT-TN87/21 ..... N88-24814 #
DOT/FAA/CT-TN87/36 ..... N88-24813 #
DOT/FAA/CT-TN87/39 ..... N88-24615 #
DOT/FAA/CT-TN87/49 ..... N88-24616 #

DOT/FAA/CT-87/18 ..... N88-24799 #
DOT/FAA/CT-87/18 ..... N88-24807 #
DOT/FAA/CT-87/34 ..... N88-24622 #
DOT/FAA/CT-88/03 ..... N88-24610 #

DOT/FAA/PM-87/19 ..... N88-24652 #

DREA-TM-87/217 ..... N88-24886 #

DRI-3-88 ..... N88-25077 #

DTIC/TR-87/4 ..... N88-25382 #
DTIC/TR-88/4 ..... N88-25382 #

DTRC-87/054 ..... N88-24881 #

DTRC/AERO-1302 ..... N88-24881 #

E-3989 ..... N88-24883* #
E-4012 ..... N88-24859* #
E-4049 ..... N88-24975* #
E-4077 ..... N88-24706* #
E-4104 ..... N88-24889* #
E-4106 ..... N88-25239* #
E-4110 ..... N88-24847* #
E-4135 ..... N88-24754* #
E-4143 ..... N88-24640* #
E-4154 ..... N88-24749* #
E-4157 ..... N88-24811* #
E-4166 ..... N88-24870* #
E-4172 ..... N88-24917* #
E-4176 ..... N88-24639* #
E-4179 ..... N88-24882* #
E-4186 ..... N88-24712* #
E-4192 ..... N88-24968* #
E-4198 ..... N88-24641* #
E-4204 ..... N88-24690* #
E-4206 ..... N88-24686* #
E-4211 ..... N88-24592* #
E-4216 ..... N88-25059* #
E-4228 ..... N88-24688* #
E-4230 ..... N88-24687* #
E-4234 ..... N88-24597* #
E-4240 ..... N88-24642* #
E-4242 ..... N88-24808* #
E-4245 ..... N88-25260* #

EEI-87-172 ..... N88-25415* #
EEI-88-183 ..... N88-25414* #

EGG-M-02187 ..... N88-24709 #
EGG-M-12287 ..... N88-24859 #
EGG-M-12487 ..... N88-24812 #
EGG-M-31686 ..... N88-24966 #
EGG-M-33687 ..... N88-25251 #
EGG-M-41087 ..... N88-24681 #

ENST-87E022 ..... N88-25180 #

EO/MO-12 ..... N88-25293 #

EOTR-88-1 ..... N88-24648 #

EPA/600/D-88/067 ..... N88-25076 #

ESA-CR(P)-2486-VOL-1 ..... N88-24841 #
ESA-CR(P)-2486-VOL-2 ..... N88-24842 #
ESA-CR(P)-2507 ..... N88-24653 #

ESA-STM-239 ..... N88-24670 #

ESD-TR-87-206 ..... N88-24647 #

ESL-TR-716148-29 ..... N88-25300* #

ESL-717220-7 ..... N88-24833 #
ESL-718048-4 ..... N88-24832 #
ESL-718048-7 ..... N88-25175 #
ESL-718109-2 ..... N88-24853 #

ESSRL-88-1 ..... N88-24826 #

ETN-88-91883 ..... N88-25179 #
ETN-88-91884 ..... N88-24839 #
ETN-88-91927 ..... N88-24892 #
ETN-88-91928 ..... N88-24891 #
ETN-88-91932 ..... N88-25052 #
ETN-88-91933 ..... N88-24663 #
ETN-88-91934 ..... N88-25008 #
ETN-88-91939 ..... N88-24810 #
ETN-88-91942 ..... N88-25009 #
ETN-88-91944 ..... N88-24651 #
ETN-88-91946 ..... N88-25127 #
ETN-88-91948 ..... N88-25186 #
ETN-88-91951 ..... N88-24959 #
ETN-88-91952 ..... N88-25068
ETN-88-91995 ..... N88-25130 #
ETN-88-91996 ..... N88-24593 #
ETN-88-92084 ..... N88-24940 #
ETN-88-92143 ..... N88-24792 #
ETN-88-92146 ..... N88-24793 #
ETN-88-92148 ..... N88-24750 #
ETN-88-92149 ..... N88-24751 #
ETN-88-92150 ..... N88-25069 #
ETN-88-92151 ..... N88-24594 #
ETN-88-92152 ..... N88-24707 #
ETN-88-92153 ..... N88-24907 #
ETN-88-92154 ..... N88-25104 #
ETN-88-92156 ..... N88-24908 #
ETN-88-92158 ..... N88-24752 #
ETN-88-92163 ..... N88-24595 #
ETN-88-92165 ..... N88-24984

ETN-88-92181 ..... N88-25180 #
ETN-88-92189 ..... N88-25201 #
ETN-88-92221 ..... N88-25324 #
ETN-88-92260 ..... N88-25217 #
ETN-88-92262 ..... N88-25218 #
ETN-88-92263 ..... N88-25219 #
ETN-88-92269 ..... N88-25220 #
ETN-88-92290 ..... N88-25202 #
ETN-88-92313 ..... N88-24928 #
ETN-88-92335 ..... N88-24669 #
ETN-88-92337 ..... N88-25063 #
ETN-88-92387 ..... N88-25025 #
ETN-88-92457 ..... N88-24734 #
ETN-88-92458 ..... N88-24733 #
ETN-88-92460 ..... N88-24909 #
ETN-88-92474 ..... N88-25020 #
ETN-88-92481 ..... N88-24650 #
ETN-88-92482 ..... N88-24697 #
ETN-88-92483 ..... N88-25422 #
ETN-88-92485 ..... N88-24726 #
ETN-88-92486 ..... N88-25084 #
ETN-88-92487 ..... N88-24840 #
ETN-88-92488 ..... N88-25299 #
ETN-88-92489 ..... N88-25311 #
ETN-88-92490 ..... N88-25085 #
ETN-88-92491 ..... N88-24585 #
ETN-88-92492 ..... N88-24995 #
ETN-88-92493 ..... N88-24586 #
ETN-88-92494 ..... N88-24996 #
ETN-88-92495 ..... N88-24704 #
ETN-88-92496 ..... N88-24587 #
ETN-88-92497 ..... N88-25409 #
ETN-88-92498 ..... N88-25405 #
ETN-88-92499 ..... N88-25410 #
ETN-88-92500 ..... N88-25411 #
ETN-88-92504 ..... N88-24693 #
ETN-88-92505 ..... N88-25061 #
ETN-88-92506 ..... N88-24725 #
ETN-88-92507 ..... N88-24894 #
ETN-88-92508 ..... N88-24895 #
ETN-88-92521 ..... N88-25257 #
ETN-88-92523 ..... N88-25221 #
ETN-88-92535 ..... N88-25124 #
ETN-88-92536 ..... N88-24787 #
ETN-88-92537 ..... N88-24896 #
ETN-88-92538 ..... N88-24703 #
ETN-88-92539 ..... N88-24788 #
ETN-88-92540 ..... N88-24993 #
ETN-88-92546 ..... N88-24994 #
ETN-88-92547 ..... N88-24596 #
ETN-88-92550 ..... N88-24841 #
ETN-88-92551 ..... N88-24842 #
ETN-88-92552 ..... N88-24653 #
ETN-88-92555 ..... N88-24670 #
ETN-88-92564 ..... N88-25053 #
ETN-88-92565 ..... N88-25074 #
ETN-88-92582 ..... N88-25240 #
ETN-88-92583 ..... N88-25090 #
ETN-88-92584 ..... N88-24985 #
ETN-88-92585 ..... N88-25258 #
ETN-88-92586 ..... N88-25241 #
ETN-88-92593 ..... N88-25242 #
ETN-88-92594 ..... N88-25259 #
ETN-88-92595 ..... N88-25243 #
ETN-88-92596 ..... N88-25187 #

FAA-APO-88-1 ..... N88-24576 #

FASAC-TAR-3120 ..... N88-24730 #

FEDC-R-87-INTOR-1 ..... N88-25316 #

FFA-TN-1986-43 ..... N88-24585 #
FFA-TN-1987-07 ..... N88-24995 #
FFA-TN-1987-65 ..... N88-24586 #
FFA-TN-1987-70 ..... N88-24996 #
FFA-TN-1988-04 ..... N88-24704 #
FFA-TN-1988-08 ..... N88-24587 #

FOA-B-30120-3.2 ..... N88-24821 #

FOA-C-30460-3.3 ..... N88-24840 #
FOA-C-30465-3.3 ..... N88-25179 #
FOA-C-30472-3.3 ..... N88-24839 #
FOA-C-30477-3 ..... N88-25299 #

FSU-TR-M-774 ..... N88-25210 #

FTD-ID(RS)T-1193-87 ..... N88-24575 #
FTD-ID(RS)T-1364-87 ..... N88-24582 #

F0231-FR ..... N88-24627 #

GAO/AFMD-88-21 ..... N88-25373 #

GAO/IMTEC-88-6BR ..... N88-24609 #

GAO/RCED-88-40 ..... N88-25060 #

GC-TR-87-1628-F ..... N88-24803 #

GRI-87/0206 ..... N88-25370 #
GRI-88/0044 ..... N88-24731 #

H-1371 ..... N88-24634* #
H-1493 ..... N88-25207* #
H-1500 ..... N88-24633* #

HDL-TR-140 ..... N88-24583 #
HDL-TR-2137 ..... N88-25345 #

ICASE-88-33 ..... N88-24916* #
ICASE-88-35 ..... N88-25247* #
ICASE-88-38 ..... N88-25246* #
ICASE-88-39 ..... N88-25249* #
ICASE-88-40 ..... N88-24608* #

ICMA-87-113-PT-1 ..... N88-25215 #

IFSR-316 ..... N88-25319 #

IFVE-OEF-87-22 ..... N88-25292 #

ILR-MITT-180 ..... N88-25052 #
ILR-MITT-185 ..... N88-24683 #
ILR-MITT-188 ..... N88-25008 #

INDU/DC/GMH/TR-88-22 ..... N88-25296 #

INIS-MF-11087 ..... N88-25262 #

IOS-253 ..... N88-25124 #

IRF-PREPRINT-100 ..... N88-25311 #
IRF-PREPRINT-101 ..... N88-25085 #

IS-T-1251 ..... N88-24736 #

ISAS-RN-352 ..... N88-25286 #
ISAS-RN-367 ..... N88-25095 #
ISAS-RN-624 ..... N88-24599 #
ISAS-RN-625 ..... N88-24673 #

ISBN-0-7988-3289-4 ..... N88-25137
ISBN-0-86098-799-8 ..... N88-25364 #
ISBN-951-754-284-4 ..... N88-25352 #
ISBN-951-754-312-3 ..... N88-24849 #
ISBN-951-754-344-1 ..... N88-24872 #

ISI/TM-88-197 ..... N88-25200 #

ISSN-0065-3713 ..... N88-24726 #
ISSN-0065-3713 ..... N88-25084 #
ISSN-0065-3713 ..... N88-25422 #
ISSN-0176-0777 ..... N88-25063 #
ISSN-0176-7739 ..... N88-24928 #
ISSN-0284-1711 ..... N88-25311 #
ISSN-0285-6808 ..... N88-24599 #
ISSN-0285-6808 ..... N88-24673 #
ISSN-0341-8561 ..... N88-25127 #
ISSN-0347-3708 ..... N88-24839 #
ISSN-0347-3708 ..... N88-24840 #
ISSN-0347-3708 ..... N88-25179 #
ISSN-0347-3708 ..... N88-25299 #
ISSN-0379-4067 ..... N88-24670 #
ISSN-0436-1199 ..... N88-24891 #
ISSN-0436-1199 ..... N88-24892 #
ISSN-0436-1199 ..... N88-24940 #
ISSN-0469-4236 ..... N88-25025 #
ISSN-0751-1353 ..... N88-25180 #

ISU-ERI-AMES-88405 ..... N88-24911* #

JINR-13-87-312 ..... N88-25306 #
JINR-14-87-353 ..... N88-25326 #

JPL-D-4643 ..... N88-24677 #

K/QT-178 ..... N88-24977 #

L-16205 ..... N88-24823* #
L-16338 ..... N88-25105* #
L-16377 ..... N88-25094* #
L-16384 ..... N88-24580* #

LA-UR-87-3090 ..... N88-25181 #
LA-UR-87-3129 ..... N88-25188 #
LA-UR-87-4072 ..... N88-24953 #
LA-UR-88-409 ..... N88-24955 #
LA-UR-88-450 ..... N88-25131 #
LA-UR-88-506 ..... N88-24912 #
LA-UR-88-599 ..... N88-24925 #
LA-UR-88-629 ..... N88-25349 #

LA-UR-88-669 ..... N88-24957 #
LA-UR-88-1025 ..... N88-25322 #

LA-10958-MS ..... N88-24884 #
LA-11161-MS ..... N88-24913 #
LA-11202-T ..... N88-24737 #
LA-11264-MS ..... N88-24947 #
LA-11276-MS ..... N88-25102 #

LBL-24263 ..... N88-25348 #
LBL-24319 ..... N88-25366 #
LBL-24649 ..... N88-25279 #
LBL-24695 ..... N88-25350 #
LBL-24749 ..... N88-25362 #

LC-74-600126 ..... N88-25428* #
LC-74-600126 ..... N88-25429* #
LC-74-600126 ..... N88-25430* #

LG87ER0083-VOL-1 ..... N88-24739 #

LIDS-TH-1730 ..... N88-25381 #

LIR/03-88/284 ..... N88-25075 #

LMSC-F24660 ..... N88-24743 #

LMSC-HEC-TR-F225755 ..... N88-24899* #

LR-31216 ..... N88-24799 #
LR-31216 ..... N88-24807 #

M-586 ..... N88-25390* #

MDC-H1383 ..... N88-25156* #

MDC-K0534 ..... N88-24876 #

ME-TSPC-TR-88-10 ..... N88-24584 #

MINTEK-M318 ..... N88-25364 #

MIT/LCS/TM-343 ..... N88-25168 #

MMS-1742 ..... N88-25254 #

MP-86-234 ..... N88-25353* #

MPIS-6/1987 ..... N88-24892 #
MPIS-7/1987 ..... N88-24891 #
MPIS-8/1987 ..... N88-24940 #

MSP-87-4 ..... N88-25173 #

MTL-TR-87-2 ..... N88-25342 #

M6-577100 ..... N88-24703 #

NADC-87133-60 ..... N88-24700 #

NAS 1.15:4044 ..... N88-24580* #
NAS 1.15:4048 ..... N88-25424* #
NAS 1.15:88270 ..... N88-24834* #
NAS 1.15:88314 ..... N88-25140* #
NAS 1.15:100053 ..... N88-24900* #
NAS 1.15:100057 ..... N88-25420* #
NAS 1.15:100066 ..... N88-24601* #
NAS 1.15:100079 ..... N88-24600* #
NAS 1.15:100080 ..... N88-24602* #
NAS 1.15:100091 ..... N88-24579* #
NAS 1.15:100332 ..... N88-24672* #
NAS 1.15:100442 ..... N88-25207* #
NAS 1.15:100445 ..... N88-24633* #
NAS 1.15:100541 ..... N88-24607* #
NAS 1.15:100565 ..... N88-25190* #
NAS 1.15:100571 ..... N88-25204* #
NAS 1.15:100575 ..... N88-25184* #
NAS 1.15:100620 ..... N88-25427* #
NAS 1.15:100627 ..... N88-24598* #
NAS 1.15:100629 ..... N88-24713* #
NAS 1.15:100809 ..... N88-24663* #
NAS 1.15:100824 ..... N88-24659* #
NAS 1.15:100875 ..... N88-25239* #
NAS 1.15:100878 ..... N88-24847* #
NAS 1.15:100894 ..... N88-24754* #
NAS 1.15:100896 ..... N88-24640* #
NAS 1.15:100903 ..... N88-24749* #
NAS 1.15:100906 ..... N88-24811* #
NAS 1.15:100907 ..... N88-24766* #
NAS 1.15:100914 ..... N88-24870* #
NAS 1.15:100920 ..... N88-24639* #
NAS 1.15:100923 ..... N88-24712* #
NAS 1.15:100926 ..... N88-24682* #
NAS 1.15:100927 ..... N88-24968* #
NAS 1.15:100929 ..... N88-24641* #
NAS 1.15:100932 ..... N88-24686* #

NAS 1.15:100933 ..... N88-24690* #
NAS 1.15:100934 ..... N88-24592* #
NAS 1.15:100936 ..... N88-25059* #
NAS 1.15:100942 ..... N88-24687* #
NAS 1.15:100945 ..... N88-24597* #
NAS 1.15:100948 ..... N88-24642* #
NAS 1.15:100951 ..... N88-24808* #
NAS 1.15:100954 ..... N88-24688* #
NAS 1.15:100957 ..... N88-24689* #
NAS 1.15:100959 ..... N88-25260* #
NAS 1.15:100982 ..... N88-25133* #
NAS 1.15:100983 ..... N88-25134* #
NAS 1.15:100990 ..... N88-24603* #
NAS 1.15:100992 ..... N88-24946* #
NAS 1.15:101000 ..... N88-25192* #
NAS 1.15:101006 ..... N88-25196* #
NAS 1.15:101139 ..... N88-25419* #
NAS 1.15:101140 ..... N88-25354* #
NAS 1.15:101141 ..... N88-24809* #
NAS 1.15:101144 ..... N88-24791* #
NAS 1.15:101146 ..... N88-25365* #
NAS 1.15:101147 ..... N88-25423* #
NAS 1.15:101149 ..... N88-25323* #
NAS 1.15:101150 ..... N88-25417* #
NAS 1.15:101174 ..... N88-25238* #
NAS 1.15:101178 ..... N88-24844* #
NAS 1.21:4012-VOL-1 ..... N88-25428* #
NAS 1.21:4012-VOL-2 ..... N88-25429* #
NAS 1.21:4012-VOL-3 ..... N88-25430* #
NAS 1.21:7011(312) N88-25141*
NAS 1.21:7037(227) N88-24578*
NAS 1.21:7039(33) N88-25388*
NAS 1.26:3941 ..... N88-25371* #
NAS 1.26:3942 ..... N88-25156* #
NAS 1.26:3943 ..... N88-25372* #
NAS 1.26:4027 ..... N88-24632* #
NAS 1.26:4154 ..... N88-24948* #
NAS 1.26:4155 ..... N88-24975* #
NAS 1.26:4157 ..... N88-25268* #
NAS 1.26:168353 ..... N88-24637* #
NAS 1.26:172048 ..... N88-25414* #
NAS 1.26:172050 ..... N88-25415* #
NAS 1.26:172053 ..... N88-24854* #
NAS 1.26:172057 ..... N88-24868* #
NAS 1.26:178281 ..... N88-25014* #
NAS 1.26:178410 ..... N88-24619* #
NAS 1.26:178411 ..... N88-24911* #
NAS 1.26:179288 ..... N88-24675* #
NAS 1.26:179336 ..... N88-24676* #
NAS 1.26:179338 ..... N88-24899* #
NAS 1.26:179339 ..... N88-24962*
NAS 1.26:179355 ..... N88-25010* #
NAS 1.26:181671 ..... N88-24918* #
NAS 1.26:181673 ..... N88-25247* #
NAS 1.26:181676 ..... N88-25248* #
NAS 1.26:181677 ..... N88-25249* #
NAS 1.26:181679 ..... N88-24606* #
NAS 1.26:182118 ..... N88-25346* #
NAS 1.26:182126 ..... N88-25016* #
NAS 1.26:182137 ..... N88-24997* #
NAS 1.26:182138 ..... N88-24976* #
NAS 1.26:182147 ..... N88-24917* #
NAS 1.26:182680 ..... N88-25244* #
NAS 1.26:182681 ..... N88-24629* #
NAS 1.26:182801 ..... N88-25327* #
NAS 1.26:182807 ..... N88-25150* #
NAS 1.26:182869 ..... N88-24736* #
NAS 1.26:182901 ..... N88-25155* #
NAS 1.26:182907 ..... N88-24746* #
NAS 1.26:182931 ..... N88-25418* #
NAS 1.26:182935 ..... N88-25129* #
NAS 1.26:182938 ..... N88-24861* #
NAS 1.26:182942 ..... N88-25425* #
NAS 1.26:182943 ..... N88-25062* #
NAS 1.26:182944 ..... N88-24983* #
NAS 1.26:182946 ..... N88-25353* #
NAS 1.26:182952 ..... N88-25183* #
NAS 1.26:182973 ..... N88-24591* #
NAS 1.26:182974 ..... N88-25300* #
NAS 1.26:182976 ..... N88-25406* #
NAS 1.26:182979 ..... N88-25024* #
NAS 1.26:182983 ..... N88-25185* #
NAS 1.26:182985 ..... N88-25384* #
NAS 1.26:183021 ..... N88-24630* #
NAS 1.26:183022 ..... N88-24915* #
NAS 1.26:183023 ..... N88-24914* #
NAS 1.26:183024 ..... N88-25092* #
NAS 1.26:183027 ..... N88-25191* #
NAS 1.26:183029 ..... N88-25093* #
NAS 1.26:183031 ..... N88-25206* #
NAS 1.26:183032 ..... N88-24644* #
NAS 1.26:183049 ..... N88-24922* #
NAS 1.26:183051 ..... N88-25408* #
NAS 1.55:2498 ..... N88-25105* #
NAS 1.55:3002 ..... N88-25390* #
NAS 1.60:2776 ..... N88-24623* #

NAS 1.60:2821 ..... N88-25013* #
NAS 1.61:1200 ..... N88-25094* #
NAS 1.71:LAR-13322-1 ..... N88-24620* #
NAS 1.71:LAR-13387-1 ..... N88-25302* #
NAS 1.71:LAR-13678-1 ..... N88-25355* #
NAS 1.71:LAR-13705-1 ..... N88-25011* #
NAS 1.71:LAR-13729-1 ..... N88-24970* #
NAS 1.71:LAR-13747-1 ..... N88-24845* #
NAS 1.71:LAR-13773-1 ..... N88-24685* #
NAS 1.71:LAR-13794-1 ..... N88-24942* #
NAS 1.71:LAR-13814-1 ..... N88-24816* #
NAS 1.71:LAR-13854-1-CU ..... N88-24821* #
NAS 1.71:LAR-13924-1-CU ..... N88-24753* #
NAS 1.71:LAR-13952-1-SB ..... N88-24910* #
NAS 1.71:LAR-13983-1 ..... N88-24628* #
NAS 1.71:MFS-28182-1 ..... N88-25357* #
NAS 1.71:MFS-28206-1-SB ..... N88-25356* #
NAS 1.71:MFS-28248-1 ..... N88-24817* #
NAS 1.71:MFS-28253-1 ..... N88-24971* #
NAS 1.71:MFS-29260-1 ..... N88-24972* #
NAS 1.71:MFS-29348-1 ..... N88-25303* #
NAS 1.71:MSC-21094-1 ..... N88-24941* #
NAS 1.71:MSC-21170-1 ..... N88-24662* #
NAS 1.71:MSC-21299-1 ..... N88-24684* #
NAS 1.71:MSC-21330-1 ..... N88-24660* #
NAS 1.71:MSC-21354-1 ..... N88-24969* #
NAS 1.71:MSC-21356-1 ..... N88-24671* #
NAS 1.71:NPO-15609-2 ..... N88-24815* #
NAS 1.71:NPO-16789-1-CU ..... N88-25281* #
NAS 1.71:NPO-16882-1-CU ..... N88-24863* #
NAS 1.71:NPO-16985-1-CU ..... N88-24814* #
NAS 1.71:NPO-17024-1-CU ..... N88-24943* #
NAS 1.71:NPO-17134-1-CU ..... N88-24864* #
NAS 1.71:NPO-17139-1-CU ..... N88-25301* #
NAS 1.71:NPO-17144-1-CU ..... N88-25305* #
NAS 1.71:NPO-17207-1-CU ..... N88-25304* #
NAS 1.71:NPO-17259-1-CU ..... N88-25358* #
NAS 1.71:NPO-17278-1-CU ..... N88-24818* #
NAS 1.71:NPO-17325-1-CU ..... N88-24846* #
NAS 1.71:NPO-17354-1-CU ..... N88-24973* #
NAS 1.71:NPO-17390-1-CU ..... N88-24944* #
NAS 1.77:20163 ..... N88-24760* #
NAS 1.77:20166 ..... N88-24763* #
NAS 1.77:20168 ..... N88-24758* #
NAS 1.77:20169 ..... N88-24764* #
NAS 1.77:20170 ..... N88-24782* #
NAS 1.77:20174 ..... N88-24765* #
NAS 1.77:20178 ..... N88-24761* #
NAS 1.77:20183 ..... N88-24869* #
NAS 1.77:20184 ..... N88-24759* #
NAS 1.77:20188 ..... N88-24710* #
NAS 1.77:20189 ..... N88-24798* #
NAS 1.77:20194 ..... N88-25285* #
NAS 1.77:20195 ..... N88-25205* #
NAS 1.77:20256 ..... N88-24797* #

NASA-CASE-ARC-11428-3 ..... N88-24692*

NASA-CASE-LAR-13322-1 ..... N88-24620* #
NASA-CASE-LAR-13387-1 ..... N88-25302* #
NASA-CASE-LAR-13678-1 ..... N88-25355* #
NASA-CASE-LAR-13705-1 ..... N88-25011* #
NASA-CASE-LAR-13729-1 ..... N88-24970* #
NASA-CASE-LAR-13747-1 ..... N88-24845* #
NASA-CASE-LAR-13773-1 ..... N88-24685* #
NASA-CASE-LAR-13794-1 ..... N88-24942* #
NASA-CASE-LAR-13814-1 ..... N88-24816* #
NASA-CASE-LAR-13854-1-CU ..... N88-24821* #
NASA-CASE-LAR-13924-1-CU ..... N88-24753* #
NASA-CASE-LAR-13952-1-SB ..... N88-24910* #
NASA-CASE-LAR-13983-1 ..... N88-24628* #

NASA-CASE-MFS-28182-1 ..... N88-25357* #
NASA-CASE-MFS-28206-1-SB ..... N88-25356* #
NASA-CASE-MFS-28248-1 ..... N88-24817* #
NASA-CASE-MFS-28253-1 ..... N88-24971* #
NASA-CASE-MFS-29260-1 ..... N88-24972* #
NASA-CASE-MFS-29348-1 ..... N88-25303* #

NASA-CASE-MSC-20549-2 ..... N88-24927*
NASA-CASE-MSC-20867-1 ..... N88-24958*
NASA-CASE-MSC-21094-1 ..... N88-24941* #
NASA-CASE-MSC-21170-1 ..... N88-24662* #
NASA-CASE-MSC-21299-1 ..... N88-24684* #
NASA-CASE-MSC-21330-1 ..... N88-24660* #
NASA-CASE-MSC-21354-1 ..... N88-24969* #
NASA-CASE-MSC-21356-1 ..... N88-24671* #

NASA-CASE-NPO-15609-2 ..... N88-24815* #
NASA-CASE-NPO-16402-2 ..... N88-24862*
NASA-CASE-NPO-16789-1-CU ..... N88-25281* #
NASA-CASE-NPO-16882-1-CU ..... N88-24863* #
NASA-CASE-NPO-16907-1-CU N88-24732*
NASA-CASE-NPO-16985-1-CU ..... N88-24814* #
NASA-CASE-NPO-17024-1-CU ..... N88-24943* #
NASA-CASE-NPO-17134-1-CU ..... N88-24864* #

NASA-CASE-NPO-17139-1-CU N88-25301* #
NASA-CASE-NPO-17144-1-CU N88-25305* #
NASA-CASE-NPO-17207-1-CU N88-25304* #
NASA-CASE-NPO-17259-1-CU N88-25358* #
NASA-CASE-NPO-17278-1-CU N88-24818* #
NASA-CASE-NPO-17325-1-CU N88-24846* #
NASA-CASE-NPO-17354-1-CU N88-24973* #
NASA-CASE-NPO-17390-1-CU N88-24944* #

NASA-CP-2498 N88-25105* #
NASA-CP-3002 N88-25390* #

NASA-CR-3941 N88-25371* #
NASA-CR-3942 N88-25156* #
NASA-CR-3943 N88-25372* #
NASA-CR-4027 N88-24632* #
NASA-CR-4154 N88-24948* #
NASA-CR-4155 N88-24975* #
NASA-CR-4157 N88-25268* #
NASA-CR-168353 N88-24637* #
NASA-CR-172048 N88-25414* #
NASA-CR-172050 N88-25415* #
NASA-CR-172053 N88-24654* #
NASA-CR-172057 N88-24668* #
NASA-CR-178281 N88-25014* #
NASA-CR-178410 N88-24619* #
NASA-CR-178411 N88-24911* #
NASA-CR-179288 N88-24675* #
NASA-CR-179336 N88-24876* #
NASA-CR-179338 N88-24899* #
NASA-CR-179339 N88-24962*
NASA-CR-179355 N88-25010* #
NASA-CR-181671 N88-24916* #
NASA-CR-181673 N88-25247* #
NASA-CR-181676 N88-25246* #
NASA-CR-181677 N88-25249* #
NASA-CR-181679 N88-24808* #
NASA-CR-182118 N88-25348* #
NASA-CR-182126 N88-25016* #
NASA-CR-182137 N88-24997* #
NASA-CR-182138 N88-24976* #
NASA-CR-182147 N88-24917* #
NASA-CR-182680 N88-25244* #
NASA-CR-182681 N88-24629* #
NASA-CR-182801 N88-25327* #
NASA-CR-182807 N88-25150* #
NASA-CR-182869 N88-24738* #
NASA-CR-182901 N88-25155* #
NASA-CR-182907 N88-24746* #
NASA-CR-182931 N88-25418* #
NASA-CR-182935 N88-25129* #
NASA-CR-182938 N88-24861* #
NASA-CR-182942 N88-25425* #
NASA-CR-182943 N88-25062* #
NASA-CR-182944 N88-24963* #
NASA-CR-182946 N88-25353* #
NASA-CR-182952 N88-25183* #
NASA-CR-182973 N88-24591* #
NASA-CR-182974 N88-25300* #
NASA-CR-182976 N88-25406* #
NASA-CR-182979 N88-25024* #
NASA-CR-182983 N88-25185* #
NASA-CR-182985 N88-25384* #
NASA-CR-183021 N88-24830* #
NASA-CR-183022 N88-24915* #
NASA-CR-183023 N88-24914* #
NASA-CR-183024 N88-25092* #
NASA-CR-183027 N88-25191* #
NASA-CR-183029 N88-25093* #
NASA-CR-183031 N88-25206* #
NASA-CR-183032 N88-24644* #
NASA-CR-183049 N88-24922* #
NASA-CR-183051 N88-25408* #

NASA-RP-1200 N88-25094* #

NASA-SP-4012-VOL-1 N88-25428* #
NASA-SP-4012-VOL-2 N88-25429* #
NASA-SP-4012-VOL-3 N88-25430* #
NASA-SP-7011(312) N88-25141*
NASA-SP-7037(227) N88-24578*
NASA-SP-7039(33) N88-25388*

NASA-TM-4044 N88-24560* #
NASA-TM-4048 N88-25424* #
NASA-TM-88270 N88-24634* #
NASA-TM-88314 N88-25140* #
NASA-TM-100053 N88-24900* #
NASA-TM-100057 N88-25420* #
NASA-TM-100066 N88-24601* #
NASA-TM-100079 N88-24600* #
NASA-TM-100080 N88-24602* #
NASA-TM-100091 N88-24579* #
NASA-TM-100332 N88-24672* #
NASA-TM-100442 N88-25207* #
NASA-TM-100445 N88-24633* #
NASA-TM-100541 N88-24607* #
NASA-TM-100585 N88-25190* #
NASA-TM-100571 N88-25204* #
NASA-TM-100575 N88-25184* #
NASA-TM-100620 N88-25427* #
NASA-TM-100627 N88-24598* #
NASA-TM-100629 N88-24713* #
NASA-TM-100800 N88-24863* #
NASA-TM-100824 N88-24659* #
NASA-TM-100875 N88-25239* #
NASA-TM-100876 N88-24847* #
NASA-TM-100894 N88-24754* #
NASA-TM-100896 N88-24640* #
NASA-TM-100903 N88-24749* #
NASA-TM-100906 N88-24811* #
NASA-TM-100907 N88-24766* #
NASA-TM-100914 N88-24870* #
NASA-TM-100920 N88-24839* #
NASA-TM-100923 N88-24712* #
NASA-TM-100926 N88-24682* #
NASA-TM-100927 N88-24966* #
NASA-TM-100929 N88-24641* #
NASA-TM-100932 N88-24686* #
NASA-TM-100933 N88-24690* #
NASA-TM-100934 N88-24592* #
NASA-TM-100936 N88-25059* #
NASA-TM-100942 N88-24687* #
NASA-TM-100945 N88-24597* #
NASA-TM-100948 N88-24642* #
NASA-TM-100951 N88-24808* #
NASA-TM-100954 N88-24688* #
NASA-TM-100957 N88-24689* #
NASA-TM-100959 N88-25260* #
NASA-TM-100962 N88-25133* #
NASA-TM-100963 N88-25134* #
NASA-TM-100990 N88-24603* #
NASA-TM-100992 N88-24946* #
NASA-TM-101000 N88-25192* #
NASA-TM-101008 N88-25196* #
NASA-TM-101139 N88-25419* #
NASA-TM-101140 N88-25354* #
NASA-TM-101141 N88-24809* #
NASA-TM-101144 N88-24791* #
NASA-TM-101146 N88-25365* #
NASA-TM-101147 N88-25423* #
NASA-TM-101149 N88-25323* #
NASA-TM-101150 N88-25417* #
NASA-TM-101174 N88-25238* #
NASA-TM-101178 N88-24844* #

NASA-TP-2776 N88-24623* #
NASA-TP-2921 N88-25013* #

NASA-TT-20163 N88-24760* #
NASA-TT-20166 N88-24763* #
NASA-TT-20168 N88-24758* #
NASA-TT-20169 N88-24764* #
NASA-TT-20170 N88-24762* #
NASA-TT-20174 N88-24765* #
NASA-TT-20178 N88-24761* #
NASA-TT-20183 N88-24869* #
NASA-TT-20184 N88-24759* #
NASA-TT-20188 N88-24710* #
NASA-TT-20189 N88-24798* #
NASA-TT-20194 N88-25285* #
NASA-TT-20195 N88-25205* #
NASA-TT-20256 N88-24797* #

NATC-TM-87-171-SA N88-24626 #

NATICK-TR-88/010 N88-24767 #

NATICK/TR-88/002 N88-25151 #

NBS/GCR-88/541 N88-24873 #

NCAR/TN-298-STR N88-25096 #
NCAR/TN-304-STR N88-25096 #

NIKHEF-H-87/17 N88-25280 #

NIPER-301 N88-24735 #

NOAA-TM-NWSTM-PR-33 N88-25119 #

NOO-TN-8222-02-87 N88-25080 #

NPS69-88-001 N88-24678 #

NRL-MR-6143 N88-24829 #
NRL-MR-6174 N88-25277 #

NRL-9056 N88-25198 #

NTSB/AAR-88/02/SUM N88-24612 #

ONERA-RF-45/7131-PY N88-24727

ONERA-RT-4/3346-M N88-24792 #

ONERA-RTS-33/7169-RY-064-R N88-24994 #

ORNL/SUB-81-95011/4 N88-24860 #
ORNL/SUB-85-27494/1 N88-24789 #

ORNL/TM-10606 N88-24790 #
ORNL/TM-10704 N88-24731 #

PB88-121900 N88-24727
PB88-124706 N88-24998
PB88-124714 N88-24705
PB88-124854 N88-[illegible]37
PB88-155262 N88-25364 #
PB88-165501 N88-25389 #
PB88-167275 N88-25060 #
PB88-167739 N88-24820 #
PB88-169073 N88-25096 #
PB88-169818 N88-24609 #
PB88-171921 N88-24849 #
PB88-172523 N88-25373 #
PB88-172721 N88-24821 #
PB88-173513 N88-25250 #
PB88-173869 N88-25097 #
PB88-178157 N88-25096 #
PB88-180302 N88-25075 #
PB88-180948 N88-25280 #
PB88-181110 N88-25225 #
PB88-181466 N88-24872 #
PB88-181953 N88-24873 #
PB88-182324 N88-24730 #
PB88-183066 N88-25163 #
PB88-185364 N88-25126 #
PB88-186325 N88-24574 #
PB88-186432 N88-25352 #
PB88-188081 N88-25119 #
PB88-188891 N88-24731 #
PB88-188958 N88-25261 #
PB88-195219 N88-25078 #
PB88-196365 N88-25370 #
PB88-910407 N88-24612 #

PDR/CFDU-IC/36 N88-24895 #

PME-FM-88-1 N88-24888 #

PML-1986-C105 N88-24734 #
PML-1987-C18 N88-24733 #
PML-1987-C31 N88-24909 #

PNL-SA-15049 N88-25351 #
PNL-SA-15072 N88-24795 #
PNL-SA-15101 N88-25057 #
PNL-SA-15177 N88-24748 #
PNL-SA-15449 N88-25058 #
PNL-SA-15482 N88-25041 #
PNL-SA-15622 N88-24804 #
PNL-SA-15670 N88-24961 #

PR-13 N88-24914* #
PR-18 N88-24915* #

PROCES-VERBAL-47/363/F N88-24705

PW/GPD-FR-19875 N88-24775 #

R-2119 N88-25121 #

RADC-TR-87-166-VOL-2 N88-24850 #
RADC-TR-88-33 N88-24717 #

RCA-PRRL-87-CR-3B N88-24948* #

REPT-7 N88-24988 #
REPT-11 N88-25088
REPT-22 N88-24767 #
REPT-47-632/F N88-24793 #
REPT-48-441/F N88-24752 #
REPT-48-442/F N88-24751 #
REPT-48-451/F N88-24750 #
REPT-87-01 N88-25211 #
REPT-87-11 N88-24593 #
REPT-162 N88-25127 #
REPT-331 N88-25250 #
REPT-1988-02 N88-25261 #

RPI-TR-87-33 N88-25169 #

RR-152 N88-24820 #
RR-322 N88-25257 #
RR-323 N88-25221 #
RR-838-M N88-25217 #
RR-852-M N88-25218 #

RR-655-M ..... N88-25219 #
RR-669-M ..... N88-25220 #

RRK-88-38 ..... N88-25363 #
RRK-87-26 ..... N88-25367 #

RTR-056-07 ..... N88-24676* #

RU-TR-171-MAE-F ..... N88-24882 #

R87-900063-F ..... N88-24675* #
R8801 ..... N88-24619* #

SAIC-87/1722 ..... N88-25123 #
SAIC-87/1868 ..... N88-25122 #

SAND-87-1136C ..... N88-24868 #
SAND-87-2067C ..... N88-24806 #
SAND-87-2314C ..... N88-24657 #
SAND-87-2509C ..... N88-24794 #
SAND-87-2552C ..... N88-25189 #
SAND-87-2768C ..... N88-24865 #
SAND-87-2862C ..... N88-25387 #
SAND-87-3136C ..... N88-24926 #
SAND-87-7172C ..... N88-24858 #
SAND-87-7173C ..... N88-24866 #
SAND-88-0033C ..... N88-25361 #
SAND-88-0047C ..... N88-25330 #
SAND-88-0276C ..... N88-24867 #
SAND-88-0426C ..... N88-25308 #
SAND-88-0542C ..... N88-24898 #
SAND-88-0612C ..... N88-25012 #
SAND-88-0622C ..... N88-25161 #
SAND-88-0669C ..... N88-24945 #
SAND-88-0765C ..... N88-24805 #
SAND-88-0843C ..... N88-24658 #
SAND-88-8600 ..... N88-24800 #

SAPR-3 ..... N88-24826 #

SC5502.AR ..... N88-25295 #
SC5508-APR ..... N88-24786 #

SD-TR-88-08 ..... N88-25083 #
SD-TR-88-22 ..... N88-24855 #
SD-TR-88-35 ..... N88-24680 #

SER-C-PREPUBL-FASC-15 ..... N88-25409 #
SER-C-PREPUBL-FASC-17 ..... N88-25411 #
SER-C-PREPUBL-FASC-18-PT-3 ..... N88-25405 #
SER-C-PREPUBL-FASC-19 ..... N88-25410 #

SERI/PR-215-3297 ..... N88-25056 #

SERI/STR-217-3309 ..... N88-25055 #

SFCC-39 ..... N88-24734 #
SFCC-42 ..... N88-24733 #
SFCC-44 ..... N88-24909 #

SNPE-NT-10/86/CRB/NP ..... N88-24707 #

SOL-88-5 ..... N88-25182 #

SYRU/DECE/TR-87/4 ..... N88-24828 #

TACOM-TR-13301 ..... N88-24964 #

TKK-F-A618 ..... N88-25352 #

TM-88-12 ..... N88-24885 #

TR-D-100-ARO ..... N88-25210 #

TR-4 ..... N88-24769 #
TR-8 ..... N88-24723 #
TR-13 ..... N88-24785 #
TR-227 ..... N88-25213 #
TR-296 ..... N88-25253 #
TR-0086(6909-05)-1 ..... N88-24855 #
TR-0086A(2935-08)-1 ..... N88-24680 #
TR-0086A(2940-05)-1 ..... N88-25083 #

TTC-87-07R ..... N88-24975* #

UCID-20297-87-3 ..... N88-24906 #

UCRL-53852 ..... N88-25273 #
UCRL-95880-REV-1 ..... N88-24961 #
UCRL-98000 ..... N88-24755 #
UCRL-98103 ..... N88-24960 #
UCRL-98211 ..... N88-25195 #
UCRL-98226 ..... N88-24658 #
UCRL-98253 ..... N88-25426 #

UCSD-88-5205 ..... N88-25185* #

UDR-TR-87-150 ..... N88-24887 #

UNC/OR/TR-87-6 ..... N88-24979 #

US-PATENT APPL-SN-190185 ..... N88-25304* #

US-PATENT-APPL-SN-013803 ..... N88-24882*
US-PATENT-APPL-SN-045743 ..... N88-24927*
US-PATENT-APPL-SN-045984 ..... N88-24958*
US-PATENT-APPL-SN-151678 ..... N88-24816* #
US-PATENT-APPL-SN-154711 ..... N88-24863* #
US-PATENT-APPL-SN-154712 ..... N88-24969* #
US-PATENT-APPL-SN-154713 ..... N88-25281* #
US-PATENT-APPL-SN-154716 ..... N88-25302* #
US-PATENT-APPL-SN-154718 ..... N88-25301* #
US-PATENT-APPL-SN-156059 ..... N88-24972* #
US-PATENT-APPL-SN-156393 ..... N88-24941* #
US-PATENT-APPL-SN-156518 ..... N88-25303* #
US-PATENT-APPL-SN-159613 ..... N88-24943* #
US-PATENT-APPL-SN-161681 ..... N88-25357* #
US-PATENT-APPL-SN-165943 ..... N88-24971* #
US-PATENT-APPL-SN-165946 ..... N88-24685* #
US-PATENT-APPL-SN-165956 ..... N88-24671* #
US-PATENT-APPL-SN-168065 ..... N88-24942* #
US-PATENT-APPL-SN-172100 ..... N88-24818* #
US-PATENT-APPL-SN-172101 ..... N88-25356* #
US-PATENT-APPL-SN-172102 ..... N88-24753* #
US-PATENT-APPL-SN-172105 ..... N88-24864* #
US-PATENT-APPL-SN-176544 ..... N88-24970* #
US-PATENT-APPL-SN-176545 ..... N88-24817* #
US-PATENT-APPL-SN-176547 ..... N88-25355* #
US-PATENT-APPL-SN-176587 ..... N88-24684* #
US-PATENT-APPL-SN-182000 ..... N88-24660* #
US-PATENT-APPL-SN-182266 ..... N88-24662* #
US-PATENT-APPL-SN-184234 ..... N88-25358* #
US-PATENT-APPL-SN-184235 ..... N88-24846* #
US-PATENT-APPL-SN-184236 ..... N88-24973* #
US-PATENT-APPL-SN-187716 ..... N88-25305* #
US-PATENT-APPL-SN-192562 ..... N88-24621* #
US-PATENT-APPL-SN-192563 ..... N88-24628* #
US-PATENT-APPL-SN-195221 ..... N88-24820* #
US-PATENT-APPL-SN-195222 ..... N88-24814* #
US-PATENT-APPL-SN-197191 ..... N88-24845* #
US-PATENT-APPL-SN-203177 ..... N88-25011* #
US-PATENT-APPL-SN-203178 ..... N88-24910* #
US-PATENT-APPL-SN-205899 ..... N88-24944* #
US-PATENT-APPL-SN-599126 ..... N88-24692*
US-PATENT-APPL-SN-727931 ..... N88-24862*
US-PATENT-APPL-SN-760374 ..... N88-24692*
US-PATENT-APPL-SN-761310 ..... N88-24815* #
US-PATENT-APPL-SN-790596 ..... N88-24927*
US-PATENT-APPL-SN-924467 ..... N88-24692*
US-PATENT-APPL-SN-930217 ..... N88-24732*

US-PATENT-CLASS-72-750 ..... N88-24927*
US-PATENT-CLASS-204-157.22 ..... N88-24732*
US-PATENT-CLASS-250-423-P N88-24732*
US-PATENT-CLASS-250-427 ..... N88-24732*
US-PATENT-CLASS-254-93-H N88-24927*
US-PATENT-CLASS-254-93-R N88-24927*
US-PATENT-CLASS-269-147 ..... N88-24927*
US-PATENT-CLASS-269-246 ..... N88-24927*
US-PATENT-CLASS-307-106 ..... N88-24862*
US-PATENT-CLASS-315-172 ..... N88-24862*
US-PATENT-CLASS-315-173 ..... N88-24862*
US-PATENT-CLASS-328-67 ..... N88-24862*
US-PATENT-CLASS-356-1 ..... N88-24958*
US-PATENT-CLASS-356-4 ..... N88-24958*
US-PATENT-CLASS-356-376 ..... N88-24958*
US-PATENT-CLASS-358-107 ..... N88-24958*
US-PATENT-CLASS-364-561 ..... N88-24958*
US-PATENT-CLASS-558-80 ..... N88-24692*
US-PATENT-CLASS-564-13 ..... N88-24692*

US-PATENT-4,550,177 ..... N88-24692*
US-PATENT-4,634,759 ..... N88-24692*
US-PATENT-4,698,518 ..... N88-24862*
US-PATENT-4,704,197 ..... N88-24732*
US-PATENT-4,736,247 ..... N88-24958*
US-PATENT-4,736,927 ..... N88-24927*
US-PATENT-4,748,263 ..... N88-24692*

USAARL-87-8 ..... N88-24635 #
USAARL-87-14 ..... N88-25153 #

USAAVSCOM-TM-87-D-3 ..... N88-24611 #

USAAVSCOM-TR-88-A-001 ..... N88-24601* #

USAFSAM-TR-87-30 ..... N88-25128 #

USGC-D-02-88 ..... N88-24618 #

UTRC/R87-957565-1 ..... N88-24992 #

UVA/525418/CHE88/101 ..... N88-24742 #

UVA/528266/MS88/102 ..... N88-24748* #

V-19/86 ..... N88-25009 #

VKI-TN-161 ..... N88-24850 #
VKI-TN-162 ..... N88-24897 #

VPI/HFL-86-1 ..... N88-25159 #

VTH-LR-509 ..... N88-24734 #
VTH-LR-514 ..... N88-24733 #
VTH-LR-517 ..... N88-24909 #

WHOI-87-55 ..... N88-24661 #

WS-333 ..... N88-25225 #

WU-249 ..... N88-25419* #

Y-2393 ..... N88-24757 #

☆ U.S. GOVERNMENT PRINTING OFFICE: 1988— 201-150/80016

FEDERAL REGIONAL DEPOSITORY LIBRARIES

ALABAMA

AUBURN UNIV. AT MONTGOMERY LIBRARY
Documents Department
Montgomery, AL 36193
(205) 271-9650

UNIV. OF ALABAMA LIBRARY
Documents Dept.-Box S
University, AL 35486
(205) 348-6046

ARIZONA

DEPT. OF LIBRARY, ARCHIVES AND PUBLIC RECORDS
Third Floor—State Cap.
1700 West Washington
Phoenix, AZ 85007
(602) 255-4121

UNIVERSITY OF ARIZONA LIB.
Government Documents Dept.
Tucson, AZ 85721
(602) 621-6433

ARKANSAS

ARKANSAS STATE LIBRARY
One Capitol Mall
Little Rock, AR 72201
(501) 371-2326

CALIFORNIA

CALIFORNIA STATE LIBRARY
Govt. Publications Section
P.O. Box 2037
Sacramento, CA 95809
(916) 324-4863

COLORADO

UNIV OF COLORADO LIB.
Government Pub. Division
Campus Box 184
Boulder, CO 80309
(303) 492-8834

DENVER PUBLIC LIBRARY
Govt. Pub. Department
1357 Broadway
Denver, CO 80203
(303) 571-2131

CONNECTICUT

CONNECTICUT STATE LIBRARY
Government Documents Unit
231 Capitol Avenue
Hartford, CT 06106
(203) 566-7029

FLORIDA

UNIV. OF FLORIDA LIBRARIES
Library West
Documents Department
Gainesville, FL 32611
(904) 392-0367

GEORGIA

UNIV. OF GEORGIA LIBRARIES
Government Reference Dept.
Athens, GA 30602
(404) 542-8949

HAWAII

UNIV. OF HAWAII LIBRARY
Govt. Documents Collection
2550 The Mall
Honolulu, HI 96822
(808) 948-8230

IDAHO

UNIV. OF IDAHO LIBRARY
Documents Section
Moscow, ID 83843
(208) 885-6344

ILLINOIS

ILLINOIS STATE LIBRARY
Information Services Branch
Centennial Building
Springfield, IL 62756
(217) 782-5185

INDIANA

INDIANA STATE LIBRARY
Serials Documents Section
140 North Senate Avenue
Indianapolis, IN 46204
(317) 232-3686

IOWA

UNIV. OF IOWA LIBRARIES
Govt. Documents Department
Iowa City, IA 52242
(319) 353-3318

KANSAS

UNIVERSITY OF KANSAS
Doc. Collect—Spencer Lib.
Lawrence, KS 66045-2800
(913) 864-4662

KENTUCKY

UNIV. OF KENTUCKY LIBRARIES
Govt. Pub. Department
Lexington, KY 40506-0039
(606) 257-3139

LOUISIANA

LOUISIANA STATE UNIVERSITY
Middleton Library
Govt. Docs. Dept.
Baton Rouge, LA 70803
(504) 388-2570

LOUISIANA TECHNICAL UNIV. LIBRARY
Documents Department
Ruston, LA 71272-0046
(318) 257-4962

MAINE

UNIVERSITY OF MAINE
Raymond H. Fogler Library
Tri-State Regional Documents Depository
Orono, ME 04469
(207) 581-1680

MARYLAND

UNIVERSITY OF MARYLAND
McKeldin Lib.—Doc. Div.
College Park, MD 20742
(301) 454-3034

MASSACHUSETTS

BOSTON PUBLIC LIBRARY
Government Docs. Dept.
Boston, MA 02117
(617) 536-5400 ext.226

MICHIGAN

DETROIT PUBLIC LIBRARY
Sociology Department
5201 Woodward Avenue
Detroit, MI 48202-4093
(313) 833-1409

MICHIGAN STATE LIBRARY
P.O. Box 30007
Lansing, MI 48909
(517) 373-1593

MINNESOTA

UNIVERSITY OF MINNESOTA
Government Pubs. Division
409 Wilson Library
309 19th Avenue South
Minneapolis, MN 55455
(612) 373-7870

MISSISSIPPI

UNIV. OF MISSISSIPPI LIB.
Documents Department
University, MS 38677
(601) 232-5857

MONTANA

UNIV. OF MONTANA
Mansfield Library
Documents Division
Missoula, MT 59812
(406) 243-6700

NEBRASKA

UNIVERSITY OF NEBRASKA - LINCOLN
Love Library
Documents Department
Lincoln, NE 68588-0410
(402) 472-2562

NEVADA

UNIVERSITY OF NEVADA LIB.
Govt. Pub. Department
Reno, NV 89557-0044
(702) 784-6579

NEW JERSEY

NEWARK PUBLIC LIBRARY
5 Washington Street
Newark, NJ 07101-0630
(201) 733-7812

NEW MEXICO

UNIVERSITY OF NEW MEXICO
Zimmerman Library
Government Pub. Dept.
Albuquerque, NM 87131
(505) 277-5441

NEW MEXICO STATE LIBRARY
Reference Department
325 Don Gaspar Avenue
Santa Fe, NM 87503
(505) 827-3826

NEW YORK

NEW YORK STATE LIBRARY
Empire State Plaza
Albany, NY 12230
(518) 474-5563

NORTH CAROLINA

UNIVERSITY OF NORTH CAROLINA AT CHAPEL HILL
Davis Library
BA/SS Documents Division
Chapel Hill, NC 27515
(919) 962-1151

NORTH DAKOTA

UNIVERSITY OF NORTH DAKOTA
Chester Fritz Library
Documents Department
Grand Forks, ND 58202
(701) 777-4629
In cooperation with North Dakota State Univ. Library

OHIO

STATE LIBRARY OF OHIO
Documents Department
65 South Front Street
Columbus, OH 43266-0334
(614) 462-7051

OKLAHOMA

OKLAHOMA DEPT. OF LIB.
Government Documents
200 NE 18th Street
Oklahoma City, OK 73105
(405) 521-2502, ext. 252

OKLAHOMA STATE UNIV. LIB.
Documents Department
Stillwater, OK 74078
(405) 624-6546

OREGON

PORTLAND STATE UNIV. LIB.
Documents Department
P.O. Box 1151
Portland, OR 97207
(503) 229-3673

PENNSYLVANIA

STATE LIBRARY OF PENN.
Government Pub. Section
P.O. Box 1601
Harrisburg, PA 17105
(717) 787-3752

TEXAS

TEXAS STATE LIBRARY
Public Services Department
P.O. Box 12927—Cap. Sta.
Austin, TX 78711
(512) 475-2996

TEXAS TECH. UNIV. LIBRARY
Govt. Documents Department
Lubbock, TX 79409
(806) 742-2268

UTAH

UTAH STATE UNIVERSITY
Merrill Library, U.M.C. 30
Logan, UT 84322
(801) 750-2682

VIRGINIA

UNIVERSITY OF VIRGINIA
Alderman Lib.—Public Doc.
Charlottesville, VA 22903-2498
(804) 924-3133

WASHINGTON

WASHINGTON STATE LIBRARY
Documents Section
Olympia, WA 98504
(206) 753-4027

WEST VIRGINIA

WEST VIRGINIA UNIV. LIB.
Documents Department
Morgantown, WV 26506-6069
(304) 293-3640

WISCONSIN

MILWAUKEE PUBLIC LIBRARY
814 West Wisconsin Avenue
Milwaukee, WI 53233
(414) 278-3065

ST. HIST LIB. OF WISCONSIN
Government Pub. Section
816 State Street
Madison, WI 53706
(608) 262-4347

WYOMING

WYOMING STATE LIBRARY
Supreme Ct. & Library Bld.
Cheyenne, WY 82002
(307) 777-5919

National Aeronautics and
Space Administration
Code NTT-4
Washington, D.C.
20546

Official Business

Penalty for Private Use, $300

SPECIAL FOURTH-CLASS RATE
POSTAGE & FEES PAID
NASA
PERMIT No. G 27

NASA
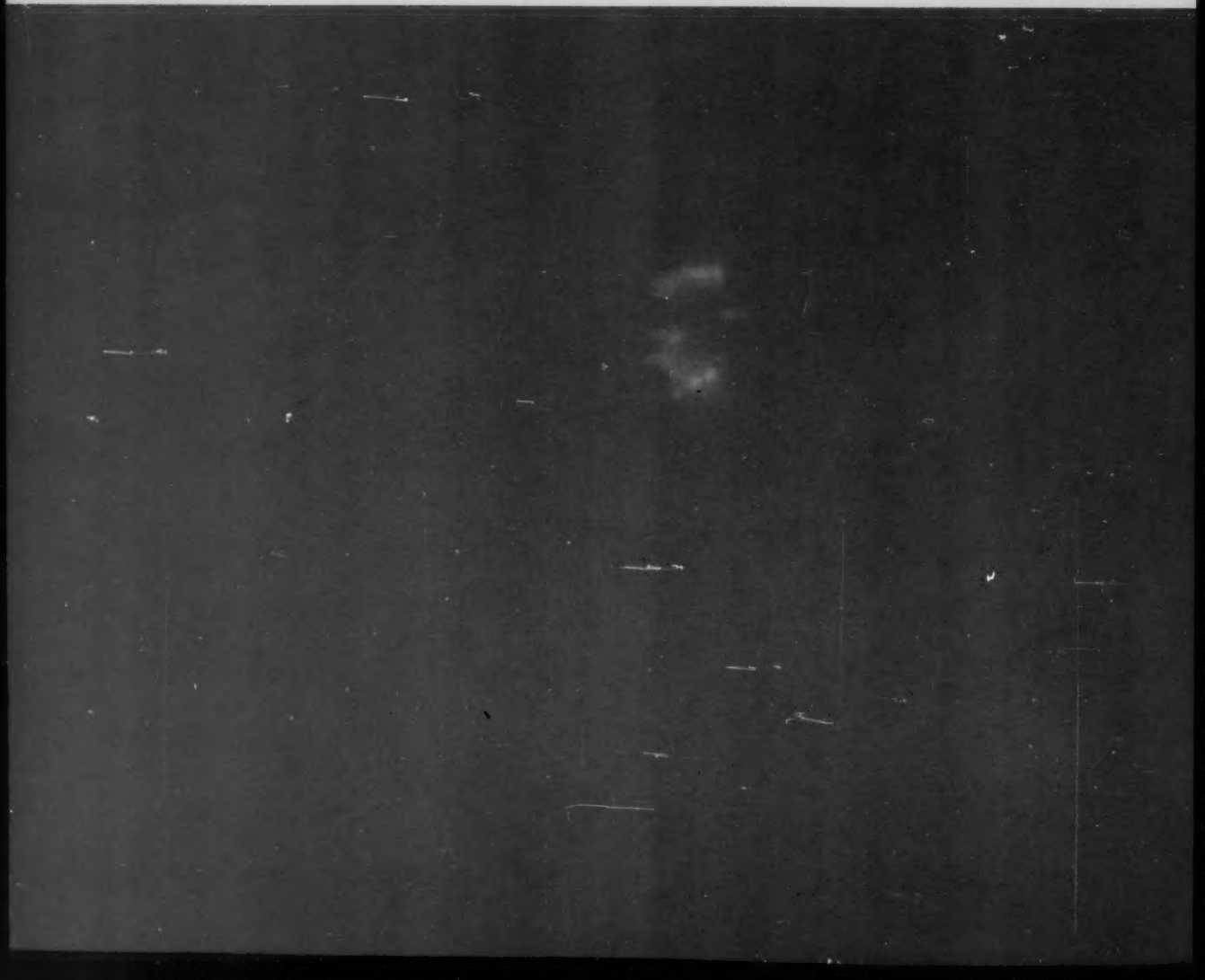
POSTMASTER: If Undeliverable (Section 158
Postal Manual) Do Not Return